TEXT FLY WITHIN THE BOOK ONLY

TEXT CROSS WITHIN THE BOOK ONLY

UNIVERSAL
LIBRARY

OU_158980

UNIVERSAL
LIBRARY

Osmania University Library

Call No. 537.2/C11P Accession No. 29635

Author Cady, W.G.

Title Piezoelectricity.

This book should be returned on or before the date last marked below

INTERNATIONAL SERIES IN PURE AND APPLIED PHYSICS
LEE A. DuBRIDGE, CONSULTING EDITOR
ADVISORY EDITORIAL COMMITTEE: E. U. Condon, George R. Harrison,
Elmer Hutchisson, K. K. Darrow

PIEZOELECTRICITY

The quality of the materials used in the manufacture of this book is governed by continued postwar shortages.

INTERNATIONAL SERIES IN PURE AND APPLIED PHYSICS

LEE A. DUBRIDGE, *Consulting Editor*

BACHER AND GOUDSMIT—ATOMIC ENERGY STATES

BITTER—INTRODUCTION TO FERROMAGNETISM

BRILLOUIN—WAVE PROPAGATION IN PERIODIC STRUCTURES

CADY—PIEZOELECTRICITY

CLARK—APPLIED X-RAYS

CONDON AND MORSE—QUANTUM MECHANICS

CURTIS—ELECTRICAL MEASUREMENTS

DAVEY—CRYSTAL STRUCTURE AND ITS APPLICATIONS

EDWARDS—ANALYTIC AND VECTOR MECHANICS

ELDRIDGE—THE PHYSICAL BASIS OF THINGS

HARDY AND PERRIN—THE PRINCIPLES OF OPTICS

HARNWELL—PRINCIPLES OF ELECTRICITY AND ELECTROMAGNETISM

HARNWELL AND LIVINGOOD—EXPERIMENTAL ATOMIC PHYSICS

HOUSTON—PRINCIPLES OF MATHEMATICAL PHYSICS

HUGHES AND DUBRIDGE—PHOTOELECTRIC PHENOMENA

HUND—HIGH-FREQUENCY MEASUREMENTS
PHENOMENA IN HIGH-FREQUENCY SYSTEMS

KEMBLE—THE FUNDAMENTAL PRINCIPLES OF QUANTUM MECHANICS

KENNARD—KINETIC THEORY OF GASES

KOLLER—THE PHYSICS OF ELECTRON TUBES

MORSE—VIBRATION AND SOUND

MUSKAT—THE FLOW OF HOMOGENEOUS FLUIDS THROUGH POROUS MEDIA

PAULING AND GOUDSMIT—THE STRUCTURE OF LINE SPECTRA

RICHTMYER—INTRODUCTION TO MODERN PHYSICS

RUARK AND UREY—ATOMS, MOLECULES AND QUANTA

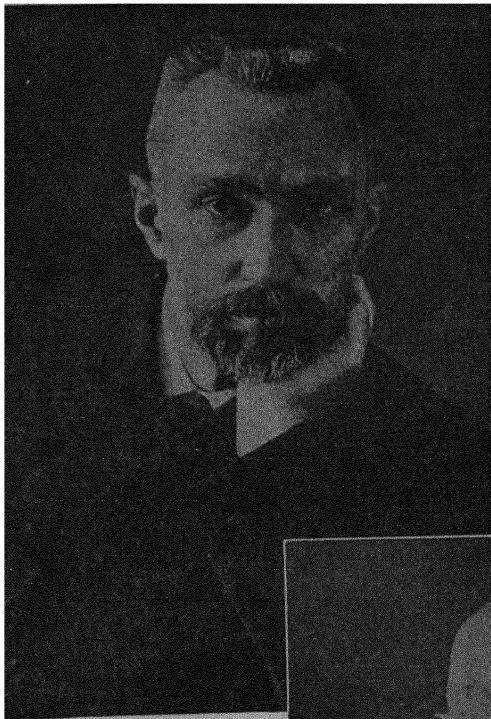
SLATER—INTRODUCTION TO CHEMICAL PHYSICS

SLATER AND FRANK—INTRODUCTION TO THEORETICAL PHYSICS

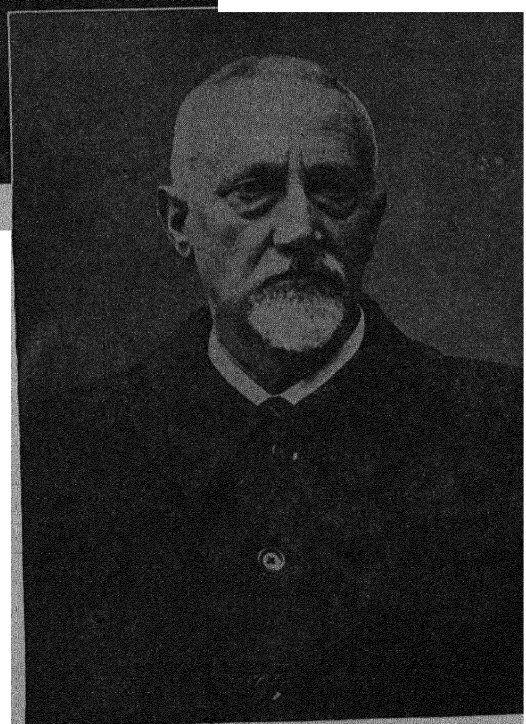
SMYTHE—STATIC AND DYNAMIC ELECTRICITY

WHITE—INTRODUCTION TO ATOMIC SPECTRA

WILLIAMS—MAGNETIC PHENOMENA



Pierre Curie, 1905



Jacques Curie, 1926

PIEZOELECTRICITY

An Introduction to the Theory and Applications of Electromechanical Phenomena in Crystals

by WALTER GUYTON CADY, Ph.D., Sc.D.
Professor of Physics, Wesleyan University

First Edition
SECOND IMPRESSION

New York *London*
McGRAW-HILL BOOK COMPANY, INC.
1946

PIEZOELECTRICITY

COPYRIGHT, 1946, BY THE
McGRAW-HILL BOOK COMPANY, INC.

PRINTED IN THE UNITED STATES OF AMERICA

All rights reserved. This book, or parts thereof, may not be reproduced in any form without permission of the publishers.

THE MAPLE PRESS COMPANY, YORK, PA.

To my dearest and most exacting critics,
the students in my classes in crystal physics

PREFACE

Interest in the physical properties of piezoelectric crystals, as well as in their practical applications, has become so great as to make the need felt for a comprehensive treatise. The present book is an attempt to meet this need, at least in part.

Piezoelectricity is related by so many ties to all branches of physics that any general text on the subject must be to some extent a treatise on crystal physics. That this book makes no attempt to comprise the whole of crystal physics is evident from the fact that such topics as metallic crystals and structure sensitiveness are hardly mentioned. Even with regard to insulating crystals the discussion is confined mainly to those with piezoelectric properties. Such matters as thermal properties and plasticity are treated, if at all, only insofar as they have a bearing on the central theme. On the other hand, it seemed desirable to include chapters on elasticity, pyroelectricity, and certain optical effects, presenting the basic principles and those special features which relate them to piezoelectric phenomena.

Considerable space has been given to the theory of the piezo resonator, its equivalent electrical network, and graphical methods for the analysis of resonator problems.

Rochelle salt and other Seignette-electrics have been treated at some length, because of the interesting problems they present and their wide range of present and future applications. The intelligent use of these crystals in technical devices is impossible without a knowledge of their properties and of the accompanying theory. The notes on ferromagnetism in the Appendix were written as an aid in interpreting the analogous effects in the Seignette-electrics. Those who desire only a brief treatment of the subject will find that various aspects of the properties and theory of Rochelle salt are summarized in the opening paragraphs of Chaps. XX, XXIII, and XXV and also in §§471 to 476 and 489 to 490.

A new formulation of piezoelectric theory, known as the "polarization theory," has recently been made by Prof. Hans Mueller and Dr. W. P. Mason in their attacks on the problem of Rochelle salt. In Chap. XI the author has shown how this and still other formulations may be derived from thermodynamic principles and has developed the polarization theory in general form, applicable to all piezoelectric crystals.

Those who use the book as a general text on the physical properties and applications of piezoelectric crystals will find their material chiefly

in Chaps. I to III, V, VII, VIII, X to XV, XVIII, XIX, and XXVIII to XXXI, supplemented by the opening sections of most of the other chapters, and by §§49 to 52 and 172 to 175.

Since the book is intended for research workers as well as for students of physics and radio amateurs who wish to learn more about crystals, it is unavoidable that some portions place more demands than others on previous acquaintance with physics, mathematics, and electric-circuit theory. Not much previous scientific training is required for understanding most of Chaps. I, II, XVI, XIX, and XXVIII, as well as the introductions to many other chapters, in which general surveys of various topics are given; Chaps. VIII, XIII, XVII, and XX may be mentioned in particular.

In general, details of electric circuits have been omitted; a few typical examples are given. Although a laboratory manual on piezoelectric crystals would doubtless be useful, limitations of space prevent the present book from going much further in this direction than to include some paragraphs on the technique of quartz and Rochelle salt.

Here and there in the book will be found material that has not been published elsewhere. This material includes some of the methods of approach and development, as well as some original contributions to the field. Mention may be made of considerable portions of Chaps. V, XI, XII, XIII, XIV, and XVII; the devices suggested in Figs. 105 and 156 and in the footnote on page 417; and some experimental results obtained by students at Wesleyan University and described in their theses.*

In general, the reference numbers in the text are the numbers of books or articles listed in the general bibliography at the end of the book. Book numbers have the prefix *B*. Special bibliographies, on electrets and on the effect of X-rays on vibrating crystals, will be found at the ends of Chaps. IX and XIII, respectively. Text references to articles in these bibliographies are in square brackets in the respective chapters.

For permission to use certain illustrations, thanks are extended to the publishers of the following books and journals and to the authors concerned: Hermann & Cie, Paris; B. G. Teubner, Leipzig; *Annalen der Physik; Bell System Technical Journal; Elektrische Nachrichten-Technik; Ergebnisse der exakten Naturwissenschaften; Helvetica Physica Acta; Proceedings of the Institute of Radio Engineers; Annals of the New York Academy of Sciences; Physics; Physical Review; Physikalische Zeitschrift; Proceedings of the Physical Society; Proceedings of the Royal Society (London); Telefunken-Zeitung; Mémoires de la Société vaudoise des sciences naturelles; Zeitschrift für technische Physik.*

* To a large extent the students' investigations were initiated by Prof. Van Dyke and carried out under his direction, as parts of an extended program of research.

Thanks are due to the following students and assistants, in addition to those mentioned in the text, for their efficient aid in experimental work, calculations, and the preparation of diagrams: H. P. Blakeslee, A. H. Butler, R. S. Cohen, C. A. Dyer, R. C. Hitchcock, G. J. Holton, H. H. Hubbell, Jr., R. I. Hulsizer, Jr., R. S. Kardas, G. H. Kent, G. A. Kolstad, J. F. Müller, D. O. North, E. T. Peabody, Miss E. Ruthven Tremain, J. E. Walstrom, M. E. White, and P. D. Zottu. Special recognition should be given to the aid rendered by Dr. H. Jaffe in experimentation and computation and particularly in the assembling of much of the material for the chapters on Rochelle salt and atomic theory. For aid in preparing the data on the structure of quartz the author is indebted to G. J. Holton.

Grateful acknowledgment is made to Dr. W. P. Mason and the Bell Laboratories for diagrams, elastic and piezoelectric equations, and unpublished experimental data; to J. K. Clapp and the General Radio Company for the use of the photograph shown in Fig. 103 and for technical information; to the Brush Development Company for Rochelle-salt crystals and much valuable information; and to the Naval Research Laboratory for access to their bibliography on crystals.

Many sections of the book have been read by the author's students, whose comments and criticisms have been very stimulating. Certain portions have been examined by Prof. Hans Mueller, Prof. V. E. Eaton, Dr. W. P. Mason, and Dr. Hans Jaffe, from whom many helpful suggestions have been received. The author is especially indebted to Prof. K. S. Van Dyke and Dr. W. M. Cady for much patient perusal of manuscript, constructive criticism, and many invaluable suggestions during the growth of the book. The careful reading of the manuscript in its final form by Lieut. F. H. Rathmann, USNR, of the Naval Research Laboratory, has also led to various emendations. To all these good friends the author is very grateful. For such errors as may still remain in the text he is responsible, not they.

WALTER GUYTON CADY.

MIDDLETOWN, CONN.,
January, 1946.

CONTENTS

Page

PREFACE ix

TABLES xix

SYMBOLS AND ABBREVIATIONS xxi

CHAPTER I

Introduction 1

CHAPTER II

Crystallography 9

General Principles—Crystallography of Rochelle Salt, Alpha- and Beta-quartz, and Tourmaline—Stereographic Projection—References.

CHAPTER III

Crystal Elasticity 39

Introduction—Primary and Secondary Effects—Thermodynamic Potentials—Stresses and Strains—Tables for the Nine Groups—Poisson's Ratio—Flexure—Torsion—Compressibility—Adiabatic Constants.

CHAPTER IV

Rotated Axes and Transformation of Elastic Constants 65

Transformation of Components of Strain and Stress—General Equations—Specialization for Certain Groups—Terminology for Crystal Cuts—Notation for Orientation of Transformed Axes—References.

CHAPTER V

Vibrations of Crystals 84

Introduction—Normal Modes—Longitudinal Vibrations of Rods—Equivalent System with Single Degree of Freedom—Harmonics—Forces Applied Locally—Effect of Cross Section—Thickness Vibrations of Plates—Conservation of Angular Momentum—Comparison of Wave Velocities for Various Types of Vibration—Flexural Vibrations—Torsional Vibrations—References.

CHAPTER VI

Elastic Constants of Crystals 116

Experimental Methods—Data for Rochelle Salt, Quartz, Tourmaline, and Other Crystals—Effects of Stress and Temperature.

CHAPTER VII

PAGE

Dielectric Properties of Crystals 160

Basic Equations, and Application to Crystals—Rotated Axes—Air Gap and Surface Impurities—Molecular Nature of Polarization—Dissipation of Energy—References.

CHAPTER VIII

Principles of Piezoelectricity 177

Introduction—Fundamental Equations—Piezoelectric Classes—Rotated Axes—Electrostriction—References.

CHAPTER IX

Special Piezoelectric Properties of Certain Crystals 200

Specialized Formulas for Rotated Axes—Values of the Piezoelectric Constants of Various Crystals—Qualitative Data on Miscellaneous Crystals—Electrets—References.

CHAPTER X

Production and Measurement of Piezoelectric Effects 236

Orientation and Electrodes—Compression, Shear, Flexure, and Torsion—Measurement of Piezoelectric Constants—Qualitative Tests.

CHAPTER XI

Alternative Formulations of Piezoelectric Theory 245

Thermodynamic Equations—Polarization, Displacement, and Molecular-field Theories—Equations of the Polarization Theory—Comparison with Voigt's Theory.

CHAPTER XII

Secondary Piezoelectric Effects 260

Correlation between Elastic and Dielectric Phenomena—Free and Clamped States—Piezoelectric Contribution to the Dielectric and Elastic Constants—Illustrations of Piezoelectric Reactions—Numerical Examples—Piezoelectric Reaction on Elastic Cycles.

CHAPTER XIII

The Piezoelectric Resonator 284

Introduction—Theory of Lengthwise and Thickness Vibrations—Equivalent Electric Constants—Effect of Gap—Overtone Frequencies—Procedure for Deriving Elastic Constants—Effects of Vibrations on X-ray Reflections—References.

CHAPTER XIV

The Electrical Equivalent of the Piezo Resonator 333

Introduction—Resonance Circle—Critical Frequencies—Effects of Gap—Resonance Curves—Insertion of Other Circuit Elements—Circle for Motional Admittance.

CHAPTER XV

PAGE

The Dynamic Measurement of Piezoelectric and Equivalent Electric Constants 384

Qualitative Tests—Methods of Quantitative Measurement—Reduction of Observations—References.

CHAPTER XVI

Properties and Technique of Quartz 406

Axes and Angles—Physical Properties—Experimental Determination of Axes—Cutting and Finishing—Mountings and Holders—References.

CHAPTER XVII

The Quartz Resonator. 435

Excitation of Lengthwise and Thickness Vibrations and Experimental Results—Unsymmetrical Effects—Effect of Gap—Flexural and Torsional Vibrations—Special Cuts and Shapes—Numerical Data—Luminous Resonators—Wave Patterns—Beta-quartz Resonators—References.

CHAPTER XVIII

Resonators from Other Crystals, and Composite Resonators 469

Theory of the Rochelle-salt Resonator—Experimental Results with Various Vibrational Modes—Other Crystals—Tourmaline—Composite Resonators —References.

CHAPTER XIX

The Piezo Oscillator. 489

Crystal Stabilizers—The Crystal-controlled Oscillator—Various Circuits—Standard-frequency Oscillators—Rochelle-salt and Tourmaline Oscillators —References.

CHAPTER XX

Rochelle Salt: History, General Properties, and Technique. 510

General Summary of Properties—Historical—Data on Chemical and Physical Properties—Production, Cutting, and Finishing—Electrodes.

CHAPTER XXI

Rochelle Salt: Piezoelectric Observations. 531

Direct Effect—Methods of Measurement—Converse Effect—Alternating Fields—Comparison of the Direct and Converse Effects—Lag, Fatigue, and Relaxation Times.

CHAPTER XXII

Rochelle Salt: Dielectric Observations. 549

Types of Permittivity—Static Fields—Unipolarity—Low-frequency Alternating Fields—Hysteresis Loops—Spontaneous Polarization—Mechanical Bias—High-frequency Fields—Effect of Hydrostatic Pressure on Susceptibility—Heavy-water Rochelle Salt.

CHAPTER XXIII

PAGE

Theory of Rochelle Salt, Part I. Interaction Theory and Dielectric Properties 580

Historical—Definitions—Rhombic and Normal Methods—Basic Equations —Application of the Interaction Theory—The Clamped Crystal between the Curie Points—Equations According to the Normal Method.

CHAPTER XXIV

Theory of Rochelle Salt, Part II. Piezoelectric and Elastic Properties, Curie-Weiss Laws, and Conclusions 603

Direct and Converse Effects—Elastic Constants—The Quadratic Effect—Curie-Weiss Laws—Summary of Theory—Experimental Confirmation—Conclusions Respecting the Polarization Theory.

CHAPTER XXV

The Domain Structure of Rochelle Salt 631

Introduction—Effect of Domain Structure on Hysteresis Loops—Polymorphism.

CHAPTER XXVI

Internal-field Theory of Seignette-electric Crystals 643

Statement of the Theory, and Application to Rochelle Salt—Correlation between Various Forms of the Theory—The Moment of Rochelle-salt Dipoles.

CHAPTER XXVII

Other Seignette-electric Crystals 654

Crystals Isomorphic with Rochelle Salt, and Mixed Tartrates—Phosphates and Arsenates—Deuterium Potassium Phosphate—Domain Structure.

CHAPTER XXVIII

Miscellaneous Applications of Piezoelectricity 667

The Crystal Filter—Various Applications of Crystals as Transducers—Ultrasonics—Piezoelectric Emitters of Ultrasonic Waves—Effects of Intense Ultrasonic Radiation—The Ultrasonic Interferometer—Optical Effects—Television Reception—References.

CHAPTER XXIX

Pyroelectricity 699

Types of Pyroelectricity—Theory of the Vectorial Pyroelectric Effect—Tourmaline—Pyroelectric Constants of Various Crystals—The Electrocaloric Effect—Tensorial Pyroelectricity—References.

CHAPTER XXX

Piezo-optic, Electro-optic, and Other Optical Effects 713

Introduction—Optical Polarization Constants—Piezo-optic Effect—Electro-optic Effects—Experimental Results—Extinction and Optical Activity —References.

CHAPTER XXXI

PAGE

Piezoelectricity in the Light of Atomic Theory 731

Binding Forces in Crystals—The Structure of Quartz, Rochelle Salt, and Primary Potassium Phosphate—Atomic Theories of Piezoelectricity—The Piezoelectric Effect According to Lattice Dynamics—References.

APPENDIX

Ferromagnetism 745

Introduction—Paramagnetism—Ferromagnetism—The Curie-Weiss Law—Generalization of the Langevin Function—Domains—Magnetism and Strain—The Hysteresis Loop—Thermal Effects—Piezomagnetism.

GENERAL BIBLIOGRAPHY 755

AUTHOR INDEX 789

SUBJECT INDEX 797

TABLES

		Page
I.	Crystal Systems and Classes	19
II.	Symbols of Faces for Right-quartz	28
III.	Grouping of Crystals According to Physical Properties	34
IV.	Elastic Constants of Rochelle Salt	122
V.	Compliance Constants of Rochelle Salt	123
VI.	Reciprocal of Young's Modulus of Rochelle Salt for Bars at 45° with the Axes Indicated	125
VII.	Linear Compressibilities of Rochelle Salt	126
VIII.	Temperature Coefficients of Frequency for 45° Rochelle-salt Bars	131
IX.	Elastic Constants of Quartz	135
X.	Dynamic Temperature Coefficients of Elastic Constants of Quartz	136
XI.	Accepted Values of the Adiabatic Elastic Constants of Quartz	137
XII.	Stiffness Coefficients q for Thickness Vibrations of Quartz Plates in Various Orientations	142
XIII.	Elastic Constants of Tourmaline	157
XIV.	Dielectric Susceptibilities for the Seven Systems	162
XV.	Effect of Surface Impurities on the Dielectric Constants of Rochelle Salt	169
XVI.	Piezoelectric Constants for Each Crystal Class	190
XVII.	Piezoelectric Strain Constant d_{11} of Quartz	217
XVIII.	Piezoelectric Strain Constant d_{14} of Quartz	219
XIX.	Dynamic Values of the Piezoelectric Constants of Quartz	220
XX.	Chief Equations of the Voigt and Polarization Theories	249
XXI.	Electromechanical Relations	265

PAGE

XXII. Equivalent Constants for Thickness Vibrations. 323

XXIII. Critical Frequencies of Resonator. 355

XXIV. Resonator Data for Wide Variations in Frequency . . . 377

XXV. Density ρ, Thermal Conductivity, and Specific Heat, for α-quartz at Various Temperatures. 411

XXVI. Resistivity of Quartz at Various Temperatures 413

XXVII. Data on Flexural Vibrations 447

XXVIII. Data on Torsional Vibrations. 450

XXIX. Summary of Data for Various Cuts of Quartz 459

XXX. The Constants of Some Typical Quartz Resonators. . . 461

XXXI. Dielectric Constants of Rochelle Salt at Various Temperatures 474

XXXII. Frequencies and Electric Constants of a Rochelle-salt X45°-Bar 478

XXXIII. Electric Conductivity of Rochelle Salt. 520

XXXIV. Dielectric Constant of Rochelle Salt at High Frequencies 572

XXXV. Calculated Values of Dipole Moments of Rochelle Salt . 65[illegible]

XXXVI. Numerical Data for Phosphates and Arsenates . . . . . 65[illegible]

SYMBOLS AND ABBREVIATIONS

References are given to sections in which the symbols are defined or first used.

A	Amplitude of vibration, real or complex, §56.
a	Coefficient of linear thermal expansion, §20.
a_{mh}, b_{mh}	Piezoelectric stress and strain constants used in the polarization theory, §189.
a, b, c	Crystallographic axes, §4.
a, **b**, **c**	Intercepts of the unit face on the a-, b-, c-axes, §4.
B	Dielectric saturation coefficient, §§449, 452.
b	Breadth of a bar or plate; electric susceptance (application to the resonator in §269).
C	Electric capacitance; for resonator, see R, L, C, C_1 below.
C_2	Capacitance of gap between crystal and electrodes, §284.
c	Wave velocity, §55; generalized symbol for an elastic stress coefficient, §201.
c_{hk}	Elastic stiffness coefficient, §26; superscripts E, P, D, and * denote the values at constant electric field, constant polarization, constant total displacement, and constant normal displacement, respectively, as explained in Chap. XII.
D	Electric displacement.
d_{mh}	Piezoelectric strain constant, §§23, 124.
E	Electric field strength, §20.
e	Thickness of a plate or bar.
e'	Electric spacing $= e + kw$, §110.
e'_r	Effective electric spacing of a resonator, §§229, 249.
e_{mh}	Piezoelectric stress constant, §§23, 124.
F	Frictional factor, §56; internal field strength, §§113, 485.
f	Frequency; $f_0 = \omega_0/2\pi$ = fundamental frequency, §58.
f_s, f_p	Frequencies at series and parallel resonance, §276.
f_m, f_n	Frequencies for maximum and minimum admittance, §279.
G	Equivalent stiffness, §62.
g	Electric conductance (application to a resonator in §269).
H	Magnetic field strength; wave constant $= fl$, §362.
h	Order of harmonic, §55; ratio of any frequency f to the fundamental frequency f_0, §61.
I	Electric current; moment of inertia, §74; magnetic polarization, §548.
J	Mechanical equivalent of heat, §23.
j	$(-1)^{\frac{1}{2}}$.
K	The Boltzmann constant, §114.
k	Wavelength constant, §56; dielectric constant = permittivity, §103.
k_l	Effective dielectric constant for lengthwise vibrations, §229.
k_m	Dielectric constant for field in any direction m; other special suffixes are explained in §§105, 107, 430.

k', k''	Dielectric constants, respectively, of a crystal free and clamped, §§104, 124, 204.
kc/sec	Kilocycles per second; occasionally, when there is no ambiguity, the term is abbreviated to kc.
L	The Langevin function, §§114, 548; self-inductance (for self-inductance of a resonator see R, L, C, C_1 below).
l	Length.
l, m, n	Direction cosines.
M	Equivalent mass of a resonator, §62.
ma	Milliamperes.
mc/sec	Megacycles per second; occasionally, when there is no ambiguity, the symbol is abbreviated to mc.
mf, mmf	microfarad, micromicrofarad.
N	Number of molecules per unit volume, §113; dynamic torsional stiffness, §74.
N_s	Static torsional stiffness, §35.
n	shear modulus, §24; measure of dissonance ($n = \omega_0 - \omega$), §58.
P	Electric polarization.
P^0	Spontaneous polarization.
p	Pyroelectric constant, §§20, 516; coefficient of the generalized Langevin function, §§114, 552.
ppm	Parts per million.
Q	Quantity of heat, §20; torque, §35; electric charge; quality factor = $\pi/\delta = \omega L/R$, §§56, 269.
Q_h	Quality factor at harmonic h, §232.
q	Electrocaloric constant, §523; coefficient of the generalized Langevin function, §§114, 552; general stiffness factor in vibrational equations, §55; thermoelastic coefficient, §§20, 23.
q', q_0	Stiffness factors with and without a gap, respectively.
R, L, C, C_1	Equivalent electric constants of a resonator, §232.
R', L', C', C_1'	Same for a resonator with gap, §232.
R_h', L_h', C_h'	Equivalent constants for overtone of order h, §232.
R_s, X_s, C_s	Equivalent series constants, §271.
R_p, X_p, C_p	Equivalent parallel constants, §273.
r	Electromechanical ratio, §233.
s	Generalized symbol for an elastic compliance coefficient, §§20, 201.
s_{hk}	Elastic compliance coefficient, §26; special superscripts same as for c_{hk}.
s_y	Scale value for admittances on the resonance circle, §266.
s_z	Scale value for impedances on the resonance circle, §270.
T	Absolute temperature; torsional compliance, §35.
t	Time; temperature in degrees centigrade.
U	Constant of the gap effect, §237.
u, v, w	Components of displacement of a particle, §26
V	Potential; potential difference.
v	Velocity of a particle in vibration, §58.
W	Equivalent frictional coefficient of a resonator, §62.
w	Total gap between crystal and electrodes, §110.
X	Generalized symbol for a stress, §§20, 201; electric reactance (for reactance of a resonator see §232).
X_h	A component of stress, §25.
X, Y, Z	Orthogonal axes, §5.
X', Y', Z'	Rotated orthogonal axes, §38.

$(X_n)_d$	Driving stress, with orientation indicated by n, in resonator theory, §228.
x	Generalized symbol for a strain, §20.
x_h	A component of strain, §26.
x, y, z	Coordinates in space.
Y	Young's modulus, §24; electric admittance (for admittance of a resonator see §§232, 265, 269).
Z	Electric impedance (for impedance of a resonator see §§232, 265, 269).
α	Damping factor or attenuation constant, §56; molecular polarizability, §113; temperature coefficient (usually with a subscript), §§85, 357.
α, β, γ	Direction cosines.
γ	Internal field constant, §§113, 484; parameter in theory of forced vibrations, §57; of thickness vibrations, §250.
δ	Logarithmic decrement per cycle, §56.
δ, ϵ	Generalized symbols for piezoelectric constants d_{mh} and e_{mh}, used when it is desirable to omit suffixes, §§20, 201, 228, 246.
ζ	Second thermodynamic potential, §23.
η	Dielectric susceptibility, §104; special suffixes and superscripts are in general the same as for k, but see also §§449, 450, 454.
η_1	Clamped susceptibility of Rochelle salt, §450.
Θ	Angular parameter for expressing general orientation of a plate, §52.
θ	Angle of rotation, §§38, 51; phase angle, §234.
θ_{jh}	Coefficients of dielectric impermeability, §106.
θ_u, θ_l	Upper and lower Curie temperatures.
ϑ	A small departure of temperature from a standard value, §20.
κ	Volume elasticity, §24.
λ	Wavelength; Lamé coefficient, §31.
μ	Moment of a dipole, §113.
ξ	First thermodynamic potential, §23; vibrational displacement of a particle, §56.
ρ	Density; radius of resonance circle, §266.
$\sum_m^h$	Summation over integral values of m from 1 to h.
σ	Surface density of electric charge; Poisson's ratio, §24; scale value for frequency, §267.
σ'	Scale value for frequency, §268.
τ	Torsional strain, §35.
Φ	Force acting on the equivalent mass M of a resonator, §62.
ϕ	Angle of azimuth, §51.
χ	Reciprocal susceptibility, §106; special suffixes and superscripts same as for η.
ψ	Angle of skew used in expressing the general orientation of a plate, §52.
$\omega = 2\pi f$	Angular velocity or pulsatance; special subscripts same as for f.
$\sim$	Cycles; cycles per second; order of magnitude.
$\approx$	Approximate equality.
$\equiv$	Identical with.

Some of the foregoing symbols, as well as others not listed, are used locally for special purposes. In such cases they are suitably defined.

PIEZOELECTRICITY

CHAPTER I

INTRODUCTION

Lorsqu'une idée nouvelle naissait dans l'esprit du Vinci, elle ne s'y engendrait pas d'elle-même et sans cause; elle y était produite par quelque circonstance extérieure, par l'observation d'un phénomène naturel, par la conversation d'un homme, plus souvent encore par la lecture d'un livre. —P. DUHEM.

Man's earliest production of an electrical effect came through the agency of mechanical forces. A mysterious attractive power was known by the ancient Greeks to be a property of *elektron* (amber) when rubbed.* In later centuries, as more was learned about electricity, its various manifestations were distinguished by special prefixes, as galvanic, voltaic, animal, frictional, contact, faradic, thermo-, photo-, ballo-, tribo-, actino-, pyro-, piezo-, or strepho-, some of which are now obsolete or abandoned.

It had long been observed that a tourmaline crystal when placed in hot ashes first attracted and then repelled them. This fact first became known in Europe about 1703, when tourmalines were brought from Ceylon by Dutch merchants, but the attracting power of the crystal seems to have been recognized in Ceylon and India from time immemorial. It was sometimes called the "Ceylon magnet," and in 1747 Linnaeus gave it the scientific name *lapis electricus*. Its electrical character was established in 1756 by Aepinus, who noted the opposite polarities at the two ends of a heated tourmaline crystal. In 1824 Brewster, who had observed the effect with various kinds of crystals, introduced the name "pyroelectricity." Among the crystals with which he found the pyroelectric effect was Rochelle salt. The first definite theory of pyroelectricity—which most subsequent investigations have tended to confirm —was that of Lord Kelvin, who, noting that Canton in 1759 had observed opposite polarities on the freshly exposed surfaces of a fractured tourmaline crystal, postulated a state of permanent polarization in every pyroelectric crystal. According to this theory the pyroelectric effect is simply a manifestation of the temperature coefficient of this polarization.

* Although a knowledge of this property of amber is frequently attributed to Thales in the sixth century B.C., the first authentic account that has come down to us appears to be in Plato's (427–347 B.C.) "Timaeus," Sec. 80c.

Following a conjecture of Coulomb's that electricity might be produced by pressure, Haüy (the "father of crystallography") and later A. C. Becquerel performed experiments in which certain crystals showed electrical effects when compressed. Their findings—especially the fact that positive results were reported with such non-piezoelectric crystals as calcite—led, however, to the conclusion that what they observed was chiefly, if not entirely, contact electricity.*

Credit may confidently be given to the brothers Pierre and Jacques Curie† for the discovery in 1880 that some crystals when compressed in particular directions show positive and negative charges on certain portions of their surfaces, the charges being proportional to the pressure and disappearing when the pressure is withdrawn.

This was no chance discovery. Pierre Curie's previous study of the relation between pyroelectric phenomena and crystal symmetry led the two brothers not only to look for electrification from pressure but to foresee in what direction pressure should be applied and in which classes the effect was to be expected. It is fitting to quote here, in translation, the opening paragraphs of their paper in which the discovery was announced.

"Those crystals having one or more axes whose ends are unlike, that is to say hemihedral crystals with oblique faces, have the special physical property of giving rise to two electric poles of opposite signs at the extremities of these axes when they

* Nevertheless, there was something prophetic in a statement by A. C. Becquerel (*Bull. soc. philomath. Paris, ser.* 3, vol. 7, pp. 149–155, 1820) quoted at the beginning of Chap. VIII.

† Pierre Curie was born in Paris on May 15, 1859. After attending the Sorbonne, where he served as preparator in physics and received the master's degree and later the degree of doctor of science, he was appointed to a professorship in the Municipal School of Physics and Chemistry in Paris in 1895, and in the same year he married Marie Sklodowska. In 1900 he became a professor at the Sorbonne. In addition to his famous work on radioactivity in collaboration with Mme. Curie and on piezoelectric and other properties of dielectrics with his brother, his researches included the principles of symmetry, the design of various measuring instruments of great delicacy, and especially the effects of temperature on magnetism. He died on Apr. 19, 1906.

Paul-Jacques Curie was born in Paris in 1855. At the age of twenty he became preparator of chemistry courses in the School of Pharmacy and later preparator in the laboratory of mineralogy under Friedel, at the Sorbonne. He was associated with Friedel in a series of publications on pyroelectricity. It was in this laboratory that he and Pierre Curie discovered piezoelectricity in 1880. For this discovery the two brothers were awarded the Planté prize in 1895. In 1893 Jacques Curie became head lecturer in mineralogy at the University of Montpelier. His last work in physics was his determination of the piezoelectric constant of quartz in 1910. Suffering from a serious deafness, he retired in 1925 and died in 1941. (The information concerning Jacques Curie was obtained through the courtesy of his son, Prof. Maurice Curie.)

are subjected to a change in temperature: this is the phenomenon known under the name of *pyroelectricity.*

"We have found a new method for the development of polar electricity in these same crystals, consisting in subjecting them to variations in pressure along their hemihedral axes."

These remarks are followed by a brief account of the preparation of flat plates cut according to the proper orientation, provided with tin-foil electrodes, and connected to an electrometer. Deflections were observed on the application of pressure to plates from the following crystals: zinc blende, sodium chlorate, boracite, tourmaline, quartz, calamine, topaz, tartaric acid, cane sugar, and Rochelle salt. In later papers the Curies described piezoelectric effects in other crystals, the first quantitative measurements of the effect in quartz and tourmaline, practical applications of piezoelectric crystals, and the verification of the converse effect, to which reference will presently be made.

Great interest was immediately aroused in scientific circles. In particular, Hankel took exception to the Curies' belief in a one-to-one correspondence between the electrical effects of thermal and mechanical deformation. He contended that the new effect obeyed special laws of its own and proposed the name "piezoelectricity," a term that was promptly accepted by all, including the Curie brothers themselves.

This question of the relation of pyro- to piezoelectricity has been the object of much discussion, especially on the part of Voigt. He pointed out that a distinction must be made between "true" pyroelectricity caused by a change in temperature alone and the "false" pyroelectricity that is due to the deformation which accompanies a change in temperature and which is therefore of piezoelectric origin. Nor does it in any sense detract from the brilliance of the Curies' discovery to say that the first manifestations of piezoelectricity were observed centuries before their time, under the guise of electrification through heat.

The pyroelectric effect is so closely related to the piezoelectric that we shall have frequent occasion to refer to it. According to the dictionary (Webster's "New International Dictionary," 1939) the two effects are thus defined:*

* So many mispronunciations of "piezoelectricity" are current that it may be well to point out that according to both British and American dictionaries the first two syllables should be pronounced like the words "pie" and "ease." Although most authorities place the accent on the first syllable, in the 1934 and 1939 editions of Webster it is shifted to the second. This change deserves general acceptance, as it makes the word a little more euphonious, besides conforming to the practice in European languages.

The prefixes "piezo-" and "pyro-" are derived from Greek words meaning "to press" and "fire," respectively.

"*Piezoelectricity.* Electricity or electric polarity due to pressure, especially in a crystallized substance, as quartz.

"*Pyroelectricity.* A state of electric polarity produced on certain crystals by change of temperature. . . ."

An electromechanical phenomenon somewhat related to piezoelectricity is *electrostriction,* for which the dictionary offers this definition:

"*Electrostriction.* A deformation produced by electric stress, as the deformation of a Leyden jar on being charged."*

Piezoelectricity may be more precisely defined as *electric polarization produced by mechanical strain in crystals belonging to certain classes, the polarization being proportional to the strain and changing sign with it.* This statement defines the *direct piezoelectric effect.* Closely related to it is the *converse effect* (sometimes called the "reciprocal" or "inverse" effect), whereby a piezoelectric crystal becomes strained, when electrically polarized, by an amount proportional to the polarizing field. Both effects are manifestations of the same fundamental property of the crystal, and they occupy a position among those physical phenomena which are *reversible.* It is therefore only for historical reasons that the term "direct" is applied to one rather than the other of these two effects.

The converse piezoelectric effect was not foreseen by the Curie brothers. In the year following their discovery of the direct effect, Lippmann discussed the application of thermodynamic principles to reversible processes involving electric quantities. He treated the special cases of electrostriction, pyroelectricity, and the Curies' recent discovery, and he asserted that there should exist a converse phenomenon corresponding to each of these effects. All these predictions have been verified. The converse of pyroelectricity is the electrocaloric effect, which, also on thermodynamic grounds, had already been predicted by Lord Kelvin in 1877. Before the end of 1881 the Curies had verified the converse piezoelectric effect, and in a later paper they showed that the piezoelectric coefficient of quartz had the same value for the converse as for the direct effect. They also called attention to the analogy between the interaction of the direct and converse effects and Lenz's law.

The converse piezoelectric effect has sometimes been treated as a special type of electrostriction. Although the dictionary definitions given above may appear to justify this treatment, the two phenomena are essentially different. So far as external effects are concerned, the distinction lies in the fact that the deformations due to electrostriction are proportional to the *square* of the applied electric field and therefore are independent of the direction of the field. That is, to show the effect a

* For more precise definitions of pyroelectricity and electrostriction see §§515 and 137.

substance need have no special peculiarity in its internal structure. Indeed, electrostriction is a universal property of dielectrics, whether in the gaseous, liquid, or solid state. The effect is always extremely minute, and we shall have but little occasion to refer to it. On the other hand, piezoelectric deformations are *directly proportional* to the electric field and reverse their sign upon reversal of field. This is possible only in substances that possess a certain inherent "one-wayness." Such substances are *anisotropic*, and the only materials with which we shall be especially concerned are those crystals which possess the requisite degree of asymmetry.

The phenomenological theory of piezoelectricity is based on thermodynamic principles enunciated by Lord Kelvin. His penetrating and many-sided applications of thermodynamics to crystals marked a great advance in the study of crystal physics. The piezoelectric formulation was carried out more completely by P. Duhem and F. Pockels and most fully and rigorously by Woldemar Voigt in 1894. To this formulation is devoted one of the chapters in Voigt's monumental "Lehrbuch der Kristallphysik,"* which appeared in 1910 and has ever since been the bible for workers in this field. By combining the elements of symmetry of elastic tensors and of electric vectors with the geometrical symmetry elements of crystals he made clear in which of the 32 crystal classes piezoelectric effects may exist, and for each class he showed which of the possible 18 piezoelectric coefficients may have values differing from zero.

For a third of a century after its discovery piezoelectricity remained a scientific curiosity, unmentioned in many textbooks, and furnishing material for a few doctor's theses. Even among crystallographers it has received less attention than pyroelectricity, although it was the chief cause of most observed pyroelectric effects, and, properly applied, it might have served as a valuable aid in crystal classification.

Then came the spur of wartime activity. In France, cradle of piezoelectricity, Langevin conceived the idea of exciting quartz plates electrically to serve as emitters, and later also as receivers, of high-frequency (h-f) sound waves under water. At the hands of Langevin and others the "echo method" has become a valuable means of locating immersed objects and of exploring the ocean bottom.

Langevin thus became the originator of the modern science and art of *ultrasonics*. Acoustic waves having frequencies of a million or more are now widely used, both for measuring various elastic and other properties of matter and for many practical applications in chemistry, biology, and industry. The source of radiation may be either a magnetostriction

* Throughout the present book, references to the "Lehrbuch" will be indicated simply by Voigt, "Kristallphysik," or "Lehrbuch."

oscillator or, more commonly, especially for the highest frequencies, a vibrating piezoelectric crystal plate (usually quartz). For investigating the properties of gases and liquids there is the acoustic interferometer, first described by G. W. Pierce in 1925. Elastic properties of liquids and solids are studied by various adaptations of the principle of optical diffraction produced by h-f compressional waves, discovered in 1932 independently by Debye and Sears and by Lucas and Biquard.

The exigency of the First World War led to experiments in various laboratories on the properties and practical applications of piezoelectric crystals. As is well known, these investigations have most fortunately borne fruit in the form of many useful peacetime devices. In the course of observing the characteristics of Rochelle-salt crystal plates for use in underwater signaling, the author was led in 1918 to examine certain peculiarities in their electrical behavior in the neighborhood of frequencies of mechanical resonance. Out of this experience arose the development of the *piezoelectric resonator* and its various uses as stabilizer, oscillator, and filter, for which quartz was soon found to be the most suitable material. Their operation involves a combination of the direct and converse effects. At the hands of many experimenters, resonators of quartz or tourmaline have been constructed that respond to frequencies from the audible range to over a hundred million cycles per second. On the purely scientific side, by means of observations with piezo resonators knowledge has been gained of the nature of vibrations in crystalline media and of the dynamic values of the elastic and piezoelectric constants. Composite resonators have also been constructed, in which, for example, a bar of metal is kept in resonant vibration by means of an attached piece of quartz. By this means the elastic constants and frictional coefficients of various solids have been determined.

Among the technical developments of resonating crystals may be mentioned their almost universal use in radio transmitting stations, either for direct control of frequency in the form of piezo oscillators or indirectly as monitoring devices. The combination in quartz of extraordinarily low damping with sufficiently strong piezoelectric properties to react upon and control the frequency of vacuum-tube generators results in a method for obtaining frequencies much more constant than is possible by electrical tuning alone. Certain disturbing effects due to coupling between different modes of vibration, and also the effect of changing temperature upon frequency, can be largely avoided by cutting quartz plates according to special orientations. This precision reaches its culmination in the *quartz clock*, in which a vibrating quartz plate or ring replaces the swinging pendulum, resulting in a timepiece more constant than the best astronomical clocks. Piezo resonators and oscillators have proved useful in many kinds of electrical measurement. Among recent appli-

cations is their use as electric filters for communication lines and radio receiving sets.

At the same time that the crystal resonator and its applications were being investigated, there was hardly less activity in the development of non-resonant applications of quartz and Rochelle salt and, to a less extent, of tourmaline. Many devices have been invented, especially in Germany and Japan, for the measurement of explosive pressures and of velocities, accelerations, forces, vibrations of machinery, etc. In the United States the progress has been chiefly in the field of acoustics, by taking advantage of the extremely great piezoelectric effect in Rochelle salt. By the ingenious adaptation of plates from Rochelle-salt crystals, microphones, telephone receivers, phonograph pickups, record cutters, and other devices have been made that are in most respects superior to their elctromagnetic predecessors.

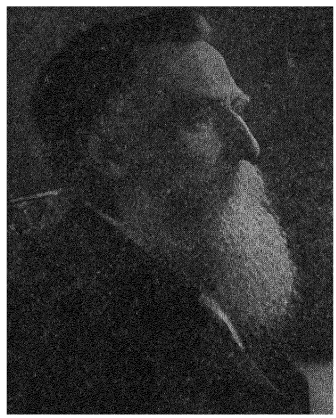
The revival of interest in piezoelectricity has led to a vast amount of research on the electrical properties of Rochelle salt. This substance has turned out to be the most remarkable of all known dielectrics and the prototype of a group of crystals known as the "Seignette-electrics." Our reasons for devoting to these what may seem a disproportionate amount of space are the close relation of their unique behavior to their piezoelectric properties, their analogy to ferromagnetic materials, and the important place they occupy in the theory of polar dielectrics. For these reasons we shall attempt in later chapters to summarize and correlate the chief results that have thus far been achieved. Investigations in this field have been most active in the United States, Russia, and Switzerland.

With respect to an *atomic theory* of piezoelectricity only modest progress has hitherto been made. Early attempts were put forward by the Curies, Riecke, and Voigt and especially by Lord Kelvin. The most rigorous treatment is that by M. Born, who in his general theory of lattice dynamics included a consideration of dielectric, pyroelectric, and piezoelectric effects. He applied his theory to a few types of cubic lattice. In 1920 he published, with E. Bormann, the first theoretical calculation of the piezoelectric constant of zinc blende.

X-ray analysis has thrown considerable light on the arrangement of atoms in quartz. By this means Bragg and Gibbs in 1925 arrived at a qualitative explanation of piezoelectric polarization in this crystal. The effect of vibrations in quartz plates upon X-ray reflection patterns has also been studied, by both the Laue and the Bragg methods. As to Rochelle salt, its structure is too complex for X-rays to be of much help in accounting for the piezoelectric properties, although they have thrown some light on the problem of the internal field. The molecular theory of the Seignette-electrics is still at a very early stage.

Piezoelectricity has been called by Voigt the most complicated

branch of crystal physics. Considered only in its phenomenological aspect, quite apart from the difficulties with which the atomic theory is beset, a complete description of the piezoelectric properties of a crystal involves a treatment in terms of three different types of directed quantities. These are electric (field and polarization), elastic (stress and



Professor Woldemar Voigt. (The portrait was obtained through the courtesy of his grandson, Dr. E. Mollwo, of the University of Gottingen.)

strain), and the piezoelectric coefficients by which they are related. In mathematical language the three types are, respectively, vectors (first-order tensors) and tensors of the second and third orders. With masterly skill and great thoroughness Voigt worked out all the essential details of these very intricate relations. He laid an impregnable and permanent groundwork for the labors of all succeeding workers in this field.*

* "Woldemar Voigt was born in 1850. He studied under F. Neumann, to whose influence his interest in crystal physics was due. In 1875 he became *Ausserordentlicher* Professor of physics at Königsberg, and in 1883 professor of theoretical physics at Göttingen, where he remained until his death in 1919. He served twice as *Rektor* of the University of Göttingen. Besides his monumental work in the physics of crystals, he made notable contributions in elasticity, thermodynamics, and magneto- and electro-optics" (translated from C. Runge, *Physik. Z.*, vol. 21, pp. 81–82, 1920).

Voigt came very near to being the originator of the piezo resonator. In the "Lehrbuch" he gave the differential equations for elastic vibrations in crystals, without, however, mentioning the bearing of the piezoelectric effect on such vibrations. He mentioned the use of h-f in the measurement of dielectric constants, recognizing the fact that anomalous results are to be expected at frequencies of molecular resonance. What he did not foresee was that similar anomalies would be found with all vibrating piezoelectric crystals whenever the applied frequency coincided with that of a normal vibrational mode of the entire crystal specimen. It was the electronic generator of h-f alternating currents, supplanting the induction coil of Voigt's day, that paved the way for the advent of the piezo resonator.

CHAPTER II

CRYSTALLOGRAPHY

An engineer gave me an ashtray
Made of a chunk of smelted bismuth.
The ore, when cooked,
Crystallizes in cubes and terraces,
Condenses in sharp stairs and corners,
Like the ruins of a mimic Cuzco.

O basic and everlasting geometry!
The cordillera itself
In the slack and purge of fire
Boils into right angles,
Takes conventional Inca pattern.
The greatest disorder on earth
Has the instinct of Perfect Form.

—CHRISTOPHER MORLEY.

1. In speaking of bismuth, it may be said at the start that the great majority of metallic elements and alloys crystallize with structures that are too highly symmetrical to show the piezoelectric effect, even if they were not conductors of electricity. Among the few exceptions are selenium and tellurium, which are commonly assigned to the trigonal holoaxial class, to which quartz belongs. A few intermetallic compounds, as MgTe and CdSe, also belong to a piezoelectric class, but they are rather salts than metals.

No familiarity with any branch of crystal physics is possible without at least a slight acquaintance with the principles of crystallography. This is especially true of piezoelectricity, if for no other reason than that without such acquaintance confusion and ambiguity are sure to arise in the specification of crystal faces, angles of cuts, etc. Until the recent growth of literature on piezo resonators, such matters as the definition of positive directions of crystal axes were minutiae that concerned only crystallographers and the few workers in the field of crystal physics. Such conventions as had been advocated were in a widely scattered state, not readily available to physicists. It is therefore not entirely surprising that so many investigators of piezoelectricity have been inclined to state their own particular "conventions" with regard to axes and angles—if indeed they did not fail altogether to be specific. It is hardly an exaggeration to say that the only general agreement seems

to have been in ignoring such definitions as had already been provided on good authority. This practice has led to considerable confusion, especially with regard to the recent oblique cuts in quartz. It is highly desirable, in dealing with elastic and piezoelectric coefficients, that a standard set of definitions concerning the positive sense of axes and of angles be universally adopted as soon as possible. It is hoped that the present treatment may prove to be a step in the right direction.

In this chapter only those crystallographic principles are given that are needed for an understanding of the succeeding portions of the book. For a general introduction to the subject the reader may consult one or more of the references given at the end of the chapter.

The ideal crystal consists of identical *unit cells*, each similarly situated with respect to its neighbors, forming a *crystal lattice*. The unit cell is the smallest parallelepiped, identical with all others in dimensions and atomic content, out of which the crystal could be constructed. The particular group of atoms contained in each cell is usually chosen to conform to the structural cell, as revealed by X-rays, whenever the structure is known. The edges of the unit cell are parallel to the crystallographic axes, and, as we shall see, its relative dimensions are simply related to the unit distances along these axes.

There are, for any given crystal, various directions in which planes, known as "net planes," can be conceived as drawn, such that each plane is populated with corresponding points of unit cells regularly arranged in rows and columns. The crystal differs from isotropic substances in external appearance, since in its normal growth certain of these planes become the faces of the crystal. A more important difference is the fact that the physical properties of a crystal vary from one direction to another. This last statement holds for all anisotropic bodies, even a piece of wood, which has different properties along and across the grain.

The belief is now held that ideal crystals exist rarely if ever. In the first place an "ideal crystal," for which there existed an *exact* correspondence between external and physical symmetry, would have to be grown in entire absence of external forces, such as gravity and stresses due to changing temperature; and second there is the possibility that the net planes may not be actually continuous throughout the crystal, *i.e.*, the crystal may have a "secondary structure," as if broken into small fragments similarly oriented and closely joined, but not quite alike in size. Since this book deals chiefly with large-scale phenomena in actual crystals, we shall be but little concerned with the question of departure from perfect homogeneity, except when we encounter the phenomenon of twinning, and the existence of a so-called "domain" structure in certain crystals.

The Law of Constancy of Angles. From what has been said it should

be clear that, however much actual crystals of the same species differ in size and in the relative development of faces, the angles between corresponding faces are constant. This *constancy of crystal angles* is a fundamental law of crystallography.

2. *Neumann's Principle.* The most fundamental principle of crystal physics is the correspondence between geometrical form and physical properties, first pointed out by F. Neumann. It is the basis of the phenomenological theory of every branch of the subject. According to this principle, when the elements of symmetry that characterize the outward form of the crystal are known, the symmetry of its physical properties can be predicted. Any given physical property, as density or thermal expansion or elasticity, may be of higher symmetry than that of the crystal form (approaching more closely to that of an isotropic body), but it cannot be of lower symmetry.

It is, of course, not to be expected that every specimen will indicate its exact classification by visible faces. Fundamentally the symmetry is that of the atomic structure of the unit cell; and while on a given specimen any of the faces constituting the external symmetry *may* be present, still the ensemble of all recorded faces is rarely if ever found. For example, crystals of quartz and Rochelle salt frequently occur without a visible trace of those faces which alone betray the asymmetry on which their characteristic piezoelectric properties depend. The extent to which such faces are developed bears no relation to the magnitude of the corresponding physical effects. When present, the faces of low symmetry in Rochelle salt are even less conspicuous than the corresponding ones in quartz; yet the piezoelectric effect is hundreds of times greater.

Neumann's principle is a rule that works both ways. From the study of physical properties the proper crystallographic classification has been made of crystals that were so rare or so imperfect that an insufficient number of faces could be identified. In some cases the morphology as indicated by the physical properties has later been confirmed through the finding of new specimens with hitherto unidentified faces.

3. *The classification of crystals* is somewhat analogous to that of plants or animals into various orders, families, genera, and species. A very important difference is that, while the number of possible biological groups is apparently limitless, the number of possible crystal groups is restricted by geometrical laws to a known finite number. The nearest approach to freedom from restriction is in the variety of atomic arrangements capable of forming crystals, and this in turn is limited only by the number of ways in which atoms can form compounds. Nevertheless, every crystal, whatever its composition, *must* belong to some one of the finite number of subdivisions.

The geometrical basis for the classification of crystals can here be outlined in only the briefest terms. Bravais showed that the number of types of polyhedron that will completely fill all space is 7. These polyhedra are usually represented in skeleton form, as an array of points, one of which comes at each vertex of the polyhedron. These seven arrays are the units of the seven *simple space-lattices*. Bravais also found that, when face-centered and body-centered polyhedra are taken into account, the number of possible space-lattices is increased to 14. Each polyhedron is a *unit cell*. It is characteristic of space-lattices that, if the entire lattice is moved without rotation until any given point reaches the position occupied by some other point in the original position of the lattice, all points are found to coincide with points in the original position. The lattice thus repeats itself, and such a translation is the simplest of all *covering operations*. Other covering operations for the space-lattices are rotations through certain angles about certain axes and reflections with respect to certain planes. From the simple lattices are evolved the seven crystal systems described below; the edges of a polyhedron are the crystallographic axes, the faces are the pinacoids, or basal planes, of the crystal. Each polyhedron of a simple Bravais space-lattice represents the class of highest symmetry (the *holohedral* class) for the system in question.

In general, the points that form the space-lattices do not represent the positions of atoms. They serve merely to define the unit cells, within which the atoms may be situated in any configuration. The symmetry characteristics of the unit cell, and hence the elements of symmetry of the crystal as a whole, depend on the arrangement of the atoms. As diverse as are the atomic configurations in the thousands of different crystals, nevertheless they can all be classified in a finite number of *space-groups*, all the configurations in each group having certain geometrical characteristics in common. Historically, the theory of space-groups was fully developed long before X-rays had made possible the determination of the arrangements of the atoms. It is a purely geometrical theory. The evolution of the space-groups out of the Bravais space-lattices consists essentially in inserting further points in the unit cell of the space-lattice, such that the pattern can be made to repeat itself by a combination of rotation and translation (*screw axes*), or of reflection in a plane and translation (*glide planes*), in addition to the cyclic axes of symmetry and reflection planes that characterize the Bravais lattices. Through the labors of Sohncke, Fedorov, Schoenflies, and Barlow, it has been proved that there are in all 230 such configurations. These configurations constitute the 230 *space-groups*.

The space-groups are divided into 32 *point-groups*, each possessing certain symmetry characteristics with respect to a point (§6). These

are the same as the 32 *classes* of the crystallographer. Each point-group is commonly designated by a symbol indicating the particular rotations about an axis and reflections in a plane that constitute the covering operations for that group. The symmetry operations for the point-group do not include translations of the lattice as a whole. On the other hand, the symmetry of a space-group is such that a symmetry operation may result in a new position related to the original one by a *translation*. A space-group may be regarded as a combining of the characteristics of the point-group with those of the space-lattice.

Although the space-group is a more fundamental picture of crystal properties than the point-group, it cannot be determined by gross measurements on crystals or by observation of their general physical properties. A more refined method is needed, and in recent years this need has been met by X-ray analysis. Since this book has to do with properties characteristic of *classes*, it is unnecessary to deal further with space-groups.*

4. Crystal faces are specified in terms of their intercepts on the three *crystallographic axes*, called by the crystallographer the *a*-, *b*-, and *c*-axes (the use of four axes and also of the symbols a_1, a_2, etc., in certain cases is considered below). In each system the axial directions are chosen so as to make the specification of the faces as simple as possible. Usually a crystallographic axis is an axis of symmetry or a line normal to a plane of symmetry or the edge between two prominent crystal faces. It is of course understood that a crystal axis is primarily a *direction* with respect to the crystal; the location of the origin is entirely arbitrary.

It is customary to take as the *unit face* for a given crystal a prominent face having intercepts a, b, c, of the same order of magnitude on all three crystallographic axes. The quantities of importance to the crystallographer are the *axial ratio* $a:b:c$† and the angles between the axes; when these have been determined, the inclinations of all possible crystal faces can be expressed at once. This definition of the axial ratio was adopted by the crystallographers long before the dimensions of the unit cell had been measured by X-ray methods. It is now known that the ratio of the three edges of the unit cell is either the same as the crystallographic axial ratio or related thereto by small integers. Any plane drawn through three points having coordinates a/h, b/k, c/l, is parallel to a net plane of the lattice and hence to a geometrically possible crystal face. In accordance with the *law of rational indices*, h, k, and l are

* The nature of space-groups and the symbols used to specify them are given in refs. B8, B14, and B53. The theory has been fully developed by Wyckoff.[B57] A good account of the history of the subject is in Tutton.[B48]

† Since the location of the origin is arbitrary, only the ratios of the intercepts are significant. Usually they are so adjusted that $b = 1$.

integers, including zero. It is only in the classes of highest symmetry that all the geometrically possible faces could occur, and even then in most cases only a relatively small number is actually found; there are the *holohedral* classes in Table I, pages 19–20. In all other classes the atomic structure of the unit cell is such that certain faces are never formed. For example, a crystal may have a face corresponding to $+a/h$, $+b/k$, and $+c/l$, but not to $+a/h$, $-b/k$, and $+c/l$. All crystals in the same class share the same fate as regards the suppression of certain faces.

The *Miller indices* are commonly used for specifying crystal faces. According to the Millerian system the unit face has the index (111) (signifying that the intercepts on the three axes are the unit distances a, b, and c), while the general formula for any face is (hkl). The symbols

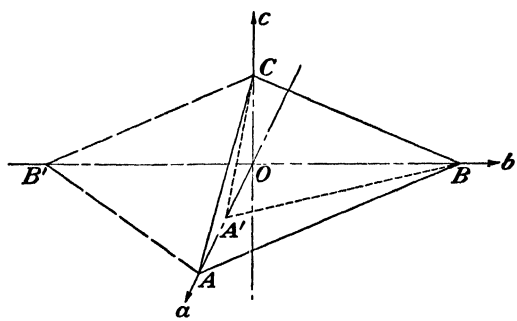


FIG. 1.—Orientations of three crystal faces, illustrating the use of the Miller indices. The axial ratio $OA:OB:OC$ is here represented as approximately that for Rochelle salt. The triangles ABC, $AB'C$, and $A'BC$ show respectively the inclinations of faces having the symbols (111) (the unit face), $(1\bar{1}1)$, and $(2\bar{1}1)$. A face through (or parallel to) $B'C$ and parallel to the a-axis would have the symbol $(0\bar{1}1)$.

h, k, l are taken in the order of the a-, b-, c- axes, and they are usually small integers, including zero. They are proportional to the *reciprocals* of the intercepts on the axes. If an intercept lies on the negative side of an axis, a negative sign is placed above the corresponding index, as illustrated in Fig. 1. By way of further example, it may be stated that (001) means a face perpendicular to the c-axis at its positive end. The corresponding face at the negative end is $(00\bar{1})$, and the two faces form the *basal pinacoid*. The face $(\bar{2}1\bar{3})$ has intercepts at $-a/2$, b, and $-c/3$.

Each face of a crystal is a member of a *form* consisting of a set of faces similarly oriented with respect to the elements of symmetry. Each form has a common form-symbol $\{hkl\}$, where h, k, and l have fixed numerical values. The various faces belonging to the form are obtained by giving to h, k, and l all the positive and negative combinations compatible with the symmetry of the crystal class. It is only in the holohedral class of each system that the form can be a complete octohedron.

A set of faces having parallel intersections is called a *zone*. A complete zone is therefore a prism. On an actual crystal the faces of the zone may be so little developed that their intersections are absent, owing to the intervention of faces of other forms.

As will be seen in §5, the axes on which the intercepts are taken in expressing the Miller indices are not orthogonal except in the cubic, tetragonal, and rhombic systems.

Of great significance physically is the possession by many crystals of *polar axes*. In crystallography a polar axis is a direction having at its two ends faces of different forms, with different numerical indices. A "one-wayness" of this sort is a sure indication of a corresponding unilateral quality for this direction with regard to the physical properties. For example, such vectorial effects as pyro- and piezoelectricity are found only with crystals having polar axes.

5. The Seven Crystal Systems. The physicist unschooled in crystallography finds himself somewhat bewildered by the diversity in nomenclature used by different authorities. This applies not only to the names of the classes but also to their grouping into systems. The geometrical nature of each of the 32 classes is of course as absolute as mathematics itself. Still, their characteristics can be expressed in various ways, depending especially on whether they are defined in terms of faces or of symmetry elements. The arrangement of the 32 classes in order of ascending or descending symmetry, and their classification into systems, is to some degree a matter of opinion. For example, while some crystallographers prefer to assign crystals having trigonal symmetry to a separate system, others regard them as a hexagonal subsystem. The number of crystal systems is accordingly given sometimes as six, sometimes as seven.

In this book the division into seven systems is adopted. As a preface to the list given below, a few general statements should be made concerning the axes and their positive directions. If a crystallographic axis is unique, as for example by the possession of trigonal symmetry, it is made the *c*-axis. In the case of a non-polar axis the positive direction is arbitrary. With a polar axis, if the crystal shows a pyroelectric effect in this direction, the positive end may be defined as that at which a positive charge appears when the crystal is heated; or if piezoelectric charges appear at the ends of the axis when the crystal is stretched in the direction of the axis, the positive end is that at which a positive charge appears on stretching.

The relations of the physicist's orthogonal X- Y-, Z-axes to the axes of the crystallographer, as used in this book, are explained below for each system. The XY-, YZ- and ZX-planes will be referred to as the *principal planes*. Except with the levogyrate (left) forms of enantio-

morphous crystals (§7), a right-handed orthogonal axial system is always to be understood.

Cubic System (also called the regular, isometric, or tesseral system). There are three orthogonal two- or fourfold axes a_1, a_2, a_3 of equal length. The (111) plane therefore has equal intercepts along the three axes. The X-, Y-, Z-axes are parallel to a_1, a_2, a_3.

Tetragonal System. Orthogonal axes are used with a_1 and a_2 of equal length, both different from c. The X-, Y-, Z-axes are parallel, respectively, to a_1, a_2, c.

Rhombic (or orthorhombic) *System.* There are three orthogonal axes a, b, c, all unequal; they are parallel to the X-, Y-, Z-axes, respectively.

Monoclinic System. More crystals belong to this system than to any other. The axes are unequal in length, the b-axis being perpendicular to the a- and c-axes, which do not form a right angle. The positive directions of a and c are outward from the obtuse angle between them, while the positive direction of b (the polar axis) is such as to make a right-handed system. The X-axis, according to Voigt's* usage, coincides with c in direction and sign, and the Z-axis with b. The Y-axis completes the right-handed orthogonal axial system, thus making an acute angle with the a-axis.†

Triclinic System. The a-, b-, c-axes are all unequal and oblique. For each species the choice of the a-, b-, c-axes, also of the orthogonal X-, Y-, Z-axes, is arbitrary.

Hexagonal System. The c-axis is the axis of sixfold symmetry. Faces are commonly specified by means of the Bravais (often called the Bravais-Miller) system. This system employs four crystallographic axes, *viz.*, the c-axis and three others perpendicular to it, called A_1, A_2, A_3, 120° apart, each being parallel to a pair of faces of the first-order prism, as shown in Fig. 3. A typical face symbol is $(hikl)$, the four letters corresponding to A_1, A_2, A_3, c, respectively. Since three parameters suffice to specify a face and since always $h + i + k = 0$, it is common practice to write as face symbol $(hi \cdot l)$, the dot signifying $k = -(h + i)$. The *orthogonal* axial system has the Z-axis coincident with c, the X-axis parallel to any one of the A-axes, and the Y-axis perpendicular to Z and X.

Since the three axes A_1, A_2, and A_3 are equivalent, the unit face makes equal intercepts on two of these axes. The axial ratio is therefore given by the single ratio $a:c$, for both the hexagonal and the trigonal system.

Trigonal System. From the crystallographic point of view the fundamental form is that of a *rhombohedron*, although in only three of the five classes is this form fully developed. Two opposite vertices of a rhombohedron lie on the trigonal (optic, or principal) axis, thus forming a three-sided pyramid at each end of the crystal. In two classes (Nos. 16 and 19), only the pyramid at one end of the trigonal axis is present for each rhombohedron. With any given kind of crystal a prominent rhombohedron (or pyramid) is selected as the primary rhombohedron (or *first-order trigonal* pyramid). If twofold axes are present (as in quartz), the rhombohedron is so chosen that the angles between the projections of its edges on the plane normal to the principal axis are bisected by these axes, as shown in Fig. 3.

The Bravais system, with four axes, may be used as with the hexagonal system. It is quite common, however, to employ the *Miller* system, according to which the faces of trigonal crystals are specified in terms of the three *Millerian axes, viz.*, the three edges of the primary rhombohedron or of the first-order trigonal pyramid (see Fig. 3). The typical face symbol is (hkl), the letters corresponding to intercepts on the Millerian a_1-, a_2-, a_3-axes, respectively. The angle between any two Millerian

* "Lehrbuch," p. 100.

† For the special convention in the case of Rochelle salt, see §481.

axes is denoted by α and is called the *Millerian angle.* If this angle were 90°, the rhombohedron would become a cube and the Millerian indices would become the usual indices for the cubic system. The trigonal and cubic systems are thus related in the sense that the trigonal rhombohedron may be regarded as a distorted cube.*

The cyclical order in which the Bravais and the Miller axes are to be taken is given in §12.

For the convenience of those who may have occasion to translate Millerian symbols into Bravais, or vice versa, the following relations are given, in which (hkl) and $(HIKL)$ or $(HI \cdot L)$ are the Miller and Bravais symbols for the same face:

$$H = (h - k); I = (k - l); K = (l - h); L = (h + k + l);$$
$$h = H - K + L = 2H + I + L;$$
$$k = I - H + L; l = -H - 2I + L = K - I + L.$$

For an orthogonal axial system we shall use, for Y- and Z-axes, the convention adopted by Voigt.† The Z-axis is the trigonal axis; either end may be taken as positive. The Y-axis is the projection of any one of the Millerian axes upon a plane normal to the Z-axis; its positive direction is outward from one of the faces of the first-order trigonal pyramid at the positive end of the Z-axis. The X-axis according to Voigt always forms a right-handed system with the other two. We shall adhere to Voigt's convention for dextrogyrate forms (§7); but for levogyrate forms, for reasons explained in §327, we shall define the positive direction of the X-axis as that which forms a left-handed system with the Y- and Z-axes.

The relation of the orthogonal X-, Y-, Z-axes to the Bravais axes is the same as for the hexagonal system.

6. The Thirty-two Crystal Classes. As shown in Table I, the numbering of classes in the order of ascending symmetry, and their grouping in systems, is taken from Rogers. The symmetry formulas in the fourth column are those of Schönflies; in the fifth column are the Hermann-Mauguin symbols. Voigt's terminology for the names of the classes is given, for the benefit of those who are acquainted with his "Lehrbuch." Voigt's class numbers are given in parentheses. The terminology introduced by Miers is also included, as the expressions are based on symmetry elements rather than on faces and hence give rather simply the symmetry relations that are essential in piezoelectricity.

A body or any one of its physical properties may be symmetrical with respect to a *point*, a *line*, a *plane*, or any combination of these. If symmetrical with respect to a *point*, the body is *centrosymmetrical* and can possess no polar properties; hence, no piezoelectric crystals are found in any of the 11 centrosymmetrical classes. With one exception, all classes devoid of a center of symmetry are piezoelectric. The single exception is Class 29, which, although without a center of symmetry, nevertheless

* This relation is discussed more fully by Voigt in the "Lehrbuch," p. 31, and in "Die fundamentalen physikalischen Eigenschaften der Kristalle in elementarer Darstellung," pp. 10–12, Leipzig, 1898.

† "Lehrbuch," p. 750.

has other symmetry elements that combine to exclude the piezoelectric property.

Symmetry with respect to a *line* is called *axial symmetry*, and the line is an *axis of symmetry*.*

A *plane of symmetry* may be likened to a mirror. In those classes having this type of symmetry, a plane passed through a crystal in the proper orientation divides the crystal in such a way that to each face on one side of the plane there corresponds a possible face on the other side, each face being the mirror image of the other with respect to the plane.

EXPLANATION OF THE SCHÖNFLIES SYMBOLS OF CRYSTAL SYMMETRY

C_n A cyclic axis of symmetry, *i.e.*, an axis such that rotation about it through an angle $2\pi/n$ results in a repetition of the figure. ($n = 1, 2, 3, 4,$ or 6.) $n = 1$ means no symmetry at all.

C_{nh} An n-fold cyclic axis with a plane of symmetry normal to it.

C_{ni} An n-fold cyclic axis with a center of symmetry.

C_{nv} An n-fold cyclic axis to which n planes of symmetry are parallel.

S_2 Every direction is a twofold cyclic axis with a plane of symmetry perpendicular to it, or an "axis of composite symmetry." The crystal has a center of symmetry and nothing else.

S_4 A fourfold cyclic axis of composite symmetry with reflection at each 90° step of rotation (alternating axis, or *Drehspiegelachse*). This means that upon rotation of 90° the figure becomes the mirror image, with respect to a plane perpendicular to the axis, of what it was before rotation. There is no center of symmetry. This type of symmetry was first described by P. Curie.

V 3 mutually perpendicular twofold cyclic axes.

V_h Symmetry V with addition of a plane of symmetry normal to each of the 3 axes.

V_d Symmetry V with 2 planes of symmetry containing the principal axis, and at 45° to the other 2 axes.

D_n Axis C_n (principal axis) with n twofold axes (secondary axes) normal to it. ($n = 3, 4,$ or 6.)

D_{nd} Symmetry D_n with n planes of symmetry containing the C_n axis and bisecting the angles between the secondary axes.

D_{nh} Symmetry D_n with a plane of symmetry normal to the C_n (principal) axis and therefore n planes of symmetry each containing the principal and 1 secondary axis.

T 3 orthogonal twofold axes and 4 threefold axes (the tetrahedral group).

T_h Symmetry T with a plane of symmetry normal to each of the twofold axes.

T_d Symmetry T with 6 planes of symmetry each containing 2 of the threefold axes.

O 3 orthogonal fourfold axes, 6 twofold axes, and 4 threefold axes (the octahedral group).

O_h Symmetry O with the planes of symmetry of both T_d and T_h.

The classes listed in Table I as pyroelectric are those possessing primary, or true, pyroelectricity. All pyroelectric crystals are also piezoelectric. As will be seen in Chap. XXIX, all piezoelectric crystals may exhibit secondary pyroelectricity.

* An axis of this type is sometimes called a *cyclic* axis, to distinguish it from the screw axis mentioned in §3.

TABLE I.—CRYSTAL SYSTEMS AND CLASSES

P = piezoelectric $\underline{P}$ = both piezo- and pyroelectric

Class No.	Names of classes: Voigt	Names of classes: Miers	Schönflies	Hermann-Mauguin	Examples
		Triclinic System			
1 $\underline{P}$	Hemihedral (2)	Asymmetrical	C_1	$\underline{1}$	Strontium ditartrate tetrahydrate
2	Holohedral (1)	Centrosymmetrical	$S_2 = C_i$	1	Copper sulphate
		Monoclinic System			
3 P	Hemimorphic (5)	Digonal polar	C_2	2	Tartaric acid
4 $\underline{P}$	Hemihedral (4)	Equatorial	$C_{1h} = C_s$	m	Potassium tetrathionate
5	Holohedral (3)	Digonal equatorial	C_{2h}	$\frac{2}{m}$	Gypsum
		Rhombic (or orthorhombic) System			
6 P	Hemihedral (7)	Digonal holoaxial	$V = D_2$	2 2 2	Rochelle salt
7 $\underline{P}$	Hemimorphic (8)	Didigonal polar	C_{2v}	m m 2	Calamine
8	Holohedral (6)	Didigonal equatorial	$V_h = D_{2h}$	$\frac{2}{m}\,\frac{2}{m}\,\frac{2}{m}$	Barite
		Tetragonal System			
9 P	Tetartohedral with inversion axis (20)	Tetragonal alternating	S_4	$\bar{4}$	$Ca_2Al_2SiO_7$
10 $\underline{P}$	Tetartohedral (18)	Tetragonal polar	C_4	4	Wulfenite
11 $\underline{P}$	Hemihedral with inversion axis (19)	Ditetragonal alternating	$Vd = D_{2d}$	$\bar{4}$ 2 m	Ammonium and potassium primary phosphates
12 P	Enantiomorphous hemihedral (15)	Tetragonal holoaxial	D_4	4 2 2	Nickel sulphate
13	Paramorphic hemihedral (17)	Tetragonal equatorial	C_{4h}	$\frac{4}{m}$	Scheellite
14 $\underline{P}$	Hemimorphic hemihedral (16)	Ditetragonal polar	C_{4v}	4 m m	Pentaerythritol
15	Holohedral (14)	Ditetragonal equatorial	D_{4h}	$\frac{4}{m}\,\frac{2}{m}\,\frac{2}{m}$	Zircon
		Trigonal System			
16 $\underline{P}$	Tetartohedral (13)	Trigonal polar	C_3	3	Sodium periodate
17	Paramorphic hemihedral (12)	Hexagonal alternating	C_{3i}	$\bar{3}$	Dolomite
18 P	Enantiomorphous hemihedral	Trigonal holoaxial	D_3	3 2	α-quartz
19 $\underline{P}$	Hemimorphic hemihedral (11)	Ditrigonal polar	C_{3v}	3 m	Tourmaline
20	Holohedral (9)	Dihexagonal alternating	D_{3d}	$\bar{3}\frac{2}{m}$	Calcite

TABLE I.—CRYSTAL SYSTEMS AND CLASSES.—(*Continued*)

Class No.	Names of classes		Schönflies	Hermann-Mauguin	Examples
	Voigt	Miers			
		Hexagonal System			
21 *P*	Tetartohedral with threefold axis (27)	Trigonal equatorial	C_{3h}	$\bar{6}$	
22 *P*	Hemihedral with threefold axis (26)	Ditrigonal equatorial	D_{3h}	$\bar{6}\,m\,2$	Benitoite
23 $\underline{P}$	Tetartohedral (25)	Hexagonal polar	C_6	6	Nephelite
24 $\underline{P}$	Enantiomorphous hemihedral (22)	Hexagonal holoaxial	D_6	6 2 2	β-quartz
25	Paramorphic hemihedral (24)	Hexagonal equatorial	C_{6h}	$\frac{6}{m}$	Apatite
26 $\underline{P}$	Hemimorphic hemihedral (23)	Dihexagonal polar	C_{6v}	6 *m m*	Silver iodide
27	Holohedral (21)	Dihexagonal equatorial	D_{6h}	$\frac{6}{m}\,\frac{2}{m}\,\frac{2}{m}$	Beryl
		Cubic (isometric or regular) System			
28 *P*	Tetartohedral (32)	Tesseral polar	T	2 3	Sodium chlorate
29*	Enantiomorphous hemihedral (29)	Tesseral holoaxial	O	4 3 2	
30	Paramorphic hemihedral (31)	Tesseral central	T_h	$\frac{2}{m}\,3$	Pyrite
31 *P*	Hemimorphic hemihedral (30)	Ditesseral polar	T_d	$\bar{4}\,3\,m$	Sphalerite
32	Holohedral (28)	Ditesseral central	O_h	$\frac{4}{m}\,\bar{3}\,\frac{2}{m}$	Sodium chloride

* No fully authentic member of Class 29 seems to be known. X-ray analysis has made it appear that the customary assignment of cuprite, sylvite, and ammonium chloride to this class is incorrect. (R. W. G. WYCKOFF, "The Structure of Crystals," pp. 209, 266, 306, New York, 1924.)

7. Enantiomorphous Crystals. In the 11 classes having no plane of symmetry, two different types of the same species may exist, those of one type being characterized by certain faces that are related to the corresponding faces of the other as the right hand is related to the left. Each type is the mirror image of the other; neither type can be made to look exactly like the other by a simple rotation.* Some species of crystals, as for example Rochelle salt, commonly occur in only one of the two possible enantiomorphous forms. In other species both forms are of frequent occurrence, as is the case with quartz.

Enantiomorphous crystals offer a good illustration of Neumann's principle, since certain directed physical properties have different signs for the two types.

* However unsymmetrical a *non-enantiomorphous* crystal may be in external appearance and physical properties, a mirror-image model would after suitable rotation be indistinguishable from the original.

In the Millerian system, the symbols are the same for a "right- " as for a "left- " crystal, if the convention given in §327 is accepted.

The right and left forms of an enantiomorphous crystal are also termed the "dextrogyrate" and "levogyrate" forms according to the sense in which they rotate the plane of polarization of light as seen by an observer looking back *toward the source* of light (§326). The prefixes *d* and *l* (or *r* and *l*) are often used, as for example *r*-quartz and *l*-quartz.

When orthogonal axes are used, ambiguities may be avoided by employing a right-handed axial system for dextrogyrate crystals, left-handed for levogyrate (§327). This practice will be followed in this book.

The 11 enantiomorphous classes are Nos. 1, 3, 6, 10, 12, 16, 18, 23, 24, 28, and 29. Of these all but the last are piezoelectric. All 11 are included among the 15 optically active classes (§538).

8. Special Crystallographic Properties of Certain Crystals. *Rhombic Digonal Holoaxial Class, No.* 6, (symmetry *V*, rhombic enantiomorphous hemihedral, sphenoidal, bi- or disphenoidal, or tetrahedral class). This is one of the 11 enantiomorphous classes. Since the *X*-, *Y*-, *Z*-axes are identical with the crystallographic *a*-, *b*-, *c*-axes, the Millerian symbols apply equally to either. The symmetry is such that either end of any two of the axes may be taken as positive. The third axis is then given the proper direction to form a right-handed system. The crystal may be rotated 180° about any one of the three axes without change in magnitude or sign of the physical properties.

The member of this class with which we have chiefly to do is *Rochelle salt*, a diagram of which is shown in Fig. 2.* Crystals are usually dextrogyrate. Axial ratio $a:b:c = 0.8325:1:0.4334$ (see §542). The most prominent and typical forms are the three pinacoids (pairs of faces normal to the three axes, marked *a*, *b*, *c* in the figure) {100}, {010}, {001}; a series of prisms $p\{110\}$, $p_1\{120\}$ not shown in the figure and $p_2\{210\}$ parallel to the *Z*-axis; two prisms $q\{011\}$ and $r\{101\}$ parallel to the *X*- and *Y*-axes, four faces each; and the primary and secondary bisphenoids $o\{111\}$ and $v\{211\}$, four faces each. The *q*-, *r*-, *o*-, and *v*-faces are often vestigial or absent. Yet it is the bisphenoids that furnish the outward and visible sign of the polarity of all three axes and of the enantiomorphous structure. Figure 2 shows a *right*-crystal, which is the only form that normally occurs. The *c* and *p* faces are usually by far the most developed.†

* Recent evidence that between the temperatures −18 and +24°C Rochelle salt should strictly be classed as monoclinic will be considered in §481. For the present we adhere to the traditional classification.

† Figure 2 is based on a drawing in Groth.[B22] In actual crystals the occurrence and relative size of many of the faces are very variable. Dr. H. Jaffe informs me that in the examination of many specimens he has found {211} the commonest of the bisphenoids, while $\{1\bar{1}1\}$ never occurs.

Following are the angles between an *a* face and the principal prismatic faces: $\angle ap_2 = 22°35'$; $\angle ap = 39°43'$; $\angle ap_1 = 58°57'$. For further data on Rochelle salt see Chaps. XX and XXXI.

To this class belong other tartrates isomorphous with Rochelle salt, which will be dealt with in Chap. XXVII.

9. *Trigonal Holoaxial Class, No.* 18 (symmetry D_3). This class is variously described as trigonal trapezohedral, holoaxial tetartosymmetrical, hexagonal trapezohedral tetartohedral, trigonal enantiomorphous hemihedral, and rhombohedral trapezohedral. As we have seen, the Millerian axes and indices are commonly used, with the primary rhombohedron as the basis, although there is doubt whether some representatives, for

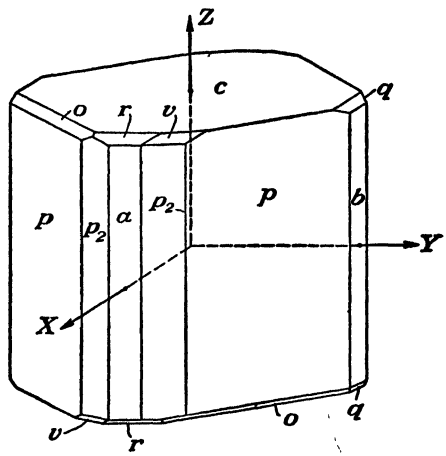


FIG. 2.—An idealized Rochelle-salt crystal. The *c*-faces (top and base of the prism) and the prismatic *p*-faces are usually the most developed. The other faces are often very small or absent.

example quartz (ref. B14), have a truly rhombohedral structure. The various alternative axial systems are shown in Fig. 3, which is drawn with special reference to *quartz*, although in principle it is applicable to all trigonal crystals. *BCDEFG* is a section of the usual prism, perpendicular to the trigonal axis *OZ*. The three pyramidal faces *ABC*, *ADE*, and *AFG* belong to the primary positive first-order rhombohedron; they are the three *R*-faces at one end of the quartz crystal, as shown in Fig. 5. The remaining pyramidal faces, *ACD*, etc., are *r*-faces, belonging to the primary negative first-order rhombohedron (ref. B47). For simplicity the pyramid is shown with hexagonal symmetry, although the *R*-faces are usually larger than the *r*. When the *R*-faces are extended, they meet along the lines AM_1, AM_2, and AM_3, which are the edges of the rhombohedron and the axes of the Millerian system. The projections of these

axes on a plane normal to the principal axis, one of which is shown as M_1N, are the Y-axes of the rectangular system. The positive direction of any Y-axis is that in which it emerges from an R-face (see Fig. 5). In Fig. 3, OZ is the Z-axis, positive upward (either end may be taken as positive). Each X-axis bisects the angle between two prismatic faces, as for example at G, forming (except with levogyrate crystals) a right-handed system with Y and Z. The X-axes are the twofold (binary or digonal) polar axes; following the Curies, they are also called *electric axes*. The name "mechanical axis" is sometimes applied to Y. In this book we

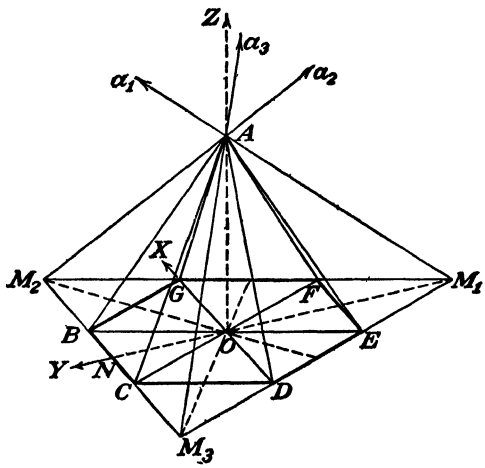


FIG. 3.—Axes for the hexagonal and trigonal systems. The Miller axes are a_1, a_2, a_3. The Bravais axes are A_1, A_2, A_3, and c, parallel respectively to GO, CO, EO, and OA. One of the three sets of orthogonal axes is shown as X, Y, and Z. Any one of the Bravais axes A_1, A_2, A_3 may be taken as an X-axis. The projections of the Miller axes upon the basal plane (normal to the Z-axis) are the Y-axes.

shall make use of the terms X-, Y-, and Z-axes almost exclusively; preparations cut with major faces normal to these axes are X-cuts, Y-cuts, or Z-cuts.

The three Bravais axes A_1, A_2, and A_3 are parallel to the three X-axes and are indicated by the lines GD, CF, and EB in Fig. 3. As usually represented, their sense is the same as that of the X-axes in a left-quartz, opposite in a right-quartz. The Bravais c-axis (OZ in the figure) coincides with the Z-axis.

10. *Alpha-quartz.* The word "crystal" is derived from the Latin *crystallum*, which in turn is from the Greek κρύσταλλος, compounded from κρύος, clear ice, and στέλλειν, to set in order.* This term was also applied

* S. I. TOMKEIEFF, On the Origin of the Name "Quartz," *Mineral. Mag.*, vol. 26, pp. 172–178, 1942. This paper points out that the word "crystallum" for quartz

in ancient times to quartz, in the belief that quartz was a form of ice. Quartz is silicon dioxide, SiO_2. Both these elements are among the most abundant, and SiO_2, in its various forms, crystalline or amorphous, is said to form about one-tenth of the earth's crust. It is a constituent in sandstones, in many of the rocks, and in other geological formations.

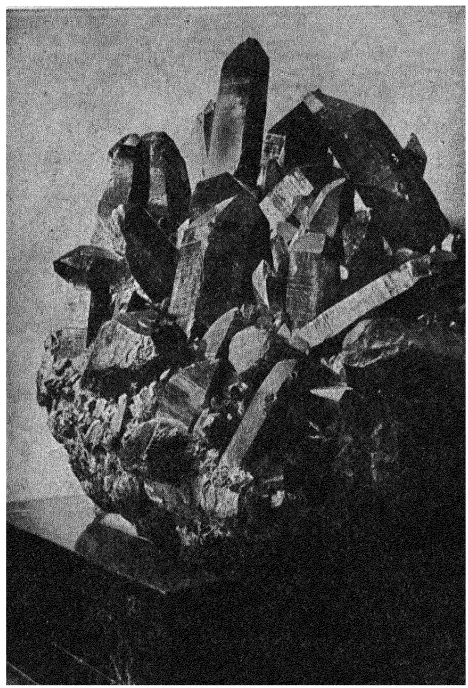


FIG. 4.—Quartz crystals in the Museum of Natural History at Geneva, Switzerland. They were found in 1868 in a cave at the side of the Rhone glacier. Mountaineers were attracted to the cave by the bright reflection of the sun from the faces of the crystals. The separate specimens (some weighing as much as 150 kg) were distributed among the chalets of the mountaineers. Later as many of the crystals as possible were purchased and reassembled, half in Geneva and half in Berne. (Courtesy of Professor Jean Weigle and of Dr. Revilliod, Director of the museum in Geneva.)

Sand consists largely of quartz grains. α-quartz ("low-quartz," or rock crystal) is only one of the numerous crystalline forms; it is the one that crystallizes at temperatures below 573°C (§14). If crystallization takes place between 573 and 870°, the form known as "beta-quartz" ("high-quartz") is produced, of hexagonal instead of trigonal structure. Among

survived until almost the end of the eighteenth century. It presents evidence that "quertz," the original spelling of "quartz," is a contraction of *Querklufterz*, or cross-vein ore, used by the miners in Saxony.

the other forms of SiO_2 are tridymite, cristobalite, and the fused amorphous form called silica or "quartz glass." The colors of such varieties as rose quartz, smoky quartz, amethyst, and other gems are due to traces of foreign matter. Unless their electric conductivity is too high or they are found to be twinned (as is often the case with amethyst), there is no technical reason why they should not be suitable for piezoelectric applications.

Our concern lies almost exclusively with α-quartz, to which we shall in general refer simply as "quartz." As abundant as SiO_2 is, in only a few regions have crystals of any considerable size and perfection been found. At present the supply comes chiefly from Brazil. Clear crystals have been found of lengths of 4 ft. or more and weighing over 100 lb. In the Smithsonian Institution in Washington is a very clear quartz sphere $12\frac{7}{8}$ in. in diameter.*

In the past, large and clear quartz crystals were fashioned into beautiful *objets d'art*, such as may be seen in the Louvre and other museums, to say nothing of spheres for crystal gazing. Too often large crystals are shattered in transportation or even purposely broken up by the laborers who collect them in remote regions. For this reason as well as because of the frequent presence of internal defects, foreign matter, and twinning, the task of determining the orientation of the axes and of selecting those portions suitable for cutting into plates, etc., is often not easy. The methods for attacking this problem are described in Chap. XVI. Pyramidal faces at both ends are rarely found, except on crystals of small size.

It is believed that natural quartz crystals were formed either by condensation of SiO_2 vapor or by the evaporation of solutions of silicates in water. Very small crystals can be produced artificially.†

* An account of this beautiful specimen is given in *Science*, vol. 71, p. 410, 1930. The various forms of quartz and their occurrence in nature, as well as descriptions of some famous quartz specimens, are treated in a popular manner in "Quartz Family Minerals," by H. C. Dake, F. L. Fleener, and B. H. Wilson, New York, 1938. P. F. Kerr and A. I. Erichsen (*Am. Mineral.*, vol. 27, pp. 487–499, 1942) describe a crystal of smoky quartz from Teofilo Otoni in Brazil, 7 ft. 2 in. long, 11 ft. 2 in. in circumference, weighing over 5 tons.

† A full account of this subject has recently been prepared by Paul F. Kerr and Elizabeth Armstrong, "Recorded Experiments in the Production of Quartz," *Bull. Geol. Soc. Am.*, vol. 54, supplement 1, pp. 1–34, 1943. Most of the experiments have been performed with steel bombs or thick-walled tubes, at pressures up to 3,000 kg/cm^2. Various temperatures, extending in some cases to over 870°C, have been used. Crystals have been produced from a large number of materials. The presence of potassium or lithium chloride and of sodium tungstate is thought to be beneficial. The largest artificial quartz crystals on record were produced by Chrustschoff in 1887 from aqueous dialyzed silica at 250 to 320°C; they measured 8 by 3 mm, reaching this size in 6 months. Most of the experiments of other workers, resulting in smaller crystals (usually a millimeter or less in size), lasted only a few days. The question is

11. As was stated in §7, quartz is enantiomorphous, both right- and left-crystals being found in nature. The two types of α-quartz are represented in Fig. 5. In addition to the faces shown, which are the most characteristic, many others have been recorded.* The trigonal symmetry is usually revealed by the larger size and greater smoothness of the R- as compared with the r-faces. It is the x- and s-faces that indicate

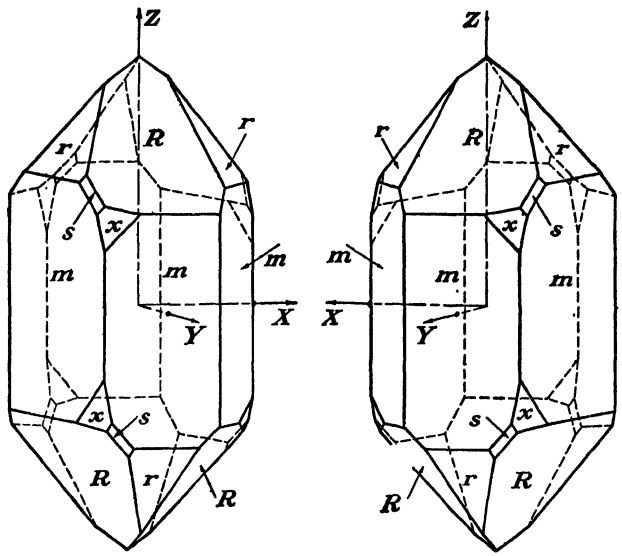


FIG. 5.—The two enantiomorphic forms of α-quartz, together with the orthogonal axial systems.

right- or left-handedness. It will be observed in Fig. 5 that in a left-quartz the normal to the edge where these two faces meet points up and to the left, while in right-quartz it points up and to the *right*. Moreover, the two non-parallel edges of an x-face converge upward toward the left in a left-quartz, upward toward the right in a right-quartz. This rule holds true on inverting the crystal end for end; hence, either end of the principal axis may be taken as the positive end of the Z-axis. In other

still open whether quartz crystals large enough for practical purposes can be grown in a reasonable time in the laboratory, instead of requiring the lapse of many years, as seems to have been the case in nature.

* A discussion of many less common faces on quartz crystals may be found in a paper by A. Descloiseaux in *Ann. chim. phys.*, vol. 44, pp. 129–316, 1855; also in "Manuel de Mineralogie," vol. 1, Paris, 1862, by the same author; see also G. Kalb, *Z. Krist.*, vol. 86, pp. 439–464, 1932, vol. 89, pp. 400–412, 1933, vol. 90, pp. 163–185, 1935. Further information on quartz is given in A. E. H. Tutton's[B48] "Crystallography and Practical Crystal Measurement" and in the book by Sosman[B47].

words, the principal axis is not a *polar* axis, as are the three X-axes. Their polarity is betrayed by the x- and s-faces, when these are present. As indicated in Fig. 5, the x- and s-faces occur (in untwinned specimens) only at alternate edges of the prism. Hence it is only at one end of each X-axis that the sx-combination can be found—and not always there, for in many specimens these faces are altogether absent. They are said to be most common in crystals from Brazil. In *twinned* crystals, on the other hand, the sx-combination may occasionally be found at both ends of an X-axis. The s-faces tend to have one pair of parallel edges relatively long and close together; moreover, the natural striations sometimes visible on an s-face always point toward an adjacent x-face.

Prismatic faces, especially on large specimens, often have parallel striations running across them in the X-direction. When present, especially on two adjacent faces, they are useful in forming a first estimate of the axial directions. These striations are alternations between very short segments of m- and r-faces; the effect is sometimes called *palisading*. They may cause a pronounced tapering of the prismatic face, the edges of which then usually converge toward an R-face. Usually the R- and r-faces are more nearly plane and perfectly oriented than the prismatic faces.

In this book we take as the positive sense of an X-axis the direction *outward from a prismatic edge at the ends of which x- and s-faces belong*, whether the crystal is right or left, as shown in Fig. 5 (see Chap. XVI for a full discussion of quartz axes and their determination). This convention, with the customary Y-axes, makes the axial system right-handed for right-quartz, left-handed for left-quartz.

The principal (Z-) axis of quartz is of the type called a "screw axis"; the SiO_2 groups occupy positions that wind themselves progressively about this axis, as explained in §540. The sense of rotation in a right-crystal is opposed to that in the levo form.

The *axial ratio* for the Bravais-Miller axes of α-quartz at room temperature is $a:c = 1:1.100$; it is the ratio OA/OB in Fig. 3, the R-face being taken as the unit face. The Millerian angle α between any two of the Miller axes has the value $93°57' \pm 2'$. The R- and r-faces make an angle of $141°47'$ with the corresponding m-faces.* The s-faces are at an angle of $24°26'$ with the principal axis. Such evidence of cleavage as there is shows itself chiefly parallel to the R- or r-faces. This can sometimes be observed when a thin plate is shattered by too intense vibration.

12. List of the Commoner Faces of Quartz Crystals, with Miller and Bravais Symbols. It is customary to number the Miller axes a_1, a_2, a_3,

* The azimuths φ and polar angles θ of the normals to the six R-faces are $\varphi = 90°$, $\theta = 51°47'$; $\varphi = 30°$, $\theta = -51°47'$; and $\varphi = -30°$, $\theta = 51°47'$. For definitions of these angles see §51.

as well as the Bravais-Miller axes A_1, A_2, A_3, in cyclical order counterclockwise as seen from the positive end of the principal (c- or Z-) axis, whether the crystal is dextro- or levogyrate. This convention is followed in Table II below and also in Fig. 6.

The names of the various faces are as follows:

m, first-order hexagonal prism.

R, primary positive first-order rhombohedron (or simply positive rhombohedron or major rhombohedron).

r, negative first-order rhombohedron (or simply negative rhombohedron or minor rhombohedron).

s, trigonal bipyramid.

x, trigonal trapezohedron.

The numbers in the first column of Table II are those of the faces marked in Fig. 6. Faces 4, 5, and 6 for m are obtained by reversing the sign of each index of faces 1, 2, and 3. The symbols for faces R, r, s, and x apply to the $+Z$-end of the crystal (the end toward the observer in Fig. 6). For the other end, all signs of indices for R and r are reversed; for the s- and x-faces, any two indices of the Miller symbol are interchanged, with corresponding changes for the Bravais symbols. Miller and Bravais symbols are denoted by M and B.

TABLE II.—SYMBOLS OF FACES FOR RIGHT-QUARTZ

No.	m-faces		R-faces		r-faces		s-faces		x-faces	
	M	B	M	B	M	B	M	B	M	B
1	$(2\bar{1}\bar{1})$	(10.0)	(100)	(10.1)	$(\bar{1}22)$	$(\bar{1}0.1)$	$(1\bar{2}4)$	$(1\bar{2}.1)$	$(4\bar{1}\bar{2})$	(51.1)
2	$(11\bar{2})$	(01.0)	(010)	$(\bar{1}1.1)$	$(2\bar{1}2)$	$(1\bar{1}.1)$	$(\bar{2}41)$	$(\bar{2}1.1)$	$(\bar{2}4\bar{1})$	$(\bar{6}5.1)$
3	$(\bar{1}2\bar{1})$	$(\bar{1}1.0)$	(001)	$(0\bar{1}.1)$	$(22\bar{1})$	(01.1)	$(41\bar{2})$	(11.1)	$(\bar{1}24)$	$(1\bar{6}.1)$

For a surface normal to an X-axis (the YZ-plane), the Miller indices are $(01\bar{1})$, $(0\bar{1}1)$; $(\bar{1}01)$, $(10\bar{1})$; $(1\bar{1}0)$, $(\bar{1}10)$. Such surfaces are not common natural faces of the crystal, but they are the major faces of the X-cuts. Surfaces normal to the Y-axes are of course simply the m-faces. A surface normal to the principal (Z-) axis (the basal plane) would have the symbol (111) or $(\bar{1}\bar{1}\bar{1})$.

Face Symbols for Left-quartz. In conformity with the principle outlined in §327, it would be logical to let the mirror image of Fig. 6 be the stereographic projection for left-quartz. This procedure would require taking the Miller and Bravais axes in clockwise instead of counterclockwise order, but it would offer the advantage of leaving the symbols of all faces the same as for right-quartz. If one adheres to the usual convention of counterclockwise order for both kinds of quartz, it is necessary to assign different symbols to corresponding s- and x-faces. For

these faces, the Miller symbols for left-quartz are derived from those for right by interchanging any two indices (or by writing all three indices in reverse order); from statements made above it is thus evident that the same face symbols hold for the s- and x-faces of left-quartz at the $+Z$-end of the crystal as for right-quartz at the $-Z$-end. The Bravais symbols for the s-faces of left-quartz are obtained from those of right-quartz by changing the signs of the first three indices; for the x-faces, the first three indices are written in reverse order with signs reversed. The open circles

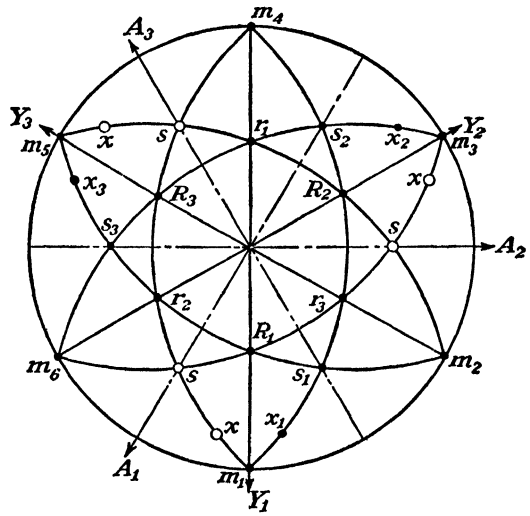


FIG. 6.—Stereographic projection of the faces seen from the $+Z$ end of a right-quartz crystal. The three Bravais axes A_1, A_2, A_3 are parallel to the X-axes of a left-quartz, antiparallel to those of a right-quartz. The Z-axis is toward the front. The axes marked Y_1, Y_2, Y_3 are the projections of the three Miller axes upon the plane of the primitive circle. The circles marked s and x (without subscripts) are the poles of these faces for a left-quartz; they are also the poles of the same faces for a right-quartz at the end facing away from the observer. For a left-quartz, the mirror image of this figure would be used, with the words "right" and "left" interchanged in the caption.

in Fig. 6 show the locations of the poles of the s- and x-faces of a left-quartz at the end toward the observer.

The angles between the normals to adjacent pairs of faces of quartz crystals are as follows, from Tutton:

mR	38°13′	mx	12°1′
RR	85°46′	mm	60°0′
Rr	46°16′	xs	25°57′
ms	37°58′	rx	54°51′
mr	66°52′		

*Stereographic Projection of a Quartz Crystal.** Figure 6 shows the arrangement of faces at the end nearer the observer for a right-quartz.

* Stereographic projections are explained in §19.

Attention is called especially to the trigonal disposition of the *s*- and *r*-faces. The *s*-faces are the more significant, since the pole corresponding to each of them comes at the intersection of two circular arcs containing also *R*- and *r*-faces. According to §19, all poles on the same arc correspond to faces in the same zone, having parallel intersections. For example, one such zone comprises the series m_1, x_1, s_1, r_3, R_2, s_2, and m_4.

13. *Ditrigonal Polar Class, No.* 19 (symmetry C_{3v}, also called trigonal hemimorphic hemihedral, rhombohedral hemimorphic, ditrigonal pyramidal, and polar ditrigonal tetartosymmetrical). The only representative of this class that need be mentioned is *tourmaline*. For further information one should consult the larger books on crystallography and especially a paper by Worobieff.*

In chemical composition tourmaline is a complex silicate of boron and aluminum and one or more of various metals. The composition, like the color, is very variable. Opaque specimens are generally useless for piezoelectric purposes owing to their relatively high conductivity. The usual form is that of a rather slender prism terminated by pyramids which often have different degrees of bluntness, owing to the predominance of different types of trigonal pyramid at the two ends. The axis of the prism is the *c*- (or *Z*-) axis; unlike that in the quartz class, it is a *polar* axis. By convention that end which becomes electrically positive on heating is called the "positive" end. Aepinus called this the *analogous* end of a tourmaline crystal, regarding the positive increase in charge as analogous to the positive increase in temperature; the opposite end he called the *antilogous* end (usually, but not always, the more pointed end). It has become common usage to apply the terms "analogous" and "antilogous" to the positive and negative ends of the polar axes of other crystals as well.

When once the positive direction of the *Z*-axis has been fixed, the *X*- and *Y*-axes are determined according to the general rule for the trigonal system given in §3.

The axial ratio of tourmaline is $a:c = 1:0.4474$.

14. *Hexagonal Holoaxial Class, No.* 24 (symmetry D_6, hexagonal enantiomorphous hemihedral, hemimorphic hemihedral, or trapezohedral). The representative of present interest is *β-quartz*, or high-quartz, the form that crystallizes at temperatures from 573 to 870°C. Above 870° it transforms to upper high-tridymite. β-quartz occurs as a natural crystal, and has been grown on a small scale artificially. When crystals of β-quartz are cooled below 573°, the outward features remain unchanged (with minute alterations in axial ratio and density), but the

* V. V. Worobieff, *Z. Krist.*, vol. 33, p. 263, 1900. A long paper, illustrated, giving a very full account of this crystal.

internal structure is that of α-quartz.* Similarly, crystals that grew as α-quartz at temperatures below 573° are inverted to β-quartz at the transition temperature, bearing still their trigonal faces, some of which now are unrelated to the internal structure. Right α-quartz becomes right β-quartz, and similarly for the left forms. A crystal may be passed up and down through the inversion point repeatedly, having the characteristic properties of a trigonal crystal on one side of the critical temperature and those of a hexagonal crystal on the other. Stresses set up on cooling, however, are likely to cause cracks; and, after cooling, the α-quartz may be found twinned. The inversion point has been precisely determined to be 573.3°.† Like α-quartz, high-quartz is enantiomorphous and has neither center nor plane of symmetry. The same axes are used as for α-quartz, but the twofold axes are now six in number.

15. Crystal Twinning. Much has been written about the analogies between crystals and living organisms, with regard to growth, disease, and many other attributes. One characteristic that crystals share with mankind is the ability to change their minds. After growing to a certain extent from the original nucleus, a crystal face may decide to change its manner of growth, henceforth taking on particles in a different orientation. If the decision is made once and for all, a *contact twin* results, each portion being entirely characteristic of the class, but with axes in different orientations. Sometimes there is such a state of vacillation that it appears as if two crystals were so intimately intergrown as to make separation impossible. This is called *penetration twinning;* the component parts may be of very irregular size and shape. Various intermediate gradations between contact and penetration twins occur. Again, the change in orientation may take place in a rhythmical manner, sometimes producing quite uniform alternating layers, leading to visible striations on the surface (*repeated*, or *polysynthetic*, twinning). In many cases twinning increases the apparent symmetry of a crystal.

In structure, the two components of a twin may be symmetrical with respect to a plane (*reflection*, or *chiral*, twins) or to a point (*inversion twins);* or one component may be relatively rotated 180° about a line called the *twin axis* (*orientational*, or *rotational*, *twins*). Still other special types of twinning are recognized.

The only example of twinning to which particular attention need be given here is that in quartz crystals. Twinning in Rochelle salt is related to the domain structure and will be treated in Chap. XXV.

* According to Sosman (ref. B47, p. 116), departures have been found with some specimens.

† BATES, F., and F. P. PHELPS, *Nat. Bur. Standards, Sci. Paper* 557, August, 1927. The transition is so sharply defined that its use as a base point on the thermometric scale is suggested.

Twinning in quartz crystals is a very important consideration in the selection of material for resonators as well as for specimens to be used in the measurement of piezoelectric coefficients. For the following statements we are indebted chiefly to Sosman's book. Orientational twinning is common; in the case of quartz this is called twinning of the *Dauphiné* type, the two components being both right or both left, but one being rotated 180° with respect to the other about the Z-axis. Also of frequent occurrence is chiral twinning, known as the *Brazil* type, with one component right, the other left, having a prismatic face $(11\bar{2}0)$ as the twinning plane. The electric axes may be in the same sense or in opposite senses, depending on whether or not there is also Dauphiné twinning. Penetration twinning is common in both the Dauphiné and the Brazilian types. Repeated twinning, especially of the Brazilian type, is often found, with layers parallel to the faces of the trigonal prism. Other less common types of twinning have been recorded.*

Twinning of the Dauphiné type is not revealed by optical tests with polarized light parallel to the optic axis (§333), since both components of the twin rotate the plane of polarization in the same sense. Since the electric axes in the two components are opposed, thereby diminishing the piezoelectric effect, this type is sometimes called *electrical twinning*. This term is also applicable to those Brazil twins in which the electric axes are opposed. The Brazil type can always be detected in polarized light and may therefore be called *optical twinning*. There are probably not many cases of optical twinning in which the electric activity is not impaired, especially when the twinning is irregular.

Many badly twinned crystals show no external evidence of anything abnormal. In the case of penetration twinning, however, it may happen that x- or s-faces occur at the ends of *adjacent*, instead of alternate, prismatic edges. If the s-faces are all inclined in the same way when seen from the front, the twinning is of the Dauphiné type; if they point alternately in opposite directions, the twinning is Brazilian. Sometimes local twinning at the surface is revealed by differences in the degree of glossiness or, on artificially polished or etched surfaces, by a line separating the twinned portions.

The question of the possible removal of twinning from quartz crystals is considered by Sosman. He points out that (for Brazilian twinning) the conversion of right- into left-quartz or the reverse must be difficult, if not impossible, since it would require on the part of each pair of oxygen atoms in the twinned region, not only a rotation of 180° about the prin-

* Twinning in quartz crystals is described at greater length by Groth[B22]; Sosman[B47]; L. Essen, *Jour. Sci. Instruments*, vol. 12, p. 256, 1935; W. A. Burgers, *Proc. Roy. Soc. (London)*, vol. 116, p. 553, 1927; and W. Bragg and R. E. Gibbs, *Proc. Roy. Soc. (London)*, vol. 109, pp. 405–427, 1925.

cipal axis, but a further change in orientation with respect to the Si atoms as well. It is true that Shubnikov and Zinserling* assert that a sharply localized stress (pressure with a steel ball) causes a (Dauphiné) twin to form on the surface of a quartz crystal, but this holds out no hope for the *removal* of twinning from the interior. Twinning in quartz is considered further in Chap. XVI.

16. Etch Figures and Their Uses. Crystal symmetry is related to chemical as well as to physical agents. Just as the rate of growth of a crystal from a solution or melt is different in different directions, so also is its rate of solution. For example, a sphere of quartz immersed in aqueous hydrofluoric acid assumes in time a flattened form having trigonal trapezohedral symmetry.

Our interest is mainly in the microscopic figures and general patterns produced by etching with a suitable solvent on a natural or artificial plane on the surface of a crystal or on a sphere fashioned from a crystal. Such figures are of great value in the identification of faces, in determining the axes of unfaced crystals and the positive directions of polar axes, in distinguishing between enantiomorphous forms, and in revealing the presence of regions of twinning.

The study of etch figures is complicated by the fact that they depend to a considerable extent on the treatment of the surface before etching, the solvent, the extent to which the solvent is kept in circulation during the etch process, the time of etching, and other factors. For etch figures on Rochelle salt see §406; for those on quartz, §335.

17. Isomorphic Mixtures. Many instances are known of two or more different compounds so closely related that their crystals not only belong to the same class but can be mingled in any proportion in the same crystal. Such a crystal may be regarded as a type of solid solution, the term *isomorphic* referring to the similarity in crystalline form of the constituents. Isomorphic mixtures, or "mixed crystals," are found especially among salts having the same acid radicals and related metals and with molecular radii and axial ratios that are not too different. Such crystals are found in nature, as for example the garnets. In the laboratory they can be produced in great variety. We shall revert to this subject in Chap. XXVII, where mixed crystals of Rochelle salt and certain isomorphic salts will be dealt with.

18. The Grouping of Crystal Classes According to Physical Properties. With respect to any given physical effect each class is characterized by certain constants that can be arranged in matrix form according to their geometrical properties. Each physical effect is a relation between two phenomena, for example, elastic stress and strain or electric field and polarization. Mathematically, each effect is treated as the

* A. SHUBNIKOV and K. ZINSERLING, *Z. Krist.*, vol. 83, pp. 243–264, 1932.

relation between two parameters, either of which may be scalar, polar vector, axial vector, or tensor.* From the types of parameter, one determines what constants exist in the most general case, and then from considerations of crystal symmetry one learns which constants may differ from zero for each class.

Those crystallographically related classes having identical matrices of constants (the magnitudes of these constants varying from one species of crystal to another) may be combined to form a "group." In general, the groups are not the same as the crystal systems, though closely related to them. Voigt distinguishes 11 chief groups (*Obergruppen*) having centrosymmetrical properties in common; for the elastic, dielectric, and piezo-optic constants the number is further reduced. Piezo- and pyroelectric phenomena do not fall into this scheme; each class possessing these properties forms a group by itself.

In Table III are presented the pertinent data for some of the branches of crystal physics. The second column gives the mathematical symbols for the physical effects involved: S = scalar, V = polar vector, V_a = axial vector, T = tensor. The third column indicates the number of groups as defined above, and the last column shows how many classes exhibit the effect named.

TABLE III

Effect	Parameters	Groups	Classes
Elastic	T, T	9	32
Dielectric	V, V	5	32
Piezo-optic	T, T	9	32
Pyroelectric (vectorial)	S, V	10	10
Pyroelectric (tensorial)	S, T	11	29
Thermal expansion	S, T	11	32
Piezomagnetic	T, V_a	11	29
Electro-optic	T, V	20	20
Piezoelectric (vectorial)	T, V	20	20
Piezoelectric (tensorial)	T, T	9	32
Internal friction	T, T	9	32

19. Stereographic Projections of Crystal Faces. If from the center of a sphere radii are drawn parallel to the normals to the faces of any crystal, they intersect the spherical surface in points known as *poles*. A *stereographic projection* is the projection of all poles of one hemisphere upon the plane of the great circle of that hemisphere, as seen by an eye at the geometrical pole of the other hemisphere. It is common practice to combine the projections of the poles of both hemispheres on one diagram. The great circle is called the *primitive circle*.

* According to common usage the term *tensor*, when not otherwise qualified, means a tensor of the second rank (a dyadic).

If the crystal has a unique axis (commonly taken as the Z-axis), the plane of the primitive circle is chosen normal to it, so that the end of the unique axis, which is now the axis of projection, appears at the center of the projection. If there is no unique axis, the axis of projection is taken parallel to the intersections of the faces belonging to some prominent zone. In what follows we shall refer to the axis of projection as the Z-axis.

The projected poles corresponding to faces parallel to the Z-axis lie on the primitive circle itself. All other poles fall in loci that are either straight lines or circular arcs passing through the ends of a diameter of the primitive circle. The poles on any such locus correspond to a set of faces that form a *zone* (§4); the edges formed by the intersections of such a set of faces are all parallel. The pole at the center of the primitive circle represents a face normal to the Z-axis (the basal plane).

Although a stereographic projection cannot show the actual form of a crystal, it is in important respects more useful than a perspective view of the crystal, since it

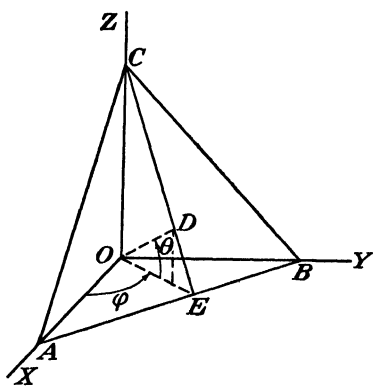


FIG. 7.—The angular coordinates φ and θ of a crystal face ABC.

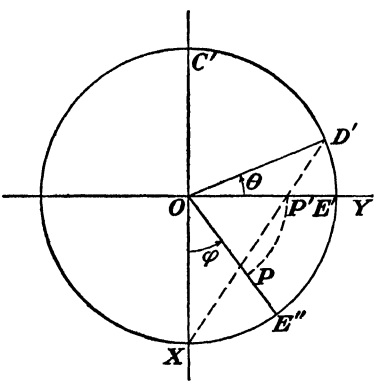


FIG. 8.—Diagram illustrating the construction of a stereographic projection.

reveals the symmetry characteristics at a glance and shows quantitatively the orientations of the various faces.

In Fig. 6 is shown a stereographic projection of a quartz crystal.

Since clear and simple directions for making stereographic projections are somewhat hard to find, the method now to be described may prove useful. The problem is to find by the smallest number of operations the location of the pole P in Fig. 8, corresponding to a face (hkl) of a crystal of given axial ratio $a:b:c$.

The method can best be explained by reference to Fig. 7, in which the (hkl)-plane is represented by the triangle ABC, the normal to which is OD. In accordance with §4, we may let the distance OA be a/h, $OB = b/k$, $OC = c/l$. Any of the digits h, k, l may be negative, in which case the corresponding distances in the figure are to be laid off in the negative directions. The angular coordinates of the direction OD are φ and θ, where $\tan \varphi = ka/hb$, and $\tan \theta = (al/ch) \cos \varphi = (bl/ck) \sin \varphi$.

If O in Fig. 7 is taken as the center of the sphere, it is evident that the pole corresponding to the face (hkl) will be at the intersection of OD with the spherical surface. The projection on the plane of the primitive circle (the XY-plane in Fig. 7) will lie on the line OE, since it is the point where the primitive circle is intersected by the line from the pole on the sphere to the point on the Z-axis where the eye is located.

The construction of the stereographic projection can now be carried out according to Fig. 8, in which OX, OY, and φ are the same as in Fig. 7, and OE'', a radius of the primitive circle, is parallel to OE. It remains to find the position of P on OE''. Instead of making a separate diagram for this purpose, it is customary to perform the construction on the same diagram. As the first step we imagine the COE-plane in Fig. 7 to coincide with the plane of the paper in Fig. 8 so that OC, OD, and OE coincide in direction with OC', OD', and OE', respectively. The line OD', making the angle θ with OE', is normal to (hkl); hence, D' is the pole of (hkl) on the sphere. The eye is

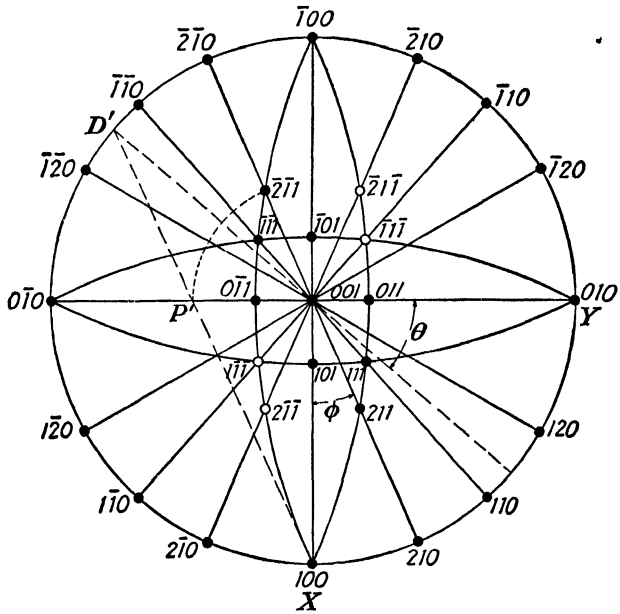


FIG. 9.—Stereographic projection of a Rochelle-salt crystal, with details of construction for the (T21) face.

located at X; hence, P' is the stereographic projection of D' on the plane of the primitive circle, which at this stage is perpendicular to the paper. OP' is the distance of the stereographic projection from the center of the circle.

Having located P', we now return the primitive circle to its original position in the plane of the paper. The second and final step in the construction consists simply in laying off on OE'' a distance $OP = OP'$. P is then the desired projection of the face (hkl).

If the stereographic projection is desired for a face belonging to a *hexagonal* or *trigonal* crystal, for which the indices are given according to the Miller or the Bravais system, it is necessary first to calculate the relative intercepts of the face on the three *orthogonal* axes. Formulas for the transformation are given, for example, by Davey (ref. B14, p. 34) and by Wolfe*.

As an example of this construction we shall find the stereographic projection of the $(\bar{2}\bar{1}1)$-face of rhombic Rochelle salt. Here $h = -2$, $k = -1$, $l = 1$. From §8 we

* C. W. WOLFE, *Am. Mineral.*, vol. 26, p. 83, 1941.

find $\mathbf{a}:\mathbf{b}:\mathbf{c} = 0.8325:1:0.4334$. Hence $\tan \varphi = ka/hb = 0.416$, $\varphi = 22°36'$,

$$\cos \varphi = 0.923$$

$\tan \theta = (l/c) \cos \varphi = -0.893$, $\theta = -41°47'$. As in Fig. 8 these angles are laid off on Fig. 9, and the pole for $(2\bar{1}1)$ is thereby located. The poles of the remaining faces of Rochelle salt are also shown. The open circles indicate faces at the end of the crystal away from the observer. This diagram reveals clearly the asymmetry of Rochelle salt with respect to all three principal planes.

Between the Curie points, Rochelle salt has the form of a *monoclinic* crystal, owing to the spontaneous strain y_z^o(§482). This strain rises from zero at -18 and $+24°C$ to a maximum of about 4′ of arc at about 5°C and represents the departure of the angle between the Y- and Z-axes from 90°. The alteration in Fig. 8 caused by so small an angular change would be quite imperceptible. Strictly, one of the two black dots representing the faces $(0\bar{1}0)$ and (010) (the two Y-faces) would be moved inward radially by a very minute amount, while the other black dot would become an open circle moved inward by the same amount.

With those systems having oblique crystallographic axes, the axial ratios do not at once lead to the distances OA, OB, and OC in Fig. 7. Nevertheless, the angles φ and θ for any face can always be calculated from goniometric measurements, so that Fig. 8 can be used for locating the position of the corresponding pole.

REFERENCES

General Books and Articles

Dale,[B13] Groth,[B22] Tutton.[B48]

Friedel, Georges: "Leçons de Cristallographie," Berger-Levrault, Paris, 1926, 602 pp.

Kalb, G.: Contributions to the Crystal Morphology of Quartz, *Z. Krist.*, vol. 86, pp. 439–465, 1933; vol. 89, pp. 400–412, 1933; vol. 90, pp. 163–185, 1935.

Kraus, E. H., W. F. Hunt, and L. S. Ramsdell: "Mineralogy, An Introduction to the Study of Minerals and Crystals," 3d ed., McGraw-Hill Book Company, Inc., New York, 1936, 638 pp.

Miers, Sir Henry Alexander: "Mineralogy, An Introduction to the Scientific Study of Minerals," 2d ed., Macmillan Company, Ltd., London, 1929, 658 pp.

Palache, Charles, Harry Berman, and Clifford Frondel: "The System of Mineralogy of James Dwight Dana and Edward Salisbury Dana," 7th ed., vol. 1, John Wiley & Sons, Inc., New York, and Chapman & Hall, Ltd., London, 1944, 834 pp.

Rogers, Austin Flint: "Introduction to the Study of Minerals," 3d ed., McGraw-Hill Book Company, Inc., New York, 1937, 626 pp.

Wyckoff, R. W. G.: "The Structure of Crystals," The Chemical Catalog Company, Inc., New York, 1924, 462 pp.

Crystallographic Properties of Quartz

Dake, Fleener, and Wilson,[B12] Sosman,[B47] Tutton.[B48]

Kraus, Hunt, and Ramsdell, reference above.

Etching and Etch Figures

I. *Quartz*

Gramont,[B21] Honess,[B16] Sosman,[B47] Bond,[63] Gaudefroy,[154] Herlinger,[220] Nacken,[337] Van Dyke,[558] Willard,[584,586] Worobieff.[592]

BAUMHAUER, H.: "Resultate der Aetzmethode," W. Engelmann, Leipzig, 1894; "Die Neuere Entwicklung der Kristallographie," Vieweg und Sohn, Brunswick, 1905.

GRAMONT, A. DE: On the Determination of the Electric Axes of Quartz with the Aid of Etch-figures, *Proc. World Eng. Cong., Tokyo*, vol. 3, pp. 417–421, 1929.

KAO, P. T.: Examination of Piezoelectric Quartz Plates, *Rev. optique*, vol. 10, pp. 153–161, 1931.

LEYDOLT, F.: On a New Method for Investigating the Structure and Composition of Crystals, with Special Reference to the Varieties of Rhombohedral Quartz, *Sitzber. Akad. Wiss. Wien. Math.-naturw. Klasse*, vol. 15, pp. 59*ff*, 1855.

MEYER, O., and S. L. PENFIELD: Results Obtained by Etching a Sphere and Crystals of Quartz with Hydrofluoric Acid, *Trans. Conn. Acad. Sci.*, vol. 8, pp. 158–165, 1889.

For further references on quartz, see list at end of Chap. XVI.

II. *Tourmaline*

WOROBIEFF.[502]

MATSUMURA, S., and A. GOTO: Relations between Etch Figures and Piezo-electric Properties of Tourmaline, *Jour. I.E.E. Japan*, vol. 53, pp. 197–199, 1933.

CHAPTER III

CRYSTAL ELASTICITY

Take from our souls the strain and stress . . . WHITTIER.

Owing to the interactions between the elastic and the electric properties of piezoelectric crystals, it may be helpful, before considering elastic phenomena by themselves, to survey the field somewhat comprehensively, including thermal effects as well. The first part of the chapter is devoted to this survey, which leads naturally to the expression for the energy of a system that is under mechanical, electric, and thermal strain, known as the *thermodynamic potential.* The subject matter of the present chapter is symbolized by the first term in that equation.

After these general preliminaries, there will follow the treatment of the purely elastic relations. As an introduction to the special elastic properties of crystals, the familiar expressions for stress and strain and for the elastic constants of isotropic solids are first reviewed. The subject of shears is considered somewhat in detail, because of their occurrence in some of the more important types of resonator and other piezoelectric devices.

After the fundamental stress-strain equations for anisotropic solids will come consideration of the properties of the nine elastic groups into which the 32 classes can be divided. Finally we shall give the equations for transformation to axial systems in any orientation, first in general form, then specialized for those groups which are of chief importance in this work.

20. Relations among Elastic, Electric, and Thermal Properties of Crystals. No study of piezoelectric phenomena can be complete without regard to the interactions between the electroelastic effects on the one hand and thermal phenomena on the other. The following chapters contain abundant evidence that the subject is of more than academic interest. The present discussion is confined to *linear* effects, thus excluding such subjects as electrostriction.

The relationships between the three types of effect are illustrated in Fig. 10. The arrangement of symbols is here based upon Voigt's theory, according to which a field E causes a piezoelectric stress $X = -\epsilon E$, where ϵ is the appropriate piezoelectric stress coefficient. Similarly a strain x causes the electric polarization $P = \epsilon x$. In like manner the pyroelectric constant p relates a change in temperature ϑ with P; the arrow from E to

δQ indicates the electrocaloric effect (variation in the quantity of heat Q on application of an electric field E), which, however, is usually expressed as a relation between the change ϑ in temperature and E (§523); the coefficient of expansion a relates ϑ with x; the line from X to δQ, with a coefficient b relating them, indicates the thermoelastic effect.* X and x are related by an equation of the form $x = -sX$, with analogous expressions for the dielectric susceptibility η and the specific heat C. The arrows indicate the directions in which the various effects usually take place. The additional arrow from P to E shows that an electric field may exist by virtue of polarization charges.

Each of the nine straight lines forming the diagram in Fig. 10 represents what may be designated as a *primary effect.* In every case, however, there is at least one other path over which the process can take place, unless certain coefficients vanish for the particular class to which the crystal belongs. Such roundabout effects may be called *secondary effects.* An outstanding instance is the "false" pyroelectric effect, due to piezoelectric action, which may be several times as great as the direct effect itself. In this case the primary, or "true," effect is indicated by the path $\vartheta \rightarrow P$, while the secondary effect follows the path $\vartheta \rightarrow x \rightarrow P$. Similarly, when an elastic compliance coefficient s is measured by observations on X and x, a piezoelectric polarization P is produced (unless $\epsilon = 0$), which if the crystal is not short-circuited gives rise to a field E, which in turn modifies the value of X; moreover, through the thermoelastic effect the temperature changes, thus affecting the value of x. While for most crystals the thermoelastic effect is very small (adiabatic correction), this is by no means true of the piezoelectric reaction upon X.

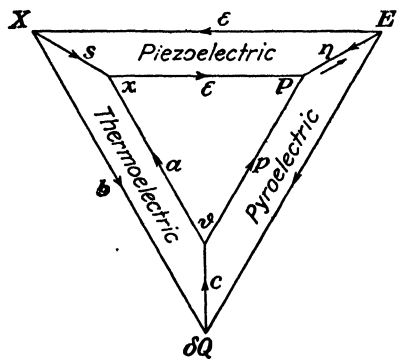


FIG. 10.—Relations between elastic, dielectric, and thermal phenomena, adapted from Heckmann[213].

This unified presentation of primary and secondary effects does not appear to have been given hitherto. The reader can easily trace out still

* This expression of thermoelastic relations in terms of a coefficient such as b relating stress to change in quantity of heat is unconventional. Usually, as on pp. 285, 286, and 784 in Voigt, the theory relates stress to *temperature*, through coefficients of thermal stress q_k; these are the coefficients employed in Eq. (1) below. In the treatment of the electrocaloric effect (§523) we shall use the symbol q to designate the electrocaloric coefficient, but there need be no confusion, since the electrocaloric q does not appear in the present chapter.

other secondary effects. The only one with which we shall be especially concerned is the relation between E and P: the susceptibility derived from measured values of P and E may be very different (especially with Rochelle salt) according to whether or not the path $E \rightarrow X \rightarrow x \rightarrow P$ is suppressed by mechanical constraints that prohibit deformation of the crystal.

21. We are thus led to another important consideration, *viz.*, the specification of the *conditions* under which any given coefficient is observed. In thermodynamics one distinguishes between the two specific heats of gases, C_p and C_v. Similarly in solids the difference between the specific heat C_X at constant stress, and C_x at constant strain, though small, is real. The necessary condition, or standard state, for the experimental determination of C_X, as well as for its use in equations, is that X and E shall be held constant: there must be no change in applied stress, of either mechanical or electrical origin. For C_x, x and P must be constant.

Of greater importance to us are the analogous remarks that may be made concerning the coefficients s and η (see also §§198, 204, and 205). Supplementing the statement made above, it may be said that the compliance coefficients s (always with appropriate subscripts) have in general different values according to the thermal and electrical state of the crystal: not only must we discriminate between the elastic coefficients at constant temperature (isothermal) and at constant entropy (adiabatic), but in each of these cases it is necessary to specify whether E or P is constant throughout the process. Frequent use will be made of the symbols s_E (or sometimes s^E)* and of s_P (or s^P) to denote constancy of field and of polarization, respectively. Other suffixes or superscripts, as D for constant electric displacement, will also be employed. Similar notation will be used for the elastic stiffness coefficients c. It is not necessary to indicate in the symbol whether T (temperature) or Q is constant. In static equations the isothermal values will be tacitly assumed; in vibrational equations, the adiabatic.

In the case of the dielectric susceptibility we shall use the symbol η' when X is constant (crystal "free"), and η'' when x is constant (crystal "clamped").

We come now to the effects represented by the *sides* of the triangles in Fig. 10. Reference has already been made to the true and the false pyroelectric effects. Similarly, one might speak of a true and a false thermal expansion effect in piezoelectric crystals: the true, or primary, effect would be observed by holding E constant. Otherwise, a secondary effect $\vartheta \rightarrow P \rightarrow E \rightarrow X \rightarrow x$ might occur, causing a piezoelectric contribution to the observed expansion.

* It is perhaps excusable, and certainly space-saving, to refer to the value of an elastic coefficient at constant field as the "isagric" value (pronounced "ice-agric").

In the case of the direct piezoelectric effect represented by $x \rightarrow P$, the standard state, tacitly assumed in the fundamental equations, is with E and ϑ constant. Strictly, if observations are not made with extreme slowness, the application of stress X causes adiabatic heating, with a false piezoelectric effect over the path $X \rightarrow \delta Q \rightarrow \vartheta \rightarrow P$. Unless the pyroelectric constant p is very large, this may be neglected in static experiments. When a pyroelectric crystal vibrates, however, the periodically varying temperature must make a pyroelectric contribution to the polarization. Such an effect deserves consideration in such crystals as Rochelle salt.

In Fig. 10, as also in Fig. 11, the portion $Xx\vartheta\delta Q$ represents the thermodynamics of solids. In a broader sense the entire figure is a thermodynamic diagram, and the development of the theory relating the various effects is along thermodynamic lines. It is in this sense that the strain-energy function about to be considered is called a "thermodynamic potential."

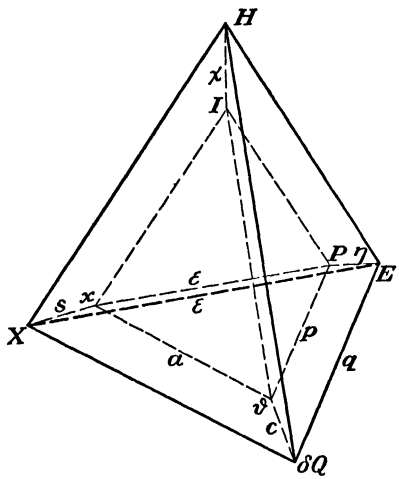


FIG. 11.—Tetrahedrons representing the relations between elastic, dielectric, thermal, and magnetic effects.

22. It is possible to extend the foregoing discussion by including other physical effects. By way of illustration we consider briefly the relation of magnetic phenomena to those already treated, even though they have but slight bearing on the field of this book. This extension requires a three-dimensional model instead of the two-dimensional Fig. 10. Such a model is shown in perspective in Fig. 11, consisting of the tetrahedron $HX\delta QE$, which we may call the *stress tetrahedron*, enclosing a smaller *strain tetrahedron* $Ix\vartheta P$. The two basic triangles $X\delta QE$ and $x\vartheta P$ are the same as in Fig. 10.

In Fig. 11, H represents the magnetic field strength, related to the magnetic polarization I (intensity of magnetization) by the equation $I = \chi H$, analogous to $P = \eta E$. The three quadrilaterals $HIxX$, $HI\delta Q\vartheta$, and $IIPE$ symbolize, respectively, the relations of magnetism to elasticity (primarily piezo magnetism, though the concept may be extended to include other magnetoelastic effects), to heat (thermomagnetic effects), and to electrostatics. The last effect is hitherto undetected, and probably undetectable, owing to the absence of appreciable magnetic permeability in insulating crystals. The purpose in mentioning these magnetic effects is to point out that, so far as they exist at all, they are subject to secondary effects and to the necessity of defining standard states, just as is the case with the elastic, electrical, and thermal effects to which we now turn.

It should be noted that in Figs. 10 and 11 the quantities δQ and ϑ are scalars, E and P vectors, X, x, H, and I tensors; in tensor analysis they are tensors of ranks 0, 1, and 2.

23. The Thermodynamic Potentials. In the treatment of problems in elasticity, Green in 1837 introduced the "*strain-energy function.*"* This function, when applied to a reversible system, is commonly called the *free energy* of the system and has been extended to include thermal and electrical as well as elastic effects. The synonymous term "thermodynamic potential" was used by Lord Kelvin and by Gibbs and applied to crystals by Duhem and by Voigt.

When the free energy is expressed in terms of *strains*, it is known as the *first thermodynamic potential* and is denoted by ξ. The negatives of its differential coefficients with respect to the components of elastic strain are the components of stress.

The free energy is also often expressed in terms of *stresses*. It is then called the *second thermodynamic potential*, denoted by ζ; the negatives of its differential coefficients with respect to the components of elastic stress are then the components of strain. These potentials are further discussed in §187. Either of these expressions for the free energy can be expanded in powers and products of the components of strain (or of stress), thus becoming the sum of homogeneous functions of various degrees. Since for an unstrained body the potential energy is a true minimum, the first-degree term vanishes. Insofar as the strains are small, as is usually the case, only quadratic terms need be retained. In elasticity, for example, this amounts to the acceptance of Hooke's law. We shall have but little occasion to consider terms of higher degree.

As a basis for further discussion in later chapters, as well as with respect to elasticity, we now write the two thermodynamic potentials in terms of mechanical, electrical, and thermal effects. A crystal plate is assumed to be subjected simultaneously to an arbitrary uniform mechanical stress, a uniform electric field in any orientation, and to be at a temperature differing from some standard temperature T by the amount ϑ; ΔS is the change in entropy corresponding to ϑ.

The frame of reference has its X-, Y-, and Z-axes parallel to the principal orthogonal axes of the crystal, as defined in Chap. II. The six terms in each equation represent the energy in terms of the elastic, dielectric, piezoelectric, thermal, thermoelastic, and pyroelectric properties of the material. Symbols of the form x_h denote components of the total strain due to all causes, while X_h, X_i are components of externally applied mechanical stress (§25); c_{hi} and s_{hi} are coefficients of elastic stiffness and compliance, respectively (§26) (their values are assumed to be

* "Mathematical Papers of the Late George Green," Macmillan & Co., London, 1871, p. 245: "In whatever way the elements of any material system act on each other, if all the internal forces exerted be multiplied by the elements of their respective directions, the total sum for any assigned portion of the mass will always be the exact differential of some function." The phrase "in whatever way" may be regarded as including thermal and electrical effects.

those which would be observed at constant electric field (§76) and at the temperature T); η''_{km} and η'_{km} are dielectric susceptibilities at constant strain and constant stress, respectively (§204); E_k, E_m are components of the field strength in the crystal, maintained constant by potentials applied to suitable electrodes; e_{mh} and d_{mh} are piezoelectric stress and strain coefficients; J is the mechanical equivalent of heat in ergs per calorie, ρ the density, C the specific heat in calories g^{-1} deg^{-1} (with solids its value is practically the same at constant stress and constant strain); q_h and a_h coefficients of thermal stress and expansion;* and p_m a pyroelectric constant.† Summations extend from 1 to the number indicated in the superscript. For all combinations of different subscripts, $s_{hi} = s_{ih}$ and $\eta_{km} = \eta_{mk}$; such commutation is not permissible with the piezoelectric coefficients. Hence in the development of Eqs. (1) and (2) there are, in the most general case, 21 elastic terms, 6 dielectric, 18 piezoelectric, 6 thermoelastic, and 3 pyroelectric. All products are scalar.‡

$$\xi = \frac{1}{2}\sum_{h}^{6}\sum_{i}^{6} c_{hi}x_h x_i + \frac{1}{2}\sum_{k}^{3}\sum_{m}^{3} \eta''_{km}E_kE_m + \sum_{m}^{3}\sum_{h}^{6} e_{mh}E_m x_h + \frac{1}{2}\frac{J\rho C\vartheta^2}{T} + \vartheta\sum_{h}^{6} q_h x_h + \vartheta\sum_{m}^{3} p_m E_m \quad (1)$$

$$\zeta = \frac{1}{2}\sum_{h}^{6}\sum_{i}^{6} s_{hi}X_hX_i + \frac{1}{2}\sum_{k}^{3}\sum_{m}^{3} \eta'_{km}E_kE_m - \sum_{m}^{3}\sum_{h}^{6} d_{mh}E_mX_h + \frac{1}{2}\frac{J\rho T}{C}(\Delta S)^2 + \vartheta\sum_{h}^{6} a_h X_h + \vartheta\sum_{m}^{3} p_m E_m \quad (2)$$

* VOIGT, pp. 285 and 772.

† *Note on the use of subscripts.* Just as the six components of stress or of strain are often conveniently indicated by the subscripts 1 . . . 6, so the three components of electric vectors are often indicated by subscripts 1, 2, 3 instead of x, y, z. In writing general expressions, applicable to all components of a given quantity, it is customary to use a letter as subscript: for example, X_h means a component of stress where h may have any value from 1 to 6. Some quantities, as, for example, elastic and piezoelectric coefficients, require (according to the convention in common use) two subscripts: d_{25} is the piezoelectric coefficient relating a field parallel to Y to the strain z_x, while d_{mh} is the general form of the coefficient, it being understood that $m = 1, 2,$ or 3, while $h = 1, 2, 3, 4, 5,$ or 6. This symbolic notation is especially useful in the writing of summations in abbreviated form.

The choice of letters to serve as generalized subscripts is entirely arbitrary; the reader soon learns that the important thing is not what the symbols for the subscripts are but where they are located.

‡ Since the field strength E is analogous to stress, and polarization to strain, the second, third, and sixth terms in Eq. (1) should in strict consistency be expressed in

The six terms of Eqs. (1) and (2) will be recognized as corresponding to the three radial and the three peripheral relations represented in Fig. 10. Our concern is mainly with the first three terms, and in the present chapter with the first term alone. Its use in obtaining the fundamental stress-strain equations will be discussed in §26.

24. In the elementary theory of elasticity the three elastic constants of an isotropic solid are Young's modulus Y, the rigidity, or shear, modulus n, and the bulk modulus, or volume elasticity, κ. These are not independent, for any one of the three can be expressed in terms of the other two by the relations given below. Expressions involving Poisson's ratio σ (transverse contraction: longitudinal extension) are also included.

$$\left.\begin{aligned} Y &= \frac{9\kappa n}{3\kappa + n} = 2n(1+\sigma) \\ n &= \frac{3\kappa Y}{9\kappa - Y} = \frac{Y}{2(1+\sigma)} \\ \kappa &= \frac{nY}{3(3n - Y)} = \frac{Y}{3(1-2\sigma)} \\ \sigma &= \frac{Y - 2n}{2n} = \frac{3\kappa - 2n}{2(3\kappa + n)} \end{aligned}\right\} \tag{3}$$

The relations between the elasticities of isotropic bodies and of crystals are discussed in succeeding sections, especially in §31.

When a solid body is in equilibrium under a given system of externally impressed forces, its state of deformation is called a *strain*, while the forces, which necessarily occur in equal and opposite pairs, give rise to a *stress*. If all parts of the body suffer the same deformation the strain is *homogeneous:* lines originally straight and parallel remain so in the strained state, though in general their lengths are changed (always in the same ratio) and their directions are altered; a square becomes a parallelogram, a sphere becomes, in the most general case, a triaxial ellipsoid.

25. Stresses and Their Components. In some texts a *stress* is defined simply as force per unit area acting on any plane in the body, with the understanding that the force may or may not be normal to the plane. In respect to elasticity, such a definition is defective, since an elastic strain is expressed in terms of one or more *pairs* of equal and opposite forces per unit area. A force per unit area is a *vector*, while a pair of equal and opposite forces per unit area is a component of a *symmetrical tensor*. Graphically, a vector is usually represented by a simple arrow; similarly,

---

terms of polarization. The energy is, in fact, so expressed in Eq. (243) (p. 252). The present formulation is chosen because it makes explicit use throughout of the parameters that occur in Voigt's theory.

a tensor component, if extensional or compressional, may be represented by an arrow with heads at both ends pointing in opposite directions.* The two heads may be thought of as representing either the oppositely directed *impressed* forces acting on opposite sides of the body under stress or an impressed force balanced at any plane by a force of *elastic reaction.*

Stresses and Stress Systems for a Homogeneous Solid in Equilibrium. A stress is defined as the force per unit area exerted by the portion of the body on one side of a surface element within it upon the portion on the other side. This definition involves the tensorial nature of the stress; for when the body is in equilibrium, there is on "the other side" an equal and opposite force, and the *pair* of forces constitutes the stress. In general, such a force can be resolved into a normal component, which is a simple *pressure* (positive or negative) and a tangential component, which is one of the pair of forces producing a *shearing stress.* Whatever the direction of the force, if the body is in equilibrium a plane can always be drawn in such a direction that the shearing stress vanishes (§28).

The origin of the stress may be purely mechanical, owing to contact of the body with some material medium: the forces acting on the surface are then called *surface tractions,* and if the strain is homogeneous the stress at the outer surface is the same as at any point in the interior. On the other hand, the stress may originate in *body forces,* exerted directly on some or all portions of the body by some agent through "action at a distance." To this type belong the piezoelectric stresses, *i.e.*, mechanical stresses in a piezoelectric crystal caused by the application of an electric field. As will be seen later, a uniform field gives rise to a homogeneous internal stress, tending to deform the crystal exactly as an equivalent mechanical stress impressed externally would tend to deform it. If the crystal is clamped, the clamping mechanism exerts forces equal and opposite to those produced by the field, so that the strain is zero.

In general, the term "impressed stress" means the sum of the mechanical and piezoelectric stresses, with respect to any surface element in the crystal.

In most practical cases the body is subjected not merely to a single stress such as we have been discussing, but rather to a system of such stresses, which may be due in part to external mechanical forces and in part to an electric field. Hence, in the most general case we have to do with a *stress system,* resolvable into *stress components* with respect to some set of axes. Such a stress system is treated as a second-order tensor. The single stress discussed above may be one such component.

Where there can be no ambiguity, we shall sometimes refer to a stress system simply as *the stress.*

* In the "Lehrbuch," p. 133, Voigt suggests a special graphical symbol for a *shearing* stress.

A body may, of course, be in equilibrium even though the impressed stress system is not homogeneous, as in the case of a flexed bar or of a body subjected to a pair of opposite collinear forces applied to limited regions on opposite sides. In general, in such cases the stress and hence the strain become distributed throughout the body in a manner that may be very complicated, especially in such anisotropic media as crystals. Nevertheless, the stress and strain at any point can always be regarded as homogeneous if a sufficiently small element of volume is taken in the body in equilibrium.

In a *vibrating body* not even small volume elements are in elastic equilibrium. Each element is subject to an unbalanced stress system, the forces on opposite sides no longer being in equal and opposite pairs. The strain in the element is determined by the lesser of the two forces in the pair; the difference between the two forces is what overcomes friction and provides the acceleration. Nevertheless, by applying D'Alembert's principle we can regard the element as being in equilibrium. The balance of forces then includes the elastic reaction, the inertial and frictional forces, and the impressed external and body forces. In the piezo resonator it is the body forces that do the driving.

Just as a force vector may be resolved into three components, so the symmetrical tensor that represents a stress system may be resolved into *six* components, *viz.*, compressions along the three coordinate axes, and shearing stresses with respect to the three planes normal to the axes. In all cases a right-handed orthogonal system is used. The six components are designated by X_x, Y_y, Z_z, Y_z, Z_x, and X_y, in each case the capital letter indicating the direction of the force and the subscript the direction of the normal to the surface on which the force acts. Frequently we shall find it convenient to use the symbols X_1, X_2, X_3, X_4, X_5, and X_6, where, for example, X_4 stands for Y_z. When a general symbol for a stress is required, X will be used without a subscript. X_x, Y_y, and Z_z are compressional components, while Y_z, Z_x, and X_y are shearing components. The latter might equally well be written Z_y, X_z, and Y_x.

Rules for the Algebraic Signs of Stresses. In agreement with Voigt we shall observe the following rule:

Normal to any surface, a stress is positive when compressional, negative when extensional.

When the term "compressional" is used in a general sense, it is with the understanding that a negative compression is an extension.

26. Strains and Their Components. The components of strain are denoted by x_x, y_y, z_z, y_z, z_x, and x_y or by x_1, x_2, . . . x_6.* They are related to the displacements as follows: If u, v, w are displacements of a

* This notation, due to Kirchhoff, is much more commonly used in piezoelectric literature than that of Love, in which x_x, etc., is replaced by e_{xx}, etc.

point whose undisturbed coordinates x, y, z become altered by strain to $x + u$, $y + v$, $z + w$, then

$$\left.\begin{aligned} x_x &= \frac{\partial u}{\partial x} & y_y &= \frac{\partial v}{\partial y} & z_z &= \frac{\partial w}{\partial z} \\ y_z &= \frac{\partial w}{\partial y} + \frac{\partial v}{\partial z} & z_x &= \frac{\partial u}{\partial z} + \frac{\partial w}{\partial x} & x_y &= \frac{\partial v}{\partial x} + \frac{\partial u}{\partial y} \\ 2\bar{\omega}_x &= \frac{\partial w}{\partial y} - \frac{\partial v}{\partial z} & 2\bar{\omega}_y &= \frac{\partial u}{\partial z} - \frac{\partial w}{\partial x} & 2\bar{\omega}_z &= \frac{\partial v}{\partial x} - \frac{\partial u}{\partial y} \end{aligned}\right\} \quad (4)$$

The last row of equations takes account of the fact that in general an arbitrary system of stresses produces a rotation of the body as a whole as well as a deformation. The amount of rotation is $(\bar{\omega}_x^2 + \bar{\omega}_y^2 + \bar{\omega}_z^2)^{\frac{1}{2}}$ radians about an axis whose direction is given by $(\bar{\omega}_x : \bar{\omega}_y : \bar{\omega}_z)$. In the case of pure shears (§27) there is no rotation.

x_x, y_y, and z_z are the *extensional* components of strain, a compression being a negative extension. *The algebraic sign of these components is positive for an extension, negative for a compression. A positive strain corresponds to a negative stress* (see §27). This rather unfortunate convention is so deeply embedded in crystal literature that we shall not attempt to uproot it. It is analogous to the custom in the theory of gases of treating an externally applied *pressure* as positive, while a change in volume is regarded as positive for an *expansion*. The nature of shearing strains and the convention with respect to signs are considered in §27.

In elastic theory Hooke's law is assumed to be valid for all types of deformation within the elastic limit. Linear equations then suffice to express the stress-strain relations. Departures from linearity in the case of certain crystals will be considered in §462.

The complete expression for the components of elastic strain of an anisotropic body in terms of components of stress is obtained by taking the derivatives of the energy function [Eq. (2)], the electric field E being constant and the change in temperature ϑ being zero. Only the first term remains,

$$\frac{\partial \zeta}{\partial X_h} = \sum_i^6 s_{hi} X_i = -x_h,$$

the negative sign conforming to the convention mentioned above. When this expression is written out in full for all six values of h and of i, we obtain the following six fundamental equations for the components of strain in terms of the components of stress and of the 36 elastic *compliance coefficients* s_{11} . . . s_{66}:*

* In strict tensor notation, the components of stress and strain, which are second-rank tensors, should be written with two subscripts and the elastic stiffness and compliance coefficients, which are fourth-rank tensors, with four. We employ the simpler notation given by Voigt.

$$\left.\begin{aligned}
-x_x &= s_{11}X_x + s_{12}Y_y + s_{13}Z_z + s_{14}Y_z + s_{15}Z_x + s_{16}X_y \\
-y_y &= s_{21}X_x + s_{22}Y_y + s_{23}Z_z + s_{24}Y_z + s_{25}Z_x + s_{26}X_y \\
-z_z &= s_{31}X_x + s_{32}Y_y + s_{33}Z_z + s_{34}Y_z + s_{35}Z_x + s_{36}X_y \\
-y_z &= s_{41}X_x + s_{42}Y_y + s_{43}Z_z + s_{44}Y_z + s_{45}Z_x + s_{46}X_y \\
-z_x &= s_{51}X_x + s_{52}Y_y + s_{53}Z_z + s_{54}Y_z + s_{55}Z_x + s_{56}X_y \\
-x_y &= s_{61}X_x + s_{62}Y_y + s_{63}Z_z + s_{64}Y_z + s_{65}Z_x + s_{66}X_y
\end{aligned}\right\} \quad (5)$$

According to elastic theory the number of independent coefficients is reduced from 36 to 21 by the relation $s_{ik} = s_{ki}$, where i and k may be any integers from 1 to 6. The 21 coefficients s_{ik} are called by Voigt the "elastic moduli." Since in English the term "modulus" is usually applied to the ratio of stress to strain, we prefer to call the s_{ik} the elastic *compliance coefficients* or simply the *compliances*. They may also appropriately be called the *elastic susceptibilities*. We have introduced them first, as they are the quantities derived directly from observation.

In order to express the stresses in terms of the strains, Eqs. (5) are solved by determinants. Each stress is then given in terms of strains and of certain functions of the compliances, which appear as coefficients of the strains. Calling these coefficients c_{11} . . . c_{66}, we have

$$\left.\begin{aligned}
-X_x &= c_{11}x_x + c_{12}y_y + c_{13}z_z + c_{14}y_z + c_{15}z_x + c_{16}x_y \\
-Y_y &= c_{21}x_x + c_{22}y_y + c_{23}z_z + c_{24}y_z + c_{25}z_x + c_{26}x_y \\
-Z_z &= c_{31}x_x + c_{32}y_y + c_{33}z_z + c_{34}y_z + c_{35}z_x + c_{36}x_y \\
-Y_z &= c_{41}x_x + c_{42}y_y + c_{43}z_z + c_{44}y_z + c_{45}z_x + c_{46}x_y \\
-Z_x &= c_{51}x_x + c_{52}y_y + c_{53}z_z + c_{54}y_z + c_{55}z_x + c_{56}x_y \\
-X_y &= c_{61}x_x + c_{62}y_y + c_{63}z_z + c_{64}y_z + c_{65}z_x + c_{66}x_y
\end{aligned}\right\} \quad (6)$$

Equations (5) and (6) are the generalized form of Hooke's law. Equations (6) can also be obtained by taking the derivative of the first term in Eq. (1) with respect to x_h.

The c_{ik} are commonly called the *elastic constants*. As with the compliances, there are 21 independent values, owing to the relation $c_{ik} = c_{ki}$. In order to avoid ambiguity and to distinguish them from the compliances one may appropriately call them the *stiffness coefficients*. They are analogous to dielectric stiffness, while the s_{ik} are analogous to dielectric susceptibility. Each stiffness coefficient is related to the corresponding compliance coefficient by an equation of the form $c_{hk} = S_{hk}/D$, where D is the determinant of all the compliance coefficients [the matrix for this determinant is evident from Eqs. (5); it appears also under Group I in §29] and S_{hk} is the cofactor of the same determinant with respect to s_{hk}.

Only in the crystal class of lowest symmetry do all 21 elastic coefficients have values differing from zero. The number decreases with ascending symmetry, becoming 3 for cubic crystals, 2 for isotropic solids, and 1 for fluids. Wherever an s_{ik} becomes equal to zero, the corresponding c_{ik} vanishes also.

The two types of elastic constant are related by the following equations, in which i and k may have any values from 1 to 6, k being different from i:

$$\sum_{k}^{6} c_{ik}s_{ik} = 1 \qquad \sum_{k}^{6} c_{ik}s_{kk} = 0 \tag{7}$$

27. Shearing Strains and Stresses. Shearing stresses and strains play an important part in piezoelectric phenomena. The model shown

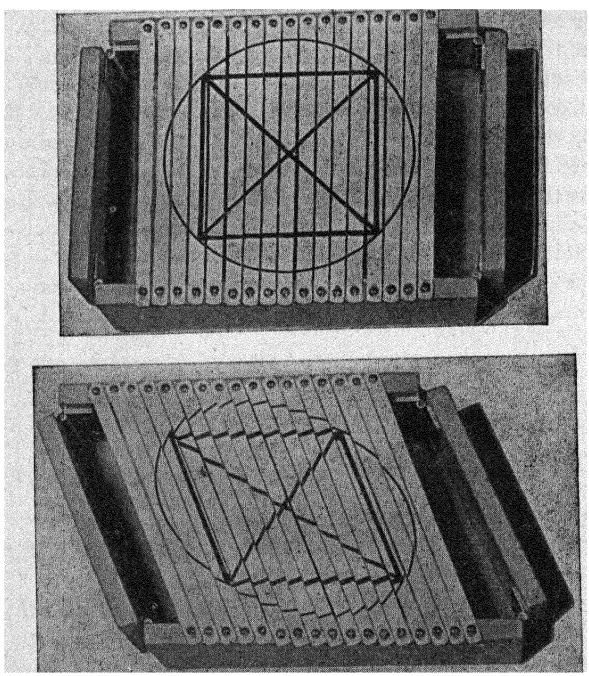


FIG. 12.—Wooden model, hinged at the corners, illustrating shears. The pattern painted on the metal cross strips shows the deformation of a circle into an ellipse.

in Fig. 12 was designed to illustrate a shearing strain. The two lines drawn at 45° to the sides remain mutually perpendicular after shearing, and they become the major and minor axes of the ellipse. If the strain is produced by moving one side while the opposite side remains fixed, it is called a *simple shear*. Adjacent cross strips, which may be considered as representing adjacent parallel planes in a three-dimensional body, slide relatively to each other. This would be equally true if one of the vertical sides of the model were moved vertically, and it would also be true if the strips were horizontal instead of vertical.

The definitions of the magnitude and sign of a component of shear can be understood from Fig. 13, which represents the base $OACB$ of a cube having edges of length OA. The X- and Y-axes are here the "axes corresponding to the shear." If a force in the X-direction is applied to the AC-face of the cube, so that the stress is X_y, the base OB being held immovable, AC will move tangentially to $A'C'$, the distance AA' being proportional to X_y, to OA, and to the compliance s_{66} of Eq. (5). All planes parallel to the face OA are rotated through an angle φ, which, for small deformations, may be taken as equal to AA'/OA. The angle φ is the measure of and numerically equal to the shearing strain, which in Fig. 13 is *positive.*

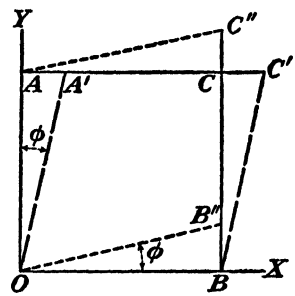


FIG. 13.—A simple shear. The measure of the shearing strain is ϕ. In this figure the strain is positive, and the plane of the diagram is the plane of shear.

A shearing strain is positive when the planes undergoing rotation are turned from the positive direction of one of the axes corresponding to the strain toward the positive direction of the other axis. Or, in a positive shear, a rectangle becomes deformed so that an acute angle lies in the quadrant between the positive directions of the two axes.

A shearing stress is positive when it tends to produce a negative shearing strain. The internal elastic *reacting* stress, which opposes an impressed shearing stress, thus has the same sign as the strain. An analogous statement may be made concerning *compressional* impressed and reacting stresses.

Figure 13 represents a *simple shear*, which involves a rotation of the body as a whole about the Z-axis. If the stress had been Y_x, of the same magnitude as before but applied vertically upward to the face BC, the deformation would have been the same but the rotation would have been in the opposite sense, as shown by the dotted lines in Fig. 13. If Y_x and X_y were applied simultaneously, the strain would be twice as great and the net rotation would be zero. Since in the macroscopic description of elastic phenomena it is immaterial whether the actual sliding takes place in one direction or the other, or in both, it is customary to use the single symbol X_y for the shearing stress in the XY-plane, whether it is to be regarded as producing a simple shear, as in Fig. 13, or a pure shear, which will now be considered. Mathematically, the identification of X_y with Y_x reduces the number of components of the general stress tensor $(X_x, Y_y, Z_z, Y_z, Z_y, Z_x, X_z, X_y, Y_x)$ from nine to six.

In a *pure shear* there is no rotation of the body as a whole. It may be regarded either as the result of two equal simple shears, as in the preceding paragraph, or as due to a compression along one diagonal of the cube face

and an extension along the other, as shown in Fig. 14. From the first point of view the deformation of the square into a rhombus is effected by the shearing stresses S_1, S_1' and S_2, S_2', which are equivalent; from the second point of view, to the mutually perpendicular compressional stress C, C' and extensional stress E, E'. The point to be emphasized is that the deformation may be regarded either as a compressional or as a shearing strain according to whether the axes of reference are parallel to E and C or to S_1 and S_2, these sets of axes differing by 45°. Geometrically, it means that by rotating the axes 45° a pure shear becomes transformed into a compression and an extension at right angles, and vice versa. The significance of this in piezoelectric applications is that a shearing stress produced piezoelectrically by an electric field can be converted into a compression in a direction 45° from the axes of shear.

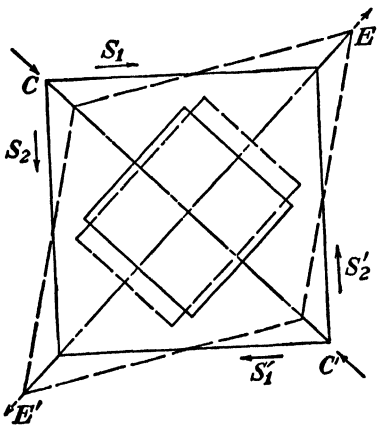


FIG. 14.—Equivalence of pure shear to combined extension and compression.

The correlation between Eqs. (4) and Fig. 13 can now be pointed out. If in Fig. 13 we let $OB = x$, $OA = y$, then $AA'/y = BB''/x$, or in differential notation $\partial u/\partial y = \partial v/\partial x$. The rotation of the body as a whole is given in the last row of Eqs. (4), and is zero when $\partial u/\partial y = \partial v/\partial x$; this is the condition for a pure shear. The second row of equations shows that in general a component of shear such as x_y is made up of two simple shears; it is "pure" or "irrotational" when these two simple shears are equal and opposite.

It is evident that such an expression as "the shear about the Z-axis" is meaningless until the axes corresponding to the shear have been specified. However, the expression is permissible with the understanding that the axes corresponding to the shear are the two orthogonal axes perpendicular to that axis about which the shear is regarded as taking place, as illustrated in Fig. 13. This latter axis is that about which the entire body rotates in a simple shear. This necessity of specifying the *axes* corresponding to a shear is analogous to that of specifying the *direction* of a compressional strain or stress.

28. ***The Ellipsoids of Elasticity.*** From the foregoing discussion it is evident that, when a solid is sheared, there are two planes in which there is no shear, but only extension and contraction. This statement may be generalized as follows, the proof being given in treatises on elasticity: In any homogeneous strain, whether all six components differ from zero or not, there is always a set of three orthogonal lines in the unstrained

state that remain orthogonal and unaltered in direction after the strain. These lines are the *principal axes* of the ellipsoid into which a sphere is transformed. This ellipsoid is the *strain ellipsoid;* its parameters are the components of strain. The radius vector in any direction is proportional to the ratio of the length of a line having this direction in the strained state, to the length of the corresponding line before strain. The planes perpendicular to the principal axes are the *principal planes*, and they are the planes in which the shearing strains are zero.

Associated with the strain ellipsoid is the *reciprocal strain ellipsoid.* This is the unique ellipsoid that can be constructed in the body in the *unstrained* state, which is transformed by the strain into a *sphere.* Its principal axes are the reciprocals of those of the strain ellipsoid; and if the strain is pure, unaccompanied by rotation of the body as a whole, its axes are coincident in direction with those of the strain ellipsoid.

In the most general type of homogeneous *pure* strain, in which all six components may be present, the strain is equivalent to three mutually perpendicular extensions, whose directions are the *principal axes* of the strain. They are also the principal axes of the reciprocal strain ellipsoid. If the strain is not pure, the principal axes of strain have to be rotated; and in general it may be said that any strain can be resolved into terms of simple extension and simple shear. The equations by which such transformations are effected are given in §38.

In most of the problems in this book we shall be concerned only with the configuration of a body after strain, without being troubled by the question whether the strain is pure or not. It is only in certain vibrational problems that the rotation of the body as a whole becomes important.

Analogous to the strain ellipsoid is the *stress ellipsoid*, the parameters of which are components of stress; the principal planes are those for which the shearing stresses vanish.

29. Elastic Constants for the Thirty-two Crystal Classes. From their fundamental nature it is evident that the elastic properties of all substances are centrosymmetrical; they can be described entirely in terms of axes of symmetry. The question whether an axis is *polar* or not has no bearing on the elastic classification. Hence all crystals have a higher degree of symmetry with respect to their elastic than to their piezoelectric properties, since the latter are dependent on polarity of axes and also on elements of symmetry other than axial. With ascending symmetry the number of independent elastic constants decreases, the criterion being the degree of *axial* symmetry. For example, if a crystal has an axis of threefold symmetry, a rotation of the system of reference by 120° or 240° is a "covering operation" with respect to which all expressions involving the elastic constants are invariant, and the number of independent constants is correspondingly reduced. It is shown by Voigt that the 32 classes fall into 11 groups (*Obergruppen*), in each of which the axial symmetry is the same. These are the same groups into which crystals are classified in the treatment of dielectric polarization, electrostriction, thermal expansion, tensorial pyroelectricity, piezomagnetism, piezo-optics, and the Kerr effect. For the elastic classification the matrices are the same in the 2 hexagonal groups and also in the 2 cubic groups.

For the present purpose we therefore need list only 9 groupings instead of 11.

Full details of the procedure are given in refs. B34, B52, and B56. We are concerned only with the results, as presented in the following tabulation. The class numbers are as in Table I (pages 19–20). The coefficients are arranged in the same order as in Eqs. (5) and (6), the subscripts indicating the *independent* coefficients. For example, the symmetry in Groups VI and VII is such that $c_{56} = c_{14}$, whence c_{14} is written in place of c_{56}. In accordance with §26, we write $c_{12}^{\dagger}$ in place of c_{21} etc., and s_{12} in place of s_{21} etc.

It must be emphasized that the coefficients in the following tabulation are the ones to use in Eqs. (5) and (6) when, and only when, *the frame of reference is the three orthogonal crystallographic axes defined in* §5. Otherwise, the *transformed* coefficients must be used, according to Chap. IV.

GROUP I, TRICLINIC SYSTEM, CLASSES 1, 2

c_{11}	c_{12}	c_{13}	c_{14}	c_{15}	c_{16}	s_{11}	s_{12}	s_{13}	s_{14}	s_{15}	s_{16}
c_{12}	c_{22}	c_{23}	c_{24}	c_{25}	c_{26}	s_{12}	s_{22}	s_{23}	s_{24}	s_{25}	s_{26}
c_{13}	c_{23}	c_{33}	c_{34}	c_{35}	c_{36}	s_{13}	s_{23}	s_{33}	s_{34}	s_{35}	s_{36}
c_{14}	c_{24}	c_{34}	c_{44}	c_{45}	c_{46}	s_{14}	s_{24}	s_{34}	s_{44}	s_{45}	s_{46}
c_{15}	c_{25}	c_{35}	c_{45}	c_{55}	c_{56}	s_{15}	s_{25}	s_{35}	s_{45}	s_{55}	s_{56}
c_{16}	c_{26}	c_{36}	c_{46}	c_{56}	c_{66}	s_{16}	s_{26}	s_{36}	s_{46}	s_{56}	s_{66}

GROUP II, MONOCLINIC SYSTEM, CLASSES 3, 4, 5

c_{11}	c_{12}	c_{13}	0	0	c_{16}	s_{11}	s_{12}	s_{13}	0	0	s_{16}
c_{12}	c_{22}	c_{23}	0	0	c_{26}	s_{12}	s_{22}	s_{23}	0	0	s_{26}
c_{13}	c_{23}	c_{33}	0	0	c_{36}	s_{13}	s_{23}	s_{33}	0	0	s_{36}
0	0	0	c_{44}	c_{45}	0	0	0	0	s_{44}	s_{45}	0
0	0	0	c_{45}	c_{55}	0	0	0	0	s_{45}	s_{55}	0
c_{16}	c_{26}	c_{36}	0	0	c_{66}	s_{16}	s_{26}	s_{36}	0	0	s_{66}

GROUP III, RHOMBIC SYSTEM, CLASSES 6, 7, 8

c_{11}	c_{12}	c_{13}	0	0	0	s_{11}	s_{12}	s_{13}	0	0	0
c_{12}	c_{22}	c_{23}	0	0	0	s_{12}	s_{22}	s_{23}	0	0	0
c_{13}	c_{23}	c_{33}	0	0	0	s_{13}	s_{23}	s_{33}	0	0	0
0	0	0	c_{44}	0	0	0	0	0	s_{44}	0	0
0	0	0	0	c_{55}	0	0	0	0	0	s_{55}	0
0	0	0	0	0	c_{66}	0	0	0	0	0	s_{66}

GROUP IV, TETRAGONAL SYSTEM, CLASSES 9, 11, 12, 15

c_{11}	c_{12}	c_{13}	0	0	0	s_{11}	s_{12}	s_{13}	0	0	0
c_{12}	c_{11}	c_{13}	0	0	0	s_{12}	s_{11}	s_{13}	0	0	0
c_{13}	c_{13}	c_{33}	0	0	0	s_{13}	s_{13}	s_{33}	0	0	0
0	0	0	c_{44}	0	0	0	0	0	s_{44}	0	0
0	0	0	0	c_{44}	0	0	0	0	0	s_{44}	0
0	0	0	0	0	c_{66}	0	0	0	0	0	s_{66}

GROUP V, TETRAGONAL SYSTEM, CLASSES 10, 13, 14

$$\begin{matrix} c_{11} & c_{12} & c_{13} & 0 & 0 & c_{16} \\ c_{12} & c_{11} & c_{13} & 0 & 0 & -c_{16} \\ c_{13} & c_{13} & c_{33} & 0 & 0 & 0 \\ 0 & 0 & 0 & c_{44} & 0 & 0 \\ 0 & 0 & 0 & 0 & c_{44} & 0 \\ c_{16} & -c_{16} & 0 & 0 & 0 & c_{66} \end{matrix} \qquad \begin{matrix} s_{11} & s_{12} & s_{13} & 0 & 0 & s_{16} \\ s_{12} & s_{11} & s_{13} & 0 & 0 & -s_{16} \\ s_{13} & s_{13} & s_{33} & 0 & 0 & 0 \\ 0 & 0 & 0 & s_{44} & 0 & 0 \\ 0 & 0 & 0 & 0 & s_{44} & 0 \\ s_{16} & -s_{16} & 0 & 0 & 0 & s_{66} \end{matrix}$$

GROUP VI, TRIGONAL SYSTEM, CLASSES 16, 17

$$\begin{matrix} c_{11} & c_{12} & c_{13} & c_{14} & -c_{25} & 0 \\ c_{12} & c_{11} & c_{13} & -c_{14} & c_{25} & 0 \\ c_{13} & c_{13} & c_{33} & 0 & 0 & 0 \\ c_{14} & -c_{14} & 0 & c_{44} & 0 & c_{25} \\ -c_{25} & c_{25} & 0 & 0 & c_{44} & c_{14} \\ 0 & 0 & 0 & c_{25} & c_{14} & \tfrac{1}{2}(c_{11} - c_{12}) \end{matrix} \qquad \begin{matrix} s_{11} & s_{12} & s_{13} & s_{14} & -s_{25} & 0 \\ s_{12} & s_{11} & s_{13} & -s_{14} & s_{25} & 0 \\ s_{13} & s_{13} & s_{33} & 0 & 0 & 0 \\ s_{14} & -s_{14} & 0 & s_{44} & 0 & 2s_{25} \\ -s_{25} & s_{25} & 0 & 0 & s_{44} & 2s_{14} \\ 0 & 0 & 0 & 2s_{25} & 2s_{14} & 2(s_{11} - s_{12}) \end{matrix}$$

GROUP VII, TRIGONAL SYSTEM, CLASSES 18, 19, 20

$$\begin{matrix} c_{11} & c_{12} & c_{13} & c_{14} & 0 & 0 \\ c_{12} & c_{11} & c_{13} & -c_{14} & 0 & 0 \\ c_{13} & c_{13} & c_{33} & 0 & 0 & 0 \\ c_{14} & -c_{14} & 0 & c_{44} & 0 & 0 \\ 0 & 0 & 0 & 0 & c_{44} & c_{14} \\ 0 & 0 & 0 & 0 & c_{14} & \tfrac{1}{2}(c_{11} - c_{12}) \end{matrix} \qquad \begin{matrix} s_{11} & s_{12} & s_{13} & s_{14} & 0 & 0 \\ s_{12} & s_{11} & s_{13} & -s_{14} & 0 & 0 \\ s_{13} & s_{13} & s_{33} & 0 & 0 & 0 \\ s_{14} & -s_{14} & 0 & s_{44} & 0 & 0 \\ 0 & 0 & 0 & 0 & s_{44} & 2s_{14} \\ 0 & 0 & 0 & 0 & 2s_{14} & 2(s_{11} - s_{12}) \end{matrix}$$

GROUP VIII, HEXAGONAL SYSTEM, CLASSES 21 TO 27

$$\begin{matrix} c_{11} & c_{12} & c_{13} & 0 & 0 & 0 \\ c_{12} & c_{11} & c_{13} & 0 & 0 & 0 \\ c_{13} & c_{13} & c_{33} & 0 & 0 & 0 \\ 0 & 0 & 0 & c_{44} & 0 & 0 \\ 0 & 0 & 0 & 0 & c_{44} & 0 \\ 0 & 0 & 0 & 0 & 0 & \tfrac{1}{2}(c_{11} - c_{12}) \end{matrix} \qquad \begin{matrix} s_{11} & s_{12} & s_{13} & 0 & 0 & 0 \\ s_{12} & s_{11} & s_{13} & 0 & 0 & 0 \\ s_{13} & s_{13} & s_{33} & 0 & 0 & 0 \\ 0 & 0 & 0 & s_{44} & 0 & 0 \\ 0 & 0 & 0 & 0 & s_{44} & 0 \\ 0 & 0 & 0 & 0 & 0 & 2(s_{11} - s_{12}) \end{matrix}$$

GROUP IX, CUBIC SYSTEM, CLASSES 28 TO 32

$$\begin{matrix} c_{11} & c_{12} & c_{12} & 0 & 0 & 0 \\ c_{12} & c_{11} & c_{12} & 0 & 0 & 0 \\ c_{12} & c_{12} & c_{11} & 0 & 0 & 0 \\ 0 & 0 & 0 & c_{44} & 0 & 0 \\ 0 & 0 & 0 & 0 & c_{44} & 0 \\ 0 & 0 & 0 & 0 & 0 & c_{44} \end{matrix} \qquad \begin{matrix} s_{11} & s_{12} & s_{12} & 0 & 0 & 0 \\ s_{12} & s_{11} & s_{12} & 0 & 0 & 0 \\ s_{12} & s_{12} & s_{11} & 0 & 0 & 0 \\ 0 & 0 & 0 & s_{44} & 0 & 0 \\ 0 & 0 & 0 & 0 & s_{44} & 0 \\ 0 & 0 & 0 & 0 & 0 & s_{44} \end{matrix}$$

For comparison the corresponding coefficients for isotropic solids are given; the choice of axes is now arbitrary.

ISOTROPIC SOLIDS

$$\begin{matrix} c & \lambda & \lambda & 0 & 0 & 0 \\ \lambda & c & \lambda & 0 & 0 & 0 \\ \lambda & \lambda & c & 0 & 0 & 0 \\ 0 & 0 & 0 & n & 0 & 0 \\ 0 & 0 & 0 & 0 & n & 0 \\ 0 & 0 & 0 & 0 & 0 & n \end{matrix} \qquad \begin{matrix} s & s_1 & s_1 & 0 & 0 & 0 \\ s_1 & s & s_1 & 0 & 0 & 0 \\ s_1 & s_1 & s & 0 & 0 & 0 \\ 0 & 0 & 0 & s_2 & 0 & 0 \\ 0 & 0 & 0 & 0 & s_2 & 0 \\ 0 & 0 & 0 & 0 & 0 & s_2 \end{matrix}$$

It will be observed that the s occurs in exactly the same way as the c in all groups except VI, VII, and VIII, for trigonal and hexagonal crystals. The symmetry of these groups requires that $c_{66} = (c_{11} - c_{12})/2$, while $s_{66} = 2(s_{11} - s_{12})$, and also that $s_{46} = 2s_{25}$ and $s_{56} = 2s_{14}$ in the trigonal groups.

30. The character of the various elastic constants is indicated in Fig. 15, in which the types of strain that can be produced by the com-

	X_x	Y_y	Z_z	Y_z	Z_x	X_y
x_x	L	T	T	L'	T'	T'
y_y	T	L	T	T'	L'	T'
z_z	T	T	L	T'	T'	L'
y_z	L'	T'	T'	S	S'	S'
z_x	T'	L'	T'	S'	S	S'
x_y	T'	T'	L'	S'	S'	S

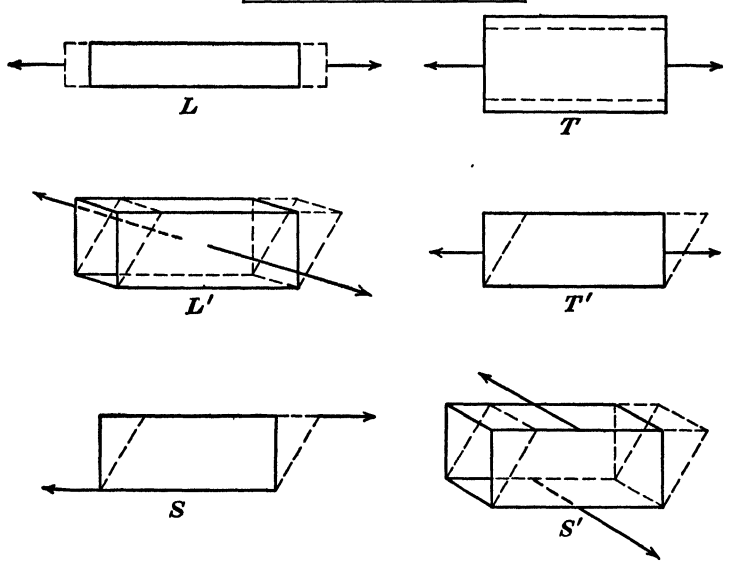


FIG. 15.—Table showing the stress-strain relation associated with each type of elastic constant. In the small schematic diagrams, arrows represent forces; dotted lines, strains.

ponents of stress are denoted by L, T, L', T', S, and S'. L (longitudinal) and T (transverse) indicate extensional strains parallel and transverse, respectively, to extensional stresses, as shown in the figure. S (shear)

and S' are shearing strains in planes to which shearing stresses are, respectively, parallel and perpendicular. L' indicates a relation between a shearing stress and an extensional strain parallel to the axis of the shear (or the converse), while in T' an extensional strain is in the plane of a shearing stress (or the converse).

All crystals, together with isotropic solids, have values differing from zero for the elastic coefficients corresponding to L, T, and S. Fluids have only compressibility, which is equivalent to writing $n = 0, T = -L$. In four of the nine groups of crystals no other elastic coefficients exist than those of the L-, T-, and S-types.

Elastic coefficients of types L and S, represented by c_{hh} or s_{hh} ($h = 1 \ldots 6$), are essentially positive. With few exceptions all compliance coefficients of type T are negative, as they must necessarily be in isotropic substances, in which the positive extension due to an extensional stress is always accompanied by a *negative* lateral extension. In all other cases the signs of elastic coefficients of crystals may be positive or negative.

31. Comparison of Isotropic Solids with Crystals. It is of some interest to compare the elastic properties of isotropic solids with those of crystals, especially crystals of cubic symmetry. In Group IX the three constants c_{11}, c_{12}, c_{44} are all independent. On the other hand the three isotropic constants c, λ, n, although forming a matrix precisely like that of cubic crystals, are not all independent. An isotropic substance has an infinite degree of symmetry about all axes. Since this statement includes hexagonal symmetry, it follows that the special relations for trigonal and hexagonal crystals noted at the end of §29 hold here also, *viz.*, $n = (c - \lambda)/2$ and $s_2 = 2(s - s_1)$. Bearing this in mind and applying Eqs. (3), we can now interpret the elastic constants Y, k, and σ in the light of the fundamental parameters given in the tabulation above, both for isotropic substances and for crystals. We thus find, as is also proved in treatises on elasticity, that, for isotropic solids,

$$Y = \frac{n(3\lambda + 2n)}{\lambda + n} \qquad n = \frac{c - \lambda}{2} \qquad k = \frac{3\lambda + 2n}{3} \qquad \sigma = \frac{\lambda}{2(\lambda + n)} \tag{8}$$

The constants λ and n are the "Lamé coefficients" of elastic theory.* n is the rigidity, while λ, to which no name seems to have been given, is a measure of the resistance offered by an isotropic solid to compressional strain in a direction at right angles to an extensional stress. In other words, it expresses the *lateral incontractibility* of a stretched solid. λ is thus related to Poisson's ratio σ; but since the combination of an extensional strain with a compressional strain at right angles to it always

*The symbol μ was originally used in place of n.

involves a shear, and hence the rigidity modulus n, it turns out that σ is a function of both λ and n, as shown in Eq. (8).

In terms of λ and n the following expressions for c, s, s_1, and s_2 in the matrices for isotropic solids in §29 are easily derived:

$$c = \lambda + 2n \qquad s = \frac{\lambda + n}{n(3\lambda + 2n)} = \frac{1}{Y} \qquad s_1 = \frac{-\lambda}{2n(3\lambda + 2n)} \qquad s_2 = \frac{1}{n} \quad (9)$$

32. *Poisson's ratio* calls for further consideration, since it occurs in the theory of vibrations of crystals. If a simple compressional stress X_x is applied to any solid, the resulting compressional strains are $x_x = -s_{11}X_x$, $y_y = -s_{12}X_x$, and $z_z = -s_{13}X_x$. If the substance is isotropic, $y_y = z_z = x_x(s_{12}/s_{11}) = x_x s_1/s$. Since by definition $\sigma = y_y/x_x$, it is evident that one may also write $\sigma = s_1/s$. As defined in this manner Poisson's ratio is a negative quantity, since, as is seen from Eq. (9), s_1 and s have opposite signs. Nevertheless, it is customary to ignore the negative sign in dealing with isotropic solids. In crystals Poisson's ratio has different values depending on the directions of stress and strain. In the case considered above the values may be denoted by $\sigma_{21} = s_{12}/s_{11}$ and $\sigma_{31} = s_{13}/s_{11}$, the second suffix in each case specifying the stress. In general, $\sigma_{hk} = s_{hk}/s_{kk}$, and the numerical value may be of either sign. Tourmaline has the smallest numerical value of σ on record (§100) and Rochelle salt the largest (§79).

In contrast to compliance coefficients of types L and S in Fig. 15, symbolized by s_{hh}, all the remaining compliance coefficients, of form s_{hk}, express a *mutual* relation between two different types of deformation. It is for this reason that such coefficients occur in expressions for the coupling between different modes of mechanical vibration, just as in magnetic coupling between oscillating circuits the mutual inductances play a part. The smaller Poisson's ratio is, the weaker are coupling effects and the more nearly do the overtones of thickness and lengthwise vibrations approach to a harmonic ratio. By taking advantage of the fact that for certain orientations of quartz plates Poisson's ratio vanishes, it is possible to eliminate certain undesired coupled vibrational modes from quartz resonators (§358).

Coefficients of the form s_{hk} or $c_{hk}(h \neq k)$ are often called *elastic cross constants*.

33. Elastic constants of crystals of types L and S, mentioned in §30, can now be further interpreted. Compliance coefficients of the L-type, *viz.*, s_{11}, s_{22}, and s_{33}, are reciprocals of Young's modulus Y in the X-, Y-, and Z-directions. This becomes evident if, for example, it is assumed that a single stress X_x is applied to a parallelepiped, as when a bar with length parallel to X is compressed endwise. Then $x_x = -s_{11}X_x$ is the compressional strain, while the other five strain components derived

from Eqs. (5) represent the other deformations caused by X_x, on the assumption that no constraints are present. The usual stress-strain relation gives at once $Y = 1/s_{11} = -X_x/x_x$. In the equations for longitudinal vibrations of rods, the stiffness factor is $1/s_{hh}$, the length of the rod lying in the h-direction. This factor holds also with close approximation for relatively *thin* plates vibrating longitudinally, even when the breadth is greater than the length.

On the other hand, if the parallelepiped were confined in a box with unyielding sides and bottom and then compressed from above by the stress X_x, the only possible strain would be $-x_x$, but in addition to X_x there would, in the general case, be five other stress components exerted by the box. From Eqs. (6) we find $x_x = -(1/c_{11})X_x$. In general, each c_{hk} is the measure of the resistance offered by the crystal to a stress X_h, when *all other strain components are prohibited*, while $1/s_{hk}$ is a measure of the resistance when these other components are permitted.

The same constraints as those imposed by a rigid box would also be present if the parallelepiped were in the form of a flat plate of infinite area, having its thickness in the h-direction, and subjected to pressure X_h. It is for this reason that c_{hh} appears as the stiffness factor for a thin piezoelectric plate vibrating in the direction of its thickness h.

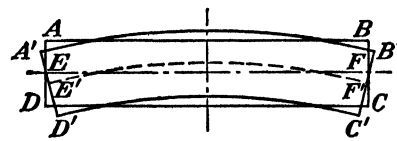


FIG. 16.—A rectangular plate $ABCD$ bent by flexure into the form $A'B'C'D'$. The plane of the figure is the plane of flexure. The surface through EF normal to the plane of the figure is the neutral surface.

With regard to coefficients of type S it need only be pointed out that, as with isotropic solids, the constants s_{44}, s_{55}, and s_{66} are the reciprocals of the moduli of torsion about the respective axes.

34. Flexure of Crystalline Plates. First we consider an isotropic plate in the form of a flat parallelepiped, bent as shown in Fig. 16. Before bending, the length $l = AB$, thickness $e = AD$, while the breadth b is perpendicular to the plane of the diagram.* If only such forces are applied as are required to cause bending in the *le*-plane, the deformation is a *pure flexure*, every section normal to b being bent in its own plane into a form like $A'B'C'D'$. The surface intersecting the paper in EF (or $E'F'$), midway between the top and bottom surfaces of the plate, is the *neutral surface*. This surface suffers neither elongation nor contraction. Above this surface (for the case shown in the figure), all linear elements parallel to l are elongated, by amounts proportional to their distances from the neutral surface; below it, they are compressed by like amounts.

* For simplicity of treatment we are assuming here that $l >> e$. The theory is more complicated when e is of the same order of magnitude as l, as will be seen in §73. There is no restriction on the ratio b/e.

All cross sections normal to l, except that through the center of the plate, become rotated without change in shape or size. It is owing to this rotation that the expression for the frequency of flexural vibrations, given in §73, contains as a factor the moment of inertia of the section perpendicular to l. From the relation between extensional forces and shears explained in §27 it is evident that the deformation represented in Fig. 16 can also be produced by suitably applied shearing stresses. This fact is important in the piezoelectric production of flexural vibrations, as will be seen in §179.

Complications arise when the plate is of crystalline material. In general, crystals have elastic cross constants not present in isotropic solids. Except in special cases these constants couple the compressional strain that characterizes the flexure with a shearing stress capable of causing torsion about the length dimension.

As an example we consider a quartz plate with its l-, b-, e-dimensions parallel to the Y-, Z-, X-axes, respectively. When the plate is flexed in the le-plane, as in Fig. 16, the strain $+y_y$ is present in the upper half, $-y_y$ in the lower. Then, by virtue of the relation $Y_z = -c_{24}y_y = c_{14}y_y$, there is a stress $+Y_z$ in the upper half, $-Y_z$ in the lower, and the combined effect of the two is to twist the plate about the Z-axis.

On the other hand, if the same quartz plate is flexed in the lb-plane, similar reasoning shows that there is no cross constant leading to torsion. This orientation is one of the special cases mentioned above.

The application of a bending moment, whether accomplished mechanically or piezoelectrically, results in a flexure accompanied by a twist, except when either (1) the length l is parallel to an axis of crystallographic symmetry or (2) the plane parallel to l and to a principal axis of the geometrical cross section (for a rectangular cross section this is the bl- or the be-plane) coincides with a plane of crystallographic summetry. This rule can also be put compactly by saying that torsion-free flexure is possible with a transformed axial system such that

$$s'_{34} = s'_{35} = 0$$

the length l of the plate being parallel to Z'.

A quartz bar or plate can be flexed without torsion if its length l lies anywhere in the YZ-plane.

A plate so oriented as to bend without torsion is also free from flexure when twisted about the same axis.

Static flexural effects in crystals have been used chiefly in the measurement of elastic constants* and in the Curie electrometer described in §122.

* The theory of flexure in crystals and its use in measurements are treated more fully in Voigt's "Lehrbuch," pp. 634, 725, 731, 751 and elsewhere.

Of greater concern in this book are flexural *vibrations*, which are treated in §§73, 179, 354, 359, 380, 396, and 503.

35. Torsion of Crystalline Prisms and Cylinders. The well-known facts for homogeneous isotropic materials will first be summarized. When equal and opposite torques $\pm Q$ are applied at the ends of a solid cylinder whose circular cross section has the radius a, the torsional strain in radians per unit length is

$$\tau = \frac{Q}{\pi n a^4}$$

where n is the rigidity.

For a circular cylinder, solid or hollow, the velocity of propagation of torsional waves is $v = \sqrt{n/\rho}$, where ρ is the density.

When in a state of torsion, each cross section of a circular cylinder rotates without deformation in its own plane. If the section is not circular, it becomes warped by torsion.

For the piezoelectric production of torsion or of torsional vibrations it is important to note that, when a solid of any material and cross section is subjected to torsion, all planes parallel to the axis of torque are in a state of shear. The manner in which advantage is taken of this fact is explained in §180.

With crystals the theory is complicated except in the case of a *circular cylinder*, for which the *torsional compliance* T is $\frac{1}{2}(s_{44} + s_{55})$ when the cylindrical axis is in the Z-direction; or, in general, when the axis is parallel to h, the compliance is $T_h = \frac{1}{2}(s_{ii} + s_{ij})$, h, i, and j signifying the X-, Y-, Z-axes taken in any order. This expression reduces to

$$T = s_2 = 1/n$$

for isotropic cylinders. For *oblique directions* transformed axes are used. For any given h-direction the i- and j-axes may have any two mutually perpendicular directions in the plane normal to h. Hence it is possible to express the torsional compliance in terms of the fundamental constants and the direction cosines l, m, n of h alone.*

$$\begin{aligned}
2T_h = s'_{ii} + s'_{jj} &= l^4(s_{55} + s_{66}) + m^4(s_{66} + s_{44}) + n^4(s_{44} + s_{55}) \\
&+ m^2n^2(4s_{22} + 4s_{33} - 8s_{23} + s_{55} + s_{66} - 2s_{44}) \\
&+ n^2l^2(4s_{33} + 4s_{11} - 8s_{31} + s_{66} + s_{44} - 2s_{55}) \\
&+ l^2m^2(4s_{11} + 4s_{22} - 8s_{12} + s_{44} + s_{55} - 2s_{66}) \\
&+ 2l^2mn(2s_{24} + 2s_{34} - 4s_{14} - 3s_{56}) + 2m^2nl(2s_{35} + 2s_{15} - 4s_{25} - 3s_{64}) \\
&+ 2n^2lm(2s_{16} + 2s_{26} - 4s_{36} - 3s_{45}) \\
&+ 2l^3[n(2s_{15} - 2s_{35} + s_{64}) + m(2s_{16} - 2s_{26} + s_{45})] \\
&+ 2m^3[l(2s_{26} - 2s_{16} + s_{45}) + n(2s_{24} - 2s_{34} + s_{56})] \\
&+ 2n^3[m(2s_{34} - 2s_{24} + s_{56}) + l(2s_{35} - 2s_{15} + s_{64})] \qquad (10)
\end{aligned}$$

* VOIGT, p. 735.

This formula, which becomes greatly simplified for the groups of higher symmetry, plays an important part in the measurement of elastic coefficients by static methods. If, according to Voigt's usage, the h-direction is taken as that of the Z'-axis, the expression above gives $2T_h = s'_{44} + s'_{55}$.

In the following equations τ is the rotational (torsional) strain in radians per unit length of the cylinder or prism, Q the torque, a and b the major and minor semiaxes of the elliptical section, $2b$ and $2e$ the breadth and thickness of the rectangular section. For rotated axes the coefficients are to be primed.

For a *cylinder of elliptical section*, axis parallel to Z,

$$\tau = \frac{Q}{\pi ab}\left(\frac{s_{44}}{a^2} + \frac{s_{55}}{b^2}\right) \tag{11}$$

On setting $a = b$ this becomes the equation for a cylinder with *circular* section of radius a:

$$\tau = \frac{Q}{\pi a^4}(s_{44} + s_{55}) = \frac{2QT}{\pi a^4} \tag{12}$$

If the material is isotropic, one has the familiar equation $\tau = 2Q/\pi n a^4$.

The general equation for a *prismatic crystal bar* of rectangular section, in any orientation, is given in Voigt.* The expression is greatly simplified when the length l (axis of torsion) is parallel to Z and the crystal symmetry is such that $s_{45} = 0$. Under these conditions, taking l, b, and the thickness e as parallel to the Z-, X-, and Y-axes, respectively, we have for the torsional strain approximately

$$\tau = \frac{3s_{55}Q}{A^2 be^3} \tag{13}$$

where, as long as $b > 3e$, $A^2 \approx 1 - 0.630(e/b)(s_{44}/s_{55})^{\frac{1}{2}}$.

If the axis of torsion is in a direction of three-, four-, or sixfold symmetry, $s_{44} = s_{55}$, and the formula becomes identical with that for an isotropic prism of the same dimensions, in which case s_{55} becomes $1/n$ for isotropic solids. In this case the coefficient A may be found approximately from $A^2 = 1 - 0.630e/b$ when $b > 3e$. For larger ratios of e to b, A may be obtained from the following values, which we have computed from data in Geiger and Scheel.†

$\frac{e}{b} =$	1	0.5	0.25	0.125
$A =$	0.895	0.926	0.947	0.968

These values of A are for isotropic solids, but the order of magnitude is the same for crystals.

* P. 644. See also ref. B19, vol. 8, p. 194.

† Vol. 8, p. 195.

In general, any cylinder or prism under a static torque Q may be said to possess a certain *static torsional stiffness* $N_s = Q/\tau$, which is a more or less complicated function of the cross section and the elastic constants. Only with isotropic solids, and in certain special cases with crystals, as exemplified by Eq. (12), do the elastic constants appear as a separate factor (modulus of rigidity). The relation of N_s to the *dynamic* torsional stiffness of vibrating rods is pointed out in §74.

The subject of torsion in crystals is more fully discussed in Voigt, in Auerbach-Hort,* and in Geiger and Scheel.†

For the treatment of torsional vibrations see §§74, 180, 356, 380, and 503.

36. Compressibility of Crystals. In general, uniform hydrostatic pressure causes both the volume and the angles of a crystal to change. Nevertheless, there is always a certain orientation in which a *parallelepiped* can be cut so that no angular distortion occurs. In all systems except triclinic and monoclinic the edges of this parallelepiped are parallel to the crystallographic axes.

In all cases the compressibility s_c is given by the equation

$$-s_c = \frac{\Delta v}{v\,\Delta p} = s_{11} + s_{22} + s_{33} + 2(s_{23} + s_{31} + s_{12}) \text{ cm}^2 \text{ dyne}^{-1} \quad (14)$$

where Δv is the change in volume caused by a change Δp in pressure.

The linear compressibility $S_l = -\Delta l/l\,\Delta p$ depends on the direction of l. For the three principal directions the formulas‡ are

$$S_x = s_{11} + s_{12} + s_{13} \qquad S_y = s_{21} + s_{22} + s_{23}$$
$$S_z = s_{31} + s_{32} + s_{33} \quad (15)$$

37. The Adiabatic Elastic Constants. As a rule, crystal vibrations are of such high frequency that the adiabatic rather than the isothermal values of the elastic constants should be used in calculations. Most of the numerical data for the fundamental constants at present available were obtained by static measurements, in which the temperature remained practically constant. The derivation of the adiabatic from the isothermal values requires a knowledge of the specific heat, which in solids may with sufficient accuracy be considered as approximately the same at constant volume as at constant pressure, and of the coefficients of expansion parallel to the three axes.

The following formulas have been derived by Voigt;§ the superscript a denotes the adiabatic constants, T is the absolute temperature, c the

* Vol. 3.
† Vol. 8.
‡ "Lehrbuch," p. 722.
§ "Lehrbuch," pp. 779*ff.*

specific heat in ergs cm^{-3} deg^{-1}, and q_h and a_h are coefficients of thermal pressure and expansion:

$$c^a_{hk} = c_{hk} + \frac{q_h q_k T}{c} \tag{16}$$

$$s^a_{hk} = s_{hk} - \frac{a_h a_k T}{c} \tag{17}$$

The adiabatic correction thus causes a slight *increase* in the stiffness of a crystal.

The quantity q is a thermo-elastic coefficient (§23) representing the increment of a component of stress exerted by the crystal when heated 1° at constant strain. Its value may be calculated from the equation

$$q_h = \sum_i c_{ih} a_i \text{ dyne cm}^{-2} \text{ deg}^{-1}$$

For all elastic groups except I and II the summation extends only over $i = 1, 2, 3$, because $a_4 = a_5 = a_6 = 0$.

CHAPTER IV

ROTATED AXES AND TRANSFORMATION OF ELASTIC CONSTANTS

Omnia mutantur, nihil interit. —OVID.

More often than not, the crystal plates and bars in technical applications have orientations that are rotated with respect to the crystallographic axes. Special formulas are therefore required by which the elastic properties of an oblique cut from any crystal can be expressed in terms of the fundamental elastic constants discussed in Chap. III.

The general transformation equations for the components of strain and stress will be given first. They will be followed by the equations for transformation of the elastic constants, including the specialization of these equations with reference to those crystal groups with which we shall be most concerned.

This chapter contains also a short account of the geometrical representation of elastic properties, the terminology for crystal cuts, and the conventions for specifying the orientation of oblique axes.

38. Transformation of Components of Strain and Stress. The process of determining which of the 21 possible elastic coefficients vanish for a crystal of given symmetry involves a rotation of the crystallographic axes through certain angles. Angular transformations of axes also play an important part in the measurement of elastic constants, in the theory and design of piezoelectric devices, and in many other problems.

The basic equations for the components x'_x, etc., of strain with respect to an axial system X', Y', Z', in terms of the components with respect to the original system X, Y, Z, are now given, with direction cosines according to the adjoining matrix.

	X'	Y'	Z'
X	l_1	l_2	l_3
Y	m_1	m_2	m_3
Z	n_1	n_2	n_3

$$
\left.\begin{aligned}
x'_x &= l_1^2 x_x + m_1^2 y_y + n_1^2 z_z + m_1 n_1 y_z + n_1 l_1 z_x + l_1 m_1 x_y \\
y'_y &= l_2^2 x_x + m_2^2 y_y + n_2^2 z_z + m_2 n_2 y_z + n_2 l_2 z_x + l_2 m_2 x_y \\
z'_z &= l_3^2 x_x + m_3^2 y_y + n_3^2 z_z + m_3 n_3 y_z + n_3 l_3 z_x + l_3 m_3 x_y \\
y'_z &= 2 l_2 l_3 x_x + 2 m_2 m_3 y_y + 2 n_2 n_3 z_z + (m_2 n_3 + m_3 n_2) y_z \\
&\qquad + (n_2 l_3 + n_3 l_2) z_x + (l_2 m_3 + l_3 m_2) x_y \\
z'_x &= 2 l_3 l_1 x_x + 2 m_3 m_1 y_y + 2 n_3 n_1 z_z + (m_3 n_1 + m_1 n_3) y_z \\
&\qquad + (n_3 l_1 + n_1 l_3) z_x + (l_3 m_1 + l_1 m_3) x_y \\
x'_y &= 2 l_1 l_2 x_x + 2 m_1 m_2 y_y + 2 n_1 n_2 z_z + (m_1 n_2 + m_2 n_1) y_z \\
&\qquad + (n_1 l_2 + n_2 l_1) z_z + (l_1 m_2 + l_2 m_1) x_y
\end{aligned}\right\} \qquad (18)
$$

It is sometimes necessary to express the unprimed components of strain or stress in terms of a given set of primed components. Following are the strain equations, in which the direction cosines are still defined according to the matrix above:

$$\left.\begin{aligned}
x_x &= l_1^2x'_x + l_2^2y'_y + l_3^2z'_z + l_2l_3y'_z + l_3l_1z'_x + l_1l_2x'_y \\
y_y &= m_1^2x'_x + m_2^2y'_y + m_3^2z'_z + m_2m_3y'_z + m_3m_1z'_x + m_1m_2x'_y \\
z'_z &= n_1^2x'_x + n_2^2y'_y + n_3^2z'_z + n_2n_3y'_z + n_3n_1z'_x + n_1n_2x'_y \\
y'_z &= 2m_1n_1x'_x + 2m_2n_2y'_y + 2m_3n_3z'_z + (m_2n_3 + m_3n_2)y'_z \\
&\qquad + (m_3n_1 + m_1n_3)z'_x + (m_1n_2 + m_2n_1)x'_y \\
z_x &= 2n_1l_1x'_x + 2n_2l_2y'_y + 2n_3l_3z'_z + (n_2l_3 + n_3l_2)y'_z \\
&\qquad + (n_3l_1 + n_1l_3)z'_x + (n_1l_2 + n_2l_1)x'_y \\
x_y &= 2l_1m_1x'_x + 2l_2m_2y'_y + 2l_3m_3z'_z + (l_2m_3 + l_3m_2)y'_z \\
&\qquad + (l_3m_1 + l_1m_3)z'_x + (l_1m_2 + l_2m_1)x'_y
\end{aligned}\right\} \quad (19)$$

The corresponding equations for transformation of stresses, using the same direction cosines, are

$$\left.\begin{aligned}
X'_x &= l_1^2X_x + m_1^2Y_y + n_1^2Z_z + 2m_1n_1Y_z + 2n_1l_1Z_x + 2l_1m_1X_y \\
Y'_y &= l_2^2X_x + m_2^2Y_y + n_2^2Z_z + 2m_2n_2Y_z + 2n_2l_2Z_x + 2l_2m_2X_y \\
Z'_z &= l_3^2X_x + m_3^2Y_y + n_3^2Z_z + 2m_3n_3Y_z + 2n_3l_3Z_x + 2l_3m_3X_y \\
Y'_z &= l_2l_3X_x + m_2m_3Y_y + n_2n_3Z_z + (m_2n_3 + m_3n_2)Y_z \\
&\qquad + (n_2l_3 + n_3l_2)Z_x + (l_2m_3 + l_3m_2)X_y \\
Z'_x &= l_3l_1X_x + m_3m_1Y_y + n_3n_1Z_z + (m_3n_1 + m_1n_3)Y_z \\
&\qquad + (n_3l_1 + n_1l_3)Z_x + (l_3m_1 + l_1m_3)X_y \\
X'_y &= l_1l_2X_x + m_1m_2Y_y + n_1n_2Z_z + (m_1n_2 + m_2n_1)Y_z \\
&\qquad + (n_1l_2 + n_2l_1)Z_x + (l_1m_2 + l_2m_1)X_y
\end{aligned}\right\} \quad (20)$$

The unprimed components of stress in terms of the primed components are given in Eqs. (21).

$$\left.\begin{aligned}
X_x &= l_1^2X'_x + l_2^2Y'_y + l_3^2Z'_z + 2l_2l_3Y'_z + 2l_3l_1Z'_x + 2l_1l_2X'_y \\
Y_y &= m_1^2X'_x + m_2^2Y'_y + m_3^2Z'_z + 2m_2m_3Y'_z + 2m_3m_1Z'_x + 2m_1m_2X'_y \\
Z_z &= n_1^2X'_x + n_2^2Y'_y + n_3^2Z'_z + 2n_2n_3Y'_z + 2n_3n_1Z'_x + 2n_1n_2X'_y \\
Y_z &= m_1n_1X'_x + m_2n_2Y'_y + m_3n_3Z'_z + (m_2n_3 + m_3n_2)Y'_z \\
&\qquad + (m_3n_1 + m_1n_3)Z'_x + (m_1n_2 + m_2n_1)X'_y \\
Z_x &= n_1l_1X'_x + n_2l_2Y'_y + n_3l_3Z'_z + (n_2l_3 + n_3l_2)Y'_z \\
&\qquad + (n_3l_1 + n_1l_3)Z'_x + (n_1l_2 + n_2l_1)X'_y \\
X_y &= l_1m_1X'_x + l_2m_2Y'_y + l_3m_3Z'_z + (l_2m_3 + l_3m_2)Y'_z \\
&\qquad + (l_3m_1 + l_1m_3)Z'_x + (l_1m_2 + l_2m_1)X'_y
\end{aligned}\right\} \quad (21)$$

We shall also have occasion to express the unprimed stress components in terms of the primed, using the matrix of direction cosines $\alpha_1 \ldots \gamma_3$ shown in §41, instead of $l_1 \ldots n_3$. In place of Eqs. (21) we then write

$$\left.\begin{aligned}
X_x &= \alpha_1^2 X_x' + \beta_1^2 Y_y' + \gamma_1^2 Z_z' + 2\beta_1\gamma_1 Y_z' + 2\gamma_1\alpha_1 Z_x' + 2\alpha_1\beta_1 X_y' \\
Y_y &= \alpha_2^2 X_x' + \beta_2^2 Y_y' + \gamma_2^2 Z_z' + 2\beta_2\gamma_2 Y_z' + 2\gamma_2\alpha_2 Z_x' + 2\alpha_2\beta_2 X_y' \\
Z_z &= \alpha_3^2 X_x' + \beta_3^2 Y_y' + \gamma_3^2 Z_z' + 2\beta_3\gamma_3 Y_z' + 2\gamma_3\alpha_3 Z_x' + 2\alpha_3\beta_3 X_y' \\
Y_z &= \alpha_2\alpha_3 X_x' + \beta_2\beta_3 Y_y' + \gamma_2\gamma_3 Z_z' + (\beta_2\gamma_3 + \beta_3\gamma_2) Y_z' \\
&\qquad + (\gamma_2\alpha_3 + \gamma_3\alpha_2) Z_x' + (\alpha_2\beta_3 + \alpha_3\beta_2) X_y' \\
Z_x &= \alpha_3\alpha_1 X_x' + \beta_3\beta_1 Y_y' + \gamma_3\gamma_1 Z_z' + (\beta_3\gamma_1 + \beta_1\gamma_3) Y_z' \\
&\qquad + (\gamma_3\alpha_1 + \gamma_1\alpha_3) Z_x' + (\alpha_3\beta_1 + \alpha_1\beta_3) X_y' \\
X_y &= \alpha_1\alpha_2 X_x' + \beta_1\beta_2 Y_y' + \gamma_1\gamma_2 Z_z' + (\beta_1\gamma_2 + \beta_2\gamma_1) Y_z' \\
&\qquad + (\gamma_1\alpha_2 + \gamma_2\alpha_1) Z_x' + (\alpha_1\beta_2 + \alpha_2\beta_1) X_y'
\end{aligned}\right\} \quad (22)$$

In most of the uses to which these formulas will be put, the transformation consists in a rotation about only one of the axes. In such a case one primed axis is identical with the corresponding unprimed, and the calculation is considerably simplified.

The angle θ through which the rotation takes place is to be taken as positive when counterclockwise as seen by an observer looking back toward the origin from the positive end of the axis of rotation.

The only exception to this rule occurs with the levo (left) types of enantiomorphous crystals, in which the rotation is positive when *clockwise.* Since, according to our convention (see §327 for quartz), one of the axes is then also reversed, a single rule for the sign of θ may be stated thus:

The angle θ through which any rotation takes place is to be taken as positive when laid off from the positive direction of one axis to the positive direction of the other, in this order: for rotations about the X- , Y- , or Z-axes, θ is positive when counted from $+Y$ to $+Z$, $+Z$ to $+X$, or $+X$ to $+Y$, respectively.

Sometimes, as in the description of certain oblique cuts, all three axes assume new directions. Although such transformations may be made in a single step, it is often advantageous to make first a rotation about one axis to the X_1- , Y_1- , Z_1-system (direction cosines $l_1 \ldots n_3$), and then by rotation about one of the primed axes to reach the final system X_2, Y_2, Z_2. If $l_1' \ldots n_3'$ are the direction cosines of the final system with respect to the primed axes and $l_1'' \ldots n_3''$ those of the final with respect to the original system, the following relations hold:

$$\left.\begin{aligned}
l_1'' &= l_1'l_1 + m_1'l_2 + n_1'l_3 & m_1'' &= l_1'm_1 + m_1'm_2 + n_1'm_3 \\
l_2'' &= l_2'l_1 + m_2'l_2 + n_2'l_3 & m_2'' &= l_2'm_1 + m_2'm_2 + n_2'm_3 \\
l_3'' &= l_3'l_1 + m_3'l_2 + n_3'l_3 & m_3'' &= l_3'm_1 + m_3'm_2 + n_3'm_3 \\
& & n_1'' &= l_1'n_1 + m_1'n_2 + n_1'n_3 \\
& & n_2'' &= l_2'n_1 + m_2'n_2 + n_2'n_3 \\
& & n_3'' &= l_3'n_1 + m_3'n_2 + n_3'n_3
\end{aligned}\right\} \quad (23)$$

When the matrix of direction cosines given in §41 is used instead of that in §38, Eqs. (23) become

$$\left.\begin{aligned}
\alpha_1'' &= \alpha_1'\alpha_1 + \alpha_2'\beta_1 + \alpha_3'\gamma_1 & \alpha_2'' &= \alpha_1'\alpha_2 + \alpha_2'\beta_2 + \alpha_3'\gamma_2 \\
\beta_1'' &= \beta_1'\alpha_1 + \beta_2'\beta_1 + \beta_3'\gamma_1 & \beta_2'' &= \beta_1'\alpha_2 + \beta_2'\beta_2 + \beta_3'\gamma_2 \\
\gamma_1'' &= \gamma_1'\alpha_1 + \gamma_2'\beta_1 + \gamma_3'\gamma_1 & \gamma_2'' &= \gamma_1'\alpha_2 + \gamma_2'\beta_2 + \gamma_3'\gamma_2 \\
& & \alpha_3'' &= \alpha_1'\alpha_3 + \alpha_2'\beta_3 + \alpha_3'\gamma_3 \\
& & \beta_3'' &= \beta_1'\alpha_3 + \beta_2'\beta_3 + \beta_3'\gamma_3 \\
& & \gamma_3'' &= \gamma_1'\alpha_3 + \gamma_2'\beta_3 + \gamma_3'\gamma_3
\end{aligned}\right\} \quad (24)$$

39. The use of the foregoing equations will now be illustrated by a few simple types of transformation, application of which is to be made in later sections.

First, assume the only *strain* to be y_z and that its components are sought with respect to axes X' parallel to X, Y' bisecting the angle between the positive directions of the Y- and Z-axes, and Z' making a right-handed system with X' and Y'. We have $\theta = 45°$, $l_1 = 1$, $l_2 = l_3 = m_1 = n_1 = 0$, $m_2 = n_3 = n_2 = -m_3 = \cos 45° = 1/\sqrt{2}$. Then, from Eq. (18), all components vanish except $y_y' = -z_z' = y_z/2$. The shear has been transformed into a positive and a negative extensional strain, each equal to half the original shear in magnitude. The application of this transformation in piezoelectric problems will appear later.

Second, let the only *stress* be Y_z. By substitution in Eqs. (20), it is found that after rotating the coordinate axes 45° about the X-axis the stress components equivalent to Y_z are $Y_y' = -Z_z' = Y_z$.

Third, still considering a rotation of $\theta = 45°$ about the X-axis, assume compressional stresses Y_y' and Z_z' applied parallel to the Y'- and Z'-axes. With respect to the original axes the equivalent stress components are $Y_y = Z_z = (Y_y' + Z_z')/2$, $Y_z = (Y_y' - Z_z')/2$. If $Z_z' = 0$, then

$$Y_y = Z_z = Y_z = \frac{Y_y'}{2}.$$

If $Z_z' = Y_y'$, Y_z vanishes and the body is compressed on four sides without being sheared. If $Z_z' = -Y_y'$ (equal compressional and extensional stresses at right angles), there is neither compression nor extension with respect to the unprimed axes, but only a shear $Y_z = Y_y'$.

40. Transformation Equations for the Elastic Constants. When it is recalled that the vanishing of certain of the elastic coefficients for any particular crystal class is due to the fact that the coefficients are defined with respect to the crystallographic axes of symmetry, it becomes evident that with respect to any other axial system all the coefficients will assume values different from zero except in certain special cases in which some degree of axial symmetry is still present. Hence, in the general transformation, however small the amount of rotation may be, all crystal

classes, even the most symmetrical, assume the elastic properties of the triclinic system.

On the other hand, it is often possible to find a new set of axes X', Y', Z' with respect to which some one of the coefficients vanishes, although it does not do so with respect to the crystallographic X- , Y- , Z-axes. Advantage of this fact is taken in certain oblique cuts of quartz in order to eliminate undesired coupling effects.

The complete theory, which is rather complicated, is given in Voigt and elsewhere. For only a few of the constants have the transformation equations been worked out for rotation about all three axes. For rotation about a single axis the equations for a considerable number of constants, both general and specialized for various crystal classes, have been derived by various authors.

While the technique described by Voigt* when once mastered leads most readily to the transformed equations, the following method is in principle simpler: Let it be required, for example, to derive s'_{hk} with respect to axes X', Y', Z', according to the equation $x'_h = -s'_{hk}X'_k$. We assume the single stress component X'_k impressed and write the six fundamental stress components $X_x \ldots X_y$ in terms of it, from Eqs. (21). These values are substituted on the right side of Eqs. (5), giving $x_x \ldots x_y$ in terms of fundamental elastic constants, direction cosines, and X'_k. The values of $x_x \ldots x_y$ in turn are substituted on the right side of the expression for x'_h in Eqs. (18); for example, if $h = 5$, the proper expression is that for z'_x. The coefficient of X'_k, which in the general case has 21 independent terms, is the desired quantity s'_{hk}.

Similarly, any coefficient c'_{hk} can be derived by assuming a single *strain* x'_h impressed, substituting in Eqs. (19), and then using Eqs. (6) and (20). The process becomes greatly simplified when the rotation is about a single axis and when for the crystal in question some of the fundamental elastic constants are equal to zero.

41. General Equations, Applicable to All Crystal Classes. Direction cosines are according to the adjoining table. When the rotation takes

	X'	Y'	Z'
X	α_1	β_1	γ_1
Y	α_2	β_2	γ_2
Z	α_3	β_3	γ_3

place about a single axis through the angle θ, the positive sign of θ is to be taken as indicated in §38. All direction cosines then reduce to 1, 0, $\pm \cos\theta$, or $\pm \sin\theta$. For brevity we shall write c for $\cos\theta$ and s for $\sin\theta$.

* Pp. 589*ff*.

ROTATION ABOUT ALL THREE AXES.

$$\begin{aligned}s'_{11} &= \alpha_1^4 s_{11} + \alpha_2^4 s_{22} + \alpha_3^4 s_{33} \\ &+ \alpha_2^2\alpha_3^2(2s_{23} + s_{44}) + \alpha_3^2\alpha_1^2(2s_{31} + s_{55}) + \alpha_1^2\alpha_2^2(2s_{12} + s_{66}) \\ &+ 2\alpha_1^2\alpha_2\alpha_3(s_{14} + s_{56}) + 2\alpha_2^2\alpha_3\alpha_1(s_{25} + s_{64}) + 2\alpha_3^2\alpha_1\alpha_2(s_{36} + s_{45}) \\ &+ 2\alpha_1^3(\alpha_2 s_{16} + \alpha_3 s_{15}) + 2\alpha_2^3(\alpha_3 s_{24} + \alpha_1 s_{26}) + 2\alpha_3^3(\alpha_1 s_{35} + \alpha_2 s_{34}) \quad (25)\end{aligned}$$

The equation for s'_{22} is derived by substituting β for α everywhere in Eq. (25); in the equation for s'_{33}, γ replaces α. In both cases all subscripts are left unaltered.

$$\begin{aligned}s'_{23} &= \beta_1^2\gamma_1^2 s_{11} + \beta_2^2\gamma_2^2 s_{22} + \beta_3^2\gamma_3^2 s_{33} \\ &+ (\beta_2^2\gamma_3^2 + \beta_3^2\gamma_2^2)s_{23} + \cdot\cdot + \beta_2\gamma_2\beta_3\gamma_3 s_{44} + \cdot\cdot \\ &+ \beta_1\gamma_1(\beta_2\gamma_3 + \beta_3\gamma_2)s_{56} + \cdot\cdot + (\beta_1^2\gamma_2\gamma_3 + \gamma_1^2\beta_2\beta_3)s_{14} + \cdot\cdot \\ &+ \beta_1\gamma_1(\beta_1\gamma_3 + \beta_3\gamma_1)s_{15} + (\beta_1\gamma_2 + \beta_2\gamma_1)s_{16} + \cdot\cdot \quad (26)\end{aligned}$$

Each missing term indicated by a dot is obtained from the term immediately preceding by raising all suffixes of both direction cosines and compliances by one step: write 2, 3, 1, 5, 6, 4 in place of 1, 2, 3, 4, 5, 6, respectively.

The equation for s'_{31} differs from Eq. (26) only in the substitution of β, γ, α for α, β, γ, respectively. For s'_{12} substitute γ, α, β for α, β, γ, respectively, leaving subscripts unchanged in both cases.

$$\begin{aligned}s'_{44} &= 4\beta_1^2\gamma_1^2 s_{11} + 4\beta_2^2\gamma_2^2 s_{22} + 4\beta_3^2\gamma_3^2 s_{33} \\ &+ 8\beta_2\gamma_2\beta_3\gamma_3 s_{23} + \cdot\cdot + (\beta_2\gamma_3 + \beta_3\gamma_2)^2 s_{44} + \cdot\cdot \\ &+ 2(\beta_1\gamma_2 + \beta_2\gamma_1)(\beta_1\gamma_3 + \beta_3\gamma_1)s_{56} + \cdot\cdot \\ &+ 4\beta_1\gamma_1(\beta_2\gamma_3 + \beta_3\gamma_2)s_{14} + \cdot\cdot \\ &+ 4\beta_1\gamma_1[(\beta_1\gamma_3 + \beta_3\gamma_1)s_{15} + (\beta_1\gamma_2 + \beta_2\gamma_1)s_{16}] + \cdot\cdot \quad (27)\end{aligned}$$

Missing terms are to be filled in as in Eq. (26). Equations for s'_{55} and s'_{66} are formed from Eq. (27) according to the rule given above for deriving s'_{31} and s'_{12} from Eq. (26).

$$\begin{aligned}c'_{11} &= c_{11}\alpha_1^4 + c_{22}\alpha_2^4 + c_{33}\alpha_3^4 \\ &+ 2[\alpha_2^2\alpha_3^2(c_{23} + 2c_{44}) + \alpha_3^2\alpha_1^2(c_{31} + 2c_{55}) + \alpha_1^2\alpha_2^2(c_{12} + 2c_{66})] \\ &+ 4\{\alpha_1^2\alpha_2\alpha_3(c_{14} + 2c_{56}) + \alpha_2^2\alpha_3\alpha_1(c_{25} + 2c_{46}) + \alpha_3^2\alpha_1\alpha_2(c_{36} + 2c_{45})] \\ &+ 4[\alpha_1^3(\alpha_3 c_{15} + \alpha_2 c_{16}) + \alpha_2^3(\alpha_1 c_{26} + \alpha_3 c_{24}) + \alpha_3^3(\alpha_2 c_{34} + \alpha_1 c_{35})] \quad (28)\end{aligned}$$

Equations for c'_{22} and c'_{33} are obtained from (28) by the rules given above for s'_{22} and s'_{33}.

$$\begin{aligned}c'_{44} &= c_{11}\beta_1^2\gamma_1^2 + \cdot\cdot + 2c_{23}\beta_2\gamma_2\beta_3\gamma_3 + \cdot\cdot \\ &+ c_{44}(\beta_2\gamma_3 + \beta_3\gamma_2)^2 + \cdot\cdot + 2c_{56}(\beta_1\gamma_2 + \beta_2\gamma_1)(\beta_1\gamma_3 + \beta_3\gamma_1) + \cdot\cdot \\ &+ 2c_{14}\beta_1\gamma_1(\beta_2\gamma_3 + \beta_3\gamma_2) + \cdot\cdot \\ &+ 2\beta_1\gamma_1[c_{15}(\beta_1\gamma_3 + \beta_3\gamma_1) + c_{16}(\beta_1\gamma_2 + \beta_2\gamma_1)] + \cdot\cdot \quad (29)\end{aligned}$$

Missing terms are supplied according to the rule following Eq. (26). For c'_{55} and c'_{66} write β, γ, α and γ, α, β for α, β, γ, respectively, leaving all subscripts unchanged. For example, the factor $\beta_2\gamma_3$ in the equation for c'_{44} becomes $\alpha_2\beta_3$ in that for c'_{66}.

$$\begin{aligned} c'_{23} = {} & c_{11}\beta_1^2\gamma_1^2 + \cdots + c_{23}(\beta_2^2\gamma_3^2 + \beta_3^2\gamma_2^2) + \cdots \\ & + 2c_{44}(\beta_2\gamma_3 + \beta_3\gamma_2)^2 + \cdots + 4c_{56}\beta_1\gamma_1(\beta_2\gamma_3 + \beta_3\gamma_2) + \cdots \\ & + 2c_{14}(\beta_1^2\gamma_2\gamma_3 + \gamma_1^2\beta_2\beta_3) + \cdots \\ & + 2\beta_1\gamma_1[c_{15}(\beta_1\gamma_3 + \beta_3\gamma_1) + c_{16}(\beta_1\gamma_2 + \beta_2\gamma_1)] + \cdots \end{aligned} \tag{30}$$

The missing terms in this equation, as well as the cyclical changes for obtaining expressions for c'_{31} and c'_{12}, are the same as with Eq. (29).

42. Rotation through Angle θ about the Z-axis. The direction cosines become reduced to $\alpha_1 = \beta_2 = \cos\theta \equiv c$, $\alpha_2 = -\beta_1 = \sin\theta \equiv s$, $\alpha_3 = \beta_3 = \gamma_1 = \gamma_2 = 0$, $\gamma_3 = 1$.*

$$\left.\begin{aligned} s'_{11} &= c^4 s_{11} + s^2c^2(2s_{12} + s_{66}) + s^4 s_{22} + 2c^3 s s_{16} + 2s^3 c s_{26} \\ s'_{22} &= s^4 s_{11} + s^2c^2(2s_{12} + s_{66}) + c^4 s_{22} - 2s^3 c s_{16} - 2c^3 s s_{26} \\ s'_{33} &= s_{33} \\ s'_{44} &= c^2 s_{44} - 2sc s_{45} + s^2 s_{55} \\ s'_{55} &= s^2 s_{44} + 2sc s_{45} + c^2 s_{55} \\ s'_{66} &= 4c^2s^2(s_{11} + s_{22} - 2s_{12}) - 4sc(c^2 - s^2)(s_{16} - s_{26}) \\ &\qquad + (c^2 - s^2)^2 s_{66} \\ s'_{12} &= c^2s^2(s_{11} + s_{22}) + (c^4 + s^4)s_{12} + sc(c^2 - s^2)(s_{16} - s_{26}) \\ &\qquad - c^2s^2 s_{66} \\ s'_{13} &= s^2 s_{23} + sc s_{36} + c^2 s_{31} \\ s'_{14} &= c^3 s_{14} - c^2 s(s_{15} - s_{46}) + s^2 c(s_{24} - s_{56}) - s^3 s_{25} \\ s'_{15} &= s^3 s_{24} + s^2 c(s_{25} + s_{64}) + c^2 s(s_{14} + s_{56}) + c^3 s_{15} \\ s'_{16} &= -2sc(c^2 s_{11} - s^2 s_{22}) + cs(c^2 - s^2)(2s_{12} + s_{66}) \\ &\qquad + c^2(c^2 - 3s^2)s_{16} + s^2(3c^2 - s^2)s_{26} \\ s'_{23} &= c^2 s_{23} - cs s_{36} + s^2 s_{31} \\ s'_{24} &= c^3 s_{24} - c^2 s(s_{25} + s_{64}) + s^2 c(s_{14} + s_{56}) - s^3 s_{15} \\ s'_{25} &= s^3 s_{14} + s^2 c(s_{15} - s_{46}) + c^2 s(s_{24} - s_{56}) + c^3 s_{25} \\ s'_{26} &= -2sc(s^2 s_{11} - c^2 s_{22}) - cs(c^2 - s^2)(2s_{12} + s_{66}) \\ &\qquad + s^2(3c^2 - s^2)s_{16} + c^2(c^2 - 3s^2)s_{26} \\ s'_{34} &= c s_{34} - s s_{35} \\ s'_{35} &= s s_{34} + c s_{35} \\ s'_{36} &= cs(s_{23} - s_{31}) + (c^2 - s^2)s_{36} \\ s'_{45} &= cs(s_{44} - s_{55}) + (c^2 - s^2)s_{45} \\ s'_{46} &= -2s^2 c(s_{25} - s_{15}) + 2c^2 s(s_{24} - s_{14}) + (c^2 - s^2)(c s_{46} - s s_{56}) \\ s'_{56} &= 2c^2 s(s_{25} - s_{15}) + 2s^2 c(s_{24} - s_{14}) + (c^2 - s^2)(s s_{46} + c s_{56}) \end{aligned}\right\} \tag{31}$$

* Equations (31) are taken from Voigt's "Lehrbuch." In the expression for s'_{66} two misprints have been corrected. The author has noted also a number of other minor misprints at various points in the "Lehrbuch."

For a rotation about the X- or Y-axis the equations are exactly as in (31), except that all digits in suffixes on both sides of the equations are raised by one and two points, respectively, as shown in the following table, in which the first column indicates the axis of rotation. For example, wherever suffix 5 occurs in Eqs. (31), 6 is to be written for rotation about the X-axis, and 4 for rotation about the Y-axis.

Z	1	2	3	4	5	6
X	2	3	1	5	6	4
Y	3	1	2	6	4	5

Nowhere does a complete set of equations for c'_{hk} for rotated axes seem to have been worked out, except in specialized form for certain crystal systems. Below is given the equation for c'_{33} for rotation about the X-axis. It is obtained from Eqs. (28) by first substituting γ for α and then setting $\gamma_1 = 0$, $\gamma_2 = -\sin\theta = -s$, $\gamma_3 = \cos\theta = c$:

$$c'_{33} = s^4c_{22} + c^4c_{33} + 2s^2c^2(c_{23} + 2c_{44}) - 4s^3cc_{24} - 4c^3sc_{34} \qquad (32)$$

43. Young's Modulus for a Crystal Bar in Any Orientation. In §33 we saw that $1/s_{11}$, $1/s_{22}$, and $1/s_{33}$ represent Young's modulus for bars parallel to X, Y, and Z. Similarly, by suitable choice of axes Eq. (25) gives the reciprocal of Young's modulus Y for any crystal in any direction. Owing to the importance of this constant we now write the same equation in another form, due to Koga[275], which is perhaps more convenient for calculation. For any direction having the direction cosines l, m, n,

$$\begin{aligned}\frac{1}{Y} = {} & l^2(l^2s_{11} + m^2s_{12} + n^2s_{13} + mns_{14} + nls_{15} + lms_{16}) \\ & + m^2(l^2s_{12} + m^2s_{22} + n^2s_{23} + mns_{24} + nls_{25} + lms_{26}) \\ & + n^2(l^2s_{13} + m^2s_{23} + n^2s_{33} + mns_{34} + nls_{35} + lms_{36}) \\ & + mn(l^2s_{14} + m^2s_{24} + n^2s_{34} + mns_{44} + nls_{45} + lms_{46}) \\ & + nl(l^2s_{15} + m^2s_{25} + n^2s_{35} + mns_{45} + nls_{55} + lms_{56}) \\ & + lm(l^2s_{16} + m^2s_{26} + n^2s_{36} + mns_{46} + nls_{56} + lms_{66}) \qquad (33)\end{aligned}$$

For example, parallel to the Y-axis, $l = n = 0$, $m = 1$, and $1/Y$ reduces to s_{22}. Equation (33) is easily specialized for any crystal group. When Young's modulus is expressed in terms of transformed axes, it is customary to take the Z'-axis as the direction of stress and strain, giving the equation

$$z'_z = -s'_{33}Z'_z, \qquad (34)$$

where Young's modulus is $1/s'_{33}$.

SPECIALIZATION OF AXIAL TRANSFORMATIONS FOR CERTAIN GROUPS OF CRYSTALS

With the groups here considered many of the coefficients vanish, so that the general expressions are greatly simplified. The following equations are obtained from the foregoing general equations, the subscripts of the various coefficients being taken from the tables in §29. The table of direction cosines is the same as in §41.

Group III, Rhombic System

44. All elastic parameters in this group are symmetrical with respect to the crystallographic axes. For example, in all polar diagrams (§49) representing the elastic properties in the principal planes (planes normal to the three crystallographic axes), the same values are repeated in all four quadrants. Of course, this is not true of planes that are oblique to all three axes.

This group includes Rochelle salt and its isomorphic relatives. The procedure for deriving the stiffness coefficients from the observed compliance coefficients according to the method outlined in §26 is especially simple for this group and will serve as an example of the general method. The L- and T-coefficients (§30) are found from the determinant

$$D = \begin{vmatrix} s_{11} & s_{12} & s_{13} \\ s_{21} & s_{22} & s_{23} \\ s_{31} & s_{32} & s_{33} \end{vmatrix} s_{44}s_{55}s_{66}$$

together with the various cofactors. Thus,

$$Dc_{11} = s_{44}s_{55}s_{66}\begin{vmatrix} s_{22} & s_{23} \\ s_{32} & s_{33} \end{vmatrix} \cdots$$

$$Dc_{23} = s_{44}s_{55}s_{66}\begin{vmatrix} s_{31} & s_{32} \\ s_{11} & s_{12} \end{vmatrix} \cdots$$

The S-coefficients (§30) are simply $c_{44} = 1/s_{44}$, $c_{55} = 1/s_{55}$, and $c_{66} = 1/s_{66}$.

Elastic Constants for Axes in Any Orientation. Direction cosines are as tabulated in §41.

$$s'_{33} = \gamma_1^4 s_{11} + \gamma_2^4 s_{22} + \gamma_3^4 s_{33} + \gamma_2^2\gamma_3^2(2s_{23} + s_{44}) + \gamma_3^2\gamma_1^2(2s_{31} + s_{55}) + \gamma_1^2\gamma_2^2(2s_{12} + s_{66}) \quad (35)$$

For s'_{11} and s'_{22}, substitute α and β, respectively, for γ.

$$s'_{44} = 4(\beta_1^2\gamma_1^2 s_{11} + \beta_2^2\gamma_2^2 s_{22} + \beta_3^2\gamma_3^2 s_{33}) + 8(\beta_2\gamma_2\beta_3\gamma_3 s_{23} + \beta_3\gamma_3\beta_1\gamma_1 s_{31} + \beta_1\gamma_1\beta_2\gamma_2 s_{12}) + (\beta_2\gamma_3 + \beta_3\gamma_2)^2 s_{44} + (\beta_3\gamma_1 + \beta_1\gamma_3)^2 s_{55} + (\beta_1\gamma_2 + \beta_2\gamma_1)^2 s_{66} \quad (36)$$

For s'_{55}, change β to α; for s'_{66}, change γ to α.

$$c'_{11} = \alpha_1^4 c_{11} + \alpha_2^4 c_{22} + \alpha_3^4 c_{33} + 2[\alpha_2^2\alpha_3^2(c_{23} + 2c_{44}) + \alpha_3^2\alpha_1^2(c_{31} + 2c_{55}) + \alpha_1^2\alpha_2^2(c_{12} + 2c_{66})] \quad (37)$$

For c'_{22} and c'_{33}, permute α to β and γ, respectively.

$$c'_{44} = c_{11}\beta_1^2\gamma_1^2 + c_{22}\beta_2^2\gamma_2^2 + c_{33}\beta_3^2\gamma_3^2 + 2c_{23}\beta_2\gamma_2\beta_3\gamma_3 + 2c_{31}\beta_3\gamma_3\beta_1\gamma_1 + 2c_{12}\beta_1\gamma_1\beta_2\gamma_2 + c_{44}(\beta_2\gamma_3 + \beta_3\gamma_2)^2 + c_{55}(\beta_3\gamma_1 + \beta_1\gamma_3)^2 + c_{66}(\beta_1\gamma_2 + \beta_2\gamma_1)^2 \quad (38)$$

The rules for c'_{55} and c'_{66} are the same as for s'_{55} and s'_{66} above.

45. Rotation about a Single Axis. All expressions for rotation about a single axis are found from the more general equations for axes in any direction, by assigning proper values to the direction cosines according to §41. Some of the following are derived more simply from Eqs. (35) to (38). In all cases the suffixes are determined by the rules following the respective equations.

Data for *rotation about the X-axis* (Y'-cut) are furnished by Mason.[335]

$$\left.\begin{aligned}
&s'_{11} = s_{11} \qquad s'_{22} = c^4 s_{22} + s^4 s_{33} + c^2 s^2 (2s_{23} + \bar{s}_{44}) \\
&s'_{33} = c^4 s_{33} + s^4 s_{22} + c^2 s^2 (2s_{23} + s_{44}) \\
&s'_{44} = (c^2 - s^2) s_{44} + 4c^2 s^2 (s_{22} + s_{33} - 2s_{23}) \\
&s'_{55} = c^2 s_{55} + s^2 s_{66} \\
&s'_{66} = c^2 s_{66} + s^2 s_{55} \qquad s'_{12} = c^2 s_{12} + s^2 s_{13} \\
&s'_{13} = c^2 s_{13} + s^2 s_{12} \qquad s'_{14} = 2cs(s_{13} - s_{12}) \\
&s'_{23} = (c^4 + s^4) s_{23} + c^2 s^2 (s_{22} + s_{33} - s_{44}) \\
&s'_{24} = 2c^2 s^2 [c^2 (2s_{23} + s_{44} - 2s_{22}) + s^2 (2s_{33} - 2s_{23} - s_{44})] \\
&s'_{34} = 2c^2 s^2 [c^2 (2s_{33} - 2s_{23} - s_{44}) + s^2 (2s_{23} - 2s_{22} + s_{44})] \\
&s'_{56} = cs(s_{55} - s_{66}) \\
&s'_{15} = s'_{16} = s'_{25} = s'_{26} = s'_{35} = s'_{36} = s'_{45} = s'_{46} = 0
\end{aligned}\right\} \quad (39)$$

Of the corresponding stiffness coefficients we give only the following, derived from Eq. (38):

$$\left.\begin{aligned}
&c'_{44} = (c^2 - s^2) c_{44} + c^2 s^2 (c_{22} + c_{33} - 2c_{23}) \\
&c'_{55} = c^2 c_{55} + s^2 c_{66} \qquad c'_{66} = c^2 c_{66} + s^2 c_{55}
\end{aligned}\right\} \quad (40)$$

For both compliance and stiffness coefficients the equations for rotation about the Y- and Z-axes are derived from the above by permutation of subscripts according to the rule and table following Eqs. (31). Among the more important examples are the following:

About the Y-axis,

$$\left.\begin{aligned} c'_{44} &= c^2c_{44} + s^2c_{66} \qquad c'_{66} = c^2c_{66} + s^2c_{44} \\ c'_{55} &= (c^2 - s^2)c_{55} + c^2s^2(c_{11} + c_{33} - 2c_{13}) \end{aligned}\right\} \tag{41}$$

About the Z-axis,

$$\left.\begin{aligned} s'_{11} &= c^4s_{11} + s^4s_{22} + c^2s^2(2s_{12} + s_{66}) \\ c'_{44} &= c^2c_{44} + s^2c_{55} \qquad c'_{55} = c^2c_{55} + s^2c_{44} \\ c'_{66} &= (c^2 - s^2)c_{66} + c^2s^2(c_{11} + c_{22} - 2c_{12}) \end{aligned}\right\} \tag{42}$$

When $\theta = 45°$, the foregoing equations become, for rotation about the X-axis,

$$\left.\begin{aligned} &s'_{11} = s_{11} && s'_{22} = s'_{33} = \tfrac{1}{4}(s_{22} + s_{33} + s_{44} + 2s_{23}) \\ &s'_{44} = s_{22} + s_{33} - 2s_{23} && s'_{55} = s'_{66} = \tfrac{1}{2}(s_{55} + s_{66}) \\ &s'_{12} = s'_{13} = \tfrac{1}{2}(s_{12} + s_{13}) && s'_{14} = s_{13} - s_{12} \\ &s'_{23} = \tfrac{1}{4}(s_{22} + s_{33} - s_{44} + 2s_{23}) && s'_{34} = s'_{24} = \tfrac{1}{2}(s_{33} - s_{22}) \\ &s'_{56} = \tfrac{1}{2}(s_{55} - s_{66}) \\ &s'_{15} = s'_{16} = s'_{25} = s'_{26} = s'_{35} = s'_{36} = s'_{45} = s'_{46} = 0 \end{aligned}\right\} \tag{43}$$

The corresponding stiffness coefficients, complete with the exception of c'_{56}, are as follows:

$$\left.\begin{aligned} &c'_{11} = c_{11} && c'_{22} = c'_{33} = \tfrac{1}{4}(c_{22} + c_{33} + 2c_{23} + 4c_{44}) \\ &c'_{44} = \tfrac{1}{4}(c_{22} + c_{33} - 2c_{23}) && c'_{55} = c'_{66} = \tfrac{1}{2}(c_{55} + c_{66}) \\ &c'_{12} = c'_{13} = \tfrac{1}{2}(c_{12} + c_{13}) && c'_{14} = \tfrac{1}{2}(c_{13} - c_{12}) \\ &c'_{23} = \tfrac{1}{4}(c_{22} + c_{33} + 2c_{23} - 4c_{44}) && c'_{24} = c'_{34} = \tfrac{1}{4}(c_{33} - c_{22}) \\ &c'_{15} = c'_{16} = c'_{25} = c'_{26} = c'_{35} = c'_{36} = c'_{45} = c'_{46} = 0 \end{aligned}\right\} \tag{44}$$

The reciprocals of s'_{22} and s'_{33} are Young's modulus for directions in the YZ-plane at $\pm 45°$ with the Y-axis. Analogous expressions for rotation about the Y- and Z-axes are obtained by the rule given above.

For any arbitrary direction having direction cosines α_1, α_2, α_3, the following equation for Young's modulus is derived from Eq. (33):

$$\frac{1}{Y} = \alpha_1^4s_{11} + \alpha_2^4s_{22} + \alpha_3^4s_{33} + \alpha_2^2\alpha_3^2(s_{44} + 2s_{23}) + \alpha_3^2\alpha_1^2(s_{55} + 2s_{31}) + \alpha_1^2\alpha_2^2(s_{66} + 2s_{12}) \tag{45}$$

For a direction X' making equal angles with all three axes, the stiffness coefficient c'_{11} is

$$c'_{11} = 0.111[(c_{11} + c_{22} + c_{33}) + 2(c_{23} + c_{31} + c_{12}) + 4(c_{44} + c_{55} + c_{66})] \tag{46}$$

This equation is used in calculating the frequency for thickness vibrations of the L-cut (§140).

Group VII, Trigonal System

46. This is the trigonal group that includes quartz and tourmaline. Direction cosines are as tabulated in §41. Although both right and left forms of crystals may occur in this group, there is no difference in the equations (see §327).

For this group, the compliance and stiffness coefficients are related by the following equations:

$$\alpha = s_{33}(s_{11} + s_{12}) - 2s_{13}^2 \qquad \beta = s_{44}(s_{11} - s_{12}) - 2s_{14}^2$$
$$\alpha' = c_{33}(c_{11} + c_{12}) - 2c_{13}^2 \qquad \beta' = c_{44}(c_{11} - c_{12}) - 2c_{14}^2$$

$$\left.\begin{array}{llllll}
2c_{11} = \dfrac{s_{33}}{\alpha} + \dfrac{s_{44}}{\beta} & c_{13} = -\dfrac{s_{13}}{\alpha} & c_{33} = \dfrac{s_{11} + s_{12}}{\alpha} & c_{66} = \dfrac{c_{11} - c_{12}}{2} \\
2c_{12} = \dfrac{s_{33}}{\alpha} - \dfrac{s_{44}}{\beta} & c_{14} = -\dfrac{s_{14}}{\beta} & c_{44} = \dfrac{s_{11} - s_{12}}{\beta} & c_{66} = \dfrac{s_{44}}{2\beta} \\
2s_{11} = \dfrac{c_{33}}{\alpha'} + \dfrac{c_{44}}{\beta'} & s_{13} = -\dfrac{c_{13}}{\alpha'} & s_{33} = \dfrac{c_{11} + c_{12}}{\alpha'} & s_{66} = 2(s_{11} - s_{12}) \\
2s_{12} = \dfrac{c_{33}}{\alpha'} - \dfrac{c_{44}}{\beta'} & s_{14} = -\dfrac{c_{14}}{\beta'} & s_{44} = \dfrac{c_{11} - c_{12}}{\beta'} & s_{66} = 2\dfrac{c_{44}}{\beta'}
\end{array}\right\} \quad (47)$$

General Formulas for Rotated Axes. For orthogonal axes in any arbitrary orientation only a few equations are found in the literature. Expressions for the remaining coefficients can be derived by the methods described in §40 and 41. Equations (48) and (49) are from Voigt.

$$s'_{33} = (1 - \gamma_3^2)^2 s_{11} + \gamma_3^4 s_{33} + \gamma_3^2(1 - \gamma_3^2)(2s_{13} + s_{44}) + 2(3\gamma_1^2 - \gamma_2^2)\gamma_2\gamma_3 s_{14} \quad (48)$$

For s'_{11} and s'_{22}, γ is changed to α and β, respectively.

$$s'_{44} = s_{44} + \alpha_3^2(2s_{11} - 2s_{12} - s_{44}) + 4\beta_3^2\gamma_3^2(s_{11} + s_{33} - 2s_{13} - s_{44}) + 4[(3\beta_1\gamma_1 - \beta_2\gamma_2)(\beta_3\gamma_2 + \beta_2\gamma_3) - \alpha_2\alpha_3]s_{14} \quad (49)$$

For s'_{55} and s'_{66}, permute α, β, γ to β, γ, α and γ, α, β, respectively.

47. Elastic Coefficients for Rotation about a Single Axis. The transformation of axes is given in terms of $\cos\theta = c$ and $\sin\theta = s$, where θ is the angle of rotation of two of the axes about the third axis. θ is positive when *counterclockwise* as seen from the positive end of the axis of rotation. In all cases the table of direction cosines in §41 is employed.

These equations* result from retaining in the general equations of §42 the special coefficients for Group VII (§29). Some of them are found in Voigt and in later publications, for example, those of Mason[332] and of Hight and Willard.[227]

* The full set of equations was furnished to the author through the courtesy of the American Telephone and Telegraph Company. In conformity with our convention respecting the definition of the positive sense of rotation, the signs of certain of the terms have been changed.

Rotation about the X-axis (Y'-cut). $\alpha_1 = 1$, $\beta_1 = \gamma_1 = \alpha_2 = \alpha_3 = 0$, $\beta_2 = \gamma_3 = c$, $\beta_3 = -\gamma_2 = s$.

$$
\begin{aligned}
s'_{11} &= s_{11}\\
s'_{22} &= c^4 s_{11} + s^4 s_{33} + c^2 s^2 (2s_{13} + s_{44}) - 2c^3 s s_{14}\\
s'_{33} &= s^4 s_{11} + c^4 s_{33} + c^2 s^2 (2s_{13} + s_{44}) + 2cs^3 s_{14} = s'_{22}[\theta \pm 90°]^*\\
s'_{44} &= 4c^2 s^2 (s_{11} + s_{33} - 2s_{13}) + (c^2 - s^2)^2 s_{44} + 4cs(c^2 - s^2) s_{14}\\
s'_{55} &= c^2 s_{44} + 2s^2 (s_{11} - s_{12}) - 4css_{14}\\
s'_{66} &= 2c^2 (s_{11} - s_{12}) + s^2 s_{44} + 4css_{14} = s'_{55}[\theta \pm 90°]\\
s'_{12} &= c^2 s_{12} + s^2 s_{13} + css_{14}\\
s'_{13} &= s^2 s_{12} + c^2 s_{13} - css_{14} = s'_{12}[\theta \pm 90°]\\
s'_{14} &= 2cs(s_{13} - s_{12}) + (c^2 - s^2) s_{14}\\
s'_{15} &= s'_{16} = 0\\
s'_{23} &= (c^4 + s^4) s_{13} + c^2 s^2 (s_{11} + s_{33} - s_{44}) + sc(c^2 - s^2) s_{14}\\
s'_{24} &= -2c^3 s s_{11} + 2cs^3 s_{33} + cs(c^2 - s^2)(2s_{13} + s_{44})\\
&\qquad - c^2 (c^2 - 3s^2) s_{14}\\
s'_{25} &= s'_{26} = 0\\
s'_{34} &= -2cs^3 s_{11} + 2c^3 s s_{33} - cs(c^2 - s^2)(2s_{13} + s_{44})\\
&\qquad + s^2 (s^2 - 3c^2) s_{14} = -s'_{24}[\theta \pm 90°]\\
s'_{35} &= s'_{36} = 0 \qquad s'_{45} = s'_{46} = 0\\
s'_{56} &= 2(c^2 - s^2) s_{14} - sc(s_{66} - s_{44})
\end{aligned}
\tag{50}
$$

$$
\begin{aligned}
c'_{11} &= c_{11}\\
c'_{22} &= c^4 c_{22} + s^4 c_{33} + 2c^2 s^2 (c_{13} + 2c_{44}) - 4c^3 s c_{14}\\
c'_{33} &= s^4 c_{11} + c^4 c_{33} + 2c^2 s^2 (c_{13} + 2c_{44}) + 4cs^3 c_{14} = c'_{22}[\theta \pm 90°]\\
c'_{44} &= c^2 s^2 (c_{22} + c_{33} - 2c_{13}) + (c^2 - s^2)^2 c_{44} + 2cs(c^2 - s^2) c_{14}\\
c'_{55} &= c^2 c_{44} + s^2 c_{66} - 2csc_{14}\\
c'_{66} &= s^2 c_{44} + c^2 c_{66} + 2csc_{14} = c'_{55}[\theta \pm 90°]\\
c'_{12} &= c^2 c_{12} + s^2 c_{13} + 2csc_{14}\\
c'_{13} &= s^2 c_{12} + c^2 c_{13} - 2csc_{14} = c'_{12}[\theta \pm 90°]\\
c'_{14} &= (c^2 - s^2) c_{14} - cs(c_{12} - c_{13})\\
c'_{15} &= c'_{16} = 0\\
c'_{23} &= (c^4 + s^4) c_{13} + s^2 c^2 (c_{11} + c_{33} - 4c_{44}) + 2cs(c^2 - s^2) c_{14}\\
c'_{24} &= c^2 (4s^2 - 1) c_{14} + cs[c^2 c_{11} - s^2 c_{33} + (c^2 - s^2)(2c_{44} + c_{13})]\\
c'_{25} &= c'_{26} = 0\\
c'_{34} &= -s^2 (4c^2 - 1) c_{14} + cs[s^2 c_{11} - c^2 c_{33} - (c^2 - s^2)(2c_{44} + c_{13})]\\
&\qquad = -c'_{24}[\theta \pm 90°]\\
c'_{35} &= c'_{36} = c'_{45} = c'_{46} = 0\\
c'_{56} &= (c^2 - s^2) c_{14} - cs(c_{66} - c_{44})
\end{aligned}
\tag{51}
$$

When $\theta = 0$, so that $c = 1$, $s = 0$, the foregoing equations apply to the Y-cut.

* The expression $s'_{22}[\theta \pm 90°]$ means that the equation for s'_{22}, for an axial rotation of $\theta \pm 90°$, is identical with the equation for s'_{33} for a rotation of θ. A similar meaning is to be attached to all bracketed angles in equations for rotated axes, whether the transformed quantities are elastic or piezoelectric coefficients.

Rotation about the Y-axis (X'-cut). $\beta_2 = 1$, $\beta_1 = \beta_3 = \alpha_2 = \gamma_2 = 0$, $\alpha_1 = \gamma_3 = c$, $-\alpha_3 = \gamma_1 = s$.

$$
\begin{aligned}
s'_{11} &= c^4 s_{11} + s^4 s_{33} + s^2 c^2 (s_{44} + 2s_{13}) \\
s'_{22} &= s_{11} \\
s'_{33} &= s^4 s_{11} + c^4 s_{33} + s^2 c^2 (s_{44} + 2s_{13}) = s'_{11}[90^\circ - \theta] \\
s'_{44} &= c^2 s_{44} + s^2 s_{66} \\
s'_{55} &= 4s^2 c^2 (s_{11} + s_{33} - 2s_{13}) + (c^2 - s^2)^2 s_{44} \\
s'_{66} &= s^2 s_{44} + c^2 s_{66} = s'_{44}[90^\circ - \theta] \\
s'_{12} &= c^2 s_{12} + s^2 s_{13} \\
s'_{13} &= (c^4 + s^4) s_{13} + s^2 c^2 (s_{11} + s_{33} - s_{44}) \\
s'_{14} &= c(1 - 3s^2) s_{14} \\
s'_{15} &= cs[2(c^2 s_{11} - s^2 s_{33}) - (c^2 - s^2)(s_{44} + 2s_{13})] \\
s'_{16} &= -3sc^2 s_{14} \\
s'_{23} &= s^2 s_{12} + c^2 s_{13} = s'_{12}[90^\circ - \theta] \\
s'_{24} &= -cs_{14} \\
s'_{25} &= 2cs(s_{12} - s_{13}) \\
s'_{26} &= ss_{14} = -s'_{24}[90^\circ - \theta] \\
s'_{34} &= 3cs^2 s_{14} = -s'_{16}[90^\circ - \theta] \\
s'_{35} &= cs[2(s^2 s_{11} - c^2 s_{33}) + (c^2 - s^2)(s_{44} + 2s_{13})] = s'_{15}[90^\circ - \theta] \\
s'_{36} &= -s(1 - 3c^2) s_{14} = -s'_{14}[90^\circ - \theta] \\
s'_{45} &= -2s(1 - 3c^2) s_{14} = 2s'_{36} \\
s'_{46} &= cs(s_{66} - s_{44}) \\
s'_{56} &= 2c(1 - 3s^2) s_{14} = 2s'_{14}
\end{aligned}
\qquad (52)
$$

$$
\begin{aligned}
c'_{11} &= c^4 c_{11} + s^4 c_{33} + 2s^2 c^2 (2c_{44} + c_{13}) \\
c'_{22} &= c_{11} \\
c'_{33} &= s^4 c_{11} + c^4 c_{33} + 2s^2 c^2 (2c_{44} + c_{13}) = c'_{11}[90^\circ - \theta] \\
c'_{44} &= c^2 c_{44} + s^2 c_{66} \\
c'_{55} &= s^2 c^2 (c_{11} + c_{33} - 2c_{13}) + (c^2 - s^2)^2 c_{44} \\
c'_{66} &= s^2 c_{44} + c^2 c_{66} = c'_{44}[90^\circ - \theta] \\
c'_{12} &= c^2 c_{12} + s^2 c_{13} \\
c'_{13} &= (c^4 + s^4) c_{13} + s^2 c^2 (c_{11} + c_{33} - 4c_{44}) \\
c'_{14} &= c(1 - 3s^2) c_{14} \\
c'_{15} &= cs[c^2 c_{11} - s^2 c_{33} - (c^2 - s^2)(2c_{44} + c_{13})] \\
c'_{16} &= -3sc^2 c_{14} \\
c'_{23} &= s^2 c_{12} + c^2 c_{13} = c'_{12}[90^\circ - \theta] \\
c'_{24} &= -cc_{14} \qquad c'_{25} = cs(c_{12} - c_{13}) \\
c'_{26} &= sc_{14} = -c'_{24}[90^\circ - \theta] \\
c'_{34} &= 3cs^2 c_{14} = -c'_{16}[90^\circ - \theta] \\
c'_{35} &= cs[s^2 c_{11} - c^2 c_{33} + (c^2 - s^2)(2c_{44} + c_{13})] = c'_{15}[90^\circ - \theta] \\
c'_{36} &= -s(1 - 3c^2) c_{14} = -c'_{14}[90^\circ - \theta] \\
c'_{45} &= c_{36} = -c'_{14}[90^\circ - \theta] \\
c'_{46} &= cs(c_{66} - c_{44}) \\
c'_{56} &= e'_{14}
\end{aligned}
\qquad (53)
$$

Rotation about the Z-axis. $\gamma_3 = 1, \gamma_1 = \gamma_2 = \alpha_3 = \beta_3 = 0,$
$\alpha_1 = \beta_2 = c, \alpha_2 = -\beta_1 = s.$

$$
\begin{aligned}
s'_{11} &= s_{11} & c'_{11} &= c_{11}\\
s'_{22} &= s_{22} = s_{11} & c'_{22} &= c_{22} = c_{11}\\
s'_{33} &= s_{33} & c'_{33} &= c_{33}\\
s'_{44} &= s_{44} & c'_{44} &= c_{44}\\
s'_{55} &= s_{55} = s_{44} & c'_{55} &= c_{55} = c_{44}\\
s'_{66} &= s_{66} & c'_{66} &= c_{66}\\
s'_{12} &= s_{12} & c'_{12} &= c_{12}\\
s'_{13} &= s_{13} & c'_{13} &= c_{13}\\
s'_{14} &= c(1 - 4s^2)s_{14} & c'_{14} &= c(1 - 4s^2)c_{14}\\
s'_{15} &= -s(1 - 4c^2)s_{14} & c'_{15} &= -s(1 - 4c^2)c_{14}\\
s'_{16} &= 0 & c'_{16} &= 0\\
s'_{23} &= s_{13} & c'_{23} &= c_{13}\\
s'_{24} &= -s'_{14} & c'_{24} &= -c'_{14}\\
s'_{25} &= -s'_{15} & c'_{25} &= -c'_{15}\\
s'_{26} &= 0 & c'_{26} &= 0\\
s'_{34} &= s'_{35} = s'_{36} = 0 & c'_{34} &= c'_{35} = c'_{36} = 0\\
s'_{45} &= 0 & c'_{45} &= 0\\
s'_{46} &= -2s'_{15} & c'_{46} &= -c'_{15}\\
s'_{56} &= 2s'_{14} & c'_{56} &= c'_{14}
\end{aligned}
\qquad (54)
$$

48. *Young's modulus* for a quartz bar in any orientation, the length having direction cosines l, m, n, from Eq. (33), is

$$\frac{1}{Y} = (1 - n^2)^2 s_{11} + n^4 s_{33} + n^2(1 - n^2)(s_{44} + 2s_{13}) + 2mn(3l^2 - m^2)s_{14} \qquad (55)$$

For any direction in the YZ-plane making an angle θ with the Z-axis ($\cos\theta = c = n$, $\sin\theta = s = -m$), this expression is identical with s'_{33} in Eqs. (50); similarly, in the ZX-plane it becomes s'_{33} from Eqs. (52); in the XY-plane it is simply s_{11} in all directions. These relations are shown graphically in Fig. 38.

Other formulas, involving different angular parameters, are found in the literature.*

49. Geometrical Representation of Elastic Properties. From the foregoing sections it is clear that each elastic constant has a definite meaning and a definite numerical value only with respect to a specific frame of reference within the crystal. If the frame of reference coincides with the three conventionally adopted orthogonal crystallographic axes, one has the "fundamental" constants.

* See, for example, Wright and Stuart[594] and Bechmann.[32]

In order to present to the eye the dependence of the elastic constants of any given crystal upon the orientation of the axial system, it is customary to make use of certain geometrical surfaces or of diagrammatic intersections of such surfaces with certain planes.

The most general elastic surface is represented by an equation of the fourth degree, in which the 21 parameters are either the stiffness or the compliance constants.* Such surfaces are of greater theoretical than practical value.

More useful are surfaces representing the magnitudes of individual constants or functions of constants in their dependence upon the orientation of the axial system. An example of considerable importance is the surface for which the radius vector in any direction is proportional to the value of Young's modulus $1/s'_{33}$ in that direction. A model of such a surface, for quartz, is shown in Fig. 37.

The construction of surfaces to represent the elastic cross constants, of types T, L', S', or T' (§30), would not be quite so simple. As can be seen from equations such as (26), these constants cannot be expressed in terms of a single direction in space. For any arbitrary direction of the Z'-axis the value of any such constant depends also on the choice of the X'- and Y'-axes. A surface representing any cross constant could be constructed, however, by laying off, for any given Z'-direction, the computed value of the cross constant in a direction parallel, say, to the X'-axis. Such a surface would be somewhat analogous to the optical index ellipsoid (§528), in which the refractive indices corresponding to waves in any direction are proportional to radius vectors perpendicular to this direction.

Owing to the difficulty in the actual construction of elastic surfaces, it is customary, and for most purposes sufficient, to prepare polar or Cartesian graphs showing the various elastic constants for rotation about a single crystallographic axis. For this purpose the equations in preceding sections for rotation about a single axis are employed. Examples of this sort, for individual crystals, are given in Chap. VI.

50. Terminology for Crystal Cuts. When a flat parallel-faced plate or bar is cut from a crystal, the term "cut" is used to designate the direction of the normal to the major faces. Thus an X-cut has the normal to its major faces parallel to the X-axis of the crystal. Similarly, Y- and Z-cuts have their faces perpendicular to the Y- and Z-axes.

Oblique Cuts. While in the earlier investigations plates and bars were usually cut with their edges parallel to the crystal axes, various oblique cuts, especially of quartz crystals, are in common use. It must be recognized first of all that the choice of crystal axes is arbitrary, so that there is no reason a priori why the physical performance of crystal

* VOIGT, p. 736.

preparations may not for many purposes be better when they are cut so that the electric field will lie in some oblique direction. Mathematically, the problem consists in carrying out a transformation of axes, resulting in an entirely different set of values of the elastic and piezoelectric constants. With respect to the new axes piezoelectric effects can be created that were not present in the original system; conversely, by suitable choice of axes certain elastic or piezoelectric effects may be eliminated. For example, Mason[332] succeeded in getting rid of an undesired mode of vibration in quartz by rotating the Y- and Z-axes through a certain angle while leaving the X-axis unchanged; several investigators have found that the frequency of vibrating quartz plates, such as are used for standards of frequency, can be made practically independent of temperature by orienting the plates in certain directions; and the author has made use of the longitudinal effect that can be realized in obliquely cut Rochelle-salt plates. As early as 1894 Pockels showed that the transverse effect can be obtained in Rochelle salt by cutting bars with their lengths at 45° with two of the crystal axes. The last-mentioned fact has found wide application.

Oblique cuts may be specified in terms of the transformed axes X', Y', or Z'; for example, an X'-cut has its normal parallel to the X'-axis. Special designations are considered in later chapters. We now give the rules for the specification of oblique cuts that will be used in this book.

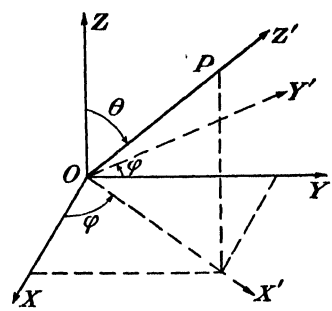


FIG. 17.—An arbitrary direction OP represented in terms of azimuth φ and polar angle θ.

51. Notation for Orientation of Transformed Axes. Many transformation formulas involve rotation about a single axis. In such cases, as in §47, we shall use θ to denote the angle of rotation and assign to it the *positive* sign when the rotation is *counterclockwise* as seen from the positive end of the axis about which the rotation takes place (except with *left*-crystals, as indicated below).

When a single direction in space is to be specified, as, for example, in equations for Young's modulus or in defining the normal to a given cut, we shall use as parameters the azimuth φ and the colatitude (polar angle) θ. They are illustrated in Fig. 17, in which OP is the specified direction. In all cases φ is positive when laid off from $+X$ toward $+Y$. The rotation φ about the Z-axis transforms the X-, Y-axes to new axes, which in Fig. 17 are called X' and Y'. The angle θ may be regarded as the result of a rotation of the Z- and X'-axes about Y'. θ is positive when the rotation is from $+Z$ toward $+X'$; if the crystal is enantiomorphous,

this statement is valid for both the right and the left forms. From the rules for right- and left-crystals given in §7, it is evident that Fig. 17 applies to a *right*-crystal, since the axial system is here right-handed; in this case θ is positive when counterclockwise as seen from the + end of the Y-axis. The diagram for a *left*-crystal would be the mirror image of Fig. 17, and θ would be positive when *clockwise* as seen from the + end of the Y-axis.

The direction defined by φ and θ is that of the Z'-axis, and with suitable values of φ and θ it may assume any orientation in space. This choice of the Z'-axis to represent a given direction explains why, for example, Young's modulus is often denoted as $1/s'_{33}$.

52. While a single direction can be specified by φ and θ without mention of transformed axes, it is necessary to make explicit use of the latter

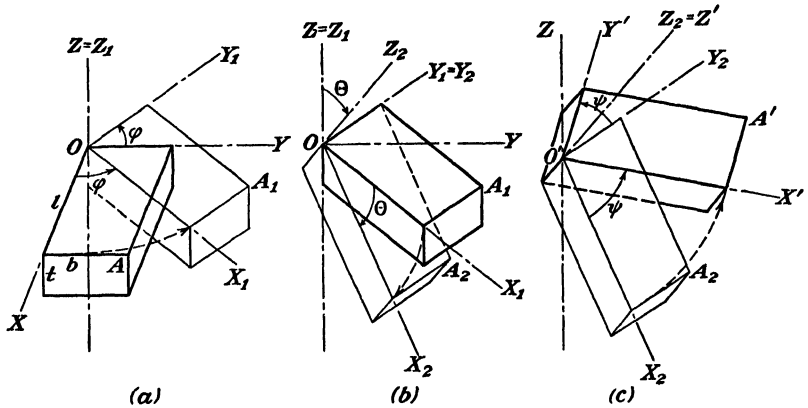


FIG. 18.—An oblique plate $O'A'$, derived by three rotations from a Z-cut OA.

when a third angular parameter is required. Thus, for specifying completely the orientation of a rectangular plate, we perform first a rotation of the X- and Y-axes about the Z-axis through the angle φ, as indicated in Fig. 18; the resulting axial system is X_1, Y_1, $Z_1 = Z$. A second rotation, about the Y_1-axis through the angle Θ, gives the axial system X_2, $Y_2 = Y_1$, Z_2. The Z_2-axis is thus defined in terms of φ and Θ and is taken as the direction of one edge of the plate. The orientation of the plate at this stage can be visualized by considering first a Z-cut plate OA with its length l and breadth b parallel, respectively, to X and Y. The first rotation, about the Z-axis, turns the plate to the position OA_1, while the second, about the Y_1-axis, brings it into the position OA_2. The thickness dimension t is now parallel to the Z_2-axis. The final orientation is brought about by a rotation around the Z_2-axis through the "angle of skew" ψ, yielding the axial system X', Y', $Z' = Z_2$.

The full specifications for an oblique plate may be given by writing the values of φ, Θ, and ψ in this order, together with the dimensions parallel to the X'-, Y'-, and Z'-axes: for example, an X-cut bar with its length parallel to the direction of maximum Young's modulus may be denoted by $X'40$ mm(0°), $Y'10$ mm (90°), $Z'1$ mm (48°36′).*

Direction Cosines. The direction cosines of the $X_2Y_2Z_2$-axial system with respect to the XYZ-axes, defined according to the accompanying matrix, are as follows:

$$\left.\begin{aligned} l_1 &= \cos\varphi\cos\Theta & l_2 &= -\sin\varphi \\ l_3 &= \cos\varphi\sin\Theta & m_1 &= \sin\varphi\cos\Theta \\ m_2 &= \cos\varphi & m_3 &= \sin\varphi\sin\Theta \\ n_1 &= -\sin\Theta & n_2 &= 0 \qquad n_3 = \cos\Theta \end{aligned}\right\} \tag{56}$$

	X_2	Y_2	Z_2
X	l_1	l_2	l_3
Y	m_1	m_2	m_3
Z	n_1	n_2	n_3

For the final $X'Y'Z'$-axes with respect to the XYZ-axes the values are

$$\left.\begin{aligned} l_1^0 &= \cos\varphi\cos\Theta\cos\psi - \sin\varphi\sin\psi \\ l_2^0 &= -\cos\varphi\cos\Theta\sin\psi - \sin\varphi\cos\psi \\ l_3^0 &= \cos\varphi\sin\Theta \\ m_1^0 &= \sin\varphi\cos\Theta\cos\psi + \cos\varphi\sin\psi \\ m_2^0 &= -\sin\varphi\cos\Theta\sin\psi + \cos\varphi\cos\psi \\ m_3^0 &= \sin\varphi\sin\Theta \\ n_1^0 &= -\sin\Theta\cos\psi \qquad n_2^0 = \sin\Theta\sin\psi \qquad n_3^0 = \cos\Theta \end{aligned}\right\} \tag{57}$$

	X'	Y'	Z'
X	l_1^0	l_2^0	l_3^0
Y	m_1^0	m_2^0	m_3^0
Z	n_1^0	n_2^0	n_3^0

REFERENCES

AUERBACH and HORT,[B1] GEIGER and SCHEEL[B29], LOVE,[B34] BOND.[64]

* The rules given above are in agreement with the conventions recently approved by the Institute of Radio Engineers (I.R.E.). The institute has recommended further that such values be assigned to φ, Θ, and ψ as will cause the orientations of the X'-, Y'-, and Z'-axes to be parallel, respectively, to the length, breadth, and thickness of the plate. For the application of this I.R.E. axial system to quartz see §327.

CHAPTER V

VIBRATIONS OF CRYSTALS

. . . sed ut unda impellitur unda
urgueturque eadem veniens urguetque priorem,
tempora sic fugiunt pariter pariterque sequuntur
et nova sunt semper.

—OVID.

53. Introduction. Voigt in his "Lehrbuch" gave the fundamental equations for vibrations in crystals, but they received no further attention until the 1920's, when the advent of the crystal resonator revived interest in the elastic properties of crystals. The author's paper in 1921 on the theory of longitudinal vibrations in damped isotropic rods was followed by another the next year on the application of this theory to the first piezoelectric resonators. The same problem was subjected to more precise analysis by Laue in 1925. Soon many other papers on crystal vibrations appeared, both theoretical and experimental, dealing with rods, plates, and rings cut from various piezoelectric crystals.

More recently much attention has been given to the theory of vibrations in quartz plates cut at various oblique angles with respect to the crystallographic axes, for the purpose of eliminating the effects of temperature on frequency or of avoiding coupling effects between different types of vibration. New methods for measuring elastic constants have been developed, of which one of the most important and interesting makes use of optical effects due to ultrasonic waves. In all this work it is important to observe the distinction between the isothermal elastic constants derived from static observations and the adiabatic constants that play a part in all vibratory phenomena.

Although the effect of piezoelectric reactions upon the elastic constants is touched upon only briefly in this chapter, mention should be made of the fact that recent measurements of the adiabatic elastic constants of Rochelle salt have led to a changed opinion as to the conditions under which the "pure" elastic constants of piezoelectric crystals, uncontaminated by piezoelectric reaction, should be measured. This consideration in turn demands a new formulation of fundamental piezo-electric theory, differing in important respects from that of Voigt. These matters are discussed in Chap. XI.

An idea of the complexity in the theory of vibrations can be gained by considering the various modes in which a parallelepiped is capable of

vibrating. To the six possible components of strain correspond six degrees of freedom, hence six of the simpler modes of vibration, the frequency for each depending on the elastic constants, density, and dimensions. The possible modes are

1. Those corresponding to one of the six strains by itself. These modes comprise compressional and shear, with their overtones.

2. Flexural (fundamental or overtone), with strains in different parts of the parallelepiped opposing each other.

3. Torsional, including overtones.

4. Coupled modes, in which two or more of the foregoing simpler modes become interlocked to form a more complex vibration. As in the analogous electric case, the coupling may be due to frictional forces, to inertia, or to elastic coupling through the elastic cross constants. The latter type of coupling is of chief importance in crystal resonators. Either fundamental or overtone frequencies may take part in the coupling. As in electrical networks, the relative importance of each of the component modes at any resonant frequency for the coupled vibration depends on the closeness of coupling and on the natural frequencies of the component modes.

No complete and rigorous theory of vibrations in solids, even for the simpler forms of isotropic bodies, has ever been formulated. A full treatment of all coupling effects and boundary conditions defies analysis. Nevertheless, the difficulties have been sufficiently overcome so that a fairly precise description can be given of compressional, shear, flexural, and torsional vibrations in crystal preparations of simple geometrical shape. For the fundamental theory the references at the end of this chapter may be consulted. We must confine ourselves mainly to the results, although the equations for rods and thin plates will be developed in some detail. Most of the expressions are basically those for isotropic solids, with such modifications as are needed to adapt them to crystals. In many important cases, especially those having to do with compressional waves, the isotropic equations can be used without alteration.

We shall give attention chiefly to two important forms of crystal vibrator, for which the theory is fortunately fairly amenable to analysis.

The first of these is the elongated rod. The theory of lengthwise compressional waves, including the effects of damping, is quite simple. The vibrations associated with the other five modes of strain, if excited at all, are of such relatively high natural frequency that coupling can be ignored; these strains are then in phase with the longitudinal strain. For vibrations of this type the effective stiffness is Young's modulus. As the order of overtones becomes high, or the length is no longer great in comparison with the other dimensions, complicated stages of coupling

are encountered, until the comparatively simple theory of thickness vibrations of a thin plate is reached.*

The second form to consider is that of a thin plate of large area. Here again, only this time for *thickness* vibrations (compressional or shear), there is no appreciable coupling with lateral effects except with high overtones of the latter—and in practice these are troublesome enough. The simple theory considers a plate of infinite lateral extent, in which case the plate may be regarded as completely constrained laterally (see §33), except that, for shear vibrations, freedom for small tangential displacements has to be allowed.

54. *Normal Modes of Vibration.* In general, when an elastic solid body is set into a state of free vibration, as by being suddenly struck, its motion, if of small amplitude, can theoretically be analyzed into a large number of "normal" vibrational modes. The number of these modes is the same as the number of degrees of freedom, which is theoretically infinite even for the simplest geometrical forms of solids. To each normal mode corresponds a "normal frequency," which, however, is *abnormal* in one particular, *viz.*, that it is usually taken as the value in absence of damping.

For any normal frequency the necessary characteristics are that all particles move in phase with simple harmonic motion and with amplitudes in constant ratios to one another. This criterion is very closely fulfilled when the viscosity is small.

The chief types of vibration, for each of which an indefinitely large number of normal frequencies (overtones) is possible, are *compressional* (called also "longitudinal" or "extensional"), *shear* ("transverse"), *flexural*, and *torsional*.

In *compressional vibrations* the motion of the vibrating particles is parallel to the direction of propagation of the wave.

In *shear vibrations* the particles move in a direction normal to the direction of propagation, *i.e.*, parallel to the wave front.

Flexural vibrations involve a bending of the specimen in a certain plane. They are sometimes, though ambiguously, called "transverse" or "lateral" vibrations. Although they are most prominent in elongated bars or in thin plates, they may be present in solids of almost any form.

Torsional vibrations are those in which a relative angular displacement about a certain axis takes place between adjacent cross sections. The direction of wave propagation is along this axis.

* The theory of elastic vibrations in the piezoelectric resonator is a little more complicated when the rod is in a state of forced vibration due to the piezoelectric effects of an impressed alternating electric field, if, as is usually the case, the field causes other components of stress than that tending to change the length of the rod. The method of dealing with this complication is given in Chap. XIII.

When the "natural frequency" for any mode of vibration is measured, the observed value is always less than the theoretical "normal value" by an amount depending on the damping to which the resonating body is subject. The observed frequency also depends somewhat upon the method of observation: it is slightly greater for free vibrations (those vibrations which, once excited, die away at a rate depending on the decrement) than for forced vibrations in which the frequency of maximum *velocity* of the particles in the resonator is observed; and this in turn is slightly greater than the frequency for maximum *amplitude* of vibration. All these observed frequencies are lower than the ideal normal frequency in absence of damping. This subject is discussed further in §58.

55. Vibrations of Crystals. In most cases here considered the vibrations can be expressed in terms of wave velocity. The fundamental equation for velocity in absence of damping is

$$c = \sqrt{\frac{q}{\rho}} \tag{58}$$

where q is the stiffness factor, which assumes different forms for different types of vibration, and ρ is the density. The problem then resolves itself into finding the proper expression for q for each type of vibration, due heed being paid to the dimensions of the vibrator. In the case of an unconstrained rectangular parallelepiped in which the direction of wave propagation is parallel to one of the edges it is permissible, to a certain degree of approximation, to consider the vibration as due to a system of stationary waves, reflection taking place at two opposite faces. To fix the ideas we assume the parallelepiped to have dimensions X, Y, Z and the wave propagation to be in the Z-direction. Then for the wave velocity and frequency of free undamped vibrations we may write

$$\left.\begin{aligned} c = f_h\lambda &= \frac{2Zf_h}{h} \\ f_h &= \frac{hc}{2Z} = \frac{h}{2Z}\sqrt{\frac{q}{\rho}} \end{aligned}\right\} \tag{59}$$

where h is the order of the overtone, which is approximately harmonic; for the fundamental frequency, $h = 1$.

Leaving flexural and torsional vibrations for later consideration, we regard for the present two extreme cases that are often approximated in practice. The first is that of thin rods, the second that of extended media, exemplified by thickness vibrations in plates of relatively large area. In general we shall be concerned only with steady-state solutions, in homogeneous rods of unvarying cross section.*

* The theory for isotropic rods of varying cross section and of varying material was given long ago by J. Stefan, in *Sitzber. Akad. Wiss. Wien., Math.-naturw. Klasse*, vol. 55, part 2, pp. 597*f.*, 1867; vol. 57, part 2, pp. 517*f.*, 1868. Recently the theory of

56. Longitudinal Vibrations of Rods. Most of the theoretical and experimental investigations with which we are concerned have to do with steady-state forced vibrations. Space permits only a statement of the principal results, with references to original papers in which a fuller treatment can be found. The discussion will be confined to rods in which both ends are free, since this is the case usually occurring with piezoelectric resonators.

In the ideal case of an infinitely thin frictionless rod, Eq. (59) may be written in the form

$$f = \frac{h}{2l}\sqrt{\frac{1}{\rho s}} = \frac{h}{2l}\sqrt{\frac{q}{\rho}} \tag{60}$$

where l is the length of the rod and $q = 1/s$ is Young's modulus. As a first approximation (lateral inertia being ignored) this equation is often very useful, especially for predetermining the length of a resonator.

We now turn to the problem of *vibrations in a thin rod* subject to frictional losses. Concerning these losses nothing further need be assumed than that there is a frictional force proportional to the velocity.* The following treatment is essentially that which was first given by the author,[92] starting with the differential wave equation and leading to simple expressions in which the resonator is regarded as having concentrated mass and elasticity, vibrating with a single degree of freedom. The method will be recognized as analogous to that used in the problem of the electric transmission line.

The well-known equation for waves in one dimension is

$$\rho \frac{\partial^2 \xi}{\partial t^2} = q \frac{\partial^2 \xi}{\partial x^2} + F \frac{\partial^3 \xi}{\partial x^2 \, \partial t} \tag{61}$$

where ξ is the displacement at time t of that cross section whose undisturbed coordinate is x.† ρ, q, and F are density, Young's modulus,

---

vibrations in composite rods driven piezoelectrically has received much attention, especially in connection with the measurement of the dynamic elastic characteristics of metals and other non-piezoelectric solids. References will be found at the end of this chapter and of the next.

* Voigt ("Lehrbuch," p. 792) discusses the coefficients of internal friction of crystals, b_{hk}, and their relation to the elastic constants. In most practical cases the internal friction is small in comparison with that due to external causes. The b_{hk} could be measured only with crystals mounted with extreme care and vibrated in vacuum. As will be seen in §242, they were introduced by Laue in his theory. The internal losses in Rochelle salt are treated in Chaps. XVIII and XX to XXV.

† In the case of longitudinal vibrations, ξ is parallel to the direction of wave propagation. Equation (61), however, holds for displacements in any direction, as long as this direction is the same for all particles in the same plane normal to the direction of propagation. This equation is therefore applicable to all modes of thickness vibration of plates as well as to longitudinal vibrations of rods.

and frictional factor. The possible dependence of q and F upon temperature, frequency, and various electrical and mechanical circumstances, is for the present left in abeyance. F is here regarded as a constant, with dimensions $(ML^{-1}T^{-1})$. In most practical cases F depends much more on losses due to mounting and to surrounding air than on the losses inherent in the crystal. The theory is in no way contingent on any assumption as to the origin of F or its constancy, except that at any frequency it must be independent of the amplitude of vibration. In general, in place of F, we shall use the logarithmic decrement δ, the quality factor Q, or the damping factor α, which are quantities related to F that can be determined at any frequency.

We first write the solution of Eq. (61) in the form appropriate for progressive waves of any wavelength λ, subject to attenuation with time. No term representing attenuation in space need be included. The solution is

$$\xi = Ae^{-\alpha t+j(kx+\omega t)} \tag{62}$$

where A is the amplitude, α and k are constants, and $\omega = 2\pi f$.

The following relations are found by substituting Eq. (62) in (61) and equating real and imaginary parts:

$$k = \frac{2\pi}{\lambda} \tag{63}$$

$$\alpha = \frac{Fk^2}{2\rho} = \frac{2\pi^2 F}{\rho\lambda^2} \tag{64}$$

k is sometimes called the "wavelength constant" and α the "attenuation constant" or "damping constant."

The velocity of progressive waves, including the effect of damping, is

$$c = \frac{\omega}{k} = \pm\sqrt{\frac{q}{\rho} - \frac{k^2F^2}{4\rho^2}} = \pm\sqrt{\frac{q}{\rho} - \frac{\pi^2F^2}{\rho^2\lambda^2}} \approx \sqrt{\frac{q}{\rho}}\left(1 - \frac{\delta^2}{8\pi^2}\right)$$
$$= \sqrt{\frac{q}{\rho}}\left(1 - \frac{1}{8Q^2}\right) \tag{65}$$

where δ is the logarithmic decrement and Q is the quality factor, given by Eq. (67). The dependence of c upon λ, and therefore on the frequency, may be called a "dispersion," analogous to optical dispersion. In most cases the second term in the expressions above is negligible in comparison with the first, so that the velocity given by Eq. (65) is practically identical with that in Eq. (58).

The instantaneous displacement at any point then becomes

$$\xi(x) = Ae^{-\frac{2\pi^2Ft}{\rho\lambda^2}}\cos\frac{2\pi}{\lambda}(x + ct) \tag{66}$$

This is the equation for the displacement at any distance x from an arbitrary origin, for progressive sinusoidal waves of length λ, traveling with velocity c in a rod of indefinite length. If free, they die away at a rate given by the exponential factor. The logarithmic decrement per period is

$$\delta = \frac{2\pi^2 F}{\rho c \lambda} = \frac{\alpha}{f} = \frac{\pi}{Q} \tag{67}$$

57. *Forced Vibrations.* A flat bar of relatively small cross section with its length l in the X-direction is excited piezoelectrically by a uniform alternating electric field parallel to the thickness of the bar. A uniform alternating stress system is thus produced. As will be seen when specific cases are encountered, this complex of stress components can be resolved into an equivalent uniformly distributed longitudinal driving stress X. The problem before us is to express the instantaneous displacement $\xi(x)$ at any point in terms of X and of any prescribed frequency. The origin of coordinates is taken at the center of the rod.

For the steady-state solution, Eq. (62) is replaced by

$$\xi = A(x)\epsilon^{j\omega t} \tag{68}$$

in which A is now a complex function of x, involving amplitude, frequency, and phase.

Upon substituting Eq. (68) in (61) it is found that

$$\frac{\partial^2 A(x)}{\partial x^2} = \gamma^2 A(x) \tag{69}$$

where

$$\gamma^2 = \frac{-\omega^2 \rho}{q + j\omega F} \tag{70}$$

The only simplifying assumption inherent in these expressions, beyond the disregard of cross section, is the same as in Eq. (62), namely, that the frictional coefficient is so small that its effect upon the distribution of strain along the length of the rod can be ignored.

If X_0 is the maximum value of the impressed stress, we may assume the instantaneous impressed stress to be

$$X = X_0 \epsilon^{j\omega t} \tag{71}$$

This equation gives also the *total* stress at the ends of the rod, where $x = \pm l/2$, so that the strain at the ends is

$$\left(\frac{\partial \xi}{\partial x}\right)_{l/2} = (x_x)_{l/2} = -\frac{X}{q} \tag{72}$$

In order to find $A(x)$ and ξ, we solve Eq. (69) for $A(x)$. The constants of integration are determined from the boundary conditions that when

$x = 0$, $\xi = 0$, and when $x = l/2$, $\partial\xi/\partial x = \epsilon^{j\omega t}\partial A(x)/\partial x = -\epsilon^{j\omega t}X_0/q$, from Eqs. (71) and (72). It can then be proved that

$$A(x) = -\frac{X_0}{q\gamma}\frac{\sinh \gamma x}{\cosh \gamma \frac{l}{2}} \tag{73}$$

The solution obtained from this assumption of a uniformly distributed periodic driving stress is the same that would be reached if one supposed a pair of equal and opposite periodic forces to be applied at the ends of the rod, the force per unit area being numerically equal to the stress X. Although the author used the latter method in his first papers on the resonator,[92,93] a method that has since been followed by others, still the treatment now considered is to be preferred, since it represents the facts more directly; moreover, as will be seen when the theory is specialized for particular crystals, it facilitates the inclusion in the theory of all the piezoelectric effects that contribute to the vibration and to the electrical characteristics of the resonator.

Equation (73) can be thrown into a more workable form, which retains high precision even for a degree of damping greatly in excess of any commonly encountered in resonators, by writing, from Eqs. (64) and (70),

$$\gamma \approx \frac{\alpha}{c} + j\frac{\omega}{c} \tag{74}$$

On substituting this value of γ in Eq. (73) and making obvious reductions one finds

$$-A(x) = \frac{X_0 c}{q\omega}\frac{\left(\sin\frac{\omega x}{c}\cos\frac{\omega l}{2c} - \frac{\alpha^2 l x}{2c^2}\cos\frac{\omega x}{c}\sin\frac{\omega l}{2c}\right) - j\left(\frac{\alpha x}{c}\cos\frac{\omega x}{c}\cos\frac{\omega l}{2c} + \frac{\alpha l}{2c}\sin\frac{\omega x}{c}\sin\frac{\omega l}{2c}\right)}{\cos^2\frac{\omega l}{2c} + \frac{\alpha^2 l^2}{4c^2}\sin^2\frac{\omega l}{2c}} \tag{75}$$

The modulus of $A(x)$ is the amplitude of ξ at any x, while the argument is the phase angle. In most cases it suffices to express the amplitude and phase of the vibration *at the ends* of the rod; we therefore set $x = l/2$ in Eq. (75) and find, after making trigonometrical reductions and rejecting as negligible the term in α^2 in the numerator (the α^2-term in the denominator must be retained owing to the vanishing of the $\cos^2$ term at resonance)

$$-A\left(\frac{l}{2}\right) = \frac{X_0 c}{2q\omega}\frac{\sin\frac{\omega l}{c} - j\frac{\alpha l}{c}}{\cos^2\frac{\omega l}{2c} + \frac{\alpha^2 l^2}{4c^2}\sin^2\frac{\omega l}{2c}} \tag{76}$$

At frequencies close to resonance all terms in Eq. (76) have to be retained.

From Eqs. (68) and (76) the longitudinal displacement at the end of the rod is found to be

$$-\xi\left(\frac{l}{2}\right) = \frac{X_0 c}{2q\omega} \frac{\left(\frac{\alpha^2 l^2}{c^2} + \sin^2 \frac{\omega l}{c}\right)^{\frac{1}{2}}}{\cos^2 \frac{\omega l}{2c} + \frac{\alpha^2 l^2}{4c^2} \sin^2 \frac{\omega l}{2c}} \sin(\omega t - \theta) \tag{77}$$

where $\tan \theta = -[\sin(\omega l/c)]/(\alpha l/c)$. $\xi(l/2)$ leads X_0 by the angle $90° - \theta$.

Equations (76) and (77) hold with high precision at all frequencies, including zero. At zero frequency α and ω vanish, and the amplitude becomes the static elongation

$$-\xi\left(\frac{l}{2}\right)_{\omega=0} = \frac{X_0 l}{2q} \tag{78}$$

58. In most practical cases interest is confined to *frequencies close to resonance.* For generality we give the equation in a form applicable to *overtones* as well as to the fundamental frequency. The overtone frequencies, in the ideal case of an infinitely thin rod here considered, are almost exactly integral multiples of the fundamental, the departure from true harmonic relation being due to the slight variation of velocity with frequency expressed in Eq. (65). This departure is so small in comparison with that due to the effect of cross section (§65) that it can usually be ignored. The resonant harmonic frequencies are then $f_{h0} = hf_0$, where $f_0 = c/2l$ is the fundamental frequency ($h = 1$) of the undamped bar and h is the order of the harmonic. As will be seen, f_{h0} is the frequency at which the *velocity* of particles in the rod is a maximum under forced vibrations. We have, from Eq. (65),

$$f_{h0} = \frac{\omega_{h0}}{2\pi} = hf_0 = \frac{hc}{2l} = \frac{h}{2l}\sqrt{\frac{q}{\rho}} \tag{79}$$

Under our present assumption that the rod is driven by a uniformly distributed stress, it is to be anticipated that large amplitudes at the ends can occur only for odd integral values of h.

For all values of h, the attenuation constant and logarithmic decrement may be written, from Eq. (67), as

$$\alpha_h = \delta_h f_h \tag{80}$$

Close to resonance we may write

$$\omega_h = \omega_{h0} - n_h \tag{81}$$

where n_h is a measure of the *dissonance* and $\omega_{h0} = 2\pi f_{h0} = h\omega_0$.

The longitudinal displacement at the end of the bar has large maxima at frequencies very close to odd integral values of h and is extremely small at even integral values of h. This fact is implicit in Eq. (77) and is brought clearly to light by making the following substitutions, valid in the neighborhood of all harmonic frequencies. We write

$$\omega \equiv \omega_h = h\omega_0 - n_h,$$

$\omega_0 = 2\pi f_0 = \pi c/l$, $\sin \omega l/c \approx (-1)^{h-1} n_h/2f_0 l$,

$$\tan \theta_h = -\frac{\sin \omega l/c}{\alpha_h l/c} \approx (-1)^h \frac{n_h}{\alpha_h},$$

and after the customary approximations for trigonometrical functions we find

For h odd,

$$-\xi\left(\frac{l}{2}\right) = \frac{2X_0c^2}{q\omega_h l} \frac{1}{\sqrt{\alpha_h^2 + n_h^2}} \sin(\omega_h t - \theta_h) \tag{82}$$

For h even,

$$-\xi\left(\frac{l}{2}\right) = \frac{X_0 l}{2q\omega_h} \sqrt{\alpha_h^2 + n_h^2} \sin(\omega_h t - \theta_h) \tag{83}$$

In writing the *maximum values* at frequencies close to harmonics, we may with sufficient accuracy set $h\omega_0$ in place of ω_h in the denominators of the equations above:

$$\xi_0\left(\frac{l}{2}\right) = \frac{-2X_0c^2}{qh\omega_0 l\sqrt{\alpha_h^2 + n_h^2}} = \frac{-2X_0c^2}{qh\omega_0 l\alpha_h} \cos\theta_h = \frac{-2X_0}{\rho h\omega_0 l\alpha_h} \cos\theta_h \; [h \text{ odd}] \tag{84}$$

$$\xi_0\left(\frac{l}{2}\right) = \frac{-X_0 l\sqrt{\alpha_h^2 + n_h^2}}{2qh\omega_0} = \frac{-X_0 l\alpha_h}{2qh\omega_0 \cos\theta_h} = \frac{-\pi^2 X_0 \alpha_h}{2\rho h l\omega_0^3 \cos\theta_h} \; [h \text{ even}] \tag{85}$$

In the absence of damping, the amplitude when $n_h = 0$ would become infinite for odd values of h and zero for even values, as is further explained in §61.

When h is odd, the amplitude $\xi_0(l/2)$ has its greatest value at a frequency $f_{ha} = \omega_{ha}/2\pi$, obtained by minimizing the product $\omega_h(\alpha_h^2 + n_h^2)^{\frac{1}{2}}$ in Eq. (82), it being remembered that $\omega_h = h\omega_0 - n_h$ and that $\alpha_h = \delta_h f_h$. To a high order of precision the result is

$$n_h \approx \frac{\alpha_h^2}{h\omega_0} \quad \text{and} \quad \omega_{ha} \approx h\omega_0\left(1 - \frac{\delta_h^2}{4\pi^2}\right) \tag{86}$$

At the fundamental frequency, $\omega_a = \omega_0(1 - \delta^2/4\pi^2)$. This expression for ω_a is similar to that for electric displacement-resonance in an oscillating electric circuit with L, C, and R in series, measured in terms of maximum voltage across the condenser as the frequency is varied.

The *velocity* of a particle at the end of the bar, for odd values of h, is the time derivative of Eq. (82):

$$v\left(\frac{l}{2}\right) = \omega_h \xi_0 \left(\frac{l}{2}\right) \cos(\omega_h t - \theta_h) \equiv v_0\left(\frac{l}{2}\right) \cos(\omega_h t - \theta_h) \tag{87}$$

where $v_0\left(\frac{l}{2}\right) = \frac{-2X_0c^2}{ql\sqrt{\alpha_h^2 + n_h^2}} = \frac{-2X_0}{\rho l \sqrt{\alpha_h^2 + n_h^2}} = \frac{-2X_0}{\rho l \alpha_h} \cos\theta_h = \omega_h \xi_0 \left(\frac{l}{2}\right)$ (88)

The velocity has its maximum value when $n_h = 0$. The angular velocity is then $\omega_{hv} = \omega_{h0}$, the same as for free vibrations in the absence of damping. Velocity resonance corresponds to *current resonance* in an oscillating circuit (§234).

When h is even, one finds from Eq. (83) for the maximum velocity in a cycle

$$v_0\left(\frac{l}{2}\right) = \frac{-X_0 l}{2q} \sqrt{\alpha_h^2 + n_h^2} \tag{89}$$

The mechanical impedances for h odd and even, as well as further analogies with electric resonance, are treated in §62.

For *damped free vibrations* at any harmonic frequency, the angular velocity ω_{hf} is found from Eq. (65):

$$c \approx \sqrt{\frac{q}{\rho}}\left(1 - \frac{\delta^2}{8\pi^2}\right)$$

Then

$$\omega_{hf} = \frac{\pi h c}{l} = \omega_{h0}\left(1 - \frac{\delta^2}{8\pi^2}\right) \tag{90}$$

This expression is similar to that for free oscillations in a series electric circuit with L, C, and R.

59. *Summary of the Critical Frequencies of a Thin Bar.* From the foregoing equations it is seen that the frequency f_{h0} of free vibrations in the absence of damping is the same as f_{hv} for velocity resonance. The expressions for the frequency f_{ha} for amplitude resonance and for f_{hf} in the case of free damped vibrations are given below.

$$f_{h0} = f_{hv} = \frac{hc}{2l} = \frac{h}{2l}\sqrt{\frac{q}{\rho}} \tag{91}$$

$$f_{ha} = f_{h0}\left(1 - \frac{\delta^2}{4\pi^2}\right) \tag{92}$$

$$f_{hf} = f_{h0}\left(1 - \frac{\delta^2}{8\pi^2}\right) \tag{93}$$

These expressions are applicable to all types of vibration in which the frequency is associated with a definite wave velocity. f_{hf} and f_{ha} converge upon f_{h0} as the damping approaches zero.

It will be observed that these three frequencies are approximately *equally spaced:*

$$f_{h0} - f_{hf} \approx f_{hf} - f_{h\alpha} \approx \frac{\delta^2}{8\pi^2} = \frac{1}{8Q^2} \tag{94}$$

For all resonators of low damping these differences are extremely small, measurable only by methods of high precision. The frequency usually observed by electrical measurements on piezoelectric resonators is f_0 (or f_{h0}), modified somewhat by the parallel capacitance of the resonator, as explained in §275.

60. *Relation between Mechanical Wavelength and Length of Bar.* It is characteristic of longitudinal vibrations in bars, as in the analogous electrical case of transmission lines containing uniformly distributed resistance, inductance, and capacitance, that with forced vibrations at any given frequency the distributions of displacement and of strain along the rod at any given instant are very nearly sinusoidal, becoming strictly sinusoidal in the absence of damping. This fact is readily shown for the case of *negligible damping* by setting $\alpha = 0$ in Eq. (75). This equation then gives the amplitude of mechanical displacement at any x directly:

$$-\xi_0(x) = -A(x) = \frac{X_0 c}{q\omega \cos \dfrac{\omega l}{2c}} \sin \frac{\omega x}{c} = -\xi_0\left(\frac{l}{2}\right) \sin \frac{2\pi x}{\lambda} \tag{95}$$

where the mechanical wavelength is $\lambda = c/f$ and $\xi_0(l/2)$ is the amplitude at the ends of the bar.

The amplitude of the *strain* at any x is found from Eq. (95):

$$x_{x0}(x) = \frac{\partial \xi_0(x)}{\partial x} = \frac{2\pi}{\lambda} \xi_0\left(\frac{l}{2}\right) \cos \frac{2\pi x}{\lambda} \tag{96}$$

At the fundamental resonant frequency, $\lambda = 2l$, so that the last equation may be written

$$x_{x0}(x) = \frac{\pi}{l} \xi_0\left(\frac{l}{2}\right) \cos \frac{\pi x}{l} \tag{97}$$

This expression gives the sinusoidal distribution of strain at resonance in the absence of damping. For the strain in a damped bar see §230.

According to Eq. (96) the strain at the ends of the rod vanishes at the frequency of resonance, *i.e.*, when l is an integral multiple of $\lambda/2$. This is for zero damping; if the damping terms in Eq. (75) were retained it would be found that $\xi_0(l/2)$ remained always different from zero and that there was no frequency at which the strain at the ends of the rod quite vanished.

The relation between the displacement ξ and length of rod l is shown in Fig. 19, in which a fixed frequency is assumed, corresponding to a fixed wavelength λ along the X-axis. Rods are pictured having the

lengths aa' and bb'. In the case of aa' the length is so short in comparison with $\lambda/2$ that the distribution of displacement is almost linear, showing that at relatively low frequencies the deformation of the rod approximates that caused by a static stress. On the other hand, rod bb' is considerably longer than $\lambda/2$, and the displacement has a maximum value at a certain distance from each end.

When the length of the rod is an odd multiple of $\lambda/2$, the condition is that of resonance. Since the amplitude then depends primarily on the damping, Eqs. (95) and (96) are no longer valid. Nevertheless, when the damping is small the strain at the ends of the rod is exceedingly small, and the form of the displacement curve is almost exactly that of a sine wave, with greatest value at the ends of the rod, diminishing sinusoidally to zero at the center, as represented, for the fundamental frequency, by

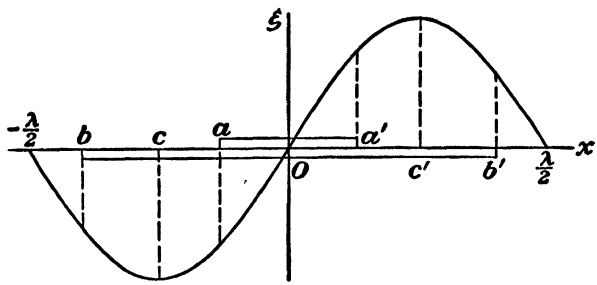


FIG. 19.—Relation between length of rod and distribution of mechanical displacement.

the range from c to c' in Fig. 19. In most piezoelectric resonators the resonance is so sharp and the variation in frequency that ordinarily need be considered is so small that within this range, so far as the distribution of displacement and strain is concerned, we may write $\lambda \approx 2l$, or, for overtone h, $\lambda \approx 2l/h$. From this it follows that, close to resonance, the sinusoidal distribution represented by the equation

$$\xi(x) = \xi\left(\frac{l}{2}\right) \sin \frac{\pi x h}{l} \tag{98}$$

holds to a high degree of precision. We shall make use of this relation in later paragraphs.

61. *Resonator Amplitudes for Wide Ranges of Frequency.* It is sometimes desirable to study the reaction of a piezoelectric resonator upon the electric circuit over a range of frequencies too wide for sufficiently accurate calculation in terms of the simple equivalent electrical network discussed in Chap. XIV. We therefore require a formula that is at least approximately correct over any desired range. So far as the purely elastic side of the problem is concerned, such a formula is given in Eq. (77),

but this is too cumbersome to be used conveniently. For most purposes the problem is treated with sufficient accuracy by solving for the resonant and non-resonant conditions separately. We first solve Eq. (77) for frequencies well removed from resonance, the damping terms being ignored [or we may set $x = l/2$ in Eq. (95)]; and second we solve Eq. (84) for the resonance frequencies themselves ($\cos \theta_h = 1$). We write $\omega = h\omega_0$, where ω_0 refers to the fundamental frequency and where h may have fractional as well as odd or even integral values. Then, noting that $\omega l/c = \pi h$, and that $\sin(\omega l/c) = 2 \sin(\omega l/2c) \cos(\omega l/2c)$, we find for the maximum value of the displacement in the first case (non-integral values of h)

$$-\xi_0\left(\frac{l}{2}\right) = -A\left(\frac{l}{2}\right) = \frac{X_0 l}{\pi h q} \tan\frac{\pi h}{2} \tag{99}$$

and in the second case ($h = 1, 3, 5, \ldots$)

$$-\xi_0\left(\frac{l}{2}\right) = -A\left(\frac{l}{2}\right) = \frac{4X_0 l^2}{\pi^3 h^3 c F} = \frac{2X_0}{\pi \rho c h \alpha_h} \tag{100}$$

If the frictional coefficient F were a constant independent of frequency the amplitude at harmonic h would be only $1/h^3$ as great as for the fundamental. In practical resonators the damping may be due to so many causes that it is better to use the last expression in Eq. (100), in which the damping factor α_h can be found experimentally at any frequency. Since there is experimental evidence (§296) that α_h increases with frequency, it can at least be said that with increasing order of harmonic the amplitude decreases proportionally to a power of h greater than unity.

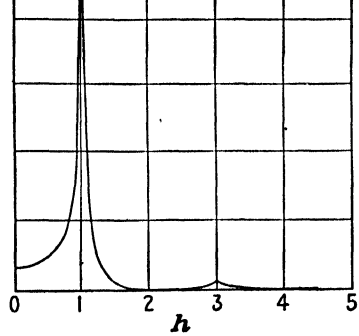


FIG. 20.—Maximum displacement at the end of a longitudinally vibrating rod, in terms of frequency. $h = f_h/f_1$, where f_h is any frequency, and f_1 is the fundamental frequency.

In schematic form the maximum displacements at $l/2$ are shown in Fig. 20 as functions of h, the driving force having constant amplitude. The exact form of the curve and, in particular, the height and sharpness of the resonance peaks depend of course upon the values of l, c, q, and F. The value at $\omega = 0$ can be calculated from Eq. (78). In Fig. 20, F is considered constant.

It remains to add a word concerning *even* values of h (see also §63). From Eq. (85) or (99) it is found that the amplitude $A(l/2)$ is zero when ω

is an even multiple of ω_0, as long as damping is neglected. By symmetry there are also $h - 1$ nodes of motion at intermediate points, between which the rod is in a state of forced vibration when periodic forces are applied at the ends. For example, the amplitude of the second harmonic is found by setting $x = l/4$ and $\omega = 2\omega_0$ in Eq. (75); $A(l/4) = -X_0 c/q\omega$. There is no resonance, since the strain at each end is limited, the value being $x_x(l/2) = -X/q$. There is also no external piezoelectric reaction due to longitudinal deformations when rods with full-length electrodes are excited at an even multiple of the fundamental frequency, since the effects of compressions and extensions in the various segments cancel exactly.*

62. *Equivalent Resonating System with a Single Degree of Freedom.* When any feebly damped mechanical system that has many degrees of freedom vibrates at or near one of its normal modes, it is sometimes advantageous to deal with vibrational problems in terms of an equivalent system having a single degree of freedom.[92] One may, for example, visualize as the equivalent system a mass at the end of a weightless spring, subject to a small frictional drag. It was the device of a simplified equivalent vibrating system that led the way to the representation of the piezoelectric resonator by certain equivalent *electrical* constants.

Whatever the type of vibrator may be, the selection of the three equivalent constants for the single-degree system is determined by the condition that at every instant the kinetic energies of the two systems must be the same. That is, the systems must agree in amplitude, phase, and decrement. This condition leaves us free to choose arbitrarily either the equivalent mass M, assumed concentrated at a point (or more generally the equivalent coefficient of inertia), or the coordinate that determines the motion of M. Usually the motion of the concentrated mass is taken as identical with the motion of that region on the boundary of the actual vibrator where the driving mechanical force is assumed to be applied. By this convention the value of M then becomes determined.

The present problem is to determine the equivalent mass, stiffness, and frictional coefficient for the case of a longitudinally vibrating rod. The fundamental frequency will be considered first. The concentrated mass M is assumed to undergo the same motion as a point at the end of the rod. The condition of equality of kinetic energies leads to the assignment to M of half the actual mass of the rod, or $M = \frac{1}{2}\rho ble$, where b, l, e are, respectively, the breath, length, and thickness.† The equivalent stiffness is defined by $G = M\omega_0^2 = \pi^2 beq/2l$, and the frictional coefficient

* Nevertheless, if the impressed frequency is lower than the resonant frequencies of *lateral* vibrational modes, there can still be a piezoelectric contribution to the polarization, as explained in §229.

† See, for example, H. Lamb, ref. B33, p. 13.

W, from Eqs. (64) and (67), by $\delta = 2\pi^2 F/\rho\lambda^2 f = W/2fM$. M, W, and G correspond to L, R, and $1/C$ in a series electric circuit having lumped, as contrasted with distributed, constants.

The equation of motion is

$$M\ddot{\xi} + W\xi + G\xi = \Phi_0 \cos \omega t \tag{101}$$

where ξ is written for $\xi(l/2)$, the displacement at the end of the rod, and Φ_0 is the maximum value of the force that acts on the equivalent mass M.

The steady-state solution of (101) is

$$\xi = \xi_0 \sin (\omega t - \theta) \tag{102}$$

in which the maximum displacement is

$$\xi_0 = \frac{\Phi_0}{\omega\sqrt{W^2 + \left(\omega M - \dfrac{G}{\omega}\right)^2}} = \frac{\Phi_0}{\omega W}\cos\theta \tag{103}$$

and

$$\tan\theta = \frac{\omega M - G/\omega}{W} = -\frac{2\pi n}{\omega_0\delta} = -\frac{n}{\alpha} \tag{104}$$

As previously, $n = \omega_0 - \omega$, and $\delta = W/2fM \approx W/2f_0M$. The *mechanical reactance* is

$$X_c = \omega M - \frac{G}{\omega} \approx -2Mn \tag{105}$$

From the foregoing equation for W, together with Eq. (67), the *mechanical resistance* may be expressed as

$$W = \frac{\rho bec\delta}{2} = \frac{\pi\rho bec}{2Q} = 2M\alpha \tag{106}$$

The *mechanical impedance* is given by

$$Z_c^2 = W^2 + X_c^2 = W^2 + \left(\omega M - \frac{G}{\omega}\right)^2 = 4M^2(\alpha^2 + n^2) \tag{107}$$

On comparing Eq. (84) with (103) one sees that the conditions for identity of the distributed-constant system with its equivalent lumped-constant system are fulfilled. Equality of damping is ensured through the definition of W, and identity of phase from the definition of $\tan\theta$. Equality of amplitude is attained by setting $\Phi_0 = -2X_0be$.

Derivations of equations for the longitudinal vibrations of damped rods, leading to results similar to the foregoing, have also been given by Vigoureux[B50,B51,567] and by Laue[309] (see §242).

63. *Equivalent Lumped Mechanical Constants for a Bar Vibrating in Harmonics.* We consider first the case in which the periodic driving stress is uniform throughout the

bar. For all values of h the effective driving force is $\Phi = -2X_0be$, just as at the fundamental frequency. The bar may be treated as consisting of h segments in series, for each of which we may write $M_1 = \rho lbe/2h$, $G_1 = M_1\omega_0^2h^2 = hG$, where G has the value given above for the fundamental frequency of the entire bar. $W_1 = 2\alpha_1 M_1$, where α_1 is the damping constant for a single segment.

As in §58, the solutions for odd and even values of h must be treated separately. *When h is odd,* the effective mass for the complete bar is $M_h = hM_1 = \rho lbe/2 = M$; $G_h = \omega_h^2 M_h = hG_1 = h^2G = \pi^2 qbeh^2/2l$; $\alpha_h = W_h/2M_h$, whence $W_h = 2M\alpha_h$. The mechanical impedance is

$$Z_h = (W_h^2 + X_h^2)^{\frac{1}{2}} = 2M(\alpha_h^2 + n_h^2)^{\frac{1}{2}} \tag{108}$$

where

$$X_h = \omega_h M_h - \frac{G_h}{\omega_h} \approx 2M_h(\omega_h - h\omega_0) = -2Mn_h \tag{109}$$

By analogy with the alternating-current (a-c) equation $I = V/Z$, one would expect to find for the velocity at $l/2$ the value $v_0(l/2) = \Phi/Z_h$. In fact, Eq. (88) for v_0 can be reduced to exactly this form through the use of the foregoing expressions. As in the case of a series resonant electric circuit, Z_h has its minimum value at the resonant frequency for which $n_h = 0$.

The situation is quite different *when h is even.* There is then destructive interference (180° phase difference) between adjacent segments of the bar. An electrical analogy is the 180° phase difference between the inductive and capacitive branches of a parallel (antiresonant) circuit. The current has a minimum value at resonance, analogous to the minimum in $v_0(l/2)$ according to Eq. (89).

In the foregoing discussion it has been assumed that the mechanical driving stress was applied uniformly throughout the rod, from $-l/2$ to $+l/2$. We may anticipate the results of the following section by remarking that, if the stress is applied from $(l/2 - l/h)$ to $l/2$ (or if it is applied to any other single one of the h segments), then when h is even the destructive interference between segments is eliminated and a *maximum* in velocity occurs at resonance. For application to the piezo resonator see §238.

64. *Rods Driven by Forces Applied Locally.* Rod-shaped piezoelectric resonators are sometimes excited by the use of electrodes covering only a portion of the length, as indicated in Fig. 21. The purely elastic part of the problem of determining the amplitude at any frequency can be solved approximately by assuming a uniformly distributed stress from x_1 to x_2 or its equivalent, *viz.*, a force $X = X_0 \cos \omega t$ per unit area of cross section, applied at x_1, and an equal and opposite force at x_2. We consider first only the frequency region close to the fundamental and omit the subscript h. The excitation of overtone frequencies is discussed in §238.

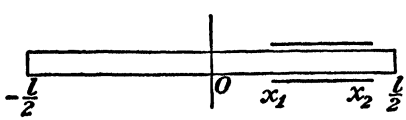


FIG. 21.—Rod maintained in longitudinal vibration by equal and opposite periodic forces at x_1 and x_2.

An approximate solution can be reached by several routes:

1. By first deriving an expression for $\xi(l/2)$ when the applied forces are symmetrically situated at $\pm l'/2$, where $l' < l$. The solution for $l' = \pm x_1$ is then subtracted from that for $l' = \pm x_2$. The final value of

$\xi(l/2)$ is half of this difference and is identical with that derived by method 2.

2. On the assumption that $l = \lambda/2$ and that the strain is sinusoidally distributed, an expression can be derived for the average input of power to the rod in terms of X_0 and $\xi_0(l/2)_{1,2}$ where the latter quantity denotes the maximum displacement at $x = l/2$ when the forces are applied at x_1 and x_2. The average power is found to be $P = \omega\xi_0(l/2)_{1,2} X_0 S_{12} \cos\theta$, where $S_{12} \equiv \frac{1}{2}\left(\sin\frac{\pi x_2}{l} - \sin\frac{\pi x_1}{l}\right)$, and θ has the value in §57. A second expression for P is then derived representing the expenditure of energy in the rod, *viz.*, $P = \omega^4 l F \xi_0^2(l/2)_{1,2}/4c^2$. Upon equating these values of P one obtains $\xi_0(l/2)_{1,2} = 4lX_0S_{12} \cos\theta/\pi^2\omega F$. If, as formerly, $\xi_0(l/2)$ denotes the displacement at $l/2$ when the driving forces are at the ends, we find for the instantaneous displacement at $l/2$ with forces at x_1 and x_2 the equation

$$\xi(l/2)_{1,2} = \xi_0(l/2)_{1,2} \sin(\omega t - \theta) = S_{12}\xi_0(l/2) \sin(\omega t - \theta) \quad (110)$$

The reduction in amplitude caused by driving the rod at points not at the ends is thus expressed by the factor S_{12}. When x_1 and x_2 are at the ends, $S_{12} = 1$ and the equation becomes identical with (82). When x_1 and x_2 are symmetrically placed, so that $x_1 = -x_2$, $S_{12} = \sin \pi x_1/l$.

3. A more rigorous treatment takes account of the fact that in a piezoelectric resonator the wave velocity in the portion of the rod between the electrodes is less than in the exposed parts (§241). Two different values of Young's modulus must therefore be included in the corresponding elastic problem. The rod has to be divided into three regimes, *viz.*, from $-l/2$ to x_1, from x_1 to x_2, and from x_2 to $+l/2$. At x_1 and x_2 the medium undergoes a discontinuous change in elastic constant and in strain, but the stress is continuous. The method of attack is analogous to that discussed by Mason,[B35,335] by Quimby,* and by Crandall.[B9] The author has derived the equation for the motion of the rod, but the form is too complicated to make the plotting of a resonance curve at all convenient. Moreover, the velocities in the three regimes are so nearly equal, at least in the case of quartz, that the result differs but little numerically from that given in Eq. (110). It need only be stated that the resonance frequency, defined for a homogeneous rod by $1/f_0 = 2l/c$, is given by the following equation when account is taken of the change in elasticity at x_1 and x_2:

$$\frac{1}{2f_0} = \frac{l'}{c} + \frac{l - l'}{c'} \quad (111)$$

where $l' = x_2 - x_1$, c = velocity between x_1 and x_2, and c_1 = velocity outside of this region.

* S. L. QUIMBY, *Phys. Rev.*, vol. 25, pp. 558–573, 1925.

65. *Effect of Cross Section on Frequency of Rods.* Rayleigh's well-known equation for the frequency of longitudinal vibration of an isotropic cylindrical rod of length l, radius $r(r << l)$, Poisson's ratio σ, gives, to the first approximation,

$$f_h = \frac{1}{2l}\sqrt{\frac{q}{\rho}}\left(1 + \frac{h^2\sigma^2\pi^2}{4l^2}\right)^{-1} \tag{112}$$

h being the order of the overtone. For example, if $\sigma = \frac{1}{3}$ and $l = 4r$, the frequency is about 2 per cent less than if the radius were negligible.

With other than circular cross sections and with anisotropic mediums the obstacles in the way of theoretical formulation multiply, but the order of magnitude of the correction is not very different from that indicated above. For isotropic bars of rectangular section (length l, breadth b, thickness e), the following equation is given by Giebe and Scheibe:[171]

$$f_h = \frac{hf_1}{\sqrt{1 + \frac{1}{3}\sigma^2\left(\frac{b^2 + e^2}{4}\right)\frac{\pi^2h^2}{l^2}}} \approx \frac{hf_1}{1 + \frac{\pi^2h^2\sigma^2(b^2 + e^2)}{24l^2}} \tag{113}$$

where f_1 is the fundamental frequency. These authors find that (113) fails to give values in agreement with experiment for quartz bars. Their experimental and theoretical investigations are treated in Chap. XVII.

The effect of cross section on longitudinal vibrations has also been treated by Ruedy.*

The basic equations from which the effect of lateral inertia on the longitudinal frequency of rectangular crystal bars in any orientation can be found have been derived by R. M. Davies.[120] The only application made by Davies is to bars from crystals of Group III (Rochelle salt), the length l of any given bar bisecting the angle between two of the crystal axes and the dimension e being perpendicular to both these axes. He finds the corrected frequency f_h for overtone h to be given (in the notation of the present section) by an equation of the form

$$\frac{(f_h)_0 - f_h}{(f_h)_0} = \frac{\pi^2h^2}{24s'^2_{22}l^2}[(s'^2_{32} + s'^2_{42})b^2 + s'^2_{12}e^2] \tag{114}$$

where $(f_h)_0$ is the frequency for a bar of negligible cross section and b is the third dimension of the bar, which may be greater or less than e. The subscripts in Eq. (114) are for a bar having its b, l, and e dimensions

* R. Ruedy, *Can. Jour. Research*, A, vol. 14, pp. 66–70, 1936.

parallel, respectively, to the Z'-, Y'-, and X-axes. Bars of this type are called elsewhere in this book the "$X45°$-cut." The transformed axes are obtained from the matrix in §41 by setting $\alpha_1 = 1$,

$$\beta_1 = \gamma_1 = \alpha_2 = \alpha_3 = 0, \qquad \beta_2 = \beta_3 = \gamma_3 = 1/\sqrt{2}, \qquad \gamma_2 = -1/\sqrt{2}.$$

The expressions for the elastic coefficients are given in Eqs. (43).

By analogous axial transformations the equations for $Y45°$- and $Z45°$-bars may be obtained. More simply, they are derived directly from (114) by permuting the subscripts according to the rule following Eqs. (31) in §42.

For an $X45°$-bar of square cross section, with $b = e = l/4$, the correction given by Eq. (114) amounts to about 2 per cent. If $b = e = l/6$, the corrections for $h = 1$, 2, 3, and 4 are roughly 1, 4, 8, and 14 per cent.

For the effect of cross section on quartz resonators, in which there are pronounced departures from the Rayleigh correction, see §349.

66. Thickness Vibrations in Crystal Plates. The general theory will now be outlined. Later, in §§93 and 253, the application of the theory to special problems will be considered.

The following paragraphs have to do primarily with plates of *infinite area*, in which the same motions are shared by all particles having the same coordinate in the direction of the normal. It is strictly not enough to specify that the lateral dimensions shall be *great* in comparison with the thickness. When the plate is finite, coupling effects between various vibrational modes distort the wave front. Attention will be paid in Chap. XVII to these coupling effects. In any event it is important to study the nature of the vibrations in the ideal case. For the application to the piezo resonator see §243.

For *isotropic solids* the velocity of compressional waves is

$$\sqrt{\frac{(\lambda + 2n)}{\rho}} = \sqrt{\frac{c}{\rho}},$$

the elastic constants λ, n, and c having the meaning indicated in §31. The velocity of transverse waves (waves of distortion) is $\sqrt{n/\rho}$. From the matrices of the crystal groups in §29 one might infer that the same equations held for crystals, on substituting the appropriate c_{hh} for c and n. This statement is hardly a rigorous proof, and indeed it is not generally true; moreover it fails to indicate the direction of vibration for transverse waves.

The general theory of the propagation of plane waves in anisotropic mediums, of which the foregoing equations are particular cases, was

first given by Green.* He showed that for any direction of propagation there are in general three possible types of wave, each with a different velocity, the three vibration directions being mutually perpendicular.

67. The form of the theory now to be considered is due to Christoffel.† Calling l, m, n the direction cosines of the normal to the plane wave surface and s the distance of this surface from an arbitrary origin, we have $s = lx + my + nz$. The displacement of a point on the surface from its normal position is ξ, with components u, v, w and direction cosines α, β, γ, so that $\xi = \alpha u + \beta v + \gamma w$.

The general equations of motion, analogous to (61) in the absence of damping, are

$$-\rho \frac{\partial^2 u}{\partial t^2} = \frac{\partial X_x}{\partial x} + \frac{\partial X_y}{\partial y} + \frac{\partial X_z}{\partial z} \tag{115}$$

with similar expressions for v and w.

Christoffel shows that these equations can be written in terms of u, v, w, and s instead of stress, by introducing new moduli $\Gamma_{11} \cdots \Gamma_{33}$, which are functions of the elastic constants c_{hk} and of l, m, n. Equation (115) then becomes

$$\begin{aligned}
\rho \frac{\partial^2 u}{\partial t^2} &= \Gamma_{11} \frac{\partial^2 u}{\partial s^2} + \Gamma_{12} \frac{\partial^2 v}{\partial s^2} + \Gamma_{13} \frac{\partial^2 w}{\partial s^2} \\
\rho \frac{\partial^2 v}{\partial t^2} &= \Gamma_{12} \frac{\partial^2 u}{\partial s^2} + \Gamma_{22} \frac{\partial^2 v}{\partial s^2} + \Gamma_{23} \frac{\partial^2 w}{\partial s^2} \\
\rho \frac{\partial^2 w}{\partial t^2} &= \Gamma_{13} \frac{\partial^2 u}{\partial s^2} + \Gamma_{23} \frac{\partial^2 v}{\partial s^2} + \Gamma_{33} \frac{\partial^2 w}{\partial s^2}
\end{aligned}$$

where‡ $\Gamma_{12} = \Gamma_{21}$, $\Gamma_{13} = \Gamma_{31}$, $\Gamma_{23} = \Gamma_{32}$, and

* G. GREEN, "Mathematical Papers," London, 1871. See also Lord Kelvin's "Baltimore Lectures," London, 1904.

† E. W. CHRISTOFFEL, *Annali di matematica pura ed applicata*, series II, vol. 8, p. 193, 1877. Christoffel's method was applied to the piezo resonator by Koga[270,271] and later by Mason,[338] Bechmann,[32,39] and Atanasoff and Hart.[12] See also Love, ref. B34, p. 298.

‡ The six moduli $\Gamma_{11} \ldots \Gamma_{33}$ correspond to the six types of strain that can be present in thickness vibrations. They are as follows: one strain of type L shown in Fig. 15 (p. 56), *viz.*, a compression normal to the surface of the plate; two strains of type T'; two of type S; and one of type S'. All other strain components are prohibited by lateral inertia. As an illustration consider an X-cut, for which $l = 1$, $m = n = 0$. The Γ are then reduced to the six fundamental constants c_{11}, c_{66}, c_{55}, c_{56}, c_{15}, and c_{16}, which will be recognized as belonging to the types mentioned above. The last three of these c are the cross constants corresponding to the first three. For an X-cut these are the only fundamental constants that play a part in thickness vibrations. Analogous statements may be made concerning other cuts, including those in oblique directions.

$$\left.\begin{aligned}
\Gamma_{11} &= l^2c_{11} + m^2c_{66} + n^2c_{55} + 2mnc_{56} + 2nlc_{51} + 2lmc_{16} \\
\Gamma_{22} &= l^2c_{66} + m^2c_{22} + n^2c_{44} + 2mnc_{24} + 2nlc_{46} + 2lmc_{26} \\
\Gamma_{33} &= l^2c_{55} + m^2c_{44} + n^2c_{33} + 2mnc_{34} + 2nlc_{35} + 2lmc_{45} \\
\Gamma_{23} &= l^2c_{56} + m^2c_{24} + n^2c_{34} + mn(c_{23} + c_{44}) + nl(c_{45} + c_{36}) \\
&\qquad + lm(c_{46} + c_{25}) \\
\Gamma_{31} &= l^2c_{15} + m^2c_{46} + n^2c_{35} + mn(c_{45} + c_{36}) + nl(c_{31} + c_{55}) \\
&\qquad + lm(c_{56} + c_{14}) \\
\Gamma_{12} &= l^2c_{16} + m^2c_{26} + n^2c_{45} + mn(c_{46} + c_{25}) + nl(c_{56} + c_{14}) \\
&\qquad + lm(c_{12} + c_{66})
\end{aligned}\right\} \tag{116}$$

The quantity sought is the stiffness factor q for insertion in Eq. (59). It enters the scene in the following secular equations, which, as shown by Christoffel, give the relations between stiffness, direction cosines, and Γ_{hk}:

$$\left.\begin{aligned}
\alpha\Gamma_{11} + \beta\Gamma_{12} + \gamma\Gamma_{13} &= \alpha q \\
\alpha\Gamma_{12} + \beta\Gamma_{22} + \gamma\Gamma_{23} &= \beta q \\
\alpha\Gamma_{13} + \beta\Gamma_{23} + \gamma\Gamma_{33} &= \gamma q
\end{aligned}\right\} \tag{117}$$

The values of q for quartz and Rochelle salt, derived from the solution of (117), are treated later.

There are three possible values of q, all of which are real; they are the roots q_1, q_2, q_3 of the cubic equation, expressed in terms of known quantities:

$$\begin{vmatrix}
\Gamma_{11} - q & \Gamma_{12} & \Gamma_{13} \\
\Gamma_{12} & \Gamma_{22} - q & \Gamma_{23} \\
\Gamma_{13} & \Gamma_{23} & \Gamma_{33} - q
\end{vmatrix} = 0 \tag{118}$$

To each of these roots corresponds a different set of values for α, β, γ, and hence a different direction for the displacement ξ. The three vibration directions are found from Eqs. (117).

When plane waves corresponding to one of the roots of Eq. (118) are propagated at a resonant frequency in a plane-parallel crystal plate of infinite area, in the direction of the normal to the plate, a condition to be satisfied at the surfaces is that the strain $\partial\xi/\partial s = 0$. For each root a system of stationary waves is theoretically possible for a crystal plate in any orientation, at a fundamental thickness frequency or at any overtone. Such vibrations can be realized in those cases where the piezoelectric properties of the crystal are such that the strain $\partial\xi/\partial s$ can be piezoelectrically produced.

Any one of the three roots of Eq. (118), say q_m, can be used in the fundamental wave equation

$$\rho\frac{\partial^2\xi}{\partial t^2} = q_m\frac{\partial^2\xi}{\partial s^2} \tag{119}$$

from which follows, in the usual manner, for the normal frequencies of a plane-parallel plate, with vibrations propagated in the direction of the thickness e, the formula

$$f_{hm} = \frac{h}{2e}\sqrt{\frac{q_m}{\rho}} \tag{120}$$

where h is the order of the harmonic.

When Eqs. (117) are solved for α, β, and γ, it is found in the general case that each of the three displacements, which we shall call ξ_1, ξ_2, ξ_3, has components both normal and parallel to the surfaces of the plate, so that no one of the waves is purely compressional or purely transverse. It is only in isotropic solids and in certain special cases in crystals that one of the three waves is strictly longitudinal and the other two strictly transverse. If the substance is isotropic, the velocities of the two transverse waves coincide and the transverse vibratory motion can have any direction whatever in the wave front, while the third wave is compressional, with displacements normal to the wave front. The general condition that one vibration direction shall be normal to the surface (compressional wave) is that $\alpha = l, \beta = m, \gamma = n$. For a vibration direction to lie *in* the surface the condition to be satisfied is $\alpha l + \beta m + \gamma n = 0$.

Elastic vibrations of the transverse type in solids are often called *shear vibrations*.

68. The Christoffel theory has been applied in the determination of vibration directions and frequencies, as well as of elastic constants, in plates of quartz, tourmaline, and Rochelle salt. The excitation takes place piezoelectrically, the plate being placed between plane-parallel electrodes that are connected to a source of alternating current of the right frequency for producing resonant vibrations. It is possible to excite any one of the three vibration modes that involves a strain capable of being caused piezoelectrically by an electric field; the latter is usually normal to the plate. The criterion can also be expressed thus: The vibrational deformation must be such as to produce a piezoelectric polarization in the direction of the driving field. Obviously, the essential question in any particular instance is whether there is a piezoelectric coefficient satisfying this condition. Examples are considered in §§351 following and §378.

In the precise measurement of elastic constants by means of thickness vibrations it is desirable to use h-f overtones rather than the fundamental vibration. This fact has recently been made evident in the case of quartz by Atanasoff and Hart,[12] who point out that at high harmonic frequencies the effects of gap, boundary conditions, and coupling between different modes are eliminated. The procedure for deriving the elastic constants from observational data is described in §§93 and 252.

The elastic properties of a non-piezoelectric solid can be studied experimentally by cementing to a flat face of the solid a plate of piezoelectric crystal. High-frequency compressional or transverse waves generated in the crystal can then be propagated in the solid, as described in §512 below.*

69. In the days when light was treated as waves in an elastic solid, the two transverse waves mentioned above became the two waves of polarized light in crystals. In isotropic media the two waves had the same velocity, the vibration direction could have any orientation in the wave front, and hence the medium exerted no polarizing effect. Compressional waves were removed from the discussion by conferring on the ether such properties that their velocity was either infinite or zero.

Even with the acceptance of the electromagnetic theory of light, the analogy with elastic waves still remains valid. It is not inappropriate, for example, to regard the two transverse waves in crystals, each with its own velocity, as an instance of elastic double refraction. Elastic wave propagation in crystals, however, is more complicated than the propagation of optical waves. This is partly due to the presence of the compressional wave, so that in all there are three wave surfaces to consider as against two in optics; and in addition there is the fact that, while three parameters (the principal refractive indices mentioned in §528) suffice to describe the optical properties of crystals, the number of elastic parameters in crystals, for the general case, is much greater. That is, there is in general no unique elastic ellipsoid in terms of which the wave velocities in all directions can be expressed† (§527). All 21 elastic constants play a part in determining the velocity. In all crystals except those of lowest symmetry, special wave directions can, however, be found for which certain constants or groups of constants are zero; as has been stated, use is made of this fact in certain oblique cuts in quartz.

One respect in which elastic waves are somewhat simpler than optical waves is dispersion. The only effect of frequency upon wave velocity, at least so far as mechanical waves of ordinary frequencies are concerned, is an extremely small diminution with increasing frequency due to friction, as indicated by Eq. (65). Molecular friction or viscosity plays a part in optics, but in a quite different manner, namely, in causing anomalous dispersion.

70. *Damped Thickness Vibrations.* The theory of the piezoelectrically driven resonator vibrating in a thickness mode, with due regard to damping, overtones, space between crystal and electrodes, and the effect of piezoelectric reaction on the elastic constant, is given in Chap. XIII. For the present it is necessary only to indicate briefly how the equations

* The fact that elastic waves in crystals can be propagated in a given direction with any one of three different velocities finds an interesting application in explaining the modified lines that are observed in the spectrum of light scattered while passing through a quartz crystal. This effect was found by E. Gross (*Compt. rend. acad. sci. U.R.S.S.*, vol. 18, p. 93, 1938), who thinks it due to local variations in the index of refraction caused by strains accompanying heat waves, according to the theory of Debye.

† Nevertheless, corresponding to any given direction of the wave normal there is a certain ellipsoid, the principal axes of which give the vibration directions and velocities of the three elastic waves (G. Green, reference on p. 104; Love, ref. B34, p. 299).

for longitudinal vibrations in damped bars may be adapted to the treatment of thickness vibrations of plates. This purely elastic theory will then serve as the basis for the later discussion.

When applied to thickness vibrations, Eq. (61) assumes the form

$$\rho \frac{\partial^2 \xi}{\partial t^2} = q_m \frac{\partial^2 \xi}{\partial x^2} + F \frac{\partial^3 \xi}{\partial x^2 \partial t} \tag{121}$$

in which the displacement ξ may make any angle with the plane of the plate and x represents the distance parallel to the thickness dimension e (the s-direction in §67) from the nodal plane at the center of the plate. q_m is the stiffness coefficient corresponding to the particular type of thickness vibration [see Eq. (119)].

Since the theory of thickness vibrations in damped plates runs exactly parallel to that for lengthwise vibrations in rods, it is unnecessary to repeat it. Just as in our theory of rods we have disregarded the effects of cross section, so here the assumption of plates of infinite area disposes of the complication due to boundary conditions. When applied to actual plates of relatively large area, the theory is still accurate enough to be of great usefulness, yielding frequencies that agree with observation to the order of 1 per cent.

Most of the equations and discussion in §§56 to 63 apply equally to plates, provided that the symbols l and e (length and thickness) are interchanged (see, for example, §254).

When thickness vibrations are used for the stabilization of radio frequencies, the lowest, or fundamental, mode is commonly used. Plates vibrating in high overtones have also recently found an important application as h-f oscillators. In crystal oscillators for the production of ultrasonic waves it is common practice to employ high overtones of compressional thickness vibrations. In the case of piezoelectrically driven plates only odd harmonics can be excited.

71. *Conservation of Angular Momentum in Shear Vibrations.* The following remarks are applicable to all shear vibrations, whether of the thickness type, in which the plane of shear is at right angles to the major surfaces of the plate, or of the "contour" type, in which the shear is in the plane of the plate.

A circumstance that must not be overlooked when plates of finite area are vibrating in a shear mode is the principle of *conservation of angular momentum.* A shearing strain involves rotation of linear elements in the crystal about a certain axis. If the vibrating plate is free, a compensating periodic rotation of the body as a whole must take place, in order to keep the total angular momentum zero. With increasing lateral dimensions the moment of inertia of the plate increases; hence, the amplitude of angular movement of the plate as a whole diminishes,

approaches zero as the area becomes indefinitely large. Thus, it is only with plates of relatively great area (if vibrating with perfect freedom) that the two major surfaces remain so fixed in orientation that the instantaneous deformation is a simple shear.

Under a static shearing stress the rectangular section $ABCD$ of a flat plate, shown in Fig. 22*a*, would become deformed into the parallelogram $A'B'C'D'$ or $A''B''C''D''$. If the stress alternated at very low frequency, these two configurations would take place alternately, the nodal plane EF remaining approximately fixed. But if the frequency had the value for the fundamental thickness vibration in direction $e = BC$, the distribution of strain and of displacement would be sinusoidal, as indicated in Fig. 22*b*, provided that the dimension AB was so great that the rotation of the plate as a whole about an axis perpendicular to the paper at O could be ignored. One may also assume that the plate is so mounted that the nodal plane EF is fixed in space. The sinusoidal distribution is exactly analogous to that described in §60 for extensional vibrations.

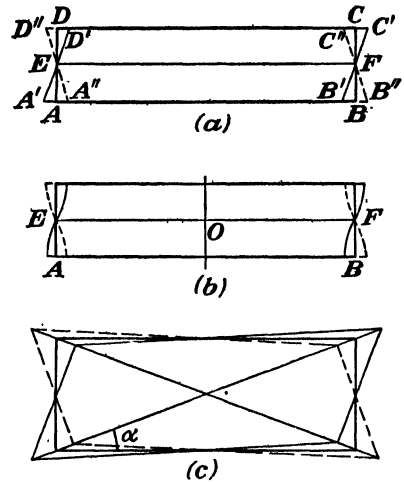


FIG. 22.—Deformation of a plate by a shearing stress: (*a*) static, (*b*) in resonant vibration with nodal plane EF fixed, (*c*) in vibration without constraint.

The rotation of the body as a whole that tends to accompany the alternating shearing strain is represented in Fig. 22*c*, where for simplicity the strained figure is shown as a parallelogram. If the unstrained figure were a square, the strain would be "pure."

The effect of this periodic rotation of the body as a whole is to make the frequency of shear vibration higher than it would be if there were no rotation, *i.e.*, if the nodal plane EF remained invariant. Considering only the case of the fundamental shear mode in a rectangular plate of length a and breadth b, it can be proved from simple dynamic principles that, when the body vibrates freely, the *diagonals of the rectangle remain invariant in direction* and also that the frequency is higher by the factor $1/\cos\ \alpha$ than it would be if the median line EF remained fixed. Since $1/\cos\ \alpha = (a^2 + b^2)^{\frac{1}{2}}/a$, it is evident that the increase in frequency approaches zero when $a >> b$, as is usually the case with thickness vibrations, where the dimension called b here is the thickness.

If $c = (q/\rho)^{\frac{1}{2}}$, where q is the stiffness constant for the shear mode and ρ is the density, the frequency is

$$f = \frac{c}{2b \cos \alpha} = \frac{c}{2ab}\sqrt{a^2 + b^2} \tag{122}$$

This formula can be extended to overtone frequencies, where fractional parts of a and b have to be taken. By a different method Mason[332] derived an approximate equation, which as modified by Sykes[498] has the following form:

$$f = \frac{c}{2}\sqrt{\frac{m^2}{a^2} + k^2\frac{n^2}{b^2}} \tag{123}$$

where a, b, and c are as in Eq. (122) and m and n are positive integers. k is an experimental constant dependent on m and n, with value unity when $m = n$. In the latter case (123) reduces to (122).

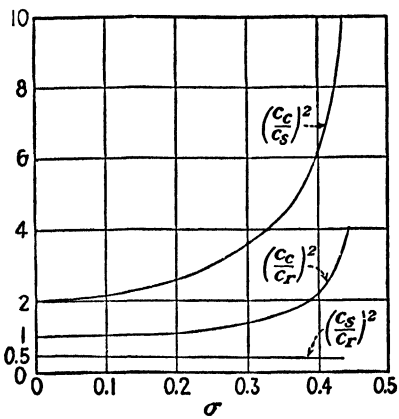


FIG. 23.—Dependence of ratios of velocities of compressional and shear waves on Poisson's ratio.

Shear vibrations of the type we have just discussed, as well as other vibrational modes in finite crystal plates, have recently been treated theoretically by H. Ekstein,[131] who compares calculations based on his theoretical formulas with the experimental results of Mason and others.

72. Comparison of Wave Velocities for Various Types of Vibration. This comparison has a bearing on the dimensioning of resonators. The velocities concerned are c_r in a thin rod, c_c and c_s (compressional and shear) in a plate of large area. The ratios c_c/c_r and c_s/c_r are not the same for all materials, even isotropic, but depend on the relations between the elastic constants.

For isotropic solids, damping being ignored, the velocities as given in §§56 and 66 can be expressed by means of the equations in §§24 and 31 in the form

$$c_r = \sqrt{\frac{Y}{\rho}} \qquad c_c = \sqrt{\frac{Y}{\rho}\frac{1-\sigma}{(1+\sigma)(1-2\sigma)}} \qquad c_s = \sqrt{\frac{Y}{\rho}\frac{1}{2(1+\sigma)}} \tag{124}$$

The ratios between the velocities are thus expressible as functions of Poisson's ratio σ. It will be noted that this quantity does not affect c_r, since the rod is assumed extremely thin. The ratios have been computed for various values of σ by F. Auerbach,* and the results are shown graphically in Fig. 23. Following are the main conclusions:

1. The smaller σ is, the more nearly does the velocity of compressional waves in an extended medium approach that for a thin rod. With increasing σ, c_c increases;

* Ref. B1, p. 289.

this may be interpreted as due to the fact that in an extended medium lateral expansions and contractions are inhibited, so that the effective stiffness coefficient becomes greater.

2. As σ approaches zero, c_s approaches $c_r/\sqrt{2}$; with increasing σ, c_s *decreases* somewhat.

3. c_c has a value approaching $c_s\sqrt{2}$ as σ approaches zero, and the ratio c_c/c_s rises rapidly with increasing σ.

Qualitatively, similar relations may be expected in crystals. It has not been found feasible to express wave velocities in crystals quantitatively in terms of Poisson's ratio, since in the general case this quantity is anisotropic and its introduction into the equations would present grave difficulties. In a few special cases, as, for example, with quartz bars or cylinders parallel to the Z-axis, a single value can be assigned to σ. Such "quasi-isotropic" vibrational conditions are considered in §§382 and 400. The bearing of Poisson's ratio on the coupling between different vibrational modes is mentioned in §§349, 357, and elsewhere.

73. Flexural Vibrations. Just as the compressional vibrations of rods and the compressional or transverse thickness vibrations of thin plates may be regarded as systems of stationary waves with characteristic velocities, so the subject of flexural vibrations may be approached by first considering the velocity of propagation of flexural waves. In contrast to the wave types previously considered, pure flexural waves have velocities proportional to the square root of the frequency [Eq. (126) below], as long as the thickness of the plate is small compared with the wavelength. With increasing frequency, as was shown by Doerffler,[124] there is a gradual transition from pure flexural waves to transverse waves of constant velocity. Pure flexural waves bear a certain analogy to ripples on the free surface of a liquid.

The simplest equation for the velocity of a flexural wave in an indefinitely long rectangular bar of solid isotropic material of breadth b, the vibratory motion taking place in the direction of thickness e (Fig. 24), is

$$c = \frac{\pi e}{\lambda\sqrt{3}}\sqrt{\frac{Y}{\rho}} = kr\sqrt{\frac{Y}{\rho}} \tag{125}$$

where λ = wavelength, Y = Young's modulus, ρ = density, k = wavelength constant $= 2\pi/\lambda$, and $r = e/(2\sqrt{3})$ = radius of gyration of the cross section be with respect to an axis through its center, normal to the plane of flexure (Fig. 24). This equation takes no account of rotational or compressional inertia. Nevertheless, it is fairly precise as long as $e << \lambda$ and was used by Doerffler[124] in experiments on quartz bars. In terms of frequency, since $c = f\lambda$, Eq. (125) becomes

$$c^2 = \frac{\pi e f}{\sqrt{3}}\sqrt{\frac{Y}{\rho}} \tag{126}$$

In the foregoing equations, as also in all the following expressions for flexural vibrations, the breadth b does not appear, as its effect is negligible.

A somewhat more accurate expression, including the effect of rotational inertia, is given by Lamb:[B33]

$$c = \frac{kr}{\sqrt{1 + k^2r^2}}\sqrt{\frac{Y}{\rho}} \tag{127}$$

Further equations for velocity are given in Geiger and Scheel.*

Coming now to flexural vibrations in bars of finite length, we are confronted first with the fact that the terminal effects are very large, so that it is not permissible to assume that the length of the bar is even approximately equal to an integral number of half waves, except for flexural modes of high order. Only vibrations in bars free at both ends are here considered. The equation commonly employed is

$$f = \frac{m^2r}{2\pi l^2}\sqrt{\frac{Y}{\rho}} \tag{128}$$

in which l is the length of the bar and m a coefficient depending on the order n of the mode. For relatively thin bars, $m = (2n + 1)\pi/2$ approximately, where n may be any positive integer. The number of nodes is $n + 1$, as shown in Fig. 24 for $n = 2$. The fundamental mode $n = 1$ is shown in Fig. 47 (page 239).

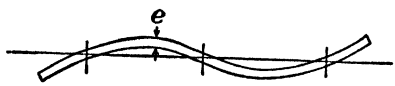


FIG. 24.—Flexural vibration of a bar of length l, thickness e, with three nodes. First overtone, $n = 2$. The plane of the diagram is the "plane of flexure."

For the first three modes of thin bars, the values of m, together with the theoretical distances d of the first nodes from the ends of the bar, expressed as fractions of l, and the relative frequencies, are:

	n	m	d	f_n/f_1
Fundamental	1	4.73	0.2242	1
1st overtone	2	7.85	0.1321	2.756
2nd overtone	3	11.00	0.0944	5.404

Doerffler[124] recorded flexural vibrations in quartz plates with orders as high as $n = 32$.

A small ratio of e to l is by no means a requirement for the existence of flexural vibrations. They have been observed when e was of the order of magnitude of l. A more complete theory, taking account of both rotational and compressional inertia, has been developed by Mason,[333] who gives equations and curves (Fig. 25) from which the coefficient m,

* Vol. 8, p. 195.

for insertion in Eq. (128), can be precisely found for any ratio of e to l up to 1. The only point at which the special properties of crystals enter is in the expression for Poisson's ratio. Mason shows that, as e approaches l, the flexural frequency gradually merges into that for compressional vibrations.

Still another formulation of the theory for isotropic materials, in which Mason's expressions are simplified and extended, with curves to aid in calculations, has been made by Thomson.*

74. Torsional Vibrations. Torsional vibrations are encountered, not only in rods of small cross section, but also in resonators of many shapes. Like flexural vibrations they are frequently present in experiments with vibrating plates, and they contribute both to the complexity of the experiment and the perplexity of the experimenter. Owing to the presence of cross constants connecting extensions with shears, coupling is likely to occur between flexural and torsional modes. In the following equations coupling effects are disregarded, as are also the second-order effects of warping of transverse planes.

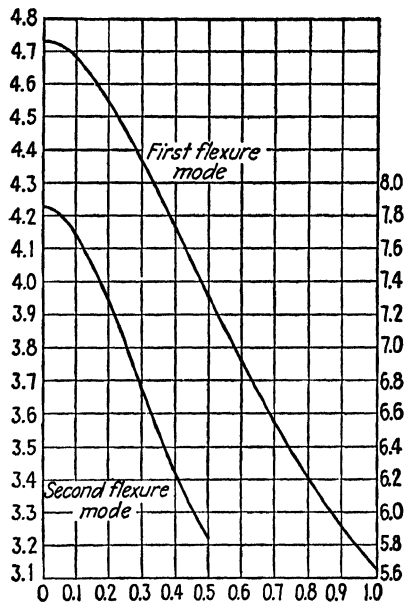


FIG. 25.—Curves for computing flexural frequencies of bars, from Mason. Abscissas are the thickness: length ratio e/l. Upper curve (ordinate scale at the left) gives m for $n = 1$; lower curve (scale at right) gives m for $n = 2$.

In investigations on torsional vibrations, end effects are less serious than with flexural vibrations, so that with sufficient precision the frequency can be expressed simply in terms of wave velocity and length of specimen, the latter being assumed cylindrical or prismatic in form. In general, the theory of longitudinal vibrations in rods can be applied directly to torsional vibrations.

Calling N the *dynamic torsional stiffness* [corresponding to q in Eq. (58)] we have for the torsional wave velocity

$$c = \sqrt{\frac{N}{\rho}} = \sqrt{\frac{N_s}{I_1}} \tag{129}$$

* W. T. THOMSON, *Jour. Acoustical Soc. Am.*, vol. 11, pp. 198–204, 1939.

where N_s is the *static* torsional stiffness as defined in §35 and I_1 is the moment of inertia about the axis of torsion for unit length of the resonator. For a circular cylinder of radius r, $I_1 = \pi\rho r^4/2$; for a rectangular bar of breadth b and thickness e, $I_1 = \rho be(b^2 + e^2)/12$. In the case of a circular cylinder, solid or hollow, $N = 1/T_h$ (§35).

For a *cylinder* or *prism* of length l, the fundamental frequency is $f_1 = c/2l$. The overtones stand very closely in harmonic relation to the fundamental as long as the cross-sectional dimensions are not too large.[162] Hence, for the harmonic of order h,

$$f_h = \frac{h}{2l}\sqrt{\frac{N_s}{I_1}} \quad (h = 1, 2, 3, \cdots) \tag{130}$$

Two expressions for the static torsional stiffness $N_s = Q/\tau$ can be obtained from Eqs. (11) and (12), for the special cases represented by these equations. For a discussion of the more general case in which the axis of torsion may have any orientation the reader is referred to Voigt.*

In the case of bars of *rectangular section* the general expression for the static torsional stiffness is

$$N_s = \frac{A^2be^3n}{3} \tag{131}$$

where A is a function of e/b as defined in §35 and n is the effective rigidity (reciprocal of the torsional compliance). For an isotropic solid n is the ordinary rigidity; for crystals it is a function of certain of the fundamental elastic constants.

The torsional frequency equation for a rectangular bar of any e and l is found from Eqs. (130) and (131) to be

$$f = \frac{Aeh}{l\sqrt{b^2 + e^2}}\sqrt{\frac{n}{\rho}} \tag{132}$$

To a degree of approximation sufficient for the identification of the torsional mode, n may be taken as the reciprocal of $\frac{1}{2}(s'_{44} + s'_{55})$, the primed compliances referring to transformed axes and the length l lying in the Z'-direction. For example, if the specimen has its length parallel to Z, n is $2/(s_{44} + s_{55})$; for length parallel to X, $n = 2/(s_{55} + s_{66})$.

For still other vibrational modes see §§359, 360, and 379.

REFERENCES

General Theory of Vibrations. AUERBACH and HORT,[B1] BARTON,[B2] CRANDALL,[B9] GEIGER and SCHEEL,[B19] LAMB,[B33] LOVE,[B34] MASON,[B35] RAYLEIGH,[B43] BECHMANN,[35,39,40] VAN DIJL,[128] EKSTEIN,[131] MCSKIMIN.[356]

* Pp. 641*f.*

Longitudinal Waves in Bars. BANCROFT,[21] BECHMANN,[35,40,41,42] CADY,[92] OSTERBERG and COOKSON.[405]

Thickness Vibrations. ATANASOFF and HART,[12] ATANASOFF and KAMMER,[13] BAUMGARDT,[30] BECHMANN,[34,35,39,40,41] KOGA,[270] LAWSON,[311,313] MASON.[335]

Flexural Vibrations. GOENS,[175,176] KELLER,[255] KRISTA,[290] MASON,[333] OSTERBERG and COOKSON, [405] PAVLIK,[409,410] THOMSON,[518] WOLF.[589]

Torsional Vibrations. BROWN,[78] GIEBE and BLECHSCHMIDT.[162]

Further references, including other vibrational modes and applications to particular crystals, are given at the end of Chap. XVII.

CHAPTER VI

ELASTIC CONSTANTS OF CRYSTALS

And oft in the hills of Habersham,
And oft in the valleys of Hall,
The white quartz shone, and the smooth brook-stone
Did bar me of passage with friendly brawl,
And many a luminous jewel lone
—Crystals clear or a-cloud with mist,
Ruby, garnet and amethyst—
Made lures with the lights of streaming stone
In the clefts of the hills of Habersham,
In the beds of the valleys of Hall. —LANIER.

In this chapter will be given the results of observations of the fundamental elastic constants of those piezoelectric crystals for which data are available, arranged according to the elastic groups. Other elastic properties of interest are included, although some matters having to do with elasticity are so closely related to the piezoelectric properties that they must be reserved for later chapters.

It is impossible, however, to avoid some reference in the present chapter to the influence of piezoelectric reactions upon the observed elastic constants. For a fuller understanding of these reactions Chap. XII should be consulted.

75. The Measurement of Elastic Constants. In general, three different methods may be used for measuring the elastic constants of solids:

1. By static deformations of specimens cut in various orientations, employing a mechanical or optical technique or a combination of the two. For details the original papers must be consulted. The results when reduced by means of the transformation equations given in Chap. V yield the isothermal values, and they are assumed to be for zero electric field (of significance only with piezoelectric materials). There is reason to suspect that in some cases, notably with Rochelle salt, insufficient precautions were taken to ensure this condition. By making the corrections noted in §37, the adiabatic can be computed from the isothermal values.

2. From observations of frequency, dimensions, and density of resonating devices made of or containing the material to be tested. Frequencies are usually so high that the elastic conditions are essentially adiabatic. Care must be taken to avoid or allow for coupling between

various vibrational modes. With piezoelectric resonators, the electrical state (dependence of elastic coefficients upon piezoelectric reaction) is dependent on the air gap, as explained in §§235 and 248, and also on the relative dimensions and orientation of the specimen. The effect of a gap on the piezoelectric reactions is always to increase the effective stiffness. It is therefore to be expected that dynamic values of the compliances, uncorrected for such reactions, will never be greater than the static values, and the dynamic values of the c's never less than the static values.

3. From the optical effects of ultrasonic waves, as described in Chap. XXX. Although the method is indirect and complicated, it appears to be capable of yielding results of precision comparable with those mentioned above. Not enough precise data on piezoelectric crystals have thus far been obtained to warrant inclusion here.

Method 1, the *static method*, gives primarily the s_{hk} constants, since they occur in the equations relating a single component of stress with the resulting strain. From them the c_{hk}'s are computed as explained in §26. By method 2, whether the quantity derived from observation is a compliance or a stiffness constant depends on the form of the resonator. Methods 2 and 3 are called *vibrational* or *dynamic* methods.

Considering not only observational errors and limitations imposed by methods of measurement but also the impossibility of preparing test pieces in exactly the right orientation, possible defects in test pieces, and variability of different crystals, there is probably some uncertainty in the third significant figure, at least in most cases. Where more than three significant figures are given in the following paragraphs, it is mainly to focus attention on the differences between isothermal and adiabatic values. Room temperature is to be understood unless otherwise stated.

76. In anticipation of the discussion in §199 a word should be said at this point concerning the "electrical state" of crystals. To a greater or lesser extent this must be taken into account in expressing the elastic constants of all piezoelectric crystals. While with most crystals, for example quartz and tourmaline, the influence of the electrical state on the elastic constants is a second-order effect that need be regarded only in work of precision, it becomes an effect of first order when the piezoelectric reactions are abnormally strong, as is the case with Rochelle salt. Hence, the following precautions become less urgent as the magnitude of the piezoelectric constants diminishes.

A definite physical meaning can be attached to the elastic constants when

1. The electric *field* is held constant when a stress is applied. In static observations this condition is usually sufficiently met by allowing a short time to elapse for the neutralization of surface polarization charges

of piezoelectric origin. With Rochelle salt, owing to the magnitude of the piezoelectric effect and the great relaxation time, many minutes may elapse after the application of stress before the final steady state of strain, with all charges neutralized, is reached. The time can be shortened by coating the entire specimen with a conducting film so thin as not to have an appreciable stiffness of its own.

In dynamic measurements, the field may be regarded as virtually constant when the electrodes by which the resonator is driven from an external source are in *immediate* contact with the surfaces of the crystal.

2. The electric *displacement* is held constant when a stress is applied (see §199).

In order to prevent the displacement from varying, there must also be provided an electric field in the crystal of the right strength and in the right direction. With relatively thin bars and plates the field is parallel to the thickness; and if the polarization also is in this direction and no conductors are in the neighborhood, the displacement remains practically zero. Under these conditions constant-displacement coefficients of elasticity can be measured, both statically and dynamically. If the polarization is not parallel to the field, only the component of displacement parallel to the field remains constant. The observed elastic constant is then s^*_{kk} or c^*_{kk}, given by Eq. (273) or (272). From these values the isagric, constant-potential, and constant-displacement values can be calculated. For the procedure in the case of thickness vibrations see §252. It would be excessively difficult to apply to the crystal a compensating field such as to hold the total displacement constant in the general case when the polarization was not parallel to the field.

3. The electric *polarization* is held constant when the crystal is under stress. The constant-polarization elastic constants are used according to the polarization theory discussed in Chap. XI. They are of practical importance chiefly in the treatment of the Seignette-electrics. As is pointed out in §§200 and 211, their numerical values agree with those at constant displacement, within the usual limits of experimental precision.

In estimating the *precision with which a specimen should be oriented* in order that its elastic constants may be measured with a desired accuracy, account must be taken of the fact that the variation of any given constant with angle of cut may depend greatly upon the axis about which the rotation is considered. For quartz, this variation is illustrated in Figs. 31 to 36 and in Fig. 38. In measuring Young's modulus parallel to the Y-axis of quartz by measurements on a bar, the error due to incorrect orientation of the length of the bar in the YZ-plane is much greater than that incurred, when the modulus parallel to X is to be determined with a bar parallel to X, by incorrect orientation in the XZ-plane. This subject is treated more fully by Giebe and Scheibe.[171] Calculations

for all rotations and all crystals can be made with the aid of the transformations treated in Chap. IV.

The effects due to coupling between different modes will be considered later, in various special cases.

In general, the values of compliance coefficients s_{hk} are expressed in square centimeters per dyne, those of stiffness coefficients c_{hk} in dynes per square centimeter. In the reduction of all static measurements to cgs units it does not matter appreciably whether g be taken as 980 or 981 cm/sec.^{2} As a rule the value adopted is 981.

Among piezoelectric crystals complete elastic data are available only for Rochelle salt, sodium ammonium tartrate, quartz, tourmaline, and sodium chlorate.

Unless otherwise stated, all numerical data in this chapter are for *constant-field* conditions.

GROUP III (RHOMBIC)

As may be seen from the table in §29, this group has nine of the possible 21 fundamental elastic constants, each independent of the rest. The rules for the axes in Class 6, to which the crystals here discussed belong, are given in §5. Unlike quartz, the crystals in Group III have qualitatively similar elastic properties with respect to all three crystallographic axes. This symmetry is already apparent in the array of constants in the table in §29. Equations for transformed axes are in §§44 and 45.

77. Rochelle Salt (Class 6, symmetry *V*). It is with Rochelle salt that consideration of the electrical state of the crystal becomes of prime importance in elastic measurements. It is stated in §76 that values of the elastic constants having a definite physical meaning can be obtained only when one of the following quantities is maintained constant when strain is applied: either the electric field, or else the electric displacement, or, as is nearly the same, the electric polarization. In the case of Rochelle salt this precaution is particularly important in all measurements involving s_{55}, s_{66}, and especially s_{44}, since these are the quantities that occur in the expressions for piezoelectric deformations. The elastic "constant" associated with the piezoelectric coefficient d_{14} and the dielectric constant η_1 in the description of the much-discussed anomalies is s_{44} or its reciprocal c_{44}. The observed isagric values of these two quantities depend to a very marked degree on temperature and electric field (§§466 and 474).

The first measurements of all nine constants were made by Mandell,[326] by a static method, in which the bending or torsion of bars cut in various orientations was observed. The constants were calculated from appropriate transformation equations such as are given in §44. Unfortunately no information is given concerning either

the temperature (except that it was held constant) or the completeness with which disturbing effects of electric fields caused by the applied stresses were eliminated. One can only assume that these very careful and painstaking observations were made at room temperature, a few degrees below the upper Curie point, and hope that sufficient opportunity was given for the piezoelectric surface charges to become neutralized by leakage. Doubt on this score has been expressed by Mueller.[378] Mandell's original results, together with the adiabatic values based on them, are given in Table IV (page 122).

Static measurements of the elastic compliances have been made more recently by Hinz,[229] whose method differed from that of Mandell in that by means of compression apparatus (optical lever) he observed the shortening of rods subjected to endwise pressures, at room temperature, stress about 30 kg/cm.^{2} Rods were cut parallel to the crystal axes and also in directions bisecting the angles between pairs of axes. Care was taken to prevent disturbing electric fields of piezoelectric origin; hence, Hinz's values may be considered as isagric. For the theory of this method the original paper should be consulted. Hinz claims a precision of ± 2.5 per cent.

Davies[120] derived equations for Young's modulus for bars in lengthwise vibration in the YZ-plane at 45° with the Y- and Z-axes, the applied alternating field being parallel to X, and also for bars similarly oriented in the ZX- and XY-planes with fields parallel to Y and Z, respectively. We designate these as $X45°$-, $Y45°$-, and $Z45°$-bars, and the corresponding values of Young's modulus as $Y_{(x45)}$, $Y_{(y45)}$, and $Y_{(z45)}$. The formulas will be found in Eqs. (45).

Unfortunately, Davies's metallic electrodes made only light contact with the crystals, so that the effective gap was pretty certainly not zero (§214). His values of Y would therefore be expected to lie between those at constant displacement and those at constant field, approximating somewhat more closely to the latter. His final results are corrected both for adiabatic conditions and for lateral inertia (§65). The values at 15°C are entered in Table VI (page 125).

Frequency measurements on a large number of $Y45°$-rods have been made by Mattiat;[355] the frequencies were corrected for lateral inertia, but the nature of the electrodes is not mentioned. From his data, presumably at room temperature, Young's modulus for this direction (in the ZX-plane at 45° to the Z-axis) is found to be $10.4(10^{10})$ dyne/cm^2 (see Table VI). His curves show the dependence of frequency on the $b:l$ ratio and also the variation with orientation of the bar in the ZX-plane.

The most reliable *dynamic* measurements of elastic constants of Rochelle salt, and indeed the only ones hitherto made that give all nine constants, are those of Mason.[335] His data are obtained from observations at 30°C of resonant frequencies of lengthwise compressional vibrations of rods and of thickness vibrations of plates in a shear mode, piezoelectrically excited in both cases. For the former observations, the rods had lengths lying in the three principal planes, at angles of 22.5°, 45°, and 67.5° with the axes, the field in each case being normal to the principal plane; these measurements yielded s_{11}, s_{22}, s_{33}, and three relations among the remaining six constants. From the thickness vibrations (page 127) were derived $s_{44} = 1/c_{44}$, $s_{55} = 1/c_{55}$, and $s_{66} = 1/c_{66}$; thus all nine compliances were evaluated and also the nine c's. All these are "constant-charge" values (§190), since the gap was large.

Following are the formulas for the stiffness coefficients q_m in the thickness-vibration experiments, derived by means of the theory outlined in §67. For each of the particular oblique cuts employed, certain of the moduli Γ vanish, whence it can be shown that the vibration which is piezoelectrically excited has a vibration direction in the plane of the plate. The electric field was normal to the plate in all cases. For a plate one

edge of which is parallel to X, the normal to its surface making an angle θ with the Y-axis, we shall call the stiffness coefficient $q_{x\theta}$; when one edge is parallel to Y and the normal is at an angle θ with the X-axis, the coefficient is $q_{y\theta}$; and when one edge is parallel to Z, the normal making an angle θ with the X-axis, $q_{z\theta}$. The formulas as derived by Mason are then

$$\left.\begin{aligned} q_{x\theta} &= c_{66}^{*}\cos^2\theta + c_{55}^{*}\sin^2\theta = c_{66}'^{*} \text{ for rotation about } X \\ q_{y\theta} &= c_{44}^{*}\sin^2\theta + c_{66}^{*}\cos^2\theta = c_{66}'^{*} \text{ for rotation about } Y \\ q_{z\theta} &= c_{55}^{*}\cos^2\theta + c_{44}^{*}\sin^2\theta = c_{55}'^{*} \text{ for rotation about } Z \end{aligned}\right\} \tag{133}$$

The values of θ used were 22.5, 45, and 67.5. From the observations of frequency, the values of the q's are found by means of Eq. (120), letting $h = 1$.

The asterisks in Eqs. (133) indicate values at infinite gap, according to §207. In solving for c_{44}^{*}, c_{55}^{*}, and c_{66}^{*}, Mason assumed these quantities to have the same values at each value of θ and also for rotation about each axis. We shall show in §207 that this procedure is not rigorously correct. Nevertheless, since the dependence of these quantities on orientation is not known, Mason's values at constant charge, indicated by "constant σ," are included without correction in Table IV, but they were not used in calculating the values for Table V.

Two years after the appearance of Mason's paper it was shown by Atanasoff and Hart[12] that precise values of the elastic constants of *quartz*, and hence presumably of other crystals, from thickness vibrations, can be obtained only by the use of high harmonic frequencies (§250). With Rochelle salt Mason observed only at the fundamental frequency, and it is impossible to say how different the elastic constants c_{44}, c_{55}, and c_{66} would have been if derived from the frequencies of high overtone vibrations. This circumstance is discussed further in §79.

78. The compliance and stiffness constants as determined by Mandell, Hinz, and Mason by the methods outlined above are assembled in Table IV. Mandell's and Hinz's isothermal values are taken from their papers, and from them the author has calculated the adiabatic values (at room temperature) from Eq. (17), taking data from §§407 and 409. The values obtained by Mandell and Hinz may be assumed to be approximately at *zero field*.

The first prominent feature in this table is the "softness" of Rochelle salt as compared with quartz (Table IX). Next we notice that the magnitude of the important constant s_{44} is not outstanding as being either very great or very small (see §474).

Owing to the peculiar nature of Rochelle salt it is impossible to make a complete comparison of the values without knowledge in every case of the age and previous condition of servitude of the crystals used. The results may be influenced also by faulty orientation and, especially in Mandell's measurements, by the sources of error mentioned above.

Hinz's static compliances agree better with Mason's dynamic than with Mandell's static values. This fact cannot be ascribed to temperature differences, for Hinz and Mandell must have observed at nearly the same temperature, a few degrees below the upper Curie point, while Mason worked at 30°C, several degrees above this point. From all

TABLE IV.—ELASTIC CONSTANTS OF ROCHELLE SALT

	Static				Dynamic
	Mandell, room temp. Isagric		Hinz, room temp. Isagric		Mason, 30°C const. σ
	Obs'd isothermal	Calc. adiabatic	Obs'd isothermal	Calc. adiabatic	Obs'd adiabatic
$cm^2\ dyne^{-1}$	$\times 10^{-12}$	$\times 10^{-12}$	$\times 10^{-12}$	$\times 10^{-12}$	$\times 10^{-12}$
s_{11}	4.69	4.65	5.23	5.19	5.18
s_{22}	3.20	3.18	3.43	3.41	3.49
s_{33}	2.82	2.80	3.24	3.22	3.34
s_{44}	6.09	6.09	9.63	9.63	7 98
s_{55}	30.6	30.6	33.7	33.7	32 8
s_{66}	8.02	8.02	11.8	11.8	10.1
s_{12}	−0.80	−0.82	−2.18	−2.20	−1 53
s_{13}	−2.18	−2.21	−1.69	−1.72	−2.11
s_{23}	+1.68	+1.66	−1.34	−1.36	−1.03
$dyne\ cm^{-2}$	$\times 10^{10}$	.....	. ....	.....	$\times 10^{10}$
c_{11}	34.7	.....	.....	.....	42.5
c_{22}	47.3	.....	.....	.....	51.5
c_{33}	80.6	.....	.....	.....	62.9
c_{44}	16.4	.....	.....	.....	12 5
c_{55}	3.24	.....	.....	.....	3.04
c_{66}	12.4	.....	.....	.....	9.96
c_{12}	−8.04	.....	.....	.....	+29.6
c_{13}	+31.6	. ....	.....	.....	+35.7
c_{23}	−34.4	.....	.....	.....	+34.2

available published data it appears that all the compliances except s_{44} decrease by an amount of the order of 0.2 per cent for each degree rise in temperature over the range from 0 to 40°C (for s_{44}, see §86). About half of the difference between Mandell's and Mason's values can thus be accounted for. On the other hand, one would expect the static values of the compliances to be *greater* than the dynamic, owing to the greater opportunity given the crystal to relax (§428). Smallest of all should be the dynamic values at constant electric charge, such as those of Mason. This relatively low value of compliance is especially to be looked for in the case of s_{44}, and indeed Mason's value is very considerably less than Hinz's. Why Mandell found s_{44} still smaller must remain a mystery.

It will be observed that Mandell's s_{23} does not agree even in sign with the other values. This fact is probably related to his small value of s_{44},

since these two constants occur together in the equations from which the final values are derived.

All things considered, we are inclined to prefer Hinz's static values to Mandell's, partly because of his greater attention to the elimination of disturbing electric fields and partly owing to his better agreement with Mason's results.

79. Best Values of the Elastic Constants of Rochelle Salt. All the constants except s_{44}, s_{55}, and s_{66} vary but little with temperature, and their variation with stress is probably also small. They are also subject to no piezoelectric correction; hence, no distinction need be made between their values at constant field, constant polarization, and constant displacement. Since, as is shown in §211, the values at constant normal displacement (which are practically the same as the constant-polarization values s^P_{hk}) of s_{44}, s_{55}, and s_{66} are less dependent on temperature than the isagric values, the values given below are those at constant normal displacement.

For s_{11}, s_{22}, and s_{33} we adopt the average of the adiabatic values of Hinz and those of Mason, from Table IV.

Mason derived his s^*_{44}, s^*_{55}, and s^*_{66} from thickness vibrations and therefrom obtained s_{23}, s_{31}, and s_{12} by means of the experimentally determined compliances $(2s_{23} + s^*_{44}) = 5.93(10^{-12})$, $(2s_{31} + s^*_{55}) = 28.6(10^{-12})$, $(2s_{12} + s^*_{66}) = 7.02(10^{-12})$. These three numerical values come from measurements of frequency of lengthwise vibrations of bars in different planes and different orientations, as stated in §77. The compliances of the bars are s'_{22} from Eqs. (39) for rotation about X, with analogous expressions for rotations about the other two axes. Since, for the reason stated in §§77 and 207, Mason's values of c^*_{44}, c^*_{55}, and c^*_{66} from his observations of thickness vibrations are subject to correction of unknown amount, his values of s_{23}, s_{31}, and s_{12} cannot be accepted. Instead, we follow Mueller's procedure* and adopt Hinz's values of s_{23}, s_{31}, and s_{12}. Then from Mason's values of $(2s_{23} + s^*_{44})$, etc., given above, the constants s^*_{44}, s^*_{55}, and s^*_{66} are calculated, all at 30°C. Their reciprocals give c^*_{44}, c^*_{55}, and c^*_{66}. These starred values hold only for X-, Y-, and Z-cuts, respectively. For the reason given in §207 they cannot be used accurately in equations involving other orientations.

We thus arrive at the following set of values at room temperature:

TABLE V

Compliance Constants of Rochelle Salt, $\times 10^{12}$

$s_{11} = 5.1(8)$ $s_{22} = 3.4(5)$ $s_{33} = 3.2(8)$ $s_{23} = -1.3(6)$

$s_{31} = -1.7(2)$ $s_{12} = -2.2(0)$

$s^*_{44} = 8.6(5)$ $s^*_{55} = 32.(0)$ $s^*_{66} = 11.(4)$

Stiffness Constants, $\times 10^{-10}$

$c^*_{44} = 11.(6)$ $c^*_{55} = 3.1(2)$ $c^*_{66} = 8.(8)$

* Ref. 378, footnotes 25 and 26.

The numbers in parentheses are of uncertain magnitude. Future experimentation may show that in some cases even the digits preceding the parentheses should be changed. The value of c_{44}^{P}, at constant polarization, is of importance in the polarization theory. Within the limits of experimental error (see §211) we may write

$$c_{44}^{P} \approx c_{44}^{*} = 11.(6)(10^{10}) \text{ dyne cm}^{-2} \tag{134}$$

The variation of c_{44}^{*} with temperature can be calculated from the data in Table I of Mason[338] (a portion of which is given in Table XXXII, page 478) or from Fig. 28. From the values of frequency the author finds, using the values of s_{22}, s_{33}, and s_{23} from Table V, a fairly uniform decrease in c_{44}^{*} from $12.5(10^{10})$ at $-12°$C to $11.0(10^{10})$ at 47.5°C. Curve H_M in Fig. 94 indicates that there is a very slight discontinuity in c_{44}^{*} at the upper Curie point.

The isagric compliance s_{44}^{E} and its dependence on temperature can be derived from s_{44}^{*} by means of Eq. (273). If the calculation is made by the use of d_{14} and k_x' from Figs. 145 and 146, values of s_{44}^{E} in agreement with Fig. 146 are obtained. For s_{55}^{E} and s_{66}^{E} see §141.

Our knowledge of the elastic constants of Rochelle salt, even at small field strengths, is still in an unsatisfactory state. There is need of more experimental data, on many plates and bars in different orientations, with strong as well as weak fields and over a wide range of temperatures including both Curie points. The resonant and antiresonant frequencies with zero gap should be observed and also the frequencies with infinite gap, together with the dielectric constants. Due attention should be given to the piezoelectric terms in the stiffness equations. In observing thickness vibrations of plates, high harmonics should be used. It is also desirable to make static observations of the elastic and dielectric properties of the same specimens, under carefully controlled conditions.

80. Young's Modulus for Bars in Various Orientations. Data for Table VI are taken chiefly from the papers cited above. All values were obtained from the resonant frequencies of lengthwise vibrations except those of Hinz, who observed the moduli directly by his static method, and of Mandell, whose values are derived from his fundamental constants. Davies observed at 15°C, Mason at 30°C, Mikhailov at 15 to 19°C, the others at room temperature.

The errors in the observed values of Y due to an error of 1° in orientation for bars in the three principal planes, with lengths at 45° to the axes, have been computed by Davies[120] as follows: in the XY-plane about 1 per cent, and in the YZ- and ZX-planes about 0.5 per cent.

Hiltscher used very short electrodes (§377) in his experiments, so that his values, like Mason's, may be regarded as practically at constant displacement. The best constant-displacement values are probably those of Mason, the best isagric values those of Hinz. Cady's and

TABLE VI.—RECIPROCAL OF YOUNG'S MODULUS OF ROCHELLE SALT FOR BARS AT 45° WITH THE AXES INDICATED
(In cm^2 $dyne^{-1}$)

	Plane		
	YZ	*ZX*	*XY*
	$\times 10^{-12}$	$\times 10^{-12}$	$\times 10^{-12}$
Cady[103]	3.31	10.2	3.97
Davies[120]	3.29	11.0	3.97
Hiltscher[228]	3.19		
Hinz[229]	3.41	9.70	4.02
Mandell[326]	3.84	8.41	3.55
Mason[335]	3.16	9.31	3.90
Mattiat[355]		9.64	
Mikhailov[367]	3.13	10.4	3.66

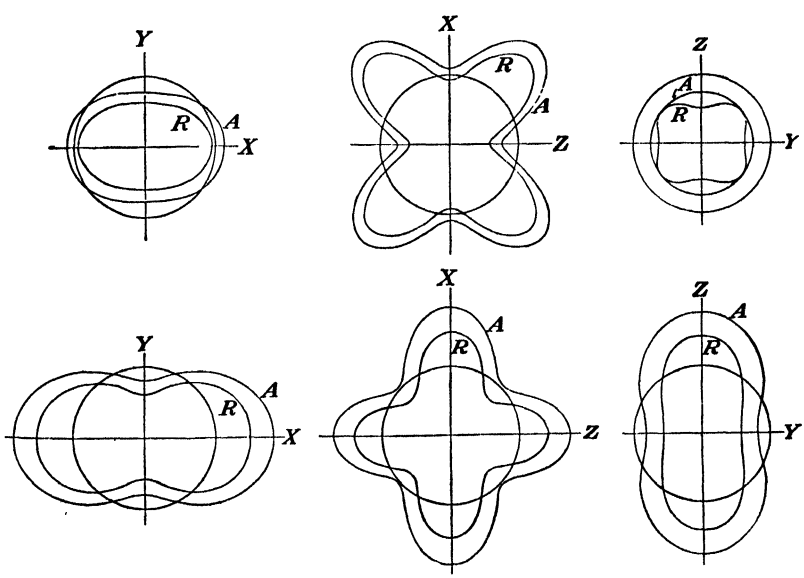


FIG. 26.—Elastic constants of Rochelle salt *R* and sodium–ammonium tartrate *A* (see §88) from Mandell. Upper diagrams: radius vectors are s'_{22}, the reciprocals of Young's modulus; radius of circle is $50(10^{-10})$ cm^2 gm^{-1} = $5.1(10^{-12})$ cm^2 $dyne^{-1}$. Lower diagrams: radius vectors are the torsional compliance *T*; radius of circle is $125(10^{-10})$ cm^2 gm^{-1} = 12.74 cm^2 $dyne.^{-1}$

Davies' dynamic measurements were made under conditions approximating those at constant field, so that their results might be expected to agree with those of Hinz, as indeed they do fairly well accept in the case of the ZX-plane, where Davies' value looks suspiciously large.

In the upper part of Fig. 26 are shown polar diagrams of the reciprocal of Young's modulus for all orientations in the three principal planes. They are taken from Mandell's papers[326,327] and are based on his measurements. The curves may be regarded as fairly representative, despite such corrections as may have to be made to Mandell's values of the elastic constants. The minimum of Young's modulus comes at about 42° with the X-axis, the value of the reciprocal being $8.50(10^{-12})$.

The diagrams in the lower part of Fig. 26 represent the modulus of torsion T for circular cylinders with lengths lying in the three principal planes. The values are derived from Eq. (10) after the latter has been specialized for the rhombic group.*

The three stiffness coefficients corresponding to the three possible modes of *thickness vibrations* in Rochelle-salt plates have been computed by Takagi and Miyake.[501] Values are shown in the form of polar diagrams, for plates whose normals are perpendicular to the Z-axis, at various angles with the X- and Y-axes.

81. *Crushing Strength of Rochelle Salt.* The only data at hand are from a single test in this laboratory.† An X-cut 45° plate 3.6 by 2.5 by 0.6 cm with carefully machined ends was stood on end while increasing forces were applied from above. Care was taken to distribute the stress as uniformly as possible. At about 130 kg/cm² the first crack appeared, running lengthwise. The plate was still standing up under 300 kg/cm² but fell apart in several pieces when removed. Apparently 100 kg/cm² is a safe compressional stress for the direction bisecting the Y- and Z-axes.

82. Compressibility of Rochelle Salt. A check on the relative reasonableness of the elastic constants as given in Table IV is provided by a calculation of the linear compressibilities in the three principal directions under uniform hydrostatic pressure, using Eqs. (15). These calcula-

TABLE VII.—LINEAR COMPRESSIBILITIES
(In 10^{-12} cm² dyne^{-1})

	Mandell	Hinz	Mason	Bridgman
X: $s_{11} + s_{12} + s_{13}$	1.71	1.36	1.54	1.36
Y: $s_{22} + s_{23} + s_{12}$	4.08	−0.09	+0.93	2.76
Z: $s_{33} + s_{13} + s_{23}$	2.32	+0.21	+0.20	1.99
Sum	8.11	1.48	2.67	6.11

* The simplified expression is in Voigt, p. 760, and also in Mandell's papers.

† This test was made by R. A. Richardson and M. C. Waltz.

tions are given in Table VII. The values from Mandell[326] and Hinz[229] are isothermal. The last column gives the initial compressibilities, derived by extrapolation from the observations of Bridgman,* which covered the range from 2,000 to 12,000 kg/cm², at temperature 30°C.

The curious discrepancies in Table VII are attributable largely to differences in the value of s_{23}, which as has previously been pointed out is closely associated with the anomalous "constant" s_{44}. On the whole, Bridgman is found to be in best agreement with Mandell, although the latter's values are somewhat greater. On the other hand, Bridgman is in good agreement with Mason, and especially with Hinz, in the X-direction. In the Y-direction Hinz's data predict a slight *expansion* under uniform pressure.

The last line in the table gives the volume compressibilities. The values of Hinz and of Mason appear very low. One is tempted to wonder whether their values of the cross constants, particularly Hinz's values of s_{12} and s_{23}, are not numerically too great.

83. Stiffness Coefficients for Thickness Vibrations. The following values are from Mason,[335] obtained directly from observed frequencies of shear modes. These are the q's which, by means of Eqs. (133), served to determine his values of c_{44}, c_{55}, and c_{66} and thence s_{44}, s_{55}, and s_{66} in Table IV. The symbol $X22.5Y$ means a plate having one edge parallel to X, its normal making an angle of 22.5° with the Y-axis, and similarly for the remaining cuts. All values are in 10^{10} dynes/cm².

Cut	Stiffness	Cut	Stiffness	Cut	Stiffness
$X22.5Y$	7.51	$Y22.5X$	10.18	$Z22\ 5X$	4.54
$X45Y$	6.34	$Y45X$	11.39	$Z45X$	7.87
$X67.5Y$	4.06	$Y67.5X$	11.99		

With these may be compared the probably less reliable values (electrodes and gap not specified) of Mikhailov:[367] $Y45X$, $12.3(10^{10})$; $Z45X$, $6.83(10^{10})$ dyne cm^{-2}.

Using Mandell's data from Table IV the author has calculated from Eq. 37 the stiffness coefficient c'_{11} for various directions of the X'-axis. The maximum value $80.4(10^{10})$ is in the Z-direction. The minimum value is $27.5(10^{10})$, with direction cosines approximately $\alpha_1 = 0.707$, $\alpha_2 = 0.612$, $\alpha_3 = 0.354$.

An idea of the configuration of the c'_{11}-surface may be gained from Fig. 27. The model† shown here for viewing stereoscopically, has radius

* P. W. BRIDGMAN, *Proc. Am. Acad. Arts Sci.*, vol. 64, p. 68, 1929.

† This "pincushion" model, designed and constructed in Scott Laboratory, consists of a carefully machined aluminum casting in the form of an octant, in which holes

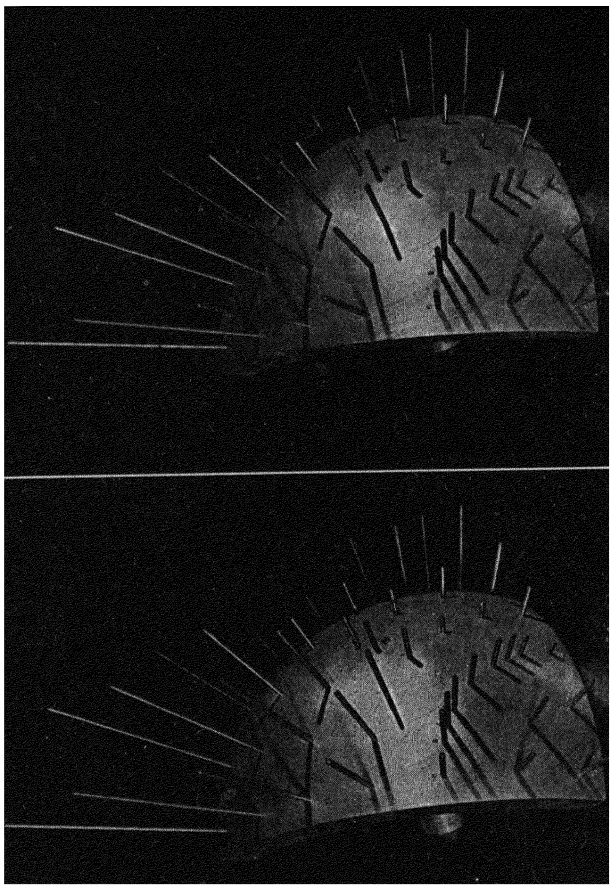


FIG. 27.—Stereoscopic view of an aluminum octant, illustrating the c'_{11}-surface for Rochelle salt. The X-axis is toward the front, the Y-axis to the right, and the Z-axis points vertically upward in the plane of the paper.

vectors (distances of tips of rods from center of sphere) proportional to the square root of c'_{11}.

are drilled radially for various latitudes and longitudes. Threaded steel rods are screwed into these holes, each projecting outward so that the distance from the center of the sphere to the tip of the rod is proportional to the calculated value of the parameter in question. The rods are threaded and can be screwed in and out at will. The apparatus is thus a *universal contour model*, capable of illustrating any physical property of any crystal so far as is possible with a single octant.

The symmetry of Rochelle salt is such that every elastic property can be completely represented by a single octant; three of the remaining octants are identical with the first; the other four are mirror images.

If the model were set up to illustrate any elastic property of quartz, a range of 30° in azimuth (longitude) about the Z-axis would suffice, together with 90° in latitude.

84. *Variability of the Elastic Constants of Rochelle Salt with Stress.* Almost the only experimental data seem to be those of Iseley,[243] who applied endwise compressions to a bar whose length bisected the angle between the Y- and Z-axes. The stresses Y'_y (§39) extended to 2.225 kg/cm^2 [about 2(10^6) dynes/cm^2]. The strain is $y'_y = -s'_{22}Y'_y$; the compliance s'_{22}, from Eqs. (43), involves s_{22}, s_{33}, s_{23}, and s_{44}. The first three of these coefficients should be sensibly constant; hence, any departure from strict proportionality between y_z and Y_z must be attributed to s_{44}, which shares in the anomalies discussed in Chap. XXIV. Iseley's curves, for temperatures 20, 22.5, and 30°C, show a slight decrease in s'_{22} with increasing Y'_y, indicating a somewhat more marked decrease in s_{44}. Although the interpretation of his data is difficult, still it can be said that his results tend to confirm quantitatively the theoretical curves in Fig. 142.

Hinz's value of s_{44} in Table IV tends to confirm the view that this quantity becomes smaller under large stresses. The value, obtained presumably at zero field, is 9.63(10^{-12}), the stress being about 30 kg/cm^2. At small stresses, according to Fig. 146 the value is about 20(10^{-12}) at room temperature. Unfortunately, Hinz does not record the dependence of his elastic constants upon stress.

Mandell[326] states that he found it necessary after each observation on the elastic constants of a bar of Rochelle salt to wait for the recovery from fatigue before using the same bar again (time not stated).

85. Temperature Coefficients of the Elastic Constants of Rochelle Salt. The behavior of s_{44} with varying temperature and stress is discussed later.* Further experimental results bearing on s_{44} will now be given, together with data on the variation of the other elastic constants with temperature.

Since the dielectric and piezoelectric anomalies of Rochelle salt are confined to fields in the X-direction and since the only elastic constant related piezoelectrically to E_x is s_{44}, one would hardly expect to find anomalies in s_{55} or s_{66} at any temperature. Nevertheless, the evidence is quite convincing that s_{55} and s_{66} (hence also c_{55} and c_{66}) have anomalous values in the neighborhood of the Curie points of the same order of magnitude as that in s_{44} at infinite gap. The results of different observers are in too good agreement, at least in order of magnitude, for the effect to be attributed to faulty orientation of the Y- and Z-cuts employed.

Owing to the large values of d_{14} and e_{14} and their dependence on temperature, the effect of the gap width w on s_{44} and on its temperature coefficient is very pronounced.† For unambiguous results with X-cut

* See especially §§462 and 474 and Figs. 142 and 146.

† Formulas for the effect of the gap on the elastic constants or on vibrational frequencies are given in Eqs. (284), (330), (355), (370), and (336).

plates the gap should be zero (with due regard to the precautions noted in §§415 and 416) or else infinitely great; spacing of a few millimeters between crystal and electrodes usually makes the gap effectively equal to infinity. It is when $w = 0$ that s_{44}, and hence the effective stiffness s_{22}' of $X45°$-bars, shows very great dependence on frequency. The data below are for bars with w large enough to give to s_{44} the value for constant normal electric displacement.

With Y- and Z-cuts a consideration of the gap is not of much importance, since the piezoelectric correction is relatively small and independent of temperature. The dependence on temperature of all elastic constants except $s_{44} = 1/c_{44}$ should be substantially the same whatever the gap may be.

All the available data on temperature coefficients are from observations of resonant frequencies of bars or plates. The earliest results of this sort, obtained in Scott Laboratory at intervals from 1928 to 1933 but not published, were confirmed by the publications of Davies[120] and Mason[335,338]. In all this work, lengthwise vibrations of 45° bars were used, leading to values of Young's modulus along lines bisecting the Y- and Z-, Z- and X-, and X- and Y-axes. The driving fields were parallel to X, Y, and Z, respectively. All these cuts yield negative temperature coefficients of frequency, in most cases with larger values below the upper Curie point θ_u than above it. On each side of θ_u the relation between frequency f and temperature t is nearly linear. There is an anomaly over a narrow region close to θ_u for each cut, usually involving a kink in the $f:t$ curve, with a reversal of sign of the temperature coefficient. This anomaly may be seen in Davies' diagrams and also in curve H_M of Fig. 94 taken from Mason's paper.

At low temperatures, observations made in this laboratory in 1929 by B. B. Doolittle, Jr., on an X-cut 45° bar, indicate a nearly constant value of the temperature coefficient $\alpha_f = \Delta f/f\Delta t$ from -44 to $+15°$C, amounting to $-920(10^{-6})$. This value agrees fairly well with that calculated from unpublished data by W. P. Mason on a similarly oriented bar (wide gap) over the range from -145 to $+48°$C: the average for the entire range is $-980(10^{-6})$, with a very slight increase between the Curie points.* The values of the effective compliance found by Mason are $2.625(10^{-12})$ at $-145°$ and $3.225(10^{-12})$ at $+48°$, with a nearly linear relation between. On the other hand, Doolittle observed a flat region in the neighborhood of the lower Curie point, where α_f became almost constant.

* The author's thanks are due to Dr. Mason of the Bell Telephone Laboratories for these data and also for those on c_{44}, c_{66} and the temperature coefficients of the various elastic constants of Rochelle salt.

For the regions *adjacent to the upper Curie point*, data are available from Davies,[120] Mason (unpublished), and Kent.* They are given in Table VIII.

TABLE VIII.—TEMPERATURE COEFFICIENTS OF FREQUENCY FOR 45° ROCHELLE-SALT BARS

Author	Cut	$-\alpha_f$	
		Below θ_u	Above θ_u
		$\times 10^{-6}$	$\times 10^{-6}$
Davies	X	957	957
Mason	X	945	918
Average	..	950	940
Davies	Y	1,500	410
Kent	Y	1,330	530
Average	..	1,400	470
Davies	Z	485	485
Kent	Z	525	468
Average	..	500	475

The averages, calculated in round numbers, are probably fairly representative from 0 to 23°C and from 24 to 40°C. Most noteworthy is the fact that below θ_u an X-cut bar has a lower coefficient than a Y-cut.

Reference has been made to the rather sudden increase in frequency as the temperature rises through the upper Curie point. This change, which is least with the X-cut, amounts to a few tenths of 1 per cent in frequency, in a temperature interval of about 1°.

Mikhailov[366] has obtained values of α_f of the same order of magnitude as those reported above, for both lengthwise and shear vibrations. Owing to uncertainty in the identification of his vibrational modes his numerical values are not quoted here.

The only further data that we find are from Mattiat,[355] who found for Y-cut 45° bars values of α_f from $-600(10^{-6})$ at 14°C to $-2{,}300(10^{-6})$ at 35°C.

Most of the quantitative work on Rochelle salt, including the measurements cited above, has been done with small fields (not over 10 volt/cm) and small stresses. It is shown in Chaps. XXIII and XXIV that under these conditions s_{44} and d_{14} are most dependent on temperature. Although observational data are lacking, it is to be expected that in vibrational observations on X-cut bars with large voltages, where

* G. H. KENT, M. A. thesis, Wesleyan University, 1933, unpublished.

saturation conditions are approached, the temperature coefficients of frequency will also diminish. Klein* has stated that he found no change in wave velocity in $X45°$-bars from 15 to 28°C and no anomaly at the Curie point. This finding, which is quite at variance with those of other observers, is possibly due to the fact that his applied voltages were relatively great.

86. From measurements of the frequencies of plates and bars with large gap, Mason has obtained the following values of the temperature coefficients, corrected for the effect of temperature on dimensions and

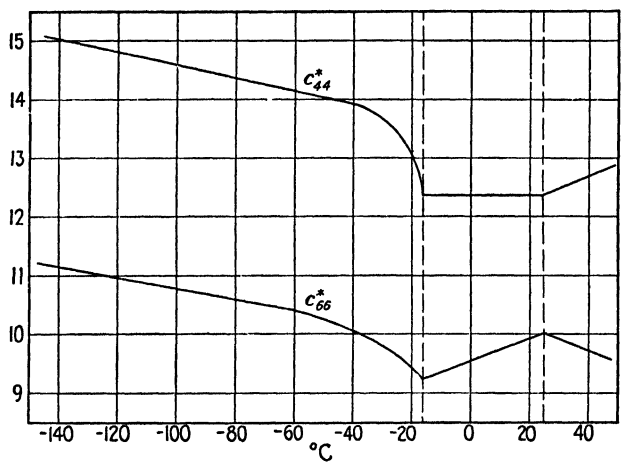


FIG. 28.—Variation of c^*_{44} and c^*_{66} of Rochelle salt with temperature, from Mason. Ordinates are in dyne $cm^{-2} \times 10^{10}$.

density. They are valid from 24 to 48°C, the basic value of the elastic constant being taken at 30° in each case. The temperature coefficients are here designated by Ts_{11}, etc., expressed, as usual, as parts per million (ppm):

$Ts_{11} = 1{,}230$	$Ts_{44} = -1{,}660$	$Ts_{12} = 5{,}240$
$Ts_{22} = 1{,}330$	$Ts_{55} = 700$	$Ts_{13} = 2{,}710$
$Ts_{33} = 890$	$Ts_{66} = 1{,}830$	$Ts_{23} = -10{,}200$

The curves in Fig. 28 show the measured values of $c^*_{44} = 1/s^*_{44}$ and $c^*_{66} = 1/s^*_{66}$, derived from the frequencies of plates cut in various orientations. The asterisk indicates constant normal electric displacement, as explained in §§207 and 253. Since the elastic constants under these conditions vary from one orientation to another and are not corrected

* E. KLEIN, The Velocity of Sound in Rochelle Salt Crystals, abstract in *Phys. Rev.*, vol. 33, p. 1095, 1929.

for the piezoelectric term in Eq. (358), they have neither the isagric nor the constant-displacement values, though they approximate more closely to the latter. The curves are of value mainly in showing qualitatively the probable dependence of the constant-displacement values on temperature.

With the exception of c_{44} and c_{66} the temperature dependence of the elastic constants has not been determined below the upper Curie point. The peculiarity in s'_{22} for a $Y45°$-bar noted above is pretty certainly attributable to an anomaly in c_{55} at θ_u. To account for the anomaly in compliance for $X45°$- and $Z45°$-bars one would expect kinks at θ_u in the curves in Fig. 28. Their absence may be due to the lack of sufficient observations close to this temperature.

87. Heavy-water Rochelle Salt. The only published data are the following, from Holden and Mason.[231] From observations of resonant frequency on an X-cut 45° bar with wide gap, they find, for the reciprocal s'^{*}_{22} of Young's modulus, a linear increase from $3.14(10^{-12})$ at $-12°$C to $3.21(10^{-12})$ at the Curie point, $+35°$. At this point occurs a sudden drop to $3.19(10^{-12})$, followed by a linear increase to $3.26(10^{-12})$ at 48°C. This dependence on temperature is similar to that for ordinary Rochelle salt shown in Fig. 94, and the numerical values are of the order of 1 per cent less than those for the ordinary salt.

To the constant s^{*}_{44} is assigned the value $7.98(^{10-12})$, the same as that given by Mason[335] for ordinary Rochelle salt, but the temperature and method of measurement are not stated.

The reciprocal s'^{*}_{11} of Young's modulus was also determined from the resonant frequencies of Y- and Z-cut bars, at 30°C. For the Y-cut, $s'^{*}_{11} = 9.93(10^{-12})$; Z-cut, $s'^{*}_{22} = 4.2(10^{-12})$. These values may be compared with those for the same cuts in ordinary Rochelle salt at 30°, from Mason:[335] $9.31(10^{-12})$ and $3.905(10^{-12})$, respectively.

88. Sodium-ammonium Tartrate. This crystal, $NaNH_4C_4H_4O_6 \cdot 4H_2O$, is isomorphic with Rochelle salt, having the NH_4 group in place of K. The density is 1.587, and the axial ratio is

$$a:b:c = 0.8233:1:0.4200.$$

The elastic properties have been investigated by Mandell,[327] using the same static method as for Rochelle salt. In the same paper are comments on the method of growing these crystals; the process is more difficult than with Rochelle salt. They have the same type of piezoelectric constants as Rochelle salt, though of smaller magnitude. Piezoelectric reactions are a less serious source of error in elastic measurements; the long relaxation time and other anomalies characteristic of Rochelle salt are absent. Following are Mandell's values, converted to cgs units:

	s_{11}	s_{22}	s_{33}	s_{44}	s_{55}	s_{66}	s_{12}	s_{13}	s_{23}
$10^{-12}\times$	5.37	3.84	3.73	8.74	36.0	11.8	−0.87	−3.43	−0.50 cm² dyne⁻¹
	c_{11}	c_{22}	c_{33}	c_{44}	c_{55}	c_{66}	c_{12}	c_{13}	c_{23}
$10^{10}\times$	53.1	34.1	77.8	11.8	2.9	8.8	18.7	51.3	21.6 dyne cm⁻²

In Fig. 26 above are Mandell's polar diagrams for the reciprocal of Young's modulus and for the modulus of torsion in the three principal planes.

In a later paper Mandell[329] gives results of experiments on the resonant frequencies of 45° bars of this crystal in the three principal planes. For the theory of these experiments and the effect of cross section on frequency the original paper should be consulted. We give here only the resulting adiabatic values of Young's modulus by this dynamical method. In each case the direction is at 45° with the axes named.

$$YZ,\ 27.9(10^{10})\quad ZX,\ 9.54(10^{10})\quad XY,\ 22.8(10^{10})\ \text{dyne cm}^{-2}$$

The corresponding values calculated from the static measurements are

$$YZ,\ 26.2(10^{10})\quad ZX,\ 10.45(10^{10})\quad XY,\ 20.6(10^{10})\ \text{dyne cm}^{-2}$$

89. Group IV. As shown in §29, this group has nine elastic constants, as in the rhombic Group III, but in the present case $s_{11} = s_{22}$, $s_{13} = s_{23}$, and $s_{44} = s_{55}$, so that the number of independent constants is six, *viz.*, s_{11}, s_{12}, s_{13}, s_{33}, s_{44}, and s_{66}. The crystallographic axes are defined in §5.

The only representative of this group on which measurements seem to have been published is *primary potassium phosphate*, KH_2PO_4. By a dynamic method Lüdy[323] has found, at 20°C, the following values, in square centimeters per dyne:

$$s_{11} = 1.9(10^{-12})\qquad s_{33} = 2.2(10^{-12})$$

No data for the other constants are at hand.

GROUP VII

According to the table in §29, this group has 12 of the 21 possible fundamental elastic constants, of which only 6 are independent. For the axes see §5.

90. α-Quartz (Class 18, symmetry D_3). The crystallography of this, the common form of quartz, as well as the conventions respecting axes and angles for right- and left-quartz, are explained in Chaps. II and XVI.

Since quartz is piezoelectric, the application of mechanical stress, at least in certain directions, to a crystal that is not artificially short-circuited gives rise to an electric field, which, in turn, affects the strain and thereby the apparent stiffness. This fact must be allowed for in measuring the elastic constants by vibrational methods, as indicated

below. In static measurements it can usually be assumed that enough time elapses for surface leakage to neutralize the electric field, so that static observations of the constants yield values that are appreciably *at constant field.*

TABLE IX.—ELASTIC CONSTANTS OF QUARTZ.

	Voigt		Atanasoff and Hart	Mason, 1943
	Isothermal	Adiabatic	Adiabatic at 35°C	Adiabatic at 25°C
$cm^2\ dyne^{-1}$	$\times 10^{-12}$	$\times 10^{-12}$	.....	$\times 10^{-12}$
$s_{11} = s_{22}$	1.298	1.295	.....	1.279
s_{33}	0.990	0.989	.....	0.956
$s_{44} = s_{55}$	2.005	2.005	.....	1.978
s_{12}	−0.166	−0.169	.....	−0 1535
$s_{13} = s_{23}$	−0.152	−0.154	.....	−0.110
$s_{14} = -s_{24} = \frac{s_{66}}{2}$	−0.431	−0.431	.....	−0.446
$s_{66} = 2(s_{11} - s_{12})$	2.93	2.93	.....	2.865
$dyne\ cm^{-2}$	$\times 10^{10}$	$\times 10^{10}$	$\times 10^{10}$	$\times 10^{10}$
$c_{11} = c_{22}$	85.1	85.4	86 75	86.05
c_{33}	105.4	105.6	106.8	107.1
$c_{44} = c_{55}$	57.1	57.1	57.86	58.65
c_{12}	6.96	7.26	6.87	5.05
$c_{13} = c_{23}$	14.1	14.4	11.3	10.45
$c_{14} = -c_{24} = c_{56}$	16.9	16.9	17.96	18.25
$c_{66} = \frac{c_{11} - c_{12}}{2}$	39.1	39.1	.....	40.5

In Table IX the first column of figures is from Voigt's static (isothermal) observations.* The second column gives the adiabatic values computed from them according to §37, for 0°C; the same values hold at all ordinary temperatures. The third column is from Atanasoff and Hart,[12] as corrected by Lawson.[312] Mason's values[340] in the last column are also from resonant vibrations, both lengthwise and thickness.†

* "Lehrbuch," pp. 752, 753.

† Atanasoff and Hart observed with high overtone frequencies, the advantages of which are pointed out in §250. Overtones as high as the 87th harmonic were used. Their quartz plates were carefully examined for twinning and oriented by means of X-rays. The plates included *X*-cut, *Y*-cut (with which they observed all three of the theoretically possible thickness modes), *R*-cut ($\varphi = 30°$, $\theta = -51°47'$), and a cut with $\varphi = 0°$, $\theta = 45°$. The electric field was in some cases in a direction parallel to the major faces of the plate. They used air-gap mountings, but the effect of the gap

There is no way of knowing how much the values in the foregoing table are influenced by systematic and observational errors and by peculiarities in the crystal specimens. The digits recorded in the table

TABLE X.—DYNAMIC TEMPERATURE COEFFICIENTS OF ELASTIC CONSTANTS OF QUARTZ

$$\alpha = \frac{1}{s_{hk}}\frac{\partial s_{hk}}{\partial T} \quad \text{or} \quad \frac{1}{c_{hk}}\frac{\partial c_{hk}}{\partial T}$$

Elastic constant	Bechmann	Mason	Koga	Atanasoff and Hart
	$\times 10^{-6}$	$\times 10^{-6}$		
$s_{11} = s_{22}$	+11.5	+11.8		
s_{33}	+180	+182		
$s_{44} = s_{55}$	+175	+195		
s_{12}	−1,125	−1,352		
$s_{13} = s_{23}$	−148	−295		
$s_{14} = -s_{24} = \frac{s_{66}}{2}$	+113	+120		
s_{66}	+233*	−134		
	$\times 10^{-6}$	$\times 10^{-6}$	$\times 10^{-6}$	$\times 10^{-6}$
$c_{11} = c_{22}$	−48	−46.5	−61	−49.7
c_{33}	−208	−204	.....	−213
$c_{44} = c_{55}$	−151	−166	−199	−169
c_{12}	−2,115	−3,300	−2,860	−3,000
$c_{13} = c_{23}$	−530	−697	.....	−580
$c_{14} = -c_{24} = c_{56}$	+82	+90.2	+110	+107
c_{66}	+144	+164	+199	+170.1

* This value is for $(s_{44} + 2s_{12})$, not s_{66}.

are taken from the original sources. Since the discrepancies between the results of the various investigators are of the order of 1 per cent, it is evident that in general the last significant figures are of little or no

was eliminated by restricting the observations to high harmonics. Their original results give the elastic constants at constant normal displacement. By use of a formula similar to Eq. (272*a*) (p. 271), Lawson converted them into the corresponding *isagric* values, which are given in Table IX. Atanasoff and Hart's paper should be consulted for their treatment of the theory of thickness vibrations as well as for experimental details.

In his determination of the elastic constants of quartz given in Table IX, Mason used *AT*-, *BT*-, and *Y*-cuts for c_{44}, c_{66}, and c_{56}. The fundamental thickness mode with zero gap was employed, uncorrected for the piezoelectric terms in Eq. (356) (p. 316). These are the values in Table IX. If they were reduced to isagric values by applying the piezoelectric correction, they would be diminished in amount by 0.2 to 0.3 per cent. Mason's data for s_{11}, s_{33}, and s_{14} were obtained with plated bars, which give the isagric values directly. The remaining *s*'s and *c*'s were calculated with the aid of c_{44}, c_{55}, and c_{66} and hence should be subjected to a piezoelectric correction.

importance. A similar remark may be made concerning Table X, except that here the discrepancies are relatively large—as is to be expected in the determination of quantities as small as temperature coefficients.

Table X gives the *temperature coefficients* of the elastic constants in ppm per degree centigrade, valid for temperatures from 20 to 70°C. In all cases corrections were made for variation of density and dimensions with temperature. The data are from Bechmann,[32] Mason[340] (claimed to be accurate within about ±2 per cent from 20 to 60°C), Koga,[272] and Atanasoff and Hart.[12] These data are discussed in §91. For temperature coefficients of quartz resonators, see §92 and Chap. XVII.

Accepted Values of the Elastic Constants of Quartz. Beyond the values given above, the most important elastic measurements are those of s_{11} and s_{33} by Perrier and de Mandrot, discussed in §95. They are probably more precise than Voigt's measurements of these constants. Their isothermal values are $s_{11} = 1.272(10^{-12})$, $s_{33} = 0.972(10^{-12})$, from which the adiabatic values are found to be

$$s_{11} = 1.269(10^{-12}) \qquad s_{33} = 0.971(10^{-12})$$

In this book we shall in general use these values, together with Voigt's for the remaining compliances. On this basis the values of the stiffness constants have been calculated,* with the results shown in Table XI.

TABLE XI.—ACCEPTED VALUES OF THE ADIABATIC ELASTIC CONSTANTS OF QUARTZ

$\times 10^{-12}$ cm^2 dyne^{-1}	$\times 10^{10}$ dyne cm^{-2}
$s_{11} = 1.26(9)$	$c_{11} = 87.(5)$
$s_{33} = 0.97(1)$	$c_{33} = 107.(7)$
$s_{44} = 2.00(5)$	$c_{44} = 57.(3)$
$s_{12} = -0.16(9)$	$c_{12} = 7.6(2)$
$s_{13} = -0.15(4)$	$c_{13} = 15.(1)$
$s_{14} = -0.43(1)$	$c_{14} = 17.(2)$
$s_{66} = 2.8(8)$	$c_{66} = 39.(9)$

The values above are all based on static observations. The first three values in each column are probably reliable within less than 1 per cent; considerably less reliance can be placed on the remaining values.

How accurately the data in Table XI may be applied in vibrational equations is not yet certain. As stated on page 138, it is not impossible that the stiffness coefficients are inherently greater (and the compliance coefficients correspondingly smaller) in the dynamic than in the static case. If so, it may well be that the values obtained by Atanasoff and Hart should be used in all h-f calculations.

Other Determinations of Elastic Constants of Quartz. In the extensive literature on quartz resonators many more or less trustworthy determinations of certain of the elastic coefficients, especially s_{11}, are

* The calculations were carried out by M. E. White.

found. Some of the more noteworthy results will now be summarized, although they do not seem to warrant a revision of the values given above.

Giebe and Scheibe[171] determined s_{11} from dynamic observations on quartz rods having lengths parallel to X or Y. They found the measurements most trustworthy when the rods were not too thin and when the elastic constant was calculated from vibrations at the third or fourth overtone frequency. Their electrodes were so small that the effective air gap was practically infinite, which necessitated, in the case of rods parallel to Y, applying a piezoelectric correction to the measured s_{11} (§235). They computed, for rods parallel to X, $s_{11} \times 1.277_5(10^{-12}) \pm 0.06$ per cent; parallel to Y (uncorrected), $s_{11} = 1.265_6(10^{-12}) \pm 0.06$ per cent. After the piezoelectric correction has been made, the latter value becomes 1.277. We may take $s_{11} = 1.277$ as their best value.

From an extensive study of the effects of cross section the same investigators derive for the ratio s_{11}/s_{33} the value 1.149, in good agreement with Voigt's value of 1.145. By the use of the value 1.149 they calculate $s_{33} = 0.968(10^{-12})$.

Giebe and Blechschmidt,[161] from the vibrations of a hollow quartz cylinder with length parallel to Z, found $s_{11} = 1.256(10^{-12})$, $s_{33} = 0.978(10^{-12})$, $s_{13} = -0.130(10^{-12})$. In a later paper[162] on the lengthwise vibrations of bars, they give $s_{11} = 1.278(10^{-12})$, $s_{44} = 2.016(10^{-12})$, $s_{12} = -0.167(10^{-12})$. These values are not corrected for the piezoelectric reaction discussed in §235. For the temperature coefficients they find, for s_{12}, $-1{,}200(10^{-6})$ and, for s_{44}, $+176(10^{-6})$.

Osterberg and Cookson[406] excited compressional lengthwise vibrations in the X-direction in a large number of plates of various shapes. Although some of the plates had breadths comparable with the lengths, all calculated values of s_{11}, for "harmonics" as well as for the fundamental frequency, lie within about ± 1.5 per cent of the mean, $1.27(10^{-12})$. From their observations on vibrations in the Z-direction (excited through elastic coupling) one finds $s_{33} = 0.963(10^{-12})$. In this latter work, however, it seems doubtful whether s_{33} was actually the only elastic coefficient that came into action.

In a comparison of Voigt's static values with the dynamic values of the foregoing constants it is noteworthy that in almost all cases the recorded dynamic compliances are less than the static even after the piezoelectric correction has been made. Whether the discrepancies are due to the numerous sources of error or to something more deep-seated cannot at present be determined. It should be noted that the dynamic values of s_{11} and s_{33} are in better agreement with those of Perrier and De Mandrot than with those of Voigt.

91. We turn now to a discussion of the *temperature coefficients* in Table X.

Bechmann has made very thorough studies of the effect of temperature on the adiabatic elastic constants of quartz, for which his papers* should be consulted. Some of his results are shown in Fig. 30. He claims, over a range from 20 to 70°C, a precision of ± 10 per cent in his measurements of the temperature coefficients, in the reduction of which due

* *Zs. Hochfrequenztech.*, 1934; *Zs. tech. Physik*, 1935.

allowance is made for the effects of temperature on dimensions and density. One cannot be very confident that the same values would be obtained from *static* observations at different temperatures, especially since one cannot be certain that in each of his measurements of frequency of plates in various orientations the effective elastic constant was of the theoretical form, unaffected by coupling with other vibrational modes.

From measurements between 25 and 95°C of frequencies of shear modes of thickness vibrations with plates in different orientations, Koga[272] derived the values given in Table X. These values are all greater than those of Mason and of Bechmann.

As is explained in §90, Atanasoff and Hart derived their temperature-coefficients from observations of high overtone frequencies of thickness vibrations. This procedure tends to minimize edge effects and coupling with undesired vibrations, difficulties from which the measurements of the other observers were less likely to be free. This fact, together with the high precision with which the observations of Atanasoff and Hart were obtained, justifies one in regarding their results as the most reliable.

Koga calculated also the average rate of change of three of the temperature coefficients over the range studied, by taking the second derivatives of his frequency equations with respect to T:

$$\frac{1}{c_{66}}\frac{\partial^2 c_{66}}{\partial T^2} = -6.1(10^{-8}) \qquad \frac{1}{c_{44}}\frac{\partial^2 c_{44}}{\partial T^2} = -1.3(10^{-6})$$

$$\frac{1}{c_{14}}\frac{\partial^2 c_{14}}{\partial T^2} = -7.7(10^{-7})$$

It is of the greatest significance that some of the temperature coefficients are positive, others negative. By cutting a plate in such an orientation that the effective stiffness coefficient q is a function of elastic constants having temperature coefficients of opposite signs, it is possible to obtain a resonator with frequency practically independent of temperature over a comparatively wide temperature range (§358).

A careful search for an *elastic aftereffect* in quartz was made by Joffé.[B30] His results show that, after secondary effects due to heating of the crystal have been eliminated, no true elastic aftereffect can be detected.

Measurements of the volume compressibility of quartz up to 12,000 kg/cm² have been made by Bridgman.* Hydrostatic pressure produces no piezoelectric polarization in quartz.

92. The Elastic Constants of Quartz at High Temperatures. Although nearly constant at ordinary temperatures, the elastic coefficients undergo very pronounced changes in the neighborhood of the α-β inversion at 573°C. The most complete data are those of Perrier

* P. Bridgman, *Am. Jour. Sci.*, vol. 15, pp. 287–296, 1928.

and De Mandrot,[413] illustrated in Fig. 29. These observers, using a static method, by flexure of thin bars, found Young's moduli $1/s_{11}$ and $1/s_{33}$ to decrease rapidly to values near $3(10^{10})$ dynes/cm^2 as the inversion point was approached, after which in the β-quartz state they rose rapidly. Above 573°, $1/s_{33}$ was found to be slightly smaller than at room temperature, while $1/s_{11}$ became even *greater* than was $1/s_{33}$ at room temperature. At ordinary temperatures they found s_{33} to increase by 0.02

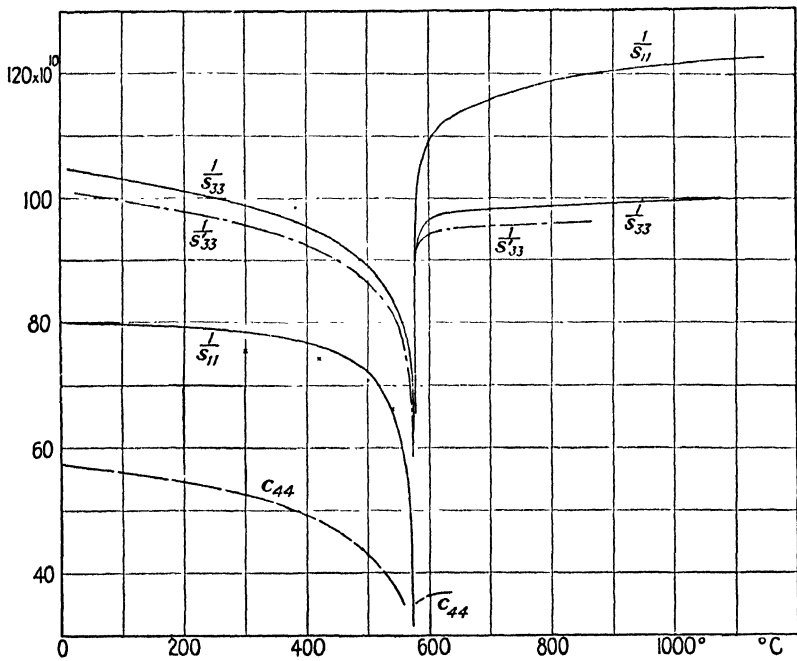


FIG. 29.—Dependence of elastic constants of quartz on temperature. Curves $1/s_{11}$ and $1/s_{33}$ are from Perrier and De Mandrot; $1/s'_{33}$ from Lawson, for the ZX-plane, at 45° to the Z- and X-axes; c_{44} from Atanasoff and Hart, and Atanasoff and Kammer. The crosses ($1/s_{11}$) are from the observations by Fréedericksz and Mikhailov.

per cent per degree rise in temperature, while for s_{11} the corresponding change was less than 0.001 per cent. A similarly small dependence of s_{11} upon temperature was also recorded by Fréedericksz and Mikhailov,[150] who used a dynamic method.

In Fig. 29 is shown also a curve relating $1/s'_{33}$ with temperature, for a Y-cut 45° quartz bar, from observations by Lawson.[311] The length of the bar bisected the angle between the X- and Z-axes; in this plane, as is clear from curve C in Fig. 33, it is immaterial whether the angle (here 45°) is taken as positive or negative. The bar was provided with

platinized electrodes and vibrated piezoelectrically at resonant lengthwise frequency. The piezoelectric effect was that represented by the equation $z'_z = d'_{23}E_y = -d_{14}E_y/2$. From the observed frequency at each temperature, with due regard to the density and dimensions, Young's modulus $1/s'_{33}$ was calculated.

Included in Fig. 29 is also a curve for c_{44}, from the observations of Atanasoff and Hart and of Atanasoff and Kammer, obtained by the method described in §90. The crosses in Fig. 29, representing $1/s_{11}$, are from a few data by Fréedericksz and Mikhailov,[150] from resonant observations on an X-cut bar in lengthwise vibration parallel to Y.

93. Stiffness Coefficients for Thickness Vibrations. We learned in §66 that when plane waves are propagated in crystals, the three mechanical displacements (vibration directions) corresponding to the three types of wave are mutually perpendicular and that in the most general case none of them is either normal or parallel to the wave front. The symmetry of quartz is such that for some types of orientation certain of the Christoffel moduli Γ disappear, so that the vibration directions for those modes lie either in the plane of the plate (shear vibrations) or normal to it (compressional vibrations).

As an example we consider the Y-cut, which, as is well known, vibrates in a shear mode (§352), with field E_y. In Eqs. (116), $l = n = 0$, $m = 1$, and certain of the c's vanish for quartz, whence $\Gamma_{11} = c_{66}$, $\Gamma_{22} = c_{11}$, $\Gamma_{33} = c_{44}$, $\Gamma_{23} = -c_{14}$, $\Gamma_{12} = \Gamma_{13} = 0$. The three roots of Eq. (118) (the order of subscripts is arbitrary) are

$$\left.\begin{aligned} q_1 &= c_{66} = \tfrac{1}{2}(c_{11} - c_{12}) = 39.1(10^{10}) \\ q_2 &= \tfrac{1}{2}(c_{11} + c_{44}) + \sqrt{\tfrac{1}{4}(c_{11} - c_{44})^2 + c_{14}^2} = 93.3(10^{10}) \\ q_3 &= \tfrac{1}{2}(c_{11} + c_{44}) - \sqrt{\tfrac{1}{4}(c_{11} - c_{44})^2 + c_{14}^2} = 49.2(10^{10}) \end{aligned}\right\} \quad (135)$$

Voigt's values of the fundamental constants, with the adiabatic correction, were used in this computation.

The vibration directions are found by solving Eqs. (117) for α, β, γ:[270]

$$\begin{array}{lll} \alpha_1 = 1 & \beta_1 = 0 & \gamma_1 = 0 \\ \alpha_2 = 0 & \beta_2 = -0.907 & \gamma_2 = -0.422 \\ \alpha_3 = 0 & \beta_3 = 0.422 & \gamma_3 = -0.907 \end{array}$$

The first of these vibration directions is therefore parallel to X and the wave is transverse, with wave front in the plane of the plate and the vibration direction also in this plane. This is the mode that is usually excited piezoelectrically; the driving stress is $X_y = -e_{26}E_y$. For the other two modes the vibration directions make angles of about 25° and −65° with the normal to the wave front.

A similar analysis for the X-cut shows that one mode (that which is commonly excited piezoelectrically) has its vibration direction normal

TABLE XII.—STIFFNESS COEFFICIENTS q FOR THICKNESS VIBRATIONS OF QUARTZ PLATES IN VARIOUS ORIENTATIONS

q = (value in table) $\times 10^{10}$ dyne cm^{-2}

θ \ φ →	30°	25° and 35°	20° and 40°	15° and 45°	10° and 50°	5° and 55°	0° and 60°	
0°	105.67 57.09 57.09	105 67 57.09 57.09	105 67 57 09 57.09	105.67 57.09 57.09	105.67 57.09 57.09	105 67 57.09 57.09	105.67 57.09 57.09	180°
15°	110.76 59.10 47.44	110.74 59.20 47.41	110.56 59.31 47.42	110.28 59 91 47.11	109 94 60.47 46.88	109.55 61.10 46.64	109.11 61.78 46 40	165°
30°	121 94 50 38 37 99	121.87 50.49 37 94	121 24 51.25 37.81	120 21 52.44 37 64	118 95 53.90 37.45	117 14 55 86 37 31	115 21 57.91 37.18	150°
45°	129 06 40.46 31.23	128 69 40.70 31.37	127 59 41.39 31 77	125.80 42.56 32 38	123 36 44.26 33 14	120 35 46.46 33 94	116 87 49.13 34 74	135°
60°	127 27 34.93 28 99	125.74 37.03 28 42	124.41 36 87 29 91	122.10 37.98 31.10	119.00 39 34 32.85	115.13 40.90 35.16	110 64 42.52 38.03	120°
75°	113 33 39.01 31 86	112.53 40.33 31.34	111 37 42.49 30 34	109.00 45 54 29 64	105.78 48.83 29.59	101 84 52.13 30.23	97.30 55.27 31 63	105°
90°	93.32 49.22 39.10	92.93 50.99 37 72	91.84 54.71 35.09	90 17 58.90 32 57	88.12 62 90 30 62	86 26 65.99 29.39	85.45 67 22 28.98	90°
105°	75 44 60 02 48.74	76.16 60.91 47 13	78.56 61 92 43.73	82 48 61 69 40.01	87 31 60.28 36 62	92.37 58.05 33.78	97.30 55 27 31 63	75°
120°	84.97 48.01 58 21	86.48 47.80 56 91	90.25 47.22 53 72	95.12 46 25 49.81	100.42 44.54 46 23	105 68 44.17 41.34	110.64 42.52 38 03	60°
135°	98.33 37.45 64.97	99 29 37.43 64 13	101.74 37.12 61.88	105.18 36.70 58.86	109.08 36.16 55.53	113 05 35.49 52 20	116.87 49.13 34.74	45°
150°	106.15 36.95 67 21	106 52 36 95 66 82	107.95 35 99 65 36	109.17 36 99 64 14	111 00 37.12 62 18	113.16 37.09 60 06	115.21 57 91 37.18	30°
165°	105 70 47.28 64.32	107.41 45.65 64.23	107.59 45 72 63.98	107 89 45.83 63.58	108 25 45 99 63 05	108 67 46.18 62 44	109.11 61.78 46.40	15°
180°	105.67 57.09 57.09	105.67 57.09 57.09	105.67 57.09 57.09	105.67 57.09 57 09	105.67 57.09 57.09	105 67 57.09 57.09	105.67 57.09 57.09	0°
	−30°	−25° and −35°	−20° and −40°	−15° and −45°	−10° and −50°	−5° and −55°	0° and 60°	↑ θ ← φ

to the plate; the two theoretical transverse modes have vibration directions in the plane of the plate, making angles of about 31° and −59° with the Y-axis.

For Y'-cuts (rotation about the X-axis) the direction of vibration that is excited in piezoelectric resonators can be shown to be parallel to X, as in the Y-cut. For this mode it is found that q is the same as Γ_{11}, which, for rotation about the X-axis ($l = 0$), and remembering that with quartz $c_{51} = c_{16} = 0$, reduces from the form given in Eqs. (116) to that in Eqs. (51):

$$q = c'_{66} = \Gamma_{11} = c_{66} \cos^2 \theta + c_{44} \sin^2 \theta + 2c_{14} \sin \theta \cos \theta \quad (136)$$

Here we have written sin θ for n, cos θ for m, θ being the angle (+ or − according to the rule in §38) between the Y-axis and the normal to the plate.

The numerical values of the three stiffness coefficients q_1, q_2, q_3 in plates with zero gap, for a large number of orientations in a quartz crystal, have been worked out by Koga[274] and are shown in Table XII. They are based on Voigt's data, with the adiabatic correction. By substitution in Eq. (112) the three theoretically possible frequencies for all these cuts can be found. Which, if any, of the three frequencies for any given cut can actually be realized must be determined by consideration of the piezoelectric constants of quartz. The direction of the normal to the plate is given in terms of φ, the angle of azimuth measured from $+X$ toward $+Y$, and the colatitude θ, as shown in Fig. 17. In copying the table from Koga's paper we have changed the values of φ to conform to the convention adopted in this book (§51).

In all cases the q's repeat themselves every 120° in azimuth; that is, ±120° may be added to every value of φ.

When values of φ at the foot of the table are used, the corresponding values of θ are at the right.

The Y'-cuts are those in the column for $\varphi = 30°$. When $\theta = 90°$, we have the Y-cut, with $q = c_{66} = 39.1(10^{10})$. The last of the three values for each θ belongs to the mode commonly observed with Y'-cuts. In order to correlate these values with those derived from Eqs. (51) for rotation about the X-axis we must set $\varphi = 90°$ in Table XII. Since $90° = -30° + 120°$, we use the values of θ at the right of the table. θ is then the same as the angle of rotation θ in Eqs. (51), for which we set $\cos \theta \equiv c$, $\sin \theta \equiv s$. The equation in (51) that applies in this case is the one for c'_{66}, which is the same as Eq. (136).

The X'-cuts (rotation about the Y-axis) are in the last column ($\varphi = 0$ and 60°). At $\theta = 90°$ we find the X-cut, with

$$q = c_{11} = 85.45(10^{10}).$$

The compressional mode persists as θ varies, at least for moderate changes in θ.

In the same paper, Koga shows some of the numerical data from Table XII in the form of polar diagrams.

For the X'-cuts a table has also been prepared by Bechmann,[32,34]

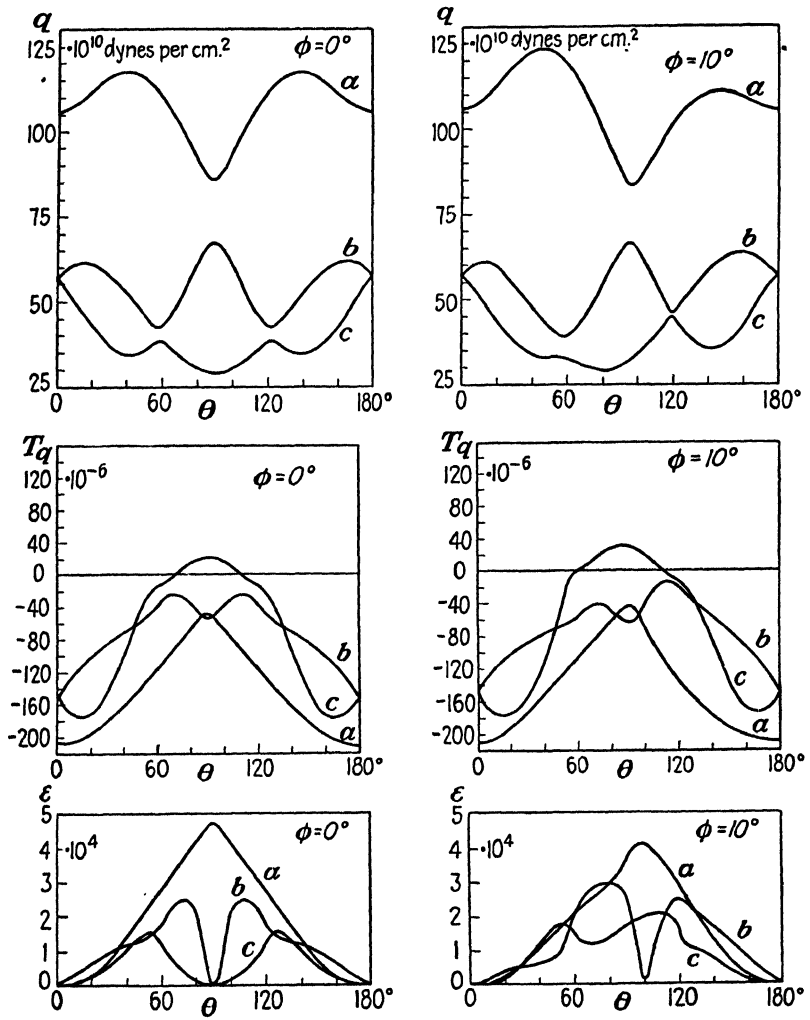
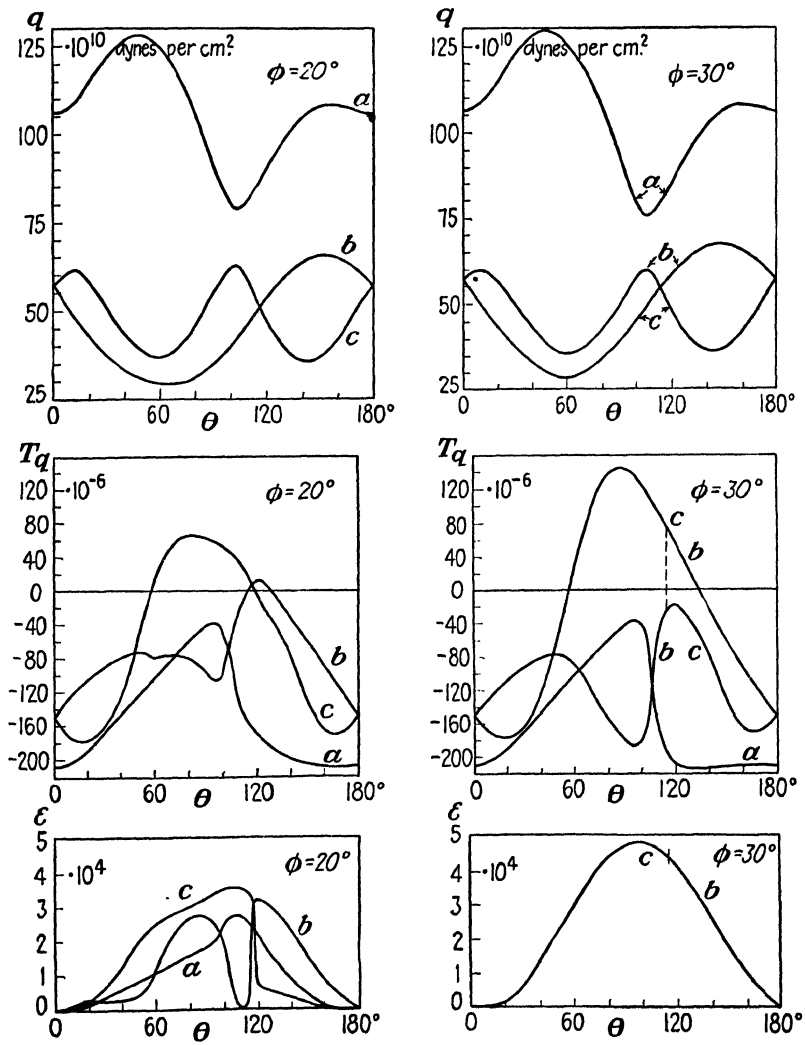


FIG. 30.—Elastic and piezoelectric constants of quarts for thickness vibrations in vibration-modes. To each q corresponds a temperature

giving the three q's for every 5° from $\theta = 0°$ to $\theta = 90°$, thus filling some of the gaps in Table XII.

In a later paper Bechmann[35] published a series of curves for the three Christoffel q's, their temperature coefficients T_q, and the effective piezoelectric constants ϵ, as functions of the polar angle θ, for azimuth $\varphi = 0$,



various directions, from Bechmann. The three values of q are for the three possible coefficient Tq, and an effective piezoelectric constant ϵ.

10, 20, and 30°. These curves* are reproduced in Fig. 30, in which φ and θ specify the direction of the normal to the plate, as in Fig. 17.

The curves for q are calculated from Voigt's adiabatic values of the fundamental elastic constants, as given in Table IX, uncorrected for piezoelectric reaction, but with due allowance for linear and volume expansion. They will be found to agree approximately with the values in Table XII, except that in some cases the values for curves b and c are interchanged. If the piezoelectric reaction were included, it would increase the values, at zero gap, by an amount varying from zero to about 0.2 per cent, depending on the value of ϵ. When $\varphi = 0$, $\theta = 90°$, we have an X-cut. At $\varphi = 30°$, $\theta = 90°$, it is a Y-cut. For most of the possible orientations, all three vibration directions make oblique angles with the surfaces of the plate. In those cases, as in the X-cut, where there is a pure compressional mode, the value of q is given by curve a.

Curve a for q at $\varphi = 0$ is the same as A in Fig. 34. Curves a, b, and c for $\varphi = 30°$ correspond to A, B, and C in Fig. 32. The mode commonly employed for cuts of this type is c.

The curves for T_q were derived from Bechmann's measurements of vibrational frequencies at temperatures from 20 to 60°C. In particular, they show the modes and orientations at which $T_q = 0$.

The curves for ϵ show the values of the piezoelectric coefficients that are effective in exciting the various modes for any orientation. It will be noted that ϵ vanishes for the Z-cut ($\theta = 0$ or 180°) and in certain other cases.

As an example may be mentioned the AT-cut, of which Bechmann was one of the independent originators. The normal to the plate is given by $\varphi = 30°$, $\theta = 55°$ (or $\varphi = 90°$, $\theta = -55°$). At this orientation $T_q = 0$; from the curve for $\varphi = 30°$, ϵ is found to be approximately $2.8(10^4)$, about half as great as for the Y-cut (for more precise data on the AT-cut see §358).

94. Diagrams of the Elastic Constants of Quartz with Respect to Rotated Axes. The variations in the elastic constants of quartz with rotation of the axial system about the X-, Y-, and Z-axes are shown in the following polar diagrams† (Figs. 31 to 36). The curves are plotted from Eqs. (50) to (54), with Voigt's isothermal values of the fundamental constants (Table IX).

In the polar diagrams the value of each s_{hk}, $1/s_{hk}$, or c_{hk} is laid off as radius vector corresponding to the angle of rotation θ; where there are negative as well as positive values, the magnitudes are measured from an arbitrarily chosen zero circle.

As an example of the use of the following diagrams we consider the Y'-cut, obtained by rotating a Y-cut about the X-axis through the angle θ. For thickness vibrations the elastic coefficient, by §93, is c'_{66}.

* Bechmann's values of the temperature coefficients of the fundamental elastic constants in Table X are from the same experimental data as Fig. 30.

† These diagrams are made available through the courtesy of Dr. W. P. Mason of the Bell Telephone Laboratories. In the present reproduction the sign of θ follows the convention adopted in §51. A few of the diagrams, necessary to complete the set, were prepared by the author.

INDEX FOR FIGS. 31 TO 36

Elastic constants of quartz for rotations about the X-, Y-, and Z-axes.
Values of s_{hk} are to be multiplied by 10^{-14} cm^2 dyne^{-1}.
Values of c_{hk} and $1/s_{hk}$ are to be multiplied by 10^{10} dyne cm^{-2}.

Fig.	Rotation about	Constants
31	X	$A, 1/s'_{11}$; $B, 1/s'_{22}$; $C, 1/s'_{33}$; $D, 1/s'_{44}$; $E, 1/s'_{55}$; $F, 1/s'_{66}$; G, s'_{12}; H, s'_{13}; I, s'_{14}; J, s'_{23}; $K, s'_{56}/2$; L, s'_{24}; M, s'_{34}
32	X	A, c'_{22}; B, c'_{44}; C, c'_{55}; D, c'_{12}; E, c'_{13}; F, c'_{14}; G, c'_{23}; H, c'_{56}; I, c'_{24}; J, c'_{34}
33	Y	$A, 1/s'_{11}$; $B, 1/s'_{22}$; $C, 1/s'_{33}$; $D, 1/s'_{44}$; $E, 1/s'_{55}$; $F, 1/s'_{66}$; G, s'_{12}; H, s'_{13}; I, s'_{23}; J, s'_{14}; K, s'_{36}; L, s'_{15}; M, s'_{45}
34	Y	N, s'_{16}; O, s'_{34}; P, s'_{24}; Q, s'_{26}; R, s'_{25}; S, s'_{46}; A, c'_{11}; B, c'_{44}; C, c'_{55}
35	Y	D, c'_{12}; E, c'_{13}; F, c'_{23}; G, c'_{14}; H, c'_{16}; I, c'_{15}; J, c'_{35}; K, c'_{16}; L, c'_{44}
36	Y	M, c'_{24}; N, c'_{26}; O, c'_{25}; P, c'_{46}
	Z	A, s'_{14}; B, s'_{15}; C, c'_{14}; D, c'_{15}

It is shown in Eqs. (51) that $c'_{66} = c'_{55}(\theta \pm 90°)$; we therefore turn to curve C for c'_{55} in Fig. 32. For any value of θ, the value of c'_{66} is the radius vector of curve C for $\theta \pm 90°$. Thus, if $\theta = -50°$, the value for $\theta = -50° + 90°$ on curve C shows that c'_{66} is approximately $32(10^{10})$ dynes/cm^2. For a more precise value the equation should be used. A glance at curve C shows the wide variation in the stiffness, and hence in the frequency of Y'-cut quartz plates as the angle is varied.

If, as is preferable, the orientation of the plate is specified in terms of the *normal* to its major surfaces, we find $\theta = 90°$ for the Y-cut. A little consideration shows that for any arbitrary angle θ beween the normal and the Z-axis, curve C for c'_{55} may be used directly to give the stiffness for thickness vibrations. By this convention the plate might more properly be called a Z'-cut, with the field parallel to the Z'-axis. Whether the Y'-cut is regarded as a Y-cut rotated $\theta°$ or as a Z-cut rotated $\theta° \pm 90°$ is a matter of definition.

95. Young's Modulus of Quartz. Approximate values for rotation about X can be obtained from Fig. 31, curves A, B, C, and for rotation about Y in Fig. 33, curves A, B, C.

Very careful static measurements of s_{11} and s_{33} have been made by Perrier and De Mandrot,[413] by means of the flexure of thin plates. They observed Young's modulus $\|Z$, $\perp Z$, also at $\pm 50°$ with Z in the YZ-plane. Their values at 15°C, in the units and terminology of Table IX (all $\times 10^{-12}$ cm^2/dyne), are $s_{11} = 1.272$, $s_{33} = 0.972$, $(s'_{33})_{+50} = 0.781$, $(s'_{33})_{-50} = 1.30$. These values of s_{11} and s_{33} are about 2 per cent lower than Voigt's isothermal values in Table IX. On the other hand, their value of $(s'_{33})_{50}$ is

very close to that calculated from Voigt's data. This fact would seem to indicate that, if their s_{11} and s_{33} are more nearly correct, Voigt's values of s_{44}, s_{13}, and s_{14}, which enter into the calculation for oblique directions (Eq. 55), are too small. All things considered, Perrier and De Mandrot's

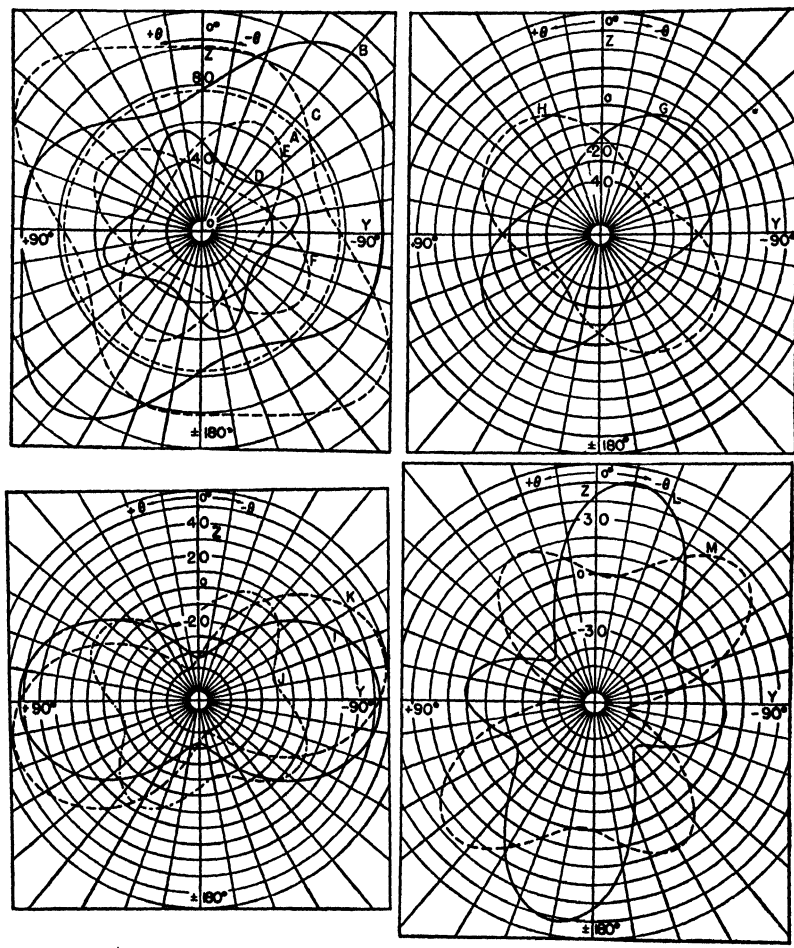


FIG. 31.—Elastic constants of quartz for rotation about the X-axis.

values of s_{11} and s_{33} are probably more reliable than Voigt's, and they are used in Fig. 38 and Table IX.

Young's modulus for various orientations is represented as a three-dimensional model in the paper by Perrier and De Mandrot, here reproduced in Fig. 37. The topographical features of the model for 15°,

typical of all ordinary temperatures, have their counterparts in Fig. 38 below. The only geometrical feature common to all the models is the fact that the equatorial section perpendicular to Z is circular. Below 573°C, sections normal to X have only a center of symmetry. There is a

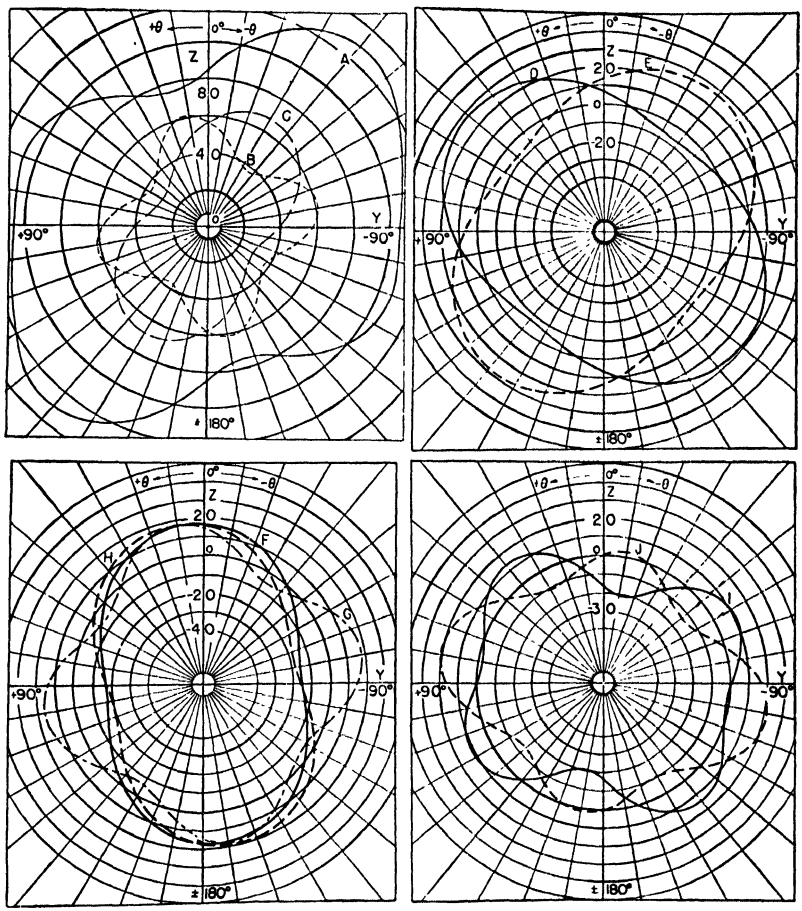


FIG. 32.—Elastic constants of quartz for rotation about the X-axis.

pronounced maximum and minimum in each of these sections, as well as a less pronounced secondary maximum and minimum, the latter being parallel to Z (see also the polar diagram in Fig. 31, curve C).

Starting at ordinary temperatures, the models contract in all directions with rising temperature, especially in the directions of the principal maxima. The maxima disappear completely at the transition point to

β-quartz. Above this point the surface dilates in all directions, but chiefly in the directions perpendicular to Z.

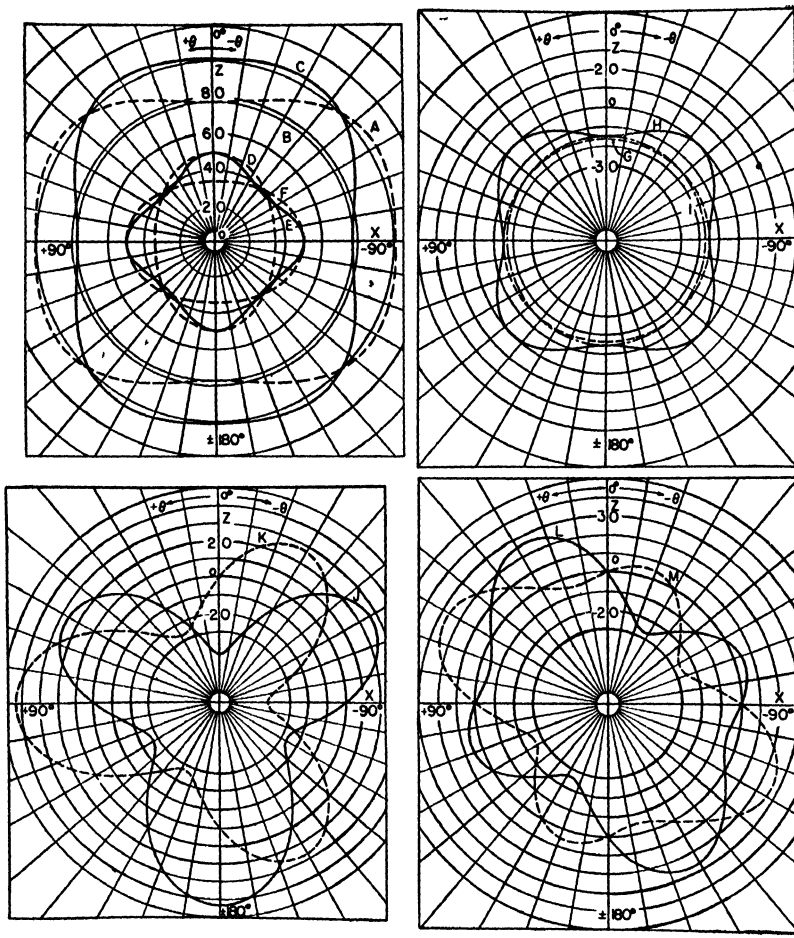


FIG. 33.—Elastic constants of quartz for rotation about the Y-axis.

96. From Fig. 38 the value of Young's modulus $Y = 1/s'_{33}$ for any direction in space can be found.* Equation (55) was used for the computation; for quartz it may be written in the form

$$s'_{33}(10^{12}) = 1{,}269 - 841\ \cos^2\theta + 543\ \cos^4\theta - 862\ \sin^3\theta\ \cos\theta\ \sin 3\varphi$$

* The calculations for these curves were made by M. E. White, using the fundamental constants from Table XI.

The azimuth φ and colatitude θ are defined according to Fig. 17. In conformity with the convention described in §327, Fig. 38 may be used without change for either right- or left-quartz.

The threefold symmetry of quartz about the Z-axis is indicated by the factor 3 in $\sin 3\varphi$. It will be observed that, at $\theta = \pm 90°$, Y has the

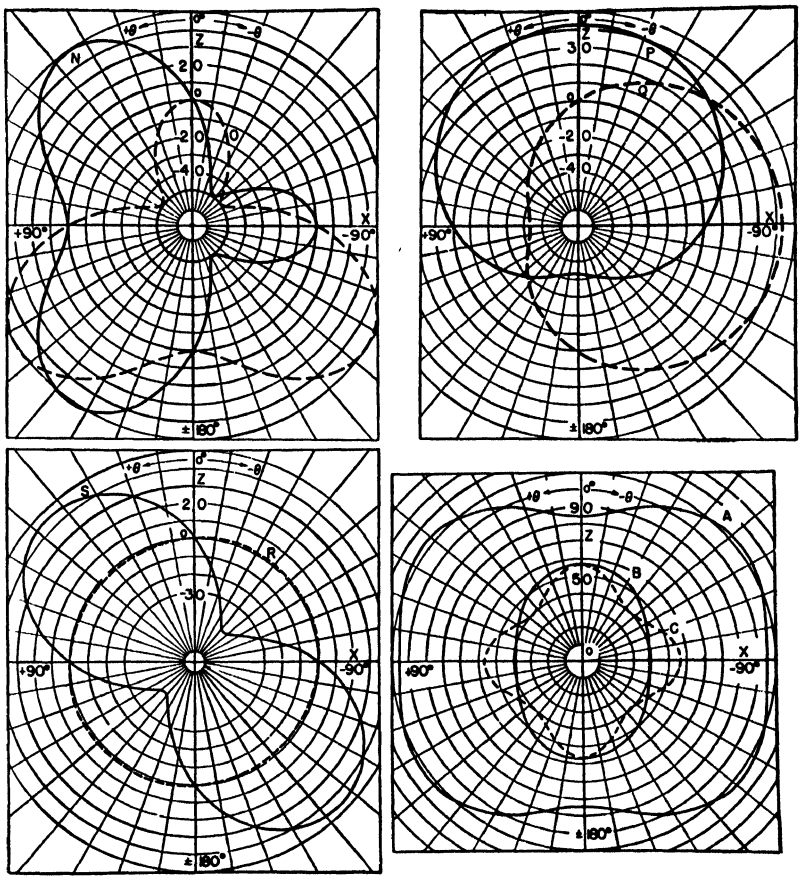


FIG. 34.—Elastic constants of quartz for rotation about the Y-axis.

same value for all azimuth angles: the elastic properties are the same for all directions in the XY-plane. When $\varphi = 0$, Y lies in the ZX-plane, and the Y-tensor is symmetrical about the Z-axis (see curve C in Fig. 33). On the other hand, when $\varphi = 30°$, Y lies in the YZ-plane and is not symmetrical about Z (see curve C in Fig. 31, also Fig. 76).

In applying Fig. 38 to values of φ outside the range from 0 to 30° the following rules may be found helpful for any given φ and θ:

If $-30° < \varphi < 0°$, use the ordinate for $-\varphi$, with the sign of θ reversed.

If $30° < \varphi < 60°$, use the ordinate for $60° - \varphi$.

If $-60° < \varphi < -30°$, use the ordinate for $60° + \varphi$ and reverse the sign of θ.

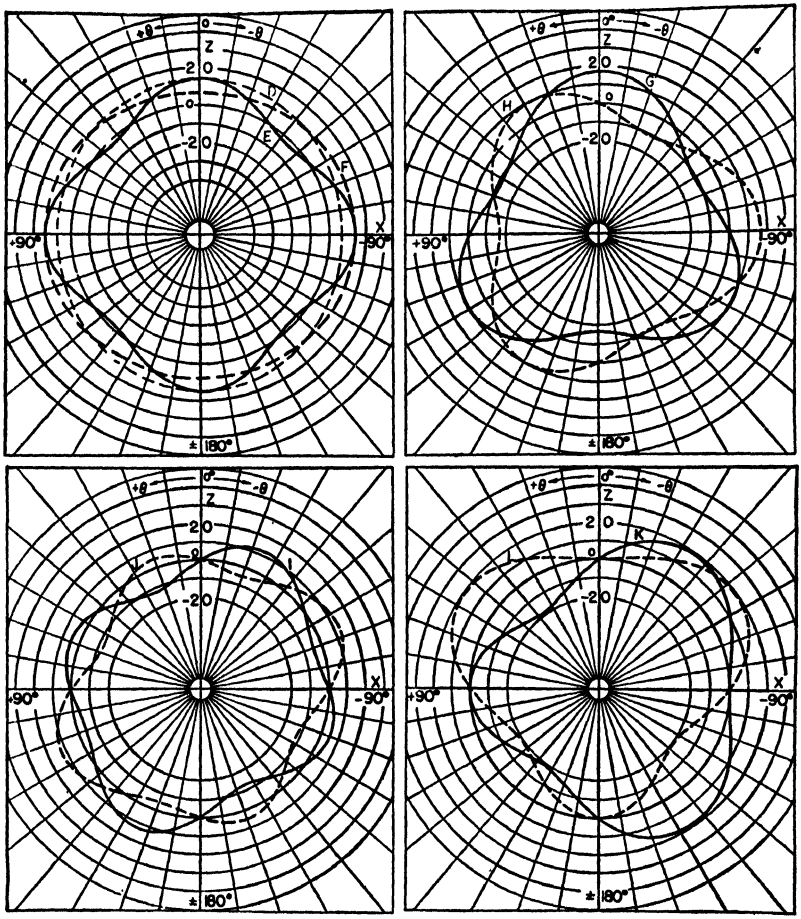


FIG. 35.—Elastic constants of quartz for rotation about the Y-axis.

If $60° < \varphi < 300°$, make use of the fact that Y is the same for $\varphi \pm 120°$ as for φ. Hence, if 120° is added to or subtracted from φ, the azimuth is brought within the range of one of the foregoing rules. In particular, if $\varphi = 90°$, the curve for 30° is used, with θ reversed.

As may be seen from Fig. 31 or 38, the largest and smallest values of Y fall in the YZ-plane. There are in this plane two maxima and two minima:

$\theta =$	48°36′	0	−9°45′	−71°4′
$10^{10}Y =$	130.8	103.0	103.2	70.3

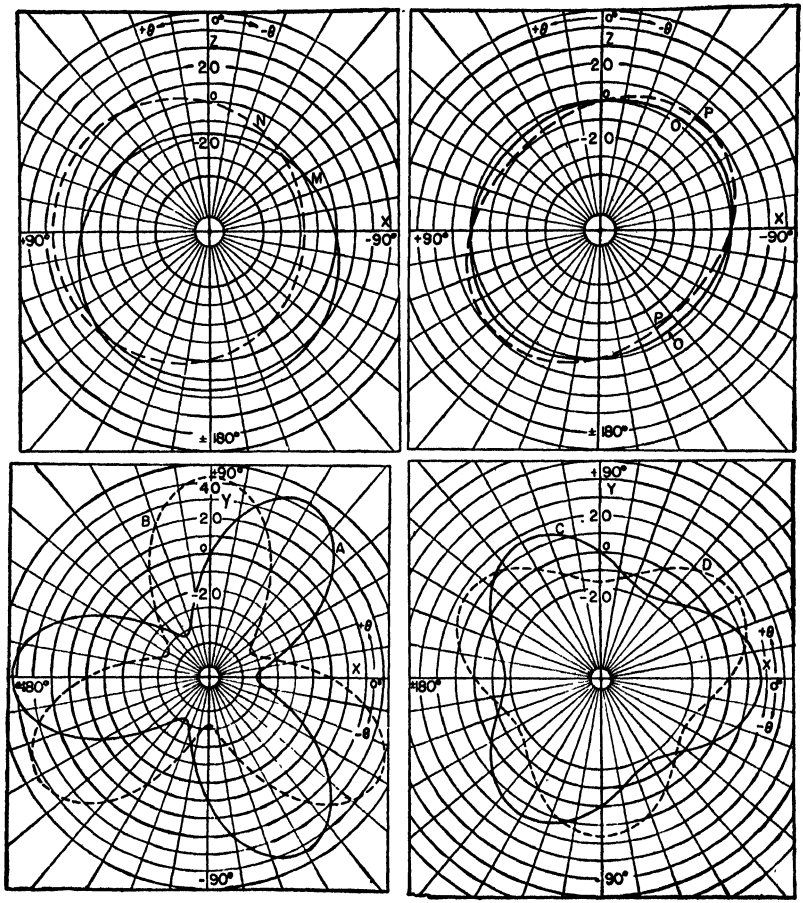


FIG. 36.—Elastic constants of quartz for rotation about the Y- and Z-axes.

Measurements of the frequency of quartz bars have been published by many observers. The most complete and trustworthy are those of Bechmann[32,35] and Mason,[340] from which their values of Young's modulus can be obtained. Bechmann's papers include the temperature coefficients for bars in various orientations, as stated in §91.

97. When a circular X-cut quartz disk is driven as a resonator, at relatively low frequencies corresponding to compressional waves propagated in the YZ-plane, it is found that for the lowest frequency there is a nodal line across the disk (revealed by lycopodium powder, §366), making an angle of about $+19°$ with the Z-axis. This angle indicates a direction of propagation parallel to the direction of *minimum* Y (Straubel[488]). In addition to more complex vibrational modes that need not be discussed here, there is also a simple compressional vibration at somewhat higher

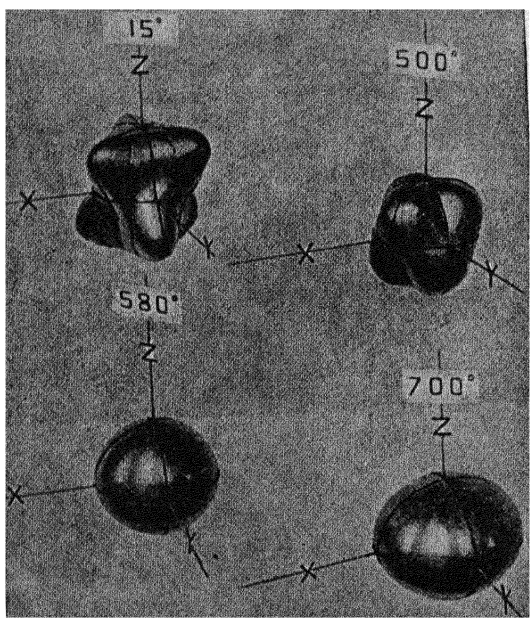


FIG. 37.—Models representing Young's modulus of quartz for all directions in space and at four different temperatures, from Perrier and De Mandrot.

frequency than that mentioned above, corresponding to *maximum* Y, with a nodal line about $-42°$ from the Z-axis. No vibration can be excited in the Y-direction in a circular plate.

These facts indicate that compressional waves tend to proceed in a direction normal to either the maximum or the minimum value of Young's modulus. The effect was first observed by Meissner[359,360,361] with rectangular plates having dimensions l, b, e parallel, respectively, to Y, Z, and X. For the fundamental compressional frequency in the Y-direction the nodal line across the center of the plate was not parallel to the breadth b, but made with b (*i.e.*, with the direction of the Z-axis)

an angle that for broad plates approximated 19°, becoming less for narrower plates. Correspondingly, the observed frequency agreed with that calculated from Young's modulus in the Y-direction only when the plate was in the form of a very narrow bar; with increasing breadth the frequency as well as the nodal line gave evidence of wave propagation that was no longer parallel to the length of the plate. This subject is discussed further in §350.

98. Modulus of Rigidity of Quartz. The compliance s'_{44} for any system of axes is given by Eq. (36). Its reciprocal is the rigidity, or

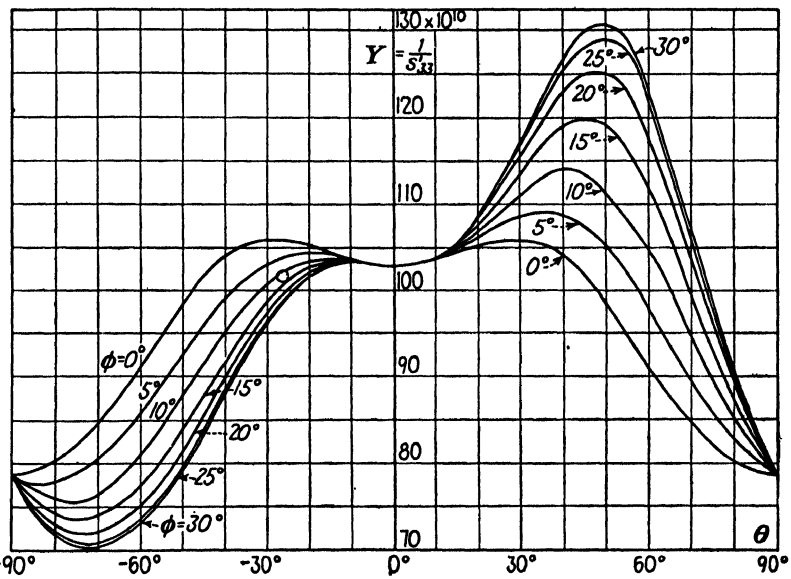


FIG. 38.—Young's modulus $Y = 1/s'_{33}$ for quartz, for azimuth φ from 0° to 30°, and polar angle θ from −90° to +90°.

resistance against shear, with respect to the axes Y' and Z'. By using the formula for s'_{44} in a somewhat modified form, with conventions of their own respecting angles, Wright and Stuart[594] have derived values for the rigidity with respect to axes Y' and Z' lying in planes containing the Z-axis. Their Fig. 21 shows in the form of curves the rigidity for three different azimuths about the Z-axis, in each case giving values for all orientations in the plane containing this axis.

Polar diagrams of the modulus of torsion for rectangular bars in different planes, with equations, are given by Voigt* and reproduced in Auerbach and Hort[B1].

* W. VOIGT, *Wiedemann's Ann.*, vol. 31, pp. 474, 701, 1887.

99. Poisson's Ratio for Quartz. The general formula for Poisson's ratio, as stated in §32, is $\sigma_{hk} = s_{hk}/s_{kk}$; it is a measure of the lateral contraction parallel to h accompanying an extension parallel to k. As long as the directions h and k are those of two of the crystallographic axes, σ is thus expressed directly in terms of fundamental constants. For specimens in oblique directions the formula given above would require a calculation of the primed compliances for each particular direction.

The calculation is simplified by the use of equations given by Wright and Stuart.[594] Using Voigt's values for the fundamental constants, they calculated σ for axes lying in planes containing the Z-axis, making various angles with this axis. Figure 22 in their paper shows the results, for three different azimuths. They draw attention to the fact that some of the more troublesome coupled vibrations can be avoided (for resonators designed for compressional vibrations) by choosing an orientation for which $\sigma = 0$. The absence of lateral motion also simplifies the problem of clamping the resonator at a nodal region without hampering the freedom of its vibrations.

From observations of frequencies of rods of varying relative dimensions and in different orientations effective values of σ have been computed by several writers. For example, Giebe and Scheibe[171] find $s_{12}/s_{11} = 0.132$, $s_{13}/s_{11} = 0.120$. Khol's value[258] of s_{12}/s_{11} is 0.135. From Voigt's data in Table IX one finds $s_{12}/s_{11} = 0.130$, $s_{13}/s_{11} = 0.119$.

Further consideration of Poisson's ratio, in its relation to coupling effects in piezoelectric resonators, will be found in Chap. XVII.

Other data on the elastic properties of quartz and of other forms of silica are given in the books by Sosman[B47] and Joffé.[B30]

100. Tourmaline (Class 19, symmetry C_{3v}). The axes for this class are defined in §5.

Below are the fundamental elastic constants, from static observations recorded in Voigt.* The difference between adiabatic and isothermal values is too small to change the last significant figure.

Dynamic values are available from various sources. For example, the experiments of Osterberg and Cookson[406] on tourmaline rods† yield $s_{11} = 38.6(10^{-14})$, $s_{33} = 60.0(10^{-14})$.

Observations of radial vibrations in circular Z-cut disks have been made by Khol,[258] from which are derived the values

$$s_{11} = 0.382(10^{-12}) \pm 0.5 \text{ per cent}, \qquad \sigma = s_{12}/s_{11} = 0.323 \pm 3 \text{ per cent}.$$

From similar observations by Petrzilka, Khol[259] calculates $s_{11} = 0.383(10^{-12})$, $s_{12}/s_{11} = 0.327$.

* P. 753.

† The quantities that they call c_{11} and c_{33} for tourmaline rods parallel to X and Z should be written as $1/s_{11}$ and $1/s_{33}$, respectively.

TABLE XIII

$\times 10^{-12}$ cm^2 dyne^{-1}		$\times 10^{10}$ dyne cm^{-2}	
$s_{11} = s_{22} =$	0.398	$c_{11} = c_{22} =$	270
$s_{33} =$	0.625	$c_{33} =$	161
$s_{44} = s_{55} =$	1.51	$c_{44} = c_{55} =$	67
$s_{12} =$	−0.103	$c_{12} =$	69
$s_{13} = s_{23} =$	−0.016	$c_{13} = c_{23} =$	8.8
$s_{14} = -s_{24} = s_{56}/2 =$	+0.058	$c_{14} = -c_{24} = c_{56} =$	−7.8

Several observers have measured the frequencies of compressional thickness vibrations of Z-cut plates. The following values of the wave constant (frequency in cycles) times (thickness in millimeters $\times 10^{-6}$) were found: Petrzilka,[415] 3.75; Matsumura and Ishikawa,[348] 3.97; Fox and Underwood,[148] 3.77; Straubel,[487] 3.52. Calling the average 3.75, we find for the average dynamic stiffness coefficient $c_{33} = 177(10^{10})$ dynes/cm^2.

Comparison with the static coefficients in Table XIII shows that all dynamic measurements recorded above yield greater stiffnesses and smaller compliances than those observed statically, just as is the case with quartz. The discrepancies are too great to be attributed to piezoelectric reactions alone.

Owing to the very small magnitudes of the cross constants, Poisson's ratio has extremely low values for tourmaline. As a consequence almost no correction for cross section is required for frequency in the longitudinal vibrations of bars. Giebe and Blechschmidt[162] found the overtone frequencies of a bar parallel to the Z-axis to stand in almost exact harmonic relation to the fundamental.

The effect of temperature on vibrational frequencies is discussed in §400.

In the "Lehrbuch"* are polar diagrams for s'_{33} in the YZ- and XZ-planes, based on Voigt's static measurements. The similarity to the C curves in Figs. 31 and 33 for quartz is close, the only qualitative difference being that, since tourmaline is not enantiomorphous, the terms "right" and "left" have no meaning.

101. Group VIII (Hexagonal). This group has nine constants, of which five are independent. The axes are explained in §5.

β-quartz (Class 24, symmetry D_6) is stable from 573 to 870°C. The only stresses that can be produced piezoelectrically are

$$Y_z = -e_{14}E_x = -c_{44}y_z$$

and

$$Z_z = +e_{14}E_y = -c_{55}z_z = -c_{44}z_z \qquad (\S168)$$

The values at different temperatures of s_{11}, s_{33}, $c_{44} = 1/s_{44}$, and s'_{33} (Y-cut 45° bar) have already been considered in §92. The first

* P. 755.

measurement of c_{44} was published in 1935 by Osterberg and Cookson,[404] who used shear vibrations of types $y_z = -s_{44}Y_z$ and $z_x = -s_{55}Z_x$ in rectangular X- and Y-cut plates, over the entire temperature range for β-quartz. They gave as their best value, at 600°C, $c_{44} = 19.9(10^{10})$ dynes/cm^2. The value diminished rapidly as the α-β transition point was approached. The value at 600° is only about half as large as that determined later by Atanasoff and Kammer.[13] As is pointed out by these authors, and also by Lawson,[311] neither the vibrational mode used by Osterberg and Cookson nor their theoretical treatment is well suited to a precise measurement of c_{44}. We therefore give preference to the work of Atanasoff and Kammer, whose results for c_{44} have already been shown in Fig. 29. These investigators found, at 600°C,

$$c_{44} = 35.76(10^{10}) \text{ dynes/cm}^2,$$

by the method described in §90. Recently, by a somewhat different method, Kammer and Atanasoff[251] determined all the elastic constants of β-quartz at 600°C, finding c_{44} practically identical with their former value.

In this last-named paper, Kammer and Atanasoff used high-harmonic vibrations of four different cuts, involving six different vibrational modes. The driving frequency was modulated at 60 cycles/sec. Each time the modulated frequency passed through the crystal frequency the quartz was set into vibration and continued for a small fraction of a second to vibrate at its own frequency while the driving frequency continued to change (the method was thus in principle similar to the "click" method described in §308). The resulting wave form was recorded on an oscillograph, and the resonant frequency thereby determined. Their results (all adiabatic) are $c_{11} = 118.4$, $c_{12} = 19.0$, $c_{13} = 32.0$, $c_{33} = 107.0$, $c_{44} = 35.8$, all $\times 10^{10}$; $s_{11} = 0.926$, $s_{12} = -0.0802$, $s_{13} = -0.252$, $s_{33} = 1.085$, $s_{44} = 2.79$, all $\times 10^{-12}$. In the YZ-plane, 45 and 50° from the Z-axis, $s'_{33} = 1.073(10^{-12})$ and $1.057(10^{-12})$, respectively.

Perrier and De Mandrot (§92) found, at 600°C, for s'_{33} at 50°, $1.075(10^{-12})$ and, for s_{33}, $1.050(10^{-12})$ (isothermal).

In the observations discussed in §92, Lawson found, at 600°C, s'_{33} at 45° to be $1.067(10^{-12})$ (adiabatic). In the same paper Lawson derives for s_{13} the adiabatic value $-0.226(10^{-12})$. Since Lawson's method was somewhat more direct than that of Kammer and Atanasoff, we are inclined to consider his values of s_{13} and of s'_{33} at 45° to be somewhat more reliable, while accepting the results of Kammer and Atanasoff for the remaining constants.

102. Group IX (Cubic). The axes for the cubic system are described in §5. Crystals in this group have nine fundamental elastic constants, of which only three have independent values.

Sodium Chlorate (Class 28, symmetry T). Voigt's static values,* reduced to cgs units, are

$$s_{11} = s_{22} = s_{33} = 2.46(10^{-12}) \qquad s_{12} = s_{13} = s_{23} = 1.25(10^{-12})$$
$$s_{44} = s_{55} = s_{66} = 8.36(10^{-12}) \text{ cm}^2 \text{ dyne}^{-1}$$
$$c_{11} = c_{22} = c_{33} = 65.0(10^{10}) \qquad c_{12} = c_{13} = c_{23} = -21.0(10^{10})$$
$$c_{44} = c_{55} = c_{66} = 11.9(10^{10}) \text{ dyne cm}^{-2}$$

Zinc Blende (Class 31_4, symmetry T_d). One of Voigt's latest papers was an account of his measurement† of the elastic constants of this crystal. His values (static method), in cgs units, are

$$s_{11} = 1.94(10^{-12}) \qquad s_{23} = -7.30(10^{-12}) \qquad s_{44} = 22.9(10^{-12}) \text{ cm}^2 \text{ dyne}^{-1}$$
$$c_{11} = 9.42(10^{11}) \qquad c_{23} = +5.68(10^{11}) \qquad c_{44} = 4.36(10^{11}) \text{ dyne cm}^{-2}$$

* "Lehrbuch," p. 741.

† W. VOIGT, *Nachr. Ges. Wiss. Göttingen, Math.-physik. Klasse*, 1918, pp. 424–450.

CHAPTER VII

DIELECTRIC PROPERTIES OF CRYSTALS

Amongst the actions of different kinds into which electricity has conventionally been subdivided, there is, I think, none which excels, or even equals in importance that called Induction. —FARADAY.

We summarize here the basic equations, first for isotropic media and then for crystals, including the case in which the crystal plate is separated by a gap from the electrodes. A short discussion is given of the molecular nature of polarization, dipole theory, and losses in dielectrics.

103. When a flat slab of any solid dielectric of large area is placed in a uniform electric field E_0, with its normal parallel to the field, the basic dielectric equations are

$$\boldsymbol{D} = k_0\boldsymbol{E}_0 = k\boldsymbol{E} = \boldsymbol{E} + 4\pi\boldsymbol{P} \tag{137}$$

where $\boldsymbol{D}$ is the electric displacement, $\boldsymbol{E}_0$ and $\boldsymbol{E}$ the field strengths outside and in the dielectric (dynes per unit charge), k_0 and k the permittivities of the surrounding medium and of the dielectric, and $\boldsymbol{P}$ the polarization (electric moment per unit volume). $\boldsymbol{E}$ is also called the "potential gradient" or in practical units the "voltage gradient" (volts per centimeter) The electrostatic cgs system of units is used except where it is otherwise specified.

Since the surrounding medium is usually air or vacuum, k_0 may be considered as having the numerical value unity. Except with reference to the dimensions of piezoelectric coefficients (§128), we shall not be concerned with the question of the dimensions of k_0 or k, and the terms "permittivity" and "dielectric constant" will be treated as synonymous

In isotropic materials the polarization is always parallel to the field; all quantities in Eq. (137) may then be written as scalars. In crystals, however, P and E may have different directions.

104. Ignoring for the present *spontaneous* polarization (§115), we have the general relation between $\boldsymbol{E}$ and $\boldsymbol{P}$,

$$\boldsymbol{P} = \eta\boldsymbol{E} \tag{138}$$

where η is the *dielectric susceptibility*, analogous to the magnetic susceptibility (§547).

From Eqs. (137) and (138) follows the relation

$$k = 1 + 4\pi\eta \tag{139}$$

We have already seen in §21 that in piezoelectric crystals k depends on the state of mechanical constraint. In later sections we shall use the symbols k' and η' for crystals that are under constant stress, k'' and η'' for constant strain. So far as one can speak of the "true" dielectric constant of a piezoelectric crystal, the value k'' at constant strain is the proper one to use. Strictly, both the constrained (constant-strain) state and the state of constant stress, including the *relaxed* state in which all external stresses are removed, are idealized conditions, which cannot be exactly realized in the laboratory. Rochelle salt is so extremely strain-sensitive that an approximation to the relaxed state sufficient for even roughly approximate results is difficult. Fortunately, with most piezoelectric crystals the values of k' and k'' differ by a very small amount, so that the distinction is of small consequence. For quartz, in directions perpendicular to the (optic) Z-axis, the difference amounts to about 2 per cent. For the present this distinction can be disregarded, since the general relations hold whether the crystal is clamped or free. Except in §114 it will be assumed that the dielectric coefficients are independent of the field. For a discussion of *differential permittivity* see §430. The quantities $\boldsymbol{P}$ and $\boldsymbol{E}$, which are vectors, are related by the coefficient η, just as in elasticity X_h and x_k are related by s_{hk} and in thermodynamics quantity of heat and temperature are related by the specific heat C (§20).

At the surface of any dielectric, whether isotropic or not, in an electric field, the quantities that are the same on both sides of the boundary are the normal component of displacement and the tangential component of field strength. Nevertheless, when this law of electric refraction is applied to crystals, it is found in general, even when the field is normal to the crystal surface, that the polarization and hence the *total* displacement are in some oblique direction.

105. The general relation between polarization and field in a crystal may be found by taking the derivative of ζ with respect to E_j in Eq. (2), letting the mechanical stresses and the temperature remain constant:

$$\frac{\partial \zeta}{\partial E_j} = \sum_k^3 \eta_{jk} E_k = P_j \qquad (j = 1, 2, 3)$$

When this expression is expanded we have the following equations due to Kelvin:*

* Voigt, p. 415.

In these equations, as in most cases throughout this book, the vectors are not

$$\left.\begin{aligned} P_1 &= \eta_{11}E_1 + \eta_{12}E_2 + \eta_{13}E_3 \\ P_2 &= \eta_{21}E_1 + \eta_{22}E_2 + \eta_{23}E_3 \\ P_3 &= \eta_{31}E_1 + \eta_{32}E_2 + \eta_{33}E_3 \end{aligned}\right\} \tag{140}$$

The subscripts 1, 2, 3 refer to the orthogonal crystallographic X-, Y-, Z-axes or, in transformed coordinates, to the X'-, Y'-, Z'-axes. Such quantities as $\eta_{hk}(h \neq k)$ may be called *cross susceptibilities*, analogous to the cross compliances s_{hk} in elasticity; they relate a field along one axis to a polarization parallel to another axis. As will be seen, these cross constants are present only in triclinic and monoclinic crystals. In all cases $\eta_{hi} = \eta_{ih}$.

Corresponding to Eqs. (140) are the following equations for components of displacement:

$$\left.\begin{aligned} D_1 &= k_{11}E_1 + k_{12}E_2 + k_{13}E_3 \\ D_2 &= k_{21}E_1 + k_{22}E_2 + k_{23}E_3 \\ D_3 &= k_{31}E_1 + k_{32}E_2 + k_{33}E_3 \end{aligned}\right\} \tag{141}$$

The dielectric constants are related to the susceptibilities thus:*

$$k_{hh} = 1 + 4\pi\eta_{hh} \qquad k_{hi} = k_{ih} = 4\pi\eta_{hi} \quad (h \neq i) \tag{142}$$

These equations make clear the distinction between the cross coefficients, of form k_{hi} or η_{hi}, and those of form k_{hh} or η_{hh}, which may be termed the *direct* coefficients; any of the former may vanish for certain crystal groups (as they do for isotropic substances), but the latter never. From $k_{hi} = k_{ih}$ it is evident that the k's and η's are *symmetric* tensors.

The greatest possible number of independent η's (or k's) is six, but in all systems except triclinic the number is less, becoming one for cubic crystals. By combining the ellipsoidal symmetry inherent in the η's (§112) with the crystalline symmetry, Voigt shows that the constants may be classified according to the seven systems, as follows:

TABLE XIV

Systems	Susceptibilities					
1	η_{11}	η_{22}	η_{33}	η_{23}	η_{31}	η_{12}
2	η_{11}	η_{22}	η_{33}	0	0	η_{12}
3	η_{11}	η_{22}	η_{33}	0	0	0
4, 5, 6	η_{11}	η_{11}	η_{33}	0	0	0
7	η_{11}	η_{11}	η_{11}	0	0	0

printed in boldface type. There will be but little occasion to use the methods of vector analysis, and wherever directional properties are considered they will be made clear by appropriate subscripts.

* VOIGT, p. 436.

The same tabulation holds also for the k's. The classification is valid only with respect to the *crystallographic* axes: in general, when rotated axes are used, the crystal loses some of its symmetry, and the number of effective constants increases. Formulas for transformation are given in §107.

106. We shall have occasion to express the components of field strength in the crystal in terms of those of polarization. If Eqs. (140) are solved for the E's, a new set of constants appears, which are functions of the η's and may be termed the coefficients of *dielectric stiffness*, χ. The three equations are

$$E_j = \sum_h^3 \chi_{jh} P_h = \chi_{j1} P_1 + \chi_{j2} P_2 + \chi_{j3} P_3 \quad (j = 1, 2, 3) \quad (143)$$

Here $\chi_{jh} = \chi_{hj}$. In order to express any χ_{jh} in terms of the η's, the method outlined in §26 is used. The general formula is

$$\chi_{jh} = \frac{S_{jh}}{D} \quad (144)$$

where D is the determinant of all the η's and S_{jh} is the cofactor with respect to η_{jh}. For example, $\chi_{13} = (\eta_{21}\eta_{32} - \eta_{31}\eta_{22})/D$. The vanishing of any η_{jh} does not necessarily imply the vanishing of the corresponding χ_{jh}. Nevertheless, in systems of higher symmetry than monoclinic, all cross susceptibilities ($j \neq h$) vanish, and $\chi_{jj} = 1/\eta_{jj}$ as long as the subscript refers to one of the crystallographic axes. With respect to rotated axes, this simple relation no longer holds in general (see §107). In an isotropic material there is but one η, so that $\chi = 1/\eta$ for all orientations.

Equations analogous to (143) can be derived from Eqs. (141), expressing the components of E in terms of those of the displacement D. The coefficients θ_{jh} in this case are of the nature of reciprocal permittivities, called by Kelvin the "dielectric impermeability":*

$$E_j = \sum_h^3 \theta_{jh} D_h = \theta_{j1} D_1 + \theta_{j2} D_2 + \theta_{j3} D_3 \quad (j = 1, 2, 3) \quad (145)$$

Expressions for the θ_{jh} in terms of the E_j will be needed for deriving the equations for elastic coefficients at constant electric displacement. They are found in the manner indicated above for the χ_{jh}. The general formula is

$$\theta_{jh} = \frac{S_{jh}}{D} \quad (146)$$

* VOIGT, p. 441.

where D is the determinant of all the k's and S_{jh} is the cofactor with respect to k_{jh}.

For brevity, it is permissible to use a single subscript x, y, or z (or 1, 2, or 3) for k, η, and θ whenever there are no cross constants, so that both field and polarization are parallel to the axis indicated (see §112 concerning the "principal susceptibilities" and footnote on page 44 for the use of subscripts). Thus $k_x \equiv k_{11}$; and for a transformed axis X' we may write k'_x, etc. Where there is no ambiguity, the subscripts may be omitted altogether.

107. Dielectric Constants with Respect to Rotated Axes. Since the symmetry of crystals (excepting triclinic) is usually lowered when the frame of reference is other than the fundamental crystallographic axes, certain cross constants of form k_{jh} and η_{jh} ($j \neq h$) may be expected to be present in the transformed system. In general, all coefficients are altered by the transformation.

The transformed coefficients occur in the expressions for the elastic constants at constant displacement and at constant polarization (Chap. XII). They must also be taken into account when the resonator theory is applied to oblique bars or plates.

By a method analogous to that outlined in §40, any η'_{jh} can be derived. The direction cosines of the rotated axes are given in §38. In terms of the fundamental susceptibilities, the value of η'_{jh} in the most general form is

$$\eta'_{jh} = l_j(l_h\eta_{11} + m_h\eta_{12} + n_h\eta_{13}) + m_j(l_h\eta_{21} + m_h\eta_{22} + n_h\eta_{23}) + n_j(l_h\eta_{31} + m_h\eta_{32} + n_h\eta_{33}) \quad (147)$$

For *quartz*, the only fundamental susceptibilities are $\eta_{11} = \eta_{22} = \eta_\perp$, and $\eta_{33} = \eta_\parallel$, perpendicular and parallel, respectively, to the Z-axis.

$$\eta'_{jh} = (l_j l_h + m_j m_h)\eta_\perp + n_j n_h \eta \quad (148)$$

For a *quartz plate, rotated through the angle θ about the X-axis*, $l_1 = 1$, $l_2 = l_3 = m_1 = n_1 = 0, m_2 = n_3 = \cos\ \theta \equiv c$, $n_2 = -m_3 = \sin\ \theta \equiv s$, so that the only susceptibilities which contribute to the polarization when the field is E'_2 in the Y'-direction (direction of thickness of plate) are

$$\left.\begin{aligned} \eta'_{22} &= m_2^2\eta_\perp + n_2^2\eta_\parallel = c^2\eta_\perp + s^2\eta_\parallel \\ \eta'_{32} &= m_3 m_2\eta_\perp + n_3 n_2\eta_\parallel = cs(\eta_\parallel - \eta_\perp) \\ \eta'_{33} &= m_3^2\eta_\perp + n_3^2\eta_\parallel = s^2\eta_\perp + c^2\eta_\parallel \end{aligned}\right\} \quad (149)$$

In quartz the difference $(\eta_\parallel - \eta_\perp)$ is so small that the cross susceptibilities in oblique fields can usually be ignored.

Similarly, one finds for the permittivities that contribute to the total polarization in a quartz plate rotated about the X-axis as indicated above, the expressions

$$k'_{22} = c^2k_\perp + s^2k_\parallel \qquad k_{33} = s^2k_\perp + c^2k_\parallel \qquad k'_{23} = cs(k_\parallel - k_\perp) \quad (150)$$

In general, any rotated permittivity k'_{jh} is expressed by an equation similar to (147):

$$k'_{jh} = (l_j l_h k_{11} + l_j m_h k_{12} + l_j n_h k_{13}) + (m_j l_h k_{21} + m_j m_h k_{22} + m_j n_h k_{23}) + (n_j l_h k_{31} + n_j m_h k_{32} + n_j n_h k_{33}) \quad (151)$$

For quartz, the coefficient relating the polarization in any direction j to an impressed field in the h-direction, or vice versa, is

$$k'_{jh} = (l_j l_h + m_j m_h) k_\perp + n_j n_h k_\parallel) \quad (152)$$

In most practical applications of quartz the effective dielectric constant is expressed in terms of the constant k' for the free crystal, taken in a direction parallel to that of the field (§§235, 247). The expression for k' is found by setting $j = h$ in Eq. (152), giving, for a field in the h-direction,

$$k'_h \equiv k' = (l_h^2 + m_h^2) k_\perp + n_h^2 k_\parallel = k'_\perp + n_h^2 (k'_\parallel - k'_\perp)$$
$$= 4.5 + 0.1 n_h^2 \quad (153)$$

where n_h is the cosine of the angle between the h-direction and the Z-axis.

108. For crystals of symmetry higher than monoclinic, the *total polarization* P produced by a uniform field E having direction cosines l, m, n can be found from Eqs. (140):

$$P = E \sqrt{(l\eta_{11})^2 + (m\eta_{22})^2 + (n\eta_{33})^2} \quad (154)$$

In general, P is not parallel to E. The divergence is greater the wider the disparity between η_{11}, η_{22}, and η_{33}. Equation (154) is applicable also when the axes are rotated; in this case all electrical quantities should be primed.

The *dielectric constant* in the direction *parallel to the field* is

$$k_N = 1 + 4\pi\eta_N,$$

where, for crystals of any class,

$$\eta_N = l^2\eta_{11} + m^2\eta_{22} + n^2\eta_{33} + 2mn\eta_{23} + 2nl\eta_{31} + 2lm\eta_{12} \quad (155)$$

The subscript N denotes the direction of the normal to the plane-parallel plate to which the field E, with direction cosines l, m, n, is applied. Equation (155) can be used for rotated axes by priming all the η's.

When the symmetry is higher than monoclinic, the polarization normal to the plate is

$$P_N = P_1 l + P_2 m + P_3 n = (l^2\eta_{11} + m^2\eta_{22} + n^2\eta_{33})E \equiv \eta_N E$$

where
$$\eta_N = l^2\eta_{11} + m^2\eta_{22} + n^2\eta_{33} \quad (156)$$

Similarly,
$$k_N = l^2 k_{11} + m^2 k_{22} + n^2 k_{33} \quad (157)$$

In order to calculate the *coefficients* $(\chi_{jh})'$ *or* $(\theta_{jh})'$ *for rotated axes,* it is usually necessary first to derive the entire matrix of transformed susceptibilities $(\eta_{jh})'$ or $(k_{jh})'$, respectively, as indicated above. The desired coefficients are then found by means of equations analogous to (144) and (146).

For *quartz* the calculation is relatively simple. For example, with plates rotated through the angle θ about the X-axis (as in the AT-cut, etc.), the only values that do not vanish are

$$(\chi_{11})' = \frac{1}{\eta_\perp}(\chi_{22})' = \frac{(\eta_{33})'}{S'_{11}} \qquad (\chi_{33})' = \frac{(\eta_{22})'}{S'_{11}} \qquad (\chi_{23})' = -\frac{(\eta_{23})'}{S'_{11}} \tag{158}$$

where $S'_{11} \equiv (\eta_{22})'(\eta_{33})' - (\eta_{23}^2)'$.
The corresponding $(\theta_{jh})'$ may be reduced to the form

$$\left.\begin{aligned} (\theta_{11})' &= \frac{1}{k_\perp} \qquad (\theta_{22})' = \frac{(k_{33})'}{k_\perp k_\parallel} = \frac{s^2 k_\perp + c^2 k_\parallel}{k_\perp k_\parallel} \\ (\theta_{33})' &= \frac{(k_{22})'}{k_\perp k_\parallel} = \frac{c^2 k_\perp + s^2 k_\parallel}{k_\perp k_\parallel} \qquad (\theta_{23})' = \frac{(k_{23})'}{k_\perp k_\parallel} = \frac{cs(k_\parallel - k_\perp)}{k_\perp k_\parallel} \end{aligned}\right\} \tag{159}$$

In Eqs. (158) and (159) the primes refer to rotated axes and do not indicate that the crystal is mechanically free. On the contrary, in some of those elastic equations in which these coefficients occur the crystal is free, and in others it is clamped (see §206).

As an example we consider the coefficients $(\theta''_{11})'$ and $(\theta''_{23})'$ for a clamped quartz plate rotated 45° about the X-axis. Coefficients of this type, with differing degrees of rotation, are used in deriving the elastic constants from thickness vibrations of cuts of AT-type. We have, from §331, $k''_\perp = 4.41$, $k''_\parallel = k_\parallel = 4.6$, $cs = 0.5$, so that

$$(\theta''_{11})' = 0.226 \qquad (\theta''_{23})' = -0.00465 \tag{160}$$

The cross constant $(\theta''_{23})'$ is small enough to be neglected in most calculations.

109. *Expressions for Energy in a Dielectric.* In Eq. (1) we saw that Voigt's expression for the energy per unit volume in terms of field components was $\frac{1}{2}\sum_k^3 \sum_m^3 \eta_{km} E_k E_m$, corresponding to $\frac{1}{2}\eta E^2$ for isotropic bodies. It can be shown from Eqs. (140) and (143) that the energy in terms of components of *polarization* is

$$\text{Energy} = \tfrac{1}{2}\sum_k^3 \sum_m^3 \chi_{km} P_k P_m$$

This expression corresponds to $P^2/2\eta$ for isotropic bodies.

110. Effect of an Air Gap on Polarization. A plane-parallel slab of dielectric of permittivity k, thickness e, and infinite area is placed between parallel electrodes spaced at a distance $e + w$ apart, w being the gap width, air or vacuum. It is immaterial whether the gap is all on one side of the dielectric, as shown in Fig. 39, or partly on each side. Let E_w be the field in the gap, E that in the slab, V the potential difference between the electrodes, V_1 the potential drop across the slab, and $\pm\sigma$ the charge density on the electrodes. Vectors are positive when to the right. E and P are assumed to be normal to the slab.

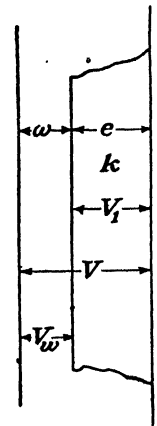


FIG. 39.—Slab of dielectric between parallel electrodes.

1. The following equations hold universally, whether the slab is piezoelectric or not, provided that the polarization is parallel to the field. If it is piezoelectric, the solution given in (2) can be superposed on that now to be considered. As in Eq. (137), the electric displacement is

$$D = kE = E_w = 4\pi\sigma = \frac{kV_1}{e} = \frac{V_w}{w} \tag{161}$$

For brevity, we let e' stand for $e + kw$; e' may be called the "electric spacing" between electrodes:

$$e' = e + kw \tag{162}$$

The following relations are easily derived:

$$E_w = \frac{kV}{e'} \tag{163a}$$

$$E = \frac{V}{e'} \tag{163b}$$

$$V_1 = \frac{eV}{e'} \tag{163c}$$

$$P = \frac{\eta V}{e'} = \frac{k-1}{k}\sigma \tag{163d}$$

$$\sigma = \frac{kV}{4\pi e'} = \frac{kV_1}{4\pi e} \tag{163e}$$

It should be noted that when $w = \infty$, $\sigma = 0$.

2. We now assume $V = 0$ and that the slab is of piezoelectric crystal, so strained as to produce a uniform polarization P_n, where the subscript n denotes a polarization normal to the slab. It is obvious that there will be polarization surface charges* $\pm P_n$ on the slab, equal and opposite induced charges on the electrodes, a field E_w in the gap in the same direction as P_n, and a depolarizing field E_n, opposed to P_n, in the slab.

* The effects of space charge in the crystal are treated in §249.

The values are found to be

$$E_w = \frac{4\pi e P_n}{e'} \tag{164a}$$

$$E_n = \frac{-4\pi w P_n}{e'} \tag{164b}$$

E_n gives rise to a counterpolarization $P' = \eta E_n$, and the total polarization is

$$P_t = P_n + P' = \frac{e + w}{e + kw} P_n \tag{165}$$

When $w = 0$ (electrodes adherent), $P_t = P_n$, and $E_n = 0$. When $w = \infty$ (slab far removed from all conductors), $P_t = P_n/k$ and $D = 0$; the displacement vanishes both outside and inside the dielectric.

If there is a potential difference V between the electrodes, its contribution to the polarization, given by Eq. (163*d*), is added to that in Eq. (165).

It should be noted that the field E_n in the crystal stands in the ratio $-w/e$ to the field E_w in the gap, independently of the dielectric constant.

111. *Impurities on Surfaces of Crystal.* The static measurement of dielectric constants involves a measurement of the charge flowing to the crystal condenser on application of a known potential difference V to the electrodes, or its removal. It is of the utmost importance that the electrodes make *immediate* contact with the substance of the crystal. Loosely fitting electrodes must be avoided (or else the gap w accurately measured), and layers of cement, if employed, must be exceedingly thin. These precautions are especially urgent with crystals of high k, as Rochelle salt. With such crystals all surface impurities resulting from the process of polishing or from dehydration must be removed (§415) if accurate results are desired.

The magnitude of the error to be expected when the crystal slab is separated from the electrodes by a thin layer of foreign material of permittivity k_w and thickness w can be deduced from the foregoing paragraphs. Under these conditions Eq. (161) becomes

$$D = kE = k_w E_w = 4\pi\sigma = \frac{kV_1}{e} = \frac{k_w V_w}{w}$$

It follows that

$$\sigma = \frac{kV}{4\pi e}\left(\frac{1}{1 + kw/k_w e}\right)$$

If the area of the condenser is A (assumed great enough for edge effects to be disregarded), the observed charge is σA. If the electrodes made immediate contact with the crystal, the observed charge would be $\sigma_0 A$, where $\sigma_0 = kV/4\pi e$. The ratio σ/σ_0 is a measure of the error incurred by

having the foreign layer present. Table XV gives approximate values of σ/σ_0 for various ratios k/k_w and w/e.

TABLE XV

$\frac{k}{k_w}$	$\frac{w}{e}$	$\frac{\sigma}{\sigma_0}$
10	0.01	0.9
10	0.001	0.99
100	0.01	0.5
100	0.001	0.9
1,000	0.01	0.1
1,000	0.001	0.5

Considering the extraordinarily large value of k_x for Rochelle salt in comparison with ordinary cements and with the dehydrated salt, one sees clearly from this table how important it is to make intimate contact between crystal and electrodes. For example, under the conditions assumed in the next to the last line—conditions quite likely to occur when e is small—the observed permittivity would be only one-tenth of the true value.

The subject of suitable electrodes for such measurements as these is treated in §416. At present all that is necessary is to point out the difficulty in having electrodes closely adherent while at the same time allowing freedom for deformation of the crystal when a field is applied. Very thin deposits of metal, such as gold foil or plated electrodes are best for this purpose.

112. *The Dielectric Ellipsoids.* The lack of parallelism between $\boldsymbol{E}$ and $\boldsymbol{P}$ is expressed mathematically by the fact that η is not a scalar, but a symmetrical tensor. Its magnitude varies with direction; it may be represented geometrically by an ellipsoidal surface given by the following equation, which is written with respect to the principal axes of the crystal:

$$\eta_{11}x^2 + \eta_{22}y^2 + \eta_{33}z^2 + 2(\eta_{23}yz + \eta_{31}zx + \eta_{12}xy) = \pm 1 \tag{166}$$

Unless the cross constants vanish, the principal axes of this ellipsoid are not coincident with the principal (crystallographic) axes. By rotating the coordinate system until it coincides with the principal ellipsoidal axes we obtain the equation

$$\eta_x x^2 + \eta_y y^2 + \eta_z z^2 = \pm 1 \tag{167}$$

where η_x, η_y, η_z are the *principal susceptibilities*. For all except triclinic and monoclinic crystals these η's are the same as the direct coefficients mentioned above.

The ellipsoid represented by Eq. (167) has the following property: If a radius vector r is drawn parallel to $\boldsymbol{E}$, then the polarization $\boldsymbol{P}$ associated with $\boldsymbol{E}$ lies in the direction of the normal to the tangential plane drawn at the point where r intersects the ellipsoidal surface. Parallel to the principal axes of the ellipsoid, and only in these directions, are polarization and displacement parallel to the field.

The reader familiar with physical optics will notice analogies between the foregoing ellipsoid and the optical ellipsoids discussed in Chap. XXX. Indeed, if instead of the static or radio-frequency (r-f) values of k we were to consider those at *optical* frequencies, we should pass directly to the optical ellipsoids; an ellipsoid having $k^{\frac{1}{2}}$ as parameter would be the Fresnel ellipsoid. Furthermore, those crystals having the three principal dielectric constants k_x, k_y, k_z [corresponding to η_x, η_y, η_z in Eq. (167)] all different (systems 1, 2, and 3 in Table XIV) are the optically *biaxial* crystals; those having two of these constants identical (systems 4, 5, 6) are *uniaxial*.

The dielectric ellipsoid for quartz, from Eq. (167), would be slightly prolate, with axis of revolution parallel to Z, and differing but little from a sphere. For Rochelle salt the ellipsoid would be a cigar-shaped figure with the long axis parallel to X.

113. The Molecular Nature of Polarization. The foregoing equations are perfectly general statistical descriptions of dielectric phenomena, in terms of quantities that are observable outside of the dielectric. They involve no hypothesis concerning the molecular nature of polarization. We shall now summarize those statements concerning the internal field and polarizability of which use will be made in the chapters on Rochelle salt and the other Seignette-electrics. For the remaining crystals, including quartz and tourmaline, there are no dielectric anomalies; the permittivities are so nearly constant over wide ranges of temperature, field, and frequency that for practical purposes no appeal need be made to molecular theory.

The actual field in a dielectric varies greatly from point to point, over distances comparable with molecular dimensions. The internal field F (also called the *local* or *molecular* field) is defined as that in a very small spherical cavity from which the molecules have been removed,* according to the Lorentz equation

$$F = E + \gamma P \tag{168}$$

where E is the statistical field (as ordinarily defined) in the dielectric, P the polarization, and γ the internal-field constant. If the medium is isotropic or of cubic symmetry, γ has the value $4\pi/3$. In crystals of symmetry lower than cubic, γ has values differing from $4\pi/3$, though of the same order of magnitude; it is usually considered as independent of temperature.

In the field F each molecule becomes polarized and assumes an electric moment μ. If $\bar{\mu}$ is the average value of μ in the direction of F and α the molecular constant known as the total molecular *polarizability*, we have the simple relation

$$\bar{\mu} = \alpha F \tag{169}$$

This linear relation suffices in most cases; non-linear effects are considered

*This definition of F, as applied to piezoelectric phenomena, is discussed in Chap. XXVI.

later. Calling N the number of molecules per cubic centimeter, one has also

$$P = N\bar{\mu} \tag{170}$$

The quantity α is the sum of the constituents $\alpha_e + \alpha_a + \alpha_d$, where α_e and α_a are due to displacements of electrons and atoms, respectively. The terms $\alpha_e + \alpha_a$ may be abbreviated to α_{ea}; they are called the *induced* or *lattice* polarizability, *Lorentz* type of polarizability, or polarizability *by distortion*. This type of polarizability, and hence the portion of the dielectric constant dependent on it, is essentially independent of temperature.

The contribution due to structural dipoles, when they are present (*i.e.*, permanent dipoles that are characteristic of the structure even in the absence of external field, causing polarization by *orientation*) is α_d. Polar structures of higher order than dipoles need not be considered here. The constituents of μ are $\bar{\mu}_{ea} = \alpha_{ea}F$ and $\bar{\mu}_d = \alpha_d F$. In the second of these equations the bar is of special significance, since in general the directions of the permanent dipole axes are widely distributed in space. The bar in the first equation is in recognition of the fact that the polarization in a crystal is not necessarily parallel to the impressed field.

In applying the foregoing expressions, especially in Chap. XXVI, the only type of dipole that will be explicitly considered is the *permanent* dipole, capable of rotation in an electric field, and designated above by μ_d. We may therefore drop the subscript d and write simply μ for the moment of a permanent dipole.

The total polarization may now be expressed as

$$P = N\bar{\mu} = N\alpha F = P_{ea} + P_d = N\mu_{ea} + N\bar{\mu}_d = N\alpha_{ea}F + N\alpha_d F \tag{171}$$

For those dielectrics in which $\gamma = 4\pi/3$, the well-known Clausius-Mosotti relation can be deduced from Eqs. (168) and (171), upon setting $E = 4\pi P(k - 1)$, where k is the dielectric constant:

$$\frac{k-1}{k+2} = \frac{4\pi}{3} N\alpha \tag{172}$$

Although in this equation α was originally meant to comprise only the lattice polarization α_{ea}, it has been extended by several writers to include dipole polarization as well (§485).

The following relation between susceptibility and molecular polarizability, derived from Eqs. (170), (171), and $P = \eta E$, will be used later, in §486:

$$N\alpha = \frac{\eta}{1 + \gamma\eta}, \qquad \text{whence} \qquad \eta = \frac{N\alpha}{1 - \gamma N\alpha} \tag{173}$$

114. *Polarization Due to Permanent Dipoles.* The theory is due to Debye,[B15,B16] who adapted to the study of dielectrics Langevin's theory

of paramagnetism. The latter is described in the Appendix, and the application of the Langevin-Debye-Weiss theory to the Seignette-electrics is considered in Chap. XXVI. We give here only those essential equations which are of a more general nature.

In brief, the theory postulates that a dielectric having a temperature-dependent dielectric constant contains dipoles which normally are in a state of disorder owing to thermal agitation. Upon application of an electric field the dipoles tend to rotate; the average rotation depends on the amount of thermal agitation, being greater at lower temperatures. A condition of statistical equilibrium is reached that determines the dipole polarization α_d. The polarization under weak fields is approximately proportional to the field, but as the latter becomes large a state of saturation is approached.

The *Langevin function* $L(a)$, employed in the Appendix with respect to phenomena involving magnetic dipoles, can be used also in the dielectric case, by the substitution of electrical for magnetic quantities. It then expresses the theoretical ratio of the average $\bar{\mu}$ [Eq. (169)] to the moment μ of the individual dipole, the latter being regarded as constant and independent of temperature. The parameter a is $\mu F/KT$, where K is the Boltzmann constant and T the absolute temperature. In its original form the Langevin function is

$$L(a) = L\frac{\mu F}{KT} = \frac{\bar{\mu}}{\mu} = \frac{P_d}{P_0} = \coth a - \frac{1}{a} \tag{174}$$

where P_0 is the polarization in infinite field, when the dipoles are completely aligned. The form of the $L(a):a$ curve is shown in Fig. 165 (page 748).

A useful approximate form of this equation, sufficiently accurate as long as F is small enough so that $a << 1$, is Eq. (556a), which we give here as well as later; it is obtained by retaining the first two terms in the expansion of (174) in powers of a.

$$\frac{\bar{\mu}}{\mu} = \frac{1}{3}\frac{\mu F}{KT} - \frac{1}{45}\left(\frac{\mu F}{KT}\right)^3 = \frac{P}{N\mu} \tag{175}$$

Equation (174), hence also the numerical coefficients in (175), is based on the assumption that the orientation of the dipoles is unrestricted in space (§552). In solids certain restrictions are present, but in all cases as long as the field is not too great one can write a generalized Langevin function in the following approximate form, from Eq. (562):

$$\frac{\bar{\mu}}{\mu} = p\frac{\mu F}{KT} - q\left(\frac{\mu F}{KT}\right)^3 = \frac{P}{N\mu} \tag{176}$$

For the original function, p and q assume the values $\frac{1}{3}$ and $\frac{1}{45}$, respectively.

Equation (174) indicates that the polarization P_d approaches saturation at high fields. It follows that the dielectric susceptibility is not a constant but decreases with increasing field strength. In paramagnetism, saturation is observable only in rare instances and with great difficulty (§548); but it is an important characteristic of ferromagnetic substances.

As in the analogous magnetic case, the dielectric properties of the Seignette-electrics in *weak fields* are of importance. In such cases the first term or at most the first two terms of the expansion of $L(a)$ in powers of a suffice.

When F is small enough for the first term to be used alone, one may write

$$\bar{\mu} = p \frac{\mu^2 F}{KT}$$

where $\mu^2 F/KT$ is the dipole contribution to the molecular polarizability. The total polarizability may now be written as

$$\alpha = \alpha_{ea} + p \frac{\mu^2}{KT} \tag{177}$$

The contributions to the polarization made by the two terms are the polarization by *distortion* and polarization by *orientation* mentioned above.

As a rule, dielectrics of large permittivity possess a structure containing dipoles. What confirms the diagnosis is the dependence on temperature shown in Eq. (177). Dipoles are aperiodically damped, and they play no part in the permittivity or refractive index at frequencies as high as in the infrared.

The following expression for polarization will be used in §484. As F becomes indefinitely large, $\bar{\mu}$ approaches μ, and from Eq. (174) $L(a)$ approaches unity. We then have, for the saturation value of the polarization by orientation in an infinite field, $P_0 = N\mu$ and, for the total polarization at any F,

$$P = N\alpha_{ae}F + P_0 L(a) \tag{178}$$

Although most investigations on saturation effects have had to do with freely rotating dipoles, still saturation is also known to occur in dielectrics containing no polar molecules (ref. B15, Chap. VI). We shall encounter instances of this among the Seignette-electrics. In such cases the Langevin function can be extended to include the α_{ae} type of polarization.*

In this chapter it is unnecessary to discuss further the effect of temperature on polarizability. The subject will be taken up in connection

* For the most part we shall use the Langevin function in the generalized form [Eq. (176)].

with the theory of Rochelle salt. It need be remarked here only that any dielectric with a very large and temperature-dependent polarizability may be suspected of having a Curie point like that of Rochelle salt.

115. Brief mention should be made in this chapter of *spontaneous polarization*, which is important in the theory of Rochelle salt. When a spontaneous polarization P^0 is present, it is to be added to the polarization P due to E. P^0 is associated with a spontaneous internal field $F_0 = \gamma P^0$. Calling F_E the term due to E, we have for the total internal field

$$F = F_0 + F_E = E + \gamma(P^0 + P) = \gamma P^0 + E(1 + \gamma\eta) \qquad (179)$$

In problems such as ordinarily arise in connection with dielectrics the only polarization is that due to E, *viz.*, $P = \eta E$. On the other hand, pyroelectric crystals may have a spontaneous polarization P^0, and piezoelectric crystals when in a state of strain have a polarization that we shall call P_h. Both P^0 and P_h (disregarding Seignette-electric anomalies) are independent of E; in any case they differ from zero even when $E = 0$.

Piezoelectric crystals may be either polar or non-polar. In the former case the application of a suitable strain produces a polarization both by distorting the lattice and by rotating the dipoles: both α_{ae} and α_d are affected. If the crystal is non-polar, only lattice distortion takes place.

When an electric field is applied to a *clamped* crystal, in which all externally observable deformation is prevented, one may assume that both types of polarization are present, though to a reduced degree. We shall see in §468 that reasons have been advanced by Mueller for believing that a clamped crystal of Rochelle salt shows no observable "ferroelectric" properties.

116. *Dissipation of Energy in Dielectrics.* A condenser may be represented as a pure capacitance in series with a small resistance, or in parallel with a large resistance, or both together. The materials selected as dielectrics for condensers usually provide a capacitance that is nearly constant over wide ranges of frequency and temperature. On the other hand, the resistance is often found to depend greatly upon these two quantities.

While the permittivities of a considerable number of piezoelectric crystals have been measured, in most cases no special need has arisen for the measurement of their dielectric losses. The only examples with which we shall have to deal are quartz and Rochelle salt. In quartz, the inherent losses, chiefly elastic, set the ultimate limit in the construction of resonators of low damping. Usually the damping introduced by mounting, air friction, etc., is greater than that characteristic of the quartz itself.

In the case of Rochelle salt both the permittivity and the internal losses vary greatly with field, temperature, frequency, and other factors as well. Rochelle salt belongs among those substances for which the *relaxation times* have been investigated. The effect is usually found among materials containing polar molecules. Although a full discussion of relaxation times lies outside the scope of this book, the following features may be briefly summarized.*

If an alternating field of constant amplitude is applied to a substance containing dipoles, as the frequency is gradually increased, certain absorption bands in the frequency spectrum are traversed, within which, owing to something of the nature of molecular friction, the polarization and hence also the permittivity decreases, remaining relatively low on the h-f side. For each of these regions there is a certain characteristic frequency $\omega_0/2\pi$, defined by the equation $\omega_0 = 2KT/b = 1/\tau$, where K is Boltzmann's constant, T the absolute temperature, b a frictional constant, and τ the relaxation time.† The permittivity begins to diminish at the beginning of the absorption band, at which point the frequency may be only a fraction of $\omega_0/2\pi$. For Rochelle salt, absorption bands in the infrared have been dealt with by Valasek.[546]

Several observers claim to have found certain characteristic relaxation times for Rochelle salt, in some cases at extremely low frequencies. References to their work will be found in §428.

Another type of absorption of energy, closely analogous to that encountered in the piezoelectric resonator, is found in the infrared and in the optical spectrum. This type is due to natural vibrational periods associated with electrons, molecules, or the crystal lattice, and is accompanied by anomalous dispersion (in the range of optical frequencies the refractive index, and hence the dielectric constant, normally *increases* with increasing frequency).

If all types of absorption are taken into account, the result is a progressive diminution in permittivity with increasing frequency, with the exception of rapid increases as the frequencies of natural vibrational modes are approached. If the dielectric is a preparation from a piezoelectric crystal, mounted without too much mechanical constraint, it will have a large number of natural vibrational frequencies depending on its dimensions, in the neighborhood of each of which it will react upon the driving circuit. The variations in electric current in such a region are exactly as if the dielectric possessed a permittivity and absorption that varied

* See refs. at the end of this chapter.

† In terms of static fields one may say that, when a constant field is impressed on the dielectric, the dipoles are held in a certain statistical state of order. Upon the sudden removal of the field it can be proved that this state of order sinks to $1/\epsilon$ of its initial value in a time equal to the relaxation time.

with frequency. As will be shown below, it is possible to represent the behavior of a piezo resonator in terms of a complex permittivity, just as is customarily done in the case of molecular vibrations. In each case the phenomenon may be described as "anomalous dispersion."

Whatever the nature of the energy absorption may be, unless the loss is small it has a perceptible effect upon the measured permittivity.

117. From observations made with a bridge, the permittivity of any dielectric can be deduced from the equation $C = kA/4\pi e$ (A = area, e = separation of electrodes, which are assumed to be in contact with the dielectric); and the equivalent parallel resistance R can be calculated and thence the equivalent conductivity of the material. If the observations are such that the measured quantity is the *admittance*, erroneous values of k may result if it is assumed that the losses can be neglected. In such cases the observed permittivity is the quantity known as the *complex permittivity*, which we shall designate as k_c and which is a function of k, R, and frequency.

The equation for complex permittivity may be derived thus: If the "complex capacitance" C_c is defined in terms of the observed admittance by the equation $Y = j\omega C_c = g - jb$, we have

$$C_c = \frac{Ak_c}{4\pi e} = -\frac{1}{\omega}(b + jg) \tag{180}$$

where k_c is the complex permittivity, b the susceptance, and g the conductance. Hence

$$k_c = -\frac{4\pi e}{\omega A}(b + jg) \approx k - j\frac{4\pi eg}{\omega A} \tag{181}$$

where, when the losses are small, k is the ordinary permittivity, given by the equation $C = kA/4\pi e = -b/\omega$. The dissipation term appears here as an imaginary quantity, instead of occupying its conventional place as the real part as in a-c theory.

Since for any network the resultant values of g and b can always be derived at any given frequency, it follows that any network can be represented as a condenser with complex permittivity. If the network is inductive, the reactive part of the permittivity will appear as negative. In particular, the equivalent network of a piezo resonator can be so represented, as will be seen in §258.

The theory of losses in dielectrics has been treated most extensively by Debye. His theory is used by Mason[338] in the treatment of dielectric hysteresis in Rochelle salt.

REFERENCES

DEBYE,[B15] DEBYE and SACK,[B16] VAN VLECK,[B49] MURPHY and MORGAN.[384]

CHAPTER VIII

PRINCIPLES OF PIEZOELECTRICITY

It would be interesting to know whether this development [of charges by stretching rubber], and that produced by compression, is progressive or sudden, whether the electrification produced by each of these operations is the same or different [in sign], what part the molecules in the interior of the body and those on the surface take in the total production; it would be especially curious and perhaps rather easy to investigate in crystalline minerals, where the aggregation of the particles, however regular in its assembly, presents in the different directions in the crystal known differences which can influence the ease, great or small, with which the electricity is separated.

—A. C. BECQUEREL, 1820.

118. Introduction. The statements in Chap. I concerning the piezoelectric effect may be summarized and extended in the following manner:

A piezoelectric crystal may be defined as a crystal in which "electricity or electric polarity" is produced by pressure; or, more briefly, as one that becomes electrified on squeezing; or as one that becomes deformed when in an electric field. The first two definitions express the direct effect, while the third expresses the converse effect.

These definitions are correct as far as they go, but they require further explanation. In the first place, if the pressure is replaced by a stretch (*i.e.*, a reversal in sign of the pressure) the sign of the electric polarity becomes reversed, also. One may ask how the crystal knows which way to become electrified. The answer is that a piezoelectric crystal must have a certain *one-wayness* in its internal structure; in other words, it must have a structural "bias" that determines whether a given region on the surface shall show a positive or a negative charge on compression. In the converse effect, the same one-wayness determines the sign of the deformation when an electric field is applied to the crystal. It is this reversal of sign of strain with sign of field that distinguishes piezoelectricity from electrostriction (§137).

Of the 32 crystal classes, there are 20 that possess this one-wayness. With all the rest there is nothing to determine the direction of the polarity on compression; hence they do not become polarized at all.*

The second consideration has to do with the relation between the applied stress and the resulting polarization. The stress may be a compression or an extension, as stated above; but it may also be a shearing stress, which, as shown in §27, is closely related to a compression. There

* This statement ignores the *tensorial* piezoelectricity mentioned in §525, which is too feeble to require consideration at this point.

is one crystal class in which a random stress of any type will produce a polarization, the direction and amount of which will, of course, vary with the stress. This is the asymmetric triclinic class, the one of lowest symmetry, of which more will be said presently. With all other classes it is only certain particular types of stress, standing in particular relations to the crystal axes, that can produce a polarization. There is no class in which the piezoelectric polarization has one and only one direction, but there are several classes in which the polarization is confined to a certain plane. Conversely, an applied field must have at least a component in this plane in order to produce any piezoelectric deformation.

Since there are six possible components of stress and three of electric polarization, it is evident that there are 18 possible relations between the mechanical and electrical states of the crystal. These relations are expressed by the 18 *piezoelectric constants*, whose values are independent and differ from zero except when (as is always the case outside of the triclinic system) the symmetry of the class is such as to make some of the constants have identical values, including zero. In some of the classes of relatively high symmetry there is but one independent constant, but it is associated with at least two types of stress and strain and with at least two components of polarization and field. However high the symmetry, as long as a crystal is piezoelectric at all, there is wide latitude in the choice of stresses, field directions, cuts, and vibrational modes. The principles that underlie the production of various types of vibration by piezoelectric excitation are treated in Chap. X.

Although the foregoing statements refer mainly to the direct effect, they can be equally well expressed in the language of the converse effect. If in the direct effect a mechanical stress of type h produces an electrical strain (polarization) in the m-direction, then by the converse effect an electrical stress (applied field strength) in the m-direction will produce a mechanical strain of type h. For each crystal class there is complete reciprocity between the two effects.

119. This chapter has to do chiefly with the presentation of Voigt's phenomenological theory of piezoelectricity. It includes a tabulation of the characteristic effects for the 20 piezoelectric classes of crystals and the equations for the piezoelectric constants with respect to rotated axes. The representation of piezoelectric properties by means of surfaces and diagrams is discussed, as an introduction to the graphical methods employed in the next chapter for showing how particular crystals vary as the axial system is rotated.

In the early part of the chapter is given a brief survey of the pioneer researches of P. and J. Curie in this field, together with Lippmann's prediction of the converse effect.

At the close is a brief section on electrostriction.

120. An Illustration of Piezoelectric Effects and Reactions. If an electric field in some arbitrary direction were applied to a hemihedral triclinic crystal, a number of things would happen. Each of the three components of field strength would excite six independent components of internal stress, known as *piezoelectric stress.* The total stress system would consist of 18 different terms, 3 terms for each of the six components of stress. The resulting strain would involve all the possible types of deformation: the lengths of all edges and all angles between edges would be changed.

Yet even with this complex state of affairs the story would by no means be at an end. On the surfaces of the crystal, if the latter were not in contact with the electrodes, would appear polarization charges due to the state of strain, from the *direct* piezoelectric effect, giving rise to an additional set of field components whereby the entire stress and strain systems became altered, and this in turn would cause still other polarization charges, and so on. The final configuration would depend on all these circumstances.

Beyond this, since our crystal is also necessarily pyroelectric, the electric field would cause certain thermal changes through the electrocaloric effect, and these in turn would both alter the elastic constants and thereby affect the deformation and also, through the pyroelectric effect, have an influence on the state of polarization. Lastly, the crystal could not escape having its state of deformation still further altered through the effect of electrostriction; and through the converse electrostrictive effect the polarization would undergo still further modification. A complete description of the final state of the crystal would include these thermal and electrostrictive effects. Fortunately they can usually be ignored.

121. It is the object of piezoelectric theory to analyze such situations as that described in the foregoing section. The piezoelectric forces are examples of the class of forces known as "body forces," acting directly on the entire substance, rather than applied mechanically to the boundaries from without. As will be seen, the problem can be solved completely when all conditions are homogeneous, *i.e.*, when all elements of volume have exactly the same temperature and the same components of field and of strain. Whenever boundary conditions have to be taken into account, the problem becomes so complicated that solutions are possible only in certain special cases.

The triclinic hemihedral class of crystals was chosen as an illustration because it represents the lowest degree of crystalline symmetry, although almost no experimental work has been done on it. The other triclinic class, having a center of symmetry, is not piezoelectric.

For generality it is customary to write the fundamental piezoelectric

equations in terms of all 18 possible coefficients. Each of the 20 piezoelectric classes is characterized, with respect to suitably chosen axes, by a definite number of coefficients, which become fewer with increasing symmetry, until in a few classes the number of *independent* constants is reduced to one. Except for the triclinic hemihedral class, in which the choice of axes is perfectly arbitrary, the fundamental piezoelectric coefficients for each class are expressed with reference to a system of orthogonal axes based upon the elements of symmetry present in that class; hence they are fewer in number than they would be for any other axial system. If, as often happens, a crystal specimen is cut in an *oblique* direction, a new system of axes has to be adopted, involving usually a great increase in the number of coefficients. That is, any transformation of axes may be expected to reduce the crystal effectively to a position of lower symmetry.

122. The Researches of the Brothers Curie. As a prelude to Voigt's theory we shall survey briefly some of the principal piezoelectric researches of Pierre and Jacques Curie.* In Chap. I an account has been given of the discovery by the two brothers in 1880 of the *direct* piezoelectric effect (electric polarization caused by mechanical deformation) and their verification in 1881 of the *converse* effect, following Lippmann's prediction. They found that from quartz crystals it is possible to cut plates in such a way that the polarization in a certain direction can be produced by a compression both *parallel* to this direction (the *longitudinal effect*) and in a suitable direction *perpendicular* to it (the *transverse effect*).

Their only quantitative results were on the constant d_{11} of quartz and d_{33} of tourmaline. Only quartz will be considered in this brief summary. They applied pressure parallel to the thickness of an X-cut quartz plate and measured the resulting charge with an electrometer, finding $d_{11} = 6.32(10^{-8})$ esu, in close agreement with the best later values. In measuring d_{11} by the converse effect they applied to the electrodes of an X-cut quartz plate a potential difference from an electrostatic Holtz machine and observed the dilatation in the Y-direction by means of a delicate amplifying lever.† Considering that the voltage was measured by means of a spark gap, it is remarkable that the value of d_{11} by this method agreed within 4 per cent with that determined by the direct effect.

Among the quartz plates used in their various experiments were some 8 cm long and only $\frac{1}{15}$ mm thick.

In the "Œuvres" are described several ingenious piezoelectric devices, intended for various types of static measurement. One of them, the

* From ref. B10, "Œuvres de Pierre Curie." In the present section this book is referred to as "Œuvres."

† "Œuvres," p. 45.

piezoelectric manometer,* employed the longitudinal effect: compression of an X-cut quartz plate in the direction of its thickness caused a deflection of the electrometer. This apparatus was intended for the measurement of pressures (for example, the stresses due to magnetostriction) and was the forerunner of some of the present-day applications mentioned in Chap. XXVIII. When the pressure was caused by the application of a large potential difference to an auxiliary system of quartz plates in contact with the one described above, the device could be used for the measurement of large potential differences. The theory of this arrangement is given in Voigt.†

A second device, which also finds occasional use today (§§354, 396), was the quartz *bilame*, or double strip.‡ Two long narrow X-cut quartz plates were cemented together like the bimetallic strips used for thermostats. In one form, the X-axes of the two plates were opposed, so that, when equal and opposite charges were placed on electrodes (films of silver) covering the outer faces of the double plate, one of the components became elongated, the other contracted, and a flexure ensued. In another form, the X-axes were not opposed, but between the two plates was placed a third electrode connected to one terminal of the high voltage to be measured, the other terminal being joined to the two outer electrodes in parallel. This device could therefore serve as a piezoelectric electrometer.§ Voigt's theory of its action is in the "Lehrbuch."‖

The simplest and best known of these early devices, for which there is still a field of usefulness, is the *quartz piézoélectrique*.¶ It consists of a single thin, elongated plate of quartz, which in the original design measured 100 by 20 by 0.5 mm parallel to the Y-, Z-, and X-axes, with its major faces silvered or coated with tin foil for electrodes. To each end was attached a strip of metal, and it was suspended vertically in a grounded metal box, with a scalepan fastened to the lower end on which weights could be placed, for applying any desired degree of tension to the quartz. The instrument thus utilized the transverse effect. The electrodes were connected to an electrometer. The device has been used for producing known charges, for the measurement of capacitances, voltages, and pyro- and piezoelectric effects, and in radioactivity.**

* "Œuvres," p. 38.

† P. 904.

‡ "Œuvres," p. 49.

§ French patent No. 183,851, May 27, 1887.

‖ P. 906.

¶ First described in Jacques Curie's doctoral dissertation, Paris, 1889 ("Œuvres," p. 554).

** See Mme. Curie, "Traité de Radioactivité," Gauthiers-Villars & Cie, Paris, 1910.

123. Fundamental Piezoelectric Theory. In the development of the fundamental theory only *isothermal* processes will be considered. It is assumed throughout that the state of the crystal is homogeneous, both electrically and mechanically, and that the equations are linear. The latter condition expresses a generalized Hooke's law, or a proportionality between stress and strain for electromechanical as well as for purely elastic phenomena. Under ordinary conditions this is found experimentally to be the case with all crystals tested, with the important exception of the Seignette-electrics.

The fundamental piezoelectric relations are derived from the third term in Eq. (1). The genesis of this term is best understood in the light of *Lippmann's theory.* As we pointed out in Chap. I, Lippmann's important contribution to piezoelectricity was the prediction of the converse effect.[316] His papers, which were devoted to the application of thermodynamic methods to electrical phenomena, with special reference to the problem of electrostriction and its converse, are remembered today chiefly because of that portion in which he states that the same reasoning, when applied to the direct piezoelectric effect discovered by the Curies, leads to the conclusion that a piezoelectric crystal when placed in an electric field must undergo a deformation. He predicted the same numerical value of the coefficient for the converse as for the direct effect.

As applied to piezoelectricity, Lippmann's reasoning may be expressed in the following manner: A piezoelectric crystal is placed in an electric field of strength E and at the same time subjected to a mechanical stress X. There are then present in the crystal an electric polarization P and a strain x. If now the field and the stress are varied by small amounts dE and dX, the total change in energy dU may be expressed as an exact differential, $dU = P\,dE - x\,dX$. The effect of electrostriction is considered in §137. Assuming the process to be reversible, we write (see §187)

$$\left(\frac{\partial P}{\partial X}\right)_E = -\left(\frac{\partial x}{\partial E}\right)_X \tag{182}$$

Since it is found, over wide ranges of pressure and with most crystals, that the relation is linear, we may set $\partial P/\partial X = -\delta$, where δ is the piezoelectric strain constant. This represents the direct effect, and the equation above says that there is a converse effect $\partial x/\partial E$, having the same constant δ with sign reversed. It is this prediction which was promptly confirmed by the Curies.

Accepting Lippmann's conclusions, Pockels, Duhem, and later, in more precise and general form, Voigt formulated the thermodynamic potentials for piezoelectricity. The physical meaning of the ther-

modynamic potentials is that, when any one of the three components of electric field strength is present simultaneously with any one of the six components of strain or stress, there is, in the most general case, a new contribution to the energy stored in the crystal, which is zero only when the corresponding piezoelectric coefficient vanishes.

124. Fundamental Piezoelectric Equations. The method that will now be employed for deriving the fundamental piezoelectric equations makes use of all the first three terms in Eqs. (1) and (2) (the remaining terms are absent because the process is assumed to be isothermal). This leads, in a more simple and perspicuous manner than that of Voigt, not only to the important *primary* equations for the direct and converse effects, but to the expressions for the *secondary* effects as well. It thus becomes easy to determine with full generality the effect of piezoelectric reactions upon the elastic and dielectric constants. The axes are the orthogonal crystallographic axes. Transformations to other axial systems are considered in §§134*ff*.

From Eq. (1) are obtained the fundamental piezoelectric equations in terms of strains. The derivatives with respect to strain and field (at constant T) are

$$\frac{\partial \xi}{\partial x_h} = \sum_i^6 c^E_{hi} x_i + \sum_m^3 e_{mh} E_m = -(X_h) \quad \text{(converse effect)} \qquad (183)$$

$$\frac{\partial \xi}{\partial E_m} = \sum_k^3 \eta''_{km} E_k + \sum_h^6 e_{mh} x_h = P_m \quad \text{(direct effect)} \qquad (183a)$$

The meaning of (X_h) is explained in §126.

The 18 quantities e_{mh} are the *piezoelectric stress coefficients* (Voigt's "piezoelectric constants").

Similarly the derivatives of Eq. (2) lead to the fundamental equations in terms of external stresses:

$$\frac{\partial \zeta}{\partial X_h} = \sum_i^6 s^E_{hi} X_i - \sum_m^3 d_{mh} E_m = -x_h \quad \text{(converse effect)} \qquad (184)$$

$$\frac{\partial \zeta}{\partial E_m} = \sum_k^3 \eta'_{km} E_k - \sum_h^6 d_{mh} X_h = P_m \quad \text{(direct effect)} \qquad (184a)$$

η'' and η' are the clamped and free susceptibilities (§204).

The 18 quantities d_{mh} are the *piezoelectric strain coefficients* (Voigt's "piezoelectric moduli").* By analogy with η' they might well be called the *piezoelectric susceptibilities*.

* In English it is customary to define a modulus as the quotient of a stress by a

In the foregoing equations, s^E_{hi} and c^E_{hi} are isagric elastic coefficients (at constant E); this type of elastic coefficient is tacitly assumed by Voigt and is required by the fact that E is the independent variable in the expressions for electrical energy.* The compliance s^E_{hi} at constant E is analogous to the susceptibility η'_{km} at constant mechanical stress (§204), while s^F_{hi}, the isopolarization compliance, is analogous to η''_{km}, the susceptibility at constant mechanical strain.

For all crystals except the Seignette-electrics the values of c^E_{hi} and s^E_{hi} may be regarded as practically independent of the magnitude of E.

125. *Interpretation of the Energy Equations.* It is desirable at this point to show how the total energy becomes allocated among the terms of Eqs. (1) and (2). Only the first three terms in each equation need be considered, since thermal changes are here ignored. The principles involved will stand out more clearly if subscripts and summations are omitted; the same conclusions are reached when the expressions are written in full. In this abbreviated form we have

$$\xi = \tfrac{1}{2}c^E x^2 + \tfrac{1}{2}\eta'' E^2 + eEx \quad . \qquad (185)$$

$$\zeta = \tfrac{1}{2}s^E X^2 + \tfrac{1}{2}\eta' E^2 - dEX \qquad (185a)$$

As was stated in §23, the crystal plate, with adherent electrodes connected to a battery, is assumed to be subjected simultaneously to a stress X of any type and to an electric field E normal to the surface of the plate. The total strain, due jointly to X and E, is x. The two equations above are alternative ways of expressing the energy stored in the plate by X and E together. In the case of Eq. (185) we may suppose that x is

---

strain. Now from Eqs. (184) and (184*a*) it is evident that d_{mh} is of the nature of a strain divided by a stress; hence it is e_{mh} rather than d_{mh} that should be called a "modulus." On the whole it seems most appropriate to call the *d*'s the *piezoelectric strain constants* (or *strain coefficients*) and the *e*'s the *piezoelectric stress constants* (or *stress coefficients*), respectively. This terminology will be used throughout the book. It is perhaps worth noting that e^2 has the dimensions of stress × permittivity. According to systematic tensor notation the *d*'s and *e*'s should be written with three suffixes instead of two, since they express relations between vectors and second-rank tensors and are therefore tensors of the third rank. Nevertheless, following Voigt's notation, which has become almost universally adopted and is in all cases sufficiently explicit, we shall use only two suffixes. Wooster[B56] introduces the fundamental piezoelectric equations in full tensor notation but later finds it expedient to abbreviate the suffixes to two symbols. Unfortunately his abbreviated suffixes are not the same as Voigt's. In §26 we have already explained the use of a single suffix instead of two for the stress and strain tensors.

Recently a very compact *matrix notation* for piezoelectric and other constants of crystals has been introduced by W. L. Bond.[64]

* The use of the isopolarization coefficients is associated with the polarization theory (§192). The relations between isagric and constant-polarization coefficients are given in §208.

produced by the application of X while $E = 0$, the plate being short-circuited. The work done per cubic centimeter is represented by the first term in Eq. (185). The application of X causes a polarization $P = ex$, which persists after E is impressed. We next clamp the plate so that further deformation is prohibited, leaving x fixed; since no motion is involved, the clamping forces do no work. Now let the battery be connected to the electrodes, producing a field E in the plate. The battery does work per cubic centimeter equal to $\eta''E^2/2$ on the dielectric; and since the field E is also associated with the polarization $P = ex$, there is in the crystal an additional energy eEx per cubic centimeter. The second and third terms in Eq. (1) are thus accounted for.

For Eq. (185*a*) one may suppose a field E to be impressed at the start, the crystal being mechanically free. A polarization $P_E = \eta'E$ is set up, and the electrical work done is $\eta'E^2/2$. The mechanical stress X is then applied, the mechanical work being $s^E X^2/2$. This operation causes a contribution $P = -dX$ to the polarization, with a corresponding additional flow of charge from the battery, involving an additional expenditure of electrical energy $-dEX$. Thus the three terms in Eq. (185*a*) are accounted for.

In a non-piezoelectric crystal d and e vanish, $\eta' = \eta''$, and in Eqs. (185) and (185*a*) the two surviving terms represent mechanical and electrical energy, which are now entirely unrelated.

126. *Interpretation of Eqs.* (183) *to* (184*a*). Equation (183) states that the total stress (X_h) is made up of two parts: first, the externally applied stress that would produce the prescribed strain if $E = 0$; second, the stress caused piezoelectrically by E (a body stress, as distinguished from an external stress). That is, the second term is equal and opposite to the external mechanical stress that would have to be added to the mechanical stress responsible for the first term, in order to hold the strain constant when the field was applied. With both strain and field prescribed, the total external mechanical stress component X_h is therefore not the (X_h) in Eq. (183), but rather

$$X_h = -\sum_i^6 c_{hi}^E x_i + \sum_m^3 e_{mh}E_m = (X_h) + 2\sum_m^3 e_{mh}E_m \qquad (186)$$

The fact that (X_h) is not the external stress, but the sum of two stresses, one external and the other internal, must be kept in mind in all uses that are made of Eq. (183). Failure to observe this distinction has led to discrepancies in the signs of certain terms in the various handbooks. No such source of confusion exists in Eqs. (183*a*), (184), and (184*a*).

Equations occur frequently in which the only stress is the internal (X_h) caused by E. In such cases, where there can be no ambiguity, the stress symbol will be written without parentheses.

Equation (183*a*) gives the polarization as the sum of two contributions, *viz.*, dielectric (as for an unstrained or clamped crystal) and piezoelectric (due to the strain). With most crystals, for which all relations are practically linear, η'' is independent of the strain and of the field strength. With the Seignette-electrics η'' is itself a function of the field strength as will be seen in §456. If there is no external stress, the strain component x_h in Eq. (183*a*) is all piezoelectric, due to the electric field, so that P_m is then the polarization in the *free* crystal, as shown in Eq. (260).

Similarly, Eq. (184) expresses the strain when an externally applied stress X and field E are both present. In Eq. (184*a*) the first term is the contribution which the applied field E makes toward the polarization in an unstressed (free) crystal; the second term is contributed by any stress that may be impressed from without. In most crystals η' is independent of field and of external stress (as long as the latter is held constant when the field is applied); in the Seignette-electrics this is not true (Chap. XXII).

As will be seen later, in the case of such a crystal as Rochelle salt, which has different symmetry elements at different temperatures, if the same piezoelectric equations are to be used at all temperatures, it is necessary to specify clearly the particular configuration of the crystal at which the strain is taken as zero. With Rochelle salt this consideration leads to the concepts of "rhombic" and "monoclinic" clamping and to the proper introduction of the spontaneous polarization P° in the equations. Although this distinction is first discussed in relation to the polarization theory, it could also be made in Voigt's formulation as treated in the present chapter. Nevertheless, in all applications of Voigt's formulation that we shall have occasion to make to the Seignette-electrics, it will suffice to employ the "normal method" of §458, whereby, at any temperature, the crystal is in a state of zero strain when it is in its undisturbed configuration, free from all stress when in zero field. By this means the Voigt equations can, for example, be applied at once to the problem of the piezoelectric resonator, without explicit introduction of either the spontaneous strain or the spontaneous polarization in the equations.

All the elastic, dielectric, and piezoelectric coefficients are more or less variable with temperature. Formal recognition might be given to this fact by retaining the fourth terms in Eqs. (1) and (2), but it is simpler to assume isothermal processes and to treat the temperature variations separately. This method is the more justifiable since for most crystals at all ordinary temperatures the piezoelectric coefficients are nearly constant.

127. We now write the piezoelectric relations in full, by expanding the summations in the second terms of the four equations (183) to (184*a*) and setting the first terms equal to zero. For the direct effect, the resulting expressions yield the polarization due to mechanical stress in the absence of an electric field; for the converse effect, they give the contributions to the stress and strain due to an impressed field, on which may, of course, be superposed the contributions due to mechanical forces. Since with most crystals the piezoelectric coefficients are independent of field and stress, it follows that, when either or both of these latter effects are present, the first terms in Eqs. (183) to (184*a*) can be retained without affecting the values of the second terms. On the other hand, there are crystals, notably Rochelle salt, in which the direct and converse piezoelectric effects are non-linear in X and E. The theoretical treatment of such cases demands the inclusion of terms of higher degree in the expressions for the free energy (§23); this procedure is indeed carried out for Rochelle salt by Mueller (§448), but in the case of most crystals it would only overcomplicate the treatment.

From Eqs. (183*a*) and (184*a*) are obtained the principal equations for the direct effect.

$$\left.\begin{aligned} P_x &= e_{11}x_x + e_{12}y_y + e_{13}z_z + e_{14}y_z + e_{15}z_x + e_{16}x_y \\ P_y &= e_{21}x_x + e_{22}y_y + e_{23}z_z + e_{24}y_z + e_{25}z_x + e_{26}x_y \\ P_z &= e_{31}x_x + e_{32}y_y + e_{33}z_z + e_{34}y_z + e_{35}z_x + e_{36}x_y \end{aligned}\right\} \tag{187}$$

$$\left.\begin{aligned} -P_x &= d_{11}X_x + d_{12}Y_y + d_{13}Z_z + d_{14}Y_z + d_{15}Z_x + d_{16}X_y \\ -P_y &= d_{21}X_x + d_{22}Y_y + d_{23}Z_z + d_{24}Y_z + d_{25}Z_x + d_{26}X_y \\ -P_z &= d_{31}X_x + d_{32}Y_y + d_{33}Z_z + d_{34}Y_z + d_{35}Z_x + d_{36}X_y \end{aligned}\right\} \tag{188}$$

It will be observed that Eqs. (187) and (188) express the electrical strain induced by a mechanical strain or stress.

Similarly, the principal equations for the converse effect, giving the mechanical stress or strain caused by an electrical stress, are derived from Eqs. (183) and (184).

$$\left.\begin{aligned} -X_x &= e_{11}E_x + e_{21}E_y + e_{31}E_z \\ -Y_y &= e_{12}E_x + e_{22}E_y + e_{32}E_z \\ -Z_z &= e_{13}E_x + e_{23}E_y + e_{33}E_z \\ -Y_z &= e_{14}E_x + e_{24}E_y + e_{34}E_z \\ -Z_x &= e_{15}E_x + e_{25}E_y + e_{35}E_z \\ -X_y &= e_{16}E_x + e_{26}E_y + e_{36}E_z \end{aligned}\right\} \tag{189}$$

In these last equations the quantities on the left are the *internal* stresses due to the E's. Henceforth the parenthesis introduced in Eq. (183) will in general be omitted, with the understanding that, unless

otherwise specified, the stress symbols in piezoelectric equations like (189) will signify *internal* stress components.

The equations for strain are

$$\left.\begin{aligned} x_x &= d_{11}E_x + d_{21}E_y + d_{31}E_z \\ y_y &= d_{12}E_x + d_{22}E_y + d_{32}E_z \\ z_z &= d_{13}E_x + d_{23}E_y + d_{33}E_z \\ y_z &= d_{14}E_x + d_{24}E_y + d_{34}E_z \\ z_x &= d_{15}E_x + d_{25}E_y + d_{35}E_z \\ x_y &= d_{16}E_x + d_{26}E_y + d_{36}E_z \end{aligned}\right\} \tag{190}$$

As one may infer from the equations above, the d's and e's are related by elastic constants. This relation is obtained by first expressing each component of stress in Eq. (188) in terms of components of strain, by Eqs. (6); the result is $P_m = \sum_i^6 \sum_h^6 d_{mi}c_{ih}^E x_h$. This expression agrees with Eq. (187) or Eq. (183a) if one writes

$$e_{mh} = \sum_i^6 d_{mi}c_{ih}^E \tag{191}$$

Similarly, it is easily proved that

$$d_{mh} = \sum_i^6 e_{mi}s_{ih}^E \tag{191a}$$

In expanded form, Eqs. (191) and (191a) become

$$e_{mh} = d_{m1}c_{1h} + d_{m2}c_{2h} + d_{m3}c_{3h} + d_{m4}c_{4h} + d_{m5}c_{5h} + d_{m6}c_{6h} \tag{192}$$

$$d_{mh} = e_{m1}s_{1h} + e_{m2}s_{2h} + e_{m3}s_{3h} + e_{m4}s_{4h} + e_{m5}s_{5h} + e_{m6}s_{6h} \tag{192a}$$

where $m = 1, 2, 3$; $h = 1, 2, \ldots 6$.

In these equations all elastic coefficients are *at constant field.* In general, whenever Voigt's piezoelectric equations are used, isagric values are assumed for the elastic constants.

128. From the foregoing equations it is seen that the dimensions of d_{mh} are polarization/stress, charge/force, or the reciprocal of electric-field strength: in the electrostatic system of units this is $[M^{-\frac{1}{2}}L^{\frac{1}{2}}Tk^{\frac{1}{2}}]$. The dimensions of e_{mh} are those of a polarization, $[M^{\frac{1}{2}}L^{-\frac{1}{2}}T^{-1}k^{\frac{1}{2}}]$. It is important to note that the only dimension of the product $e_{mh}d_{mh}$ is $[k]$. Using the practical system of units, we may express d_{mh} in terms of coulombs per kilogram weight and e_{mh} in coulombs per square centimeter.*

* The conversion factors for passing from the electrostatic cgs system to other systems are as follows: The parentheses indicate the units in which the quantities

It is more customary, however, to use the electrostatic cgs system, with d_{mh} in statcoulombs per dyne and e_{mh} in statcoulombs per square centimeter.

It will be observed, with both the d's and the e's, that the first figure in the subscript indicates the direction of the field or polarization, while the second expresses the type of stress or strain. Hence it is not true, as with the elastic constants, that $d_{mh} = d_{hm}$. For example, if d_{24} has a value different from zero, this means that an electric polarization parallel to Y is associated with a shear in the YZ-plane. Whenever any d equals zero, the corresponding e also necessarily vanishes and vice versa. In the case of coefficients associated with shears (*i.e.*, when the second figure in the subscript is 4, 5, or 6), it is possible, owing to the presence of both + and − signs in the c's and s's, for d_{mn} and e_{mn} to have opposite signs.

129. From Eqs. (187) to (190) the following useful qualitative rule can be deduced. It holds universally for all piezoelectric crystals, irrespective of the signs of the d's and e's.

The direction of the polarization (*i.e.*, the algebraic sign of P) *associated with a given strain is always the same, whether strain and polarization are due to mechanical forces* (direct effect) *or to an impressed electric field* (converse effect).

For example, if a tourmaline crystal is compressed in the X-direction, $x_x = x_1$ is negative. Since for tourmaline e_{21} and d_{21} are positive, it follows from Eqs. (187) ($P_y = e_{21}x_x$) that the component of polarization in the Y-direction is negative. Now let a field E_y in the negative Y-direction be applied: again P_y, which in this case is $\eta_{22}E_y$, is negative, and from Eqs. (190) ($x_x = d_{21}E_y$) we see that x_x is also negative. The rule can also be verified for the Z-component of polarization (for a strain x_x, $P_1 = 0$ in tourmaline); and the rule can be expressed in terms of stress instead of strain.

130. *Effect of Spontaneous Polarization on the Piezoelectric Constants.* A crystal belonging to any pyroelectric class has a single polar axis, which implies the presence of a spontaneous, or permanent, polarization P°. The question suggests itself whether, even in an isothermal process, an alteration in the surface polarization charges may not take place when the crystal is deformed, owing to a possible dependence of P° upon the

---

are expressed.

$$d_{mh}[\text{esu}] = d_{mh}\left[\frac{\text{statcoul}}{\text{dyne}}\right] = 3(10^9)d_{mh}\left[\frac{\text{coul}}{\text{dyne}}\right]$$

$$= 3(10^4)\,d_{mh}\left[\frac{\text{coul}}{\text{newton}}\right] = 300d_{mh}\left[\frac{\text{cm}}{\text{volt}}\right] = 3{,}060d_{mh}\left[\frac{\text{coul}}{\text{kg weight}}\right]$$

$$e_{mh}[\text{esu}] = e_{mh}\left[\frac{\text{statcoul}}{\text{cm}^2}\right] = 3(10^9)e_{mh}\left[\frac{\text{coul}}{\text{cm}^2}\right] = 3(10^5)e_{mh}\left[\frac{\text{coul}}{m^2}\right]$$

strain. Such alteration would affect the value of one or more of the piezoelectric coefficients. As ordinarily measured, the latter include this effect whenever it is present.

The theory is discussed by Voigt,* with the conclusion that any abnormally large piezoelectric coefficient may owe its magnitude to this effect. The criterion is whether P° is large in comparison with e. Data for tourmaline indicate that spontaneous polarization does not have a dominating effect on its piezoelectric properties. In Rochelle salt P°, while large, is small in comparison with e_{14}, hence the hugeness of the piezoelectric effect cannot even in this case be attributed solely to P°. The part played by P° in Rochelle salt is treated in later chapters.

131. Specialization of the Constants for the Thirty-two Crystal Classes. The twenty piezoelectric classes have already been indicated in Table I, §6. As stated there, all are devoid of a center of symmetry (hemimorphic); they are also all either hemihedral or tetartohedral.

The matrices of the piezoelectric coefficients† are shown in Table XVI. It should be recalled that the first figure in the subscript indicates the direction of the electric vector, the second the component of elastic strain or stress. For all classes not listed below, all d's and e's are zero. The coefficients are arranged in the same order as in Eqs. (187) and (188), the subscripts indicating *independent* values, as in §29.

TABLE XVI

TRICLINIC SYSTEM

Class 1, Asymmetric, C_1

e_{11}	e_{12}	e_{13}	e_{14}	e_{15}	e_{16}	d_{11}	d_{12}	d_{13}	d_{14}	d_{15}	d_{16}
e_{21}	e_{22}	e_{23}	e_{24}	e_{25}	e_{26}	d_{21}	d_{22}	d_{23}	d_{24}	d_{25}	d_{26}
e_{31}	e_{32}	e_{33}	e_{34}	e_{35}	e_{36}	d_{31}	d_{32}	d_{33}	d_{34}	d_{35}	d_{36}

MONOCLINIC SYSTEM

Class 3, Digonal Polar, C_2

0	0	0	e_{14}	e_{15}	0	0	0	0	d_{14}	d_{15}	0
0	0	0	e_{24}	e_{25}	0	0	0	0	d_{24}	d_{25}	0
e_{31}	e_{32}	e_{33}	0	0	e_{36}	d_{31}	d_{32}	d_{33}	0	0	d_{36}

Class 4, Equatorial, C_{1h}

e_{11}	e_{12}	e_{13}	0	0	e_{16}	d_{11}	d_{12}	d_{13}	0	0	0
e_{21}	e_{22}	e_{23}	0	0	e_{26}	d_{21}	d_{22}	d_{23}	0	0	d_{26}
0	0	0	e_{34}	e_{35}	0	0	0	0	d_{34}	d_{35}	0

RHOMBIC SYSTEM

Class 6, Digonal Holoaxial, V

0	0	0	e_{14}	0	0	0	0	0	d_{14}	0	0
0	0	0	0	e_{25}	0	0	0	0	0	d_{25}	0
0	0	0	0	0	e_{36}	0	0	0	0	0	d_{36}

* "Lehrbuch," pp. 815, 842, 871.

† In Voigt's tabulation in his "Lehrbuch" (p. 829), there are a few misprints.

Class 7, Didigonal Polar, C_{2v}

0	0	0	0	e_{15}	0	0	0	0	0	d_{15}	0
0	0	0	e_{24}	0	0	0	0	0	d_{24}	0	0
e_{31}	e_{32}	e_{33}	0	0	0	d_{31}	d_{32}	d_{33}	0	0	0

TETRAGONAL SYSTEM

Class 9, Tetragonal Alternating, S_4

0	0	0	0	e_{15}	0	0	0	0	0	d_{15}	0
0	0	0	e_{15}	0	0	0	0	0	d_{15}	0	0
e_{31}	e_{31}	e_{33}	0	0	0	d_{31}	d_{31}	d_{33}	0	0	0

Class 10, Tetragonal Polar, C_4

0	0	0	e_{14}	e_{15}	0	0	0	0	d_{14}	d_{15}	0
0	0	0	e_{15}	$-e_{14}$	0	0	0	0	d_{15}	$-d_{14}$	0
e_{31}	e_{31}	e_{33}	0	0	0	d_{31}	d_{31}	d_{33}	0	0	0

Class 11, Ditetragonal Alternating, V_d

0	0	0	e_{14}	0	0	0	0	0	d_{14}	0	0
0	0	0	0	e_{14}	0	0	0	0	0	d_{14}	0
0	0	0	0	0	e_{36}	0	0	0	0	0	d_{36}

Class 12, Tetragonal Holoaxial, D_4

0	0	0	e_{14}	0	0	0	0	0	d_{14}	0	0
0	0	0	0	$-e_{14}$	0	0	0	0	0	$-d_{14}$	0
0	0	0	0	0	0	0	0	0	0	0	0

Class 14, Ditetragonal Polar, C_{4v}

0	0	0	e_{14}	e_{15}	0	0	0	0	d_{14}	d_{15}	0
0	0	0	$-e_{15}$	e_{14}	0	0	0	0	$-d_{15}$	d_{14}	0
e_{31}	$-e_{31}$	0	0	0	e_{36}	d_{31}	$-d_{31}$	0	0	0	d_{36}

TRIGONAL SYSTEM

Class 16, Trigonal Polar, C_3

e_{11}	$-e_{11}$	0	e_{14}	e_{15}	$-e_{22}$	d_{11}	$-d_{11}$	0	d_{14}	d_{15}	$-2d_{22}$
$-e_{22}$	e_{22}	0	e_{15}	$-e_{14}$	$-e_{11}$	$-d_{22}$	d_{22}	0	d_{15}	$-d_{14}$	$-2d_{11}$
e_{31}	e_{31}	e_{33}	0	0	0	d_{31}	d_{31}	d_{33}	0	0	0

Class 18, Trigonal Holoaxial, D_3

e_{11}	$-e_{11}$	0	e_{14}	0	0	d_{11}	$-d_{11}$	0	d_{14}	0	0
0	0	0	0	$-e_{14}$	$-e_{11}$	0	0	0	0	$-d_{14}$	$-2d_{11}$
0	0	0	0	0	0	0	0	0	0	0	0

Class 19, Ditrigonal Polar, C_{3v}

0	0	0	0	e_{15}	$-e_{22}$	0	0	0	0	d_{15}	$-2d_{22}$
$-e_{22}$	e_{22}	0	e_{15}	0	0	$-d_{22}$	d_{22}	0	d_{15}	0	0
e_{31}	e_{31}	e_{33}	0	0	0	d_{31}	d_{31}	d_{33}	0	0	0

HEXAGONAL SYSTEM

Class 21, Trigonal Equatorial, C_{3h}

e_{11}	$-e_{11}$	0	0	0	$-e_{22}$	d_{11}	$-d_{11}$	0	0	0	$-2d_{22}$
$-e_{22}$	e_{22}	0	0	0	$-e_{11}$	$-d_{22}$	d_{22}	0	0	0	$-2d_{11}$
0	0	0	0	0	0	0	0	0	0	0	0

Class 22, Ditrigonal Equatorial, D_{3h}

e_{11}	$-e_{11}$	0	0	0	0	d_{11}	$-d_{11}$	0	0	0	0
0	0	0	0	0	$-e_{11}$	0	0	0	0	0	$-2d_{11}$
0	0	0	0	0	0	0	0	0	0	0	0

Class 23, Hexagonal Polar, C_6

0	0	0	e_{14}	e_{15}	0	0	0	0	d_{14}	d_{15}	0
0	0	0	e_{15}	$-e_{14}$	0	0	0	0	d_{15}	$-d_{14}$	0
e_{31}	e_{31}	e_{33}	0	0	0	d_{31}	d_{31}	d_{33}	0	0	0

Class 24, Hexagonal Holoaxial, D_6

0	0	0	e_{14}	0	0	0	0	0	d_{14}	0	0
0	0	0	0	$-e_{14}$	0	0	0	0	0	$-d_{14}$	0
0	0	0	0	0	0	0	0	0	0	0	0

Class 26, Dihexagonal Polar, C_{6v}

0	0	0	0	e_{15}	0	0	0	0	0	d_{15}	0
0	0	0	e_{15}	0	0	0	0	0	d_{15}	0	0
e_{31}	e_{31}	e_{33}	0	0	0	d_{31}	d_{31}	d_{33}	0	0	0

Cubic System

Class 28, Tesseral Polar, T

0	0	0	e_{14}	0	0	0	0	0	d_{14}	0	0
0	0	0	0	e_{14}	0	0	0	0	0	d_{14}	0
0	0	0	0	0	e_{14}	0	0	0	0	0	d_{14}

Class 31, Ditesseral Polar, T_d

0	0	0	e_{14}	0	0	0	0	0	d_{14}	0	0
0	0	0	0	e_{14}	0	0	0	0	0	d_{14}	0
0	0	0	0	0	e_{14}	0	0	0	0	0	d_{14}

Voigt's method* for determining the matrices given above consists, in brief, in writing the general equations for the piezoelectric surfaces (§136) and then applying to them the various elements of symmetry of the different classes; for example, if a crystal has an n-fold axis of symmetry, the equations must be invariant for a rotation of $2\pi/n$ of the system of reference about this axis. Certain of the 18 parameters from each class then vanish, excepting only Class 1. Owing to certain differences between the equations in terms of the e's and those in terms of the d's (involving the definitions of the components of strain and stress), it turns out that, while in most cases the matrices for the d's are exactly similar to those for the e's, exceptions occur in those classes having a threefold cyclic axis of symmetry. These classes are Nos. 16, 18, 19, 21, and 22; for each of them, in the last column of the d-matrix, $2d_{11}$ and $2d_{22}$ are the parameters corresponding to e_{11} and e_{22} in the e-matrix. It will be recalled that an analogous situation exists with the s's and the c's in the trigonal and hexagonal groups.

132. Discussion of the Piezoelectric Effects. The general piezoelectric matrix is shown in symbolic form in Fig. 40, in which L and T

* "Lehrbuch," pp. 820–833.

stand for the longitudinal and transverse compressional effects, and L_s and T_s may be termed the longitudinal and transverse shear effects. This figure should be compared with the analogous one for the elastic effects (Fig. 15, on page 56).

Strain / Polarization		1	2	3	4	5	6
		x_x	y_y	z_z	y_z	z_x	x_y
1	P_x	L	T	T	L_s	T_s	T_s
2	P_y	T	L	T	T_s	L_s	T_s
3	P_z	T	T	L	T_s	T_s	L_s

FIG. 40.—The four types of piezoelectric effect.

In place of the strain components at the top of the figure, components X_x . . . X_y of stress might have been written; and E_x, E_y, E_z (converse effect) may replace the P's, which signify the direct effect; L, T, etc., may thus represent either the e's or the d's. For example, in the upper right-hand corner of the figure, T_s may represent either $P_x = e_{16}x_y$, $P_x = -d_{16}X_y$, $X_y = -e_{16}E_x$, or $x_y = d_{16}E_x$.

If the coefficient corresponding to any one of the L's differs from zero, then a compression in a direction corresponding to this L causes a polarization in the same direction. This is the *longitudinal effect*, which is present in all crystals having d_{11}, d_{22}, or d_{33} or the corresponding coefficients for rotated axes.

In the *transverse effect* T, the polarization is at right angles to the associated compressional strain; these coefficients may be called the *transverse piezoelectric coefficients.*

In effects of the type L_s we have the polarization parallel to the axis of shear (§27), *i.e.*, normal to the plane of shear; these may be termed *longitudinal shear effects.*

Finally T_s represents a polarization in the plane of shear ("transverse" to the axis of shear).

Coefficients of types T and T_s may appropriately be called the piezoelectric "cross constants," by analogy with the elastic and dielectric cross susceptibilities (§§32, 105).

Among quartz resonators, as well as in other piezoelectric applications, are found examples of all four effects.

All classes have at least two constants; Classes 12 and 24 have only two, both of the L_s-type, but they are numerically alike, so that they have only one *independent* constant. Also, in Classes 22, 28, and 31 the number of independent constants is one.

Four groups of classes have identical matrices (numerical values being disregarded). They are Nos. 6, 11, 28, 31; 12, 24; 9, 26; 10, 23.

133. Piezoelectric Effects Due to Hydrostatic Pressure. If a crystal or crystal preparation, of any form, is under uniform hydrostatic pressure Π, it is easily proved that the components of piezoelectric polarization are

$$\left.\begin{aligned} -P_1 &= (d_{11} + d_{12} + d_{13})\Pi \qquad -P_2 = (d_{21} + d_{22} + d_{23})\Pi \\ -P_3 &= (d_{31} + d_{32} + d_{33})\Pi \end{aligned}\right\} \quad (193)$$

The remaining d's are absent, since uniform pressure introduces no shearing stresses. Hence, crystals possessing only coefficients of the types L_s and T_s shown in Fig. 40 do not become polarized under uniform pressure. Even with crystals having coefficients represented in Eqs. (193), the d's may have such values as to make all three parentheses vanish.

If for any crystal class the components of polarization do *not* all vanish under hydrostatic pressure, there is a resultant polarization in a direction that Voigt calls the *piezoelectric axis* of the crystal. Just half the piezoelectric classes have such an axis, *viz.*, those which are also pyroelectric. All other classes show no polarization under hydrostatic pressure. For example, quartz does not show it, while tourmaline does (piezoelectric axis parallel to the Z-axis; see the "*Lehrbuch*,*" and also §165.) The case of Rochelle salt is considered in §483.

Piezoelectric Constants for Rotated Axes. The process of deriving the piezoelectric constants for any system of rotated axes is similar to that for the elastic constants, as described in §40. Only the results need be given. For convenience the scheme of direction cosines is here repeated in Fig. 41.

	x'	y'	z'
x	α_1	β_1	γ_1
y	α_2	β_2	γ_2
z	α_3	β_3	γ_3

FIG. 41.

134. *General Transformation to Axes in Any Orientation.* The only expressions that have been worked out in full appear to be those given in Voigt.†

$$\begin{aligned} e'_{11} = {} & \alpha_1^3 e_{11} + \alpha_2^3 e_{22} + \alpha_3^3 e_{33} + \alpha_1^2[\alpha_2(e_{21} + 2e_{16}) + \alpha_3(e_{31} + 2e_{15})] \\ & + \alpha_2^2[\alpha_3(e_{32} + 2e_{24}) + \alpha_1(e_{12} + 2e_{26})] + \alpha_3^2[\alpha_1(e_{13} + 2e_{35}) + \alpha_2(e_{23} + 2e_{34})] \\ & + 2\alpha_1\alpha_2\alpha_3(e_{14} + e_{25} + e_{36}) \end{aligned} \quad (194)$$

* P. 878.

† Pp. 838, 840.

The equation for d'_{11} is obtained from that for e'_{11} by substituting d for e everywhere and omitting the factor 2 wherever it occurs. From the equations for e'_{11} and d'_{11}, expressions for e'_{22} and d'_{22} or for e'_{33} and d'_{33} are found by changing α to β or γ, respectively, leaving all subscripts on the right unaltered. The expression for d'_{33} is given in Eq. (198).

Any transformed d'_{kh} may be derived by the following method (an analogous treatment would give e'_{kh}): The transformed coefficient may be defined by an equation of the form $-P'_k = d'_{kh}X'_h$

$$(k = 1, 2, 3; h = 1, 2, \cdots 6).$$

The first step is to find the stresses $X_x \ldots X_y$ equivalent to X'_h from Eqs. (20). Then by means of Eqs. (188) we express P_x, P_y, and P_z in terms of $X_x \ldots X_y$ and the fundamental piezoelectric strain coefficients; this gives the components of the polarization, due to X'_h, parallel to the original axes. From them are formed the expressions for the components parallel to the rotated axes. Parallel to X' the component is

$$P'_x = \alpha_1 P_x + \alpha_2 P_y + \alpha_3 P_z = -d'_{1h} X'_h \tag{195}$$

Since P_x, P_y, P_z all contain X'_h as a factor, d'_{1h} is thus expressed in terms of direction cosines and fundamental piezoelectric constants, for any of the six values of h. Similarly, by writing the equations for P'_y and P'_z, expressions for d'_{2h} and d'_{3h} are found. A simpler method for deriving the transformed constants for $h = 1$, 2, or 3 is given in §136.

135. *General Transformation about a Single Axis.* Following are Voigt's equations for the transformed piezoelectric stress constants, for rotation through *an angle θ about the Z-axis.* The direction cosines become reduced to $\alpha_1 = \beta_2 = \cos\theta \equiv c$, $\alpha_2 = -\beta_1 = \sin\theta \equiv s$,

$$\alpha_3 = \beta_3 = \gamma_1 = \gamma_2 = 0,$$

$\gamma_3 = 1$. The positive sense of θ follows the rules given in §38.

From Eqs. (196), expressions for rotation about the X- or Y-axis are obtained by cyclical changes in all suffixes on both sides of the equations according to the following table, leaving all else unaltered. For example, the suffix 24 for rotation about the Z-axis

Z	1 2 3	4 5 6
X	2 3 1	5 6 4
Y	3 1 2	6 4 5

becomes 35 for rotation about the X-axis and 16 for rotation about the Y-axis.

$$
\begin{aligned}
e'_{11} &= c^3e_{11} + s^3e_{22} + c^2s(e_{21} + 2e_{16}) + cs^2(e_{12} + 2e_{26}) \\
e'_{12} &= cs^2(e_{11} - 2e_{26}) + s^3e_{21} + c^3e_{12} + c^2s(e_{22} - 2e_{16}) \\
e'_{13} &= ce_{13} + se_{23} \qquad e'_{14} = cs(e_{24} - e_{15}) + c^2e_{14} - s^2e_{25} \\
e'_{15} &= c^2e_{15} + s^2e_{24} + sc(e_{14} + e_{25}) \\
e'_{16} &= -c^2s(e_{11} - e_{12}) + c(1 - 2s^2)e_{16} - s(1 - 2c^2)e_{26} + cs^2(e_{22} - e_{21}) \\
e'_{21} &= -c^2s(e_{11} - 2e_{26}) + c^3e_{21} - s^3e_{12} + cs^2(e_{22} - 2e_{16}) \\
e'_{22} &= -s^3e_{11} + c^3e_{22} + cs^2(e_{21} + 2e_{16}) - c^2s(e_{12} + 2e_{26}) \\
e'_{23} &= ce_{23} - se_{13} \qquad e'_{24} = c^2e_{24} + s^2e_{15} - sc(e_{14} + e_{25}) \\
e'_{25} &= c^2e_{25} - s^2e_{14} + cs(e_{24} - e_{15}) \\
e'_{26} &= c(1 - 2s^2)e_{26} + s(1 - 2c^2)e_{16} + c^2s(e_{22} - e_{21}) + cs^2(e_{11} - e_{12}) \\
e'_{31} &= c^2e_{31} + s^2e_{32} + 2sce_{36} \qquad e'_{32} = c^2e_{32} + s^2e_{31} - 2sce_{36} \\
e'_{33} &= e_{33} \qquad e'_{34} = ce_{34} - se_{35} \\
e'_{35} &= ce_{35} + se_{34} \qquad e'_{36} = (c^2 - s^2)e_{36} + cs(e_{32} - e_{31})
\end{aligned}
\tag{196}
$$

The corresponding equations for the piezoelectric strain coefficients d'_{11} . . . d'_{36} for rotation about the Z-axis are obtained directly from Eqs. (196) by simply writing d_{hk} in place of e_{hk}, whenever $h = 1, 2, 3$ and $k = 1, 2, 3$; but when $h = 1, 2, 3$ and $k = 4, 5, 6$, $d_{hk}/2$ is to be written in place of e_{hk}. This rule applies to both primed and unprimed coefficients. For example, $d'_{36}/2 = (c^2 - s^2)d_{36}/2 + cs(d_{32} - d_{31})$. The transition to rotation about the X- or Y-axis is made in the same way as with the e's.

When the general equation for any d_{hk} or e_{hk} has once been derived, that for $d_{(h+1)(k+1)}$ or $e_{(h+1)(k+1)}$ is found by changing α to β, β to γ, γ to α, leaving all subscripts on the right side of each equation unaltered. This rule may be applied also to the equations for the general rotation specialized for any class, with the following important reservation: It is not valid in those cases where two different constants have the same numerical value and where for the sake of simplification a single symbol is used for both. Thus, for example, in Eqs. (221) the rule is not applicable because we have written $-e_{14}$ for e_{25} and $-e_{11}$ for e_{26}; but it is applicable to all equations for general rotation of axes in Class 6 or indeed in any class where no two constants become identical.

The rule as stated is of course not applicable to the equations given for rotation about a *single* axis.

The specialization of the foregoing equations to the various crystal classes is given in later sections.

136. Piezoelectric Surfaces and Diagrams. For the purpose of determining which piezoelectric constants differ from zero in the various crystal classes, Voigt made use of three relations between the e_{hk}, also three between the d_{hk}, each of which could be represented by a certain "piezoelectric surface." One of them is a trivector (tensor of the third rank) surface, involving all 18 constants; it is of the third degree and

essentially the same as the expression for e'_{11} (or d'_{11}) given by Eq. (194) or that for d'_{33} that we derive below in Eq. (198). The other two surfaces are represented by equations of the second and first degrees and need not concern us further.*

The piezoelectric surfaces that are usually represented graphically, as intersections with the three principal planes, and as illustrated in later paragraphs, are derived from Eqs. (197) and (198) below. If a pressure Z'_z is applied, parallel to the Z'-axis of a rectangular system of axes X', Y', Z' in any orientation, it follows from Eqs. (22) and (188) that

$$\left.\begin{aligned} -P_x &= Z'_z(d_{11}\gamma_1^2 + d_{12}\gamma_2^2 + d_{13}\gamma_3^2 + d_{14}\gamma_2\gamma_3 + d_{15}\gamma_3\gamma_1 + d_{16}\gamma_1\gamma_2) \\ -P_y &= Z'_z(d_{21}\gamma_1^2 + d_{22}\gamma_2^2 + d_{23}\gamma_3^2 + d_{24}\gamma_2\gamma_3 + d_{25}\gamma_3\gamma_1 + d_{26}\gamma_1\gamma_2) \\ -P_z &= Z'_z(d_{31}\gamma_1^2 + d_{32}\gamma_2^2 + d_{33}\gamma_3^2 + d_{34}\gamma_2\gamma_3 + d_{35}\gamma_3\gamma_1 + d_{36}\gamma_1\gamma_2) \end{aligned}\right\} \quad (197)$$

If the pressure is parallel to X' or to Y', we write X'_x or Y'_y in place of Z'_z and α or β in place of γ.

Next we find the component of polarization P'_z parallel to Z'_z:

$$\left.\begin{aligned} P'_z &= P_x\gamma_1 + P_y\gamma_2 + P_z\gamma_3 \\ &= -Z'_z[d_{11}\gamma_1^3 + d_{22}\gamma_2^3 + d_{33}\gamma_3^3 \\ &\quad + \{(d_{21} + d_{16})\gamma_2 + (d_{31} + d_{15})\gamma_3\}\gamma_1^2 \\ &\quad + \{(d_{32} + d_{24})\gamma_3 + (d_{12} + d_{26})\gamma_1\}\gamma_2^2 \\ &\quad + \{(d_{13} + d_{35})\gamma_1 + (d_{23} + d_{34})\gamma_2\}\gamma_3^2 \\ &\quad + (d_{14} + d_{25} + d_{36})\gamma_1\gamma_2\gamma_3] \\ &= -Z'_z d'_{33} \end{aligned}\right\} \quad (198)$$

where d'_{33}, given by the expression in braces, is the transformed piezoelectric strain constant. The same equation can be used for d'_{11} or d'_{22} by changing γ to α or β; P'_z then becomes P'_x or P'_y, and for Z'_z we write X'_x or Y'_y. Equation (198) expresses the *longitudinal effect* for rotated axes. It gives the electrical strain in any direction due to a mechanical stress in the same direction and is the piezoelectric analogue to Eq. (34) for Young's modulus. P'_z is called the *longitudinal polarization* corresponding to a compression Z'_z in the direction γ_1, γ_2, γ_3.

Similar expressions may be written for the *transverse polarizations* P'_x and P'_y:

$$P'_x = P_x\alpha_1 + P_y\alpha_2 + P_z\alpha_3 = -Z'_z d'_{13} \quad (199)$$

$$P'_y = P_x\beta_1 + P_y\beta_2 + P_z\beta_3 = -Z'_z d'_{23} \quad (199a)$$

If the applied stress is X'_x, the transverse polarizations are

$$P'_y = P_x\beta_1 + \cdots = -X'_x d'_{21},$$

$P'_z = P_x\gamma_1 + \ldots = -X'_x d'_{31}$; similarly, in terms of Y'_y we obtain the expressions for d'_{12} and d'_{32}.

* For a more complete discussion of piezoelectric surfaces see Voigt, pp. 820*f.* and 840, also ref. B20, vol. 1, pp. 366*f.*

These expressions for the polarization produced by uniform compression in various directions are of special importance. As has been stated, the components of polarization parallel and perpendicular to the direction of compression represent, respectively, the longitudinal and the transverse effects. For the longitudinal effect with respect to arbitrary axes the strain constants are d'_{11}, d'_{22}, and d'_{33}. If we consistently let the Z'-axis be the direction of compression, attention need be paid only to d'_{33}, the variation of which, as the Z'-direction is allowed to vary, will then completely describe the longitudinal effect for all orientations. The constants d'_{13} and d'_{23} will then suffice for the transverse effect, since they give the polarization components along the X'- and Y'-axes. Illustrations of the distribution of these quantities in space will be found in the discussions of particular types of crystal.

For a given value of Z'_z, if P'_z as given by Eq. (198) is plotted as a radius vector with direction cosines γ_1, γ_2, γ_3, the resulting surface is the trivector surface mentioned above; and if $Z'_z = 1$ dyne/cm^2, any radius vector gives the numerical value of d'_{33}. In this case we have, for any given crystal, the characteristic piezoelectric surface for d'_{33}. A similar surface could be constructed for d'_{66}, and of course likewise for d'_{11}, d'_{22}, d'_{44}, and d'_{55}. It would not be convenient, however, to construct surfaces for the remaining constants, since the polarization parallel to any radius vector would then not have a value uniquely associated with that direction.

Nevertheless, if the transformation of axes consists in a rotation about a *single axis*, a polar diagram for any of the 18 constants can be drawn in a plane perpendicular to this axis, in which the radius vector gives uniquely the value of the constant for all orientations about the axis. Such diagrams are shown later for some of the more important crystals.

137. Electrostriction. In the most general sense, the term *electrostriction* in dielectrics applies to any interaction between an electric field and the deformation of a dielectric in the field. With this broad interpretation, the word includes the phenomena of piezoelectricity, and indeed some writers have called the converse effect "electrostriction." This usage can lead only to confusion and should not be encouraged. Most authorities have adopted the wiser practice of reserving the term for those phenomena in which the deformation is independent of the direction of the field and *proportional to the square of the field.* All observed relations between field and deformation can be assigned either to this type, which is properly called electrostriction, or to the type in which the relations are *linear*, which includes the phenomena of piezoelectricity. In the former type the relation between field and deformation is centrosymmetrical; in the latter it is not.

In all references to electrostriction in this book the quadratic effect is meant.

Quadratic electrostriction is the mechanical analogue of the Kerr quadratic electro-optic effect. It is distinguished from the linear or piezoelectric effect in two important respects. First, it is a common property of all materials, whether gaseous, liquid, or solid. Second, the effect is so minute that, although it is always present in piezoelectric phenomena, it can usually be completely ignored. Only in fields stronger than 20,000 volts/cm can it be comparable with the effects of piezoelectricity. Its presence in quartz has been studied by Tsi-ze, as stated in §159.

The deformation of a dielectric in an electric field, apart from the piezoelectric effect, is determined partly by the Maxwell stresses, which are the only ones mentioned in reference to electrostriction in many textbooks, and partly by any dependence that the dielectric may have upon the strain. In an electric field the dielectric tends to assume a configuration such as to reduce the total energy to a minimum. If, as is usually the case, the dielectric constant decreases as the volume increases, the Maxwell stresses and the varying dielectric constant conspire to make the volume increase when a field is applied. With some substances, however, the dielectric constant decreases with *decreasing* volume. In such cases, the state of minimum energy may be accompanied by a *diminution* in the volume despite the Maxwell stresses.*

REFERENCES

Encycl. Math. Wiss., ref. B17, vol. 5, part 2 (by F. Pockels).

GEIGER and SCHEEL, ref. B19, vol. 13 (by H. Falkenhagen).

GRAETZ., ref. B20, vol. 1 (by E. Riecke).

VOIGT.[B52]

WINKELMANN, ref. B54, vol. 4, part 1 (by F. Pockels).

TERPSTRA, P.: Piezoelectricity and crystal structure, *Nederland. Tijdschr. Natuurkunde*, vol. 8, pp. 275–288, 1941; *Chem. Centralblatt*, vol. 1, p. 847, 1942; *Tijdschr. Nederland. Radiogen.* vol. 9, pp. 71–84, 1941.

* References to the literature on electrostriction down to 1928, with some numerical results, are given in the "International Critical Tables," vol. 6, 1929, and reproduced in *Proc. I.R.E.*, vol. 18, pp. 1247–1262, 1930. To these references may be added J. H. Jeans, "The Mathematical Theory of Electricity and Magnetism" and W. Wien and F. Harms, ref. B53, vol. 10. In recent years the subject has been treated by H. Osterberg and J. W. Cookson, ref. 407 and *Phys. Rev.*, vol. 51, pp. 1096–1101, 1937; also by G. Bruhat and M. Pauthenier, *Jour. phys. radium*, vol. 10, pp. 209–218, 1929.

CHAPTER IX

SPECIAL PIEZOELECTRIC PROPERTIES OF CERTAIN CRYSTALS

Ich aber schneyd Edelgestein
Auff meiner scheiben gross und klein,
Als Granat, Rubin und Demut,
Schmarack, Saphyr, Jacinthn gut,
Auch Calcidonj und Perill,
Schneyd auch der Fürsten Wapen viel,
Die man setzt in die Petschafft Ring,
Sunst auch viel Wappen aller ding.

—HANS SACHS.

For those piezoelectric classes that include crystals on which quantitative observations have been made, the general expressions given in the last chapter will now be specialized and the outstanding piezoelectric features described. Numerical values of the piezoelectric constants will be given, so far as they are recorded in the literature and appear to be trustworthy. For quartz and Rochelle salt, however, the data presented in this chapter are supplemented by the more detailed discussion in chapters devoted to those crystals.

For each class that is now to be considered, the characteristic piezoelectric features, based on Table XVI, will be summarized. The equations for rotated axes are taken from various soufces; some of them have been worked out by the author. Wherever necessary, these equations have been modified to conform to our conventions respecting the sense of rotation and the positive directions of axes, as shown in §51. When any class is mentioned as being also pyroelectric, the combined effects of *primary* and *secondary* pyroelectricity are meant; all piezoelectric crystals have tertiary pyroelectric properties (§515).

The piezoelectric properties of each class can be presented equally well by Eqs. (187), (188), (189), or (190), with the aid of the matrices in Table XVI. Equations 189, for the converse effect, have been chosen here, owing to their importance in the theory of resonators.

The precision in the measurement of the piezoelectric constants may be inferred from the number of significant figures. Hardly any data are available concerning systematic errors and differences between individual specimens. Measurements are so difficult, and the results are so uncertain, that in many cases one cannot even be sure of the first significant figure.

For some of the classes a few crystals are named as examples, with which positive results have been observed, though only qualitatively. Reference to qualitative observations on a large number of crystals is made in §172. All values are in electrostatic cgs units (§128).

138. Class 3, Monoclinic Digonal Polar (Hemimorphic) (symmetry C_2). This class is also pyroelectric. There are eight independent piezoelectric constants. The equations for the converse effect are

$$\left.\begin{array}{lll} -X_x = e_{31}E_z & -Y_y = e_{32}E_z & -Z_z = e_{33}E_z \\ -Y_z = e_{14}E_x + e_{24}E_y & -Z_x = e_{14}E_x + e_{25}E_y & -X_y = e_{36}E_z \end{array}\right\} \quad (200)$$

Further data, including expressions for the components of polarization produced by pressure in various directions, are given in Voigt.* Pavlik[411] shows how an orientation can be found for which certain piezoelectric shearing stresses vanish; he also gives some transformation equations for constants of Classes 3 and 4.

Tartaric Acid, $C_4H_6O_6$. The following values are from Tamaru:[503]

$$\left.\begin{array}{llll} d_{14} = -24 & d_{15} = 28 & d_{24} = 28.5 & d_{25} = -36.5 \\ d_{31} = 1.95 & d_{32} = 5.95 & d_{33} = 6.45 & d_{36} = 3.8 \end{array}\right\} \text{ all } \times 10^{-8}$$

Despite its strong piezoelectric properties this crystal, perhaps on account of its comparatively easy cleavage, has not found piezoelectric applications, beyond that suggested below.

Cane Sugar, $C_{12}H_{22}O_{11}$. Holmann[232] finds

$$\left.\begin{array}{llll} d_{14} = 1.3 & d_{15} = -1.3 & d_{24} = -7.2 & d_{25} = -3.7 \\ d_{31} = +2.2 & d_{32} = +4.4 & d_{33} = -10 & d_{36} = -2.6 \end{array}\right\} \text{ all } \times 10^{-8}$$

By applying hydrostatic pressure to tartaric acid and cane sugar, Lawson and Miller† have observed the quantity $(d_{31} + d_{32} + d_{33})$ for each of these crystals, finding good agreement with the values given above.

For resonator experiments with beet sugar see §381.

Terpstra‡ has recently found that crystals of brushite, $CaHPO_4$, are piezoelectric and that they should be assigned to Class 3. Other examples of this class are milk sugar, lithium sulphate, and the tartrates of Na, K, and NH_4.

139. Class 6, Rhombic Digonal Holoaxial (Hemihedral) (symmetry V). This is the class to which Rochelle salt in the parelectric state (§434) belongs. The class is not pyroelectric. There are three piezoelectric constants, all independent. The three stresses associated with them are

$$-Y_z = e_{14}E_x \qquad -Z_x = e_{25}E_y \qquad -X_y = e_{36}E_z$$

* Pp. 873*f*.

† A. W. Lawson and P. H. Miller, Jr., Piezometer for Transient Pressure, *Rev. Sci. Instruments*, vol. 13, pp. 297–298, 1942.

‡ P. Terpstra, *Z. Krist.*, vol. 97, pp. 229–233, 1937.

Whatever the direction of the electric field, the only strains that it can cause, with respect to the X-, Y-, Z-axes, are the three indicated by the equations above. Similarly, only stresses that involve one or more of these three components can produce an electric polarization. In general, a compression in any *oblique* direction causes a polarization having a component parallel to this direction (longitudinal effect). Only in special cases can the *total* polarization be made parallel to the direction of compression.

If e_{14}, e_{25}, and e_{36} (and hence d_{14}, d_{25}, and d_{36}) do not all have the same sign, there is always a component of polarization at right angles to the compression; this fact was first pointed out by Pockels[428] for Rochelle salt. That is, there is in this case no axial orientation for which both d'_{12} and d'_{13} in Eqs. (201) can be made to vanish.

Following are the equations for d'_{hk}, *axes in any orientation* (direction cosines as in Fig. 41):

$$
\left.\begin{aligned}
d'_{11} &= \alpha_1\alpha_2\alpha_3(d_{14} + d_{25} + d_{36}) \\
3d'_{12} &= (\alpha_1\beta_2\beta_3 + \alpha_2\beta_3\beta_1 + \alpha_3\beta_1\beta_2)(d_{14} + d_{25} + d_{36}) \\
&\quad + \beta_1\gamma_1(d_{25} - d_{36}) + \beta_2\gamma_2(d_{36} - d_{14}) + \beta_3\gamma_3(d_{14} - d_{25}) \\
3d'_{13} &= (\alpha_1\gamma_2\gamma_3 + \alpha_2\gamma_3\gamma_1 + \alpha_3\gamma_1\gamma_2)(d_{14} + d_{25} + d_{36}) \\
&\quad - \beta_1\gamma_1(d_{25} - d_{36}) - \beta_2\gamma_2(d_{36} - d_{14}) - \beta_3\gamma_3(d_{14} - d_{25}) \\
3d'_{14} &= [\alpha_1(\beta_2\gamma_3 + \beta_3\gamma_2) + \alpha_2(\beta_3\gamma_1 + \beta_1\gamma_3) + \alpha_3(\beta_1\gamma_2 + \beta_2\gamma_1)] \\
&\qquad (d_{14} + d_{25} + d_{36}) + (\alpha_1^2 + 2\gamma_1^2)(d_{25} - d_{36}) \\
&\qquad + (\alpha_2^2 + 2\gamma_2^2)(d_{36} - d_{14}) + (\alpha_3^2 + 2\gamma_3^2)(d_{14} - d_{25}) \\
d'_{22} &= \beta_1\beta_2\beta_3(d_{14} + d_{25} + d_{36}) \\
3d'_{26} &= 2(\alpha_1\beta_2\beta_3 + \alpha_2\beta_3\beta_1 + \alpha_3\beta_1\beta_2)(d_{14} + d_{25} + d_{36}) \\
&\quad - \beta_1\gamma_1(d_{25} - d_{36}) - \beta_2\gamma_2(d_{36} - d_{14}) - \beta_3\gamma_3(d_{14} - d_{25}) \\
d'_{33} &= \gamma_1\gamma_2\gamma_3(d_{14} + d_{25} + d_{36}) \\
3d'_{35} &= 2(\alpha_1\gamma_2\gamma_3 + \alpha_2\gamma_3\gamma_1 + \alpha_3\gamma_1\gamma_2)(d_{14} + d_{25} + d_{36}) \\
&\quad + \beta_1\gamma_1(d_{25} - d_{36}) + \beta_2\gamma_2(d_{36} - d_{14}) + \beta_3\gamma_3(d_{14} - d_{25}) \\
3d'_{36} &= [\gamma_1(\alpha_2\beta_3 + \alpha_3\beta_2) + \gamma_2(\alpha_3\beta_1 + \alpha_1\beta_3) + \gamma_3(\alpha_1\beta_2 + \alpha_2\beta_1)] \\
&\qquad (d_{14} + d_{25} + d_{36}) + (\gamma_1^2 + 2\beta_1^2)(d_{25} - d_{36}) \\
&\qquad + (\gamma_2^2 + 2\beta_2^2)(d_{36} - d_{14}) + (\gamma_3^2 + 2\beta_3^2)(d_{14} - d_{25})
\end{aligned}\right\} \quad (201)
$$

By following the rule given in §135, one can obtain the equations for all the remaining d'_{hk} directly from the expressions above. As an example of this we have included the equation for d'_{36}, which is arrived at by permutation from that for d'_{14}.

The rule for writing the equation for any e'_{hk} from the corresponding d'_{hk} in Eqs. (201) is as follows: Substitute e_{hk} for d_{hk} (both primed and unprimed) when $h = 1$, 2, or 3 and $k = 1$, 2, or 3; when $h = 1$, 2, or 3 and $k = 4$, 5, or 6, substitute $2e_{hk}$ for d_{hk}.

Any one of the equations for d'_{11}, d'_{22}, and d'_{33} may be taken as an expression for the *longitudinal effect.** For example, d'_{11} occurs in the equation $P'_x = -d'_{11}X'_x$, showing that a compression X'_x in any arbitrary direction α_1, α_2, α_3 causes a polarization P'_x in this same direction. Theoretically, the longitudinal effect vanishes only with the vanishing of at least one of these direction cosines, *i.e.*, when the direction of compression is perpendicular to at least one of the crystallographic axes. Practically, the effect is relatively small until α_1, α_2, and α_3 become approximately equal (see §140).

Equations (201) and the corresponding equations for e_{hk} hold also for Classes 11, 12, 24, 28, and 31.

Equations for e'_{hk}, Rotation about the X-axis. $\alpha_1 = 1$,

$$\beta_1 = \gamma_1 = \alpha_2 = \alpha_3 = 0,$$

$\beta_2 = \gamma_3 = c$, $\beta_3 = -\gamma_2 = s$. The corresponding expressions for d'_{hk} are obtained by writing d_{hk} in place of e_{hk} when $h = 1, 2, 3$ and $k = 1, 2, 3$; but when $h = 1, 2, 3$ and $k = 4, 5, 6$, $d_{hk}/2$ must be written in place of e_{hk}. This rule applies to both primed and unprimed coefficients.

$$\left.\begin{array}{llll} e'_{11} = 0 & e'_{12} = 2cse_{14} & e'_{13} = -2cse_{14} & \\ e'_{14} = (c^2 - s^2)e_{14} & e'_{15} = e'_{16} = 0 & & \\ e'_{21} = e'_{22} = e'_{23} = e'_{24} = 0 & & e'_{25} = c^2e_{25} - s^2e_{36} & \\ e'_{26} = cs(e_{25} + e_{36}) & e'_{31} = e'_{32} = e'_{33} = e'_{34} = 0 & & \\ e'_{35} = -cs(e_{25} + e_{36}) & & e'_{36} = c^2e_{36} - s^2e_{25} & \end{array}\right\} \qquad (202)$$

By changing the suffixes cyclically according to the scheme in §135, the equations for rotation about the Y- or Z-axis may be derived from Eqs. (202).

If the angle of rotation about the X-axis is 45°, $s = c = 1/\sqrt{2}$, and we have the transformed constants suitable for use, for example, in problems dealing with vibrations of X-cut 45° bars:

$$e'_{12} = e_{14} \qquad e'_{13} = -e_{14} \qquad d'_{12} = \frac{d_{14}}{2} \qquad d'_{13} = -\frac{d_{14}}{2} \qquad (203)$$

For an electric field parallel to X these are the only constants. Similar equations hold for 45° rotations about Y or Z.

The relations between the piezoelectric strain and stress coefficients are especially simple for crystals of Class 6. Since $c_{44} = 1/s_{44}$, $c_{55} = 1/s_{55}$, $c_{66} = 1/s_{66}$, Eqs. (192) and (192a) reduce to

* The existence of a longitudinal effect in crystals of this class seems to have been generally overlooked, in spite of the fact that the Curies probably employed it in their discovery of piezoelectricity in Rochelle salt; moreover, it is clearly implied in the equations subsequently derived by Voigt. The author was guilty of this oversight in 1930 (ref. 102), and it appears in the literature as late as 1937 (ref. 228).

$$d_{14} = e_{14}s^E_{44} \qquad d_{25} = e_{25}s^E_{55} \qquad d_{36} = e_{36}s^E_{66} \tag{204}$$

There is nothing very critical in the orientation of X-cut 45° bars of Rochelle salt. An error of a degree in any angular parameter reduces the piezoelectric effect to an extent not over about half of 1 per cent. On the other hand, Y- and Z-cut plates should be oriented with great care if effects due to d_{14} are to be excluded.

140. As an illustration of the use of formulas for rotated axes may be mentioned the "L-cut," in which the normal to the crystal plate makes equal angles with all three crystallographic axes. The direction of the normal is taken as the X'-axis; the Y'-axis lies in the XY-plane, at 45° to the X- and Y-axes. According to Fig. 41 the direction cosines of the normal are $\alpha_1 = \alpha_2 = \alpha_3 = 0.5774$. The general equation for the longitudinal effect in this class is found, from Eqs. (201), to be

$$d'_{11} = \alpha_1\alpha_2\alpha_3(d_{14} + d_{25} + d_{36}) \tag{205}$$

In the present case this reduces to

$$d'_{11} = 0.192(d_{14} + d_{25} + d_{36}) \tag{206}$$

Equation (206) shows that a longitudinal effect exists in Rochelle salt for all orientations in which $\alpha_1\alpha_2\alpha_3$ differs from zero, reaching a maximum when $\alpha_1 = \alpha_2 = \alpha_3$. The same statement is true of all crystals in Classes 6, 11 28, and 31; for Classes 12 and 24 the right side of Eq. (206) vanishes.

Experiments with Rochelle-salt oblique cuts of this type are described in §§378 and 504.

141. Rochelle Salt, $NaKC_4H_4O_6{\cdot}4H_2O$. Outside the two Curie points (approximately −18 and +24°C), this crystal clearly belongs to Class 6. Its monoclinic character (Class 3) between these points is discussed in Chap. XXV. It possesses primary pyroelectricity in the monoclinic form, but not in the rhombic. We consider first d_{25} and d_{36}, which show no anomalies.

d_{25} and d_{36} have been measured by Pockels[428] at room temperature, by Valasek[545] at 0°C (both used static compression of 45° bars), and by Mason[335] at 30° by the antiresonance method* described in §311.

	d_{25}	d_{36}
	$\times 10^{-8}$	$\times 10^{-8}$
Pockels	−165	+35
Valasek	−138	+28.3
Mason	−169	+39.4

* Dr. Mason informs the author that his latest observations give $d_{25} = -176(10^{-8})$.

Valasek also observed the variation with temperature, finding an increase in the numerical values from −60 to +30°C amounting to $0.68(10^{-8})$ per degree for d_{25} and $0.031(10^{-8})$ for d_{36}. These results, together with the dependence of d_{14} on temperature, are shown in Fig. 106.

When the foregoing results are reduced to 0°C by the use of Valasek's temperature coefficients (assuming Pockels's data to be at 20°C), the following values are found:

	d_{25}	d_{36}
	$\times 10^{-8}$	$\times 10^{-8}$
Pockels	−151	34.4
Valasek	−138	28.3
Mason	−149	38.5
Average values at 0°C	$-146(10^{-8})$	$34(10^{-8})$

Again using Valasek's temperature coefficients, we find for the average values at 20°C

$$d_{25} = -160(10^{-8}) \qquad d_{36} = 35(10^{-8}) \tag{207}$$

in close agreement with Pockels's original data.

Values of the piezoelectric stress coefficients e_{25} and e_{36} are obtained from Eqs. (204). We must first find the isagric values of s^E_{55} and s^E_{66}, starting with $s^*_{55} = 32.0(10^{-12})$ and $s^*_{66} = 11.4(10^{-12})$ from §79, Table V (the asterisks indicate that the values are for infinite gap). From Eqs. (273), (205), and (488), it is found that at room temperature

$$s^E_{55} = 35.3(10^{-12}) \qquad s^E_{66} = 11.6(10^{-12})$$

From Eqs. (205) and (204) we obtain finally

$$e_{25} = -4.5(10^4) \qquad e_{36} = 3.0(10^4)$$

The first measurement of d_{14} was by Pockels,* who found values from $340(10^{-8})$ to $1{,}180(10^{-8})$. Further experimental data, obtained under static and l-f conditions, are treated in Chaps. XXI and XXIV. The theory is discussed in Chaps. XI, XXIII, and XXIV, where it will be shown that the piezoelectric constants according to the "polarization theory" are nearly free from the variability with temperature and stress for which d_{14} is notorious. The abnormal behavior of d_{14} is summarized

* Ref. 428. Pockels's results were obtained with three $X45°$-plates, each 6 by 6 by 3 mm, compressed by a force of about 100 g parallel to a long edge. The temperature is not mentioned. Pockels attributed the wide range of values to lack of uniformity in the stress, but variations in temperature may well have been a contributing cause.

in §§370, 402, and 403 and Chap. XXV. Although there is no such thing as a "normal" or "standard" value for either d_{14} or e_{14}, fairly definite values can be given to their counterparts b_{14} and a_{14} in the polarization theory.

142. *Piezoelectric Constants of Rochelle Salt According to the Polarization Theory.* The constant b_{14} is obtained from Eq. (495*b*), $b_{14} = d_{14}/\eta'_x$, and a_{14} from Eq. (495), $a_{14} = b_{14}c^P_{44}$. d_{14} and η'_x are known within perhaps ± 10 per cent for small fields and small stresses (initial values, with linear relations), except close to the Curie points. Information is still lacking on their dependence on mechanical and electric stress, and under large stresses their values between the Curie points are complicated by hysteresis. From the parallelism between d_{14} and η'_x, b_{14} and a_{14} may be expected to show but small dependence on Y_x and E_x. The values given below are to be regarded as *initial* values.

From his treatment of Mason's vibrational experiments Mueller[378] calculates d_{14} (see §474) and thence finds, from 24.7 to 47.5°C, values of b_{14} from $5.7(10^{-7})$ to $6.4(10^{-7})$, with an average of $6.2(10^{-7})$. Between the Curie points, as is evident in Fig. 146, b_{14} rises to higher values; the same applies to a_{14}. Provisionally, at least, the value of b_{14} given below may be accepted. The values of b_{25} and b_{36} are calculated from Eqs. (205) and (488*a*), by the use of Eq. (242): $b_{25} = d_{25}/\eta'_y$, $b_{36} = d_{36}/\eta'_z$.

a_{14} is the same as Mueller's f_{14}. From Mason's experimental data Mueller calculated a_{14} from d_{14}, η'_x, and c^P_{44} (or, in our notation, from b_{14} and c^P_{44}). The results are shown in Fig. 146, from which the average value is seen to be around $7.5(10^4)$. Mason's f_{14} is expressed according to his charge theory, as explained in §190. Mason's value, which we shall here call f^σ_{14} (σ = charge density), is 4π times the value f^D_{44} according to the displacement theory. From §189 it is seen that $f^\sigma_{14} = (k'' - 1)a_{14}/k''$, where a_{14} is the constant according to the polarization theory, whence a_{14} is about 1 per cent greater than f^σ_{14}.

Now for f^σ_{14} Mason gives the value $7.8(10^4)$ in his first paper[335] and also in his book,[B35] although in his second paper,[338] by a method apparently less open to criticism,* he finds the value $7.5(10^4)$; this value was found to show no measurable drift with temperature from -10 to $+50$°C. Whatever value is adopted, it must satisfy the relation

$$a_{14} = b_{14}c^P_{44}.$$

If one accepts $b_{14} = 6.4(10^{-7})$ and $c^P_{44} = 11.6(10^{10})$, one finds

$$a_{14} = 7.4(10^4).$$

* Mason writes $f^\sigma_{14} = 4\pi e_{14}/K_1$, where K_1 is the clamped dielectric constant. He gets e_{14} from $e_{14} = d_{14}/s_{44}$, but apparently he uses s^P_{44} instead of s^E_{44} in this equation [see Eq. (204)]. As may be seen from his equations (54) and (55), his K_1 is also in error. The correct relation between K_F and K_1 [our k' and k''; see Eqs. (521) and (521*b*)] does not involve s'_{12}.

In calculating a_{25} and a_{36}, we use the values of c_{55} and c_{66} from Table V, which may be assumed to be approximately the constant-polarization values. Then from Eq. (ix), Table XX, we have $a_{25} = b_{25}c^P_{55}$ and $a_{36} = b_{36}c^P_{66}$.

The final values are as follows, all with a probable precision of ± 10 per cent:

$$a_{14} = 7.4(10^4) \qquad b_{14} = 6.4(10^{-7})$$
$$a_{25} = -7.1(10^4) \qquad b_{25} = -23(10^{-7})$$
$$a_{36} = 4.7(10^7) \qquad b_{36} = 5.4(10^{-7})$$

Not only are these constants nearly independent of temperature, but all in the same column are of the same order of magnitude and, indeed, of the same order as the corresponding constants for quartz. The close relationship between piezoelectric and dielectric phenomena comes again to light here: the b-constants are functions of quotients (Voigt piezoelectric strain constant)/(susceptibility), and since large values of d_{hk} are associated with large η'_k the quotients are much more nearly alike than are the d_{hk} for different crystals and for different effects in the same crystal.

143. *Heavy-water Rochelle Salt.* The properties of this crystal, including dielectric and elastic, are described in §444. The piezoelectric values below are derived from observations by Holden and Mason[231] on 45° X-, Y-, and Z-cut bars vibrating in resonance. d_{14} is calculated by means of Eq. (452) (page 388);* similar formulas are used for d_{25} and d_{36}. The coefficient a_{14} of the polarization theory is derived from Eq. (495d).

Temperature, deg C	d_{14}	a_{14}
	$\times 10^{-6}$	$\times 10^4$
−15	5.8	7.1
+ 4	4.2	7.0
34	84	7.2
48	6.4	7.8

The form of the curve relating d_{14} with temperature, show in Holden and Mason's paper, is similar to that for ordinary Rochelle salt. a_{14} is nearly independent of temperature, with a mean value of about $7.3(10^4)$, approximately the same as for ordinary Rochelle salt.

* This formula is probably more accurate than that used by Holden and Mason and yields values somewhat different from theirs. Values of η'_z are from their Fig. 5, in substantial agreement with Hablützel's data, which are shown in Fig. 134.

Holden and Mason find for d_{25} and d_{36}:

$$d_{25} = -220(10^{-8}) \qquad d_{36} = 40(10^{-8})$$

These two values are both somewhat greater than those for ordinary Rochelle salt in §141. d_{25} shows a slight increase with temperature.

144. Sodium-ammonium Tartrate, $NaNH_4C_4H_4O_6{\cdot}4H_2O$. Elastic and other data for this crystal are given in §88. The following piezoelectric constants were measured by Mandell,[328] who also measured the elastic constants:

$$d_{14} = 56(10^{-8}) \qquad d_{25} = -149.5(10^{-8}) \qquad d_{36} = 28.3(10^{-8})$$

This tartrate is isomorphic with Rochelle salt, but it shows none of the piezoelectric anomalies of the latter, beyond a certain fatigue effect and dependence on moisture in the surrounding air. Mandell found no appreciable change in piezoelectric response from -17 to $+30°C$. Above 30°C the crystal gradually becomes conducting.

Mixed crystals of the $Na(NH_4)$ and NaK tartrates can be grown in all proportions. Their properties are discussed in Chap. XXVII.

145. Class 10, Tetragonal Polar (Tetartohedral) (symmetry C_4). Not pyroelectric. There are seven piezoelectric constants, with four independent values:

$$\left.\begin{aligned} -X_x = e_{31}E_z \qquad -Y_y = e_{32}E_z = e_{31}E_z \qquad -Z_z = e_{33}Z_z \\ -Y_z = e_{14}E_x + e_{15}E_y \qquad -Z_x = e_{15}E_x + e_{25}E_y = e_{15}E_x - e_{14}E_y \end{aligned}\right\} \quad (208)$$

The only crystal in this class on which piezoelectric measurements have been made is *barium antimonyl tartrate*, $Ba(SbO)_2(C_4H_4O_6)_2{\cdot}H_2O$. Veen[563] found $d_{33} = 11(10^{-8})$.

146. Class 11, Ditetragonal Alternating (Hemihedral with Inversion Axis (symmetry V_d). Not pyroelectric. There are three piezoelectric constants, of the same types as those in Class 6, but two of them have identical values:

$$-Y_z = e_{14}E_x \qquad -Z_x = e_{14}E_y \qquad -X_y = e_{36}E_z \qquad (209)$$

All the transformation equations given above for Class 6 hold for Class 11 also.

At the present time the importance of this class, from the piezoelectric viewpoint, lies in the fact that some of its representatives have Seignette-electric properties related to those of Rochelle salt. As shown by Busch[88] these are the primary phosphates and arsenates of potassium and ammonium. Their dielectric properties and the possible transitions to other crystallographic classes at certain temperatures are treated in Chap. XXVII.

The piezoelectric constant d_{36} of KH_2PO_4 has been measured statically by Lüdy[322] by means of a string electrometer, and by Bantle and Caflisch,[26] who used a ballistic galvanometer. At the Curie point, 122°K (−151°C), a value as high as 60,000 (10^{-8}) was determined. With increasing temperature the value falls, very rapidly at first and then more slowly, to 50(10^{-8}) at 20°C. Below 122°K the value decreases to 10,000 (10^{-8}) at the temperature of liquid air. It is in the region below 122°K that KH_2PO_4 takes on Seignette-electric properties, analogous to those of Rochelle salt between the Curie points. In this region d_{36} depends on stress as well as on temperature, as is shown by the fact that the polarization: stress curve is non-linear, with an approach toward saturation when the stress is around 40 kg/cm².

Similar results with the converse effect were obtained by Arx and Bantle.[11] They found that below the Curie point, exactly as with Rochelle salt, an alternating electric field gave rise to a hysteresis loop. From this it appears that d_{36} is not a single-valued quantity below 122°C, except with very weak fields. As with Rochelle salt, there is a "Curie-Weiss law" for d_{36} in the neighborhood of the upper Curie point.[26] The properties of KH_2PO_4 are described further in Chap. XXVII.

147. Class 12, Tetragonal Holoaxial (Enantiomorphous Hemihedral) (symmetry D_4). Not pyroelectric. There is only one independent piezoelectric constant, $e_{14} = -e_{25}$. The transformation equations given above for Class 6 become especially simple when applied to Class 12.

Classes 12 and 24 possess a unique piezoelectric property, which follows from the fact that for both of them $e_{25} = -e_{14}$ and $e_{36} = 0$. The result is that for these two classes there is no direction in which a compression can be applied which will cause any component of polarization parallel to the compression: *there is no longitudinal effect in Classes* 12 *and* 24. This conclusion follows at once from the equation for d'_{11}, d'_{22}, or d'_{33} in (201). On the other hand, the transverse effect with respect to transformed axes does not vanish; this may be seen, for example, from the equation for d'_{12} in (201).

The only representative of Class 12 that need be mentioned is nickel sulphate, $NiSO_4 \cdot 6H_2O$. Its cleavage is so easy and its instability is such that it cannot be recommended for piezoelectric applications.

148. Class 18, Trigonal Holoaxial (Enantiomorphous Hemihedral) (symmetry D_3). Not pyroelectric. The chief representative is α-quartz. There are five piezoelectric constants, with only two independent values:

$$\left.\begin{aligned} -X_x = e_{11}E_x \qquad -Y_y = e_{12}E_x = -e_{11}E_x \qquad -Y_z = e_{14}E_x \\ -Z_x = e_{25}E_y = -e_{14}E_y \qquad -X_y = e_{26}E_y = -e_{11}E_y \end{aligned}\right\} \quad (210)$$

Of these equations, the first represents the longitudinal effect, the second the transverse effect, discovered in quartz by the Curie brothers.

The first gives the driving stress for thickness vibrations, the second that for lengthwise vibrations, in X-cut plates. The last equation plays a part in thickness vibrations of Y-cut plates. In the theory of oblique cuts various combinations of the constants occur. The possible vibrational modes that can be excited piezoelectrically in quartz are discussed in Chap. XVII.

Following are the expressions relating the piezoelectric stress and strain constants, specialized from Eqs. (191) and (191a):

$$e_{11} = d_{11}(c_{11} - c_{12}) + d_{14}c_{14} \tag{211}$$
$$e_{14} = 2d_{11}c_{14} + d_{14}c_{44} \tag{211a}$$
$$d_{11} = e_{11}(s_{11} - s_{12}) + e_{14}s_{14} \tag{211b}$$
$$d_{14} = 2e_{11}s_{14} + e_{14}s_{44} \tag{211c}$$

Equations (188) become reduced to

$$-P_x = d_{11}(X_x - Y_y) + d_{14}Y_z \quad -P_y = -(d_{14}Z_x + 2d_{11}X_y)$$
$$P_z = 0 \tag{212}$$

For crystals in this class the summation in Eq. (265), for fields parallel to either X or Y ($m = 1$ or 2), becomes reduced to

$$\sum_i^6 e_{mi}d_{mi} = 2e_{11}d_{11} + e_{14}d_{14} \tag{213}$$

This expression occurs in the relation between the free and clamped dielectric constants. For fields parallel to Z the piezoelectric effect vanishes, so that $k_z' = k_z''$.

Let the dimensions of an X-cut plate be e, l, and b parallel to the X-, Y-, and Z-axes, e being small in comparison with b and l. Then if a compressional force $F_x = blX_x$ is applied, the piezoelectric charge on electrodes covering the major faces is

$$Q_x = blP_x = -\frac{bld_{11}F_x}{bl} = -d_{11}F_x \tag{214}$$

If the applied compression is $F_y = beY_y$, the charge is

$$Q_x = blP_x = \frac{bld_{11}F_y}{be} = \frac{d_{11}F_yl}{e} \tag{215}$$

Equations (214) and (215), which express the longitudinal and transverse effects respectively, were verified by the Curie brothers. It should be noted especially that in the longitudinal effect the charge is independent of the area to which the force is applied, while in the transverse effect the charge is proportional to the ratio of length to thickness of plate.

149. In the measurement of d_{11} a question may arise concerning the effect on the precision with which d_{11} is determined, when the pressure

is applied to a *small portion only* of the surface and also when the electrodes do not cover the entire YZ-faces. So far as the longitudinal effect is concerned, if the force F_x and the total charge Q_x are observed, the constant d_{11} is given by Eq. (214): $d_{11} = -Q_x/F_x$. In order that all of the piezoelectric charge may be observed, the electrodes must cover at least as much of the crystal as is in a state of strain; but it is not necessary to assume that all lines of elastic stress are parallel to the X-axis. Nevertheless, in order to minimize the danger of producing a flexure of the plate, with the attendant polarization, it is better to distribute the pressure uniformly over the entire surface and to let the electrodes extend to the edges of the plate.

When, as is more common, d_{11} $(= -d_{12})$ is measured by the transverse effect, it is customary to apply a pressure, parallel to Y, to an X-cut plate having its length and breadth parallel to Y and Z, and provided with electrodes in immediate contact with the two faces normal to X. The pressure may, of course, be either a compression or an extension. The latter is preferable, since bending or buckling of the plate is thereby avoided. In order to avoid troublesome edge corrections, the electrodes should cover the entire *breadth* of the plate, parallel to Z, but they need not extend to the ends: it is sufficient to let the quantity l in Eq. (215) represent the length of the electrodes.

Corresponding to Eqs. (214) and (215), the following expressions hold for the elongations produced when a potential difference V esu is applied to an X-cut plate having a thickness e parallel to X and length l parallel to Y:

$$\Delta e = d_{11}V \qquad \Delta l = d_{12}\frac{l}{e}V = -d_{11}\frac{l}{e}V \tag{216}$$

An expression for d_{14} similar to Eq. (215) can be written if it is assumed that the applied stress is Y_z. Such a stress could theoretically be realized with an X-cut plate by impressing upon the two faces normal to the Y-axis a pair of tangential tractive forces $\pm F_y = \pm beY_z$, the directions of these forces being parallel to the Z-axis. From Eqs. (212) there would result

$$Q_x = blP_x = -\frac{bld_{11}F_y}{be} = -\frac{l}{e}d_{14}F_y \tag{217}$$

The similarity of this expression to (215) is obvious. In practice, such a shearing stress as this is usually attained by applying a compression to an obliquely cut plate. It was thus that Voigt determined d_{14} for quartz, using X-cut rectangular plates rotated $22\frac{1}{2}$ and 45° about the X-axis. Calling Z'_z the impressed stress, we have for the resulting polarization, from Eqs. (221),

$$-P_x = d'_{13}Z'_z = -Z'_z(s^2d_{11} + scd_{14})$$

When d_{11} has been determined by means of Eq. (214) or (215), d_{14} can be calculated from the observed P_x and Z'_x.

150. Piezoelectric Constants, Class 18, for Rotated Axes. For the transformation to axes in any desired orientation the methods of §134 are employed, retaining only those constants that are characteristic of this class. For example, from Eq. (194) it follows that

$$e'_{33} = \gamma_1(\gamma_1^2 - 3\gamma_2^2)e_{11} \tag{218}$$

where γ_1 and γ_2 are direction cosines for the Z'-axis. In terms of azimuth φ and colatitude θ of the Z'-axis, as defined in §51, this equation may be written thus:

$$e'_{33} = e_{11} \cos 3\varphi \sin^3 \theta \tag{218a}$$

Similarly, from Eq. (194) or (198),

$$d'_{33} = \gamma_1(\gamma_1^2 - 3\gamma_2^2)d_{11} = d_{11} \cos 3\varphi \sin^3 \theta \tag{219}$$

For this class hardly any general transformation formulas for the piezoelectric constants, applicable to axes in all orientations, are available. In a recent paper Mason and Sykes[343] give the equation for d'_{31} for any axial system, the axial directions being specified in terms of the angles φ, Θ, and ψ according to §52:

$$d'_{31} = d_{11} \sin \Theta[\cos 3\varphi(\cos^2 \Theta \cos^2 \varphi - \sin^2 \psi) - \sin 2\psi \sin 3\varphi \cos \Theta] - \frac{d_{14}}{2}(\sin^2 \Theta \sin 2\psi) \tag{220}$$

The relations between φ, Θ, ψ, and the direction cosines are given in §52.

151. The most useful transformation formulas are those for rotation about a *single axis.* They may be derived from Eqs. (196). *About the X-axis,* the direction cosines defined in Fig. 41 become $\alpha_1 = 1$,

$$\beta_1 = \gamma_1 = \alpha_2 = \alpha_3 = 0,$$

$\beta_2 = \gamma_3 = c$, $\beta_3 = -\gamma_2 = s$. The transformed constants are

$$\left.\begin{array}{ll}
d'_{11} = d_{11} & e'_{11} = e_{11} \\
d'_{12} = -c^2d_{11} + scd_{14} & e'_{12} = -c^2e_{11} + 2sce_{14} \\
d'_{13} = -s^2d_{11} - scd_{14} = d'_{12} \quad [\theta \pm 90°] & e'_{13} = -s^2e_{11} - 2sce_{14} = e'_{12} \quad [\theta \pm 90°] \\
d'_{14} = 2csd_{11} + (c^2 - s^2)d_{14} & e'_{14} = cse_{11} + (c^2 - s^2)e_{14} \\
d'_{15} = d'_{16} = 0 & e'_{15} = e'_{16} = 0 \\
d'_{21} = d'_{22} = d'_{23} = d'_{24} = 0 & e'_{21} = e'_{22} = e'_{23} = e'_{24} = 0 \\
d'_{25} = 2csd_{11} - c^2d_{14} & e'_{25} = cse_{11} - c^2e_{14} \\
d'_{26} = -2c^2d_{11} - csd_{14} & e'_{26} = -c^2e_{11} - cse_{14} \\
d'_{31} = d'_{32} = d'_{33} = d'_{34} = 0 & e'_{31} = e'_{32} = e'_{33} = e'_{34} = 0 \\
d'_{35} = -2s^2d_{11} + csd_{14} = d'_{26} \quad [\theta \pm 90°] & e'_{35} = -s^2e_{11} + cse_{14} = e'_{26} \quad [\theta \pm 90°] \\
d'_{36} = 2csd_{11} + s^2d_{14} = -d'_{25} \quad [\theta \pm 90°] & e'_{36} = cse_{11} + s^2e_{14} = -e'_{25} \quad [\theta \pm 90°]
\end{array}\right\} \tag{221}$$

Rotation about the Y-axis. $\beta_2 = 1, \beta_1 = \beta_3 = \alpha_2 = \gamma_2 = 0,$

$$\alpha_1 = \gamma_3 = c \qquad -\alpha_3 = \gamma_1 = s.$$

$$\begin{aligned}
d'_{11} &= c^3 d_{11} & e'_{11} &= c^3 e_{11}\\
d'_{12} &= -cd_{11} & e'_{12} &= -ce_{11}\\
d'_{13} &= cs^2 d_{11} & e'_{13} &= cs^2 e_{11}\\
d'_{14} &= c^2 d_{14} & e'_{14} &= c^2 e_{14}\\
d'_{15} &= 2c^2 s d_{11} = 2d'_{13} \quad [90^\circ \pm \theta] & e'_{15} &= c^2 s c_{11} = e'_{13} \quad [90^\circ \pm \theta]\\
d'_{16} &= -csd_{14} & e'_{16} &= -cse_{14}\\
d'_{21} &= -d'_{16} & e'_{21} &= -2e'_{16}\\
d'_{22} &= 0 & e'_{22} &= 0\\
d'_{23} &= d'_{16} & e'_{23} &= 2e'_{16}\\
d'_{24} &= -sd_{11} = d'_{12} \quad [90^\circ \pm \theta] & e'_{24} &= -sc_{11} = c'_{12} \quad [90^\circ \pm \theta]\\
d'_{25} &= -(c^2 - s^2)d_{14} & e'_{25} &= -(c^2 - s^2)e_{14}\\
d'_{26} &= 2d'_{12} & e'_{26} &= c'_{12}\\
d'_{31} &= \frac{d'_{15}}{2} & e'_{31} &= c'_{15}\\
d'_{32} &= d'_{24} & e'_{32} &= e'_{24}\\
d'_{33} &= s^3 d_{11} = d'_{11} \quad [90^\circ \pm \theta] & e'_{33} &= s^3 c_{11} = e'_{11} \quad [90^\circ \pm \theta]\\
d'_{34} &= -d'_{16} & e'_{34} &= -e'_{16}\\
d'_{35} &= 2d'_{13} & e'_{35} &= e'_{13}\\
d'_{36} &= -s^2 d_{14} = -d'_{14} \quad [90^\circ \pm \theta] & e'_{36} &= -s^2 e_{14} = -e'_{14} \quad [90^\circ \pm \theta]
\end{aligned} \tag{222}$$

Rotation about the Z-axis. $\gamma_3 = 1, \gamma_1 = \gamma_2 = \alpha_3 = \beta_3 = 0,$

$$\alpha_1 = \beta_2 = c \qquad \alpha_2 = -\beta_1 = s.$$

$$\begin{aligned}
d'_{11} &= c(1 - 4s^2)d_{11} = d_{11}\cos 3\theta & e'_{11} &= c(1 - 4s^2)e_{11} = e_{11}\cos 3\theta\\
d'_{12} &= -d'_{11} & e'_{12} &= -e'_{11}\\
d'_{13} &= d'_{15} = 0 & e'_{13} &= e'_{15} = 0\\
d'_{14} &= d_{14} & e'_{14} &= e_{14}\\
d'_{16} &= d'_{21} & e'_{16} &= e'_{21}\\
d'_{21} &= s(1 - 4c^2)d_{11} = -d_{11}\sin 3\theta & e'_{21} &= s(1 - 4c^2)e_{11} = -e_{11}\sin 3\theta\\
d'_{22} &= -d'_{21} & e'_{22} &= -e'_{21}\\
d'_{23} &= d'_{24} = 0 & e'_{23} &= e'_{24} = 0\\
d'_{25} &= -d_{14} & e'_{25} &= -e_{14}\\
d'_{26} &= -d'_{11} & e'_{26} &= -e'_{11}\\
d'_{31} &= d'_{32} = d'_{33} = 0 & e'_{31} &= e'_{32} = e'_{33} = 0\\
d'_{34} &= d'_{35} = d'_{36} = 0 & e'_{34} &= e'_{35} = e'_{36} = 0
\end{aligned} \tag{223}$$

152. Polarization Produced in Crystals of Class 18 by Uniform Pressure in Any Direction. Let the pressure be Z'_z, parallel to a Z'-axis having any direction cosines $\gamma_1, \gamma_2, \gamma_3$; the result may also be expressed in terms of azimuth φ and colatitude θ (Fig. 17). It follows from Eqs. (212) and (22) or from Eq. (197) that the components of polarization are

$$\left.\begin{aligned} P_x &= -[(\gamma_1^2 - \gamma_2^2)d_{11} - \gamma_2\gamma_3 d_{14}]Z'_z \\ &= -[d_{11}\sin^2\theta(\cos^2\varphi - \sin^2\varphi) + d_{14}\sin\theta\cos\theta\sin\varphi]Z'_z \\ P_y &= \gamma_1(2\gamma_2 d_{11} + \gamma_3 d_{14})Z'_z \\ &= \sin\theta\cos\varphi(2d_{11}\sin\theta\sin\varphi + d_{14}\cos\theta)Z'_z \\ P_z &= 0 \end{aligned}\right\} \tag{224}$$

The total polarization, given by $P^2 = P_x^2 + P_y^2$, lies always in the XY-plane; it can be resolved into two components, parallel and perpendicular to Z'. The former of these, which may be called P_l, expresses the longitudinal effect for oblique pressures in quartz or in other crystals of Class 18.

$$P'_z = P_l = \gamma_1 P_l + \gamma_2 P_2 = -d_{11}\sin^3\theta\cos 3\varphi \cdot Z'_z = -d'_{33}Z'_z \tag{225}$$

where
$$d'_{33} = d_{11}\sin^3\theta\cos 3\varphi \tag{226}$$

as in Eq. (219).

When $\theta = 90°$ and $\varphi = 0$, 120, or 240°, $d'_{33} = d_{11}$, Z'_z becomes X_x parallel to one of the electric axes, P_l becomes P_x. This is the maximum value that P_l can assume with given Z'_z; and in these special orientations P_l is also the *total* polarization. In general, there are components of polarization both parallel and perpendicular to Z'_z, except for certain special orientations that will be considered in the following paragraphs.

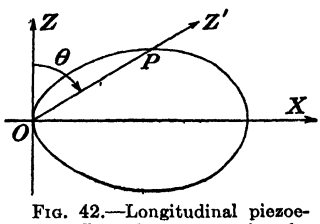


FIG. 42.—Longitudinal piezoelectric effect for quartz in the ZX-plane (from Voigt). Radius vectors are proportional to d'_{33}.

We pass now to the specialization of Eq. (226) for the three principal planes. For *pressures in the YZ-plane*, $\varphi = 90°$, and $d'_{33} = 0$ for all values of θ; no longitudinal polarization P_l is produced by pressures perpendicular to the X-axis, but only P_x as given by Eqs. (224). If the pressure is *in the ZX-plane*, $\varphi = 0$ and

$$d'_{33} = d_{11}\sin^3\theta \tag{227}$$

The polar diagram representing d'_{33} for quartz as a function of θ, from Eq. (227), is shown in Fig. 42, in which the radius vector OP is proportional to d'_{33} and hence to $P'_z = -d'_{33}Z'_z$. For negative values of θ, d'_{33} becomes negative, but its numerical value is still correctly given in Fig. 42.

The trigonal character of this crystal class is evident from the occurrence of the angle 3φ in Eq. (226) and is nicely brought to light when we consider the longitudinal effect *in the XY-plane.* Here $\theta = 90°$, so that

$$d'_{33} = d_{11} \cos 3\varphi \tag{228}$$

The polar diagram (Fig. 43) is now in the form of a cloverleaf, with $d'_{33} = d_{11}$ when the pressure is parallel to one of the axes X_1, X_2, or X_3. With respect to any one of the three X-axes, say X_1, d'_{33} takes on both + and − values as φ varies. These changes in sign, as well as the numerical values for quartz, are shown in Fig. 44. If one were to take X'_x or Y'_y as the pressure instead of Z'_z, Fig. 43 would of course represent d'_{11} or d'_{22}.

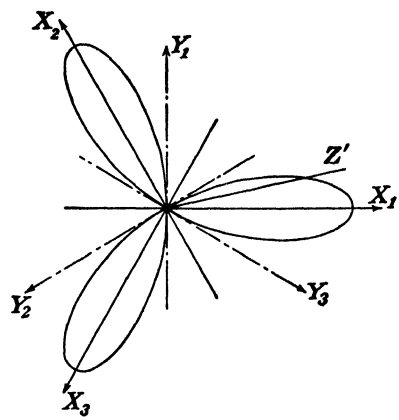


FIG. 43.—Longitudinal piezoelectric effect for quartz in the XY-plane (from Voigt). Radius vectors are proportional to d'_{33}.

One may imagine a model based on Eq. (226) constructed to represent d'_{33} in all orientations. Its surface would be of the third degree, *viz.*, the trivector surface mentioned in §136, of which the intersections with the ZX- and XY-planes are represented by Figs. 42 and 43. Such a surface would be like three almonds placed with their small ends in contact.*

An interesting relation between polarization P and compressional stress holds when the latter is *normal to the Z-axis.* Like the effects described in the foregoing paragraphs, it depends on the fact that for this class $d_{12} = -d_{11}$. By setting $\theta = 90°$ in Eqs. (224) we find

$$P_x = -d_{11} Z'_z \cos 2\varphi,$$

$P_y = d_{11} Z'_z \sin 2\varphi$, whence $P^2 = P_x^2 + P_y^2 = d_{11}^2 Z_z'^2$. From these expressions it is seen at once that, when the pressure is parallel to either an X- or a Y-axis ($\varphi = 0$), P is parallel to X; that, when the pressure is in a direction $\pm 45°$ from an X-axis, P is parallel to Y; and hence that, as the direction of the pressure varies in the XY-plane, P rotates in space while maintaining always the same numerical value $d_{11} Z'_z$. It is easy to show that P rotates *twice as rapidly* as Z'_z, and in the *opposite direction.* This relation for the *total* polarization must not be confused with that for

* A photograph of the "almond" model is reproduced in a paper by Günther.[197]

the *longitudinal* polarization depicted in Fig. 43, which shows that as the pressure is rotated through 360° there are six positions in which the component of P parallel to the pressure vanishes.

153. Polarization Produced by a Uniform Field Normal to the Z-axis. In the last paragraph it was shown that a compressional stress normal to the Z-axis produces a polarization that is constant in amount, but not parallel to the stress except in certain special azimuths. On the other hand, a uniform electric *field* normal to the Z-axis causes a polarization not only constant in amount but also *parallel to the field.* This fact follows from the symmetry of this crystal class and is true whether the crystal is clamped (constant strain) or free to deform itself in the field. Hence a sphere of quartz or a circular cylinder with its axis parallel to Z, mounted so as to rotate freely about the Z-axis and placed between plane-parallel electrodes that are also parallel to the Z-axis and sufficiently remote to ensure that the field is uniform, will show no tendency to orient itself in any particular direction, except insofar as its cross section departs slightly from the circular form as a result of extension or compression along an X-axis. Even with fields of several thousand volts per centimeter, x_x is only of the order of 10^{-6}. If an orientation due to a uniform field is ever observed, it is very much more likely to be caused by some slight eccentricity in the mounting than to an increase in diameter in the direction of one of the X-axes.

Since, according to most observers, the dielectric constant of quartz is slightly greater along the Z-axis than at right angles to it, it follows that a quartz sphere free to assume *any* orientation in a uniform electric field will tend to set itself with the Z-axis in the field direction.

The assertion has been made* that a circular Z-cut quartz disk in an electric field parallel to its plane tends to rotate so as to bring one of its electric axes into parallelism with the field. Their explanation, based on a hypothesis concerning the deformation of the unit cell in a uniform field, is not valid. If experimental errors were eliminated in their observations, one must attribute the rotation to non-uniformity in the electric field. The electrodes were relatively small and close to the edge of the plate on each side. The piezoelectric strain was small except in the regions nearest the electrodes. The crystal was therefore effectively in a state of partial constraint, neither uniformly clamped nor entirely free. Near the electrodes the stresses are greatest, but they are largely neutralized by elastic reaction from the neighboring regions. The strain that may be expected to predominate is the extensional x_z, the extension being nearly radial, in the direction of the X-axis that happens to be closest to the line joining the electrodes. According to §204, this strain provides a slight increment to the susceptibility in the X-direction,

* A. Meissner and R. Bechmann, *Z. tech. Physik*, vol. 9, pp. 430–434, 1928.

whereupon the disk tends to set itself with the direction of maximum susceptibility parallel to the field.

154. Alpha-quartz. The crystallographic properties are described in §11, and the definition of the I.R.E. axial system, adopted in this book for enantiomorphous crystals, is to be found in §327. All values given below are in terms of this system, according to which the signs of d_{11} and d_{14} are the same for a right- as for a left-quartz, *viz.*, the same signs that Voigt would have assigned to a *right-quartz* according to his axial convention.*

TABLE XVII.—PIEZOELECTRIC STRAIN CONSTANT d_{11} OF QUARTZ
(Static values)

No.	Source	Ref.	d_{11}	Effect
			$\times 10^{-8}$	
1	P. and J. Curie, 1881	B10, 117	6.32	Direct, *L*, *T*
2	Czermak, 1887	118	6.3	Direct, *L*
3	Riecke and Voigt, 1892	435	6.45	Direct, *L*
4	Pockels, 1894	428	6.27	Direct, *T*
5	Nachtikal, 1899	386	6.54	Direct, *L*
6	J. Curie, 1910	B11	6.90	Direct, *T*
7	Veen, 1911	563	6.32	Direct, *T*
8	Hayashi, 1912	210	6.31	Direct, *L*
9	Röntgen and Joffé, 1913	440	6.94	Direct, *T*, *L*
10	Tsi-Ze, 1927	523	6.4	Converse, *T*, *L*
11	Seidl, 1932	456	6.90	Direct, *T*
12	Günther, 1932	194	6.35	Converse, *T*
13	Knol, 1932	262	6.83	Direct, *L*
14	Osterberg and Cookson, 1935	407	6.22	Converse, *T*
15	Clay and Karper, 1937	112	6.80	Direct, *L*
16	A. Langevin, 1939	305	7.10	Direct, *T*(?)
17	Lüdy, 1939	322	6.54	Direct, *T*

In Tables XVII and XVIII are given those values of d_{11} and d_{14} found in the literature, measured by *static* methods, that can be regarded as representative. All are for room temperature. The fourth column indicates whether the direct or the converse effect was employed and also whether the impressed stress (or the observed strain) was parallel to X (longitudinal effect L) or parallel to Y (transverse effect T). It can be assumed that in no case was the deformation great enough to show a departure from linearity.

* That the signs of d_{11} and d_{14}, *according to Voigt's conventions respecting axes*, must be reversed on passing from right- to left-quartz, is made clear on p. 861 of the "Lehrbuch." Readers of the "Lehrbuch" have no way of knowing that the values of these constants, given on p. 869, were obtained with *left*-quartz, unless they consult the original paper of Riecke and Voigt.[435]

In about half the measurements listed in Table XVII the direct longitudinal effect was used, with compression and polarization both parallel to X. Where the transverse effect was employed, the polarization was produced in most cases by *tension* parallel to Y, rather than by compression, a procedure that is preferable in order to avoid bending of the plate. The transverse effect gives d_{12}; all experimental data confirm the relation $d_{12} = -d_{11}$. Osterberg and Cookson observed the deformations under a 60-cycle *alternating* field; this frequency is so low that their result may properly be included among the static values.

Most of the systematic sources of error, such as faulty orientation of the plate, twinning or other defects in the crystal, and imperfect insulation, tend to make the observed values of d_{11} too small. It is quite probable that the larger values recorded in Table XVII from 1910 on are due to more successful attention to these matters. Of all the observations recorded, none seem to exceed Nos. 6 and 9 in care and skill; it is probably not by mere chance that these are also among the largest values. Langevin emphasizes the fact that his large value was obtained only with very perfect plates. He states, for example, that on removal of a small twinned region from one of his plates the value of d_{11} rose from $5.77(10^{-8})$ to $6.83(10^{-8})$. Though the details of his method are not given, his results can be accepted as very reliable.

All things considered, the value $d_{11} = 6.9(10^{-8})$ seems a conservative one to adopt, in agreement with the opinions of Sosman* and of Voigt and Fréedericksz.[576] More measurements of high precision, with accurately oriented plates of greatest perfection, are much to be desired; it may well be that such measurements will confirm the large value observed by Langevin.

A critical discussion of some of the papers cited in Table XVII is given in Sosman's book. In the "Lehrbuch"† Voigt seems to accept the mean of the observations of Riecke and Voigt and of Pockels as the best value of d_{11}, namely, $-6.36(10^{-8})$.‡ Although still widely used, this value should henceforth be superseded by that given above.

Measurements of d_{11} have also been published by a number of other observers. Those of Dawson[121] and of Fox and Fink,[143] while apparently less precise than those recorded in Table XVII, are of the same order of magnitude. Gramont§ obtained $d_{11} = 6.37$, 6.37, and $6.40(10^{-8})$ with three different samples, but experimental details are lacking.

155. *Experimental Values of d_{11} for Quartz by Static Methods.* Values from various sources are given in Table XVIII.

* Ref. B47, p. 559.

† P. 870.

‡ The negative sign, as used by Voigt, arose from his convention respecting axial directions, for which see §327.

§ Ref. B21, p. 51.

TABLE XVIII.—PIEZOELECTRIC STRAIN CONSTANT d_{14} OF QUARTZ
(Static values)

No.	Source	Ref.	$-d_{14}$	Method
			$\times 10^{-8}$	
1	Riecke and Voigt, 1892	435	1.45	X-cut plate
2	Pockels, 1894	428	1.93	X-cut plate
3	Voigt and Fréedericksz, 1915	576	2.25	Torsion
4	Osterberg and Cookson, 1935	407	2.24	X-cut plate, 60~
5	Langevin and Solomon, 1935	307	2.1	Torsion
6	Gibbs and Tsien, 1936	159	2.04	Torsion

Owing to the comparatively small magnitude of d_{14} and to increased experimental difficulties, less precision can be expected in the measurement of this constant than in that of d_{11}. Observations 3, 5, and 6 were made by applying torsion to quartz cylinders. Although less reliance can be placed on such indirect data than on those obtained with flat plates, still the uniformly high values are significant. On the one hand, we have the fact pointed out above in connection with d_{11}, that most sources of error tend to make the values too small. On the other hand, observations 1 and 2, yielding the lowest values, were made with especial care and skill. The mean of observations 1 and 2, $1.69(10^{-8})$, was adopted by Voigt* and has been widely quoted. In view of the later publications, however, it seems best to adopt for the present the value $d_{14} = -2.0(10^{-8})$.

156. The following are to be recommended as the best values to date for the piezoelectric strain constants of quartz:

$$d_{11} = +6.9(10^{-8}) \qquad d_{14} = -2.0(10^{-8}) \tag{229}$$

The values according to the polarization theory are given in §158.

The piezoelectric stress constants of quartz are found from Eqs. (211) and (211a), using the values of d_{11} and d_{14} given above, together with the elastic constants from Table XI:†

$$e_{11} = +5.2(10^4) \qquad e_{14} = +1.2(10^4) \tag{230}$$

157. *The Piezoelectric Constants by Dynamic Methods.* Some of the more important results are given in Table XIX. They are derived by methods described in §310. The first two data are of relatively low

* "Lehrbuch," p. 870.

† In Voigt's "Lehrbuch" (p. 870), the values of e_{11} and e_{14} as calculated from his data are in error. They should read $e_{11} = -4.69(10^4)$, $e_{14} = -1.18(10^4)$.

precision and are included as of historical interest. The most trustworthy values are probably those of Van Dyke and Mason.

TABLE XIX.—DYNAMIC VALUES OF THE PIEZOELECTRIC CONSTANTS OF QUARTZ

No.	Source	Ref.	e_{11}	d_{11}
			$\times 10^{+4}$	$\times 10^{-8}$
1	Andreeff, Fréedericksz, and Kazarnowsky, 1929	4		6.51
2	Fujimoto, 1929	152		6.1
3	Fréedericksz and Mikhailov, 1932	150		5.55
4	Nussbaumer, 1932	395		6.84
5	Van Dyke, 1935	554		6.70
6	Mason, 1943 [also $d_{14} = -2.56(10^{-8})$ and $e_{14} = +0.97(10^4)$]	340	5.01	6.76

No theoretical reason is known for any difference between static and dynamic values of the piezoelectric constants. Until the dynamic methods have proved themselves further and it is certain that possible sources of error have been eliminated, it seems best to adopt the values of the constants given in Eqs. (229) and (230).

158. *Piezoelectric Constants of Quartz According to the Polarization Theory.* From Eq. (242), together with the piezoelectric constants in Eqs. (229) and (230) and the dielectric constants from §331, one finds

$$\left.\begin{aligned} a_{11} &= \frac{e_{11}}{\eta_x''} = 19(10^4) & a_{14} &= \frac{e_{14}}{\eta_x''} = 4.4(10^4) \\ b_{11} &= \frac{d_{11}}{\eta_x'} = 2.5(10^{-7}) & b_{14} &= \frac{d_{14}}{\eta_x'} = -0.72(10^4) \end{aligned}\right\} \tag{231}$$

As in Voigt's theory, the other constants are $a_{12} = a_{26} = -a_{11}$, $b_{12} = b_{26}/2 = -b_{11}$, $a_{25} = -a_{14}$, $b_{25} = -b_{14}$.

159. *Dependence of d_{11} upon Stress.* Under ordinary conditions this effect is small. For larger stresses the results are conflicting. Nachtikal[386] found that d_{11} was linear in X_x,

$$d_{11} = 6.54(10^{-8}) - 1.05(10^{-16})X_x \tag{232}$$

where, as usual, X_x is in dynes per square centimeter. According to this equation, a load of 1 kg/cm² decreases d_{11} by 0.16 per cent. The paper by Clay and Karper[112] records d_{11} as constant up to 10 kg/cm², but slightly less at 15 kg/cm². Finally, Karcher[274] found d_{11} to be constant to within 0.1 per cent for pressures up to 3,500 kg/cm².

In experiments on the converse effect, Tsi-Ze[523] found d_{11} to decrease according to an exponential law as E_x increased, being nearly constant until E_x reached a value of

about 40 esu. In experiments with the *transverse* effect, at $E_x = 20$ esu, d_{11} was diminished by about 9 per cent, and at 500 esu the diminution was about 40 per cent.* Values of the same order of magnitude were obtained with the longitudinal effect, indicating that in both cases the deformation approached a state of saturation as the field became very great. If his data are accepted, one must conclude that, *for the same deformation*, the diminution in d_{11} caused by the converse effect is very much greater than that by the direct effect. For example, Tsi-Ze's Table V for the longitudinal effect indicates, for a field strength of 268 esu, a strain $x_x \approx 10^{-5}$. To produce this strain mechanically would require a stress $X_x \approx 8(10^6)$ dynes/cm^2; and when this value is inserted in Nachtikal's Eq. (232), d_{11} is found to be diminished by only 1.2 per cent, whereas according to Tsi-Ze's data the diminution corresponding to this same strain is 43 per cent. Evidently the piezoelectric effect in quartz under large mechanical and electrical stresses merits further investigation.

No data are at hand concerning the dependence of d_{14} upon stress.

160. *Dependence of d_{11} upon Temperature.* Although the observations are somewhat less discordant than those on the effect of pressure just described, there is so much disagreement among authors as to lead one to suspect that in many cases it was not only the temperature coefficient of d_{11} that was being measured.

Qualitatively, most observers are agreed that d_{11} is greater at room temperature than at very low or very high temperatures.† *Below room temperature* Lissauer‡ found d_{11} to vary not over 2 per cent down to −192°C (liquid air). Onnes and Beckman[396] found d_{11} to decrease about 1.2 per cent from room temperature to that of liquid air and 0.2 per cent from that point to the temperature of liquid hydrogen. Langevin and Moulin[306] observed a greater rate of decrease, *viz.*, a value of d_{11} 5.8 per cent lower at −60 than at 0°C; these last figures indicate a temperature coefficient $\alpha = 9.7(10^{-4})$.

Pitt and McKinley[426] observed the dependence of d_{11} on temperature from 4 to 813°K by means of both a static and a dynamic method. In the latter a quartz X-cut plate 24 by 24 by 0.81 mm was in a piezo-oscillator circuit By the static method d_{11} was found to decrease by 1.3 per cent as the temperature fell from 296 to 83°K; there was a total decrease of 12 per cent in passing from 296 to 4.2°K. Observations by the dynamic method were made all the way from 4.2°K to 540°C. On

* At the larger field strengths Tsi-Ze found the deformations to be due in part to electrostriction (§137), the effect of which was eliminated by reversing the field. His general equation for deformation as a function of field strength is open to criticism, since it proceeds from the theoretically insecure assumption that the variation of d_{11} is proportional to the potential drop across the crystal rather than to the field-strength and that the constant of proportionality is independent of the thickness of the plate.

† Osterberg (*Phys. Rev.*, vol. 49, pp. 552–553, 1936) asserted that the piezoelectric "activity" *increased* as the temperature decreased from that of the room to −175°C.

‡ Voigt, p. 862.

cooling below 14°K there was no change in d_{11} down to 5.5°K, at which point a sudden decrease occurred. d_{11} was nearly constant from 5.5°K to 200°C, at which point a gradual decrease began, and the response ceased at 540°C. The authors think it might be possible, however, to detect an effect up to α-β-inversion temperature. On the return from high to low temperature they found no trace of the lag in piezoelectric activity that had been reported by Dawson.[121]

Above room temperature, d_{11} was found by Perrier[412] to be nearly constant to 200° and then to decrease until it disappeared at 579°C, reappearing with decreasing temperature at 576° (579° is Perrier's value for the transition temperature from α- to β-quartz; the value now usually assigned is 573°). A similar hysteresis on cooling was also reported by Dawson,[121] who however recorded also a maximum in d_{11} at about 60°C, followed by a rapid decrease, until the value became extremely small between 300 and 480°, differing results being obtained with different crystals. According to Andreeff, Fréedericksz, and Kazarnowsky,[4] d_{11} decreases by 17 per cent as the temperature rises from 15 to 500°C; Fréedericksz and Mikhailov[150] found d_{11} to be practically constant to 187°C, followed by a rapid decrease. A linear decrease of 10 per cent was observed by A. Langevin[304] as the temperature increased from 20 to 200°C, beyond which his observations did not extend.* Langevin's results yield a temperature coefficient $\alpha = -5.5(10^{-4})$, in fair agreement with $-3.5(10^{-4})$ computed from the data of Andreeff, Fréedericksz, and Kazarnowsky quoted above. A still smaller temperature coefficient was measured by Clay and Karper,[112] who found, from 17 to 90°C,

$$\alpha = -7(10^{-6});$$

this result is in substantial agreement with Perrier's observations and those of Fréedericksz and Mikhailov. Röentgen and Joffé,[440] whose apparatus was capable of detecting a change as small as 0.1 per cent, could observe no effect of temperature on d_{11} from 15 to 25°C.

Observations of the lengthwise frequency of an X-cut quartz bar (length parallel to Y) have been made by Van Dyke[553] at temperatures from −80 to +40°C. He finds the effective piezoelectric coefficient† ϵ to decrease from $5.57(10^4)$ at −80°, slowly at first, then more rapidly, reaching the value $5.27(10^4)$ at 40°. The temperature coefficient is ten

* This result was obtained by a zero-deflection (constant-potential) method. Langevin tried first a deflection method, which yielded a maximum in d_{11} at about 60°C. He attributes this maximum, as well as that recorded by Dawson, to errors introduced by deformation of the apparatus.

† It follows from §228 that the effective piezoelectric coefficient for a quartz bar in this orientation is not e_{11}, as stated by Scheibe (ref. B45, p. 70) but $\epsilon = d_{11}/s_{11}$. The difference between ϵ and e_{11}, though small, is not negligible.

times as great at 40° as at −80°, having the value $\alpha_\epsilon = \partial\epsilon/\epsilon\,\partial t = 10(10^{-4})$ at room temperature. From this and the relatively small temperature coefficient of s_{11} one finds for d_{11} a value of $\alpha_{d_{11}}$ around $10(10^{-4})$.

On the whole, it seems probable that the piezoelectric constant d_{11} of quartz has a very flat maximal value around room temperature and that the rate of decrease is of the order of magnitude of 0.1 per cent per degree down to the lowest temperatures on the one hand and up to approximately 200° on the other. It is also certain that $d_{11} = 0$ at the alpha-beta transition point, 573°C.

As to d_{14}, no observations on the temperature dependence seem to have been made. One can be certain, however, that d_{14} does not vanish at 573°C but carries on as the surviving coefficient of β-quartz (§168).

161. *Effect of Radiation from Radium on d_{11} for Quartz.* Laimböck* exposed a quartz plate to the beta and gamma rays from 94 mg of radium. The value of d_{11} was found to increase at a rate roughly proportional to the time, the total increase in 7 days amounting to about 12 per cent. The constant gradually returned to its original value. The effect was less pronounced after repeated radiation.

162. Piezoelectric Constants of Quartz for Rotation about the Three Axes. The curves shown in the succeeding figures are calculated from Eqs. (221) to (223), with $d_{11} = +6.9(10^{-8})$, $d_{14} = -2.0(10^{-8})$.

Figure 44 gives d'_{12}, d'_{14}, d'_{25}, and d'_{26} for rotation about X, and d'_{11} for

$$(\theta \pm 180°)$$

rotation about Z. The following rules apply to this figure:

For *rotation about* X, the ordinate for any θ is the same as for

$$(\theta \pm 180°).$$

For *rotation about* Z, the ordinate for any θ is the same as for $(\theta \pm 120°)$.

Of the constants d'_{hk} for *rotation about* X not shown in Fig. 44, the value of d'_{13} for any θ is the same as that for d'_{12} at $(\theta \pm 90°)$; similarly, the values of d'_{35} and $-d'_{36}$ for any θ are the same as those for d'_{26} and d'_{25}, respectively, at $(\theta \pm 90°)$. All the remaining d'_{hk} vanish except

$$d'_{11} = d_{11}.$$

Of the constants for *rotation about* Z not shown in Fig. 44, all vanish except $d'_{12} = d'_{26} = -d'_{11}$ and $d'_{16} = d'_{21} = -d'_{22} = d_{11} \cos 3(\theta + 30°)$. That is, the value of d'_{16}, d'_{21}, or $-d'_{22}$ for any θ is the same as that of d'_{11} for $(\theta + 30°)$.

The curves for d_{hk} for *rotation about* Y are given in Fig. 45. If the desired angle of rotation lies outside the range from −90 to +90°, the

* J. LAIMBÖCK, *Mitt. Inst. Radiumforschung*, No. 221a, 1928.

following rules are observed: For d'_{11}, d'_{12}, and d'_{13}, the value for any θ is the *negative* of the value for $(\theta \pm 180°)$. For d'_{14}, d'_{16}, and d'_{25} the ordinate

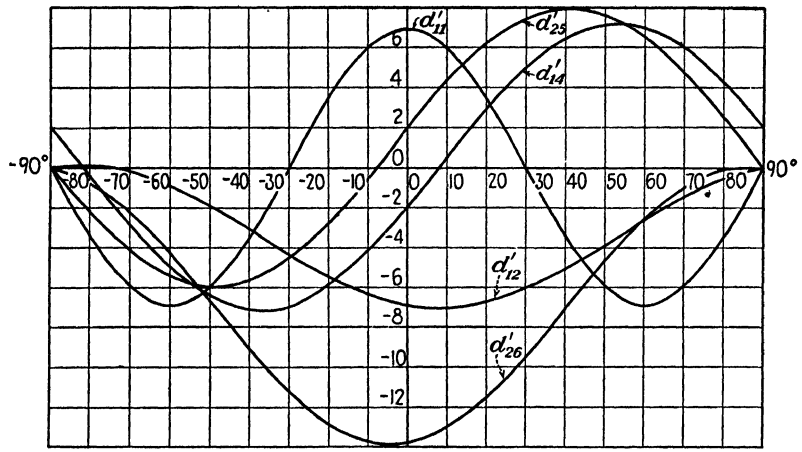


FIG. 44.—Piezoelectric constants of quartz for rotated axes. d'_{12}, d'_{14}, d'_{25}, and d'_{26} are for rotation about the X-axis, d'_{11} for rotation about the Z-axis.

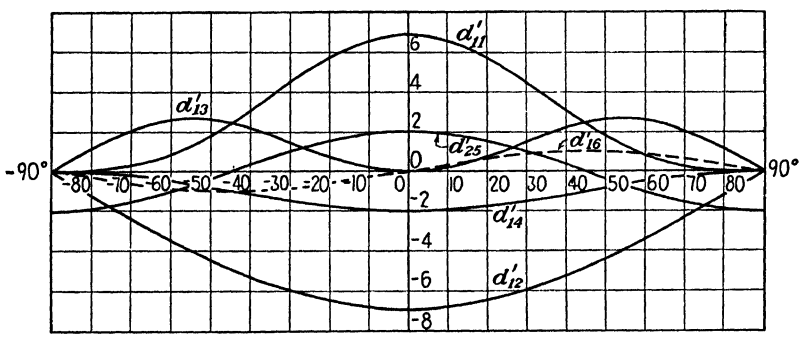


FIG. 45.—Piezoelectric constants of quartz for rotation about the Y-axis.

for any θ is the same as for $(\theta \pm 180°)$. For the remaining constants one finds, for any given θ,

d'_{15}, twice the value of d'_{13} for $(90° \pm \theta)$
$d'_{21} = -d'_{23} = d'_{34} = -d'_{16}$ $\quad d'_{22} = 0$
$d'_{26} = 2d'_{12}$ $\quad d'_{35} = 2d'_{13}$
d'_{24} and d'_{32}, same as d'_{12} for $(90° \pm \theta)$
d'_{31}, same as d'_{13} for $(90° \pm \theta)$
d'_{33}, same as d'_{11} for $(90° \pm \theta)$
d'_{36}, same as d'_{14} for $(90° \pm \theta)$

Other Crystals in Class 18. Veen[563] measured d_{11} for the following crystals in this class:

Benzil, $C_{14}H_{10}O_2$	$24(10^{-8})$
Patchouli camphor, $C_{15}H_{26}O$	$0.14(10^{-8})$
Rubidium tartrate, $Rb_2C_4H_4O_6$	$8(10^{-8})$

163. Class 19, Trigonal Ditrigonal Polar (Hemimorphic Hemihedral) (symmetry C_{3v}). The most important example is tourmaline. Crystals in this class are pyroelectric, the Z-axis being the polar axis. Table XVI shows that there are eight piezoelectric constants, with four independent values e_{15}, e_{22}, e_{31}, and e_{33}:

$$\left.\begin{aligned} -X_x &= e_{21}E_y + e_{31}E_z = -e_{22}E_y + e_{31}E_z \\ -Y_y &= e_{22}E_y + e_{32}E_z = e_{22}E_y + e_{31}E_z \\ -Z_z &= e_{33}E_z \qquad -Y_z = e_{24}E_y = e_{15}E_y \\ -Z_x &= e_{15}E_x \qquad -X_y = e_{16}E_x = -e_{22}E_x \end{aligned}\right\} \tag{233}$$

The large number of constants offers a wide selection in the manner of producing a desired deformation and in exciting the various vibrational modes. Nevertheless, owing to the high cost of large specimens, the only effect that has hitherto been put to practical use is the longitudinal effect parallel to the Z-axis, since in this case only a small amount of crystal material is required.

164. Piezoelectric Constants, Class 19, for Rotated Axes. All the transformed constants can be derived by the methods described in §134. Only a few of the results need be given here.

For a Z'-axis in any direction, with direction cosines γ_1, γ_2, γ_3, the constant for the longitudinal effect is

$$d'_{33} = \gamma_3(\gamma_1^2 + \gamma_2^2)(d_{31} + d_{15}) + \gamma_2(\gamma_2^2 - 3\gamma_1^2)d_{22} + \gamma_3^3 d_{33} \tag{234}$$

When expressed in terms of the colatitude θ and azimuth φ, as in Fig. 17, Eq. (234) becomes

$$d'_{33} = (d_{31} + d_{15}) \cos\theta \sin^2\theta - d_{22} \sin^3\theta \sin 3\varphi + d_{33} \cos^3\theta \tag{234a}$$

From this equation, for any crystal in this class a three-dimensional model could be constructed, the surface of which would be the surface of the third degree mentioned in §136. We shall consider only the intersections of this surface with the three principal planes.

For pressures in the YZ-plane, $\varphi = 90°$, and we have from Eq. (234a)

$$d'_{33} = s^3 d_{22} + c^3 d_{33} + cs^2(d_{31} + d_{15}) \tag{235}$$

where $c \equiv \cos\theta$ and $s \equiv \sin\theta$.

For pressures in the ZX-plane, $\varphi = 0$, whence

$$d'_{33} = c^3 d_{33} + cs^2(d_{31} + d_{15}) \tag{235a}$$

If the pressure is in the XY-plane, $\theta = 90°$, so that

$$d'_{33} = -\sin 3\varphi d_{22} \qquad (235b)$$

Equations (235) and (235a) are shown graphically in Fig. 46.* It will be observed that Eqs. (235) and (235a) differ only in the term containing d_{22}, and this constant is so small that curves (a) and (b) in Fig. 46 are nearly alike. The presence of d_{22} makes curve (a) slightly unsymmetrical, with a short segment below the Y-axis.

In interpreting Fig. 46(a) it must be remembered that, since Z'_z is a tensor, the polarization P'_z produced by Z'_z at any θ has the same sign as at $\theta \pm 180°$; that the Z'-axis is positive in the direction outward from the

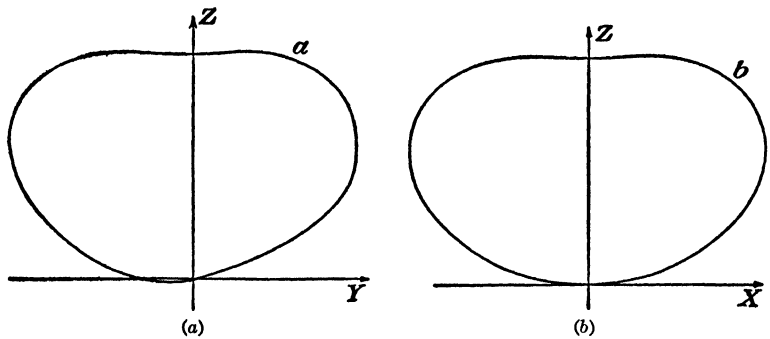


FIG. 46.—Longitudinal piezoelectric effect for crystals of Class 19 (C_{3v}). Radius vectors are proportional to d'_{33}.

origin O at any θ; and that P'_z is positive when in the direction of $+Z'$. It thus becomes clear that Fig. 46(a) gives a complete picture of d'_{33}, and hence of $P'_z = -d'_{33}Z'_z$, for all possible directions of pressure in the YZ-plane and that (for tourmaline) the positive direction of P'_z is always *toward* the origin. Similar remarks are applicable to (b) and to the diagram for the XY-plane.

The entire piezoelectric surface of tourmaline, of which Fig. 46 shows two of the principal sections, would look like a slightly unsymmetrical apple standing on its calyx end. Grouped around the calyx end would be three very small bulges, with depressions between.

* The curves in this figure are based on Voigt's diagrams for tourmaline. In order to emphasize the asymmetry, the effects of the d_{22}-terms have been purposely exaggerated by the author; hence the curves are only qualitatively correct. For other crystals of this class, with constants of different signs and relative magnitudes, (a) and (b) might present a quite different appearance. The diagram for the XY-plane would always consist of three lobes, like those for quartz (Fig. 43), but with the X- and Y-axes interchanged. The radius vectors in the XY-plane depend on d_{22} alone; owing to the smallness of this constant, the diagram (for tourmaline) would be very much smaller than (a) and (b).

165. Tourmaline. This crystal has already been briefly described in §13.

In measuring the piezoelectric constants, Riecke and Voigt[435] applied pressures in various directions to plates whose edges were parallel to the X-, Y-, and Z-axes and also to plates having one edge parallel to X, the other edges of the parallelepiped being at $\pm 45°$ to Z. They used Brazilian tourmaline, as did also Röntgen,[439] who made a similar determination some years later. Different specimens yielded values differing by about 2 per cent. Röntgen's measurements, as is admitted by Voigt,[572] are probably the more accurate.

	Riecke and Voigt	Röntgen
	$\times 10^{-8}$	$\times 10^{-8}$
d_{15}	11.0	———
d_{22}	−0.69	−0.94
d_{31}	0.74	0.96
d_{33}	5.8	5.4

Other observers have measured only d_{33}. Nachtikal[386] found

$$d_{33} = 5.6(10^{-8})$$

at small pressures, while at larger pressures he stated that

$$d_{33} = 5.60(10^{-8}) + 1.77(10^{-16})Z_z,$$

where Z_z is in dynes per square centimeter. Not much importance can be attached to this observation of the effect of pressure, in view of the work of Keys,[257] who found d_{33} to be only $5.4(10^{-8})$ at 100 atm pressure. Veen[563] found an average of $d_{33} = 5.3(10^{-8})$ for different crystals, and Fox and Fink[143] an average of $5.1(10^{-8})$; a recent measurement on black California tourmaline by R. C. Cook* gives $d_{33} = 4.8(10^{-8})$. Considering the variability in the composition of tourmaline, these differences are not surprising. For good crystals, there are probably no better data at present than those of Röntgen.

In the paper referred to above, Cook also describes a determination of the quantity $(d_{31} + d_{32} + d_{33}) = (2d_{31} + d_{33})$, which by Eq. (193) is the coefficient in the expression for the polarization produced by hydrostatic pressure. The measurement was made by a dynamic method on a black California tourmaline, the hydrostatic pressure being due to acoustic waves in the air surrounding the crystal. The resulting value for $(2d_{31} + d_{33})$ was $6.7(10^{-8})$, in fair agreement with $7.3(10^{-8})$

* R. C. Cook, *Bur. Standards Jour. Research*, vol. 25, pp. 489–505, 1940.

calculated from the data of Riecke and Voigt and $8.0(10^{-8})$ from Koch's observations.* Both Koch and Riecke and Voigt used green Brazilian tourmaline.

Keys, in the paper cited above, also computed the pyroelectric polarization due to adiabatic heating of the tourmaline crystal when hydrostatic pressure was suddenly applied and found it to be only $\frac{1}{300}$ of the piezoelectric polarization.

The coefficient d_{33} was found by Lissauer† to be constant within 2 per cent over a temperature range from +19 to −192°C.

166. Piezoelectric Stress Constants of Tourmaline. By applying Eq. (191) to tourmaline, with c_{ik} taken from Table XIII and d_{mi} from the values of Riecke and Voigt above, we find‡

$$\begin{aligned} e_{15} &= d_{15}c_{44} - 2d_{22}c_{14} = +7.40(10^4) \\ e_{22} &= d_{22}(c_{11} - c_{12}) - d_{15}c_{14} = -0.53(10^4) \\ e_{31} &= d_{31}(c_{11} + c_{12}) + d_{33}c_{13} = +3.09(10^4) \\ e_{33} &= 2d_{31}c_{31} + d_{33}c_{33} = +9.60(10^4) \end{aligned}$$

167. *Lithium Trisodium Molybdate.* Veen[563] found this crystal quite strongly piezoelectric: $d_{11} = 14(10^{-8})$.

168. Class 24, Hexagonal Holoaxial (Enantiomorphous Hemihedral) (symmetry D_6). Not pyroelectric. There is only one independent piezoelectric constant, $d_{14} = -d_{25}$, as in Class 12. The absence of a longitudinal effect in any direction for this class has already been mentioned under Class 12 (§147).

The piezoelectric equations are

$$-Y_z = e_{14}E_x \qquad -Z_x = e_{25}E_y = -e_{14}E_y$$

The only representative of this class that need be considered is *β-quartz*. The transition of quartz from the alpha to the beta form at 573°C has been discussed in §14. The atomic structure is treated in Chap. XXXI.

The erroneous statement has sometimes been made that β-quartz is not piezoelectric. Still, the fact that β-quartz belongs to this class is enough to make it certain that shears in the YZ- and ZX-planes can be produced piezoelectrically, provided that e_{14} is sufficiently large to give an observable effect.

The effect has been observed by Osterberg and Cookson,[404] who succeeded in making resonators of β-quartz vibrate from the transition

* P. P. Koch, *Ann. Physik*, vol. 19, pp. 567–586, 1906.

† Voigt, p. 866.

‡ "Lehrbuch," p. 870.

temperature to 847°C. Both X-cut and Y-cut plates were made to vibrate piezoelectrically, in y_s- and z_s-modes, respectively.

Lawson[310] observed the piezoelectric effect in β-quartz qualitatively by the powder method (§172). He also made use of the effect in his determination of the elastic constant s_{13}, described in §§92 and 101.

No measurements of the magnitude of d_{14} for β-quartz have been published.

169. Class 28, Cubic Tesseral Polar (Tetartohedral) (symmetry T). Not pyroelectric. There are three piezoelectric constants, all of the shear type and of the same numerical value,

$$-Y_z = e_{14}E_x \qquad -Z_x = e_{25}E_y = e_{14}E_y \qquad -X_y = e_{36}E_z = e_{14}E_z$$

The equations for rotated axes are the same as for Class 6.

Mention need be made here only of *sodium chlorate*, $NaClO_3$, the optical and piezoelectric properties of which were investigated by Pockels.[428] His measurements gave

$$d_{14} = -4.8(10^{-8})$$

170. Class 31, Cubic Ditesseral Polar (Hemimorphic Hemihedral) (symmetry T_d). Crystals in this class have no primary pyroelectricity, but strong secondary effects have been reported for boracite. The piezoelectric constants are the same as for Class 28.

Zinc blende, ZnS, is one of the forms of zinc sulphide, known also as *sphalerite*. Another form, *wurtzite*, belongs to Class 26 (see §522).

Two measurements of d_{14} for zinc blende have been made. The first was by Veen,[563] who measured d'_{11} for compression in a direction normal to (111), that is, making equal angles with all three axes. His average value for two specimens was $-4.75(10^{-8})$. From Eq. (206) one finds $d_{14} = -8.24(10^{-8})$. From the fact that his d_{11} for quartz recorded in the same paper (see Table XVII) was very low, it seems probable that his value of d_{14} for zinc blende is also too small. The negative sign has been verified by Coster, Knol, and Prins,[114] who also showed that the polarity of the axis normal to (111) was indicated by differences in the X-ray reflections at the opposite ends of this axis.

The second measurement of d_{14} was by Knol,[262] who found the value $-9.8(10^{-8})$. Laying greater weight on this value we adopt for zinc blende

$$d_{14} = -9.7(10^{-8})$$

From this value, together with the elastic constant c_{44} from §102, we find by the use of Eq. (191)

$$e_{14} = d_{14}c_{44} = -4.2(10^4)$$

Zinc blende has the distinction of being the first crystal for which a value of e_{14} was predicted from the lattice theory (§546). Born calculated $e_{14} = -2.3(10^5)$, about five times the observed value; to have arrived at the same order of magnitude at all was an achievement.

Ammonium chloride, NH_4Cl, which was known to have an anomaly in the specific heat at $-30.5°C$, was found by Bahrs and Engl[15] to become piezoelectric when the temperature was lowered to this point, the full value of $d_{14} = 0.337(10^{-8})$ being attained at $-32.5°C$.

171. *Boracite,* $B_{16}O_{30}Cl_2Mg_7$, is one of the crystals in which piezoelectricity was first observed by the Curie brothers. No quantitative measurements of d_{14} seem to have been made.

The crystal boracite is usually assigned to the present class, T_d. In fact, it has sometimes been given as the typical example of the class. However, optical and pyroelectric investigation have revealed that boracite crystals at ordinary temperatures really consist of rhombic domains (Class C_{2v})* with the polar axes parallel to any one of the four space-diagonals of the unit cube of the apparent cubic symmetry. Above 275°C the crystal is truly cubic. The indication is that all apparently cubic crystals of boracite have developed above the temperature of 275°C. The analogy to the strictly hexagonal habit of quartz crystals grown above 573°C is obvious.

The elastic and dielectric properties of boracite do not seem to have been investigated hitherto. The transition from a pyroelectric to a non-pyroelectric class at 275°C leads one to suspect the possibility of Seignette-electric properties (§471). The preliminary search for such properties, now to be described, has given negative results.

Six boracite crystals, all from Sehnde near Hanover in Germany, were studied in this laboratory in 1937.† The crystals showed the cubic dodecahedron with an indication of one of the tetrahedra that reveal the symmetry T_d. Three of the crystals were clear and free of any but minor surface intergrowth. The distance between opposite dodecahedron faces was 5.1 mm in the smallest and 7.2 mm in the largest crystal.

A plate was cut from one of the crystals with its major faces perpendicular to a cube diagonal, and the dielectric constant of this plate determined as a function of temperature from room temperature up to 315°C. The expectation of finding a dielectric anomaly near the transformation point (275°C) was not fulfilled. The dielectric constant was found to be about 6 at room temperature with an average temperature coefficient of +0.10 per cent per degree centigrade without any irregularity near the transformation point. It did not seem necessary to repeat the experiment on plates of different orientation, since, above the transformation point, the crystal is truly cubic and should have the same dielectric constant in all directions.

* Groth B[22]; see also the papers by Mehmel, *Z. Krist.*, vol. 87, pp. 239–263, vol. 88, pp. 1–25, 1934.

† These observations were made by Dr. H. Jaffe.

The clear crystals in an uncut state were submitted to the "click" test for piezoelectric resonances (§308). The "spectrum" of frequencies, in kilocycles per second, for a crystal with a distance of 5.1 mm between opposite dodecahedron faces was as follows: 841, strong; 1,050, several, weak; 1,356, strong; 1,442, strong; 1,670, several; also 2,630 and other responses at higher frequencies. Change of orientation produced only minor changes in the frequencies and some shift of relative intensity. The other crystals gave very similar spectra, with the individual frequencies shifted inversely proportional to the linear dimensions. If we regard the lowest strong resonance, 841 kc, as a fundamental resonance related to the thickness of the crystal, we obtain a frequency constant of 4,250 kc·mm. The same value ±1 per cent was found with the other two crystals studied. From this value and the thickness of the crystal the velocity of wave propagation is found to be around $8.5(10^5)$cm/sec, indicating an elastic stiffness even greater than that of quartz.

It is unfortunate that clear crystals of boracite, larger than those described above, are very rare.

172. Piezoelectric Investigations of Other Crystals. One of the author's earliest observations on resonating crystals, in 1919, was that of the click heard in a telephone receiver in an oscillating circuit of variable frequency to which the crystal electrodes were connected, whenever the frequency was tuned through a natural frequency of the crystal.[93] In these experiments it was found that clicks were heard even when a small irregular fragment of quartz, of unknown orientation, was placed between the electrodes. This click method (§308) was later developed by Giebe and Scheibe[164] into the "powder method" for detecting piezoelectric properties in a large number of crystals of different kinds. By using an oscillating circuit of sufficiently high variable frequency, they were able to secure responses when very small granular fragments of the crystals were placed between the electrodes.*

The wide applicability and simplicity of the powder method gave great impetus to the search for piezoelectric properties. Whenever resonant responses are obtained, it can reasonably be assumed that the crystal is piezoelectric. Negative results *may* indicate that the crystal in question belongs in a non-piezoelectric class; on the other hand, they may be due to too great conductivity of the crystal, to excessive damping, or to the fact that piezoelectric properties, though present, are too weak to be detectable. These uncertainties are doubtless responsible for most of the discrepancies among the results of different observers. The method of Giebe and Scheibe has become of great value, on the one hand for identifying the piezoelectric property in crystals already supposed to belong to piezoelectric classes and for determining whether it is "strong" or "weak," and on the other hand, within limits, for determining the class to which a given crystal should be assigned; for example, the existence of the piezoelectric property is a sure sign that a crystal has no

* For a discussion of apparatus and circuits see Scheibe.[B45]

center of symmetry. The method has also been used to throw light on the relation of piezoelectric properties to chemical constitution and on the structural changes that take place at certain transitional temperatures; for example, Hettich[221] found evidence of such transitional effects with camphor, potassium iodate, and pentaerythritol. The last-named crystal has been the object of much discussion, but it now seems clear that it belongs in Class 14.*

Mention may also be made of iodyrite (silver iodide, AgI), which at ordinary temperatures belongs in Class 26 (hexagonal, C_{6v}); it becomes cubic around 145°C and is also cubic "at low temperatures."†* Up to 145° it has a *negative* coefficient of expansion. In spite of the fact that it is a semiconductor, Hettich and Steinmetz recorded a strong response by the method of Giebe and Scheibe.

The class to which topaz is usually assigned is not piezoelectric. Yet Alston and West‡ have reported traces of piezoelectricity in this crystal.

By the methods mentioned above the different kinds of crystals examined for piezoelectric effects are now numbered in the hundreds, including many organic substances. A few examples have been mentioned in previous paragraphs. A complete list would be of little value without the accompanying discussion, for which reference must be made to the original papers,§ to the book by Scheibe,[B45] to various handbooks,[B19,B20,B54] and to the "International Critical Tables,"‖ in which references to the literature are given.

The most recent addition to the list of piezoelectric crystals is that of Bond,[65] who used the powder method for testing several hundred different minerals. Among those with which he obtained positive results, the

* See H. Mark and K. Weissenberg, *Z. Krist.*, vol. 65, p. 499, 1927, and *Z. Physik.*, vol. 47, p. 301, 1928; H. Seifert, *Berl. Ber.*, vol. 34, pp. 289–293, 1927; A. Schleede and A. Hettich, *Z. anorg. allgem. Chem.*, vol. 172, pp. 121–128, 1928 (etch figures on pentaerythritol crystals are shown in this paper); A. Hettich,[221]; and W. A. Wooster, *Z. Krist.*, vol. 74, *Referatenteil*, p. 105, 1930.

† Groth.[B22]

‡ N. A. Alston and J. West, *Proc. Roy. Soc.* (*London*) (*A*), vol. 121, pp. 358–367, 1928; see also Wooster, ref. B56, p. 230.

§ Among the various investigations, in many of which use was made of the powder method, are the following: E. Giebe and A. Scheibe;[164] A. Hettich;[221,222] A. Hettich and A. Schleede;[223,224] A. Hettich and H. Steinmetz, *Z. Physik*, vol. 76, pp. 688–706, 1932; S. B. Elings and P. Terpstra, *Z. Krist.*, vol. 67, pp. 279–284, 1928; W. Schneider, *Z. Physik*, vol. 51, pp. 263–267, 1928; E. Hertel and K. Schneider, *Z. physik. Chem.* (*B*), vol. 12, pp. 140–150, 1931; G. Greenwood and D. Tomboulian, *Z. Krist.*, vol. 81, pp. 30–37, 1932; G. Greenwood, *Z. Krist.*, vol. 91, pp. 235–242, 1935; H. Seifert, *Z. Krist.*, vol. 81, pp. 396–468, 1932; W. A. Wooster, *Z. Krist.*, vol. 74, *Referatenteil*, p. 105, 1930; A. L. W. E. van der Veen, thesis, Delft, 1911; R. Lucas, *Compt. rend.*, vol. 178, p. 1890, 1924.

‖ Vol. 6, p. 209, 1929.

following do not appear to have been recorded hitherto as responding piezoelectrically, although some are known to be pyroelectric: clinohedrite, cronstedtite, edingtonite, epistilbite, epsomite, langbeinite, leucophanite, meliphanite, shortite, stibiotantalite, struvite, tiemannite, wurtzite, and zunyite. Bond recorded negative results with iodyrite, which had been reported by Greenwood and Tomboulian (footnote, page 232) as active; and, contrary to the observations of Hettich and Steinmetz and of Greenwood and Tomboulian, he found scolecite to be active.

173. Somewhat similar to the method described in §185, in which the direct effect is used for the testing of small crystal fragments, is that of Bergmann:[52] a periodic pressure at audio frequency is impressed upon a single fragment or on a collection of fragments. The pressure is derived from the stem of a tuning fork, either struck or electrically driven. Electrodes placed above and below the crystal specimens are connected to an amplifier. Observations on single fragments make a rough determination of the piezoelectric axes possible.

Still another variant of the powder method is described by Engl and Leventer.[132] Small crystal grains, screened to approximately the same size, were immersed in benzene in a small glass "calorimeter" with a capillary tube in which the rise in height of the liquid indicated a rise in temperature. An electric field of variable high frequency was impressed, which caused a slight increase in temperature when the grains vibrated in resonance. The results are claimed to be of greater quantitative value than those by the usual powder method.

174. Piezo- and Pyroelectric Effects from Non-crystals. A short account will now be given of certain investigations with substances which are commonly considered amorphous or which at least do not have the structure of homogeneous crystals. References, indicated by numbers in brackets, will be found at the end of this chapter.

Electrets. It was Heaviside who first suggested this term for materials having a permanent electric polarization, by analogy with "magnets." The word is now generally applied to certain waxes, solidified while in a strong electric field (usually several thousand volts per centimeter), the properties of which were first discovered by Eguchi.[5] The material is usually a mixture of carnauba wax and resin, sometimes with the addition of beeswax. The preparations are usually in the form of flat plates, having a permanent polarization in the direction of the thickness. Unlike pyroelectric crystals, in which the permanent polarization is normally screened by compensating charges on the surface, the electret has uncompensated positive and negative surface charges on its opposite faces that give rise to an external field persisting for years. If the charges are annulled by short-circuited electrodes, recovery takes place some

hours after the removal of the electrodes. In a very moist atmosphere the external field due to the electret is diminished, but it recovers in dry air. The full charge density is of the order of 10 esu/cm². This is twice as great as can be produced by friction on hard rubber.[16]

Uniform heating or cooling causes a change in the polarization and hence in the surface charges. This is a pyroelectric effect, the polarization in general becoming weaker with increasing temperature.[1] For the effect of hydrostatic pressure, see ref. [14].

A piezoelectric effect has also been reported:[1] upon transverse pressure or extension, a change takes place in the surface charges, dependent on the sign of the stress. The order of magnitude of the effect is the same as with crystals.[3]

X-ray studies of the structure of electrets have been made by Brain,[3] Ewing,[6] and Good and Stranathan.[9]

The most commonly accepted *theory of electrets* is that molecular dipoles in the molten wax become oriented by the electric field and hold their parallel orientation after the wax sets. The experiments of Thiessen, Winkel, and Herrmann,[16] however, indicate that the polarization may be a space-charge effect due to the wandering of ions before solidification of the wax. A serious problem is the explanation of the persistence of an external field in spite of leakage and of ions in the surrounding air. Adams[1] suggested that this effect may be due to very slow decay in the polarization. On reasonable assumptions he found that the presence of uncompensated surface charges and their recovery after removal could be accounted for if the decay amounted to only 1 per cent in a year.

Applications of Electrets. Gemant[7],[8] mentions possible applications to electrometers and as a bias for the grids of electron tubes. Nishikawa and Nukiyama[11] describe the use of an electret in a condenser transmitter.

175. *Other "Piezoelectric" Effects from Non-crystalline Materials.* Several observers[3],[12],[15] have noted that mechanical pressure causes the appearance of electric charges on the surfaces of rubber,* paraffin, glass, and other materials, including even wood. Considering the erratic and qualitative character of most of this testimony and the likelihood that the results were due largely to contact potentials, such observations should not be taken too seriously as indicating anything that can properly be called a piezoelectric effect. One reads even of "muscular piezoelectricity," with the suggestion that the closing of the sensitive plant[4] and the activity of the electric eel[13] may be manifestations of piezoelectricity!

It has been stated by Meissner and Bechmann† that electrets possess-

* A microphone made from frozen rubber is described by E. Gerlash in U. S. patent 2,231,159.

† See footnote *, p. 216.

ing marked piezoelectric and pyroelectric properties can be made by impregnating a wax (especially asphaltum) with powdered quartz and letting it harden while in a strong electric field. Whatever contribution the quartz made to the pyroelectric effect in their experiments must have been due to a temperature gradient. As for the piezoelectric effect, these authors found that the presence of the quartz powder rendered the electrets more permanent rather than more responsive to pressure.

REFERENCES ON ELECTRETS

[1] ADAMS, E. P.: *Jour. Franklin Inst.*, vol. 204, pp. 469–486, 1927.

[2] BÖNING, P.: "Elektrische Isolierstoffe," Vieweg & Sohn, Brunswick, Germany, 1938, 140 pp.

[3] BRAIN, K. R.: *Proc. Phys. Soc.* (*London*), vol. 36, pp. 81–93, 1924.

[4] BUCHANAN, F.: *Nature*, vol. 108, p. 340, 1921.

[5] EGUCHI, M.: *Phil. Mag.*, vol. 49, pp. 178–192, 1925.

[6] EWING, M.: *Phys. Rev.*, vol. 36, p. 378, 1930 (abst.).

[7] GEMANT, A.: *Rev. Sci. Instruments*, vol. 11, pp. 65–71, 1940.

[8] GEMANT, A.: *Phys. Rev.*, vol. 61, pp. 79–83, 1942.

[9] GOOD, W. M., and J. D. STRANATHAN: *Phys. Rev.*, vol. 56, pp. 810–813, 1939.

[10] NADJAKOFF, G.: *Physik. Z.*, vol. 39, pp. 226–227, 1938.

[11] NISHIKAWA, A., and D. NUKIYAMA: *Proc. Imp. Acad.* (*Tokyo*), vol. 4, pp. 290–291, 1928.

[12] RICHARDS, H. F.: *Phys. Rev.*, vol. 22, pp. 122–133, 1923.

[13] RUSSELL, E. W.: *Nature*, vol. 108, p. 275, 1921.

[14] SHEPPARD, G. E., and J. D. STRANATHAN: *Phys. Rev.*, vol. 60, pp. 360–362, 1941.

[15] SHUBNIKOV, A., and B. BRUNOVSKIJ: *Bull. Acad. Sci. Leningrad*, 1928, pp. 367–374.

[16] THIESSEN, P. A., A. WINKEL, and K. HERRMANN: *Physik. Z.*, vol. 37, pp. 511–520, 1936.

SUPPLEMENTARY

DODDS, W. J., and J. D. STRANATHAN: *Phys. Rev.*, vol. 60, p. 360, 1941.

GEMANT, A.: *Phil. Mag.*, vol. 20, suppl., pp. 929–952, 1935.

GROSS, B.: *Phys. Rev.*, vol. 66, pp 26–28, 1944.

JOHNSON, O. J., and P. H. CARR: *Phys. Rev.*, vol. 42, p. 912, 1932 (abst.).

NUMAKURA, H.: *Rept. Elec. Research Inst.* (*Tokyo*), vol. 3, pp. 112–129, 1932.

TIKU, T.: *Proc. Tokyo Math.-Phys. Soc.*, vol. 14, pp. 63–88, 1932.

TURPAIN, A., and M. DUREPAIRE: *Compt. rend.*, vol. 189, pp. 739–741, 1929.

CHAPTER X

PRODUCTION AND MEASUREMENT OF PIEZOELECTRIC EFFECTS

Es beruht also auch die durch Druckänderungen erzeugte Elektrizität auf einem besonderen Vorgange, und ich habe sie deshalb als Piezoelektrizität unterschieden.

—HANKEL.

The last two chapters have dealt with the general phenomena of piezoelectricity. The basic equations and their specialization to some of the crystal classes have been given, as well as the numerical values of piezoelectric constants.

We shall attempt in the present chapter to outline certain practical considerations that may be of service to the experimenter, in the selection and orientation of specimens and in the arrangement of electrodes, for the production of piezoelectric deformations of any desired type. Although experimental details are outside the scope of this book, methods of measurement and qualitative testing are briefly treated at the end of the chapter.

176. Orientation of Specimens and Location of Electrodes for Producing Piezoelectric Deformations. The rules that will now be given are stated from the point of view of the converse effect, whereby a deformation is produced by applying an electric field to the crystal. Whatever arrangement is effective for the converse effect is also equally advantageous for the direct effect.

The deformations fall into two groups, resonant and non-resonant, which require somewhat separate treatment, although the basic principles are identical. In either case, when the kind of crystal, type of deformation, and size and shape of specimen have been chosen, the first consideration is the orientation of the specimen with respect to the crystal axes, *i.e.*, the manner in which the specimen is to be cut from the available parent crystal. The decision often depends on the size of the given crystal, as well as on the available piezoelectric coefficients and on the desirability of selecting a mode of excitation that permits the use of electrodes spaced only a short distance apart, in order to produce as strong a field as possible with a given voltage.

Usually the first step is to seek, in the table of piezoelectric coefficients for the particular class (§131), a coefficient d_{hk} such that a field E_h will produce the desired strain x_k ($k = 1$ to 6, Fig. 40). Often one must

resort to oblique cuts, using the formulas for rotated axes given in §134 and elsewhere.

Non-resonant deformations include static deformations and also those vibrational devices in which the frequency is so far below the resonant frequency of the specimen that the deformation is essentially the same as in the static case. In simple extensions and shears, the strains are so nearly uniform that they are most effectively produced by applying electric fields that are uniform throughout the specimen, by the use of electrodes that completely cover the faces normal to the field.

Resonant Deformations. For exciting vibrations in any desired mode, the orientation of the specimen and direction of field are governed for the most part by the same rules as those for non-resonant deformations.

Except for the purpose of generating ultrasonic acoustic waves or of studying vibrational modes, piezoelectric resonators are designed for producing certain electric reactions on the circuit in which they are placed. They function then purely as circuit elements, and the mode of vibration is important only insofar as it affects the problem of mounting the crystal in such a way as to secure the least frictional damping. Nevertheless, it is always true that the amount of reaction on the circuit is proportional to the amplitude of vibration. Hence, in most cases maximum effectiveness is secured when the electrodes cover as much as possible of the area of the crystal. In general, the field is most effective at an antinode of strain (node of vibrational motion).

For experimental research and for other special purposes, although not often in practical applications, very small electrodes are sometimes used, covering only a small portion of the crystal surface. In fact, if full-sized electrodes are not used it is better to make them as small as possible, for this reason: As has already been stated in §64, the elastic stiffness is not the same in the region between electrodes as in the region outside, a fact which complicates the relation between observed and calculated frequencies unless the electrodes are so small—or else so remote from the crystal—that the stiffness is essentially the same as that of an electrodeless crystal.

In general, it may be said that any electric field of suitable frequency, of large or small extent, uniform or not (unless it happens to cause, in different regions, piezoelectric stresses that cancel one another), will excite vibrations if there is a d_{hk} relating a component E_h of the field to a strain x_k characteristic of or bound by coupling to a possible vibrational mode. The actual distribution of vibrational stresses and strains in all cases is essentially that which is typically associated with the vibrational mode, irrespective of the region where the field is applied.

177. Compressional Strains. These call for piezoelectric constants of type L or T (Fig. 40); both types, of forms d_{hh} and d_{hk} (h and k = 1, 2,

or 3), are found in 12 classes of crystals; Class 14 has two constants of type T but none of type L. Thus with 13 classes there is at least one crystallographic axis parallel to which a field can be applied so as to produce an extension at right angles to the field (transverse effect), and in all but one of these classes the same field produces also an extension (+ or −) parallel to the field (longitudinal effect). Each of the remaining seven piezoelectric classes has at least one constant of type L_s; with all, a transverse extensional effect (T-effect with transformed axes) can be realized on application of an *oblique* field; with all but two (Classes 12 and 24, §147), the longitudinal effect can also be thus realized. The corresponding constants are found by means of the transformation formulas; examples will be found in §§184 and 139.*

Compressional vibrations can be produced with the field parallel to the vibrational direction (L-effect), or perpendicular to it (T-effect). The first of these arrangements is used for obtaining *thickness vibrations* in plates of relatively large area, with electrodes covering the entire major surfaces. It can also be used for generating *lengthwise vibrations* in plates or rods, but it is inefficient for this purpose owing to the large separation between electrodes. For lengthwise vibrations it is customary to use the T-effect, with the field parallel to the thickness of the specimen. With either manner of exciting lengthwise vibrations, overtone frequencies as well as the fundamental can be produced; but here again the T-effect is to be preferred, since the length of the electrodes can then be made to fit the desired overtone. The latter type of excitation is illustrated in Fig. 53.

Sometimes it is desired to excite compressional vibrations in crystals such as Rochelle salt, which have neither an L-effect nor a T-effect with respect to the crystallographic axes. In such cases, as has been stated above, various oblique cuts may be used, so oriented that with respect to the transformed axes the original L_s- or T_s-shearing effects give rise to longitudinal or transverse compressional effects. The application of this principle is made in §139 and elsewhere.

178. Shearing Strains. Shearing strains can be produced piezoelectrically by the L_s-effect (Fig. 40), with field parallel to the axis of shear, or by the T_s-effect, with field parallel to the plane of shear.

Thirteen classes have at least one L_s-coefficient with respect to the crystallographic axes; for the remainder, an L_s-effect can be secured by rotating the axial system about one of the axes, except in Classes 9 and 26.

So far as mechanical effects are concerned, shearing strains are useful chiefly for producing flexure and torsion in elongated crystal plates.

* It will be recalled from §27 that an extension can always be regarded as a combination of two shears, and vice versa. Whether a piezoelectric deformation is represented in one way or the other is a matter of convenience.

Examples are considered in §§354, 356, and 380. Among piezoelectric resonators (Chap. XVII) those of the shear type are now of the greatest importance.

179. Flexural Strains. It has been shown in §34 that the chief elastic characteristics are a compression in one half of the specimen (usually a plate or bar), an extension in the other half, and shearing stresses in the plane of flexure. These features are shown in Fig. 47, in which the plane of the diagram is the plane of flexure and also the plane of shear. Flexure can be produced piezoelectrically by means of either (1) compressional stresses in the l-direction, applied to the upper or the lower portion of the plate (or to both, if one of the stresses is compressional and the other extensional); or (2) two opposite shearing stresses applied to the right and left halves of the plate shown in Fig. 47, the axes corresponding to the shear being parallel to l and e. If we assume that the compressional strain, with respect to the crystal axes, is of type x_k and

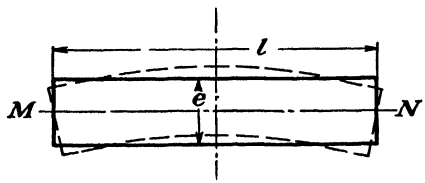


FIG. 47.—Plate in a state of flexure.

that the shear is of type x_i, then it is clear that flexure can be produced by a field having a component in the direction h, if the piezoelectric constant d_{hk} or d_{hi} differs from zero.

Non-resonant applications of flexure have to do chiefly with the conversion of electrical impulses or l-f currents into mechanical movements, or vice versa. Much greater movements are thus obtainable than by the simple compressional effects. For this purpose, instead of producing flexure piezoelectrically in a single plate, it is usually found more effective to use a *double plate* of the type first introduced by the Curie brothers (§122). The two thin crystal slabs are so oriented and the field in each is so disposed that one slab becomes elongated while the other contracts, thus meeting the requirements stated above for the production of flexure. This device, called a "bimorph," now consists usually of two plates of Rochelle salt and is described in §503.

Flexural Resonators. The flexural-vibration frequencies of thin plates are far lower than those ordinarily obtainable by compressional or shearing modes. Many different types of flexural resonators have been investigated, of both quartz and Rochelle salt, and some have found practical application in piezo oscillators of relatively low frequency and in the production of acoustic waves (§396).

Flexural vibrations in quartz and Rochelle salt are treated in Chaps. XVII and XVIII. The theory of these vibrations is considered in §73.

180. Torsional Strains. As we have seen in §35, when a solid is in a state of torsion, the particles are displaced in planes normal to the axis of torque, and shearing strains are set up; the plane of shear (Fig. 13) at any point contains a line parallel to the axis of torque and the line along which the particle moves; it is *not* the plane normal to the axis. These two directions correspond to the axes of shear (§27). Since the material is sheared in opposite senses on opposite sides of the axis of torsion, it is evident that, if a single piece of crystal is to be brought piezoelectrically into a state of torque, the electric field producing the shears must have opposite directions on these two sides; at least, the field must not have the same direction and magnitude in both regions. For piezoelectric excitation of torsion it is therefore necessary to choose such a d_{hk} that a field E_h in the proper direction will produce the requisite shearing strain x_k. The desired end cannot be attained if E_h is uniform throughout the crystal or if it is directed uniformly through the specimen in a direction normal to the axis of torsion.

This difficulty can be overcome in various ways. One method, applicable at least to quartz and mentioned in §356, is to use a specimen in the form of a hollow circular cylinder with cylindrical electrodes inside and outside, so that the field is radial. Another expedient, described in §356, is to apply oppositely directed fields to different portions of the specimen.

A third method, which finds practical application in the Rochelle-salt "twisters," makes use of two elongated flat plates cemented together with a common electrode of metal foil between (§503). The polarities of the plates are both in the same direction; but since the electric fields are in opposite directions, two opposing shears are produced, which result in a torsion of the combination.

This third method is used in various l-f devices; the other two methods have been employed both statically and for resonant vibrations. As will be seen in Chap. XVII, it is possible by suitable placing of electrodes to excite overtone torsional vibrations as well as the fundamental mode. The equations for torsional deformations and vibrations are given in §§35 and 74.

181. *Special Forms of Vibrating Devices.* In addition to the crystal plates, rods, and cylinders mentioned above, other forms have been made to vibrate piezoelectrically. They include spheres (§360), tuning forks (§385), and saucerlike shapes (§508).

The use of obliquely cut plates for special purposes has already been referred to in §50. It need only be added at this point that the decrease in the piezoelectric effect which often accompanies the use of oblique

fields is much more than compensated by the advantages offered by such cuts. Moreover, the low decrements that can be attained by suitable mounting of specimens, especially in the case of quartz, is of greater importance in resonators than an especially large piezoelectric effect.

182. *Disturbing Effects in Crystal Resonators.* At certain frequencies, compressional, shearing, flexural, and torsional vibrations, in fundamental or overtone modes, singly or in combination, may be present in specimens of almost any shape. For the production of any one type of vibration it is by no means necessary that the electrodes be placed for most efficient excitation. If the driving current is of the proper frequency, a stray component of alternating field is likely to be present somewhere in the specimen in such a direction as to cause a mechanical stress of the type necessary to excite vibrations of any of the four types. Moreover, through the presence of elastic cross constants (§32), purely mechanical coupling effects exist between different types of vibration, so that modes may occur that are not directly excited by piezoelectric action. An example of such indirectly excited modes is the compressional vibrations parallel to the Z-axis in quartz (§348).

Considering the multiplicity of possible vibrational modes, the variety of ways in which they can be excited, and the fact that close coupling between modes can affect the vibrations over a considerable range of frequency, it is no wonder that very complicated vibrational patterns have so often been observed by means of dust figures or otherwise and that the frequency spectrum of a resonator is so complicated.

We leave this subject with two words of admonition to all who attempt to identify vibrational modes in crystals. First, when the crystal is connected as a resonator, it is very important that the tube generating circuit be so well filtered that only a voltage of a single frequency is impressed on the crystal. Second, it is generally rash to assume that a particular mode is present because a resonant frequency of the right value has been observed. It is always desirable, and usually not difficult, to locate the nodal regions by one or more of the methods described in §§366 to 368 and thus to determine the mode in which the crystal is vibrating and whether other modes are also present. In no branch of crystal experimentation is self-criticism a more important virtue than here.

183. The Measurement of Piezoelectric Constants. In §75 it is stated that elastic constants can be measured by either a static or a dynamic method. The same is true of the measurement of piezoelectric constants, but there is a wider range of methods. For whereas in elasticity there are only mechanical stresses to be applied, in piezoelectricity observations can be made by applying either a mechanical stress (direct effect) or an electric stress (converse effect). For most crystals, with the

exception of quartz and Rochelle salt, the values were obtained only by the static direct effect, yielding the piezoelectric strain coefficients d_{hk}. As will be seen in Chap. XXI, the constant d_{14} of Rochelle salt has been observed both statically and in a l-f alternating electric field by the converse effect. In Chaps. XV and XVIII we shall consider the derivation of the piezoelectric constants of quartz and Rochelle salt from observations on resonators, which involve a combination of the direct and converse effects, and sometimes yield e_{hk} rather than d_{hk}.

It is beyond the scope of this book to go into detail concerning the experimental methods of measuring the piezoelectric constants statically, although certain precautions, which to a large extent are applicable to all crystals, are pointed out in §§411 and 417. Theoretical details are given in Voigt's "Lehrbuch," and excellent accounts of experimental methods, with diagrams of apparatus, will be found in references B45 and B51. Measurements are made by the use of a ballistic galvanometer, electrometer, or thermionic voltmeter or, for the converse effect, by observing the deformation of the specimen. Those who undertake the precise determination of piezoelectric constants would do well to examine as many as possible of the original papers from which the values given below are derived.*

184. A word should be said, however, concerning the measurement of d_{14}, d_{25}, and d_{36}, since reference will be made to it later, especially in connection with Rochelle salt. It is enough to consider d_{14}, since the treatment of d_{25} and d_{36} is exactly analogous. The constant d_{14} occurs in equations of the type $P_x = -d_{14}Y_z$ or $y_z = d_{14}E_x$, which means that in order to observe d_{14} a shearing stress Y_z or an electric field E_x must be applied to an X-cut plate, the resulting P_x or y_z being observed. The second of these equations was used by Sawyer and Tower,[449] who observed the strain y_z directly; the spontaneous y_z in Rochelle salt has been observed by Mueller.[378]

In the main the direct effect has been utilized, with $P_x = -d_{14}Y_z$. Owing to the difficulty in applying a simple shear to a crystal plate it is customary to apply an endwise compression to a rectangular plate, the length of which bisects the angle between the positive senses of the Y- and Z-axes. If this direction is called Y' and the compressional stress Y'_y, one can easily prove by simple geometry that $P_x = -d_{14}Y'_y/2$. This equation also follows from §39, where it was shown that for 45° cuts $Y_z = Y'_y/2$. The same result is also reached by expressing the piezoelectric constant in terms of transformed axes Y' and Z', these axes resulting from a rotation of 45° about the X-axis. We then write

* The reader is referred especially to the paper by Lüdy,[322] for measurements by the direct effect. For the converse effect, various techniques are described in the references mentioned in Chap. XXI (see also L. M. Myers[385]).

$P_x = -d'_{12}Y'_y$ and find from Eqs. (203) that $d'_{12} = d_{14}/2$. This equation for P_x expresses the *transverse effect* in a 45° X-cut plate.

If the direction of pressure is rotated 90° in the YZ-plane, so that the compression is parallel to the *breadth* of the plate, the equation is

$$P_x = -d'_{13}Z'_z = \frac{d_{14}Z'_z}{2}$$

by Eq. (203). The sign of the shearing strain y_z is thereby reversed. For the same pressure the same value of P_x results, but with reversed sign.

This simple method for measuring d_{14}, d_{25}, and d_{36} is not in general applicable with crystals having still other piezoelectric constants, since, as may be seen from Eqs. (196), such constants may cause a further contribution to the polarization.

In all measurements of piezoelectric coefficients by application of a stress X_h, it is essential that the crystal be free from all other mechanical constraints. According to Eq. (188), any such constraint may contribute to the value of P_m and therefore to the observed d_{mh}.

When the strain coefficients d_{hk} for any crystal have been determined, it is necessary to know the values of the elastic constants before the e_{hk} can be calculated, and vice versa. Equations (192) and (192*a*) are to be used for this purpose. If these equations are applied to rotated axial systems, the primed values of elastic as well as of piezoelectric constants must of course be employed.

For dynamic methods for the determination of piezoelectric constants are §§310 following.

185. Qualitative Tests of Piezoelectric Specimens. In the methods now to be described the direct piezoelectric effect is used. The specimen is subjected to compression, which may be either static or of low frequency. In either case the crystal does not resonate. Methods making use of the resonating property are described in §§172 and 308.

If the crystallographic class of the specimen is known, the specimen can be so oriented and the electrodes so placed, in accordance with the principles outlined earlier in this chapter, that a suitable compression will liberate charges on the electrodes. In the absence of such knowledge, various positions of electrodes and directions of compression must be tried until an arrangement is found that works. The compressional method has been used mostly with X-cut plates of quartz, which can by this means be explored for twinned regions and defects.

In the form most commonly adopted, the plate to be tested lies on a large horizontal electrode, and pressure is applied locally on the upper surface by means of a rod carrying at its lower end a metallic knob that serves as the other electrode. This knob is connected either to a

string electrometer, as in Dye's arrangement*, or to a sensitive electronic voltmeter, in which case a stage of amplification can also be employed. Due attention must be given to the problems of insulation and screening. Devices of this sort have been described by Dawson,[121] Meissner,[361] and Tsi-Ze.[524]

If a pulsating pressure is applied to the plate, a vacuum-tube detector and telephone receiver or loud-speaker can be substituted for the voltmeter. This device was described by the author[94] in 1922. The periodic pressure was derived from a glass rod in contact with a small buzzer, and it was shown that the device could be used for testing a single plate, for comparing an unknown plate with a standard, or for matching two plates with respect to polarity. Similar arrangements, using a tuning fork or loud-speaker mechanism in place of the buzzer, were later described by Bergmann[52] and by Rosani.†

* VIGOUREUX, ref. B51, p. 21. See also SCHEIBE, ref. B45, p. 4.

† S. ROSANI, *Alta Frequenza*, vol. 3, pp. 643–649, 1934.

CHAPTER XI

ALTERNATIVE FORMULATIONS OF PIEZOELECTRIC THEORY

A theory of physics is not an explanation. It is a system of mathematical propositions, deduced from a small number of principles, which have for their aim to represent as simply, as completely and as exactly as possible, a group of experimental laws.
—P. DUHEM.

186. Voigt's theory, while fully capable of giving a phenomenological description of all piezoelectric effects, is not the only possible formulation. It offers the advantage of mathematical simplicity, and for this reason, as well as because of its almost universal adoption in the literature, it is employed throughout most of this book.

In recent years three suggestions have been made toward a new formulation. In each case the purpose was to give a more reasonable description of the anomalous behavior of Rochelle salt than was afforded by Voigt's theory. Mueller[376] in 1935 proposed that the piezoelectric strain should be regarded as proportional to the molecular field F rather than to the macroscopic field E, while later Mason[335] considered the piezoelectric stress proportional to the density of *charge* on the electrodes. In view of the experimental results of Mason and others, both Mueller[378] and Mason[338] have more recently treated the stress as proportional to the *polarization*.

These hypotheses, calling for a revision of the entire formulation of piezoelectric theory, are so important as to require careful consideration. For, however anomalous the behavior of Rochelle salt may be, it seems most reasonable to assume that its fundamental piezoelectric properties are of the same nature as those of other crystals. The fact that with Rochelle salt these properties are so largely dependent on conditions easily realized in the laboratory then serves to determine the most reasonable form of theory, not alone for Rochelle salt, but for all other piezoelectric crystals as well.

No new form that may be given to the theory can be expected to reveal new truths, so long as both forms are founded on the same fundamental principles. One form differs from another only in the choice of parameters, and they are mutually convertible. In each case the same raw materials go into the mill, and the only difference in the product is that it appears in different packages. The criterion is to be sought in experiment: that form of theory will survive which defines its piezo-

electric, elastic, and dielectric coefficients in such a way that they are found experimentally to be most nearly *constant* under varying conditions.

187. The formulation of modifications of Voigt's theory can best be introduced by means of the differential expressions for the thermodynamic potentials involving elastic and electrical effects. The potentials themselves, which represent the free energy of the crystal in terms of strains (ξ) or of stresses (ζ), were discussed in §23; use has been made of their partial derivatives in §§26, 105, and 124.

On the assumption that all processes are reversible and isothermal, we may write the exact differentials in the following equations in terms of the fundamental electrical and mechanical quantities:

$$d\xi_{P,X} = P\,dE - X\,dx \tag{236}$$
$$d\xi_{E,X} = E\,dP - X\,dx \tag{236a}$$
$$d\zeta_{E,x} = E\,dP - x\,dX \tag{236b}$$
$$d\zeta_{P,x} = P\,dE - x\,dX \tag{236c}$$

These four equations are analogous, respectively, to the well-known thermodynamic expressions for the internal energy, the Helmholtz free energy, the Gibbs free energy, and the enthalpy of a reversible system; the quantities P, E, x, and X are analogous, respectively, to absolute temperature, entropy, volume, and pressure in ordinary thermodynamics.

Although the foregoing equations are not written in vector notation, it is of course understood that E and P are vectors, while X and x are second-rank tensors. The nature of these parameters is made explicit when appropriate suffixes are introduced.

Since each of the equations (236) to (236*c*), like Eqs. (1) and (2), is an exact differential, we may take derivatives and write a set of equations analogous to Maxwell's relations. Just as each derivative in Maxwell's relations represents a thermomechanical constant characteristic of the material, so in Eqs. (237) to (237*c*) each derivative represents a characteristic electromechanical constant*:

$$\left(\frac{\partial P}{\partial x}\right)_E = -\left(\frac{\partial X}{\partial E}\right)_x \equiv \epsilon \tag{237}$$
$$\left(\frac{\partial E}{\partial x}\right)_P = -\left(\frac{\partial X}{\partial P}\right)_x \equiv a \tag{237a}$$
$$\left(\frac{\partial E}{\partial X}\right)_P = -\left(\frac{\partial x}{\partial P}\right)_X \equiv -b \tag{237b}$$
$$\left(\frac{\partial P}{\partial X}\right)_E = -\left(\frac{\partial x}{\partial E}\right)_X \equiv -\delta \tag{237c}$$

* Equations (237) to (237*c*) express the *differential* values of ϵ, δ, a, and b and are valid whether the electromechanical relations are linear or not, as long as they are

Equations (237) and (237*c*) express the converse and direct piezoelectric effects according to Voigt's theory, with ϵ and δ as the corresponding coefficients (see also §123). In the other two equations the foundation is laid for the *polarization theory*, with coefficients a and b, which is further discussed in §192.

It must be emphasized that Eqs. (236) to (237*c*) no more *predict* a piezoelectric effect than the thermodynamic equations referred to above predict the existence of a coefficient of thermal expansion. Their service consists in giving expression to the relation between the effect, when it exists, and its converse. The material world is so constituted that the *thermomechanical* effects are universal, while a linear *electromechanical* effect is a very special property. Nor do Eqs. (237) to (237*c*) establish the *law* relating electrical to mechanical phenomena. If the relations were quadratic, the equations would represent the electrostrictive effect and its converse (§137). This effect is so small that we may disregard it. The assumption that we have to do only with a *linear* effect is based on the experimental fact that, with almost all piezoelectric crystals that have been tested, direct proportionality has been observed. There is but little doubt of the general validity of this assumption except among the "Seignette" crystals.

The foregoing equations are special cases of a general *reciprocity theorem:* among reversible processes, whenever there are two primary effects $m = a_1M$, $n = b_1N$, together with a secondary effect $m = a_2N$, then there exists also the supplementary relationship (converse effect) $n = b_2M$.[316] This theorem can be further generalized to include any number of primary effects.* Some of its consequences have already been considered in §20.

188. Still other formulations of piezoelectric theory are possible, depending on the choice of parameters for the dielectric term. We make use of the following relations:

$$D = kE = \frac{k}{\eta}P = \frac{k}{K}F \tag{238}$$

In the last of these expressions F is the *molecular* field and K is an abbrevi-

reversible. When the relations are linear, these four quantities are constant (at a given temperature). For the linear case, the equations give relations identical with those expressed in Eqs. (183) to (184*a*) and (244) to (245*a*). The only difference is that they are in abbreviated symbolic form, without explicit introduction of the various components. Each subscript indicates the quantity that is held constant.

* "Lehrbuch," p. 189. The special form assumed by this theorem in the piezoelectric case is as follows: We let $m \equiv P$, $n \equiv X$, $M \equiv E$, $N \equiv x$, $a_1 \equiv \eta$, $b_1 \equiv -c$, where c is an elastic stiffness constant. Then the primary effects are $P = \eta E$ and $X = -cx$; according to the theorem, if there exists the relation $P = \epsilon x (\epsilon \equiv a_2)$, then there exists also the converse relation $X = -\epsilon E$.

ation for $(1 + \gamma\eta)$, by analogy with $k = 1 + 4\pi\eta$ (see §113). D is the electric displacement.

A few of the ways in which the thermodynamic potentials may be expressed with the aid of Eq. (238) are now given. A single accent (η', k', K') denotes the value at constant stress, a double accent the value at constant strain.

$$\left.\begin{aligned} d\xi_{P,x} &= \frac{1}{\eta''} P\,dP - X\,dx \\ d\zeta_{P,X} &= \frac{1}{\eta'} P\,dP - x\,dX \end{aligned}\right\} \tag{239}$$

$$\left.\begin{aligned} d\xi_{D,x} &= \frac{1}{k''} P\,dD - X\,dx \\ d\zeta_{D,X} &= \frac{1}{k'} P\,dD - x\,dX \end{aligned}\right\} \tag{240}$$

$$\left.\begin{aligned} d\xi_{F,x} &= \frac{1}{K''} P\,dF - X\,dx \\ d\zeta_{F,X} &= \frac{1}{K'} P\,dF - x\,dX \end{aligned}\right\} \tag{241}$$

Equations (239) correspond to (236*a*) and (236*b*); they are basic for the *polarization theory*. Equations (240) and (241) are the fundamental expressions for two other possible modes of treatment, which may be called the *displacement theory* (D-theory) and the *molecular-field* theory (F-theory).

189. The relative merits of the various formulations will be discussed below. Anticipating the conclusion that the polarization theory (P-theory) is to be preferred on theoretical grounds (though not always for practical use), we summarize its main equations, in parallel columns with Voigt's, in Table XX. For the P-theory a and b denote coefficients corresponding to Voigt's e and d, while the superscript P attached to the elastic coefficients means *at constant polarization*.

For each crystal class the matrix of the a's and b's is exactly the same as for the e's and d's, as are also the equations for transformation to rotated axes; this fact is made evident in Eqs. (*xi*) and (*xii*) of the table. The meaning of the symbol (E_m) is explained in §194.

The equations for the P-theory are based on Eqs. (237*a*) and (237*b*). Equation (xi) in Table XX is derived by equating the expressions for X_k in (iv) for the two theories and setting $P_m = \sum_h^3 \eta''_{mh} E_h$. By an analogous process Eq. (xii) is derived from (vii).

By the use of Eq. (143) it can also be shown that

$$a_{mk} = \sum_h^3 e_{hk}\chi''_{mh}, \qquad \text{and} \qquad b_{mk} = \sum_h^3 d_{hk}\chi'_{mh} \tag{242}$$

TABLE XX.—CHIEF EQUATIONS OF THE VOIGT AND POLARIZATION THEORIES

Voigt's theory	Eqs.	P-theory
$\left(\frac{\partial P}{\partial x}\right)_E = -\left(\frac{\partial X}{\partial E}\right)_x = \epsilon$	(i)	$\left(\frac{\partial E}{\partial x}\right)_P = -\left(\frac{\partial X}{\partial P}\right)_x = a$
$\left(\frac{\partial P}{\partial X}\right)_E = -\left(\frac{\partial x}{\partial E}\right)_X = -\delta$	(ii)	$\left(\frac{\partial E}{\partial X}\right)_P = -\left(\frac{\partial x}{\partial P}\right)_X = -b$
$\xi = \sum_m^3 \sum_k^6 e_{mk} x_k E_m$	(iii)	$\xi = \sum_m^3 \sum_k^6 a_{mk} x_k P_m$
$\frac{\partial \xi}{\partial x_k} = \sum_m^3 e_{mk} E_m = -(X_k)$	(iv)	$\frac{\partial \xi}{\partial x_k} = \sum_m^3 a_{mk} P_m = -(X_k)$
$\frac{\partial \xi}{\partial E_m} = \sum_k^6 e_{mk} x_k = P_m$	(v)	$\frac{\partial \xi}{\partial P_m} = \sum_k^6 a_{mk} x_k = (E_m)''$
$\zeta = -\sum_m^3 \sum_k^6 d_{mk} X_k E_m$	(vi)	$\zeta = -\sum_m^3 \sum_k^6 b_{mk} X_k P_m$
$\frac{\partial \zeta}{\partial X_k} = -\sum_m^3 d_{mk} E_m = -x_k$	(vii)	$\frac{\partial \zeta}{\partial X_k} = -\sum_m^3 b_{mk} P_m = -x_k$
$\frac{\partial \zeta}{\partial E_m} = -\sum_k^6 d_{mk} X_k = P_m$	(viii)	$\frac{\partial \zeta}{\partial P_m} = -\sum_k^6 b_{mk} X_k = (E_m)'$
$e_{hk} = \sum_m^6 d_{hm} c^E_{km}$	(ix)	$a_{hk} = \sum_m^6 b_{hm} c^P_{km}$
$d_{hk} = \sum_m^6 e_{hm} s^E_{mk}$	(x)	$b_{hk} = \sum_m^6 a_{hm} s^P_{mk}$
	(xi)	$e_{hk} = \sum_m^3 a_{mk} \eta_{mh}''$
	(xii)	$d_{hk} = \sum_m^3 b_{mk} \eta_{hm}'$

It is unnecessary to give the full tabulation for the other forms of theory that have been mentioned. The equations for the D-theory are obtained from those for the P-theory by writing k' and k'' in place of η' and η'', and D in place of P; for the F-theory we substitute $k' = 1 + \gamma\eta'$ for η', $k'' = 1 + \gamma\eta''$ for η'', and F for P. Otherwise, the equations are all identical. For Mason's charge theory[335, 340, B35] one would substitute $k'/4\pi$ for η', $k''/4\pi$ for η'', and the charge density σ for P.

As was stated in §186, that form of theory is to be preferred which defines its piezoelectric coefficients in such a way as to be the most nearly constant under varying physical conditions. The principal clue to the search is Mason's observation[335] that the resonant frequency, and hence the stiffness, of a 45° X-cut Rochelle-salt plate separated by a wide gap from the electrodes is nearly independent of temperature, while when the electrodes are adherent [so that no depolarizing field (§199) can be built up] there is a very pronounced temperature dependence. According to Voigt's theory the piezoelectric reaction upon the stiffness varies from zero at zero gap to a limiting value at infinite gap; Mason's result could then be explained only on the not too plausible assumption that the temperature coefficient of stiffness was just such as to neutralize that of the piezoelectric reaction with large gaps.

190. Abandoning Voigt's theory, Mason[335] assumed that the true stiffness, unaffected by piezoelectric reaction, was that observed with the widest possible gap; the decrease in frequency with decreasing gap he ascribed to piezoelectric reaction, *i.e.*, to a piezoelectric stress *proportional to the charge* on the electrodes, since the charge increases (at the same electrode voltage) as the gap diminishes. He thus arrived at a new definition of the piezoelectric stress coefficient, $f_{14} = -Y_x\sigma_x$, replacing Voigt's $e_{14} = -Y_xE_x$.

Although Mason's original elaboration of his theory is open to serious criticism,[378] one of his outstanding results consists in finding f_{14}, as he defines it, practically independent of temperature. Taken together with his results concerning the stiffness, this fact suggests very strongly that, if the piezoelectric stress is not proportional to the charge on the electrodes, it is at any rate proportional to some closely related quantity. The employment of the charge or charge density σ as a parameter seems unreasonable on theoretical grounds, because

$$\sigma = \frac{D}{4\pi} = \frac{(E + 4\pi P)}{4\pi},$$

thus involving implicitly both E and P.

One must recognize, as is pointed out in §199, that, as the gap between resonating crystal and electrodes increases indefinitely, the electrical quantity that approaches zero is theoretically the displacement, so that at wide gaps the observed stiffness is very approximately that at *zero electric displacement.* From a purely pragmatic point of view this fact points to the adoption of the charge theory or the equivalent displacement theory, just as Voigt made the pragmatic assumption that stress is proportional to field. Nevertheless, one should not confuse that which is most easily measurable with that which is most fundamental; and if the proportionality of stress with field has to be abandoned, it

appears fundamentally more logical to assume proportionality with polarization than with a parameter that involves both P and E. By the same argument the use of the displacement D or of the internal field F as parameter is ruled out. A step in the direction of the F-theory was taken by Mueller[376] when he assumed the polarizability of Rochelle salt to be due partly to piezoelectric strain and this in turn to be proportional to F. Nevertheless, he did not develop this concept further.

191. We are thus left with the polarization theory as the one to be preferred as an alternative to Voigt's theory. It has been put to experimental test only with Rochelle salt, and here its fundamental hypothesis, that stress is proportional to polarization, is almost identical with that of the charge theory, according to which stress is proportional to charge. For the charge is proportional to the electric displacement, and owing to the very high susceptibility of Rochelle salt the displacement is very nearly proportional to the polarization. Moreover, when the stiffness is derived from the frequency of crystals vibrating with a wide gap, as in Mason's measurements, the depolarizing effect is so strong that the net polarization, like the displacement, is almost zero, so that both forms of theory give practically identical values of the "true" stiffness. The small difference is discussed in §211.

We may therefore accept Mason's dynamic measurements of the elastic constants of Rochelle salt, use of which has been made in §79, as being free from appreciable piezoelectric reaction. The advantages of the P-theory over Voigt's theory in the case of Rochelle salt are that the coefficients a_{14} and b_{14} are more nearly independent than are Voigt's e_{14} and d_{14} of both temperature and field (§474).

With *normal piezoelectric crystals* any one of the foregoing forms of theory could also be applied. For such crystals σ, E, D, F, and P are proportional, not because of *large* values of k, but because with them k is practically *constant*. It is this constancy of k, along with that of the piezoelectric constants, and the very low piezoelectric reaction on the stiffness, that makes well-nigh futile any thought of using observations on normal crystals to decide whether any alternative theory is preferable to Voigt's. For such crystals it is more expedient to continue to employ the Voigt theory. The special field in which the polarization theory is appropriate is that where there is pronounced variability in at least one of the coefficients d_{mh} with temperature.

192. The Polarization Theory. It is an interesting historical fact that in formulating for the first time the general equations for the converse effect, Pockels[427] expressed the piezoelectric strains in terms of components of *polarization*. Not until later did Duhem and Voigt come to use the field instead of the polarization in their equations. At that time, however, the reasons for advocating a general polarization theory

were unknown. In his lattice theory, discussed in §546, Born expressed the piezoelectric and elastic relations in terms of polarization.

When written in terms of polarization instead of field, the two thermodynamic potentials for isothermal changes [Eqs. (1) and (2)] become*

$$\xi = \tfrac{1}{2}\sum_{h}^{6}\sum_{i}^{6} c^{P}_{hi}x_h x_i + \tfrac{1}{2}\sum_{k}^{3}\sum_{m}^{3} \chi''_{km}P_kP_m + \sum_{m}^{3}\sum_{h}^{6} a_{mh}P_m x_h \qquad (243)$$

$$\zeta = \tfrac{1}{2}\sum_{h}^{6}\sum_{i}^{6} s^{P}_{hi}X_h X_i + \tfrac{1}{2}\sum_{k}^{3}\sum_{m}^{3} \chi'_{km}P_kP_m - \sum_{m}^{3}\sum_{h}^{6} b_{mh}P_m X_h \qquad (243a)$$

These two expressions for the free energy contain only *linear* terms. The non-linear term that describes saturation effects is introduced in §451.

When the energy equations are applied to the Seignette-electrics, recognition must be given to the fact that between certain temperatures there is a *spontaneous polarization*, associated with a *spontaneous strain*, which makes a contribution to the energy. The introduction of this contribution in the equations, as well as the inclusion of a term representing non-linear effects, can be presented most clearly in a specific case. We therefore refer the reader to the treatment of Rochelle salt in Chaps. XXIII and XXIV and pass at once to the fundamental piezoelectric equations of the polarization theory, analogous to Eqs. (183) to (184*a*) in Voigt's formulation. They are derived from Eqs. (243) and (243*a*).

$$\frac{\partial\xi}{\partial x_h} = \sum_{i}^{6} c^{P}_{hi}x_i + \sum_{m}^{3} a_{mh}P_m = -(X_h) \qquad (244)$$

$$\frac{\partial\xi}{\partial P_m} = \sum_{k}^{3} \chi''_{km}P_k + \sum_{h}^{6} a_{mh}x_h = (E_m)'' \qquad (244a)$$

$$\frac{\partial\zeta}{\partial X_h} = \sum_{i}^{6} s^{P}_{hi}X_i - \sum_{m}^{3} b_{mh}P_m = -x_h \qquad (245)$$

$$\frac{\partial\zeta}{\partial P_m} = \sum_{k}^{3} \chi'_{km}P_k - \sum_{h}^{6} b_{mh}X_h = (E_m)' \qquad (245a)$$

* After the author had developed this general theory, Mueller's 1940 papers,[378,380,381] appeared, introducing for Rochelle salt a coefficient f_{14} identical with the author's a_{14}. Mueller here adopts the principle of the polarization theory, but he does not go beyond the consideration of the special constants for Rochelle salt with fields parallel to x. He recognizes the effect of piezoelectric reaction on s_{44} and c_{44}, but his use of s_{44} for constant field and of c_{44} for constant polarization is confusing. As far as they go, his results agree with the present treatment. Following is the correlation between Mueller's symbols and the author's:

Mueller	f_{14}	χ_1	κ_1	χ^0_1	κ^0_{cl}	κ^0_1	d^0_{14}	s_{44}	c_{44}
This book	a_{14}	χ_1	η'	χ''_s	η''_s	η'_s	$(d_{14})^s_0$	s^E_{44}	c^P_{44}

The piezoelectric terms in these equations are the same as in Table XX, Eqs. (iv), (v), (vii), and (viii).

Equation (244) may be regarded as the basic equation of the polarization theory. As Mueller has pointed out, it has a certain logical superiority over Voigt's corresponding Eq. (183), in that it involves only the internal parameters x_h and P.

If there is no spontaneous polarization, the P's in the foregoing equations are components of polarization due to the impressed field, at constant strain in Eqs. (244) and (244a) and at constant stress in (245) and (245a).

193. *Dimensions of a_{mh} and b_{mh}.* These quantities correspond to e_{mh} and d_{mh} of Voigt's theory, the dimensions of which were given in §128. The dimensions of a_{mh} are $[M^{\frac{1}{2}}L^{-\frac{1}{2}}T^{-1}k^{-\frac{1}{2}}]$, the same as for a field strength. b_{mh} is of the nature of field strength/stress, with dimensions $[M^{-\frac{1}{2}}L^{\frac{1}{2}}Tk^{-\frac{1}{2}}]$, the same as for the reciprocal of a polarization. In the practical system of electric units a_{mh} may be expressed in volts per centimeter and b_{mh} in volts cm dyne^{-1}. In general, we shall use electrostatic cgs units, as in the case of d_{mh} and e_{mh}.

Following are some of the conversion factors relating the piezoelectric constants according to the Voigt theory (e_{mh} and d_{mh}), the polarization theory (a_{mh} and b_{mh}), the displacement theory (a^D_{mh} and b^D_{mh}), and Mason's charge theory (f_{mh} and g_{mh}) (see §189). Special conversion factors for the Voigt constants are given in §128. For simplicity we confine the discussion to crystals that, like Rochelle salt, have only one piezoelectric constant with respect to a field parallel to any one of the crystallographic axes; each summation in Table XX that concerns us here is thus reduced to a single term.

With all quantities in electrostatic cgs units the following relations hold:

$$a_{mh} = \frac{1}{\eta''_m}\, e_{mh} \qquad b_{mh} = \frac{1}{\eta'_m}\, d_{mh}$$

$$f_{mh} = \frac{4\pi}{k''_m}\, e_{mh} = \frac{k''_m - 1}{k''_m}\, a_{mh} \qquad g_{mh} = \frac{4\pi}{k'_m}\, d_{mh} = \frac{k'_m - 1}{k'_m}\, b_{mh}$$

$$a^D_{mh} = \frac{1}{4\pi} f_{mh} \qquad b^D_{mh} = \frac{1}{4\pi}\, g_{mh}$$

Converting to practical electrical units,

$$a_{mh}\left[\frac{\text{volt}}{\text{cm}}\right] = 300 a_{mh}\left[\frac{\text{statvolt}}{\text{cm}}\right]$$

$$b_{mh}\left[\frac{\text{volt} \cdot \text{cm}}{\text{dyne}}\right] = 300 b_{mh}\left[\frac{\text{statvolt} \cdot \text{cm}}{\text{dyne}}\right]$$

$$g_{mh}\left[\frac{\text{volt} \cdot \text{cm}}{\text{dyne}}\right] = 300 g_{mh}\left[\frac{\text{statvolt} \cdot \text{cm}}{\text{dyne}}\right] = \frac{113(10^{11})}{k'_m}\, d_{mh}\left[\frac{\text{coul}}{\text{dyne}}\right]$$

194. *Interpretation of Eqs.* (244) *to* (245*a*). To Eq. (244) the same reasoning applies as was used in §126 in explanation of Eq. (183); for the present case it may be paraphrased as follows: In (244) the total stress component (X_h) is made up of two parts: (1) the externally applied stress that would produce the prescribed strain if $P = 0$; (2) the part caused piezoelectrically by P. The latter is a body stress, as distinguished from an external stress. That is, the second term is equal and opposite to the external mechanical stress that would have to be added to the mechanical stress responsible for the first term, in order to hold the strain constant when the polarization was applied. With both strain and polarization prescribed, the total external mechanical stress component is therefore, not the (X_h) in Eq. (244), but rather

$$X_h = -\Sigma c^P_{hi} x_i + \Sigma a_{mh} P_m = (X_h) + 2\Sigma a_{mh} P_m \tag{246}$$

We see also that, when $(X_h) = 0$, there must be an external stress $X_h = 2\Sigma a_{mh} P_m$, with a strain given by $-\Sigma c^P_{hi} x_i = \Sigma a_{mh} P_m$. The fact that (X_h) is not the external stress, but the sum of two stresses, one external and the other internal, must be kept in mind in all uses that are made of Eq. (244).

Just as in Eq. (244) (X_h) is not an externally impressed stress component, so in Eqs. (244*a*) and (245*a*) $(E_m)''$ and $(E_m)'$ are not components of the actual impressed field. In (244*a*) $(E_m)''$ is a component of the field that would produce the same total polarization in a clamped crystal that is given by the prescribed values of the P_k and x_h. If all $x_h = 0$ and if there is no spontaneous polarization, we have simply the dielectric equations (143) for a clamped crystal, and $(E_m)'' = E_m$, the actual field; and if all $P_k = 0$, $(E_m)''$ is a component of the field that would cause in a clamped crystal the polarization due to x_h.

In Eqs. (245) and (245*a*), the X's are externally applied stresses. The interpretation of $(E_m)'$ is analogous to that of $(E_m)''$ above.

195. The following considerations will serve further to make clear the relation between $(E_m)''$ and the actual field E_m. We restrict ourselves to the case in which the only component of the actual field is E_m and assume that there are no cross susceptibilities, so that in the unstrained (clamped) crystal the only polarization is $P_m = \eta''_{mm} E_m$. Then if an arbitrary strain is also impressed, the total polarization, from Eq. (183*a*), according to Voigt's notation, is

$$(P_m)_t = \eta''_{mm} E_m + \sum_h^6 e_{mh} x_h = P_m + \sum_h^6 e_{mh} x_h \tag{247}$$

whence

$$E_m = \chi''_{mm} (P_m)_t - \chi''_{mm} \sum_h^6 e_{mh} x_h = \chi''_{mm} P_m \tag{248}$$

On the polarization theory, the corresponding expression, from Table XX, Eq. (xi), is

$$E_m = \chi''_{mm}(P_m)_t - \sum_h^6 a_{mh}x_h = \chi''_{mm}P_m \tag{248a}$$

Under the same conditions Eq. (244a) becomes

$$(E_m)'' = \chi''_{mm}P_m + \sum_h^6 a_{mh}x_h \tag{248b}$$

Then, since P_m is the polarization due to E_m alone, we have $\chi''_{mm}P_m = E_m$, whence the following relation holds:

$$(E_m)'' = E_m + \sum_h^6 a_{mh}x_h = \chi''_{mm}(P_m)_t \tag{248c}$$

The equivalent field $(E_m)''$ is thus seen to be the sum of the actual field E_m due to the potential difference between the crystal surfaces and the quasi-field due to the deformation. It is also easily proved that

$$\frac{(E_m)''}{E_m} = \frac{(P_m)_t}{P_m}.$$

Analogous expressions are readily derived for the case where an arbitrary *stress system* is impressed, the crystal being free to deform itself when E is applied. Corresponding to Eqs. (247), (248a), and (248c), one finds

$$(P_m)_t = \eta'_{mm}E_m - \sum_h^6 d_{mh}X_h = P_m - \sum_h^6 d_{mh}X_h \tag{249}$$

$$E_m = \chi'_{mm}(P_m)_t + \sum_h^6 b_{mh}X_h = \chi'_{mm}P_m \tag{250}$$

$$\begin{aligned}(E_m)' &= E_m - \sum_h^6 b_{mh}X_h = \chi'_{mm}(P_m)_t \\ &= \chi'_{mm}P_m - \sum_h^6 b_{mh}X_h \end{aligned} \tag{250a}$$

As before, we find also that $\dfrac{(E_m)'}{E_m} = \dfrac{(P_m)_t}{P_m}$.

From Eqs. (248c) and (250a) it is evident that $(E_m) = E_m$ in two special cases: (1) when the crystal is clamped so that there is no strain, *i.e.*, when a mechanical stress system is applied such as to prevent deformation when the field is applied; (2) when the crystal is entirely free to deform itself in the field, *i.e.*, when all impressed mechanical stresses vanish.

Equations (247) and (250a) give the actual field E_m in the crystal when the strain (or stress) system and the total polarization are prescribed. By introducing the cross susceptibilities these expressions can be generalized to the following forms, supplementing Eqs. (244a) and (245a):

$$E_m = \sum_k^3 \chi''_{km}(P_k)_t - \sum_h^6 a_{mh}x_h \tag{251}$$

$$E_m = \sum_k^3 \chi'_{km}(P_k)_t + \sum_h^6 b_{mh}X_h \tag{251a}$$

Since the foregoing equations are to be applied in §452 to Rochelle salt, with the field in the X-direction, we can set $m = 1$, $h = 4$, $X_h = Y_s$, $x_h = y_s$ and drop the subscript m from P, E, η, and χ. The following expressions are valid only for *small* stresses and fields. Otherwise, non-linear effects are present, for which see §452. For a crystal under a prescribed strain y_s and field E,

$$P_t = \eta''E + e_{14}y_s \tag{252}$$

$$E = \chi''P_t - \chi''e_{14}y_s = \chi''P_t - a_{14}y_s \tag{253}$$

$$(E'') = \chi''P + a_{14}y_s = E + a_{14}y_s = \chi''P_t \tag{253a}$$

where P is the polarization due to E when $y_s = 0$.

For a crystal under prescribed *stress* Y_s and field E,

$$P_t = \eta'E - d_{14}Y_s \tag{254}$$

$$E = \chi'P_t + \chi'd_{14}Y_s = \chi'P_t + b_{14}Y_s \tag{255}$$

$$(E)' = \chi'P - b_{14}Y_s = E - b_{14}Y_s = \chi'P_t \tag{255a}$$

where P is the polarization due to E when $Y_s = 0$.

Whether the crystal is clamped or free, (E) is related to E by the equation

$$\frac{(E)}{E} = \frac{P_t}{P}.$$

We can now derive, in terms of the polarization theory, expressions for the components of polarization in the *direct effect*, analogous to Eqs. (187) and (188) according to Voigt. We assume zero field in the crystal and also $P^\circ = 0$* and therefore set $P_k = 0$ in (244a) and (245a), then multiply each of the three components (E_m) by the appropriate susceptibility and add them according to Eqs. (140). The three components of piezoelectric polarization P_n ($n = 1, 2, 3$) are thus obtained:

$$P_n = \sum_m^3 \eta''_{nm}(E_m)'' = \sum_m^3 \sum_h^6 \eta''_{nm}a_{mh}x_h \quad \text{(constant strain)} \tag{256}$$

$$P_n = \sum_m^3 \eta'_{nm}(E_m)' = -\sum_m^3 \sum_h^6 \eta'_{nm}b_{mh}X_h \quad \text{(constant stress)} \tag{256a}$$

* The special expressions when P° is present are worked out for Rochelle salt in §459.

From Eqs. (xi) and (xii) in Table XX, these expressions can be reduced to Eqs. (187) and (188). As always, η''_{nm} and η'_{nm} denote susceptibilities at constant strain and constant stress, respectively.

When there are no cross susceptibilities, $n = m$, and the field and polarization are parallel. For given strain and given stress the polarizations are then

$$P_m = \eta''_{mm} \sum_{h}^{6} a_{mh} x_h \qquad \text{and} \qquad P_m = -\eta'_{mm} \sum_{h}^{6} b_{mh} X_h \qquad (257)$$

The same expressions can also be derived by taking derivatives of Eqs. (243) and (243*a*) with respect to E_m. Equations (256), (256*a*), and (257) give the *actual* polarizations when the electrodes are adherent to the crystal and short-circuited (field = 0). Otherwise, the contributions due to the field must be added.

196. Comparison of the Polarization Theory with Voigt's Theory. From the point of view of the polarization theory, the positions of the parameters "electric field" and "polarization" in Figs. 1 and 48 would have to be interchanged. Although this alteration would logically lead to corresponding changes in the formulation of pyroelectric theory, we need not concern ourselves with this problem, since Voigt's formulation seems quite adequate for this purpose.

When an electric field is applied to a piezoelectric crystal, it is in general impossible to make direct measurements of both stress and polarization. In observations of the *direct* effect, with electrodes closely adherent to the crystal, this is possible, and here all forms of the theory give identical results. With the *converse* effect, on the other hand, if we attempt to measure the piezoelectric stress, as for example by observing the externally applied stress necessary to reduce the strain to zero, we thereby alter the polarization by an amount that cannot be measured directly. Likewise, the polarization cannot be measured without involving a change in stress. We are confronted with a sort of piezoelectric "principle of uncertainty."

At this point we must pause to consider what quantities can be regarded as observable. There is first of all the mechanical *strain*, which, on paper at least, is perfectly determinate and measurable under all circumstances. Next the electric susceptibilities, η'' at constant strain and η' at constant stress, both of which are measurable (though somewhat indirectly) and which have a perfectly definite meaning independent of all theory. The field strength E is directly measurable with flat plates of sufficient area and with adherent electrodes. The polarization, as has been stated, is directly measurable only with the direct effect, using adherent electrodes.

The piezoelectric stress has a value independent of theory only when the crystal is so clamped that no deformation can take place. In this case, for the same field, all equations of the type of (iv) in Table XX give identical numerical values, and the components of stress are equal and opposite to those of the external constraint. The electrodes are here assumed to be adherent and maintained at a fixed potential difference. If now the constraints are removed, the field remains unchanged, but the polarization, by Eq. (v), is increased. According to the *Voigt* theory the stress remains unchanged and there is still no piezoelectric reaction, while the *polarization* theory asserts that there *is* a piezoelectric reaction and that the stress is thereby increased. Now this increased stress is that which would actually be observed if known forces could be applied from without such as to reduce the strain to zero *at constant polarization.* This particular effect, like all other piezoelectric phenomena, can be described in terms of *any* of the alternative forms of theory. Of itself it furnishes no criterion whatever for choice between the various forms.

The stress-strain relations according to the polarization theory may be illustrated by a simple example. A stress X_E is applied to a piezoelectric crystal, producing a certain strain x. If the *field* is held constant, as for example by short-circuiting the crystal so that $E = 0$, the observed stress X_E (at constant E) will be relatively small.

If the experiment is repeated with the *polarization* held at zero, the observed stress X_P will be greater. According to the *Voigt theory* this fact is explainable thus: The strain gives rise to a polarization P, which is present when $E = 0$ and which does not affect X_E. To make $P = 0$ it is necessary to apply a negative field $-E'$ sufficient to produce a counter-polarization $-P$ that will neutralize $+P$. This negative field also causes a *negative stress,* to overcome which a stress X_P greater than X_E must be applied externally to produce the same strain.

According to the *polarization theory* this negative piezoelectric stress, being proportional to P, is present when $E = 0$ but not when $P = 0$. Its effect is, by Eq. (vii) in Table XX, to *increase the strain;* hence, for the same strain, X_E is less than X_P by an amount equal to the piezoelectric stress.

Equations for the elastic constants in terms of the polarization theory are given in §208.

197. The following correlation between the Voigt and polarization theories may be helpful. In comparing Eqs. (184) and (245), we may assume that the crystal is subjected simultaneously to a stress system X and a field E in any direction. There is then a polarization P due partly to X, partly to E. If the resulting strain x is to be expressed in terms of X and E, the Voigt theory is used, with isagric compliances and with

piezoelectric constants d_{mh}. On the other hand, when X and P are given it is simpler to use the polarization theory, with compliances s^P_{hi} and piezoelectric constants b_{mh}. The fact that, for the same stress, field, and strain, the two theories require the use of different compliances follows from the circumstance that x is due in part to E as well as to X and that the former of these contributions has a different form according to whether it is expressed in terms of E or of P.

The exact equivalence of Eqs. (184) and (245) can be shown in general form from the relations already given between the various coefficients. A simple example is afforded by Rochelle salt (or any crystal in Classes V, V_d, D_4, D_6, T, or T_d). If the field is E_x, the only piezoelectric coefficients to consider are d_{14} and $b_{14} = d_{14}/\eta'$ [Eq. (242)]. Assuming the only mechanically impressed stress to be Y_z, we have from Eq. (184), by Voigt's theory,

$$-y_z = s^E_{44} Y_z - d_{14} E_x \tag{258}$$

and from Eq. (245), by the polarization theory,

$$-y_z = s^P_{44} Y_z - b_{14} P_x \tag{259}$$

On substituting d_{14}/η' for b_{14} and making use of the relations $s^P_{44} = s^E_{44}\eta''/\eta'$ from Eq. (520) and $P_x = \eta' E_x - d_{14} Y_z$ from Eq. (184a), we find

$$-y_z = s^E_{44}\left(\frac{\eta''}{\eta'} + \frac{d^2_{14}}{s^E_{44}\eta'}\right) Y_z - d_{14} E_x$$

Then since $d_{14}/s^E_{44} = e_{14}$ from Eqs. (204) and $\eta' = \eta'' + e_{14}d_{14}$ from Eq. (264), the expression for y_z is easily reduced to the form given in (258). For simplicity, these expressions have been written without regard to the phenomenon of saturation in Rochelle salt. The complications that arise from this cause are treated in Chaps. XXIII and XXIV.

CHAPTER XII

SECONDARY PIEZOELECTRIC EFFECTS

Primary causes are unknown to us; but are subject to simple and constant laws, which may be discovered by observation, the study of them being the object of natural philosophy. —FOURIER.

Whenever a piezoelectric crystal is under mechanical stress, an electric polarization is produced by the direct effect, which, except under special boundary conditions, gives rise to an electric field. According to Voigt's theory, this field, through the action of the converse effect, causes certain components of strain in addition to those due to the mechanical stress. Similarly, an impressed electric field causes a primary polarization, superposed on which is a secondary polarization due to the state of strain produced piezoelectrically by the field. The state of affairs is further complicated when electric and mechanical stresses are impressed simultaneously.

These secondary effects are sometimes sources of great annoyance. On the other hand, they can also be turned to good account, as for example in the piezoelectric resonator, a device in which they play a very essential part. Whether for good or ill, they are usually present, so that it becomes important to examine somewhat closely their general theory, as well as their operation under certain special conditions.

198. Correlation between Elastic and Dielectric Phenomena. In the formulation of physical laws, close similarities between the statements expressing widely differing phenomena are of very frequent occurrence. The correspondences are sometimes chiefly in form, as when Ohm's law is compared with its magnetic analogy; and sometimes they express identity of underlying principles, an illustration of which is found in the application of electric-circuit theory to acoustic problems.

There are some interesting analogies between mechanical phenomena in elastic bodies and the electrical effects in dielectrics. Since piezoelectricity deals with a system of relations between these two domains, it is worth while to inquire to what extent the relations can be made symmetrical in form and also in how far the correspondences thus disclosed may be regarded as of more than merely formal significance. It can be foreseen at the outset that full symmetry in the mathematical formulation is impossible, for the following reasons:

1. Elastic stresses and strains are tensors, while electric fields* and polarizations are vectors, the field being characterized by a potential gradient.

2. Across the boundary between two media it is the normal elastic *stress* that is continuous, while in the electric case the continuity is in the electric *displacement* and not in the field. Furthermore, an elastic stress is defined as force per unit area, while the electric stress, or field strength, is force per unit charge.

3. An elastic stress exists only in a material medium; there is no "elastic field" in a vacuum corresponding to the electric field. On the other hand, an electric field can act directly on a charge without an intervening material medium.

According to molecular theory, when a mechanical pressure is applied to the plate, the outer electrons of adjacent atoms become crowded together, and the thickness of the plate is decreased, while at the same time certain other related deformations take place. The latter depend on the form of the unit cell, *i.e.*, on the crystal structure. In an ordinary dielectric no polarization results. Equilibrium is reached when the interatomic forces become equal and opposite to those caused by the pressure. This complex of *short-range, highly divergent* inner fields constitutes the elastic reacting stress and determines the compliance s. In a piezoelectric plate, a *polarization* is caused by the deformation; the resultant electric field depends upon conditions at the boundaries. It is for this reason that the fundamental piezoelectric equations in Table XXI (page 265) express the polarization, rather than the field, as a function of impressed mechanical stress.

If now instead of a mechanical stress we impress upon the plate an electric stress, in the form of a uniform field, this field, which may originate in distant charges, acts at *long range* upon the charges in the dielectric, giving rise to a polarization $P = \eta E$. The quantities η and P may be regarded as the dielectric "compliance" and "strain," respectively, analogous to s and x in the equation $x = -sX$. As in the mechanical case, equilibrium is attained when the forces of restitution between the displaced charges have become sufficiently great. If the plate is not piezoelectric, no mechanical deformation takes place; we are here ignoring the electrostrictive effect, which depends on the square of the field and is usually negligible in comparison with the piezoelectric effect.

In a piezoelectric plate thus stressed electrically, the particles become systematically displaced, in a manner depending on the crystal symmetry, so as to deform the crystal. Equilibrium is reached when the restoring elastic stress $X' = -cx$ balances the piezoelectric stress $X = -\epsilon E$ (c and ϵ are elastic and piezoelectric stress coefficients).

* The terms electric *field*, or *field strength*, and *electric stress* are used synonymously.

199. Mechanical and Electrical Boundary Conditions. In piezoelectric problems, the elastic boundary conditions are of importance when an electric field is impressed, and the electrical boundary conditions when a mechanical stress is impressed. Conditions are here assumed isothermal throughout the present discussion. Just as an applied electric field produces in a piezoelectric crystal a polarization that depends on the state of mechanical relaxation, so when mechanical stress is applied the amount of yield depends on the state of electrical relaxation; the analogous quantities in the crystal are the dielectric susceptibilities and the elastic constants, *i.e.*, the electrical and mechanical compliances.

With respect to *elastic conditions* the two standard states may be defined as *clamped* and *free*. In the *clamped state*, whenever an electric field is impressed a system of mechanical stresses is postulated such as to prevent all alterations in strains (§216). The crystal may then be regarded as having all its surfaces firmly attached to a surrounding medium of infinite rigidity. In the *free state* the surrounding medium has infinite compliance (air or vacuum), a condition that can be approximately realized with suitable mounting; the crystal is then free from external stress, and the piezoelectric strain $x = \delta E$ can assume its full theoretical value. Measurements of dielectric constant are ordinarily made with the dielectric approximately in this state. If all relations are linear, the same value of the dielectric constant will be observed if the mechanical stress system is not zero but maintained constant during the experiment.

Electrically, by analogy, the crystal should be considered *clamped* when conditions are such that there is no polarization or, more generally, when the polarization is constant. This state can be brought about by providing a counter-field of such intensity as to neutralize the polarization caused by mechanical stress [Eq. (290)]. To a certain degree of approximation a crystal may be considered as *electrically clamped* when it is *isolated*, *i.e.*, so remote from all conductors that the depolarizing field due to polarization charges on the surface reduces the net polarization to a small value. In the case of such a crystal as Rochelle salt, in which the dielectric constant is very large, this depolarizing effect reduces the polarization almost to the vanishing point (§211). An *isolated* crystal is then practically in the "electrically clamped" state.

Of great importance is the *electrically free state*, in which the surrounding medium has infinite dielectric susceptibility. This condition is realized very simply by making the entire surface equipotential, as by providing short-circuited electrodes or by allowing time for surface charges to be neutralized by leakage. There is then no field in the crystal; and if the crystal is piezoelectric and is mechanically stressed, the piezoelectric polarization is not diminished by counter-polarization.

Static measurements of elastic constants of crystals are customarily made with the specimens in the electrically free state. The same values would be observed (if all relations were *linear*) if the electric field were different from zero but maintained constant throughout the experiment. The values of elastic constants under constant-field conditions may be called *isagric* values, with symbols s^E_{hk} and c^E_{hk} when it is necessary to be specific.

Under certain experimental conditions the crystal when deformed by a mechanical stress is in a state of *constant electric displacement.* This situation is encountered, for example, when the stress is applied to a relatively thin plate cut in such an orientation that the piezoelectric polarization is parallel to the thickness, the plate being far removed from all conductors. From the principle of continuity of displacement normal to the boundary between two media, it is clear that in the crystal, as at infinity, the displacement is zero. According to §214, there is still a polarization in the crystal, which causes a contribution to the displacement, but this contribution is neutralized by the depolarizing field. Even in a thin crystal, however, the displacement never vanishes at the edges. Fortunately, in most crystals, including quartz, the dielectric constant is large enough so that edge corrections do not have to be made with bars or plates that are reasonably thin in the field direction.

200. A serious complication arises from the fact that in crystals of low symmetry and in oblique cuts from crystals of high symmetry the polarization is in general not parallel to the field. In such cases an impressed stress may cause a polarization, and hence a displacement, with components *at right angles to the field.* If the specimen is in the form of a thin bar or plate, the component of displacement parallel to the field and to the thickness can become neutralized by the depolarizing field when the crystal is sufficiently far from conductors. If the lateral dimensions are relatively large, the other components are not neutralized but are almost as great as in a short-circuited crystal. That is, while short-circuiting makes the *field* zero, absence of electrodes does not ensure that the *displacement* will be zero.

The foregoing remarks apply particularly to the determination of elastic constants from observations of resonant frequencies. If, as is often the case in such observations, the gap between crystal and electrodes is zero, the deformation of the specimen is without influence on the field in the thickness direction; for this is the driving field, impressed from without. There is no lateral field except one of negligible magnitude due to polarization charges at the edges. Hence no component of the piezoelectric polarization is neutralized, and there is no depolarizing field to contribute to the total stress or strain. That is, from observations at *zero gap* the *isagric* elastic constants are determined. As will

be shown in Chap. XIII, their derivation from lengthwise vibrations of bars is quite simple; on the other hand, certain piezoelectric corrections have to be applied in the case of thickness vibrations.

When observations are made with a very wide gap, the effective elastic constants as deduced from the resonant frequencies are essentially those at *constant displacement*, if field and polarization are parallel. When the polarization is not parallel to the field, the effective constants are those for a constant-displacement component normal to the surfaces of the plate; their value is then intermediate between the constant-displacement and the constant-field values. Formulas for the latter type of elastic constant, which should be used whenever the fundamental (isagric) constants are to be derived from vibrational data, are given below.

Numerically, the elastic constants at constant displacement are very close to those at constant polarization (see the comparisons for Rochelle salt and quartz in §211). Since, as we have seen, they cannot in general be observed directly, it is advisable to consider the isagric values as standard, as has indeed been the practice in the past. The only exceptions are the Seignette-electrics, for which there are good reasons for considering the values at constant polarization as more fundamental (§191).

The formulas in the following pages are based on the assumption that the area of the crystal plate is infinite. With finite plates, owing to the lack of uniformity in field, polarization, and displacement near the edges, the formulas offer only a more or less close approximation. The greater the dielectric constant, the smaller can the lateral dimensions be without introducing serious errors.

In summary, it may be said that the two principal mechanical states are *clamped* (constant strain) and *free* (constant external stress, usually zero) and that the two principal electrical states are *isolated* (subject to depolarizing field) and electrically *free* (short-circuited, or electric field held constant). Static measurements of dielectric and elastic constants are usually made respectively with external mechanical stresses and internal (macroscopic) electric fields as near zero as possible. In a vibrating resonator, the crystal is usually mechanically free with respect to certain stresses but not to others.

201. Bearing in mind the general considerations that have just been discussed, we turn to their mathematical formulation. The chief relations between electrostatic and mechanical phenomena for piezoelectric crystals, so far as our present needs are concerned, are grouped together in Table XXI. On the right side of each equation is the independent variable in terms of which that on the left side is expressed. For the sake of simplicity summations and subscripts are omitted, and all effects

are assumed to be linear. The basic piezoelectric equations are (*c*), (*d*), (*c'*), and (*e'*), the direct and converse effects being at the right and left, respectively. Each equation in the table, including these four, holds rigorously only for a specified state of the crystal. Thus the familiar elastic equations (*a*) and (*b*), as well as (*c'*) and (*e'*), assume the crystal to be electrically free, so that the elastic constants *s* and *c* have their isagric values. In (*e*), (*f*), and (*a'*) the crystal is mechanically free, so that η and *k* are identical with the η' and k' of Eqs. (264) and (265), while (*b'*), (*d'*), and (*f'*) are for a completely isolated plate of large area. Beside each equation in one column is placed its counterpart in the other column, with electric strain substituted for mechanical strain, etc. The limitations of each equation, together with the effect of secondary reactions, will be discussed below. In general, whenever a departure is made from the standard state for each equation, piezoelectric reactions enter in (secondary effects) that depend on boundary conditions, often adding serious complications to the problem. The equations that may best be regarded as fundamental are (*a*), (*a'*), (*c*), and (*c'*), all the rest being derivable from them.

Voigt treats numerous special problems in which boundary conditions are considered; but, except for a brief discussion of a plate under combined electric and mechanical stresses ("Lehrbuch," pages 915–920), he does not introduce secondary effects into his theory, although on pages 817 and 920 he recognizes that they would have a quantitative effect on his results. In most of the special cases that he treats, secondary effects are absent.

TABLE XXI.—ELECTROMECHANICAL RELATIONS

Mechanical Effects		Electrical Effects	
$x = -sX$	(*a*)	$P = \eta E$	(*a'*)
$X = -cx$	(*b*)	$E = -\frac{4\pi}{k} P$	(*b'*)
$x = dE$	(*c*)	$P = -dX$	(*c'*)
$X = -eE$	(*d*)	$E = \frac{4\pi d}{k} X$	(*d'*)
$x = \frac{d}{\eta} P$	(*e*)	$P = ex$	(*e'*)
$X = -\frac{e}{\eta} P$	(*f*)	$E = -\frac{4\pi e}{k} x$	(*f'*)

Eqs. (*a*) and (*b*), in which *s* and *c* are isagric, symbolize the fundamental stress-strain elastic relations at constant field. Corresponding to (*a*) is Eq. (*a'*) for dielectric stress and strain in a mechanically free crystal.

Although Eq. (*b'*) is of a more special character than (*a'*), it is included in Table XXI, partly for the sake of the symmetrical relationships and partly because we shall have occasion to refer to it later (§214). In

(b') the crystal is isolated and in zero external field, and hence the total electric displacement must be zero; P is an *impressed* polarization, which may be due to a mechanical strain (piezoelectric effect) or to a change in temperature (pyroelectric effect), or the substance may be an electret (§174).

Equations (c), (d), (c'), and (e') are abbreviated forms of the fundamental piezoelectric equations (187) to (190). The fact that (d) and (e') are not symmetrical, one being in terms of stress and the other of strain, testifies to the lack of complete correspondence. Equation (d') bears the same relation to (d) that (b') does to (b). It holds for an isolated piezoelectric crystal subjected to stress X and is derived from (b') and (c'). It is expressed more specifically in §§207, 212, and 214. Equation (e) is the complement to (e'), expressing strain in terms of polarization (*cf.* §189). It is derived from (c) and (a') and is used in Chap. XXIII. Equations (f) and (f') are included to complete the symmetry in Table XXI. Equation (f), which is the basic equation of the polarization theory, is derived from (d) and (a'), and Eq. (f') from (b') and (e').

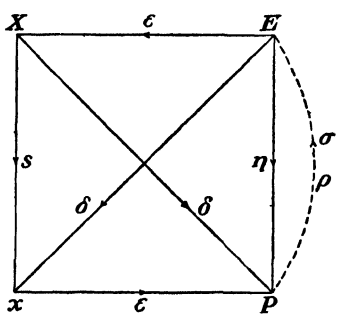


FIG. 48.—Interaction between elastic and electric effects.

202. The effects represented in Table XXI are shown graphically in Fig. 48, taken from the upper portion of Fig. 10, in which the arrows indicate the usual sequence from cause to effect. The arrows $X \rightarrow P$ and $x \rightarrow P$ represent the direct piezoelectric effect, from Eqs. (f') and (e'), Table XXI, $E \rightarrow x$ and $E \rightarrow X$ the converse effect, from (c) and (d). The arrows $E \rightarrow P$, from (a'), and $X \rightarrow x$, from (a), apply normally to the electrically and mechanically free states, respectively.

Figure 48 shows also the genesis of the secondary effects. For example, when the crystal is mechanically clamped and a field E is applied, the resultant X and x are both zero and we have simply Eq. (a'). If the crystal is mechanically free, the arrows $E \rightarrow x$ and $x \rightarrow P$ indicate a piezoelectric contribution to the total polarization [Eq. (263)]. The surface charge σ due to P, or in some cases the space charge ρ, gives rise to an additional component of E (or, if E is held constant, to an additional charge on the electrodes), as indicated by the curved arrow, leading to a change in the effective value of the dielectric constant (§204). The curved arrow corresponds to Eq. (b').

Similarly, when the crystal is electrically free (electrodes short-circuited), the resultant field is zero and Eq. (a) remains unmodified. On the other hand, if the crystal is isolated, the arrows $X \rightarrow P$, $P \rightarrow E$,

$E \rightarrow x$ indicate the process whereby the strain, and thence the effective elastic compliance, is influenced by secondary piezoelectric action. The theory of these reactions, which are of great importance in the piezoelectric resonator, will now be considered.

203. Theory of Isothermal Piezoelectric Reactions. The following treatment corresponds in part to the paragraphs on secondary effects in Voigt's "Lehrbuch,"* with certain changes in notation. It is assumed, as is approximately the case except with the Seignette-electrics, that the susceptibility and the piezoelectric coefficients d and e are constant, *i.e.*, that all relations are linear. The peculiar characteristics of the Seignette-electrics are considered in Chaps. XXIII and XXIV. In order to minimize boundary effects, a plane-parallel piezoelectric plate of thickness small in comparison with its other dimensions is assumed, the electric field and polarization being normal to the large surfaces. A more general solution would involve very grave complications, tending to obscure the physical significance. So far as first-order effects are concerned, the present treatment is applicable to most experimental situations. The equations are sufficiently general to apply under the conditions specified above to a plate in any orientation, in any non-conducting piezoelectric crystal, so long as linear relations between stress and strain hold in both the electric and the elastic equations.

A system of orthogonal axes X, Y, Z in any orientation is assumed. All elastic and electric coefficients are expressed with respect to these axes. The six stress components $X_x \ldots X_y$ are denoted by $X_1 \ldots X_6$, and the strain components by $x_1 \ldots x_6$.

204. The Piezoelectric Contribution to the Dielectric Constant. Mention has already been made in §§104 and 124 of the distinction between the dielectric constant k'' of a clamped crystal, and k' of the crystal when mechanically free or under constant stress. The effective k of vibrating plates usually lies somewhere between these two limiting values. The unaccented symbols k and η are used in this book where there can be no ambiguity or where no special distinction is needed. This was also the practice of Voigt, who used a primed symbol for the dielectric constant of the free crystal in his brief treatment of secondary effects.†

The very important relation between k'' and k' is found by combining Eqs. (183a) and (184) for the direct and converse effects. We assume the fields to be in the h-direction and seek an expression, in terms of the clamped susceptibility, for the polarization in the m-direction due to the joint action of E_h and a stress X_k. On substituting x_h from (184) in

* Pp. 916–919.

† "Lehrbuch," p. 917.

(183a) and making appropriate changes in subscripts, one finds, by means of Eq. (191a),

$$P_m = E_h\left(\eta''_{hm} + \sum_i^6 e_{mi}d_{hi}\right) - \sum_i^6 e_{mi}s^E_{ik}X_k$$

$$= E_h\left(\eta''_{hm} + \sum_i^6 e_{mi}d_{hi}\right) - d_{mk}X_k \tag{260}$$

Now, from Eq. (184a),

$$P_m = \eta''_{hm}E_h - d_{mk}X_k \tag{261}$$

From these two equations the desired result follows:

$$\eta'_{hm} = \eta''_{hm} + \sum_i^6 e_{mi}d_{hi} \tag{262}$$

In most practical cases the polarization is exactly or very nearly parallel to the field, so that $h = m$, and for brevity a single subscript m may be written in place of mm:

$$P_m = \eta'_m E_m - d_{mk}X_k \tag{263}$$

$$\eta'_m = \eta''_m + \sum_i^6 e_{mi}d_{mi} \tag{264}$$

$$k'_m = 1 + 4\pi\eta'_m = k''_m + 4\pi\sum_i^6 e_{mi}d_{mi} \tag{265}$$

$$k''_m = 1 + 4\pi\eta''_m \tag{266}$$

Equations (264) and (265) when applied to Rochelle salt for fields in the X-direction take the following form, of which frequent use will be made:

$$\eta'_x = \eta''_x + e_{14}d_{14} \tag{267}$$

$$k'_x = 1 + 4\pi\eta'_x = k''_x + 4\pi e_{14}d_{14} \tag{267a}$$

According to Eqs. (260) and (261), the value of η'_{hm} is independent of the stress X_k. This independence holds whenever, as in the cases here considered, all relations are linear. Then, and only then, can one call η' the susceptibility *at constant stress*, as in §124. In Rochelle salt, for example, the relations are non-linear, and it is necessary to specify the value of the stress—usually zero—in order to give η' a definite meaning (see §450).

If some, but not all, of the components of strain are prohibited, as happens in certain vibrational problems to be considered later, the corresponding terms in the summation disappear. The susceptibility then has a value somewhere between η' for a free crystal and η'' for a clamped crystal.

205. The Piezoelectric Contribution to the Elastic Constants. This effect has already been mentioned repeatedly. As we have seen, the elastic coefficients depend on the electrical state of the crystal, which in turn is conditioned by the polarization due to the deformation.

The relations between the elastic compliance and stiffness coefficients under conditions of constant field, constant electric displacement, and constant polarization will now be derived in general form. The isagric coefficients s_{hk}^E and c_{hk}^E relate strain to stress when there is no potential gradient in the crystal. Their values are commonly measured by static methods, or by lengthwise vibrations when the field is perpendicular to the direction of vibration, with full-sized electrodes closely adherent to the crystal. The constant-displacement coefficients s_{hk}^D and c_{hk}^D hold in certain cases for a completely isolated crystal*, while the constant-polarization coefficients s_{hk}^P and c_{hk}^P play an important part in the polarization theory (Chaps. XI and XXIII).

The constant-displacement and constant-polarization tensors have the same form as the isagric tensor, with the same number of elastic constants for a given crystal class. They transform to rotated axes in the same way, permitting the use of the transformation equations in Chap. IV.

206. *Elastic Coefficients at Constant Electric Displacement.* We consider a piece of crystal of any form, subjected to a homogeneous stress system in which all six components $X_1 \ldots X_6$ may be present. If the entire surface of the specimen is kept at a fixed potential, for example by a grounded metallic coating, the constants relating strain components with stress components are the isagric $s_{11}^E \ldots s_{66}^E$. Although the field in the crystal is zero, there is present a polarization with components given by Eq. (183*a*).

The following equations can be applied to a rotated axial system by expressing all parameters with respect to the rotated axes. In order to obtain the coefficients s_{hk}^D, one may in theory impress upon the crystal, while it is thus stressed, a field in the proper direction and of such strength as to maintain the electric displacement at the value zero. If the stress system is left constant, this field will change the strain components according to Eq. (184), and from the new strains the s_{hk}^D can be calculated.

* The crystal may be bare and far removed from all conductors, or it may have adherent coatings that are disconnected from the circuit and free from stray capacitive effects. In the latter case one may say that the adherent electrodes are connected to an infinite impedance. Thus, in a static field or with thickness vibrations, a crystal plate may be plated on both sides and still be "isolated," with a compliance s_{hk}^D. The plated bar in lengthwise vibration requires a special treatment, as will be seen in §286. The terms "plated" and "unplated" are, however, sometimes employed to denote zero gap and infinite gap.

The equations are derived most conveniently by assuming a single stress component X_k, which gives rise to three components of piezoelectric displacement of form $D_m = 4\pi P_m = -4\pi d_{mk} X_k$, by Eq. (184*a*). To neutralize D_m we need $D'_m = -D_m = 4\pi d_{mk} X_k$. To each D'_m there correspond three components of the requisite field E':

$$E'_j = \sum_m^3 \theta'_{jm} D'_m = 4\pi X_k \sum_m^3 \theta'_{jm} d_{mk}$$

by Eq. (145). The accented θ' signifies a *free* crystal (constant stress).

Each E'_j causes a strain component $x'_h = d_{jh} E'_j$. Hence for all three components of E' we have

$$x'_h = 4\pi X_k \sum_j^3 \sum_m^3 d_{jh} d_{mk} \theta'_{jm}$$

This strain is to be added to that due to X_k at zero field, giving for the total strain component of type x_h at constant displacement the expression

$$x_h = -s^D_{hk} X_k = -X_k (s^E_{hk} - 4\pi \sum_j^3 \sum_m^3 d_{jh} d_{mk} \theta'_{jm}) \tag{268}$$

Hence,
$$s^D_{hk} = s^E_{hk} - 4\pi \sum_j^3 \sum_m^3 d_{jh} d_{mk} \theta'_{jm} \tag{269}$$

An analogous expression for c^D_{hk} is found by starting with the strain x_k given, in which case we use θ'' to represent the dielectric impermeability of a *clamped* crystal:

$$c^D_{hk} = c^E_{hk} + 4\pi \sum_j^3 \sum_m^3 e_{jh} e_{mk} \theta''_{jm} \tag{270}$$

If the crystal has no dielectric cross constants, all θ_{jm} vanish except those for which $j = m$. Then, as in the analogous case of the susceptibilities (§106), $\theta_{mm} = 1/k_m$, so that

$$s^D_{hk} = s^E_{hk} - 4\pi \sum_m^3 \frac{d_{mh} d_{mk}}{k'_m} \qquad c^D_{hk} = c^E_{hk} + 4\pi \sum_m^3 \frac{e_{mh} e_{mk}}{k''_m} \tag{271}$$

Finally, if the only component of displacement is that in the m-direction,

$$s^D_{hk} = s^E_{hk} - \frac{4\pi d_{mh} d_{mk}}{k'_m}, \qquad c^D_{hk} = c^E_{hk} + \frac{4\pi e_{mh} e_{mk}}{k''_m} \tag{271a}$$

207. *Elastic Coefficients at Constant Normal Displacement.* These are the effective constants for a resonator in thickness vibration with infinite

gap. From §199 it follows that, as the gap approaches infinity, the component of displacement normal to the plate, which will be called D^*, approaches zero at all points in the crystal (thin bar or plate) and at every instant during the cycle. The vanishing of D^* in the crystal is brought about by the fact that the piezoelectric polarization due to the strain gives rise to polarization charges, from which all lines of force turn back through the crystal, producing a depolarizing field of the right magnitude to make the normal displacement zero both inside and outside the crystal. Whatever the strain may be, there is no polarization charge "free" (as there is when the gap $w < \infty$) to send lines of force across toward the electrodes. For this reason Mason[B35,340] uses the superscript Q to designate the elastic coefficients at "constant charge," when the gap is infinite. We shall follow Lawson[313] in writing s^*_{hk} and c^*_{hk} for the elastic constants at infinite gap, corresponding to constant (usually zero) D^*. The significance of c^*_{hh} as the effective stiffness in thickness vibrations is treated in §§248 and 253.

For c^*_{hk} we seek the total stress X_h corresponding to a given strain x_k. Letting the thickness direction be m, we are concerned only with the polarization component $P_m = e_{mk}x_k$. P_m causes a depolarizing field $E'_m = -4\pi P_m/k''_m = -4\pi e_{mk}x_k/k''_m$, and E'_m gives rise to a stress component $X'_h = -e_{mh}E'_m = 4\pi e_{mk}e_{mh}x_k/k''_m$. k''_m is the clamped dielectric constant (see §204). X'_h tends to diminish x_k; hence, to hold x_k constant, we must write

$$X_h = -c^E_{hk}x_k - \frac{4\pi e_{mk}e_{mh}}{k''_m}x_k \equiv -c^*_{hk}x_k$$

where

$$c^*_{hk} = c^E_{hk} + \frac{4\pi e_{mk}e_{mh}}{k''_m} \tag{272}$$

It may be noted that if $h \neq k$ and if e_{mk} and e_{hk} have opposite signs, c^*_{hk} is numerically smaller than c^E_{hk}.

When $h = k$, we find

$$c^*_{hh} = c^E_{hh} + \frac{4\pi e^2_{mh}}{k''_m} \tag{272a}$$

For the application of this equation to thickness vibrations see §250.

By an analogous method one finds, for the compliance coefficient (for k'_m see §204),

$$s^*_{hk} = s^E_{hk} - \frac{4\pi d_{mk}d_{mh}}{k'_m} \tag{273}$$

When $h = k$, this expression becomes

$$s^*_{hh} = s^E_{hh} - \frac{4\pi d^2_{mh}}{k'_m} \tag{273a}$$

Equations (273) and (273a) are identical with (298a) and (298) when in the latter equations the gap w becomes infinite. c^*_{hk} and s^*_{hk} are identical with c^D_{hk} and s^D_{hk} in the special case where the piezoelectric polarization is parallel to the thickness, and there are no cross constants. This statement can be verified by letting m have a single value in Eqs. (269) and (270), with $j = m$.

When the foregoing equations are applied to an oblique bar or plate, all symbols for physical quantities are to be primed. For example, Eq. (272) becomes $c'^*_{hh} = c'^E_{hh} + 4\pi e'^2_{mh}/(k''_m)'$, where, as in the most general case of thickness vibrations, h may specify a direction that is oblique with respect to the rotated axes, while m specifies the direction normal to the plate. This fact leads to a complicated expression for the effective e'_{mh} [see Eq. (344), page 311]. Fortunately, for most oblique cuts in common use h lies in the plane of the plate, at right angles to m, so that the transformation equations for the piezoelectric constant given in Chaps. VIII and IX can be used directly.

It is important to consider whether the elastic coefficients at constant normal displacement constitute a transformable tensor system. For example, one may ask whether it is correct, for rotation of a Y-cut Rochelle-salt plate about the X-axis, to write according to Eq. (40)

$$c'^*_{66} = c^*_{66} \cos^2 \theta + c^*_{55} \sin^2 \theta \tag{274}$$

The answer is yes, provided that c'^*_{66}, c^*_{66}, and c^*_{55} are all at constant displacement with respect to a field *making the same angle θ with the Y-axis.* This condition would require special expressions for c^*_{66} and c^*_{55}, and these expressions would vary with θ. No fixed values independent of θ can be assigned to c^*_{66} and c^*_{55} such that these quantities can be used in equations for rotated axes. The same is true of all the other stiffness and compliance constants that involve a piezoelectric term.

From what has been said it is evident that it is impossible to derive a set of single-valued elastic constants c^*_{hh} from observations of the frequency of thickness vibrations of plates cut in different orientations and driven by means of remote electrodes (as in Mason's experiments with Rochelle salt, described in §77), unless suitable piezoelectric corrections are applied, and even then each c^*_{hh} would have a value depending on whether the field direction m in Eq. (272a) was parallel to X, to Y, or to Z. Observations made with a wide gap can be used to determine the *isagric* constants by one of the methods described in §252; for the reduction of such observations the formulas in this chapter are suitable.

208. *Elastic Coefficients at Constant Polarization.* The derivation is exactly similar to that in §206, using P_m instead of D_m, and $E_j = \sum_m^3 \chi'_{jm} P'_m$ from Eq. (143). The result is

$$s^P_{hk} = s^E_{hk} - \sum_j^3 \sum_m^3 d_{jm} d_{mk} \chi'_{jm} \tag{275}$$

$$c^P_{hk} = c^E_{hk} + \sum_j^3 \sum_m^3 e_{jm} e_{mk} \chi''_{jm} \tag{276}$$

Corresponding to Eqs. (271*a*) one has, for a single direction $j = m$,

$$s^P_{hk} = s^E_{hk} - \frac{d_{mh} d_{mk}}{\eta'_m} \tag{277}$$

$$c^P_{hk} = c^E_{hk} + \frac{e_{mh} e_{mk}}{\eta''_m} \tag{278}$$

If $h = k$, these equations reduce to

$$s^P_{kk} = s^E_{kk} - \frac{d^2_{mk}}{\eta'_m} \qquad c^P_{kk} = c^E_{kk} + \frac{e^2_{mk}}{\eta''_m} \tag{279}$$

The constant-polarization coefficients in terms of those at constant normal displacement. From Eqs. (272), (273), (277), and (278),

$$s^P_{hk} = s^*_{hk} - \frac{d_{mh} d_{mk}}{k'_m \eta'_m} \qquad c^P_{hk} = c^*_{hk} + \frac{e_{mh} e_{mk}}{k'_m \eta'_m} \tag{280}$$

The two terms on the right in such equations as (273) or (277) correspond, respectively, to the arrows $X \to x$ and $X \to P \to E \to x$ in Fig. 48. The latter path indicates the process of piezoelectric reaction mentioned at the end of §202. There is an obvious analogy between the effect of piezoelectric reactions on the *elastic* compliance in (273) or (277) and its effect on the *dielectric* compliance (susceptibility) expressed in Eq. (262). In each case there is a term arising from the combined action of the direct and converse piezoelectric effects. The influence of a depolarizing field on the elastic constants is analogous to that of mechanical constraint on the dielectric constants. In the first case the crystal becomes stiffer mechanically; in the second case it becomes stiffer electrically.

A crystal of large k is electrically soft, just as large s means mechanical softness.

209. *An Important Special Case.* If the deformation is of the type L or S in Fig. 15, so that $h = k$, and if the piezoelectric class is such that Eq. (191*a*) has but a single term, with $i = h$, then $d_{mh} = d_{mk} = e_{mh} s^E_{hh}$ and, from Eq. (191), $e_{mh} = d_{mh} c^E_{hh}$. Hence $c^E_{hh} = 1/s^E_{hh}$, and Eq. (271) reduces to

$$s^D_{hh} = s^E_{hh} \left(\frac{k'_m - 4\pi d_{mh} e_{mh}}{k'_m} \right)$$

Hence, from Eq. (265), we find

$$\frac{s^D_{hh}}{s^E_{hh}} = \frac{c^E_{hh}}{c^D_{hh}} = \frac{k''_m}{k'_m} \tag{281}$$

Under the same conditions and by use of Eqs. (277) and (262), we obtain

$$\frac{s^P_{hh}}{s^E_{hh}} = \frac{c^E_{hh}}{c^P_{hh}} = \frac{\eta''_m}{\eta'_m} \tag{282}$$

210. *Relations between the Elastic Coefficients According to the Polarization Theory.* All the foregoing expressions can be written in terms of the polarization theory, by applying the same reasoning to the equations in §192. Only the following need be given here:

$$s^E_{hk} = s^P_{hk}\left(1 + \sum_m^3 \sum_j^3 a_{mk} b_{jk} \eta'_{mj}\right) \tag{283}$$

Equations (521) and (521*a*), specialized for Rochelle salt, can be derived from Eq. (283).

211. *Specialization to Rochelle Salt and Quartz.* In later chapters we shall have to do with Rochelle-salt X-cut plates subjected to a stress Y_x, producing a strain $y_x = -s_{44}Y_x$. It is therefore of interest at this point to compare the values of s^E_{44}, s^P_{44}, and s^D_{44} for this crystal. A similar comparison will also be made for s_{11} in quartz.*

For Rochelle salt, one finds, from Eqs. (271) and (279),

$$s^D_{44} = s^E_{44} - \frac{4\pi d^2_{14}}{k'_x} \qquad s^P_{44} = s^E_{44} - \frac{d^2_{14}}{\eta'_x} \tag{284}$$

That these two values are practically identical is seen by writing

$$s^D_{44} - s^P_{44} = 4\pi d^2_{14}\left(\frac{1}{4\pi\eta'_x} - \frac{1}{k'_x}\right) = \frac{d^2_{14}}{\eta'_x k'_x} \tag{284a}$$

At all temperatures this difference is of the order of $0.03(10^{-12})$, as may be verified from Figs. 145 and 146. Since s^P_{44} is of the order of 10^{-11}, it is evident that s^D_{44} does not differ from s^P_{44} by more than about 0.35 per cent, an amount too small to distinguish experimentally. It is this fact which justifies us in accepting for $c^P_{44} = 1/s^P_{44}$, in §79, the value derived from observations on an *isolated* crystal. On the other hand, the difference $s^D_{44} - s^E_{44} (\approx s^P_{44} - s^E_{44})$ is very large, as may be seen by substituting values from Figs. 145 and 146 in Eq. (279) or (283). For Rochelle salt, Eq. (283) reduces to $s^E_{44} = s^P_{44}(1 + a_{14}b_{14}\eta'_x)$. The smallest value of s^E_{44}, at 47.5°C, is greater than s^P_{44} by a factor of 1.35, and it approaches infinity (for small stresses) at the Curie points.

Following is the relation between c^D_{44} and c^P_{44} for Rochelle salt according to the polarization theory:

$$c^D_{44} = c^P_{44} - \frac{a^2_{14}\eta''_x}{k''_x} \tag{285}$$

* For the cases considered here the constant-displacement values are the same as those at constant *normal* displacement, according to §207.

where η_x'' and k_x'' are the values for a clamped crystal. Similarly,

$$c_{55}^D = c_{55}^P - (a_{25}^2\eta_y''/k_y''),$$

and $c_{66}^D = c_{66}^P - (a_{36}^2\eta_z''/k_z'')$.

In *quartz*, the piezoelectric effect is so small that s_{11}^E, s_{11}^D, and s_{11}^P are identical within about 1 per cent. Thus, from Eqs. (271*a*), s_{11}^D is about 1.03 per cent less than s_{11}^E, and c_{11}^D is 0.87 per cent greater than c_{11}^E. On the other hand, owing to the low diclectric constant of quartz, the difference $s_{11}^D - s_{11}^P$ is not, as with Rochelle salt, negligible in comparison with $s_{11}^D - s_{11}^E$. That is, to the degree of precision attainable in quartz, the compliance at constant polarization cannot be regarded as practically identical with that at constant displacement (isolated crystal). This fact is, however, of little practical consequence, since the equations of the polarization theory are not commonly applied to quartz.

Neglecting edge effects, it follows from §199 that for an X-cut Rochelle-salt plate the coefficient s_{44}^E is observed when the gap w is zero, while s_{44}^D is observed when the plate is isolated ($w = \infty$). The fact that s_{44}^P is practically identical with s_{44}^D is a consequence of the large value of k_x, which causes the depolarization to be practically complete when $w = \infty$. How nearly complete the depolarization is can be seen from Eq. (294), according to which the net polarization in an isolated stressed plate is only $1/k_x'$ of the full value attained when $w = 0$.

212. Illustrations of Piezoelectric Reactions. As a background for the treatment of various piezoelectric applications in later chapters, the secondary effects present in some special cases will now be considered. As before, we have to do with a flat plate of relatively large area. If the electrodes are parallel to the plate, the field is normal to the plate, *i.e.*, parallel to the thickness dimension e, which we have assumed to be in the m-direction. In general, the polarization is not parallel to e, partly because the material is anisotropic with dielectric cross constants k_{ij} [$i \neq j$, Eq. (141), page 162] and partly because any mechanical stress causes a piezoelectric polarization with components perpendicular to e. As a first approximation we regard the area of the plate as infinite, so that the lateral components of polarization can be ignored. Throughout the present discussion we need consider only the component P_m.

Inside the plate the field is E_m; outside, where the medium has a dielectric constant $k^\circ = 1$, the field is E_m°. Then, if σ is the surface density of any true charges (*i.e.*, other than polarization charges) that may be on the surfaces and P_m is the polarization in the plate, including that of piezoelectric origin as well as that due to E_m, one may write the general equation

$$E_m = E_m^\circ - 4\pi P_m - 4\pi\sigma \tag{286}$$

The sign of σ is to be taken as that on the face toward the positive direction of the m-axis. The free charges may be upon metallic electrodes in contact with the plate, or they may be compensating charges resulting from surface or body leakage.

If now a stress X_k is impressed, while the crystal is still free to deform itself in the field, the value of P_m from Eq. (263) may be substituted, giving

$$\begin{aligned} E_m &= E_m^\circ - 4\pi(\eta'_m E_m - d_{mk}X_k) - 4\pi\sigma \\ &= \frac{1}{k'_m}(E_m^\circ + 4\pi d_{mk}X_k - 4\pi\sigma) \end{aligned} \tag{287}$$

Throughout this chapter all elastic constants, unless otherwise specified, have the *constant-field values.*

213. CASE I. Plate of thickness e in contact with electrodes on which a *stress* X_k *and a potential difference* $V = eE_m$ are impressed. In Eq. (287) the field E_m° outside the electrodes has no effect on the conditions between them, so that the charge density on the electrodes becomes*

$$\sigma = -\frac{k'_m E_m}{4\pi} + d_{mk}X_k \tag{288}$$

The strain is

$$x_k = \frac{d_{mk}V}{e} - s_{kk}^E X_k \tag{289}$$

The polarization remains as in Eq. (263). The strain x_k caused by X_k can be reduced to zero by applying a field

$$E_m = \frac{s_{kk}^E}{d_{mk}} X_k \tag{290}$$

This field depends *inversely* on the piezoelectric strain constant, while by Eq. (263) the field necessary to reduce the *polarization* to zero depends *directly* on this constant.

If there is no external stress, the crystal is *mechanically free* and behaves as a dielectric with

$$\sigma = -\frac{k'_m E_m}{4\pi} \qquad \text{and} \qquad P_m = \eta'_m E_m$$

For a *clamped* plate the polarization, from Eqs. (264) and (266), is

$$P_m = \eta''_m E_m = E_m(\eta'_m - \sum_i^6 e_{mi}d_{mi}) \tag{291}$$

If $E_m = 0$ (electrodes short-circuited), then under an impressed X_k we have simply, from (263), (288), and (289), $\sigma = d_{mk}X_k$, $P_m = -d_{mk}X_k$, and $x_k = -s_{kk}^E X_k$. This is the special case in which the fundamental piezoelectric polarization equation holds without modification.†

* *Cf.* VOIGT, p. 918, Eq. (298).

† VOIGT, p. 919.

214. CASE II. Like Case I, only the electrodes are separated by a distance $e + w$, leaving a total gap w (which may be divided between the two sides) between crystal and electrodes. As before, both lateral dimensions are assumed to be large in comparison with the thickness. In Eq. (287) the free charge $\sigma = 0$, and both E_m and E_m° are dependent in part upon V and in part upon the surface polarization charges due to x_k or X_k. The quantity $e + k'_m w$, which, as in §110, may be regarded as the *electrical distance* between the electrodes, will be denoted by the symbol e'.

The treatment of the problem is slightly different according to whether there is impressed on the crystal a single *stress* X_k, as in Case I, or a single *strain* x_k. As we shall see in §244, the assumption that the *stress* is given lends itself most conveniently to the solution of the problem of the *bar* vibrating lengthwise, while for thickness vibrations of a *plate*, owing to the presence of lateral constraints, there is but a single *strain* to consider.

a. A single extensional stress X_k is impressed upon an elongated plate or bar whose relatively small thickness dimension is in the direction m. The only strain that concerns us is x_k, extensional, in the direction of the length of the bar. The electric field is in the m-direction. For example, with a quartz X-cut bar having its length parallel to the Y-axis, the subscript $k = 2$, $X_k = Y_y$, $x_k = y_y$, and the electric field is parallel to X, so that $m = 1$.

We seek an expression for the *effective elastic compliance* of the crystal in a gap. From Eqs. (164*a*) and (163*b*) the total field in the crystal, including the contributions due to V and X_k, is

$$E_m = \frac{V}{e'} - \frac{4\pi w(P_m)}{e'} = \frac{V}{e'} + \frac{4\pi w d_{mk} X_k}{e'} \tag{292}$$

where $(P_m) = -d_{mk}X_k$. By substituting this value of E_m in Eq. (287) and setting $\sigma = 0$, we find for the field in the gap

$$E_m^\circ = \frac{k'_m V}{e'} + \frac{4\pi c(P_m)}{e'} = \frac{k'_m V}{e'} - \frac{4\pi e d_{mk} X_k}{e'} \tag{293}$$

The second term on the right in Eq. (292) is the *depolarizing field.* As w increases, the depolarizing field becomes greater, approaching as a limit the value given below for $w \to \infty$.

When $w \to 0$, Eqs. (292) and (293) are both reduced to (286). In the crystal the field is simply V/e, while in the (infinitesimal) gap it is $k'V/e - 4\pi d_{mk}X_k$.

When $w \to \infty$ while V remains finite, $E_m \to 4\pi d_{mk}X_k/k'_m$, and $E_m^\circ \to 0$. This is the case for a stressed crystal completely isolated in space. It is easily proved that the principle of continuity of displacement is satisfied, the displacement approaching zero inside as well as outside the crystal.

Nevertheless, the polarization does not then approach zero. Its value at infinite gap is*

$$P_m^{\infty} = -d_{mk}X_k + \eta'_m E_m = -\frac{d_{mk}X_k}{k'_m} \tag{294}$$

or only $1/k'_m$ of the value when $w = 0$ and $V = 0$, as given at the end of Case I. The analogy with the effect of magnetic depolarization upon a magnetic shell is obvious.

In Eqs. (288) and (289) of the "Lehrbuch," Voigt treats the case in which the crystal is placed in an external field of constant value E_m°. His results, represented in Eqs. (295) and (296) with appropriate changes in subscripts and on the assumption that the surrounding medium has a dielectric constant of unity, can be derived from Eqs. (292) to (294). The crystal plate may be considered as in a very wide gap, with V large enough to produce an arbitrary E_m°. It is then easily proved that

$$E_m = \frac{E_m^{\circ}}{k'_m} + \frac{4\pi d_{mk}X_k}{k'_m} \tag{295}$$

$$P_m = \frac{l}{k'_m}(\eta' E_m^{\circ} - d_{mk}X_k) \tag{296}$$

When X_k is constant, we see that the crystal behaves, with respect to variations in E_m°, like an ordinary dielectric with dielectric constant k'_m.

We return to the case where w is finite. The total strain component x_k is due in part to the two field constituents in Eq. (292). With the aid of Eq. (184) one finds

$$x_k = \frac{d_{mk}V}{e'} + \frac{4\pi w d_{mk}^2 X_k}{e'} - s_{kk}^E X_k \tag{297}$$

If, as is usually the case, V is independent of x_k, the *effective compliance of a crystal with gap w*, when a stress X_k is applied, may be written as

$$s_{kk}^w = -\frac{\partial x_k}{\partial X_k} = s_{kk}^E - \frac{4\pi d_{mk}^2 w}{e'} \tag{298}$$

Similarly, one can derive the more general equation

$$s_{hk}^w = -\frac{\partial x_h}{\partial X_k} = s_{hk}^E - \frac{4\pi d_{mk}d_{mh}w}{e'} \tag{298a}$$

When the gap is infinite, the last two equations became identical with Eqs. (273*a*) and (273), since the only depolarizing field is parallel to the thickness of the bar.

* "Lehrbuch," p. 917, Eq. (291).

These equations show how the compliance departs from the isagric value when there is a gap. For example, if $w = 0$ or if the crystal has no d_{mk}, $s^w_{kk} = s^E_{kk}$. As the gap increases, then if $d_{mk} \neq 0$, the compliance goes down, and, in the case of a resonator, the natural frequency increases. As the gap becomes indefinitely large, s^w_{kk} approaches the value given by Eq. (273*a*). This condition may be very approximately realized when w is still of the order of magnitude of e. Analogous equations may be derived for the other compliance coefficients. When $w = 0$, Case II reduces to Case I.

215. CASE II*b*. A thin plate of infinite extent, with thickness e in the m-direction, is subject to a *single extensional strain* x_m. This situation will be encountered in the theory of thickness vibrations (§243). Here we consider only the static case, where x_m is uniform throughout the plate. As in (*a*), the plate lies between parallel electrodes, with a gap w. A potential difference V is impressed on the electrodes, causing a contribution to the field in the m-direction in the crystal, of magnitude

$$E_m = \frac{V}{e''}$$

where

$$e'' \equiv e + k''_m w \tag{299}$$

The clamped dielectric constant k''_m is used here, in accordance with §104, because the *strain* is prescribed.

As in Eq. (292), there exists also in the crystal a depolarizing field due to the strain x_m, of value $-4\pi w(P_m)/e''$, where now $(P_m) = e_{mm}x_m$. Hence the total field in the crystal is

$$E_m = \frac{V}{e''} - \frac{4\pi w(P_m)}{e''} = \frac{V}{e''} - \frac{4\pi w e_{mm} x_m}{e''}$$

The stress X_m required to produce the prescribed x_m when V is given is the sum of two constituents, one of which is that due to E_m, while the other is that causing x_m at zero field. That is,

$$X_m = e_{mm}E_m - c^E_{mm}x_m = \frac{e_{mm}V}{e''} - \left(\frac{4\pi w e^2_{mm}}{e''} + c^E_{mm}\right)x_m \tag{300}$$

The *effective stiffness* of a crystal of infinite area, thickness e, and gap w, under a static pressure, is therefore

$$c^w_{mm} = c^E_{mm} + \frac{4\pi w e^2_{mm}}{e''} \tag{301}$$

When $w = \infty$, this equation becomes identical with Eq. (272*a*) (setting $k = m$), since, as $w \to \infty$, $w/e' = w/(e + k''_m w) \to 1/k''_m$.

216. CASE III. Crystal of any form, *completely clamped*, with field E_h impressed. A system of external mechanical stresses is applied, such

that each of the components of stress $X_k = -e_{hk}E_h$ is neutralized by a stress $-X_k$, reducing the strain to zero. This does not reduce the *polarization* to zero, for a polarization $P_h = \eta''_h E_h$ still persists. For all crystal classes with which we are concerned, there are no polarization components other than P_h for a given E_h, so long as E_h is parallel to one of the three orthogonal crystal axes. For the general case, the components of P are given by Eq. (140) [see also Eq. (154)].

217. CASE IV. Equation (292) may be used to derive the field and resultant polarization in a *stressed crystal having adherent electrodes connected to an external capacitance*, as, for example, an electrometer or the deflecting plates of an oscillograph. It is necessary only to set $V = 0$ and to replace the capacitance of the gap $C_w = A/4\pi w$ (see Case II above) by the external capacitance C. A is here the area of the crystal, and for the capacitance of the crystal we have $C_e = k'_h A/4\pi e$. From these two equations it follows that $w/e' = C_e/k'_h(C_e + C_w)$, whence from (292) we have

$$E_h = \frac{4\pi d_{hk} X_k}{k'_h} \cdot \frac{C_e}{C_e + C} \tag{302}$$

The resultant polarization is $-d_{hk}X_k + \eta'_h E_h$, or

$$P_h = -d_{hk}X_k \left(1 - \frac{4\pi\eta'_h}{k'_h} \cdot \frac{C_e}{C_e + C}\right) \tag{303}$$

When $C = 0$, Eq. (303) reduces to (294); when $C = \infty$, it becomes the fundamental equation (c') in Table XXI.

218. CASE V. Crystal plate of large area A having adherent electrodes on which *fixed charges* $\pm Q$ are placed. The charge density is $\sigma = Q/A$. If the plate is clamped, the field strength is $E_1 = -4\pi\sigma/k''$ (specific subscripts are here unnecessary). When the plate is released, the field becomes reduced to $E_2 = -4\pi\sigma/k' = -4\pi\sigma/(k'' + 4\pi\Sigma ed)$ [*cf.* Eq. (265)]. We may say that the reduction in field strength is due to the increase in the effective dielectric constant. It would be equally correct to say that it is due to an *induced counter-field*, proportional to the strain, of amount $E' = (4\pi\sigma/k'')(4\pi\Sigma ed/k')$, a relation that is easily verified.

The foregoing paragraphs contain many instances of the piezoelectric analogy to Lenz's law, which, as commonly understood, may be expressed by saying that an induced current flows in such a direction as to oppose the cause that produced it, the amount of reaction depending upon the resistance of the electric circuit. In the case of the piezoelectric effect the statement is as follows: A piezoelectrically induced field has such a direction as to oppose the stress that produced it, the amount of reaction depending upon the freedom of the crystal from mechanical constraint.

219. Numerical Examples. The magnitude of the secondary effects will now be illustrated, quartz being taken as an example of relatively low piezoelectricity and Rochelle salt as the most strongly piezoelectric substance known. In each case an X-cut plate of large area is considered, the electric field and polarization being in the X-direction. The values of d_{14}, s^E_{44}, and k'_x for Rochelle salt are taken from Figs. 145 and 146 at 5°C and are typical for small electric and elastic stresses. The figures for larger stresses near a Curie point would give a still more striking contrast with quartz. The symbol Σed signifies the summation $\sum_h^6 e_{1h}d_{1h}$, which for quartz is $2e_{11}d_{11} + e_{14}d_{14}$[Eq. (213)], while for Rochelle salt it is simply $e_{14}d_{14}$.

Quantity	Quartz	Rochelle salt
d	$d_{11} = 6.9(10^{-8})$	$d_{14} = 10.4(10^{-6})$
e	$e_{11} = 5.2(10^4)$	$e_{14} = \dfrac{d_{14}}{s_{44}} = 65(10^4)$
s^E	$s^E_{11} = 1.30(10^{-12})$	$s^E_{44} = 16(10^{-12})$
Σed	0.0069	6.75
k'_x	4.5	190
η_x	0.282	15
$\eta_{x''}$	0.276	8.2
k''_x	4.46	104
s^D	$s^D_{11} = 1.29(10^{-12})$ $= 0.992s^E_{11}$	$s^D_{44} = 8.8(10^{-12})$ $= 0.55s^E_{44}$

The table shows clearly how little influence the piezoelectric effect has on the dielectric constant and compliance of quartz as compared with Rochelle salt. Consider, for example, the effect of clamping on the dielectric constant. In quartz, k''_x is about 2 per cent less than k'_x, while in Rochelle salt, for the example cited, k''_x is only about half as large as k'_x. If the field in Rochelle salt were such as to bring the polarization to the knee of the P:E curve, then between the Curie points k''_x would be but a small fraction of k'_x.

220. Piezoelectric Reaction on Elastic Cycles. It is helpful to an understanding of piezoelectric reactions to consider the energy expended electrically when a piezoelectric crystal is put through a cycle of stress and release, even though experimental data are lacking. We shall here treat the problem as static rather than vibrational and assume, to fix the ideas, that we have an m-cut plate with electrodes covering its opposite faces, the electrodes being either left insulated or connected through a resistance R. Energy lost through internal mechanical friction may be ignored. A uniform stress X_k is applied, where k may be identical with m. The piezoelectric polarization is $P_m = -d_{mk}X_k$.

If the electrodes are insulated ($R = \infty$) and there is no external field, the strain x_k is given by Eq. (268),

$$x_k = -s^D_{kk}X_k \tag{304}$$

where, by Eq. (271),

$$s^D_{kk} = s^E_{kk} - \frac{4\pi d^2_{mk}}{k'_m} \tag{304a}$$

For the field due to P_m we have

$$E_m = \frac{4\pi d_{mk}X_k}{k'_m} \tag{304b}$$

It is this depolarizing field that is responsible for the second term in (304a).

When the electrodes are connected through a resistance, unless the resistance is extremely great, the depolarizing field E_h will disappear within a short time after the application of X_k. We have then the case represented in Eq. (289) when $V = 0$:

$$x_k = -s^E_{kk} X_k \tag{304c}$$

For simplicity we now drop the subscripts k and h and write $s' = s'^D_{kk}$, $s_o = s^E_{kk}$, $x' = -s'X$, $x_o = -s_o X$, $E = 4\pi\delta X/k$, and $s' = s_o - 4\pi\delta^2/k$.

When X is applied, the energy expended is, for electrodes insulated ($R = \infty$),

$$W_i = -\tfrac{1}{2}x'X = \tfrac{1}{2}s'X^2 = \tfrac{1}{2}X^2\left(s_0 - \frac{4\pi\delta^2}{k}\right) \tag{304d}$$

and, for short-circuited electrodes ($R = 0$),

$$W_0 = -\tfrac{1}{2}x_0 X = \tfrac{1}{2}s_0 X^2 \tag{304e}$$

In neither of these processes is there any loss of energy. In the case of W_i there is a storage of both elastic and electrical energy in the stressed plate, all of which is returned when X is removed. In the case of W_0 a current flows without loss of energy, since $R = 0$ and the electrodes are at all times at the same potential.

The two processes are illustrated in Fig. 49, in which, for clarity, the ratio x_0/x' is greatly exaggerated. The lines OA and OB correspond, respectively, to Eqs. (304*d*) and (304*e*), the energies being given by the areas of the triangles OAX and OBX. For the electrostatic energy when $R = \infty$ one finds, from Eq. (304*b*),

$$W_e = \frac{kE^2}{8\pi} = \frac{2\pi\delta^2 X^2}{k} \tag{304f}$$

Since this is identical with the second term on the right in (304*d*), it follows that the energy stored electrically when $R = \infty$ is the same as the excess of W_0 over W_i. This excess is represented by the area of the triangle OBA.

After the point A has been reached upon applying the stress while $R = \infty$, if the electrodes are connected through a finite resistance R, the additional work in passing from A to B depends upon R. If $R = 0$ and if the circuit is non-inductive, the discharge and consequent relaxation of the plate are instantaneous, so that the stress drops at once to zero (point x' in Fig. 49). If the stress is applied again in such a manner that its relation to the additional strain $x_0 - x'$ is linear, the line $x'B$ results, and the additional work done is the area of the triangle $x'BA$. But this equals the area OBA, which has been proved to represent the energy W_e. Thus in this special case, and then only, the total work done is the same as if the crystal had been short-circuited from the start.

For any value of R greater than zero, a further increment of work is necessary to compensate for the loss $\int i^2 R\, dt$ in the circuit. As R increases, the loss rises from zero to a certain extreme value, which is attained when R is so great, and hence the rate of relaxation so slow, that the full stress X is applied during the entire increase in strain from x' to x_0. The additional work is then $-(x_0 - x')X$, and this, by Eqs. (304*d*) to (304*f*), is just twice W_e, being represented by the rectangle $x'x_0BA$.

From these considerations it is a natural step to the construction of the ideal cycle of operations represented by the parallelogram $OABC$ in Fig. 49. Along OA mechanical stress is applied while $R = \infty$; along AB the electrodes are connected through a high resistance; $R = \infty$ again along BC while the stress is removed; and finally a

resistance is connected, allowing the crystal to return along CO to its unstrained state. The total loss in energy is $2W_e$, the area of the parallelogram. The points of analogy with the Carnot cycle—as well as the essential differences—are sufficiently obvious.

Similarly, a hysteresis loop can be constructed for the case in which an alternating stress is applied to a crystal having electrodes connected through a constant resistance.

The analogous problem of the energy losses when an *electric* stress is applied to the crystal by connecting the electrodes to a battery suggests itself. Corresponding to

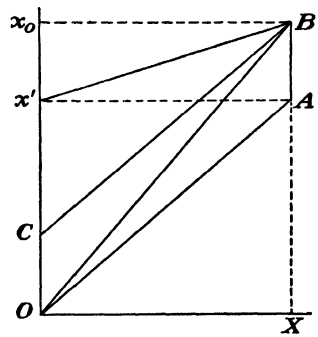


FIG. 49.—Relation between stress and strain for a piezoelectric crystal.

the insulated and short-circuited states in the foregoing treatment are, according to §199, the mechanically clamped and free states. Cycles similar to those described above can be drawn, the coordinates being polarization and field strength. The energy that disappears is accounted for partly by dielectric losses and partly by internal friction in the crystal and in the external system that controls the clamping. Examples of this sort will be found in Chaps. XXII and XXIII.

In order to illustrate Lippmann's theorem, Poynting and Thomson* discuss a piezoelectric cycle of a form somewhat analogous to Fig. 49.

* Ref. B42, p. 157.

CHAPTER XIII

THE PIEZOELECTRIC RESONATOR

They gather also peerles by the sea side, and Diamondes and Carbuncles vpon certein rockes; and yet they seke not for them; but by chaunce finding them they cutt and polish them. —Sir Thomas More.

221. Introduction. In the most general sense, a piezoelectric resonator, or piezo resonator, is an elastic solid body consisting partly at least of piezoelectric crystalline material, capable of being excited to resonant vibration by an alternating electric field of the proper frequency. In its simplest form it is a single piece of crystal, usually cut to a prescribed size, shape, and orientation, but even a rough fragment or an entire crystal can be made to resonate. When one or more pieces of piezoelectric crystal are cemented to non-piezoelectric material, for example a metal bar or plate, usually for the purpose of obtaining resonance at relatively low frequency, we have a *composite* resonator. The field is applied by means of electrodes, so situated that the field will be in the proper direction to excite the desired mode of vibration. With all types of resonator, the electrodes may be separated from the crystal by gaps, or they may be attached directly to the crystal.

The electric field drives the resonator through the action of the *converse* piezoelectric effect. When the crystal vibrates, the periodic deformation causes periodic piezoelectric charges on the electrodes, through the *direct effect*, that react on the driving circuit. It is this reaction, present only when the resonator is vibrating, that gives the device its greatest usefulness.

The cooperation of the direct and converse effects has an analogy in the electric motor, which is driven by an electric current and which when running develops a counter emf that reacts on the driving circuit. The analogy with the synchronous motor is especially close, since here, as in the crystal, both the amount and the phase of the reaction have to be considered. Where the analogy breaks down is in the fact that the crystal, unlike the synchronous motor, can be "driven" to an appreciable extent only at or near a definite frequency.* The phase relation in the case of the synchronous motor depends on the load. With the piezo

* In most cases, as the applied frequency is varied, resonance occurs at a large number of distinct frequencies, depending on the possible vibrational modes that can be excited by a field in the given direction. The frequency corresponding to any one of these modes may be taken as the "definite frequency."

resonator the load usually includes only the losses in the resonator itself. Considered as a motor, the resonator "idles." The phase angle between resonator-reaction and applied emf is determined by the difference between the driving frequency and the natural frequency of the resonator, and at a given frequency it depends also on the losses.

The piezo resonator may also be thought of as a *vibrating condenser.* At very low frequencies, including zero, it behaves as a pure capacitance, at least for most crystals now in practical use, since in them the dielectric losses at low frequency are negligible. There is, of course, some piezoelectric deformation even in a l-f field, but it is insignificant in comparison with the deformation near resonance. That is, the resonator, like all other vibrating systems, is in a state of *forced* vibration at all frequencies of the driving force. As the applied frequency is increased until the value corresponding to the lowest natural mode of the resonator is approached, the amplitude of the deformation increases, passes through a maximum at a certain frequency, and then decreases. With further increase in frequency a whole spectrum of maxima of various heights is encountered, corresponding to various vibrational modes and their overtones, up to frequency values many times greater than that of the first maximum.

The mechanical vibrations in the neighborhood of a resonant frequency depend on the inertia, elastic compliance, and damping losses of the vibrating crystal. Similarly, its electric reaction on any electric circuit to which it is connected is the same as if the crystal were replaced by a certain "equivalent network," containing an inductance, capacitance, and resistance, corresponding to the mechanical inertia, compliance, and frictional resistance of the crystal and proportional to them.

From the engineering point of view, a piezoelectric resonator is an electromechanical *transducer.**

222. The usefulness of the piezo resonator in a wide range of practical application arises from its extremely sharp resonance, together with the lucky circumstance that crystals of convenient size can be made to resonate at frequencies over the entire range from 50 to $3(10^8)$ cycles per second; this is a range of over 20 octaves. Still higher resonant frequencies have been observed, but they do not yet seem to have reached the stage of practical application.

To these advantages should be added the fact that in quartz crystals we possess a piezoelectric material that combines almost ideal elastic qualities with great mechanical strength and durability. By the use of certain oblique cuts, quartz resonators for almost any frequency can be made with frequencies practically independent of temperature over a very broad temperature range.

* For a treatment of the piezoelectric transducer, both resonating and nonresonating, see ref. B35.

The most widely used resonators are in the form of rectangular parallelepipeds with the electric field in the thickness direction. If the slab is relatively long and narrow, it is called a *bar* or *rod* and is used mostly for *lengthwise* compressional vibrations of relatively low frequency. For a given crystal and orientation the fundamental frequency is inversely proportional to the length. *Plates* with both length and breadth large in comparison with the thickness are used in one of two ways. The first depends on the fact that certain cuts can be made to execute *thickness vibrations*, the resonant frequency being inversely proportional to the thickness; such resonators are used in the higher range of frequencies. Rectangular plates with breadth comparable with the length can also be made to vibrate in a shear mode, the shear taking place in the plane of the plate (*contour vibrations*). The frequency is of the same order of magnitude as that of a bar of length comparable with the length or breadth of the plate. The temperature coefficient of frequency practically vanishes over a very wide range of temperature in the case of properly oriented quartz plates vibrating in this mode.

223. Thus far we have spoken only of the piezo *resonator*, without mention of the piezo oscillator or of the piezo stabilizer. In general, every piezoelectric device that has a natural frequency and is not too highly damped, when vibrated electrically at or near this frequency, is a resonator. This statement is true even when the crystal controls the frequency, as in a piezo-oscillator circuit. In a more restricted sense it is sometimes called a "resonator" only when it does nothing but resonate. This condition is realized when it is so loosely coupled to the driving circuit that its reaction on the driver is negligible. Such circuits are used in studying the properties of the crystal, and to some extent in frequency measurement.

The term *piezo oscillator* is properly applied to an amplifying circuit that of itself is incapable of oscillating because of too little regeneration or an unfavorable phase angle, but that oscillates when a piezo resonator is inserted in it or is coupled to it, the frequency being determined by one of the vibrational modes of the resonator. Such a circuit is said to be *crystal controlled.*

Sometimes a piezo resonator is connected to a circuit that is capable of oscillating by itself, for the purpose of holding the frequency constant within narrower limits than would otherwise be possible. The circuit is then said to be *piezoelectrically stabilized* or *crystal stabilized*, and the resonator operates as a *crystal stabilizer.*

The present chapter has to do with the theory of piezo resonators consisting of bars in lengthwise vibration and plates in thickness vibration. It includes a discussion of the manner in which the dielectric constants of a piezoelectric crystal vary with frequency. At the

close is an account of the effect of piezoelectric vibrations on X-ray reflections.

Further properties of the resonator, including those of crystals vibrating in other modes, will be considered in later chapters, as well as the application of the theory to particular crystals, with some experimental results.

224. *Notes on the History of the Piezo Resonator.* The first to make an important application of piezoelectricity was P. Langevin, who, in the investigation of his quartz-metal "sandwich" described in §506, recognized the resonating properties as early as 1917. A. M. Nicolson described experiments on resonance in Rochelle-salt crystals in November, 1919, including observation of the effective series capacitance over a certain range in frequency and of the minimum in current at the resonant frequency. The publications of Langevin and of Nicolson say nothing concerning the fact that the reaction of the crystal on the circuit makes possible the application of the crystal, when vibrating in a normal mode, as a frequency standard, constant-frequency oscillator, or filter.

The author observed the minimum in capacitance together with the reaction of a Rochelle-salt plate on the driving circuit in August, 1918, and experimented with his first quartz resonator in January, 1919. In the succeeding months he investigated the properties and possible applications of the piezo resonator as well as methods of mounting the crystal plates. The first public account of the device was given to the American Physical Society on Feb. 26, 1921; on this occasion the uses of the resonator as a standard of frequency, as a filter, and as a coupling device between circuits were mentioned. At the meeting on Apr. 23, 1921, the piezoelectric stabilizer for h-f generating circuits was first publicly described; and on Dec. 28, 1921, came the first paper on the piezo oscillator, in which lengthwise vibrations of a quartz bar were used.

The various steps mentioned above are described in the following patents:

(*A*) P. Langevin, French patent 505,703, application Sept. 17, 1918, issued Aug. 5, 1920; also British patent 145,691 of July 28, 1921.

(*B*) P. Langevin, U. S. patent 2,248,870, application June 21, 1920, issued July 8, 1941.

(*C*) A. M. Nicolson, U. S. patent 1,495,429, application Apr. 10, 1918, issued May 27, 1924.

(*D*) A. M. Nicolson, U. S. patent 2,212,845, divisional application Apr. 13, 1923, based on the foregoing, issued Aug. 27, 1940.

(*E*) W. G. Cady, U. S. patent 1,450,246, application Jan. 28, 1920, issued Apr. 3, 1923.

(*F*) W. G. Cady, U. S. patent 1,472,583, application May 28, 1921, issued Oct. 30, 1923.

(*A*) is Langevin's original patent on the use of a vibrating quartz sandwich for submarine signaling. In it he mentions tuning the driving circuit to the natural frequency of the quartz-steel transducer but says nothing about the reacting or controlling properties of the latter. Nicolson's first patent (*C*) had to do chiefly with acoustic applications of Rochelle salt. One of these, illustrated in his Fig. 11, was the use of a Rochelle-salt crystal, connected to an oscillating circuit, for modulating a carrier wave. The circuit was not claimed to be vibrating in resonance with the crystal. Nothing was said about the use of the crystal as a resonator.*

* Recently the author was informed by Dr. Nicolson that he found in September, 1917, that the circuit represented in his Fig. 11 must have been oscillating at a fre-

(*E*) is the original patent on the piezo resonator, in which the uses of the resonator as a frequency standard, coupler, and filter are mentioned, together with an explanation of the various effects. In (*F*), which followed soon after, various piezo-oscillator circuits are described. Shortly after the appearance of (*E*), Nicolson filed a divisional application based on Fig. 11 in (*C*), in which the doctrine of inherency was invoked to claim that this figure embodied the principle of the piezo resonator, oscillator, coupler, and filter. The result was (*D*). When patent (*B*), on "piezoelectric signaling apparatus," was issued, it contained claims for the use of a quartz crystal as a "frequency-determining element." Litigation has resulted in legal decisions in favor of Nicolson over (*B*) as well as over (*E*) and (*F*).

225. Alternating-current Notation. A few of the standard definitions and symbols are given here, for reference in this and later chapters.

We consider a resistance R, self-inductance L, and capacitance C, in series with an alternating emf. $V = V_0 \cos \omega t$, where $\omega = 2\pi f$.

$$\left.\begin{aligned}
\text{Reactance} &= X = \omega L - \frac{1}{\omega C} \\
\text{Impedance} &= Z = \left\{R^2 + \left(\omega L - \frac{1}{\omega C}\right)^2\right\}^{\frac{1}{2}} \\
\text{Vector impedance} &= \boldsymbol{Z} = R + jX \\
\text{Conductance} &= g = \frac{R}{Z^2} \\
\text{Susceptance} &= b = \frac{X}{Z^2} \\
\text{Admittance} &= Y = \frac{1}{Z} \\
\text{Vector admittance} &= \boldsymbol{Y} = g - jb \text{ (see below)} \\
\text{Maximum current} &= \text{current amplitude} = I_0 = \frac{V_0}{Z} = V_0 Y
\end{aligned}\right\} \quad (305)$$

The emf is usually written in exponential notation as $V = V_0 \epsilon^{j\omega t}$. The vector current is

$$\boldsymbol{I} = \frac{\boldsymbol{V}}{\boldsymbol{Z}} = \boldsymbol{V}\boldsymbol{Y} = V_0 \epsilon^{j\omega t}(g - jb) \qquad (305a)$$

The real part of this expression is the instantaneous current I:

$$I = V_0 Y \cos(\omega t - \varphi) \qquad \left(\tan \varphi = \frac{X}{R} = \frac{b}{g}\right) \qquad (305b)$$

For the peak value (maximum in a cycle or current amplitude), we have $I_0 = V_0 Y$.

---

quency determined by a natural mode of the Rochelle-salt crystal. It is most unfortunate that the evidence was not published. In view of this statement, however, it appears that Nicolson was the first to construct a crystal-controlled oscillator—unless, indeed, Langevin's circuit was to some extent crystal controlled. Such findings were entirely unknown to the author in his investigations described above.

Whenever the vector emf is written in the form $V = V_0\epsilon^{j\omega t}$, it is customary to regard the vector diagram as rotating counterclockwise and to take as the instantaneous V the real part of V: $V = V_0 \cos \omega t$. Sometimes one finds the emf given as $V = V_0\epsilon^{-j\omega t}$. In this case the vector rotates clockwise, but the real part is the same as for $V_0\epsilon^{+j\omega t}$. Nevertheless, as is clearly seen when time derivatives have to be taken, the opposite sense of the rotation requires that the signs of X, b, and φ be taken as opposite to those when $V_0\epsilon^{+j\omega t}$ is used. This fact is not always made clear in texts on alternating currents.

A simple example will illustrate this statement. If the circuit is a pure capacitance C in series with $V = V_0\epsilon^{-j\omega t}$, then, if the instantaneous charge is Q,

$$I = dQ/dt = C\,dV/dt = -j\omega CV,$$

while if $V = V_0\epsilon^{j\omega t}$ we should write $I = +j\omega CV$. The discrepancy is removed by writing $b = +\omega C$ in the former case.

226. Theory of the Piezo Resonator. A rigorous theory for a crystal resonator of any form and orientation, vibrating in any desired mode, would have to take account of all boundary conditions, size and position of electrodes, losses due to the dielectric and mounting, non-linear effects, coupling between different modes of vibration, non-uniformity of electric field, and, when the electrodes are separated by a gap from the crystal, the effects of the gap, including possible resonance effects in the air itself. While no such general theory has been attempted, special problems involving most of these considerations have been attacked by many writers. Some of these special cases will be considered later.

In practice, the commonest types of piezo resonator are the *bar*, vibrating compressionally lengthwise, and the *plate*, in which the wave propagation is normal to the major surfaces although the vibration direction may have any orientation. Other types involve *flexural vibrations*, *torsional vibrations*, and the *contour vibrations* mentioned above.

In principle, it is always possible to express the amplitude of vibration at any frequency in terms of the effective driving stress, together with the physical constants of the material and the dimensions of the specimen. The corresponding electrical problem is the calculation of the equivalent electric constants in the neighborhood of a resonant frequency. Just as the spectroscopist is interested in both frequencies and intensities of spectral lines, so here the study of the resonator involves both resonant frequencies and vibrational (or current) amplitudes. Resonant frequencies are usually only slightly dependent on the damping. On the other hand, in expressing such quantities as sharpness of resonance or the shape of the resonance curve, on which the usefulness of the resonator depends, the damping factor must be introduced.

In the present chapter it is assumed that all stress-strain relations, both electrical and mechanical, are linear. The treatment of non-linear effects has been carried out only for Rochelle salt and will be considered in Chaps. XXIII and XXIV.

We shall restrict ourselves to the theory of lengthwise vibrations of bars and thickness vibrations of plates. While these two types of resonator have much in common, they differ in such significant particulars that they are better treated separately. Theories of the flexural and torsional resonator could be developed along the lines indicated for the bar.

In all cases the resonator is assumed to be in the form of a parallelepiped with edges parallel to the axes of reference and with the field parallel to one of these axes. If the reference axes are the crystallographic axes, for any given crystal the elastic and piezoelectric constants that come into play are given directly by the tables in §§29 and 131. For oblique cuts all parameters must be those appropriate to the particular axes employed; they may be computed from the transformation equations already given in Chaps. IV, VI, and VIII.

LENGTHWISE COMPRESSIONAL VIBRATIONS OF BARS

227. The length l of the bar is in the n-direction, and the compressional stress and strain are denoted by X_n and x_n, respectively. As in the treatment of lengthwise vibrations in Chap. V, we take the origin at the center of the bar and denote the distance from the origin, along the axis of the bar, by x. The section of the bar is rectangular, with dimensions small in comparison with l. The electric field E_i is in the i-direction, normal to a pair of the lateral faces.* The electrodes are assumed to cover the entire surface of the bar normal to the i-axis, though they may be separated from it by a total gap w. The breadth and thickness of the bar are denoted by b and e. We assume that $b << l$ and that the ratio b/e is great enough to make the driving field sensibly uniform over the cross section. For excitation it is necessary that there be a piezoelectric constant d_{in} such that $x_n = d_{in}E_i$.

228. *The Driving Stress for Lengthwise Vibrations.* This quantity is defined as that alternating mechanical stress, denoted by $(X_n)_d$, which, applied uniformly throughout the bar, would produce the same vibration of type x_n as is actually produced by the alternating field E_i. $(X_n)_d$ then takes the place of the stress X in §§57 following, while in place of

* Under certain conditions lengthwise vibrations can also be excited by placing the electrodes so as to produce a field parallel to the length of the bar. In this case the electric field is parallel to the direction of wave propagation, and the theory is more complicated because of the presence of a space charge. As will be seen in §349, quartz resonators of this type have been described by Giebe and Scheibe.

Young's modulus Y we shall use the symbol $q' = 1/s^w_{nn}$; this is the effective value assumed by Young's modulus when there is a total gap w between crystal and electrodes, as given below in Eq. (330).

In general, E_i causes six components of piezoelectric stress:

$$X_1 = -e_{i1}E_i \cdots X_6 = -e_{i6}E_i.$$

Through elastic coupling each of them contributes to $(X_n)_d$. Thus X_h tends to cause a strain component $-s^E_{nh}X_h$, and the sum of all six strain components is $x_n = -\Sigma s^E_{nh}X_h \equiv -s^E_{nn}(X_n)_d$. We seek the value of the effective piezoelectric stress coefficient ϵ, given by $(X_n)_d = -\epsilon E_i$. We have

$$(X_n)_d = \frac{1}{s^E_{nn}} \sum_h^6 s^E_{nh}X_h = -\frac{E_i}{s^E_{nn}} \sum_h^6 s^E_{nh}e_{ih} = -\epsilon E_i \tag{306}$$

Hence,

$$\epsilon = \frac{1}{s^E_{nn}} \sum_h^6 s^E_{nh}e_{ih} \tag{307}$$

If the resonator is partly clamped (see §372) or if the dimensions are such that some of the six stresses are prevented by inertia from becoming effective, some of the terms in the summation will be absent. In a thin bar undergoing longitudinal vibration all six terms are present (though in most cases certain of the e_{ih} vanish for the particular crystal used). It follows from Eq. (191a) that, for a field parallel to i,

$$\epsilon = \frac{d_{in}}{s^E_{nn}} \tag{308}$$

This expression will be used throughout in the theory of the bar. Its value is independent of the gap.

As an illustration of the formula for $(X_n)_d$ may be mentioned the quartz X-cut resonator with length parallel to Y, which was the earliest type and is still widely used. For it, when $w = 0$, $\epsilon = d_{12}/s^E_{22} = -d_{11}/s^E_{11}$, while the driving stress is $(Y_y)_d = -\epsilon E_x = -d_{11}E_x/s^E_{11}$.

In all cases only the component of polarization parallel to the field need be considered. From §110 it is seen that a potential difference V applied to the electrodes causes a field strength $E_i = V/e'_r = V/(e + k_l w)$ (for k_l see next section). Hence, from Eq. (306), on writing $V = V_0 e^{j\omega t}$, we have

$$(X_n)_d = -\frac{\epsilon V_0 e^{j\omega t}}{e'_r} \tag{309}$$

229. The Dielectric Constant for Lengthwise Vibrations. At very low frequencies the dielectric constant has the value k'_i for a free crystal.

The lowest normal mode, leaving aside flexural and torsional vibrations, is the fundamental lengthwise mode. As the frequency of this mode is approached, the longitudinal strain x_n due to the state of vibration begins to be appreciable, becoming many times greater than the static strain $x_n^E = d_{in}E_i$ that tends to be caused by the instantaneous E_i. Since the normal modes corresponding to all the components of strain except x_n have frequencies that are high in comparison with the fundamental lengthwise frequency, all such components of strain are practically proportional to and in phase with E_i. With respect to these components, then, the crystal is still free, and they all contribute to the value of the dielectric constant. On the other hand, with increasing frequency the static strain x_n^E gradually merges into the vibrational strain x_n, which is treated in a separate equation. Hence the polarization ϵx_n^E must be subtracted from that characteristic of the free crystal in forming the expression for the effective dielectric constant. We have therefore, for the polarization due to E_i,

$$P_i^E = \eta_i' E_i - \epsilon x_n^E = \eta_i' E_i - \epsilon d_{in} E_i = \left(\eta_i' - \frac{d_{in}^2}{s_{nn}^E}\right) E_i \equiv \eta_l E_i \quad (310)$$

where the effective susceptibility is $\eta_l = \eta_i' - \epsilon d_{in}$. The effective dielectric constant is therefore*

$$k_l = 1 + 4\pi\eta_l = k_i' - 4\pi\epsilon d_{in} = k_i' - \frac{4\pi d_{in}^2}{s_{nn}^E} \quad (311)$$

In a quartz X-cut resonator k_l is about 1 per cent less than k_x'. In a Rochelle-salt X-cut 45° bar, k_l is only about half as large as k_x'.

The value of k_l given by Eq. (311) is to be used everywhere in the theory of lengthwise vibrations, except in the expression for the stiffness q', as explained in §235. The symbol k_l indicates the dielectric constant that determines the driving field for *lengthwise* vibrations when a potential difference V is applied to the electrodes. In terms of k_l the "electric spacing" (§110) is

$$e_r' = e + k_l w \quad (312)$$

230. Polarization and Current in the Resonator. The instantaneous piezoelectric polarization at any distance x from the center and at any frequency is derived from the general expression for the strain $x_n(x)$ at the same point. The X-direction, which is that of the length of the bar, may have any orientation with respect to the crystallographic axes. For the lengthwise compressional vibrations here considered, x_n means the lengthwise compressional strain.

* This equation, for a quartz X-cut bar, was first derived by Vigoureux.[567] Similar expressions have been used by Mueller[378] and by Mason.[B35,340]

In order to find an expression of sufficient generality for x_n we must go back to §57, where the mechanical displacement ξ at any x is given by Eq. (68). With the aid of Eqs. (71) and (73) we find (writing q' in place of q for the stiffness)

$$x_n(x) = \frac{\partial \xi(x)}{\partial x} = -\frac{(X_n)_{d0}}{q'} \frac{\cosh \gamma x}{\cosh (\gamma l/2)} \epsilon^{j\omega t} \tag{313}$$

where l is the length of the bar, q' is given by Eq. (330), and

$$(X_n)_d = (X_n)_{d0}\epsilon^{j\omega t}$$

is the instantaneous driving stress, taking the place of X in the earlier section. At zero frequency $(X_n)_d$ becomes a *static* stress, the static strain being approximately $-(X_n)_d/q'$. Equation (313) shows that the actual strain at any point when the crystal vibrates is this static strain multiplied by the factor $\cosh \gamma x/\cosh (\gamma l/2)$. This is the factor by which the amplitude of vibration is in excess of the static elongation.

From the equations that follow it can be proved that, for the same driving force, the ratio of the static to the resonant amplitude of mechanical displacement is $\delta/4\pi$, where $\delta = \alpha/f$ is the logarithmic decrement per period. The same ratio holds for the strain at the center and for the current.

In terms of maximal displacement $\xi_0(l/2)$ at the end of the bar, the maximal vibrational stress is $-\pi q' l \xi_0(l/2)$.

The piezoelectric polarization* at any point is $P_i(x) = \epsilon x_n(x)$. It gives rise to a piezoelectric displacement D_p, which, when there is a gap, is equal to the corresponding field $(E_w)_p$ in the gap, and is given by Eq. (164*a*):

$$D_p(x) = (E_w)_p(x) = 4\pi P_i(x) \frac{e}{e_r'} \tag{314}$$

The total displacement $D(x)$ at any x is the sum of $D_p(x)$ and the contribution due to the driving field E_i, *viz.*, $k_i V/e_r'$ by Eq. (163*b*). The current density at any x is $\partial D/4\pi\partial t$, and the total current I is the integral of this expression over the breadth b and length l of the bar: from Eqs. (309), (313), and (314) one finds

$$\begin{aligned} I &= \frac{j\omega b V_0}{4\pi e_r'} \epsilon^{j\omega t} \int_{-l/2}^{l/2} \left(k_i + \frac{4\pi\epsilon^2 e}{q' e_r'} \frac{\cosh \gamma x}{\cosh (\gamma l/2)} \right) dx \\ &= j\omega V_0 \epsilon^{j\omega t} \left(\frac{k_i b l}{4\pi e_r'} + \frac{2b\epsilon^2 e}{q'\gamma e_r'^2} \tanh \frac{\gamma l}{2} \right) \end{aligned} \tag{315}$$

* In general, the polarization has components at right angles to the thickness e, but they have no effect on the current.

This equation holds at all vibrational frequencies up to those at which coupling between overtone lengthwise vibrations and vibrations in lateral directions begins to cause complications, and for any degree of damping for which Eq. (74) in §57 is valid.

When $w = 0$ (electrodes adherent), then as $f \to 0$,

$$\tanh\left(\frac{\gamma l}{2}\right) \to \frac{\alpha l}{2c},$$

$\gamma \to \alpha/c$, and by Eq. (311) $k_l \to k_i'$, the value for a free crystal.

The quantity in the parentheses in Eq. (315), multiplied by $j\omega$, represents an electrical admittance. The first term is capacitive, while the second is the vibrational contribution, which is variable in phase with respect to V. Use will be made of this fact in deriving the constants of the equivalent electrical network.

A curve relating I with frequency would show a series of maxima like those in Fig. 20. The relative heights of successive maxima would depend on the nature of the damping. From the relations between F, α, and δ in Eq. (67), it can be shown that the ratio of the maximum occurring at the fundamental frequency f_0 (for which $h = 1$) to that occurring at any harmonic frequency $f_h = hf_0$ is h^2 if F is independent of the frequency; the ratio is h if δ is independent of frequency; and the current is the same at all harmonic frequencies if α is independent of frequency.

Not much is known of the dependence of damping on frequency. Usually the viscosity inherent in the crystal is overshadowed by losses due to the mounting, and these may well vary more or less erratically from one type of mounting to another. On the whole it can be pretty confidently expected that the current maxima will diminish at a pronounced rate with increasing order of harmonics.

By the use of a system of h pairs of short electrodes, properly connected and distributed uniformly along the length of the bar, the current corresponding to overtone h can be increased (see §239).

231. Equation (315) can be put into a useful approximate form, (1) when the damping is negligible, (2) in the neighborhood of a resonant frequency.

1. *When damping is neglected,* Eq. (74) reduces to $\gamma = j\omega/c = j\pi f/lf_0$, where c is the wave velocity and f_0 the fundamental frequency for maximum particle velocity and maximum piezo current (§234). Since now $\tanh(\gamma l/2) = \tanh(j\omega l/2c) = j \tan(\pi f/2f_0)$, it is found from Eq. (315) that

$$I = \frac{j\omega blV_0 e^{j\omega t}}{e_r'}\left(\frac{k_l}{4\pi} + \frac{2\epsilon^2 f_0 e}{\pi f q' e_r'} \tan\frac{\pi f}{2f_0}\right) \tag{316}$$

This equation can be used at all vibrational frequencies, except that it becomes infinite when f is an odd multiple of f_0. The frequency for parallel resonance, which we call f_p, is found by setting $I = 0$ and solving for f. A more convenient expression for f_p, in terms of the equivalent electric constants, is given by Eq. (398).

2. In making the approximations for frequencies close to resonance, we denote the order of the harmonic by h ($h = 1, 2, 3, \ldots$), as in §58. The fundamental frequency $f_1 = \omega_1/2\pi$ will, however, still be denoted by $f_0 = \omega_0/2\pi$. If the width b of the bar is not greater than $l/4$, where l is the length, a true harmonic ratio for overtones can be assumed to a first order of approximation. The correction for the frequencies of overtones is given in §65. By Eq. (64) the damping constant is $\alpha_h = h^2\alpha$, if the frictional coefficient F in Eq. (61) is regarded as constant. If, as is probable, F varies with frequency, α_h must be found experimentally.

For the factor γ in the denominator of Eq. (315) one may write with sufficient approximation $j\omega_h/2f_0l$. Near resonance, where $n_h << \omega_h$, one has $\omega_h = \omega_{h0} - n_h$ [Eq. (81)]. After obvious reductions it is found that

$$\tanh \frac{\gamma l}{2} \approx 4f_0 \frac{\alpha_h + j(-1)^{h-1}n_h}{[1 + (-1)^h]8f_0^2 + [\alpha_h^2 - (-1)^h n_h^2]} \tag{317}$$

With even integral values of h this expression becomes extremely small and the current approaches that flowing to an ordinary non-vibrating condenser. That is, when full-length electrodes are used, as is here assumed to be the case, the response of the resonator is negligibly small in the neighborhood of even harmonics. For the excitation of even harmonics by short electrodes see §238.

In what immediately follows we shall be concerned only with odd harmonics. When h is near an odd integer, Eq. (317) becomes

$$\tanh \frac{\gamma l}{2} \approx 4f_0 \frac{\alpha_h + jn_h}{\alpha_h^2 + n_h^2}$$

With these substitutions in Eq. (315) the equation for current is

$$I = \frac{\omega_h b l V_0 \epsilon^{j\omega_h t}}{e_r'} \left(j \frac{k_l}{4\pi} + \frac{4\epsilon^2 \omega_{h0} e}{\pi^2 q' h^2 e_r'} \frac{\alpha_h + jn_h}{\alpha_h^2 + n_h^2} \right) \tag{318}$$

On rearranging terms and making the approximation

$$\omega_{h0}\omega_h \approx \omega_{h0}^2 = h^2\omega_0^2 = h^2\pi^2 q'/\rho l^2,$$

one finds

$$\begin{aligned} I &= V_0 \epsilon^{j\omega_h t} \left[\frac{4\epsilon^2 b e}{\rho l e_r'^2} \left(\frac{\alpha_h}{\alpha_h^2 + n_h^2} + j \frac{n_h}{\alpha_h^2 + n_h^2} \right) + j\omega_h \frac{k_l b l}{4\pi e_r'} \right] \\ &= V_0 \epsilon^{j\omega_h t}(g' - jb' - jb'') \equiv V_0 \epsilon^{j\omega_h t} Y_1' \end{aligned} \tag{319}$$

where $g' \equiv 4\epsilon^2 b e \alpha_h / \rho l e_r'^2 (\alpha_h^2 + n_h^2)$, $b' \equiv -4\epsilon^2 b e n_h / \rho l e_r'^2 (\alpha_h^2 + n_h^2)$, and $b'' \equiv -\omega_h k_l b l / 4\pi e_r'$.

232. The Equivalent Electrical Constants. In Eq. (319), Y_1' represents an electrical vector admittance, of which the first component is a conductance g', while b' and b'' are constituents of a susceptance.* Since b' and g' contain n_h and α_h, they must originate in the *vibrations*, while b'' is a parallel susceptance independent of the state of vibration.

The electrical impedance corresponding to the vibrational terms is

$$Z' = \frac{1}{g' - jb'} = R_h' + jX_h'$$

where, as is easily verified,

$$R_h' = \frac{\rho l e'^2}{4\epsilon^2 be}\,\alpha_h \qquad X_h' = \frac{-\rho l e'^2}{4\epsilon^2 be}\,n_h \tag{320}$$

The negative sign results from the definition $n_h = h\omega_0 - \omega_h$ and indicates that on the h-f side of resonance, where n_h is negative, the reactance X_h' is positive.

Since ω_h is close to $h\omega_0$, it follows that the reactance X_h', which must be of the form $\omega_h L_h' - 1/\omega_h C_h'$, can with sufficient accuracy be written as $X_h' = -2L_h' n_h$. This expression leads at once to the *equivalent self-inductance* L_h',

$$L_h' = \frac{\rho l e'^2}{8\epsilon^2 be} \tag{321}$$

L_h' is independent of the value of h, just as was the case with the equivalent mass M in §63.

The value of the equivalent capacitance C_h' in series with L_h' is found from the relation $\omega_{h0}^2 L_h' C_h' = 1$:

$$C_h' = \frac{8\epsilon^2 ble}{\pi^2 q' e_r'^2 h^2} \tag{322}$$

In parallel with the $R_h' L_h' C_h'$ series chain is the capacitance C_1' represented by the last term in Eq. (319):

$$C_1' = \frac{k_t bl}{4\pi e_r'} \tag{323}$$

All the foregoing electrical quantities are expressed in cgs electrostatic units.

To avoid confusion, we use the primed symbols q', R_h', L_h', and C_h' for the equivalent constants at harmonic h *when there is a gap*, as in Fig. 50. When the gap is zero, the primes are omitted. The reason for the use of the primes will become more apparent when we come to the two alternative networks shown in Fig. 56.

* The symbol for susceptance must not be confused with the b that denotes the breadth of the bar.

When there is no gap, the expressions for the electric constants become

$$\left.\begin{aligned} R_h &= \frac{\rho l e}{4\epsilon^2 b}\,\alpha_h & L_h &= \frac{\rho l e}{8\epsilon^2 b} \\ C_h &= \frac{8\epsilon^2 b l}{\pi^2 q_0 e h^2} & C_1 &= \frac{k_l b l}{4\pi e} \end{aligned}\right\} \tag{324}$$

where now q_0 is the stiffness at zero gap, with value $1/s^E_{nn}$. The dependence of the four parameters upon the gap w is expressed by the factor $e'_r = e + k_l w$ and, in the case of C'_h, by the factor q'.

It should be noted especially that C'_h decreases as the gap increases, approaching the value zero at infinite gap, while L'_h approaches infinity. The increase in frequency as the gap goes from zero to infinity is due to the factor for mechanical stiffness in the expression for C'_h, which increases from q_0 when $w = 0$ to $q' = q^*$ when $w = \infty$. For quartz this increase is small; for Rochelle salt (§377) it is very large.

From the foregoing equations, together with Eq. (67), it is seen that the damping constant α_h can be variously expressed as

$$\alpha_h = \frac{R'_h}{2L'_h} = f_h \delta_h = \frac{\pi f_h}{Q_h}$$

Q_h and δ_h would be constants of the material of the resonator if the frictional coefficient F in §56 were constant. The dependence of Q_h on frequency, and hence on the dimensions of the resonator, is discussed in §296.

Most, if not all, types of piezo resonator, vibrating in the neighborhood of a natural frequency, can be represented electrically by a series RLC- (or $R'L'C'$-) chain in parallel with a fixed capacitance. The network is shown in Fig. 50, and the representation of the behavior of the resonator by means of a circle diagram is considered in Chap. XIV.

233. *The Electromechanical Ratio.* In §62 expressions were given for the equivalent lumped mechanical constants of the bar: $W_h = \rho l b e \alpha_h$, $G_h = \pi^2 Y b e h^2/2l$, $M_h = \rho b l e/2$. As stated previously, Young's modulus Y is denoted by q in the present discussion. Comparison of these quantities with the expressions for R'_h, C'_h, and L'_h in Eqs. (320), (322), and (321) shows that they are related in the following manner:

$$Z'_h = r(Z_c)_h \qquad R'_h = rW_h \qquad C'_h = \frac{1}{rG_h} \qquad L'_h = rM_h \tag{325}$$

where

$$r = \frac{e'^2_r}{4\epsilon^2 b^2 e^2} = \frac{(e + k_l w)^2}{4\epsilon^2 b^2 e^2} \tag{326}$$

is the *electromechanical ratio** and Z_c is the motional impedance. When the gap $w = 0$, the ratio is simply $1/(4\epsilon^2 b^2)$. For every type of piezo reso-

* In a former paper[107] the author used the symbol r' for this ratio when there was a gap between electrodes and crystal and r for the case of zero gap. It is simpler to use r for all values of gap, including zero.

nator, as with every transducer in general, there exists a corresponding ratio expressing the relationship between the two forms of energy involved. The expression for r in the case of thickness vibrations is given in §255.

From the foregoing equations it is clear that the quality coefficient Q may be expressed as either $\omega M_h/W_h$ or $\omega L_h'/R_h'$.

The electromechanical ratio r may be taken as a measure of the *activity* of the crystal as a resonator (for its relation to the *capacitance ratio* C_1/C see §280). For example, the amplitude of the piezo current I_p in Fig. 50 is proportional to the coefficient $4\epsilon^2 be/\rho l e_r'^2$ in Eq. (319), and this coefficient, from Eq. (326), is $1/r\rho lbe = 1/r\tilde{M}$, where $\tilde{M}$ is the equivalent mass defined above.

234. The electrical network equivalent to the crystal bar with gap, vibrating longitudinally in the neighborhood of harmonic h, is shown in Fig. 50. Since all electrical quantities are functions of the properties of the bar and independent of frequency, this network may be considered as completely replacing the crystal in any circuit, so long as the frequency

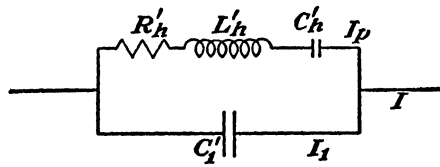


FIG. 50.—Electrical equivalent of a piezo resonator in the neighborhood of harmonic h.

remains sufficiently close to f_{h0}. The frequency f_{h0} is that at which $n_h = 0$ and the reactance $X_h' = \omega_{h0}L_h' - 1/\omega_{h0}C_h'$ vanishes. At this frequency the current has its maximum value. The alternative network, with $R_hL_hC_hC_1$ in series with the gap capacitance C_2, is explained in Chap. XIV.

The two components of the current I, represented by the two terms on the right in Eq. (318), are now seen to be the currents I_1 and I_p in Fig. 50. I_p is the *piezo current* in the $L_h'R_h'C_h'$-branch, proportional to and in phase with the *vibrational velocity*. For frequencies close to the fundamental resonant frequency this fact is readily seen by comparing Eq. (319) with (87). For this purpose the vibrational part of Eq. (319) may be rationalized into the form

$$I_p = \frac{4V_0\epsilon^2 be}{\rho l e_r'^2\sqrt{\alpha_h^2 + n_h^2}} \cos(\omega_h t - \theta_h) \tag{327}$$

where $\tan\theta_h = (-1)^h n_h/\alpha_h$.

The velocity at the end of the rod is given by Eq. (87), which, on writing $(X_n)_d = -\epsilon V/e_r'$ from Eq. (309) in place of X_0, becomes

$$v\left(\frac{l}{2}\right) = \frac{2\epsilon V_0}{\rho l e_r'\sqrt{\alpha_h^2 + n_h^2}} \cos(\omega_h t - \theta_h) \tag{328}$$

The velocity is in phase with I_p, and except at very low frequencies it is also very nearly in phase with the total current I.

The ratio of the values of I_p and $v(l/2)$ is seen from (326) to (328) to be

$$\frac{I_p}{v\left(\frac{l}{2}\right)} = \frac{2ebe}{e'_r} = \sqrt{\frac{1}{r}} \tag{329}$$

It must be emphasized that the network shown in Fig. 50 is valid only as long as the resonator can be treated as having a single degree of freedom. It fails also when the frequency approaches zero.

235. The Effect of the Gap on the Elastic Constant in Lengthwise Vibrations. In Eq. (298), a formula is given for the effective compliance for compressional strains in the k-direction, applicable to a bar lying between short-circuited electrodes that are separated from the bar by a total gap w. When the subscripts are altered to conform to the notation in the foregoing paragraphs, this equation becomes*

$$s^w_{nn} = s^E_{nn} - \frac{4\pi d^2_{in} w}{e'} \equiv \frac{1}{q'} \tag{330}$$

where $e' = e + k'w$.

Equation (330) gives the proper value of q' to use in all equations for lengthwise vibrations when there is a gap, except in the case of a *plated* crystal with gap, which is considered in §286.

According to Eq. (330) the compliance at zero gap is the pure elastic constant s^E_{nn}. This statement is in conformity with Voigt's development of piezoelectric theory, which says that the piezoelectric reactions vanish when the field is unaffected by the state of strain. That this is not the only logical point of view has already been seen in Chap. XI, where reasons are given for considering the "pure" elastic constants of Rochelle salt as those observed at infinite gap. Moreover, the theory of thickness vibrations in all crystals indicates that the elastic stiffness at infinite gap, rather than that at zero gap, should be regarded as free from piezoelectric reaction (§251). For these reasons it is worth while to see what form Eq. (330) assumes when the gap correction is measured from $w = \infty$ instead of from $w = 0$.

* In Eq. (330) the proper dielectric constant is not k_t, as elsewhere in the theory of lengthwise vibrations [see the discussion of Eq. (312)], but has the value k' for an unconstrained crystal. The reason may be seen from the derivation of Eq. (298), according to which the field to which the piezoelectric term is due is proportional to and in phase with the instantaneous stress. With respect to this field the crystal behaves as if unconstrained, just as when an l-f field is applied externally.

At infinite gap s^w_{nn} assumes the value for constant normal displacement given by Eq. (273a):

$$s^*_{nn} = s^E_{nn} - \frac{4\pi d^2_{in}}{k'} \tag{331}$$

From this equation and (330) one finds

$$s^w_{nn} = s^*_{nn} + \frac{4\pi d^2_{in}}{k'} - \frac{4\pi d^2_{in} w}{e + k'w} = s^*_{nn} + \frac{4\pi d^2_{in} e}{k'e'} \tag{331a}$$

Thus, when s^4_{nn} is taken as the pure elastic compliance, the value for gap w is greater than s^*_{nn} by $4\pi d^2_{in}e/k'e'$. When $w = 0$, the compliance* becomes, as before, simply s^E_{nn}.

With the aid of Eq. (311), a relation can be found between s^*_{nn}, s^E_{nn}, and the dielectric constants k' for a free crystal and k_l for a bar in lengthwise vibration:

$$\frac{s^E_{nn}}{s^*_{nn}} = \frac{k'}{k_l} \tag{332}$$

This expression is analogous to Eqs. (281), (282), and (521b).

236. Since s^E_{nn} and s^*_{nn} are inversely proportional to the squares of the resonant frequencies, f_0^2 at zero gap and f_∞^2 at infinite gap, respectively, we may derive from (331) the following equations, which will be used later as a step in calculating the frequency of a Rochelle-salt bar at infinite gap:

$$\frac{f_\infty^2}{f_0^2} - 1 = \frac{s^E_{nn}}{s^*_{nn}} - 1 = \frac{k' - k_l}{k_l} = \frac{4\pi d^2_{in}}{k_l s^E_{nn}} \tag{333}$$

This expression has an important relation to the frequency f_p at antiresonance when the gap is zero. This frequency is the higher of the two at which the reactance vanishes; when R is small, the current sinks almost to zero. With good approximation, therefore, the condition for antiresonance can be found by setting $I = 0$ in Eq. (316). When $w = 0$, we have $e'_r = e$ and $q' = q_0 = 1/s^E_{nn}$, giving, with the aid of Eq. (308),

$$\frac{\pi f_p}{2f_0} \cot \frac{\pi f_p}{2f_0} = -\frac{4\pi\epsilon^2 s^E_{nn}}{k_l} = -\frac{4\pi d^2_{in}}{k_l s^E_{nn}} \tag{334}$$

where i specifies the field direction and n, at right angles to i, specifies the direction of the length of the bar.

From Eqs. (333) and (334) we have finally

$$\frac{\pi f_p}{2f_0} \cot \frac{\pi f_p}{2f_0} = 1 - \frac{f_\infty^2}{f_0^2} \tag{335}$$

* For a comparison with the effective stiffness of a *plate*, see §251.

237. Effect of Gap upon Frequency of Lengthwise Vibrations. As before, f_{h0} denotes the resonant frequency (maximum particle velocity and maximum piezo current) at harmonic h. For gaps w and 0 we have

$$(f_{h0}^w)^2 = \frac{h^2}{4l^2\rho s_{nn}^w} \qquad (f_{h0}^0)^2 = \frac{h^2}{4l^2\rho s_{nn}^E}$$

where s_{nn}^w is given by Eq. (330). It follows that

$$\frac{1}{(f_{h0}^0)^2} - \frac{1}{(f_{h0}^w)^2} = \frac{16\pi l^2\rho d_{in}^2 w}{h^2 e'} \tag{336}$$

When d_{in} is large, as in Rochelle salt, this rigorous expression must be used as it stands. It finds an important application in the determination of d_{in}. Usually observations are made first with zero gap, and then with a very large gap ($w \to \infty$), in which case

$$\frac{1}{(f_{h0}^0)^2} - \frac{1}{(f_{h0}^\infty)^2} = \frac{16\pi l^2\rho d_{in}^2}{h^2 k'} \tag{336a}$$

With such crystals as quartz, f_{h0}^w differs from f_{h0}^0 by only a few tenths of 1 per cent. Equation (336a) can then be reduced to the simpler form

$$\frac{f_{h0}^w - f_{h0}^0}{f_{h0}^0} \equiv \frac{\Delta f_{h0}}{f_{h0}^0} \approx \frac{2\pi d_{in}^2 w}{s_{nn}^E e'} \equiv U\frac{w}{e'} \tag{336b}$$

where $U = 2\pi d_{in}^2/s_{nn}^E$ is a constant for the crystal and $e' = e + k'w$.

It will be noted that the relative variation of frequency with gap is the same for harmonic h as for the fundamental frequency (see also §285).

The case of a *plated* crystal with gap is treated in §286.

238. The Use of Short Electrodes in Lengthwise Vibrations. Full-length electrodes are desirable only at the fundamental frequency, when, with a given alternating potential difference, maximum amplitude of vibration or maximum reaction upon the electric circuit is to be attained or sometimes, in the measurement of the physical constants of the resonator, when it is important to apply the driving stress uniformly to all parts of the crystal.

At the *fundamental frequency*, a shortening of the electrodes diminishes the response of the crystal. Nevertheless, a very considerable shortening can take place with relatively small loss in response, as long as the electrodes are symmetrically placed. This fact is illustrated in Fig. 51, in which the ends x_1 and x_2 of the electrodes of length l' are at equal distances from the center. The curve represents the sinusoidal distribution of vibrational stress, which has a maximum at the center; in the neighborhood of resonance and with small damping, the curve falls practically to

zero at the ends. The applied piezoelectric stress is most effectual over the region where the vibrational stress is greatest. If the driving field near the ends of the bar is absent, there is but little diminution in amplitude of vibration.

Harmonic Frequencies. In §58 we learned that when the driving stress is uniform over the entire length of the bar, as is the case with full-length electrodes, large resonant amplitudes are built up only when the

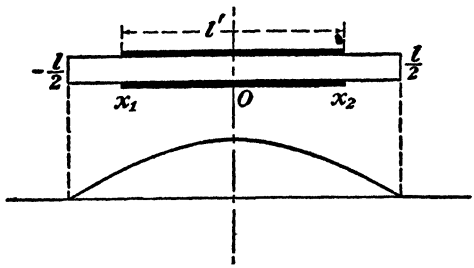


FIG. 51.—Excitation of lengthwise vibrations by short electrodes.

order h of the harmonic is odd. In Fig. 52 the curve shows the distribution of stress in a bar when $h = 3$. The impressed field between the electrodes tries to make the three segments AB, BC, CD vibrate in phase, while the curve shows that, as long as the segments are parts of a continuous bar, there must be between adjacent segments a vibrational phase difference of 180°. Such a phase difference is impossible when the electrodes are continuous. In effect, all segments but one neutralize

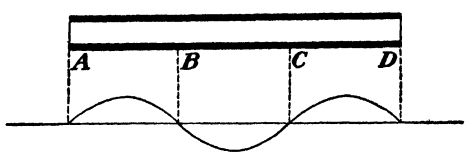


FIG. 52.—Piezoelectrically driven bar vibrating at harmonic $h = 3$.

one another, so that the resulting vibration is substantially the same as if the electrodes covered only one segment.

If h were even, the neutralization would be complete. For example, in Fig. 52 one might imagine the bar to extend only from A to C, with $h = 2$. In each of the two segments there would be feeble forced vibrations, as explained in §61, but the piezoelectric reaction on the driving circuit would vanish (see also §63).

239. By the use of *short electrodes*, however, intense vibrations, with correspondingly strong electric reactions, can be secured at any value of h, even or odd. For example, the fourth harmonic can be excited by

means of any one of the four pairs of electrodes shown in Fig. 53. The bar should be supported at one or more nodes of motion. More than one pair of electrodes may be used, suitably connected in series or parallel. With a given voltage, if $AB'CD'$ are connected to one side of the line and $A'BC'D$ to the other, a large amplitude results. From what has been said above, the spaces between adjacent electrodes, as A and B, cause but little loss in amplitude. The reaction on the electric circuit is four times that of a single short segment.

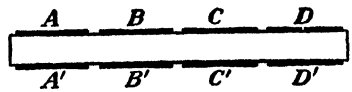


FIG. 53.—Bar with electrodes for excitation of the fourth harmonic frequency.

Resonators like that shown in Fig. 53 with any number of pairs of electrodes can be prepared by silvering or evaporating a uniform metallic deposit on the opposite sides of the bar and then dissolving away metal in the proper regions to produce the desired number of pairs of separate electrodes.

An arrangement like that in Fig. 53 is discussed by Sokolov,[473] Hehlgans,[217] and Williams.[587]

A bar with two pairs of electrodes can be used as a coupling device between two circuits, in which case it serves as a very narrow pass band filter (§500).

By the use of a single pair of short electrodes at one end of the bar, as at AA' in Fig. 53, the fundamental and a large number of harmonics, both even and odd, can be excited. This arrangement was first described by the author in 1925.[97] In the same year Giebe and Scheibe[163] described the use of short electrodes for the excitation of the luminous effects mentioned in §365. Since the intensity of the reaction on the driving circuit diminishes as h increases (with short electrodes near one end of the bar), it is found that the response for all values of h including unity is of the same order of magnitude, as long as the length l' of the electrodes is not too much greater than the half wavelength of the vibration in the bar. This fact makes such an arrangement useful as a reference standard for a large number of nearly harmonic frequencies.

240. Theory of the Lengthwise Resonator with Short Electrodes. In Eq. (110) it was shown that reducing the length of the electrodes from full length l to $(x_2 - x_1) = l'$ (see Fig. 21) caused the amplitude of vibration at the fundamental mode to be diminished by a factor S_{12}, where

$$S_{12} = \tfrac{1}{2}\left(\sin\frac{\pi x_2}{l} - \sin\frac{\pi x_1}{l}\right) \tag{337}$$

Evidently the fundamental mode can still be excited, though weakly, with short electrodes close to one end. It is easily proved that, with l' prescribed, S_{12} is a maximum when x_1 and x_2 are equidistant from the

center, thus confirming the statement made on page 302 concerning the most effective position of the electrodes. For this symmetrical placing of the electrodes, we may drop the subscript in Eq. (337) and write

$$S = \sin \frac{\pi l'}{2l} \tag{337a}$$

Expressions will now be given for current and equivalent electric constants at the fundamental frequency for a resonator with a pair of symmetrical electrodes of any length separated from the crystal bar by a total gap w. The derivation is exactly like that of Eq. (315) with these exceptions: (1) the factor S must be applied to the driving stress; (2) the integration must take place from $-l'/2$ to $+l'/2$. The result is

$$I = SV_0 e^{j\omega t}\left(j\omega \frac{l'bk_r'}{4\pi e_r'} + \frac{4\epsilon^2 beS}{\rho l e_r'^2}\frac{\alpha + jn}{\alpha^2 + n^2}\right) \tag{338}$$

where, instead of k_t as given by Eq. (311), we now have for the effective dielectric constant, with short electrodes and gap,

$$k_r' = k_t' - \frac{4qd_{in}^2 e}{e_r'}\left(\pi - 2\cos\frac{\pi l'}{2l}\right) \tag{339}$$

The corresponding equivalent electric constants, in cgs electrostatic units, are found, by the method of §232, to be

$$\left.\begin{aligned} R' &= \frac{\rho l e_r'^2 \alpha}{4\epsilon^2 beS^2} \qquad L' = \frac{\rho l e_r'^2}{8\epsilon^2 beS^2} \qquad C' = \frac{8\epsilon^2 lbeS^2}{\pi^2 q' e_r'^2} \\ C_1' &= \frac{k_r' bl'}{4\pi e_r'} \end{aligned}\right\} \tag{340}$$

where $e_r' \equiv e + k_r' w$.

These values agree with those deduced by a different method by Starr,[476] who, however, disregards the losses (α and R are left out of account) and considers only the case in which the gap $w = 0$. Starr gives formulas for determining the proper value of l' when it is desired to avoid the excitation of some one harmonic.

The foregoing expressions are applicable to a bar of length l vibrating at any harmonic frequency, with h pairs of electrodes, each pair having a length l_1'. It can be proved that in this case the electric constants for *each segment* are

$$\left.\begin{aligned} R_h' &= \frac{\rho l e_r'^2 \alpha}{4\epsilon^2 beh \sin^2(\pi l_1' h/2l)} \qquad L_h' = \frac{\rho l e_r'^2}{8\epsilon^2 beh \sin^2(\pi l_1' h/2l)} \\ C_h' &= \frac{8\epsilon^2 ble}{\pi^2 q' e_r'^2 h} \qquad C_{1h}' = \frac{k_r' bl_1'}{4\pi e_r'} \end{aligned}\right\} \tag{340a}$$

When h pairs of segments are connected in parallel, the values for the entire resonator are

$$R' = \frac{R'_h}{h} \qquad L' = \frac{L'_h}{h} \qquad C' = hC'_h \qquad C'_1 = hC_1 \tag{341}$$

When the gap $w = 0$, it is necessary only to write e in place of e' in all the foregoing equations and to drop the prime accents from R', L', C', and C'_1.

241. If calculations of highest precision are required when the electrodes are of less than full length, account has to be taken of the fact that in the regions covered by the electrodes the elastic stiffness is somewhat smaller than in the exposed regions, as was pointed out in §64.

The optimum length of electrodes depends on the object in view. For maximal amplitude of vibration with constant impressed alternating voltage and for maximal control in a piezo-oscillator circuit at fundamental frequency, full-length electrodes should be used. In such measurements as that of the frequency of a bar with infinite gap, a close approach to the ideal condition of infinite gap can be made by the use of very short electrodes. For the excitation of overtones short electrodes are indicated, as explained above.

There remains the important class of cases discussed in §280, in which it is desirable to make the ratio $C:C_1$ as large as possible. It will now be shown that in the case of bars a slight increase can be brought about by making the electrodes approximately three-fourths as long as the bar. From Eqs. (340), for zero gap ($e'_r = e$) and fundamental frequency ($h = 1$), one finds

$$\frac{C}{C_1} = \frac{32\epsilon^2 l}{\pi q_0 k_r'} \frac{S^2}{l'} \tag{342}$$

where $32\epsilon^2 l/\pi q_0 k_r'$ is practically constant and S is given by Eq. (337*a*). On equating the derivative $\partial/\partial l'$ to zero, we find that C/C_1 is a maximum when $\tan \pi l'/2l = \pi l'/l$, whence $l'/l \approx 0.75$. In this case, $S = 0.92$ and C/C_1 is about 14 per cent greater than when $l' = l$.

If l' is made still shorter, the ratio C/C_1 begins to decrease again. On the other hand, the ratio L/C becomes continuously greater as l' is diminished.*

242. *Laue's Formulation of Resonator Theory.* In 1925 Laue[309] published a thorough treatment of the problem of piezoelectric lengthwise vibrations in a quartz X-cut bar with length parallel to Y, subject, however, to the same limitations as in the theory presented here, *viz.*, that the bar is so thin that no correction for finite cross section need be made, that there is no coupling with other vibrational modes, and

* For further discussion of the ratio l'/l see Mason[335] and Starr.[476]

that overtone frequencies are harmonics of the fundamental. The electrodes are assumed to be adherent to the crystal. The equation of motion is derived from a consideration of the various potential and kinetic energies. The only losses appearing in the equation are those inherent in the quartz. Two frictional coefficients are introduced, *viz.*, α, a function of Voigt's frictional coefficients* b_{ik} and of the elastic and piezoelectric constants; and β, a function of the b_{ik}-coefficients and elastic constants. Comparison of Laue's equation (16) with Eq. (61) shows that the frictional factor F in (61) is identical with Laue's β/s_{11}^2. We have not attempted to express F in terms of the fundamental frictional coefficients of quartz, since the latter usually play but a small part in determining the actual damping.

If sufficiently precise measurements could be made of resonance in a quartz bar mounted without friction in a vacuum, Laue's equations would doubtless be found useful for determining the frictional coefficients of the crystal. In particular, mention should be made of his equation (23) for the amplitude at the ends of the bar, (25) for the phase difference between motion and driving field, and (26) for the piezoelectric capacitance.

In comparing Laue's theory (as Laue himself does) with that in the author's 1922 paper,[93] one must understand that the author was then concerned only with first-order effects, with the object of providing an approximate theory for a new device. In the form in which the author's formulation of the theory now stands, as set forth in §§227 to 231, equations are derived that are identical with Laue's (23), (25), and (26), save for one point: his equations (25) and (26) contain terms in $(\alpha + \epsilon_{11}\beta)$, absent in the author's theory, which have an effect on the phase angle and on the piezoelectric capacitance. This expression arises from the assumption that the vibrations are to some extent influenced by the shearing stress $Y_z = -e_{14}E_x$ [see Laue's equation (12a)]. The assumption rests on fundamental theory and is perfectly sound. Nevertheless, this term involves only the losses in the crystal, which may ordinarily be completely neglected. The assumption of perfect uniformity in the electric field and the ignoring of the correction for cross section probably involve errors greater than that incurred by the disregard of this expression.

The Laue method has been applied by Sokolov[473] in the study of the production of overtone frequencies in the lengthwise vibrations of bars, by Bechmann[39] in the theory of thickness vibrations of plates, and by others.

THICKNESS VIBRATIONS OF PLATES

243. The first to deal with thickness vibrations of piezoelectric plates was P. Langevin, who in 1915 employed X-cut quartz plates for generating h-f acoustic waves (§506). It was this work of Langevin's that later led the author to investigate the possibility of using piezoelectric crystals as resonators and oscillators.

The use of thickness vibrations for the control of frequency was first described by G. W. Pierce[423] in 1923. For this purpose he used an X-cut quartz plate. With this cut the vibrations are compressional (§93), the plate becoming alternately thicker and thinner. The experimental evidence of this mode of vibration is that acoustic waves in the air are emitted from the surface; that small particles of sand or of lycopodium

* "Lehrbuch," p. 792.

can be seen to dance up and down when the plate is horizontal; and that optical interference patterns can be observed, as described in §367.

The first general treatment of the theory of thickness vibrations for all crystals and all cuts was published by Koga[270,271] in 1932. He introduced the Christoffel method for calculating the stiffness, as well as the piezoelectric contribution to the stiffness. Overtone frequencies are included, but both gap and damping are assumed to be zero.

In the theory of thickness vibrations for a piezo resonator with gap and damping, published by the author[107] in 1936, expressions were derived for the equivalent electric constants, the elastic coefficients, and the resonator current, including the gap effect. This treatment of the theory did not include overtones. It was shown that at the fundamental frequency the polarization, space charge, and electric field have approximately the distribution illustrated in Fig. 54. In the derivation of the gap correction to the elastic constant, the residual strain due to the field at the surfaces of the plate was recognized. This strain, although it is responsible for the effect of gap on frequency, was nevertheless assumed to be so small as to justify the assumption that in the vibrational equations the strain and space charge could still be regarded as sinking practically to zero at the surfaces of the plate. As will be seen, the more rigorous theories of Bechmann and of Lawson, which take complete account of the strain at the boundaries, show that the author's earlier results are correct except for a negligible second-order effect.

In Bechmann's paper[39] general equations are derived for thickness vibrations in plates cut in any orientation from any piezoelectric crystal. Gap, damping, and overtone frequencies are all taken into account, and the departure of the overtones from the harmonic relation is given. Expressions are derived for the equivalent electric constants.

Lawson[313] is concerned only with resonant frequencies (normal modes) of the fundamental and overtones. The gap effect is included, but not the damping. Like Bechmann, Lawson uses the Christoffel method for finding the effective stiffness for any crystal and cut.

244. In the following treatment the plate is assumed to be plane-parallel, with infinite lateral dimensions and with infinite plane electrodes separated from the crystal surfaces by a total gap w. This assumption eliminates the complications due to a finite boundary, and it ensures that the lateral constraints due to inertia will prohibit all strains except that which is involved in the thickness vibrations. The chief difference between the theories of lengthwise and thickness vibrations is that in the former case we deal with a single *stress* and in the latter case with a single *strain*.

The present theory does not take account of the fact that in a *finite* plate the boundary conditions have a marked influence on the vibrations.

In the first place the velocity of wave propagation is not the same near the edges as in the center of the plate. Beyond this, coupling may exist between the thickness mode and overtones of all other possible modes. The elastic conditions are so complex that many resonant frequencies can be observed, all comprised within a narrow band in the neighborhood of the ideal thickness frequency. The frequency spectrum varies with small amounts of edge grinding and also with temperature. One of the most important and difficult problems in the technique of preparing crystal plates for piezo-oscillator circuits is to lap a plate and grind its edges in such a way as to give it an outstanding thickness response of the desired frequency at a certain temperature, with the further requirement that changing the temperature shall not cause this response to give way to another at a slightly different frequency.

At the fundamental frequency f_0 the mechanical wavelength λ is approximately $2e$ (for the departure from exact equality see §250). The velocity of wave propagation is $\sqrt{q/\rho} = \lambda f_0 \approx 2ef_0$. q is the effective stiffness, a function of the fundamental elastic constants, modified somewhat by space-charge effects and by the presence of the gap. ρ is the density, and f_0 the fundamental frequency, defined as the frequency at which the velocity of a particle and the current I_p in the vibrational branch of the equivalent network have maximum values. As is shown in §255, the equivalent network is the same as that in Fig. 50.

When the plate is driven at the frequency of an overtone of order h, the basic formula is

$$f_{h0} \approx \frac{h\sqrt{q/\rho}}{2e} \tag{343}$$

As will be seen, the overtone frequencies are not quite exact multiples of the fundamental.

Since it is not possible, as it is with lengthwise vibrations, to apply the electrodes to a single one of the h segments into which the plate may be considered as divided, there is no means by which resonant vibrations can be excited at even harmonics. Hence only odd values of h need be considered, at least for perfect plates in uniform fields.

There are circumstances under which a plate may conceivably vibrate in a thickness mode at or close to an even harmonic frequency. The shape, size, and location of the electrodes may be such as to produce a driving field in the plate that varies in the direction of the thickness. Or the plate may be twinned or have other defects such that the excitation is not uniform. Finally, the plate may be in contact with an electrode of considerable mass, so that in effect one has a composite resonator. It would appear that one or more of these circumstances

must have been present in a recent observation by Parthasarathy, Pande, and Pancholy.* In optical diffraction experiments according to the method of Debye and Sears described in §511, using an X-cut quartz plate as the ultrasonic source, these investigators found diffraction patterns (of relatively low intensity) at frequencies that were approximately 2, 4, 6, and 8 times the fundamental.

A complication arises from the fact that, whereas a bar has only one value of Young's modulus, a plate has in general *three* different stiffness coefficients q for thickness vibrations, corresponding to three different possible types of vibration.

245. *The Three Types of Vibration.* We learned in §66 that, when plane waves are propagated in the direction normal to the surface of the plate, the vibration direction, in which the particles move in simple harmonic motion, must lie in one of three mutually perpendicular directions, which are determined by the elastic constants of the crystal and the direction of propagation. In general, to each of these vibration directions there corresponds a different wave velocity. Thus for a plate in a given orientation any one of three different types of wave is theoretically possible, each traveling with a different velocity. The plate has, in the most general case, not one fundamental thickness frequency, but three; each of the three vibration directions may make an oblique angle with the direction of propagation. It is only in certain special cases—which, however, are readily realized and are in wide use—that one of the vibration directions is parallel to the direction of propagation (compressional waves) or perpendicular to it (transverse or shear waves).

In practice, when the fundamental elastic constants of the crystal and the orientation of the plate are known, the three values of q and the direction cosines α, β, γ of the vibration direction can be found from Eqs. (117) and (118). If the plate is referred to an axial system X', Y', Z', with X' as the direction of the thickness, the only strain (assuming infinite area) corresponding to any q is $\partial\xi/\partial x'$, where ξ is the instantaneous mechanical displacement in the vibration direction. This strain can be resolved into components x'_x, z'_x, and x'_y, which in turn can be resolved into components with respect to the X-, Y-, Z-axes.† If the crystal has a piezoelectric coefficient capable of exciting at least one of these components, the vibrational type in question can be excited. In the

* S. PARTHASARATHY, A. PANDE, and M. PANCHOLY, A New Phenomenon in the Piezo-electric Oscillations of a Quartz Crystal, *Jour. of Scientific and Industrial Research*, vol. 2, no. 5, June, 1944, 2 pp.

† The strain x'_x respresents an extensional displacement normal to the surface, while z'_x and x'_y are shears in planes containing x'. Lateral inertia prevents all other strains.

general case, the effective piezoelectric stress coefficient, which we shall call ϵ, is a function of all the fundamental stress coefficients. The formula for ϵ is given in Eq. (344). The numerical values of q for *quartz* plates in various orientations have already been given in Table XII (page 142).

In lengthwise vibrations, the trifling effect of damping being disregarded, when the field is at right angles to the length of the bar, the strain at the ends vanishes at the frequency of velocity resonance. Such is not the case at the surfaces of a plate in thickness vibration, except when the gap between plate and electrodes is infinitely great, on one side at least. With a finite gap, as will be seen, the electric field at the surfaces due to the space charge in the crystal causes a small residual strain at all frequencies, even in the absence of damping. As the gap increases from zero to infinity, the resonant frequencies undergo a slight increase. The effect can be expressed conveniently as a contribution to the effective stiffness.

In addition to the effect of the gap, the effective stiffness receives a further contribution from the field in the interior of the crystal. This piezoelectric contribution is independent of the gap.

The foregoing general statements will be better understood in the light of the theory that will now be developed.

246. In the following formulation of the theory we shall use a procedure as nearly parallel as possible to that for lengthwise vibrations, assuming that the elastic stiffness is known.*

The thickness dimension of the plate lies in the s-direction, with direction cosines l, m, n. The electric field E is in the same direction. The origin is at the center of the plate, and the distance from the origin, in the s-direction, is denoted by x. The X-axis thus coincides with the s-direction; in general, it is *not* the crystallographic X-axis. The surfaces of the plate are at $x = \pm e/2$, where e is the thickness.

Of the three possible types of vibration, that one will usually be selected for which the effective piezoelectric coefficient ϵ has the greatest value according to Eq. (344). If we let $\xi(x)$ represent the mechanical displacement of a particle at distance x from the origin, the strain is $x_\xi = \partial\xi(x)/\partial x$, where the subscript ξ denotes the strain corresponding to the variation of ξ in the X-direction. The direction cosines of ξ, and hence of the vibration direction, are α, β, γ derivable from Eqs. (117). The direction cosines of the normal to the plate are l, m, n.

Under these conditions the effective piezoelectric stress coefficient, as derived by Bechmann,[39] is

* For the determination of elastic constants from observations of frequency, see §252.

$$\begin{aligned}\epsilon = \alpha[&e_{11}l^2 + e_{26}m^2 + e_{35}n^2 + (e_{25} + e_{36})mn \\ &+ (e_{31} + e_{15})nl + (e_{21} + e_{16})lm] \\ + \beta[&e_{16}l^2 + e_{22}m^2 + e_{34}n^2 + (e_{32} + e_{24})mn \\ &+ (e_{14} + e_{36})nl + (e_{12} + e_{26})lm] \\ + \gamma[&e_{15}l^2 + e_{24}m^2 + e_{33}n^2 + (e_{34} + e_{23})mn \\ &+ (e_{13} + e_{35})nl + (e_{14} + e_{25})lm] \end{aligned} \quad (344)$$

This coefficient ϵ is employed in expressing the piezoelectric polarization $P = \epsilon x_\xi$.

With the simpler cuts the procedure does not have to be so complicated as that indicated above. For example, in the case of an X-cut quartz plate, we know that a field E_x causes a stress $-e_{11}E_x$, whence we conclude that the effective piezoelectric constant is e_{11}. This conclusion is confirmed on setting $\alpha = 1$ and $l = 1$ in Eq. (344) and discarding the piezoelectric constants that vanish in quartz. Also, thanks to the lateral constraints in an infinite plate, the only strain is x_x, so that from the equation $X_x = -c_{11}x_x$ we conclude that the value of q is c_{11}. This finding is confirmed by application of the Christoffel method.

Similarly, in a Z-cut quartz plate $l = m = 0$, $n = 1$, whence from Eq. (344) since for quartz $e_{35} = e_{34} = e_{33} = 0$, it follows that $\epsilon = 0$ and that direct excitation of thickness vibrations is impossible.

247. *The Dielectric Constant for Thickness Vibrations.* This quantity cannot be derived it the same way as for lengthwise vibrations, chiefly because the polarization is not uniform in the field direction. Instead, we make use of the fact that all strains except x_ξ are prohibited, so that the only possible increase in the dielectric constant above the value for a clamped crystal would be that due to the strain x_ξ. According to the method adopted here, the entire piezoelectric polarization appears in the equations as a function of x_ξ. Any piezoelectric contribution, of the form of $e_{mi}d_{hi}$ in Eq. (262), that the strain makes to the susceptibility is thus taken care of, leaving as the effective susceptibility only the *clamped* value η''. The *effective dielectric constant* is therefore

$$k'' = 1 + 4\pi\eta''$$

The Clamped Dielectric Constant. Since the electric field, like the thickness dimension, lies in the s-direction and the only component of polarization with which we are concerned is in this same direction, we can use Eq. (265), in the form

$$k_s'' = k_s' - 4\pi \sum_i^6 e_{si}d_{si} \quad (345)$$

If the dielectric constant k_s' for the unclamped plate is measured at a low non-resonant frequency and the piezoelectric constants e_{si} and d_{si}

are known (transformed to a rotated axial system if the plate is oblique), k_s'' can be calculated.

If the piezoelectric constants are not known, one can measure k_s'' directly by using a very high frequency, as explained in §374.

248. *The Effective Stiffness.* By the method described in §66 the stiffness for thickness vibrations is deduced from the fundamental elastic constants. If, as is usually the case, the values of the latter have been measured at constant field, the derived value is also isagric and will henceforth be denoted by q^E. Owing to the piezoelectric reaction that is now to be considered, a correction term has to be added to q^E in order to give q', the effective stiffness.*

The derivation requires no assumption concerning the distribution of strain beyond considering the only spatial variation of strain to be in a direction parallel to the field. It is assumed that ϵ is known. In the notation explained above, we let $x_\xi(x)$ be the strain at any x. Then, in general, there is a space charge $\rho(x) = -\partial P(x)/\partial x = -\epsilon\, \partial x_\xi(x)/\partial x$. Poisson's equation gives

$$\frac{\partial^2 V(x)}{\partial x^2} = -\frac{\partial E(x)}{\partial x} = -\frac{4\pi\rho(x)}{k''} = \frac{4\pi\epsilon}{k''}\frac{\partial x_\xi(x)}{\partial x}$$

whence

$$E(x) = -\frac{4\pi\epsilon x_\xi(x)}{k''} + C \tag{346}$$

where $E(x)$ is the field at x due to the space charge. The constant C is a function of the distribution of ρ from $-e/2$ to $+e/2$. It represents the field at the surfaces of the plate. In general, the distribution of ρ is such that there is a polarization charge on each outer surface, with a surface density σ, and the constant C may be regarded as the contribution $-4\pi\sigma/k''$ made by σ to the field.

The field $E(x)$ causes a piezoelectric stress $X'_\xi(x) = -\epsilon E(x)$. X'_ξ is of the nature of a *body stress*, balanced by an equal and opposite elastic restoring stress.† It is the latter that is to be added to the constant-field elastic stress $-q^E x_\xi(x)$, where q^E is the appropriate isagric elastic coefficient. The total stress at x is now

$$X_\xi(x) = -q^E x_\xi(x) - \frac{4\pi\epsilon^2 x_\xi(x)}{k''} + \epsilon C \equiv -q x_\xi(x) + \epsilon C \tag{347}$$

where

$$q = q^E + \frac{4\pi\epsilon^2}{k''} \tag{347a}$$

* The expression for the effective stiffness was first derived by the author[107] in 1936. The problem was attacked independently by Baumgardt[30] in 1938, who, however, failed to take all factors into account.

† See the discussion of Eq. (186), §126.

This expression holds for all thickness vibrations, including overtones. The term ϵC, not containing $x_\xi(x)$ as a factor, does not contribute directly to this expression for the effective stiffness. As will be seen, ϵC includes the effect of the gap, and its influence on the frequency can be expressed either as an effective change in thickness or, indirectly, as a further contribution to the effective stiffness.*

Equation (347*a*) is a special case of Eq. (272*a*), which expresses the stiffness coefficient c^*_{hh} at *constant normal electric displacement*, relating the stress X_h with the strain x_h when the electric field in the crystal is in the m-direction.

249. In order to evaluate the stress ϵC it is necessary to know the field distribution throughout the plate. For this purpose we start with the assumption that the distribution of strain x_ξ is sinusoidal in the X-direction, passing through zero at intervals of $\lambda/2$. The piezoelectric polarization $P = \epsilon x_\xi$ has a similar sinusoidal form, as is shown in Fig. 54. For the narrow band of frequencies in the region of resonance the difference between the thickness e of the plate and the half wavelength is too small to be appreciable in the figure. The electrodes are at A' and B', with a total gap $w = A'A + B'B$. The potential difference between the electrodes is here assumed to be zero. In the actual resonator the instantaneous driving field due to the impressed voltage between the electrodes would have to be added to the values shown in the figure, but this would not affect the present argument. Figure 54 represents conditions at the fundamental frequency. For an overtone frequency the portion from A to B may be taken as representing a single segment of the plate. The following equations hold at the fundamental frequency and odd (approximate) harmonics ($h = 1, 3, 5, \ldots$). As a first approximation it is assumed that e is $h\lambda$, where λ is the wavelength.

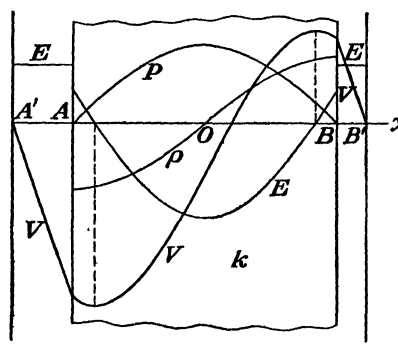


FIG. 54.—Distribution of polarization P, space charge ρ, field strength E, and potential V, in a resonator for thickness vibrations. The origin is at O, and the thickness of the plate is AB.

At any x the instantaneous strain (§246) is $x_\xi(x) = x_\xi(0) \cos(\pi hx/e)$, where $x_\xi(0)$ is the maximum strain (this is a maximum in space, *viz.*, at the origin, and not the maximum in a cycle). The polarization due to the strain is $P = \epsilon x_\xi(0) \cos(\pi hx/e)$. The space-variation of P gives rise

* For a comparison with the effective stiffness of a *bar*, see §251.

to a space charge,* of value

$$\rho = -\frac{\partial P}{\partial x} = \frac{\pi h \epsilon x_\xi(0)}{e} \sin \frac{\pi h x}{e} \equiv \rho_0 \sin \frac{\pi h x}{e}$$

The field in the crystal due to this distribution of space charge can be derived by a method previously given by the author.[106,†] The value at any x, for a crystal of thickness e, vibrating at such a frequency that the wavelength of the elastic wave is $2e/h$, is

$$E(x) = -\frac{4\rho_0 e}{hk''}\left(\cos\frac{\pi h x}{e} - \frac{2e}{\pi h e_r'}\right) = -\frac{4\pi\epsilon x_\xi(0)}{k''}\left(\cos\frac{\pi h x}{e} - \frac{2e}{\pi h e_r'}\right) \quad (348)$$

where e_r' has the value

$$e_r' = e + k''w \quad (348a)$$

This expression is the special form assumed by Eq. (346) when the distribution of x_ξ and of ρ is sinusoidal. Comparison with Eq. (346) shows that

$$C = \frac{8\epsilon e x_\xi(0)}{hk'' e_r'} = E\left(\frac{e}{2}\right) = -\frac{4\pi\sigma}{k''}$$

At infinite gap $C = 0$.

From Eq. (347) the stress due to C is

$$\epsilon C = \frac{8\epsilon^2 e x_\xi(0)}{hk'' e_r'} = -\frac{4\pi\epsilon\sigma}{k''} \quad (349)$$

Since the gap is included in e', it is clear that the stress ϵC is responsible for the effect of the gap on the resonant frequency f_0. The space charge *in* the crystal affects f_0 through the term $4\pi\epsilon^2/k''$ in Eq. (347), while the surface charge *on* the crystal affects f_0 through the stress ϵC.

250. The effect of this stress, or of the C-field, has been expressed in various ways. Bechmann[39] shows that the resonant frequency is very approximately expressed (in the notation of this book) by

$$\omega_{h0} = \frac{\pi h(1 - \gamma_h)}{e}\sqrt{\frac{q}{\rho}} \quad (350)$$

where

$$\gamma_h = \frac{16\epsilon^2 e}{\pi h^2 k'' q e_r'} \quad \text{(Bechmann's } \gamma_n\text{)} \quad (350a)$$

* Here we encounter a fundamental difference between thickness and lengthwise vibrations. In the bar the instantaneous polarization varies sinusoidally at resonance from one end of the bar to the other but *does not vary in the direction of the field* (as long as the field is at right angles to the bar). Space charge is present in the bar only when the electrodes are at the ends.

† The effects of space charge on the performance of resonators seem to have been considered first by Laue,[309] who found it to be negligible in his theory of the bar vibrating lengthwise. The subject was considered later in papers by Giebe and Scheibe,[169,171] Kobzarev,[265] and Koga.[270]

and h is an odd positive integer. The factor $(1 - \gamma_h)$ is very slightly less than unity. The quantity γ_h diminishes rapidly with increasing h and approaches zero (owing to e_r') as the gap approaches infinity. Hence, for large values of h the overtone frequencies approach harmonic ratios, a fact that was utilized by Atanasoff and Hart in their determination of the elastic constants of quartz (§90).

One may say that the effect of our constant C in Eq. (349) is to increase the effective thickness of the plate from e to $e/(1 - \gamma_h)$. This concept is used explicitly by Lawson,[313] who uses in place of e a length s_r, given approximately by

$$\frac{1}{s_r} = \frac{1}{e} - D_r - eD_r^2 \tag{351}$$

where $D_r \equiv 16\epsilon^2/\pi h^2 k'' q e_r'$. Ignoring the term eD_r^2, which is usually negligibly small, one sees that Lawson's D_r is identical with Bechmann's γ_h/e and that $(1 - \gamma_h)/e$ is identical with $1/s_r$. We write

$$e_h \equiv s_r \approx \frac{e}{1 - \gamma_h} \tag{352}$$

to denote the *effective thickness* of the plate in the neighborhood of a resonant frequency corresponding to any odd integral value of h. Then, in agreement with both Bechmann and Lawson, we may express the frequency thus:*

$$\omega_{h0} = 2\pi f_{h0} = \frac{\pi h}{e_h}\sqrt{\frac{q}{\rho}} \tag{353}$$

where, by Eq. (347a), $\qquad q = q^E + \dfrac{4\pi\epsilon^2}{k''}$

As an alternative to Eq. (350) one may put the factor $(1 - \gamma_h)$ under the radical sign. Then, from Eqs. (347a) and (351),

$$\omega_{h0} = \frac{\pi h}{e}\sqrt{\frac{q(1 - \gamma_h)^2}{\rho}} \approx \frac{\pi h}{e}\left(\frac{q^E + \dfrac{4\pi\epsilon^2}{k} - \dfrac{32\epsilon^2 e}{\pi h^2 k'' e_r'}}{\rho}\right)^{\frac{1}{2}} \equiv \frac{\pi h}{e}\sqrt{\frac{q'}{\rho}} \tag{354}$$

* At one point Bechmann's theory differs from that of all others who have derived the piezoelectric contribution to the stiffness. In place of $4\pi\epsilon^2/k''$ he finds $8\pi\epsilon^2/k''$, which must be regarded as an error. Moreover, as far as one can judge from experimental values of stiffness, for example, those of Atanasoff and Hart,[12] it appears that the isagric stiffness, when calculated from the observed q by the equation

$$q^E = q - 4\pi\epsilon^2/k'',$$

agrees better with Voigt's static values than does $q^E = q - 8\pi\epsilon^2/k''$.

where the *effective stiffness*, including the gap effect, is, to a high degree of approximation,

$$q' = q^E + \frac{4\pi\epsilon^2}{k''} - \frac{32\epsilon^2 e}{\pi h^2 k'' e'_r} = q^E + \frac{4\pi\epsilon^2}{k''}\left(1 - \frac{8e}{\pi^2 h^2 e'_r}\right) \tag{355}$$

This equation, with $h = 1$, is the one derived by the author[107] by another method, to express the effective stiffness q' for a plate with gap. Within experimental errors it yields values of the frequency in agreement with those derived from Lawson's and Bechmann's formulas.

At *zero gap*, $e'_r = e$, and Eq. (355) leads to the following expression for the effective stiffness q_0:

$$q_0 = q^E + \frac{4\pi\epsilon^2}{k''} - \frac{32\epsilon^2}{\pi h^2 k''} \equiv q - \frac{32\epsilon^2}{\pi h^2 k''} \tag{356}$$

where q has the value given in Eq. (347*a*).

When the gap is infinite and also when the order of harmonic h is sufficiently high, the third term in Eq. (355) vanishes; q' then becomes identical with q in Eq. (347*a*) and has the same form as Eq. (272*a*), as it should, since, when $w = \infty$, there is no electric displacement normal to the plate. In the general case of thickness vibrations, however, it has been shown in §246 that the mechanical displacement ξ may make any angle with respect to the coordinates. Hence, assuming as in Eq. (272*a*) that the thickness direction is denoted by m, it is evident that the elastic coefficient relating the strain $\partial\xi/\partial m$ to the corresponding stress belongs to an axial system different from that in terms of which the dimensions of the plate are expressed. In those special cases in which ξ is normal or parallel to the plate, Eq. (272*a*) becomes identical with (347*a*), since ϵ then simplifies to e_{mh}, the subscript h denoting the particular type of strain. In the more general case the obliquity of ξ is taken care of by giving the proper value to ϵ, from Eq. (344).

When elastic constants are to be determined by observation of the frequency of thickness vibrations, account must be taken of the fact that, for the stiffness q occurring in the basic formula $f = (q/\rho)^{\frac{1}{2}}/2e$, the value designated by q' in Eq. (355) is to be used. Whatever the gap may be, this q' is neither the isagric nor the constant-displacement stiffness but depends on the gap. The isagric value is q^E, while the constant-displacement value q^* is $q^E + 4\pi\epsilon^2/k''$, as we have stated in the discussion following Eq. (347*a*). Both these values can be found when q', ϵ, k'', e, h, and w are known.

251. *A Comparison between the Elastic Constants for Thickness and Lengthwise Vibrations.* First it must be recalled that the elastic state of a bar in lengthwise vibration can be described as involving only a single *stress* (§§57 and 244), while with

a plate in thickness vibration we have to do with a single *strain*. It is for this reason that compliance constants are appropriate for the bar and stiffness constants for the plate.

The chief difference between the two types of resonator, with respect to the piezoelectric reaction, arises from the fact that in the bar the strain is uniform in the field direction (assuming the field to be perpendicular to the length of the bar), while in the plate the strain in the field direction varies sinusoidally. For the bar an equation similar to (346) can be derived, but the boundary conditions are such that the constant C, which depends on the gap, assumes at zero gap a value that reduces the piezoelectric field to zero. It is for this reason that the compliance at zero gap has the isagric value s^E_{nn}. On the other hand Eq. (348) shows that in the plate the field does not vanish at zero gap (set $e'_r = e$ in this equation); the constant C is such that there is no value of w at which the stiffness has the isagric value.

It has been shown that, if the stiffness of the plate is defined as q in Eq. (347a), it is necessary in the frequency equation (353) to introduce an "effective thickness" e_h in place of the actual thickness e. A similar process could be carried out in the case of the bar, if for the compliance at all gaps one were to take the constant-displacement value s^*_{nn} given by Eq. (331); the correct resonant frequency would then be given by substituting in the frequency equation in §237 a suitable "equivalent length" l_h in place of l. The equation would then be $(f^w_{h0})^2 = h^2/4l_h^2\rho s^*_{nn}$. When $w = \infty$, $l_h = l$.

In summary, it is seen that the stiffness q^* at constant normal displacement [the q of Eq. (347a) for plates or $1/s^*_{nn}$ of Eq. (331) for bars], when used in the equation for frequency along with the actual dimension of the resonator (e or l), gives the correct value of the resonant frequency when the gap is infinite, for both plate and bar. As w diminishes from ∞ to 0, if the dimension of the plate is left uncorrected in the formula, the decrease in frequency has to be explained by saying that the effective stiffness decreases from q^* to $q^E = 1/s^E_{nn}$ in the case of the bar and to the value q_0 in Eq. (356) in the case of the plate. The objection to this explanation is that it makes the stiffness, and therefore the wave velocity, depend upon both gap and order of harmonic. If the wave velocity is to be regarded as an intrinsic property of the material, it becomes necessary to consider q^* as the true stiffness under all circumstances. This consideration requires us to insert a factor [$(1 - \gamma_h)$ in the case of the plate] in the frequency equation to take care of the apparent variation in stiffness; this factor may be interpreted as a small correction to the dimension of the resonator in the direction of wave propagation.

For practical purposes it is convenient to regard the effective stiffness as variable with the gap and, in the case of the plate, variable with the order of harmonic. No correction factor is then needed for e or l. For the plate we use q' as given in Eq. (355). For the bar, the effective compliance is s^w_{nn}, given by Eq. (330), a value that we have used in the theory of lengthwise vibrations.

252. Procedure for Deriving the Elastic Constants from Observations of the Frequency of Thickness Vibrations. Now that the effect of piezoelectric reactions on the stiffness in thickness vibrations has been treated, we are in a position to indicate how the fundamental isagric constants (or, if desired, the constants at constant polarization) may be calculated from measurements of frequency.

It is desirable to avoid having to make a correction for gap or for the effective thickness e_h in Eq. (353). According to Eq. (355) one can either observe with a gap so wide that $e'_r \to \infty$ or excite the plate at a high

harmonic ($h = 7$ at least) or both. The equation for effective stiffness q is then (347a). Plated crystals ($w = 0$) may be used, although the metallic coating affects the frequency somewhat. With thickness vibrations this source of error is eliminated by observing at a high harmonic frequency. The lateral dimensions of the plate should be sufficiently great to avoid coupling with other modes and to permit the use of the theory for infinite plates. A safe minimum value for the ratio of lateral dimension to half wavelength is perhaps 20. The shape of the plate, and the orientation of its edges are usually quite arbitrary as long as they are not such as to encourage coupling effects. Most investigators have used square plates.

Unless otherwise stated, it will be assumed that the plate is between two electrodes of large area, so that the driving field is normal to the surface.

It is perhaps needless to say that for precise results the plate must be made accurately plane-parallel, and its thickness and density must be known to the necessary order of precision. The plate should be free from optical and electrical twinning and so mounted as to leave the major faces free from external stresses. A simple and satisfactory mounting consists simply in standing the plate on edge. The orientation of the normal to the plate should be accurately determined, preferably by X-rays.

The oscillator circuit must be capable of fine frequency regulation and sufficiently stable to prevent reaction from the crystal. The latter should therefore be very loosely coupled to the oscillator. Theoretically, the observed frequency f_{h0}, from which q is found by the use of Eq. (343), should be that at which the current in the LCR-branch of the equivalent network is a maximum. Practically, a sufficiently close approximation is reached by observing either (1) the frequency for maximum current to the resonator, for example by means of a vacuum-tube voltmeter, or (2) the frequency at the bottom of the "crevasse" (§316). To avoid disturbances from varying temperature, the current to the crystal should be extremely small.

253. *First Method.* It is assumed that the observed values of q have the form of Eq. (347a), the gap effect having been eliminated. We have seen that q is the effective stiffness at *constant normal electric displacement.* Its value may be reduced to q^E with the aid of Eq. (344), in which case the solution of a set of equations of the form of (118) gives the isagric constants at once. There must be at least as many values of q as there are constants to be derived. Usually the same vibrational mode is used, with cuts rotated by different amounts about some one axis. The mathematical calculation is carried out in the same manner as in the second method below. The coefficient ϵ must be calculated for each

orientation, a process that is often more laborious than that now to be described.

A *second method* consists in leaving q uncorrected and applying the correction to the coefficients c_{hk} separately.

Whichever method is selected, it is advantageous to express the Γ's in Eqs. (118) with respect to a system of axes of which one is normal to the plate. We may assume the X'-axis to be thus chosen; it is then, of course, parallel to the thickness. Using primed symbols in Eqs. (116), we now have $l' = 1, m' = n' = 0$. Analogous and equally simple expressions are formed by letting $m' = 1$ or $n' = 1$. When $l' = 1$, all terms but the first in Eqs. (116) vanish. In place of Eq. (118) we have, after interchanging rows and columns in the determinant,

$$\begin{vmatrix} c'_{11} - q & c'_{15} & c'_{16} \\ c'_{15} & c'_{55} - q & c'_{56} \\ c'_{16} & c'_{56} & c'_{66} - q \end{vmatrix} = 0 \tag{357}$$

This equation is to be solved for q, giving in general three different expressions for q, each being a function of the c'_{hk}. From a knowledge of the piezoelectric properties of the crystal one usually knows by inspection which of the three q's is effective in any given case. This is especially true when Eq. (357) is factorable, so that one value of q is simply c'_{11}, c'_{55}, or c'_{66}. In any case the vibration direction ξ, and hence the strain $\partial\xi/\partial x'$ (§67), can be found from Eq. (117).

If the first method mentioned above is used, the piezoelectric correction is applied to q. The c'_{hk} in Eq. (357) are then isagric, and from them the fundamental isagric constants can be found by means of the formulas for rotated axes.

In the second method each c'_{hk}, like the uncorrected q, has a value corresponding to constant normal displacement, which in Eq. (272) has been denoted by c^*_{hk}:

$$c^*_{hk} = c'^E_{hk} + \frac{4\pi e'_{1h} e'_{1k}}{k''_{x'}} \tag{358}$$

Each c'_{hk} in Eq. (357) is to be replaced by the right-hand side of Eq. (358), every c'^E_{hk} having first been expressed in terms of the fundamental isagric constants by the formulas for rotated axes. If in all there are n such fundamental constants in Eq. (357), there must be at least n observed values of q, each for a different orientation.

An example of the application of the foregoing theory to quartz is given in §93 and to Rochelle salt in §§77 and 207.

Sometimes the number of fundamental elastic constants that can be determined with a given set of crystal plates in different orientations can be extended by observing q with the driving field *parallel* to the surfaces

of the plate. Other piezoelectric constants of the crystal are thus brought into play, leading to another of the three possible solutions of Eq. (357), which remains unchanged, whatever may be the direction of the driving field.

254. The Electrical Characteristics of a Plate in Thickness Vibration. The mechanical driving stress is

$$X_\xi = -\epsilon E_1 = -\frac{\epsilon V}{e_r'} = -\frac{\epsilon V_0 \epsilon^{j\omega t}}{e_r'} \tag{359}$$

where E_1 is the driving field, V is the impressed potential difference between the electrodes, ϵ is given by Eq. (344), and $e_r' = e + k''w$. With the aid of this expression, a general equation for the amplitude of mechanical vibration can be derived, by a method analogous to that in §57 for a bar. Of greater interest is the expression for the current to the resonator, which will now be derived.

As in the case of the bar, the current per unit area is $(\partial D/\partial t)/4\pi$, where D is the vector sum of two components of electric displacement. For the plate, one component is $D_1 = k''E_1 = k''V/e_r'$, the displacement in the *clamped* plate due to the impressed field. The other component is D_v due to the state of strain. From Eq. (348),

$$D_v = E_w = k''E\left(\frac{e}{2}\right) = \frac{8\epsilon e x_\xi(0)}{he_r'} \tag{360}$$

where E_w is the field in the gap.

The strain $x_\xi(0)$ at the origin is now to be derived from the general equation (313). One replacing x_n by x_ξ, l by e, and setting $x = 0$, one has, with the aid of Eq. (359),

$$x_\xi(0) = -\frac{X\xi_0 \epsilon^{j\omega t}}{q' \cosh(\gamma e/2)} = \frac{\epsilon V_0 \epsilon^{j\omega t}}{q' e_r' \cosh(\gamma e/2)} \tag{361}$$

From Eq. (74) this expression, after obvious approximations,† becomes

$$x_\xi(0) = -j\frac{2\omega_0 \epsilon V_0 \epsilon^{j\omega t}}{\pi q' e_r'} \frac{\alpha_h + jn_h}{\alpha_h^2 + n_h^2} \tag{361a}$$

where the fundamental frequency is $f_0 = \omega_0/2\pi$, α_h is the damping constant at the frequency $f = f_h = \omega_h/2\pi$, $n_h = \omega_{h0} - \omega_h$, and $f_{h0} = \omega_{h0}/2\pi$ is the resonant frequency (maximum particle velocity and maximum piezo current) at harmonic h.

* Advantage was taken of this fact by Atanasoff and Hart[12] in their observations with quartz plates.

† Since $c = 2f_0 e = \omega_0 e/\pi$, Eq. (74) may be written as $\gamma \approx (\pi/\omega_0 e)(\alpha + j\omega)$. It is then easily proved that $\cosh \gamma e/2 \approx (\pi/2\omega_0)(n + j\alpha)$. At harmonic h, ω has the value ω_h.

The value of $x_\xi(0)$ from Eq. (361a) is now substituted in (360) to give D_v. From this and the foregoing expression for D_1 we obtain, for the instantaneous current flowing to a plate of area A,

$$I = \frac{\omega_h A V_0 e^{j\omega t}}{4\pi e_r'}\left(jk'' + \frac{16\epsilon^2 e\omega_{h0}}{\pi q' e_r' h^2}\frac{\alpha_h + jn_h}{\alpha_h^2 + n_h^2}\right)$$

or, since $\omega_h \approx \omega_{h0} = \pi ch/e$, where $c = (q'/\rho)^{\frac{1}{2}}$,

$$I = \frac{chA V_0 e^{j\omega t}}{4ee_r'}\left(jk'' + \frac{16\epsilon^2 c}{q' e_r' h}\frac{\alpha_h + jn_h}{\alpha_h^2 + n_h^2}\right) \tag{362}$$

Except for the difference in notation, this equation can be shown to be in complete agreement with Bechmann's corresponding expression[40] [his equation (55)], if in place of n_h one writes $n_h(1 - \gamma_h)^2$. For all practical purposes the difference is negligible.

255. Equivalent Electric Constants for Thickness Vibrations. As we did in the case of Eq. (319) for lengthwise vibrations, so here we write Eq. (362) in the form

$$I = V_0 e^{j\omega t}(g' - jb' - jb'') \equiv V_0 e^{j\omega t} Y_1'$$

where

$$g' = \frac{4\epsilon^2 c^2 A \alpha_h}{q' e e_r'^2(\alpha_h^2 + n_h^2)}$$

$$b' = -\frac{4\epsilon^2 c^2 A n_h}{q' e e_r'^2(\alpha_h^2 + n_h^2)}$$

$$b'' = -\frac{chAk''}{4ee_r'} = -\frac{\omega_h A k''}{4\pi e_r'}$$

For the vibrational terms (those containing α and n), the electrical impedance is

$$Z' = \frac{1}{g' - jb'} = R_h' + jX_h'$$

where, on substituting q'/ρ for c^2, one has

$$\left.\begin{aligned} R_h' &= \frac{\rho e e_r'^2}{4\epsilon^2 A}\alpha_h = \frac{\pi^2 h^2 e_r'^2}{8\epsilon^2 e A} F \\ X_h' &= -\frac{\rho e e_r'^2}{4\epsilon^2 A} n_h = \omega_h L_h' - \frac{1}{\omega_h C_h'} \end{aligned}\right\} \tag{363}$$

The two expressions for R_h are valid, whatever may be the dependence of the damping constant α or of the frictional coefficient F [Eqs. (61) and (67)] upon frequency. If F is constant, R_h varies with h^2.

As in §232, one finds, with the aid of Eq. (354), for L_h' and C_h' the expressions

$$\left.\begin{aligned} L'_h &= \frac{\rho e e'^2_r}{8\epsilon^2 A} \\ C'_h &= \frac{8\epsilon^2 A e}{\pi^2 h^2 q e'^2_r (1-\gamma_h)^2} = \frac{8\epsilon^2 A e}{\pi^2 h^2 q' e'^2_r} \end{aligned}\right\} \tag{364}$$

For the non-vibrational branch of the network we have

$$C'_1 = \frac{k'' A}{4\pi e'_r} = \frac{k'' A}{4\pi(e + k'' w)} \tag{365}$$

The discussion of the equivalent electric constants in §§232 to 234 applies equally to thickness vibrations. In particular, the *electromechanical ratio* r for thickness vibrations has a value that will now be derived. We need first the expression for the lumped mechanical constants, *viz.*, the mechanical resistance W_h, stiffness G_h, and mass M_h, for any harmonic h. By the method outlined in §§62 and 63 they are found to be

$$\left.\begin{aligned} W_h &= \rho e A \alpha_h \qquad M_h = \frac{\rho A e}{2} \\ G_h &= \omega^2_{h0} M_h = \frac{\pi^2 A h^2 q (1-\gamma_h)^2}{2e} \end{aligned}\right\} \tag{366}$$

On comparing these values with the equivalent electric constants from Eqs. (363) and (364) we find for the *electromechanical ratio*

$$r = \frac{Z'_h}{(Z_c)_h} = \frac{R'_h}{W_h} = \frac{1}{C'_h G_h} = \frac{L'_h}{M_h} = \frac{e'^2_r}{4\epsilon^2 A^2} \tag{367}$$

where Z_c is the mechanical impedance.

This ratio depends, through e'_r, on the gap, but it is independent of the order of harmonic.

The equivalent electrical network for thickness vibrations is the same as for lengthwise vibrations, illustrated in Fig. 50 and discussed more fully in Chap. XIV.

In the table on page 323 are the values assumed by the mechanical and electric constants for gaps zero and infinity.

Electrically, the crystal becomes a more and more feeble resonator as $w \to \infty$, but the product $L'_h C'_h$ is always such that the resonant frequency has the values given in the table.

256. Effect of Gap upon Frequency of Thickness Vibrations. As in §237 we let f^w_{h0} and f_{h0} denote the resonant frequencies at gaps w and zero. For γ_h we write γ^w_h and γ^0_h. Then, from Eqs. (350) and (350*a*),

$$f^w_{h0} - f_{h0} \equiv \Delta f_{h0} = \frac{h}{2e}\sqrt{\frac{q}{\rho}}\,(\gamma^0_h - \gamma^w_h)$$

and

$$\frac{\Delta f_{h0}}{f_{h0}} \approx \frac{16\epsilon^2 w}{\pi h^2 q e'_r}\,(1 + \gamma^0_h + \gamma^{0^2}_h) \tag{368}$$

TABLE XXII

Constant	$w = 0$	$w = \infty$
W_h	$\rho e A \alpha_h$	$\rho e A \alpha_h$
M_h	$\frac{\rho A e}{2}$	$\frac{\rho A e}{2}$
G_h	$\frac{\pi^2 A h^2}{2e}\left(q - \frac{32\epsilon^2}{\pi h^2 k''}\right)$	$\frac{\pi^2 A h^2 q}{2e}$
R_h'	$R_h = \frac{\rho e^3 \alpha_h}{4\epsilon^2 A}$	∞
L_h'	$L_h = \frac{\rho e^3}{8\epsilon^2 A}$	∞
C_h'	$C_h = \frac{8\epsilon^2 A}{\pi^2 h^2 e(q - 32\epsilon^2/\pi h^2 k'')} \equiv \frac{8\epsilon^2 A}{\pi^2 h^2 e q_0}$	0
C_1'	$C_1 = \frac{k'' A}{4\pi e}$	0
f_{h0}	$\frac{h^2}{4\rho e^2}\left(q - \frac{32\epsilon^2}{\pi h^2 k''}\right)$	$\frac{h^2 q}{4\rho e^2}$

If $\Delta' f_{h0}$ is defined as $f_{h0}^{\infty} - f_{h0}^{w}$, where f_{h0}^{∞} at infinite gap is taken as the basic frequency, the expression becomes

$$\frac{\Delta' f_{h0}}{f_{h0}^{\infty}} = \gamma_h^w = \frac{16\epsilon^2 e}{\pi h^2 k'' q e_r'} \tag{369}$$

Lawson's analysis introduces a second-order term, according to which the gap correction, in the present notation, is

$$\frac{\Delta' f_{h0}}{f_{h0}^{\infty}} = \frac{16\epsilon^2 e}{\pi h^2 k'' q e_r'}\left(1 + \frac{16\epsilon^2 e}{\pi h^2 k'' q e_r'}\right) \tag{369a}$$

Unless ϵ is very large, the last fraction is insignificant, so that Eq. (369) suffices for use in any investigation in which f_{h0}^{∞} is taken as the basic frequency.

For experimental tests it is usually more convenient to use Eq. (368). If, as is the case with most crystals, $\gamma_h^0 << 1$, this equation becomes

$$\frac{\Delta f_{h0}}{f_{h0}} \approx \frac{16\epsilon^2 w}{\pi h^2 q e_r'} \equiv U \frac{w}{h^2 e_r'} \tag{370}$$

where $U = 16\epsilon^2/\pi q$ is a constant for the crystal. As will be shown in §353, the total change in frequency for quartz, as w increases from 0

to ∞, is of the order of 1 per cent at the fundamental frequency, when $h = 1$.

Equation (370) shows that with increasing h the gap correction rapidly becomes negligible. With h as large as 7 or 9, the frequency can usually be considered as independent of the gap, and from then on the overtones have practically harmonic ratios, as explained in §250.

From observations of the gap effect in thickness vibrations an approximate value of the piezoelectric constant can be derived by means of Eq. (370).

For any given gap the ratio $\Delta' f_{h0}/f_{h0}$ is very approximately equal to $C_h'/2C_1'$. When $w = 0$, the ratio becomes $C_h/2C_1$, where C_h and C_1 are the values at *zero* gap. But, according to Eq. (401), $C_h/2C_1$ is the relative difference between the frequencies for parallel resonance and series resonance. Thus the foregoing results for thickness vibrations illustrate the general fact concerning series and parallel resonance stated in §291 after Eq. (439*a*). For further statements concerning the ratio $C_h'/2C_1'$ and its relation to the electromechanical ratio r, see §280.

257. The Maximum Safe Resonator Current. The maximum current depends on the maximum strain that the crystal can undergo before breaking, and this in turn depends on the vibrational mode. As an example of the calculation we consider the case of lengthwise vibrations in an X-cut quartz bar, length parallel to Y. From the tensile strength of 1,000 kg/cm^2 given in §328 and the elastic compliance $s_{11} = 1.30(10^{-12})$ one finds for the breaking strain $y_y \approx 0.0013$. Rupture may be expected to start at the center of the bar, where the strain is greatest. The relation between $(y_y)_0$ at this point and the piezo current I_p can be found with the aid of Eqs. (88), (97), and (329). At the fundamental resonant frequency ($h = 1$) and zero gap one finds

$$I_p = 2ebc(y_y)_0 \text{ esu} \tag{371}$$

where $c = \sqrt{q/\rho}$ and b is the breadth of the bar. For quartz the effective piezoelectric coefficient ϵ is $e_{11} = 5.2(10^4)$, while $c = 5.4(10^5)$ cm/sec. Hence, if $(y_y)_0 = 0.0013$, we have $I_p = 7.3b(10^7)$ esu $= 24b$ ma. Thus, if $b = 1.5$ cm, $I_p = 36$ ma. At resonance I_p may be taken as the current to the entire resonator, since the portion in the parallel capacitance C_1 is then relatively small.

Since the piezo current I_p is approximately proportional to the strain at all frequencies in the resonance range, the value calculated above holds also when, as in most types of piezo oscillator, the crystal is vibrating near its antiresonant frequency. The only difference is that in order to produce the same I_p the voltage across the crystal must be higher, causing the current in C_1 to be greater. Therefore, near antiresonance the total safe current can be greater than at resonance.

The foregoing estimate of I_p gives the maximum possible value at resonance under ideal conditions. The value would be different for other cuts and other modes of vibration. In actual cases overtones of various modes, as well as defects in the crystal, are likely to produce localized stresses sufficient to cause fracture at currents far below the ideal value.

In general, larger currents per square centimeter of electrode area can be used with thickness than with lengthwise vibrations. With some thickness resonators of average size, currents as great as 100 ma can be used safely. Nevertheless, the experimenter would do well not to let the crystal current exceed 20 ma/cm^2 with thickness vibrations or 10 ma/cm^2 with lengthwise vibrations. Not only does this precaution safeguard the crystal, but it also avoids undue heating and consequent change in frequency.

258. Anomalous Dispersion in the Resonator. Just as a crystal is often regarded as a single large molecule, so the macroscopic dielectric properties of a piezo resonator at radio frequencies simulate the molecular behavior of matter in the infrared and optical regions. While this similarity is shown to some extent also by such electromagnetic devices as telephone receivers, the analogy is closer in the case of piezoelectric resonators.

We saw in §116 that when the particles of which a substance is composed have a natural frequency in the optical spectrum, the substance exhibits *anomalous dispersion* for radiation in the neighborhood of this frequency. The medium becomes highly absorptive, and the index of refraction, and hence the dielectric constant, increases with increasing frequency to a maximum, decreases to a minimum, finally approaching a value somewhat lower than that on the l-f side of resonance. Since, in electrical language, the vibrating system possesses both reactance and resistance, it is customary to express both the refractive index and the dielectric constant as complex quantities, as is shown in Eq. (181) for the dielectric constant.

In the following sections we shall first show how the equivalent electrical admittance of the entire resonator can be expressed in terms of a complex dielectric constant and then trace the dependence of this constant upon frequency. The dielectric constant and resistance (or decrement) of the resonator correspond to the refractive index and coefficient of absorption in the optical case. The discussion will be confined to lengthwise vibrations, but in principle it is applicable to piezo resonators vibrating in any other mode.

In its most general form the complex dielectric constant k_c would be written as in Eq. (181), with b (susceptance) and g derived from Eq. (315). Since such an expression would be complex in more than one sense, it is simpler and equally instructive to take advantage of the very

low damping in piezo resonators, by writing one expression valid at frequencies sufficiently removed from resonance, and another for the resonance region.

259. Except in the immediate neighborhood of a resonance frequency, the parenthesis in Eq. (316) may be used to represent the complex dielectric constant. It is assumed that the field strength is small, so that we have to do only with the *initial* value. First it should be noted that it is the *real* part of k_c that represents the dielectric constant in the ordinary sense. In Eq. (316) the imaginary term is omitted, since the impedance of the crystal is almost exactly a pure reactance except over a

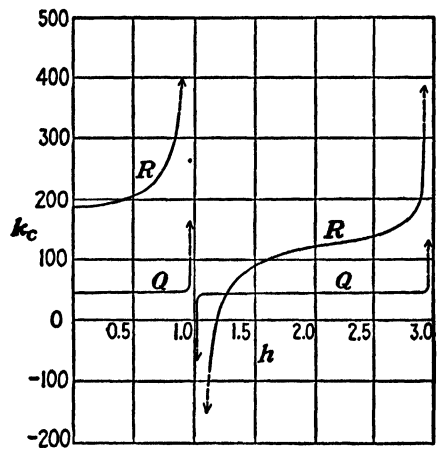


FIG. 55.—Variation of dielectric constant k_c with frequency of lengthwise vibrations. Curve Q is for quartz, R for Rochelle salt. The curves are drawn approximately to scale, except that the resonance for quartz is made to appear less sharp than would be the case with a typical quartz resonator, and that the ordinates for quartz are multiplied ten times. The data for Rochelle salt are from Mason's observations on a 45° X-cut bar, with low field strength, at 5°C. Energy losses, which limit the values of k_c at resonance, are not represented in this figure.

very narrow region close to resonance. k_c is then given very approximately by the real quantity

$$k_c = k_l + \frac{8q'd_{in}^2}{h} \tan \frac{\pi h}{2} \tag{372}$$

The dependence of k_c on frequency is governed by $h = f/f_0$, where f_0 is the fundamental frequency, f is any frequency higher than the fundamental, and h is any real positive number, integral or fractional, greater than unity. The equation shows that, as f increases indefinitely, k_c diminishes, with anomalous values in the neighborhood of frequencies for which h is an integer. This k_c is the value associated with the equivalent series capacitance C_s of the entire resonator (§271).

The variation of k_c with frequency, for lengthwise vibrations in quartz and Rochelle salt, is shown in Fig. 55 for values of h up to 3. Negative values correspond to inductive reactance.

In the case of Rochelle salt it is evident that the "anomaly" due to the fundamental resonance frequency ($h = 1$) extends over an extremely wide range of frequency. This fact is the result of the large piezoelectric constant of Rochelle salt. The quantity k_t, which we have called the "effective dielectric constant," can be identified on the curve at $h = 2$, where the crystal is driven at double frequency, as explained in §321. At zero frequency $k_c = k' = 190$. Most noteworthy is the fact that the crystal does not return to this value after the fundamental resonance, at least not until the frequency approaches the value for which $h = 3$, where the current has its second maximum.

Qualitatively the same behavior is shown by the quartz resonator. The outstanding difference is that in quartz at all frequencies, except very close to resonance, the departure of the dielectric constant from its static value is hardly perceptible. This contrast with the more pronounced curvature in the case of Rochelle salt has practically nothing to do with relative energy losses. Except over frequency bands too narrow to be indicated clearly in Fig. 55, the crystal, whether of quartz or of Rochelle salt, is essentially a pure reactance.

260. The variation of k_c close to resonance will next be considered. For this purpose we may use Eq. (319) and the network shown in Fig. 50. Let the admittance of the RLC-branch, in the notation of §232,* be denoted by $Y = g' - jb'$ and that of C_1 by $Y_1 = -jb_1 = j\omega C_1$. The admittance of the entire resonator is then

$$Y_1' = g_1' - jb_1' = g' - j(b' + b_1) = \frac{R}{Z^2} - j\left(\frac{X}{Z^2} - \omega C_1\right) \qquad (373)$$

As in §232, the complex dielectric constant is found by writing $Y_1' = j\omega C_c = j\omega blk_c/4\pi e$, whence from Eq. (373), for frequencies in the neighborhood of resonance,

$$k_c = -\frac{4\pi e}{\omega bl}[(b' + b_1) + jg'] = -\frac{4\pi e}{\omega bl}\left(\frac{X}{Z^2} - \omega C_1 + j\frac{R}{Z^2}\right) \qquad (374)$$

With the aid of Eq. (320) the real part of this expression can be proved identical with Eq. (372), as long as R can be neglected. Close to resonance the effect of R becomes appreciable, in determining the shape and finite height of the resonance peak.

* For simplicity the primes and the subscript h are dropped from R, L, C, C_1, and Z in this section.

A plot of the *dissipation component* $-j4\pi eg'/\omega bl$ of quartz against frequency, with the scale used in Fig. 55, would appear as nothing more than a horizontal straight line of very small ordinate value, rising abruptly to high values at $h = 1$ and 3. In Rochelle salt the same is true if g' is computed for the mechanical losses alone.* Nevertheless, this process would not correctly represent the dielectric behavior of Rochelle salt, owing to the presence of a resistance, which Mason calls R_0, in the C_1-branch of Fig. 50. Mason's[338] equation (63) amounts to an expression for the complex dielectric constant, but numerical data are not available for its complete evaluation (see §375).

As the frequency is increased beyond the limit shown in Fig. 55, other resonant values are encountered, at each of which the net value of the dielectric constant on the h-f side is less than on the low. These resonant values correspond to odd integral values of h up to the point where other h-f modes, compressional, torsional, flexural, or shear, depending on the lateral dimensions, begin to enter. Considering only lengthwise compressional modes, one sees from Eq. (372) that with increasing frequency the dielectric constant approaches the value k_l, which by Eq. (311) is $k_l = k_i' - 4\pi d_{in}^2/s_{nn}$. This is also the value that would be measured at all even values of h. At very high frequencies the vibrational reaction due to lengthwise compressional vibration is negligible, even at odd values of h.

If a crystal had only one piezoelectric constant, namely, that associated with compressional lengthwise vibrations, the value of k_l given above would be that of the completely clamped crystal: it would therefore be expected to hold until the optical range of frequencies was approached. In general, however, owing to the possession of other piezoelectric constants, before extremely high frequencies are reached the bar resonates in other modes, as stated above. As long as the frequency is low with respect to these other modes, then as was shown in §229 the piezoelectric strains corresponding to these modes are proportional to and in phase with the driving field. They therefore contribute to the polarization and to the effective dielectric constant. It is this effect which gives to k_l a value somewhat greater than that of the clamped dielectric constant. When with increasing frequency these other modes come successively into resonance, the crystal in effect becomes progressively more and more clamped, owing to the inertial reaction of all modes of lower frequency, until at very high frequencies, which for crystals of ordinary size are of the order of 10^7, the only vibrations are high overtones of negligible amplitude. When this stage is reached, the crystal may be regarded as completely clamped. The best values of the clamped dielectric constant

* See Mason,[338] Eqs. (57).

k'' are obtained by this method. Such measurements on Rochelle salt are discussed in §442.

From the foregoing statements it is clear that the effective dielectric constant k_l holds for all frequencies within which only compressional lengthwise vibrations need be considered. A theoretical formulation that took account of other vibrational modes and of coupling effects would lead to a different expression for k_l.

If it were possible to increase the frequency up to that of the optical range, the dielectric constant would be found to diminish still further, suffering a drop whenever a characteristic molecular frequency was passed,* until in the visible spectrum, where the refractive index is of the order of 1.5, the dielectric constant would be reduced to the order of 2.

261. Effects of Piezoelectric Vibrations on X-ray Reflections.† *a. Observations with Quartz.* In 1931 Fox and Carr[8] observed that the Laue spots due to a beam of X-rays passing through an X-cut or Y-cut quartz plate became more intense when the plate was vibrated piezoelectrically. The effect was found with all vibrational modes investigated by them, and it varied in amount with the amplitude of vibration.

This subject received considerable attention in the succeeding years. On the experimental side, the fine structure of the spots, which appears when the quartz plate is vibrating, has been studied by Cork[6] and by Barrett and Howe[1]. The latter investigators made a Laue survey of an entire X-cut plate vibrating in its thickness mode, which threw light on the highly complex nature of this mode. For further experiments on the effect of thickness vibrations see refs. [6], [9], [16], and [19].

The increase in intensity caused by the *lengthwise* vibrations of X-cut plates (compressional waves in the Y-direction) has been observed by Bertsch[2] and by Colby and Harris,[5] using the Laue method. On the other hand, Blechschmidt and Boas[2a] could find no change in intensity.

The foregoing results, obtained by the observation of Laue spots, indicate that the cause of the increase in intensity lies in the body of the crystal and is not merely a surface phenomenon. On the other hand, when an increase in intensity is sought by *Bragg* reflections, it is found, as would be expected, that the condition of the surface of the crystal is important. No increase in intensity of the radiation reflected from a *polished* surface is observed; but if the damage done to the surface by

* From the measurement of X-ray intensities H. Staub[478] has calculated a *Reststrahlen* wavelength in Rochelle salt of about 100μ. Valasek[543] predicted an absorption band at 55μ, while W. W. Coblentz ("Investigations of Infra-red Spectra," Carnegie Institution of Washington, 1905–1908) recorded an absorption band at 4.2μ. Much remains to be done with Rochelle salt in the infrared.

† Reference numbers in this section are to papers listed at the end of the chapter.

polishing is removed by etching in H_2F_2, the crystal when vibrating does show an increase in intensity, provided that the reflection does not take place from a region on the surface where there is a node of strain. These conclusions are confirmed by the observations of Colby and Harris.[5] For observations by the Bragg method see also refs. [3], [6], and [9].

On the effects of grinding and etching the surfaces, see refs. [1], [4], [6], [9], and [16]. For plates in various orientations, see refs. [12] and [19]; in the latter paper the modes of vibration are investigated by X-rays.

The increase in intensity mentioned above is confined to the characteristic radiation from the target. According to Jauncey and Bruce[14] vibrations have no effect on the diffuse radiation. The characteristic lines have been found by Colby and Harris[5] to be widened as well as increased in intensity by vibration. For a theoretical treatment see the paper by Weigle and Bleuler.[21]

From the first it has been recognized that the increased intensity of the diffracted beam when the plate vibrates is due to a decrease in extinction. The strains due to vibration have an effect somewhat analogous to that produced by polishing the surface, which destroys or disarranges the lattice in the superficial layers and allows the X-rays to penetrate more deeply. The best evidence indicates that vibration reduces the *secondary* extinction, by setting up inhomogeneous strains, warping the lattice, or causing disturbances among the inhomogeneities that are normally present in the crystal.[10],[14],[17],[18],[19]

There is evidence that *static* as well as dynamic strains cause an increase in the intensity of the Laue spots from quartz crystals. The effect was observed by Barrett and Howe[1] and by Fukushima[13] with strains produced mechanically and by Sakisaka and Sumoto,[20] who employed thermal strains. The same effect was observed by Kakiuchi[15] when the strain was caused by a static electric field.

Although it has nothing to do with the question of increase in the intensity of X-ray reflections, mention may be made here of the fact that piezoelectric strains have been calculated from their effect on Bragg reflections, by Dolejsek and Jahoda.[7] The results were found to be in agreement with the values derived from the field strength and the known piezoelectric constant. The same method as applied to Rochelle salt is mentioned in §422.

b. Results with Other Crystals. Both Rochelle salt and tourmaline show an increase in intensity of Laue spots when vibrating, though the effect is much weaker than with quartz.*

* For Rochelle salt see refs. [6] and [10]; for tourmaline, refs. [10] and [16].

The use of X-rays in the precise determination of crystal axes is mentioned in §341.

REFERENCES ON X-RAYS AND VIBRATING CRYSTALS

[1] BARRETT, C. S., and C. E. HOWE: X-ray Reflection from Inhomogeneously Strained Quartz, *Phys. Rev.*, vol. 39, pp. 889–897, 1932.

[2] BERTSCH, C. V.: X-ray Studies of Crystals Vibrating Piezoelectrically, *Phys. Rev.*, vol. 49, pp. 128–132, 1936.

[2a] BLECHSCHMIDT, E., and W. BOAS: Laue Reflexion Photographs with Vibrating Quartz Rods, *Z. Krist.*, vol. 85, p. 329, 1933.

[3] BRUCE, W. A., and G. E. M. JAUNCEY: Dependence of Diffuse Scattering of X-rays from Quartz upon the Angle between the Crystal Axis and the Plane of Scattering, (abstract) *Phys. Rev.*, vol. 49, pp. 418–419, 1926.

[4] COLBY, M. Y., and S. HARRIS: Effect of Etching on the Relative Intensities of the Components of Double Laue Spots Obtained from a Quartz Crystal, *Phys. Rev.*, vol. 43, pp. 562–563, 1933.

[5] COLBY, M. Y., and S. HARRIS: An X-ray Study of a Long X-cut Quartz Crystal Vibrating under the Transverse Piezoelectric Effect, *Phys. Rev.*, vol. 46, pp. 445–450, 1934.

[6] CORK, J. M.: Laue Patterns from Thick Crystals at Rest and Oscillating Piezoelectrically, *Phys. Rev.*, vol. 42, pp. 749–752, 1932.

[7] DOLEJSEK, V., and M. JAHODA: Variations of Lattice Dimensions in Piezoelectric Crystals Produced by Electrostatic Forces, *Compt. rend.*, vol. 206, pp. 113–115, 1938.

[8] FOX, G. W., and P. H. CARR: The Effect of Piezoelectric Oscillation on the Intensity of X-ray Reflections from Quartz, *Phys. Rev.*, vol. 37, pp. 1622–1625, 1931.

[9] FOX, G. W., and J. M. CORK: Regular Reflection of X-rays from Quartz Crystals Oscillating Piezoelectrically, *Phys. Rev.*, vol. 38, pp. 1420–1423, 1931.

[10] FOX, G. W., and W. A. FRASER: X-ray Extinction in Piezoelectrically Oscillating Crystals, *Phys. Rev.*, vol. 47, pp. 899–902, 1935.

[11] FOX, G. W., and J. R. FREDERICK: Further Study of X-ray Diffraction in Quartz, *Phys. Rev.*, vol. 53, pp. 135–136, 1938.

[12] FOX, G. W., and D. W. STEBBINS: Effect of Quartz Filters on the Distribution of Energy in Laue Patterns, *Phys. Rev.*, vol. 55, pp. 405–408, 1939.

[13] FUKUSHIMA, E.: The Relation between the Mechanical Strain and the Intensity of X-rays Reflected by a Quartz Plate, *Bull. Inst. Phys. Chem. Research (Tokyo)*, vol. 15, pp. 1–14, 1936.

[14] JAUNCEY, G. E. M., and W. A. BRUCE: Diffuse Scattering of X-rays from Piezoelectrically Oscillating Quartz, *Phys. Rev.*, vol. 54, pp. 163–165, 1938.

[15] KAKIUCHI, Y.: The Increase of X-ray Reflection from Quartz Due to a Strong Electric Field, *Phys. Rev.*, vol. 54, p. 772, 1938.

[16] KLAUER, F.: Röntgen-Laue-diagrams from Piezoelectrically Vibrating Crystals, *Physik. Z.*, vol. 36, pp. 208–211, 1935.

[17] LANGER, R. M.: X-ray Reflections from Oscillating Crystals, *Phys. Rev.*, vol. 38, pp. 573–574, 1931.

[18] LANGER, R. M.: Passage of X-rays through Oscillating Crystals, *Phys. Rev.*, (abstract) vol. 49, p. 206, 1936.

[19] NISHIKAWA, S., Y. SAKISAKA, and I. SUMOTO: X-ray Investigation of the Mode of Vibration of Piezoelectric Quartz Plates, *Sci. Papers Inst. Phys. Chem. Research*

(*Tokyo*), vol. 25, pp. 20–30, 1934; see also *Phys. Rev.*, vol. 38, pp. 1078–1079, 1931, and vol. 43, pp. 363–364, 1933.

[20] SAKISAKA, Y., and I. SUMOTO: The Effects of the Thermal Strain on the Intensity of Reflection of X-rays by Some Crystals, *Proc. Phys.-Math. Soc. Japan*, vol. 13, pp. 211–217, 1931.

[21] WEIGLE, J., and K. BLEULER: Theory of the Influence of Ultrasonic Waves on the Diffraction of X-rays by Crystals, *Helv. Phys. Acta*, vol. 15, pp. 445–454, 1942.

CHAPTER XIV

THE ELECTRICAL EQUIVALENT OF THE PIEZO RESONATOR

Mit leisem Finger geistiger Gewalten
Erbauen sie durchsichtige Gestalten;
Dann im Kristall und seiner ewigen Schweignis
Erblicken sie der Oberwelt Ereignis.

—GOETHE.

262. Introduction. In the foregoing chapter we learned that the electrical characteristics of a resonator for lengthwise or thickness vibrations, in the neighborhood of any resonant frequency, can be expressed in terms of four fixed parameters, represented in Fig. 50. Most, if not all, types of piezo resonator can be represented by the same network. In the present chapter some of the properties of this network and of other equivalent networks will be considered, with special reference to variations in frequency, gap, and the constants of the crystal.

The "equivalent network" of any electromechanical system is generally understood to mean an assemblage of R-, L-, and C-values, each independent of frequency, so interconnected that when the assemblage is substituted for the actual system in any electric circuit its effect on the circuit will be the same as that of the electromechanical system itself, at least over a certain range of frequency. In the case of the piezo resonator the electric constants of the equivalent network are chosen so as to represent the electrical behavior of the resonator in the neighborhood of a particular characteristic vibration frequency of the crystal. The frequency range over which the equivalent electric "constants" may be treated as actually constant depends largely on the nearness of other vibrational modes. In general, a crystal resonator having a given form and orientation possesses a large number of characteristic vibrational modes, each occurring at a different frequency, for each of which the resonator may be treated as if it had a single degree of freedom, with a particular set of equivalent electric constants. The equivalent network has different parameters for each mode.

Several years before the first resonators had been made from piezoelectric crystals, it was shown theoretically by Butterworth* that any mechanical vibrating device driven by a periodic emf across a condenser presents to the driving circuit an equivalent electrical impedance con-

* S. BUTTERWORTH, *Proc. Phys. Soc.* (*London*), vol. 27, pp. 410–424, 1915.

sisting of a certain resistance, inductance, and capacitance in series, the whole being shunted by a second capacitance. This paper had not come to the attention of the author[93] when he first dealt with the theory of the piezo resonator in 1922; the existence of an equivalent electrical combination was recognized, but the only combination arrived at was a resistance and a capacitance, either in series or in parallel, with values that varied with the frequency (see §§271 and 273).

The equivalent network universally adopted for the piezo resonator today was derived from the author's basic equations by Van Dyke[547,550,552] independently of Butterworth's work, but leading to the same network, as shown in Fig. 50. The equivalent electric constants in Van Dyke's network, as in Butterworth's, are *independent of the frequency.*

A little later Dye,[127,*] starting with Butterworth's theorem, derived the same network as Van Dyke and treated the theory of the piezo resonator very completely, including the effects of the gap between crystal and electrodes. Since then many papers have appeared on the subject, to some of which references will be made in due course.

It has already been shown that the Butterworth-Van Dyke-Dye network represented in Figs. 50 and 56*b* is applicable both to bars in lengthwise vibration and to plates in thickness vibration and also that, by proper choice of the equivalent constants, the same network holds when there is a gap of any width (but see §285 for the limitation in the case of unplated bars). Although the detailed theory has not been worked out for other types of resonator, there can hardly be any doubt of the universal validity of Butterworth's theorem as applied to piezoelectric vibrators, in that a piezo resonator of any type can be represented by the same form of equivalent network.

263. We shall now consider the method introduced by Dye and developed further by Watanabe,[581] by which the electric constants of a crystal with gap are equivalent to those of the crystal with zero gap, in series with which is still another condenser representing the gap. For greater simplicity, consideration of overtone frequencies will be left out of account for the present. The proper notation for overtones can be introduced at any point if desired.

The crystal and its equivalent networks are illustrated in Fig. 56. The total gap is w. The electrodes are connected to the external circuit at p and q. The equivalent constants, the gap being taken into account,

* In this paper Dye shows as an alternative network a resistance, inductance, and capacitance in *parallel*, representing the vibrational portion of the equivalent network at zero gap, in series with which is a capacitance corresponding to C_1 in Fig. 50 and another capacitance representing the gap. For a general treatment of equivalent networks see T. E. Shea, "Transmission Networks and Wave Filters," New York, 1929.

are, as before, represented by R', L', C', and C_1'; they are the same as the R_h', L_h', C_h', and C_1' of §§232 and 255. R, L, C, and C_1 are the corresponding values when $w = 0$, so that in Fig. 56c C_2 represents the capacitance of the gap. The relations between the constants in (*b*) and (*c*) are given in §284.

Throughout this discussion the assumption is made that R', L', C', and C_1' are independent of the electric field strength and of the amplitude of vibration. In other words, it is assumed that the fundamental elastic and dielectric constants are actually constant. This assumption is fully justified with such crystals as quartz or tourmaline, over all ranges of stress encountered in practice. In the case of Rochelle salt, unless the stresses are held at very low values, allowance must be made for the non-linearity between stress and strain, both mechanical and electrical.

The diagrams *b* and *c* are two different ways of representing the electrical characteristics of the crystal with gap shown in diagram *a*. As

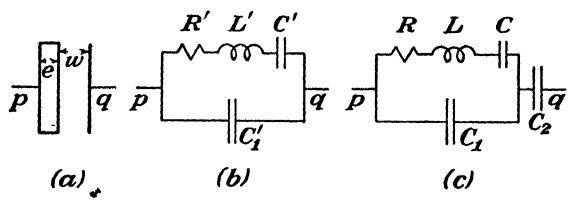


FIG. 56.—A crystal with gap, and its two equivalent networks.

will be seen in §284, by proper choice of parameters the two networks can be made equivalent, as long as the surface of the crystal exposed to the gap is always an equipotential surface; for in this case the crystal acts as if it had adherent electrodes, while the gap is a simple air condenser. Such is indeed the case with thickness vibrations, at least if the complications due to coupled modes are disregarded. As will be seen in §286, it is also the case with lengthwise vibrations of a bar when the surfaces exposed to the gap are provided with a conducting coating; if the bar is bare, the gap capacitance C_2 requires a correcting factor.

The electrical equivalents for the same crystal at several frequencies may be combined in a single network. For example, if, in addition to the vibrational mode represented by *RLC* in Fig. 56c, there are other modes or overtones represented electrically by series chains $R_1L_1C_1$, $R_2L_2C_2$, . . . , these chains, all in parallel, may be connected in parallel with *RLC*. In the neighborhood of any one resonant frequency the impedances of all but one chain are practically infinite, unless two resonant frequencies happen to come too close together. It must be recalled that C_1 has a slightly different value for each mode, as may be seen from Eqs. (311) and (323).

264. The Response Frequencies of the Resonator. There are several cases to consider, most of which are of some importance in practice.

1. The crystal is set into vibration, electrically or mechanically, and then left to itself, with the terminals p and q in Fig. 56 on open circuit (or connected to an infinite impedance). To find the frequency of free vibration and the rate of decay, one may imagine that an initial charge has been placed on the condenser C'. The discharge takes place around the path $R'L'C'$ in *series* with C_1'. The frequency of free vibration is given by $\omega^2 = 1/L'C_f - R'^2/4L'^2$, where $C_f = C'C_1'/(C' + C_1')$. The oscillographic record of the rate of decay of a vibrating quartz plate described in §320 was obtained under these circumstances. Although this frequency differs but little from the resonant frequency given by $\omega_0^2 = 1/L'C'$, still the distinction cannot be ignored.

2. The crystal is excited as in (1) but vibrates freely with *pq short-circuited.* The $R'L'C'$ chain is now connected to a zero impedance, C_1 is inoperative, and the frequency of the decaying vibrations is given by $\omega^2 = 1/L'C' - R'^2/4L'^2$, a value slightly lower than that in (1).

3. The terminals p and q are connected to a generator of variable frequency and zero internal impedance. This is the case assumed in the theoretical treatment, where an alternating potential difference of constant amplitude V_0 is impressed on the network. It is approximately realized in some experimental methods. The network has two degrees of freedom, with two characteristic frequencies. These are the well-known frequencies of *series* and *parallel resonance,* concerning which more will be said later.

4. Usually the terminals p and q are connected to a circuit on which the resonator reacts more or less strongly. The potential drop across the resonator may then vary greatly with the frequency, but the characteristics of the resonator, including the frequencies for series and parallel resonance, are the same as in (3).

The further discussion of the electrical properties of the piezo resonator can be better understood with the aid of the graphical representation, to which we now turn.

265. The Resonance Circle. The use of a circular locus for representing admittances or impedances of resonators offers many advantages.* In schematic form it makes the performance of a resonator under varying conditions evident at a glance, and it is a valuable aid in writing or interpreting equations. When carefully drawn to scale, such a diagram can often be used for deriving quantitative results, thus eliminating much laborious computation.

* The representation of the characteristics of a vibrating system by means of a circular locus was introduced in 1912 by Kennelly and his collaborators in their studies of the telephone receiver. The method is fully treated in Kennelly's "Electrical Vibration Instruments," New York, 1923.

In general, the resonance circle represents correctly the performance of a resonator over the range of frequencies in which the resonating element can be regarded as having a single degree of freedom. If the device has several resonant frequencies, a separate diagram can be drawn for each; or by a suitable choice of scale values the same diagram can be made to serve for different vibrational modes, including harmonics of the fundamental.

The characteristic electrical property of the piezo resonator is the equivalent series chain *RLC* in Fig. 56. Its admittance is very low except close to the resonant frequency defined by $\omega_0 = 2\pi f_0 = (1/LC)^{\frac{1}{2}}$. We start with the graphical representation of the *RLC*-branch, the gap being zero, and then show how the graph can be extended to more complicated networks. In the following discussion all equations and diagrams are applicable to any overtone, if to R, L, C, and C_1 are assigned the appropri-

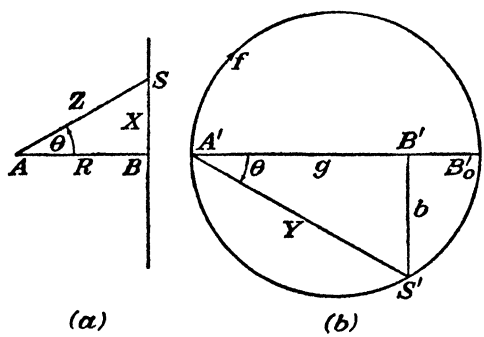


FIG. 57.—Impedance and admittance of R, L, and C in series.

ate values. They are also applicable to a crystal with gap, if for R, L, C, and C_1 are substituted the appropriate R', L', C', and C_1'. The limits within which the approximations in the equations are valid are given in §294.

The impedance of R, L, and C in series depends on the frequency as shown in Fig. 57*a*, where $X = \omega L - 1/\omega C \equiv BS$ and $Z^2 = R^2 + X^2$, or, in vector notation, $Z = R + jX$. As ω varies from 0 to ∞, $R \equiv AB$ remains constant, while the point S moves up the X-axis from $X = -\infty$ to $X = +\infty$. At the resonant frequency the phase angle $\theta = 0$, $X = 0$, and $Z = R$. Figure 57*b* represents the admittance $Y = 1/Z$ at the same frequency. We have $Y = g - jb$, where the conductance is

$$g = \frac{R}{Z^2} \equiv A'B'$$

and the susceptance is $b = X/Z^2 \equiv B'S'$. If X is positive,

$$\theta = \tan^{-1}\frac{X}{R} = \tan^{-1}\frac{b}{g}$$

is positive on both diagrams, but it is laid off clockwise in (*b*) instead of counterclockwise. At the resonant frequency, $g = 1/R$; we shall denote this value of the conductance by g_0.

In Fig. 57*b* the value of g_0 is represented by $A'B'_0$. At any frequency, $Y = 1/Z = \cos\theta/R = g_0 \cos\theta$. But this is the polar equation of a *circle* of diameter $g_0 = 1/R$. The circle itself is seen in the figure, and its circumference is the locus of $Y = A'S'$ as the frequency varies. When $f = 0$, S' is at A' and $Y = 0$. As f increases, S' travels clockwise around the circle, returning to A' at $f = \infty$.

The reason for thus emphasizing the admittance is that it must be used, graphically or analytically, when any circuit element, such as C_1 in Fig. 50 or 56, is connected in parallel with *RLC*. In the study of the resonator we seek a simple means for surveying its performance over the resonance range, when it is connected to any alternating circuit. Since both impedances and admittances have to be considered, there is a pronounced advantage in the use of a *single diagram* to represent both these quantities, instead of the two separate diagrams shown in Fig. 57.

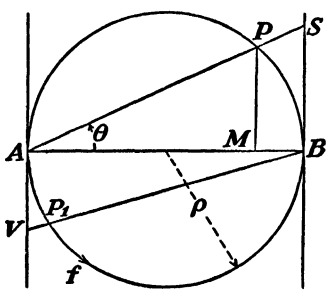


FIG. 58.—Impedance and admittance vectors combined in the same diagram.

266. In constructing any vector diagram, a unit vector, or scale value, must be selected for the particular physical quantity that is to be represented. By the proper choice of scale values the two diagrams in Fig. 57 can be superposed, with AB and $A'B'_0$ in coincidence. The result is seen in Fig. 58, where, as before, AS represents the impedance at any frequency f. A circle is drawn with an arbitrary radius ρ, expressed in convenient units of length. If the diameter $2\rho = AB$ represents R, the scale value is $s = R/AB = R/2\rho$ ohms per unit length (or esu per unit length). The reactance is $s \cdot BS$, the impedance is $s \cdot AS$, while $\tan\theta = BS/AB$ gives the phase angle.

In order that the admittance may be represented on the same diagram, we must select a scale value of admittances, say s_y, such that AB shall represent $g_0 = 1/R$. The value is

$$s_y = \frac{(1/R)}{AB} = \frac{1}{2\rho R} = \frac{s}{R^2} \tag{375}$$

reciprocal resistance units per unit distance, as for example mhos per centimeter. Then, since $Y = \cos\theta/R$ and $\cos\theta = AP/AB$, we have $Y = s_y \cdot AP$. The components of impedance are $R = s \cdot AB$ and $X = s \cdot BS$; those of admittance are $g = s_y \cdot AM$ and $b = s_y \cdot MP$.

Geometrically, we have performed an *inversion* of the vector AS with respect to a *circle of inversion** (not shown in the diagram) with center at A and radius AB. According to the principle of inversion, which in this case amounts to a statement of the fact that $(AB)^2 = AS \cdot AP$, any point S on the line $BS \perp AB$ inverts into the point P, where AS cuts the circle having AB as diameter. If AS represents an impedance for the RLC chain, AP represents, in magnitude and phase, the corresponding admittance.

The present procedure requires one departure from the usual graphical convention for admittances, in that a positive susceptance, like a positive reactance, is drawn *upward*. This practice need lead to no confusion, especially since the sign of θ is always the same for a susceptance as for the corresponding reactance. As the frequency increases from zero through f_0 to $f = \infty$, S moves upward from $-\infty$ through B (minimum impedance) to $+\infty$, while P moves *counterclockwise* around the circle from A through B (maximum admittance) and back to A. The phase angle θ is negative below the line AB ($f < f_0$, capacitive reactance), changing through zero to positive above AB ($f > f_0$, inductive reactance).†

267. *Frequency Calibration of the Resonance Circle.* In the applications of the graphical method that are to come, we shall treat the resonance circle for the admittance of the RLC branch of the resonator as the *fiducial circle*. Any vector drawn from the origin at A in Fig. 58 to a point on the circumference, as AP, represents the admittance Y of RLC:

* *The principle of inversion.* With respect to a circle of radius a and center at O, two points P and P' are said to be *mutually inverse* if they are situated on the same radius, one inside and the other outside the circle, at such distances that $OP \cdot OP' = a^2$. The circle is called the *circle of inversion*, and its center is the *center of inversion*. If the principle is applied to all the points of any geometrical figure in the plane of the circle of inversion, the inverse of this figure is obtained. It is easily proved that by inversion any circle is transformed into another circle, including the limiting case of a straight line. Every straight line is transformed into a circle passing through the center of inversion O. We shall have occasion repeatedly to make use of the fact that any given circle transforms into itself when it is tangential to a radius of the circle of inversion at a point on the circumference of the latter. Any two points on the given circle are then mutually inverse when they are on the same straight line through the center of inversion.

For the mathematical principles of inversion see, for example, Graustein, "Introduction to Higher Algebra," New York, 1930, or Ziwet and Hopkins, "Analytic Geometry and Principles of Higher Algebra," New York, 1922. For applications to alternating currents, see Lee, "Graphical Analysis of Alternating Current Circuits," Baltimore, 1928. For applications to vibrating systems, see Kennelly, "Electrical Vibration Instruments," New York, 1923. For applications to piezoelectric resonator circuits, see Vigoureux [B50,B51] and also refs. 127 and 581.

† The use of a single resonance circle to represent both admittances and impedances was introduced by the author[105] in 1933. In the paper cited will be found certain applications beyond those described in this book.

$Y = s_y \cdot AP$. As will be seen, the parallel capacitance C_1 of the resonator or any series or parallel external impedance can be represented graphically in such a manner that a resultant vector can be drawn for the impedance or admittance of the entire combination. The circle itself may function as the locus of either admittances or impedances, and the distribution of frequencies around the circle will vary according to the total network. Nevertheless, by simple graphical operations, the frequency corresponding to any vector, as, for example, the frequency for minimum impedance for a given network, can be determined in terms of the frequency distribution around the fiducial circle.

It is therefore desirable at this point to show how the fiducial circle may be calibrated for frequency, when R, L, and C are given.

To each point on the fiducial circle there corresponds a particular frequency; for example, at P in Fig. 58 the frequency $f = \omega/2\pi$ is somewhat higher than the resonant value $f_0 = \omega_0/2\pi = 1/2\pi LC$ at B. We shall show that the distance BS, measured upward or downward from B to the point S where the line AP produced cuts the vertical axis through B, is very nearly proportional to the frequency difference $f - f_0$. A linear scale of frequencies can therefore be constructed on the vertical axis through B.

The desired expressions can best be derived by starting with the phase angle θ in Fig. 58.

$$\tan \theta = \frac{BS}{2\rho} = \frac{X}{R} = \frac{\omega^2 LC - 1}{\omega CR} = \frac{L(\omega^2 - \omega_0^2)}{\omega R} \tag{376}$$

This equation is rigorous for all values of ω. With such crystals as Rochelle salt, for which ω varies very considerably over the resonant range, the expression cannot be further simplified. BS is proportional to ω only for values of ω close to ω_0; for larger values of $\omega - \omega_0$, if L, C, R, ρ, and BS are given, ω must be found by solving a quadratic equation. On the other hand, if ω is given, BS is easily calculated, and thence the location of P on the circle is found.

If ω is so close to ω_0 as to permit the approximation $(\omega + \omega_0) \approx 2\omega$, Eq. (376) can be written in the following simplified form:

$$\frac{BS}{2\rho} \approx \frac{2L(\omega - \omega_0)}{R} \equiv -\frac{2Ln}{R} \tag{377}$$

where

$$n \equiv \omega_0 - \omega = 2\pi(f_0 - f) \tag{377a}$$

It follows that the frequency difference can be expressed as

$$f_0 - f \approx \frac{n}{2\pi} = -\frac{R}{8\pi\rho L} BS \equiv \sigma \cdot BS \tag{378}$$

where the *scale value for frequency* is

$$\sigma \equiv -\frac{R}{8\pi\rho L} \quad \text{(cycles sec}^{-1}\text{)/(unit dist.)} \quad (378a)$$

Unit distance, measured upward or downward from B, therefore corresponds to a frequency difference σ, so that a *linear scale* of frequencies can be constructed along this vertical line.* Close to resonance the scale is extremely accurate; it is in error by 1 per cent when f differs from f_0 by 2 per cent. It is amply sufficient for quartz resonators at all frequencies that ever need be considered.

The positive direction of BS is upward, corresponding to negative values of n (the h-f side of resonance).

A series of graduations, for a particular resonator, could be marked on the circle itself, but such a scale would be very wide open near B, becoming more and more closed as A was approached from either direction. It is much more convenient to find the frequency corresponding to any point P by the method described above.

268. In many cases it is necessary to find the frequency for a point P on the left side of the circle, as is the case, in fact, with most piezo oscillators. When the line APS is drawn, the point S may be inconveniently far above or below B. A good estimate of the frequency can then be made by the following geometrical artifice: For such a point as P_1 in Fig. 58 the point corresponding to S, say S', would come at an inconveniently great distance below B, on the prolongation of AP_1. Instead of drawing AP_1S', one may draw the line BP_1V. Then, by similar triangles, $BS'/AB = AB/AV$, whence $BS' = 4\rho^2/AV$, and

$$n = 2\pi\sigma \cdot BS' = \frac{-2\pi R}{8\pi\rho L} \cdot \frac{4\rho^2}{AV} = \frac{-R\rho}{L \cdot AV} = \frac{-2\alpha\rho}{AV} \equiv \frac{2\pi\sigma'}{AV} \quad (379)$$

where $$\sigma' = \frac{-R}{2\pi L} = \frac{n}{2\pi} AV = 4\rho^2\sigma \quad \text{(cycles sec}^{-1}\text{)(unit dist.)} \quad (379a)$$

The frequency difference $f_0 - f$ $(= n/2\pi)$ corresponding to any point on the left side of the circle is σ'/AV. Conversely, the location on the circle of the point corresponding to a given f can be found by means of Eq. (379) or (379a).

By the use of σ or σ', as defined by Eqs. (378a) and (379a), the graphical method yields values of n correct within 1 per cent as long as n is not over 2 per cent of f_0. For very large and very small frequencies the operating point on the circle is too close to A for reliable measurements of the distance AV. In such cases it is better not to use the graphical method but rather to derive the relations between the various parameters

* This linear scale was described by E. Mallett, "Telegraphy and Telephony," p. 135, London, Chapman & Hall, Ltd., 1929.

and the frequency analytically, using the geometrical relations as a guide. The derivations are usually quite simple, since far from resonance the terms in R can be left out. A numerical example is given in §300.

If R'_h is written for R', etc., in the treatment of the resonance circle in the foregoing sections, all expressions become applicable to a resonator vibrating near the harmonic h.

269. Resonance Diagram for the Crystal Resonator. We have shown that the impedance or the admittance of the *RLC*-branch of the resonator network can be represented by means of the resonance circle (Fig. 58). From this figure a resonance curve of the ordinary sort can be derived, by plotting frequencies as abscissas and admittances as ordinates. The circular diagram is simpler, even for the *RLC*-branch alone, and it becomes very much more convenient when the effect of the parallel capacitance C_1 is included.

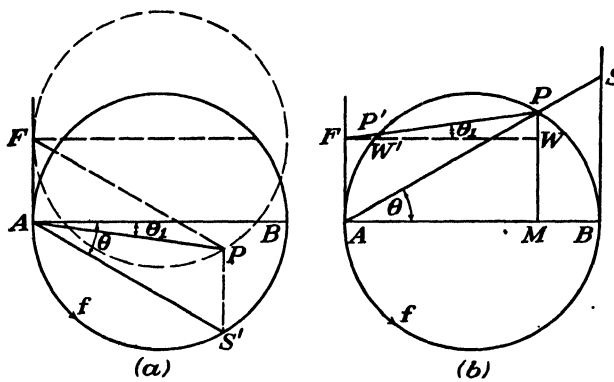


FIG. 59.—Vector diagram for resonator admittance, (*a*) by the usual convention, (*b*) by the method adopted in this book. The arrow *f* indicates the direction of increasing frequency.

The admittance of C_1 is $Y_1 = -jb_1 = j\omega C_1$, with absolute value $Y_1 = \omega C_1$. The vector admittance of the entire resonator is

$$Y'_1 = Y + Y_1 = g - jb - jb_1$$

We consider first the manner in which it has been customary in the past to represent such an admittance. In Fig. 59*a*, AS' represents $Y = g - jb$, b being inductive in this particular case. To Y is to be added vectorially $Y_1 = -jb_1$, a capacitive admittance represented by AF drawn upward. The resultant AP of AF and AS' represents Y'_1. If the point S' has a circular locus with varying frequency, the compounding of AS' with AF requires that the locus be moved upward, to the position indicated by the dotted circle. Such a shift in the resonance circle would be intoler-

able in dealing with resonator problems in which the location of the point F is variable. The difficulty is overcome simply by the expedient shown in Fig. 58, *viz.*, laying off the angle θ *upward when positive*, as shown in Fig. 59*b*. The capacitive admittance Y_1 still points upward. By this means the line FP represents at once the resultant admittance Y_1', the angle θ_1 being the phase angle for Y_1', drawn upward when Y_1' is inductive, downward when it is capacitive. We now have

$$\left.\begin{array}{lll} RLC \text{ branch} & \left\{\begin{array}{ll} R = 2\rho s = \dfrac{1}{2\rho s_y} & X = s \cdot BS \\ Z = s \cdot AS & Y = s_y \cdot AP \\ g = s_y \cdot AM & b = s_y \cdot MP \end{array}\right. & \\ C_1 \text{ branch} & g_1 = 0 & b_1 = -\omega C_1 = -s_y \cdot AF \\ RLCC_1 & \left\{\begin{array}{l} g_1' = g \\ Y_1' = s_y \cdot FP \end{array}\right. & b_1' = b + b_1 = s_y(MP + WM) = s_y \cdot WP \\ & s_y = \dfrac{1}{4\rho^2 s} & \end{array}\right\} \quad (380)$$

The point A in Fig. 59*b* is the origin for vectors representing the impedance or admittance of the RLC-branch, while F is the origin for the admittance of the network consisting of C_1 in parallel with RLC. Of considerable importance is the ratio AF/AB; considering only the magnitude, and using the relation $Q = \omega L/R$, we have

$$\frac{AF}{AB} = \frac{AF}{2\rho} = \omega C_1 R = \frac{C_1}{CQ} \quad (381)$$

As the frequency increases from zero to infinity and the operating point P travels around the circle, the distance AF varies uniformly from zero to infinity. Nevertheless, over the usual resonant range of such crystals as quartz, the variation in frequency is so slight that F may practically be regarded as a fixed point. The use of the graphical method is thus greatly simplified, without perceptible sacrifice of accuracy.

On the other hand, very strongly piezoelectric crystals, like Rochelle salt, undergo variations in frequency as great as 50 per cent within the range that has to be considered. In such cases a separate position must be assigned to F at each frequency.

In general, the assumption is made throughout this chapter that in the graphical treatment the frequency varies so little over the range considered that one may write, in place of the expression in Eqs. (380),

$$b_1 = -\omega_0 C_1 = -s_y \cdot AF \approx \text{const.} \quad (382)$$

where $\omega_0 = (1/LC)^{\frac{1}{2}}$.

The admittance of the resonator, in general form without approximations, is

$$Y_1' = \frac{R}{Z^2} - j\left(\frac{X}{Z^2} - \omega C_1\right) \tag{383}$$

In dealing with resonators in which the resonant range is very narrow, we may set $\omega = \omega_0 - n$ in the expressions for X and Z and with negligible error write $\omega_0 C_1$ in place of ωC_1. Equation (383) then takes the form

$$Y_1' \approx \frac{R}{R^2 + 4n^2L^2} + j\left(\frac{2nL}{R^2 + 4n^2L^2} + \omega_0 C_1\right) \tag{384}$$

For a circle of fixed radius ρ and with given L and C, if the effective value of R is diminished by improved mounting, s_y is increased and $AF = -\omega C_1/s_y$ becomes smaller. From Eq. (378a) it is seen that σ is diminished, making BS greater for the same n and giving a more open scale of frequency over the greater part of the resonance circle.

270. *The Impedance Circle.* The manner in which the same resonance circle is used not only for the admittance but also for the *impedance* of the entire resonator is shown in Fig. 59b. If a graphical representation is sought for the resonator with an external impedance in series (for example, the gap between crystal and electrodes), it is necessary first to find on the diagram the vector representing $Z_1' = 1/Y_1'$, as will now be explained. Z_1' can then be added vectorially to the external impedance.

Since Z_1' is the reciprocal of Y_1', we make use of the method of inversion to find the point P' inverse to P. This second inversion is performed with respect to F, the circle of inversion (which need not be drawn) having the radius FA and center at F. The geometrical relation involved is $(FA)^2 = FP \cdot FP'$. The point P inverts into P', where the straight line FP cuts the circle. For some locations of P it is evident that $FP' > FP$, corresponding to the fact that a smaller admittance means a larger impedance.

By the principle of inversion, wherever P may be on the circle, the distance FP' is inversely proportional to FP; it is therefore directly proportional to the impedance Z_1'. This fact can be proved in the present instance very simply without appeal to inversion theory, by writing

$$Z_1' = \frac{1}{Y_1'} = \frac{1}{s_y \cdot FP} = \frac{FP'}{s_y(AF)^2} \equiv s_z \cdot FP' \tag{385}$$

where

$$s_z = \frac{1}{s_y(AF)^2} = \frac{1}{2\rho R\omega^2 C_1^2} = \frac{s_y}{\omega^2 C_1^2} \tag{385a}$$

is the scale value for the impedance of $RLCC_1$. s_z is a function of the constants R and C_1 and of the fixed diameter 2ρ; it is also a function of ω, but over the resonance range the relative variation in frequency is so

minute that s_s may be treated as a constant. For the same reason it is usually allowable to consider AF as constant over the resonance range: although the impedance of the RLC branch varies enormously, that of C_1 remains practically constant for all frequencies that commonly come into play.

271. When s_y is taken as unit vector, the entire diagram in Fig. 59*b* is an *admittance diagram*, with AF and AP representing the admittances of C_1 and RLC, respectively; FP represents the admittance of $RLCC_1$. On the other hand, with s_z as unit vector, the figure becomes an *impedance diagram*, for which the following relations hold, including that given in Eq. (385):

$$\text{Impedance of } C_1 = -\frac{1}{\omega C_1} = s_z \cdot AF \tag{386}$$

$$\text{Impedance of } RLCC_1 = Z_1' = s_z \cdot FP' = R_s + jX_s \tag{387}$$

R_s and X_s are the *equivalent series resistance and reactance* of the entire resonator $RLCC_1$. Their values* can be proved to be (see Fig. 59)

$$R_s = s_z \cdot FW' = \frac{R}{(1 - \omega C_1 X)^2 + \omega^2 C_1^2 R^2} \tag{388}$$

$$X_s = s_z \cdot W'P' = \frac{X - \omega C_1 (R^2 + X^2)}{(1 - \omega C_1 X)^2 + \omega^2 C_1^2 R^2} \tag{389}$$

The values of X_s at series and parallel resonance are considered in §276.

In many cases it is more convenient to use these formulas in the approximate form obtained by setting $\omega = \omega_0 - n$, where $\omega_0^2 = 1/LC$:

$$R_s \approx \frac{R}{(1 + 2\omega_0 L C_1 n)^2 + \omega_0^2 C_1^2 R^2} \tag{390}$$

$$X_s \approx \frac{-2Ln(1 + 2\omega_0 L C_1 n) - \omega_0 C_1 R^2}{(1 + 2\omega_0 L C_1 n)^2 + \omega_0^2 C_1^2 R^2} \tag{391}$$

When n lies outside of a certain range, depending on the various parameters and on the desired precision, the effect of R^2 becomes inappreciable. The formulas then become

$$R_s \approx \frac{R}{(1 + 2\omega_0 L C_1 n)^2} \tag{392}$$

$$X_s \approx \frac{-2Ln}{1 + 2\omega_0 L C_1 n} \tag{393}$$

These expressions are valid until n becomes so large that the approximation involved in the denominator is no longer justified.

* These values correspond to those given by Eqs. (*a*) and (*b*) in Dye, ref. 127, p. 403, and to R_1' and X_1' in the author's earlier paper.[105]

Unless R is extremely small, it may be found that the terms in R^2 have to be retained over the entire range of frequencies that usually has to be considered. This fact will be found exemplified in §301.

It is sometimes convenient to treat the resonator as equivalent to a *resistance R_s in series with a capacitance C_s*. The latter is found from the equation

$$C_s = -\frac{1}{\omega X_s} = -\frac{1}{\omega s_z \cdot W'P'} \tag{394}$$

For all points on the admittance circle lying above the line FW, $W'P'$ is positive and C_s is negative.

When R is very small, C_s can be shown, by means of Eqs. (389) and (394), to have, at any ω, the value

$$C_s \approx \frac{C_1 + C - LC_1C\omega^2}{1 - LC\omega^2} \tag{394a}$$

272. *The Frequency Scale for the Impedance Circle.* Turning once more to Fig. 59*b*, we find that, as the point P on the admittance circle travels counterclockwise from A back to A, the inverse point P', whose location represents the impedance, moves *clockwise* from A back to A. The distribution of frequency around the circle is also different from that when the circle is regarded as an admittance locus. It is not necessary, however, to construct a special frequency scale for impedances, if the following simple procedure is adopted.

For every point P' on the impedance circle there is an inverse point P, situated on the straight line through F and P'. P' and P correspond, respectively, to the impedance and admittance of the resonator at the same frequency. When P' is given, one need only locate the inverse point P, draw the line APS (or BPV according to Fig. 58), and find the frequency from Eq. (378) or (379). This graphical method is sufficiently accurate for most purposes, and it obviates the laborious calculations that would otherwise be needed to determine the frequency corresponding to any impedance value of the resonator.

273. The resonator $RLCC_1$ can also be represented as a resistance R_p *in parallel with a capacitance C_p*. Like R_s and C_s, R_p and C_p are dependent on the frequency. From Fig. 59*b* and Eqs. (380) it is seen that at the frequency corresponding to any point P,

$$R_p = \frac{1}{g_1'} = \frac{1}{s_y \cdot FW} \tag{395}$$

and

$$X_p = \frac{1}{b_1'} = \frac{1}{s_y \cdot WP} = -\frac{1}{\omega C_p} \tag{395a}$$

C_p is negative at frequencies above the broken line FW in Fig. 59.

At frequencies well removed from resonance, R_s and R_p can be ignored. At high frequencies C_s and C_p converge toward the common value C_1. At low frequencies they converge toward the common value $(C_1 + C)$. This subject is further discussed in §§300 and 258.

In Fig. 59 and in most of the diagrams that are to follow, the length of the line AF is greatly exaggerated beyond the value that would be characteristic of a typical piezo resonator. The ratio $AF:AB$ is $\omega C_1 R$. The resistance R is usually so small that the ratio is of the order of 1:100. As will be seen, the length AF becomes greater when a gap is present, but even then, with the small gaps usually employed, the ratio remains small. It would be difficult to illustrate the principle of the resonator without exaggerating the length of AF.

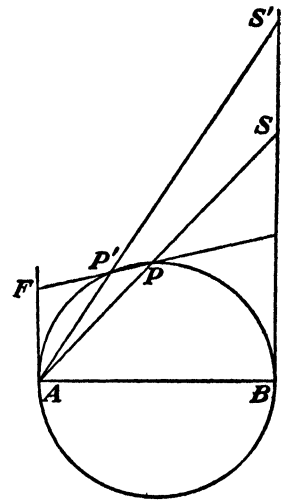


FIG. 60.—Two mutually inverse points on the admittance circle, with the corresponding points S and S' on the frequency scale.

274. *A Relation between Mutually Inverse Points.* The following relation will find application later. Consider any two mutually inverse points on the admittance circle, as P and P' in Fig. 60. Calling the corresponding frequencies $f = \omega/2\pi$ and $f' = \omega'/2\pi$, we have from Eq. (378) $n = \omega_0 - \omega = -2\pi\sigma \cdot BS$ and $n' = \omega_0 - \omega' = -2\pi\sigma \cdot BS'$. From geometrical considerations, with the aid of the equation $4\pi^2 f_0^2 LC = 1$, it can be proved that

$$SS' = 4\rho^2/AF - 2BS, \text{ or } f' - f = 4\rho^2\sigma/AF - 2(f - f_0),$$

whence

$$f' + f = \frac{4\rho^2\sigma}{AF} + 2f_0 = \frac{1}{8\pi^2 f_0 LC_1} + 2f_0 = 2f_0\left(1 + \frac{C}{4C_1}\right) = \text{const.} \tag{396}$$

Thus *the sum of the frequencies for any two mutually inverse points is a constant*, insofar as σ and AF can be regarded as constants, which is very approximately true over the ordinary range of resonance.

275. The Critical Frequencies of the Resonator. We now consider the critical points on the resonance circle for admittances, giving at the same time a number of useful approximate formulas relating the various frequencies.

The critical points are shown in Fig. 61. At *point B* the frequency is $f_0 = 1/2\pi(LC)^{\frac{1}{2}}$, corresponding to maximum admittance of the *RLC*-branch and (with constant voltage) maximum current I_p in that branch.

At B the parallel resistance R_p has its minimum value [see Eq. (395)]. On the *impedance* circle, B is the point at which the series resistance R_s has its greatest value: for if B replaces P' in Eq. (387), $Z_1' = s_z \cdot FB$, with components $R_s = s_z \cdot AB$ and $X_s = s_z \cdot AF$; *i.e.*, AB is the largest value that FW' in Eq. (388) can have. The frequency corresponding to B on the impedance circle is not f_0 but has a value higher than f_0, *viz.*, the value for the point P_7 on the admittance circle; P_7 is the inverse of B. It is easily proved that this maximum value of R_s is related to R by the equation $(R_s)_{max} = 1/R\omega_7^2 C_1^2 \approx 1/R\omega_0^2 C_1^2$.

Consider next the mutually inverse points P_3 and P_4 on the horizontal (conductance or resistance) axis through F. At both points the resonator acts as a *pure resistance*. At P_3 the admittance, now a pure conductance,

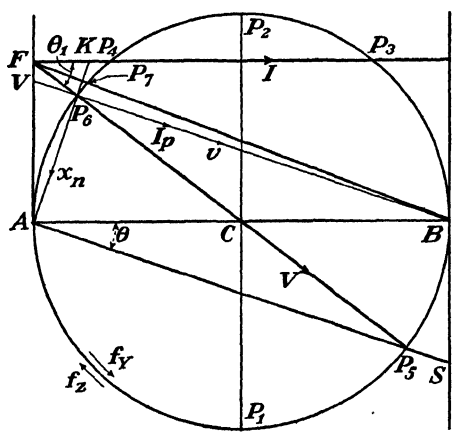


FIG. 61.—The critical points on the resonance circle. The curved arrows f_Y and f_Z show the directions in which the frequency increases around the circle, for admittances and impedances, respectively.

is large. The frequency at P_3 is commonly called the frequency for *series resonance*, since, if C_1 is relatively small (as is the case with a typical piezo resonator), F is close to A, and P_3 is so close to B that the frequency differs only by an extremely small amount from f_0, which is the series-resonance value for the RLC-branch. On the other hand, at P_4 we have the condition for *parallel resonance* (antiresonance), in which C_1 plays an important part. The admittances at series and parallel resonance are $s_y \cdot FP_3$ and $s_y \cdot FP_4$, respectively, while the impedances are $s_z \cdot FP_4$ and $s_z \cdot FP_3$, respectively. If AF is small, the ratio $FP_4 : FP_3$ is extremely small.

At P_3 and P_4, as may be seen from Eqs. (388), (389), (394), and (395), $X_s = 0$, $X_p = \pm\infty$, $C_s = \infty$, $C_p = 0$. At P_3, $R_s = s_z \cdot FP_4$ and $R_p = 1/(s_y \cdot FP_3) = R_s$; at P_4, $R_s = s_z \cdot FP_3$ and $R_p = 1/(s_y \cdot FP_4) = R_s$.

276. *Frequencies and Reactances at Series and Parallel Resonance.* The frequencies are derived from Eq. (383) or by setting $X_s = 0$ in Eq. (389). On solving for ω, one finds, to a first order of approximation in R,

$$\omega_s^2 = \frac{1}{LC} + \frac{R^2 C_1}{L^2 C} \tag{397}$$

$$\omega_p^2 = \frac{1}{LC} + \frac{1}{LC_1} - \frac{R^2}{L^2}\frac{C_1 + C}{C} \tag{398}$$

where ω_s and ω_p are the values at series and parallel resonance, respectively (points P_3 and P_4). Hence,

$$\omega_s = 2\pi f_s \approx \frac{1}{\sqrt{LC}}\left(1 + \frac{R^2 C_1}{2L}\right) \tag{399}$$

$$\omega_p = 2\pi f_p \approx \frac{1}{\sqrt{LC}}\left(1 + \frac{C}{2C_1} - \frac{R^2(C_1 + C)}{2L}\right) \tag{399a}$$

$$\omega_p - \omega_s \approx \frac{1}{\sqrt{LC}}\left(\frac{C}{2C_1} - \frac{R^2(2C_1 + C)}{2L}\right) \tag{400}$$

If the damping is very small, so that $R \to 0$, ω_s approaches the value $\omega_0 = (1/LC)^{\frac{1}{2}}$, while ω_p approaches $(1/LC)^{\frac{1}{2}}(1 + C/2C_1)$. Then also

$$\frac{\omega_p - \omega_s}{\omega_s} \approx \frac{C}{2C_1} \tag{401}$$

This expression can be shown to be approximately equal to γ_h in Eq. (350*a*).

The smaller the ratio C/C_1, the closer together are the frequencies at series and parallel resonance.

In dealing with such crystals as quartz, with which the ratio C_1/C is over 100, the approximate equations (399) to (400) are usually sufficient. On the other hand, cases may arise where higher precision is desired or where, as with Rochelle salt, the ratio C_1/C is not so great, so that $\omega_p - \omega_s$ is no longer small in comparison with ω_s. The following more rigorous expressions, derived from (397) and (398), should then be used:

$$\omega_p^2 - \omega_s^2 = \frac{1}{LC_1} - \frac{R^2}{L^2}\frac{2C_1 + C}{C} \tag{402}$$

In most cases where this formula finds application R is so small that

$$\left.\begin{aligned} \omega_p^2 - \omega_s^2 &\approx \frac{1}{LC_1} = \frac{C}{LCC_1} = \omega_s^2 \frac{C}{C_1} \\ \frac{\omega_p^2 - \omega_s^2}{\omega_s^2} &= \frac{\omega_p^2}{\omega_s^2} - 1 = \frac{f_p^2}{f_s^2} - 1 \approx \frac{C}{C_1} \end{aligned}\right\} \tag{403}$$

The statement has sometimes been made that the series reactance X_s of a piezo resonator is zero at series resonance and infinite at parallel

resonance. The latter part of the statement would be true only if the resistance R were strictly zero. Equation (389) shows that as long as $R > 0$ the reactance cannot become infinite at any frequency but passes through *the value zero at both series and parallel resonance.*

If $R = 0$ in Eqs. (388) and (389), one finds

$$R_s = 0 \qquad X_s = \frac{X}{1 - \omega C_1 X} \tag{404}$$

Then $X_s = 0$ when $X = 0$, and $X_s = \infty$ when $X = 1/\omega C_1$, where $\omega^2 = (C_1 + C)/LC_1C$; this is the value of ω_p^2 in Eq. (398) when $R = 0$.

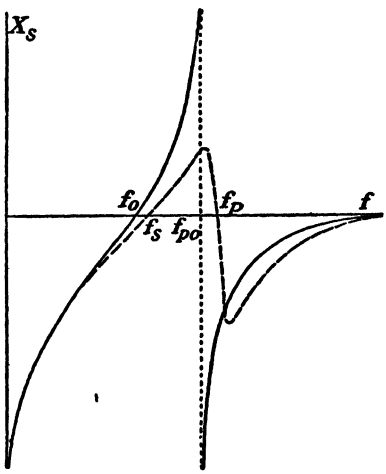


FIG. 62.—Variation with frequency of the series reactance X_s of a resonator. The full line is for $R = 0$.

The variation of X_s with frequency is illustrated qualitatively in Fig. 62. When $R = 0$, $X_s = 0$ at the frequency $f_0 = 1/2\pi(LC)^{\frac{1}{2}}$ and changes from $+\infty$ to $-\infty$ at the frequency f_{p0} given by

$$\omega^2 = \frac{(C_1 + C)}{LC_1C}$$

When $R > 0$, X_s has a finite maximum and minimum, with zero values at f_s and f_p. For reasonably small values of R, the frequency difference $(f_p - f_s)$ between antiresonance and resonance does not differ appreciably from $(f_{p0} - f_0)$.

277. The *quadrantal points* are at P_1 and P_2. Although they cannot conveniently be determined experimentally, still they have a certain physical significance, especially because of their relation to the damping. They are the points for which $\theta = \pm 45°$, the resistance and reactance of the *RLC*-branch being here numerically equal. They are therefore also the half energy points for the current in the *RLC*-branch and, by §305, for the mechanical energy of vibration. This fact leads to the equations

$$\omega_2 \approx \sqrt{\omega_0^2 + \alpha^2} + \alpha \qquad \omega_1 \approx \sqrt{\omega_0^2 + \alpha^2} - \alpha \tag{405}$$

where ω_2 and ω_1 refer to the points P_2 and P_1, and $\alpha = R/2L$. When α is small, one has

$$f_2 - f_0 \approx f_0 - f_1 \approx \frac{\alpha}{2\pi} \approx f_0 \frac{\delta}{2\pi} \tag{406}$$

where δ is the logarithmic decrement.

On the *admittance* diagram P_1 and P_2 are the points for maximum positive and negative values, respectively, of the parallel capacitance C_p (§273). On the *impedance* diagram they are the points for maximum positive and negative values of the series capacitance C_s.

278. The points for *maximum and minimum admittance* of the entire resonator $RLCC_1$ are sometimes used in the measurement of the electric constants. They are the points P_5 and P_6, obtained by drawing a line from F through the center of the circle C. Letting Y_m and Y_n denote maximum and minimum values of Y_1', we find

$$Y_m = s_y \cdot FP_5 \qquad Y_n = s_y \cdot FP_6 \qquad Z_m = s_z \cdot FP_5 \qquad Z_n = s_z \cdot FP_6 \quad (407)$$

The frequencies corresponding to P_5 and P_6 on the impedance diagram are the same as for P_6 and P_5 on the admittance diagram, since these are mutually inverse points.

279. *Equations for ω_m, ω_n, Y_m, and Y_n.* These expressions could be derived by applying to Eq. (383) the condition for maximum and minimum admittance of $RLCC_1$ with variable ω. It is less laborious, and equally precise, to base the calculation on the graphical representation as shown in Fig. 61. In that figure let it be assumed that F has the location corresponding to ω_n for minimum admittance Y_n, so that $s_y \cdot AF = -\omega_n C_1$. Then P_6, where FC cuts the circle, marks the point on the circle at which ω has the value ω_n. Taking advantage of the fact that $\angle FCA = 2\theta$ and also that $s_y \cdot 2\rho R = 1$ (§269), one finds

$$\tan 2\theta = \frac{AF}{AC} = \frac{\omega_n C_1}{s_y \cdot \rho} = 2\omega_n C_1 R$$

A similar expression holds for the frequency of maximum admittance, with ω_m in place of ω_n; θ and AF are then somewhat smaller than in the case of ω_n, but this fact need not be taken into account, since neither θ nor AF appears in the final solution. A single equation can now be written, valid for the frequencies f_m and f_n:

$$\tan 2\theta = 2\omega C_1 R \quad (408)$$

The two values of ω are found by eliminating θ between this equation and (376). Upon discarding terms of order higher than R^2 we find

$$\omega_m^2 \approx \frac{1}{LC}\left(1 - \frac{R^2 C_1}{L}\right) = \omega_0^2\left(1 - \frac{R^2 C_1}{L}\right) \quad (409)$$

$$\omega_n^2 \approx \frac{1}{LC}\left(1 + \frac{C}{C_1} + \frac{R^2(C_1 + C)}{L}\right) = \omega_0^2\left(1 + \frac{C}{C_1} + \frac{R^2(C_1 + C)}{L}\right) \quad (409a)$$

Even in Rochelle salt, for which $R^2 C_1/L$ is much greater than for quartz, ω_m is extremely close to ω_0.

When, as is usually the case, the terms in R^2 can be ignored, one finds

$$\frac{\omega_n^2 - \omega_m^2}{\omega_m^2} = \frac{f_n^2 - f_m^2}{f_m^2} \approx \frac{C}{C_1} \tag{410}$$

For quartz, in which $C << C_1$, one may write with sufficient precision,

$$\frac{\omega_n - \omega_m}{\omega_m} = \frac{f_n - f_m}{f_m} \approx \frac{C}{2C_1} \tag{410a}$$

Equations (410) and (410*a*) are identical with (403) and (401), showing that the frequency difference between maximum and minimum admittance is nearly the same as that between resonance and antiresonance. The approximation becomes closer the smaller the value of R.

In passing, it may be noted that f_n is approximately the resonant frequency of a circuit consisting of R, L, C, and C_1, all in series.

In deriving Y_m and Y_n we make use again of the graphical relations in Fig. 61. We have*

$$Y_n = s_y \cdot FP_6 = s_y(FC - \rho) = s_y\left(\frac{\rho}{\cos 2\theta} - \rho\right) = \frac{\dfrac{1}{\cos 2\theta} - 1}{2R}$$

On combining this expression with Eq. (408) it is found that

$$Y_n \approx \omega_n^2 C_1^2 R \tag{411}$$

or, from Eq. (409*a*),

$$Y_n \approx \frac{RC_1}{LC}(C_1 + C) = \omega_0^2 C_1 R(C_1 + C) \tag{411a}$$

A similar procedure leads to

$$Y_m = s_y \cdot FP_5 \approx \frac{1}{R}(1 + \omega^2 C_1^2 R^2) \tag{411b}$$

Obviously Y_n vanishes with R, as it should for parallel resonance, while the impedance Z_n is extremely close to R as long as R is small. Y_n is usually so small and the minimum so flat that it is not easy to measure f_n with precision.

The difference between the two admittances is

$$Y_m - Y_n \approx \frac{1}{R} - \frac{C_1 R}{L} \tag{412}$$

* The fact that F does not have the same location at both maximum and minimum admittance, so that strictly F, P_6, C, and P_5 are not collinear, introduces no error in the present reasoning.

When R is small, this difference approximates $1/R$, a result that follows also from the principle of inversion on the assumption that the distance AF in Fig. 61 is appreciably the same at each frequency.

The ratio Y_m/Y_n is

$$\frac{Y_m}{Y_n} \approx \frac{LC}{R^2C_1(C_1 + C)} \approx \frac{1}{\omega_0^2R^2C_1(C_1 + C)} \tag{413}$$

When, as in quartz, $C_1 >> C$, this becomes

$$\frac{Y_m}{Y_n} \approx \frac{1}{\omega_0^2C_1^2R^2} \tag{413a}$$

an expression that will be used in §317.

The foregoing derivations offer a good illustration of the usefulness of the graphical representation. The same procedure can be applied to a crystal with a gap of any width, using the primed parameters R', L', C', and C_1'.

280. *The Capacitance Ratio.* When the damping is small, it is seen from Eqs. (401), (409a), and (410a) that the ratio $C/2C_1$ is approximately equal to $(f_p - f_s)/f_s$, $(f_n - f_0)/f_0$, or $(f_n - f_m)/f_m$. This ratio is a measure of the excellence of a resonator. Instead of $C/2C_1$, however, it has become customary to use the ratio C_1/C, which we shall call the *capacitance ratio.** As will be seen in §283, it is the ratio of the energies stored in the electrical and mechanical systems. A small capacitance ratio means high activity. From Eqs. (322), (323), (364), and (365) one finds, for both lengthwise and thickness vibrations, at harmonic h and with a gap w,

$$\frac{C_1'}{C_h'} = \frac{\pi kq'h^2e_r'}{32\epsilon^2e} \tag{414}$$

or, at the fundamental frequency and no gap ($h = 1$, $w = 0$),

$$\frac{C_1}{C} = \frac{\pi kq_0}{32\epsilon^2} \tag{414a}$$

where the electric spacing e_r', effective dielectric constant k, stiffness q, and piezoelectric constant ϵ have the appropriate values in each case. These expressions do not involve the dimensions of the resonator. The larger ϵ is, the greater the activity and the greater the spread between resonance and antiresonance. If a crystal cut is twinned or otherwise defective, the values of k, q, C_1' and frequency may be normal, but the low activity will be betrayed by abnormally small values of $(f_p - f_s)$,

* The importance of the ratio C_1/C was first recognized by Dye (ref. 127, p. 426), who called it the "piezoelectric ratio."

with a correspondingly large value of L_h' and of the electromechanical ratio r.

Relation of the Electromechanical Ratio to the Capacitance Ratio. If the value of r, first for lengthwise vibrations from Eq. (326) in §233, then for thickness vibrations from Eq. (367) in §255, is combined with Eq. (414), there results in each case

$$\frac{C_1'}{C_h'} = \frac{\pi k q h^2 A^2}{8 e_r' e} r \qquad (415)$$

where A is the area of the plate in thickness vibrations, and of the cross section be in lengthwise vibrations. Since the fraction on the right is substantially constant, it is seen that r *is proportional to the capacitance ratio.* When $h = 1$ and $w = 0$,

$$\frac{C_1}{C} = \frac{\pi k q A^2}{8 e^2} r \qquad (416)$$

Inspection of the equations shows that in order to secure a low ratio C_1/C a crystal of high ϵ should be chosen, with no gap. With a crystal of given material, for example quartz, ϵ depends on the angle of cut, and for most of the cuts of low temperature coefficient the angle is such that ϵ is considerably reduced in value (§361). The question is then what can be done to reduce C_1/C when ϵ, k, and q are prescribed.

One expedient is to connect an inductance to the crystal in such a way as to neutralize C_1; this is done in some filter circuits. In the case of a bar in lengthwise vibration, C_1/C can be diminished by about 20 per cent by making the electrodes three-fourths as long as the bar, as was shown in §241. With plates in thickness vibration nothing is gained by making the electrodes smaller, since the effect of this is equivalent to increasing the gap.

It is to be noted that the expression for the capacitance ratio does not involve either R or Q. For the same C_1/C, a resonator will of course be more sharply selective the smaller R is; R can be made small by suitable mounting and by placing the crystal in a vacuum. Anything that increases the effective value of C_1, such as stray capacitances or a condenser in series or parallel, reduces the activity.

281. *Summary of Data on the Critical Frequencies.* The results derived in the foregoing sections are summarized and extended in Table XXIII. The encircled numbers indicate the order of increasing frequency, while in the second column are noted the points on the admittance circle in Figs. 61 and 67. Frequencies are expressed in terms of relative differences $\Delta f/f_0 = (f_c - f_0)/f_0$, f_c being the critical frequency. For I and I_p see Fig. 50.

TABLE XXIII

No.	Point	Frequency symbol	Critical condition	Equation	$\frac{\Delta f}{f_0}$
①	P_1	f_1	max. X_p	(406)	$-\frac{R}{2}\sqrt{\frac{C}{L}}$
②	P_5	f_m	max. Y_1', min. Z_1', max. I	(409)	$-\frac{R^2C_1}{2L}$
③	B	f_0	$X = 0$, max. Y, min. R_p, max. I_p, max. velocity	$\omega_0^2 = \frac{1}{LC}$	0
④	P_3	f_s	$X_s = 0$, $X_p = \pm\infty$	(399)	$\frac{R^2C_1}{2L}$
⑤	P_2	f_2	min. X_p	(406)	$\frac{R}{2}\sqrt{\frac{C}{L}}$
⑥	P_8	..	max. X_s	See §300	
⑦	P_4	f_p	$X_s = 0$, $X_p = \pm\infty$	(399a)	$\frac{C}{2C_1} - \frac{R^2(C_1+C)}{2L}$
⑧	P_7	..	max. R_s	See §300	
⑨	P_6	f_n	min. Y_1', max. Z_1', min. I	(409a)	$\frac{C}{2C_1} + \frac{R^2C_1}{2L}$
⑩	P_9		min. X_s	See §300	

The following pairs of points are mutually inverse: P_1 and P_9, P_5 and P_6, B and P_7, P_3 and P_4, P_2 and P_8.

It should be noted that those critical points which are most used in resonator calculations fall into two groups, *viz.*, P_5, B, and P_3, for all of which the frequency is very nearly the same, coming closer to f_0 the smaller R is, and P_4, P_7, and P_6, which also differ among themselves but little in frequency. Within the limits of precision usually attainable the frequency difference between P_6 and P_5, P_7 and B, or P_4 and P_3 may be taken as the interval between antiresonance and resonance; in §280 it has been pointed out that the three ratios $(f_p - f_s)/f_s$, $(f_n - f_0)/f_0$, and $(f_n - f_m)/f_m$ are all substantially equal to $C/2C_1$. Strictly, the distance AF in the circle diagrams, given in Eqs. (380), should be greater for antiresonance than for resonance in the ratio $(1 + C/2C_1):1$. For quartz resonators this ratio is about 1.005 and need not be taken into account.

In the measurement of the electrical characteristics of resonators, points P_5 and P_6 are of chief importance. Piezo oscillators, with the exception of some recent circuits, usually operate at relatively high frequency, in the neighborhood of P_4, the antiresonant point (see §389 and Fig. 61). As has been stated, in most resonators the ratio of the distance AF to the diameter of the circle is so small that at the higher frequencies the graphical method can serve only as a guide in making calculations. For example, at very high and very low frequencies X_s

can be obtained from Eq. (389), in which with sufficient precision one can set $R = 0$. The value is then

$$X_s \approx \frac{X}{1 - \omega C_1 X} \tag{417}$$

As long as $n << \omega_0$, $X \approx -2Ln$; in this case

$$X_s \approx \frac{-2Ln}{1 + 2L\omega_0 C_1 n} \tag{417a}$$

In extension of Table XXIII one more critical frequency may be mentioned, *viz.*, that for *free vibrations*, which plays a part in certain methods of measurement, as will be seen in §320. From Eq. (65) or Eq. (93) one finds, for the fundamental frequency of free vibrations of any resonator, the expression

$$f_f^2 = f_0^2\left(1 - \frac{\delta^2}{4\pi^2}\right) = f_0^2\left(1 - \frac{R^2}{4\omega_0^2 L^2}\right) = f_0^2\left(1 - \frac{R^2 C}{4L}\right)$$

Hence,

$$\frac{f_f - f_0}{f_0} \approx -\frac{R^2 C}{8L} \tag{418}$$

When R is reasonably small, this value is too small to detect by ordinary means. It is less than the value for point P_5 in Table XXIII in the ratio $C/4C_1$. In the example discussed in §298, with $C_1 = 31.9$ esu, the frequency for free vibrations would be lower than f_0 by about 0.0004 cycle/sec.

From Table XXIII it is evident that all frequencies are more or less dependent on the resistance R of the RLC-branch of the resonator network. Nevertheless, in a well-mounted resonator the terms in R are extremely small. It will be noted that as R approaches zero the frequencies at points P_1, P_5, P_3, and P_2 all converge on the common value f_0; in practice, these points may all be found to lie within a single cycle per second. Also, P_4 and P_6 fall very close together when R is small, so that, for both points, $\Delta f/f_0 \approx C/2C_1$. If R could be made to vanish entirely, X_s would become infinite instead of zero at P_4.

The entire range of values assumed by X_s on passing through resonance from very low to very high frequencies is illustrated and discussed in §300.

282. *Phase Relations.* The following relation holds between the phase angle θ, the damping constant $\alpha = R/2L$, and the frequency difference $n_m = \omega_0 - \omega_m$ for maximum admittance Y_m [see Fig. 61 and Eq. (376)]:

$$\tan\theta = \frac{BS}{2\rho} = \frac{AV}{2\rho} = \frac{FK}{AF} = \frac{FP_6}{AF} = \frac{Y_n}{\omega C_1} = \frac{-n_m}{\alpha} \tag{419}$$

In Fig. 61 the horizontal line through F is the one on which points P_3 and P_4 fall, for series and parallel resonance, respectively. At these points the resonator is a simple resistance, and the current I is in phase with the potential difference V impressed on the resonator. If the vector representing I is drawn parallel to FP_3, then the vector for V, at any frequency f, is parallel to the line that represents the admittance Y_1' at this frequency. For example, at the frequency represented by P_5 in Fig. 61, I leads V by the angle $P_3FP_5 = \theta_1$. The current I_p in the RLC branch leads V by the angle θ; since by geometry $\theta = \angle BAP_5 = \angle BP_6P_5$, it is clear that the phase of I_p (for point P_5) is given correctly by the direction P_6B. Since according to §234 the particle velocity v is in phase with I_p (a relation that holds for all types of piezo resonator), it is clear that P_6B gives also the phase of v. The mechanical strain, indicated as x_n, lags 90° behind v and is therefore represented by a vector parallel to P_6A.

Similar relations hold for all points around the circle. In all cases the current vector I is parallel to FP_3. The *lengths* of the various lines are not proportional to I, I_p, V, v, and the strain x_n; the lines indicate only relative *phases*.

283. *The Distribution of Energy in the Resonator.* In §125 consideration was given to the allocation of the energy in a piezoelectric crystal under combined electric and mechanical stress among the various terms in the energy equation. Somewhat analogous reasoning can be applied to the equivalent $RLCC_1$ network. The simplest case is that of thickness vibrations, in which, as shown in §247, the parallel capacitance C_1 is that of the clamped crystal. At any instant when a field is applied to the crystal, the energy stored in C_1 is electrical energy at constant strain, while that stored in C represents the work done in mechanical deformation. The energy lost per second in friction is I_p^2R. If there are appreciable dielectric losses, another resistance must be added to the network in series with C_1, as explained in §302; this step was taken by Mason[338] in his treatment of the Rochelle-salt resonator.

284. Relations between the Equivalent Electric Constants with and without a Gap. It was stated in §263 that the electrical properties of a piezo resonator can be represented by either of the two networks shown in Fig. 56. If A is the area of the electrodes (equal to bl in the case of full-sized electrodes), then as long as the surfaces of the crystal exposed to the gap are equipotential, the capacitance of the gap is

$$C_2 = \frac{A}{4\pi w} \tag{420}$$

For either lengthwise or thickness vibrations there is a simple relation between the oft-appearing ratio e/e_r' and the capacitances C_2 and C_1.

It will be recalled that e is the crystal thickness and w the gap and that $e'_r = e + kw$, where k is represented by k_l or k'' for lengthwise or thickness vibrations, respectively. For either type, $C_1 = kA/4\pi e$. It is easily shown that

$$\frac{e}{e'_r} = \frac{C_2}{C_1 + C_2} \tag{421}$$

We seek the relations between the four constants R'_h, L'_h, C'_h, and C'_1 for gap w and the corresponding values R_h, L_h, C_h, and C_1 for $w = 0$. From equations in §232 and §255, for both *lengthwise and thickness* vibrations,

$$\frac{R'_h}{R_h} = \frac{L'_h}{L_h} = \left(\frac{e'_r}{e}\right)^2 = \left(\frac{C_1 + C_2}{C_2}\right)^2 \tag{422}$$

$$\frac{C'_h}{C_h} = \left(\frac{e}{e'_r}\right)^2 \frac{q_0}{q'} = \left(\frac{C_2}{C_1 + C_2}\right)^2 \frac{q_0}{q'} \tag{422a}$$

$$\frac{C'_1}{C_1} = \frac{e}{e'_r} = \frac{C_2}{C_1 + C_2} \tag{423}$$

where q_0 and q' are the stiffness coefficients for gaps 0 and w, respectively.

Equations (420) to (423) are theoretically correct for all crystals and all gaps, as long as the performance of the resonator can be represented by an *RLC*-chain in parallel with a pure capacitance C_1. They will now be used as a test for the equivalence of the two alternative networks shown in §263, Fig. 56. A simple circuit analysis shows that, if the networks (*b*) and (*c*) are equivalent, then, with the subscript h inserted for generality,

$$\left.\begin{aligned} \frac{R'_h}{R_h} = \frac{L'_h}{L_h} = \left(\frac{C_1 + C_2}{C_2}\right)^2 \qquad \frac{C'_1}{C_1} = \frac{C_2}{C_1 + C_2} \\ \frac{C'_h}{C_h} = \frac{C_2}{C_1 + C_2}\,\frac{C_2}{C_h + C_1 + C_2} \end{aligned}\right\} \tag{424}$$

or

$$\frac{C_h}{C'_h} = \left(\frac{C_1 + C_2}{C_2}\right)^2 + \frac{C_h}{C_2}\left(\frac{C_1 + C_2}{C_2}\right) = \left(\frac{e'_r}{e}\right)^2 + \frac{C_h}{C_2}\frac{e'_r}{e} \tag{424a}$$

These equations were first given by Watanabe.[581]* They agree in all particulars with Eqs. (422) to (423), provided that the dependence of the elastic stiffness on the gap is such that

$$\frac{q_0}{q'} = \frac{(C_1 + C_2)}{(C_h + C_1 + C_2)}$$

* Equivalent networks of substantially the same type had previously been treated by K. S. Johnson and T. E. Shea, *Bell System Tech. Jour.*, vol. 4, p. 52, 1925. For a general discussion of equivalent networks see T. E. Shea, "Transmission Networks and Wave Filters," New York, 1929.

As we shall see, this is the case with thickness vibrations, but not always with lengthwise vibrations.

In the case of *thickness vibrations* it is found from Eqs. (421), (355), (356), (364) and Table XXII, together with $C_1 = k''A/4\pi e$, that

$$\frac{q_0}{q'} = \frac{C_1 + C_2}{C_h + C_1 + C_2} \tag{425}$$

From this equation and (422*a*) it follows that

$$\frac{C_h'}{C_h} = \frac{C_2}{C_1 + C_2} \frac{C_2}{C_h + C_1 + C_2} \tag{425a}$$

in agreement with Eq. (424).

285. *The Gap Effect in Lengthwise Vibrations in Terms of the Equivalent Network.* We shall deal first with the case of the *unplated bar.* This is the case commonly encountered in practice, in which the bare bar is placed between electrodes, with or without a gap. The use of a plated bar with gap is considered later. If the gap is zero, it makes no difference whether the surfaces presented to the electrodes are plated or not.

In the first place, it must be pointed out that, while the equations in §232 for the equivalent constants R_h', L_h', and C_h', for a bar separated from the electrodes by a gap w, are theoretically entirely correct for any integral value of h, still these constants do not agree with those derived by considering the resonator as an $RLCC_1$-mesh in series with C_2; in other words, Eqs. (424) are not satisfied. The discrepancy arises from two separate causes. One is the fact that the vibration direction of the bar is perpendicular to the electric field and (practically) independent of the thickness. The effective stiffness q', though a function of the gap, is independent of the order of harmonic, as may be seen from Eq. (330). But, according to Eq. (425), q', being a function of C_h, should contain h in order to satisfy Eqs. (424). It is thus evident that the latter equations, if valid at all for bars, are *valid only at the fundamental frequency*, when $h = 1$. This statement holds for both plated and bare bars.

The other contributing cause of the discrepancy mentioned above has specifically to do with the *unplated* bar with a gap. The strain x_n discussed in §230 and hence the piezoelectric polarization and the depolarizing field all vary along the length of the bar. As a consequence, the surfaces of the unplated crystal are not equipotential except when $w = 0$. This complication does not affect the ratio e_r'/e; as long as $h = 1$, Eqs. (422) and (423) are in agreement with the corresponding expressions in (424). As far as they are concerned, the $R'L'C'C_1'$ and $RLCC_1C_2$ networks are equivalent. But with Eq. (422*a*) the situation is different; for when the ratio q_0/q' is calculated from Eq. (330), there results a value that does not agree with Eq. (425). One finds, namely, from (330), that

$1/q_0 = s^E_{nn}$, $1/q' = s^E_{nn}(1 - 4\pi\epsilon^2 s^E_{nn} w/e')$, so that, with the aid of Eq. (324), $q_0/q' = 1 - \pi^2 Ce/8C_2e'$, where $C_2 = bl/4\pi w$. With such crystals as quartz, for which the piezoelectric reaction is relatively small, one may write as an approximation

$$\frac{q'}{q_0} = 1 + \frac{\pi^2 Ce}{8C_2e'} \tag{426}$$

Now with the aid of Eq. (423) Eq. (425) may be written in the form

$$\frac{q'}{q_0} = 1 + \frac{C}{C_2}\left(\frac{e}{c'_r}\right) \tag{426a}$$

Equation (426*a*) must be satisfied if the $RLCC_1C_2$ network is to be equivalent to $R'L'C'C'_1$; yet Eq. (426), which represents the actual stiffness ratio, fails to satisfy it by the factor $\pi^2/8$ in the second term. This factor is a consequence of the sinusoidal distribution of that portion of the polarization in the bar which is due to the state of strain. The contribution of the field in the gap due to the state of strain also has a sinusoidal distribution, which can be allowed for by substituting for C_2 in Eq. (426) the value

$$C_2^* = \frac{8}{\pi^2} C_2 \tag{427}$$

When this is done and when C_2^* replaces C_2 in Eq. (426*a*), the two expressions are brought into approximate agreement, with crystals for which, as with quartz, $e'_r \approx e'$.

It does not follow, however, that C_2^* can replace C_2 completely in the equivalent network. For example, in the expression for e/e'_r in Eq. (423), one must still use $C_2 = bl/4\pi w$. Not only is the combined use of both C_2 and C_2^* troublesome, but it would lead to grave complications in applying the graphical methods described earlier in this chapter to a bar with gap. If there is a gap, it is best to derive R', L', and C' directly from the equations in §232, which have the added advantage of being applicable for any value of h. If there is no gap, $q' = q_0$ and both C_2 and C_2^* drop out of consideration, so that the graphical method is then entirely applicable to bars.

We have discussed the problem of the unplated bar with gap at some length because it has been common practice to assume that its electrical characteristics are correctly described in terms of $RLCC_1$ in series with C_2. The magnitude of the error so incurred can be found from Eqs. (426) and (426*a*). In general, for crystals with small piezoelectric reaction, $(q'/q) - 1 = (f_w^2/f_0^2) - 1 \approx 2\,\Delta f/f_0$ where f_w is the frequency when the gap is w and $\Delta f \equiv f_w - f_0$. Calling $(\Delta f)_1$ the value from Eq. (426), which is theoretically correct, and $(\Delta f)_2$ that from the equivalent network

theory in Eq. (426*a*), we find that

$$(\Delta f)_1 = \frac{\pi^2 e_r'}{8e'} (\Delta f)_2$$

Since, when the piezoelectric reaction is small, $e_r' = e + k_l w$ differs but little from $e' = e + k'w$, it follows that the network theory predicts a variation of frequency of the unplated bar with gap that is too small by the factor $\pi^2/8$, approximately.

286. *The Gap Effect in a Plated Bar.* In order to make the two networks shown in Fig. 56 strictly equivalent for lengthwise vibrations, it is necessary to make the crystal surfaces facing the gap equipotential, as can be done by *plating them lightly with metal.* Then, for any gap w, the gap capacitance $C_2 = bl/4\pi w$ can be used in Eqs. (424). These equations give R', L', and C' when R, L, C, and C_1 are known, and the graphical methods described in §§288 and 289 are applicable. As in the case of the bare bar, this equivalent-network method can be applied only at the fundamental frequency, for which $h = 1$.

The dependence of frequency on w in the case of a plated bar can be found most conveniently by an expression derived by the author[107] for the effective stiffness q',

$$q' = q_0 \left(1 + \frac{32\epsilon^2 w}{\pi q_0 e'}\right) = \frac{1}{s_{nn}^E} + \frac{32 d_{in}^2 w}{\pi (s_{nn}^E)^2 e'} \tag{428}$$

The difference between this q' and that given by Eq. (330) for a bare bar is due to the fact that when the surfaces are made equipotential the distribution of the depolarizing field is changed.

Equation (428) gives the value of q' to use in Eq. (322) for C', when the crystal is plated. It becomes $1/s_{nn}^E$, as it should, when the gap is zero. The degree of approximation in Eq. (428) should be amply accurate for quartz, but not for Rochelle salt.

By the method that was used in deriving Eq. (336*b*) it is found that the relative variation of frequency with gap, for a bar whose opposite faces have been made equipotential by *plating*, is

$$\frac{\Delta f_0}{f_0} \approx \frac{16 d_{in}^2 w}{\pi s_{nn}^E e'} \equiv U \frac{w}{e'} = U \frac{w}{e + k'w} \tag{429}$$

where $U = 16 d_{in}^2/\pi s_{nn}^E$.

When $w = \infty$, the relative increase in resonant frequency over that when $w = 0$ is, for the plated bar, $16 d_{in}^2/\pi s_{nn}^E k_l$. This value* is greater than that for an unplated bar, as derived from Eq. (336*b*), by the factor $\pi^2/8$.

* The air-gap equation given by Dye (ref. 127, p. 426) can be reduced to Eq. (429). Dye did not take account of the distinction between the dielectric constant of a free crystal and k_l for a vibrating bar nor of the distinction between the gap effects with bare and plated bars.

287. Summary on the Application of Equivalent Network Theory to Plates and Bars. In summary, it may be said that the equations for the equivalent network, including C_2, together with the graphical representation, are applicable to thickness vibrations of plates at the fundamental frequency or any overtone thereof; and also to lengthwise vibrations of *plated* bars at the fundamental frequency.

If the bar is not plated, the equations for the equivalent electrical network of a resonator with gap, and the graphical representation, are valid only as a first approximation. If there is no gap, they become entirely valid. But in no case can the method of the equivalent network of the type treated here be employed at overtone frequencies of bars.

288. Resonance Diagram for a Piezo Resonator with Gap. Thus far the graphical method has been applied only to the simple $RLCC_1$ network. The graphical construction will now be explained whereby the equivalent values R_h', L_h', C_h', and C_1', as well as the critical frequencies, can quickly be determined for a resonator with gap, or with a condenser C_2 in series, when R_h, L_h, C_h, and C_1 at zero gap are given. The assumption is made that Figs. 56*b* and *c* are equivalent, which means that Eqs. (424) are valid. As has been shown, this assumption is fully justified with thickness vibrations and with lengthwise vibrations when the bar has its surfaces plated; and, as shown in §285, it holds approximately for an unplated bar cut from a crystal such as quartz, of relatively low piezoelectric constant. With all lengthwise vibrations in which the vibration direction is normal to the electric field, only the value $h = 1$ can be used (§285).

In the following sections we shall omit the subscript h, with the understanding that it can be restored when any harmonic frequency is to be considered. The procedure consists in inverting the admittance diagram for $RLCC_1$ to an impedance diagram, inserting C_2, and inverting back to an admittance diagram. As will be seen, the two inversions entail a change in the distribution of frequencies around the circle.

Using the same notation as in previous sections, we let the admittance of C_1 be represented by $AF = -\omega C_1/s_y$ in Fig. 63. The resonance circle is primarily the locus of *admittances* for the $RLCC_1$ combination. On this circle we let the frequencies at B and at any point P be f_0 and f, respectively. Then, in accordance with Eq. (387), the same circle can be regarded as an *impedance* locus, in which the impedance of $RLCC_1$ is $Z_1' = s_z \cdot FP'$.

In order to represent graphically the connection of C_2 in series, we lay off a distance FF' such that $s_z \cdot F'F = -1/\omega C_2$. The vector sum of $F'F$ and FP' is $F'P'$, and the impedance of $RLCC_1C_2$ is

$$Z_2' = s_z \cdot F'P' \tag{430}$$

The same circle that is the locus of admittances for $RLCC_1$ is now

serving as the locus of *impedances* for $RLCC_1C_2$; to every point P on the former circle there corresponds a point P' on the latter. A line drawn from F' to any point on the circle gives the impedance of $RLCC_1C_2$ at some particular frequency.

From Eq. (386) and the foregoing statements it is seen that

$$-s_z \cdot AF' = \frac{1}{\omega C_1} + \frac{1}{\omega C_2} \tag{431}$$

289. Figure 63 can be inverted into an *admittance* diagram for $RLCC_1C_2$ by performing an inversion with F' as center. The operation

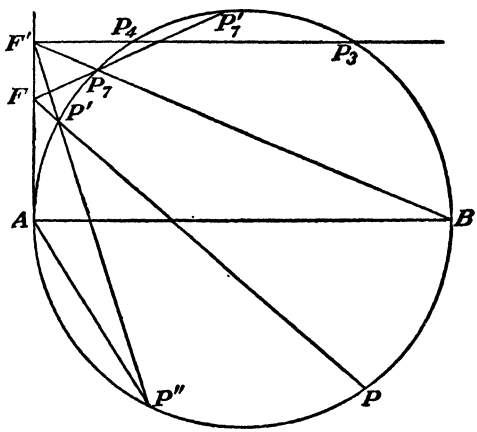


FIG. 63.—Resonance diagram for a resonator with a gap or condenser in series.

consists simply in producing $F'P'$ to cut the circle at P''. The circle is now the admittance locus for $RLCC_1C_2$, with F' as origin. Besides the shift in origin, the introduction of C_2 has brought about two further changes: there is a new admittance scale value s_y', given by

$$s_y' = \frac{1}{s_z(AF')^2} = s_y\left(\frac{AF}{AF'}\right)^2 \tag{432}$$

and the frequency distribution around the circle is altered. The new distribution of frequency will be explained in the next section.*

* The foregoing statements can be generalized in the following manner: When the origin of vectors has to be shifted owing to the introduction of an impedance or admittance into the circuit, the scale value remains unchanged. On the other hand, if with respect to the new origin an *inversion* is performed to pass from admittances to impedances or the reverse, a new scale value is required. One example of this is the introduction of the new scale value s_y' in Eq. (432); another example will be found in §303.

The admittance of $RLCC_1C_2$ at the frequency corresponding to P on the admittance circle for $RLCC_1$ is found from Eqs. (430) and (432) and $(F'P')(F'P'') = (AF)^2$ to be

$$Y_2' = \frac{1}{Z_2'} = s_y' \cdot F'P'' \tag{433}$$

This is the graphical equation for Y_2'. The analytical equation is of the same form as Eq. (383) or (384), with the circuit elements primed to indicate the presence of C_2:

$$\mathrm{Y}_2' = \frac{R'}{Z'^2} - j\left(\frac{X'}{Z'^2} - \omega C_1'\right) \tag{433a}$$

or, in the neighborhood of resonance, where $\omega = \omega_0 - n$,

$$Y_2' \approx \frac{R'}{R'^2 + 4n^2L'^2} + j\left(\frac{2nL'}{R'^2 + 4n^2L'^2} + \omega_0 C_1'\right) \tag{433b}$$

R', L', C', and C_1' are given by Eqs. (423) and (424). Y_2' is the sum of two admittances, one of which is the vector $F'A$, practically constant over the resonant range, while the other is AP'', which has a circular locus. Since this is exactly the condition that obtained in the case of the diagram for $RLCC_1$, it is clear that the new diagram, with F' as origin, represents a series chain, which we call $R'L'C'$, in parallel with a fixed capacitance C_1'. From Eqs. (431) and (432), C_1' has the value

$$C_1' = \frac{C_1C_2}{C_1 + C_2} = C_1\left(\frac{e}{e_r'}\right) = -s_y'\frac{AF'}{\omega} \tag{434}$$

in agreement with Eqs. (424). The other relations in Eqs. (424) also have their graphical counterparts. The expression for R'/R is verified with the aid of Eqs. (385a), (431), and (432):

$$R' = \frac{1}{2\rho s_y'} = R\left(\frac{C_1 + C_2}{C_2}\right)^2 \tag{434a}$$

When the frequency scale for the admittance circle for $RLCC_1C_2$ has been determined, L' and C' can be calculated. Their values are found to be identical with those in Eqs. (424):

$$L' = L\left(\frac{C_1 + C_2}{C_2}\right)^2 \tag{434b}$$

$$C' = C\frac{C_2^2}{(C_1 + C_2)(C + C_1 + C_2)} \tag{434c}$$

From the foregoing statements it is evident that a diagram such as Fig. 63, with the origin of vectors at F', may be thought of as representing either the $RLCC_1$ network in series with C_2 or the equivalent simple

network $R'L'C'C_1'$. In the former case, AF' represents $\omega C_1C_2/(C_1 + C_2)$, and, in the latter case, $\omega C_1'$, which by Eq. (434) amounts to the same thing. All vectors and all frequencies are the same from either point of view. It must be remembered, however, that the insertion of C_2 changes the various scale values, since, as has been shown, the latter are functions of C_2. In §§302 to 304 we shall discuss the more general case of a resonator in series or parallel with any arbitrary impedance.

290. *Effect of C_2 on Resonator Frequencies.* When a gap or an external capacitance C_2 is in series with the resonator and the vectors for admittance or impedance are laid off from an origin at F' in Fig. 63 according to the preceding paragraphs, the frequency scale value σ, as defined by Eq. (378a), remains unaltered, since the damping constant

$$\alpha = \frac{R}{2L} = \frac{R'}{2L'}$$

remains unchanged. Nevertheless, all frequencies are shifted clockwise around the circle in a manner that will now be explained.

For the simple $RLCC_1$ network it was shown in §267 that frequencies are determined graphically in terms of frequency differences above or below the frequency at point B on the circle, measured on a linear scale on the vertical axis through B, Fig. 58. When C_2 is included, the frequency at B no longer has the same value as before but is increased by a certain amount depending on C_2 and on whether the vectors are taken as representing impedances or admittances.

When C_2 is in, we shall denote the frequency at B by f_0' and find the difference $f_0' - f_0$. Only the procedure for an *admittance* diagram need be worked out in detail; the value of $f_0' - f_0$ for an impedance diagram is found by analogous steps. The relation between f_0 (the frequency at B for $RLCC_1$ alone) and f_0' is easily found by the following graphical method. The same method can be applied to finding the frequency corresponding to any other point on the admittance circle for $RLCC_1C_2$.

When there is a gap, the frequency at point B on the admittance diagram is that at which the particle velocity and the current in the $R'L'C'$-branch have maximal values, just as is the case when the gap is zero and we write RLC in place of $R'L'C'$.

In Fig. 63 the admittance at point B on the admittance circle for $RLCC_1C_2$ is $s_y' \cdot F'B = Y_2'$, the frequency at this point being f_0'. On performing inversions one finds $s_z \cdot F'P_7 = Z_2'$, $s_z \cdot FP_7 = Z_1'$, and $s_y \cdot FP_7' = Y_1'$. Hence P_7' marks the point of frequency f_0' on the admittance circle for $RLCC_1$. But this is the fiducial circle, the calibration of which was explained in §267. On the fiducial circle the frequency at B is f_0. The frequency difference $f_0' - f_0$ can be found graphically according to §267. Analytically, since $\omega_0^2 = 1/LC$ and $\omega_0'^2 = 4\pi^2 f_0'^2 = 1/L'C'$,

one finds from Eqs. (434b) and (434c) that

$$f_0' - f_0 \equiv \Delta f = f_0\left(\sqrt{\frac{C + C_1 + C_2}{C_1 + C_2}} - 1\right) \tag{435}$$

291. The relative change in frequency due to the gap is

$$\frac{\Delta f}{f_0} = \sqrt{1 + \frac{C}{C_1 + C_2}} - 1 \tag{436}$$

If, as is the case with quartz, $C << (C_1 + C_2)$, one finds approximately*

$$\frac{\Delta f}{f_0} \approx \frac{C}{2(C_1 + C_2)} = \frac{e}{e_r'}\frac{C}{2C_2} \tag{436a}$$

When this equation is applied to an unplated bar, $C_2^* = 8C_2/\pi^2$ should be used in place of C_2, according to §285.

Equation (436a) can be shown to agree with Eq. (368) except for a small difference due to the nature of the approximations involved.

The frequency f_0' is that at which the particle velocity and the current in the $R'L'C'$ branch have maximal values. As may be seen by applying a simple graphical construction to Fig. 64, f_0' lies between the frequencies for maximum and minimum admittance f_m' and f_n' shown in Fig. 64, and it may properly be called the *response frequency* when the gap is so great that there is no longer any series resonance in the usual sense.

When the gap is small enough for the resonator to exhibit parallel and series resonance (as explained in §294), then, if R is small, f_0' is practically indistinguishable from f_s'.

In order to express the difference $\omega_p' - \omega_s'$ between parallel and series resonance when there is a gap, we may substitute the values of L' and C' from Eq. (424) in the equation $\omega_0'^2 = 1/L'C'$, assuming, as stated above, that $\omega_s' \approx \omega_0' = 2\pi f_0'$. The result is

$$\omega_s'^2 \approx \frac{1}{LC}\left(\frac{C + C_1 + C_2}{C_1 + C_2}\right) = \omega_s^2\left(\frac{C + C_1 + C_2}{C_1 + C_2}\right) \tag{437}$$

From Eqs. (398) (with all quantities primed), (423), and (424), it is found that

$$\omega_p'^2 \approx \frac{1}{L'C'} + \frac{1}{L'C_1'} \approx \omega_s'^2\left[1 + \frac{CC_2}{C_1(C + C_1 + C_2)}\right] \tag{438}$$

whence

$$\frac{\omega_p' - \omega_s'}{\omega_s'} \approx \frac{C'}{2C_1'} \approx \frac{CC_2}{2C_1(C + C_1 + C_2)} \tag{438a}$$

These expressions for ω_p' and ω_s' hold only for small gaps and low piezoelectric constants, as explained in §§294 and 295.

* This approximate relation was also given by Dye[127] in his equation (22).

Relation between f_p and f_0' When the Gap Is Infinite. From Eq. (438*a*) or (401), it is seen that at zero gap, when $C << C_1$ and R can be ignored,

$$\frac{f_p}{f_s} - 1 \approx \frac{C}{2C_1} \tag{439}$$

At infinite gap, writing f_∞ for f_0' in Eq. (435) and setting $C_2 = 0$, one finds

$$\frac{f_\infty}{f_0} - 1 \approx \frac{C}{2C_1} \tag{439a}$$

It follows, since $f_0 \approx f_s$, that $f_\infty \approx f_p$.

That is, *the frequency for parallel resonance when the gap is zero is approximately the same as the response frequency when the gap approaches infinity.*

It must be clearly understood, however, that this statement holds good only when R is small and the piezoelectric constant is small enough to make $C << C_1$. With quartz this condition is fairly well met. On the other hand, in Rochelle salt f_∞ may be far greater than f_p, as will be seen in §375.

292. Equation (438*a*) is sufficiently accurate for the small gaps usually employed in resonators. For larger gaps, where w is of the order of magnitude of e, the resistance R cannot be ignored. In fact, when w increases beyond a certain limit, the resonator becomes capacitive at all frequencies. There are then no longer any frequencies for series and parallel resonance, since these terms are defined as the frequencies at which the reactance vanishes. For all values of w, however, there are a maximum and a minimum value of admittance, the values of f_m and f_n depending on w.

As the gap increases from zero, the interval $\omega_p - \omega_s$, at first relatively large, gradually diminishes, becoming zero at a value of w that can be found by equating the numerator on the right of Eq. (389) to zero and deriving the condition under which X has a single value. This condition is

$$2\omega C_1' R' = 1 \tag{440}$$

With the aid of Eqs. (422) and (423), Eq. (440) can be written in terms of C_2 and the constants for zero gap, giving

$$C_2 = \frac{2R\omega C_1^2}{1 - 2R\omega C_1} \tag{440a}$$

or, since $C_2 = bl/4\pi w$,

$$w = \frac{e}{k}\left(\frac{2\pi e}{R\omega_0 kbl} - 1\right) \tag{440b}$$

As an example, Eq. (440*b*) may be applied to the quartz bar mentioned in §298. It is found that the critical value of w is about 0.5 cm. If the gap is greater than this, the admittance of the resonator is entirely capacitive.

293. The foregoing statements may be verified by inspection of Fig. 64. In the notation of §§269, 270, 288, and 289,

$$AF = -\frac{\omega C_1}{s_y} = -\frac{1}{\omega C_1 s_z},$$

$FF' = -1/C_2 s_z$. When $w = 0$, $FF' = 0$ and the frequencies for maximum and minimum admittance f_m and f_n fall at points P_m and P_n, obtained by drawing a line from F through the center C of the circle. As w increases from zero, F' moves upward from F (usually F has practically the same location for both f_m and f_n). When F' coincides with F_1, w has the critical value given by Eq. (440*b*), and the frequencies for series and parallel resonance merge at P_2. At this point $Y_m = Y_n = s'_y \cdot F_1P_2$, where s'_y is given by Eq. (432). The corresponding frequency on the fiducial circle (§267) comes where a straight line from P_2 to F cuts the circle.

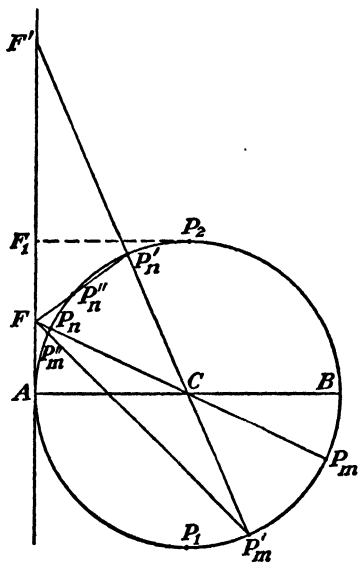


FIG. 64.—Effect of increasing gap on maximum and minimum admittance of a resonator.

For larger values of w, F' falls above F_1, and there is no longer either series or parallel resonance. For a given location of F', the maximum and minimum admittances are $Y'_m = s'_y \cdot F'P'_m$ and $Y'_n = s'_y \cdot F'P'_n$, while $Z'_m = s_z \cdot F'P'_m$ and $Z'_n = s_z \cdot F'P'_n$. For the $RLCC_1$ network, the impedance corresponding to P'_n is $Z'_1 = s_z \cdot FP'_n$, and on the fiducial circle the admittance at the same frequency is $Y'_1 = s_y \cdot FP''_n$. On the fiducial circle, therefore, the frequency for maximum admittance, when w is such that F' comes in the position indicated in Fig. 64, falls at P''_n. Similarly, the frequency for minimum admittance falls at P''_m. The introduction of a gap has caused the point for maximum admittance to move clockwise from P_m to P'_m, while the point marking the frequency has moved counterclockwise; the frequency increases from the value at P_m to that at P''_n. The frequency for minimum admittance increases from the value at P_n to that at P''_m.

At infinite gap, $FF' = \infty$ and P'_m and P'_n coincide with P_1 and P_2.

The frequencies are thus still further increased, to values that can be represented graphically by the method described above or calculated by means of Eq. (425) or, depending on the type of resonator, by means of (330), (336a), (370), or (429).

When the gap is so large that the admittance Y_2' of $RLCC_1C_2$ is capacitive at all frequencies, the variation of Y_2' with frequency is as shown qualitatively by Fig. 65, in which f_m' and f_n' are the frequencies at P_m' and P_n' in Fig. 64. As w approaches infinity, the frequency difference $f_m' - f_n'$ decreases toward a very small but definite limit, while Y_2' approaches zero. It is true that the line representing Y_2' in Fig. 64 becomes infinitely long, but it must be noted that the scale value s_y' varies in such a manner as to make Y_2' itself diminish toward zero. Although the response of the resonator, as indicated by the crevasse or the click method, theoretically vanishes at infinite gap, still the stray electrostatic coupling can be enough to produce a response even when the resonator is entirely disconnected from the oscillating circuit. A narrow bar 2 or 3 cm long suspended by a thread in the neighborhood of the tuning condenser or coil can still cause an audible click when the oscillator frequency passes through the resonant value. The response is due to the minute change in capacitive admittance from a maximum at f_m' to a minimum at f_n'.

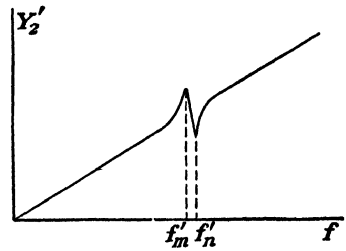


FIG. 65.—Variation of resonator admittance with frequency when the gap is large.

294. *The Failure of Approximate Equations When the Gap Is Large.* Many of the formulas given in this chapter, including some that have been used by various investigators in the measurement of the constants of resonators and of crystals, are approximations. One approximation is the treatment of R as a very small quantity or ignoring it altogether. A second approximation rests on the assumption that the resonance phenomena under discussion are comprised within a band of frequencies so narrow that the frequency difference $n = \omega_0 - \omega$ is small in comparison with ω_0.

We have now to examine the validity of a third assumption, mentioned in the text but not yet fully explained. This is the assumption that the gap between crystal and electrodes is small enough to make such equations as those in §§276 and 279 sufficiently accurate:

$$\frac{f_n - f_m}{f_m} \approx \frac{f_p - f_s}{f_s} \approx \frac{C'}{2C_1'} \tag{441}$$

The electric constants are primed to indicate the presence of a gap.

In deriving the equations in §276 by the binomial theorem the condition for sufficient approximation is that $4\omega^2 C_1'^2 R'^2 << 1$, that is,

$$\omega C_1' R' << 0.5 \tag{442}$$

From Eqs. (422) and (423) this expression may be written as

$$\frac{e_r'}{e} = 1 + \frac{kw}{e} << \frac{0.5}{\omega C_1 R} \tag{442a}$$

The smaller R is, the greater can the gap w be without violating this inequality. In many practical cases the approximate equations referred to are accurate only when w is very much less than the critical value given by Eq. (440*b*), for which $\omega_p - \omega_s$ vanishes. That is, w must be small enough to make the distance AF' in Fig. 64 only a small fraction of AF_1. For quartz the allowable gap width w is of the order of magnitude of the crystal thickness e or less.*

As an example we consider the quartz bar described in §298. Here $\omega C_1 R = 0.03$; hence, by Eq. (442*a*), $w << 0.5$ cm. For values of w greater than this the more rigorous equations should be used.

The limitation imposed on the equations as w increases does not in any way affect the applicability of the *graphical* method. By means of a graphical construction the various frequencies and admittances can be determined at all gaps with as much precision as any graphical method permits.

We return now to the approximate equations (441). From §§232 and 255 it is found that $C'/2C_1'$ is proportional to e/e_r', vanishing at infinite gap. That Eq. (441) breaks down completely when w is large is clear from the foregoing discussion. This equation predicts that $(f_n - f_m)$ and $(f_p - f_s)$ gradually approach zero with increasing w, whereas in fact $(f_p - f_s)$ vanishes at a certain finite w, while $(f_n - f_m)$ remains greater than zero at all gaps.

295. Finally a fourth approximation consists in the assumption that C in the *RLC*-branch of the resonator is small in comparison with C_1. While most of the equations are independent of this assumption, still it must be made if the equations in §284 for the equivalent network of a bar in *lengthwise* vibration are to hold with any precision, as will soon be shown. The expressions in §284 are accurate for plates in *thickness* vibration whatever values C and w may have. The following discussion has to do only with lengthwise vibrations in bars:

The ratio C/C_1 is large when the piezoelectric constant is large, as

* The reason why Eq. (397), for example, is accurate only when the gap is small may be expressed by saying that, even though R may be very small at zero gap, still, with increasing gap, R' rapidly becomes large (primed symbols are used when there is a gap).

may be seen from Eq. (322). This is the case with Rochelle salt. With quartz, as explained in §288, the equivalent network equations and the corresponding graphical treatment can be used with fair accuracy at all gaps, whether the bar is bare or plated, since C/C' is very small.

When C is not small in comparison with C_1 or, as in Rochelle salt at certain temperatures, is even greater than C_1, the outstanding consequences are as follows: (1) By Eq. (401), the difference in frequency $(\omega_p - \omega_s)$ between antiresonance and resonance is relatively large. (2) The frequency f_∞ at infinite gap, instead of being approximately equal to f_p, according to the statement following Eq. (439a), is much greater than f_p.

This second consequence does not follow at all from the simple network equations (424). The reason, as already stated in §284, is that they are accurate only when the elastic compliance varies with the gap in a particular manner, a condition that is not fulfilled in the case of the bar.

The reason why a large piezoelectric constant brings about a relatively great value of f_∞ is evident at once from an inspection of Eq. (331). That it is also so much greater than f_p cannot be seen from the elastic equations, but it follows from Eq. (335).

The experimental confirmation of the foregoing statements will be found in §375.

296. *Resonance Conditions for Thickness Vibrations in Very Thin Plates or at High Harmonic Frequencies.* In most types of piezo oscillator the resonator vibrates at a frequency at which its reactance is inductive. One must therefore make sure that the effect of the gap or of an external reactance connected in any way to the resonator is not to deprive the resonator of its region of inductive reactance. From the last section it is clear that the condition that must be satisfied if the resonator with gap is to have an inductive region is that the origin of admittance vectors F' in Fig. 64 shall be below the point F_1, for which $AF_1 = AB/2$.

If there is no gap, the origin is at F. For most resonators, the ratio AF/AB is relatively very small. We shall now investigate certain cases in which AF may become so great, even with zero gap, as to make the resonator capacitive at all frequencies.

From Eqs. (380) it follows that in general, when $w = 0$, $AF/AB = AF/2\rho = \omega_h C_1 R_h$, where ω_h is approximately h times the fundamental frequency f_0 and R_h is given in Table XXII. As long as $\omega_h C_1 R_h < 0.5$, there is a range of frequencies over which the resonator is inductive. Now from Table XXII we find, on writing $\omega_h \approx \pi h(q_0/\rho)^{\frac{1}{2}}/e$,

$$\omega_h C_1 R_h = \frac{hk'' e \sqrt{q_0 \rho}}{16\epsilon^2} \alpha_h \tag{443}$$

This expression can also be written in terms of the quality factor $Q_h = \pi f_h/\alpha_h$:

$$\omega_h C_1 R_h = \frac{\pi h^2 k'' q_0}{32\epsilon^2 Q_h} \tag{443a}$$

Either Q_h or the damping factor α_h may be taken as a measure of the resonator losses. Since they include both mounting losses and dissipation of energy in the crystal, theory can predict neither their amount nor their dependence on frequency. Obviously, if α_h is independent of frequency, Q_h cannot be. If experiment shows α_h to be constant, Eq. (443) indicates that $\omega_h C_1 R_h$ is proportional to the product he. The resonator will have an inductive region when $\omega_h C_1 R_h$ does not exceed 0.5, that is, when

$$he \gtrless \frac{8\epsilon^2}{k''\alpha_h \sqrt{q_0/\rho}} \tag{444}$$

This expression sets the limit to the order of harmonic h for a given e or to the thickness e itself at the fundamental frequency; above this limit the reactance of the resonator can be only capacitive.

On the other hand, if Q_h should turn out to be independent of frequency, one would conclude from Eq. (443a) that, when $\omega_h C_1 R_h \gtrless 0.5$,

$$h^2 \gtrless \frac{16\epsilon^2 Q_h}{\pi k'' q_0} \tag{444a}$$

In this case the resonator would become capacitive at a comparatively low value of h; but at the fundamental frequency it would have an inductive region for all values of e, unless Q_h were so excessively low that h could not even equal unity.

As an example we consider a quartz plate 1 mm thick, with a fundamental frequency around $3(10^6)$. In round numbers we may take $\epsilon = 5(10^4)$, $k'' = 4.5$, $q_0 = 90(10^{10})$, $\rho = 2.65$. Then, if $\alpha_h = 1{,}000$ at all frequencies, Eq. (444) shows that h can have any value up to about 30. But if Q_h has the value 10,000 at all frequencies, h cannot exceed 5. Such experimental data as are available indicate that the latter of these alternatives is more nearly correct.* That is, while Q and the logarithmic decrement δ appear to be independent of frequency, α_h increases with the frequency.

297. *Distribution of Potential in Crystal and Gap.* The current I from p to q in Fig. 56 is

$$I = \frac{V}{Z_2'} = \frac{V_1}{Z_1'} = V_2 \omega C_2 \tag{445}$$

where Z_2', Z_1', and $1/\omega C_2$ are the impedances of $RLCC_1C_2$, $RLCC_1$, and C_2,

* See Mason and Fair.[341]

respectively. The potential drops V_1 across the crystal and V_2 across the gap, in terms of the total drop V, are

$$\frac{V_1}{V} = \frac{Z_1'}{Z_2'} \qquad \frac{V_2}{V} = \frac{1}{\omega C_2 Z_2'} \tag{446}$$

$Z_1' = 1/Y_1'$ is given by Eq. (383) or (384) and $Z_2' = 1/Y_2'$ by Eq. (433*a*) or (433*b*).

The dependence of the relative magnitudes of V_1 and V_2 upon frequency is brought to light clearly by means of the resonance circle in Fig. 63. It is shown in §288 that for any frequency, such as that corresponding to point P on the admittance circle for $RLCC_1$, the following relations hold: $Z_1' = s_z \cdot FP'$, $Z_2' = s_z \cdot F'P'$, and $\omega C_2 = -1/(s_z \cdot F'F)$. Considering magnitudes only, one has, from Eq. (446),

$$\frac{V_1}{V} = \frac{FP'}{F'P'} \qquad \frac{V_2}{V} = \frac{F'F}{F'P'} \tag{447}$$

As represented in Fig. 63, P comes at a frequency very close to the resonant value f_0 at B. As the frequency increases, P moves counterclockwise around the circle, while P', the point inverse to P with respect to F, moves clockwise, causing a decrease in $F'P'$ and an increase in FP'. V_1 therefore increases, until at a certain frequency the ratio $FP'/F'P'$ has a maximal value. Since the position of F' does not vary perceptibly with frequencies near resonance, this maximal value comes when the line $F'P'P$ passes through the center of the circle. This construction at once determines the position of P and therefore the frequency at which the voltage across the crystal, and also across the gap, is a maximum with constant V for a given C_2. This is the frequency at which the impedance of the entire network is a minimum.

For a given V, this maximal ratio V_2/V depends on C_2 and has its greatest possible value at a certain critical value of C_2. The geometrical problem is to find that position of F' that makes $FF'/F'P_1$ a maximum, P_1 being the new location of P' on the straight line from F' to the center of the circle. It is easily proved that this condition is satisfied when FP_1 is tangent to the circle, so that FP_1F' is a right angle. Since now $AF = FP_1$, it follows that at this frequency the reactance of C_1 is numerically equal to the impedance of $RLCC_1$.

When C_1 is relatively small and the gap is such that C_2 has the critical value, the potential drop across the gap may be many times greater than the applied potential V. Dye,[127] who made a study of this effect, found the increase to be as much as thirtyfold. If V is of the order of 50 volts, a glow discharge may be seen in the space between electrodes and crystal, with either lengthwise or thickness vibrations.

298. A Typical Resonance Curve. The characteristics of a typical resonator are shown in Fig. 66. Qualitatively, they illustrate the performance of all piezo resonators. Numerical data are for the same X-cut quartz bar $N2$, in lengthwise vibration, and with a small gap, that has been mentioned in previous papers.[93,550] The dimensions are $X1.4$

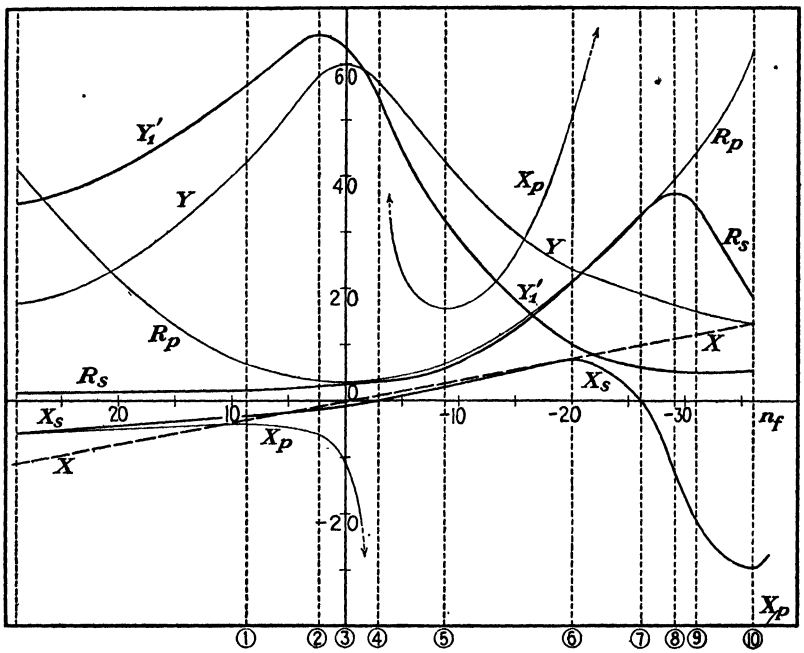


FIG. 66.—Some characteristic curves of a piezo resonator of frequency 89.87 kc. Abscissas are departures from resonance, in cycles per second. Frequency increases from left to right. Ordinates shown in the figure are to be multiplied by 10^6 esu for Y and Y', and by $5(10^{-9})$ esu for X, X_s, X_p, R_s and R_p. The vertical dotted lines are marked to correspond to points on the circumference of the circle in Fig. 67 (first column in Table XXIII).

mm, $Y30.7$ mm, $Z4.1$ mm, fundamental frequency $f_0 = 89.87$ kc/sec, $\omega_0 = 5.65(10^5)$. The equivalent electric constants are

$$L = 137 \text{ henrys} = 1.52(10^{-10}) \text{ esu}$$
$$R = 15{,}000 \text{ ohms} = 1.67(10^{-8}) \text{ esu}$$
$$C = 0.0228 \text{ mmf} = 0.0205 \text{ esu}$$
$$C_1 = 3.54 \text{ mmf} = 3.19 \text{ esu}$$

The product $\omega C_1 R$, which according to Eq. (381) determines the ratio $AF:AB$ in Fig. 67, is only about 0.03. Although this value is much larger than is common with modern, well-mounted resonators, still it is so small that its use would bring the point F so close to A as to crowd the

critical points in the neighborhood of F very close together. The performance of the resonator can be shown more instructively by arbitrarily multiplying C_1 by a suitable factor. In the present case the factor 10 has been chosen, so that the value of C_1, for the purpose of illustration, is assumed to be $C_1 = 31.9$ esu. The effect is the same as if an external capacitance of 28.7 esu were placed in parallel with the crystal.

299. The graphical procedure for obtaining the ordinates of the various curves is illustrated in Fig. 67. In constructing this diagram, a

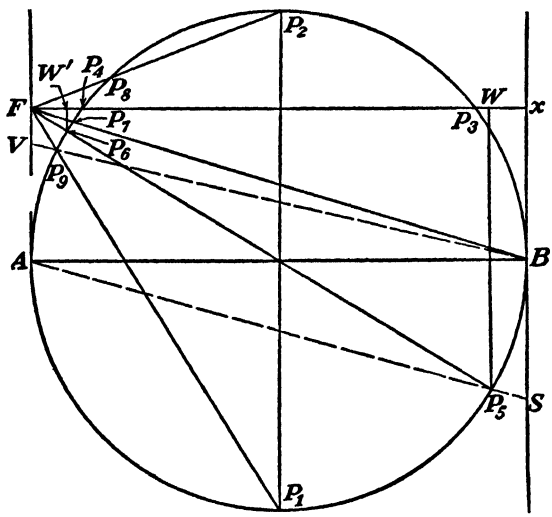


FIG. 67.—Resonance circle used in deriving the data for Fig. 66.

circle was first drawn with diameter $AB = 2\rho = 16$ cm. From the data above, together with $\rho = 8$ cm, it was found from Eqs. (375), (385a), (378a), and (379a) that $s_y = 3.75(10^6)$, $s_z = 1.16(10^{-8})$,

$$FA = \frac{\omega C_1}{s_y} = 4.8 \text{ cm},$$

$\sigma = 0.544$ cycle sec^{-1} cm^{-1}, $\sigma' = 96$ cycles sec^{-1}cm. Values plotted in Fig. 66 were obtained for the critical points shown in Fig. 61 and for a few other selected points, so that smooth curves could be drawn with enough accuracy to illustrate the characteristics of the resonator. For example, in the case of point P_5, the distance BS was measured, and $n_f = \sigma \cdot BS$ was calculated, where $n_f = f_0 - f_5$, f_0 is the frequency at B, and f_5 the frequency at P_5. This value of n_f (2.4 cycles/sec) was plotted as abscissa in Fig. 66. At this frequency, $Y = s_y \cdot AP_5$, $Y_1' = s_y \cdot FP_5$ (maximal value of Y_1').

The values of R_s, R_p, X_s, and X_p (§§271, 273) for points P_5 and P_6 were obtained by dropping perpendiculars on the line Fx in Fig. 67 from P_5 and also from P_6, the point inverse to P_5. In the notation of Fig. 59, these perpendiculars are P_5W and P_6W' (P_5 and P_6 correspond to P and P' in Fig. 59*b*). Then, according to Eqs. (388), (389), and (395*a*), $R_s = s_z \cdot FW'$, $R_p = 1/(s_y \cdot FW)$, $X_s = s_z \cdot W'P'$, and $X_p = 1/(s_y \cdot WP)$.

The same process was used for the other points, except that for points on the left side of the circle (as, for example, P_9) it was more convenient to use the frequency scale value σ' and to measure AV instead of BS, as explained in §268. In such cases the value of n_f is given by $n_f = \sigma'/AV$.

300. As may be seen from Fig. 66, Y has a maximum at $n_f = 0$, while the maximum of Y_1' comes at a slightly lower frequency. The maximum of R_s comes at the frequency corresponding to the point P_7 inverse to B, for which point $FW' = Fx = AB$. As may be easily verified, this maximum value is $(R_s)_{max} = 1/RC_1^2\omega^2$. R_p has its minimum value when $n_f = 0$. X_s becomes zero at points P_3 and P_4, where the resonator is a pure resistance; its maximum value is at the frequency corresponding to the point P_8 inverse to P_2, while its minimum is at P_9, inverse to P_1 (see also Fig. 62). X_p has a maximum at P_1, a minimum at P_2, and becomes infinite at P_3 and P_4; a vestige of X_p coming up from $-\infty$ can be seen in the lower right-hand corner.

Over a range of frequencies considerably beyond that shown in Fig. 66, the distance $AF = -\omega C_1/s_y$ remains practically constant. At still lower frequencies the point F approaches A, while it moves upward without limit on the h-f side. Moreover, at very high and very low frequencies the distance AV, in terms of which frequencies are expressed, becomes too small to measure accurately. Recourse must be had then to the algebraic equations, which become very simple at frequencies far enough from resonance for certain terms in R to be ignored. It is convenient to write $\omega = h\omega_0$, where h is a multiplying factor greater or less than 1. The admittance of RLC can be written as

$$Y \approx \frac{1}{X} = \frac{\omega_0 L(h^2 - 1)}{h}$$

For Y_1', X_s, and R_s, we use Eqs. (383), (388), and (389). By this means the following values have been computed, providing an extension of the data in Fig. 66, all in esu.

The table on page 377 illustrates the extent to which the various quantities are affected as the frequency departs widely from resonance. The admittance Y sinks to $\frac{1}{200}$ of its maximum value when the frequency is off resonance by 2 per cent. Y_1', like Y, gradually becomes a pure capacitive admittance. Since at very low frequencies $Y \to 1/X \to \omega C$, it is evident from Eq. (383) that $Y_1' \to (C + C_1)$. On the h-f side, $Y_1' \to C_1$.

$$C_s = -\frac{1}{\omega X_s}$$

tends toward the limiting values $(C_1 + C)$ and C_1 on the l-f and h-f sides, respectively. Considered as a condenser, the resonator has a series capacitance C_s that diminishes from $(C_1 + C)$ at low frequency to C_1 at high frequency; this is equivalent to saying that the dielectric constant defined as $k = 4\pi C_s/A$ undergoes a diminution on passing through the resonant region, with anomalous values in the resonant region itself (see §258). It will be noted, however, that C_s differs from its limiting

TABLE XXIV

h	f	Y	Y_1'	X_s	$\frac{X}{R}$	R_s	C_s
	kcs	$\times 10^6$	$\times 10^6$	$\times 10^{-8}$		$\times 10^{-12}$	
0.5	4,494	0.0077	9.05	−11	7,750	0.012	32.2
1.02	9,167	0.303	18.1	− 5.5	198	4.65	31.5
1.5	13,481	0.0140	27.2	− 3.7	4,300	0.0044	31.8

values (31.92 and 31.9) perceptibly, even for detuning as great as that indicated by $h = 0.5$ and $h = 1.5$. The large ratio X/R shows that the resonator has a very low power factor even for detuning as low as 2 per cent. Corresponding to this fact are the low values of R_s, which are practically negligible in comparison with R.

In an actual quartz resonator the diminution of C_s from $(C_1 + C)$ to C_1 with increasing frequency would be much more pronounced than is indicated by the data above. Even so, the diminution in quartz is less than 1 per cent; on the other hand, in Rochelle salt the diminution is very large.

The arbitrary assignment to C_1 of a value ten times the actual value for the crystal in question has served its purpose in making the steps in the graphical method easier to follow. Qualitatively it has not made the resulting curves less instructive. On the quantitative side it may be said that, if C_1 were smaller, the maximum of Y_1' would come closer to that of Y, with respect to both magnitude and frequency. The minimum of Y_1' would be lower and would come at a higher frequency. The frequency scale itself would remain unchanged, but the interval $\omega_p - \omega_s$ between the two values for $X_s = 0$ would be increased almost proportionately to the decrease in C_1. From Eq. (400) it can be shown that, if instead of the fictitious value 31.9 we had used 3.19 for C_1, $f_p - f_s$ would have been about 290, instead of the value 23.3 shown in Fig. 66.

301. *Effect of R upon the Performance of the Resonator.* As was stated in §269, the smaller R is, the larger is s_y (for a circle of the same diameter)

and the smaller σ and σ' become. Therefore, as R diminishes, the frequency scale becomes more wide open, fewer cycles are comprised on the right side of the circle between the quadrantal points, and the resonance is sharper. The maxima of Y and Y_1' are higher, and the minimum of Y_1' is lower. The difference between the frequencies for series and parallel resonance is greater when R is made smaller, as may be seen from Eq. (400).

In the discussion following Eq. (393) the necessity for retaining R in the expressions for R_s and X_s over a relatively wide range of frequencies is emphasized. This fact is well illustrated in the foregoing example. For instance, if X_s for point P_7 in Fig. 66 or 67 is calculated from Eq. (389), it is found that the terms in R^2 form the chief contribution to both numerator and denominator. It is only at considerably higher frequencies or at correspondingly low frequencies that the simpler equation (393) can be used.

302. Graphical Method for the Insertion of Other Circuit Elements. As the basic resonator network only the $RLCC_1$ combination need be considered. If there is a gap, the primed values shown in Fig. 56*b* should be used.

In the present section the method will be outlined briefly, leaving specific applications until later.

a. A Resistance R_1 in Series with C_1. This case occurs when there are losses in C_1; such losses in Rochelle salt are discussed by Mason.[338] We have $Z_1 = R_1 - j(1/\omega C_1)$, $Y_1 = R_1/Z_1^2 + j(1/\omega C_1 Z_1^2) = g_1 - jb_1$. Hitherto R_1 has been ignored, and, as in Eq. (380), we have set

$$AF = -\frac{\omega C_1}{s_y},$$

with $\omega C_1 = b_1$ and $g_1 = 0$. When R_1 is included, we can no longer use F as the origin of vectors for the resonator. Instead, it is necessary to choose as origin a new point, represented as O'' in Fig. 68, such that

$$AF'' = -\frac{b_1}{s_y} = \frac{1}{s_y \cdot \omega C_1 Z_1^2} \qquad O''F'' = \frac{g_1}{s_y} = \frac{R_1}{s_y \cdot Z_1^2} \tag{448}$$

The presence of R_1 makes AF'' smaller than AF in the ratio

$$\frac{AF''}{AF} = \frac{1}{1 + R_1/(s_y \cdot Z_1^2)}.$$

O'' is to be used as the origin for all vectors for $RLCC_1R_1$ in the same way that F was used in preceding sections for $RLCC_1$.

303. *b. An Impedance Z_2 in Series with $RLCC_1$.* Let the point P (Fig. 68) on the Y-circle for RLC be given, at any frequency f, and let it be required to find the vector representing the impedance of $RLCC_1Z_2$

at this frequency. The impedance of $RLCC_1$ is $Z_1' = s_z \cdot FP'$. Draw the line OF of such length that $s_z \cdot OF = Z_2 = R_2 + jX_2$, so that

$$s_z \cdot OM = R_2, \qquad s_z \cdot MF = X_2.$$

As represented in Fig. 68, X_2 is capacitive. If it were inductive, M would lie below F.

The vector sum of Z_2 and Z_1' is Z_2', given by the equation $Z_2' = s_z \cdot OP'$. Its components are $R_2' = s_z \cdot OW$ and $X_2' = s_z \cdot WP'$. P' is the point on the impedance circle for $RLCC_1Z_2$ at which the frequency is the same as at P on the original admittance circle for RLC.

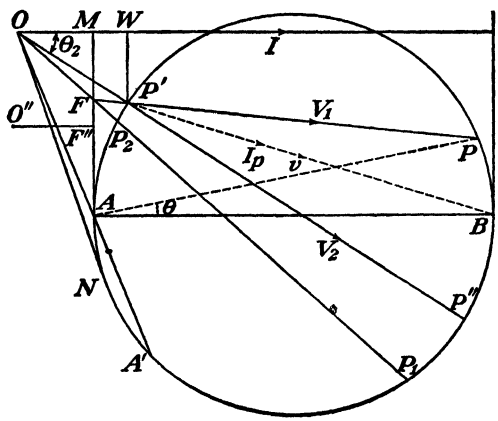


FIG. 68.—Resonance diagram for a resonator with an impedance in series.

The admittance diagram for $RLCC_1Z_2$ is obtained by inverting P' into P'', with O as center of inversion, and ON (tangent to the resonance circle at N) as radius of the circle of inversion. ON need be drawn only when the scale value s_y'' for admittances of $RLCC_1Z_2$ is desired:

$$s_y'' = \frac{1}{(s_y \cdot ON^2)}$$

The admittance of $RLCC_1Z_2$ at frequency f is then $Y_2' = s_y'' \cdot OP''$.

The method described in §282 for representing *phase relations* can be applied to the present case. We let V_1 and V_2 be the potential difference across $RLCC_1$ and $RLCC_1Z_2$, respectively. With this notation, the phase relations are as indicated in Fig. 68.

With regard to the distribution of frequencies around the admittance circle for $RLCC_1Z_2$, it is to be noted first that, upon the addition of Z_2, A inverts into A', which becomes the point for zero and infinite frequency. At P_1 and P_2, on the prolongation of OF, frequencies are the same as

on the original admittance circle for RLC. All frequencies that, on the RLC circle, lie on the lower (l-f) portion between A and P are now compressed into the arc $A'P''$. The frequencies corresponding to all points on the admittance circle with Z_2 out (origin at F) are, when Z_2 is in, shifted in both directions away from P_2 toward P_1.

This extension of the graphical method is useful in investigating the effect of the impedance of the circuit to which the resonator is connected on the critical frequencies and on the performance of the resonator. For example, the maximum and minimum impedances of $RLCC_1Z_2$ are found simply by drawing a line from O through the center of the circle. The frequencies at series and parallel resonance are determined by the points where the horizontal line through O cuts the circle. If AM is greater than the radius of the circle, these points no longer exist, and the circuit is capacitive (or inductive if AM is drawn downward) at all frequencies.

If it is desired to find the frequency corresponding to any point P'' on the admittance circle for $RLCC_1Z_2$, the method described for locating P'' when P is given is worked backward. First P' is found, on the line $P''O$; then $FP'P$ is drawn; and the desired frequency is that for P on the RLC circle. This frequency is determined as described in §267.

It may happen that Z_2 cannot be regarded as constant over the range of frequencies considered. For example, as in §316, Z_2 may be arbitrarily varied so as to hold the current in some part of the circuit at a maximum value; or Z_2 may contain elements that are either sharply tuned or subject to variation with current, as is the case with tube impedances. In such cases it is necessary to determine the locus of the origin O in Fig. 68, whereby the position of O at any given frequency is known. Such a method is described in §324.

The graphical treatment can also be extended without difficulty to cover the case where an arbitrary impedance is connected *in parallel* with either $RLCC_1$ or $RLCC_1C_2$. This and other features of the graphical method have been discussed elsewhere by the author.[105]

304. *c. A Capacitance C_3 in Parallel with $RLCC_1C_2$.* As in §288, the capacitance C_2 in series with $RLCC_1$ may be either the gap or an external condenser. In either case the admittance locus is the circle in Fig. 63, with $s'_y \cdot AF' = -\omega C'_1$ from Eq. (434) and with a frequency scale for $RLCC_1C_2$ determined according to §290. The addition of C_3 (condenser or capacitance of connecting wires, etc.) in parallel with $RLCC_1C_2$ simply necessitates moving the origin upward exactly as in the case of C_2, only now the new origin F'' is determined by the equation $s'_y \cdot FF' = -\omega C_3$, or $s'_y \cdot AF'' = -\omega(C'_1 + C_3)$. The frequency distribution is still that for $RLCC_1C_2$, but the critical points when C_3 is in are shifted in such a manner that series resonance, corresponding to point P_3 in Fig. 61,

comes at a frequency very slightly higher than when C_3 is out; the same is true of the frequency for maximum admittance. The frequencies for parallel resonance and for maximum impedance are *lowered* by the presence of C_3. That is, a parallel capacitance diminishes the frequency interval between series and parallel resonance.

These relations are easily derived analytically. The equation for series resonance, analogous to Eq. (397), is*

$$\omega_s'^2 = \frac{1}{L'C'} + \frac{R'^2C_3'}{L'^2C'} = \frac{1}{LC}\left(1 + \frac{C}{C_1 + C_2} + \frac{R^2C_{123}(C + C_1 + C_2)}{LC_2^2}\right) \quad (449)$$

where L', C', and R' are given by Eqs. (424), $C_3' = C_1' + C_3$, and

$$C_{123} = C_1C_2 + C_2C_3 + C_3C_1$$

R is usually small enough to justify the approximation

$$\omega_s'^2 \approx \frac{1}{LC}\left(1 + \frac{C}{C_1 + C_2}\right) \quad (450)$$

This expression is the same as Eq. (437) for $RLCC_1C_2$, showing that the presence of C_3 is practically without effect on the frequency for series resonance.

The frequency for parallel resonance, when R is small, is found most readily by applying Eq. (383) to the $R'L'C'C_1'$ network, setting $R' = 0$ and $Z' = X' = (\omega^2L'C' - 1)/\omega C'$. Then, for $RLCC_1C_2C_3$,

$$Y_3' \approx -j\left(\frac{\omega C'}{\omega^2L'C' - 1} - \omega C_1' - \omega C_3\right)$$

The condition for parallel resonance is that $Y_3' = 0$. By the use of Eqs. (424) one then finds

$$\omega_p'^2 \approx \frac{1}{L'C'}\left(1 + \frac{C'}{C_1' + C_3}\right) \approx \frac{1}{LC}\left[1 + \frac{C(C_2 + C_3)}{C_1C_2 + C_2C_3 + C_3C_1}\right] \quad (450a)$$

The last expression involves the approximation

$$C + C_1 + C_2 \approx C_1 + C_2$$

305. *The Resonance Circle for Motional Admittance.* From Eq. (329) it is seen that a proportionality exists between the current I_p in the RLC branch of a resonator for lengthwise vibrations and the particle velocity v at the ends of the bar. A similar relation can be proved for thickness

* The symbol ω_s' is used in order to avoid confusion with ω_s, the value for the $RLCC_1$ network alone.

vibrations. This proportionality is expressed in Eqs. (325) and (367), for lengthwise and thickness vibrations, as a fixed ratio between the electrical impedance Z_h of the *RLC* branch and the mechanical impedance $(Z_c)_h$. A corresponding ratio must hold for piezo resonators of other types as well. It follows that the same admittance circle, with the same scale of frequencies, can be used for the mechanical admittance, as that which has been described in the case of the electrical admittance. Since we are dealing here only with the *RLC* branch, the origin of vectors is at A on the resonance circle, for example in Fig. 58. Any electric vector divided by the electromechanical ratio r gives the corresponding mechanical vector. That is, the scale value for mechanical admittances is $s_c = rs_y$.

On the circle for mechanical admittance, the maximum admittance comes at point B, where the particle velocity is a maximum and the frequency is defined as f_0. In accordance with Eq. (94), the frequency f_a for maximum amplitude of vibration is lower than f_0 by the amount $f_0\delta^2/8\pi^2$, where δ is the logarithmic decrement per period. From Table XXIII it is seen that the frequency f_a is only $C/4C_1$ as far from f_0 as is the frequency for maximum electrical admittance, at point P_5; at P_5 the frequency is already extremely close to f_0.

If there is a gap between crystal and electrodes, the resonance circle in Fig. 63 is used, with F' as origin for electric vectors. The presence of the gap (represented by a shift of origin from F to F') changes the maximum particle velocity and also the distribution of frequencies around the circle. The frequency for maximum particle velocity, though somewhat higher than when there is no gap, still comes at point B in Fig. 63. By §§58 and 234 the amplitude of vibration ξ_0 at the boundary of the resonator, in terms of the peak current $(I_p)_0$ in the *RLC* branch, is

$$\xi_0 = \frac{e'_r}{2\epsilon bew}(I_p)_0 \tag{451}$$

306. *The Electrical and the Mechanical Theories of a Resonator with Gap.* The *electrical theory* may be defined as that which regards the electric and elastic properties of the resonator as those characteristic of zero gap, while the gap itself is represented as a series capacitance C_2, as illustrated in Fig. 56*c*. The equivalent network is $RLCC_1C_2$.

On the other hand, the *mechanical theory* treats the electric and elastic properties as dependent on the gap. The equivalent network is $R'L'C'C'_1$ as shown in Fig. 56*b*, in which all four parameters are functions of the gap. The elastic stiffness, which occurs as a factor in C', is different from that which occurs in C when there is no gap. In the following discussion we shall use q_w for the stiffness when there is a gap w and q_0 for the value when $w = 0$. According to the electrical theory the stiffness is q_0 at all values of the gap.

The equivalence of the two theories has already been proved. It remains only to show how each requires a somewhat different description of the vibrational process.

Let f_0 be the resonant frequency for $RLCC_1$ as observed when there is no gap, and let f_w be the resonant frequency when the gap is w. Then, under constant impressed voltage, if the frequency f_0 is applied while the gap is w, there is no resonance. According to the electrical theory the crystal is being driven at its resonant frequency, its impedance is low, but the drop in voltage takes place mostly in the gap so that the amplitude of vibration is small. According to the mechanical theory the stiffness of the crystal, in the presence of the gap, is so great that the applied voltage causes only forced vibrations of small amplitude.

Similarly, when the impressed frequency is f_w, the electrical theory states that there is electric resonance although the crystal itself is not in mechanical resonance: the impedance of the crystal is large, so that the potential drop across it is relatively large, resulting in forced vibrations of great amplitude. On the other hand, the mechanical theory states that the crystal is vibrating in resonance, with low impedance, and that the large drop in potential across it is produced piezoelectrically by its own deformation.

The difference in the point of view is due to the different definitions of the stiffness of the crystal. Which view to adopt is a matter of convenience. In any case, when the crystal with gap is in resonance, $f_w > f_0$, so that the $RLCC_1$ combination is inductive, while C_2 is, of course, capacitive. Over a certain range of values of C_2 the potential drop across C_2 and also the corresponding drop across the crystal may be many times greater than the applied voltage V. The condition for maximum voltage across the gap is shown graphically in §297.

CHAPTER XV

THE DYNAMIC MEASUREMENT OF PIEZOELECTRIC AND EQUIVALENT ELECTRIC CONSTANTS

A vibrating system of one degree of freedom when set in motion by the interaction of charged bodies on an electrostatic field behaves as a series combination of inductance, resistance and capacity. —S. BUTTERWORTH.

307. Although the technique of electrical measurements lies outside the scope of this book, it is desirable to indicate the principles on which are based the applications of standard methods of measurement at radio frequencies to the crystal resonator. The choice of method depends on the size of the quantity to be observed and on the required precision, as well as on simplicity and the desirability of obtaining results in a short time by as few observations as possible.

The measurement of elastic constants has been treated in §§75 and 252. In §§183 and 184 we have considered briefly the measurement of piezoelectric constants by static methods.

In the present chapter the "click" method is first described, in which use is made of the audible response of a resonator as the impressed frequency passes through resonance. There follows an outline of the methods available for determining, from observations with circuits of various types, the piezoelectric constants of any crystal, and the electric constants of the equivalent network for any piezo resonator. Lastly we shall discuss the reduction of such observations, with particular reference to the use of graphical methods.

For the methods described below, the most indispensable feature of the equipment is a generator with extremely fine frequency regulation over the resonance range of the crystal. The generator must be sufficiently stable to hold its frequency and voltage constant, at any given setting, during the time needed for a series of observations; means must be provided for measuring accurately small changes in frequency; and the generated frequency should be immune against reaction due to the varying impedance of the crystal. The generator may be a power oscillator of 50 to 250 watts, very loosely coupled to a secondary circuit containing the crystal; or it may be a low-power oscillator connected through an amplifier to the crystal, the stages of amplification being so designed as to prevent reaction. For the more precise measurements it may be necessary to adjust the frequency within a small fraction of a cycle per

second. The importance of avoiding harmonics in the output voltage is emphasized in §379.

308. The Click and Key-tapping Methods. Before coming to the quantitative measurements of the piezoelectric and equivalent electric constants, we describe some simple circuits that are useful for qualitative tests of piezoelectric crystals, such as those mentioned in §172. These circuits also provide a means for making an approximate determination of crystal frequency in terms of a frequency meter and for calibrating a frequency meter when one or more resonators of known frequency are available. Those who are just beginning the study of crystal resonators can learn much about their performance by experimenting with these simple devices.

For demonstrating the principle of the *click method* it is convenient to use a low-power tube oscillator with inductive feedback and with a telephone receiver or loud-speaker in the anode circuit; either the grid or the anode circuit may be tuned. The frequency must be continuously variable over a considerable range on each side of crystal resonance. As a resonator, a small X-cut quartz bar (length parallel to Y) may be chosen. For lengths of 10 to 40 mm the fundamental lengthwise frequency varies, in round numbers, from 300,000 to 75,000 cycles/sec. If the anode voltage is low enough to avoid danger of fracture, the crystal, which may be mounted loosely between fixed electrodes, can be connected directly across the tuning element. As the tuning condenser is varied through the setting corresponding to crystal resonance, a characteristic *click* is heard, which has more of a musical quality the lower the frequency and the smaller the damping of the resonator. The sound is due to the fact that the resonator is set into vibration when the condenser reaches the critical setting and continues to vibrate for a fraction of a second. During this time it acts as a generator, impressing on the tube circuit an alternating voltage at its own resonant frequency and producing beats with the oscillating current already present. A d-c meter in the anode circuit will also respond at crystal resonance.

The click can also be heard with the crystal at other locations in the oscillating circuit, for example in series with the grid, with a high-resistance leak in parallel. One can usually hear an audible response with one electrode of the crystal disconnected. Indeed, it may suffice to suspend the bar, without electrodes, from a thread and let it hang close to the coil or to a binding post of the tuning condenser. Enough energy is absorbed and reradiated to produce the beats.

When the click method is used with thickness vibrations, one hears, on tuning through the frequency at which the response should come, not a single click, as in the case of the bar, but rather a whole volley of clicks. A very large number of responses may be heard in a narrow range of

frequency around the expected value. This complexity is due chiefly to various elastic couplings, as stated in §244. The procedure for reducing the number of responses, and for obtaining a single dominating frequency of resonance, as is necessary in efficient piezo oscillators, is mentioned in §352.

If the oscillating circuit is already calibrated, or of too high power, it is better to place the crystal in a loosely coupled secondary circuit, as shown in Fig. 69. L_1 is the output coil of the oscillator. L_2C_3 should be tuned approximately to the crystal. The click is heard in the telephone receiver T. A d-c milliammeter may be used in place of T. If desired, the crystal may replace the grid condenser C_4.

In the earlier experiments, the author sometimes used a contact detector (galena or molybdenite) and telephone receiver in place of the

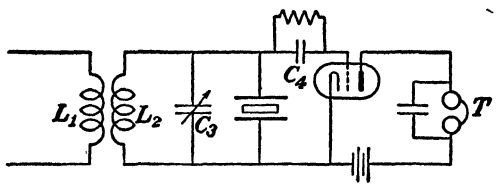


FIG. 69.—Circuit for resting a resonator by the click method.

detecting tube shown in Fig. 69. Moreover, it was found that L_1 could be the coil of a buzzer-driven wavemeter; in this case L_2 picked up trains of decaying waves, and the buzzer tone, heard continuously in T, underwent a change in quality when the wavemeter was tuned through crystal resonance.

With the circuits that have been described, somewhat greater precision can be gained by setting the tuning condenser of the generator circuit as closely as possible to the critical value and then suddenly varying it by a small amount. The setting is altered by small stages until the click is just heard. By performing this operation with both increasing and decreasing settings, a fairly precise mean value can be obtained.

309. This last expedient leads naturally to the *key-tapping method*, whereby the rapid turning of a variable condenser back and forth is avoided. All that is necessary is to place in parallel with the tuning condenser in the oscillating circuit a small auxiliary variable condenser in series with a key. The auxiliary condenser should be set at such a value that when the key is pressed the frequency f is changed to a value f_1 such that $f - f_1$ is a frequency in the audible range. The key should be on the grounded side in order to avoid a troublesome knock on closing. The key is tapped repeatedly as the tuning condenser is slowly varied. When a setting is reached such that, with the key open, the resonator is set into vibration, then on closing the key a beat note, of longer or

shorter duration, is heard. This note has a very sharp maximum at the resonant frequency. It is, of course, also possible to listen for maximum loudness of the beat note on *opening* the key.

Either the click method or the key-tapping method is a helpful adjunct to the equipment for measuring resonator constants by the methods outlined in §§315 to 321. Owing to the extreme sharpness of resonance of a good crystal, it is usually quite difficult to find the adjustment of the oscillator corresponding to the very narrow band of frequencies to which the crystal responds. If provision is made for listening to the click, this adjustment can be arrived at very quickly.

DYNAMIC MEASUREMENT OF PIEZOELECTRIC CONSTANTS

The methods that have been employed may be classified as follows:

a. The gap method, involving measurements of frequency of a resonator at two different gaps, usually $w = 0$ and $w = \infty$.

b. The antiresonance method, by which the gap (commonly zero) is fixed while the frequencies at resonance and antiresonance are observed.

c. The resonance-curve method, by which the piezoelectric constant is derived from the value of the equivalent R, L, or C.

d. The elongation method, by which the maximum elongation of a bar at resonance is measured.

e. The composite-bar method, by which the crystal under investigation is vibrated by means of a second crystal of known constants.

Either lengthwise vibrations of bars or thickness vibrations of plates may be used. The chief equations for each case will now be given. For generality, we assume the bar or plate to be oblique, so that all constants are primed, indicating transformed axes.

310. *a. The Gap Method.** Owing to the difficulty in measuring small gaps with precision, as well as to the lack of close agreement between observations and theory noted in §§349 and 353, no gain in precision can be expected by using gaps other than zero and infinity.

Bars. Only the fundamental lengthwise frequency need be considered. For gaps zero and infinity we have

$$(s'_{nn})^E = \frac{1}{4l^2\rho f_0^2} \qquad (s'_{nn})^* = \frac{1}{4l^2\rho f_\infty^2}$$

With negligible error f_0 and f_∞ may be regarded as frequencies at either maximum admittance of the resonator or maximum amplitude of vibration.

* This method was first used by the author[107] for measuring d_{25} of Rochelle salt. Soon after this, Mikhailov[368] used it for d_{14} of Rochelle salt, obtaining a result in good agreement with that by method *c*.

The solution is somewhat different according to whether or not, when $w = \infty$, the surfaces of the bar normal to the electric field are plated with a metallic coating to render them equipotential. If the surfaces are bare, Eqs. (332) and (333) are to be used, giving

$$(d'_{in})^2 = \frac{k'}{16\pi l^2 \rho}\left(\frac{1}{f_0^2} - \frac{1}{f_\infty^2}\right) \tag{452}$$

where i indicates the field direction and k' is the dielectric constant of the free crystal for the particular orientation, measured at a non-resonant low frequency.

Thus when k'_i is known, d'_{in} can be found from the frequencies at zero and infinite gap. The precision with which $(d'_{in})^2$ can be measured by this method depends on that of k'_i and of the frequency difference $(f_\infty - f_0)$; and, as in all other methods, it is limited also by the fact that the ideal conditions assumed in the equations never can be exactly realized in practice.

The large value of the dielectric constant k_x of Rochelle salt makes it permissible, for an X-cut bar from this crystal, to write Eq. (452) in the form

$$(d'_{12})^2 \approx \frac{\eta'}{4l^2\rho}\left(\frac{1}{f_0^2} - \frac{1}{f_\infty^2}\right), \tag{452a}$$

where $\eta' = k'/4\pi$. In calculating d_{14} for Rochelle salt from Mason's observations, Mueller[378] used this equation.

When a *plated bar* is used, the stiffness at infinite gap, from Eq. (428), is

$$q_\infty = \frac{1}{s^E_{nn}} + \frac{32 d^2_{in}}{\pi (s^E_{nn})^2 k'} \tag{453}$$

From this equation, together with (311) and the relation $q_0 = 1/s^E_{nn}$ for zero gap, one finds

$$\frac{k'_i}{4\pi (d'_{in})^2} \approx 4l^2\rho f_0^2\left(\frac{8}{\pi^2}\frac{f_\infty^2}{f_\infty^2 - f_0^2} + 1\right) \tag{454}$$

This approximation is valid only for crystals with small piezoelectric constants, like quartz.

As an example of the foregoing method, we calculate d_{11} for quartz from the author's observations on a quartz X-cut bar with dimensions X0.152 cm, Y4.04 cm, Z1.40 cm. The unclamped dielectric constant is $k' = 4.5$. When the bar is bare, the observed frequency for $w = 0$ is $f_0 = 6.65(10^4)$. Extrapolation of observed frequencies for $w = \infty$ gives $f_\infty - f_0 = 298$. Similarly for the same bar when plated, $f_0 = 6.65(10^4)$, $f_\infty - f_0 = 240$. On substitution of these values in the foregoing equa-

tions we find, for the bare and plated bars, $6.45(10^{-8})$ and $6.42(10^{-8})$, respectively. Although the values are comparatively low, owing probably to defects in the bar, they show at least that the formulas give practically identical results for bare and plated bars.

Plates. By observing the frequencies f_0 and f_∞ of thickness vibrations, the following expression can be derived from Eq. (355) for the effective piezoelectric constant ϵ:

$$\epsilon^2 = \frac{\pi e^2 \rho k''}{8} (f_\infty^2 - f_0^2) \tag{455}$$

where e is the thickness and k'' the clamped dielectric constant for the particular orientation. Except with the simplest cuts the derivation of the fundamental e_{mh} from ϵ is impossible. In general, observations with several plates in different orientations would be necessary. When it is considered that k'' cannot be calculated without a previous knowledge of at least the approximate values of the piezoelectric constants or observed without the use of extremely high frequency (§247), it becomes clear that it is not advisable in general to attempt to determine the piezoelectric constants by the gap method with thickness vibrations. No such determination seems to have been undertaken.

311. *b. The Antiresonance Method.* The frequencies f_s and f_p for series and parallel resonance (resonance and antiresonance) are observed at a fixed gap, preferably zero.

The desired expressions can be derived from the approximate equation (401) when the piezoelectric constants are small. If the piezoelectric reaction is large, as in Rochelle salt, it is better to start with the more rigorous equations (397) and (398), in which it is usually allowable for the present purpose to set $R = 0$. One thus finds, to a high degree of precision,

$$\frac{\omega_p^2 - \omega_s^2}{\omega_s^2} = \frac{C}{C_1} = \frac{f_p^2 - f_s^2}{f_s^2} \tag{456}$$

From Eqs. (324) and Table XXII it is found that C/C_1 has the same form for both lengthwise and thickness vibrations. If f_p and f_s are observed at harmonic h, $C_h/C_1 = 32\epsilon^2/\pi h^2 k q_0$, whence, since $q_0 = 4l^2\rho f_s^2/h^2$,

$$\epsilon^2 = \frac{\pi k l^2 \rho}{8} (f_p^2 - f_s^2)^2 = \frac{\pi h^2 k q_0}{32} \frac{C_h}{C_1} \tag{457}$$

For thickness vibrations, we write k'' for k and let l represent the thickness. For lengthwise vibrations (with which only $h = 1$ should be used) k becomes k_l and l is the length of the bar. ϵ is the effective piezoelectric constant for the particular orientation. In order to obtain the fundamental piezoelectric constants, observations with several different

orientations are usually necessary. In the case of bars, the effective piezoelectric strain coefficient (d'_{in} in the preceding paragraphs) can be found directly from ϵ by the relation $d'_{in} = \epsilon/q_0$.

This method is simple and fairly accurate. The chief difficulty, aside from the determination of k, is that the antiresonant f_p is not sharp. It is the method used by Mason[340] in measuring d_{11} and d_{14} for quartz.

312. *c. The Resonance-curve Method.* While methods *a* and *b* use only two observed frequencies, method *c* offers the advantage of increased accuracy, in that by means of a resonance curve or of the resonance circle a large number of observations at different frequencies can lead to an accurate measurement (§315) of the equivalent L, R, or C. Then Eqs. (324) or those in Table XXII (page 323) can be solved for ϵ, from observations on bars or plates, respectively. The simplest expression to use is that for L or C, although the values of d_{11} obtained by Andreeff, Fréedericksz, and Kazarnowsky, by Fréedericksz and Mikhailov, and by Van Dyke, in Table XIX (page 220) were obtained from R. Nussbaumer's value in the same table was derived from observations with a crevasse circuit (§316), which is essentially an equivalent-network method.

No sharp distinction can be drawn between methods *b* and *c* except insofar as *c* can make use of more observational data. For example, the last part of Eq. (457) is written for use with method *c*. From this equation can be derived an expression for d'_{in} in terms of k', applicable to a bar vibrating at its fundamental lengthwise frequency. By writing $k \equiv k_l = k' - 4\pi(d'_{in})^2/s^E_{nn}$, we find, since $\epsilon = d'_{in}/s^E_{nn}$,

$$(d'_{in})^2 = \frac{\pi s^E_{nn} k' C}{4(8C_1 + \pi^2 C)} = \frac{\pi^2 s^E_{nn}}{8bl} C \tag{458}$$

where C and C_1 are in esu.

313. *d. The Elongation Method.* This method is hardly suitable for plates but has been used by Fujimoto* with a quartz X-cut bar, for determining d_{11}. The method is the dynamic analogue of the static measurement of piezoelectric constants by the converse effect. The amplitude of vibration ξ_0 at one end of the bar at resonance is observed with an optical interferometer. From Eqs. (67), (324), (329), (87), and (406), one finds for the effective piezoelectric constant, with sufficient precision,

$$\epsilon = \frac{I_0}{2b\omega_0\xi_0} = \frac{V_0}{2b\omega_0 R\xi_0} = \frac{M\omega_0^2\xi_0}{2bQV_0} = \frac{M\omega_0\xi_0}{2bV_0}(\omega_2 - \omega_1) \tag{459}$$

* T. Fujimoto, *Proc. World Eng. Congr., Tokyo*, vol. 20, pp. 399–416, 1929. The value of $d_{11} = \epsilon/s_{11}$ in Table XIX was calculated by the author from Fujimoto's data. For a more complete treatment of the application of the interferometer to resonator measurements, with experimental data, see H. Osterberg[299] and S. H. Cortez.[113] Preliminary observations by this method were made by E. M. Thorndike (Willbur Fiske Scholar thesis, Wesleyan University, 1926).

Any one of these expressions may be used, depending on which electrical quantities are observed. I_0 and V_0 are maximum current and voltage at resonance, R is the resistance in the equivalent network, $M = \rho ble/2$ is the equivalent mass, and Q is the quality factor from Eq. (67). ω_2 and ω_1 are the angular velocities at the two quadrantal points (§277); if observations are made at a sufficient number of frequencies for plotting the resonance circle, $(\omega_2 - \omega_1)$ can be determined with considerable precision.

This method calls for practically the same electrical equipment as method *c*, in addition to means for measuring the elongation. It is therefore not to be recommended, except as a check on the other methods and on the theory.

314. *e. The Composite-bar Method.* This method was introduced by Mason[338] for determining the piezoelectric constant a_{14} (his f_{14}) of Rochelle salt. He cemented an X-cut 45° Rochelle-salt bar endwise to a quartz bar of which the constants were accurately known. The bars had a common lengthwise resonant frequency, and the system was driven by an oscillator connected to the quartz. The quartz had also a pair of small auxiliary electrodes that could be connected to an amplifier of high impedance for comparing the voltage drop E_q across the quartz with E_R across the Rochelle salt. For this purpose the Rochelle-salt bar, otherwise bare, had a pair of small electrodes plated on at its center. The Rochelle salt was set in vibration by the quartz. Since the layer of cement came at a loop of motion, it was under very little strain. In evaluating the observations it was necessary to estimate the ratio of the strains y_{yq} and y_{yR} on either side of the joint. Mason's formula may be written as follows:

$$a_{14} = \frac{8\pi(c^D_{44})_R(d'_{12})_q}{k'_q} \frac{(s'_{22})_R}{(s'_{22})_q} \frac{e_q}{e_R} \frac{y_{yq}}{y_{yR}} \frac{E_R}{E_q} \tag{460}$$

where s'_{22} is the effective stiffness in each case and e_q and e_R are the thicknesses of the bars. Using an 18.5° quartz bar (§357) of known d'_{12} and k', Mason found $a_{14} = 7.6(10^4)$ at 30°C; for the dependence on temperature see §474.

This method is, of course, applicable to any piezoelectric crystal from which a bar can be so cut that its piezoelectric constant can be expressed in terms of the elongation of the bar. It offers the great advantage that the dielectric constant of the crystal under investigation need not be known, so far as the constant a_{in} according to the polarization theory is concerned. Nevertheless, in order to find d_{in} from a_{in} the dielectric susceptibility must be known, according to Eq. (xi) or (xii) in Table XX (page 249). For example, in the case of Rochelle salt at 30°C we may use Eq. (495*b*). Then, if $s^D_{44} = 1/c^D_{44} = 1/11.6(10^{10})$, $\eta' = 25$ from Fig. 146, and $a_{14} = 7.6(10^4)$, we find $d_{14} = 16(10^{-6})$.

Method *e* involves rather serious sources of error. As is recognized by Mason, the absolute value of the result cannot be considered very accurate, but relative values over a range of temperatures can be compared with good precision.

315. Determination of the Constants of the Equivalent Network. The methods outlined above for the measurement of piezoelectric constants had to do with a property of the material. We shall now describe methods for finding the electric constants of a resonator of given dimensions. From them, in turn, the mechanical and electric constants of the material can be derived.

The present discussion is applicable to any form of piezoelectric resonator that can be represented by an equivalent electrical network $RLCC_1$, as illustrated in Fig. 50 or 56. We omit the prime accents, with the understanding that the symbols stand for the over-all values, including the effect of the gap when there is one. In general, any change in gap or in the size or placing of the electrodes will affect the values of R, L, C, and C_1. Most of the experimental work mentioned below was done with quartz resonators.

The parameters of greatest practical importance in resonators are the capacitance ratio C_1/C (§280) and $Q = \omega_0 L/R = 1/\omega_0 CR$. These quantities can be calculated when C_1, C, and R have been determined, or they can be expressed directly in terms of observed quantities as indicated below.

The various experimental methods that have been used for determining the electric constants are classified below, though there is a certain amount of overlapping. We cannot go into details here concerning tubes, circuits, shielding, temperature control, and other matters of technique, important as they are. Particular attention should, however, be drawn to one source of error so easily overlooked that the trustful observer may not suspect that it is ruining his results. This circumstance is the presence of harmonic frequencies in the voltage applied to the crystal. A harmonic component of more than negligible size can affect the readings of meters, and in addition it may excite undesired vibrations that react upon the characteristics of the particular mode that is being investigated. It is highly desirable to know the wave form of the generator and to provide such filtering circuits as may be necessary to ensure a practically pure sinusoidal supply to the crystal.

One other troublesome effect should be mentioned, which is present with crystals that have an appreciable temperature coefficient of frequency. As resonance is approached, the crystal vibrates more vigorously, and more of the driving energy is expended in heating the crystal. Even though the resonator may be under temperature control, this body heating changes the constants of the crystal, thus altering the resonant

frequency. A continuous curve can still be obtained, but it is distorted, since the characteristics of the crystal are a function of the ordinates of the curve. The distortion does not prevent the derivation of a correct value of the decrement from the curve. On the other hand, the values of R, L, and C for any particular temperature cannot be determined unless certain corrections are applied to the curve or unless the current can be made small enough to avoid perceptible heating. This effect has been studied by Walstrom in the investigation mentioned in §316; see also Hatakeyama.[209]

316. *a. The Crevasse,* or Parallel-impedance, Method.* This method was first used by the author,[93] and later by Dye[127] in his very thorough

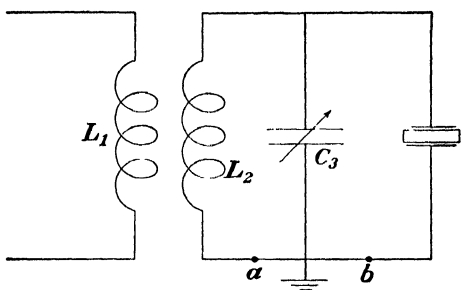


FIG. 70.—Crevasse circuit for measurement of resonator constants.

investigation of the electric properties of the piezo resonator. Dye's paper should be consulted for its treatment of many refinements, in both theory and experiment. Watanabe[581] gives a full discussion of the use of the resonance circle. The method has been employed by many others for the measurement of resonator constants. The circuit is shown in Fig. 70. The output coil L_1 of a generator with fine frequency control is loosely coupled to the secondary circuit containing the crystal. The L_2C_3 circuit should be capable of being tuned both sides of crystal frequency.† As the impressed frequency is varied in small steps, C_3 may be varied so as to make the current in L_2 always a maximum, or it may be left at that constant value for which the L_2C_3 circuit resonates at the natural frequency f_0 of the crystal. The current in L_2 and that flowing to the crystal can be measured by thermoelements at a and b, or readings can be taken on a tube voltmeter connected across the crystal. In any

* The term "crevasse," first used by Dye, was suggested by the form of the response curve, as illustrated in Fig. 75.

† The tuning condenser is designated by C_3 to distinguish it from the air-gap capacitance C_2 that may be present in the equivalent network of the crystal.

case a complete resonance curve can be obtained, from which the crystal constants can be derived.*

Instead of placing the crystal in a separate secondary circuit, Bechmann[43] and Builder[81] connected it directly to the tuned output element of the oscillator itself. The disadvantage in this method is the reaction of the crystal upon the oscillator frequency.

According to a hitherto unpublished method used in this laboratory,† the crystal is connected across the output of an amplifier in such a manner that a practically constant voltage of variable frequency is impressed upon it. The current to the crystal is observed with a thermoelement, and the results are plotted as a resonance curve, from which the decrement can be calculated.

The graphical treatment of the crevasse circuit is given in §322.

317. *b. The Filter, or Series-impedance, Method.* The simple measuring circuit described by Heegner[216] belongs properly in this category. In its simplest form it contains a pickup coil loosely coupled to an oscillator, the crystal, and a thermoelement in series. With certain refinements this device has been used in this laboratory by Newark and Peabody‡ for measuring the maximum and minimum impedances of quartz bars, from which resonance circles were plotted and the equivalent constants were calculated.

Some modifications of Heegner's method are described by Heegner himself, and also by Meissner,[359,360] including the use of a triode in place of the thermoelement.

According to the method that seems at present to be preferable, the crystal is connected as a filter between a variable-frequency oscillator and a receiving circuit, which may be a tube voltmeter (preceded, when necessary, by a suitable attenuator and amplifier) or a detector. The latter is used when only frequencies are to be observed. In one form or another this method has been described by Mason,[332] Booth,[69] and Mason and Fair.[341] When a tube voltmeter is used, the circuit is as represented in Fig. 71. The variable frequency from the oscillator O is impressed across the resistance R_1, and the drop across R_2 is measured by the tube voltmeter V. In order to minimize the stray capacitance of the crystal leads, R_1 and R_2 are made very small and are placed close to the crystal.

* Applications of the crevasse method will be found in the references at the end of the chapter. All who study these papers with a view to using the special techniques described in them should be very discriminating with regard to the extent to which certain small quantities are dropped as being negligible. For example, the expressions derived by Mme. Székely[500] and applied experimentally by Mme. Nussbaumer[395] are valid only at frequencies so far from resonance that the ratio BS/AB in Fig. 59 is large.

† J. E. Walstrom, M. A. thesis, Wesleyan University, 1934.

‡ A. F. Newark, M. A. thesis, Wesleyan University, 1931; E. T. Peabody, M. A. thesis, Wesleyan University, 1933.

For determining the crystal constants it suffices to observe the frequencies f_m and f_n together with the corresponding maximum and minimum voltmeter readings V_m and V_n. These are the values at which the resonator admittance Y_1' has its maximum and minimum values Y_m and Y_n (§278). From Eq. (407) and Fig. 61 it is seen that $Y_m = s_y \cdot FP_5$, $Y_n = s_y \cdot FP_6$. By the principle of inversion, $FP_5 \cdot FP_6 = AF^2 = \omega_0^2 C_1^2/s_y^2$. For a quartz resonator the ratio AF/AB is very small and P_5 is so close

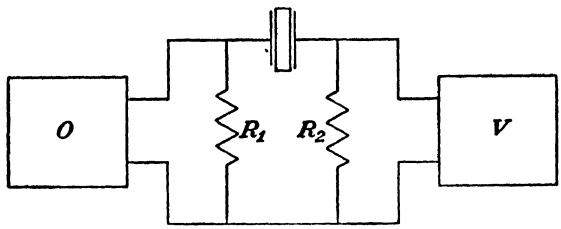


FIG. 71.—Series impedance circuit for measuring resonator constants.

to B that one can write $FP_5 \approx AB = 1/s_y R$. Therefore

$$\frac{Y_m}{Y_n} = \frac{V_m}{V_n} = \frac{FP_5}{FP_6} \approx \frac{1}{R^2\omega_0^2 C_1^2} \tag{461}$$

From this equation R follows at once. In order to determine

$$Q = \frac{\omega_0 L}{R}$$

it is necessary to find L. For this purpose we use Eq. (410a), which, since ω_0 is extremely close to ω_m, may be written in the form

$$\frac{1}{2LC_1\omega_0} \approx \omega_n - \omega_m$$

From this equation and (461) it follows that

$$Q = \frac{\omega_0 L}{R} = \frac{\omega_0}{2(\omega_n - \omega_m)}\sqrt{\frac{V_m}{V_n}} = \frac{f_0}{2(f_n - f_m)}\sqrt{\frac{V_m}{V_n}} \tag{462}$$

As is shown in §281, both f_0 and f_m very nearly coincide with the frequency for series resonance, while f_n is almost exactly that for parallel resonance (antiresonance).

As an alternative method, Mason and Fair replace the voltmeter with a detecting circuit by means of which f_m and f_n are determined. Since f_m is extremely close to the frequency at which the impedance of the crystal becomes simply the R of the RLC-branch, it is possible to find R by substitution of a known resistance in place of the crystal, while the frequency

is held at the value f_m. When R is known, Q is found with the aid of Eq. (403):*

$$Q \approx \frac{f_m}{2\pi(f_n^2 - f_m^2)C_1R} \tag{462a}$$

Mason and Fair describe still another variant of the method, whereby Q is found from V_n, f_n, and any frequency f near resonance together with the corresponding voltage V.

318. *c. The Bridge Method.* The crystal forms one arm of a h-f bridge, and its impedance at various frequencies is measured. Van Dyke and Thorndike used a bridge in their "three-crystal method," which required two auxiliary crystals nearly identical with the one being tested. One auxiliary crystal was in a piezo-oscillator circuit and served as a fixed standard. The other, in a separate piezo-oscillator circuit, supplied the driving current for the bridge; by adjustments of this circuit the frequency could be varied over the necessary range, which was very small. By the use of mixer and beat-counter circuits the applied frequency was very precisely known. From the resulting resonance curve the electric constants of the test crystal were determined.†

A bridge connection was also used by Van Dyke[548] in determining the equivalent network of the crystal by measurements of the Lissajous figures obtained with a cathode-ray oscillograph.

319. *d. The Substitution Method.* By means of a two-way key the crystal may be replaced by a variable resistance or a combination of resistance and reactance in a suitable measuring circuit. Günther,[197] adapting a method due to Pauli, placed the crystal in a secondary circuit, but instead of replacing it by a known impedance he measured the change in resonant frequency when the resistance or inductance of the circuit was varied by a known amount. Becker[45] found the equivalent constants of the crystal by substituting for it a known capacitance and resistance in parallel.

Bechmann[43] placed the crystal between the tubes of a two-tube oscillating circuit, so that in effect his was a filter method. He deter-

* It is here assumed that f_m and f_n are equal, respectively, to f_s and f_p within the limits of precision. That this assumption is justified, at least for quartz, can be seen by applying Eq. (396) to the pairs of mutually inverse points P_3P_4 and P_5P_6 in Fig. 61. The frequencies are f_s at P_3, f_p at P_4, f_m at P_5, and f_n at P_6. From Eq. (396),

$$f_s + f_p = f_m + f_n$$

Now for quartz $f_s \approx f_m$, whence $f_p \approx f_n$.

† The advantages gained, in both convenience and accuracy, by using two matched crystals, one as an oscillator of slightly variable frequency and the other as test crystal in a secondary circuit, should be obvious. The third matched crystal is not needed when there is available a secondary frequency standard with equipment for precise checking of the calibration of the oscillator.

mined the equivalent constants by substituting a known resistance for the crystal or by connecting a known inductance and capacitance in series.

320. *e. The decay method* has been used by several experimenters. Van Dyke[551–554] excited vibrations in a crystal and then allowed them to decay while the crystal was connected through an amplifier to a cathode-ray oscillograph in such a way that the decay took place virtually while the crystal was on open circuit. By a special timing arrangement amplitudes of vibration could be compared at known intervals. The logarithmic decrement was thus found directly. It was by this method that he observed the extremely low decrements mentioned in §363. A similar method has been used by Bosshard and Busch,[73] H. A. Brown,[76] and Becker.[46]

Chaikin[111] let the current from the vibrating crystal pass through a contact detector and ballistic galvanometer. He used a rotating disk carrying a contact to give suitable time intervals and thus measured the decrement. This method has been employed by Rziankin[442] and also by Gockel;[173] the latter substituted a Helmholtz pendulum for the rotating disk. The ballistic galvanometer method is open to the objection that the impedance in series with the crystal is not infinite, so that the measured quantity is not the true open-circuit decrement.

321. The Effective Parallel Capacitance C_1. C_1 is usually derived from measurement of the crystal capacitance at a frequency low enough for the crystal vibrations to be inappreciable, say at 1,000 cycles/sec. The quantity thus measured is, however, the capacitance of the *free* crystal (plus the effect of leads and mounting), and for precise results it should be diminished by a certain amount, in order to allow for the fact that the effective dielectric constant of the crystal when vibrating near resonance is less than that of the free crystal. This diminution depends on the type of resonator.

For an unplated bar, if the frequency f_0 at zero gap and f_∞ at infinite gap are known and also the free dielectric constant k', the effective constant k_l can be found from Eq. (332):

$$\frac{s^E_{nn}}{s^*_{nn}} = \frac{f_w^2}{f_0^2} = \frac{k'}{k_l} \tag{463}$$

k_l is also the type of dielectric constant to use in expressions for the equivalent network of a flexural resonator. In the case of bars in lengthwise vibration it can be measured directly by applying an alternating voltage at twice the fundamental frequency, as described in §371.

In the case of *thickness vibrations* with the field in the m-direction, the effective dielectric constant is k''_m as for a clamped crystal. One can

measure the capacitance $(C_1')_0$ of the free crystal at low frequency and then write $C_1 = k_m''(C_1')_0/k_m'$. For the calculation of k_m'' see §247, where it is also suggested that C_1 for the clamped crystal can be measured directly by using a very *high* frequency.

322. Reduction of Observations for the Determination of the Electric Constants. We are concerned here chiefly with those methods which yield the values of the impedance Z_1' or the admittance $Y_1' = 1/Z_1'$ of the entire resonator at various frequencies. These quantities are defined in §269. The simplest and most widely used procedure, sufficiently precise for most purposes, is to observe the maximum and minimum values Y_m and Y_n (§278), together with the corresponding frequencies f_m and f_n. At these frequencies the resonator is practically a pure resistance.

Before considering this special case further we shall deal with the more general problem, in which measurements are made, at a number of known frequencies in the resonant range, of Y_1' and its components g_1' and b_1' $(Y_1' = g_1' - jb_1')$. It is by this means that the most precise results can be attained.

In this book the term *resonant frequency* usually refers to the frequency f_0 for maximum mechanical admittance, identical with that for maximum electrical admittance of the *RLC* branch (§275). The resonant frequency actually measured is usually f_m, the value for maximum admittance of the entire network (§279). The only other critical frequency near resonance that is readily found is f_s, at series resonance (§276); here the reactance b_1' vanishes, and the resonator becomes a pure resistance. As may be seen from Table XXIII, the differences $(f_0 - f_m)$ and $(f_s - f_0)$ are proportional to R^2, becoming vanishingly small for well-mounted quartz resonators;* with resonators subject to large losses, whether by friction in the mounting, radiation, or the nature of the crystal itself, these differences may have to be recognized. For almost all purposes it suffices to assume that within the limits of error the resonant frequency, as measured by a frequency meter, is $f_0 = f_s = f_m$. Moreover, from the footnote on page 396, it is seen that with equal precision one may set $f_p = f_n$. The quantity that must be measured with highest precision is the frequency *difference* $f_0 - f$, not the absolute value of f_0.

From §269 and Fig. 59 we have the following relations: For the entire $RLCC_1$ network,

$$\omega_0 C_1 = s_y \cdot AF \qquad Y_1' = s_y \cdot FP \qquad g_1' = s_y \cdot FW \qquad b_1' = s_y \cdot WP \quad (464)$$

* For a quartz bar with logarithmic decrement $1(10^{-5})$ the quantity $(f_0 - f_m)/f_0$ is less than one part in thirty million. If Fig. 61 were drawn to scale, the point F for most resonators would come so close to A that points P_1, B, and P_2 would be practically indistinguishable.

For the *RCL* branch, $Y = g - jb$, where

$$Y = s_y \cdot AP \qquad g = s_y \cdot AM = g_1' \qquad b = s_y \cdot MP \tag{465}$$

$$b = b_1' - \omega_0 C_1 \tag{465a}$$

$$\tan \theta_1 = \frac{b_1'}{g_1'} \qquad \tan \theta = \frac{b}{g} = \frac{b_1' - \omega_0 C_1}{g_1'} \tag{465b}$$

Although it is theoretically possible to derive the electric constants from observations at any two different frequencies, still it is preferable to use a large number of observed values of g_1' and b_1' and then to plot a resonance circle. A convenient scale value s_y is arbitrarily selected, and, for each frequency, FW and WP are laid off with F as origin. A point P is thus located at each frequency. All such points should lie on a circular locus, the center C of which is at a distance $AF = \omega_0 C_1/s_y$ below the horizontal axis through F. If the center does not fall at this level, it may indicate an error in the measurement of C_1; nevertheless, the ratio AF/AB is usually so small that a rough agreement is sufficient. If the locus is not circular and no source of error in the electrical measurements can be found, the discrepancy may be traced to varying temperature of the resonator, especially since the temperature depends on the varying amplitude of vibration as well as on the surrounding air, as explained in §315. In the case of Rochelle salt both the piezoelectric and dielectric constants vary with temperature, and a variation in either of these constants will displace the point P. If the circular locus is not tangent to the vertical axis through F, an additional resistance component must be sought. With Rochelle salt this component may be inherent in C_1 itself. The graphical method for allowing for the resistance of the thermoelement is described in ref. 107.

If for no other reason, the plotting of the circular locus is useful for detecting sources of error and checking the consistency of the observations.

When the circular locus has been drawn, its diameter AB gives the value of R by the relation

$$R = \frac{1}{s_y \cdot AB} \tag{466}$$

323. In order to find L, C, and Q, one must make use of the frequency measurements. The frequency is most conveniently introduced by means of the formula for frequency scale value σ [Eq. (378*a*)]. Usually the observed frequency for maximum admittance may be taken as identical with f_0. If very high precision is sought, the following procedure is recommended: Let $f' = \omega'/2\pi$ be the frequency for which b_1' is nearest to zero. Values of $n' = \omega' - \omega$ for the various observed frequencies are tabulated. Assuming C_1 and R to have been determined and b_1' and g_1' to be known at each frequency, we can express σ by the following formula,

which is easily derived:

$$\sigma = \frac{s_y R(\omega - \omega')}{2\pi(\tan\theta' - \tan\theta)} \tag{467}$$

For each observed frequency, σ is calculated, and the average taken. When σ has thus been determined and f_0, the frequency at point B in Fig. 59, has been found, the frequency corresponding to any point on the circle can be found according to §267. This knowledge is useful in predicting the performance of the resonator when it is to be connected to a given external impedance.

From this average value of σ, L is found from Eq. (378):

$$L = -\frac{s_y R^2}{8\pi\sigma} \tag{468}$$

If it is desired to calculate ω_0 very precisely, the following formula may be used for each observed ω:

$$\omega_0 = \frac{\omega \tan\theta' - \omega' \tan\theta}{\tan\theta' - \tan\theta} \tag{469}$$

The final value of ω_0 is the average of the values thus obtained.

C is to be calculated from $\omega_0^2 = 1/LC$, and Q from the equation

$$Q = \frac{\omega_0 L}{R} = -\frac{s_y R \omega_0}{8\pi\sigma} \tag{470}$$

The foregoing procedure is necessary only when the highest possible precision is sought. For most practical purposes it suffices to use Eqs. (412) and (410a):

$$\left.\begin{aligned} R &= \frac{1}{Y_m - Y_n} \qquad C = \frac{2C_1(f_n - f_m)}{f_m} \\ Q &= \frac{\pi}{\delta} = \frac{2\pi f_m L}{R} = 2\pi f_m L(Y_m - Y_n) \end{aligned}\right\} \tag{471}$$

L is found from $L = 1/\omega_m^2 C$.

If observations are made with a gap, the symbols R', L', and C' should be used in Eqs. (471). R, L, and C can then be calculated by use of the equations in §232 or §255.

An alternative, but more laborious, procedure for precise determination of the electric constants has been described by Dye.[127]

324. The foregoing section has dealt only with the circle diagram for the resonator by itself. It is often helpful to add to this diagram the other constants of the measuring circuit. Light is thus thrown on the performance of the circuit as a whole, and conclusions can be drawn concerning the best values of the circuit constants.

As an example we consider the *crevasse circuit* (Fig. 70). Since the induced emf is effectively in series with L_2, the circuit may be represented as in Fig. 72. R_2 is the resistance of L_2. The emf is applied at the points a and b, and we seek the graphical representation of the impedance between them. Qualitatively, the diagram can be constructed as in Fig. 73, and useful conclusions can be drawn without knowledge of the exact values of the various constants. For application to a quantitative problem it is best to start with the known value of R and to draw a circle of convenient diameter AB. The scale value for admittances is then $s_y = 1/(R \cdot AB)$.

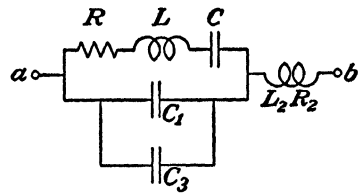


FIG. 72.—Equivalent crevasse circuit with crystal represented by $RLCC_1$. The voltage is applied at a and b.

In building up the diagram for the other parameters we lay off $AF = -\omega_0 C_1/s_y$ and $FF' = -\omega_0 C_3/s_y$. For any point P on the fiducial circle (§267), corresponding to some frequency in the resonant range, the admittance Y_2' of $RLCC_1C_3$ is given by $s_y \cdot F'P = Y_2'$.

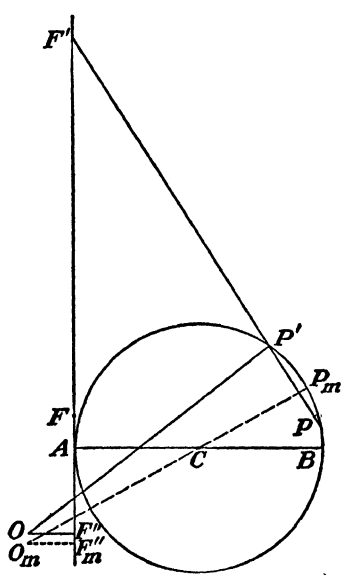


FIG. 73.—Resonance circle diagram for the crevasse circuit.

Since L_2 is in series with $RLCC_1C_3$, it is necessary to treat the problem from here on in terms of impedances, according to method b, §303. The impedance of $RLCC_1C_3$ is $Z_2' = 1/Y_2' = s_z \cdot F'P'$, where

$$s_z = \frac{s_y}{\omega^2(C_1 + C_3)^2}$$

and P' is the point inverse to P with respect to F'. To this must be added vectorially the external impedance of L_2R_2, namely, $s_z \cdot F'F'' = \omega L_2$,

$$s_z \cdot OF'' = R_2.$$

The vectorial sum is $OP' = Z_3/s_z$, where Z_3 is the impedance of

$$RLCC_1C_3L_2R_2.$$

We have left out of account the correction, usually small, for a thermoelement or other measuring device in the circuit; this correction has been treated in a former paper.[107]

Before considering what happens to OP' while the crystal is vibrating and the frequency is varied over the resonant range, it is necessary to

show how the resonance curve for the tuned circuit $L_2R_2C_3C_1$ alone can be derived. Such a curve can, of course, be found experimentally by clamping the crystal to suppress its vibrations or by removing it temporarily from the circuit and connecting a known capacitance of value C_1 in its place. Either procedure effectively makes the diameter AB shrink to zero, so that the resonator admittance is simply $-\omega C_1 = s_y \cdot AF$. Now observations are hardly ever extended over a frequency range of more than $0.01f_0$. With a good resonator and a fiducial circle of reasonable size, AF is usually so short that its variation with ω can be ignored.

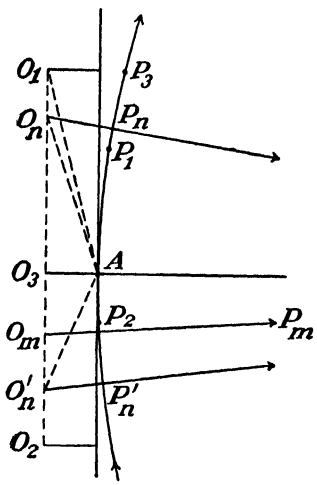


FIG. 74.—Vector diagram for resonance curve of $L_2R_2C_3C_1$.

As the frequency passes through the resonant range with the crystal vibrating, the operating point on the circle goes around nearly the whole circumference, the point F remains practically fixed, but the changes in FF' and $F'F''$ with frequency cannot be ignored. C_3 is likely to be so great that FF' is several times as large as AB and hundreds of times greater than AF. Hence, as the frequency increases from a value f_1 on the l-f side of resonance to f_2 on the other side, the origin O does not, like F, remain practically fixed but moves downward through a range that amounts to perhaps a tenth of AB. Small as this range is, it plays a vital part in the resonance phenomena.

If the crystal does not vibrate, the impedance Z_3 becomes $s_z \cdot OA \equiv Z_2$. The variation of this quantity with frequency can best be seen from Fig. 74, which is an enlarged view of the portion near the point A in Fig. 73. Suppose O to move from O_1 to O_2 as the frequency increases through the resonance range from f_1 to f_2. Each vector O_1A, O_nA, etc., is proportional to the impedance of $L_2R_2C_3C_1$, and its reciprocal gives the admittance $Y_2 = 1/(s_z \cdot OF)$, which, under constant impressed voltage, is proportional to the current I_2 in L_2. A plot of $1/OA$, Y_2, or I_2 against f will therefore be the resonance curve for $L_2R_2C_3C_1$. The peak of the curve is at the frequency for which OA is a minimum. The origin O is then at O_3, and the resonant frequency for $L_2R_2C_3C_1$, say $f'_0 = \omega'_0/2\pi$, is given by $\omega'_0L_2 = 1/\omega'_0(C_3 + C_1)$. f'_0 is usually not far from f_0, but it is not necessarily equal to f_0. Indeed, the C_3L_2 circuit may be so detuned that f'_0 lies far outside the range of frequencies constituting the "resonant range" of the crystal.

Such a curve, with different parameters from those arbitrarily

assumed in Fig. 74, which is purely schematic, is shown in Fig. 75. This figure is based on experimental data from Dye* for a 44-kc X-cut bar in lengthwise vibration. The broken line is the resonance curve for $L_2R_2C_3C_1$, with $f_1 = 44{,}000 - 120$, $f_2 = 44{,}000 + 120$, and f_0' at about $44{,}000 - 70$, corresponding to the minimum impedance O_3A in Fig. 74.

When the crystal vibrates, the impedance vector Z_3 for $RLCC_1L_2R_2C_3$ at any frequency is obtained by drawing a line from the appropriate location of O to the point on the circle for the particular frequency in question. It must be remembered that we are now dealing with an *impedance* circle (§§270, 303), around which the frequency increases in a *clockwise* direction. As the frequency increases from a low value f_1 to

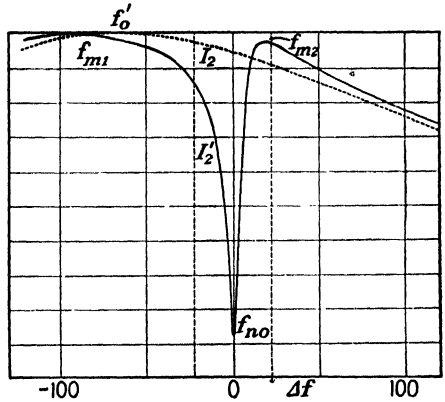


FIG. 75.—Resonance curves for I_2 and I'_2 in the crevasse circuit, from Dye. The frequency is $44{,}000 + \Delta f$.

a high value f_2, the operating point on the circle travels clockwise from some such position as P_1 to P_2 in Fig. 74. Z_3 is proportional to O_1P_1 at frequency f_1, to O_3P_3 at the frequency of resonance for $L_2R_2C_3C_1$, and finally to O_2P_2 at f_2 (to avoid confusion these lines are not shown in the figure). As the frequency increases from f_1, a value is soon reached for which the line O_nP_n passes through the center of the circle. This is the frequency for minimum Z_3 or maximum Y_3, corresponding to maximum current I_2' in L_2 with the crystal vibrating.

The full curve in Fig. 75 shows I_2' as function of f. The maximum just referred to comes at f_{m1}, about $(44{,}000 - 90)$ cycles/sec. Here I_2' is slightly greater than I_2, corresponding to the fact that in Fig. 74 $O_nP_n < O_nA$. A second maximum in I_2' comes at $(44{,}000 + 40)$ cycles/sec, corresponding to $O_n'P_n'$ in Fig. 74; at this frequency, f_{m2}, the points O and P again find themselves on a line passing through the center of the circle.

* Ref. 127, Fig. 6.

Within the small range of intervening frequencies the operating point swings around the circle, and the impedance Z_3 passes through a very sharp maximum at a frequency depending on C_3 (if L_2 is fixed), but always very close to f_0. This maximum Z_3 determines the minimum I_2' at the bottom of the crevasse, the frequency here being denoted by f_{n0}. The graphical relations can now be understood best with the aid of Fig. 73. It will be recalled that in this figure $s_z \cdot OP' = Z_3$ at the frequency for which P' has the position shown on the impedance circle. If now the frequency is increased slightly, P' moves clockwise around the circle, O moves downward, and at a certain frequency the line OP' passes through the center C of the circle. This position of the line is marked O_mCP_m in Fig. 73; it is here that Z_3 has its greatest possible value, for given values of L_2 and C_3. The smaller R_2 can be made, the sharper is the bottom of the crevasse and the larger the value of I_2' at this point. In general, if C_3 is set at a relatively large value, so that f_0' is less than f_0 by 2 or 3 per cent, the bottom of the crevasse comes at a frequency slightly lower than f_0, and I_2' is relatively small at this point. When C_3 is decreased until f_0' has the value shown in Fig. 75, the bottom of the crevasse is at frequency f_{n0}, less than f_0 by an extremely small amount. f_{n0} coincides with f_0 when f_0' is almost, but not quite, as great as f_0. It is here that the minimum of I_2' has its greatest possible value. As C_3 is still further decreased, f_{n0} becomes slightly greater than f_0 and the minimum value of I_2' diminishes again.

The foregoing conclusions, based on the graphical method, are in agreement with Dye's analytical treatment, as illustrated in Fig. 7 in his paper.

For determining the resonator constants by the crevasse method it is usually amply accurate to have $f_0' = f_0$ within a few parts in a thousand and to assume that $f_{n0} = f_0$ at the bottom of the crevasse.

325. *Impressed Voltage in Parallel with L_2.* As has been stated in §316, in a few cases the coil L_2 has been connected directly to the oscillator output. The voltage is then applied effectively to the coil, C_3, and the resonator, all *in parallel*. The vector representing the coil has components $s_y \cdot F'F'' = b_2$, $s_y \cdot OF'' = g_2$, where b_2 and g_2 are the susceptance and conductance of L_2R_2. In the graphical treatment, following the path indicated above, no impedance diagram is necessary; the problem is handled entirely in terms of admittances. To this extent the graphical method is considerably simplified. Each vector like OP' in Fig. 73 is now proportional to the *admittance* Y_3 of the entire network. For any given L_2 and C_3, as the frequency is gradually varied it is found that there are two minimum values of Y_3, with one sharp maximum between them. They correspond to the two minima and one maximum in Z_3

when L_2 is in series with the rest of the network. The "crevasse" is converted into a sharp "pinnacle."

It can be shown that the frequency difference between the two values of minimum Y_3 is greater the larger the value of L_2 and that it can be made several times greater than the difference $f_p - f_s$ between the parallel- and series-resonance frequencies of the resonator alone. It was for this reason that Builder[81] adopted this method in his measurement of resonator constants.

REFERENCES ON MEASUREMENT OF CONSTANTS OF THE EQUIVALENT NETWORK

Crevasse Method. ANDREEFF, FRÉEDERICKSZ, and KAZARNOWSKY,[4] BECHMANN,[38,43] BOELLA,[56,57] BUILDER,[81] CADY,[93] DYE,[127] GÜNTHER,[196] HEEGNER,[214] KOBZAREV,[265] LUCAS,[320] MATTIAT,[355] MELIKIAN and PIETROVA,[363] NUSSBAUMER,[395] SCHIFFERMÜLLER,[152] SZÉKELY,[500] UST'YANOV,[539] WATANABE,[581] ZELYAKH and VELIKIN.[601]

Filter Method. HUND,[B28] BOOTH,[69] GÜNTHER,[195] MASON,[332] MASON and FAIR,[341] MEISSNER,[359,360]

Bridge Method. HUND,[B28] GIEBE and SCHEIBE,[170] VAN DYKE,[548] VAN DYKE and THORNDIKE.[559]

Substitution Method. BECHMANN,[43] BECKER,[45] GÜNTHER.[197]

Decay Method. ARKHANGEL'SKAYA,[8] BECKER,[46] BOSSHARD and BUSCH,[73] BROWN,[76] CHAIKIN,[111] GOCKEL,[173] RZIANKIN,[442] VAN DYKE.[551–554]

Unclassified. HATAKEYAMA,[209] NIESSEN.[392]

In most of the foregoing references the theory of the method is given. The general theory is discussed by Vigoureux in ref. 567.

CHAPTER XVI

PROPERTIES AND TECHNIQUE OF QUARTZ

Marmoreum ne sperne globum. Spectacula transit
regia, nec rubro vilior iste mari.
informis glacies, saxum rude, nulla figurae
gratia: sed raras inter habetur opes.

—CLAUDIUS CLAUDIANUS.

Because of its physical stability and its superior elastic properties, quartz is the only piezoelectric crystal that has found important applications as a resonator. Its behavior as a resonator will be treated in the next chapter. For the present we shall be concerned first with the conventions respecting axes and angles and with those physical properties that are not treated in Chaps. II, VI, IX, XXX, and XXXI. Later in the chapter will be found a description of methods for orienting raw crystals, cutting and finishing of plates, and mounting in holders.

326. Axes and Angles for Right- and Left-quartz. Through the voluminous literature on the properties of quartz crystals there runs, like a crack in an otherwise clear crystal, an amazing ambiguity concerning the distinction between right- and left-quartz, the positive sense of the directions of the X- and Y-axes, and the positive sense of angles of rotation. This subject has been discussed at some length in two recent papers[110,558], and a committee of the I.R.E. has agreed upon a system of conventions to be recommended for general adoption.* The recommendations of this committee concerning the three matters named above are in agreement with the suggestions in the paper by Van Dyke and the author,[110] and they are followed in this book.

The distinction between right and left (dextro- and levogyrate) crystals has been pointed out in §7. The ambiguity in definition had its origin in the writings of Herschel and Biot, who used opposite definitions of the sense of rotation of a beam of plane-polarized light.† The convention now adopted is that of Biot, according to which a crystal is called *right when the direction of rotation appears clockwise to an observer looking back through the analyzer toward the source of light* (see also §538). This definition has the advantage that if a given crystal is "right"

* The report of this committee was approved by the directors of the institute on June 7, 1944.

† SOSMAN, ref. B47, p. 649.

crystallographically, as judged by the s- and x-faces shown in Fig. 5 or Fig. 76, it is also "right" optically.

In all that has to do with the making of oblique cuts of quartz for special purposes or with the study of physical properties in oblique directions, the distinction between right and left specimens must be clearly borne in mind. Failure to do so will almost inevitably lead to false results. In many situations the difference between right and left is equivalent to that between right and *wrong*.

327. The I.R.E. Axial System. Until recently most writers, including Voigt, have used a right-handed orthogonal system of axes for both forms of quartz. This practice has the serious disadvantage of requiring, on passing from a right- to a left-crystal, a change in sign of all piezoelectric constants and of certain terms in the equations for transformed axes. These annoyances and possible sources of error are completely avoided by the adoption of a *right-handed axial system for right-quartz, left-handed for left-quartz.*

The advantages of such an arrangement were pointed out by Koga as early as 1929.* A similar proposal was made later by Mason and Willard† and independently by Cady and Van Dyke.[110]‡ This system of axes was also used by Builder and Benson[82] in 1938.

The convention by which right-handed and left-handed frames of reference are used, respectively, for right- and left-quartz will be referred to as the *I.R.E. system.* Under this system, all equations, together with all direction cosines, are exactly the same for both forms of quartz. In general, it is sufficient in diagrams, etc., to represent a right-handed system of axes, as for right-quartz. Not until the time comes to lay off angles on an actual specimen is it necessary to give heed to the question of enantiomorphism. Then, if the specimen is left-handed, one need only reverse the direction of the X-axis and observe the rule given below for the positive sense of angles.

The change in axes from right- to left-handed on passing from a right- to a left-quartz is a logical accompaniment to the corresponding change in the external appearance and physical properties of the crystal. If a photograph were taken of a right-quartz crystal showing the right-handed XYZ-axial system together with all equations, curves, polar diagrams, and models illustrating its physical properties including elastic and piezoelectric, then the mirror image of this picture, obtained, for example, by making a photographic print with the film reversed, would be an exact reproduction of a left-quartz together with its physical properties.

* KOGA, I., *Jour. Inst. Elec. Engrs. Japan*, July, 1929, pp. 49–92; *Electrotech. Jour. (Japan)*, 1938, pp. 287–289.

† W. P. MASON and G. W. WILLARD, *Proc. I.R.E.*, vol. 28, p. 428, 1940.

‡ This paper was written in 1939, but publication was delayed.

These considerations are made clear in Fig. 76, which shows an end view and also a cross section in the YZ-plane, for both right- and left-quartz. In the upper diagram the positive direction of the Z-axis, in the lower diagram the positive direction of the X-axis, points toward the observer.

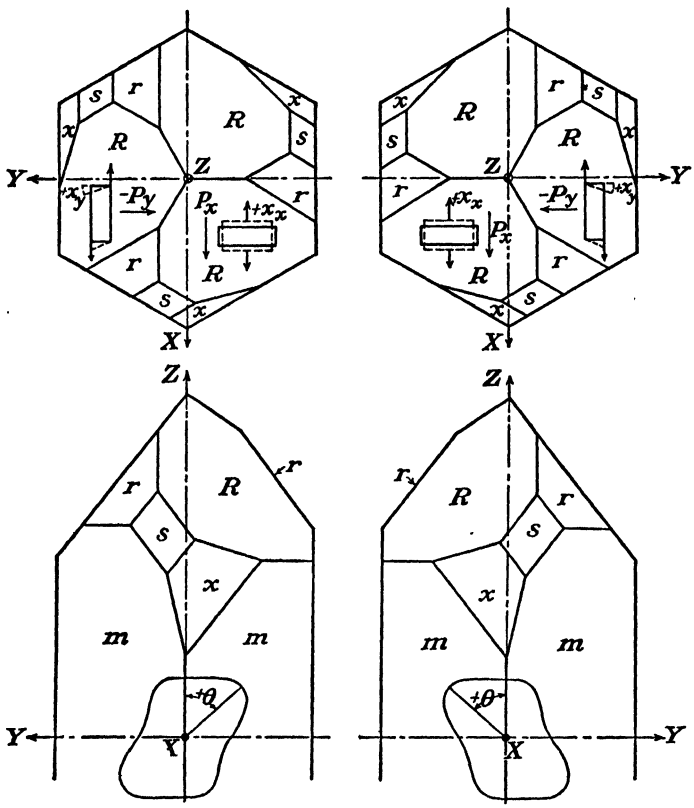


FIG. 76.—Left- and right-quartz, showing strains x_x and x_y, with accompanying polarizations P_x and P_y, also showing the positive sense of the angle of rotation θ.

The Y- and Z-axes have already been defined in §5. As may be seen from Fig. 76, *the positive end of an X-axis emerges from the crystal at each of the three prismatic edges where s- and x-faces may be found.* This is the end at which a positive charge appears when the x_x-strain is positive, *i.e.*, when the specimen is *stretched* in the X-direction. These statements hold for both right- and left-quartz.

Figure 76 shows an X-cut being stretched so that there is an extensional strain in the X-direction and accompanying contraction in the Y-direc-

tion. The arrow P_x indicates the positive direction of the ensuing electric polarization, in conformity with the statement above that a positive strain is associated with a positive charge at the positive end of the X-axis. *Compressional strains and stresses do not change sign in the mirror image.*

Positive Sense of Rotation for Quartz Axes. The general definition of positive and negative angles given in §38 is, according to the convention here adopted, to be applied to right-quartz. For a *left*-quartz the angle of rotation is to be considered as positive when *clockwise* as seen by an observer looking back toward the origin from the positive end of the axis of rotation.

These statements may be combined in the following single rule, applicable to both types of quartz crystals:

The angle of rotation is to be called positive when the sense of rotation is from $+X$ to $+Y$, from $+Y$ to $+Z$, or from $+Z$ to $+X$. In the I.R.E. system this definition is valid for both right- and left-quartz. An equivalent statement, following the usual convention for rotational vectors, is that a positive angle of rotation is related to the positive sense of the axis of rotation as the direction of twist of a screw is related to the direction of advance, the screw being right-handed for a right-quartz, left-handed for a left-quartz.

As an illustration of the rule for rotated axes there are shown in Fig. 76 polar diagrams of the distribution of Young's modulus in the YZ-plane. This quantity is the reciprocal of the compliance coefficient s'_{33} obtained by rotating the Y- and Z-axes through various angles θ about the X-axis. The maximum value is in the direction approximately perpendicular to an r-face, and the corresponding angle θ, according to the I.R.E. system, is about $+48°$ for both right- and left-quartz (§96).

In the upper portion of Fig. 76 is a section of a Y-cut plate undergoing a positive shearing strain x_y, together with the associated electric polarization P_y. Tangential forces are indicated by arrows. From the equation $P_y = e_{26}x_y = -e_{11}x_y$ and the sign of e_{11} as given below, it is seen that P_y is negative. The piezoelectric shear x_y produced by a field E_y in the positive direction of the Y-axis has the same sign for left- as for right-quartz. A similar statement applies also to all other piezoelectric shears.

The Signs of Elastic and Piezoelectric Constants. According to Voigt's notation, all elastic coefficients have the same signs for left- as for right-quartz, but the signs of all piezoelectric constants change in passing from right to left. Under the I.R.E. system, Voigt's notation for the elastic coefficients remains unchanged.

Voigt assigns negative numerical values to the constants d_{11}, e_{11}, and e_{14} for left-quartz and a positive value to d_{14}. These signs are with

respect to a right-handed axial system. While other observers have obtained values differing in magnitude from Voigt's, there has been no disagreement as to sign. For a right-quartz the signs, according to Voigt, are reversed, *viz.*, $d_{11}+$, $e_{11}+$, $d_{14}-$, $e_{14}+$. According to the I.R.E. convention, adopted in this book, the signs of the piezoelectric constants for *both types of quartz* are those which Voigt would have assigned to a *right*-quartz; they are opposite to those commonly quoted. Voigt's statement that his observations were made on a left-quartz is so inconspicuous* as to be easily overlooked, and those who made later determinations seem to have been more interested in numerical magnitudes than in signs.

328. Some Physical Properties of Quartz.† Little is known concerning the effects of traces of impurity and of previous treatment on the physical properties. At all events, such effects are probably slight, except in the case of the electrical resistivity. Nevertheless, the discrepancies between the results of different observers may have been due in part to real differences between the various specimens used.

The *hardness* of quartz is 7 on the Mohs scale. Ichikawa‡ states that a surface cut normal to the optic axis is much softer than the natural faces. The *crushing strength* has been found by Bridgman§ to vary from 33,000 to 40,000 kg/cm^2, depending on the confining pressure. When the crushing stress was reached, the crystal specimen became reduced to a fine powder. Sosman[B47] states that at atmospheric pressure the crushing strength is around 24,000 kg/cm^2 and also that for small specimens a tensile strength of about 1,000 kg/cm^2 may be expected.‖ The tensile strength is slightly greater parallel than perpendicular to the optic axis.

Fracture. The atoms of quartz are so closely bound together in all directions that there are no planes of easy cleavage. There are, however, two tendencies that can often be observed. The first is a peculiar shell-like curved portion of the broken surface, called *conchoidal fracture.* The second is fracture approximately parallel to one of the faces of the major rhombohedron or, to a smaller extent, the minor rhombohedron.¶ This type of fracture is sometimes encountered on heating or when plates vibrated piezoelectrically are shattered by the application of too high a voltage. The author first observed this latter effect in 1920. Since then it has been recorded by others, for example Wright and Stuart,[594] Seidl,[455]

* "Lehrbuch," p. 861.

† All data are for *α-quartz* unless otherwise noted. Certain data on the β-modification (at temperatures above 573°C) will be found elsewhere in this book. For a full discussion of β-quartz see Sosman.[B47]

‡ S. Ichikawa, *Am. Jour. Sci.*, vol. 39, pp. 455–473, 1915.

§ P. W. Bridgman, *Jour. Applied Phys.*, vol. 12, pp. 461–469, 1941.

‖ From this figure and the elastic compliance of quartz the breaking extensional *strain* for a quartz bar is found to be of the order of 0.001.

¶ See H. W. Fairbairn, *American Mineralogist*, vol. 24, pp. 351–368, 1939.

Booth,[69] Gramont,[B21] Van Dyke,[555] Sanders,[446] Shubnikov,[463] and, especially, Straubel.[488] Gibbs and Tsien[159] observed a *spiral* fracture in the case of a torsionally vibrating hollow quartz cylinder with length parallel to the optic axis. Rivlin* found that, after a Z-cut plate had been suitably rough-ground, it showed a hexagonal pattern when held close to the eye while the observer viewed a point source of light. He attributed the effect to comparatively easy fracture in planes belonging to zones $\{10 \cdot l\}$ and suggested it as a means for locating the X-axes. Rivlin's pattern can be seen easily with the aid of the rodoscope described in §339. The grinding on the Z-surface should be done by hand, using very coarse carborundum (45 to 60 mesh) and water, and applying rather heavy pressure in short, curving strokes in random directions. In 1930 Shubnikov had already observed the formation of small triangular pits when a Z-surface had been struck with a sharp steel point. He found that subsequent etching with H_2F_2 made the outlines more distinct. A similar effect produced by dropping a steel ball on to the Z-surface is mentioned by Hawk.†

Luminescence is observed when prismatic edges of two quartz crystals are struck together in a dark room. The effect is not as bright as with sugar crystals.

329. The physical properties of quartz have been discussed very exhaustively by Sosman.[B47] A few of the data from his book, for *density*, *thermal conductivity*, and *specific heat*, are assembled in Table XXV.

TABLE XXV.—DENSITY ρ IN GM CM^{-3}, THERMAL CONDUCTIVITY IN CAL CM^{-1} SEC^{-1} DEG^{-1}, AND SPECIFIC HEAT IN CAL GM^{-1} DEG^{-1}, FOR α-QUARTZ, AT VARIOUS TEMPERATURES

Temperature, deg. C	ρ	Thermal conductivity		Specific heat
		$\parallel Z$	$\perp Z$	
−50	2.655	40	20.5	0.1412
0	2.651	32	17.0	0.1664
50	2.646	25.5	14.9	0.1870
100	2.641	21	13.1	0.2043

The symmetry of quartz is such that the thermal and electrical conductivities have only two principal values, parallel and perpendicular to the Z-axis, just as is the case with the dielectric and optical constants. For oblique directions the values vary ellipsoidally between the two principal values.

* R. S. RIVLIN, *Nature*, vol. 146, pp. 806–807, 1940.

† H. W. N. HAWK, U. S. patent 2,264,380, 1941.

As the best mean value at 20°C Sosman adopts $\rho = 2.649 \pm 0.2$. Recently Miller and Du Mond* have found $\rho = 2.64822 \pm 0.00005$ at 25°. For most calculations it suffices to call $\rho = 2.65$ at ordinary temperatures.

The temperature coefficient of density $(\partial\rho/\partial t)/\rho$ as calculated by Mason and Sykes[343] is $-36.4(10^{-6})$.

For *β-quartz*, $\rho = 2.518$ at 600°C.†

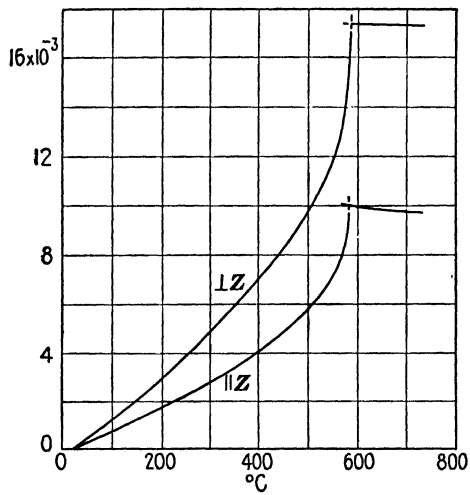


FIG. 77.—Thermal expansion of alpha- and beta-quartz, from Jay. Upper curve $\perp Z$-axis, lower curve $\parallel Z$-axis. Ordinates indicate expansion per unit length, starting at 18°C.

The *coefficient of thermal expansion* has been thoroughly investigated by Jay,‡ by an X-ray method, over a wide range of temperature. His results, shown in Fig. 77, include data on β-quartz. His values are in general agreement with those obtained by optical methods. In the neighborhood of room temperature the coefficients of expansion parallel and perpendicular to the optic axis are found from Jay's results to be 9.0 (10^{-6}) and 14.8 (10^{-6}) per degree, respectively.

More recently, the thermal expansion perpendicular to the optic axis has been measured by Nix and MacNair§ by means of their "inter-

* P. H. MILLER, JR., and J. W. M. DU MOND, *Phys. Rev.*, vol. 57, pp. 198–206, 1940.

† A. L. DAY, R. B. SOSMAN, and J. C. HOSTETTER, *Am. Jour. Sci.*, vol. 37, pp. 1–39, 1914.

‡ A. H. JAY, *Proc. Roy. Soc. (London) (A)*, vol. 142, pp. 237–247, 1933.

§ F. C. NIX and D. MACNAIR, *Rev. Sci. Instruments*, vol. 12, pp. 66–70, 1941. The dilatometer described in this paper should prove useful for measuring piezoelectric as well as thermal dilatations at all temperatures.

ferometric dilatometer." Their results are in substantial agreement with Jay's.

330. Electrical Properties of Quartz. Quartz is an excellent insulator, except at high temperatures. Such *electrical conductivity* as it has is much greater parallel than perpendicular to the optic axis. Parallel to the optic axis the conductivity is largely electrolytic at high temperatures, owing to traces of impurities. The data in the following table are from Sosman;[B47] they indicate only the order of magnitude. Observations of conductivity at various temperatures and under various voltages

TABLE XXVI.—RESISTIVITY OF QUARTZ AT VARIOUS TEMPERATURES
In ohm cm^{-1}

Temperature, deg C	Resistivity	
	$\parallel Z$	$\perp Z$
20	10^{14}	$200(10^{14})$
100	$8(10^{11})$	
1000	$5(10^{4})$	$10(10^{4})$

have been made more recently by Altheim.* Joffé[B30] found that exposure of a specimen to the radiations from radium caused a gradual increase in conductivity, so that after "many days" the initial value was exceeded many times.

The *electric strength* of quartz parallel to the optic axis is given by Austen and Whitehead† as $6.7(10^6)$ volts/cm. This value agrees well with the observations of von Hippel and Maurer,‡ who find that the electric strength increases almost linearly from about $4(10)^6$ volts/cm at $-80°C$ to $7(10^6)$ at $+60°C$. The value is slightly greater parallel than perpendicular to the optic axis.

331. The recorded measurements of the *dielectric constant* of quartz show a spread of several per cent. It is not yet known to how great an extent this may be due to actual differences between individual speci-

* OLGA G. VON ALTHEIM, *An. Phk.*, vol. 35, pp. 417–444, 1939. For further investigations on the conductivity of quartz see E. Darmois and R. Radmanèche, *Jour. phys. rad.*, vol. 7, pp. 16S, 17S, 1936; N. G. Rahimi, *Jour. phys. rad.*, vol. 9, pp. 291–296, 1938; E. G. Rochow, *J. Applied Phys.*, vol. 9, pp. 664–669, 1938; H. Saegusa and T. Matsumoto, *Japan Jour. Phys.*, vol. 11, p. 61, 1936; H. Saegusa and K. Saeki, *Sci. Repts. Tohoku Univ.*, vol. 18, pp. 231–244, 1929; H. Saegusa and S. Shimizu, *Elec. Rev. (Japan)*, vol. 18, pp. 69*f.*, 1930; H. Saegusa and S. Shimizu, *Sci. Repts. Tohoku Univ.*, vol. 20, pp. 1–35, 1931; Seidl;[456] S. Shimizu, *Phil. Mag.*, vol. 13, pp. 907–934, 1932.

† A. E. W. AUSTEN and S. WHITEHEAD, *Proc. Roy. Soc. (London)* (A), vol. 176, pp. 33–50, 1940.

‡ A. VON HIPPEL and R. J. MAURER, *Phys. Rev.*, vol. 59, pp. 820–823, 1941.

mens. At least it can be said that the constant is slightly greater parallel to the optic axis than perpendicular to it and that there is no great change with frequency outside the experimental errors. Jaeger's values* were slightly greater at high than at low frequency. On the other hand, Doborzynski,† whose paper contains a comparison of the results of many observers, found from his own measurements at 50 cycles/sec that $k_\parallel = 4.66$, $k_\perp = 4.55$. At $5(10^6)$ cycles/sec he found $k_\parallel = 4.58$, $k_\perp = 4.41$. All things considered, we are inclined to accept the "most probable" values recommended by Sosman, *viz.*,

$$k_\parallel = 4.6 \qquad k_\perp = 4.5 \tag{472}$$

The value of $k_\parallel$ is independent of strain. 4.5 is the value of $k_\perp$ for a *free* crystal.

To calculate the *clamped dielectric constant* $k''_\perp$ of quartz for a field perpendicular to the optic axis we specialize Eq. (265) in §204. Using the values of the piezoelectric constants given in §156, we obtain

$$k'_\perp = k''_\perp + 4\pi(2e_{11}d_{11} + e_{14}d_{14}) = k''_\perp + 0.087 \tag{473}$$

Calling $k'_\perp = 4.5$, we thus have

$$k''_\perp = 4.41 \tag{474}$$

For lengthwise vibrations of an X-cut quartz bar with length parallel to the Y-axis, the effective dielectric constant k_l is derived from Eq. (311) in §229, using for s^E_{nn}, from §90, $s^E_{nn} = s^E_{22} = s^E_{11} = 1.269(10^{-12})$:

$$k_l = 4.5 - 0.047 = 4.45 \tag{474a}$$

The dielectric constant for a field in any oblique direction N having the direction cosines l, m, n is given in §108, Eq. (157):

$$k_N = l^2k_{11} + m^2k_{22} + n^2k_{33}$$

For quartz, $k_{11} = k_{22} = k_\perp$, $k_{33} = k_\parallel$. Hence one can write, setting $n = \cos\theta$ according to Fig. 17,

$$k_N = (1 - n^2)k_\perp + n^2k_\parallel = k_\perp + (k_\parallel - k_\perp)\cos^2\theta \tag{474b}$$

For the free crystal this expression becomes

$$k'_N = 4.5 + 0.1\cos^2\theta \tag{474c}$$

The dielectric constant is the same in all azimuths; the only variation is with the angle of altitude.

* SOSMAN.[B57]

† D. DOBORZYNSKI, *Bull. Intern. Acad. Polon. Sci. Lettres*, ser. A, no. 6-8A, pp. 320–349, 1937.

Dependence of the Dielectric Constant on Temperature. Parallel to the optic axis the constant hardly changes from 0°C to about 100°C, after which it increases, slowly at first and then more rapidly, until at 300° the value is about 13. From here on up to 750°C there is practically no further change.

Perpendicular to the axis the constant is unchanged up to 300°, with a very slight increase from 300° to about 500°, where a rather sharp upward turn takes place until at 800° the value is about 12.*

Dependence of the Dielectric Constant on the Electric Field Strength. The results obtained by Saegusa and Nakamura† are as follows: $k_{\parallel}$ is independent of the field strength up to 2,000 volts/cm, showing an increase from there on; $k_{\perp}$ shows no variation up to 12,000 volts/cm.

EXPERIMENTAL DETERMINATION OF THE AXES OF QUARTZ CRYSTALS

332. Under this heading are to be included the methods for distinguishing right- from left-crystals and for locating twinned regions, as well as the use of polarized light, etching, and X-rays for determining the axial directions.

For both experimental research and industrial uses it is important to know the orientation of the preparation, whether bar, rectangular plate, or some other form, with respect to the crystallographic axes. The allowable tolerance depends, of course, on the purpose in hand. For demonstrations, qualitative tests, and the construction of piezo oscillators when the demand for precision is modest, results may be satisfactory if the orientation is in error by several degrees. The specimens used in the pioneer work on resonators were far from being accurately oriented.

The demand for greater constancy of frequency in radio transmitters that arose in the 1920's led first to thermostatic control of temperature of the X- and Y-cuts of quartz crystals that were then employed and later to the use of various oblique cuts. Such cuts can now be made with a vibrational frequency almost independent of temperature, although for some purposes temperature control is still used. The orientation of plates with zero temperature coefficient is quite critical; in some cases the tolerance is no more than a few minutes of arc.

In the past, quartz crystals were available that were developed with enough perfection to enable plates to be cut with good precision by reference to the natural faces. Even then, however, it was necessary to use optical tests for twinned regions and often also in order to know

* Sosman, ref., B47 p. 524.

† H. Saegusa and K. Nakamura, *Sci. Repts. Tohoku Univ.*, vol. 21, pp.411–438, 1932.

whether a crystal was right or left. Entirely untwinned specimens have always been rare.

The demand for quartz crystals has now become so great that much of the raw material consists of poorly faced specimens, broken fragments devoid of natural faces, or "river quartz," which, while it may be of good quality inside, looks externally like a rounded cobblestone, with an almost opaque exterior.

Many techniques have been developed for determining the directions of the crystallographic axes without making use of natural faces. The following data are sought:

1. The direction of the optic (Z-) axis.
2. The hand of the crystal, whether right or left.
3. The positive direction of either the X- or the Y-axis.

Usually it is most convenient to obtain the first two data by an optical method. When once the optic axis has been determined within a few degrees, the etch method offers a quick and simple means for a more precise orientation; it indicates also whether the crystal is right or left, reveals twinned regions on the etched surface, and shows the positive directions of the transverse axes. For highest precision, X-rays are used.

Piezoelectric or pyroelectric tests have often been used for finding the locations and positive ends of the X-axes.*

Such methods are useful mainly in making very rough preliminary orientations of raw crystals after the direction of the optic axis has been approximately found. They cannot be included among the methods of precision.

333. Optical Tests of Quartz. The effects employed are chiefly extinction and optical activity, both of which are described in Chap. XXX. The optical constants of quartz are given in §534.

Immersion Liquids. Polished plane-parallel plates can, of course, be tested without immersion. If a specimen is irregular and unpolished, the light is refracted and scattered on entering and leaving the crystal unless the latter is immersed in a transparent liquid having at least approximately the same refractive index as quartz. For precise work in which the optic axis is to be parallel to the light beam, the index of the liquid should approximate closely to that of the ordinary ray, *viz.*, 1.544, and the liquid should be in a tank with parallel sides of plane strain-free glass. For approximate tests one need not be quite so particular. A clear lubricating oil is often sufficient.

The ideal immersion liquid would be transparent, colorless, non-volatile, non-inflammable, non-corrosive, and non-toxic, with the desired refractive index. No available liquid has all these virtues. Nitrobenzene makes a fair match but is toxic. Monobrombenzene is somewhat better, as is also a mixture of nitrobenzene with carbon tetrachloride, or of carbon disulphide with benzene. Tetralin is sometimes used, and also methyl salicylate or cedar oil. Very satisfactory results are obtained

*See, for example, L. H. Dawson.[121]

with tricresyl phosphate.* Recently a special liquid with refractive index 1.541 to 1.547 has become available.†

Preliminary Inspection. This step may be combined with the next following. The specimen is examined for cracks, phantom growths, "feathers," and inclusions, in a strong beam of transverse light, preferably with the crystal in the immersion liquid. Portions containing more than minute traces of imperfection should be rejected, since imperfections may make the finished plate more fragile and may also distort the elastic waves when the resonator vibrates. There appears to be no objection to the use of smoky quartz or of crystals that are otherwise tinted with impurities. With river quartz it may be necessary to grind or cut "windows" at various points before the preliminary inspection can be made.

Rough Determination of the Optic Axis and Detection of Optical Twinning. The crystal is immersed and examined between crossed polaroids in a beam of diffuse light, which may be white.‡ Rotating the crystal about the beam as axis will cause the transmitted light to change from light to dark four times in a complete rotation, owing to extinction, until an orientation is found for which the field remains bright on rotation. The optic axis is then approximately parallel to the beam. Extinction begins to be less complete when the optic axis is within 20° of the beam.§

When the crystal is thus viewed in plane-polarized light in a direction sufficiently close to that of the optic axis, if there is no twinning the field looks nearly uniform, except for differences in color or brightness due to differences in optical path through various portions of the crystal. If

* Sold under the trade name of Lindol. It is clear, colorless, and neither volatile nor inflammable. The refractive index is about 1.561 at 11.5°C and 1.555 at 25°C. To some individuals it is said to be a skin irritant. In any case, the liquid should be free from the ortho form, which is toxic. Tricresyl phosphate has been used in Scott Laboratory for quartz testing for many months without ill effects.

† Obtainable from the Socony Vacuum Oil Company. See also the list of liquids given by W. L. Bond.[66]

‡ If the ends have already been cut off with fairly plane surfaces approximately normal to the optic axis, as can be done if the crystal has natural faces, the examination for twinning can be made without complete immersion. A piece of ordinary glass can be placed in contact with each cut surface, with a smear of the immersion liquid between.

§ An instrument devised in this laboratory for the approximate determination of the optic axis without the necessity of dipping the hands in the immersion liquid is the *flicker polariscope.* The crystal is clamped in a holder that can be rotated about horizontal axes by rods extending down into the immersion liquid. The light beam passes vertically upward through the bottom of the glass jar containing the liquid. Above and below the jar are crossed polaroids, mounted in disks that are rotated synchronously by a chain drive about once per second. Periodic flashes of light are seen when the quartz is in place, which become a steady glow when the optic axis is parallel to the beam. A precision of 2 or 3° is easily obtained. With certain refinements settings can be made closer than 1°.

optical twinning is present, it is revealed by a sharply defined pattern, usually in the form of many triangles crowded together or streaks parallel to the X-axes, showing brilliant colors if the light source is white. The twinned regions are seen more often around the edges than in the center of the field. Their depth in the crystal can sometimes be estimated by tilting. Stereoscopic devices have also been used for the localization of twinned regions.

The approximate locations of twinned regions can be marked on the crystal and such portions discarded when the crystal is cut. Some crystals show a boundary separating the right from the left form. The boundary can be marked and the two regions utilized separately.

River quartz can usually be cleaned sufficiently by scouring to allow the optic axis to be found approximately by the method just described. A cut roughly normal to the optic axis is then made at each end, after which the crystal can be immersed again and examined for twinning.

There are also methods for finding the approximate direction of the optic axis by orienting the crystal for *maximum* extinction, instead of absence of extinction.

If the crystal is not more than about 3 cm in length parallel to the optic axis and is placed between polaroids in diffuse light, as described above, traces of the rings mentioned in the next section are usually visible to the eye placed close to the crystal.

334. *Determining the "Hand" of a Quartz Crystal in Convergent Polarized Light.* The apparatus is very simple and need not be of high optical quality. White light may be used, with or without a color filter, although with large crystals a mercury or sodium arc is to be preferred.

By means of a lens somewhat wider than the crystal, the light is converged to a cone of which the apex falls in the crystal, the outermost rays making an angle of 15° or so with the optic axis of the system. Unless the crystal is a polished Z-cut slab, which is usually not the case, it must be immersed. For large crystals the focal length of the lens may be from 5 to 10 in.; a condenser lens of the sort used in theater spotlights is suitable. A polarizer is placed between the light source and the crystal.

An observer looking at the quartz through an analyzer sees a system of more or less concentric rings. With an accurate Z-cut plate of any thickness greater than 0.5 mm, plane-parallel and untwinned, the rings are concentric circles centered on the beam if the optic axis is parallel to the beam. The rings are distorted if the crystal is irregular, and they are broken in outline, with abrupt changes in color or brightness, if there is twinning.

If now the analyzer is rotated, the rings either expand or contract according to the "hand" of the quartz. The rule is as follows:

\\ *When the analyzer is turned clockwise, if the rings expand, the quartz*

is right; if they contract, the quartz is left. The clockwise rotation is from the viewpoint of an observer looking back toward the source of light.*

If the crystal is twinned, some segments of the rings may expand while others contract.

If white light is used and if the crystal is not more than about 2 cm thick parallel to the optic axis, the hand of the quartz can also be judged by observing the succession of colors in the clear field inside the circles, as the analyzer is turned. On clockwise rotation of the analyzer, a right-quartz shows a gradual change from red through yellow and green to violet. With a left-quartz the succession is reversed. This method can be used with plates that are too thin to show the expansion of the rings.

Finding the Orientation of the Optic Axis by Convergent Light. The apparatus is similar in principle to that just described but is constructed with more precision and with the addition of a lens and eyepiece between the analyzer and the eye. Means must be provided for a fine angular adjustment of the crystal until the ring pattern is symmetrical and for correlating its position with the axis of the optical system. A precision of 1 min of arc has been claimed for this method.† A refinement of the method, in which use is made of Airy's spirals, has been described by Booth.[69]

335. Etching Tests of Quartz. The solvent commonly used is hydrofluoric acid, H_2F_2, since most other solvents, for example hot alkalis, act very slowly and there is no evidence that they produce better etch figures.‡ For most purposes commercial 48 per cent acid at room temperature is suitable, although in some cases, as will be seen, greater dilution gives better results. The time of etching may vary from half an hour to several hours, depending on the orientation of the surface to be etched and on the manner of examining the result.

Among common materials attacked but little, if at all, by H_2F_2 are paraffin, rubber, lead, and copper. Small-scale etching is conveniently carried on in a dish or tray lined with paraffin or in an old rubber battery

* The hand of a *Z*-cut slab of any thickness up to at least 2 cm can be determined with no apparatus beyond two small pieces of polaroid. If the faces of the slab are unpolished, they can usually be made sufficiently transparent by merely moistening. The crystal is held close to the eye, with a polaroid on each side, in light from the sky or from any bright diffuse source. A portion, at least, of the system of colored rings can be seen, and their expansion or contraction on rotating the analyzing polaroid can be observed. Moreover, by making use of the partly polarized light from the sky, the polarizer can be dispensed with. By a little juggling one can even contrive to use a piece of glass, for example a spectacle lens, as analyzer.

† A. Biot, *Ann. Soc. sci. Bruxelles*, vol. 58, pp. 98–100, 1938.

‡ Recently a new etch solvent for quartz, free from the more objectionable properties of H_2F_2, has become available under the name of Quartz-Etch, the base of which is said to be ammonium bifluoride. Preliminary tests in this laboratory indicate that the etch figures and refraction images are inferior to those obtained with H_2F_2.

jar. Copper implements and racks are useful for holding and handling crystals. Most uniform results are attained by rocking the container during etching; a motor drive is easily contrived and greatly to be recommended. The acid loses strength both by evaporation and use and has to be renewed rather frequently. There is also some evidence that acid containing considerable amounts of the products of solution does not make as good etch patterns as freshly prepared acid.

Provision should be made for drawing off the vapor from the acid and for neutralizing it if necessary. Every possible precaution must be taken to guard against even slight contact of the acid with the skin, since hydrofluoric acid burns are very serious.

Etching takes place most rapidly on surfaces normal to the Z-axis, less rapidly at the ends of a Y-axis (prismatic faces) and the positive ends of the X-axes, and very slowly at the negative ends of the X-axes.

Etching tests are useful for determining whether a crystal is right or left; for locating, on the etched surface, regions of optical and electrical twinning; and for determining approximately the orientation of any specimen or cut with respect to the crystallographic axes. Several techniques are available: (*a*) microscopic examination; (*b*) production of large-scale patterns on a quartz sphere; (*c*) light reflection; (*d*) light refraction.*

336. *a. Microscopic Examination of Etched Surfaces.*† We consider first the etch figures on surfaces normal to the X-, Y-, and Z-axes and their relation to the hand of the crystal and to optical and electrical twinning. Although the figures usually observed differ widely in size and in degree of perfection, still certain characteristic forms can be recognized. These forms appear best after etching for an entire day and require no special preliminary treatment of the surface beyond enough lapping to remove gross roughness.

As illustrated in Fig. 78, at the positive end of the X-axis the figures resemble narrow hysteresis loops, which merge to form closely packed grooves parallel to the Z-axis. At the negative end are parallelograms with one pair of sides parallel to Z. The polar character of the X-axis is here clearly in evidence. The Y-axis is not polar, and the figures at its ends, for crystals of the same hand, are alike except for orientation; this difference can be traced to the polarity of the X-axis. The same remarks apply to the figures on faces normal to the Z-axis. In each of

* A technique for making replicas of etched surfaces, suitable for microscope slides, has been described by V. J. Schaefer, *Phys. Rev.*, vol. 62, pp. 495–496, 1942.

† Perplexing discrepancies are found in the literature. The outlines of etch figures on the m-faces (Y-cuts) in Groth (ref. B22, Table III) do not agree with those shown by O. Meyer and S. L. Penfield in *Trans. Conn. Acad. Arts Sci.*, vol. 8, pp. 158–165, 1889, and both are at variance with the results of very careful tests made in this laboratory.

the six diagrams the etch figures at the right and left of the vertical axis illustrate *optical* twinning.

The figures at the ends of the Z-axis (*i.e.*, on Z-cut surfaces) are due to minute pyramids or pits with triangular bases (see Plate 6 in the paper by Booth[69]). They vary greatly in appearance with time of etching, illumination, and microscope focus. On prolonged etching they undergo characteristic changes.*

If electrical twinning (§15) is present, some regions of the same hand are rotated 180° about the Z-axis with respect to the rest of the crystal. For example, a left-quartz may show etch figures like a_1 and a_2 on the same X-surface, b_1 and b_2 on the same Y-surface, and c_1 and c_2 on the same

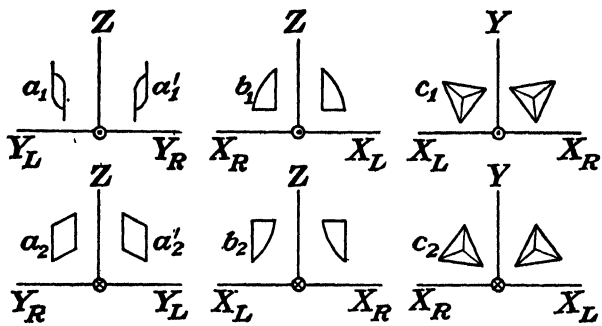


FIG. 78.—Typical idealized microscopic etch figures for right- and left-quartz, on surfaces normal to the X-, Y-, and Z-axes. Upper row is for surfaces from which the positive end of one axis points toward the observer. In the lower row the positive end points away from the observer. Figures for left-quartz are to the left of the vertical axis in each case, for right-quartz to the right. The symbol Y_L indicates the positive direction of the Y-axis for left-quartz, etc. The magnification is of the order of 200 diameters. The patterns are shown in their actual orientation on the crystal surface, and not as they appear under the microscope.

Z-surface. Electrically twinned regions are generally bordered by irregular lines. Both elastic and piezoelectric properties are different on opposite sides of the border; hence, electrically twinned plates are not suitable for resonators.

In *optical twins* there are two different possibilities, according to whether the two components have the positive ends of the X-axes or of the Y-axes pointing the same way (see Fig. 76). In the former case, a surface normal to X may show a_1 and a_1' on different areas, while the corresponding surface on the other side of the crystal shows a_2 and a_2'. If the Y-axes point the same way, a_1 and a_2 may be seen on one side of the crystal, a_1' and a_2' on the other. Analogous remarks may be made concerning the figures on Y-surfaces. As to the Z-surfaces, if the X-axes (or Y-axes) point the same way, the figures are always mirror

* HONESS, ref. *B* 6.

images with respect to X (or Y). It seems to be a common convention to call the type of twinning when the Y-axes point the same way simply "optical twinning," while the term "combined optical and electrical twinning" is used in the other case.

If the X-axes point the same way in an optically twinned crystal, the piezoelectric properties are the same on both sides of the boundary, but not the elastic properties. If the X-axes are oppositely oriented (in which case the Y-axes are similarly oriented), the elastic properties, but not the piezoelectric, are the same on both sides of the boundary. In either case optical twinning beyond a very small amount makes a specimen undesirable for resonators.

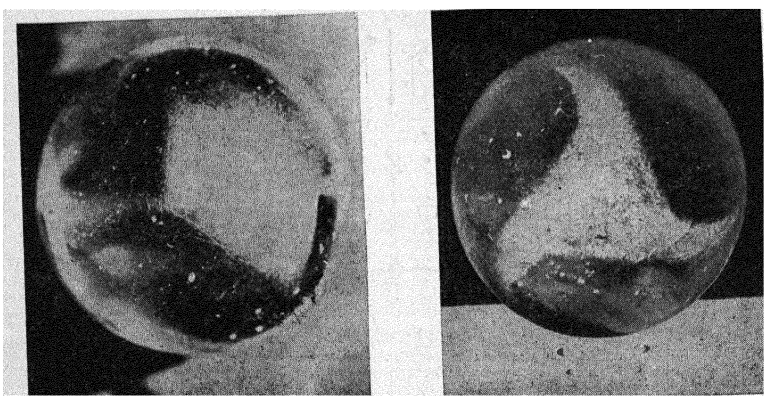


FIG. 79.—Etch pattern on a 50-mm sphere of left-quartz, from Van Dyke. (*a*) View toward an *m*-face, with an *R*-face above it; (*b*) view along the optic axis.

Etched surfaces in other orientations show a great variety of characteristic figures, often very difficult to identify under the microscope. In practical cases it is much better to identify cuts and axes by reflected or refracted light rather than microscopically. The advantage thus gained is that the effects of multitudes of etch facets become integrated, yielding more dependable results than is possible from the examination of individual etch figures.*

337. *b. Large-scale etch patterns on a quartz sphere* have recently been described by Van Dyke.[558]† Figure 79, taken from his paper, shows the appearance of an initially polished sphere after several hours of etching in H_2F_2. The entire surface has been more or less attacked, but certain

* Excellent microphotographs of etch figures on quartz surfaces in many orientations appear in a paper by Bond.[63]

† References to the literature on the subject are given in this paper.

areas, notably near the negative ends of the X-axes, are so little etched that the formation of etch facets can be detected only by the "sheen" in light reflected at the proper angle. On the other hand, the roughening of the surface marked out by the "tripus" in Fig. 79*b* is quite conspicuous. In general, the outlines of the pattern are determined not so much by marked differences in amount of etching as by changes in the sheen, indicating that the orientations of the facets formed in the process of etching, as well as the speed of solution, are strongly dependent on the angle at which the sphere cuts across the lattice structure.

When viewed by reflected light, five well-defined areas can be distinguished. Most prominent is the tripus at each end of the optic axis.

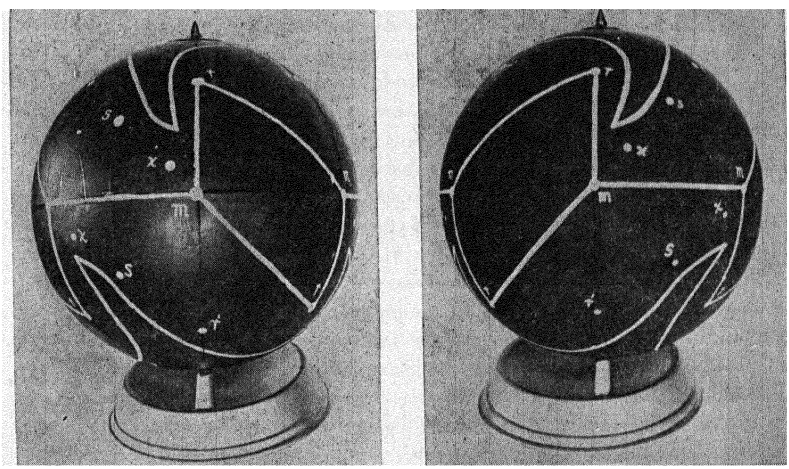


FIG. 80.—Models of left- and right-quartz showing outlines of etch patterns and the poles of various faces, from Van Dyke. Left-quartz is at the left. The optic axis is vertical.

The other three areas are parallelograms uniformly spaced around the equator. These parallelograms are linked by etched "bars," which are broadest midway between the parallelograms. The center of each bar marks the pole on the sphere of the positive end of an X-axis; the negative ends of the X-axes are at the centers of the parallelograms.

When the fine structure is examined under a microscope, at the ends of the axes characteristic figures, more or less like those in Fig. 78, can be recognized. It is from the facets forming these figures that the sheen originates. It is significant that the small-scale parallelograms in Fig. 78 are seen over the region outlined by the large-scale parallelograms, while the trigonal markings for Z-cuts are present on the trigonal tripus.

By means of a reflection goniometer or a rodometer, the characteristics

of the etch pattern on any part of the sphere can be investigated quantitatively according to methods *c* and *d*.

Van Dyke has constructed models, illustrated in Fig. 80, in which are marked the outlines of the principal etched areas. One sees that the *s*-faces come above and below the middle of a bar ($+X$-axis) and that the four corners of the parallelograms are the poles of *m*- and *R*-faces. The long sides of the parallelograms are arcs of great circles on which the poles of all faces lie. Portions of the tripus at each end of the *Z*-axis can be seen. The tips of the tripus curl clockwise or counterclockwise according to whether the crystal is right or left.

338. *c. Reflection Methods for the Examination of Etched Surfaces.* An etched surface shows a characteristic sheen in reflected light when the beam strikes it in certain particular directions. By the use of a suitable reflection goniometer the orientations of the various groups of etch facets with respect to the specimen can be determined. This method has been used for determining the axes of quartz from etched surfaces.*

339. *d. Refraction Methods.* The first to observe refraction patterns from etched quartz crystals seems to have been Nacken.[387] Later Herlinger[220] developed a "photogoniometer" for studying both reflection and refraction patterns, and still later the refraction patterns were investigated by Gramont, who introduced some novel techniques. Although Gramont's theory is at some points open to criticism, his work pointed the way to methods of considerable usefulness for determining the axial directions and the hand of unfaced quartz crystals.

Refraction patterns present a wide diversity of form, depending on the direction of the emergent beam with respect to the crystal axes. For any given orientation, the pattern is the result of rays from facets of different inclinations and azimuths. Some of the facets are not plane, but have a characteristic curvature (or possibly a set of nearly parallel etch surfaces), producing streaks or brushes of refracted light; reflection effects may also play a part in the formation of the observed refraction pattern.

Refraction patterns may be seen with little or no apparatus. An etched plate or slab cut in any orientation is simply held close to the eye, and a point source of light (a frosted lamp a few meters away will do) is viewed through it. The etched surface may face either toward or away from the eye. If the opposite surface is not polished, it can be covered with a piece of glass with a drop of immersion liquid between.

An improvement on this method consists in placing the crystal, with the etched surface horizontal, between the eye and a point source of light located a few millimeters below the crystal. A pinhole over a

* See, for example, Gaudefroy,[164] Herlinger,[220] and Willard;[586] also P. D. Gerber, U. S. patent 2,218,489.

frosted light bulb can be used. If the crystal is in the form of a flat plate, the lower surface, if not polished, can be laid on a piece of glass with a drop of immersion liquid between. Large specimens can be supported with the lower portion immersed in the liquid. A diverging cone of light traverses the crystal, and the rays reaching the eye from any point on the etched surface come from those facets located at this point which have the right orientation. The greater the divergence of the rays from the source and the larger the etched surface, the less necessary it is to place the eye close to the crystal. The focal plane of the observed pattern appears to lie a centimeter or so below the etched surface, as can be shown by a simple construction according to geometrical optics.*

A very sharp and bright pattern is seen when the point of light is produced by letting the rays from an automobile headlight bulb pass upward into the open end of a microscope objective of focal length around 2 mm. From the focal point just above the objective lens the rays diverge in a wide cone. Crystals several centimeters thick, placed just above the focal point, can be examined by this means. The eye can be at any distance above the crystal, but with thick crystals the head must be moved from side to side in order to see the complete pattern. A device of this sort is called a *rodoscope* (from the Latin *rodere*, to eat away).

340. A more precise means for examining refraction patterns is the use of a narrow beam of parallel rays instead of a diverging cone. The beam passes vertically upward through the crystal, emerging from a surface that has been suitably ground and etched. To prevent refraction and scattering of light where the beam enters the crystal, the lower portion of the latter is placed in an immersion liquid. The light is refracted by etch facets on the small area of the surface through which the beam emerges, producing a pattern that can be photographed or examined visually on a translucent screen. This pattern is determined by the orientation of the crystallographic axes with respect to the beam and is practically independent of the inclination of the etched surface. Hence, by tilting the crystal about horizontal axes and rotating it about the vertical axis, until certain well-defined features of the pattern conform exactly to a previously determined standard, the directions of all three axes with respect to the framework of the instrument become known.

This procedure is best carried out with a specimen on which an etched surface has been prepared that is normal to the optic axis within 10° or so. When the optic axis is parallel to the beam, the refraction pattern has the appearance of a three-pointed star, which varies greatly

* Refraction patterns according to the method just described are discussed by R. S. Rivlin, *Proc. Phys. Soc.* (*London*), vol. 53, pp. 409–412, 1941, and also by G. W. Willard.[586]

with time of etching, together with three characteristic *spots.** After the etching has progressed far enough to make these spots visible, their positions remain practically unchanged over long periods of etching. Although they were observed long ago by Nacken,[337] their importance has only recently been appreciated. When the optic axis is parallel to the beam of light, the three spots fall at the vertices of an equilateral triangle, and from their positions the X- and Y-axes, with their positive directions, are determined. The pattern is similar to that seen in the rodoscope, but rotated by 180°.

An instrument for orienting crystals by this method has been called a *rodometer.*† By its use the crystallographic axes of any specimen of quartz can be determined easily and quickly within a degree, and in trained hands settings can be reproduced within +15 min of arc. At the same time the refraction pattern indicates the hand of the crystal, locates twinned regions on the crystal surface, and tells whether the twinning is optical or electrical.

341. Orientation of Quartz Crystals and Plates by X-rays. As we have seen, it is possible with apparatus of high quality to determine the optic axis within a few minutes of arc by purely optical methods. Such methods, however, cannot determine the X- and Y-axes. For approximate orientations of these axes it is most convenient to use a beam of light reflected or refracted at an etched surface. By the use of the rodometer all three axes can quickly be determined with a single setting. Nevertheless, no etch method can provide as accurate an orientation as is required for precise investigations in the laboratory or for meeting modern commercial demands. It is here that X-rays are indispensable, since by their use complete orientations, precise within a few minutes of arc, can be made very quickly. An accuracy of $\pm 1'$ can be attained with X-ray apparatus of high precision.

But little use has been made of the Laue method for quartz crystals, since it is applicable only to thin cuts. Koga and Tatibana‡ have used this method; in their paper are a list of atomic planes and two photographs of Laue patterns. The back-reflection method§ has been used to a limited extent. The Bragg reflection method is chiefly employed, with K_α-rays

* Before etching, the surface should be ground with carborundum (grain about 100), with random strokes in all directions. To bring out the spots most distinctly it has been found best to mix three parts commercial (about 50 per cent) hydrofluoric acid with one part water and to etch for 2 to 3 hr.

† W. G. Cady, *Proc. I.R.E.*, vol. 28, p. 144, 1940 (abst.); H. H. Hubbell, Jr., *Phys. Rev.*, vol. 59, p. 473 (abst.). The use of the spots for the orientation of quartz, as well as many features in the technique, were introduced by G. J. Holton (distinction thesis, Wesleyan University, 1941). A more complete account of the construction and use of the rodometer is given by Holton.[333]

‡ I. Koga and M. Tatibana, *Electrotech. Jour.* (*Japan*), vol. 3, pp. 38–39, 1939.

§ A. B. Greninger, *Z. Krist.*, vol. 91, pp. 424–432, 1935.

from a copper target. The choice of atomic plane in the crystal depends on the orientation of the surface to be tested, whether normal to X, Y, or Z or in some oblique direction. "Glancing" angles up to 30° or more are used. The specimen under investigation is tilted until a response is observed in a meter actuated by an ionization chamber or Geiger counter. A full description of the method has been given by Bond and Armstrong.[68]

342. Cutting and Finishing of Quartz Plates. Formerly muck saws were used for cutting quartz, in which a rotating disk of copper or soft steel dipped into wet carborundum powder. At present diamond-charged disks are preferred, the cutting edge being kept wet by kerosene or a special coolant. In the laboratory quartz cutting can be done with such a disk mounted on the arbor of a milling machine. For small work, the author has had good success with a very thin carborundum grinding wheel mounted in a lathe.

Omitting the various details of quantity production, we pass at once to the "blank" as it comes from the saw, in approximately the right orientation but slightly oversize. It is good practice at this stage to test the blank for twinning, if this test has not already been carried out on the thin "wafer" from which, in some cases, the individual blanks are cut. The blank is lightly etched and examined by reflected light. Twinned regions are revealed by differences in the sheen.

The blank must next be lapped to the desired dimensions (or frequency) and to precise orientation, with occasional X-ray tests. For l-f crystals (lengthwise or contour vibrations), the length and breadth are of chief importance.

For *thickness modes* the thickness of the plate is the determining factor, and the plate must be of uniform thickness, usually within 0.0005 mm. Plates as thin as 0.2 mm are in practical use. For best performance, the four narrow peripheral faces have to be carefully lapped; they are sometimes also slightly beveled at the edges. Owing to coupling between different modes, a very slight change in length or breadth of the plate may affect the activity very greatly. The final contour lapping is a matter of trial and error, except in the case of certain cuts for which the optimal contour can be predetermined.

Lapping machines are of various types, some of which lap one side only of a "nest" of several plates, while others lap both sides at once. A drill press is easily converted into a machine for lapping one side at a time; in this case the plate or plates to be lapped are cemented to a flat metal plate. Small-scale lapping can be done by hand on a slab of plate glass or, better, on a trued cast-iron surface. The fluid may be water, soap and water, or a special oil. The process is carried out in several stages, depending on how much the crystal has to be reduced. Usually carborundum is used, of successive degrees of fineness down to 600.

The final fine lapping is done with emery or aluminum oxide. Polishing is, as a rule, neither necessary nor desirable. The finishing touches are usually performed by hand. Etching is also often employed to bring the crystal to exactly the desired vibrational frequency. Etching also removes loose particles of quartz and decreases the damping.[188]

The removal of a single layer of silicon atoms (§540) from a 1,000,000-cycle X-cut quartz plate 3 mm thick would increase the frequency by about 0.1 cycle/sec, an amount that is significant in precision oscillators. One of the fortunate characteristics of quartz is that the atoms are so well bonded as not to be easily removed.

343. Resonator Mountings and Holders. Since nearly all piezo resonators are of quartz, the subject of mountings, including the types

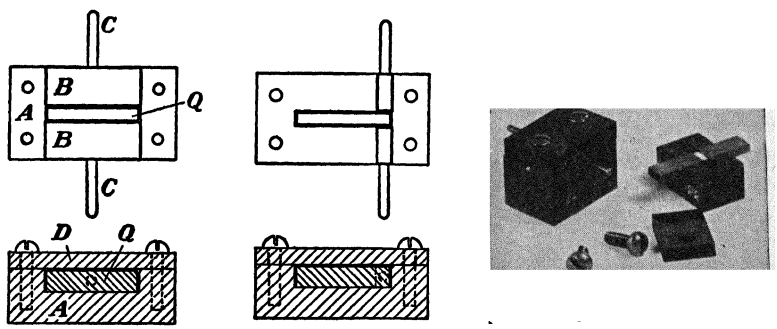


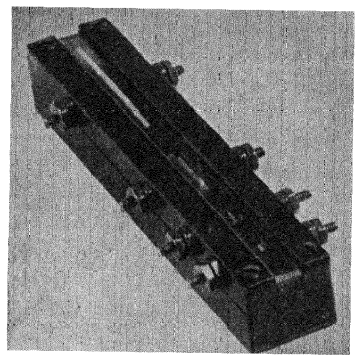
FIG. 81.—The earliest mountings for quartz resonators. The bars Q were all X-cut, length parallel to Y. The housings A and covers D were of hard rubber or bakelite, with brass electrodes B. (*a*) Full-length electrodes. (*b*) Short electrodes, for excitation of the fundamental and of both even and odd overtones. (*c*) Two small resonators, for frequencies 757 and 860 kc/sec.

used for piezo oscillators, is considered here. The guiding principles are the same whatever piezoelectric substance may be used.

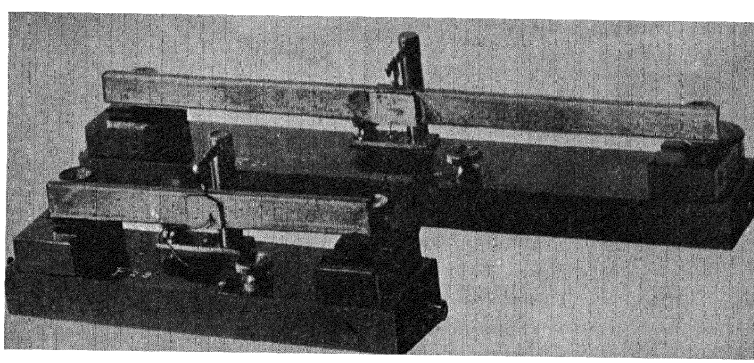
In the author's earliest experiments with resonators, bars of quartz or Rochelle salt were used, with tinfoil coatings cemented to the sides. The bars were laid flat on the table, suspended from fine wires, or placed on soft pads of cotton. It was soon found that resonance was much sharper when the tinfoil coatings were removed and the crystal stood on edge between rigid brass electrodes, with a small air gap on each side. In some cases the bars were held by silk threads tied around them at the center, in order to leave them more free to vibrate in the gap between the electrodes. Some of the quartz bars used in the early 1920's, together with typical holders, are illustrated in Fig. 81. At that time, since it was not foreseen that quartz plates could be made to resonate in thickness vibration, only lengthwise vibrations of bars were investigated. In

order to push the frequency as high as possible, some of the bars were only a millimeter long.

Some of the resonators used by the author in 1923 for comparisons with standard frequency meters in government laboratories in the United



(*a*)



(*b*)

FIG. 82.—Early types of piezo-resonators. (*a*) Four *X*-cut quartz bars, lengths 1.76, 3.60, 12.02, and 30.3 mm, parallel to *Y*. Frequencies 1.523, 762.0, 235.9, and 91.66 kc/sec, respectively, in a common holder. (*b*) Two steel bars, 180 and 90.5 mm long, 9.8 × 3.2 mm in cross section, each driven by a pair of small *X*-cut quartz plates. Frequencies 14.43 and 28.94 kc/sec. See description in §383.

States, Italy, France, and England are shown in Fig. 82. These were the first international frequency comparisons to be made by means of crystal standards. Since then, a number of such comparisons have been carried out, with improved resonators and higher precision (see the references at the end of Chap. XIX). In the primitive mountings used in 1923, the quartz bars lay loosely in the bottoms of pockets between the elec-

trodes. The damping was relatively high, and the frequency varied with slight displacements of the crystal. Moreover, there was no control of the temperature. The precision was about 0.1 per cent; today the minimum requirement is at least ten times better than this.

With increasing demands for constancy of frequency, the development of crystal holders has kept pace with that of crystals and circuits. In technical journals and patent literature can be found enough material for a treatise on mountings and holders alone. We can do no more here than discuss some of the principal features, especially of the more recent types. A few references on the subject will be found at the end of the chapter.

Crystal mountings and holders may be classified according to whether they are designed for use in oscillator circuits, stationary or portable; or for use as filters, including receiving sets; or as frequency standards. They differ also according to the mode of vibration of the crystal. Mountings of special types, as for flexural vibrations, luminous resonators, and ring-shaped crystals for quartz clocks, will be considered in later sections, with references to the original papers for details.

Of the four parameters R, L, C, and C_1 of the equivalent network, L and C are affected only to a minute extent by the character of the mounting. In recent years, through various improvements in the construction of holders, R has been greatly reduced in value and made practically free from variation due to mechanical shock and other service conditions. The effects of stray capacitances on C_1 have been reduced. At the same time, the newer holders are not less rugged and portable than the earlier types.

For the controlling crystals in *oscillator circuits*, the main requirements are constancy of frequency, ruggedness, and ability to stand fairly high voltage. Constancy of frequency demands, of course, a high Q and, in the case of portable sets, immunity against vibration. Variations in temperature are compensated in various ways. In the first place, the use of cuts having a low temperature coefficient of frequency (§357) has become almost univeral, making the use of temperature control unnecessary for most practical purposes. When such control is needed, for example to prevent condensation of moisture or to compensate for extreme variations in ambient temperature, small thermostats and heaters are sometimes built into the holder. For still more precise control, in transmitting stations and especially for frequency standards, the holder may be mounted in a special thermostatically controlled oven.

344. *Holders for Crystals in Thickness Vibration.* The crystal plates are usually square, rectangular, or circular. In the earlier types the crystal lay loosely on one electrode, held down by gravity, either with a small gap between it and the upper plane electrode, or else subjected to

slight pressure from the upper electrode, the gap being eliminated. While such mountings are most convenient for laboratory experiments, they have proved to be unsuited to modern service conditions, owing to variations in frequency and damping when the plate moves about in the holder and also because of a tendency for metal to rub off onto the crystal.

A typical holder of more modern design uses the *pressure mounting.* It has a horizontal carefully lapped electrode upon which the crystal rests. In one type the other electrode, which presses on the crystal, is slightly recessed on its lower face, so as to clamp the crystal at its four corners or around its circumference if it is circular, leaving a gap of the order of 0.2 mm between crystal and upper electrode. For frequencies above 10 megacycles, it has been found feasible to clamp the crystal, for example by bolts passing through holes at the four corners. An advantage in corner clamping is that it suppresses flexural modes. The smaller the gap, the greater the power that can be controlled in the crystal circuit, but the more sensitive the frequency to minute variations in gap width.

In another type the gap is eliminated, and the upper electrode is pressed against the crystal by a spring. The damping is greater in such mountings than when there is a gap; but even in gap mountings the damping due to contact with the lower electrode is great enough to be objectionable in precise work. The pressure can, however, be surprisingly great without preventing the crystal from vibrating. For example, Booth and Dixon[70] state that a piezo oscillator with area about 6 cm^2 (either X-cut or Y-cut) will function despite a force as great as 1.6 kg on the upper electrode. The damping caused by pressure is less noticeable with shear vibrations than in the case of X-cuts, where the thickness vibrations are compressional.

In mountings of the type just described, especially when the upper electrode presses against the crystal, a "threshold effect" has sometimes been observed; *i.e.*, the crystal fails to oscillate until the voltage reaches a critical value depending on the friction to be overcome. In mountings for resonators and filters, this effect must be avoided as far as possible. It is less objectionable in the case of oscillators.

Other types of gap mounting have been devised. For example, the electrodes are sometimes held at the desired distance apart by spacers of insulating material with low coefficient of expansion, as fused silica or pyrex glass; crystalline quartz has also been used.[358] Three separate spacers may be used, or a continuous ring of the proper thickness inside which the crystal is laid. *Adjustable gaps* have also been employed,* one or both of the electrodes being held by a micrometer screw. The advantage in this arrangement is the possibility of varying the frequency at will over a range of one-tenth of 1 per cent or so. For laboratory

* For a recent form, see ref. 43.

purposes, the author has, for many years, found this device very useful. On the other hand, it is not now generally considered desirable for constant-frequency circuits, since the desired frequency can be attained with a fixed gap by suitable dimensioning of the crystal, the frequency then being more stable. Moreover, the mounting with adjustable electrodes has more stray capacitance and is bulkier.

For greater constancy of frequency as well as smaller damping, the crystal plate, if not too thin, is sometimes clamped at three or more points at its outer edges.* Three minute cavities are drilled in the plate edgewise—two on one side and one on the other if the plate is rectangular—and in these cavities are seated the pointed ends of spurs that extend inward from the housing. The plate is thus held only at points in the nodal plane and does not touch either electrode. Bechmann[43],† describes mountings in which the quartz plates, oriented for zero temperature coefficient, are of circular form, beveled outward to a sharp edge all around the circumference. The edge lies in the nodal plane and fits into notches in three short rods, two of which are fixed while the other is pressed against the crystal by a spring. Each electrode is adjustable; but when the proper adjustment has been made, the entire mounting can be sealed in an evacuated holder. Mountings of this type are made for frequencies of 250 to 10,000 kc/sec.

Modern mountings usually have electrodes of some such material as monel metal, stainless steel, or duralumin. The housing is tightly sealed and waterproof.

345. In recent years the tendency to employ *plated crystals*‡ has been increasing, involving a special type of mounting, with metallic electrodes evaporated onto the crystal surfaces, specially designed lead wires, and hermetically sealed housings, either evacuated or filled with dry air.§ The metallic deposits on the crystal are usually of aluminum, silver, or gold, about 0.0005 mm thick. The crystal surfaces should first be etched to remove loose material left after lapping. By a special process, the ends of the phosphor-bronze lead wires, which also sustain the weight of the crystal, are attached firmly to the centers of the electrodes. The size and shape of these wires are predetermined and carefully adjusted, so that the wires will have the proper compliance for protecting the crystal against shocks, while at the same time not absorbing appreciable energy from the h-f vibrations of the crystal. The frequency is thus

* See, for example, L. Essen.[135]

† See also Heaton and Lapham.[212] Quartz plates with beveled edges, supported at points in the nodal plane, were used in this laboratory by K. S. Van Dyke in 1925.

‡ The first to use thin metallic films on the crystal were the Curie brothers. In some of their early devices they employed silver electrodes, deposited chemically.

§ See, for example, A. W. Ziegler, U. S. patents 2,218,735, Oct. 22, 1940, and 2,275,122, Mar. 3, 1942.

made more stable, while damping and stray capacitances are reduced to a minimum. The assembly of crystal and leads is mounted in a tube of glass or metal, with a standard plug-in base. In some forms the tube contains also a small thermostat and heater.

346. *Special Mountings for Low-frequency Crystals.* We are concerned here with bars in lengthwise vibration, and broad rectangular plates vibrating in a l-f mode. The general requirements and basic construction are similar to those for thickness vibrations. The crystal is now usually plated on both sides, thus eliminating the gap. Since a lengthwise-vibrating bar has a nodal region at the center, it can be firmly clamped here without too much damping. Until recently the commonest method in commercial mountings has been the use of a pair of metal knife-edges to clamp the crystal, one on each side extending in the direction of the breadth. For greater security each side is sometimes supported by two knife-edges close together. Still another method of clamping, designed especially for filters, consists in having two small metallic hemispheres pressed by springs against the crystal on each side.

In order to prevent possible displacement of the crystal, a type of mounting has been devised[69] in which a shallow groove is cut across the crystal on one side, into which a knife-edge fits, while a point contact presses against a countersunk hole on the other side. In a modification of this method two small steel balls press against conical holes in the bar on one side and one similar ball on the other.

Knife-edge mountings are applicable to bars down to about a centimeter in length (frequency around 300 kc).

In the case of broad plates vibrating in l-f shear modes, knife-edges interfere with the freedom of vibration. The plate is therefore supported by one or more pairs of pressure pins on each side.

Most recent of all is the *wire-supported type* of mounting,[188] in which the plated crystal is held by specially designed wires soldered to its surfaces, as described in §345. Crystals so mounted and properly aged are said to hold their frequency constant within 2 or 3 parts per million.

347. The Aging of Quartz Resonators. Soon after quartz began to be used as a precise standard of frequency, it was observed that for some weeks or even months after a plate had received its final lapping and was mounted in its holder the resonant frequency underwent a slow drift. It is well established that this drift persists after all possibility of change in the position of the electrodes has been removed and that it is due to the surface layers of the finished plate. A final etching of the surfaces has been found beneficial. Bechmann[44] found that aging can be hastened by repeated heating. It has now become standard practice to put the finished plate through several cycles of heating and cooling, for example between 25 and 115°C.[188]

REFERENCES

Physical Properties of Quartz

Dake, Fleener, and Wilson, [B12] Gramont,[B21] Scheibe,[B45] Sosman,[B47] Vigoureux,[B50,B51] Voigt,[B52] Baldwin[16,17] (popular accounts), Bond and Armstrong,[68] Willard.[584,585]

Hund, A.: "Phenomena in High-frequency Systems," McGraw-Hill Book Company, Inc., New York, 1936.

Testing, Preparation, and Mounting of Plates

Beckerath,[47] Bokovoy,[62] Bond,[67] Druesne,[126] Greenidge,[188] Shore,[462] Sykes,[499] Thurston,[519] Tolansky,[521] Venkov.[564]

Elbl, L. A.: Crystal Holder Design, *Electronics*, vol. 16, pp. 134–138, October, 1943; Quartz Crystal Finishing, *Electronics*, vol. 17, pp. 122–125, 288, 290, January, 1944; Crystal Testing Techniques, *Electronics*, vol. 17, pp. 120–123, 380–382, August, 1944.

Florisson, C.: Improvements in Frequency-Stabilizers, L'Onde élec., vol. 10, pp. 131–135, 1931.

Schaffers, T. W. M.: The Q-Lap, *Communications*, vol. 24, pp. 40–42, 80, Apr., 1944.

Optical Properties and Optical Methods of Testing

Myers,[B38] Sosman,[B47] Tutton,[B48] Wood,[B55] Arnulf,[9] Biot,[54] Booth,[69] Buisson,[85] Kao,[253] Modrak,[371] Van Dyke.[558]

References on the etching of crystals are given at the end of Chap. II.

Very recently the following publication has appeared, too late for discussion in the text of this book. It should be consulted by all who are interested in the use of quartz crystals as resonators and oscillators.

Symposium on Quartz Oscillator-plates, *American Mineralogist*, vol. 30, pp. 205–468, May-June, 1945. This symposium comprises the following papers:

Frondel, Clifford: "History of the Quartz Oscillator-plate Industry," 1941–1944, pp. 205–213.

Van Dyke, Karl S.: The Piezoelectric Quartz Resonator, pp. 214–244.

Stoiber, Richard E., Carl Tolman, and Robert D. Butler: Geology of Quartz Crystal Deposits, pp. 245–268.

Gordon, Samuel G.: The Inspection and Grading of Quartz, pp. 269–290.

Lukesh, Joseph S.: The Effect of Imperfections on the Usability of Quartz for Oscillator-plates, pp. 291–295.

Parrish, William, and Samuel G. Gordon: Orientation Techniques for the Manufacture of Quartz Oscillator-plates, pp. 296–325.

Parrish, William, and Samuel G. Gordon: Precise Angular Control of Quartz-cutting by X-rays, pp. 326–346.

Gordon, Samuel G., and William Parrish: Cutting Schemes for Quartz Crystals, pp. 347–370.

Parrish, William: Methods and Equipment for Sawing Quartz Crystals, pp. 371–388.

Parrish, William: Machine Lapping of Quartz Oscillator-plates, pp. 389–415.

Frondel, Clifford: Final Frequency Adjustment of Quartz Oscillator-plates, pp. 416–431.

Frondel, Clifford: Effect of Radiation on the Elasticity of Quartz, pp. 432–446.

Frondel, Clifford: Secondary Dauphiné Twinning in Quartz, pp. 447–460.

Glossary of Terms Used in the Quartz Oscillator-plate Industry, pp. 461–468.

CHAPTER XVII

THE QUARTZ RESONATOR

. . . this electric force, that keeps
A thousand pulses dancing. . . .
—TENNYSON.

The earliest resonators, crudely cut and crudely mounted, could be depended on for a precision in frequency of about 0.1 per cent. This precision was much higher than that of most wavemeters of two decades ago. Soon, however, there came an increasing demand for constancy of frequency in radio transmitters. This demand was met by the introduction of the piezo oscillator, together with temperature control of the crystal and improvements in its preparation and mounting. In 1929 the first quartz resonators of low temperature coefficient appeared. Since then, the intensive study of the elastic and thermal properties of quartz has led to the discovery or predetermination of many useful cuts for all radio frequencies, and with resonant frequencies so little dependent on temperature that thermostatic control is unnecessary.

In the present chapter the principal cuts and their properties and uses are described, with illustrative numerical data.

Excitation of the Simpler Modes of Vibration in Quartz. We shall here apply the rules outlined in Chap. X to quartz, in order to ascertain how an electric field may be applied to preparations of various forms and orientations, for the excitation of lengthwise, thickness, flexural, and torsional vibrations.

I. LENGTHWISE COMPRESSIONAL VIBRATIONS OF BARS

348. The earliest resonators were in the form of bars, using compressional lengthwise vibrations. Since the author's first experiments, which were made with bars of both Rochelle salt and quartz, it has been recognized that this type of piezo resonator offers the advantage of well-defined response frequencies, free from the effects of undesired vibrational modes. The simplest example is that of an X-cut bar with length parallel to Y, as used statically by the Curie brothers and dynamically by many others. Here the strain of primary importance is $y_y = d_{12}E_x$.

If l is parallel to X, lengthwise excitation can be brought about by placing electrodes at the ends of the bar or by applying a field parallel to X over a portion of the bar, as was done by Giebe and Scheibe (§349). For intermediate orientations of l in the XY-plane this excitation can

also be used, or the field may be applied across the bar in the XY-plane so that it has a component in the X-direction.

A bar with length parallel to Z cannot be *directly* excited in lengthwise vibration; such vibrations are, however, possible through elastic coupling, by applying an alternating field of the right frequency parallel to X. This experiment does not seem to have been performed with a thin bar, but the principle was verified by Hund,[238] who observed compressional vibrations in the Z-direction in a rectangular plate in which the applied field was parallel to X.

For a bar in any arbitrary orientation, the effective piezoelectric constant has a different value according to whether the vibrations are excited by a field *parallel* or *perpendicular* to the length. We shall dispose of the former and less usual case first. Here the shape and orientation of the cross section are of no consequence. Although no complete theory for this type of excitation has been developed, still one knows at least that the piezoelectric constant must be of the type d'_{33}, if the length of the bar is taken as parallel to the rotated Z'-axis. Equation (219) for d'_{33} shows that this constant involves d_{11} alone. It vanishes only when $\varphi = \pm 30°$ or $\pm 90°$ (projection of l on the XY-plane parallel to a Y-axis) or when $\theta = 0°$ (l parallel to Z).

In the usual case the exciting field is *perpendicular to* l, and the orientation of the cross section must be considered. Since no general equations for d'_{hk} in all orientations are available, we shall consider each of the principal planes separately. The problem is analogous to that of producing lengthwise vibrations in oblique bars of Rochelle salt (§371).

There is always an optimum orientation for E and hence for e. *If l lies in the YZ-plane*, the only possible excitation is by E_x, and X-cuts rotated about the X-axis must be used. If l is taken as parallel to the Y'-axis, making the angle θ with the Y-axis, the strain characteristic of this type of vibration is $y'_y = d'_{12}E_x$, where, by Eqs. (221),

$$d'_{12} = -c^2 d_{11} + scd_{14} \tag{475}$$

When $\theta = 0$, $d'_{12} = -d_{11} = d_{12}$ and we have the ordinary case of a bar parallel to Y. When $\theta = 90°$, $d'_{12} = 0$ and no direct excitation is possible ($l \parallel Z$). Otherwise, both d_{11} and d_{14} contribute to d'_{12}.

If l lies in the ZX-plane, one can in general let the thickness e, parallel to which the field is to be applied, have such an orientation that the field will be E_y, or a component of E_z, or a resultant of the two. A simple case is that of a rotated Y-cut, analogous to the rotated X-cut mentioned above: if l is parallel to Z', making the angle θ with Z, the strain equation is $z'_z = d'_{23}E_y$, where, by Eqs. (222),

$$d'_{23} = -csd_{14} \tag{476}$$

Lengthwise excitation by a field parallel to Y is therefore possible except when l is parallel to Z or X. When $\theta = 45°$, $d'_{23} = -d_{14}/2$ and the excitation is of exactly the same nature as for an X-cut 45° Rochelle-salt bar [Eq. (203)]. No observations seem to have been made on bars with l inclined obliquely in the ZX-plane, but compressional vibrations of this type have been observed by Wright and Stuart[594] in circular Y-cut plates and discussed by Bechmann.[36]

If l lies in the XY-plane, we may let l and e be parallel to Y' and X', respectively, so that

$$y'_y = d'_{12}E'_x = -d_{11}E'_x \cos 3\theta \tag{477}$$

by Eqs. (223), where θ is the angle between Y' and Y. When $\theta = 0$, we have the X-cut with l parallel to Y. Lengthwise vibrations can be excited at all angles in the XY-plane except when l is parallel to Z, making $\cos 3\theta = 0$.

The elastic stiffness calculated from observations of the frequency of a narrow bar of known length is the isagric Young's modulus, provided that the gap is zero. Consideration of the depolarizing effect of the electric field and of the value of the effective piezoelectric constant is needed only when there is a gap, according to Eq. (330). As long as the dimensions of the cross section are not over one-tenth of the length, the correction for finite cross section is inappreciable.[340] Bechmann's derivation of Young's modulus for various orientations from observations with narrow quartz bars has been mentioned in §96.

One other quantity occurring in the equations for vibrations of bars is the effective dielectric constant k_l, given by Eq. (311). This quantity is a little smaller than the free dielectric constant k'_i. The difference, at least for quartz, is slight and has been ignored by some writers. For any arbitrary orientation, k'_i is the same as k'_N in Eq. (474c). A rough approximation to the values of d_{in} and s^E_{nn} for the orientation in question is usually sufficient. The value of k_l for an X-cut quartz bar with length parallel to Y is given by Eq. (474a).

A full discussion of coupling effects between different modes lies outside the scope of this book. Some of the more important references on the subject are given at the end of this chapter.

349. Experimental Results with Lengthwise Vibrations. Working with rectangular quartz bars with lengths parallel to X or Y, Giebe and his associates[162,169,171] investigated the dependence of frequency upon cross section, for the fundamental and various overtones.* They derived formulas for frequency and for the departure of overtone frequencies

* We have discussed the excitation of overtones in bars in §238. The theory is treated further by Sokolov.[473]

from harmonic relations. Their theory involves coupling effects, Poisson's ratio, and the piezoelectric correction to the stiffness. Their electrodes were very small, since the bars were intended to show the luminous effects described in §365. For the bars with length parallel to Y, the small electrodes were placed at the center, so that the field was in the X-direction. When the length was parallel to X, two pairs of electrodes were used, as illustrated in Fig. 88B, giving rise to a field parallel to X at the center of the bar. Giebe and Blechschmidt[162] observed frequencies at different temperatures and calculated from them the temperature coefficients of s_{11} and s_{44}. The principal results of all these investigations are given in more detail by Scheibe.[B45]

Frequencies of thin rods in many orientations and at different temperatures have been observed by Bechmann.[32] From his results, already

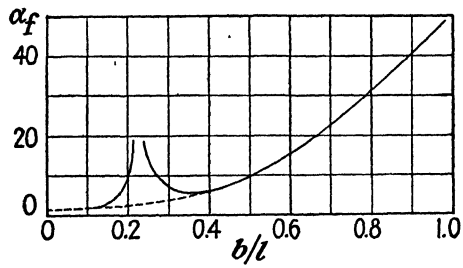


FIG. 83.—Dependence of the temperature coefficient α_f of an X-cut bar (length parallel to Y) on the ratio b/l, from Mason. For this bar $e = 0.05\ l$. Abscissas represent b/l; ordinates are in parts per million per degree centigrade.

referred to in §96, one can find the dynamic value of Young's modulus for any orientation in space, together with its temperature coefficient (summary in Scheibe[B45]).

All quartz bars or plates in lengthwise vibration, whatever the orientation may be, have negative temperature coefficients of frequency (see §357), the value becoming zero in certain special cases. For an X-cut bar with length parallel to Y, the first recorded value was that of Powers,[431] who found $\alpha_f = -5(10^{-6})$. Considering that Powers' bar had a b/l ratio of about 0.17, his αf fits satisfactorily on the curve in Fig. 83, which represents the dependence of α_f on b/l, as found by Mason.[332] The anomaly between 0.15 and 0.4 is due, according to Mason, to coupling with the second flexural mode in the YZ-plane. α_f is smallest for very narrow plates; it is also less for thick than for thin plates (X-direction). If the cross section is square ($e = b$), $\alpha_f = 0$ when $b/l = 0.272$. Qualitative agreement with Mason's results will be found in Table 13 in Scheibe's book.[B45] Booth[69] agrees with Mason in finding $\alpha_f = -2(10^{-6})$ for very narrow bars with length parallel to Y.

The *dependence of frequency on the gap width w*, for a bar at room temperature, has been investigated* by Dye[127] and the author.[107] According to Eq. (336*b*) there should be a linear relation between w and the relative change in frequency with gap, the coefficient U being the same for all gaps. The experiments yield a value of U about 15 per cent smaller than that predicted by theory and also a progressive decrease in U with increasing gap. Possible explanations of the discrepancy are discussed in the author's paper. The observed frequency increases by about one-half of 1 per cent as the gap is increased from zero to a very large value.

Lengthwise vibrations of quartz plates having a breadth b comparable with the length l have been studied by Petrzilka,[417,418] Bechmann,[36,41,42,44] and Mason.[332,340] Petrzilka used both rectangular and circular Z-cut plates, with electrodes so placed as to provide a driving field perpendicular to Z. His paper contains photographs of the wave patterns obtained. He identified, at suitable frequencies, the three vibrational modes predicted by theory and from his results calculated the elastic modulus and Poisson's ratio.†

Mason measured the variation in frequency of an X-cut 18.5° rectangular plate (see Table XXIX) as the ratio b/l was increased from 0.1 to 1. There was a general decrease of about 12 per cent, due to coupling with a flexural mode and with compression parallel to b. An anomaly occurred for values of b/l from 0.2 to 0.3, owing to close coupling with the flexural mode. Mason points out that the Rayleigh correction for cross section (§65) is incomplete when applied to quartz, since it does not take account of the coupled modes.‡

The problem was also analyzed by Bechmann, who derived, for a rectangular plate in any orientation, a cubic equation of which the roots give the three fundamental frequencies: compressional vibrations parallel to l and b, and a shearing mode. His theory does not include flexural vibrations and coupling between modes, but his experimental results reveal the presence of these effects, for various cuts. They show a general agreement with the work of Mason mentioned above.

350. *Unsymmetrical Effects with Lengthwise Vibrations.* From Figs. 31 (curve C), 33 (curve C), and 38, it is clear that in quartz Young's modulus $Y = 1/s'_{33}$ varies greatly with orientation. For any given polar angle θ except 0° and $\pm 90°$, Y varies with the azimuth φ. For all values of φ, Y varies with θ. In particular, in the YZ-plane, $Y(10^{-10})$ varies from 130.2 at $\theta = 48°36'$ to 70.3 at $\theta = -71°4'$.

* Among other papers in which the gap effect in bars is treated are those by Koga,[268] Watanabe,[581] and Grossmann and Wien,[189] but the data are either insufficient or taken with the crystal in the generating circuit. Results obtained by the latter method are not characteristic of the crystal alone.

† For a critical study of Petrzilka's values see Lonn[319] and Ekstein.[131]

‡ See also Scheibe, ref. B45, p. 92, and Giebe and Blechschmidt, ref. 161.

Through the combined effects of the fundamental elastic constants that occur in Eq. (55) for Young's modulus,* the wave pattern for lengthwise vibrations is such that, at the fundamental frequency, the nodal plane crosses the center of the bar at right angles only when the bar is very narrow or, if it has an appreciable breadth b, only when the length lies in the direction of maximum or minimum Y. In a broad plate the nodal line, revealed for example by lycopodium powder, may make a very pronounced angle with the b-direction. Meissner, who first observed this effect,[361] found that in an X-cut circular disk there were two directions along which compressional waves were propagated. These directions made angles $\theta = 48°$ and $-71°$, corresponding to the directions of maximum and minimum Young's modulus. In a rectangular plate with length in the direction $\theta = -71°$ Straubel[488] found the nodal line to be parallel to the breadth.

It is only when the length of the plate is parallel to the direction of maximum or minimum Y that the amplitude of vibration is the same at all portions of the end faces. This fact was ascertained by Meissner[359] by means of lycopodium powder, and by Bücks and Müller,[79] who made a vibrational survey of X-surfaces of plates both with length parallel to Y and at $\theta = -71°$, by observing under a microscope the movements of small specks on the silvered quartz.†

The asymmetry in the wave pattern is further revealed by another effect discovered by Meissner[359] and by Tawil.[506] This effect is an *air blast* directed outward from certain regions at the boundary of the plate, chiefly at the ends. The simple harmonic motion at the ends has a rectifying effect on the air molecules, drawing them in tangentially when the end surfaces recede and expelling them normally when the same surfaces advance—an effect already known in hydrodynamics. Meissner found the blast strong enough to blow out a candle and turn a pinwheel. The air blasts have been discussed further by Bücks and Müller,[79] Harding and White,[204] Hight,[225] Straubel,[485] Wachsmuth and Auer,[577] and Wright and Stuart.[594] Some very interesting photographs are shown in Straubel's paper.

* The constant chiefly responsible for the obliquity of the nodal plane is s_{44}. It tends to produce a contour shear mode, as described in §359. The 18.5° cut mentioned in §357 was designed to eliminate this shear mode.

† The microscopic method has been employed in this laboratory by G. W. Scott, Jr. (distinction thesis, 1934), R. L. Brown (M. A. thesis, 1936) and R. I. Hulsizer (M. A. thesis, 1942). The latter measured the vibrational directions and amplitudes at a large number of points, thus finding the distribution of strain and of piezoelectric polarization. From the integrated polarization a value of the electric current was derived, of the same order of magnitude as the observed value. He used X-cut plates with $\theta = 0°$ and $-71°$, also a GT-cut, recording especially the evidences of coupling between different vibrational modes.

The air blast issues symmetrically from the ends of the plate only when the length is in the direction of maximum or minimum Young's modulus. Otherwise, and especially when l is parallel to the Y-axis and of about the same magnitude as b, the blast is very unsymmetrical, as indicated by Fig. 84.

In order to demonstrate the effect of these unsymmetrical air currents Meissner[359] constructed a "quartz motor," consisting of a plate like that shown in Fig. 84, pivoted at the center so as to rotate in its own plane. A similar device is described by Tawil.[506] In this connection may be mentioned the rotation of a quartz sphere 4 cm in diameter observed by Van Dyke.[548,549,556] The sphere rested on the periphery of a 3-mm hole in a brass plate, which served as the lower electrode. When excited at the frequencies of certain vibrational modes, the sphere turned so as to select

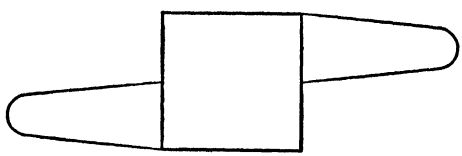


FIG. 84.—Air blasts from an X-cut quartz plate.

a vertical axis about which it then rotated. Since the effect took place also in vacuum, it must have been due to a frictional creeping where the quartz touched the brass. This fact, together with Gramont's observation[181] that a plate mounted according to Meissner rotated better in vacuum than in air, indicates that Meissner's rotation was due at least in part to a periodic frictional effect at the pivot rather than to reaction from the air. Gramont describes still other forms of quartz motor.

Van Dyke[549] found that his quartz sphere could also be made to slide along a straight track or to travel continuously along a circular track. These motions were due chiefly to reaction from the surrounding air. He found the principal resonant frequencies to be in the ratios 1, 1.47, 1.61, 1.83, 2.12, 2.18, 4.12, where the lowest frequency was approximately that of a bar parallel to Y with length equal to the diameter of the sphere, having a wave constant $H \approx 2{,}780$ kc sec^{-1} mm. At reduced pressures he observed and photographed characteristic luminous patterns (§365) at the various frequencies, and made a motion-picture record of the changes in pattern as the frequency was varied.

The rotational and translational effects mentioned above are doubtless related to the tendency of an X-cut quartz plate, whether in lengthwise or thickness vibration, to slide in one direction or another on the horizontal surface on which it rests. A motion of this sort was noted in unpublished observations by the author as early as 1923; in some cases at

a critical frequency the quartz slid completely out from the space between the fixed electrodes. Many others have since then observed the effect.*

This ease in sliding on the part of a vibrating quartz plate points to a decrease in friction (§364) between the crystal and other surfaces in contact with it.

Hirschhorn† observed a motion of translation in an X-cut quartz bar suspended by a thread between electrodes. Here it was not a question of friction against a solid surface; it is not certain how much of the effect was due to the piezoelectric field surrounding the crystal and how much to the effort of the quartz, like any other dielectric, to move into the strong part of the field between the electrodes.

Instead of observing the air-blast given off from a vibrating crystal, N. H. Williams,[587] used the opposite procedure: he set a quartz bar into vibration by means of the ultrasonic air waves from a jet of air through a nozzle. The ultrasonic "noise" excited many overtones as well as the fundamental vibration in a bar with length parallel to Y. Short electrodes and also multiple electrodes like those described in §239 were connected to an amplifier.

II. PIEZOELECTRIC EXCITATION OF THICKNESS VIBRATIONS

351. Vibrations of at least one of the three types described in §§66, 93, and 245 can be excited in a quartz plate in any orientation. In a Z-cut the field must be applied edgewise, parallel to X or Y, the strains being $y_s = d_{14}E_x$ or $z_x = d_{25}E_y$. Such vibrations in a Z-cut have been observed by Atanasoff and Hart.[12] For all other orientations the field can be parallel to the thickness. Equation (344) for the effective piezoelectric constant ϵ (applicable when the field is parallel to the thickness), when specialized for quartz, becomes

$$\epsilon = \alpha(e_{11}l^2 + e_{26}m^2 + e_{25}mn) + \beta[e_{14}nl + (e_{12} + e_{26})lm] + \gamma(e_{14} + e_{25})lm \tag{478}$$

When $m = n = 0$, we have an X-cut with $\alpha = 1$ (compressional mode parallel to X), and $\epsilon = e_{11}$. When $l = n = 0$, the plate is a Y-cut, with $\alpha = 1$ (vibration direction parallel to X, hence a shear mode[98]), and $\epsilon = e_{26} = -e_{11}$. A Z-cut corresponds to $l = m = 0$, in which case $\epsilon = 0$, showing that thickness vibrations cannot be generated with the field in the thickness direction.

The effective stiffness is given by Eq. (355). For the clamped dielectric constant we have, in the XY-plane, from Eq. (474), $k''_{\perp} = 4.41$ and, from Eq. (472), parallel to Z, $k''_{\parallel} = k_{\parallel} = 4.6$. When the field is oblique, in the N-direction, the rotated k''_N is calculated from an equation similar

* See, for example, Shaw's observations.[461]

† S. I. Hirschhorn, *Z. Physik*, vol. 44, pp. 223–225, 1927.

to Eq. (474c),

$$k_N'' = 4.41 + 0.19 \cos^2 \theta \tag{479}$$

where θ is the angle between N and Z.

352. Some Experimental Results with Thickness Vibrations. With bars in lengthwise vibration it is not difficult, by proper dimensioning, to avoid coupling with other modes. Modes of lower frequency (flexural or torsional) are usually not troublesome, while all others have too high frequencies to introduce undesired resonances. The situation is very different with thickness vibrations, since even with careful dimensioning of the contour it is difficult to avoid coupling with *overtones* of various l-f modes. This fact is notoriously true of the X-cut.

The elimination of disturbing frequencies is the most difficult problem in the design and construction of thickness-mode resonators. The

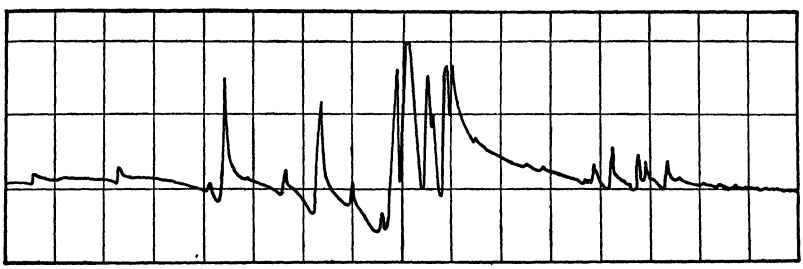


FIG. 85.—Resonance curve for an X-cut 1,500 kc/sec quartz plate in thickness vibration, from Bechmann,[37] showing many resonant frequencies over a range of about 30 kc/sec.

undesired modes, if close to that for which the resonator is designed, can cause serious disagreement between theoretical and experimental values of frequency and its temperature coefficient. By accurate lapping, dimensioning, and edge grinding it is possible to obtain a strong response frequency, corresponding to a vibrational mode that is sufficiently removed from adjacent modes so that it will control the frequency of an oscillator over the desired range of temperature (see §244). The oblique cuts that are most used on account of their low temperature coefficients of frequency are also largely free from the coupling effects that are responsible for the disturbing frequencies.

An example of the complicated frequency spectrum encountered with an X-cut plate is seen in Fig. 85.

The X-cut was first used for thickness vibrations by Pierce. The strain equation is $x_x = d_{11}E_x$. When tested as a resonator, it usually has a large number of response frequencies, strong and weak, in the neighborhood of the calculated value. As an oscillator it selects some one of these frequencies but tends on slight provocation to shift to a

different frequency. By any one of the methods described in §366 it can, when vibrating at any resonant frequency, be shown to have a very complicated wave pattern, due to coupling with overtones of modes of lower frequency. Thus, while the mode of vibration is nominally compressional, many parts of the surface have vibration directions with tangential components; and they may also be out of phase with the true compressional vibration. Nevertheless, as a whole the motion of the major faces is in the direction of the thickness. It is for this reason that X-cuts are usually employed as ultrasonic emitters. Owing to the disadvantages just mentioned and to their larger temperature coefficient of frequency, X-cuts are now but little used in piezo oscillators. The value of α_f is usually given as between $-20(10^{-6})$ and $-22(10^{-6})$.

When there is a gap between an X-cut quartz plate and either electrode, stationary air waves are produced when the gap is an integral multiple of the acoustic half wavelength. This effect is the basis of the ultrasonic interferometer (§510). The influence of the gap on the performance of resonators has been investigated by Dye,[127] Koga,[268] Vigoureux,[B50,B51] and others. The loss of energy at the critical gap values is serious, and the coupling of the crystal to the air waves reacts on the frequency. This dynamic effect of the air gap of course vanishes in vacuum mountings. It has nothing to do with the characteristic effect of gap on frequency discussed below.

For a *Y-cut* with the field parallel to Y, the strain equation is

$$x_y = d_{26}E_y = -d_{11}E_y$$

In a relatively thin plate the vibration direction is parallel to X, and the vibration is of the shear type.[98] Since there is little or no motion normal to the surface, the plate (as with all shear-type plates) can be more firmly clamped than an X-cut without stopping the vibration.* For the same reason there is less trouble from stationary air waves in the gap. Clamping also helps eliminate coupled vibrations of the type $z_x = d_{25}E_2$. Still, as with the X-cut, troublesome couplings are present, and the plate when used as an oscillator tends to jump from one frequency to another closely adjacent. Moreover, the temperature coefficient of frequency is even greater than for the X-cut; values have been observed from $+60$ to $+90(10^{-6})$, depending on dimensions and coupling with other modes.

It was this large temperature coefficient which led several investigators to experiment with *oblique* cuts, culminating in cuts of the types

* Using the interferometer method described in §313, Straubel[490] found that there was a slight movement normal to the surface of a Y-cut plate in thickness vibration. This effect was presumably due to coupling with other modes, which it should be possible to eliminate by proper dimensioning.

described in §§357 following. Like the Y-cut, these newer cuts vibrate in a shear mode. Oblique cuts now in common use have almost exactly constant frequency over a considerable range of temperature, while at the same time the coupling effects are reduced.

353. *Effect of the Gap Width on Frequency.* One method for varying the frequency of a piezo oscillator is to vary the gap. A variation of a few tenths of 1 per cent can thus be brought about, most of which takes place while the gap is very small. Equation (370) shows that an approximately linear relation should hold between the relative change in frequency and $w/(e + k''w)$, the coefficient U being a constant. The author's experiments[107,*] indicate that, as in the case of the lengthwise vibrations mentioned above, U decreases as the gap increases. The departure of U from the theoretical value appears to be least with plates which are good resonators and with those which are relatively free from coupling, as, for example, the BT- and AC-cuts; for these cuts almost the exact theoretical value was found at small gaps, although at large gaps the discrepancy amounted to as much as 30 per cent. The observed U was far below the theoretical value for the two X-cut plates employed, both of which were rather poor resonators. For Y-cut plates the deficiency in U was of the order of 20 per cent.

In Eq. (355) it is seen that three terms are necessary in general to express the effective stiffness for thickness vibrations. As an illustration of the relative magnitudes of these terms we may consider the Y-cut, for which it is shown in §351 that $\epsilon = -e_{11} = -5.2(10^4)$, while from Eq. (474) $k'' = 4.41$. The isagric stiffness coefficient is

$$q^E = c_{66}^E \approx 40(10^{10})$$

Hence, for zero gap Eq. (355) becomes, for a Y-cut plate,

$$q' = \left(40 + 0.77 - \frac{0.62}{h^2}\right) 10^{10}$$

The second term is here 1.9 per cent of q^E. At the fundamental frequency, $h = 1$, and the third term is 1.5 per cent of q^E. At the fifth "harmonic," $h = 5$, and the third term is only 0.06 per cent of q^E.

The presence of a gap decreases the third term, which vanishes at infinite gap.

It was pointed out in §250 in connection with Eqs. (350) and (350a) that, as the order h of the overtones of thickness vibrations increases, the theoretical relation between the overtone frequencies becomes

* Further data were also obtained by Booth and Dixon,[70] Dye,[127] Koga,[268,274,276] Matsumura and Hatakeyama,[344] Namba and Matsumura,[388] and Vigoureux.[B51] As far as they go, they corroborate the present statements.

more nearly harmonic. This has been confirmed in the case of quartz by Atanasoff and Hart (§90) and also by Bergmann.[52]

For thickness vibrations in special cuts see §358. The use of thickness vibrations in ultrasonics is described in §507.

III. PIEZOELECTRIC EXCITATION OF FLEXURAL VIBRATIONS

354. According to §179, a state of flexure can be produced by applying an electric field in such a way as to cause the portion *ABFE* of the bar shown in Fig. 86 to expand in the direction *AB* while the portion *EFCD* contracts. The same result is reached by applying fields to the right and left portions of the bar so as to cause opposite *shears* in *AGHD* and *GBCH*. In either case, if the field alternates with the proper frequency, flexural vibrations result.

With suitable arrangements of electrodes, overtone frequencies can also be excited. For example, Fig. 87 shows the state of deformation

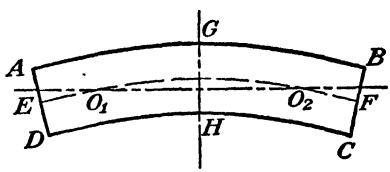


FIG. 86.—First flexural mode. The nodes O_1 and O_2 are 0.224 of the length from each end.

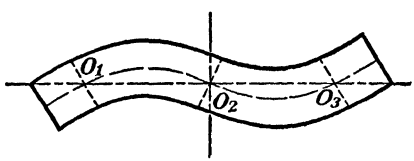


FIG. 87.—Second flexural mode. Node O_2 is at the center. Nodes O_1 and O_3 are 0.132 of the length from each end.

for the second mode (first overtone), in which, instead of two nodes O_1 and O_2 as in Fig. 86, there are three nodes O_1, O_2, O_3. However many nodes there may be, the extensional strain at any instant has the same sign in either half of the bar (lower or upper in the figure) from one *node* to the next, while the shear has the same sign from one *loop* to the next. At the ends, the extension has the same sign as the adjacent interval between nodes. Appreciation of these facts is essential in the proper placing of electrodes.

For best results the bar should be supported at one or more nodes. It will respond as a resonator even if the field is applied to only a small part of the bar, as long as this part lies entirely, or chiefly, in a region where the instantaneous strain has the same sign. For an oscillator the electrodes, preferably plated, must of course be relatively large, and for very low decrement the bar should be mounted in vacuum, since the loss of energy to the surrounding air is considerable.

With quartz crystals both constants $d_{11}(= -d_{12} = -d_{26})$ and $d_{14}(= -d_{25})$ can be used in obtaining the extensional or shearing stresses needed for exciting flexural vibrations. An even greater choice of excitations is possible when the bar or plate is cut obliquely. An idea of the

different possibilities can be gained from Fig. 88. Electrodes of opposite sign are distinguished by heavy and light lines. Electrodes of the same sign are usually connected in parallel. Field directions are indicated by arrows. The end view in each case shows the cross section in the form of a square, with the thickness e equal to the breadth b. *The plane of flexure, in which vibration takes place, is always le.* The greater the ratio

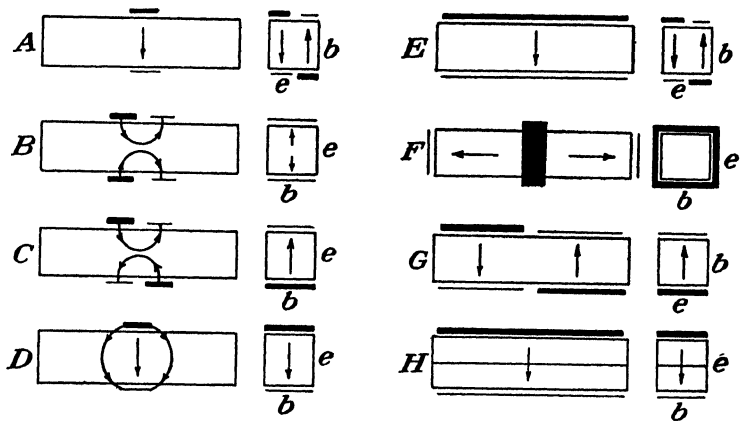


FIG. 88.—Locations of electrodes for exciting flexural vibrations. In the elongated rectangles motion takes place in the plane of the paper in all cases except A, E, and G, where it is perpendicular to the paper.

l/e, the lower the frequency. The breadth b has no appreciable effect on the frequency. Experiment shows that flexural vibrations can still be obtained even when e is as great as l, although when e is relatively large a special form of theory is required, as indicated in §73. From the figure and Table XXVII it is evident that in some cases the same bar or plate can be used for flexure in more than one plane, according to the

TABLE XXVII

Fig.	Direction of length	Direction of field	Plane of flexure	Number of nodes	Strain equation
A	Y	X	YZ	Even	$y_y = d_{12}E_x$
B	Y	X	XY	Odd	$y_y = d_{12}E_x$
C	X	X	ZX or XY	Even	$x_x = d_{11}E_x$
D	X	X	XY	Odd	$x_x = d_{11}E_x$
E	Y	X	YZ	2	$y_y = d_{12}E_x$
F	Y	Y	XY	2	$x_y = d_{26}E_y$
G	X or Z	Y	ZX	2	$z_x = d_{25}E_y$
	Y or Z	X	YZ	2	$y_z = d_{14}E_x$
H	Y	X	YZ	2	$y_y = d_{12}E_x$

arrangement of the electrodes. The nature of the piezoelectric excitation in each case is shown in this table.

In Fig. 88, *A*, *B*, *C*, and *D* represent resonators described by Giebe and Scheibe.[166–170] The electrodes are very short, in order to show the luminous effect at resonance in various overtones when the resonators are used as frequency standards. The field parallel to *X* needed for excitation in *B*, *C*, and *D* is the *X*-component of the stray field indicated by the curved arrows. Such excitation is necessarily weak.

E is Harrison's arrangement,[205] which is similar to Giebe and Scheibe's device *A* and was discovered independently and published in the same year. Harrison used two pairs of full-length electrodes for more efficient excitation of the first flexural mode. By using four pairs of electrodes (each set of two pairs covering approximately half the length of the resonator), he excited the second mode. When observing the first mode at reduced air pressure he found a series of luminous striations crossing the exposed surface of the bar near the center (see also Harrison and Hooper[208]).

F and *G* in Fig. 88 represent modes that have been observed by the author. They include flexure in all three principal planes. As may be seen from Table XXVII these arrangements make use of the shearing piezoelectric effect rather than compression. In *F* the central electrode is a girdle surrounding the bar, and from it the field in the quartz extends in both directions to electrodes (connected in parallel) opposite the ends. While this excitation is comparatively weak, that in *G* is much stronger, since the field is normal to the plane of flexure instead of parallel to the length of the bar.

Figure 88*H* represents a "Curie strip," consisting of two *X*-cut quartz plates cemented together with polarities opposing. When the field E_x is applied, one plate expands lengthwise while the other contracts. The resonator vibrates flexurally as a unit. With two plates, each 4 by 1 by 0.05 cm, cemented with Canada balsam, the author in 1927 found resonance at a frequency of about 400 cycles/sec. Resonance was indicated by lycopodium powder, by an audible note, and by response in the anode circuit of a tube to the input of which the resonator was connected. The use of the Curie strip in a piezo oscillator is mentioned in §396. The static theory is treated by Voigt.*

355. The excitation of flexural vibrations of low frequency is most efficient when the field is parallel to the thickness *e*, since this is the dimension which must be made small if the frequency is to be low. The breadth *b* can then be made large, permitting the use of electrodes of large area. This case can be realized by a modification of Fig. 88*C*, as illustrated in Fig. 89. The driving field is no longer the stray field parallel to *X*, but

* "Lehrbuch," p. 906.

the relatively strong field parallel to Y. Each half of the plate is subject to a shearing stress $X_y = -e_{26}E_y$; and since these stresses have opposite signs, a state of flexure results. With $l = 7.4$ cm, $e = 0.1$ cm, $b = 2$ cm, the author has observed a resonant frequency of 1,050 cycles/sec. This seems to be the lowest recorded frequency for a bar of uniform cross section with the field in the thickness direction. Still lower frequencies were obtained by Gruetzmacher,[191] but in his resonator the quartz was left very thick at the ends, having the form of a thin strip only in the central portion. This was therefore not a "bar" in the ordinary sense.

With the cut shown in Fig. 89, *even* modes of flexural vibration can be excited by full-sized electrodes covering the entire *lb*-faces. This is because the bar is then divided into an *odd* number of segments, sheared alternately in opposite senses.

Flexural quartz resonators can be used for controlling the frequency in a piezo-oscillator circuit. For example, a circuit like that in Fig. 99 was made to oscillate at crystal frequency with the Y-cut 1,050-cycle bar described above.

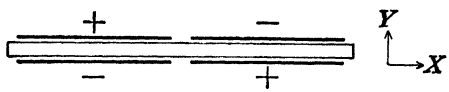


FIG. 89.—Y-cut quartz plate for low-frequency flexural vibrations. The length l is parallel to X, and the thickness e is parallel to Y. The plane of flexure is XY.

The same principles that have been described for quartz can, of course, be applied to other piezoelectric crystals. As long as the ratio l/e is large, frequencies can be calculated by Eq. (128).

References on flexure and flexural vibrations are given at the end of the chapter. Some of the applications are treated in §§368 and 396. Theory and application of static flexure are considered by Voigt* and by Voigt and Fréedericksz;[576] vibrational theory will be found in the papers by Doerffler,[124] Mason,[333] Thomson,[518] and Tykocinski-Tykociner and Woodruff.[537]

Flexural resonators have been proposed by Giebe and Scheibe [B45] as standards of frequency from 1 to 20 kc.

IV. PIEZOELECTRIC EXCITATION OF TORSIONAL VIBRATIONS

356. According to §180, the torsion of a cylinder or prism involves opposite shears on opposite sides of the axis, the plane of shear containing the axial direction. In quartz, torsional vibrations have been produced with the axis of the specimen parallel to X, Y, or Z. Oblique directions could, of course, also be chosen. The same arrangements of electrodes may be used as in Fig. 88; we can therefore indicate the methods of excitation by reference to that figure and Table XXVIII.

* "Lehrbuch," 1928 ed., p. 965; also ref. 573.

TABLE XXVIII

Method	Fig. 88	Direction of length	Direction of field	Number of nodes	Strain Equation
I	*A*	*X*	*Y*	Odd	$x_y = d_{26}E_y$
II	*A*	*Y*	*Y*	Even	$x_y = d_{26}E_y$
III	*C*	*Y*	*Y*	Odd	$x_y = d_{26}E_y$
IV	*F*	*Z*	*X* and *Y*	Odd	$\begin{cases} y_z = d_{14}E_x \\ z_x = d_{25}E_y \end{cases}$
V	*F*	*Y*	*X*	Odd	$y_z = d_{14}E_x$
VI	*F*	*X*	*Y*	Odd	$z_x = d_{25}E_y$

Methods I, II, and III were devised by Giebe and Scheibe.[169]* In method II it is the stray fields extending to right and left along the length of the bar (parallel to *Y*) that are effective.

Method IV is described by Hund and Wright,[242] who used a circular cylinder with length parallel to *Z*. The field entering the quartz from the girdling electrode had components $\pm E_x$ and $\pm E_y$, which produced in the adjacent regions the shears requisite for torsion. In some of their experiments they used, in place of electrodes at the ends, girdles surrounding the cylinder spaced at a certain distance from the center.

Method V was realized experimentally in this laboratory in 1931. The piezoelectric excitation is due to the component of field parallel to *X* entering the bar from the girdling electrode on opposite sides in opposite directions, according to $y_z = d_{14}E_x$. Instead of a girdling electrode, two small plane electrodes could be used, one at each end of the *X*-axis. Evidence of the torsional mode was provided, not only by agreement between observed and calculated frequencies, but also by the fact that fine sand sprinkled on the vibrating bar formed a lengthwise nodal line along the center.

Method VI, which has not yet been tried, is similar to method V.

Of all the methods for producing torsional vibrations in a bar, the most effective is method I in Table XXVIII, especially if the electrodes extend the full length of the bar, as in Fig. 88*E*. If the bar has a rectangular cross section, the field should be parallel to the smallest dimension *e* (the field direction is shown parallel to *b* in Fig. 88*E*). In order that this arrangement shall produce torsion, the crystal cut must be such that the field parallel to *e* will cause a shear in the *el*-plane with respect to axes parallel to *e* and *l*. With quartz, oblique cuts (the possibilities of which have not yet been explored) being excluded, the only torsional excitation by this method is with the length *l* parallel to *X*. In a crystal such as Rochelle salt, in which d_{14}, d_{25}, and d_{36} are all present, torsional

* See also Giebe and Blechschmidt.[162] In the latter paper the theory is discussed as well as the effect of temperature on frequency.

vibrations should be very efficiently producible in a bar with two pairs of electrodes as described above, the length of the bar being parallel to one of the crystal axes and the breadth and thickness making angles of 45° with the other two axes.

Any bar cut so that it responded torsionally with electrodes divided along the length, as in Fig. 88*E*, would also respond flexurally if the electrodes were divided transversely as in Fig. 88*G*.

Method I has been applied by Giebe and Scheibe to circular cylinders. As a more efficient means of excitation they employed four concave electrodes running parallel to the axis. An analogous arrangement for a rectangular bar is described by Giebe and Blechschmidt.[162]

Experiments with hollow quartz cylinders (axes parallel to *Z*) have been described by Tawil, by Tsi-Ze and Tsien, and by Zacek and Petrzilka, using a combination of inner and outer electrodes. It was in the course of these experiments that Tawil observed an effect which he attributed to "strephoelectricity," later shown by Langevin and Solomon to be completely explained in terms of d_{14}. Tsi-Ze and his associates also used their resonator as an oscillator in a Pierce circuit. Experiments on various modes of vibration of quartz cylinders, both solid and hollow, are described by Benoit; the cylinders were used in piezo-oscillator circuits.

Torsional resonators may be supported at a node or nodes, or, according to Giebe and Blechschmidt,[162] the bar or cylinder may be held by a pointed rod at each end, fitting into a small conical cavity at the center of the section. As with flexural resonators, it is not always necessary to provide the full quota of electrodes or to place them exactly as shown in Fig. 88. Local excitation over any region where the strain is all of the same nature should be enough to produce a response, although in some cases a strong alternating field may be required.

General formulas for the calculation of frequency are given in §74. Special formulas for quartz will be found in Giebe and Blechschmidt.[162]

357. Quartz Resonators of Special Cuts and Shapes. The resonators now to be described were designed to reduce the effect of temperature on frequency or to reduce coupling with undesired vibrational modes. In some cases both aims can be attained satisfactorily in the same device. Out of the large number of solutions of the problem, the choice of resonator depends on the frequency, the capacitance ratio, the extent to which the effective piezoelectric constant is diminished by rotation, the tolerance with respect to temperature effects, and the use to which the resonator is to be put—frequency standard, power oscillator, filter, etc.

Temperature changes affect the frequency, not only by causing small alterations in density and dimensions of the resonator, but also, and chiefly, by changing the values of the various elastic constants that determine the vibration. All the quartz compliance constants of type

L or S in Fig. 15, except s_{66}, have positive temperature coefficients, while the cross constants s_{12} and s_{13} have negative coefficients. By the use of oblique cuts, for which the effective elastic constants are certain functions of the fundamental ones, and in some cases by taking advantage also of the coupling between different modes, it is possible to have negative and positive temperature coefficients neutralize one another in such a way as to reduce the effective coefficient to zero. This reduction can be accomplished in many ways, for various vibrational modes and various ranges of frequency.

Unfortunately, the various temperature coefficients present in the frequency formulas usually lead to an expression for the temperature coefficient of frequency containing the square and higher powers of the temperature difference. As a consequence, the temperature coefficient can, by varying the orientation, be made strictly zero only at one particular frequency, if at all. It is only by finding an orientation such that the coefficient of the square term vanishes (terms of higher order being relatively small) that the frequency can be made practically independent of temperature over a considerable range of temperatures. This end has been attained in the GT-cut mentioned below.

We use the abbreviation α for temperature coefficient, with a designating subscript when necessary. Thus the temperature coefficient of s_{11} may be written $\alpha_{s_{11}} = (1/s_{11})\ \partial s_{11}/\partial t$, or that of frequency $\alpha_f = (1/f)\ \partial f/\partial t$ s_{11} and f being taken at some standard temperature. The curve relating f to t can be expressed by an equation that usually contains both the first and higher powers of t. $\alpha_f = 0$ wherever the curve is parallel to the axis of temperatures. If the flat portion of the curve is narrow, it may be necessary for sufficiently constant frequency outside a very small temperature range to use a thermostat. The broader the flat portion, the less important is thermostatic control.

Both the original X-cut and the Y-cut that began to compete with it about 1927 have large temperature coefficients and give much trouble from the tendency to jump from one frequency to another. The era of resonators with low α_f began in 1929. In that year Marrison[330] described a piezo oscillator of high precision containing a Y-cut ring-shaped crystal vibrating at 100 kc, with $\alpha_f < 10^{-6}$. The use of a ring had already been introduced by Giebe.[160,167,168]

Essen[137,138,139] later used a quartz ring as a frequency standard, his ring having its axis parallel to Z. A compressional circumferential mode was used, with three complete wavelengths spaced around the mean circumference. A proper ratio of inner to outer diameter reduced α_f to 10^{-6} or less over a range of 30°C. The frequency was 100 kc.

It was also in 1929 that Lack[298] described a specially dimensioned Y-cut devised by R. A. Heising, in which the shear mode with its positive

α_f was coupled to a flexural overtone mode with negative α_f in such a way as to give a zero coefficient at a certain temperature.

In 1932 and 1933 Matsumura and Kanzaki[351,352] showed that a value of α_f approaching zero for lengthwise vibrations in an X-cut bar could be reached by inclining the length l of the bar at the angle $\varphi = -20°$ to the Y-axis and at the same time giving the ratio b/l an optimal value of about 0.5. Their critical angle $\varphi = -20°$ corresponds to $\theta = +110°$ for $1/s'_{33}$ in curve C, Fig. 31, or to $\theta = +20°$ for $1/s'_{22}$ in curve B; it is practically the angle for minimal Young's modulus. This angle is so close to that for the so-called 18.5° cut that they may be credited with having first appreciated the advantage of this cut.

The 18.5° cut was first described in 1934 by Mason.[332,340] It is an X-cut rectangular plate with length making an angle of 18.5° with the Y-axis, this angle being measured in the direction from $+Y$ toward $+Z$, as shown in Fig. 92. At this angle the coupling between the lengthwise and shear modes (§349), which would otherwise be troublesome in a plate that did not have a very small b/l ratio, disappears.* The b/l ratio chosen for use as a filter is not such as to make α_f approach zero. The plate vibrates in a compressional mode parallel to one of the longer dimensions.

Somewhat similar characteristics are possessed by Mason's −5° plate,[343] illustrated in Fig. 92. Of all the series of X-cut bars with lengths in the YZ-plane it has the lowest temperature coefficient of frequency. This fact, together with its low C_1/C ratio and the fact that it can serve either as a lengthwise or flexural resonator, makes it useful as a filter crystal.

All the resonators so far described are for relatively low frequencies, of the order of 60 to 200 kc.

358. In the development of resonators for higher frequencies, for which thickness vibrations are used, notable innovations were made in 1934. By one of the coincidences that are so frequent in scientific and technological history, there appeared independently, from four widely separated sources, papers on the temperature characteristics of thickness vibrations in quartz plates containing the X-axis, the normals to the plates

* The angles +18.5° and −5° for these two cuts are expressed in conformity with the rule stated in §51 for rotation about a single axis. In the earlier publications of the Bell Laboratories they were given as −18.5° and +5°. The signs of θ for the AT-, BT-, CT-, DT-, GT-, MT-, and NT-cuts, as given in this book, likewise conform to §51.

The nature of the coupling mentioned above is indicated by the expression $y'_y = -s'_{24}Y'_x$, the length, breadth, and thickness of the plate being parallel, respectively, to Y', Z', and X. The compliance s'_{24}, which represents the coupling between the y'_y- and y'_x-strains, contains s_{44} as a chief constituent. It is the vanishing of s'_{24} at 18.5° (see curve L in Fig. 31) that characterizes this cut.

lying in the YZ-plane at various angles θ with the Y-axis.* All these investigators—Koga[272] in Japan, Bechmann[32] and Straubel[491,492,493] in Germany, and Lack, Willard and Fair[299] in New York—showed that $\alpha_f = 0$ when θ is approximately $-35°$ or $+49°$ (see Fig. 92).

Previously to his work cited above, Koga[270] had experimented with his R- and R'-cuts in thickness vibration. These cuts are parallel to the R- and r-faces of the crystal (Fig. 76) and are not very far removed from the AT- and BT-orientations mentioned below. Bechmann considered the effect of the b/l ratio on α_f; he also found that α_f had a zero value for X-cuts rotated about the Y-axis by an angle somewhere between 50 and 70°. Lack, Willard, and Fair investigated the discontinuities in frequency of thickness vibrations in a Y-cut with changing temperature. They found the discontinuities to be due to coupling between the x_y-strain, which is the essential one for thickness vibrations in this cut, and overtones of the z_x-strain. The stress-equation is $-X_y = c_{66}x_y + c_{56}z_x$, c_{56} being a measure of the coupling. When the plate is rotated about X by the angle θ, the expression becomes $-X'_y = c'_{66}x'_y + c'_{56}z'_x$. Lack, Willard, and Fair found that when $\theta = -31°$ or $+60°$ the coefficient c'_{56} vanishes. Plates of these orientations vibrate in a very pure x'_y-shear mode free from anomalies as the temperature changes. Owing to the freedom from parasitic vibrations, local stresses are reduced to a minimum, so that higher voltages can be applied without danger of fracture. Lack, Willard, and Fair called these cuts the AC and BC, respectively.

Although the temperature coefficients of the AC- and BC-cuts are low, they do not vanish. At $\theta = -35°15'$, however, α_f vanishes at 45°C, changing from negative to positive at this temperature (see Fig. 90). Following Lack, Willard, and Fair, this is now commonly called the *AT-cut* (see Fig. 92). At $\theta = +49°$, α_f vanishes when the temperature is 25°C, changing from positive to negative at this temperature (the *BT-cut.*) The AT and BT have orientations so close to those of the AC and BC that they partake of the advantages of the latter to a large extent and are commonly used.

All four of the cuts just mentioned are examples of "rotated Y-cuts" or "Y'-cuts." In each case the electric field is parallel to the thickness

* The symbol θ has been used very loosely in the literature, to signify rotation about any axis, in either sense, and measured from any fiducial direction according to some convention adopted, and not always clearly specified, by each individual writer. In this book we use θ for a single rotation about any one of the three crystallographic axes X, Y, or Z, according to the definition in §51. In the present discussion θ is the angle between the Y-axis and the normal to the plate, positive when the rotation is about the X-axis from $+Y$ toward $+Z$. For the most general rotation, in which three angles must be specified, we use φ, Θ, and ψ, where Θ is the angle about the Y_1-axis in §52. The conventions used by various writers are shown in a comparative table in ref. 110.

and makes the angle θ with the Y-axis. The axes of the rotated plate are X, Y', and Z', with Y' parallel to the thickness and X and Z' parallel to l and b (or b and l). The effective piezoelectric constant ϵ of §246 becomes e'_{26} [Eq. (221)], and the driving stress is $X'_y = -e'_{26}E'_2$, where E'_2 is the instantaneous driving field. With increasing θ, e'_{26} diminishes; hence the capacitance ratio, given by the reciprocal of Eq. (414), also diminishes.

The AT-cut has a higher capacitance ratio than the BT-cut (normal to the surface is closer to the Y-axis, so that e'_{26} is greater), but the BT-cut has a higher frequency for the same thickness. Both the AT- and BT-cuts are subject to coupling between odd shear and even flexural modes in the XY'-plane.*

It is commonly found that plates are most active when their surfaces are plane or very slightly convex. The slightest concavity lowers the activity and makes the frequency spectrum more complex. As an example may be mentioned an experiment by Koga and Tatibana,[283] who explored the surface of a BT-cut in a piezo-oscillator circuit by having one of the electrodes of small size and moving it to various parts of the surface. Finding the frequency to be somewhat higher near the edges, they prepared a plate with a concave surface, hoping thereby to make all parts vibrate in more exact synchronism. The result was failure to oscillate at all.

359. Low-frequency Resonators in the Form of Broad Plates. Some of the types to be considered make use of compressional vibrations parallel to l or b, as in the case of thin rods. Other types involve shears in the plane of the plate, the frequency depending on both b and l. Such modes of vibration are often called "contour modes" or "face shear modes" (see §71). Owing to the large b/l ratio various coupling effects have to be considered.†

The CT- and DT-cuts, due to Hight and Willard,[227] are the l-f counterparts of the AT- and BT-cuts. The piezoelectric excitation is of the type $z'_x = d'_{25}E'_y$. The vibration is essentially of a shear mode in the

* By an "odd shear mode" is meant a thickness mode in which the major surfaces do not move to and fro as units in the X-direction but are divided into an odd number of segments, adjacent segments being joined by lines parallel to Z'. For example, the frequency might be that of three plates, each of dimensions b parallel to Z' and approximately $l/3$ in the X-direction. As with lengthwise vibrations of bars at odd harmonic frequencies (§238), these odd shear modes can be excited with electrodes covering the entire crystal, only in this case, since the frequency depends primarily on the thickness, the odd modes differ but little in frequency from the fundamental thickness shear. As to the "even flexural modes," they have been described in §355, where it was shown that they can be excited by full-sized electrodes. It is the similarity in strain distribution of these shear and flexural modes that accounts for the coupling between them. The coupling can be suppressed by suitable dimensioning.

† Various contour modes in Y-cut plates are discussed by Builder and Benson.[88]

plane of the plate, and the frequency depends on the contour (usually rectangular) rather than the thickness. The edge dimensions are parallel to X and Z'. The fundamental elastic equation is $z'_x = -s'_{55}Z'_x$. For the CT- and DT-cuts the angles θ for zero α_f are $-38°$ at 41°C and $+52°$ at 50°C respectively (see Table XXIX). These angles are within a few degrees of those for the AT- and BT-cuts. The CT-cut has a better capacitance ratio than the DT-cut and is usually preferred. Both cuts have good freedom from coupling with undesired modes; their frequencies are constant to within 1 part per million from 20 to 30°C.

The GT-cut. The most remarkable of the l-f cuts of low temperature coefficient is the GT-cut, introduced in 1940 by Mason.[336] Without thermostatic control the frequency remains constant within 1 ppm from 0 to 100°C. This cut may be thought of as a CT-cut with the angle θ (see explanation of Table XXIX) increased from $-38°$ to approximately $-51°$, followed by a rotation of the rectangular plate in its own plane until the edges make angles of $\pm 45°$ with the X- and Z'-axes. Its vibrational mode is best understood, however, by starting with a narrow Y-cut 45° bar, the length of which bisects the angle between the X- and Z-axes. The piezoelectric lengthwise strain is $z'_z = d'_{23}E_y$, analogous to the 45° Y-cut bar in Rochelle salt. The elastic equation is $z'_z = -s'_{33}Z'_z$. Since from Fig. 33 the s'_{33}-curve is symmetrical about the Z- and X-axes, the 45° angle may be taken in either sense. Such a bar has a negative α_f. If now the breadth b is progressively increased, the b-and l-compressional modes become more and more closely coupled. At the same time α_f diminishes in magnitude, becoming positive at sufficiently large b. Mason found, not only that there is a certain b/l ratio for which $\alpha_f = 0$, but that, at a certain value of θ, α_f remains approximately equal to zero over a very wide range of temperature. When $\theta = -51°7.5'$ and $b/l = 0.859$, the center of the flat region falls at 25°C. By edge grinding, both frequency and α_f can be adjusted independently, and by slight variation of θ the center of the flat portion of the frequency:temperature curve can be varied. A suitable value of thickness is chosen in order to avoid coupling with a flexural mode. In vacuum this cut has Q up to 330,000. It is used for frequency standards, filters, and receivers.

The MT- and NT-cuts of Mason and Sykes[343] are l-f rectangular plates used in filters and oscillators. Their orientations can be explained by considering first an X-cut plate with its *length* at an angle θ (see explanation of Table XXIX) $-8.5°$ from $+Y$. We may call the direction of length the Y'-axis, the breadth b being parallel to Z'. The plate is now to be rotated through an angle A about Y' so that the positive end of the Z'-axis moves toward $+X$. For the MT- and NT-cuts the angle A

has the values 40° and 50°, respectively.* These orientations permit the MT-cut to vibrate in its lengthwise mode, with low α_f, while the NT-cut has low α_f when vibrating flexurally, according to Harrison's arrangement shown in Fig. 88E. Depending on the dimensions, the MT-cut is used at frequencies from 50 to 100 kc/sec, and the NT-cut from 4 to 50 kc/sec. When the NT-cut is used as an oscillator, as for example in frequency modulation, at these low frequencies, a circuit similar to that in Fig. 99 is employed.

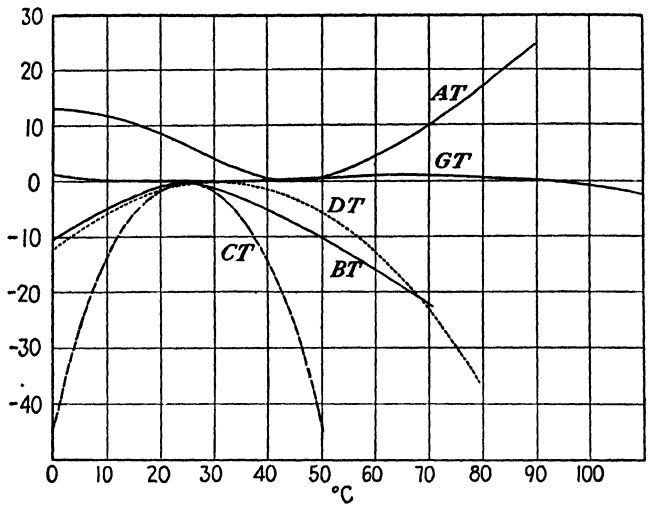


FIG. 90.—Dependence of the temperature coefficient α_f upon frequency, for some cuts of low α_f, from Mason, ref. 340. Ordinates are frequency changes in ppm.

Still other cuts of low temperature coefficient have been described, for example the ET- and FT-cuts of Hight, described by Mason,[337] and the YT-cut of Yoda,[595,596] which is similar to the BT-cut. Yoda states that he experimented with a plate so thin that its fundamental thickness mode gave a wavelength of only 4.7 m (64 megacycles/sec.).

The MT- and NT-cuts described above are examples of cuts obtained by a *general rotation*, in which the normal to the plate makes oblique angles with all three crystallographic axes. The general rotation has been treated by Bechmann[35] and Mason.[337] Further examples are the V-cuts of Bokovoy and Baldwin.† These are similar to the AT- and BT-cuts, but rotated 5° around the Z-axis.

* In their paper, Mason and Sykes describe the properties of the set of cuts that they call the "MT series," in which θ lies between 0° and −8.5° and A between 34° and 50°.

† S. A. BOKOVOY and C. F. BALDWIN, Australian patent 21,959, 1935, and British patent 457,342, 1936. See also Builder[80] and Baldwin and Bokovoy.[18]

The temperature coefficients of frequency of some of the more important cuts are shown in Fig. 90. For all cuts except the *GT* the coefficient vanishes or has a low value only when the temperature is held close to a certain value. For example, with the *AT*-cut this value* is 45°C. The *GT*-cut has a very low coefficient over the entire temperature range; *i.e.*, the second derivative of frequency with respect to temperature is nearly zero over the whole range.

360. *The Straubel Contour and Quartz Spheres.* A circular *X*-cut plate excited in compressional vibration along a diameter gives a complex frequency-spectrum. Straubel[484,486,488] conceived the idea of shaping an *X*-cut plate so that the radius in any direction in the plane of the plate is proportional to the square root of Young's modulus in that direction. The result is the contour illustrated in Fig. 91. A compressional wave starting at the center reaches all points on the circumference at the same instant. Such radial waves can be excited by electrodes covering the major surfaces in the usual way. Straubel found a single well-marked resonant frequency, free from disturbing modes; the lycopodium test (§366) showed a single nodal spot at the center. Even with thickness vibrations a plate of this shape is somewhat freer from multiple frequencies than round or rectangular plates.

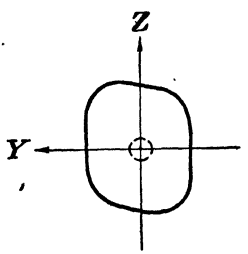


FIG. 91.—The Straubel contour.

Quartz spheres have been experimented with as resonators. The modern crystal gazer, instead of trying to divine the future, observes modes of vibration. We have already referred in §350 to the experiments of Van Dyke. Kamienski[250] has also examined various vibrational modes and measured the temperature coefficient of frequency. The modes are too complex and the labor in fashioning a sphere of quartz too great for this type of resonator to offer promise of practical applications.

361. Table XXIX gives the orientations of some typical cuts, together with the frequency constant *H*, the effective piezoelectric constant ϵ, and the frequency range within which each cut is commonly used. The data are taken chiefly from Mason[340] and Bond.[66] For the cuts from *AT* to *GT*, θ is the angle between the *Y*-axis and the normal to the plate, positive when measured from $+Y$ toward $+Z$; it is also the angle between the *Z*-axis and the *plane* of the plate, positive when laid off from $+Z$ toward $-Y$, as indicated in Fig. 92. For the *MT*-, *NT*-, 18.5°, and −5° cuts, θ is the angle between the *length* of the plate and the *Y*-axis, measured from $+Y$ toward $+Z$, as in Fig. 92.

The angles φ, Θ, and ψ in the table specify the orientations according to the I.R.E. convention, as explained in §52. With respect to the

* By a slight change in angle this critical temperature can be altered.

rotated axial system the length, breadth, and thickness in each case are parallel to X', Y', and Z', respectively.

For the X-cut in Table XXIX, the first line is for a broad plate in compressional thickness vibration, the second line for a narrow bar in

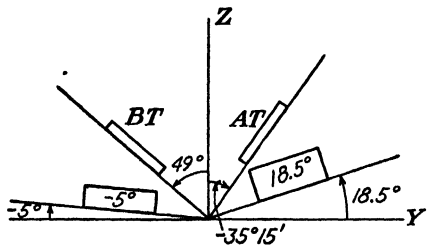


FIG. 92.—Angular orientations of some oblique cuts of quartz.

lengthwise vibration. Similarly, the first line for Y is for the shear thickness mode, and the second for the l-f shear mode in the plane of the plate. Through the process of rotation these two modes become the thickness mode of the AT- and BT-cuts and the contour mode of the CT- and DT-cuts.

TABLE XXIX.—SUMMARY OF DATA FOR VARIOUS CUTS

Cut	Mode	θ	φ	Θ	ψ	H kc sec^{-1} mm	ϵ	Range kc sec^{-1}
X	x_x	.....	0°	90°	90°	2,870	$e_{11} = 5.2(10^4)$	
X	y_y	.....	0°	90°	90°	2,700	$\frac{d_{11}}{s_{11}} = 5.4(10^4)$	
Y	x_y	.....	90°	90°	90°	1,954	$e_{11} = 5.2(10^4)$	
Y	z_z	.....	90°	90°	90°	.....	$e_{14} = 1.2(10^4)$	
AT	$x'_{y'}$	−35°15′	−90°	54°45′	90°	1,662	$e'_{26} = 2.9(10^4)$	1,000–5,000
BT	$x'_{y'}$	+49°	90°	41°	90°	2,549	$e'_{26} = 2.8(10^4)$	2,000–>13,000
CT	$z'_{x'}$	−38°	−90°	52°	90°	3,080	$e'_{25} = 3.0(10^4)$	100–1,000
DT	$z'_{x'}$	+52°	−90°	−38°	90°	2,060	$e'_{25} = 1.8(10^4)$	70–500
GT	$z'_{z'}$	−51°8′	−90°	38°52′	±45°	3,292	.....	100–1,000
MT	$y'_{y'}$	− 8.5°	6°40′	50°28′	79°36′	.....	.....	50–500
NT	$y_{y'}$	− 8.5°	9°25′	40°40′	77°40′	.....	.....	4–50
18.5°	$y'_{y'}$	+18.5°	0°	90°	108°	2,554	$d'_{12} = 7.0(10^{-8})$	Filter
−5°	$y_{y'}$	−5°	0°	90°	85°	.....	.....	Filter

A word must be added concerning the piezoelectric constants for rotated plates in Table XXIX. The subscripts attached to these constants are applicable as long as the plates are considered as Y'-cuts with the electric field parallel to Y'. In terms of the I.R.E. notation the thickness is parallel to Z' for all cuts; in order to be consistent with this system

the piezoelectric constants would have to have different subscripts. For example, the constant for the AT- and BT-cuts would be written e'_{35}, with analogous changes in all the other constants, including also those for the X- and Y-cuts. The numerical values would of course remain unchanged.

By making use of high overtones of thickness vibration, as described in §397, the range of practicable frequencies for the AT-cut is extended to 150,000 kc.

362. Numerical Data on Quartz Resonators. Experimental data from various sources, for bars in lengthwise vibration and plates in thickness vibration, are assembled in Table XXX. The fundamental mode was excited in each case. Quantities in parentheses are calculated by the author from the published data. The wave constant H is defined as $H = fl$ for bars and as $H = fe$ for plates, where f is in kilocycles per second and l and e are in millimeters. The number of meters, h, per millimeter can be calculated from the equation $h = 300{,}000/H$. In all cases the gap was zero, or close to zero, so that q_0 is the effective stiffness at zero gap.

In the table, Nos. 1, 8, 9, and 10 are from Vigoureux.[B51] Number 2 is the bar discussed in §298; the large R and low Q are due to frictional losses in the primitive form of holder in which the bar was mounted. Numbers 3 to 7 are from Mason.[B35,340] The angles specified give the deviation θ of the length l from the Y-axis, as indicated in Fig. 92 for the $-5°$ and 18.5° cuts.* These five examples illustrate the wide variations in H and q_0 for bars in different orientations.

Numbers 11 to 14 are from Bechmann.[37] The high values of Q are evidence of the excellent mounting of these plates. The value of C_1/C is calculated from the theoretical formula (414a)' in §280, in which it is assumed that $C_1 = kA/4\pi e$ esu. From C_1/C and Bechmann's values of C, C_1 is calculated.

In No. 4, C_1/C is the value given by Mason.[340] The same value can be derived from Eq. (414a)' using his data. The very large values of C_1/C occurring in the table are probably due to low effective values of the piezoelectric constant.

For *flexural resonators*, values of R, L, C and $\delta = \pi/Q$ are given by Rohde and Handrek,[438] whose paper must be consulted for details. They find that, for resonators of frequencies of 1,000 to 60,000 cycles/sec, R ranges from 22(10^5) to 1.6(10^5) ohms, C from 0.005 to 0.0027 mmf, L from 500 (10^4) to 0.26(10^4) henrys, δ from 0.00022 to 0.00034. Some of these resonators have two nodes, others three.

* For these five cuts the I.R.E. orientation angles (§52) are $\varphi = 0$, $\Theta = 90°$, $\psi = 90° + \theta$.

TABLE XXX.—THE CONSTANTS OF SOME TYPICAL QUARTZ RESONATORS

No.	Cut	l	b	e	f_0	R	L	C	C_1	$\frac{C_1}{C}$	Q	H	g_0
		mm	mm	mm	kc/sec	ohms	henrys	mmf	mmf			kc sec^{-1} mm	dyne cm^{-2} $\times 10^{-10}$
1	X-bar	62.2$\parallel Y$	7.5	1.5	44	1,640	(216)	0.06	8.7	145	(37,000)	(2,740)	(79.6)
2	X-bar	30.7$\parallel Y$	4.1	1.4	89.9	15,000	137	0.0218*	3.54	173	5,150	2,750	80.6
3	X-bar 79.5°	24.03	2.5	0.502	130.7	—	—	—	—	—	—	3,141	(105)
4	X-bar 18.5°	20.0	2.5	0.502	127.7	—	—	—	—	137	—	2,554	(69.2)
5	X-bar 0.9°	19.97	2.99	0.502	135.2	—	—	—	—	—	—	2,705	(77.5)
6	X-bar −18°	20.02	2.95	0.50	155.4	—	—	—	—	—	—	3,111	(102.5)
7	X-bar −42.6°	20.0	2.95	0.50	174.8	—	—	—	—	—	—	3,495	(129.5)
8	X-plate	16.40$\parallel Y$	15.64$\parallel Z$	6.15	472	2,100	(28.2)	0.004	1.93	460	(40,000)	(2,900)	(89.0)
9	X-plate	Disk, diam. 48.5 mm		7.52	389	400	(9.25)	0.018	9.6	530	(57,000)	(2,920)	(90.8)
10	X-plate	Disk, diam. 9.43 mm		0.58	4,980	4.6	(0.00725)	0.14	26.3	190	(50,000)	(2,890)	(88.5)
11	X-plate	Disk, diam. 25.0 mm		1.89	1,500	12.7	0.181	0.0622	(10.2)	(164)	(134,000)	2,838	85.46
12	Y-plate	Disk, diam. 25.0 mm		1.28	1,500	8.4	0.056	0.2011	(15.0)	(75)	(63,000)	1,919	39.10
13	BT	Disk, diam. 25.0 mm		1.66	1,500	35.0	0.391	0.0288	(11.9)	(413)	(105,000)	2,492	65.99
14	AT	Disk, diam. 25.0 mm		1.10	1,500	24.2	0.119	0.0945	(17.9)	(189)	(46,500)	1,657	29.23

* See p. 374

363. *The High Q of Quartz.* It is well known that the energy losses in quartz resonators are due, as a rule, chiefly to friction and air waves in the mounting and to vibrations imparted by the crystal to its supports. It has been shown by Van Dyke[554] that a considerable amount of damping is also caused by losses at the surfaces of the crystal, when these surfaces have simply been ground or lapped smooth, owing to microscopic cracks and other imperfections. If the surfaces are etched before mounting, these losses are greatly reduced, while a final polishing causes a still further diminution. Van Dyke's results obtained with an X-cut bar (frequency 67.5 kc/sec) are given below. The bar was silvered and suspended by a fine wire attached exactly at the center, serving also as a lead to the silver coating.

With surfaces ground, in air at atmospheric pressure, $Q = 25{,}000$; in hydrogen at atmospheric pressure, $Q = 101{,}000$; in vacuum,

$$Q = 180{,}000 \text{ to } 290{,}000.$$

With surfaces etched, in vacuum, $Q = 490{,}000$; etched and polished, in vacuum, $Q = 580{,}000$, corresponding to a logarithmic decrement of $5.4(10^{-6})$.

For a quartz bar in the primary frequency standard at the Reichsanstalt (§399), Scheibe* found the decrement to be from $13(10^{-6})$ to $18(10^{-6})$.

These decrement values for quartz are lower than the smallest value that we find recorded for a gravity pendulum.†

If compressional waves of frequency 67.5 kc/sec were impressed on the end of a quartz bar of indefinite length, for which the logarithmic decrement was $5.4(10^{-6})$, they would travel about 70 km before the amplitude was reduced to 1 per cent of that at the source.

For some of the vibrational modes of a Y-cut quartz *ring* Van Dyke[557] found values of Q of over a million.

The highest Q that we find recorded for a tuning fork is about 500,000, for a 480-cycle fork.‡

364. *Reduction in Friction at the Surface of a Vibrating Crystal.* When an X-cut quartz plate vibrates near resonance, the friction between it and the surface of a solid with which it is in contact is greatly reduced. This effect was described by Straubel[486] in 1931. In the same year frictional experiments were carried out in this laboratory by Hagen,§ based on earlier unpublished observations by Van Dyke. Hagen used

* A. Scheibe and E. v. Ferroni, *Physik. Z.*, vol. 39, pp. 257–258, 1938.

† H. Gockel and M. Schuler (*Z. Physik*, vol. 109, pp. 433–458, 1938) give $19.1(10^{-6})$ for the logarithmic decrement per cycle of a Schuler pendulum.

‡ E. Norrman, *Proc. I.R.E.*, vol. 20, pp. 1715–1731, 1932.

§ J. P. Hagen, M.A. thesis, Wesleyan University, 1931.

several different methods, including the measurement of the drag exerted on the quartz by a rotating brass disk on which it rested and also the effect of vibration on the angle of repose when the quartz rested on an inclined plane. When Hagen's experiments were performed in air, the friction was reduced to about half the normal value. In vacuum the effect almost disappeared, indicating that a layer of air between the surfaces was a necessary condition for the reduction in friction. On the other hand, Hagen found that the friction of a *pivot* supported by a bearing that rested on the vibrating quartz was reduced by about one-half even in vacuum.

365. Luminous Resonators. In a well-mounted resonator, driving voltages of only a few volts can cause local strains so great that the accompanying piezoelectric polarization gives rise to a charge density on the surface large enough to produce close to the surface a field sufficiently strong to ionize the air. The result is a visible glow. This effect was observed at atmospheric pressure in this laboratory in the course of the early experiments, but the results were not published. Since then, many others have also encountered it.

In 1925 Giebe and Scheibe[163] published the first of a series of papers on the luminous resonator. With rods parallel to X or Y, using very short electrodes according to §349, they were able to obtain luminosity at the fundamental lengthwise frequency and odd overtones up to the 33d order. The order can be determined by counting the number of luminous regions. Thus a single rod can serve as a frequency standard for a large number of frequencies. By proper placing of the electrodes even orders can also be excited. For the lower range of frequencies, 1,000 to 20,000, they used flexural modes, according to §354.

As standards of frequency, a precision as high as 1 part in 10^6 is claimed for the luminous resonators. The crystals are mounted in bulbs containing air or, for brighter effects, a mixture of Ne and He, at a pressure of a few millimeters.

The luminous resonator is connected in series with a pickup coil coupled to a generator of finely controllable frequency. The right setting of the generator is first found approximately with fairly close coupling. For the final precise adjustment the coupling is made as loose as possible.

366. Wave Patterns on Quartz Resonators. A vibrational survey of a resonator can be made by the use of probes, polarized light, or optical interference or by observing the movements of a liquid or of solid particles in contact with the surface.

The probe method consists in touching the resonator lightly at various points with a slender rod, to locate the nodal regions. Vibrations are suppressed least when contact is at the nodes. This method, much used by the author from the first, is described by Wright and Stuart. Its

use can go a long way in helping to avoid false conclusions as to modes of vibration.

In 1922 the use of *lycopodium powder* on quartz resonators was first described.[93] When this powder is dusted onto the surface, it tends to be shaken away from loops of motion and to collect at the nodes. Fine sand or other pulverized material can also be used. In some cases the powder is seen to move in small vortices or whirls, or to be projected violently from the surface. Wachsmuth and Auer[577] describe an experiment in which they found lycopodium to be projected as much as 50 cm. In this connection may be mentioned the experiments of Bücks and

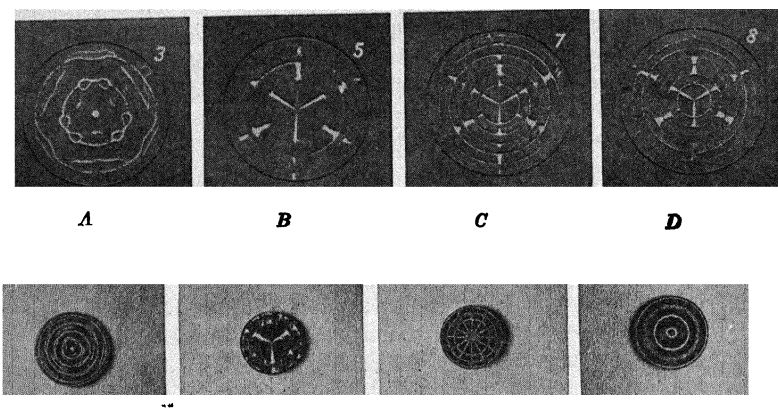


FIG. 93.—Lycopodium patterns on *Z*-cut disks vibrating in various modes, from Petrzilka. *A*, *B*, *C*, *D*, quartz. *E*, *F*, *G*, *H*, tourmaline.

Müller,[79] who observed the projection of smoke from the vibrating surface.

Many papers have appeared on the study of vibrational patterns of quartz by the use of lycopodium. Some of them contain very beautiful photographs of the lycopodium figures, examples of which are shown in Fig. 93, from Petrzilka.[417] Patterns *A*, *B*, *C*, *D* are from circular *Z*-cut quartz plates, excited by electrodes arranged around the circumference. For comparison, some of Petrzilka's patterns obtained with *Z*-cut tourmaline plates are also shown[415] (see §382). From the similarity in the elastic properties of quartz and tourmaline one would expect a similarity in the wave patterns, as is indeed made evident to some extent in the figures.* For a discussion of these and many other patterns, which were

* In comparing the patterns it must be understood that the vibrational modes are not necessarily the same in each quartz pattern as in the tourmaline pattern below it. The pictures were selected solely because of superficial similarities.

obtained in a test of Love's theory of radial and circumferential waves, Petrzilka's original papers must be consulted.

Complex patterns, such as those on the surface of an X-cut in thickness vibration, can be observed by *covering the surface with oil* or immersing the crystal in a shallow bath of oil. When viewed in a beam of reflected light, the oil surface is seen to be covered with minute irregularities. Crossley[116] found water on the surface to be quickly vaporized and that a ferroferricyanide solution left a sediment with a distinct pattern.* The oil method has been used by Tawil.[515] Bücks and Müller found that a drop of alcohol placed on the surace was shot off in a fine spray, forming striations between the vibrating surface and the plane electrode.

367. *The interference method* was introduced in 1927 by Dye and later applied by many others.† Dye produced a set of interference fringes between the non-vibrating polished quartz surface and a glass plate just above it. When the plate vibrated, the fringes were distorted, and from their appearance one could judge the quality of the resonator and the amplitude of vibration (normal to the surface) at different points. By an ingenious stroboscopic arrangement, using a synchronously flashing helium lamp, clear images of the distorted fringes were obtained, free from blurring.

Dye's method has been modified by Strong[497] and by Straubel,[490,491] whose optical system was so arranged that the entire field remained dark when the plate was not vibrating. Osterberg[398–402] describes interferometric methods, based on Dye's work, for studying various types of vibration. Osterberg and Cookson devised a "multiple interferometer"[407] for observing the vibrational patterns on all six faces of a rectangular parallelpiped. They used this method (see §313), applied to a quartz plate undergoing forced vibrations at 60 cycles/sec, for obtaining, by the converse effect, the values of d_{11} and d_{14} given in Table XVIII.

Mention may be made here also of the use of the "schlieren" method by Petrzilka and Zachoval[421] and by Schaaffs.[450]

368. *The polarized light method* was first used by Tawil[505,507,509–511] and later by several others.‡ Tawil placed his vibrating quartz plate, along with a second compensating quartz plate, between a crossed polarizer and analyzer, so that the field was dark except when the resonator vibrated. Vibrations caused certain portions of the field to be

* See also Sanders.[447]

† References at the end of this chapter. An account of Dye's work, with illustrations, is given by Rayner.

‡ K. Eichhorn, *Z. tech. Physik*, vol. 17, pp. 276–279, 1936 (he used a synchronized Kerr cell and calculated the stresses in flexural vibrations); P. T. Kao,[253] R. Moens and J. E. Verschaffelt, *Compt. rend.*, vol. 185, pp. 1034–1036, 1927; K. Grant,[187] Petrzilka,[414] Wachsmuth and Auer,[577] L. Bruninghaus, *Jour. phys. rad.*, vol. 6, pp. 159–167, 1935.

illuminated, leaving the nodal regions dark. The effect arises from the rotation of the plane of polarization by the stressed quartz, as explained in §538. Tawil and his followers investigated various vibrational modes by this method.

Many of the recorded wave patterns are so complex as to defy analysis. Compressional, shear, flexural, and torsional modes or certain of their overtones may be inextricably coupled at any given resonant frequency. It is only by a careful study of the resulting nodal patterns that conclusions—mostly qualitative—can be drawn concerning the contributing modes and their coupling.

Finally, brief mention may be made of the fact that the distribution of vibrational amplitude in quartz plates can be studied by the observation of air blasts, as described in §350, and also by means of ultrasonic waves.[B5,B24,422]

369. Beta-quartz Resonators. Increase in temperature past the transformation point at 573°C deprives quartz of all piezoelectric coefficients except d_{14}, $d_{25} = -d_{14}$, e_{14}, and $e_{25} = -e_{14}$. The possible piezoelectric stresses, as given in §168, are therefore $Y_z = -e_{14}E_x$ and $Z_x = e_{14}E_y$. The cuts and modes of excitation are similar to those for Rochelle salt or for the *CT*- and *DT*-cuts in quartz described in §359.

Such resonators have been investigated by Osterberg and Cookson.[404] Their use by these workers and also by Atanasoff and Hart, Atanasoff and Kammer, and Lawson, for the determination of elastic constants of quartz at high temperatures, is described in §§90, 92, and 101.

Osterberg and Cookson succeeded in making plates of β-quartz operate as piezo oscillators.

REFERENCES

OBLIQUE CUTS AND TEMPERATURE COEFFICIENTS, SIMPLE MODES

General. SCHEIBE,[B45] VIGOUREUX,[B50,B51] BECHMANN,[32,39,44] BROWN and HARRIS,[71] BUILDER,[80] GIEBE and SCHEIBE,[167,170] GRAMONT and BÉRETZKI,[183] KOGA,[272–274,276] MASON,[332,337,340] NAMBA and MATSUMURA,[389] SANDERS,[447] STRAUBEL,[491–493] SYKES,[498] VECCHIACCHI.[560]

Lengthwise Vibrations. GRAMONT,[B21] SCHEIBE,[B45] VIGOUREUX,[B50,B51] BECHMANN,[42,44] BUNING,[86] DYE,[127] GIEBE and BLECHSCHMIDT,[162] GIEBE and SCHEIBE,[167,172] MATSUMURA and KANZAKI,[350–352] MEISSNER,[359] NAMBA and MATSUMURA,[388] POWERS,[431] SANDERS.[447] A. HUND, "Phenomena in High-frequency Systems," McGraw-Hill Book Company, Inc., New York, 1936.

Thickness Vibrations. SCHEIBE,[B45] VIGOUREUX,[B50,B51] BECHMANN,[32,36,43,44] GERTH and ROCHOW,[156] GIBBS and THATTE,[158] HATAKEYAMA,[209] KOGA,[272] LACK,[298] NAMBA and MATSUMURA,[388] TSI-ZE and KENG-YI.[526]

AT-cut, BT-cut. LACK, WILLARD, and FAIR,[299] MASON,[337,340] MASON and SYKES,[343] SANDERS,[447] YODA,[595,596]

CT-cut, DT-cut. HIGHT,[226] HIGHT and WILLARD,[227] MASON and SYKES.[343]

GT-cut. MASON,[336,340]

V-cut. BALDWIN and BOKOVOY,[18] BENSON,[51] BUILDER,[80] SANDERS.[447]

Ring-shaped Resonators. ESSEN,[137] GIEBE and SCHEIBE,[167,168] MARRISON,[330,331] VAN DYKE.[557]

COUPLING EFFECTS BETWEEN DIFFERENT MODES

BALDWIN,[16] BECHMANN,[43,44] BUILDER and BENSON,[84] EKSTEIN,[131] GIEBE and BLECHSCHMIDT,[162] GIEBE and SCHEIBE,[165] HITCHCOCK,[230] LACK,[298] LACK, WILLARD, and FAIR,[299] LISSÜTIN,[317] MASON,[332,340] MATSUMURA and HATAKEYAMA,[345–347] NAMBA and MATSUMURA,[388] SANDERS,[447] SCHIFFERMÜLLER,[452] SYKES.[498]

CONTOUR MODES AND OTHER COMPLEX MODES

BECHMANN,[36] BUILDER and BENSON,[84] EKSTEIN,[131] FOX and HUTTON,[144] GIEBE and SCHEIBE,[166,169,171] KOGA and SHOYAMA,[281] LONN,[319] PETRZILKA,[414,417,418] SYKES.[498]

LUMINOUS RESONATORS

GRAMONT,[B21] SCHEIBE,[B45] VIGOUREUX,[B50,B51] GALOTTI,[153] GIEBE,[160] GIEBE and SCHEIBE,[163,165,170,172] HARRISON and HOOPER,[208] HEHLGANS,[217] JIMBO,[248] MITSUI,[370] MÖGEL,[373,374] NAMBA and MATSUMURA,[388] SKELLETT,[470,471] VAN DYKE,[556] WRIGHT and STUART,[594] ZAKS and UFTIUJANINOV.[599]

FLEXURAL VIBRATIONS

Theory. DOERFFLER,[124] MASON,[333] OSTERBERG and COOKSON,[405] SYKES,[498] THOMSON,[518] TYKOCINSKI-TYKOCINER and WOODRUFF,[537] VOIGT and FRÉEDERICKSZ.[576]

Equivalent Electric Constants. ROHDE,[437] ROHDE and HANDREK.[438]

Temperature Coefficients. ROHDE,[437] ROHDE and HANDREK.[438]

Use as Frequency Standard. SCHEIBE.[B45]

Use in Filters. ROHDE,[437] ROHDE and HANDREK.[438]

Use in Oscillators. ROHDE,[437] ROHDE and HANDREK.[438]

Luminous Resonator. ZAKS and UFTIUJANINOV.[599]

Curie Strip. GRAMONT and BÉRETZKI (frequencies down to 50∼).[185]

Miscellaneous Experiments. DOERFFLER,[124] EICHHORN,[130] GIEBE and SCHEIBE,[166–170] GRUETZMACHER,[191] HARRISON,[205] HARRISON and HOOPER,[208] JIMBO,[248] KRISTA,[290] NAMBA and MATSUMURA,[388] OSTERBERG,[399,400] TAWIL,[512] TYKOCINSKI-TYKOCINER and WOODRUFF.[537]

TORSIONAL VIBRATIONS AND STATIC TORSIONAL EFFECTS

Theory. GIEBE and BLECHSCHMIDT,[162] LANGEVIN and SOLOMON,[307] VOIGT and FRÉEDERICKSZ,[576] ZACEK and PETRZILKA.[598]

Use in Oscillators. BENOIT,[49] HUND and WRIGHT,[242] TSI-ZE and MING-SAN,[527] TSI-ZE and TSIEN,[530] TSI-ZE, TSIEN, and SUN-HUNG.[536]

Miscellaneous Experiments. BENOIT,[49] GIBBS and TSIEN,[159] GIEBE and BLECHSCHMIDT,[162] GIEBE and SCHEIBE,[166,167,169,170] HUND and WRIGHT,[242] TAWIL,[515] TSI-ZE and SUN-HUNG,[528,529] TSI-ZE and TSIEN,[533] ZACEK and PETRZILKA,[598] A. HUND, "Phenomena in High-frequency Systems," McGraw-Hill Book Co., Inc., New York, 1936.

Static Effects. TAWIL,[508,513,514] TSI-ZE and TSIEN.[531,532,534, 535]

Hollow Cylinders. BENOIT,[49] TSI-ZE,[525] TSI-ZE and MING-SAN,[527] TSI-ZE and SUN-HUNG,[528,529] TSI-ZE and TSIEN,[530–535] TSI-ZE, TSIEN, and SUN-HUNG,[536] ZACEK and PETRZILKA.[598]

Resonator Experiments with Polarized Light

Cady,[104] Kao,[253] Moens and Verschaffelt,[372] Petrzilka,[414] Tawil,[505,507,509,510] Tsi-Ze and Tsien,[530,533] Tsi-Ze, Tsien, and Sun-Hung,[536] Wachsmuth and Auer.[577]

Examination of Vibrating Plates with the Optical Interferometer

Scheibe,[B45] Vigoureux,[B51] Dye,[128] Kotlyarevski and Pumper,[289] Osterberg,[398–402] Petrzilka and Zachoval,[421] Rayner,[433] Schaaffs,[450] Schumacher,[453] Straubel,[490,491] Strong,[497] Wataghin and Sacerdote.[580]

CHAPTER XVIII

RESONATORS FROM OTHER CRYSTALS, AND COMPOSITE RESONATORS

For they marueyle that annye men be soo folyshe as to haue delyte and pleasure in the glysterynge of a lytyll tryfelynge stone, whyche maye beholde annye of the starres, or elles the soone yt selfe.—SIR THOMAS MORE.

Although quartz is almost the only material used at present for piezo resonators, much experimental work has been done with resonators from Rochelle salt and tourmaline. The former of these two has found some application in filters, and the latter in piezo oscillators of very high frequency. The phosphates and arsenates mentioned in Chap. XXVII have properties that recommend them as resonators; concerning them, however, judgment must be withheld until more data are available.

After a discussion of the effect of the anomalies of Rochelle salt upon its usefulness as a resonator, the resonator equations for lengthwise vibrations of 45° bars will be given. The discussion is confined to the case in which the driving field is small, since only then are the various stress-strain relations linear. The behavior of Rochelle-salt resonators with varying gap and also at very high frequencies is considered. Some experimental results are discussed, not only for lengthwise vibrations, but for other modes as well.

The resonating properties of a few other crystals are described, with special reference to tourmaline. Lastly, an account is given of the composite type of resonator, which consists most commonly of a metallic bar vibrated by having a bar of piezoelectric crystal attached to it.

370. The Rochelle-salt Resonator. Rochelle salt offers a very wide range of choice in orientations, shapes, and vibrational modes for resonators. The mechanical and thermal limitations of this crystal have restricted its practical application as a resonator. On the other hand, the experimental study of resonators has contributed greatly to our knowledge of the physical properties of Rochelle salt. Moreover, Rochelle-salt resonators are easily constructed and operated, affording some striking and instructive demonstrations.

Since the only piezoelectric strain coefficients are d_{14}, d_{25}, and d_{36}, it is impossible to obtain by direct piezoelectric excitation lengthwise vibrations parallel to the X-, Y-, or Z-crystallographic axes or thickness vibrations in plates normal to these axes.* In general, however, both

* We are here leaving out of account the possibility of exciting feeble compressional vibrations of type x_x, y_y, or z_z, through the quadratic effect discussed in §464.

types of vibration are possible in any *oblique* cut, since with respect to obliquely rotated axes the necessary piezoelectric coefficients are always present except in certain special cases. The formulas for the rotated coefficients are given in §§139 and 140. Flexural and torsional vibrations can be excited in practically any cut.

The anomalies of Rochelle salt, summarized in §402, are present only in the X-cut or in any cut in which the electric field has a component parallel to X. As long as the field is normal to X, which usually means a Y-cut or a Z-cut, there is no appreciable trouble from variability of the elastic, piezoelectric, and dielectric constants with field and stress. The change in elastic properties with temperature, while causing a rather large temperature coefficient of frequency, is fairly uniform. Although the decrements are an order of magnitude greater than in quartz, still for these cuts the equations and approximations given in Chap. XIII are usually entirely applicable.

It is when the field in the resonator has a component parallel to X, and of course most of all in the X-cut, that the anomalies have their field day, at least between the Curie temperatures and in the regions just outside of them. Some of the anomalies, however, can be avoided even between the Curie points when the field strength is restricted to a few volts per centimeter; most of the experimental work has been done with weak fields. As long as the field is weak, the dependence of strain and polarization upon the field is very nearly linear, so that the elastic and piezoelectric coefficients can be treated as constants. According to the domain theory we may define a "weak" field as one too weak to cause reversals of domains. As will be seen in §434, reversals of domains, as indicated by the beginning of the steep part of the polarization curve, do not take place as long as the field strength does not exceed 50 volts/cm, except close to the Curie points, where it rapidly sinks to a value which theoretically is zero. Between the Curie points it is best to keep the peak value of the driving field below 10 volts/cm, especially when there is a gap between crystal and electrodes, since near resonance the field in the crystal may be very greatly in excess of the driving field. At temperatures well outside the Curie points all relations are linear, so that the limitation to weak fields is removed—except for the danger of overheating or fracturing the crystal.

Between the Curie points, if the field is allowed to become so great that the relations are not linear, the elastic, dielectric, and piezoelectric constants vary in the course of each cycle (see also §426). The mechanical driving stress is then no longer proportional to the field. Even if the applied voltage is strictly sinusoidal, overtone vibrations will be present. This non-linear effect has been proposed by Wologdin[590] for application in a Rochelle-salt frequency multiplier. The analysis of

results obtained with Rochelle-salt resonators in large fields would be very difficult, and it does not seem to have been attempted.

Between the Curie points, when the vibrations are sufficiently vigorous, reversals of the spontaneous polarization in each half cycle may take place, especially in regions where the strain is greatest. The electric and elastic behavior are affected thereby, so that an anomaly in the frequency is to be expected, as well as pronounced damping. As was shown first by Mueller[380] and later in greater detail by Matthias,[353] the frequency of any mode involving s_{44}, in a plate with zero gap, is increased by application of a steady biasing field parallel to X, approaching a constant value when the biasing field is around 1,500 volts/cm. At the same time, as shown by Matthias, the damping is greatly reduced. These effects are attributable to the fact that the biasing field tends to prevent the reversals of the spontaneous polarization. Unfortunately, the crystal breaks or melts before a field can be applied great enough to prevent the reversals entirely. Matthias's work is treated further in §376.

Even in weak fields the Rochelle-salt resonator is not free from anomalies. Especially is this true when the electrodes are in contact with the crystal, since the elastic compliance then has its isagric value, which is extremely dependent on temperature.* It is only with large gaps that the X-cut resonator is nearly free from dependence on temperature.

A complication in the Rochelle-salt resonator to which attention should be given in future is the phenomenon of lag discussed in §427. From an inspection of the oscillographic data in Chap. XXII as well as Fig. 117 and the table on page 553 it appears that from about 500 cycles/sec upward the polarization is reduced by the lag, the effect increasing with rising frequency. One would expect the amplitude, and perhaps other properties, to be affected thereby. A start at the theoretical solution of this problem has been made by Mason.[338]

371. Resonator Equations for Rochelle-salt X-cut 45° Bars. Most of the experimental work with Rochelle-salt resonators has been done with lengthwise vibrations in bars. Other orientations and vibrational modes will be considered later. The present section is written in the notation for X-cut 45° bars. For other orientations all that is necessary is to make suitable changes in the coefficients. The gap is here assumed to be zero; its effect is treated in §377. Although a complete theory would include dielectric losses and the non-linear effects mentioned above, we shall here assume the field strength to be low enough for all effects to be linear. The parallel capacitance C_1 can then be regarded as free from dielectric loss; *i.e.*, the only resistance in the resonator is in the *RLC*-branch.

* See §§79, 200, 211, and 466 for the isagric coefficients and their relation to the constant-displacement and constant-polarization values.

The symbols d_{14} and e_{14} signify the *initial* piezoelectric coefficients, denoted in §§459 and 460 by $(d_{14})_0$ and $(e_{14})_0$ or, between the Curie points, by $(d_{14})_0^s$ and $(e_{14})_0^s$. The following equations hold at all temperatures, though the parameters vary greatly with temperature.

Since we are dealing only with X-cuts, the subscript x can be omitted from symbols for electrical quantities without confusion. And since the gap is zero, it is to be understood that all elastic quantities have their *isagric* values, unless otherwise specified.

The general equations for Rochelle-salt X-cut 45° bars are derived from Eqs. (186), (183*a*), (184), and (184*a*). When the strain and field are prescribed,

$$\left.\begin{aligned} Y'_y &= -c'_{22}y'_y + e'_{12}E = c'_{22}y'_y + e_{14}E \\ Z'_z &= -c'_{33}z'_z + c'_{13}E = -c'_{33}z'_z - e_{14}E \\ P &= \eta''E + c'_{12}y'_y + c'_{13}z'_z = \eta''E + e_{14}(y'_y - z'_z) \end{aligned}\right\} \tag{480}$$

When stress and field are prescribed,

$$\left.\begin{aligned} -y'_y &= s'_{22}Y'_y - d'_{12}E = s'_{22}Y'_y - \tfrac{1}{2}d_{14}E \\ -z'_z &= s'_{33}Z'_z - d'_{13}E = s'_{33}Z'_z + \tfrac{1}{2}d_{14}E \\ P &= \eta'E - d'_{12}Y'_y - d'_{13}Z'_z = \eta'E - \tfrac{1}{2}d_{14}(Y'_y - Z'_z) \end{aligned}\right\} \tag{480a}$$

η'' and η' are the clamped and free susceptibilities as defined in §450.*

Strictly, Eqs. (480) and (480*a*) are for *static* conditions. Equation (480) expresses the basic relations on which the theory of thickness vibrations rests, and also the special case treated in §372. Equations (480*a*) correspond to the case of lengthwise vibrations in a free bar, with which we are concerned in the present section.

We seek first the expression for the effective piezoelectric stress coefficient ϵ, from Eq. (307). Taking the length of the bar parallel to the Y'-axis, 45° from the Y-axis, we have, for the longitudinal isagric compliance, s'_{22} [Eqs. (43)]. The only fundamental piezoelectric coefficients to consider when the field is parallel to X are d_{14}, and $e_{14} = d_{14}/s_{44}$. With respect to the transformed axes the coefficients are, from Eqs. (203),

$$d'_{12} = \frac{d_{14}}{2} \qquad d'_{13} = -\frac{d_{14}}{2} \qquad e'_{12} = e_{14} \qquad e'_{13} = -e_{14}$$

In Eq. (307) we set $n = 2$, $i = 1$, $h = 2$ and 3, obtaining, with the aid of Eqs. 43,

$$\epsilon = (s'_{22}e'_{12} + s'_{23}e'_{13}) = \frac{e_{14}s_{44}}{2s'_{22}} = \frac{d_{14}}{2s'_{22}} \tag{481}$$

* Outside the Curie points, η'' and η' are the same as η_1 and η'. Between these points $\eta'' \equiv \eta_s''$ and $\eta' \equiv \eta_s'$ [Eqs. (499) and (504*a*)]. No thought need be given to these distinctions in the present section, since the equations are equally valid at all temperatures.

Without repetition of the intermediate stages in Chap. XIII the current may be written at once, from Eq. (315),

$$I = j\omega V\left[\frac{bl}{4\pi e}\left(k' - \frac{\pi d_{14}^2}{s'_{22}}\right) + \frac{bd_{14}^2}{2\gamma e s'_{22}}\tanh\frac{\gamma l}{2}\right] \tag{482}$$

This expression is valid at all frequencies. The effective dielectric constant is

$$k_l = k' - \frac{\pi d_{14}^2}{s'_{22}} \tag{483}$$

whence the effective susceptibility is found to be

$$\eta_l = \eta' - \frac{d_{14}^2}{4s'_{22}} \tag{483a}$$

Anticipating the results of the polarization theory as given in Eqs. (495*b*) and (522*c*), we find from Eq. (483*a*) that the reciprocal susceptibility, in terms of the *polarization theory*, is given by

$$\chi_l = \frac{1}{\eta_l} = \chi' + \frac{b_{14}^2}{4s'^P_{22}} = \chi' + \frac{a_{14}^2}{4s'^P_{22}c'^P_{44}} \tag{483b}$$

This equation shows that $\chi_l - \chi'$, like $\chi_1 - \chi'$ in Eq. 497, is a constant independent of temperature, insofar as a_{14} is temperature-independent.

Equation (483*b*) offers the advantage of having all quantities except χ' practically independent of temperature and stress. χ_l can be proved identical with Mason's[338] χ_{LC}, which he calls the value for "longitudinal clamping." This quantity can be measured by Mason's ingenious expedient of using the double frequency, as may be seen by writing $\omega = 2\pi(2f_0)$ and $c = 2f_0 l$ in Eq. (74) for γ and substituting this γ in Eq. (315). The last term vanishes, and the current is the same as if the crystal were a simple condenser with a dielectric constant k_l given by Eq. (483). The constant k_l is the same as Mueller's[380] ϵ_H.

At frequencies not too close to resonance, the damping can usually be ignored. With sufficient precision the electrical admittance Y'_1 for longitudinal vibrations at the fundamental frequency is then, from Eq. (316),

$$Y'_1 = j\omega\left(\frac{blk_l}{4\pi e} + \frac{bld_{14}^2 f_0}{2\pi f e^2 s'_{22}}\tan\frac{\pi f}{2f_0}\right) \tag{484}$$

In the resonance range we specialize Eq. (319) for the present case and find for the admittance

$$Y'_1 = \frac{bd_{14}^2}{\rho l e (s'_{22})^2(n^2 + \alpha^2)}(\alpha + jn) + j\omega\frac{blk_l}{4\pi e} \tag{484a}$$

where $\alpha = \pi f/Q = f\delta$ and $n = \omega_0 - \omega$.

The equivalent electric constants are

$$\left.\begin{aligned} L &= \frac{\rho l e (s'_{22})^2}{2bd_{14}^2} \\ C &= \frac{2d_{14}^2 bl}{\pi^2 e s'_{22}} \\ R &= \frac{\rho a l e (s'_{22})^2}{d_{14}^2 b} \\ C_1 &= \frac{blk_l}{4\pi e} \\ X &= \omega L - \frac{1}{\omega C} = \frac{\rho l e (s'_{22})^2 n}{\pi d_{14}^2} \end{aligned}\right\} \tag{485}$$

Values of η_l, η'', and k'' for a few temperatures, with the electric field in the X-direction, are given in Table XXXI; they are derived from the same data as Figs. 145 and 146. The values of $k'' = 1 + 4\pi\eta''$ fit in fairly well with the h-f values of k_x in Table XXXIV (page 572). Outside the Curie points $\eta'' \equiv \eta_l$; between them, $\eta'' \equiv \eta_s''$. k'' is the dielectric constant to use in the equations for thickness vibrations (§378).

TABLE XXXI

t, deg C	η_l	η''	k''
5	9.6	8.2	104
24.7	30	22	280
31.0	13	11	140
47.5	5.3	4.9	62

372. Rochelle-salt X-cut 45° Bar with Lateral Clamping. If the bar could be so clamped that all motion in the Z'-direction was prevented (clamping parallel to X is not essential), while freedom to vibrate in the Y'-direction was still allowed, its behavior would be described by the following equations. In some forms of mounting this condition may be approximated. If there is any lateral constraint at all, the solution may be expected to lie between the condition of complete lateral constraint and that of complete freedom postulated in the preceding equations.

Since the only permitted strain is y'_y, the appropriate elastic coefficient is c'^E_{22} rather than s'^E_{22}, just as in the case of thickness vibrations of a plate of large area. The following substitutions are to be made in the general equations in §§228 to 237: $q = c'^E_{22}$, $\epsilon = e'_{12} = e_{14}$, $(X_n)_d = (Y'_y)_d = -e_{14}E$.

In order to find the effective dielectric constant for lateral clamping we proceed as in the derivation of η_l in Eq. (310). The subscript i, which now denotes the X-direction, will be dropped. For ϵ and x_n^E we write e_{14} and $(y'_y)^E$. Since the strain z'_s is prohibited, the polarization component $e'_{13}(z_s)^E$ as well as $e_{14}(y'_y)^E$ must be subtracted from the polarization $\eta' E$ of the unclamped crystal, where $(z'_s)^E$ is $d'_{13}E$, the static strain due to the instantaneous impressed field E. Since the only strain is y'_y, we have $(y'_y)^E = -(Y'_y)_d/c'_{22} = e_{14}E/c'_{22}$, so that, in place of Eq. (310), the expression for polarization becomes

$$P^E = \left(\eta' - \frac{e_{14}^2}{c_{22}'} - e_{13}'d_{13}'\right) E \equiv |\eta_l| E$$

The bars indicate lateral clamping. On substituting $e_{14}d_{14}/2$ for $e_{13}'d_{13}'$, $d_{14}c_{44}$ for e_{14}, and making use of the equation $\eta' = \eta'' + e_{14}d_{14}$ and of the expressions for c_{22}' and c_{23}' in Eqs. (44), one finds for the laterally clamped susceptibility

$$|\eta_l| = \eta'' + d_{14}^2 c_{44}\left(\frac{c_{22}' - 2c_{44}}{2c_{22}'}\right) = \eta'' + d_{14}^2 \frac{c_{44}c_{23}'}{2c_{22}'} \tag{486}$$

The laterally clamped dielectric constant is

$$|k_l| = 1 + 4\pi|\eta_l| \tag{486a}$$

The equation for the current to the resonator is found from Eq. (315), on substituting e_{14}, $|k_l|$, c_{22}', and e, for ϵ, k_l, q', and e', respectively:

$$I = j\omega V\left(\frac{bl}{4\pi e}|k_l| + \frac{2e_{14}^2 b}{\gamma e c_{22}'}\tanh\frac{\gamma l}{2}\right) \tag{486b}$$

Outside the resonant range the admittance is approximately

$$Y_1' = \frac{j\omega bl}{4\pi e}|k_l| + \frac{2e_{14}^2 blf_0}{\pi e f c_{22}'}\tan\frac{\pi f}{2f_0} \tag{486c}$$

At frequencies close to resonance,

$$Y_1' = \frac{A\alpha}{n^2 + \alpha^2} + j\frac{An}{n^2 + \alpha^2} + j\omega\frac{bl|k_l|}{4\pi e} \tag{486d}$$

where $A = 4be_{14}^2/\rho le$.

The equivalent electric constants are

$$\left.\begin{aligned} L &= \frac{\rho le}{8be_{14}^2} & C &= \frac{8e_{14}^2 bl}{\pi^2 e c_{22}'^E} \\ R &= \frac{\rho\alpha le}{4e_{14}^2 b} & C_1 &= \frac{bl|k_l|}{4\pi e} \\ X &\approx -\frac{n}{A} = -\frac{\rho len}{4be_{14}^2} \end{aligned}\right\} \tag{486e}$$

373. Equivalent Mechanical Constants of 45° Bars. Whether there is lateral clamping or not, the equivalent mechanical constants can be found from Eqs. (104) to (107). The equivalent mass is $M = \rho ble/2$; the mechanical resistance is $W = 2M\alpha = 2MAR$ [A as in Eq. (486*d*)]; the mechanical reactance is $X_c = -2Mn = 2MAX$; mechanical stiffness factor $G = 2MA/C$; mechanical impedance $Z_c = 2MAZ$. The constant $2MA$ is the reciprocal of the electromechanical ratio r (page 297).

Comparison of the Driving Stresses. As we have seen, the driving stress for the free bar is $(Y_y')_d = -d_{14}E/2s_{22}'^E$, and for lateral clamping it is $(Y_y')_d = -e_{14}E$. The ratio of these is $s_{44}^E/2s_{22}'^E$, the value of which

for temperatures around 20°C is about 1.6, approaching a value of about 2 at the Curie point. Hence the driving stress is considerably greater in the case of the free bar.

Comparison of the stiffness factors shows that the resonant frequency for lateral clamping should be nearly twice as great as that of the free bar.

374. Rochelle Salt at Very High Frequencies. As we have seen, the Rochelle-salt X-cut 45° bar has the two piezoelectric constants d'_{12} and d'_{13}. As long as *only lengthwise modes* are considered, the contribution made by d'_{13} to the dielectric constant, at any instantaneous field strength, is the same as if the field were static, and the effective susceptibility η_l of the resonator is given by Eq. (483*a*). With increasing frequency, vibrational effects become more and more nearly negligible, so that the observed impedance approaches that due to η_l alone.

When the frequency rises to the region where lateral resonances involving d'_{13} appear, the observed susceptibility approaches the clamped value, as explained in §260. For Rochelle salt between the Curie points this is the value η''_s for monoclinic clamping, which can either be derived from observations at very high frequency or calculated from vibrational data at the fundamental lengthwise frequency. The latter process was carried out in determining $\chi''_s = 1/\eta''_s$ for Fig. 145. In that figure it is seen that at about 5°C χ''_s has a maximum of about 0.128, whence η''_s has a minimum value of about 7.8 at this temperature, yielding a dielectric constant in the neighborhood of 100. This value is in good agreement with the results of h-f measurements described in §442, and with Mueller's estimate, which he reaches by a somewhat different route on page 573 of his paper III.[380]

Experimental Results with Rochelle-salt Resonators. Most investigations have had the purpose of determining elastic constants and temperature coefficients, for which only observations of resonant frequencies are needed. In much of the earlier work the importance of special precautions in the treatment of crystals and the placing of electrodes was not understood, and the failure to mention these details makes the quantitative results of comparatively little value.

375. Lengthwise Vibrations. Almost all the recorded resonator experiments have been with 45° bars. The elastic constants thus determined by Cady, Davies, Hiltscher, Mason, Mattiat, and Mikhailov are given in Table VI (page 125). Hiltscher[228] observed at both fundamental and overtone lengthwise frequencies.

Mattiat[355] observed the dependence of the frequency of Y-cut bars on the ratio b/l of breadth to length and also the dependence of the frequency constants of X- and Y-cut bars on the angle between l and the Z-axis, obtaining approximate agreement with the values calculated from Mandell's elastic constants as given in Table IV or Fig. 26.

Mikhailov[367] measured d_{14} and k_l (§229) at temperatures from 0 to 40°C, by methods *a* and *c*, §310, using three *X*45° bars. He found the expected parallelism between the curves for d_{14} and k_l as functions of temperature. His results with d_{14} are mentioned in §474.

Reference has already been made in Chaps. VI, IX, and XXIV to Mason's observations of lengthwise vibrations in Rochelle-salt bars, which are the most complete and accurate to be found. The use that we have made of his results with bars in different orientations, for determining the "best" values of the elastic constants of Rochelle salt, has been described in §79. The present section has to do with his observa-

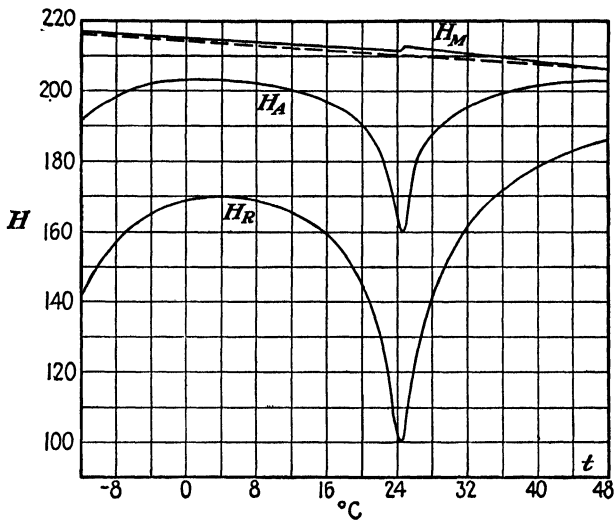


FIG. 94.—Dependence of the frequency-constant H on temperature, for a Rochelle salt *X*45° bar, from Mason. H is in kc sec^{-1} mm. The curves marked H_R and H_A are for resonance and antiresonance when $w = 0$. H_M is for the response frequency when $w = \infty$.

tions at the fundamental lengthwise frequency on a single *X*45°-bar, from which much information can be gained concerning the behavior of Rochelle salt at different temperatures. The bar had dimensions $l = 2.014$ cm, $b = 0.418$ cm, $e = 0.104$ cm. The electrodes were of gold, evaporated onto the surfaces in vacuum, so that the gap was strictly zero. The exciting field was restricted to a few volts per centimeter, so that only the initial values of the elastic and electric coefficients came into play; non-linear effects were not investigated. As stated in §474, these observations were used in preparing the data for Fig. 146. In Mason's paper[338] on hysteresis phenomena is a tabulation, for temperatures from −12° to 47.5°C, of the resonant and antiresonant frequencies f_R and f_A (our f_s and f_p, which, when the damping is small, are

seen from Table XXIII to be very nearly the same as f_m and f_n); also the "f_M-constant" in cycles sec^{-1} cm for the same bar with infinite gap; and $q = \omega_s L/R$ (our Q).

By multiplying f_R and f_A (expressed in kilocycles per second) by the length l in millimeters one obtains the frequency constants H_R and H_A in kc sec^{-1} cm. Their values, together with H_M for infinite gap ("f_M-constant" divided by 100), are shown in Fig. 94. Most noticeable are the low minima in frequency at the upper Curie point, the wide differences between the resonant and antiresonant frequencies when $w = 0$ (owing to the low capacitance ratio C_1/C, which in turn is due to the large value of d_{14}), and the very small dependence on temperature of the frequency at infinite gap.* This last feature, first observed by Mason, is the experimental foundation of the polarization theory,† as explained in §189.

TABLE XXXII.*—FREQUENCIES AND ELECTRIC CONSTANTS OF A ROCHELLE-SALT $X45°$-BAR

$l = 2.014$ cm $\quad b = 0.418$ cm $\quad e = 0.104$ cm

Temp. °C	f_R kc/sec^{-1}	f_A kc/sec^{-1}	R ohms	L henrys	C mmf	C_1 mmf	R_0 ohms	C_1/C	k_t	Q
−9.0	79.10	99.51	1300	0.066	61.5	106.0	649	1.72	148.0	25
+5.0	84.20	100.63	2600	0.0939	38.2	89.2	1850	2.34	124.8	19
20.5	71.82	95.20	900	0.0537	91.8	121.0	985	1.32	169.0	27
23.7	56.12	84.13	200	0.0415	194.0	156.5	430	0.805	219.0	73
24.7	52.00	81.60	60	0.0345	271.0	186.0	308	0.685	260.0	188
31.0	82.55	99.00	65	0.0934	40.0	93.0	209	2.32	130.0	745
47.5	94.15	100.90	2250	0.425	6.8	46.5	1480	6.9	65.0	112

* The values from the fourth column on are from recent data kindly furnished by Dr. Mason.

The broken line in Fig. 94 shows H_M as calculated from observed values of f_R and f_A by the use of Eq. (335) (f_R, f_A, and f_M are practically identical with f_0, f_p, and f_∞). The agreement with the observed H_M is excellent.

In Table XXXII are shown some of Mason's numerical results with this crystal. The values of the equivalent electric constants should be compared with those of quartz in Table XXX, due allowance being

* Mueller[381] has expressed the view that the slight slope and the kink in the curve for H_M may be due to the morphic effects described in §464.

† This constancy of frequency implies that the elastic constant s_{44}, which by Eqs. (43) occurs in the expression for s'_{22}, is nearly independent of temperature. When the gap is infinite, the elastic constants are those at constant normal electric displacement. It is shown in §§207 and 211 that for a Rochelle-salt X-cut bar the value s^*_{44} at constant normal displacement is, within the limits of experimental error, identical with s^D_{44}, the value at constant total displacement, and with s^P_{44}, the value at constant polarization. Thus the conclusion is reached that s^P_{44} is nearly independent of temperature and that c^P_{44} (the reciprocal of s^P_{44}) is to be taken as the "true" stiffness coefficient of Rochelle salt rather than c^E_{44}.

made for differences in dimensions. Outstanding are the much lower values of C_1/C and of Q in Rochelle salt. Close to the Curie point, C becomes greater than C_1. Rochelle salt evidently functions best as a resonator in the neighborhood of 30°C, where Q is largest. Above this temperature the low Q and high R and R_0 are due to increasing electrical conductivity.

R_0 is a resistance that according to Mason's theory* of hysteresis in Rochelle salt[338] is a property of the dielectric, distinct from the resistance R that corresponds to the vibrational losses. The variation of R_0 with temperature is similar to that of R. Curves with R_0 and k_l plotted against temperature are in Fig. 6 of Mason's paper.† R_0 has a broad maximum at about 5°, sinking to a flat minimum around 30°C.

The reason for the wide spread of values of f_R, f_A, and f_M for Rochelle salt has already been given in §295. The variation of these quantities with temperature should be compared with the general properties of this crystal, as set forth in Chaps. XX to XXV.

We return for a moment to the consideration of the low values of Q, and correspondingly large R in Table XXXII. Although these values of R were not great enough to affect perceptibly the frequencies and the elastic constants deduced therefrom, still it should be pointed out that not all observers have found so low a Q. For example, Mattiat,[355] in a table containing values of R, L, C, C_1, and Q for a number of X- and Y-cut 45° Rochelle-salt bars of different sizes, records Q from 1,300 to 3,600. Gockel's results[173] (see also §381) give $Q = 7{,}300$ for an $X45°$-bar. Unpublished observations in this laboratory by Van Dyke gave $Q = 2{,}200$ for an $X45°$-bar 21.3 by 5.6 by 2.1 mm, at 55 kc/sec. Both Mattiat and Van Dyke observed at room temperature.

Mason's results led him to the conclusion that "practically all hysteresis and dissipation effects are associated with the clamped dielectric properties of the crystal." This view is substantially in agreement with Mueller's, as stated in §468, that the anomalies in Rochelle salt lie in the properties of the clamped crystal.

376. The contrast between the variability of frequency, together with high energy losses, in the case of vibrational modes involving s_{44}, and the freedom from these troublesome characteristics with those modes from which this compliance coefficient is absent has recently been pointed out by Matthias.[353] By tests with an optical lever, luminous effects in partial vacuum, photoelastic effects in polarized light, and lycopodium particles, he found relatively flat resonance and small increase in amplitude at resonance for the "temperature-dependent" modes (*i.e.*, those

* Reference to this theory is made in §428.

† The numerical data in Mason's Fig. 6 differ somewhat from his more recent values in Table XXXII.

involving s_{44}). He showed that an X-cut 45° bar with zero gap (silver electrodes deposited in vacuum) had a much lower decrement and a frequency much higher and less dependent on temperature when a steady biasing field of 1,500 volts/cm was superposed on the driving voltage, as already stated in §370. Without a biasing field the decrement for temperatures between the Curie points was relatively low with small driving voltage, reached a maximum at a voltage corresponding to the steep portion of the polarization curve, and at high voltages approached the value recorded above the upper Curie point. For the details of these experiments, together with the theory, Matthias's paper should be consulted. In agreement with Mason[338] he attributes the damping in X-cuts chiefly to dielectric rather than to mechanical losses.

377. *The Gap Effect in Rochelle Salt.* Owing to the large size of the dielectric constant, the frequency increases at a much greater rate than with quartz resonators, as the gap increases from zero. The value for infinite gap is closely approximated even while the gap is less than the thickness of the plate. Calling f_w and f_∞ the frequencies corresponding to gaps w and ∞ and letting α represent a number small in comparison with unity, one can prove from Eq. (336) that $f_w = (1 - \alpha)f_\infty$ when

$$\frac{w}{e} \approx \frac{2\pi d_{in}^2}{s_{nn}^{\infty} k'^2 \alpha} \tag{487}$$

When this expression is applied to an X-cut 45° bar at 20°C, one has $d'_{12} = d_{14}/2 = 1.2(10^{-8})$; $s'_{22} = 3.16(10^{-12})$; $k' = 480$. Then $w/e \approx 12/\alpha$; and if $\alpha = 0.01$, $w/e \approx 0.12$. That is, at this temperature the frequency is within 1 per cent of the value for infinite gap when the gap width is only one-eighth of the thickness of the bar.

A *visible glow* analogous to that for quartz described in §365 has been observed with Rochelle-salt X-cut 45° bars by Hiltscher.[228]. His bars had electrodes of small area, so that most of the crystal surface was exposed. At both fundamental and overtone lengthwise frequencies the glow was observed when the bar was driven as a resonator, in air at a pressure of 0.3 to 0.6 mm.

378. Thickness Vibrations of Rochelle-salt Plates. The special equations for plates of Rochelle salt can be adapted from the theory in Chap. V. Rochelle-salt plates cut normal to the crystallographic axes cannot be piezoelectrically excited in thickness vibration. Theoretically, this type of vibration, both shear and compressional, can be excited in practically all *oblique* cuts. The activity of the resonator depends on the cut, being very low for small angles of rotation. The Christoffel theory has been applied to Rochelle salt by Mason[335,*] and by Takagi and Miyake.[501] The latter

* Also U. S. patents 2,178,146 (1939) and 2,303,375 (1942). Reference to Mason's experimental results with shear thickness vibrations has been made in §77.

investigators give experimental results on shear vibrations in a plate with normal perpendicular to a (110) face of the crystal.

Compressional thickness vibrations can also be generated in oblique plates. The only record of such vibrations is that of the author,[108] obtained with the L-cut described in §140.

379. Contour Modes in Rochelle-salt Plates. In vibrations of this type the exciting field normal to the plate causes a shearing stress in the plane of the plate, like the "contour modes" in quartz described in §359. Most experimenters have used relatively thin rectangular or square plates with edges parallel to the crystallographic axes. According to the axis selected for the normal to the major surfaces, the piezoelectric stress is of the type $Y_z = -e_{14}E_x$, $Z_x = -d_{25}E_y$, or $X_y = -e_{36}E_z$. The frequency depends essentially only on the major dimensions a and b, not on the thickness, and is given by Eq. (122). For the X-, Y-, and Z-cuts the reciprocal stiffness $1/q$ is s_{44}, s_{55}, or s_{66}, respectively. If there is no gap, the isagric values are to be used. The piezoelectric contribution to the stiffness when there is a gap has not been formulated, but the presence of a gap must certainly cause an increase in effective stiffness and hence in frequency.

Vibrations of this type have been described by Busch,[87] Mikhailov,[367] Mueller,[379,382] N. Takagi and associates,* and Taschek and Osterberg.[504] The pronounced change in frequency of X-cut plates near the upper Curie point, common to all vibrational modes in Rochelle salt in which the compliance s_{44} plays a part, was first observed by Busch in contour vibrations.

Observations in this laboratory on many rectangular plates of all three cuts have yielded results in agreement with Eq. (122). The plates were in a secondary circuit, and resonant frequencies were observed. The largest of these plates had dimensions X 0.485, Y 7.8, Z 12.0 cm, with a fundamental contour frequency of 22.6 kc/sec.† As a further test of the formula some of the plates were progressively reduced in length or breadth, with results in agreement with theory. From the dimensions and frequencies the compliance constants were calculated. Approximate agreement with the accepted values was found, but the results are not considered sufficiently precise for inclusion here.

In the experiments just described, as well as in those discussed in the next section, it was found highly important to apply to the crystal a voltage in the form of a pure sine wave. Harmonic frequencies were almost certain to excite undesired vibrational modes and cause misleading

* *Electrotech. Jour.* (*Japan*), vol. 4, pp. 95–96, 186, 232–233, 1940.

† These observations and those recorded below on flexural and torsional vibrations were made by P. D. Zottu at intervals from 1928 to 1932. The author's thanks are due the Brush Development Company for the Rochelle-salt plates.

responses. For this reason, in all the later work the supply from the tube oscillator was carefully filtered. For identifying vibrational modes, reliance was not placed on agreement between observed and calculated frequencies alone. In most cases the wave patterns were examined directly. For this purpose the plate lay horizontally on the lower electrode, usually with a few grains of sand between to provide a sort of roller bearing and diminish the friction. Nodal patterns were formed by lycopodium powder or fine sand sprinkled on the top of the plate. The upper electrode was then adjusted closely above the powder. By the use of a gauze electrode or an electrode of relatively small size, the formation of the patterns could be observed.

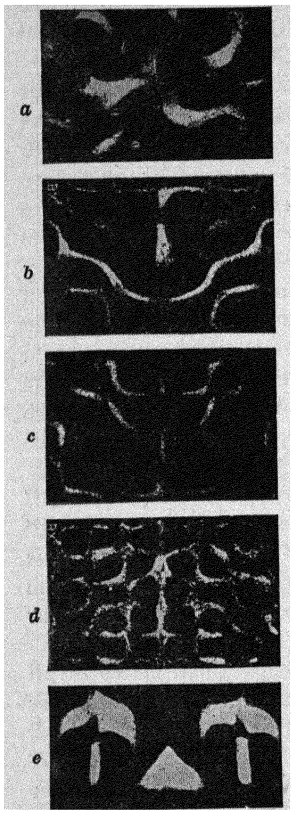


FIG. 95.—Dust patterns on X-cut Rochelle salt plates vibrating in complex modes. a, b, c, and d are from a plate X 0.48 cm, Y 7.8 cm, Z 12.0 cm. The frequencies are a, 27,300; b and c, close to 37,000; d, 54,300 cycles/sec. e has dimensions X 0.485 cm, Y 6.60 cm, Z 12.0 cm, frequency 27,500 cycles/sec. In some cases the dust particles moved in whirls or vortices, which persisted as long as the vibration continued.

When the supply was not filtered the patterns were very complex; some of them are shown in Fig. 95. With a well-filtered supply voltage, the pure contour shear mode described above gave rise to a more or less irregular nodal region in the center of the plate, such movements as the particles exhibited being chiefly in the plane of the plate. A pure flexural mode was recognized by two or more transverse nodal bands extending across the plate, and a torsional mode by a nodal line running lengthwise, midway between the lateral edges.

When the finger was touched to a vigorously vibrating portion of the surface, the crystal felt exceedingly slippery, and a sensation of warmth was felt at the finger tip.

380. Flexural and Torsional Modes in Rochelle-salt Plates. *Flexural vibrations* are easily excited, either in 45° bars or in rectangular plates with edges parallel to the crystal axes, using any one of the three cuts. The 45° bars are provided with electrodes as in Fig. 88E, the length l and breadth b being at 45° with two axes and the thickness e parallel to the third axis. Flexure takes place in the le plane. Piezoelectric excitation is through the transformed constants d'_{12}, d'_{23}, or d'_{31}, corresponding to an l-axis in the direction of Y', Z', or X',

respectively. Vibrations of plates in all these orientations have been observed by the author.

For plates cut according to the second method mentioned above, the electrodes are placed as shown in Fig. 89. In the case of quartz (if the edges of the plate are parallel to the crystal axes), there is but one orientation yielding flexural vibrations by this type of excitation. In Rochelle salt, l may be parallel to X, Y, or Z, the field being applied in the b-direction, with opposite senses in the two halves of the plate. Flexure takes place in the le-plane. When l is parallel to one axis, e may be parallel to either of the other two axes, giving in all six different possibilities. Depending on the cut, the driving stress is $Y_z = -e_{14}E_x$, $Z_x = -e_{25}E_y$, or $X_y = -e_{36}E_z$. With plates of various sizes, measurements of flexural vibrations have been made in this laboratory with all six arrangements. In each case the electrodes were separated from the crystal by small gaps. Plated electrodes could of course be used.

Torsional vibrations have been observed in this laboratory with bars parallel to X, Y, and Z. In each case a girdling electrode surrounded the bar at its center, as in Fig. 88*F*. As explained in §356 for quartz, the effective field components are those which enter the crystal from the girdle in a direction perpendicular to the length.

As stated in §356, more effective torsional excitation should be possible in a bar with length l parallel to one of the crystallographic axes, but with a rectangular cross section rotated 45° about this axis. The electrodes should be disposed as in Fig. 88*E*.

381. Resonator Results with Other Crystals. By the method mentioned in §320 Gockel measured at room temperature the logarithmic decrements of resonators prepared from the following crystals (the numbers in parentheses are logarithmic decrements in units of 10^{-4}): quartz (0.53), tourmaline (1.69), asparagine (1.63), urotropine (1.80), rhamnose (2.62), Rochelle salt (4.30). These values were obtained with the specimens mounted in vacuum. For the cuts employed and for further details the original paper should be consulted. The recorded decrements are almost unbelievably low, except for quartz and tourmaline.

Pavlik[411] has derived equations for the purpose of orienting plates from crystals in the two monoclinic piezoelectric classes so as to avoid the piezoelectric excitation of shearing stresses with respect to the axes of the plates. He describes resonator experiments with plates cut from crystals of beet sugar. Those who use his results should not forget that shearing effects can arise through elastic coupling even if they are not directly excited by the applied electric field.

Mandell[329] measured the frequencies of $X45°$, $Y45°$, and $Z45°$ bars of sodium-ammonium tartrate in lengthwise vibration. The bars served as piezo oscillators in a Pierce circuit. Discrepancies with the calculated

values amounted to as much as 5 per cent in some cases. This fact is not surprising, since there must have been at least a small effective air gap (the electrodes made only light contact with the crystal surfaces); moreover, the vibrational frequencies of the bars in the Pierce circuit, owing to the large piezoelectric constants and consequent large differences between resonant and antiresonant frequencies, were probably considerably above the true resonance values. Experiments with resonators made from certain phosphates and arsenates are mentioned in §499.

382. *Tourmaline Resonators.** The density of tourmaline varies from 2.94 to 3.24 gm/cm^3, depending on the composition of the specimen. A fair average value is 3.1. Parallel to the Z-axis the dielectric constant of the unconstrained crystal is 7.1; perpendicular to Z it is 6.3 ± 0.2.†

The eight piezoelectric constants offer a wider variety of direct excitation than do the five constants of quartz. The largest is $d_{15} = d_{24}$, which is almost twice as great in magnitude as d_{11} in quartz. By means of the excitation represented by $z_x = d_{15}E_x$, it should be possible to excite shear thickness vibrations in an X-cut plate.‡ The only tourmaline resonators that have been used extensively are of the Z-cut, in which compressional thickness vibrations are produced in accordance with $Z_z = -e_{33}E_z$. As has been pointed out by Giebe and Blechschmidt,[162] the relatively low values of the elastic cross constants responsible for coupling effects give to tourmaline resonators comparative freedom from undesired vibrational modes.

Tourmaline resonators were introduced in 1928 by Henderson.[219] Their use as piezo oscillators is described in §400, where further numerical data and references to the literature will be found. Various vibrational modes have been investigated by Petrzilka[415,416,419,§] with the aid of lycopodium patterns and the luminous effects at low pressure, as well as by frequency measurements. His papers contain many excellent photographs of nodal patterns, some of which are reproduced in Fig. 93. Further experiments with tourmaline resonators are described by Straubel,[490] Osterberg and Cookson,[406] Modrak,[371] and Khol.[258,259]

383. Composite Resonators. Among the earliest experiments with piezo resonators were tests made with metal bars excited in longitudinal vibration by means of crystals.‖ At first a single X-cut 45° Rochelle-salt

* Tourmaline plates are obtainable from the Premier Crystal Laboratories, New York, N.Y.

† "International Critical Tables," vol. 6, 1926. The measurements were made at audio frequency.

‡ See the calculations in Koga.[270] In this paper Koga derives the equations for thickness vibrations of tourmaline plates.

§ See also the discussion of his results by E. Lonn.[319]

‖ Master's theses by G. W. Bain, 1922, and H. C. Palmer, 1925, Wesleyan University; W. G. Cady, *Phys. Rev.*, vol. 21, pp. 371–372, 1923 (abst.). See also refs. 96

bar 1 to 2 cm in length was cemented endwise to a steel rod about 15 cm long. When the current from a tube oscillator was supplied to the crystal and tuned to the longitudinal frequency of the rod, the latter vibrated as a resonator, with energy derived from the reaction of the crystal. The successful results obtained with this device encouraged further investigation. It was soon found that a flat steel bar from 10 to 20 cm in length could be driven by means of a pair of quartz plates cemented on opposite sides at the center. Two such resonators are shown in Fig. 82; the construction is seen in outline in Fig. 96.

Resonators like that in Fig. 96 have been used in this laboratory with bars of various metals, glass, and fused silica, for obtaining dynamic values of Young's modulus for these materials. A quartz-steel resonator of this type has been made to serve as a piezo oscillator when provided with two pairs of quartz plates, the pairs connected, respectively, to the input and output of an amplifier.

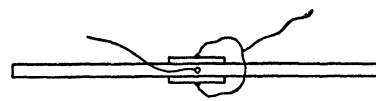


FIG. 96.—Quartz-steel resonator, 1923. The quartz plates are cemented to the flat sides of the steel bar; their outer tin-foil coatings are connected in parallel. The hook from which the bar is suspended serves as one terminal.

By the use of Rochelle-salt plates instead of quartz, a steel bar over a meter long has been driven as a resonator at its natural frequency, giving a loud musical note. A brass tube about a meter long, with four X-cut 45° Rochelle-salt bars at its center, clamped between two metal rings surrounding the bar, has been found to be especially useful as an acoustic generator with a frequency of 2,150 cycles/sec, for experiments with Kundt's tubes. The sound is emitted from a brass disk soldered across one end of the brass tube. The tin-foil coatings of two oppositely situated crystal bars are connected to the input of an amplifier, while the amplifier output is connected through a step-up transformer to the other pair of bars, the latter thus being the ones that drive the brass tube.†

In the composite resonators described above the size of the crystal element is made relatively small in order that the frequency and damping may be as nearly as possible characteristic of the vibrator to which the crystal is attached. Although this arrangement provides rugged and efficient resonators, the attachment of the crystal at a point of maximum stress is not well adapted to the precise measurement of the characteristics of the material of the bar.

---

and 97. The earliest of all piezoelectric devices that can be called "resonators" was Langevin's quartz-steel "sandwich" mentioned in §§224 and 506. References on composite resonators will be found at the end of this chapter.

† A device similar to this is described in R. M. Sutton's "Demonstration Experiments in Physics," New York, 1938.

384. The first step toward using the composite resonator for a more precise measurement of the elastic constants of various solids was taken in 1925 by Quimby, who developed the theory of vibrations in a solid bar driven by a quartz bar cemented to it at one end. The length of the quartz bar was parallel to Y, with the driving field parallel to X. His immediate object was a determination of the viscosity in rods of aluminum, copper, and glass. In his method there was no special relation between the lengths of the two components of the resonator.

The advantage gained by having the cement joint come at a node of stress was pointed out by Balamuth in 1934. Balamuth's technique has been followed by numerous other investigators (see references at end of chapter). The results have yielded data on the elastic constants, and their dependence on temperature, of a large number of solids, including metallic single crystals in the form of bars. In most cases the specimen under test was excited in lengthwise compressional vibrations by an X-cut quartz bar. On the other hand, Brown, Good, Rose, and in some of their observations Hunter and Siegel used torsional vibrations; the quartz was in the form of a cylinder with length parallel to X, provided with four electrodes according to the method of Giebe and Scheibe, as described in §356. Grime and Eaton (using flexural vibrations) and Schenk (using longitudinal vibrations) employed the quartz only as a detector, not as a driver. Boyle and Sproule examined the dust patterns on the end of a relatively thick vibrating bar, finding a configuration similar to the well-known Chladni figures. Their work makes it clear that false conclusions respecting the elastic constants of a bar may be drawn unless the bar is sufficiently thin.

In Mason's book the theory of the composite resonator, considered as an electromechanical transducer, is developed with reference to both longitudinal and torsional vibrations. Original data on the elastic properties of various materials are also presented. Some of these materials are plastics of high viscosity, for the measurement of which a special arrangement of crystals and circuit is described.

385. *Crystal-driven Tuning Forks.* The author has maintained a 2,048-cycle tuning fork in vibration by the use of X-cut 45° Rochelle-salt bars and an amplifying circuit.[95] Several different arrangements were used. In the first, a bar of size 4.6 by 1.5 by 0.4 cm was cemented endwise between the stem of the fork and a rigid base. The bar had two pairs of tin-foil coatings, connected to the input and output of a four-stage untuned resistance-coupled amplifier. When the fork was once started, it continued to vibrate with energy supplied by the amplifier at twice the fork frequency. In the second method each prong of the fork had cemented to it near the tip the end of a crystal bar with a single pair of coatings, the bars extending outward in the plane of the fork. One bar

was connected to the amplifier input, while the other, which supplied energy to the fork, was connected to the amplifier output. Here again the fork continued to vibrate after being lightly struck. The driving force was supplied by the inertial reaction of the bars. Third, a "cartridge" consisting of the crystal bar mentioned above with two pairs of coatings in a small holder, connected to the amplifier, maintained the fork in vibration when merely held in contact with one prong.

Although not a composite resonator, the quartz tuning fork of Koga[267] may be mentioned at this point. This was a 1,000-cycle fork fashioned from a single crystal and maintained in vibration piezoelectrically with the aid of suitable electrodes and an amplifier.

386. *A Quartz-Liquid Resonator.* Fox and Rock[147] cemented an X-cut quartz plate to the bottom of a cylindrical jar of water. By means of thickness vibrations at about 2.5 megacycles/sec stationary waves were produced between the quartz and a reflecting piston, and the characteristics of the resulting composite resonator were measured. With 200 stationary waves present, a value of $Q = 3{,}680$ was observed, whereas for the quartz in air Q was only 418. In comment, it may be said that the low Q in air was undoubtedly due to the cement and that, while the resonance of the water column greatly reduced the decrement, still 3,680 is too low a value of Q to warrant the expectation of practical applications. The attempts of these investigators to make a resonator of variable frequency by this method did not lead to promising results, since the response became relatively weak when the frequency departed appreciably from the natural frequency of the quartz.

REFERENCES

Rochelle-salt Resonators

Most of the papers on this subject have already been mentioned in the text. To them may be added the following references: Mason,[B35,335] Cady,[103,108] Stamford.[475]

Composite Resonators

Mason,[B35] Brown,[78] Fox and Rock.[147]

Balamuth, L.: A New Method for Measuring Elastic Moduli and the Variation with Temperature of the Principal Young's Modulus of Rocksalt between 78°K and 273°K, *Phys. Rev.*, vol. 45, pp. 715–720, 1934.

Bailou, J. W., and S. Silverman: Young's Modulus of Elasticity of Fibers and Films by Sound Velocity Measurements, *Jour. Acous. Soc. Am.*, vol. 16, pp. 113–119, 1944.

Boyle, R. W., and D. O. Sproule: Oscillation in Ultrasonic Generators and Velocity of Longitudinal Vibrations in Solids at High Frequencies, *Nature*, vol. 123, p. 13, Jan. 5, 1929.

Cooke, W. T.: The Variation of the Internal Friction and Elastic Constants with Magnetization in Iron, Part I, *Phys. Rev.*, vol. 50, pp. 1158–1164, 1936.

Good, W. A.: Rigidity Modulus of Beta-brass Single Crystals, *Phys. Rev.*, vol. 60, pp. 605–609, 1941.

GRIME, G., and J. E. EATON: Determination of Young's Modulus by Flexural Vibrations, *Phil. Mag.*, vol. 23, pp. 96–99, 1937.

HUNTER, L., and S. SIEGEL: The Variation with Temperature of the Principal Elastic Moduli of NaCl near the Melting Point, *Phys. Rev.*, vol. 61, pp. 84–90, 1942.

IDE, J. M.: Some Dynamic Methods for Determination of Young's Modulus, *Rev. Sci. Instruments*, vol. 6, pp. 296–298, 1935.

QUIMBY, S. L.: On the Experimental Determination of the Viscosity of Vibrating Solids, *Phys. Rev.*, vol. 25, p. 558, 1925.

QUIMBY, S. L.: New Experimental Methods in Ferromagnetism, (abstr.) *Phys. Rev.*, vol. 39, pp. 345–353, 1932.

QUIMBY, S. L., and S. SIEGEL: The Variation of the Elastic Constants of Crystalline Sodium with Temperature between 80°K and 210°K, *Phys. Rev.*, vol. 54, pp. 293–299, 1938.

READ, T. A.: The Internal Friction of Single Metal Crystals, *Phys. Rev.*, vol. 58, pp. 371–380, 1940.

RINEHART, J. S.: Temperature Dependence of Young's Modulus and Internal Friction of Lucite and Karolith, *Jour. Applied Phys.*, vol. 12, pp. 811–816, 1941.

ROSE, F. C.: The Variation of the Adiabatic Elastic Moduli of Rocksalt with Temperature between 80°K and 270°K, *Phys. Rev.*, vol. 49, pp. 50–54, 1936.

SCHENK, D.: Measurement of the Damping in Vibrating Steel Rods, *Z. Physik*, vol. 72, pp. 54–67, 1931.

SHEAR, S. K., and A. B. FOCKE: The Dispersion of Supersonic Waves in Cylindrical Rods of Polycrystalline Silver, Nickel and Magnesium, *Phys. Rev.*, vol. 57, pp. 532–537, 1940.

SIEGEL, S., and S. L. QUIMBY: The Variation of Young's Modulus with Magnetization and Temperature in Nickel, *Phys. Rev.*, vol. 49, pp. 663–670, 1936.

ZACHARIAS, J.: The Temperature Dependence of Young's Modulus for Nickel, *Phys. Rev.*, vol. 44, pp. 116–122, 1933.

CHAPTER XIX

THE PIEZO OSCILLATOR

Over earth and ocean, with gentle motion,
This pilot is guiding me.

—SHELLEY.

The stabilizing effect of a crystal on a circuit that is already oscillating will be considered first. This effect will lead naturally to the principle of the piezo oscillator, in which the crystal not only controls the frequency but is also an essential element in the maintenance of oscillations. Several types of piezo oscillator are described, with chief emphasis on the Pierce and Pierce-Miller circuits and some of their modifications.

By far the most important crystal for piezo oscillators is quartz, and most of the data on circuits, tubes, etc., are based on the assumption that quartz will be used. In §400, Rochelle-salt and tourmaline oscillators are treated. The chapter closes with a brief reference to the literature on the mathematical theory of the piezo oscillator.

387. Crystal Stabilizers. Any piezo resonator connected to an oscillating circuit tends to control the frequency. Having made this rather strong statement, we must state its limitations. In the first place, the controlling action is negligible except in the neighborhood of frequencies corresponding to natural modes of vibration of the crystal. If a tube circuit oscillating at frequency f contains a crystal, say in parallel with the tuning condenser, and if the crystal is clamped so that it cannot vibrate, the only effect is to add a little to the total capacitance; the amount added is substantially the parallel capacitance C_1 of the equivalent network shown in Fig. 50.

When the crystal is unclamped, the alternating potential drop makes it vibrate mechanically. If f is far from any characteristic frequency of the resonator, the amplitude is practically imperceptible. Nevertheless, the phase of the vibration and the consequent piezoelectric reaction of the crystal on the circuit are always such as to make the variation of frequency with change in tuning capacitance, or in any other circuit parameter, less than it would be in absence of the crystal. This fact is a sort of Lenz's law for the crystal-controlled oscillator.

As the oscillating frequency approaches one of the characteristic frequencies of the resonator, the vibrational amplitude and the electric reaction increase to a certain maximum; and on the other side of crystal

resonance the reaction diminishes approximately to the previous low value. For a measure of the reaction we may take the equivalent parallel reactance X_p or capacitance C_p, §273. As illustrated in Fig. 66, C_p rises to a maximum with increasing frequency, followed by a minimum. The stabilizing effect increases with C_p, which in turn increases with the size of the resonator. A very small crystal has a maximum C_p so small in comparison with other circuit capacitances that the stabilization is imperceptible. Thus a crystal bar 1.5 by 0.5 by 0.2 mm, although it resonates very nicely for lengthwise vibrations at a frequency around 2,000 kc, would make a poor showing if placed in control of a power oscillator.

In the foregoing statements we have made use of the concept of the equivalent network. With most resonators the parameters of the network are practically constant, and the electric behavior of the resonator can be fully described in terms of the network, whether the resonator is used as an oscillator or filter or for any other purpose. The crystal does nothing that could not be accomplished by an actual network containing a resistance, inductance coil, and condensers having the same values as the equivalent network. It is the impossibility of constructing such a physical network, not to mention having it stay constant if it could be constructed, that puts the crystal into a position of unique usefulness. Numerical data for quartz resonators will be found in §362.

It must be remembered that the network has different constants for each vibrational mode and that for any given mode it is applicable only over a range of frequencies undisturbed by other modes. It would be a superhuman task to derive a single equivalent network applicable to all modes.

Thus far we have discussed chiefly the stabilizing effect of a resonator in a circuit that oscillates independently of the presence of the resonator. Such a circuit, as has been stated in §223, is said to be *crystal stabilized*, and a resonator when so employed is called a *stabilizer*. The action of the stabilizer will now be explained more fully.

388. Only the case need be considered in which the crystal is in parallel with the tuning condenser of a tube oscillator, as shown in Fig. 97. The experiment is instructive and easily performed. The oscillator shown here is of the simple magnetically coupled type with tuned grid circuit, though other types may be used equally well; L_2 and C_2 must be such that the circuit can be tuned through the frequency f_0 of one of the crystal modes. Variations in frequency are observed by listening to the beat note between this circuit and a constant-frequency oscillator very loosely coupled to it.

The relation between the frequency f of the oscillator and the setting of C_2 is shown qualitatively in Fig. 98. The total capacitance

$C_t = C_2 + C_p$ (the effective parallel resistance R_p can here be ignored) is related to f by a continuous curve.* As C_2 is decreased, the frequency rises, rapidly at first and then more slowly as f_0 is approached, becoming almost constant in the neighborhood of the point A. At A comes a sudden break, the frequency jumping abruptly to point B. From there on the frequency is related to C_2 by the line BD. On decreasing C_2, the path $DBEF$ is followed, with another region of stabilization in the neighborhood of E.

The explanation may be expressed either in terms of the equivalent network $RLCC_1$ or of the effective parallel parameters C_p and R_p. In

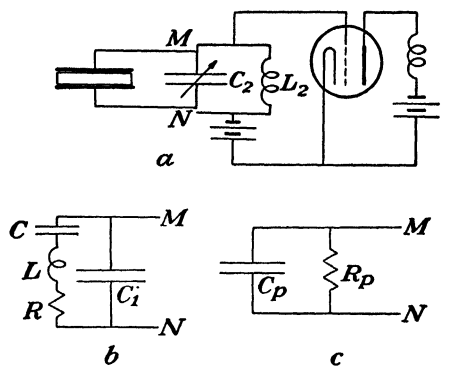


FIG. 97.—Circuit for showing the stabilizing effect of a crystal in parallel with the tuning condenser C_2 of an oscillating circuit. *b* is the customary equivalent network of the crystal, and *c* represents the crystal as a capacitance and resistance in parallel.

the former case we regard the network $RLCC_1$ as coupled to the tuning circuit C_2L_2; if the network has small damping, it tends to pull the circuit into step with its own frequency of series resonance f_0. The theory has been treated by Watanabe,[581] who showed that the coefficient of coupling between the two tuned circuits is approximately $C/(C_2 + C_1)$ and that, from observations of stabilization, the values of both C and R of the equivalent network can be calculated. The results are not very precise, owing to various effects of the tube circuit.

The stabilizing effect is explained most simply in terms of C_p. As may be seen from Fig. 66, $C_p = 1/\omega X_p$ varies with frequency in the manner indicated in Fig. 98. The maximum and minimum are higher and sharper the smaller the value of R and the greater the value of C (*i.e.*, the greater the size of the resonator). The frequencies at these two extreme values of C_p come at the quadrantal points P_1 and P_2 on

* The symbol C_2 in Figs. 97 and 98 must not be confused with the C_2 denoting the capacitance of the gap that may be present between crystal and electrodes. When a gap is present, its effect is to be regarded as included in the values of R, L, C, and C_1.

the resonance circle, as shown in Fig. 61 or 67. When C_2 is decreased to the point A, C_p cannot become any greater, the crystal loses control, and the frequency springs from A to B, and similarly at E. No oscillations are possible between P_1 and P_2.

Using the crystal $N2$ mentioned in §298, the author has found that close to the points A and E in Fig. 98 the variation in frequency for a

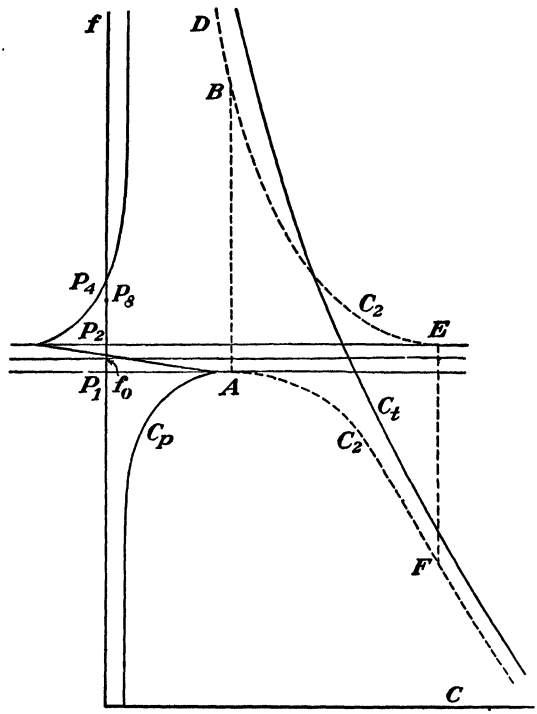


FIG. 98.—Stabilizing action of a resonator as the turning capacitance C_2 is varied.

small change in C_2 (or in filament current or any other variable) was only one-thirtieth as great as when the crystal was absent.

The crystal-stabilized circuit was first arrived at in 1920 as one stage in the search for a crystal-controlled oscillator. While the stabilizer has found some application,* its usefulness is far less than that of the piezo oscillator, to which we now turn.

389. The Crystal-controlled Oscillator. Although the circuits described in the following sections may be used with any piezoelectric crystal, particular reference is made to quartz, as this is the only

* See, for example, Heegner,[214] Handel, Krüger, and Plendl,[202] Kusunose and Ishikawa,[297] Watanabe.[581]

material in common use for the purpose. The various cuts of quartz and their properties have been discussed in Chap. XVI.

The piezo oscillator may be considered as evolved out of the stabilizing circuit just described. The tuning circuit C_2L_2 in Fig. 97 is transferred to the anode circuit of the tube, replacing the tickler coil and becoming the tank circuit, as shown in Fig. 100*a*. The only reactance connected to the grid is that of C_p, the equivalent parallel capacitance of the resonator. If the oscillating circuit is regarded as consisting of C_p in series with the grid-anode capacitance and the impedance Z_2 of the anode circuit, oscillations will be generated if C_p can assume a value that makes the total reactance vanish. Usually this condition requires that the crystal be vibrating near a resonant frequency. For stable oscillations the operating point must be on a region of the C_p-curve in Fig. 98 where $\partial C_p/\partial f$ is positive, since otherwise an increase in f will not be neutralized by a corresponding increase in C_p. At first sight it might appear that the tube would oscillate with a frequency slightly below that at P_1 if Z_2 had an inductive value lying between certain limits. Actually, this is impossible, since on the l-f side of resonance the crystal is vibrating in the wrong phase. On the h-f side, however, just above P_2 (between P_2 and the frequency for antiresonance) stable oscillations can occur if Z_2 is inductive. C_p is here negative, and the crystal operates as an inductance, automatically selecting that point on the curve which makes the total circuit reactance zero. Z_2 must of course lie between certain inductive limits, but a good resonator has such a wide range of values of negative C_p that the tolerance in Z_2 is very wide. Usually a tank circuit is employed, tuned to the optimum inductive reactance.

In terms of the equivalent series reactance X_s, the condition for stable oscillations is that $\partial X_s/\partial f$ shall be positive and that the frequency shall come between resonance and antiresonance. This consideration restricts the operating range to a region on the l-f side of point P_s, Figs. 66 and 67, between P_s and P_2. We return to this subject in §392.

It is shown by Hight and Willard, according to Llewellyn's theory and confirmed by their experiments, that the frequency is most nearly independent of small changes in the circuit reactances, plate voltage, and change of tube when the reactance of the tank circuit is numerically equal to the tube resistance R_p between cathode and plate and at the same time $R_p = (\mu + 1)R_g$, where μ is the amplification factor and R_g the cathode-grid resistance. At the optimal setting of C_2 the frequency is a maximum. A further improvement in stability is brought about by tuning a small variable condenser between grid and anode to secure an additional adjustment to maximal frequency.

390. Some Early Types of Piezo Oscillator. One of the earliest circuits, devised by the author in 1921, operates by means of piezo-

electric feedback. It is essentially an amplifier with input and output coupled through a crystal with two pairs of electrodes, as shown in Fig. 99. In the earliest form a three-stage resistance-coupled amplifier was used, but it was found by Van Dyke in 1922 that a single tube was quite sufficient.* The original crystal was an X-cut quartz bar, of size $X0.15$, $Y3.9$, $Z0.7$ cm, having a fundamental lengthwise frequency of about 70 kc. With two pairs of electrodes suitably connected, the circuit oscillated at the first overtone, approximately twice the fundamental frequency. Neither coil nor condenser was necessary: the anode circuit contained only a resistance of 12,000 ohms and was slightly capacitive from stray effects. Reversing one pair of electrodes caused the oscillations to take place at the fundamental frequency. Watanabe[581] has made a theoretical study of this type of oscillator; his results are in agreement with the foregoing statements and prove moreover that when the anode circuit is made *inductive* the connections in Fig. 99 give rise to the *fundamental* frequency, while reversing one pair of electrodes gives rise to the first overtone. His investigation shows also on which side of resonance the oscillating frequencies lie.

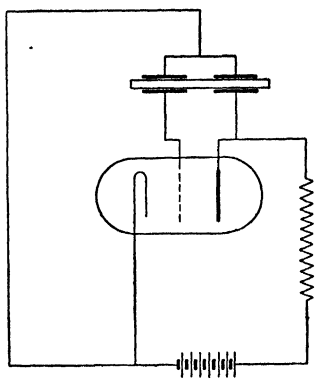


FIG. 99.—The earliest type of crystal-controlled oscillator consisting of an amplifier with input and output coupled through a crystal.

In another type of oscillator first described by the author, a tuned grid circuit was used, the coil in the grid circuit being very loosely coupled to a coil in the anode circuit. The crystal replaced the blocking condenser between the tuning element and the grid. A modification of this arrangement has been used by Horton and Marrison.[234]

The author has also used the piezoelectric feedback for driving metal rods at audio frequencies (§383). The same principle is used in oscillators described by Rohde,[436] Rohde and Handrek,[438] and Mason and Sykes.[343]

391. The Pierce and Pierce-Miller Circuits. These two circuits, especially the latter, are in very wide use. In the Pierce circuit the crystal is between grid and anode of a vacuum tube, while in the Pierce-Miller circuit it is between grid and filament.† In simple form, without

* See also Mallet and Terry.[325]

† G. W. PIERCE, U. S. patent 1,789,496, application Feb. 25, 1924, issued Jan. 20, 1931; J. M. MILLER, U. S. patent 1,756,000, application Sept. 10, 1925, issued Apr. 22, 1930. Pierce's paper[423] describes only the grid-anode connection, for which the reactance in the anode circuit has to be capacitive, as explained in §394. Hence the

the modifications to which reference will be made later, it is illustrated in Fig. 100. In *a* the crystal is between grid and filament. The action of the crystal in controlling the frequency has already been explained in §389, in terms of the equivalent parallel capacitance C_p. In principle, the device is a tuned-grid tuned-plate circuit with the crystal replacing the tuning elements in the grid branch. Feedback takes place through the capacitance between grid and plate, shown by dotted lines. The alternating potential on the grid comes from the charges liberated piezoelectrically by the vibrating plate.

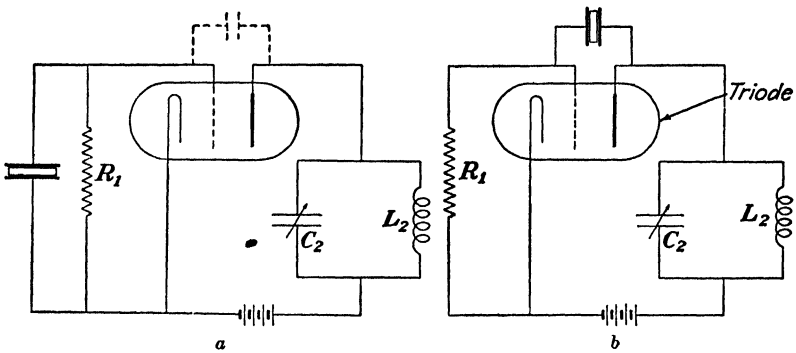


FIG. 100.—Piezo-oscillator circuits. *a*, the Pierce-Miller circuit; *b*, the Pierce circuit.

The tank circuit L_2C_2 should be tunable over a considerable range on either side of the crystal frequency. A high L_2/C_2-ratio gives a large harmonic content, which for some purposes is advantageous. If one starts with C_2 at its setting for lowest capacitance (Fig. 100*a*), the circuit usually does not oscillate and the anode direct current is large. As C_2 is increased, oscillations set in at a certain point and the direct current diminishes. The oscillation current increases with C_2, until a critical value is reached at which oscillations cease.

In the Pierce-Miller circuit just described, the crystal vibrates at a frequency slightly below its antiresonant frequency, according to the

---

coil used by Pierce in his anode circuit must have had enough distributed capacitance to make this circuit act like a condenser. J. M. Miller first recognized this fact. He also—independently of Pierce—made a circuit oscillate with the crystal between grid and filament, and he introduced the tunable element in the anode circuit (L_2C_2 in Fig. 100*a*), with a tap to L_2 to increase the output current.[115,369,461]

Although a recent legal decision has awarded to Pierce the priority for the grid-filament connection, it can hardly be denied that Miller deserves at least to share in the credit. In the literature both circuits of the types shown in Fig. 100 are commonly called "Pierce circuits." In this book, also, this term is sometimes applied generically to circuits of either type, but when special mention of the grid-filament connection is made we refer to the "Pierce-Miller circuit."

statement in §389. Strictly, the antiresonant frequency in question is that of the crystal and all associated capacitances, including those contributed by the tube itself. For satisfactory operation the impedance of this combination at antiresonance should be as high as possible, a condition which requires that the Q of the crystal shall be as large as possible. When oscillating, the tube provides the negative resistance necessary to neutralize the positive resistance component of the impedance. The smaller the associated capacitances, the greater is the antiresonant impedance and the better the oscillator. The magnitude of this antiresonant impedance is a useful *index of performance* for the oscillator.

Instead of the Q of the RLC-branch of the crystal network, use is sometimes made of the antiresonant Q_a, which is the ratio of the inductive reactance to the effective resistance of the crystal and associated capacitances at the frequency of antiresonance. This Q_a is much smaller than Q: for example, with a BT-cut of quartz for 5 to 10 megacycles, Q may be of the order of 500,000, while Q_a is only around 10,000.

The circuit with the crystal *between grid and plate* is shown in Fig. 100*b*. This circuit is of the ultraudion type, the tuning element being replaced by the crystal. Feedback takes place through the crystal itself, the tank circuit serving to determine the optimum (capacitive) reactance.

392. Without reference to the equivalent network, the action of the vibrating crystal in maintaining the oscillations may be explained as follows: Let it be assumed that the crystal is connected as in Fig. 100*a* or *b* but not vibrating. There is then an unvarying electron current through the tube, with a fixed positive static charge on the anode and a negative charge on the grid. Owing to the potential difference between grid and filament (or between grid and anode), the crystal is statically deformed to a slight extent through the converse piezoelectric effect. If now any small momentary disturbance occurs, causing the grid to become more negative, the deformation increases. The crystal has in effect received a shock excitation, which makes it vibrate;* by the direct piezoelectric effect it impresses an alternating voltage on the grid, which soon dies down if nothing occurs to maintain it. But this alternating voltage on the grid causes a variation in the anode current at the same frequency, thereby varying the anode potential by an amount and phase angle depending on the impedance in the plate circuit. If this impedance lies within a certain range of values, the effect becomes cumulative. At each surge of current to the grid, the anode changes its potential in such a way as to increase the intensity of the surge, thus compensating for the energy losses in the crystal and in the grid circuit and causing the amplitude of vibration to build up instead of decrease. This continues until a balance is reached, just as in any other oscillating device. Part of the energy of the anode supply has become converted into a-c energy through the medium of the crystal vibrations. Unless the crystal vibrates, the circuit will not oscillate.

Owing to the high Q of the crystal, its resonating range is very narrow. Hence the generator, when once started, will hold its frequency extremely constant. Within

* The mechanical inertia of the resonator plays a part strictly analogous to the electromagnetic inertia, or self-inductance, of the equivalent circuit.

wide limits, any change in circuit conditions, as for example a variation in C_2, filament temperature, or anode voltage, can affect the frequency only to the extent of causing the crystal to vibrate at a different point on its resonance curve. An equivalent statement is that the L of the resonator is so extremely great and its C so extremely small, in comparison with the effective inductance and capacitance of the rest of the circuit, that under no conditions can the frequency depart far from $(1/2\pi)(LC)^{-\frac{1}{2}}$.

393. *The Minimum Size of Crystal for a Piezo Oscillator.* For a given frequency, the length of a bar or the thickness of a plate may be considered as fixed. The question is then how narrow the bar can be, or how small the area of the plate, and still control the frequency in a Pierce circuit. In either case, it becomes a question of minimum size of electrodes, the latter being assumed to cover the entire crystal surface. Since a resonator, however small, has an inductive reactance over a certain frequency

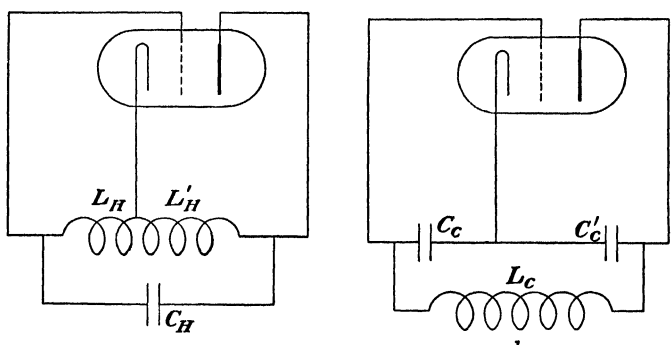


FIG. 101.—*a*, Hartley oscillator; *b*, Colpitts oscillator.

range as long as the damping is sufficiently low, there is no theoretical reason why it should not control the frequency in a Pierce circuit. There are, however, two very practical reasons for a lower limit. The first is the difficulty in mounting an extremely small resonator so as to have a sufficiently high Q. The second reason is that a minimum oscillating grid current is necessary; and if the electrode area were very small, too high a voltage would be required across the crystal. The relation of crystal resistance to the condition for oscillations is discussed by Watanabe[581] and Vigoureux.[B50,B51]

394. A piezo-oscillator circuit may be shown to function as either a Hartley or a Colpitts oscillator, depending on the location of the crystal. These two general types of oscillator are shown schematically in Fig. 101, in which *a* corresponds to Fig. 100*a*: when the crystal is between grid and filament, it vibrates on the h-f side of resonance and therefore has an inductive reactance. The crystal corresponds to L_H, and the inductively tuned tank circuit to L'_H, while the grid-plate capacitance corresponds to C_H.

With the crystal between grid and anode we have in effect a Colpitts circuit. If the grid circuit is capacitive (in practice a condenser is often connected across R_1), corresponding to C_c, and if the tank circuit is also capacitive, corresponding to C'_c, oscillations can take place on the h-f side of crystal resonance. The crystal now replaces L_c.

For the higher range of frequencies, for which thickness vibrations are chiefly employed, the grid-filament connection seen in Fig. 100*a* is chiefly used. The same circuit can of course be employed also for low frequencies, though for this purpose the grid-plate connection is often preferred.

In the simple Pierce-Miller circuit, as in all crystal-controlled oscillators, best results are obtained with tubes of high amplification. The 801 triode is suitable, with the plate voltage held to 300 volts or less, in order not to endanger the crystal. The maximum safe crystal current is considered in §257.

395. Modifications of the Pierce-Miller Circuit. The simple circuits shown in Fig. 100, using a triode tube, have a rather low output of power, and the frequency is not sufficiently constant to meet the exacting requirements of practical service. As in all oscillators, the power increases with the plate voltage, as does also the current to the crystal. Since the crystal current is proportional to the amplitude of vibration, there is danger of breaking the crystal if the plate voltage is much greater than about 250 volts. As to the frequency, any slow drift or sudden fluctuation in circuit conditions, due, for example, to variations in supply voltages or in temperature, may change the value of the grid-plate capacitance or of the anode impedance and thus force the crystal to operate at a different frequency in order to satisfy the condition for oscillations. Moreover, unless the resonator has zero temperature coefficient, the resonant frequency of the crystal itself will vary with changes in the current flowing to it. Best frequency stability in this simple circuit is obtained by the use of a relatively low ratio of L_2 to C_2 in the tank circuit, especially for the higher frequencies.

The power output can be increased to several watts by substituting a r-f choke and biasing battery for the resistance R_1 in Fig. 100*a*.* A proper choice of bias on the control grid is important, since the current to the crystal increases with the amount of bias. As an alternative to the biasing of the grid by R_1 alone, the "cathode bias" illustrated in Fig. 102 has been introduced, by which the potential between grid and filament is controlled by the d-c potential drop through a resistance R_2 in series with the (indirectly heated) cathode. This arrangement, which may be used without R_1 but with a choke in parallel with the crystal, is found to make

* A. Crossley, U. S. patent 1,696,626, (1928), also ref. 115. Crossley has obtained as much as 100 watts output from a single tube at frequencies from 3,000 to 4,000 kc.

the crystal start oscillating more easily. A combination of grid-leak bias with cathode bias is often employed, at least with triodes. The cathode bias alone is recommended for frequencies over 1,500 kc.

The criteria in the selection of tubes are high amplification, low grid-anode capacitance, small current to the crystal, and sufficient power output.

Among the various present-day piezo-oscillator circuits, which for the most part are of the Pierce-Miller type, we illustrate only one, in Fig. 102. This circuit is widely used in amateur transmission and is well suited to general laboratory use. The tube may be either a tetrode (in which case the suppressor grid in the figure is omitted) or a pentode.

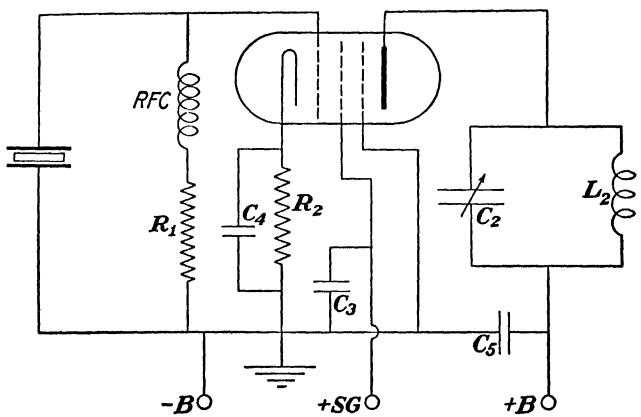


FIG. 102.—Pentode piezo-oscillator.

The advantages offered by these tubes are high amplification, greater power without fracturing the crystal, and higher frequency stability from the action of the screen grid. With a high L_2/C_2 ratio the harmonics are very pronounced. When a pentode is used, the suppressor grid may be grounded, or for greater power it may be given a small positive potential.* As represented in the figure, both grid-leak and cathode bias are used. If the grid-plate capacitance provides insufficient feedback, a very small auxiliary condenser may be connected between grid and plate. To safeguard the crystal, such capacitance should be as small as possible. The L_2/C_2 ratio is usually greater than in triode circuits.

Push-pull piezo oscillators have been used with both triodes and

* Suitable pentodes are the 41, 42, 6F6, and 802 or the beam types 6L6 and 807. With maximum plate voltage on the latter, the output should be at least 10 watts for frequencies over 1,500 kc/sec. The following typical values of circuit elements shown in Fig. 102 are taken from the "Radio Amateur's Handbook": C_2, maximum 100 mmf, with L_2 designed for the frequency used; C_3 and C_5, 1,000 mmf or more; C_4, 0.01 mf; R_1, 10,000 to 50,000 ohms; R_2, 250 to 400 ohms.

tetrodes.* In some of his experiments Harrison used crystals with four electrodes, oscillations taking place through piezoelectric feedback as described in §390. In other cases, the crystals had two electrodes, and oscillations were maintained as in the Pierce-Miller circuit. Harrison's oscillators seem especially well suited to l-f oscillations, including those controlled by plates vibrating flexurally. He was able to obtain an output of 5 watts at 50 kc/sec, with a flexural resonator. The power derived from two tubes in push-pull may be as much as $1\frac{1}{2}$ times that from a single tube. It is a characteristic of push-pull circuits that all *even* harmonics are eliminated.

396. Low-frequency Piezo Oscillators. For crystal control, any of the l-f types of piezo resonator described in Chaps. XVII and XVIII can be used. In practical applications quartz is employed almost exclusively; the usefulness of Rochelle salt is mainly for experimental work and demonstration. The various types may be classified as follows:

1. Lengthwise vibrations of bars or plates. Owing to the scarcity and cost of large quartz plates and the impracticability of making oscillators with very short bars, the usual limits of frequency for this type are from 80 to 300 kc/sec.

2. Broad plates, usually a rotated cut as described in §358, vibrating in a contour shear mode. They can be used from about 70 to 1,000 kc/sec.

3. Flexural vibrations, either of the type introduced by Harrison,[205] with two or more pairs of electrodes, or of one of the types described in §354, with a single electrode pair. The practicable range in frequency is from 1 to 100 kc/sec.

4. Torsional vibrations. The frequency range is about the same as for flexure. No practical application of this mode seems to have been made.

5. Flexural vibrations of a Curie double strip, in which two very thin quartz bars are cemented together, as described in §354. By this method Gramont and Béretzki[185,186] have obtained oscillations at frequencies down to 50 cycles/sec.†

6. Beats between two h-f piezo oscillators, using two different crytals or a single crystal with two regions of different thickness, according to Hund.[238–241] This method seems to have been used mainly in experimentation‡ rather than in routine practice.

*Push-pull piezo oscillators have been described, for example, by Harrison[207] and Koga.[266] See also I. F. Byrnes, British patent 277,008 (1927) and U.S. patent 1,722,196 (1929).

† An interesting demonstration of the acoustic waves from these oscillators was a feature in the French building at the New York World's Fair in 1939.

‡ The first suggestion leading to method 6 was made by Pierce.[423] See also Koga

Other l-f quartz cuts for piezo oscillators are described in §§357 and 359.

Whatever form of oscillating circuit is employed, it must be remembered that the l-f crystals have relatively large mass and rather low activity and are easily broken by overvoltage. Good practice calls for the use of low-power tubes, high L/C ratio in the anode circuit, and a high grid-leak resistance.

Among the available circuits, the Pierce form is commonest, though the "tritet" (see reference to Lamb[300,301] at end of chapter) and bridge circuits can also be used. Gramont and Béretzki mention the use of a relaxation circuit for their very low frequencies.* The mechanically tuned feedback has been employed by Harrison[207] for his flexural oscillators and by Rohde[437] for lengthwise vibrations.

Piezo oscillators employing torsional vibrations are described by Tsi-Ze and Tsien,[530] Tsi-Ze, Tsien, and Sun-Hung,[536] and Hund and Wright.[242]

397. High-frequency Piezo Oscillators. For this purpose only thickness vibrations are used, generally of the shear type, cut at an angle for low temperature coefficient. For the same cut, the fundamental frequency varies inversely as the thickness.

In recent years attempts to increase the frequency have been stimulated partly by the demand for shorter waves in communication and partly by the success of Straubel in 1931 in obtaining very high frequencies from tourmaline oscillators (§400). In the years following Straubel's investigations the experimental work of Fox and Underwood,[148] Osterberg and Cookson,[403] Yoda,[596] Gramont and Béretzki,[186] Koga,[278] as well as Uda and Watanabe,[538] offered convincing evidence that quartz plates could be made to oscillate at frequencies practically as high as tourmaline. This fact, together with the high cost of even small tourmaline plates and their relatively high temperature coefficient of frequency, has practically ruled tourmaline out of consideration for generating short waves in radio.

In some of the experiments just referred to, the quartz plate was less than 0.1 mm thick. Kamayachi and Watanabe report results with a plate only 0.015 mm thick, the wavelength being 1.8 m. Gramont and

---

and Yamamoto;[284] Gramont and Béretzki;[184] A. Wertli, A Quartz-controlled Heterodyne Note Generator, *Helv. Phys. Acta*, vol. 6, p. 495, 1933; and Gramont.[182] Cases have been recorded in which a plate of uniform thickness vibrated simultaneously with two modes of nearly the same frequency, causing two separate output frequencies, which could be detected as a beat note. See, for example, F. Bedeau and J. de Mare, *Compt. rend.*, vol. 185, pp. 1591–1593, 1927; Sabbatini,[444] and Vigoureux.[568]

* On the use of relaxation oscillators, see also Hund,[239] Eccles and Leyshon,[129] and Kao.[252]

Béretzki have pointed out that, in order to match the input impedance of the tube, a very thin plate should have a small area. They recommend a ratio of diameter to thickness between 30 and 40.

On the whole it has not been found practicable to use quartz plates of a thickness smaller than about 0.2 mm, corresponding to 15 megacycles for the fundamental frequency. For still higher frequencies it has been customary to use frequency-multiplying circuits, the fundamental frequency being controlled by a quartz plate of convenient thickness, for example 1 mm.

The complication of frequency-multiplying circuits can be avoided by causing the crystal itself to vibrate at a high "harmonic" frequency. Crystal control of this type with a relatively low order of harmonics was achieved by some of the investigators named above. Nevertheless, in the past there has been the difficulty that the order of harmonics, at least so far as the ordinary Pierce-Miller circuit is concerned, is strictly limited by the considerations in §296. Very recently these obstacles have been surmounted by Mason and Fair,[141,341] who placed a quartz plate (AT or BT) in a capacity bridge* between grid and ground. By this means the harmful effect of the parallel capacitance C_1 was eliminated. For further details of the circuit the original papers must be consulted. By using the 23d harmonic of an AT-cut a frequency of 197 megacycles/sec was obtained by Mason and Fair; and by doubling the frequency they could go as high as 300 megacycles (1-m waves).

398. Other Crystal-controlled Circuits. Many circuits have been described, mostly modifications of the Pierce-Miller circuit. They include transmitter circuits of various powers and frequencies, primary and secondary standards of frequency, monitors, multivibrators, frequency multipliers and dividers, and receiving circuits. Some involve the attempt at making the crystal vibrate at its resonant frequency instead of on the inductive side of the resonance curve.† At the end of the chapter are a few references selected from the very extensive literature.

Two forms of piezo oscillator use other than purely electromechanical means for coupling the crystal to the oscillating circuit. One employs a beam of sound, the other a beam of light. Wheeler and Bower[583] described a circuit in which the controlling crystal is a large quartz bar in flexural vibration, the vibrations being maintained by acoustic waves from a telephone membrane, which in turn is vibrated by the output current from the amplifier to which the crystal is connected. The light-beam method, devised by the author,[104] makes use of an X-cut quartz bar in lengthwise vibration, through which a beam of polarized light

* Bridge methods for balancing out the parallel capacitance C_1 have long been known, especially for receiving circuits; see also Builder and Benson.[82]

† See, for example, the papers by Heegner[216] and Boella.[58]

passes parallel to the Z-axis. The light, modulated by the periodic strains in the crystal, falls on a photoelectric cell, the current from which is amplified and connected to the resonator electrodes.*

In two-way telegraphic communication, the detector at the receiving end can have coupled to it a low-power piezo oscillator, controlled by a crystal having a frequency differing by, say, 1,000 cycles/sec from that at the sending end. A heterodyne note of great purity is thus produced.

Special mention should be made of a "bridge-stabilized" piezo oscillator of very high constancy,† described by Meacham.[357] The crystal forms one arm of a bridge, of which the other three arms are resistances. One diagonal of the bridge is coupled inductively to the input of an amplifying tube, the other to the output. Meacham's analysis shows that the crystal vibrates at its resonant frequency, acting as a filter. The circuit is stabilized against all fluctuations by having one of the resistance arms of the bridge thermally controlled. Over a period of several hours the change in frequency has been found to be less than ± 2 parts in 10^8. In addition to its commercial applications this circuit has proved itself superior to a chronometer when used as a time standard for gravity measurements.

399. Standard-frequency Piezo Oscillators and Quartz Clocks. Under this heading are included primary and secondary frequency standards, portable frequency monitors, and the quartz clock.

Our only concern here has to do with the crystals employed for these purposes. As a guide to the literature on circuits and temperature control, a list of references is given at the end of this chapter.

For all the purposes named above the chief requirements with respect to crystals are very low damping and small variation of frequency with temperature. Modes of vibration other than that selected for operation are not troublesome as long as they are not close to the latter. On the other hand, more attention must be paid to the mounting, especially in primary standards and quartz clocks, than in any other use to which crystals are put.

A primary frequency standard is a formidable and elaborate apparatus in a fixed location. It is essentially a crystal-controlled oscillator of highest precision, with amplifiers and circuits for multiplying and subdividing the crystal frequency. Usually the output at one of the lower

* In *Engineering* (London), vol. 124, p. 841, 1927, is an account of the measurement of the frequency of a vibrating quartz plate placed between crossed nicols in such a manner that a beam of light, modulated by the crystal, was reflected by a rotating mirror of known angular velocity.

† Oscillators of this type are now obtainable from the General Radio Company, Cambridge, Mass. A brief analysis of the theory is given in the *Gen. Radio Experimenter*, vol. 18, no. 2, pp. 6–8, May, 1944.

demultiplied frequencies—say 1,000 cycles/sec—drives a synchronous motor geared to a dial, so that time intervals can be precisely determined and comparisons made with other crystal-controlled standards and with pendulum clocks. Such a device is called a "crystal clock" or a "quartz clock."

It is now recognized that quartz clocks, at least over limited lengths of time, are more precise than the best astronomical pendulum clocks. Indeed, small variations in the rate of astronomical clocks, due to fluctuations in the earth's rotation, have been revealed by comparisons with quartz clocks.

Primary standards usually consist of three or more independent crystal-controlled oscillators. The advantages of this arrangement are continuity of service if one oscillator stops, as by the burning out of a tube; the possibility of detecting any irregularity in the performance of any one oscillator; and increased precision over long periods of time.*

A discussion of the methods and technique of making frequency comparisons with standards cannot be undertaken here.

The secondary standard is like the primary, except that it is usually of less high precision and that the clock feature may be omitted.

The crystal monitor is a small portable low-power secondary standard with a restricted range of frequencies. In some forms it has a scale to read frequencies directly.

At the National Bureau of Standards there are seven quartz-controlled primary standard oscillators, *viz.*, six with 100 kc/sec *GT*-cuts in bridge-stabilized circuits, and one with a special doughnut shape at 200 kc/sec in a modified Pierce circuit. The crystal in each unit is kept at constant pressure in a small sealed metal box, in a constant-temperature oven. For the better units the short-time variations under normal operating conditions are less than ± 2 parts in 10^9. The drift of frequency in a month is less than 2 parts in 10^9, with a daily drift of less than 10^{-10}.†

The crystal-controlled standard at the National Physical Laboratory in England, according to the most recent publication,[139,69] contains a 100 kc/sec ring, as described in §357. In vacuum, at constant temperature, the stability is $\pm 4(10^{-10})$ during hourly periods and $1(10^{-8})$ during monthly periods. The "long-period stability" is stated by Essen‡ to be $2(10^{-8})$.

According to Scheibe[B45] the four quartz clocks at the Physikalisch-Technische Reichsanstalt make use of quartz bars with lengths parallel

* See E. W. Brown and D. Brouwer, Analysis of Records Made on the Loomis Chronograph by Three Shortt Clocks and a Crystal Oscillator, *Monthly Notices, Roy. Astron. Soc.*, vol. 91, pp. 575–591, 1931.

† For this information the author is indebted to Dr. J. H. Dellinger.

‡ Ref. 69, p. 131.

to X or Y (§349). The frequency is 60 kc/sec. The bars are separated from the electrodes by 1-mm gaps and are mounted in vacuum with thermal control. For these clocks the daily variation is claimed to be less than $2(10^{-10})$, the monthly variation about $3(10^{-9})$.

In the primary standards of the General Radio Company* an X-cut 50-kc quartz bar with length parallel to Y is used, as illustrated in Fig. 103. The dimensions are $X = 9.4$ mm, $Y = 54.4$ mm, $Z = 7.0$ mm, with R around 2,700 ohms and Q around 85,000. The temperature coefficient of frequency is from $-0.7(10^{-6})$ to $-1.5(10^{-6})$. The electrodes are of chemically deposited silver, protected by copper or gold plating or both. In ordinary industrial service the short-period stability is of the order of 2 to 3 parts in 10^9. After 3 to 4 weeks of initial drift period the oscillators settle down to a slow long-time drift, usually an increase in frequency of 1 or 2 parts in 10^6 for a year. Crystals that have run for some years appear to have no systematic drift, but only fluctuations of unknown origin amounting to 1 or 2 parts in 10^7.

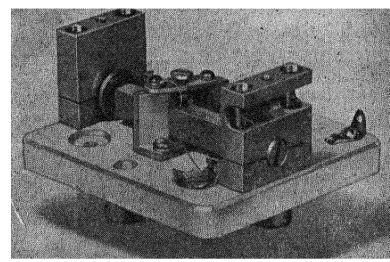


FIG. 103.—X-cut quartz bar for primary standard of frequency. The bar is clamped between two resilient pads at the mid-points of the YZ-surfaces. A baffle at each end is adjusted for quarter-wave resonance, removing at least 90 per cent of the loss due to acoustic radiation from the ends of the bar. The radiation from the sides is negligible. (*Courtesy of the General Radio Company.*)

The General Radio monitors employ AT-cut plates in frequencies from 500 to 5,000 kc/sec. The plates are mounted in holders with adjustable gaps. Electrodes are chromium plated.

400. Piezo Oscillators with Rochelle-salt and Tourmaline Crystals. Owing to the large piezoelectric constants of Rochelle salt, bars of this material, either X-, Y-, or Z-cuts, can easily be made to vibrate in a Pierce-Miller circuit. Nevertheless, for mechanical and thermal reasons they are unsuitable for practical applications. While much has been published on their performance as resonators, chiefly for the purpose of determining the dynamic elastic and piezoelectric constants, still the only mention we find in the literature on their use as piezo oscillators is in papers by Pierce[423] and Mikhailov.[366]

* This information was kindly furnished by Mr. J. K. Clapp. He states also that X-cut bars inclined at $\theta = +18°$ and $-48°$ from the Y-axis have higher Q's, but also higher temperature coefficients. At $\theta = -5°$ the temperature coefficient averages less than at $\theta = 0°$, but Q is quite low. When a 50-kc bar with length parallel to Y operates at its second "harmonic" frequency, Q is considerably greater, and at 60°C the temperature coefficient is zero.

*Tourmaline oscillators** were introduced by Straubel in 1931, when he obtained an output of 5 watts at 7 m wavelength and succeeded in getting crystal control down to 2 m. In his second paper he reported direct control at 80 cm (thickness only 0.01 mm) but found it preferable to use crystal control at 2 m, followed by a threefold frequency multiplication. In his third paper he described the stabilization of a magnetron at 1.6 m.

Wavelengths around 1.6 m were also attained by Awender and Bussman and by Kühnhold.

Various circuits were used by the experimenters listed at the end of this chapter, including the Pierce, push-pull, and stabilizing circuits. Several determinations of temperature coefficient of frequency have been made, with an average of about $-40(10^{-6})$. For the same thickness, tourmaline gives a frequency about 35 per cent higher than quartz. The frequency constant is about 3,750 kc sec^{-1} mm.

Besides having a high temperature coefficient, tourmaline crystals rise considerably in temperature while vibrating. Heierle finds an increase of 10°C in temperature in 1 hr (see also Booth and Dixon). These facts do not favor the use of tourmaline as compared with quartz for high frequencies.

In all the foregoing experiments, Z-cuts of tourmaline were used, the plates being in the form of circular disks a few millimeters in diameter. The thickness vibrations were compressional, with a strain given by the equation $z_z = d_{33}E_z$. The outstanding advantage offered by tourmaline, emphasized by Straubel and by Petrzilka, is that since the elastic properties are symmetrical about the Z-axis, very pure compressional waves are propagated in the Z-direction. There is therefore less trouble from undesired vibrational modes and parasitic frequencies than in the case of quartz.

401. Theory of the Piezo Oscillator. The earliest attack on the problem of the crystal oscillator was made by Terry[517] in 1928, in a paper that had to do mainly with the conditions for stability of frequency. In this treatment, circuit resistances are included, but a linear tube characteristic is assumed. In the years that followed numerous other treatments of the theory appeared,† each containing certain simplifying assumptions. One of the most thorough was that of Vigoureux,[B50,B51,568] who derived formulas for frequency and current in terms of crystal, tube, and circuit parameters, in good agreement with experiment.

Special mention should also be made of Llewellyn's paper in 1931,[318] which contains an analysis of the Hartley, Colpitts, and other circuits,

* See list of references at end of chapter.

† A list of some of the more important contributions is given at the end of this chapter.

with special reference to the conditions for frequency stability. Application is made to crystal control.

Both Vigoureux's and Llewellyn's conclusions will be found helpful in understanding the functioning of the Pierce circuit and in predetermining the various constants.

In the papers by Watanabe and Usui are applications of the resonance circle to their analyses. Watanabe discusses at length the effect of a gap in series with the crystal.

REFERENCES

On the subject of piezo oscillators some hundreds of papers, as well as countless patents, have been published, in various languages. An exhaustive bibliography would be so long as to defeat its own purpose. The classified lists below are a selection of representative papers, sufficiently recent to be of practical use, from which, it is hoped, not too many milestones are missing. For further references the reader must consult texts on radio and the various scientific, technical, and amateur journals. Much helpful information is contained in such publications as the "Radio Amateur's Handbook," the "Radio Handbook," and the bulletins of the General Radio Company, the Radio Corporation of America, and the Bliley Electric Company.

Piezo-oscillator Theory

Vigoureux,[B51] Boella[56,57] Handel,[200,201] Heegner,[215,216] Jefferson,[247] Koga,[268] Petrzilka and Fehr,[420] Smirnov,[472] Terry,[517] Usui,[540] Vigoureux,[568] Watanabe,[581] Wheeler,[582] Wright.[593]

Piezo-oscillator Circuits

Scheibe,[B45] Bechmann,[31,33,36,38,43] Benson,[50] Boella,[58] Booth,[69] Borsarelli,[72] Builder and Benson,[82] Cady,[104] Harrison,[206,207] Hayasi and Akasi,[211] Heegner,[216] Hight and Willard,[227] Jackson,[244] Kishpaugh and Coram,[260] Koga,[268,280] Koga and Yamamoto,[284] Koga, Yamamoto, Nisio, Harasima, and Ikezawa,[285] Kusunose and Ishikawa,[297] Lack,[298] Lamb,[300,301] [the "tritet" oscillator, for which see also I. Koga and W. Yamamoto, *Electrotech. Jour.* (*Japan*), vol. 4, pp. 110–115, 1940] Lamb,[302] Llewellyn,[318] MacKinnon,[324] Meacham,[357] Meahl,[358] Nelson,[390] Pavlik[408] Pinciroli,[425] Pontecorvo,[429] Poppele, Cunningham, and Kishpaugh,[430] Sabaroff,[443] Takagi and Nakase,[502] Vecchiacchi,[561] Wheeler and Bower.[583]

Performance of Piezo Oscillators, Dependence of Frequency on Circuit Conditions

Hund,[B27,B28] Moullin,[B37] Scheibe,[B45] Vigoureux,[B51] Amari,[2] Anderson,[3] Antseliovich,[6,7] Boella,[56,57] Booth,[69] Booth and Dixon,[70] Borsarelli,[72] Brown and Harris,[77] Builder,[80] Builder and Benson,[82] Dye,[127] Goodman,[179] Heegner,[215,216] Hight and Willard,[227] Hovgaard,[235] Koga,[268,274] Koga and Shoyama,[282] Lamb,[302] MacKinnon,[324] Namba and Matsumura,[388] Sabbatini,[444] Thurston,[520] Vecchiacchi,[560,562] Watanabe.[581]

Piezo Oscillators for very High Frequencies

Fair,[141] Fox and Underwood,[148] Gramont and Béretzki,[186] Kamayachi and Watanabe,[249] Koga,[278] Mason and Fair,[341] Osterberg and Cookson,[403] Uda, Honda, and Watanabe.[538]

Frequency Standards and Quartz Clocks

Scheibe,[845] Vigoureux,[850,851] Essen,[139] Gramont,[182] Jimbo,[248] Koga,[277] Marrison,[330,331] Mason,[336] Vecchiacchi.[562]

Adelsberger, U.: Equipment for Emission of Standard Frequencies from the German Transmitter, *Hochfrequenztech. Elektroakustik*, vol. 53, pp. 146–150, 1939.

Adelsberger, U.: Very Accurate Measurements of Time and Frequency, *Elek. Nachr.-Tech.*, vol. 12, pp. 83–91, 1935.

Clapp, J. K.: "Universal" Frequency Standardization from a Single Frequency Standard, *Jour. Optical Soc. Am.*, vol. 15, pp. 25–47, 1927.

Clapp, J. K., and J. D. Crawford: Frequency Standardization, *QST*, vol. 14, pp. 9–15, March, 1930.

Decaux, B.: Measurements of Frequency at the Laboratoire National de Radioélectricité, *L'Onde élec.*, vol. 15, pp. 411–439, 1936.

Dobberstein, H.: On the Performance of Two Commercial Quartz Clocks, *Z. Instrumentenk.*, vol. 61, pp. 188–191, 1941.

Dobberstein, H.: Small Quartz Clocks, *Z. Instrumentenk.*, vol. 62, pp. 296–301, 1942.

Essen, L.: International Frequency Comparisons by Means of Standard Radio-frequency Emissions, *Proc. Roy. Soc. (London)*, vol. 149, pp. 506–510, 1935.

George, W. D.: Production of Accurate One-second Time Intervals, *Jour. Research Nat. Bur. Standards*, vol. 21, pp. 367–373, 1938.

Hall, E. L., V. E. Heaton, and E. G. Lapham: The National Primary Standard of Radio Frequency, *Jour. Research Nat. Bur. Standards*, vol. 14, pp. 85–98, 1935.

Harnwell, G. P., and J. B. H. Kuper: A Laboratory Frequency Standard, *Rev. Sci. Instruments*, vol. 8, pp. 83–86, 1937.

Jatkar, S. K. K.: Absolute Frequency of Piezoelectric Quartz Oscillators, *Jour. Indian Inst. Sci.*, vol. 22A, pp. 1–17, 1939.

Loomis, A. L.: Precise Measurement of Time, *Monthly Notices Roy. Astron. Soc.*, vol. 91, pp. 569–575, 1931.

Loomis, A. L., and W. A. Marrison: Modern Developments in Precision Time-keepers, *Electrical Engineering*, vol. 51, pp. 542–549, 1932.

Meacham, L. A.: High-precision Frequency Comparisons, *Bridge of Eta Kappa Nu*, vol. 36, pp. 5–8, February–March, 1940.

Mickey, L., and A. D. Martin: Development of Standard Frequency Transmitting Sets, *Jour. Research Nat. Bur. Standards*, vol. 12, pp. 1–12, 1934.

Rohde, L., and R. Leonhardt: Quartz Clock and Standard Frequency Generator, *Elek. Nachr.-Tech.*, vol. 17, pp. 117–124, 1940.

Scheibe, A.: Quartz Clocks: Constructional Outline, Rate and Frequency, *Arch. f. tech. Messen*, part 122, sheets T114–115, 1941.

Scott, H. J.: A Precise Radio-frequency Generator, *Bell Labs. Record*, vol. 11, pp. 102–108, 1932.

Stansel, F. R.: A Secondary Frequency Standard Using Regenerative Frequency-dividing Circuits, *Proc. I.R.E.*, vol. 30, pp. 157–162, 1942.

Tomlinson, G. A.: Recent Developments in Precision Time-keeping, *Observatory*, vol. 57, pp. 189–195, 1934.

Vigoureux, J. E. P., and H. E. Stoakes: All-electric Clock, *Proc. Phys. Soc. (London)*, vol. 52, pp. 353–357, 1940 (discussion pp. 357–358).

Wheeler, L. P., and W. E. Bower: A New Type of Standard Frequency Piezoelectric Oscillator, *Proc. I.R.E.*, vol. 16, pp. 1035–1044, 1928.

Crystals in Frequency Modulation

Doherty,[125] Koga,[284] Morrison.[275]

Tourmaline Oscillators

Awender and Bussman,[14] Booth and Dixon,[70] Fox and Underwood,[148] Heierle,[218] Kühnhold,[291] Leithaüser and Petrzilka,[314] Matsumura and Ishikawa,[348] Matsumura, Ishikawa, and Kanzaki,[349] Osterberg and Cookson,[403] Petrzilka,[419] Straubel.[487,489,494–496]

CHAPTER XX

ROCHELLE SALT: HISTORY, GENERAL PROPERTIES, AND TECHNIQUE

And thou, Rochelle, our own Rochelle, proud
city of the waters,
Again let rapture light the eyes of all thy
mourning daughters.
As thou wert constant in our ills, be joyous
in our joy;
For cold, and stiff, and still are they who
wrought thy walls annoy.

—MACAULAY.

402. Summary of Properties. Rochelle salt (*sel de Seignette*) is so important as a dielectric on both theoretical and technical grounds that it will be considered somewhat at length. Like quartz, Rochelle salt is enantiomorphous, but it is usually of the right-handed form, produced from the natural tartaric acid of grapes. Tartaric acid occurs chiefly in the dextro form, although the levo form as well as the optically inactive mesotartaric and racemic acids can be produced artificially. Together with a few other more or less related crystals Rochelle salt possesses properties so unique that they are sometimes given a special name, the *Seignette-electrics* (the terms "ferroelectric" and "Rochelle-electric" are also found in the literature).

In this summary we shall consider only Rochelle salt itself. Its outstanding feature, which pointed the way to the discovery of other remarkable properties, is the huge piezoelectric effect, unapproached by any other known substance. Notwithstanding its rather poor mechanical strength and low temperature of disintegration (55°C), Rochelle salt finds important applications, especially in the field of acoustics. Of chief scientific interest are its electric anomalies.

These anomalies are confined to effects observed with fields in the X-direction and shearing stresses in the YZ-plane. The piezoelectric constants d_{25} and d_{36}, though larger than for most other crystals, exhibit no special peculiarities, nor do the dielectric constants for the Y- and Z-directions, both values of the latter being in the neighborhood of 10 and having small temperature coefficients.

For electric fields in the X-direction the dielectric properties of

Rochelle salt exhibit the much discussed *ferromagnetic analogy*. Just as iron and other ferromagnetics are characterized by maximum permeability at a certain temperature—the Curie point, above which the permeability decreases rapidly—so in Rochelle salt there is also a critical temperature, called by analogy the "Curie point,"* at which a similar change takes place in the dielectric constant k_x' of the free crystal. In iron the Curie point is around 770°C, while for Rochelle salt it is about 24°C, only slightly above room temperature. By analogy with the ferromagnetic and paramagnetic states of iron below and above 770°C, respectively, the terms "Seignette-electric" (or "Rochelle-electric," or "ferroelectric") and "parelectric" are applied to the corresponding states in Rochelle salt. In contrast to iron, however, the Seignette-electric state is confined to the region between approximately −18°C and +24°C. The lower critical temperature is called the "lower Curie point"; like the upper Curie point, it is characterized by a maximum in the dielectric constant k_x' of the free crystal.†

In the Seignette-electric region the relation between polarization and field is non-linear, and the crystal shows dielectric hysteresis. The strictly parelectric state, in which hysteresis disappears and the polarization is proportional to the field, is found only above +32° and below −26°C. Between these temperatures and the Curie points the properties of the crystal are somewhat affected by the nearness of the Seignette-electric region. We shall designate the upper and lower Curie points by θ_u and θ_l, respectively. It will be shown later that the values of these temperatures are changed by mechanical constraint and by the application of hydrostatic pressure.

403. Some of the principal features of the piezoelectric and dielectric properties will now be further summarized.

The Direct Piezoelectric Effect. By the static methods that have usually been employed, widely varying values of d_{14} have been observed, depending not only on temperature, but on the electrodes, surface impurities, previous history of the specimen, and certain effects of lag and fatigue as well. Between the Curie points the curve relating polarization with stress shows saturation at large stresses (the effective stress is Y_z, although by the usual technique this shearing stress is brought about by compression of the specimen in a direction bisecting the angle between the Y- and Z-axes). Near the Curie points, values of d_{14} as high as $26{,}000(10^{-8})$ have been reported.

The Converse Effect. Experimental data are more complete and con-

* The term "Curie point" was first used with reference to Rochelle salt by Valasek [542]

† As will be seen later, the maxima in k_x' at the Curie points are observed only with relatively weak fields.

sistent than with the direct effect. The curves relating strain with field between the Curie points are quite similar to the dielectric polarization and hysteresis curves. Outside the Curie points the strain: field relation is linear. In general, the values of d_{14} derived from the converse effect have been found to be several times greater than those from the direct effect.

Dielectric Properties. Between the Curie points, hysteresis is observed in the relation between P_x and E_x. Over most of this region the reversible portion (first, or initial, stage) extends to the order of ± 50 volts/cm, for frequencies from around 200 to 10,000 cycles/sec. In this initial stage the initial susceptibility $\eta_0 = P_x/E_x$ is practically independent of E_x, varying only with temperature.* As the amplitude of E_x is increased, the second stage enters in: domains tend to become polarized in the same direction, the virgin curve turns steeply upward, and the hysteresis loop has steeply sloping sides. It is here that the greatest values of the permittivity k_x are found (up to 200,000; what is observed is here the *differential* value k_d, §430). Then at $E_x \sim 150$ comes the knee of the polarization curve, followed by the region of saturation (third stage), in which the differential susceptibility is approximately the same as the initial η_0. Different specimens give different results at small E_x, perhaps owing to differences in domain structure, but they usually agree fairly well in the saturation region. The hysteresis loops are broadest in the neighborhood of 0°C, gradually becoming narrower and smaller as the Curie points are approached, where hysteresis disappears. For several degrees outside the Curie points, however, the $P:E$ relation remains non-linear. At very low frequencies, and especially under static fields, the second stage begins at smaller values of E_x. Under these conditions the effects of lag and fatigue are observed both in dielectric observations and in measurements of the converse piezoelectric effect, just as with the direct effect.

When observations, by bridge or oscillograph, are made at increasingly high frequencies, the dielectric constant is found to decrease progressively, with an anomaly at each resonant vibrational frequency of the crystal. The value at radio frequencies so high that the wavelength λ is small in comparison with the dimensions of the crystal can be taken as a measure of k_x'' for a clamped crystal; it is of the order of 100 except close to the Curie points, where it rises to a value around 230. The effects of periodic deformation of the crystal are then practically eliminated. For it must be remembered that at frequencies for which λ is of the order of the crystal dimensions, even when the crystal is not vibrating in resonance, it is still in a state of forced vibration, and the piezoelectric reaction increases the value of k_x above that for a clamped crystal. It is this piezo-

* For the sake of simplicity we here omit the subscript x from the symbol η.

electric reaction, for example, that accounts for the rapid increase in k_x with field along the sides of the hysteresis loop.

When the crystal specimen is more or less constrained, as by mechanical clamping, the values of d_{14} and of k_x are reduced. The hysteresis loop becomes smaller and is greatly deformed, the area of the loop finally vanishing when the clamping stress becomes sufficiently great. An interesting feature is that the slope of the *initial* part of the polarization curve is not altered by pressure, although it includes a wider range of field than when the crystal is free. It is also found that the more completely a crystal is clamped, the less are its electrical and elastic properties affected by temperature.

This last fact is of importance in connection with many technical applications of Rochelle-salt crystals, in which the freedom of the crystal to deform itself in the field is to some extent inhibited. The result of such constraint is to make the crystal less temperature sensitive; and although under such conditions the extremely high values of d_{14} of which Rochelle salt is capable cannot be realized, still they are large enough for practical purposes.

The thermal, optical, elastic, and electrical properties of Rochelle salt, especially at the Curie points, have been objects of much study and speculation. In the foregoing paragraphs we have touched only on some of the outstanding electric and piezoelectric features. In Chaps. XXIII and XXIV it will be seen that at the Curie points the piezoelectric constant d_{14}, the dielectric constant k'_x of the free crystal, and the elastic compliance s_{44} (all at small fields) become, theoretically, infinitely great.

The Domain Structure of Rochelle Salt. The best evidence indicates that a Rochelle-salt crystal, like iron, is made up of distinct domains, each of which possesses, between the Curie points, a *spontaneous electric polarization* having a flat maximum of about 740 esu at 5°C, diminishing to zero at θ_u and θ_l. Some of the domains are polarized in one direction, some in the other, along the X-axis. The domains appear to be of the order of a centimeter in size, enormously greater than those in iron. The spontaneous polarization is accompanied by a spontaneous strain.

In the following chapters the properties of Rochelle salt will be discussed in more detail, and an attempt will be made to correlate some of the chief results of various investigators. The theoretical aspects of the Seignette-electric crystals are summarized in §471.

404. Historical. In 1672 Pierre de la Seignette, an apothecary of La Rochelle on the coast of France, produced a new salt of tartaric acid. According to Macquer's "Dictionnaire de chymie," published in Paris in 1777, this substance came to be known as *sel de Seignette, sel polycreste,*

tartarus natronatus, or *sel de la Rochelle.* From the same source* we learn that

"Ce sel a été d'abord composé pour l'usage de la Médecine à l'imitation du tartre Soluble ordinaire ou sel végétal, par M. Saignette, Apothicaire de la Rochelle, qui l'a mis en grande vogue, & qui l'a tenu secret tant qu'il a pu. MM. Boulduc & Geoffroy en ayant depuis découvert & publié la composition, tous les Apothicaires ont commencé dès-lors à faire du sel de Saignette, exactement le même que celui de la Rochelle."

While the medicinal virtues as well as the chemical properties of Rochelle salt became universally recognized, nothing remarkable in its physical properties seems to have been observed until 1880. In that year the Curie brothers included it in their first pioneer researches on the piezoelectric effect.

The first quantitative measurements of the piezoelectric effect in Rochelle salt were made in 1894 by Pockels; his results are not in bad agreement with those of later observers. In the course of his experiments, Pockels also discovered the Kerr effect in this crystal, as well as the anomalous dielectric behavior in the *a*-direction. Unfortunately, there had appeared previously a paper by Borel, giving low and quite normal values for all three dielectric constants, which seems to have held the question of the anomaly in abeyance for a quarter of a century.

Interest in the physical properties of Rochelle salt, from the standpoint of their application in h-f underwater signaling, was revived in 1917. Investigations in this country were made independently by J. A. Anderson, A. M. Nicolson and the author.

In the work of Anderson and the author, experiments were performed with tin-foil-coated *X*-cut 45° plates cut from crystals that were grown by R. W. Moore (§412). Each observed the deflection of a ballistic galvanometer as a function of applied electric and mechanical stresses, together with the fact that marked differences exist between individual plates, even from the same crystal. Anderson found the polarization to depend upon the sign of the applied voltage and also upon the sign of the mechanical stress. This was the first observation of what is now known as the unipolarity of Rochelle salt (§433). He also made the first record of hysteresis effects with Rochelle salt. Among his most significant results was the fact that the ballistic throw upon application of a given electric field was increased by mechanical pressure up to a certain value of the pressure and that above this point the throws, for the same field, diminished.

In this laboratory the wet-thread method was used for cutting Rochelle-salt crystal plates.† The author's chief experimental results were as follows: For the first time, Young's modulus was determined for stresses at 45° to the *Y*- and *Z*-axes, from observations on vibrating rods. The dielectric constant, for *X*-cut plates at

*Vol. 3, p. 122.

†The suggestion that led to this device, which has since been widely used, originated with one of the author's students, P. E. Eckstorm.

high frequency, was found to be around 80. The importance was noted of having the electrodes closely adherent. Piezoelectric fatigue caused by mechanical stress and recovery on application of an electric field or after baking at 55°C were observed. A decrease was found in the piezoelectric effect in the neighborhood of 23°C (first observation of the Curie point). It was found that different plates under various conditions gave values of d_{14} from 3.4 (10^{-8}) to 40 (10^{-8}), thus foreshadowing the enormous values found by later observers.

The anomalous behavior of Rochelle salt as revealed in these two investigations is for the most part explained in the light of the investigations discussed in later chapters.

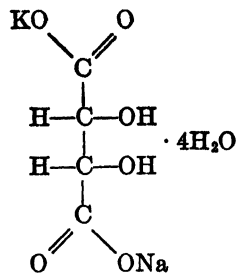
The first descriptions of technical applications of Rochelle-salt crystals, with information on the properties and methods of producing crystals, were published by A. M. Nicolson in 1919. Nicolson's crystals were of the composite, or "hourglass," type, produced by the rapid cooling of a saturated solution. His experiments were with entire crystals, and he laid great emphasis on treatment with alcohol and heat. Although this type of crystal preparation is now obsolete, his papers are of interest in so far as they record some of the earliest observations of the electric response to various stresses and the converse; the dependence of the reactance of Rochelle-salt crystals on frequency; and the evidence of hysteresis.

These early investigations were followed a few years later by a series of important papers by J. Valasek, in which the characteristic dielectric and piezoelectric properties were very thoroughly treated, although some of his conclusions have been subject to revision. It was he who introduced the term "two Curie points" for Rochelle salt. His most important contribution was the pioneer work on the analogy between the dielectric properties of Rochelle salt and ferromagnetism, an idea that seems to have been first conceived by W. F. G. Swann.

Widespread interest in the internal properties and structure theory of this substance began about the year 1929. Initial impetus came from the Physical-Technical Institute in Leningrad, through the publications first of Shulvas-Sorokina, later of I. Kurchatov and his collaborators. This has been followed by many investigations, both theoretical and experimental, outstanding among which are those of Scherrer and his associates in Zurich, of Fowler in England, and of Mueller and Mason in this country.

Recently the investigations have been extended to "heavy-water" Rochelle-salt crystals containing deuterium oxide in place of ordinary water.

405. General Chemical and Physical Properties. Rochelle salt, or sodium potassium tartrate tetrahydrate, is the sodium potassium salt of tartaric acid with four molecules of water of crystallization. Its formula is $NaKC_4H_4O_6 \cdot 4H_2O$.



As the structural formula indicates, the molecule, and hence the crystal, is enantiomorphous. Since only the dextro form of tartaric acid occurs commonly in nature, it is in general true that all Rochelle salt crystals are right-handed. All data here presented refer, therefore, to the so-called "*d*-Rochelle salt" (dextro). Hence there is no twinning of the Brazil type (§15) in Rochelle-salt crystals, as is so often the case with quartz.

The molecular weight of Rochelle salt is 282.184; the density at 25°C is 1.775 ± 0.003 (W. P. Mason[335,*]). The solubility per liter of water at 0°C is 1.50 moles (420 g.); at 30°, it is 4.90 moles (1,390 g). It has been stated by Hedvall† that the velocity of solution undergoes an abrupt change at the upper Curie point. The growth of crystals from solution must take place at temperatures below 40°C, since above this temperature sodium tartrate is deposited. The crystal itself changes at 55.6° to a mixture of Na and K tartrates and their saturated solution, and at 58° these salts are completely dissolved in the water.‡ This is what has commonly been referred to as the "melting" of the Rochelle-salt crystal. The process is irreversible.

For the axial ratio and structure of Rochelle salt, see §542.

406. *Etch Figures on Rochelle Salt.* The following account of tests made by the author may be helpful in determining the axial directions in plates cut from this crystal. Very characteristic figures are easily produced by lightly moistening a polished surface. When being dried, a face normal to the *X*-axis is found to be covered with fine striations parallel to the *Z*-axis. On faces normal to the *Y*- and *Z*-axes minute rectangular pyramids ("etch hills"), sometimes truncated, extend upward from the surface. Some characteristic forms for the *XY*-plane are shown in Fig. 104, as seen from above. The *X*-axis bisects the projection on the *XY*-plane of the acute angle α, which has a value of roughly 60°. On a

* The estimate of precision was kindly furnished by Dr. Mason. Within the probable error the value given above holds from 15 to 35°C.

† In a discussion of P. Scherrer's paper.[451]

‡ J. Docters Van Leeuwen, Z. physik. chem., vol. 23, pp. 33–55, 1897; J. F. G. Hicks and J. G. Hooley, *J. Am. Chem. Soc.*, vol. 60, pp. 2994–2997, 1938.

face normal to the Y-axis the pyramids are of the same general nature as in Fig. 104, the longer dimensions of the base being in most cases parallel to the Z-axis.

Owing to the strong polarity in the X-direction, one might expect marked differences in the etch figures on opposite sides of an X-cut plate. On the contrary, the striations look just alike. It was hoped that the domain structure might be revealed by the arrangement of the etch figures, especially on the X-faces. All that can be said at present is that a cursory examination gives no indication of domains. It is possible that a minute inspection, perhaps with the aid of the rodometer, would yield positive results.

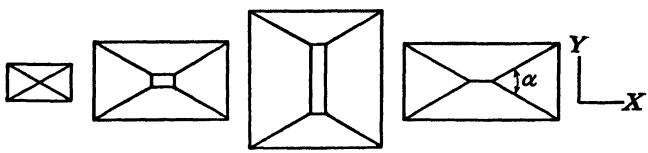


FIG. 104.—Etch figures on a Rochelle salt surface normal to the Z-axis. In each case the X-axis is horizontal, the Y-axis vertical.

407. *Thermal Expansion.* Observations by Vigness[566] indicate an almost exactly linear dependence of dimension upon temperature along each of the three crystallographic axes. The only peculiarity is a very slight bend at the upper Curie point for the Y- and Z-directions, for which there is no obvious explanation. Vigness's expansion coefficients have the following values: in the X-direction, 12 to 35°C, $58.3(10^{-6})$; Y-direction, 12 to 24°C, $35.5(10^{-6})$, 24 to 35°, $39.7(10^{-6})$; Z-direction, 14 to 24°C, $42.1(10^{-6})$, 24 to 35°, $43.6(10^{-6})$. The coefficient of *volume* expansion calculated from these data is approximately 0.00014. Earlier observations by Valasek[543] are in fair agreement with those of Vigness.

On the other hand, Hablützel[198] does not find this normal behavior. In particular, he finds an anomaly in the direction bisecting the Y- and Z-axes, which, as will appear in §482, can be understood as a converse piezoelectric effect due to the spontaneous polarization.* Hablützel also recorded certain anomalies in the X-direction, a possible explanation of which will be found in §464.

To some degree these discrepancies may also be due to different electrical states of the crystals used by different observers in their measurements of thermal dilatations. According to §199, the value of the strain caused by a given stress depends on whether or not the electrodes attached to the crystal are short-circuited. Since a thermal strain may be regarded as the result of thermal stress, it follows that reproducible results can be

* This anomaly had been predicted by E. P. Harrison (*Nature*, vol. 120, p. 770, 1927).

attained only when the specimen is maintained in a definite electrical state. It can usually be assumed that thermal observations take place so slowly that the surface of the specimen is substantially equipotential at all times.

The *thermal conductivity* of Rochelle salt is several times lower than that of quartz.*

408. *The Dielectric Constants in the Y- and Z-directions.* According to Table XIV (page 162), crystals of the rhombic system have three principal dielectric susceptibilities η_{11}, η_{22}, η_{33}. Different values of the permittivities k_x, k_y, k_z along the crystallographic axes are therefore to be expected. k_x, the *enfant terrible*, will be dealt with in later sections. Concerning k_y and k_z the data are fairly consistent and indicate no anomalies. Mueller[376] recorded values of $k_y = 10$, $k_z = 9.6$, with temperature coefficients +0.007 for k_y, +0.003 for k_z. Measurements over a wide range of temperatures have been made by Hablützel.[199] He finds the values for ordinary and heavy-water Rochelle salt to be almost identical. From −180° to +40°C his value of k_y increases pretty uniformly from 6 to 10, with a flat region between the Curie points. Over the same temperature range k_z increases from about 5.3 to 10. At 20°C, $k_y \approx 9.4$ for both forms of Rochelle salt; the values of k_z are 9.5 and 9.8, respectively, for ordinary and heavy-water Rochelle salt. The temperature coefficients are of the same order of magnitude as those of Mueller.

Probably the best values at present are those of W. P. Mason,[B35] for which, unfortunately, the only datum concerning temperature is that the values "vary little with temperature."

Mason's values are to be recommended for use at ordinary temperatures.‡

$$k_y' = 9.8 \qquad k_z' = 9.2 \tag{488}$$

The primes indicate that these values are for *mechanically free* crystals. The corresponding susceptibilities from the equation $k' = 1 + 4\pi\eta'$ are

$$\eta_y' = 0.70 \qquad \eta_z' = 0.65 \tag{488a}$$

The susceptibilities η_y'' and η_z'' for *clamped* crystals are found from Eq. (262), together with values of d_{25}, d_{36}, e_{25}, and e_{36} from §141:

$$\eta_y'' = 0.63 \qquad \eta_z'' = 0.64 \tag{488b}$$

* From unpublished observations by Dr. H. Jaffe at the Brush Development Company.

‡ Since writing this section the author has been informed by Dr. Mason that his most recent determination of k_y' yields a value somewhat greater than the one quoted here. From observations of the frequency of a *Y*-cut 45° bar he finds for k_y' the value 11.1 from −10° to +24°C, followed by a linear increase to 12.5 at 45°C.

409. *Anomaly in the Specific Heat.* Just as ferromagnetic theory led to the expectation of a sharp rise in the specific heat of iron at the upper Curie point (§556), which has been fully verified, so by the analogous argument several investigators have looked for a corresponding effect with Rochelle salt. It is easy to prove that, while an anomalous value of specific heat is to be expected in the neighborhood of either Curie point, the theoretical magnitude is extremely small. As in the case of ferromagnetism, the increase above the normal value of the specific heat c at the Curie point is

$$\Delta c = \frac{\gamma}{2} \frac{\partial P_0^2}{\partial T} \text{ erg cm}^{-3} \text{ deg}^{-1}$$

where γ is the internal field constant, P_0 the spontaneous polarization, and T the temperature. From his data on the variation of P_0 with T, Mueller[382] finds that this expression, for Rochelle salt at the upper Curie point, reduces to

$$\Delta c = 4.0\gamma(10^4) \text{ erg cm}^{-3} \text{ deg}^{-1} = 0.15\gamma \text{ cal mole}^{-1} \text{ deg}^{-1}$$

At the lower Curie point the theoretical value is a little greater, with sign reversed.

For any reasonable value of γ, these theoretical values are very small. This fact was confirmed by the very careful observations of A. J. C. Wilson,[588] who measured the specific heat of Rochelle salt from $-30°$ to $+30°$C. He found that this quantity could be well represented by the equation $c = 1.290 + 0.0031t$ joule g^{-1} deg^{-1} (t in degrees centigrade) for single crystals; the mean deviation of individual points was 0.3 per cent. At the lower Curie point a small anomaly in the right direction was found, the value of Δc amounting to somewhat less than 1 cal mole^{-1} deg^{-1}. No anomaly at the upper Curie point could be detected by the calorimetric method used; these observations indicate that if any exists it must be much smaller than 1 cal mole^{-1} deg^{-1}.* When these results are compared with Mueller's expression for Δc above, it appears that γ is of the order of magnitude of 1, and certainly not appreciably greater than the Lorentz factor $4\pi/3$.

As to the absolute value of c, Wilson's value is about 11 per cent smaller than that of Rusterholz,[441] but it agrees within one-half of 1 per cent with the value given by Kobeko and Nelidov.[264] The "International Critical Tables" give 1.37 joule g^{-1} deg^{-1} ± 2 per cent as the specific heat of Rochelle salt.

The specific heat of Rochelle salt from 15 to 340°K has been investi-

* Observations on the specific heat of Rochelle salt by Wildberger are in agreement with these findings (A. Wildberger, Diplomarbeit, Zurich, 1938; cited by P. Scherrer, *Z. Elektrochem.*, vol. 45, p. 173, 1939).

gated by Hicks and Hooley.* They find a sudden change at the decomposition point at 328.78°K (55.6°C, §405), but no anomaly at either Curie point.

410. *Electrical Conductivity and Dielectric Strength; Magnetic Properties.* The values of conductivity for the X-direction given in Table XXXIII were obtained by Valasek[542,543] using direct current. From $-65°$ to $+35°$, field strengths up to 10,000 volts/cm were used; the remaining data were obtained with a Wheatstone bridge at low voltage. After tin-foil electrodes had been attached with shellac to the well-dried crystal, the whole was coated with paraffin.

TABLE XXXIII

Temperature, Deg C	Conductivity, Mho cm^{-1}
−65	2.0×10^{-14}
−40	3.6×10^{-14}
−20	5.4×10^{-14}
0	9.0 and 5.0×10^{-14}
+20	22.0 and 11.0×10^{-14}
30	11×10^{-13}
35	1.0×10^{-11}
43	5.0×10^{-9}
47	3×10^{-8}
49	5×10^{-8}
51	5×10^{-7}
53	6×10^{-5}
54	1.7×10^{-4}
57 and over	5×10^{-4}

The two values at 0° and +20° were obtained by reversing the emf and are related to the unipolarity of the crystal (prevalence of domains polarized in one direction: see §433). Somewhat higher values of conductivity were recorded by B. and I. Kurchatov[293]; from data in Oplatka's paper[397] it appears that his crystals had a conductivity thousands of times greater than Valasek's. Moisture on the surface can affect the apparent conductivity enormously. On the other hand, a dehydrated surface or a layer of cement between crystal and electrode may cause the observed conductivity to be much too low. This was probably not the case with Valasek's data in Table XXXIII, since his values agree approximately with those obtained at the Brush Laboratories.† Moreover, the anomalous values in the region of spontaneous polarization could hardly have been so pronounced if the high resistance had been due chiefly to the shellac. From Table XXXIII it follows that at room temperatures, with a dielectric constant of 10^3, several minutes would be required

* J. F. G. HICKS and J. G. HOOLEY, *J. Am. Chem. Soc.*, vol. 60, pp. 2994–2997, 1938.

† The author is indebted to the Brush Laboratories for this information.

for the charges to fall to half values if there were no other leakage than that through the body of the crystal.

It is probable that the data in Table XXXIII are not representative of Rochelle salt exposed to the air under ordinary conditions.

Between the Curie points, the observations of hysteresis may be complicated by conduction effects. If the humidity is excessive, both the height and the width of hysteresis loops are increased, and the tips of the loops tend to become rounded off. The latter effect can be detected on some of the oscillograms shown in later paragraphs. Observations of dielectric constant, coercive field, and dielectric losses can easily be somewhat falsified by the presence of leakage.

According to Vigness[566] exposure to X-rays causes a roughening of the surface as well as a yellow coloration.

Mueller finds that a properly annealed and dried crystal (§415) has a *dielectric strength* in air better than 20 kv/cm. No such value as this can be depended on for plates that are not carefully prepared. Naturally the danger of breakdown is very greatly increased if even the minutest flaws are present. According to Gorelik* a Rochelle-salt plate under oil at high hydrostatic pressure will withstand 600 kv/cm.

Magnetic Properties. Rochelle salt is diamagnetic. The only measurements appear to be those of Lane,[303] who finds the magnetic mass susceptibility to be $-0.54(10^{-6})$ in all directions, independently of temperature. This value does not vary more than 0.25 per cent between 10 and 30°C. Thus the "ferromagnetic analogy" of Rochelle salt does not involve any *magnetic* anomaly.

411. *Requirements for Reproducible Results.* Among the following, requirements 2 and 3 should always be observed. The others are important chiefly in measurements of precision.

1. Homogeneous crystal material. The crystal should be crystallographically and optically as perfect as possible, free from the flaws mentioned in §414.

2. Clean and smooth surfaces, well dried, yet with surface layers not deprived of their water of crystallization. The drying is of importance to avoid surface conduction; on the other hand, the material close to the surface should not become a dehydrated layer of relatively low dielectric constant. For example, if $k_x = 10{,}000$ for the crystal and if a dehydrated or otherwise damaged surface layer only 0.001 mm thick has $k_x = 10$, the thickness of the crystal being 10 mm, the measured value of k_x will be in error by 10 per cent.

3. From the foregoing paragraph it follows that the electrodes should make extremely close contact with the crystal in order that the applied

* B. Gorelik, Electric Breakdown in Rochelle Salt, *Jour. Tech. Phys.* (*U.S.S.R.*), vol. 10, pp. 369–375, 1940.

potential drop shall be impressed on the crystal, and not largely on the surface layers.

4. Freedom from mechanical stresses caused by electrodes or mounting. This requirement is due to the piezoelectric sensitiveness and to the close interaction between piezoelectric and dielectric effects.

5. Constant and uniform temperature. Rochelle salt is very sluggish in attaining equilibrium (§427) so that for reproducible results it may be necessary, after a change in temperature, to wait several hours before making observations.

The means of fulfilling these requirements as completely as possible, together with further technical details, will now be discussed. Their disregard undoubtedly accounts for many of the discrepancies between the results of the different observers.

412. *Production of Rochelle-salt Crystals.* Rochelle-salt crystals are always grown from a solution. Supersaturation may be caused by cooling or by evaporation. In the latter case, the solution may be either placed in a desiccator or subjected to reduced pressure. Although the cooling method is more commonly employed and seems to be the only one used on a commercial scale, nevertheless for scientific purposes the evaporation method is to be preferred, since the temperature may be held approximately constant, internal elastic stresses being thus avoided.

Crystallization by cooling. R. W. Moore* produced very beautiful and perfect Rochelle-salt crystals, measuring several centimeters in the smallest dimension, by suspending one or more minute Rochelle-salt-crystal "seeds" in a jar of solution, which in turn was placed in a larger jar of water provided with electric heater and thermostat. The temperature was allowed to drop 0.1°C per day at first, the rate increasing to 0.6° per day as the crystals grew. The same process is also described in detail by Schwartz.[454,] † For the suspension, silk threads have commonly been used, although Hiltscher[228] used a fine silver wire. Hiltscher also caused the seed to rotate slowly in the solution.

The largest and most flawless Rochelle-salt crystals hitherto recorded are produced by the Brush Development Company.‡ According to the patent specifications, seeds, often several centimeters long, are laid in a depression on the bottom of a tank of saturated solution, which is very slowly rocked about a horizontal axis. The solution is saturated at 35°C but is heated to a somewhat higher temperature before the cooling process commences. Crystallization is more rapid if a suitable hydrogen-

* R. W. Moore, *Jour. Am. Chem. Soc.*, vol. 41, p. 1060, 1919; U.S. patent 1,347,350.

† See also H. Hinz[229] and P. Vadilov (*Jour. Expil. Theoret. Phys. U.S.S.R.*, vol. 6, pp. 496–500, 1936) for comparison of various methods.

‡ B. Kjellgren, U.S. patents 1,906,757 and 1,906,758 (also reissues 19,697 and 19,698).

ion concentration is maintained, for example, by the addition of KOH or of NaOH, corresponding to one-tenth normal solution. Sugar or formaldehyde is also sometimes added. It is found that growth takes place most rapidly in the direction of flow of the liquid, and the seed is also correspondingly oriented in order to have the long dimension of the finished crystal parallel to the desired axis. Seeds are usually placed with their X-axes vertical; each finished crystal is in the form of a long prism parallel to the Z-axis. The crystallizing process requires several days, the temperature being allowed to fall gradually and uniformly by thermostatic control. On being taken from the bath, the crystal may be rinsed with dilute alcohol and dried with a soft cloth. Single crystals weighing more than 2 kg have been grown by this method.

The method of Christopher* may also be mentioned, according to which a seed, suitably oriented, is placed in a Rochelle-salt solution between parallel glass plates, so that the finished crystal is in the form of a flat slab. For example, if a plate of large dimensions in the Y- and Z-directions is desired, the X-axis of the seed should be perpendicular to the glass plates.

The properties of the finished crystal are of course independent of its shape and of the orientation of the seed. A crystal plate cut in any particular orientation with respect to the crystal axes will theoretically—and so far as is known also experimentally—give the same results whatever may have been the shape of the crystal as determined by conditions of growth.

Crystallization by evaporation. Kurchatov[B32] places the solution, containing a seed, in a desiccator in the presence of concentrated H_2SO_4 or P_2O_5 at approximately constant temperature. In 5 to 6 days crystals weighing about 100 g are produced. The method of Busch[87] differs from this in that the solution, which is kept at a temperature constant to within 0.01°C by means of a thermostat, is connected to a trap immersed in CO_2 snow. The rate of evaporation is controlled by varying the pressure over the solution. An initial pressure of 50 mm Hg is recommended, changing to 25 mm toward the end of the process. Several 50-g crystals are produced from such a solution in 2 weeks.

Seidl and Huber[460] use a similar method, with liquid air instead of CO_2. The Moore patent mentioned above includes a description of crystallization at constant temperature by passing a current of dry air over the solution. For Stilwell's method see §478.

Further details on the process of crystallization of Rochelle salt and other Seignette-crystals may be found in papers by Bloomenthal,[55] Busch,[88] and Hinz.[229]

* J. H. CHRISTOPHER, U.S. patent 1,746,144 (1930).

413. *The Cutting of Rochelle-salt Crystals.* Mandell[326] finds it advisable not to cut the crystals until a month has elapsed after growth. Others do not appear to have observed this precaution. Most experimenters have used a wet thread or wet stretched rubber band. Details of this procedure are given by Busch,[87] David,[119] Staub,[478] and Hinz.[229] The author, who first used this method, has had good success with the apparatus shown in Fig. 105.

A stout endless linen thread is passed four times over a system of pulleys, so that from one to four cuts can be made at a time. The presence of a single large knot where the ends are joined is avoided by splaying the fibers at each end of the thread into three slender strands. These strands are tied separately with the knots staggered. The driving pulley, fixed to the shaft at *A*, has four grooves and is itself

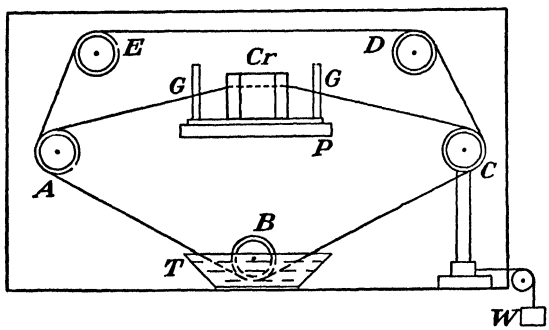


FIG. 105.—Machine for cutting Rochelle-salt crystals by means of a wet thread.

driven by a small motor at such a rate as to move the thread at a speed of about 15 cm/sec. The distance *AC* is about 40 cm If fewer than four cuts are made, the unused turns pass over idler pulleys at *D* and *E*, which are simply glass tubes on brass rods. Pulley *C* is mounted on a post, the base of which fits on a track, so that the tension can be regulated by the weight *W*. The tension should be quite large to ensure an accurate cut. The lower part of the pulleys at *B* dips slightly into water in a flat tray *T*. Across the top of the tray is a strip of wood (not shown in the figure) carrying a piece of thick felt against which the threads rub in order to wipe off excess water. The crystal *Cr* is held in place by adjustable clamps on a brass plate *P*, fastened to the back of the apparatus, and the threads are guided by vertical brass rods *GG*. It is a wise precaution to give the crystal a waterproof coating, especially on the lower surface, before clamping it in place. About half an hour is required to make a cut of 5 by 5 cm. With some crystals there is a pernicious tendency for the thread to wander from the path prescribed by the guides, as if avoiding a hard or relatively insoluble region in the interior of the crystal. As was stated in §404, the electrical and elastic properties also have sometimes been found to depend on the region from which a specimen was cut.

Rochelle-salt crystals can also be cut with a suitably constructed saw. Ordinary hack saws, whether coarse or fine, are not suitable, since they produce large chips and cracks. However, for cutting small specimens, a

jeweler's No. 6 hack saw, dry or moistened with water, is quite suitable. A band saw can also be used, if the teeth are sharp and well set, so as to make a cut somewhat wider than the thickness of the saw. An ordinary ½-in. metal-cutting saw with 14 teeth per inch, having every tooth set, has been found in this laboratory to be entirely suitable; a woodcutting blade about ¼ in. wide also gives good results. In any case, all traces of salt should be removed from the teeth after use.*

414. *Flaws in Rochelle-salt Crystals.* When visible flaws are present in Rochelle-salt crystals, they may usually be attributed to too rapid cooling or non-uniform crystallization, to some disturbance in the course of the crystallizing process, or to impurities in the solution. Flaws may appear as fine streaks or as phantom planes within the crystal, parallel to one or more of the crystallographic faces. There are no well-defined cleavage planes. With the very flawless Brush crystals, such cleavage as there is seems to take place most easily in planes approximately perpendicular to the *Z*-axis. In less perfect crystals there sometimes seems to be a tendency for cracks to start most easily in planes *containing* the *Z*-axis, so that *Z*-cut plates are the most fragile.† This is especially the case when such plates contain phantom planes, for the latter, so far as the author's experience extends, are found mostly parallel to the *Z*-axis. There may be some relation between these facts and the observation made on one occasion while a cut was being made by the wet-thread method at an angle oblique to the *Z*-axis, when the thread tended very decidedly to follow a course parallel to this axis. Moreover, it has been found that fracture, at least along phantom planes, becomes very much easier with plates that have been kept in a desiccator long enough for a large amount of superficial dehydration to take place. This seems to indicate that dehydration and consequent weakening can take place along these almost invisible flaws.

In his experiments on Rochelle salt under hydrostatic pressure, Bancroft[20] found that a sudden change in pressure, even though small, almost invariably cracked the crystal.

It is not at all impossible that some of the erratic results that have been reported for Rochelle salt are due to the presence of minute cracks or other flaws originating in the growth or treatment of the crystal. Such imperfections may be expected to affect the elastic properties and thus the electric reactions; and insofar as they introduce local peculiari-

* For a description of the band-saw method used on a large scale by the Brush Development Company, see U.S. patent 1,764,088 by C. B. Sawyer (also Canadian pat. 302,528). For large crystals, the saw here described moves with a speed of 500 ft/min; a scraper removes excess material from the teeth. It is important that the saw be at approximately the same temperature as the crystal.

† The great fragility of Z-cut plates is also mentioned by Mandell (ref. 326, p. 632).

ties in the state of hydration, they may alter the dielectric properties as well. Variable behavior on the part of the same specimen may then be brought about by changes in temperature or humidity.

A special contributing cause of the fragility of Rochelle-salt crystals probably lies in the fact that they consist of domains of varying size and of opposite electric polarization. With changing temperature these domains tend to undergo opposite shearing strains, causing large stresses at the interfaces.

415. *Grinding and Finishing of Preparations.* After a plate has been cut from the parent crystal, it usually has to be reduced to a definite size and shape, with due regard to exactness of orientation. Large specimens should be handled carefully, since cases are on record in which cracks were started from the heat of the hand.

For demonstrations, qualitative tests, and many technical applications, a very small amount of smoothing and truing suffice. Any one of several techniques may be used, provided that care is always taken not to overstress or overheat the specimens. For example, preliminary grinding may be done with rather coarse garnet paper, followed by finer garnet- or sandpaper. It is an aid both to speed and to accuracy to have the grinding paper glued to a flat disk, which can be rotated by a motor or lathe at the rate of one or two turns per second. A method preferred in this laboratory consists in the use of a 12-in. curved-tooth flat file, of the type designed for filing soft metals. By this means the surfaces can easily be made so flat and true that, except when extreme accuracy is required, little or no subsequent treatment is needed, except the final polishing.

For the local truing of crystal surfaces a razor blade is also found useful. Hinz[229] describes a special form of plane in which the cutting edge is that of a razor blade. Some workers (Körner,[287] Vigness,[565] Busch[87]) have trued their plates by rubbing them on moist ground glass.

Many procedures have been used for lapping Rochelle-salt plates. The simplest is to rub the plate on a damp, thin silk cloth stretched on a plane surface; since this process leaves the surface covered with minute etch pits, it cannot be used for optical purposes.* Staub[478] lapped the surfaces with pumice powder, finally cleansing them with pure water (for X-ray reflections); Schwartz[454] used pumice powder mixed with saturated Rochelle-salt solution; Evans,[140] fine carborundum powder and paraffin. Stamford[475] recommends rubbing the plates on a ground-glass lap, using fine pumice powder and turpentine at first, followed by methylated spirit. Holden and Mason[231] lap the surface first with carborundum and machine oil; the resulting powdery surface is dissolved

* Prof. Hans Mueller informs the author that for optical work good results are obtained by polishing the surface with optical rouge in nujol.

off in the solution used for growing crystals and warmed above the saturation point, after which a fresh surface is crystallized on for about 5 min.

One important advantage in fine lapping is that it removes minute irregularities and broken fragments that would otherwise form an undesirable layer between crystal and electrodes.

For ordinary purposes no special aging process is necessary. Earlier workers advised treatment with alcohol; for example, Valasek[544] has stated that his crystals, after immersion in alcohol, showed a great increase both in piezoelectric activity and in dielectric constant. There is, however, no indication that these values were any greater than those obtained by other observers with normal crystals. If the surface layers are dehydrated or otherwise impaired, it seems possible that alcohol treatment may increase either the conductivity or the dielectric constant close to the surface, thus yielding values more nearly characteristic of the normal crystal.

Those who experiment with home-grown crystals containing visible flaws may also find protracted soaking of the crystal or plate in very pure alcohol helpful in removing water from the flaws, since the presence of water may render the crystal practically inactive. Accidental cracks can sometimes be healed—though perhaps not permanently—by prompt application of pressure.

In order to avoid dehydration of surface layers, preparations should not be kept long in a desiccator, nor at low pressure. Disregard of this consideration doubtless accounts for some of the discrepancies in published results. There is probably no better procedure in preparation for quantitative work than that of Mueller,[376] who annealed his preparations several hours at 45°C and then dried them for 20 min over phosphorus pentoxide. This dries the surface sufficiently without causing dehydration. But if there is any possibility that the surface is dehydrated, the outer layers should be washed off before this is done.

Under normal atmospheric conditions Rochelle-salt crystals are not deliquescent, nor do they desiccate. The reason is that at room temperature the vapor pressure is only about one-third of that of pure water, while the vapor pressure of the saturated solution is somewhat less than nine-tenths of that of water.* Nevertheless, the amount of H_2O present in the crystal is quite variable; according to Valasek[541] the weight of a crystal may vary with the humidity of the surrounding air by as much as 5 per cent. Crystals and plates cut from them that have stood unprotected on cabinet shelves in this laboratory for over twenty years show no loss in transparency or sharpness of outline. Such disintegration

* H. H. Lowry and S. O. Morgan, *Jour. Am. Chem. Soc.*, vol. 46, pp. 2192–2196, 1924.

as has been observed in certain cases is due either to extremely dry air or to chemical or electrolytic action caused by contact with other materials. Plates to which metallic coatings have been cemented seem to be subject to attack, as are also plates wrapped in ordinary paper or cheap cotton batting. Crystals are not permanently injured by moist air as long as the relative humidity is below 86 per cent.

If Rochelle-salt crystals or plates cut from them are to be preserved over long periods of time, it is advisable to wrap them in very clean, soft paper or paraffin paper. Ground surfaces had best be glazed over first by treatment with water as indicated above. Plates that are not intended for use as resonators may be coated with "ambroid," shellac, rubber cement, varnish, or paraffin.* Of these, the author prefers ambroid. Some such protection is especially desirable for plates to which metal coatings are attached, since when exposed to the atmosphere the coated plates seem to disintegrate more rapidly than if left uncoated.

If it is desired to keep otherwise unprotected plates under very constant conditions, they may be sealed in a jar containing saturated solution of Rochelle salt[477,565] or in a container in which the humidity is under control; Schwartz[454] uses slightly diluted sulphuric acid for this purpose. In all such cases due regard should be given to the dependence of vapor pressure upon temperature. In a paper giving many useful technical details Körner[287] states that he coats his plates with an alcohol-free cement immediately after they have been sufficiently dried in vacuum or in a desiccator.

416. *Electrodes for Rochelle-salt Plates.* The choice of electrodes depends on the use to which the plates are to be put. For quantitative observations of the properties of the crystal it is essential, as was pointed out in §111, that the electrodes make extremely close contact with the crystal surfaces and that at the same time the crystal be free from mechanical stresses. For crystals used in acoustic applications the former of these requirements is the more important. It is important to have the electrodes cover the entire face of the crystal, since otherwise the outlying portions diminish the piezoelectric strain. The following types of electrodes have been used by different observers:

1. Finely divided metal particles. This includes molten Wood's metal or Rose metal sprayed onto the crystal (Nicolson) and evaporated silver deposited on the crystal in vacuum (Valasek). Neither process has been widely used.

2. Liquid electrodes. Körner,[287] Goedecke,[174] Schwartz[454] and Hablützel,[199] have used mercury, while Kobeko and Kurchatov[263] and Errera[134] have used saturated Rochelle-salt solution. Although this

* Special treatment of Rochelle-salt plates with a waterproof coating is described by J. H. Ream in U.S. patent 2,324,024 (1943).

method removes the possibility of a layer of low dielectric constant between electrode and crystal, still the technique involves objectionable mechanical stresses.

3. Metal-foil electrodes are most commonly used. For precise measurements the foil must be exceedingly thin to avoid mechanical constraint. Cements containing alcohol should be avoided; most of the recent experimenters have used a dilute solution of Canada balsam in xylol. Sawyer and Tower[449] used beeswax in benzol with the addition of a little rosin. Sawyer (U.S. Patent 1,994,487) recommends the addition of powdered carbon to the Canada balsam–xylol cement, to render the layer of cement conductive; his procedure is to apply the electrode, rub it down into close contact, bake at a temperature well below 55°C, and then rub again with a warm pad. A layer of colloidal graphite on the crystal, covered with metal foil, is advocated by Kurchatov and by Seidl and Huber,[460] while Valasek[544] has used amalgamated tin "squeegeed" on to the polished surfaces.*

In this laboratory it was found several years ago that a very satisfactory material for electrodes is gold leaf. The polished crystal surface is lightly moistened by breathing upon it and then brought down carefully over a horizontal sheet of gold leaf, which adheres very smoothly and firmly. The same procedure was later described by Körner[287] and Busch.[88] Aluminum leaf 0.003 mm thick has been used by the Zurich school. Electric connection with the circuit is established in various ways, for example by having the connecting wires soldered to thin, flexible metal foil, which touches the electrode lightly. It has been found that delicate contact between the gold-leaf electrode and the hairspring from a clock serves excellently; it is especially useful in h-f resonator experiments. H. Mueller[376] states that "electrodes of conducting paint, graphite or metal foil were found equally suitable and gave the same results. The tinfoil electrode, provided it is properly attached, was found most convenient."

The newest method of all, and perhaps the best, is the use of gold electrodes evaporated onto the crystal surface in vacuum, as described in §444.

In order to avoid secondary effects from stresses near the boundaries of plates, in all work of precision the electrodes should cover the entire surface. An alternative method is that of David,[119] who secured a uniform electric field and at the same time immunity from edge effects by the use of a "guard ring" kept at the same potential as the electrode proper. To this end the inner portion of each electrode is separated from the outer by a gap 0.5 mm wide. David's comparative tests show

* "Graphoil" electrodes are described by A. L. Williams in U.S. patent 2,106,143 (1938).

this precaution to be of some importance. So far as securing a uniform field is concerned, the method is not needed, since owing to the large dielectric constant, at least in the X-direction, the field is sufficiently homogeneous if the electrodes cover the entire surface.*

Owing to the interaction of dielectric and piezoelectric effects, the mounting of the crystal should be so designed as to introduce no disturbing stresses either before or after the application of an electric field. This may be accomplished by suspending the plate freely or by letting it rest on supports so located as not to hamper the deformation of the plate.

In the case of plates that are not intended for precise measurements, many of the above precautions may obviously be disregarded.

While Rochelle-salt plates of various cuts function strongly as resonators and oscillators, still on mechanical and thermal grounds it seems unlikely that they will find applications as standards of frequency.

* The use of guard rings to prevent surface leakage is described by J. P. Arndt in U.S. patent 2,289,954.

CHAPTER XXI

ROCHELLE SALT: PIEZOELECTRIC OBSERVATIONS

Sel de Seignette.—La forme hémièdre la plus ordinaire est un tétraèdre $b^{\frac{1}{2}}$; les axes d'électricité polaire sont dirigés d'un sommet de ce tétraèdre à la base opposée; ils ne coïncident donc avec aucun des axes cristallographiques; quant à leur direction exacte, nous ne l'avons pas encore déterminée: la prévoir théoriquement ne nous a pas été possible, le tétraèdre étant irrégulier, et la trouver expérimentalement demanderait une série de mesures très délicates des quantités d'électricité développées suivant des directions voisines; du reste, cela n'a pas d'importance pour la question qui nous occupe; il suffit de savoir que l'axe va du sommet à un point de la base du tétraèdre; le pôle positif par contraction est situé vers le sommet.

—P. and J. CURIE.

Piezoelectric observations fall into two general classes, according to whether they are made by means of the direct or the converse effect. The experimental investigations from various sources described in this chapter illustrate some of the anomalies of Rochelle salt and the general resemblance of piezoelectric to dielectric effects. In addition to the determinations, under various conditions, of the piezoelectric constant d_{14} recorded here, other determinations from observations with h-f vibrations will be given in later chapters.

THE DIRECT PIEZOELECTRIC EFFECT IN ROCHELLE SALT

In this chapter we are concerned mainly with stresses in the YZ-plane and polarizations in the X-direction.* So much of the published material is only qualitative, fragmentary, or obtained under questionable conditions, that reliable data with properly prepared specimens over wide ranges of stress and temperature are still lacking. From the close relationship between the piezoelectric and dielectric coefficients it is natural to anticipate a similarity between the curve of polarization vs. pressure and that of polarization vs. electric field, including the case in which the mechanical or electric stress is carried through a complete cycle. While the electrical case has been investigated with some thoroughness, surprisingly little attention has been paid to the mechanical.

417. *Methods of Measurement.* For static observations, both electrometer and ballistic galvanometer have been used. Dynamic measurements are described in §§310 and 375. For static measurements of d_{14}, d_{25}, and d_{36}, rectangular X-, Y-, or Z-cut 45° plates are used, and compressions are applied parallel to one pair of edges of the major surfaces,

* For d_{21} and d_{26} see §§141 and 418.

as explained in §184. For example, in the case of the X-cut, we may suppose the length l of the plate to be parallel to the Y'-axis, along which the stress $Y'_y = F/eb$ is applied, F being the force in dynes parallel to Y'; b and e are the breadth and thickness of the plate in centimeters. If Q (esu) is the total charge liberated, we have, for the piezoelectric polarization, $P = Q/bl = -d'_{12}Y'_y = -d'_{12}F/be$, whence $d'_{12} = -Qe/Fl$. Then, from Eqs. (203), $d_{14} = 2d'_{12} = -2Qe/Fl$. The same final equation holds also for d_{25} and d_{36}.

The galvanometer method is sufficiently sensitive and does not require a knowledge of the capacitance of the crystal specimen. This is a great advantage in view of the uncertainty in the dielectric constant and its variability with changing field. At temperatures high enough for electrical conductivity to be troublesome the galvanometer method has been found preferable. Schwartz[454] called attention to the importance of connecting a condenser of large capacitance in parallel with the crystal when the electrometer method was used. With this precaution he obtained identical results by the two methods. Mandell[328] corrected his electrometer readings for the error due to leakage by extrapolation to the value for zero time. No observations with such crystals as Rochelle salt should be made without due regard to these or equivalent precautions.

Pockels in his early investigations observed that upon compressing a 45° bar the polarization in the X-direction required a considerable time to reach its full value. According to Shulvas-Sorokina[465] from 3 to 4 min are required when the pressure is not over 1 kg/cm^2. With large pressures no such effect is observed. This piezoelectric lag is very like the dielectric effect described in §431 and suggests that the underlying cause may be the same (*cf.* also §84). Nevertheless, Schwartz,[454] whose observations of dielectric lag are shown in Fig. 117, does not appear to have found the effect in his piezoelectric measurements.

On the other hand, Pockels found the discharge upon removal of pressure to be *instantaneous*. In view of this, it is astonishing that all later observers made their measurements upon *application* of pressure.

418. *Dependence of the Direct Piezoelectric Effect upon Stress and Temperature.* Neither Pockels, Valasek, nor Mason, whose measurements of d_{25} and d_{36} are in fair agreement (§141), reported any dependence of these quantities upon stress. From the general absence of anomalies in the Y- and Z-directions none is to be expected. Nevertheless, Schwartz found d_{25} and d_{36} to *increase* as the compressional stress on 45° bars increased up to 6 kg/cm^2. Greater significance would be attached to this statement were it not that Schwartz's values of d_{25} and d_{36} are in very poor agreement with those of Pockels, Valasek, and Mason.

The dependence of d_{25} and d_{36} upon temperature is shown in Fig. 106, from Valasek.[545] The numerical data for d_{25} and d_{36} have already

been given in §141. Valasek's curve for d_{14} (stress not specified) fails to show the expected maxima at the two critical temperatures, probably owing to the use of relatively large stresses (§480). These maxima have been observed by Schwartz,[454] who, like Valasek, fails to state the stress. Similar observations by Shulvas-Sorokina are discussed below.*

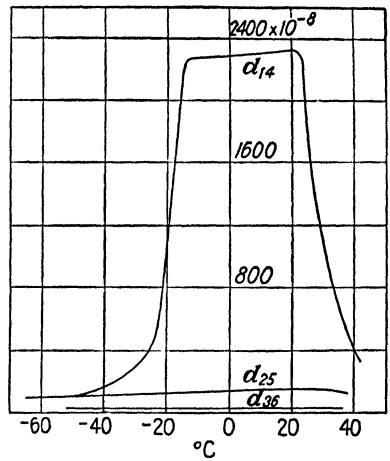


FIG. 106.—Dependence of piezoelectric strain coefficients of Rochelle salt upon temperature, from Valasek.

The earliest observation that the piezoelectric polarization is not a linear function of stress except outside the Curie points appears to have been made by Iseley,[243] as shown in Fig. 107. He applied compressional stresses Y_y' (§39) to an X-cut 45° bar and measured the piezoelectric charge with a ballistic galvanometer. The normal behavior of the crystal at the higher temperatures and the approach to saturation at temperatures between the Curie points are very evident. The greatest charge recorded was at 22.25°C (approximately the right temperature for the upper Curie point), with a stress of 2.225 kg/cm², beyond which the observations did not extend. From Fig. 107 the value of d_{14} under these conditions is found to be about 17,000(10^{-8}). A still

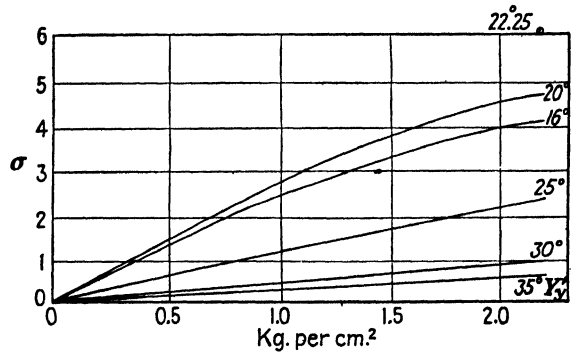


FIG. 107.—Curves relating charge-density σ in 10^{-8} coulombs/cm² with stress Y_y' in kilograms per square centimeter, for various temperatures, from Iseley.

* Using Schwartz's apparatus, Körner[288] measured d_{14}, d_{25}, and d_{36}, but the quantitative interpretation of his results is uncertain.

greater value would doubtless be found at smaller stresses. Iseley's elastic observations on the same crystal are discussed in §462.

Figures 107 and 108 represent almost all the published data on the polarization-stress relation. Mention should be made also of the work of Schwartz,[454] in whose paper is a curve in which, unlike Figs. 107 and 108, the polarization at 18.8°C has a very low value for pressures up to about 1 kg/cm², followed by a gradual rise. In view of the theory outlined in §480, as well as the form of the curves relating polarization to field and of those relating strain to field in the converse effect described in §422, this observation seems reasonable enough; it is unfortunate that others have not corroborated it. Figure 108,* from a paper by Shulvas-

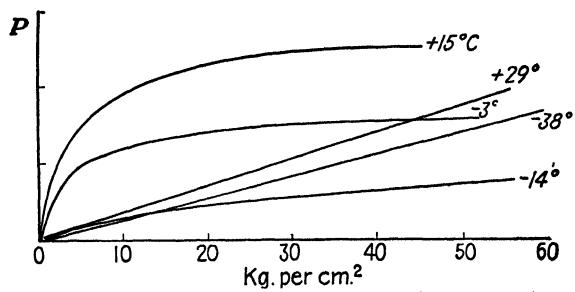


FIG. 108.—Polarization P_x as a function of pressure, at various temperatures, from Shulvas-Sorokina. Ordinates are in arbitrary units, not the same for all the curves.

Sorokina,[465] covers a wide range of stresses and temperatures, but it suffers in value from failure to state the unit of polarization, which is not the same for all curves. It can at least be regarded as definitely established that the piezoelectric polarization curve shows saturation in the range of spontaneous polarization and that there may be an inversion in the curve at low pressures. If this is true, the analogy with the polarization curves obtained with applied *field* is complete. The linear relation between P_x and stress outside the Curie points, changing to a saturation curve between these points, is fully in accord with theory. It will be observed that, from pressures of 50 kg/cm² on, saturation (rotation of dipoles) is practically complete, which means that the differential piezoelectric coefficient approaches zero at large stresses.

These relations are presented in an instructive manner in Fig. 109, also from Shulvas-Sorokina.[465] The outstanding features are the enormous value of d_{14} (26,000 × 10^{-8}) between the critical temperatures *at small pressures*, the effects of saturation, and the low and uniform value of d_{14} outside the critical temperatures. The only unaccountable feature is the comparative flatness of the curves at the lower Curie point. From

* From Shulvas-Sorokina's data we have computed Y_s for Figs. 108 and 110 and d_{14} for Fig. 110.

Fig. 109 the saturation polarization is calculated as about 1,000 esu, of the same order, though nearly twice as great, as the dielectric saturation polarization discussed in §438. In collaboration with Posnov[469] the same author later finds the value to be 940 esu.

419. The value of 26,000(10^{-8}) for d_{14} is the largest we find published as obtained by the direct effect, except that the author, from observations on an L-cut plate as described in §140, derived values as high as 32,500(10^{-8}). The maximum observation by Shulvas-Sorokina, mentioned below, for which no numerical value is stated, may have been still higher. For the very large values obtained by the converse effect

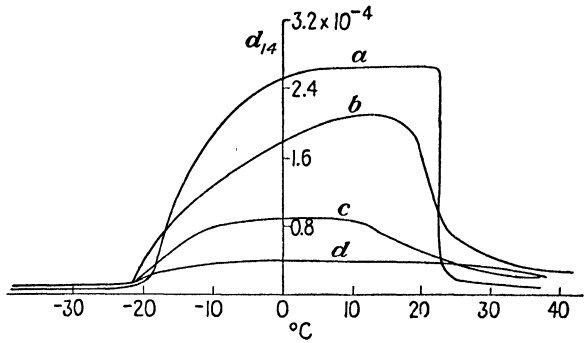


FIG. 109.—Dependence of d_{14} on temperature, from Shulvas-Sorokina. Stress Y_x for curve a is 0.5 kg/cm²; b, 4 kg/cm²; c, 15 kg/cm²; d, 25 kg/cm².

see §423. The value of 26,000(10^{-8}) is ten times as great as Valasek's in Fig. 106. To account for such discrepancies one must take into account the variability of the piezoelectric constant with pressure, differences between different specimens, and such systematic sources of error as faulty mounting and depolarizing effect of surface layers. Since the various sources of error tend to make the observed value of d_{14} too small, it may be said that in general the highest recorded values are the most representative.

In a later paper[466] Shulvas-Sorokina reports that, by careful temperature regulation and application of pressures not exceeding 2 kg/cm², a very sharp and narrow maximum in d_{14} is found at 22.5°C. The height of the maximum is found to be less with thick than with thin crystal plates; this is attributed to lack of uniformity of temperature in the thick crystals. She finds the maximum in k_x to come at exactly the same temperature. At 38 kg/cm², however, there is no trace of a maximum at the Curie point. Correspondingly, the maximum in k_x disappears when the field strength exceeds 300 volts/cm. With pressures above 50 kg/cm² the piezoelectric properties were found to be the same at *all* temperatures.

The dependence of piezoelectric polarization upon stress is further shown in Fig. 110, from Shulvas-Sorokina.[465] The data are for 3°C, and they illustrate the importance of keeping the stress small if the greatest piezoelectric effect is to be realized. The sudden drop in d_{14} from the very large initial value of about $26(10^{-5})$ esu, shown at 2 kg/cm² in Fig. 110, does not seem to have been confirmed by other observers.

It was observed by Shulvas-Sorokina[467] that when a periodic mechanical stress was applied to a Rochelle-salt plate the value of d_{14} diminished rapidly as the frequency was increased from 10 cycles/sec. This observa-

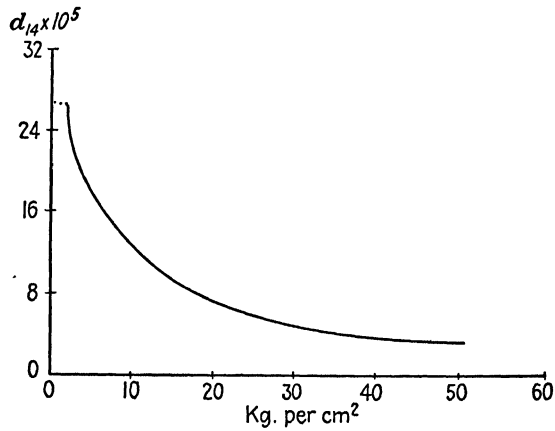


FIG. 110.—Dependence of d_{14} on pressure at 3°C, from Shulvas-Sorokina. Y_s is in kilogram per square centimeter.

tion can be correlated with the facts concerning "lag" discussed in §427. In a later paper[468] Shulvas-Sorokina describes experiments, with theoretical interpretation, in which periodic mechanical pressures up to 10 gm/cm² at frequencies from 3 to 3,000 ~ were impressed.

420. The following early observations by Valasek[541] made at room temperature should be mentioned here, since they afford a qualitative confirmation of the theory discussed in §459. With a ballistic galvanometer he measured the charge Q liberated when a force $F = Y'_y be$ was applied to an X-cut 45° plate, according to §417. The distinguishing feature of these experiments was that the force was applied while the plate was in a known electric field. The total polarization is then $P^t = P^0 + P^E + P^F$, where P^0 is the spontaneous polarization and P^E and P^F are the contributions due to the field and to F. The results are shown in Fig. 111, in which the ordinates are $Q = blP^F$. It is seen that the maxima of P^F occur at certain negative values of E; that these negative values become greater with increasing stress; and that, for the same stress, P^F is greater for large negative values of E than for large positive

values. Either because a long time was allowed to elapse between successive observations or because E was not carried through a complete cycle, P^F appears in Fig. 111 (the dotted curve being disregarded) as a single-valued function of E. In a later paper,[542] Valasek describes similar observations, made in rapid succession, in which E was varied through a complete cycle. The result is illustrated qualitatively in Fig. 111 for the largest stress, the full line indicating the form of the curve for increasing E, while the dotted curve indicates the form for decreasing

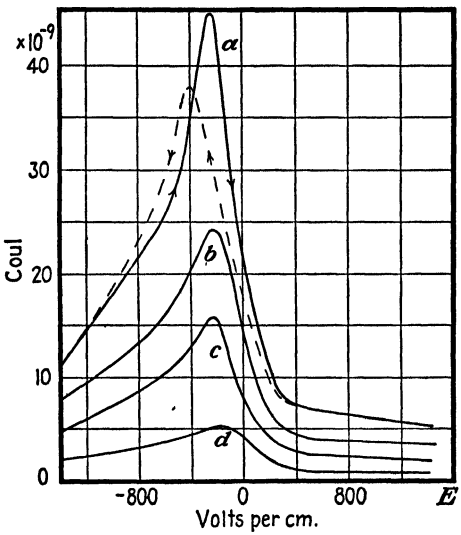


FIG. 111.—The direct effect in Rochelle salt. Piezoelectric response for various stresses with crystal in an electric field, from Valasek. Ordinates are in 10^{-9} coulomb, abscissas in volts per centimeter. Curve *a*, force F = 880 g; *b*, 660 g; *c*, 350 g; *d*, 140 g.

E.* This result, as well as the other features mentioned above, can be interpreted in the light of the discussion in §462 and by reference to Fig. 139, on the assumption that a stress Y_s is equivalent to a field strength $-E/b_{14}$.

421. *Unipolarity in the Direct Piezoelectric Effect.* Although the effect of unipolarity has recently been observed in connection with the *converse* effect (§422), little attention seems to have been given to its influence on the *direct* effect since the pioneer work of Anderson, to which reference was made in §404. Anderson used square X-cut plates with edges at 45° with the Y- and Z-axes. The sign of the strain y_s was

* This loop may be said to illustrate a sort of mixed piezoelectric and dielectric hysteresis. Piezoelectric hysteresis loops, by both the direct and the converse effect, are discussed in §§422 and 492.

reversed by changing the direction of pressure 90° in the YZ-plane, as explained in §184. He found that with some specimens the polarization was increased many times upon reversal of the sign of the stress. Later observations by Vigness are described in the next section. The explanation of the effect, in terms of the domain theory, will be found in §§462 and 477.

THE CONVERSE EFFECT

In the Seignette-electrics there are anomalies in the converse effect similar to those in the direct effect previously discussed, demanding special experimental and theoretical investigation. We are here concerned chiefly with Rochelle-salt plates having the field in the X-direction. The theoretical discussion is reserved for §460.

For measuring the piezoelectric constants of crystals the converse effect offers the advantage that no correction need be made for leakage of charge through or over the surface of the specimen. As always, it is important that the electrodes lie in immediate contact with the crystal: no appreciable layer of impurities, cement, or, in the case of such crystals as Rochelle salt, dehydrated material must be allowed to intervene. In order to satisfy this condition without hindering the deformation of the crystal, very thin electrodes should be used, as for example of evaporated gold.

The principal experimental work is that of Sawyer and Tower,[449] Bloomenthal,[55] Vigness,[565,566] Norgorden,[393,394] and Hinz.[229] In broad outline it may be said that greater values of d_{14} have been observed than with the direct effect; that the mechanical strain produced by an applied field, like the electric strain (polarization), shows both saturation and hysteresis, and depends on temperature in a manner similar to the dielectric and the direct piezoelectric effects; and that the phenomena of fatigue and unipolarity are present. Bloomenthal and Hinz applied static fields, while the other observers measured maximum strains under alternating fields. In most cases the change in length Δl of 45° X-cut bars or plates was observed. The basic formula is

$$y_x = 2\frac{\Delta l}{l} = d_{14}E \tag{489}$$

422. *Static Fields.* Vigness's plates had the l-dimension normal to the (021) faces of the crystal, hence 40°53′ from the Z-axis. This is near enough to 45° to permit the substitution in Eq. (489) of Δl. Vigness calculated Δl from observations of X-ray reflections. This seems to be the only investigation in which X-rays have been used for the measurement of piezoelectric deformations. The method appears to be reliable, provided that one can be sufficiently certain as to the lattice planes

from which reflections occur. A drawback is the formation of superficial imperfections or disintegration of the crystal after some hours of exposure, which causes a broadening of the lines on the photographic plate. Vigness found good agreement between the X-ray data and those obtained with a microscope. His chief results are shown in Figs. 112 and 113. The curves are of the same form as those shown in Fig. 118 for the dielectric effect and in Figs. 106 to 110 for the direct piezoelectric effect. The conspicuous features are the characteristic behavior near the upper Curie point and the extremely large value of d_{14}—around ten

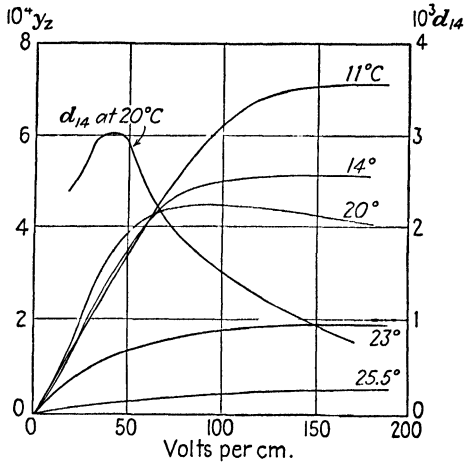


FIG. 112.—Converse piezoelectric effect in Rochelle salt, from Vigness.[565] Dependence of strain, also of d_{14}, upon static field. If $2\Delta r$ is the total change in length r of an X-cut plate observed on reversal of field, the mean strain corresponding to the field strength shown in the figure is $y_z = 2\Delta r/r$.

times as large as the values recorded for the direct effect. Although Vigness's observations do not include the initial value of d_{14}, still it appears from the strain curve for 20°C in Fig. 112 that around this temperature the comparatively low initial value of d_{14} begins to increase at a field strength of the order of 10 volts/cm. This increase at low fields, characteristic of *static* observations, is similar to that for the dielectric constant, as mentioned in §431.

The importance of a consideration of lag and fatigue (§427) in interpreting piezoelectric data is brought out in the following observations by Vigness.[565] With small fields (27 volts/cm) deformation and recovery are slow, occupying several seconds. With larger fields (165 volts/cm) the deformation is almost instantaneous up to nearly the full value, followed by a slow exponential creep that may last for hours. After long application of a large field, recovery requires more than a minute.

After application of a field in one direction, a field in the opposite direction causes a greater deformation than if the first field had not been applied.

Vigness claims to have found experimental evidence for the existence of three different relaxation times in Rochelle salt: (1) a small fraction of a second, which makes possible the acoustic and h-f vibrations; (2) a relaxation time reaching a maximum of about 15 sec at 164 volts/cm, 7.5 sec at 27 volts/cm, a little above 0°C, falling to zero at each Curie point; (3) a longer relaxation time, lasting for minutes or hours (see also §427).

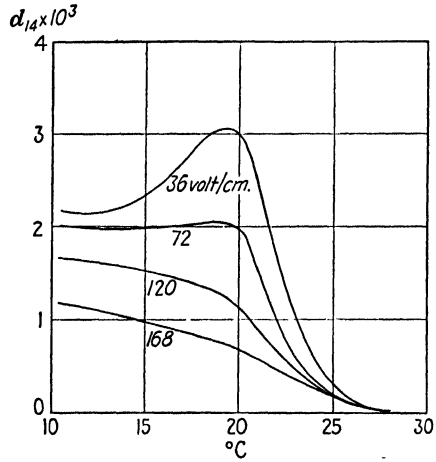


FIG. 113.—Converse effect in Rochelle salt, from Vigness.[565] Dependence of d_{14} upon temperature for various field strengths.

Mention is made in §§421 and 433 of the unipolar effect in the dielectric and the direct piezoelectric properties of Rochelle salt. It has been found by Vigness[566] that the magnitude of the strain in X-cut plates in the converse effect is not always the same upon reversal of sign of the electric field. It may be several times greater in one direction than in the other. This unipolarity with respect to strain in an electric field is analogous to the dielectric unipolarity discussed in §433. It was in effect an observation of the *spontaneous strain* and was used later by Jaffe (§482), in making the first calculation of the actual value of this quantity.

Bloomenthal used a combined optical and mechanical lever system for measuring the change in length of 45° X-cut bars of Rochelle salt containing 0.37 per cent of $C_4H_4O_6T1Na \cdot 4H_2O$. The field strength E was varied in steps through a cycle between -400 and $+400$ volts/cm. The plot of $y_x : E$ forms a hysteresis loop except at temperatures above the upper Curie point. The temperature range was from about 10 to 35°C.

The coefficient d_{14} at each temperature was computed from the maximum slope of a curve like that shown in Fig. 151. The maximum value, which comes at 19°, is $70(10^{-5})$. The time of recovery from the residual strain with field removed was not recorded. For pure Rochelle salt, his values of d_{25} and d_{36}, and also of d_{14} for temperatures above 25°C, agree with those of Valasek shown in §418.

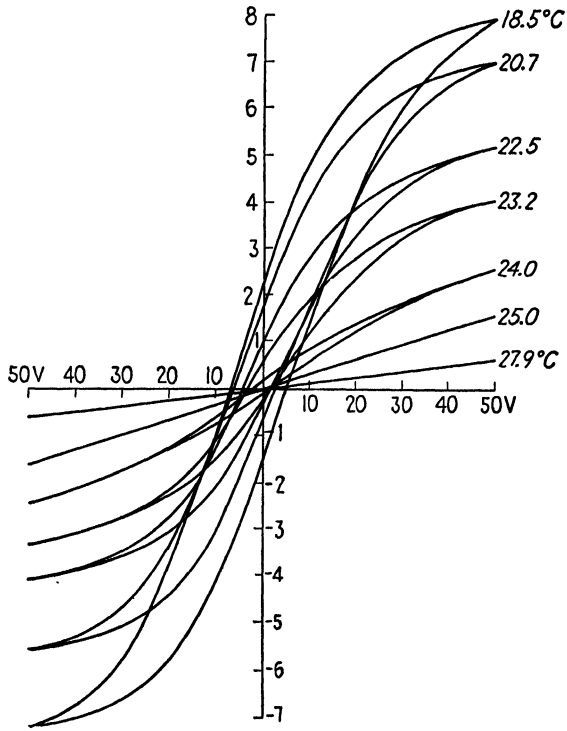


FIG. 114.—Converse effect in Rochelle salt, from Hinz. Abscissas are in volts applied to the 45° X-cut plate. Maximum field strength, for 50 volts, was 285 volts/cm. Ordinates multiplied by 0.00145 give the elongation in mm; when multiplied by $4.35(10^{-5})$ they give the piezoelectric strain y_x.

Hysteresis loops for the converse effect have been obtained by Hinz,[229] who observed the change in length of an X-cut plate 40 by 15 by 1.75 mm, to which potential differences up to 50 volts (E to 285 volts/cm) were applied. The potential was reversed after each step of 10 volts. An optical lever with rotating mirror was used, as in the measurement of the elastic constants (§77). The electrodes were of tin foil cemented on with "Acetonlack." The results, shown in Fig. 114, are in general agreement with those of Vigness and Bloomenthal. The observed elongations

are proportional to the strain $y'_y = y_z/2 = d_{14}E/2 = b_{14}P^2/2$. From these relations, together with Eq. (500) or (512*b*), a theoretical explanation is found for the "saturation effect" made evident by these curves for temperatures between the Curie points. Hinz shows also a curve relating the change in length of plate at maximum field strength (ordinates of the tips of the loops in Fig. 114) with temperature; the form is somewhat similar to Valasek's direct-effect curve (Fig. 106) for the corresponding range in temperature, but with a less steep drop at the Curie point. This discrepancy may be due to lack of sufficient freedom from constraint in Hinz's crystal plate or to the relatively high field strength that he employed.

Comparison of Fig. 114 with the oscillograms shown in Figs. 123, 124, and 125 reveals the close parallelism between mechanical strain and electric strain in their dependence on the field strength. In particular, one notices similar saturation characteristics and a similar dependence on temperature.

It will be observed that the loops in Fig. 114 are not quite symmetrical about the horizontal axis. This fact points to some degree of unipolarity in the crystal—the effect is too large to be ascribed to electrostriction.

By applying to Fig. 114 the equation $y_z = d_{14}E$, one can calculate, at each temperature, either the differential $(d_{14})_d = dy_z/dE$ from the slope of the curves or the over-all d_{14} corresponding to the peak value of E. The over-all value diminishes from $36(10^{-5})$ at 18.5°C to $3.1(10^{-5})$ at 27.9°C.

Above the Curie point one can calculate the coefficient b_{14} of the polarization theory (§452) by the formula $b_{14} = y_z/P = y_z/\eta' E$. For example, from Fig. 145 one finds, at 27.9°C, $\eta' \approx 32$, whence from Fig. 114, $b_{14} = 6.5(10^{-7})$, in fair agreement with the value $6(10^{-7})$ from Fig. 146. Below the Curie point the calculation is impossible, since the susceptibility under the conditions of Hinz's experiments is not known. Moreover, if, as seems probable, especially in view of the experiments of Vigness,[565,566] the piezoelectric strain in the Seignette-electric region is as dependent on the specimen and on its mode of treatment as is the polarization when observed with static fields, one cannot expect the hysteresis loops in Fig. 114 to be generally reproducible.

For an estimate of the spontaneous strain y_z^0 from Fig. 114 see §482.

423. *Alternating Fields.* Sawyer and Tower[449] observed the shear in an X-cut plate with edges parallel to the Y- and Z-axes. A surface normal to the Z-axis was cemented to a metal block, and the maximum displacement of the opposite face in the Y-direction was observed with a microscope when a 60-cycle field was applied. The amplitude of shear y_z is the quotient of this displacement by the length of the plate in the Z-direction. The result is shown in Fig. 115. Especially noticeable is

the fact that the converse effect fails to appear in this figure at field strengths below 50 volts/cm. The experiments of Norgorden, which will be considered presently, show that strains are indeed produced by fields below 50 volts/cm, although they are too small to have been made evident by the method of Sawyer and Tower. Except at low voltages there is fair agreement between Sawyer and Tower's a-c results and those of Vigness under static conditions.

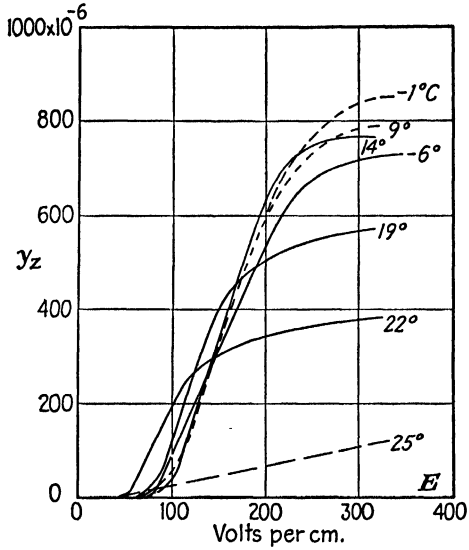


FIG. 115.—Dependence of strain upon field in an X-cut Rochelle-salt plate, for various temperatures (Sawyer and Tower). To avoid confusion, only the upper portion of the curve for −1°C is shown.

The strain in Fig. 115 approaches saturation at a value between $4(10^{-4})$ and $9(10^{-4})$, depending on the temperature in the same manner as the dielectric constant shown in Fig. 123.

From the slopes of the curves in Fig. 115 the maximum differential values of d_{14} may be calculated. For example, at 14° it is found to be about $200(10^{-5})$, of the order given by the preceding authors. The maximum over-all value, obtained from the tangent drawn from the origin to the curve at 14°, is about $100(10^{-5})$, four times as great as the maximum for the direct effect shown in Fig. 109.

424. With frequencies from 30 to 4,000 ~ and maximum fields from 5 to 47 volts/cm, Norgorden[393,394] observed the maximum change in length of a 45° X-cut cube over a temperature range from 13 to 35°C. The cube edge was 2 cm in length. Mueller's method (§§415,416) was followed for annealing the crystal and for attaching the electrodes to the faces

normal to the X-axis. One of the 45° faces also carried an electrode which served as one plate of a condenser, the other plate being fixed in close proximity. These condenser plates, across which was a bias of 184.2 volts, were connected to an amplifier so that as the crystal vibrated the maximum strain could be calculated from the amplifier output. The circuits were carefully shielded electrically.

Norgorden's work is in effect a study of the *initial converse* $(d_{14})_0$, as defined in Eq. (512). While his results are of great value qualitatively, the numerical values of d_{14} are so low that they cannot be accepted as typical. In the first place, they are hundreds of times smaller than those of Vigness, a fact that can be only partly accounted for by the fact that Vigness used a static method. Second, these values are only about one-third as large as those shown in Fig. 146, with which they can fairly be compared in spite of the difference in method. If, notwithstanding Norgorden's precautions, surface layers of low dielectric constant were on his crystals, the recorded field strengths would be too high and the calculated d_{14} too low. Excessive mechanical constraint from cemented electrodes would also make d_{14} too small.

With this reservation, one may summarize Norgorden's results as follows: Like its analogue, the initial dielectric constant k_0 (§434), $(d_{14})_0$ is nearly constant up to at least 50 volts/cm. The relation between the reciprocal strain $1/y_z$ and the temperature interval $(T - \theta_u)$ is linear, at a given field strength, on both sides of the Curie point. We have here the first, and so far the only, confirmation of the Curie-Weiss law for the piezoelectric effect (see §467).

Norgorden's observations show also a tendency toward saturation in d_{14} with increasing field, as is to be expected from Eq. (512*b*) and from the analogy with the dielectric constant. He finds the strain to be nearly independent of frequency from 100 to 4,000 ~.

COMPARISON OF THE DIRECT AND CONVERSE EFFECTS

425. Let us suppose that a stress Y_z is impressed on a Rochelle-salt crystal in zero electric field, at some temperature between the Curie points, causing a strain y_z and a polarization P. Then let a field E be applied of such magnitude as to bring the strain back to zero. We inquire first how the polarization P' due to E compares with P.

For the direct effect, $P = -d_{14}Y_z = d_{14}y_z/s_{44} = e_{14}y_z$. For the converse effect, we may write $y_z' = d_{14}'E$ and $P' = \eta E$, where the primes indicate the converse effect. The symbol d_{14}' allows for the possibility that the piezoelectric strain coefficient may have different values in the direct and converse effects. η is the effective susceptibility, which in ordinary piezoelectric crystals would be denoted by η' (constant stress) but which in Rochelle salt depends on both Y_z and E, and is usually less

than η'. Then if $y'_z = -y_z$,

$$\frac{P}{P'} = -\frac{d_{14}d'_{14}}{\eta s_{44}} = -\frac{e_{14}d'_{14}}{\eta}$$

With *ordinary crystals* $\eta = \eta'$ and $d'_{14} = d_{14}$, whence

$$e_{14}d'_{14} = e_{14}d_{14} = \eta' - \eta''$$

by Eq. (516). Then $P/P' = -(\eta' - \eta'')/\eta'$; and since usually

$$(\eta' - \eta'') << 1$$

it follows that $P << P'$.

On the other hand, in Rochelle salt, owing to the large value of d_{14}, for certain ranges of temperature and of field, $\eta' >> \eta''$, so that P' can be nearly as large as P. That is, the same strain is then associated with nearly the same polarization in both the direct and converse effects.

It must be emphasized that equality in y_z in the two effects is defined in terms of the external configuration of the crystal (more properly, of the domain). Yet the fact that in the direct effect the field can be zero, which is not the case in the converse effect, indicates that the internal forces in the unit cell, and hence the arrangement of atoms in the cell, cannot be the same in the two cases. In terms of dipole theory one may say that in the direct effect the mechanical stress turns the dipoles, while in the converse effect the rotation of dipoles in the applied field deforms the lattice.

One would suppose that this disparity in lattice configuration in the two cases might make the process irreversible and explain the fact that the observed values of d_{14}, at least under static or l-f conditions, have usually been found greater in the converse than in the direct effect. Nevertheless, doubt is cast on this view by Vigness's observation of the same value of the strain whether the measurement was by X-rays or microscope. For by X-rays only strains in the primary lattice can be observed; and since the microscope, which yields the same y_z, measures the change in external configuration due to the field, one must conclude that approximately the same strain in the primary lattice is produced by the converse as by the direct effect. One can go no further at present than to say that the relatively large values of d_{14} by the converse effect *may* be found to be due entirely to the absence of some of the sources of error that tend to make the value by the direct effect too small. If after the elimination of all sources of error there is still found a disparity between the values of d_{14} in the two effects, one can only conclude that the piezoelectric process is thermodynamically irreversible.

A better comparison between the two effects would be possible if observations were made with the same specimen, leading to curves for

$P:Y_z$ and $y_z:E$ at various temperatures, especially between the Curie points; and it would be better yet if the $P:E$ curve were included, with P observed at the same time as y_z. For lack of any such comprehensive study as this, we can only summarize some of the fragmentary results recorded in this chapter. We note first that the piezoelectric strain in the converse effect, which as has been seen leads to a larger d_{14} than does the direct effect, also shows, like the polarization curve, three stages. In the first stage, up to fields of about 40 volts/cm or less, y_z is relatively small. Then, as is shown by Figs. 114 and 115, comes a rapid rise, followed by an approach to saturation. On the other hand, Figs. 107 and 108 for the direct effect show only a rapid rise in the piezoelectric polarization at small stresses, followed by saturation. Only the observations of Schwartz, mentioned in §418, indicate the existence of a first stage of low polarization.

426. *The Effective Value of d_{14} in Piezo Resonators.* At high frequency and in weak fields, very large values of d_{14}, such as those observed by Vigness, Bloomenthal, and Hinz in static fields or those of Sawyer and Tower at 60 $\sim$ with fields above 50 volts/cm, are not to be expected. One would rather expect to find values of the order indicated in Fig. 146. It should be pointed out that the d_{14} derived from observations on resonators is due to the combined action of the direct and converse effect, as shown in §221.

Concerning the performance of resonators in strong fields very little is known. One may expect d_{14} in the Seignette-electric region to vary throughout the cycle, somewhat as is suggested by the form of the curves in Fig. 114. The effect of this non-linearity on the resonator performance is mentioned further in §§370 and 480. The only practical application of strong fields in vibrating crystals is found in certain types of transducer, and here again next to nothing is known concerning the effect of the performance of mechanical work on the effective value of d_{14}.

427. Lag and Fatigue. The more important experimental results, some of which are recorded in §§417 to 424 and 431 to 437, will now be summarized.

The term *lag* refers to the slow development of electric or mechanical strain on the application of electric field or mechanical stress. It is somewhat dependent on the *fatigue*, which means the state of the crystal as a result of previous electrical or mechanical treatment. Both terms are used chiefly with respect to static observations.

Observations of Lag. (*a*). *In charging a Rochelle-salt condenser*, the amount of charge for a given field strength E_x is found to increase with the charging time t_c as long as t_c is only a few thousandths of a second. For values of t_c from a few seconds to several minutes the charge is the

same, and on discharge the entire amount is given up rapidly enough to be observed with a ballistic galvanometer. With strong fields (over 400 volts/cm) the full charge is reached in about 0.01 sec, while with fields corresponding to the steep part of the polarization curve the growth of charge is more gradual.

With thick plates the saturation polarization has been found to be attained at smaller fields than with thin plates; but if fields lower than the saturation values are applied, the thick plates require a longer charging time than the thin (Kurchatov). The thick crystals also discharge more slowly.

b. Lag in piezoelectric observations. In the *direct effect* the full polarization P_x corresponding to a given stress Y_z may require several minutes to develop; on the other hand, the discharge is instantaneous (§417). In the *converse effect*, if the impressed field is small, both the piezoelectric deformation y_z and the recovery on removal of the field are slow. With large fields the deformation is almost instantaneous, but recovery may require more than a minute (§422).

c. Lag in elastic observations. Iseley[243] found that, on the application of compression to a 45° X-cut bar, as much as 30 sec. was required for the full attainment of the strain. Mandell[326] records a similar experience.

Observations of Fatigue. Both dielectric and piezoelectric fatigue (§404) have been observed, though the latter has been but little investigated. Dielectric fatigue consists in a reduction in the discharge after prolonged application of a field. Recovery is very slow, but it can be hastened by application of an opposing field. It is also stated that fatigue can be avoided by the use of "solution" electrodes; if this turns out to be generally true, it must point to conditions at the surface rather than in the interior of the crystal as the seat of the fatigue effect.

In his measurements of the elastic constants of Rochelle salt and of ammonium–sodium tartrate crystals (§§78, 88), Mandell encountered elastic fatigue; unfortunately, quantitative particulars are lacking.

Observations in Alternating Fields. Corresponding to the increase in polarization with longer application of a field is the observed diminution when an alternating field is used. Up to about 50 or 100 cycles per second there is a transition state, beyond which the results are not very different up to 10,000 cycles per second (see §§432, 436, 438). Similar results are found with the converse piezoelectric effect (§422).

428. Relaxation Times. It is probable that in most if not all of the observations on lag and fatigue the electrodes were separated from the normal Rochelle-salt structure by cement or dehydrated layers. Not only is the field in the crystal reduced thereby (§411), but in such layers there may also be depolarizing effects that affect the observations. For example, the wide discrepancy between Kurchatov's and Schwartz's

results, as shown in Fig. 117, does not strengthen the view that the lag effect is a property inherent entirely in the crystal.

The slow adjustments due to surface layers are not the only effects present in Rochelle salt that must be taken into consideration before one can begin explaining anomalies by the theory of relaxation times in the Debye sense. Non-linearity in the $P_x : E_x$ relation; interaction effects (§448); hysteresis, with attendant readjustments of boundaries between domains*—all these may depend upon time in ways that can fully account for most of the observed effects of lag and fatigue. Mueller[380] goes so far as to assert that "the existence of a relaxation time longer than 10^{-6} second is not justified by any experiment."

As instances of attempts to throw the responsibility for observed effects onto relaxation times may be mentioned certain conclusions of Vigness[565,566] (§422), Norgorden (§424), Staub,[477] Shulvas-Sorokina and Posnov (§437), Shulvas-Sorokina,[467] and Goedecke.[174,†] The last two of these papers contain a mathematical treatment of the problem.

In an alternating field, Rochelle salt reacts like a capacitance associated with a resistance. The power factor may be affected by any or all of the following: (1) true relaxation times; (2) energy required to reverse domains; (3) shifting of the boundaries of domains; (4) leakage of charge through or over the surface of the crystal; (5) vibration of the crystal as a whole. Power losses are too complicated to make a complete analysis possible.

The problem has been attacked empirically by Mason,[B35,338] who treats not only the dielectric constant but the piezoelectric and elastic constants as well as complex quantities. He derives an expression for the impedance of a crystal vibrated at any frequency, involving Debye's theory of relaxation times, but does not apply it quantitatively. The equivalent network of the crystal according to Mason is discussed further in §375.

In §425 we touch upon the question of the reversibility of the piezoelectric process in Rochelle salt. One might hope that light would be thrown on this problem by the observations of energy losses in vibrating crystals under various conditions. On the one hand, there is the intimate relationship between the piezoelectric and the dielectric constants. On the other hand, it is the square of the piezoelectric constant d_{14} that appears in the resonator equations, and this square is really the product of the direct- and converse-effect values of d_{14}. The analytic and experimental separation of these two contributions would not be easy.

* For the magnetic analogy see C. W. Heaps, *Phys. Rev.*, vol. 54, pp. 288–293, 1938.

† He reports relaxation times of the order of 10^{-4}, 10^{-5}, and 10^{-6}, which correspond to the smallest of Vigness's values in §422.

CHAPTER XXII

ROCHELLE SALT: DIELECTRIC OBSERVATIONS

As often happens, the phenomena which are the easiest to observe are the most difficult to interpret. —E. C. STONER.

429. This chapter has to do chiefly with fields in the X-direction. The dielectric constants in the Y- and Z-directions, which have no anomalies, were treated in §408.

The dielectric properties of Rochelle salt for fields parallel to the X-axis are very complex. The dielectric constant varies enormously with temperature, field strength, and mechanical strain. The literature is so extensive that it is impossible to do more than select and correlate some of those data which are most significant and trustworthy. Beyond the material in this chapter, further observations are recorded in §474 and Chap. XVIII.

Whenever the subscript x is omitted, it is to be understood that fields and polarizations are in the X-direction.

Owing to the large value of d_{14} and its reaction upon the permittivity, dependable values of k_x are difficult to obtain, since it is not easy to mount the crystals with their adherent electrodes in a manner sufficiently free from external stress. It is partly for the latter reason that most observers have failed to record the extremely large k_x that is to be expected at the Curie points. Much of the experimental work, especially that prior to about 1934, is of only qualitative value, and there has been a considerable amount of premature theorizing. Especially conspicuous is the lack of trustworthy quantitative data with static fields; perhaps this is because experience soon taught that more reproducible results could be obtained with alternating currents, though even here the observations of different workers are often far from harmonious. One reason for discrepancy doubtless lies in differences between unrecorded "room temperatures," an unfortunate circumstance, since such temperatures are so little removed from the upper Curie point. Other reasons, which will be made clear in the following discussion, are differences in thickness and degree of unipolarity of different specimens, previous history of the specimens used, differences in electrodes and in the cement between electrodes and crystal, and surface impurities on the crystals. Some of these sources of discrepancy are not present in alternating fields. The only results under static fields

that can fairly be compared with those obtained with l-f alternating current are at smallest and largest fields.

The *permittivity* has usually been deduced from observations of polarization P, at various field strengths E, temperatures, and degrees of mechanical constraint. Observations may be classified as follows: (1) Under static fields, polarization curves obtained by a point-by-point method, usually with ballistic galvanometer; it is chiefly by this means that the phenomena of lag, fatigue, and unipolarity have been studied. (2) Observations at low frequencies, up to 1,000 or in a few cases up to 10,000~. The three effects just mentioned, which vary from crystal to crystal, are mostly eliminated. The most nearly reproducible results are obtained by this method, using an a-c bridge or oscillograph. (3) At high frequency, with the crystal in or coupled to a tube generator circuit. The principal disturbing effects in Cases (2) and (3) are resonance with various vibrational modes and heating of the crystal.

As long as the frequency is sufficiently far from resonance with any vibrational mode, methods (2) and (3) may be assumed to give approximately the dielectric constant corresponding to the tips of the hysteresis loop. Depending on the circuit employed, the bridge method gives either the equivalent parallel capacitance C_p of the resonator or the equivalent series value C_s, as defined in §§271 and 273. These two quantities differ very widely in the resonance range but approach equality in either direction away from this range. Sufficiently far from resonance one may therefore write $k = 4\pi e C_p/A = 4\pi e C_s/A$, where e and A are thickness and area of plate and C_p and C_s are in esu. That the departure from resonance may have to be very great before the value of k thus derived is even approximately free from the effect of resonance is pointed out in §259.

430. Definitions and Symbols. We shall have occasion to use several different expressions for permittivity and susceptibility, illustrated in Fig. 116 (*cf.* Fig. 168 for the magnetic analogy). In the first place there is the "normal," or "over-all," permittivity k_x at a point such as A (the subscript x will often be omitted, since only X-polarizations are here considered), defined as $k = 1 + 4\pi\eta$, where $\eta = P/E$. In some cases, especially in the discussion of hysteresis loops, the *differential permittivity* $k_d = 1 + 4\pi\eta_d$ will be used, where $\eta_d = \partial P/\partial E$ (the slope of the curve at any point) is the *differential susceptibility;* the point in this case may be on the virgin curve or on the hysteresis loop. The *initial permittivity* k_0 (susceptibility η_0) is the differential permittivity for $E = 0$. The *saturation permittivity* k_{ds} is the differential value k_d with large fields, on the linear portion of the polarization or hysteresis curves, while the value of k_d at the steepest portion of the curve is denoted by k_{dm}. The *reversible permittivity* k_r is the limiting value of the quantity

$1 + 4\pi\,\delta P/\delta E$ observed when a *small alternating* field is applied at any point on the $P:E$ diagram. The vanishingly small variations in P are then linear and show no hysteresis; the slope of the short $P:E$ lines, from which the reversible permittivity is calculated, is that of the hysteresis curve which has its tip at the point in question. Unfortunately, in the literature it has not always been made clear which of the foregoing definitions of permittivity was meant. All that has been said concerning the different permittivities applies equally to the susceptibilities.

All the types of permittivity are derivable from data obtained with ballistic galvanometer or oscillograph. Alternating-current bridge

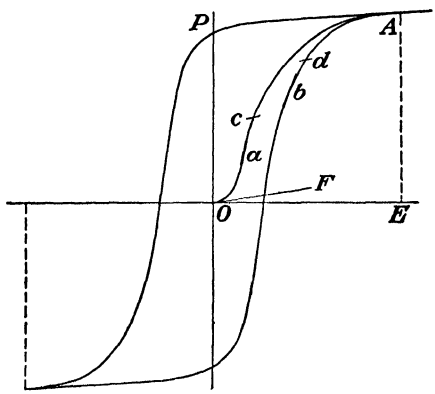


FIG. 116.—Types of permittivity. The "normal" value is $1 + 4\pi P/E$ at A. The differential permittivity is indicated at a and b, reversible permittivity at c and d. Differential and reversible values unite at large fields to become the saturation permittivity, and at small fields to become the initial permittivity at the origin.

observations give the "normal" value, which obviously varies widely with the field strength employed, becoming the initial value when the field is small. Unless otherwise specified, k will be understood to denote the normal value for the mechanically free crystal.

With Rochelle salt, in many cases it is sufficiently accurate to write $k \approx 4\pi\eta = 4\pi P/E$ (or $4\pi\,\partial P/\partial E$).

Most of the observations recorded here lie in the region of spontaneous polarization. Outside this region, except close to the Curie points, the anomalies disappear. The best data outside the Curie points have been obtained with alternating current and are considered later in this chapter.

431. Observations with Static Fields. In the earlier publications, for example by Valasek[541] and Kurchatov,[B32] one finds polarization curves, but they are of little quantitative value owing to the incompleteness in the data. We shall discuss here only enough of the very meager material to illustrate the salient facts.

The general form of the polarization curve as well as the effect of lag (§427) is illustrated in Fig. 117, curves *a* and *b* from Schwartz.[454] The resemblance to a magnetization curve with its three stages is evident. The highest values of polarization, around 500 esu, are of the same order as the saturation values obtained by other methods. From about 500 volts/cm on, the polarization is independent of the charging time. In order to show how variable the results by ballistic methods are, curve *c*, based on Kurchatov's observations,* is included in Fig. 117. This curve is at 0°C, charging time 0.07 sec, thickness of crystal plate 7.2 cm; the thickness of Schwartz's crystal is not stated. Kurchatov, like Schwartz, finds the polarization to increase with charging time.

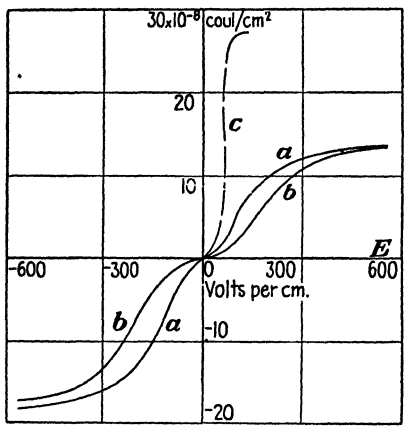


FIG. 117.—Polarization P for short charging times (field parallel to X). Curve *a* is for charging time 0.148 sec, curve *b* for 0.007 sec, temperature 19°C, from Schwartz. Curve *c* is from Kurchatov, charging time 0.07 sec, temperature 0°C.

A second example is Fig. 118 in which the charging time is 10 sec. The difference lies chiefly in the somewhat stronger polarization. In this figure is shown also the permittivity $k_x \approx 4\pi P/E$ as function of field strength (*cf.* Fig. 127).

Owing to the danger of error caused by lag and the conductivity of the crystal, most observers have measured the static polarization in terms of discharge rather than of charge. It has been found that as long as the charging time does not exceed a few minutes, the entire discharge is so nearly instantaneous that a ballistic galvanometer can be used.

When the charging time is allowed to run into hours instead of minutes, the *fatigue effect* is encountered. In such cases the discharge is not sensibly instantaneous, but a considerable portion of the charge is returned slowly, at a rate depending on the time of charge, and lasting sometimes for days. The effect is also dependent on the strength of the charging field.

Since the entire charge is returned sooner or later[397] (*i.e.*, there is no *permanent* remanence as result of a polarizing field), it may be concluded that the area of a hysteresis loop, at sufficiently low frequency, should be zero. That is, there should be no hysteresis if the observations with increasing and decreasing fields were made by a step-by-step

* Ref. B32, Fig. 24; see also §432.

method, sufficient time for complete adjustment to take place being allowed to elapse at each stage. This is by no means the case at the speed with which such observations are commonly made (*cf.* §422). For example, Valasek's observations* with a ballistic galvanometer (time intervals between observations not stated) yielded typical hysteresis loops in good agreement with those obtained by alternating current.

The field necessary to reverse the domains, when measured slowly by the d-c method, is several times smaller than by a-c (§436). The

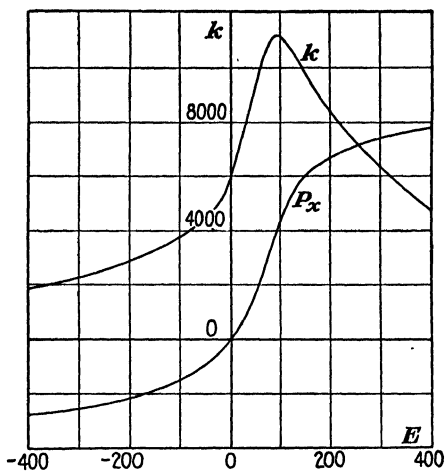


FIG. 118.—Polarization P and permittivity k for Rochelle salt at 20.3°C, as functions of field strength E (in volts/cm) in the X-direction. The polarization is in arbitrary units; at 400 volts/cm the estimated value is about $18(10^{-8})$ coul/cm^2. From Oplatka, ref. 397.

smallest recorded value, less than 15 volts/cm (presumably at room temperature), seems to be that of B. and I. Kurchatov.[293] This observation means that with static fields the initial permittivity k_0 extends over a range of less than 15 volts/cm.

432. Both fatigue and lag are illustrated in the following table from Valasek,[544] from observations at 20°C, charging field 900 volts/cm. The first two data may be compared with Fig. 117; from them it is evident

Charging Time, Sec	Discharge, Galvanometer Divisions
0.03	2.15
0.50	2.46
180	2.47
1,200	2.33
5,800	1.94

* Ref. 541.

that the charging process is over in about a second. The last two show the effect of fatigue, not all the charge being instantaneously discharged through the galvanometer.*

Valasek also records some interesting observations on the removal of fatigue by an opposing field. Thus, the effect of a field of 100 volts/cm applied for 24 hr in one direction can be eliminated by subsequent application for 20 min of an equal field in the opposite direction. He also finds that the discharge through a ballistic galvanometer after application of a field in a given direction is greater after the crystal has been strongly fatigued in the opposite direction. Further effects of fatigue are discussed by David.[119]

Kurchatov's explanation[295] of the fatigue effect is that it is due to the migration of ions into the surface layers of the crystal: when the crystal is short-circuited through a galvanometer, the ions migrate very slowly back again. He found that fatigue was absent when solution electrodes were used (see §427).

Mention should be made of certain differences in behavior between thick and thin plates, even though their significance lies mainly in directing attention to the importance of avoiding even minute surface layers or gaps between crystal and electrodes. Such layers form a region of relatively low permittivity, as was pointed out in §111. They therefore make the actual field strength in the crystal less than that computed from the potential difference V and thickness e; moreover, they give rise to a depolarizing field that hastens the discharge. The situation is further complicated if the surface layer is a partial conductor. Thin plates should show these effects more than thick ones. This dependence on thickness was indeed found to be the case by Kurchatov[295] and by Kurchatov and Shakirov,[296] who also offered the explanation given above. A few of their representative results will now be summarized, illustrating the fundamental dielectric properties of Rochelle salt as well as the effect of surface layers. They found, for example, that while for plates of all thicknesses the final state of charge corresponding to the applied field was in general attained in a few hundredths of a second—except that with increasing thickness longer charging times were required when the field strength was relatively weak—there was a marked difference in the case of discharge. Provided that the crystals were not left charged long enough for fatigue to set in, it was found that for thin crystals the times of charge and of discharge were about equal, but that the discharge was much slower in the case of thick crystals; for a crystal 7.2 cm thick it amounted to 30 sec. The same crystal, on application of 130 volts/cm, became fully charged in 0.02 sec, while with 45 volts/cm the charge had not attained one-tenth of its final value in 0.07 sec.

* Somewhat similar observations are recorded by Oplatka.[397]

Using a series of plates from 0.23 to 7.2 cm in thickness, the time of charge being 1 to 2 min, Kurchatov found that the approach to saturation required very much higher applied potentials with thin than with thick plates, in accordance with the explanation offered above. He also found the initial permittivity, with $E = 0.1$ volt/cm, to be 1,340, whereas with alternating current at 50 $\sim$ or 500 $\sim$ it was only 150.

The following conclusions seem justified: (1) that the characteristic properties of Rochelle salt can be studied better with thick than with thin plates, unless the effects of surface layers are completely eliminated; (2) that, insofar as it is desirable to avoid the effects of lag and fatigue, polarization measurements with alternating currents should be more reliable and reproducible than those made with static fields, and the effect of differences in thickness should be less pronounced. In the following sections we shall see that this expectation is realized.

No investigator seems to have measured k_x by a ballistic method over the entire range of spontaneous polarization, with a crystal so well prepared and mounted and with a field strength of such a value that the highest attainable values were recorded. At 15°C B. and I. Kurchatov[293] observed a differential value of 190,000, with a very pure crystal that showed saturation at only 15 volts/cm. With a strong field (value not specified) Schwartz[454] found k_x to reach maxima of about 4,000 and 3,500 at the upper and lower Curie temperatures, respectively, with almost equally high values between; obviously, his observations corresponded to points too far along on the polarization curve to show the highest values of k_x. From the theory one would expect that at either Curie point an extremely small field would cause a relatively great polarization, yielding a very large value of k_x. Between the Curie points the coercive force, though small, is greater than at the critical temperatures, with a corresponding decrease in k_x. Yet even here very large differential values of k_x are to be expected—as witness that of 190,000 at 15°.

433. *Static Observations on Unipolarity.* This characteristic of Rochelle salt was discovered by Anderson (§404). The reader may already have noted a peculiarity in Figs. 117 and 118: the polarizability of Rochelle salt along the X-axis is not symmetrical upon reversal of field, although the symmetry of rhombic crystals is such that both directions along the X-axis are equivalent.

This effect is a consequence of the spontaneous polarization of the crystal, by virtue of which there exists, between the Curie points, a "natural moment" for each domain in the direction of the X-axis. As is explained in Chap. XXV, in this region the crystal is properly to be considered *monoclinic.* In any given specimen, unless the opposing domains happen exactly to neutralize one another, there is a resultant

moment. Under ordinary circumstances the polarization charges may be assumed to be neutralized by equal and opposite compensating surface charges.

If now a unipolar crystal consisting of a single domain is provided with electrodes to which an external potential is applied and if the field thus impressed is opposed to the spontaneous polarization, the latter undergoes a more or less sudden *reversal* when the field reaches a certain value. Enough charge must flow to remove the compensating charges mentioned above in addition to polarizing the crystal to an extent depending on its susceptibility. On the other hand, if the impressed field is in the same direction as the spontaneous polarization, these compensating charges remain and the charge flowing to the electrodes is much less. For the same applied voltage the apparent susceptibility is greater in the former case than in the latter. This effect is further discussed in connection with Fig. 139. If, as is practically always the case, several domains with opposing polarities are present, some trace of the effect will be found unless the domains are exactly balanced.

The degree of unipolarity may be expected to be greater with small specimens than with large. Large plates should show unipolarity in opposite senses over different portions of the surface, corresponding to the pyroelectric patterns described in §521. Such regions were identified by Kurchatov[B32] on a large crystal that showed as a whole no unipolarity: by moving a small electrode across the surface he found regions of very unsymmetrical polarizability.

Evidences of unipolarity were also recorded by Valasek[541] and by Frayne.[149]

The Dielectric Constant of Rochelle Salt at Low Frequencies. The range of frequencies considered here extends from 50 or less to 10,000 cycles/sec. Since the effects of lag and unipolarity are inappreciable, the results are more consistent and reproducible than those obtained under static conditions. As a rule, for frequencies in this range no effects from resonant vibrations need be feared. As the frequency increases from 50 to 10,000 the results differ mainly in increasing width of the hysteresis loops, as will be seen in §436.

434. Observations of the Initial Dielectric Constant k_0' of Free Crystals at Small Field Strength. When the field is sufficiently weak, the relation between P and E is linear, without appreciable hysteresis. The range of linearity depends on the temperature. The critical field strength at which the $P:E$ curve begins to turn upward is zero at the Curie points, increasing rapidly to an indefinitely large value outside these points. In the Seignette-electric region the available data indicate that the value is of the order of 50 volts/cm except close to the Curie points, for frequencies at least from 50 to 10,000 cycles/sec. Under

static conditions (point-by-point method with ballistic galvanometer) the field range is smaller.

In the parelectric regions the values of k_0' obtained by different observers are in very close agreement. The agreement is not so good in the Seignette-electric region, especially in the middle of the region where the values are smallest. Among those who have published values of k_0' (in most cases by a bridge method) may be mentioned Frayne,[149] Errera,[134] Schwartz,[454] Kurchatov and Eremeev,[292] B. and I. Kurchatov,[293] David,[119] Bradford (§474), Mueller,[376] Bancroft,[20] Hablützel,[198] and Mason.[335] Further reference to some of these measurements will be

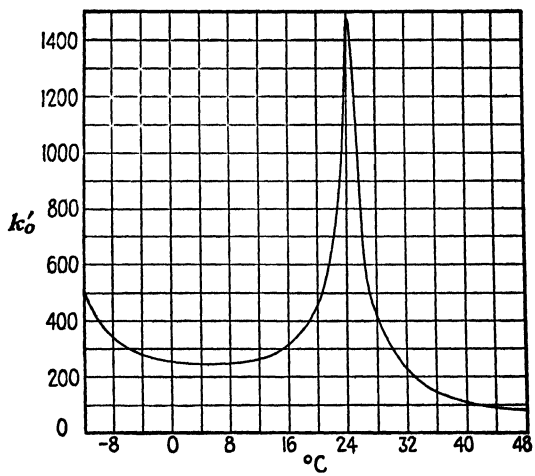


FIG. 119.—Initial free dielectric constant k_0' of Rochelle salt, field parallel to the X-axis, from Mason, ref. 335. The field strength was not over 5 volts/cm.

made in the paragraphs immediately following. Bradford's values are shown in Figs. 145 and 147, Bancroft's in Fig. 132, and Hablützel's in Figs. 134 and 135.

A typical curve showing the dependence of k_0' on temperature is given in Fig. 119, obtained with a 1,000-cycle bridge.

The most careful and complete measurements of the initial dielectric susceptibility η' at low fields (less than 10 volts/cm), chiefly outside the Curie points, are those of Mueller,[376] who used a 1,000-cycle bridge method, and of Hablützel (§444). Mueller's observations, extending from $-140°$ to $-18°$, and from $+21°$ to $+50°$C, verify the Curie-Weiss laws discussed in §465. The results at the higher temperatures are shown in Fig. 120. From 25 to 32° the following relation holds (all temperatures centigrade):

$$\chi' = \frac{1}{\eta'} = \frac{t - t_c}{C} \tag{490}$$

where $t_c = 23.0 \pm 0.5°$ and $C = 178 \pm 5$. t_c is the "Curie temperature" and C the "Curie constant."

Above 34° the crystal is well outside the influence of the Seignette-electric range, in a region which, by analogy with paramagnetism, may

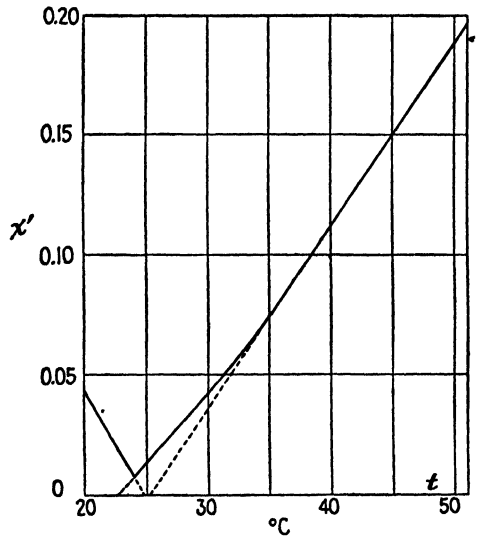


FIG. 120.—Reciprocal susceptibility $\chi' = 1/\eta'$ at high temperatures, from Mueller.

be called the *parelectric* range. Here the relation is very strictly linear; from 34 to 50° Mueller finds $t_c = 25.3 \pm 0.05$°C and $C = 136 \pm 0.5$.

The corresponding relation for the range below the lower Curie point, from −18° to −28°, is

$$\chi' = \frac{1}{\eta'} = \frac{t_c' - t}{C'} \tag{490a}$$

where $t_c' = -17.9°$ and $C' = 93.8$.

Data for the entire low-temperature range down to −140°C are shown in Fig. 121. It will be observed that χ' rises almost linearly until the temperature −160° is reached, after which it assumes the constant value 2.1, corresponding to a dielectric constant of 7.

The slight bend in the curve for χ' at about 33° in Fig. 120 was found also by Mueller in a similar relation for the Kerr effect. Such bends are also encountered in the experimental curves for magnetic susceptibility.

Mueller's values of the two Curie points are the temperatures at which the lowest values of χ' were recorded. These values are adopted in this book, *viz.*,

$$\theta_l = -18°\text{C} \qquad \theta_u = +23.7°\text{C}$$

Mueller derived the same value of θ_u from the Curie-Weiss law in the Kerr effect.

Attention is called especially to the linear relation shown in Fig. 120 just below the Curie point: in accordance with theory (§465), the downward slope is just twice as steep as the upward slope above the Curie point. The Curie point is to be taken as the temperature at which the two lines meet. In an ideal crystal, with sufficiently small field strength,

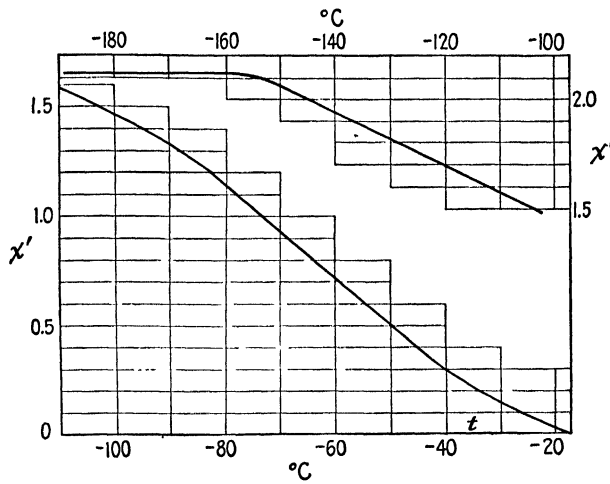


FIG. 121.—Reciprocal susceptibility $\chi' = 1/\eta'$ at low temperatures, from Mueller.

the two lines would be expected to converge on the axis of abscissas, indicating an infinite susceptibility at the Curie temperature. In the actual crystal, t_c and t_c' are not quite the same as the Curie temperatures.

These observations of Mueller are in excellent agreement with those of Hablützel, illustrated in Fig. 135.

An experimental and theoretical study of initial susceptibility has been made by Shulvas-Sorokina[468] with fields up to 12 volts/cm and frequencies from 3 to 3,000 ~.

Further data on the susceptibility between the Curie points are discussed in connection with Fig. 145.

435. Observations in Stronger Fields: Oscillograms and Hysteresis Loops. *The Oscillograph Circuit.* In most of the oscillographic work

referred to below, the horizontal deflection of the electron beam in a cathode-ray oscillograph is sinusoidal in time and proportional to the supply potential, while the vertical deflection is proportional to the charge on a condenser in series with the crystal and hence approximately proportional to the polarization in the crystal. The result is not a correct hysteresis loop, since the impedance of the crystal is variable; the potential drop across the crystal is not sinusoidal and hence not proportional to the abscissas. The ideal circuit, discussed by David, would have the crystal connected directly to one pair of deflection plates, so that the corresponding deflection would be proportional to the field in the crystal. This has not been found feasible, and all the experimenters used circuits that are in principle of the type shown in Fig. 122.*

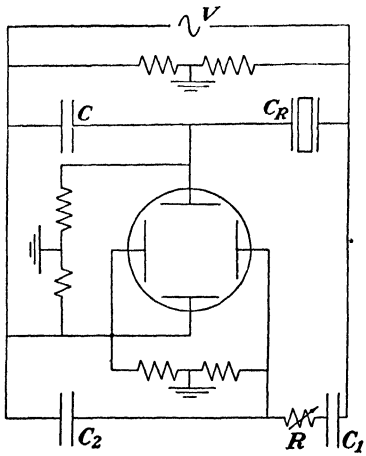


FIG. 122.—Oscillograph circuit for Rochelle-salt hysteresis curves, from Mueller.

The resistance R corrects for the power loss in the crystal C_R. Since the resistance across C is very high, the instantaneous charges on C and C_R are approximately equal, so that the vertical sweep (ordinates of the curves) is approximately proportional to the polarization P in the crystal. If the vertical scale value (oscillograph sensitivity) is $s_y = V_c/y$ volts/cm, where V_c = instantaneous volts across C and y is the deflection of the electron beam in centimeters, the polarization is given by

$$P = \frac{CV_c}{A} = \frac{Cs_y y}{A}$$

A being the area of the crystal plate in square centimeters. The horizontal sweep is proportional to the potential drop across C_2, and this in turn is proportional to V, provided that R is sufficiently small. Calling V and V_c the instantaneous voltages across the entire circuit and C, respectively, we have, approximately, for the drop across C_R,

$$V_R = V - V_c = \frac{C_1 + C_2}{C_1} s_x x - s_y y$$

where s_x and x are the horizontal scale value and deflection. If, as was the case with Sawyer and Tower, resistances R_1 and R_2 were used in

* The circuit shown in Fig. 122 is Mueller's modification[876] of that introduced by Sawyer and Tower.[449]

place of the condensers C_1 and C_2, the ratio $(C_1 + C_2)/C_1$ would be replaced by $(R_1 + R_2)/R_2$. Setting r for this ratio, we have in either case

$$V_R = rs_x x - s_y y$$

This equation can be used to compute the potential drop across the crystal corresponding to any measured point x, y on the actual curve.

436. *Some Typical Hysteresis Loops.* The most complete series of hysteresis loops, for temperatures from −19.5° to +27°C and frequencies from 100 to 100,000 cycles/sec, are those of Hablützel.[198] In §444 we discuss the similar loops obtained by him with heavy-water Rochelle salt. His photographs show that, up to 10^4 cycles/sec, variations in

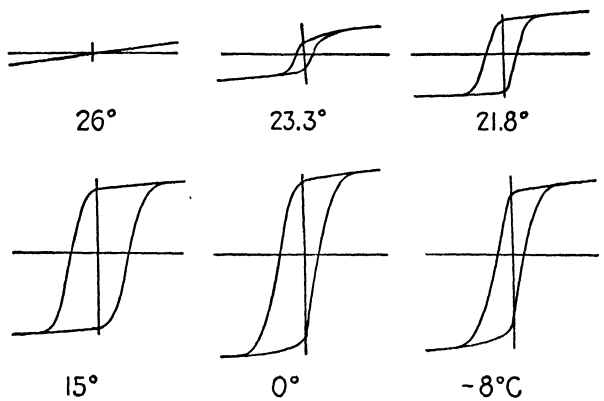


FIG. 123.—Rochelle-salt hysteresis curves, 60 cycles a-c, from Sawyer and Tower. *X*-cut plate 85 × 85 mm, 5 mm thick. Abscissas in volts/cm, max 387; ordinates are proportional to polarization.

frequency have but little effect on the form of the loops. From that point on, the width of the loop begins to increase, the polarization at saturation is less, and the loop becomes distorted. The distortion sometimes appears in the form of ripples, which may be due to natural vibrational frequencies or to shock excitation induced by the rapid variations in polarization.

The oscillographic records shown in the following figures are in general agreement with those made by Hablützel under similar conditions, except that in most cases the steep portions are less nearly vertical and the saturation regions less flat. It will be observed that the hysteresis loops are widest from 0 to 10°C, becoming narrower and smaller as the Curie points are approached. At temperatures outside these points the hysteresis vanishes.

Figure 123 shows oscillograms at 60 cycles by Sawyer and Tower;

those of David, obtained by a closely similar method at 50 cycles, are illustrated in Fig. 124.

Owing to the very large permittivity it is usually sufficient, even with thick plates, to compute this quantity from the simple formula for capacitance, $C = kA/4\pi e$. Only under extreme conditions of temperature or mechanical stress should there be any appreciable gain in precision by the use of a guard ring[119] or by applying Kirchhoff's correction for the edge effect.[87] Nevertheless, David claimed a slight improvement in the form of the hysteresis loop when a guard ring was used.

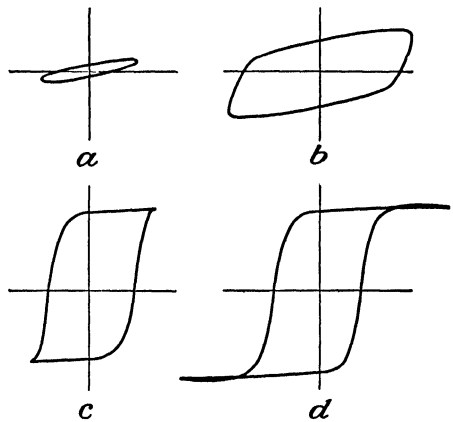


FIG. 124.—Rochelle-salt hysteresis curves, slightly retouched, 50 cycles a-c, from David. X-cut plate 20 × 20 mm, 9 mm thick, edges at 45° with the Y- and Z-axes, at room temperature. For a, b, c, d the maximum field strengths are, respectively, 30.7, 61.4, 123, and 384 volts/cm; remanence at zero field 0.76, 0.75, 23.8, and 23.1 × 10^{-8} coul/cm^2.

Figure 123 shows the effect of varying the temperature. In Fig. 124 the effect of varying the maximum voltage (presumably at room temperature) is seen.

Examination of all available data indicates that the coercive force E_c with alternating fields rises gradually from zero at the Curie points to a maximum somewhere between 5 and 15°C, of the order of 200 volts/cm, as shown in Fig. 147 (for the theory, see §482). Mueller finds that it is greater with thick plates, as shown in Fig. 125, while according to David it varies with maximum field strength. Hablützel[198] finds no dependence of E_c upon thickness.

The forms of the curves in the foregoing figures are in full agreement with theory. Especially noticeable are the disappearance of hysteresis, the small polarization, and the linear relation between polarization and field at 26° in Fig. 123, *i.e.*, at a temperature slightly above the upper Curie point. Figures 124 and 127 indicate that even in the range of spontaneous polarization the observed polarization is almost linear

and reversible for maximum field strengths up to about 50 volts/cm. We see here the first stage in the process of polarization described in §431. At 61.4 volts/cm in Fig. 124*b* the hysteresis is already large. This observation is at variance with that of Kobeko and Kurchatov,[263] who found no hysteresis with their crystal even up to 70 effective volts/cm.

The second stage in the polarization process is that in which the polarization increases rapidly with increasing field. The differential permittivity k_d has here its greatest value, owing to the contribution made by the piezoelectric deformation. This stage lasts until the knee

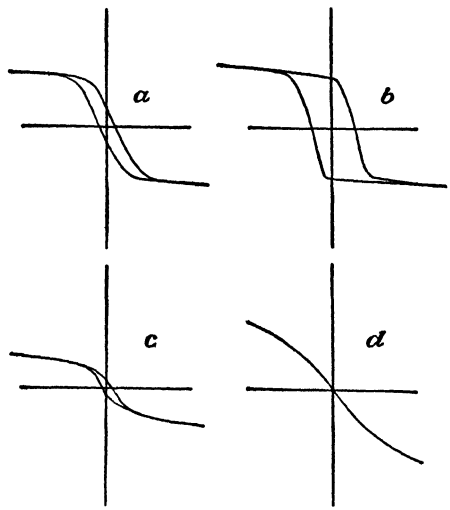


FIG. 125.—Rochelle-salt hysteresis curves, 500 cycles a-c, from Mueller. Curve *a*, *X*-cut plate 3 mm thick at 0°C; *b*, thickness 12 mm, 0°C; *c*, at 22°; *d*, below the lower Curie point.

of the curve is reached, at about 150 volts/cm. From this point on we have the third stage, characterized by an approach to saturation, with a value of the differential permittivity k_{ds} of the same order as that in the first stage, as is shown in Fig. 124, curves *a* and *d*.

From any of the curves the over-all permittivity $k = 4\pi P/E$, the initial permittivity k_0, or the differential permittivity $k_d = 1 + 4\pi \partial P/\partial E$, may be calculated. For example, from the slope in Fig. 123 at 26° we find k of the order of 650, in fair agreement with 740 as calculated from Eq. (490). Values of k corresponding to the tips of the curves in Fig. 123 have been calculated, to show how the over-all dielectric constant varies with temperature, the field strength having a maximum value of 387 volts/cm in each case.

Temperature, deg C.....	26	23.3	21.8	15	0	−8
k.....	650	1,430	2,250	3,900	4,710	4,250

At room temperature and 387 volts/cm Fig. 127 indicates a value of k twice as great as do the data above. Possibly David's crystal was less constrained than Sawyer and Tower's.

From the slope of the "saturation" portion of the curve for 15° in Fig. 123 the saturation permittivity k_{a_s} is estimated as about 330; the corresponding value from Fig. 124 at room temperature is about 200.*

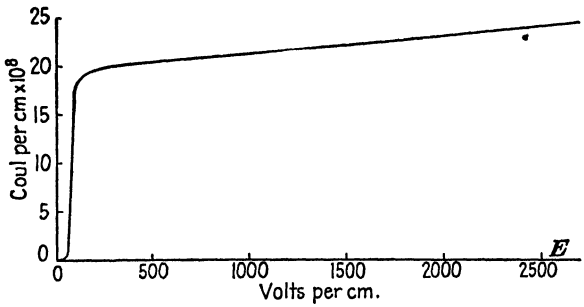


FIG. 126.—Polarization of Rochelle salt at room temperature, from David. The abscissa for each point is the maximum field strength at 50 cycles/sec, and the ordinate is the corresponding polarization.

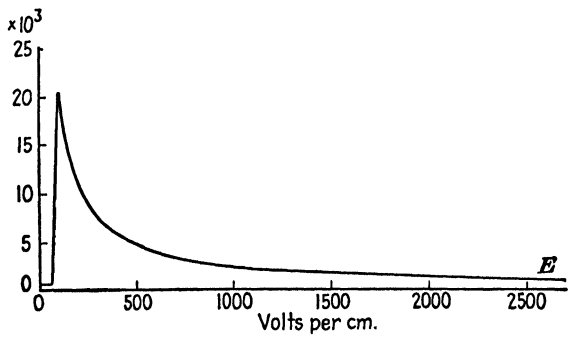


FIG. 127.—Dielectric constant of Rochelle salt as a function of field, 50 cycles/sec. from David. The curve is derived from Fig. 126.

In these curves, as in all polarization curves with Rochelle salt, complete saturation is never observed. Only under enormously large fields could the susceptibility be made to approach zero.

As in the analogous case with magnetic hysteresis loops, the highest permittivities are found along the steep portions of the curves. For example, the highest value of the differential permittivity derived from Fig. 123 is at least 200,000; the highest value from Fig. 124, about

* One would expect the value at room temperature to be *greater* than at 150°. The discrepancy must be due to causes other than the properties of Rochelle salt.

100,000; and the highest value observed by Kurchatov was 190,000 by a ballistic method.

The dependence of polarization on field strength is represented in another manner by David in the paper cited. Figure 126, obtained by plotting the extreme tips of hysteresis curves at different maximum fields, shows clearly the three stages in the growth of polarization, again recalling the magnetic analogy. From Fig. 126 David has derived Fig. 127, showing the dependence of k_x upon field strength. The data for these curves were presumably obtained at room temperature. The fact that as long as the peak value of the field strength is below 50 volts/cm the value of k_x as thus obtained is small and independent of the field is of special significance, as was pointed out in §§403 and 434. David finds that in this range the initial permittivity k_0 is from 400 to 500 and that hysteresis is almost if not entirely absent (*cf.* Fig. 124*a*). This value of k_0 is larger than that found by other observers. For example, B. and I. Kurchatov[293] assign to the initial permittivity at 15°C the value of 150 and state that it holds up to 70 maximum volts/cm. From Fig. 119, the value at 15°C is about 250.

437. *Other Observations with Alternating Fields.* The contrast between the effects of weak and strong fields is illustrated in Fig. 128. Curve *a*, from B. and I. Kurchatov,[293,B32] was obtained with fields not exceeding 15 volts/cm at 50 ~, by a bridge method. Values of k_0 from 100 to 400 are found except in the regions close to the Curie points. Sharp maxima were found at −15° and +22.5°; the Kurchatovs considered the Curie points to be thus determined. These temperatures differ somewhat from Mueller's values of −18° and +23.7° (§434), which he obtained from both dielectric and optical observations. An extremely sharp maximum at the upper Curie point is also recorded by Shulvas-Sorokina,[466] of exactly the same form as in the analogous case for iron. Such maxima are to be expected with weak fields, in view of the theoretical vanishing of the coercive force at the Curie points. Curve *a* agrees satisfactorily with Fig. 147.

Curve *b* is from ballistic observations by Schwartz,[454] with strong fields and long times of charge. In accordance with theory (§455) the values at the Curie points are lower than in curve *a*, but between these points they are higher. Curve *c*, also from Schwartz, at maximum field strength of 10 volts/cm, frequency 500, represents the initial permittivity k_0. In the range of spontaneous polarization, k_0 is in the neighborhood of 250, rising to maxima of 500 and 850 at the lower and upper Curie points. At 20° the value is about 350, in good agreement with that calculated from Mueller's observations (§434). It is impossible to say whether Schwartz's failure to record high maxima at the Curie points, comparable with those of B. and I. Kurchatov, is due to his

slightly weaker field or to greater mechanical constraint. The latter is a plausible explanation, since his plate was clamped between the cells that held the mercury electrodes.

In a stronger field (100 to 1,200 volts/cm), Kobeko and Kurchatov[263] found, on the other hand, in agreement with Valasek and Schwartz,[454] an almost uniformly high value of k_x between the Curie points, falling off sharply outside of this range. The theoretical explanation of this is given in §479. Their paper is among the first to give data on dielectric saturation at large field strengths.

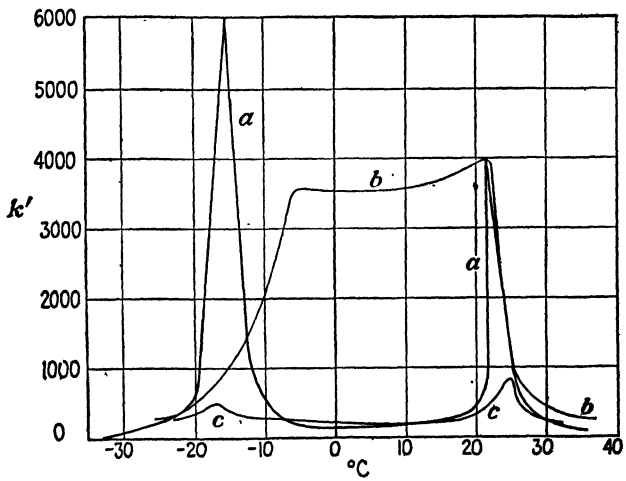


FIG. 128.—Effects of temperature on the dielectric constant of Rochelle salt. Curve *a* from Kurchatov, *b* and *c* from Schwartz.

A very curious dependence of dielectric constant upon frequency at very low frequencies has been reported by Shulvas-Sorokina and Posnov.[469] They find a sharp maximum in k at a frequency between 2 and 30 cycles/sec, the value of the frequency depending on field strength, temperature, and thickness of plate. They offer a theoretical explanation in terms of relaxation times, support for which is found in the slow growth of piezoelectric polarization under small mechanical stresses (§427).

438. *The Spontaneous Polarization $P°$.* The earliest estimates were made from the remanent polarization in hysteresis loops obtained by a step-by-step method, using static fields. From the work of Valasek[541,542] and Frayne,[149] as well as from Figs. 117 and 118, values may be derived ranging from 30 to 180 esu. These values are not unreasonable for temperatures just below the Curie point; they are on the whole probably too small, owing to the leakage of charge between observations. The most reliable data are from oscillograms of hysteresis loops at frequencies

from 50 to 1,000 cycles/sec. Mueller's curve for P^0 in terms of temperature, obtained by this method, is shown in Fig. 147. It is in excellent agreement with Hablützel's observations (Fig. 136). Fair approximations to these values may be deduced from the observations of Kobeko and Kurchatov and from the oscillograms of Sawyer and Tower, of David, and of Mueller, which were shown in previous sections.

At temperatures well outside the region of spontaneous polarization the results of all observers show that hysteresis is absent and that the polarization is directly proportional to the field. For temperatures only slightly outside the Curie points there is still some variation with field. The effect at low temperature is shown in Fig. 125*d*. Under extremely large magnetic fields certain paramagnetic substances show an analogous dependence of permeability upon field strength.

439. *Hysteresis Loops with Mechanical Bias.* If while in an alternating electric field the crystal is also kept under a constant mechanical stress of such a nature as to produce a fixed piezoelectric polarization on which the polarization due to the field is superposed, the hysteresis loops are distorted and unsymmetrical. Such curves, first mentioned by Valasek, have been recorded by Sawyer and Tower,[449] David,[119] Mueller,[376] and others. Ballistic observations of the effects of mechanical or electrical bias have been made by Anderson (§404), Valasek,[542] and Schwartz.[454]

Some of the results are shown in Figs. 129 and 130. The interpretation of the oscillograms is further discussed in §441. Sawyer and Tower cemented their crystal plate between two thick aluminum plates; the others applied mechanical pressures at 45° to the Y- and Z-axes by means of flat blocks of solid material.* We shall use the term "single constraint" for equal and opposite pressures along one of the two 45° directions, and "double constraint" for two pairs of pressures, one pair along each of the 45° directions. Under the single constraint a piezoelectric polarization becomes superposed upon that due to the electric field, thus shifting the position of the origin on the hysteresis loop. Unless the mechanical arrangement is such as to keep the stress actually constant throughout the cycle, the oscillograms are of more qualitative than quantitative value. Under double constraint, if the pairs of pressures are always equal they produce equal and opposite contributions to the polarization. The bias is thus reduced to zero. This restores the symmetry, but the polarization recorded on the oscillograms is diminished, since the crystal is no longer free.

* As is shown in §139, a pressure Π at 45° causes a shearing stress $Y_s = \Pi/2$. The resulting polarization is $P = -d_{14}Y_s = d_{14}\Pi/2$, subject to correction for capacitance connected to the crystal. All the investigators named used rectangular (in most if not all cases square) X-cut plates with edges at 45° to the Y- and Z-axes.

The following conclusions may be drawn from Figs. 129 and 130. Any constraint, whether single or double, flattens the hysteresis loop, until under heavy pressure the polarization is so suppressed that the

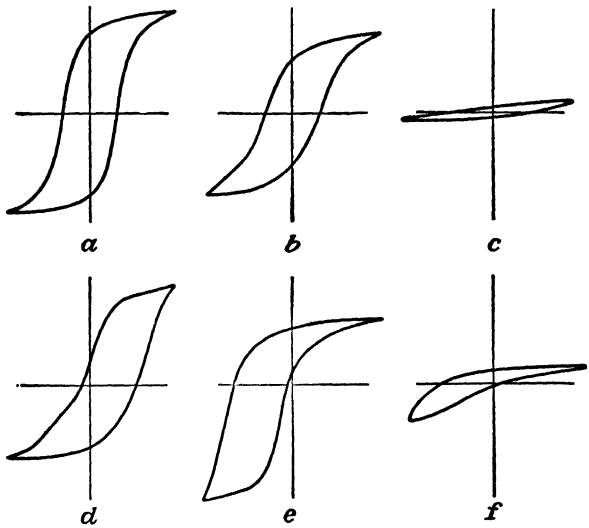


FIG. 129.—Effect of mechanical constraint on the hysteresis curves for Rochelle salt at 500 cycles, 0°C, from Mueller. Maximum field strength 2,000 volts/cm. Curve *a*, free crystal; *b*, double constraint, pressure 1 kg/cm²; *c*, double constraint, 7 kg/cm²; *d*, single constraint, 2 kg/cm²; *e*, single constraint, 3 kg/cm², applied in a direction 90° from that in *d*; *f*, single constraint, 7 kg/cm² in same direction as in *e*.

loop approaches a straight line having approximately the slope of the "saturation" portion of the unconstrained curve. The effective permittivity then becomes the same as the differential permittivity at saturation, which in §436 was seen to be of the order of 200. The fact that 200 is also the order of magnitude of the (monoclinically) clamped

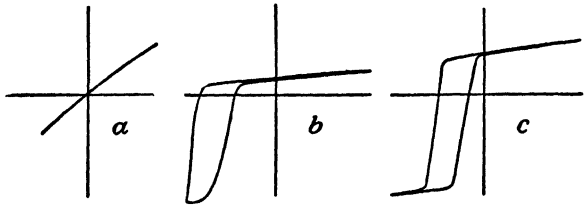


FIG. 130.—Effect of single constraint on Rochelle-salt hysteresis curves at pressure 8.35 kg/cm², from David. Maximum volts per cm: *a*, 383; *b*, 768; *c*, 1532. Frequency 50 cycles.

dielectric constant, as may be seen from the curve for χ_s'' in Fig. 145 at 20°C, is evidence that David's constraint was sufficient to cause the crystal to be very effectively clamped.

Sawyer and Tower[449] also obtained oscillograms with a constrained plate, finding a dielectric constant of 430 at 15°. This value agrees fairly well with that which they found for the unconstrained plate at saturation, but it is so much greater than the value for a clamped crystal derived from Fig. 145 as to indicate that the constraint was far from complete.

The characteristic effect of a *single* constraint is the *asymmetry* that it introduces in the hysteresis loop, and is especially conspicuous in Fig. 130*b* and *c*. Furthermore, Fig. 130*a* shows that the range of field strengths over which the initial permittivity is practically constant is greatly extended by a single constraint: the maximum field strength for this curve is 383 volts/cm, whereas in §436 the value for a free crystal was only 50. On the other hand, David finds that the initial permittivity is diminished by a single constraint and that the diminution is made greater by repeated mechanical loading.

If the mechanical bias used in conjunction with a-c experiments is to be constant throughout the cycle, the natural frequency of the mechanical pressure system must be higher than that of the crystal. Or if the pressure is simply due to the gravitational weight of a certain mass, the maximum acceleration of the face of the crystal plate must be less than 980 cm/sec^2.

A little consideration shows that, if the mechanical pressure varies cyclically, the effective bias at one end of the hysteresis loop will be greater than at the other. The loop is thus still further deformed. Furthermore, a variable pressure causes variable piezoelectric charges to be liberated, which produce a disturbing periodic field unless the resistances in the bridge arms are sufficiently low.

Friction between the pressure blocks and the crystal must tend to suppress the slight periodic changes in dimensions and thus to reduce the polarization. This fact may possibly account for the observed reduction in polarization under double constraint.

David also made oscillograms with the plate under a *hydrostatic* pressure (in oil) of 35 kg/cm^2. The curves were exactly the same as when the crystal was free. This result was to be expected, except insofar as the hydrostatic pressure brought the crystal to a slightly different position relative to the two Curie points (§443).

440. *Experiments on the equivalence of mechanical and electrical bias* have been made by David. He found that when, instead of mechanical pressure, a d-c source was connected across the crystal while it was in the oscillograph circuit the same asymmetrical curves were obtained. The asymmetry of mechanical origin could be completely removed by application of a field E_b opposing the piezoelectric polarization. Some idea of the number of volts per centimeter equivalent to 1 kg/cm^2 can be

gained from the asymmetry of the curves in Fig. 129 and 130; it appears to range from about 70 to 300. A value of the same order of magnitude as this is derived from the equation $E_b = -Y_z/b_{14}$ in §462, where b_{14} is the piezoelectric strain coefficient according to the polarization theory. In each case the equivalent bias is derived from the estimated horizontal displacement of the origin from the center of the loop. The *sum* of the piezoelectric and purely electric polarizations never exceeds the usual saturation value.

In this connection may be mentioned an experiment of Mueller's,[376] who made measurements, with a low-voltage a-c 1,000-cycle bridge, of the capacitance of a crystal on which there was superposed at the same time a much greater direct potential difference E of various positive and negative values up to ± 800 volts/cm. This potential was put through a step-by-step cycle of increasing and decreasing values in both directions. The bridge measurements gave values of the reversible permittivity $k_r = 1 + 4\pi\delta P/\delta E$ (§430). When plotted in the form of a curve (Mueller's Fig. 22), they gave evidence of hysteresis in the $P:E$ relation. This result is in agreement with that of Valasek, obtained with a ballistic galvanometer, mentioned in §431.

441. *Explanation of the Biased Hysteresis Loops.* It has been stated that the effect of bias, whether electrical or mechanical, is to shift the origin. This is represented in Fig. 131, in which the normal unbiased loop has the total sweep AB in field strength. If a large biasing polarization of value E_1O_1 is imposed on the crystal, the origin for the new curve is at O_1, this being the point on the virgin curve corresponding to the given bias. The bias then has the abscissa OE_1. The same sweep in field strength as before is now represented by A_1B_1, and the resulting loop extends from M_1 to N_1. If the sweep in field strength were a little less, from A_1' to B_1', the loop would extend from M_1' to N_1'. The point O_2 represents the origin for a small amount of bias, and the loop for a small horizontal sweep is then somewhat as indicated by M_2N_2.

The location of the origin with respect to the hysteresis loops is not the same in Figs. 129 and 130 as in the schematic drawing of Fig. 131. The reason for this lies in the fact that in oscillograph circuits of the type shown in Fig. 122 the bias, whether electrical or mechanical, does not cause a biasing static charge on the condenser C. In Fig. 122 the resistance across C, high though it is, prevents this. Hence, taken around the cycle, $\int V_C\, dt = 0$. This result is independent of the time scale of abscissas, which is usually sinusoidal. If the hysteresis loop were redrawn to a *linear* time scale having abscissas proportional to the time, it would be found that *equal areas* would be described on each side of the horizontal axis. With a sinusoidal time scale this is still approximately true, as can be verified from the curves. In Fig. 131

the distorted loops have the locations where they would be recorded if the biasing polarization were accompanied by a corresponding fixed charge on the condenser C of Fig. 122. Distorted hysteresis loops such as these have their analogy in magnetism, when a ferromagnetic substance is subjected to the combined action of a fixed and an alternating magnetic field.

By a suitable choice of bias and of horizontal sweep, all the single-contraint curves in Figs. 129 and 130 can be qualitatively reproduced on Fig. 131. The equivalence of biases produced electrically and

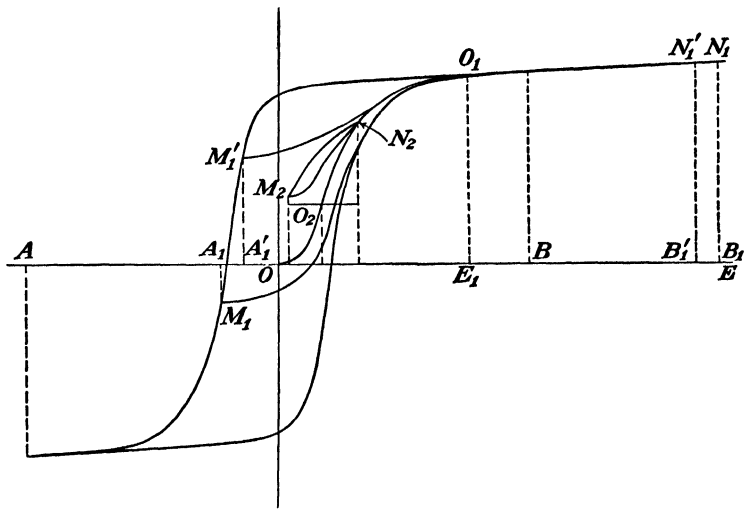


FIG. 131.—Hysteresis loops with various amounts of bias. Coordinates are field strength E and polarization P.

mechanically is thus made evident. The relation between electrically and mechanically produced polarizations is discussed in Chap. XXIV on the polarization theory, especially in §§459 and 462.

442. The Dielectric Constant of Rochelle Salt at High Frequencies. If observations could be made with specimens so small as not to resonate mechanically at any frequency within the range of investigation, the dielectric constant measured would be that of the free crystal. This procedure is not practicable; in all the h-f observations mentioned below, resonance conditions were encountered.

We saw in §258 that the measured dielectric constant is always abnormally high on the l-f side of resonance (just as in optical anomalous dispersion) and abnormally low on the h-f side. The expression for the complex dielectric constant in terms of the mechanical and electrical characteristics of the crystal is derived in §258. At the highest fre-

quencies the configuration of the crystal is that described in §450 as "rhombic clamping" outside the Curie points and as "monoclinic clamping" between these points. The concept of rhombic clamping between the Curie points is of only theoretical significance.

Data on values of the dielectric constant k_x are assembled in Table XXXIV. For comparison, some of the l-f values recorded by the same investigators are included, although in most cases they do not appear to be typical of Rochelle salt at low frequency.

TABLE XXXIV

Author	Ref.	Temp., deg C	Maximum field strength, volt cm^{-1}	Frequency, kc sec^{-1}	k_x	Electrodes
Frayne	149	Room	3	8	140	Tinfoil
				40,000	100	Tinfoil
Errera	134	Room	113	0.68	390	Solution
				1,000	100	Solution
Busch	87	0	50	20	225	Mercury
				160	120	Mercury
Bantle and Busch	24	0	?	6,100	100	Tinfoil(?)
				750,000	100	Tinfoil
Evans	140	16–17	45	300	114	Mercury
				2,000	114	Mercury
Hablützel	198	0	8.5	0.1	200	Vaporized
				10	200	gold
Mason	338	20	<5	1	460	"Plated"
				160	140	"Plated"

Most noteworthy is the approach of k_x to a value of the order of 100 at the highest frequencies. It is here that the value of the dielectric constant of the "free" crystal approaches that of the crystal clamped, which we denote by k_x''. At the lower ends of the frequency ranges the discrepancies in k_x as between different observers can be attributed to differences in frequency, mechanical constraint, and field strength, and also perhaps to the effect of surface layers.

Supplementing the data in Table XXXIV it may be said that Frayne, whose observations had to do only with the *initial* permittivity k_0, found maxima for this quantity at both Curie points at all frequencies; he found also that, below −80°C, k_0 was approximately 12 at all frequencies (*cf.* Fig. 121). Errera found a fairly uniform diminution in k_x with increasing frequency, except of course in the various resonance regions. From 1.6 to 20 kc/sec he observed that k_x was increased by about 100 per cent as the field strength increased from 56 to 226 maximum volts/cm. This fact indicates that at these frequencies the steep portion of the polarization curve comes at higher field strengths than it does at lower frequencies.

Busch's observations were made at several different temperatures from 6 to 36°C. His data point to a permittivity in the neighborhood of 100 at the highest frequencies, but at the lower frequencies the values range from about 110 at 36° to 450 at 23°. Bantle and Busch found a maximum in k_x at 23° even at the highest frequencies.

The value from Mason at 1 kc/sec is from Fig. 119. Hablützel's value is from his paper on heavy-water Rochelle salt (which contains much valuable information on ordinary Rochelle salt as well), discussed in §444.

Zeleny and Valasek[600] have also made observations of permittivity at frequencies from 30 to 10^7 cycles/sec at 0°C. They found a general downward drift from 62,000 to 220 as the frequency increased, but otherwise it is difficult to fit their observations into the picture presented above, since their large values of k_x are not reconcilable with the low field strength of only 8.75 volts/cm and, moreover, they report *negative* values of k_x at 10^7 cycles/sec, a frequency far too high for reactions from mechanical resonance. As suggested by Bantle and Busch, this observation may have been due to the self-inductance of the leads to the crystal.

443. Effect of Hydrostatic Pressure on the Susceptibility of Rochelle Salt. The measurements at hand are those of Eremeev, quoted by Kurchatov,[B32] and of Bancroft.[20] Eremeev's results are in the form of polarization curves obtained with 50-cycle alternating current for field strengths extending to 1,800 volts/cm. At 15°C, for any given field strength, the polarization and hence the susceptibility increase with increasing hydrostatic pressures up to 5,000 kg/cm²; at still higher pressures they decrease, and the flattening of the curves at high field strengths gradually disappears, until at 8,000 kg/cm the polarization is proportional to the field. Since a linear polarization curve is characteristic of the region outside the Curie points, it is apparent that high pressure shifts these points so that at 15° the crystal is no longer in the Seignette-electric region. Similar tests at 31°C showed that, while P is proportional to E up to 2,000 kg/cm², it begins to take on saturation characteristics at higher pressures; at 3,000 kg/cm² the curve at 31° is exactly like that at atmospheric pressure and 22.5°. Thus a pressure of 3,000 kg/cm² raises the upper Curie point by about 9°. Kurchatov interprets this result as evidence that the Curie point, on the absolute temperature scale, is proportional to the concentration of the dipoles; for from the elastic constants of Rochelle salt the increase in density for 3,000 kg/cm² amounts to 3 per cent, and this fraction of the absolute temperature is 9°.

By Bancroft's method a precise determination of the shift of both Curie points is made possible. He used 1,000-cycle alternating current with 2 rms volts applied to the crystals (field strength about 8 volts/cm). Three

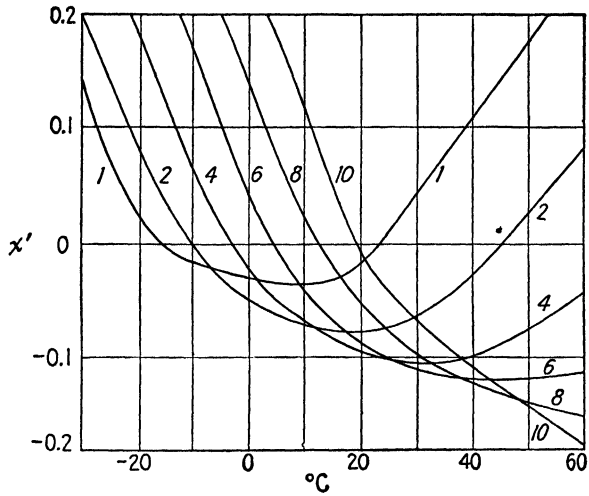


FIG. 132.—Dependence of the reciprocal initial susceptibility of a free crystal of Rochelle salt in the X-direction upon temperature and hydrostatic pressure, from Bancroft's data. Positive values of χ' correspond to the region outside the Curie points, where the susceptibility of the free crystal is $\eta' = 1/\chi'$. Between the Curie points χ' is negative, and the observed susceptibility of the free crystal, by Eq. (499), is $\eta_s' = 1/\chi_s' = -1/(2\chi')$. Curve 1 is for atmospheric pressure. The numbers beside the other curves denote the number of thousands of kilograms per square centimeter.

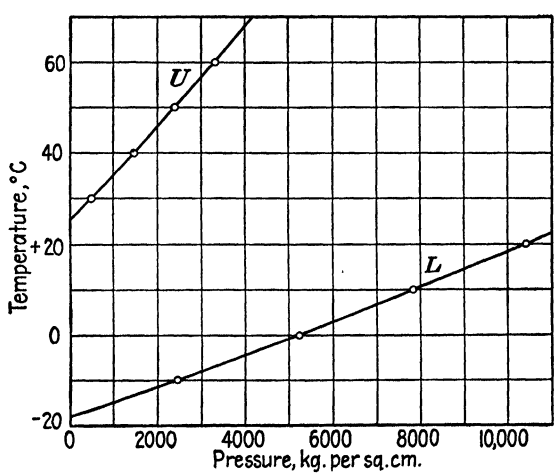


FIG. 133.—Dependence of the upper and lower Curie temperatures on hydrostatic pressure, from Bancroft. U = upper, L = lower Curie point.

crystals were used, of thicknesses 0.424, 0.356, and 0.313 cm. Temperatures were measured to $\pm 0.1°C$, and pressures were accurate to ± 10 kg/cm^2. X-cut crystals were suspended in such a way as to eliminate mechanical constraints and to yield reliable values of the initial susceptibility η' and η_s' the X-direction. The results are shown in Fig. 132, taken from Mueller.[381] The agreement with Mueller's values[376] is better than 5 per cent. Bancroft found the following approximate relations between the Curie temperatures and pressure (p in kg/cm^2):

$$\theta_u = 24.5° + 1.073p(10^{-2})$$
$$\theta_l = -19.4° + 3.769p(10^{-3})$$

Under increasing pressure both Curie points are raised and the interval between them becomes greater, as is seen in Fig. 133. According to this diagram there should be found at about 12,000 kg/cm^2 a *lower* Curie point at the same temperature as that of the upper Curie point at atmospheric pressure. Under suitable pressure there can be a Curie point at any temperature above $-18°C$.

Although Bancroft's paper does not record the observed values of susceptibility at the Curie points, it is evident from his Fig. 2 that they were finite, though very large, and that, the higher the Curie-point temperature, the greater the measured susceptibility.

Since Kurchatov's data do not indicate with sufficient precision the susceptibility at small field strengths, direct comparison of his results with Bancroft's is impossible. So far as one can judge from Kurchatov's results at high field strength, the agreement with Bancroft is satisfactory.

For details of Bancroft's theoretical treatment of his results the original paper must be consulted. He correlates his results with an equation of Fowler's[142] for the dependence of susceptibility on temperature and arrives at the conclusion that the increase in the Curie temperatures under pressure is a volume effect, due to distortion of the crystal lattice under pressure. For further discussion of these results see §470.

444. Heavy-water Rochelle Salt. The investigation of the effects of substituting deuterium for hydrogen in Rochelle salt is important from its bearing on the part played by hydrogen atoms in the dielectric phenomena. Hablützel[198] was the first to publish results, followed a few months later by Holden and Mason[231]. In both cases the crystals were prepared by dissolving in highly concentrated D_2O ordinary Rochelle salt that had been thoroughly desiccated at a high temperature (Hablützel, 40°C; Holden and Mason, 100°C). From this solution the crystals were grown. According to Hablützel, not only does the water of crystallization in these crystals consist of D_2O, but the hydrogen atoms in the OH groups (§405) are replaced by deuterium, so that the formula

becomes $NaKC_4H_2D_2O_6 \cdot 4D_2O$. The density, according to Holden and Mason, is 1.830 ± 0.003. Gold films were evaporated onto the crystals in vacuum in all these experiments, except that at high frequency Hablützel found it necessary to use mercury electrodes, owing to minute sparks betweeh the gold films and the wires with which they made light contact. Hablützel found that the loss of water of crystallization was negligible when the crystals were in vacuum for the short time necessary for the deposition of gold.

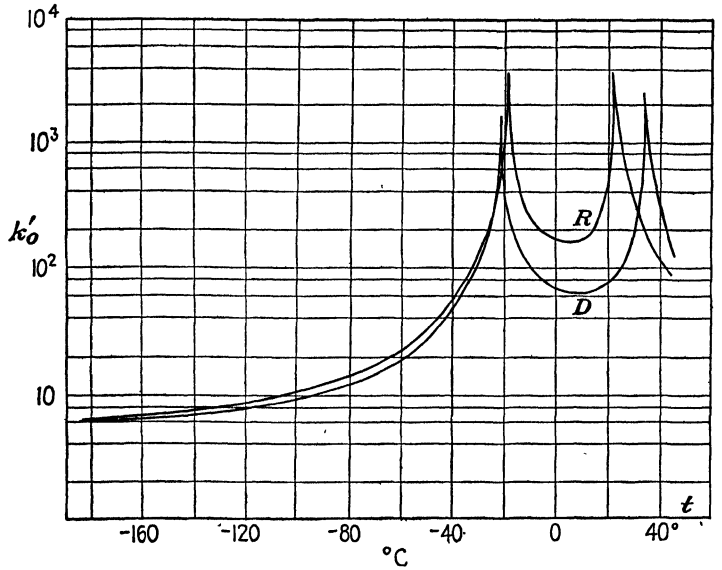


FIG. 134.—Dielectric constant of Rochelle salt (curve *R*) and deuterium-Rochelle salt (curve *D*), as functions of temperature, from Hablützel. Below 40°C, $E = 50$ volts/cm, $f = 1{,}000$ cycles. Above 40°C, $E = 4$ volts/cm, $f = 900$ cycles.

Dielectric Constant. In both papers a bridge method is described, with relatively low frequencies, and with a voltage so low that the measured constant is the initial permittivity k_0. For observations at higher voltages, Hablützel used a cathode-ray oscillograph.

In Fig. 134 are shown Hablützel's values of the initial dielectric constant k_0 for fields parallel to X, for both ordinary and heavy-water Rochelle salt. The values for ordinary Rochelle salt run somewhat lower than those that we have adopted for Fig. 147; those for deuterium–Rochelle salt are in satisfactory agreement with Fig. 5 in Holden and Mason's paper.

Hablützel finds the Curie points for the deuterium salt to lie at −22°C (251°K) and +35°C (308°K); Holden and Mason find −23° and

+35°. Hablützel's values of k_0 at the Curie points are approximately 4,000 at each point for ordinary Rochelle salt; approximately 2,300 and 1,550 at the upper and lower temperatures, respectively, for the deuterium salt.

From his results Hablützel calculated the reciprocal susceptibility χ', which is shown as a function of temperature outside the Curie points in Fig. 135. The curve for ordinary Rochelle salt agrees completely with Mueller's findings (Figs. 120 and 121). That for the deuterium salt is similar, being nearly linear close to the Curie points, in accordance with the Curie-Weiss law.

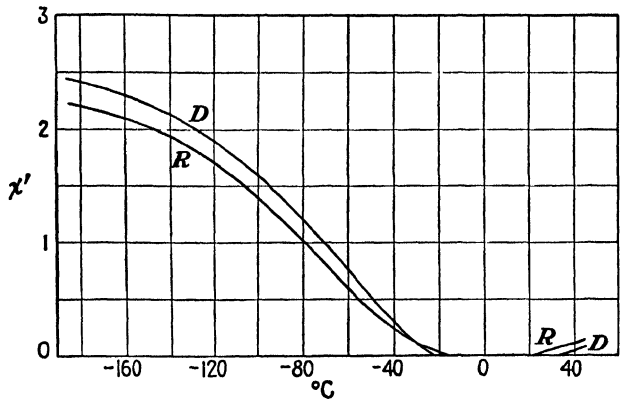


FIG. 135.—Dependence of reciprocal susceptibility upon temperature, illustrating the Curie-Weiss laws outside the Curie points, from Hablützel. R = Rochelle salt, D = deuterium-Rochelle salt.

With fields of 8.5 volts/cm parallel to X, the dielectric constant k_0 of both ordinary and deuterium–Rochelle salt was found by Hablützel at 0°C to be practically the same for frequencies from 100 to 10,000 cycles/sec. The values are approximately 200 for ordinary Rochelle salt (Table XXXIV) and 65 for the deuterium salt.

Hysteresis and Saturation. Hablützel's paper contains two series of very instructive oscillograms. The first series was recorded with 2,000 volts/cm maximum, 50 cycles, at various temperatures from −19.5° to +37.5°C, for both kinds of Rochelle salt. Those for ordinary Rochelle salt are in general agreement with the oscillograms pictured in this chapter; they differ from the latter chiefly in that the steep slopes of the hysteresis loops are more nearly vertical, thus approximating more closely to the ideal loop in Fig. 167. The absence of hysteresis at temperatures outside the Curie points is clearly shown.

For the deuterium salt the loops are both higher and broader than for the ordinary crystal, indicating considerably greater hysteresis loss,

greater coercive force, and a higher spontaneous polarization. The remanent polarization, which, as we saw in §438, is a measure of the spontaneous P^0, is shown in Fig. 136, while Fig. 137 indicates the coercive field strength, plotted in terms of temperature. From Fig. 136 we find, for ordinary Rochelle salt, maximum $P_0 \approx 735$ esu/cm^2 at about

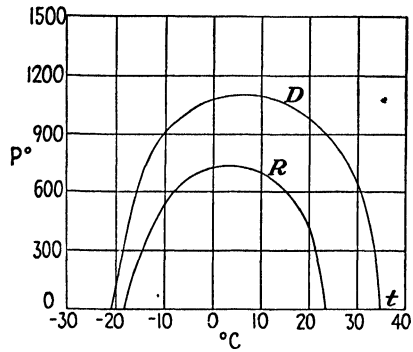


FIG. 136.—Remanent polarization P° as a function of temperature, from Hablützel. R = Rochelle salt, D = deuterium-Rochelle salt. Ordinates are in esu.

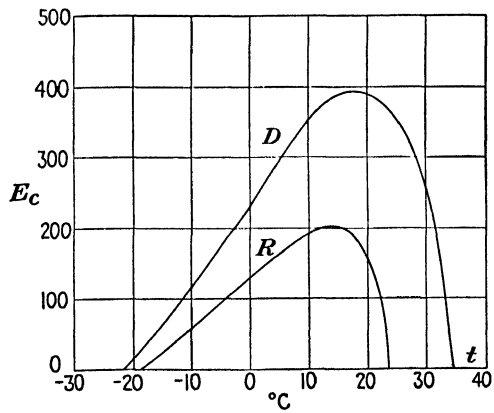


FIG. 137.—Dependence of coercive field strength on temperature, from Hablützel. R = Rochelle salt, D = deuterium-Rochelle salt. Ordinates are in volts/cm.

3°C, in good agreement with Mueller's value of 740 in Fig. 146. The deuterium salt has $P^0 \approx 1{,}110$ esu/cm^2 at about 6°C.

According to Fig. 137, the coercive field strength for ordinary Rochelle salt has a maximum value of 200 at about 15°C (*cf.* §436). Hablützel finds, contrary to Mueller, that the coercive field strength does not depend on the thickness of the plate. Mueller's coercive field values, shown in Fig. 147, are about twice as large as Hablützel's (see §479).

Hablützel's second series of oscillograms, made at room temperature

with 3,000 maximum volts/cm, show the effect of increasing frequency on the form of the hysteresis loops. From 100 to 1,000 cycles/sec there is not much change. From there on, the loops become broader, the maximum slope is less, higher voltages are required for saturation, until at 100,000 cycles/sec the maximum field strength is insufficient for saturation and the curves show pronounced asymmetry. Hysteresis is present at all frequencies.

Fields Parallel to Y and Z. Hablützel's values are given in §408. Holden and Mason assign the value 18.0 to k_y at 30°C, which is so large that its correctness is doubtful. For k_z they find the value 10.4. The piezoelectric constants are given in §143.

CHAPTER XXIII

THEORY OF ROCHELLE SALT, PART I. INTERACTION THEORY AND DIELECTRIC PROPERTIES

Regola che mai, o raro falla: Non si multi dove non è difetto, perchè non è altro che disordine. Dove però tutto è disordine, meno vi rimane del vecchio, meno vi rimane del cattivo. —MACHIAVELLI.

After a brief account of the historical development there will follow, in this chapter and the next, a formulation of the "interaction theory," based chiefly on the researches of H. Mueller. The formulation is as free as possible from molecular assumptions and general enough to apply to all crystals exhibiting the ferromagnetic analogy; thus it is well suited to serve as a basis for discussion of the more specialized theories of the various Seignette-electrics, of which Rochelle salt is the original and so far the most important member.

It is historically interesting to recall that the first attempt at a quantitative theory of ferromagnetism employed a method that had been developed for the study of *electric* dipoles. That theory, grown to maturity, has now returned to the field of dielectrics.

The ferromagnetic analogy in Rochelle salt seems to have been first discussed in a paper by Valasek.[542]

The foundation for the theory of Rochelle salt was laid by I. Kurchatov. From observations of the dielectric constant of this crystal, made by himself and his collaborators, he was led to formulate a theory, based on the earlier work of Langevin, Debye, and Weiss, in which Rochelle salt was treated as possessing dielectric properties analogous to the magnetic properties of ferromagnetic substances. A brief account of his theory, as well as of the somewhat parallel work of Fowler, can most appropriately be given in this chapter, even though their theoretical investigations were of a molecular nature.

445. *Kurchatov's Theory.* In an important paper by Kobeko and Kurchatov in 1930[263] appeared the first formulation of Rochelle-salt theory in mathematical terms similar to those employed in the Langevin-Weiss theory of ferromagnetism. From the dependence of the dielectric constant upon temperature, these authors concluded that Rochelle salt must contain rotatable dipoles, each having a moment that they computed to be of the order of 10^{-18} esu and a molecular field of the order of 10^7 volts/cm.

This molecular theory was elaborated by Kurchatov and his associates in later papers and is now available in Kurchatov's book. Reference to their experimental work is made in other chapters. The theory, as set forth in Chap. XXVI, is based on Debye's theory of electric dipoles, an essential feature of which is Langevin's treatment of the effect of thermal agitation [Eq. (556)], originally derived for paramagnetism and adapted by Debye to the analogous electrical problem. It is assumed, as in the case of paramagnetism, that the dipoles are free to rotate in all directions, like those of a gas. The dipolar property is supposed to reside in the H_2O molecules, a hypothesis that was first suggested by Valasek. Kurchatov shows that the electric interaction between dipoles causes an internal field of sufficient magnitude to account for spontaneous polarization below a critical temperature, without the need of invoking anything corresponding to the exchange forces. as was the case with ferromagnetism.

The Kurchatov theory predicts a critical temperature (the upper Curie point) at which the dielectric susceptibility η_{11} parallel to the X-axis has an infinite value and below which the crystal is in a state of spontaneous polarization. In order to account for the lower Curie point it postulates a "reciprocal action" between dipoles which leads to the formation of mutually neutralizing chains, so that the number of dipoles effective in producing a spontaneous polarization decreases with decreasing temperature. The fact that most dipolar crystals fail to exhibit Seignette properties is explained on the supposition that in them the reciprocal action is so strong as to prevent orientation by an external field.

It is noteworthy that this theory postulates separately polarized domains analogous to those in iron, but erroneously supposed to be, just as in iron, of submicroscopic size. Those peculiarities which have come to be recognized as due to a *large-scale* domain structure were attributed by Kurchatov to imperfections in the crystal. To Rochelle salt and those crystals isomorphic with it that possess similar electric properties, Kurchatov applied the term "Seignette-electrics."

446. *Fowler's Theory.* The route followed by R. H. Fowler[B18,142] in arriving at an expression for the dielectric constant as a function of temperature is that of "cooperative states," a concept similar to the "cooperative phenomena" introduced by Zwicky and which, though without precise formulation, enters into Kurchatov's theory of Rochelle salt. According to Fowler's theory there exist, for each dipole of a Rochelle-salt crystal, certain preferred positions, owing to the effect of neighboring dipoles. The energy of each dipole is a function of the amount of rotation present. The dipoles are subject to a restraining field that becomes more effective as the temperature decreases. This is

closely similar to Kurchatov's hypothesis of a decrease in the effective number of dipoles.

The dipoles are assumed to be the molecules of the water of crystallization. Above the upper Curie point there is complete disorder and no spontaneous internal field. Between the Curie points a certain portion of the dipoles form groups or filaments, their polarities oriented in either the positive or the negative direction of the X-axis. This is the cooperative state, giving rise to a field that prevails throughout an entire domain. Whichever orientation prevails determines the spontaneous polarization, the value of which depends on the temperature. Below the lower Curie point the dipoles become "frozen" in small local groups with external fields so weak that spontaneous polarization disappears. Cooperation is here replaced by association.

The internal field constant γ is assumed by Fowler to have different values parallel and perpendicular to the X-axis of the crystal. In the region of spontaneous polarization the energy of interaction between dipoles is found (in agreement with Kurchatov) to be of the right magnitude to account for the large internal field. An expression is derived for the dielectric constant, which, on substitution of suitable trial values for certain parameters that cannot be quantitatively determined from theory, gives a dependence on temperature over a range extending beyond both Curie points that agrees at least qualitatively with experiment. It predicts, in agreement with Kurchatov's theory, infinite permittivity at the two Curie points. Fowler considers the rotation of dipoles in Rochelle salt as a special case of the large group of recently discovered oscillation-rotation transitions in various solids, for example in halogen hydrides and ammonium salts.

The theories of Kurchatov and of Fowler, interpreting the state of spontaneous polarization as one stage in the progressive transition from complete disorder at high temperatures toward complete order as the temperature is diminished, may still play an important part in the theory of the Seignette-electrics. Their greatest defect is the failure to take account of the deformation of the lattice in an electric field; *i.e.*, they ignore the effect of the piezoelectric property on the dielectric constant, which was pointed out by Cady,[100] and later developed very fully by Mueller in a series of papers that will presently be discussed.*

447. Mueller's Theory. The chief observational materials out of which a theory of Rochelle salt is to be built are the following:

1. Normal dielectric and piezoelectric properties for fields perpendicular to the X-axis, at all temperatures.

* Critical comparisons of the various theories of Rochelle salt are found in Mueller's papers.[376,378,382]

The following phenomena are confined to fields and polarizations in the X-direction:

2. For fields of certain strengths parallel to the X-axis, the dielectric susceptibility η_x and the piezoelectric constant d_{14} rise to enormously high values over a certain temperature range. Their behavior is normal at temperatures well outside of this range.

3. Within this temperature range the dielectric polarization, as well as the direct and converse piezoelectric effects, shows saturation and hysteresis.

4. There is a time lag in the response to electric or mechanical stress, together with certain effects dependent on the previous history of the crystal.

5. The existence of a spontaneous polarization P^0 parallel to X, accompanied by a spontaneous strain y_x^0, between two well-defined temperatures, the lower and upper Curie points, θ_l and θ_u. Maxima in P^0 and y_x^0 are found at about 5°C.

6. Between the Curie points the strain x_x is proportional to the square of the polarization P_x.

7. Linear relations exist outside the Curie points and over small ranges between these points, between temperature and the dielectric, piezoelectric, and elastic constants (the Curie-Weiss laws).

8. For small fields and stresses the susceptibility η' of the free crystal, the piezoelectric constant d_{14}, and the isagric elastic compliance s_{44}^E, tend toward infinite values at the Curie points, with minima at about 5°C. Also, the ratio d_{14}/η' is nearly constant.

9. The compliance coefficient s_{44} of an isolated crystal (§199) is very nearly independent of temperature.

10. Between the Curie points anomalous optical effects are observed.

11. Rochelle salt consists normally of domains some millimeters in extent, characterized by opposite spontaneous polarizations (always along the X-axis) in adjacent domains. Related to this is the unipolarity sometimes observed, especially in small plates.

Most of the properties of Rochelle salt—as in the analogous case of iron—are characteristic of the single domain, although some require the assumption of adjacent domains of opposing polarities for their explanation.

Many details of considerable importance have been omitted in the list above. Among other phenomena to be considered in the theoretical treatment are the properties of clamped crystals, the possible change in specific heat at the Curie points, the effect of hydrostatic pressure on the Curie points, and the modification of Rochelle salt by isomorphic mixtures and by heavy water.

The earlier theories of the anomalous electric behavior of Rochelle

salt proceeded from the ferromagnetic analogy and attributed the anomalies to the rotation of free dipoles. From this concept grew the first theory of Mueller,[376] which related the dielectric and piezoelectric effects to the strong internal field accompanying the dipoles, although the dipole moments and rotations were not explicitly introduced. In this form the theory was in excellent agreement with observations outside the Curie points but was not adapted to a quantitative description of effects between these points.

As Mueller pointed out in his second paper,[378] there is no conclusive evidence of the existence of freely rotating dipoles in Rochelle salt. As will be seen in Chap. XXXI, the X-ray analysis of Beevers and Hughes suggests the presence of strain-sensitive bonds that may have dipole moments in terms of which the anomalies of Rochelle salt can be explained. We return to a consideration of dipoles in Chap. XXVI.

448. In his later papers Mueller disregarded the internal field, finding that a satisfactory description of essential phenomena over the entire temperature range could be derived from the following hypotheses:

1. Piezoelectric stresses are proportional to the *polarization* rather than to the field.

2. The electric field strength E is not linear in the polarization P. As a first-order approximation to the non-linearity he introduces a term in P^3.

3. For the anomalous behavior of Rochelle salt the dielectric properties of the unstrained (clamped) crystal are held chiefly responsible. In terms of these properties alone, without invoking any abnormalities in the "true" piezoelectric and elastic coefficients, the peculiar dielectric, elastic, and piezoelectric behavior of the free crystal, including the existence of two Curie points and the spontaneous polarization between these points, finds an explanation. The most fundamentally important critical temperature is that in the neighborhood of 5°C, at which temperature maxima or minima occur in the spontaneous polarization, spontaneous deformation, clamped and free susceptibilities, piezoelectric constant d_{14}, and elastic compliance s^E_{44}; the optical properties also undergo a change at this temperature.

This "interaction" theory of Mueller's is more strictly phenomenological than his earlier one. Although he suggests possible theoretical explanations,[380] his equations are empirical, based on his own observations and those of others. The effects of temperature are expressed in terms of experimentally verified linear relations between the various physical constants and temperature, relations that in the last analysis can be traced to the dependence of the clamped dielectric susceptibility upon temperature. This dependence is of the same form as the Curie-Weiss law in magnetism and strongly suggests an analogous origin.

The germs of the interaction theory, already present in Mueller's first paper (1935), were gradually developed in his papers II, III, and IV (1940) and extended so as to include a quantitative treatment of phenomena between the Curie points.

449. We now undertake a unified presentation of the interaction theory, assembling first the fundamental equations.

Mueller's treatment is expressed in terms of the *polarization theory* of piezoelectricity, which has already been developed in Chap. XI. The present treatment involves the further assumption that the observed relation between polarization P and field strength E requires the addition to the energy functions ξ and ζ of a term in P^4, which contains a new saturation coefficient B. There is, moreover, the assumption of a *quadratic piezoelectric effect* between the Curie points, originating in the monoclinic character of Rochelle salt in this region. Since this effect is dependent on the spontaneous strain, it is not conveniently expressed in the energy equations but will be considered in §464.

The Curie points are defined as the temperatures between which there are a spontaneous polarization P^0 and a spontaneous strain y_z^0. This interval is the *Seignette-electric* region, in which the free crystal takes on monoclinic properties.

The theoretical development that is to follow will perhaps be better understood if at this point we indicate the manner in which the experimental data are used to test the theory. In all cases the electric fields and polarizations are parallel to the X-axis, and the observations extend over a wide range of temperatures. First, and most essential, are the observations of the initial susceptibility η_0' of the free crystal and the dependence of susceptibility on field strength, from which the saturation constant B is derived. Beyond this are observations of P^0 (from hysteresis loops and also from pyroelectric measurements), of y_z^0, and of the compliances s_{44}^E and s_{44}^P from resonating bars. From these data are derived the piezoelectric constants d_{14}, e_{14}, a_{14}, and b_{14}, as well as a theoretical expression for the saturation coefficient B. In particular, the clamped dielectric stiffness χ_1 is derived from η', a_{14}, and b_{14}; thereby Mueller's assertion that χ_1 sinks to a very low minimum in the neighborhood of 5°C can be tested.

In his theory, Mueller reverses the experimental sequence indicated above, gives a theoretical reason for the extraordinary variation of the clamped dielectric constant with temperature, and shows that the spontaneous polarization and all other anomalies are a necessary consequence of this variation. That is, the clamped dielectric constant, deprived of all piezoelectric characteristics, turns out to be the culprit responsible for the abnormal behavior of Seignette-electric crystals (but *cf.* §468).

450. *Definitions.* Before entering upon the theory, it is necessary to supplement by the following special definitions the explanation given in §194 of the various symbols in Eqs. (243) to (245*a*). We consider first the dielectric stiffness coefficients χ'' and χ'. With normal piezoelectric crystals these are independent of strain and of stress, respectively, and also independent of the field strength E. In Rochelle salt, χ'' is a function of the strain, χ' a function of the stress, and both depend on temperature (their dependence on field is taken care of by the terms in B). The treatment is simplified by defining $\eta'' = 1/\chi''$ as the susceptibility of a clamped crystal at *zero strain* instead of merely at constant strain; we shall use the special symbols $\eta_1 = 1/\chi_1$ for the initial susceptibility at zero rhombic strain (see the discussion of rhombic clamping below). For a free crystal (zero stress) outside the Curie points, $\eta' = 1/\chi'$ is the initial susceptibility; in the Seignette-electric region, as indicated below, we write $\eta' = 1/\chi_s'$. In the energy equations (243) and (243*a*) the dielectric terms therefore represent the electrical energy at zero strain and zero stress, respectively. The effects of strain and stress on the energy are to be regarded as contained in the piezoelectric terms.

As to the strains, unless it is otherwise stated, we shall let y_z signify the strain as for a rhombic* crystal, at all temperatures. The reason for mentioning only y_z is that the theory is concerned only with fields E_x parallel to X, and for this direction the only piezoelectric constant for Rochelle salt outside the Curie points is d_{14}, so that y_z is the only strain associated with E_x. It is true that in the monoclinic phase there are three more piezoelectric constants associated with E_x; but they are relatively small, and their possible effect on the behavior of the crystal is postponed to §464. Between the Curie points, where the crystal is properly regarded as monoclinic, y_z would normally be the strain with respect to the monoclinic configuration, which is not the same as the rhombic configuration, owing to the presence of the spontaneous strain y_z^0. When the crystal is so clamped that the rhombic strain is zero, *i.e.*, so that the crystallographic b- and c-faces are at right angles, we shall use the term *rhombic clamping*. At temperatures outside the Curie points this means that the crystal is clamped while in its unstressed state. Between the Curie points, where the b- and c-faces in the absence of stress are at an angle differing from 90° by y_z^0, rhombic clamping implies a stress system such that, starting with the crystal free at the given temperature, these faces are constrained to be at 90°.

On the other hand, it is sometimes desirable to conceive of the

* The alternative term "orthorhombic" would be especially appropriate here, since it implies that the crystallographic a-, b-, and c-axes are mutually perpendicular, as stated in §5.

crystal as clamped, at a given temperature between the Curie points, while in the monoclinic state, with the spontaneous strain present and not neutralized by the clamping stress. This type of clamping will be called *monoclinic clamping;* the corresponding susceptibility will be denoted by $\eta_s'' = 1/\chi_s''$ (§456).

In general the clamping, whether rhombic or monoclinic, is to be regarded as *complete,* in the sense that the infinitely rigid clamping device is so attached to the crystal as to prohibit all components of strain when an electric field is applied.*

In conformity with the foregoing statements we shall follow Mueller and write the basic equations as if Rochelle salt were rhombic at all temperatures. *Between the Curie points* this assumption involves letting P, in some of the terms, include the spontaneous polarization P^0; y_s then signifies the strain measured from the state of rhombic clamping, *i.e.,* with the b- and c-faces mutually perpendicular; for χ'' we use χ_1 as defined above, and χ', as will be seen, assumes the special value χ_s', where the *subscript indicates the value between the Curie points* (the Seignette region).† This procedure is the more permissible because the monoclinic piezoelectric coefficients that are not present in the rhombic state of the crystal are very small. We shall refer to this method of describing the phenomena in Rochelle salt as the *rhombic method.* As will be seen, it offers the advantage of presenting a unified treatment, valid at all temperatures. Its chief usefulness will be in the development of Mueller's theory in the present chapter. When it is applied to the treatment of practical problems at temperatures between the Curie points, there is a certain awkwardness in having to regard the strain as zero only when the crystal is under stress, and *vice versa.* As long as the field is small, so that all relations are linear, such problems are better dealt with by the *normal method,* which is described in §458.

The concept of rhombic clamping employed in the present chapter defines a sort of dielectric ground state for the crystal, which, though not experimentally realizable, is, according to the theory, the state in which the crystal possesses its fundamental susceptibility, free from piezoelectric influence.

451. Energy equations like (243) and (243a), specialized for Rochelle salt, for fields in the X-direction, are given below. The subscript x

* In his earlier papers, Mueller regards the clamped state as that in which only y_s is suppressed; this might be called *partial rhombic clamping.* In his fourth paper,[381] he recognizes the distinction between this type of clamping and the complete rhombic clamping defined above. Outside the Curie points the distinction vanishes; in the monoclinic phase, the distinction is small enough to be ignored in formulating the basic equations.

† This subscript s must not be confused with the subscript ds defined in §430 to indicate the differential permittivity at saturation.

will be omitted in the case of symbols denoting electrical quantities. In accordance with the statement in §449, each equation is now to include a term in P^4. This term suffices to account qualitatively for the non-linear relations observed in Rochelle salt and yields expressions which, except for the complications introduced by the multi-domain structure in the Seignette-electric region, agree fairly well with experiment up to moderately large fields of perhaps 200 volts/cm. In order to describe the observed flatness of the saturation portion of the polarization curve in larger fields a different theoretical function would be necessary. One might, for example, write $f_1(P)$ in place of BP^4 in Eqs. (491) and (491a), and $f(P) = \partial f_1(P)/\partial P$ in place of BP^3 in (492a), (492c), and succeeding equations. The form of $f(P)$ would have to be determined experimentally.

The equations assume different forms according to whether the rhombic method or the normal method is followed. Outside the Seignette-electric range the two methods are identical. Under each method y_s represents the strain, with the understanding that in the rhombic method it is measured from the configuration of rhombic clamping, while in the normal method it is measured from the configuration of the unstressed crystal in zero field at the temperature in question.

From all that has been said it should be clear that the *rhombic method*, to which most attention will be given, treats Rochelle salt as if it were a rhombic crystal at all temperatures, while the *normal method* recognizes the configuration of the free crystal between the Curie points as being monoclinic. Each method pays due regard to spontaneous polarization and spontaneous strain, but in a different way. Methods analogous to these may prove to be useful in the case of other Seignette-electric crystals.

With Rochelle salt between the Curie points one ought strictly to include in the term for piezoelectric energy the piezoelectric constants mentioned above that are theoretically present in monoclinic hemimorphic crystals, but not in crystals of the rhombic sphenoidal class to which Rochelle salt belongs in the parelectric regions. In a first-order discussion such terms may be disregarded as of small magnitude; a special treatment of them will be found in §464.

Throughout this chapter the theory will be concerned mainly with the ideal single-domain crystal. Outside the Curie points there are no domains, and theory accords well with observation. The interactions between domains are so little understood that it is not feasible to introduce them in the basic theory. One must therefore be prepared to use the theory, insofar as it is applied to the Seignette-electric region, rather as a qualitative than a quantitative description of phenomena. Nevertheless, as will be seen, certain quantitative deductions can be

made, and the theory serves as a basis for the later discussion of actual multi-domain crystals.

452. Basic Equations for Rochelle Salt, Field Parallel to X. In the elastic term of the equation for the free energy in terms of *strains*, which is to be derived from Eq. (243), §192, with the addition of a term in P^4, the strain must be expressed as $(y_z - y_z^0)$. This is because part of the energy is due to the mechanical constraint needed to bring the crystal initially to the rhombically clamped state. Since when $y_z = 0$ the clamping neutralizes P^0, the latter quantity does not appear in the expression for polarization, but only P^E, the polarization due to the impressed field E when $y_z = 0$.* One thus obtains

$$\xi = \tfrac{1}{2}c_{44}^P(y_z - y_z^0)^2 + \tfrac{1}{2}\chi_1 P^{E2} + \tfrac{1}{4}BP^{E4} + a_{14}P^E y_z \qquad (491)$$

The free energy in terms of *stresses* assumes the crystal mechanically free except for the externally applied y_z. The dielectric energy, expressed by the second and third terms in Eq. (491a), is due to the polarization P when $Y_z = 0$, and this polarization now includes P^0, since P^0 is no longer suppressed by clamping, so that $P = P^E + P^0$.

We thus obtain, by specializing Eq. (243a) for the present case and adding the term in P^4,

$$\zeta = \tfrac{1}{2}s_{44}^P Y_z^2 + \tfrac{1}{2}\chi' P^2 + \tfrac{1}{4}BP^4 - b_{14}PY_z \qquad (491a)$$

The derivatives of Eqs. (491) and (491a) are

$$\frac{\partial \xi}{\partial y_z} = c_{44}^P y_z - c_{44}^P y_z^0 + a_{14}P^E = -(Y_z) \qquad (492)$$

$$\frac{\partial \xi}{\partial P^E} = \chi_1 P^E + BP^{E3} + a_{14}y_z = (E)'' \qquad (492a)$$

$$\frac{\partial \zeta}{\partial Y_z} = s_{44}^P Y_z - b_{14}P = -y_z \qquad (492b)$$

$$\frac{\partial \zeta}{\partial P^E} = \chi' P + BP^3 - b_{14}Y_z = (E)' \qquad (492c)$$

These four equations are similar to Eqs. (244) to (245a), specialized for Rochelle salt. The symbols $(E)''$ and $(E)'$ are discussed below.

Attention is called first to Eq. (492b), which expresses the strain due to the combined effects of a mechanical stress and an electric polarization. If there is no electric field, $P = P^0$; and if also $Y_z = 0$, we find

$$y_z = b_{14}P^0 \equiv y_z^0$$

y_z^0 is the spontaneous strain, measured from the configuration of rhombic

* Owing to the non-linearity expressed by the term in P^{E4}, we cannot define P^E as the polarization due to E at constant strain. P^E has a definite meaning only when $y_z = 0$.

clamping. This part of the total strain is still present when Y_z and E are impressed, so that y_z is the total strain measured from the rhombically clamped state, just as in Eqs. (492) and (492*a*).

Equation (492) can be simplified by the substitution of $b_{14}P^0$ for y_z^0. Also in (492) we can write the *externally applied stress* Y_z in place of (Y_z) by changing the sign of $a_{14}P^E$, according to Eq. (246).

It is to be noted also, since P^E is the polarization when $y_z = 0$, that in Eq. (492*a*) E can be written in place of $\chi_1 P^E + BP^{E3}$. The term $a_{14}y_z$ is equivalent to a field, and y_z causes a further contribution to the polarization, which in Voigt's terminology would be $P = e_{14}y_z$. We shall call P_t the sum of P^E and this contribution. Similarly, in Eq. (492*c*) we shall call P_t the total polarization due to E, P^0, and Y_z.

Equations (492) to (492*c*) then assume final form as the basic equations that will be used in further developments:

$$-Y_z = c_{44}^P y_z - a_{14}(P^0 + P^E) \tag{493}$$

$$(E)'' = \chi_1 P^E + BP^{E3} + a_{14}y_z = E + a_{14}y_z = \chi_1 P_t + BP_t^3 \tag{493a}$$

$$-y_z = s_{44}^P Y_z - b_{14}P \tag{493b}$$

$$(E)' = \chi' P + BP^3 - b_{14}Y_z = E - b_{14}Y_z = \chi' P_t + BP_t^3 \tag{493c}$$

Some of the foregoing expressions, without the non-linear terms, have been anticipated in Eqs. (252) to (255*a*). The nature of the quantities $(E)''$ and $(E)'$ has been explained in §194. That $(E)''$, for example, is not the actual field in the crystal can be seen from the fact that the strain y_z produces primarily a polarization. If y_z gives rise to a field, the latter depends on boundary conditions. The term $a_{14}y_z$ in Eq. (493*a*) is not a constituent of the actual field E, but when added to E it gives the *equivalent field* $(E)''$. The total polarization P_t, which includes the contribution due to y_z, is expressed in terms of $(E)''$. Similar remarks apply to the equivalent field $(E)'$ in Eq. (493*c*) when the crystal is free and the *stress* is prescribed.

In further interpretation of these equations, it may be stated that in Eq. (493), when $y_z = 0$ and $E = 0$, $Y_z = a_{14}P^0$ is the clamping stress needed to bring the crystal to the state of rhombic clamping. When $Y_z = 0$, the crystal is free, and $c_{44}^P y_z = a_{14}(P^0 + P^E)$; if there is no external field, $c_{44}^P y_z = a_{14}P^0$. Hence from Eq. (495*b*) it follows that $y_z = b_{14}P^0$. This y_z is the spontaneous strain y_z^0, so that we may write

$$y_z^0 = b_{14}P^0 \tag{494}$$

This relation also follows directly from Eq. (493*b*). In fact, since from Eq. (495*b*) $a_{14}s_{44}^P = b_{14}$, and furthermore $c_{44}^P = 1/s_{44}^P$, it follows that Eq. (493*b*) is only another way of writing (493). For the numerical value of y_z^0 see §482.

In Eq. (493*a*) the equivalent field $(E)''$ is the sum of the actual field E

and that which would produce in a rhombically clamped crystal a polarization equal to the polarization due to the prescribed y_s. A curve relating P_t to $(E)''$ has, depending on the temperature, a form like curve c or e in Fig. 138.

Similarly, $(E)'$ in Eq. (493c) is the sum of E and the field that would produce in a free crystal a polarization equal to that due to the prescribed Y_s. A curve relating P_t to $(E)'$ would look like curve a, b, or d in Fig. 138.

In Eq. (493b), y_s is the strain due to the combined action of the external stress Y_s and of $P = P^0 + P^E$, where P^E is the contribution to the polarization caused by the applied field E when $Y_s = 0$. When $Y_s = 0$ and $E = 0$, $y_s = b_{14}P^0$, as we have seen in Eq. (494). When $y_s = 0$ (rhombic clamping), the clamping stress is

$$Y_s = b_{14}P/s^P_{44} = b_{14}c^P_{44}(P^0 + P^E)$$

In Eqs. (493a) and (493c), when $P_t = 0$, $(E) = 0$. In the case of the rhombically clamped crystal ($y_s = 0$) it follows from (493a) that then $E = 0$. If y_s has some arbitrary value, E is the applied field necessary to make $P_t = 0$. Similarly in (493c), if $P_t = 0$ and Y_s is prescribed, E is again the applied field necessary to make $P_t = 0$.

From Eqs. (204) and (242), and (ix) to (xii) in Table XX, one finds for Rochelle salt

$$b_{14} = a_{14}s^P_{44} \tag{495}$$

$$d_{14} = e_{14}s^E_{44} \tag{495a}$$

$$d_{14} = b_{14}\eta' = a_{14}s^P_{44}\eta' \tag{495b}$$

$$e_{14} = a_{14}\eta'' = b_{14}c^P_{44}\eta'' \tag{495c}$$

$$a_{14} = e_{14}\chi'' = \frac{d_{14}}{\eta''s^E_{44}} = \frac{d_{14}}{\eta's^P_{44}} \tag{495d}$$

$$b_{14} = d_{14}\chi' = \frac{d_{14}}{\eta'} \tag{495e}$$

In these equations the symbols d_{14}, e_{14}, $\eta' = 1/\chi'$ and $\eta'' = 1/\chi''$ are written in the form that we have adopted for piezoelectric crystals in general. They represent here *initial* values, valid only with small stresses and weak fields. Where it is necessary in order to avoid ambiguity the subscript 0 will be attached to these symbols.

With Rochelle salt, owing to the presence of spontaneous polarization and of non-linearity between the Curie points, the expressions containing the symbols mentioned above assume a form different from that in the parelectric regions. In such cases the subscript or superscript s will be used to designate the Seignette-electric region. Where there is no ambiguity the indices s and 0 may be omitted.

In the parelectric regions, in conformity with §450, we shall write

$\eta_1 = 1/\chi_1$ in place of $\eta'' = 1/\chi''$, while still retaining η' and χ'. As will be seen in §454 χ' and η' do not correspond to observable quantities between the Curie points.

Equations (495) to (495*e*) are perfectly general. They are applicable equally to the rhombic or to the normal method.

453. Application of the Interaction Theory. In the remainder of this chapter the equations will be written according to the rhombic method, in which the strain is measured from the condition of rhombic clamping. The basic equations are (493) to (495*e*).

The first application to be made of the basic equations is in expressing χ' in terms of χ_1 outside the Curie points.

If Eq. (493*b*) is applied to an unstressed crystal, $Y_z = 0$ and $y_z = b_{14}P$, where P is due to E alone. Since in Eq. (493*a*) y_z is arbitrary, we may substitute $b_{14}P$ for it and find, since P is now the total polarization P_t, $E + a_{14}b_{14}P = \chi_1 P + BP^3$, whence $E = (\chi_1 - a_{14}b_{14})P + BP^3$. P is the polarization due to E in the *free* crystal, and the last equation is equivalent to (493*c*) when $Y_z = 0$. Thus we have

$$E = (\chi_1 - a_{14}b_{14})P + BP^3 = \chi' P + BP^3 \tag{496}$$

where

$$\chi' = \chi_1 - a_{14}b_{14} \tag{496a}$$

The equivalence of the last equation to Eq. (264) in §204 will be made clear in §461. It is important to note that, since a_{14} and b_{14} are nearly independent of temperature, χ' and χ_1 differ by a nearly constant amount, as is shown in Fig. 145.

In Fig. 138,* curve *d* represents Eq. (496) for a free crystal, and curve *e* is from Eq. (493*a*) for a clamped crystal with $y_z = 0$, both at 31.5°C. From Eq. (496) it is seen that the values of E for these curves differ by the amount $a_{14}b_{14}P$. For example, at $P = 400$, the distance KH represents $a_{14}b_{14}P$.

We are now prepared to begin the consideration of the variation of the properties of Rochelle salt with temperature. The interrelationships expressed in Eqs. (493) to (495*e*) are such that, when the temperature dependence of any one of the four parameters χ_1, χ', s^E_{44}, or d_{14} is established, the dependence of the rest follows. This subject is treated further in §§468 and 472. For the present we shall abide by Mueller's hypothesis that the seat of the anomalies lies in the rhombically clamped dielectric susceptibility $\eta_1 = 1/\chi_1$. The observed dielectric constant of the *free* crystal varies with temperature in the manner shown in Fig. 147 or Fig. 143; k' and χ' are related by $k' = 1 + 4\pi/\chi'$. By

* Figures 138 and 139 are for a *single-domain* crystal. Multi-domain crystals are treated in §479.

means of Eq. (496a) χ_1 can be found at any temperature when χ' is known.

The hypothesis concerning χ_1 involves the assumption that the structure of Rochelle salt is such that χ_1 depends on temperature according to the upper curve in Fig. 143, and in particular that it diminishes

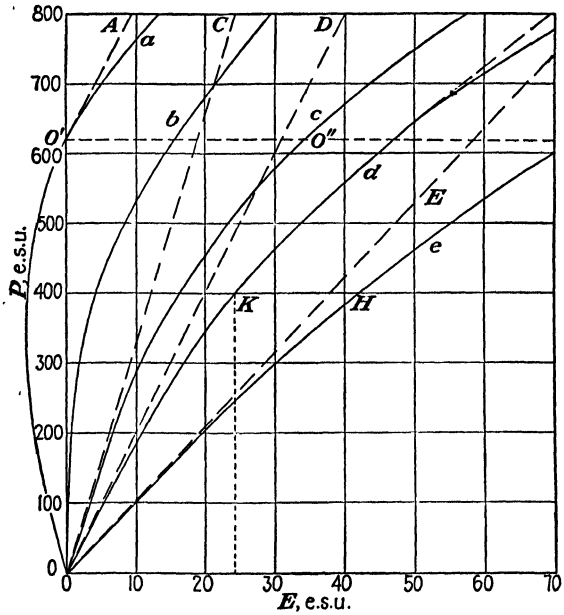


FIG. 138.—Theoretical polarization curves for Rochelle salt. Curve a, at 15°, crystal free; curve b, at the upper Curie point, crystal free; curve c, at 15°, crystal clamped; curve d, at 31.5°, crystal free; curve e, at 31.5°, crystal clamped.

as the Seignette-electric region is approached from either direction, with a finite value at each Curie point. From Eq. (496a) it is seen that $\chi' = 0$, and hence $k' = \infty$, when $\chi_1 = a_{14}b_{14}$. In the Seignette-electric region $\chi_1 < a_{14}b_{14}$.

In Fig. 138 we have plotted, approximately to scale, curves showing the relation between polarization P and applied field E for free and clamped crystals,* at two different temperatures. In curve e, above the upper Curie point, the initial slope OE at the origin gives $\eta_1 = 1/\chi_1$.

* The curves in Fig. 138 are drawn to scale from Mason's observations as summarized in Table 2 of Mueller's second paper[378] and illustrated in Figs. 145 and 146. For curve d the temperature 31.5°C was chosen because at that temperature the initial χ' of the free crystal happens to have the same value, 0.05, as the initial χ_s' (§450) at 15°, as shown in curve a. The lines $O'A$ and OD are therefore parallel. All curves were plotted on the assumption that B has the value $6.5(10^{-8})$; the true

At higher temperatures the slope decreases; in general, outside the Curie points the effect of the B-term in Eq. (496) or (493a) is very small at all attainable field strengths. As the temperature decreases, with a corresponding decrease in χ_1, the slope increases, until at 15°C it is represented by the line OC. At 5°C the slope would reach its maximum value (§469). The polarization curve for the clamped crystal at 15°, representing Eq. (493a) with $y_s = 0$, is curve c.

This change with temperature of the curve for the clamped crystal is accompanied by a similar change in the curve for the free crystal. Thus at the Curie point, where $\chi_1 = a_{14}b_{14}$, we see that $\chi' = 0$, and from Eq. (496) it is seen that the curve for the free crystal coincides with curve b, which represents BP^3. This curve has an infinite slope at the origin, indicating that $\partial P/\partial E \rightarrow \infty$ as $E \rightarrow 0$. The infinite dielectric constant of the free crystal at the Curie point θ_u is thus accounted for (similar reasoning leads to a like conclusion at θ_l); at the same time it becomes clear that very large observed values at the Curie points are to be expected only when E is very small.

454. A curious state of affairs is encountered when χ_1 in Eq. (496) becomes less than $a_{14}b_{14}$, *i.e.*, when χ' is negative and the temperature passes below θ_u. The curve for the free crystal, which is already tangent to the axis of ordinates at θ_u, becomes, so to speak, pushed still farther to the left, with a bulge in the negative direction starting at the origin. Close to the Curie point this negative segment is small, with a large negative initial slope. With decreasing temperature the negative slope $(1/\chi')$ diminishes and the height of the negative segment increases, until at 15°C curve a is reached. The maximum height would be found at a temperature around 5°C.

Obviously, χ' cannot be the reciprocal susceptibility of a free crystal between the Curie points, for it implies a positive polarization produced by a negative field. The theory is saved from disaster by the fact that at O' the curve returns to the positive side of the ordinate axis. At O' there is present in the crystal a polarization, although the impressed field is zero. We are thus led by the fundamental equations to the concept of a *spontaneous polarization* in Rochelle salt between the Curie points. We may conclude further that any crystal having a clamped reciprocal susceptibility χ_1 that becomes equal to $a_{14}b_{14}$ (or its equivalent for the class to which the crystal belongs) at a definite temperature must have a Curie point with infinite susceptibility for the free crystal at this temperature, together with a spontaneous polarization when χ_1 is less than $a_{14}b_{14}$. The quantity χ_1 itself can be of quite normal

value at temperatures above θ_u is probably greater than this. The equation for curves a, b, and d is (496) with appropriate values of χ'. For curves c and e we set $y_s = 0$ and $P_t = P$ in Eq. (493a), with $\chi_1 = 0.030$ and 0.094, respectively.

magnitude. It is the condition $\chi_1 < a_{14}b_{14}$ that accounts for all the abnormalities.

In terms of χ_1 the spontaneous polarization P^0 is found by setting $E = 0$ in Eq. (496), whence

$$BP^{0^2} = -\chi' = a_{14}b_{14} - \chi_1 \tag{497}$$

Outside the Curie points, P^0 in this equation becomes imaginary and there is no spontaneous polarization. The curve for P^0 as a function

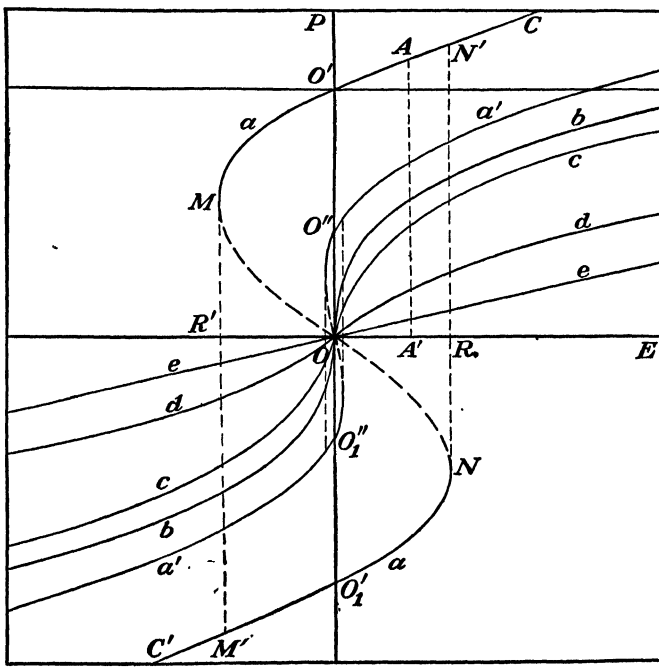


FIG. 139.—Qualitative curves illustrating the theoretical dependence of P on E for a free single-domain Rochelle-salt crystal at different temperatures. Curve a is for 5°, a' for 22°, b for the Curie point θ_u, c for 26°, d for 31.5°, and e for 40°C.

of temperature is shown in Fig. 147. It rises rapidly from the Curie points to a flat maximum at about 5°C; the value shown at the maximum is Mueller's "observed" value of 740 esu, from his third paper.[380] Using this value in Eq. (497), together with B, a_{14}, and $b_{14} = a_{14}s^E_{44}$ from the same paper, one finds, at 5°, $\chi_1 = 0.037$. This quantity is appreciably greater than the hypothetical value at 5° in Fig. 143, but the margin of uncertainty in both theory and observation is considerable.

In Fig. 138, only positive values of polarization are shown. The complete graph for Eq. (496) [same as (493c) with $Y_s = 0$] is shown in

Fig. 139, in which curve a is for 5°C, with maximum $P^0 = OO'$. Curves a', b, and c correspond to temperatures around 22°, θ_u (approximately 24°), and 26°; curves d and e are for 31.5° and 40°. Considering first curve a, we see that if the crystal consists of a single domain with P^0 positive the total polarization when $E = 0$ is P^0. As E increases in the positive direction, the portion $O'C$ of the curve is traversed, and the observed polarization P^E is the ordinate measured from an axis of abscissas through O'. The equation relating P^E to E is obtained by substituting in Eq. (496) $P = P^E + P^0$. Then, with origin at O, we have

$$E = \chi'(P^E + P^0) + B(P^E + P^0)^3 \tag{498}$$

Equation (498) is the form assumed by (493c) when $Y_z = 0$.

When $P^0 = 0$, (498) is the polarization: field equation for temperatures in the parelectric regions, and χ' is the actual reciprocal initial susceptibility. In the Seignette-electric region, where χ' is negative, the observable initial susceptibility (§450) $\eta_s' = 1/\chi_s'$ (slope of curve a, Fig. 138, at O') is found by taking the derivative of E with respect to P^E and then setting $P^E = 0$:

$$\begin{aligned}\chi_s' &= \chi' + 3BP^{0^2} = \chi_1 - a_{14}b_{14} + 3BP^{0^2} \\ &= 2(a_{14}b_{14} - \chi_1) = -2\chi' = -\frac{2D_{14}}{c_{44}^P} = 2BP^{0^2}\end{aligned} \tag{499}$$

The last expression is Eq. (11c) or (17) in Mueller's paper III; D_{14} is defined in Eq. (522a).

On substituting $-\chi_s'/2$ for χ' in Eq. (498), we find, for the Seignette-electric region,

$$\begin{aligned}E &= -\tfrac{1}{2}\chi_s'(P^E + P^0) + B(P^E + P^0)^3 \\ &= \chi_s' P^E + 3BP^{E^2}P^0 + BP^{E^3} \\ &= B(2P^{0^3}P^E + 3P^0P^{E^2} + P^{E^3})\end{aligned} \tag{500}$$

This equation gives the relation between P^E and E according to the *normal method* described in §458.

P^0 is the spontaneous polarization at the given temperature; it may have either of the two values $\pm(\chi_s'/2B)^{\frac{1}{2}}$ given by Eq. (499).

Equation (500) gives the theoretically observed P^E for any E, with origin at O' in Fig. 138 or 139, for a single-domain crystal polarized in the positive direction OO'.

In the last part of (500), the substitution of $2BP^{0^2}$ for χ_s' follows from Eq. (499). The same substitution may also be made in the equations that are to follow. In this manner the quantity on the left-hand side of the equation is represented in terms of P^0 as the only parameter that varies materially with temperature. The variation of P^0 with temperature is fairly well known, as shown by Fig. 147 and Eq. (526). It must

still be remembered, however, that the equations in the present sections apply to the idealized single-domain crystal, with hysteresis loops of the form represented by $M'NN'M$ in Fig. 139, in which the coercive field is far in excess of the E_c found in practice.

If the spontaneous polarization P^0 is negative, then for curve a, Fig. 139, the origin is to be taken at O_1' instead of at O', and in Eq. (500) the negative sign is to be attached to P^0. The form of the hysteresis loop is the same whether P^0 is + or −; the only difference is in the position of the origin of coordinates. This statement remains substantially true also when, as is practically always the case, the crystal has a multi-domain structure (see §479).

The *over-all susceptibility* $(\eta_s')_n$ of the free crystal (§430), which is the ratio P^E/E for any given value of E, is found from Eq. (500):

$$\frac{1}{(\eta_s')_n} = (\chi_s')_n = \chi_s' + BP^{E2} + 3BP^E P^0 \tag{501}$$

This susceptibility is the one derived directly from observations with a ballistic galvanometer.

The slope at any point on the $P:E$ curve is the *differential susceptibility* $(\eta_s')_d$; from Eq. (498) it is given by

$$\frac{1}{(\eta_s')_d} = (\chi_s')_d = \frac{\partial E}{\partial P^E} = \chi' + 3B(P^E + P^0)^2 \tag{501a}$$

The observed *differential permittivity* discussed in §436 would, according to the present theory, be equal to $1 + 4\pi(\eta_s')_d$.

455. If the field strength E applied to a *single-domain* crystal is increased from zero in the *negative* direction from O' in Fig. 139, a point of instability is reached at M. The spontaneous polarization P^0 is here abruptly reversed by the field, the observed polarization jumps from M to M', continuing along $M'C'$ as E becomes more negative. On the return trip the path $C'M'NN'C$ is followed. This process should be compared with the magnetic analogy described in §555. Along the paths MM' and NN', χ_d' becomes theoretically infinite.

We thus find a theoretical explanation of the dielectric hysteresis in Rochelle salt. According to the theory outlined here, the coercive field E_c (= OR' or OR, for points M and N in Fig. 139) is found from the value of the polarization at M or N, for which $\partial E/\partial P = 0$. Thus from Eqs. (496) and (497) it follows that, at M, $P_M = P_0/\sqrt{3} = 0.577P^0$. Then on substituting this value for P in Eq. (496) one finds

$$E_c = -\frac{2}{3\sqrt{3}} BP^{03} = -0.385BP^{03} \tag{502}$$

This theoretical value of the coercive field is many times greater

than that which is actually observed. The explanation, which lies in the ease of reversal of domains, is treated in §479, where the theoretical and experimental hysteresis loops will be compared in greater detail. For the present it suffices to point out the following features of Figs. 138 and 139: (1) Since the data for Fig. 138 at 15°C were based on observations of susceptibility of a free crystal at weak fields (§453 and Fig. 145), the slope $O'A$ of curve a at O' may be taken as representative of the values to be expected with weak direct or l-f alternating fields up to about 10 volts/cm. (2) Even with fields as high as 10 esu = 3,000 volts/cm, the polarization does not rise much beyond P^0. (3) Insofar as Eq. (496) is applicable to very strong fields, it indicates that complete saturation, if it exists at all, cannot be expected until the polarization has reached a value several times greater than P^0.

Figure 139 illustrates the gradual diminution in P^0 and E_c from maximum values at 5° to zero at the Curie point θ_u (see also Fig. 147). Above the temperature θ_u, polarizations are measured from a horizontal axis through the origin at O. In the Seignette-electric region the origin is displaced vertically by an amount equal to P^0; for example, if P^0 happens to be negative, the origin is at O_1' for 5° and at O_1'' for 22°C. At O_u, $\chi' = 0$, so that the equation for curve b is simply $E = BP^3$.

Above θ_u there is no hysteresis. With increasing temperature χ' increases (*cf.* Fig. 145), the term BP^3 becomes less and less important, and the curves become approximately straight lines, as is shown by the line e in Fig. 139. In practice, the relation between P and E is found to be linear, for all attainable values of E, from about 32° on.

Figure 139 explains qualitatively a peculiarity noted in Fig. 128 and elsewhere, that while with weak fields the susceptibility

$$\eta' = \frac{1}{\chi'} = \left(\frac{\partial P}{\partial E}\right)_0$$

approaches infinity at θ_u, with relatively *low* values on either side of θ_u, still when E is large the over-all value P/E (for the same E) rises continuously from low values in the parelectric regions to high values between the Curie points.

For a discussion of hysteresis in multi-domain crystals see §479.

456. *The Clamped Crystal between the Curie Points.* Rhombic clamping is always to be understood in this chapter unless monoclinic clamping is specifically mentioned. In Fig. 138 we have already seen $P:E$ curves for the clamped crystal at 31.5 and 15°C. Since according to the polarization theory, as expressed in Eqs. (493*a*) and (493*c*), the expressions for the polarization curves for a clamped crystal ($y_z = 0$) differ from those for a free crystal ($Y_z = 0$) only in the initial slope (χ_1 and χ', respectively), it is clear that the curves in Fig. 139 may also be used

to illustrate qualitatively the $P:E$ relation for clamped crystals. The straight line e then gives this relation in the neighborhood of $+35°$ and $-30°$C; curve d is representative for $+30°$ and $-25°$C; curve c for $+28°$ and $-20°$C. There is no peculiarity at either Curie point (see the curve for χ_1 in Fig. 143), but between $+28°$ and $-20°$ the curves lie between c and b, coming closest to b at about 5°C, where χ_1 is a minimum. Below $-30°$ and above $+35°$ the curves are linear, lying between e and the E-axis. Curves a and a' in Fig. 139 are for a free crystal and have no place in the present discussion.

Since with rhombic clamping the spontaneous polarization P^0 is suppressed (§459), the quantity P in Eq. (493a) is the polarization due to the field E alone. On setting $y_x = 0$ in (493a) we have, therefore, for the rhombically clamped crystal at any temperature,

$$E = \chi_1 P + BP^3 \tag{503}$$

Between the Curie points the concept of *monoclinic* clamping has both theoretical and practical significance. The configuration of the crystal under monoclinic clamping at any temperature is given by the spontaneous strain y_x^0, measured from the configuration at rhombic clamping as zero: $y_x^0 = b_{14}P^0$. A second relation between y_x^0 and P^0 is found by setting $E = 0$ in Eq. (493a) and writing P^0 for P_t:

$$(E)_0'' = a_{14}y_x^0 = \chi_1 P^0 + BP^{0^3} \tag{504}$$

This equation is illustrated graphically in Fig. 138, in which curve c may be taken as typical for a clamped crystal between the Curie points. The ordinate is now P^0, the abscissa is $(E)_0'' = a_{14}y_x^0$, and the point is O''.

Just as O is the origin for the $P:E$ curve for rhombic clamping, so under monoclinic clamping the origin is at O''. The relation between the applied E and the observed polarization P^E, which is the contribution made by E to the total polarization, is found as follows: From Eq. (493a), $(E)'' = E + a_{14}y_x^0 = E + (E)_0'' = \chi_1 P_t + BP_t^3$, where now $P_t = P^0 + P^E$. On substituting the value of $(E)_0''$ given above and expanding, we arrive at the relation

$$\begin{aligned} E &= (\chi_1 + 3BP^{0^2})P^E + 3BP^0P^{E^2} + BP^{E^3} \\ &= \chi_t''P^E + 3BP^0P^{E^2} + BP^{E^3} \end{aligned} \tag{504a}$$

This equation is illustrated by a curve such as curve c in Fig. 138, with O'' as origin. The coefficient of P^E in the first term determines the slope at O''; it is the reciprocal initial susceptibility for monoclinic clamping, which may be written

$$\chi_t'' = \chi_1 + 3BP^{0^2} \tag{505}$$

Equation (504*a*) expresses the relation between P^E and E according to the *normal method* described in §458.

From Eqs. (497) and (499), χ_s'' can also be expressed thus:

$$\chi_s'' = \frac{1}{\eta_s''} = \chi_s' + a_{14}b_{14} = \chi_1 + \tfrac{3}{2}\chi_s' = 3a_{14}b_{14} - 2\chi_1 = \chi_1 - \frac{3D_{14}}{c_{44}^P} \quad (505a)$$

The definition of D_{14} is given* in §463 [Eq. (522*a*)]. This relation between χ_s'' and χ_s' for the region of spontaneous polarization should be compared with Eq. (496*a*).

We shall find use also for the expression for the *over-all susceptibility* $(\eta_s'')_n$ or its reciprocal, for monoclinic clamping between the Curie points. From Eq. (504*a*),

$$\frac{1}{(\eta_s'')_n} = (\chi_s'')_n = \frac{E}{P^E} = \chi_s'' + 3BP^0P^E + BP^{E^2} \quad (505b)$$

457. *Further Remarks on the Clamped Dielectric Constant.* When the statement is made, as in §442, that the value of the dielectric constant observed at very high radio frequencies approximates that of the clamped crystal, it should be obvious, in the light of the foregoing theory, that the word "clamped" implies rhombic clamping in the parelectric regions and monoclinic clamping in the Seignette-electric. Practically all available experimental values were obtained with small fields. An idea of the dependence of the initial clamped dielectric constant on temperature can be obtained from the curves in Fig. 145 for χ_1 and χ_s''.

According to Eqs. (503) and (504*a*), the clamped dielectric constant may be expected to decrease with increasing field, except at temperatures well removed from the Curie points. Thus far the only experimental evidence has been indirect, from the fact that the susceptibility η_x' for the free crystal does show saturation; and since, by Eq. (267),

$$\eta_x' = \eta_x'' + e_{14}d_{14}$$

η_x'' must have the same characteristic.

Although reliable data on virgin curves, either static or by alternating current, are lacking, still one can draw certain conclusions concerning the clamped dielectric constant from the hysteresis loops shown in Chap. XXII. From the linearity of the saturation portions of these loops it is evident that the differential permittivity k_{ds} approaches a constant and relatively small value at large E. It is not unreasonable to inquire whether this k_{ds} may not be identical with the clamped dielectric constant. This will be the case if, when E is large, d_{14} becomes so small that the product $e_{14}d_{14}$ no longer makes an appreciable contribution to the susceptibility. That the polarization is subject to very great

* The last expression in Eq. (505*a*) is the same as (9c) in Mueller's paper III.

saturation under large mechanical and electric stresses is evident from Figs. 108 to 115. Nevertheless, the data do not suffice to prove convincingly that at the strongest fields appearing on the hysteresis loops the product $e_{14}d_{14}$ is in truth negligible.

On the experimental side two values of k_{ds} have been given in §436: at 15°C, $k_{ds} = 330$; at 20° (estimated), $k_{ds} = 200$. Values of the clamped constant k_s'' can be derived from the curve for χ_s'' in Fig. 145: at 15°C, $k_s'' \approx 120$; at 20°, $k_{ds}'' \approx 195$. These values are for small fields; at large E they would be smaller. This evidence, though slight, indicates that k_{ds} is somewhat greater than the clamped dielectric constant.

Mueller's theory does not throw light on this question, because, as stated in §451, the cubic equations that describe the non-linear effects are not valid up to large values of E and do not predict the constancy in k_{ds} at saturation.

From the theory in Chap. XXV and especially from §479, it is evident that the polarization of the free crystal in a given static field and its variation with the field must depend very greatly on the domain structure of the specimen. This fact doubtless accounts in large measure for the wide variety of polarization curves and values of k_x' recorded by different observers. On the other hand, the clamped dielectric constant, although not directly measurable, still must be regarded as independent of domains.

458. Equations for Rochelle Salt according to the Normal Method. This is the method referred to in §450 as being preferable to the rhombic method when the field is weak and relations are linear. It is simply the method that would be applied to any normal piezoelectric crystal devoid of anomalies. Strains are measured from the normal configuration of the crystal at any given temperature, whether the configuration is rhombic or monoclinic. The reason why this method is not as well suited as the rhombic method to the treatment of large fields and large stresses can be illustrated by considering the relation between polarization and field for a free crystal between the Curie points. In Fig. 139, the origin is at O for curves representing Eq. (493c) by the rhombic method. Such curves, for example curve a, are centrosymmetrical with respect to the point O. When $E = 0$, there is a spontaneous polarization in the domain equal to $+P^0$ or $-P^0$, represented by OO' or OO_1'. As E increases from zero, if P^0 is positive the observed polarization is the ordinate, say P^E, measured from a horizontal axis through O'. As was stated in §454, the slope of the curve at O' gives the observed initial susceptibility at the temperature in question. The curve is not symmetrical about any axis through O'. This lack of symmetry is indicated by the term in P^{E^2} in Eq. (500). Corresponding to this lack of symmetry is the fact that the energy equation for the normal method would not be as simple

as Eqs. (491) and (491*a*) for the rhombic method, except at temperatures outside the Curie points. Nevertheless, as long as the field is so weak that only the first power of P^E need be retained in the derivatives of the energy equations, all equations are equally simple by either method. Outside the Curie points, even when higher powers of P are included, the two methods are identical.

Similar considerations apply to the clamped crystal. In this case, if we regard curve *c* in Fig. 138 as typical of a clamped crystal between the Curie points, the origin is at O by the rhombic method, with initial susceptibility $\eta_1 = 1/\chi_1$. By the normal method the origin is at O'', and the initial (actually observed) susceptibility is $\eta_s'' = 1/\chi_s''$. Equation (504*a*), for a clamped crystal, corresponds to a curve with origin at O'', and it shows the asymmetry characteristic of the normal method in the region of spontaneous polarization.

Since the normal method deals with actually observed initial susceptibilities, it is well suited to the treatment of practical problems in which only small stresses and weak fields occur.

Following are the basic equations according to the normal method, for small stresses and weak fields, analogous to Eqs. (493) to (493*c*):

$$-Y_s = c_{44}^P y_s - a_{14} P^E \tag{506}$$

$$(E)'' = \chi_1 P^E + B P^{E3} + a_{14} y_s = E + a_{14} y_s = \chi_1 P_t + B P_t^3 \tag{506a}$$

$$-y_s = s_{44}^P Y_s - b_{14} P^E \tag{506b}$$

$$(E)' = \chi' P^E + B P^{E3} - b_{14} Y_s = E - b_{14} Y_s = \chi' P_t + B P_t^3 \tag{506c}$$

CHAPTER XXIV

THEORY OF ROCHELLE SALT, PART II. PIEZOELECTRIC AND ELASTIC PROPERTIES, CURIE-WEISS LAWS, AND CONCLUSIONS

The history of physics shows that the search for analogies between two categories of distinct phenomena has perhaps been, of all methods employed for the construction of physical theories, the method which is most certain and most fruitful.

—P. DUHEM.

Our exposition of the interaction theory is brought to a conclusion in this chapter, with a discussion of the distinguishing characteristics of Seignette-electric crystals and with a presentation of the experimental evidence for the findings of the interaction theory.

Piezoelectric Properties of Rochelle Salt for Fields Parallel to the *X*-axis. It was stated in §191 that the main experimental justification for the polarization theory lies in the approximate temperature-independence of a_{14} and b_{14}. We consider now the effect of electric and mechanical stress on these constants and also on the Voigt constants e_{14} and d_{14}. In Eqs. (493*a*) and (493*c*) for the direct effect, the non-linearity is expressed, at least to a first approximation, by the term in B, so that a_{14} and b_{14} are not required to show a dependence on stress. In Eqs. (493) and (493*b*) for the converse effect, B does not appear explicitly, yet the non-linearity of the relation between Y_z (or y_z) and E is deducible from the fact that P is non-linear in E, as is shown by the equations for the direct effect. We may therefore confidently expect, as is, indeed, indicated by Mason's observations,[338] that a_{14} and b_{14} will be found approximately constant under all circumstances. This being the case, it follows that d_{14} and e_{14} must be very variable with temperature, field, and mechanical stress.

459. Direct Effect. The assumption that the application of Y_z is equivalent to the application of a biasing field $-b_{14}Y_z$ makes it easy to find the relation between Y_z and the polarization that it causes when $E = 0$ in a single-domain crystal; that is, we find thus the equation for the *direct effect* in terms of stress, a relation that in Rochelle salt is non-linear. In Eq. (493*c*) P is the polarization due to E when $Y_z = 0$; hence, when $E = 0$, we have $(E)' = -b_{14}Y_z$. This expression now represents the abscissa for Fig. 139 or for the curve *a* or *d* in Fig. 138, with

origin at O. The equation for the curve in all cases, between or outside the Curie points, is*

$$-Y_s = \frac{\chi' P_i}{b_{14}} + \frac{BP_i^3}{b_{14}} \tag{507}$$

where P_i is the polarization due to Y_s when $E = 0$, plus the spontaneous P^0. The segment MN in Fig. 139 is ignored. Outside the Curie points $P^0 = 0$.

In the Seignette-electric region the relation between Y_s and the polarization P that it causes is expressed more directly by shifting the origin to O' (Fig. 139; see also Fig. 140). This is done by writing

$$P_i = P + P^0$$

and making use of Eq. (499):

$$-b_{14}Y_s = \chi_s' P + 3BP^0P^2 + BP^3 \tag{508}$$

The similarity of Eq. (508) to (500), (504a), (510), and (511) should be noted. In §460 we shall find analogous expressions for d_{14} and e_{14}. All these expressions apply only to single-domain crystals. For multi-domain crystals see §479.

The effective *differential piezoelectric constant* is given by

$$\frac{1}{(d_{14})_d} = -\frac{\partial Y_s}{\partial P} = \frac{1}{b_{14}}(\chi_s' + 6BP^0P + 3BP^2) \equiv \frac{1}{(d_{14})_0^s} + \frac{6BP^0P + 3BP^2}{b_{14}} \tag{509}$$

Outside the Curie points this becomes $(\chi' + 3BP^2)/b_{14}$. The initial value at small Y_s between the Curie points is

$$(d_{14})_0^s = \frac{b_{14}}{\chi_s'} = b_{14}\eta_s' \tag{509a}$$

which is the form assumed by Eq. (495b) in the Seignette-electric region. In the parelectric regions we have, in agreement with Eq. (495b),

$$(d_{14})_0 = \frac{b_{14}}{\chi'} = b_{14}\eta' \tag{509b}$$

From the last two equations it is evident that at the Curie points, where η_s' and η' become infinite, the initial value of the piezoelectric constant must also approach infinity, since b_{14} does not vanish. The over-all value of d_{14} is given by Eq. (512b) below.

The equation for the *direct effect in terms of strain* is a relation between y_s impressed on an unclamped crystal and the polarization that it pro-

* This is equivalent to Mueller's Eq. (3c) in his third paper,[380] with a correction in sign.

duces, while $E = 0$. *Outside the Curie points* we simply set $E = 0$ in Eq. (493*a*) and write P for $P_t : a_{14}y_z = \chi_1 P + BP^3$. Except close to the Curie points, the second term is relatively small and the relation is nearly linear. *Between the Curie points* $P_t = P^0 + P$, and y_z, which we now call $\bar{y}_z$, is measured from the normal, or monoclinic, configuration. Since in the foregoing equations y_z is measured from the configuration of rhombic clamping, it follows that $\bar{y}_z = y_z - y_z^0$. Now, from Eq. (493*a*), when $E = 0$, $a_{14}y_z^0 = \chi_1 P^0 + BP^{03}$. Hence from (493*a*) and (505) we find

$$a_{14}\bar{y}_z = \chi_s'' P + 3BP^0P^2 + BP^3 \quad (510)$$

This relation is represented graphically by curves of the form of curve *c* in Fig. 138. P and $\bar{y}_z$ are measured from an origin at O'', and P is an increment added to or subtracted from P^0.

Attention should be called to the contrast between Eqs. (510) and (508): in (510) the strain is prescribed and the coefficient of P is χ_s'', while (508), with the stress prescribed, has the coefficient χ_s'. If y_z is due to Y_z, P is the same in the two equations.

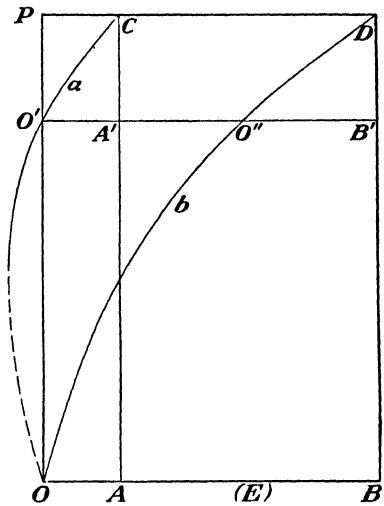


FIG. 140.—Rochelle salt between the Curie points. Curve *a*, polarization in terms of mechanical stress; curve *b*, polarization in terms of strain. The abscissa (*E*) represents $-b_{14}Y_z$ for curve *a*, $a_{14}y_z$ for curve *b*.

These relations are illustrated in Fig. 140, in which curve *a* represents Eq. (508) and curve *b* Eq. (510). For any arbitrary polarization P on curve *a*, $OA \equiv -b_{14}Y_z$, $A'C \equiv P$. For curve *b*, $OB \equiv a_{14}y_z$, $B'D \equiv P$. The origins are at O' and O'', and $OO' \equiv P^0$. The reciprocal slopes at O' and O'' are χ_s' and χ_s''.

Any observed piezoelectric polarization P, measured from P^0, is thus given by Eq. (510) in terms of strain and by (508) in terms of stress, according to the normal method. In both cases $E = 0$; therefore the quotient $-y_z/Y_z$ gives the isagric compliance s_{44}^E at zero field [see Eq. (517)].

The distinction between curves *a* and *b* in Fig. 140 becomes important when an electric field is applied to a crystal already under mechanical stress. The abscissas for both curves are thereby increased by an amount E, but the polarizations are no longer the same. This is because curve *a* represents a *free* crystal, which, as long as the stress Y_z is con-

stant, is free to be deformed by the field, while in curve b the crystal is clamped if y_z remains constant.

Equation (510) can be used to prove that, when the strain is reduced by clamping from y_z^0 to $y_z = 0$ (rhombic clamping), the spontaneous polarization is also suppressed. Remembering that y_z in (510) is measured from y_z^0, we seek the value of y_z required to make $P = -P^0$ and thus reduce the total polarization to zero. Calling this strain y_z' and setting $P = -P^0$ in (510), we find by the use of Eqs. (504) and (505) that

$$a_{14}y_z' = -\chi_z''P^0 + 2BP^{0^3} = -P^0(\chi_1 + BP^{0^2}) = -a_{14}y_z^0 \quad (510a)$$

Hence $y_z' = -y_z^0$, and the strain is reduced to the condition of rhombic clamping.

In §439 the effects of mechanical constraint on the form of the hysteresis loops have been considered. The nature of these effects becomes clear from a consideration of Figs. 138 and 139. A constraint may consist in clamping the crystal at some arbitrary strain or in impressing a fixed stress on a crystal that is otherwise free to deform itself in the electric field, or it may be of a more complicated sort. If we regard the impressing of a fixed strain or stress as equivalent to impressing a fixed biasing field on the crystal, certain conclusions can be drawn at once. It will be recalled that in Fig. 138 curve c is for a crystal at 15° clamped with $y_z = 0$ and that for monoclinic clamping the origin of the theoretically observed polarization curve is at O'', with initial susceptibility χ_z''. If the crystal is clamped with any arbitrary $+y_z$, the origin becomes displaced to a point farther up on curve c, having an abscissa displaced to the right of O'' by the amount $a_{14}y_z$. Wherever the origin falls, the portion of the curve traversed when any not too large alternating voltage is applied is not far from a straight line; hence for a clamped crystal between the Curie points there is no hysteresis, but only a practically linear polarization curve.

The result is quite different when the mechanical bias is a *constant stress*, as was approximately the case with Figs. 129 and 130. Equation (493c) is to be used with a constant value assigned to Y_z. The polarization curves are then the same as in Fig. 139, with the origin displaced by the amount $b_{14}Y_z$ to the right or left from O according to the sign of Y_z. If the origin is at A', the polarization, including that due to Y_z, will be at A (curve a at 5° being taken as an example). A is then the origin for the observed polarization curve. As E is varied to the right and left from A, a distorted curve results, like those in the oscillograms.

From what has been said, it follows that a small mechanical bias, whether constant strain or constant stress, may be expected to cause an increase or decrease in the observed susceptibility, according to the sign of the bias. On the other hand, a *large* bias of either sign,

exceeding the limits of the hysteresis loop, should cause always a decrease in susceptibility.

460. Converse Effect. Just as Eq. (507), relating a stress to the polarization that it causes, expresses the direct effect, so from Eq. (500) one can express the converse effect, with the strain produced by E as a function of E. All that is necessary is to substitute for P^E its equivalent in terms of the associated strain, which by setting $Y_z = 0$ in Eq. (493b) is found to be y_z/b_{14}. The converse effect is then expressed as*

$$E = \frac{\chi'_z}{b_{14}} y_z + \frac{3BP^0}{b_{14}^2} y_z^2 + \frac{B}{b_{14}^3} y_z^3 = \frac{y_z}{(d_{14})_n^z} \tag{511}$$

This non-linearity between y_z and E has been verified by several observers, as has been shown in Chap. XXI.

For small E and Y_z, at any temperature outside the Curie points, the initial $(d_{14})_0$ is found from Eqs. (495), (497), (509b), and (522a):†

$$(d_{14})_0 = b_{14}\eta' = \frac{a_{14}}{D_{14}} \tag{512}$$

Between the Curie points, from Eqs. (495), (499), (509a), and (522a),

$$(d_{14})_0^z = b_{14}\eta'_z = -\frac{a_{14}}{2D_{14}} \tag{512a}$$

For any E and Y_z the differential $(d_{14})_d$ is given by Eq. (509). The *over-all value* of d_{14} between the Curie points, which would be obtained experimentally from observations of P by the *direct effect* with a ballistic galvanometer on applying a stress Y_z, is found from Eq. (508):

$$\left(\frac{1}{d_{14}}\right)_n^z = -\frac{Y_z}{P} = \frac{1}{b_{14}}(\chi'_z + BP^2 + 3BP^0P)$$
$$= \frac{1}{(d_{14})_0^z} + \frac{1}{b_{14}}(BP^2 + 3BP^0P) \tag{512b}$$

For the treatment in the case of multi-domain crystals see §479. Outside the Curie points Eq. (512b) holds, with $P^0 = 0$ and χ' in place of χ'_z. From Eqs. (493b) and (500) it is easily proved that (512b) holds also for the *converse effect*,‡ in which case P is the polarization due to E in the free crystal [see also Eq. (511)].

* By means of Eq. (493b), this expression is easily seen to be an extension of Eq. (3b) in Mueller[380] (in the latter equation the sign of E_x should be changed).

† Equation (522a) may be anticipated here, since its derivation is independent of the present discussion.

‡ For experimental data on the converse effect, including observations of hysteresis, see Chap. XXI.

Expressions symmetrical with the foregoing are easily derived for e_{14}. First there are the initial values

$$(e_{14})_0 = a_{14}\eta_1 \qquad \text{and} \qquad (e_{14})_0^s = a_{14}\eta_s'' \tag{513}$$

outside and between the Curie points, respectively; the relation between $\eta_1 = 1/\chi_1$ and $\eta_s'' = 1/\chi_s''$ is given in Eq. (505a). The differential value $(e_{14})_d = a_{14}\eta_d''$ is found from Eq. (510):

$$\left(\frac{1}{e_{14}}\right)_d^s = \frac{\partial y_z}{\partial P} = \frac{1}{a_{14}}(\chi_s'' + 3BP^2 + 6BP^0P)$$
$$= \frac{1}{(e_{14})_0^s} + \frac{1}{a_{14}}(3BP^2 + 6BP^0P) \tag{513a}$$

Outside the Curie points we write χ_1 in place of χ_s'' and set $P^0 = 0$.

From Eq. (510) the *over-all value* $(e_{14})_n^s = P/y_z$ can be found, where $P = (e_{14})_n^s y_z$ is the polarization due to the impressing of a strain y_z of any magnitude:

$$a_{14} = \chi_s''(e_{14})_n^s + 3BP^0y_z(e_{14})_n^{s2} + By_z^2(e_{14})_n^{s3} \tag{513b}$$

The solution of this cubic equation would give $(e_{14})_n^s$ for any y_z in terms of the practically constant a_{14}. The dependence of e_{14} on strain is here made evident, while the dependence on temperature is introduced through χ_s'' and P^0. The over-all value can also be expressed in terms of P:

$$\frac{1}{(e_{14})_n^s} = \frac{y_z}{P} = \frac{1}{a_{14}}(\chi_s'' + BP^2 + 3BP^0P) = \frac{1}{(e_{14})_0^s} + \frac{1}{a_{14}}(BP^2 + 3BP^0P) \tag{513c}$$

461. *A Correlation between the Voigt and Polarization Theories.* The general relation between the free and clamped susceptibilities according to Voigt's theory, as applied to Rochelle salt for fields in the x-direction, is found from Eq. (264) to be $\eta' = \eta'' + e_{14}d_{14}$. With Rochelle salt, as we have seen, a distinction must be made between the initial, over-all, and differential susceptibilities. We now write the expressions for the relations between the initial and over-all susceptibilities, both between and outside the Curie points.

From Eqs. (496a), (501), (505a), and (505b), the difference between the free and clamped over-all dielectric stiffnesses between the Curie points is the same as that between the initial values χ_s' and χ_s'':

$$(\chi_s')_n - (\chi_s'')_n = \chi_s' - \chi_s'' = \chi' - \chi_1 = -a_{14}b_{14} \tag{514}$$

In terms of e_{14} and d_{14}, $a_{14}b_{14}$ can be expressed by means of Eqs. (509a), (509b), and (513):

Between the Curie points, $a_{14}b_{14} = (e_{14})_0^s(d_{14})_0^s\chi_s'\chi_s''$ (515)
Outside the Curie points, $a_{14}b_{14} = (e_{14})_0(d_{14})_0\chi'\chi_1$ (515*a*)

The corresponding equation in terms of over-all values can be found from Eqs. (512*b*) and (513*c*), but it is less simple. The Voigt theory does not lend itself easily to expressing the relation between the susceptibilities except for the initial values.

From Eqs. (514), (515), and (515*a*) one arrives at an independent proof of Eq. (264), particularized for the regions between and outside of the Curie points:

Between the Curie points, $\eta_s' - \eta_s'' = (e_{14})_0^s(d_{14})_0^s$ (516)
Outside the Curie points, $\eta' - \eta_1 = (e_{14})_0(d_{14})_0$ (516*a*)

The symmetry between Eqs. (514) on the polarization theory and Eqs. (516) and (516*a*) on Voigt's theory is obvious. The choice of expression for the difference between the susceptibilities is a matter of convenience.

462. The Elastic Constants s_{44} and c_{44}. Experimental evidence indicates that the constant-polarization value $s_{44}^P = 1/c_{44}^P$ is nearly independent of stress and temperature (§375). On the other hand, the isagric $s_{44}^E = 1/c_{44}^E$ varies greatly with both temperature and stress. The relation between s_{44}^E and s_{44}^P for large stresses is most simply expressed in terms of the Voigt coefficient $(d_{14})_n^s$, in which n signifies the over-all value given in Eq. (512*b*), applicable to large as well as to small stresses; outside the Seignette-electric region the superscript s disappears. The desired relation is obtained by assuming P_t to be held equal to zero while Y_s is applied, so that $y_s = -s_{44}^P Y_s$. The field strength needed to make $P_t = 0$ during this process is $E = +b_{14}Y_s$ by Eq. (493*c*). This E causes an additional strain, which we call $y_s^E = (d_{14})_n^s E = b_{14}(d_{14})_n^s Y_s$. With $E = 0$, y_s^E is absent, and the total strain is

$$y_s - y_s^E = -[s_{44}^P + b_{14}(d_{14})_n^s]Y_s \equiv -s_{44}^E Y_s$$

or

$$s_{44}^E = s_{44}^P + b_{14}(d_{14})_n^s = s_{44}^P - \frac{Pb_{14}}{Y_s} \tag{517}$$

where P is the polarization due to Y_s when $E = 0$.* When Y_s is small, (517) becomes identical with (522*c*), since in the latter equation d_{14} is the initial value.

The isagric relation between y_s and Y_s, for zero field, can also be obtained by combining Eqs. (508) and (510), with the aid of (495):

$$y_s = -s_{44}^E Y_s = \frac{-b_{14}}{a_{14}} Y_s + b_{14}P = -s_{44}^P Y_s + b_{14}P \tag{518}$$

where P is given by Eq. (508).

* Equation (517) is a special case of Eq. (283).

Experimental curves of the form suggested by this equation are shown in Fig. 142.

By making use of Eq. (517), together with the relations $y_z = -s^E_{44}Y_z$, $s^E_{44} = 1/c^E_{44}$, and $s^P_{44} = 1/c^P_{44}$, one arrives at the following expression for s^E_{44} in terms of strain, in which the relation between P and y_z is given by Eq. (510):

$$\frac{1}{s^E_{44}} = c^E_{44} = c^P_{44}\left(1 - \frac{b_{14}P}{y_z}\right) \quad . \tag{519}$$

If a Rochelle-salt crystal could hold out under a sufficiently great stress, the isagric stiffness would approach the value for constant polarization. This fact can be seen from Eq. (517) or (519), for owing to the non-linear relation between stress and polarization the second term on the right approaches zero with increasing stress.

Equation (517), valid at all temperatures, states that the strain when $E = 0$ is that which would be produced by Y_z at constant polarization plus a term proportional to the polarization caused by Y_z. Since according to Eq. (517) saturation effects are present, it follows that a curve relating y_z with Y_z would show saturation, as is indeed the case in Fig. 142 and as was found experimentally by Iseley.[243] Thus not only are there mechanical and electrical saturation effects under an impressed electric *field*, as expressed in Eqs. (500) and (511), but also under an impressed mechanical *stress*.

As will be seen later in Eq. (528), a relation can be written between y_z and Y_z, valid above θ_u, in which the temperature enters explicitly.

If the assumption that Y_z produces the same polarization as a field $E = -Y_z/b_{14}$ is justified, then at a critical value of Y_z there should be a sudden reversal of P^0. If Y_z were put through a cycle of positive and negative values, one would therefore expect to find the relation between P and Y_z or between y_z and Y_z in the form of a hysteresis loop. The coercive stress would be $(Y_z)_c = -E_c/b_{14}$, of the order of 0.2 kg/cm^2.

The slope $-dy_z/dY_z$ of the y_z:Y_z curve (with constant E) at any point may be called the *differential compliance* $(s^E_{44})_d$, by way of analogy with the differential susceptibility. The over-all compliance is of course $s^E_{44} = -y_z/Y_z$. By the same reasoning as in the discussion of mechanical bias in §459, so here it may be shown that the observed value of s^E_{44} should be less when a large constant biasing field E is impressed on the crystal. Such was indeed found to be the case by Mueller[380] in experiments on vibrating Rochelle-salt crystals: the resonant frequencies, which involve s^E_{44}, were found to be greater the larger the biasing constant field was made (see also §466).

No observations on this strain:stress hysteresis seem to have been made. The only pertinent data are those of Iseley, discussed in §418;

while they have the same form as the $P:E$ curves, they throw no light on the question of hysteresis. In any case, the analogy between Y_s and E must not be pushed too far: when Y_s is impressed, the lattice moves the dipole (or its equivalent), while the converse takes place when E is impressed. A very simple expression relating s^E_{44} to s^P_{44} is found when Y_s is so small that powers of P higher than the first can be omitted. From Eqs. (510) and (508) one finds with the aid of Eq. (495*b*), for *small* Y_s,

$$s^E_{44} \approx \frac{b_{14}}{a_{14}} \frac{\chi''_s}{\chi'_s} = s^P_{44} \frac{\chi''_s}{\chi'_s} = s^P_{44} \frac{\eta'_s}{\eta''_s} \tag{520}$$

The same relation follows directly from Eq. (495*d*). Since s^P_{44} is a finite constant nearly independent of temperature and $\eta'_s = \infty$ at the Curie points, it follows that for small stresses s^E_{44} should approach infinity at these points. This deduction from the theory is confirmed by the observations described in connection with Fig. 141.

Since for Rochelle salt $s^E_{44} = 1/c^E_{44}$ and $s^P_{44} = 1/c^P_{44}$, it follows from Eqs. (520) and (505*a*) that the isagric and isopolarization stiffness coefficients for small stresses are related thus:

$$\frac{c^P_{44}}{c^E_{44}} = \frac{s^E_{44}}{s^P_{44}} = \frac{\chi''_s}{\chi'_s} = \frac{\eta'_s}{\eta''_s} = 1 + \eta'_s a_{14} b_{14} \tag{521}$$

Similar reasoning for the region *outside* the Curie points leads to the analogous relations

$$\frac{c^P_{44}}{c^E_{44}} = \frac{s^E_{44}}{s^P_{44}} = \frac{\chi_1}{\chi'} = \frac{\eta'}{\eta_1} = 1 + \eta' a_{14} b_{14} \tag{521a}$$

463. In interpreting the results of experiments with *isolated* plates (electrodes far removed from crystal), account must be taken of the fact mentioned in §§190 and 199, that deformations then take place at constant electric displacement* D. The relation between s^E_{44} and s^D_{44}, the value at constant displacement, is readily found by specializing Eq. (281) for fields parallel to X in Rochelle salt:

$$\frac{s^E_{44}}{s^D_{44}} = \frac{k'}{k''} \tag{521b}$$

This equation gives the ratio of the compliance at zero gap (adherent electrodes) to that at infinite gap, for small stresses. In adopting as the value of s^P_{44} that derived from observations with a wide gap we disregard the fact that the ratio η'_s/η''_s in Eq. (521) or η'/η_1 in Eq. (521*a*) is not quite the same as k'/k'' in Eq. (521*b*). However, in the least favorable

* The present chapter has to do only with X-cut plates of Rochelle salt, in which the polarization and displacement are parallel to the field. Under these conditions s^D_{44} is identical with the quantity s^*_{44} derived from Eq. (273*a*).

case, when k' has its smallest value, of the order of 75, the difference amounts to only about one-half of 1 per cent, which is not greater than the uncertainty in the observed value (see also §211).

From Eqs. (499), (505a), (520), and (521), s^E_{44} between the Curie points for small stresses may be expressed in the following ways:

$$s^E_{44} = \frac{\chi''_s}{c^P_{44}\chi''_s - a^2_{14}} = -\frac{\chi''_s}{2D_{14}} = -\frac{\chi_1}{2D_{14}} + \frac{3}{2c^P_{44}} = (\eta'_s\chi_1 + \tfrac{3}{2})s^P_{44} \quad (522)$$

where $$D_{14} \equiv \chi_1 c^P_{44} - a^2_{14} = \frac{1}{s^E_{44}\eta' - d^2_{14}} = -c^P_{44}BP^{0^2} \quad (522a)$$

The parameter D_{14}, a function of the fundamental dielectric, elastic, and piezoelectric constants, plays a prominent part in Mueller's expression of his theory. The third of the expressions in (522) is identical with Eq. (11a) in his third paper.[380]

Outside the Curie points the equations are analogous but somewhat simpler:

$$s^E_{44} = \frac{\chi_1}{D_{14}} = \eta'\chi_1 s^P_{44} \quad (522b)$$

The last expression is equivalent to Eq. (521a) and also to Eqs. (4a) and (4c) in Mueller's paper II.

The general equations (275) and (276) as applied to s_{44} and c_{44} in Rochelle salt can also be derived from Eqs. (521) and (495b). Between the Curie points, for small stresses,

$$s^E_{44} = s^P_{44} + a_{14}b_{14}s^P_{44}\eta'_s = s^P_{44} + b^2_{14}\eta'_s = s^P_{44} + d^2_{14}\chi'_s \quad (522c)$$

$$c^E_{44} = c^P_{44} - a^2_{14}\eta''_s = c^P_{44} - e^2_{14}\chi''_s = c^P_{44} - \frac{e^2_{14}}{\eta''_s} \quad (522d)$$

Outside the Curie points the same equations hold, with η', χ', η_1, and χ_1 substituted for η'_s, χ'_s, η''_s, and χ''_s.

464. The Quadratic Piezoelectric Effect in Rochelle Salt. In a monoclinic crystal with constant angle β (corresponding to y_z in Rochelle salt), there is a linear converse piezoelectric effect expressed* by

$$x_x = b_{11}P_x \qquad y_y = b_{12}P_x \qquad z_z = b_{13}P_x$$

Since we are concerned here only with fields parallel to X, the monoclinic coefficients b_{26} and b_{35} (or d_{26} and d_{35}) play no part. In Rochelle salt the monoclinic angle is not constant but is represented by the spontaneous strain $y^0_z = b_{14}P^0$ mentioned in §456; moreover, under electric or mechanical stress the strain can be altered by amounts even greater than y^0_z. According to Mueller's theory,[381] the extent to which Rochelle salt becomes monoclinic is measured by the departure of the configuration

* For the monoclinic terminology employed here, see §450.

of the crystal from the unstressed rhombic form. Thus even outside the Curie points the crystal takes on monoclinic characteristics when subjected to a shear y_z, and the magnitude of the monoclinic coefficients b_{11}, b_{12}, and b_{13} is assumed to be directly proportional to y_z, as shown by the equations $b_{11} = \varphi_1 P_x$, $b_{12} = \varphi_2 P_x$, $b_{13} = \varphi_3 P_x$, where φ_1, φ_2, and φ_3 are constants. We are thus led to the following quadratic piezoelectric equations, in which the subscript x is omitted from P, with the understanding that only polarizations in the X-direction need be considered.

$$x_x = \varphi_1 P^2 \qquad y_y = \varphi_2 P^2 \qquad z_z = \varphi_3 P^2 \tag{523}$$

Beyond these there are also $y_z = b_{14} P$, $z_x = x_y = 0$.

When a field E is applied at a temperature between the Curie points, $P = P^0 + P^E$, where P^E is the polarization caused by E. It is sufficient to consider x_x alone, for which, if $E = 0$, we have $(x_x)_0 = \varphi_1 P^{0^2}$. If E is present, $x_x = (x_x)_0 + (x_x)_E = \varphi_1 (P^0 + P^E)^2$, whence

$$(x_x)_E = \varphi_1 P^E (2P^0 + P^E) \tag{523a}$$

Several deductions can be made from this equation. (1) Outside the Curie points, where $P^0 = 0$, $(x_x)_E = \varphi_1 P^{E^2}$; this irreversible converse quadratic effect was observed by Mueller[381] at 25.5°C. (2) As long as E is less than the coercive E_c, there should be, between the Curie points, a reversible linear converse effect $(x_x)_E = 2\varphi_1 P^0 P^E$ of large magnitude. This effect does not seem to have been observed. (3) If $E > E_c$, the polarization P^0 has the same sign as E, and both the linear and the quadratic terms in Eq. (523a) are irreversible.

From his observations Mueller estimates φ_1 of the order $-1.2(10^{-9})$ cm³/erg. The crystal contracts in the X-direction for a sufficiently large field of either sign; this contraction at 3,000 volts is of the same order as that caused by a pressure of 100 atm (§82).

Mueller finds in this quadratic effect an explanation of the anomalous thermal expansion of Rochelle salt in the range of spontaneous polarization, to which reference has been made in §407. He also discusses an analogous quadratic optical effect.[381]

The production of the strains x_x, y_y, and z_z makes a contribution to the specific heat, and it also suggests slight changes in a_{14}, c^P_{44}, and B at the Curie points.[380,381]

To such effects as those treated in this section, in which new physical constants come into being in a crystal as the result of a deformation, Mueller gives the name "morphic effects."* Pushed to its logical

* The magnitude of d_{11}, calculated from Mueller's values of x_x and E_x by the equation $d_{11} = x_x/E_x$, is quite astonishingly large, except at fields of only a few volts per centimeter. Thus we find, from Mueller's data, $d_{11} = 500(10^{-8})$ when $E_x = 1$ esu,

conclusion, this concept is equivalent to asserting that a crystal belongs to its assigned class only as long as it is free from stress of any sort. When under strain it possesses a different, usually a lower, set of elements of symmetry. Attention is called to this fact in §531 in connection with the piezo-optic effect (see also §482). With most phenomena in the great majority of crystals, morphic effects are doubtless of a high order, thus escaping detection.

Mueller also points out that the quadratic effects of the type described differ in principle from electrostriction, since they occur only when the strain y_z is not suppressed. Moreover, their magnitude in Rochelle salt is thousands of times greater than any known electrostrictive effect.*

465. The Curie-Weiss Laws. For ferromagnetic substances above the Curie point, as is seen from Eq. (561), the Curie-Weiss law is

$$k_m = C/(T - \theta)$$

where k_m is the magnetic mass susceptibility, C a constant, and T any absolute temperature above the Curie temperature θ. By proper choice of C, the volume susceptibility may be written in place of k_m. Over a narrow range just below the Curie point the susceptibility is $k_m/2$, as shown in §552.

In §552 it is proved that the linear relations between $1/k_m$ and temperature, both above and below the Curie point, are independent of the coefficients p and q in the generalized Langevin function [Eq. (562)]. In the first form of his theory of Rochelle salt, as will be seen in §485, Mueller postulated a cubic equation relating the polarization P with the molecular electric field F, together with an expression similar to Weiss's Eq. (557). The molecular-field theory led to the Curie-Weiss law for the dielectric susceptibility in exactly the same manner as in the magnetic case.

The interaction theory that has been discussed in the foregoing sections does not of itself predict the Curie-Weiss law or any other depend-

---

rising to $1{,}600(10^{-8})$ when $E_x = 10$ esu. These values are of the order of d_{14} itself. It must be noted, however, that this is not a true longitudinal effect in the ordinary sense, for the following reasons: (1) Since the effect is *quadratic* in E_x, the strain x_x maintains the same sign (a contraction) on reversal of E_x when $E_x > E_c$. (2) Being "morphic," it is a converse effect only. There can be no morphic direct effect involving d_{11}, since neither in the rhombic nor in the monoclinic system is there an elastic coefficient s_{14}. For this reason there should be no piezoelectric contribution from the morphic d_{11} to the dielectric constant at any temperature, although Mueller holds that there should be an effect on the dielectric constant of the *clamped* crystal. It is also conceivable that Rochelle salt, being monoclinic between the Curie points, may in this region also possess small but measurable coefficients d_{11}, d_{12}, d_{13}, d_{26}, and d_{35} that are not morphic (see §483).

* See also Matthias.[353]

ence of electric or piezoelectric properties upon temperature. Such prediction is impossible without some form of molecular theory. Hence on the basis of the interaction theory the Curie-Weiss law has to be accepted as an experimental fact. From it, as will now be shown, can be deduced certain other linear relations that have an important bearing on the general theory.

The discovery of the Curie-Weiss law for Rochelle salt may be credited to Kurchatov and Eremeev.[292] As explained in §§434 and 444, it has been most exactly established by the experiments of Mueller and Hablützel. According to Eq. (490), the initial reciprocal susceptibility above θ_u is given by

$$\chi' = \frac{t - t_c}{C} \tag{524}$$

When this value is substituted in Eq. (498), the following equation results, giving the relation between P and E for any temperature for the first few degrees above θ_u:*

$$E = \frac{t - t_c}{C} P + BP^3 \tag{524a}$$

In his paper I, Fig. 10, Mueller shows a set of experimental $P:E$ curves for temperatures from 24.3 to 31.2°, which are in full agreement with Eq. (524a) for $t_c = 23°$, $C = 170$, $B = 10(10^{-8})$. The values of these three constants are not far from those given in connection with Eq. (490), which are based on other data. The curves have forms varying between that of curve c, Fig. 139, at the lowest temperature, and that of curve e at the highest.

Below θ_u the Curie-Weiss law, expressed by Eq. (490a), is illustrated in Fig. 120. The slope of the $\chi':t$ curve is here twice as great as that above θ_u; this agrees with theory, since according to Eq. (499) $\chi_s' = -2\chi'$, where χ_s' is the initial value in the Seignette-electric range.

Since from Eqs. (496a) and (505a) $\chi_1 = \chi' + a_{14}b_{14}$ (rhombic clamping) and $\chi_s'' = \chi_s' + a_{14}b_{14}$ (monoclinic clamping), it follows that the Curie-Weiss relation holds for the clamped as well as for the free crystal, for a few degrees on each side of θ_u. Above and below θ_u we find, from Eqs. (499) and (524),

$$\chi_1 = \frac{t - t_c}{C} + a_{14}b_{14} = \frac{t - (t_c - a_{14}b_{14}C)}{C} \approx \frac{t - 18^0}{C} \tag{525}$$

$$\chi_s'' = \frac{2(t_c - t)}{C} + a_{14}b_{14} = \frac{t_c - (t - a_{14}b_{14}C/2)}{C/2} \tag{525a}$$

The slopes of the lines representing these equations, as indicated in Figs. 143 and 145, are $1/C$ and $-2/C$, respectively. The constant C

* Ref. 376, Eq. (38).

is the same for the clamped as for the free crystal. The significance of the temperature 18° in Eq. (525) is pointed out in §468.

The linear relations between χ' (or χ_1) and temperature lead to other linear relations, or Curie-Weiss laws, for all physical quantities dependent on the susceptibility. They will now be summarized.

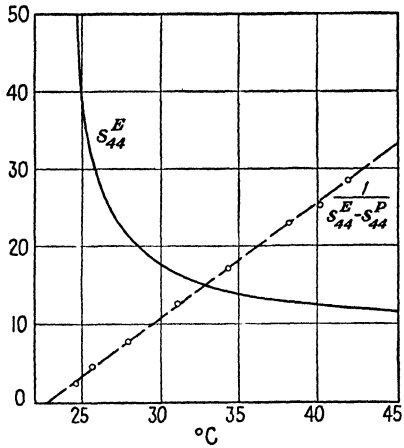


FIG. 141.—The Curie-Weiss law for the elastic compliance s^E_{44} of Rochelle salt, from Mueller. For the curve the ordinates should be multiplied by 10^{-12}; for the straight line, by 10^{10}. The circles are from Mason's experimental data.

466. For the *spontaneous polarization* P^0 we find from Eqs. (497) and (524)

$$P^{0^2} = \frac{t_c - t}{BC} \equiv h(t_c - t) \qquad (526)$$

where h is a constant. This equation expresses the parabolic form of the curve for P^0 in Fig. 147. It is necessary, however, to assign different values to h for the right and left portions of the "parabola." According to Mueller[376] the values are approximately $1.5(10^4)$ and $2.65(10^4)$ for the higher and lower temperatures, respectively.

From Eqs. (502) and (526) an analogous expression is derived for the *coercive field* E_c.

For the *elastic compliance* s^E_{44} the following expressions for the value with small stress follow from Eqs. (495*b*), (499), (522*c*), and (524): Outside the Curie points,

$$s^E_{44} - s^P_{44} = \frac{Cb^2_{14}}{t - t_c} \equiv \frac{\sigma}{t - t_c} \qquad (527)$$

where C is the "electric Curie constant" and $\sigma = Cb^2_{14}$ is the "elastic Curie constant" (Mueller). Between the Curie points,

$$s^E_{44} - s^P_{44} = \frac{Cb^2_{14}}{2(t_c - t)} \qquad (527a)$$

For $t_c = 23°$ and $Cb^2_{14} = 66.7(10^{-12})$, Mueller[378] finds Eq. (527*a*) very exactly in accord with experiment at temperatures above θ_u, as is evident from Fig. 141. The curve for s^E_{44} is derived from Mason's observations,* which are illustrated also in Fig. 146. From this curve, together with the constant $s^P_{44} = 1/c^P_{44}$, values of $1/(s^E_{44} - s^P_{44})$ are plotted. They are

* See §§375 and 474.

a linear function of temperature, thus confirming Eq. (527*a*). Of special interest in Fig. 141 is the pointing of s_{44}^E toward an infinite value at the Curie point, according to the prediction in §462. The physical meaning of this fact is that at the Curie point Rochelle salt is in an unstable condition, which makes it elastically "soft" with respect to small stresses, just as it is dielectrically soft, with a dielectric constant approaching infinity, on the application of a small field. It was pointed out in §455, in explanation of Fig. 128, that close to the Curie points the dielectric constant is smaller in large than in small fields; similarly, as the mechanical stress Y_z is increased from a very small value at a temperature close to either Curie point, the crystal becomes stiffer (see §§459 and 462). That is, the phenomenon of saturation is most striking close to a Curie point. No static elastic observations are at hand indicating abnormally large values of s_{44}^E under small stresses. In agreement with Mason, Busch[87] observed a decrease of 30 per cent in the resonant frequency of a vibrating Rochelle-salt plate as the temperature passed through the upper Curie point. The magnitude of the observed effect depends on how small the field is, as well as on the elastic constants other than the temperature-sensitive s_{44}^E that enter into the expression for the frequency.

From Eq. (527) and the general equations of the polarization theory given above, Mueller[380] has derived the following expression for the relation between Y_z and the strain y_z that it causes *at zero field*, valid for the first 10° above θ_u:

$$Y_z = (Y_z + c_{44}^P y_z)\frac{\Delta t}{\sigma c_{44}^P} + (Y_z + c_{44}^P y_z)^3\left(\frac{\Delta t}{\sigma c_{44}^P} + 1\right)\frac{B}{\chi_1 a_{14}^2} \qquad (528)$$

where $\Delta t = t - \theta_u$ and $\sigma = Cb_{11}^2$ as in Eq. (527). A plot of this theoretical curve is shown in Fig. 142 for several temperatures.

There are no experimental data with which a quantitative comparison can be made, except at small stresses. The observations of Iseley[243] on a 45° X-cut bar yield curves relating y_y' to Y_y' that have the form of those in Fig. (142); hence they may be regarded as a qualitative verification of the saturation effect expressed in Eq. (528), since by Eqs. (43) the compliance $s_{22}' = -y_y'/Y_y'$ contains $s_{44} = 1/c_{44}$.

The values of s_{44}^E calculated from the initial slopes of the curves in Fig. 142 agree closely with the values in Fig. 141 for the same temperatures.

467. For the *piezoelectric coefficient* $(d_{14})_0$ under small stresses, a Curie-Weiss law is to be expected, owing to the close relationship between d_{14} and η'. Above θ_u we have, from Eq. (495*b*), $d_{14} = b_{14}\eta'$, whence from Eq. (524) it follows that

$$(d_{14})_0 = \frac{b_{14}C}{t - t_a} \qquad (529)$$

Below θ_u, where $\eta_s' = -\eta'/2$, the corresponding expression is

$$(d_{14})_0^s = \frac{b_{14}C}{2(t_c - t)} \tag{529a}$$

These two equations show clearly the relation between the Voigt piezoelectric coefficient d_{14}, which is highly variable with temperature, and the piezoelectric constant b_{14} according to the polarization theory, which is found experimentally to be almost independent of temperature. The product of b_{14} by the electric Curie constant C may be called the *piezoelectric Curie constant.*

Satisfactory confirmation of Eqs. (529) and (529*a*) is found in the experiments of Norgorden, described in §424.

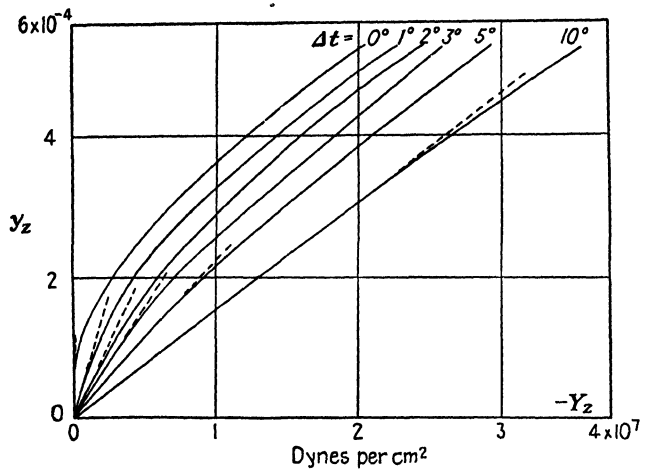


FIG. 142.—Theoretical isagric stress-strain relation for shear in the YZ-plane of Rochelle salt, above the Curie point, from Mueller.

Mueller[378,381] also finds linear relations corresponding to the Curie-Weiss law for the Kerr effect and for the monoclinic strain x_x described in §464.

In the foregoing paragraphs little has been said concerning the Curie-Weiss laws *below the lower Curie point.* Inasmuch as the law holds with respect to the dielectric susceptibility below θ_l, it can hardly be doubted that linear relations like those given above hold for all the physical quantities involved.

The dependence of the dielectric, elastic, and piezoelectric coefficients on temperature over the entire range between the Curie points is treated in §474.

468. Theory of Rochelle Salt between the Curie Points. From Eqs. (495*b*), (497), and (522*c*) it is clear that between the Curie points

the spontaneous polarization P^0, the compliance s^E_{44}, and the piezoelectric coefficient $(d_{14})_s$ can all be expressed by equations in which the only quantity that varies with temperature is the initial susceptibility η'_s. Hence any theory that accounts for the dependence on temperature of η'_s, or indeed of any one of these four quantities, will at the same time explain the temperature dependence of the other three. In §§445 and 446 we have referred to the early attempts of Kurchatov and of Fowler to find a relation between susceptibility and temperature. More recent attacks on this problem have been made by Mueller[376,378,380,381] and by Busch.[88] Like Busch (§485), Mueller in his first paper used a method closely analogous to that of Weiss in ferromagnetism, in which the concept of the molecular field F was involved. Mueller's explanation of the Curie points and of the variability of susceptibility with temperature, which he accomplished by postulating a slight effect of temperature on the molecular polarizability, will be discussed in Chap. XXVI.

For the present we are concerned with Mueller's later theory, according to which Rochelle salt possesses a single anomaly, inherent in the clamped crystal. The type of constraint is that which in §450 we have called "rhombic clamping," by which all strains are prohibited, including in particular, between the Curie points, the spontaneous strain y^0_2. As may be seen from Eq. (510*a*), this clamping completely neutralizes the spontaneous polarization P^0. The fundamental dielectric properties of Rochelle salt are regarded as inhering in the rhombically clamped crystal, in which the prohibition of strains ensures the absence of all piezoelectric deformations.

The particular property on which the theory depends is expressed by the Curie-Weiss law for χ_1 in Eq. (525) and is illustrated by the high-temperature portion of the χ_1 line in Fig. 143. Starting at the highest temperature, χ_1 slopes downward linearly, threatening to vanish at about 18°C; and if the crystal were not piezoelectric, χ_1 *would* vanish at this temperature, rising again at temperatures below 18°C, somewhat as indicated by the dotted lines.*

By Eq. (497) the χ' line for the free crystal is at a nearly constant distance $a_{14}b_{14}$ below the χ_1 line, with the consequence that $\chi' = 0$ at about 24°C and also at some temperature below 18°C. The presence of the two Curie points is thus accounted for.

* The infinite susceptibility of the completely clamped crystal, implied in the vanishing of χ_1, seems at first sight paradoxical, since large susceptibilities are usually associated only with *free* crystals. The physical explanation probably lies in the unstable state of the clamped crystal. The spontaneous polarization P^0, which the crystal would possess at 18° if free, is suppressed. Just as the introduction of an extremely small strain y_2 would cause a relatively large polarization to develop, so a weak field may so deform the crystal lattice as to produce the same result. The same explanation may be offered for the low value of χ_1 at 5°C.

469. It is pertinent at this point to quote from Mueller's paper IV, on the possible nature of the hypothetical transition in the neighborhood of 18°C and on the reason why the course of the χ_1 line between the Curie points, as calculated from observations on the free crystal, has the particular form shown in Fig. 143.

"If the crystal of Rochelle salt were not piezoelectric it would show only a single transition point. The two Curie points and the large number of dielectric, piezoelectric, optical, caloric and thermal anomalies of the free crystal can all be explained

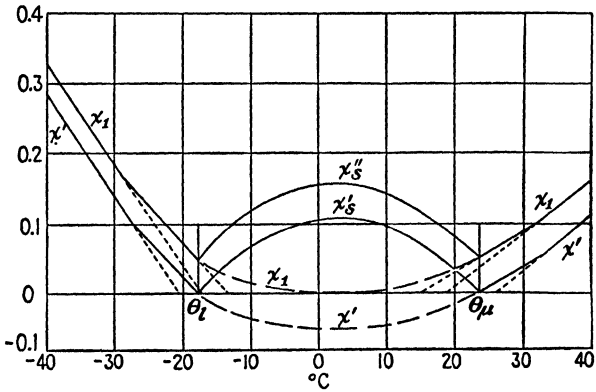


FIG. 143.—Schematic diagram of the dependence of the reciprocal susceptibilities on temperature, for small fields, from Mueller. It is based on measurements of χ' outside the Curie points, from Figs. 120 and 121, and of χ'_s between these points. From these values, χ' between the Curie points was calculated from Eq. (499) and χ_1 from Eq. (496a), χ'_1 ($\equiv 1/\eta''$) is the dielectric stiffness for rhombic clamping; χ''_s is for monoclinic clamping, calculated from Eq. (505a). The ordinate differences $\chi'_1 - \chi$ and $\chi''_s - \chi'_s$ are approximately constant and equal to $a_{14}b_{14}$.

on the basis of laws which are logical extensions of the laws of classical crystal physics. There remains, therefore, only the problem of understanding the nature of the transition of the clamped crystal. This transition is characterized by a high maximum of the [rhombically clamped] dielectric constant, but the available evidence does not indicate any changes of the internal energy or of the structure. The temperature gradient of the birefringence is altered but there is no sudden change of the optical constants. These peculiarities indicate that the transition can involve only a change of the position or of the dynamics of the protons of either the OH groups or the water of crystallization. The transition may be similar to those in HBr, HI, H_2S, PH_3.* It differs, however, from the modifications of these crystals by the fact that the transition of Rochelle salt produces no change of the specific heat. To account for this we propose the hypothesis that the transition is suppressed, i.e., with decreasing temperature the crystal approaches a transition point without actually reaching it, because in the initial stages of the transition secondary effects are created which suppress the modification and the crystal remains in its original state because at lower temperature the protons have not sufficient energy to change their positions."

* For a review of these transitions see A. Eucken, *Z. Elektrochem.*, vol. 45, p. 126, 1939. See also J. A. Hedvall and R. W. Pauly, *Z. physik. Chem.*, vol. 29, *Abt.* B, pp. 225–230, 1935.

In explaining the nature of this suppression of the transition point, Mueller advances the hypothesis that it is related to the piezoelectric morphic effects discussed in §464. One may carry this suggestion somewhat beyond the point where Mueller leaves it, by considering that in the clamped crystal between the Curie points these morphic effects (the development of strains x_x, y_y, and z_z when a field E_x is applied) try to assert themselves just as y_z does. Although suppressed by the clamping stresses so far as the *external* configuration is concerned, they may be accompanied by changes in the *internal* structure of such a nature that the polarization, when a field E_x is applied, is less than it would be if only the strain y_z were concerned. The whole question concerning the tendency toward a transition point in the clamped crystal at 18°C and of its suppression cannot be satisfactorily answered until more is known about the lattice structure of Rochelle salt.

Whatever the mechanism may be, the result is a rounding off of the χ_1 line to a minimum at about 5°C. It is therefore at this temperature, according to Mueller's theory, that the maxima in χ'_s and P^0 occur, together with hysteresis curves of greatest width and greatest energy loss.

If the χ_1 line actually touched the horizontal axis in Fig. 143, the rhombically clamped Rochelle-salt crystal would have a single Curie point like that in ferromagnetic materials, with infinite clamped dielectric constant at this point. On the other hand, the two Curie points of the unconstrained *heavy-water* Rochelle-salt crystal are so far apart that the χ_1 line would certainly intersect the horizontal axis twice.* The clamped crystal would therefore still have two Curie points with a spontaneous polarization between them.

470. One conclusion that can be drawn from Fig. 143 is that a *partial mechanical constraint* would be expected to draw the Curie points of Rochelle salt closer together. In §204 we have shown that a partial constraint diminishes the effective piezoelectric contribution to the susceptibility, yielding a value intermediate between those of a free and a fully clamped crystal. The effect in the case of Fig. 143 would be a decrease in the vertical separation of the χ_1 and χ' lines: if the χ_1 line remained constant, the χ' line would move vertically upward so that its intersections with the horizontal axis, at θ_l and θ_u, would be separated by a smaller interval. No systematic investigation of this effect seems to have been made, although it was mentioned by Mueller[376] as a possible explanation of the lack of agreement on the part of different observers as to the values of θ_l and θ_u. From the hysteresis loops in Fig. 129,

* That this is so can be seen from the fact that the elastic and piezoelectric properties of ordinary and heavy-water Rochelle salt are so nearly the same, as shown in §§87 and 143, that the vertical separation of the χ' and χ_1 lines for the heavy-water variety is nearly the same as in Fig. 143.

however, it is evident that mechanical constraint at least makes the $P:E$ curve approximate that of a fully clamped crystal. The only experimental data on the Curie point of a partially constrained crystal are those of Mason,[338] who finds the maximum susceptibility of a "longitudinally clamped" vibrating crystal to come at a temperature that, from his diagrams, appears to be substantially the same as for a free crystal, about 24°C. Mason used an X-cut 45° bar with full-length plated electrodes, to which a voltage of twice the fundamental lengthwise-vibration frequency was applied. The piezoelectric contribution to the polarization, so far as lengthwise movements are concerned, was thus neutralized (§61), while lateral movements were allowed to develop. The dielectric constant was indeed found to lie between the values for a free and a clamped crystal; it is difficult to see why this degree of constraint should not have been accompanied by an easily detectable decrease in the temperature for maximum dielectric constant, unless it be that the constraint imposed by inertia in the dynamic case differs, in its effect upon the temperature dependence of the dielectric susceptibility, from the constraint due to static externally applied clamping stresses. In this connection it may be recalled that under the constraining effect of *hydrostatic* pressure both Curie points are *raised* (§443), whereas a consideration of Fig. 143 led us to expect that *externally* applied mechanical constraint would increase θ_l but decrease θ_u. The discrepancy becomes resolved if we assume, with Bancroft, that the observed raising of the Curie points under hydrostatic pressure is due, not to mechanical constraints in the ordinary sense, but rather to distortion of the crystal lattice under pressure.

471. *What Is a Seignette-electric?* We conclude this consideration of the theory of Rochelle salt with a brief retrospect to the essential Seignette-electric phenomena, as described in the foregoing chapters. In spite of the knowledge acquired through the observations with mixed tartrates (§491) and the phosphates and arsenates (§493), conclusions must still be drawn chiefly from Rochelle salt. The investigations on the mixed tartrates have contributed to the dipole theory (§490) without throwing new light on Mueller's interaction theory. For lack of piezoelectric and elastic data on the phosphates and arsenates, it is not yet possible to say how completely all the details of the interaction theory apply to them. It can at least be said that no observations hitherto recorded on crystals other than pure Rochelle salt contradict any of the following statements:

So far as macroscopic observations are concerned, a Seignette-electric crystal may be defined as having a critical temperature, on one side of which the dielectric properties exhibit non-linearity and hysteresis (the *Seignette-electric* region), while on the other side there is no hysteresis

and the relation between polarization and field is nearly or quite linear (the parelectric region). The possession of such a critical temperature, or Curie point, is the basic criterion. Rochelle salt has two such points; some of the isomorphic mixtures as well as the phosphates and arsenates may have only an upper Curie point. Possibly a crystal with only a lower Curie point will one day be discovered, or one that is stable only in the Seignette-electric temperature range, so that no Curie point is observable.

Among the directly observed concomitant effects, at least in Rochelle salt, may be mentioned the following:

1. A Curie-Weiss law for dielectric, elastic, and piezoelectric effects on both sides of the Curie point.

2. The crystal is piezoelectric on both sides of the Curie point.

3. A reversible spontaneous polarization on one side of the Curie point, falling to zero at that point.

4. The crystal is pyroelectric in the region of spontaneous polarization (but see §521).

5. In the region of spontaneous polarization, abnormally large values of the dielectric constant of the free crystal, the piezoelectric constant, and the isagric elastic constant, as well as large dielectric losses (§375), are observed under certain field strengths and stresses. As the Curie point is approached, these three quantities tend toward infinite values under small field strengths and stresses.

6. At all temperatures the dielectric and piezoelectric constants become diminished by mechanical constraints.

7. Except with occasional very small specimens, the crystal has, in the region of spontaneous polarization, a multi-domain structure with opposing polarizations in adjacent domains.

The interaction theory leads to the following conclusion, which is at least partly corroborated by experiment:

8. The *clamped* crystal obeys a dielectric Curie-Weiss law. Beyond this, the anomalous behavior of the clamped crystal with varying field and temperature is such as to furnish, through the equations of the interaction theory, a description of all the other anomalies.

It is too early to say whether all the effects 1 to 8 are essential properties of all Seignette-electric crystals. It is hardly conceivable that the ferromagnetic analogy can exist without 3 and 6. It appears possible, however, that the essential features of the analogy might be present in a single-domain crystal, so that 7 cannot be regarded as a necessary characteristic.

According to the interaction theory, a Seignette-electric crystal is one which, from §453, has $\eta_1 > a_{14}b_{14}$ in a certain range of temperature. The corresponding condition according to the dipole theory, from §485,

is $\alpha_M > 1/\gamma$. This correspondence is discussed in §486. The two expressions are equivalent inasmuch as each postulates the attainment at a certain temperature of a critical polarizability in excess of a certain value. It is only when this condition is fulfilled that there can be a spontaneous polarization and a spontaneous strain, which can be reversed by an applied field, giving rise to the appearance of abnormally large values of the dielectric, piezoelectric, and elastic constants.

One may ask why Seignette-electric properties are not observed in more cases among crystals. The answer is partly that very few crystals have been investigated over wide ranges of temperature and partly that these properties are due to a fortuitous combination of circumstances. Iu the first place, the polarizability must be great enough to satisfy the condition mentioned above. This is a necessary condition, but it is not sufficient; for although it implies an instability and a structural modification at a certain temperature, still of itself it does not give assurance that the crystal, on one side or the other of the critical temperature, will have a symmetry low enough for spontaneous polarization to be possible. Furthermore, on both sides of the critical temperature, the substance must be a solid dielectric with homogeneous crystalline structure.

472. Owing to the impossibility of experimenting with a completely clamped crystal, Mueller's theory of Rochelle salt, based, as we have seen, on the assumption of a suppressed transition in the neighborhood of 18°C, must remain a matter of hypothesis. If, as was pointed out at the beginning of this section, a theoretical explanation could be established for the dependence of any one of the quantities P^0, s^E_{44}, $(d_{14})_s$, or η'_s upon temperature, it would serve as well as χ_1 for the basic parameter.

For example, a molecular theory of the spontaneous polarization P^0 that predicted the correct dependence of P^0 on temperature could be used as the starting point, and with the aid of the foregoing equations the various elastic, piezoelectric, and dielectric properties could be expressed in terms of this theory. To illustrate this fact, we tabulate below the principal dielectric equations: at the left, the various quantities are expressed in terms of χ_1; at the right, in terms of P^0. It is assumed that a_{14}, b_{14}, B, and C are determined experimentally and that Eq. (526) is established on a molecular-theoretical basis, giving the spontaneous polarization in agreement with experiment.

FUNDAMENTAL EQUATIONS

$\chi' = \chi_1 - a_{14}b_{14}$	(497)	$\chi' = -BP^{0^2}$	(497)
$BP^{0^2} = a_{14}b_{14} - \chi_1$	(497)	$\chi_1 = a_{14}b_{14} - BP^{0^2}$	(497)
$\chi'_s = 2(a_{14}b_{14} - \chi_1)$	(499)	$\chi'_s = 2BP^{0^2}$	(499)

DEPENDENCE ON TEMPERATURE

$$\chi' = \frac{t - t_c}{C} \qquad (524) \qquad P^{0s} = \frac{t_c - t}{BC} = -\frac{\chi'}{B} = \frac{\chi'_s}{2B} \quad \begin{cases} (526) \\ (497) \\ (499) \end{cases}$$

$$\therefore \chi' = \frac{t - t_c}{C} = -BP^{0s} \quad \begin{cases} (526) \\ (497) \\ (499) \end{cases}$$

$$\chi'_s = \frac{2(t_c - t)}{C} \qquad (499) \qquad \chi'_s = \frac{2(t_c - t)}{C} = 2BP^{0s} \quad \begin{cases} (526) \\ (497) \\ (499) \end{cases}$$

$$\chi_1 = \frac{t - t_c}{C} + a_{14}b_{14} \qquad (525) \qquad \chi_1 = a_{14}b_{14} - BP^{0s} \qquad (497)$$

$$\chi''_s = \frac{2(t_c - t)}{C} + a_{14}b_{14} \qquad (525a) \qquad \chi''_s = a_{14}b_{14} + 2BP^{0s} \qquad (499), (505a)$$

473. The existence of a spontaneous polarization on one side of the Curie point but not on the other suggests a change from a pyroelectric to a non-pyroelectric class at this temperature. In terms of crystal energy, one may regard the crystal as having a state of minimum energy U for one of these two configurations, represented by curve A in Fig. 144 and by curve B for the other configuration. If B were lower than A at all temperatures, the state corresponding to A would not exist at all. If $B > A$ above some temperature θ_u, becoming less than A below this temperature, a change will take place in lattice configuration and crystal classification; and if B corresponds to a configuration in which there is a spontaneous polarization, there will be an upper Curie point at θ_u. If the two curves happen to have a second intersection at a lower temperature θ_l, there will be a lower Curie point here.

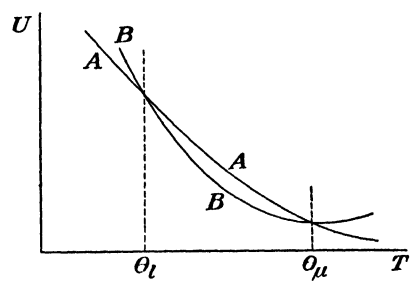


FIG. 144.—Two overlapping states of minimal energy.

Similarly, if there were theoretical grounds for treating the temperature dependence of either s^E_{44}, $(d_{14})_s$, or η'_s as the cornerstone of the theory of Rochelle salt, a table of relationships analogous to the foregoing could be drawn up, in terms of which all the parameters could be expressed. With η'_s, P^0, and the experimental values of a_{14}, b_{14}, and B given, it can be seen from Eq. (499) that the minimal value and absence of Curie points for χ_1 follow necessarily. The behavior of the clamped crystal would then appear, not as the cause of the anomalies, but as an incidental circumstance.

474. Experimental Confirmation of the Theoretical Curves in Fig. 143. The only complete data available at present are those derived by Mueller[378,380] from observations by Mason. Following Mueller, we use here for the dielectric constant of the free crystal and for the spontaneous polarization the values obtained by Bradford,* which are in substantial

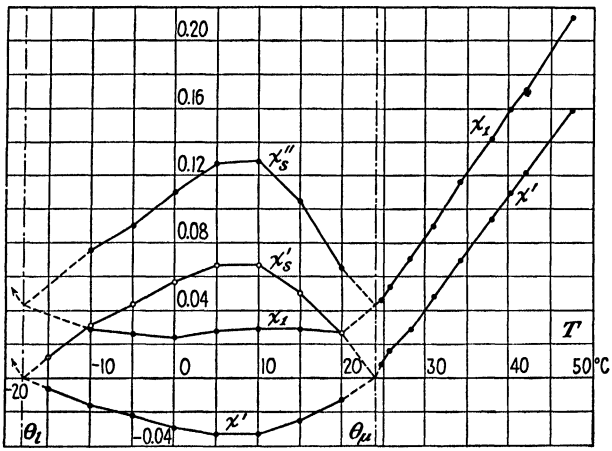


FIG. 145.—Reciprocal susceptibilities of Rochelle salt for free and clamped crystals as functions of temperature. Bradford's observations, as reported by Mueller.

agreement with the results of other observers. All values are "initial," obtained with small fields.

From Mason's resonance observations with an X-cut plated 45° bar, values of d_{14} and s_{44}^E are derived at each temperature. From these data, with the aid of Eqs. (497), (499), (505a), and (522b) and with

$$c_{44}^P = 11.6(10^{10})$$

dynes/cm², Figs. 145 and 146 have been drawn. The saturation coefficient B is obtained from χ_s' and P^0 by means of Eq. (499).

In Fig. 145 the observed quantities are χ' and χ_s', for the free crystal above and below θ_u. χ_1 for rhombic clamping,† χ_s'' for monoclinic clamping, and χ' between the Curie points are all derived by means of the equations mentioned above. The general similarity with Fig. 143, in which the curves between the Curie points are based on Mueller's theory, should be especially noted. The only obvious discrepancy lies in the value of χ_1, which in Fig. 145 fails to have a minimum close to zero. Now χ_1 is calculated from the equation

$$\chi_1 = \chi' + a_{14}b_{14} = -\frac{\chi_s'}{2} + a_{14}b_{14}$$

* E. B. BRADFORD, B.S. thesis, Massachusetts Institute of Technology, 1934.

† Outside the Curie points χ_1 is identical with $1/\eta_x''$.

It may be that $a_{14}b_{14}$, which we have taken from Mueller's calculations, is too large. At present one can only say that experimental verification of Mueller's hypothesis concerning the extremely low minimum in χ_1 is still lacking. At θ_u, however, χ_1 in Fig. 145 is in good agreement with Mason's[378] Fig. 7; and χ_s'' agrees well with Mason's curve for a (monoclinically?) clamped crystal.

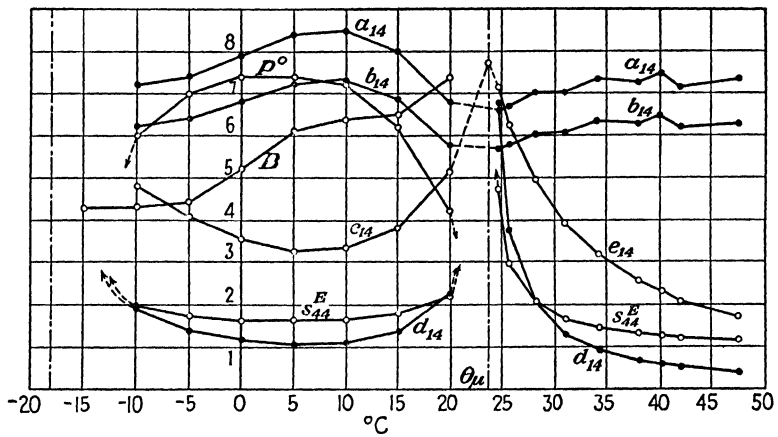


FIG. 146.—Electric and elastic constants of Rochelle salt as functions of temperature, from Mueller, calculated from Mason's observations. Ordinates are to be multiplied by the following factors:

Quantity	a_{14}	b_{14}	P^0	B	e_{14}	s_{44}^E	d_{14}
Factor	10^4	10^{-7}	100	10^{-8}	$2(10^5)$	10^{-11}	10^{-5}

In both Figs. 145 and 146 the dotted lines indicate gaps in the observational data that were used in the construction of these curves. The arrows show the trend to be expected beyond the observed limits. Of the values in Fig. 146, P^0 and s_{44}^E may be accepted with a fair degree of confidence as being representative of average well-prepared Rochelle salt crystals to within a few per cent. From Fig. 142 it is evident that with larger fields, and hence with larger stresses, considerably smaller values of s_{44}^E would be observed. The relatively low values of s_{44}^E obtained by Mandell and by Hinz (Table IV) were probably due to the use of large stresses.

In calculating d_{14} Mueller employed the gap method described in §310 [Eq. (452)], the essential data being the frequencies f_0 and f_∞ at series resonance, for gaps $w = 0$ and $w = \infty$, together with the density ρ, length l, and the dielectric constant. e_{14} is calculated from $e_{14} = d_{14}/s_{44}^E$; a_{14} and b_{14} are found from Eq. (495b), and s_{44}^E from f_0.

As is shown in §142, Mason, by a different method, found a_{14} to be practically independent of temperature. If his finding is accepted, one must conclude that the gap method employed in Mueller's calculation is

incapable of yielding correct results with Rochelle salt. On the other hand, there may be unsuspected temperature dependencies among the various quantities appearing in Eq. (495*d*), which, if introduced, would confer on a_{14} a variation with temperature. All that can confidently be said at present is that the variability of a_{14} and b_{14} with temperature is at least an order of magnitude lower than that of e_{14} and d_{14}.

It will be observed that e_{14} depends less on temperature than does d_{14}. Instead of approaching infinity at the Curie points, e_{14} has at θ_u the value a_{14}/χ_1. In §546 reasons are given for considering the piezoelectric stress

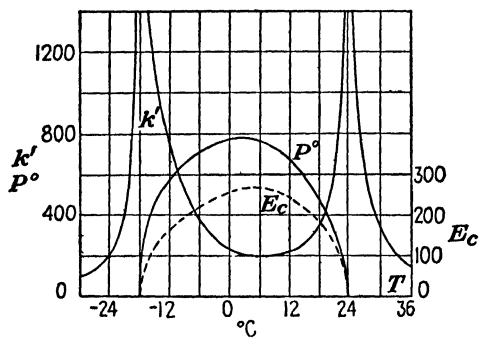


FIG. 147.—Dielectric constant k' at small fields, spontaneous polarization P^0, and coercive field E_c (in volts per centimeter), for Rochelle salt, from Bradford. Frequency 1,000 cycles per second.

coefficient e_{hk} in general of more fundamental significance than the strain coefficient d_{hk}.

The observations of Bradford* on which Fig. 145 is based are presented in another form in Fig. 147, taken from Mueller.[382] The curve for $k' = 1 + 4\pi\eta'$ corresponds to $\chi' = 1/\eta'$ and $\chi'_s = 1/\eta'_s$ in Fig. 145. P^0 is the same as in Fig. 146. The values of E_c may be compared with the data recorded in §436.

The dynamic value of d_{14} has also been measured by Mikhailov[368] from 0 to 40°C, by the use of $X45°$-bars with a small gap and a field of 1 to 2 volts/cm. His curve relating d_{14} to temperature is like that in Fig. 146, but the values over most of the range are only about one-third as large, owing possibly to the presence of the gap.

It has already been pointed out in §426 that relatively small values of d_{14} are to be expected when weak fields are used at frequencies as high as those in resonators. Comparison of Fig. 146 with the experimental results obtained with static and l-f alternating fields, as recorded in Chap. XXII, shows that in the h-f dynamic case this expectation is

* See footnote, p. 626.

fulfilled. According to §480, the discrepancies between the curve for d_{14} in Fig. 146 and Figs. 106, 109, and 115 are explained simply by the fact that in the resonator experiments the field and stress were so small that d_{14} never exceeded its initial value. As the Curie points were approached, this initial value became very large; midway between these points it was very small indeed in comparison with the values that it attains under larger stresses, and especially in static fields, as illustrated in Fig. 106.

475. Conclusions Respecting the Polarization Theory. In the foregoing pages we have given, with certain elaborations, an account of Mueller's interaction theory of Rochelle salt, in terms of the polarization theory, which was developed independently by Mueller and the author from premises first suggested by Mason. While the interaction theory might have been written in terms of Voigt's field theory, still the concepts of the polarization theory provide a description of the properties of Rochelle salt (and, without much doubt, of all other Seignette-electrics as well) that presents a clearer picture of the physical nature of the phenomena. The chief experimental justification lies in the fact that the coefficients a_{14} and b_{14} are found to have values nearly, if not quite, independent of temperature, and probably also independent of stress. a_{14} and b_{14} are therefore to be regarded as the true piezoelectric constants. As has been seen, the "constants" d_{14} and e_{14} vary enormously with both stress and temperature.

On the other hand, if the "true" dielectric constant is defined as that which would be observed with a clamped crystal, this constant so defined is not linear in E or independent of temperature, although the dependence on temperature is small in comparison with that of the free crystal.

Mueller has pointed out[382] that effects that are not directly related to the electric properties may be expected to vary linearly with temperature if at all, except for very slight changes at the Curie points and small effects caused by an electric field. An example of such a property is the elastic compliance s^D_{44} at constant electric displacement. s^D_{44} is the quantity derived from measurements of the elastic stiffness of a completely isolated crystal (§463), and it is found to have a very slight dependence on temperature, with a minute anomaly at the upper Curie point (§375). The compliance s^P_{44} at constant polarization, which plays an important part in the polarization theory, is numerically practically identical with s^D_{44} (§211).

In the basic equations (493) to (493*c*) of the polarization theory no provision is made for variation of s^P_{44} with stress. A linear relation is assumed between stress and strain at constant polarization. The justification for this assumption lies in the approximate agreement of theory with observation as far as present experimental data go.

476. *Comparison of the Polarization Theory with Voigt's Field Theory.* As has been stated, both "theories" are only different ways of describing the same phenomena. If it were not for the great dependence of the elastic and piezoelectric constants of Rochelle salt on temperature, the polarization theory would probably never have arisen. The superiority of the polarization theory lies entirely in the fact that the elastic coefficients at constant polarization, and the piezoelectric coefficients when defined in terms of polarization rather than of field, are practically independent of temperature. The polarization theory does not reveal these facts; it only takes advantage of them. In particular, it gives clearer expression than does the field theory to this very important fact: To a high degree of approximation the piezoelectric strain, at all temperatures and up to the attainable limits of saturation, is *proportional to the polarization.* Mathematically, this statement is equivalent to saying that a_{14} and b_{14} are approximately constant, whereas e_{14} and d_{14}, which relate stress and strain with the *field*, vary greatly with temperature.

In the theoretical treatment of practical applications, whenever the polarization rather than the field can conveniently be used as the electrical parameter, the polarization theory is to be preferred. Voigt's formulation, using e_{14} and d_{14}, is to be used when the phenomena can more conveniently be described in terms of the applied field. For example, the latter is the case in dealing with the piezoelectric resonator. The question of the applicability of the polarization theory to piezoelectric crystals other than Rochelle salt is dealt with in §191.

CHAPTER XXV

THE DOMAIN STRUCTURE OF ROCHELLE SALT

La donna è mobile
Qual piuma il vento, . . .

—"RIGOLETTO."

477. Frequent reference has been made in the preceding chapters to the hypothesis that between the Curie points Rochelle salt, like iron, normally consists of an aggregate of distinct domains. The experimental evidence will now be examined, and the bearing of domain structure on dielectric and piezoelectric observations will be discussed. An account is included of Jaffe's theory of polymorphism in Rochelle salt, leading to the conclusion that Rochelle salt is properly to be regarded as monoclinic in the Seignette-electric region.

The remark has been made by Debye* that a sample of unmagnetized iron is analogous to a mixture of microcrystalline tourmaline crystals with random orientations. The analogy is still closer if Rochelle salt is substituted for tourmaline.

The first suggestion that the spontaneous polarization in Rochelle salt might be due to *groups* of atoms having different orientations of the same probability in the lattice seems to have been made by Debye in the discussion of a paper by Dorfman.† This idea, adopted by Kurchatov and verified by Mueller and others, made the ferromagnetic analogy even more complete.

The experimental evidence is of several sorts. First, there is the electrical Barkhausen effect indicating discontinuous jumps in the process of polarization as the field is gradually increased; it constitutes an additional item in the long list of magnetic analogies (§555). This effect in Rochelle salt was described by Kluge and Schönfeld[261] and also by Mueller.[376] It is observed only between the Curie points.

Second may be mentioned the pyroelectric tests with Bürker's powder (§517), which reveal discrete regions of opposite polarity. The pyroelectric effect would be zero if the domains were very small and their polarities were equally divided in opposite directions. One evidence of the minute size of the domains in iron lies in the fact that iron is not pyromagnetic.

* "Handbuch der Radiologie," vol. 6, p. 750, 1925.

† J. DORFMAN, in "Magnetisme," *Rapports 6ème Conseil phys. (Inst. Solvay)*, 1930 (pub. 1932), pp. 381–387.

From the size of the regions observed in his pyroelectric tests (§521), Mueller concludes that the domains in Rochelle salt are of the order of 1 cm in extent, enormously greater than in the case of ferromagnetism. His small crystals appeared to consist of single domains. That the domains are much less numerous than in iron is indicated by the relatively small number of Barkhausen "clicks," though it must be admitted that they are still sufficiently numerous to make one suspect that, if each domain is of the order of 1 cm^3, its polarity does not become reversed all in one jump. The effects of domain structure are manifest only between the Curie points.

To account for the large size of the domains, Mueller offers a hypothesis that may be stated thus: In the process of growth the crystal is constantly surrounded by a conducting liquid, which makes the surface equipotential and prevents the development of an opposing field. On the contrary, the domains in iron, while still very small, find themselves in the presence of opposing magnetic fields, which prevent further growth.

A necessary consequence of the presence of fairly large domains is *unipolarity*, which has sometimes been found, especially with small crystals or, as recorded by Kurchatov,[B32,294] in portions of a large crystal. In §433 unipolarity is further considered.

The domains in Rochelle salt preserve their individuality to a remarkable degree. Kurchatov states that after the large crystal, to which reference has just been made, had been kept for several hours at 40°C and then allowed to cool, the diminution in unipolarity was very slight. It would appear that the state of thermal disorder at high temperatures is unable to destroy either the configuration of the domains or the characteristic direction of the polarity in each domain, even though above the Curie point the spontaneous polarization is gone, only to reappear as the temperature passes downward through the critical temperature. This view is confirmed by Mueller's remark that no permanent reversal of the spontaneous field has ever been observed by him, even when a crystal was cooled while in a reversing field of 1,000 volts/cm. It is an interesting question whether the magnetic domains in iron also retain their individuality after being heated above the Curie point.

The persistence in polarity of individual domains can perhaps be explained in terms of the large mechanical stresses at the boundaries of adjacent domains when the crystal is in an electric field. Such stresses would tend to restore the original configuration and the original polarities on removal of the field. But a *single-domain* specimen might be expected to have its polarity permanently reversed by a strong reversing field.

Another consequence to be expected from the stresses between domains is that such stresses will prevent the isagric compliance s_{44}^E for

very small stresses from being as great with a multi-domain crystal as in a single domain (§462 and Fig. 141).

478. *Can Large Single-domain Crystals Be Produced?* When a Rochelle-salt crystal is grown by the method of cooling from a hot solution, the gradual lowering of temperature must give rise to internal stresses. Since the solution is usually considerably above the upper Curie point at the start, the stresses may be expected to be especially large as the temperature passes through this point. It is conceivable that such stresses are an important factor in the breaking up of the crystal into domains. If this is the case, then it seems possible that, by growing crystals at a *constant temperature* between the Curie points, single domains, or at least multi-domain crystals with larger domains, might result. As has been stated in §412, a few experimenters have used crystals grown by evaporation at constant temperature. Although it must be admitted that the properties of such crystals do not appear to be recognizably different from those in the case of growth by cooling, still there is not found in the literature a satisfactory answer to the question whether the domain structure is dependent on the method of growth.

A little light was thrown on this problem by W. S. Stilwell, who compared the pyroelectric patterns formed on crystals grown by evaporation at a constant temperature between the Curie points with those on crystals grown by cooling.* Seeds were placed in a 1,500-cm^3 flask containing a saturated solution at 1.8 $\pm$ 0.02°C. This flask, together with a large coil of copper tubing through which ice water was circulated, was immersed in a large container of water surrounded with good thermal insulation. In this container were also a heating coil, thermostat, and stirrer. An exhaust pump in constant operation kept the pressure of the air above the solution at a few millimeters of mercury. The water evaporated from the crystallizing flask was condensed in a second flask, which was cooled by a mixture of dry ice and alcohol.

The best crystal was grown to a size of 18.5 by 18 by 12 mm in 16 days. It is impossible to say what sort of domain structure this specimen might have been found to possess if it could have been tested at the temperature at which it was grown. It may be that in warming up to room temperature after removal from the solution and then in having its temperature changed by a few degrees during the pyroelectric test it took on a multiple-domain structure. At any rate, when it was sprinkled with a mixture of red lead and sulphur, it showed the presence of many domains. These appeared to be predominantly in the form of flat slabs of the order of 1 mm thick, with their planes normal to the Y-axis. Instead of being relatively large, the domains were found to be actually smaller than those observed by the same method on crystals grown by

* W. S. Stilwell, thesis for distinction, Wesleyan University, 1939.

cooling [crystals grown by R. W. Moore (§412), and from the Brush Development Company].

While these tests are not fully conclusive, they do not offer a hopeful prospect for the growth and permanence of single-domain Rochelle-salt crystals.

479. Effect of Domain Structure on the Hysteresis Loops. In Fig. 139 we have shown idealized curves for a single-domain crystal. It will be recalled that, if the spontaneous polarization P^0 is represented by OO', then when the field E is impressed the observed polarization is given by Eq. (500) and illustrated by curve a, with origin at O'. Since the domain is already polarized at the start, there is no "virgin curve."

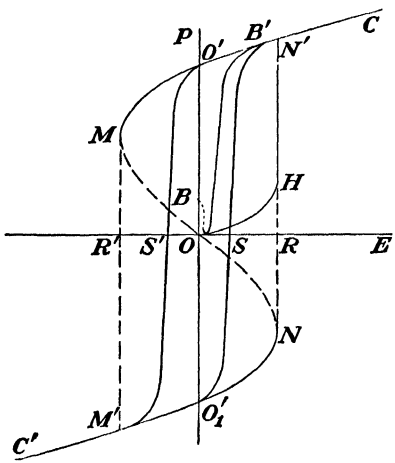


FIG. 148.—Theoretical hysteresis loop for a multidomain Rochelle-salt crystal.

If a crystal contains a number of domains whose positive and negative spontaneous polarizations just balance, it shows no unipolarity as a whole. Such a case is represented theoretically in Fig. 148, in which OO' and OO'_1 are the average positive and negative values of P^0. In the ideal case, such as has hitherto been treated, the + and − domains make separate contributions to the observed polarization. As E increases from zero in the positive direction, the contribution of the positive domains is represented by $O'N'C$, with O' as origin; that of the negative domains is $O'_1NN'C$, with O'_1 as origin, the portion NN' representing the sudden reversal of the negative domains. The total observed polarization, which can now be depicted with origin at O, is half the sum of the two contributions, or $OHN'C$. The form of the virgin curve thus finds a theoretical explanation. If now E is put through a cycle from + to − and back, the hysteresis loop $CO'MM'C'O'_1NN'C$ results, exactly as in Fig. 139, where only domains of a single sign were considered. If the average + and − spontaneous polarizations do not exactly cancel, the foregoing discussion need be modified only to the extent of moving the origin to a position somewhat above or below O in Fig. 148.

Even with a single-domain crystal it is probable that local inhomogeneities would facilitate the reversal of polarity, so that the virgin curve would begin to turn upward at some such point as B, and the coercive force E_c would be $OS = -OS'$ instead of $OR = -OR'$. The

corners of the loop would become rounded, leading to the form indicated in Fig. 148. The diminution of E_c must be still greater in a multi-domain crystal, in which the spontaneous deformation of each domain is hindered by adjacent domains. A field applied in either dirdction finds it easier to reverse those domains which oppose it, especially if, as in the case of iron (§555), some domains can grow at the expense of others.*

As to the actually observed field values, it will be recalled from §432 that under static excitation saturation has been recorded with a field strength as low as 15 volts/cm, while in a-c measurements from 50 to 1,000 cycles/sec the coercive field E_c is found to vary from zero at θ_u to about 200 volts in the neighborhood at 15°C, according to Hablützel. Mueller, as shown in Fig. 147, finds E_c to have a maximum of about 270 volts/cm at 5°C. Such discrepancies are not surprising in view of the variability in the domain structure. The foregoing values are only of the order of one-tenth as great as that calculated with the aid of Eq. (502). This fact does not invalidate the data in Fig. 147, which are based on actual measurement. It only goes to show that Eq. (502), which does not involve the domain structure, is incapable of furnishing the correct value of the coercive field.

In Fig. 128 it is seen that between the Curie points the dielectric constant is very much higher with moderately strong than with weak fields, just as is the case with the permeability of iron. As in the case of iron, the explanation lies in the shape of the polarization curve $OBB'C$ in Fig. 148. It is obvious that from point B on, the ratio $P:E$, and hence the dielectric constant of the free crystal, increases with increasing E up to the knee of the curve and remains relatively large up to very great values of E.

The foregoing account of dielectric hysteresis in Rochelle salt assumes that the energy loss per cycle, represented by the area of the loop, is involved in the work done in reversing the domains. This description is necessarily only qualitative; moreover, it does not take account of those viscous losses which may be independent of the reversal of domains. Nevertheless, the view that domain reversal plays an essential part in the phenomenon of hysteresis is not incompatible with the theory of hysteresis in Rochelle salt advanced by W. P. Mason, which is discussed in §375.

In Fig. 148 it will be observed that the initial slope, for $E = 0$, is the same at points O, O', and O'_1. Hence, so far as *small* fields are concerned, the observed dielectric properties of Rochelle salt are the same whether the specimen consists of a single domain or not, and all that has

* A painstaking, if not fully convincing, theory of domain structure has been attempted by David.[119]

been said from §452 on, concerning effects at weak fields and small stresses, becomes applicable to all specimens.

In a single-domain crystal or in a multi-domain crystal having a preponderance of spontaneous polarization of one sign, it is theoretically impossible, owing to the reversal of domains, to find any field strength whatever that will reduce the net polarization to zero.

480. A word is needed concerning the bearing of domain structure on the piezoelectric coefficient d_{14}. Outside the Curie points Rochelle salt is always rhombic dextrogyrate, and the sign of d_{14} is positive. In the Seignette-electric region, where the crystal is monoclinic enantiomorphous, d_{14} is still positive, retaining the same sign whether the domain has a positive or negative spontaneous polarization. The sign of d_{14} would be negative only in a left-crystal. Owing to the close relationship between the susceptibility of a free crystal and d_{14}, it follows that the interaction between domains will have an effect on d_{14} similar to that on the susceptibility.

When the dielectric constant of Rochelle salt is measured with a low-voltage a-c bridge while a relatively large static field is impressed on the crystal, the value is diminished to an extent depending on the static field. An inspection of Fig. 148 shows this. The phenomenon is analogous to the effect of a mechanical bias discussed in §459. This effect has been recorded by Errera[134] and also by Mueller.[376]

In §§453 and 459 it was shown that the quantities $a_{14}y_z$ and $-b_{14}Y_z$ are equivalent to E in the production of polarization. It follows that when, as can be the case in Rochelle-salt resonators, there are periodic changes in strain or stress of sufficient magnitude for non-linear effects to be appreciable, the polarization:strain or polarization:stress curves must have the form indicated in Fig. 148. Some evidence of this is afforded by Figs. 112, 114, and 115. Unfortunately, no data are available for comparing, with the *same crystal*, the dependence of P_x on the mechanical stress Y_z, the dependence of the strain y_z on the electric stress E_x, and that of P_x on E_x, over wide ranges of these stresses.

We are now in a position to consider the dependence of the over-all piezoelectric coefficient $(d_{14})_n^s$ upon stress, in a multi-domain crystal. According to Eq. (512*b*), in a single-domain crystal this coefficient has its largest value at small stresses, when P is small, up to the point where the stress is great enough to cause a reversal of P^0. In the usual case of a multi-domain crystal, when static stresses of varying magnitude are applied, the $P:Y_z$ relation should be similar to the $P:E$ virgin curve in Fig. 148, with $(d_{14})_n^s = -P/Y_z$. Obviously, $(d_{14})_n^s$ is small up to the point B and has an approximately constant value identical with $(d_{14})_0^s$ in Eq. (509*a*). With increasing Y_z it increases rapidly toward a saturation value. This effect is to be expected over the temperature range in

which hysteresis is present. Such experimental evidence as can be found is mentioned in §418. In particular, it follows from the dependence of P^0, and hence of the size of the hysteresis loop, upon temperature that under large stresses $(d_{14})_n^s$ is greatest midway between the Curie points, sloping gradually downward through the Curie points; at these points $(d_{14})_n^s$ fails to show maxima when the stress is large, as is illustrated in Fig. 106.

Similar results are indicated by theory for the converse effect, in which case the hysteresis loops are plotted with y_s- and E-coordinates, and $(d_{14})_n^s = y_s/E$, as in Fig. 114.

Evidence for the existence of domains in Seignette-electric crystals other than Rochelle salt will be found in §498.

481. Polymorphism in Rochelle Salt. It has been pointed out by Jaffe[246] that whenever a transition takes place from a non-pyroelectric to a pyroelectric crystal class at a definite temperature an infinite value of the electric susceptibility is to be expected at this temperature, provided that the transition does not involve latent heat. In an earlier paper[245] Jaffe also discusses the question whether the Weiss region in iron should not be considered as tetragonal paramorphic rather than cubic, even though a single crystal, with its random orientations of domains, is externally cubic. It may be added that in 1916 Perrier[412] attempted to correlate the high-low inversion in quartz with the ferromagnetic Curie point and looked for a sharp maximum in the permittivity. That the result was negative can now be understood from the fact that neither high nor low quartz possesses primary pyroelectricity.

The rhombic system has three mutually perpendicular axes of unequal lengths. Hitherto Rochelle salt has always been assigned to the rhombic hemihedral (or bisphenoidal) class, No. 6, from goniometric measurements made presumably at room temperature and hence in the Seignette-electric range. In this class each of the three crystallographic axes is a twofold symmetry axis, which precludes the possibility of a polar axis. This means, physically, that it is impossible for any scalar agent, as temperature or hydrostatic pressure, to give rise to a vectorial phenomenon such as magnetic or electric polarization or for a linear electro-optic effect to exist in this class. Hence, in accordance with Neumann's principle as elaborated by Voigt, any pyroelectricity exhibited by this class must be of the "false" type.

Outside the region of spontaneous polarization the physical properties of Rochelle salt are entirely in accord with its rhombic hemihedral symmetry. Within this region, on the other hand, as was emphasized by Jaffe,[245] there are several one-way effects indicating that the X-axis is physically a polar axis and therefore should be so regarded crystallographically: spontaneous internal field, pyroelectricity (§521), unipolar

conductivity (§410), asymmetry in polarizability (§433) and in the converse piezoelectric effect §(422), and a linear electro-optic effect.[376]

These effects are all characteristic of the domain, just as the large internal field in iron is a domain property. If in Rochelle salt as in iron the domains were very small, with their polarities distributed at random in space or equally divided along the + and − X-directions, none of the effects associated with a polar axis would be externally observable, and there would be no doubt about assigning Rochelle salt to the rhombic hemihedral class. For example, consider the pyroelectric effect, which Mueller found to be very strong in the range of spontaneous polarization. In view of what has been said, we must conclude either that this effect is only "apparent" as a result of the spontaneous polarization, or that between the Curie points Rochelle salt belongs properly to a class of lower symmetry. The latter view seems clearly the logical one, at least in the case of a crystal consisting of a single domain. The spontaneous polarization makes the X-axis a polar axis of symmetry in the physical sense; we shall now show that this is also true in the crystallographic sense.

In assigning Rochelle salt in the region between the Curie points to the appropriate class we confine the discussion to the single domain. The only rhombic class other than hemihedral that is piezoelectric is the hemimorphic, and this is excluded because of the absence of d_{14}. The proposals of Valasek[543] and of Taschek and Osterberg[504] in this regard are therefore of no avail. Now, if the X-axis is recognized as a polar axis, the Y- and Z-axes can no longer be axes of symmetry. With only one twofold axis of symmetry left the crystal must be monoclinic hemimorphic. It will be recalled that, while in both the rhombic and monoclinic systems the three axes are unequal, the rhombic system has its axes mutually perpendicular. On the other hand, in the monoclinic system one axis is perpendicular to each of the other two, the latter forming an angle different from 90°. Thus the transition from rhombic to monoclinic involves crystallographically only a change in the angle between two axes, in this case the Y- and Z-axes. These are the considerations that lead to the assignment of Rochelle salt to the monoclinic hemimorphic class.

According to the usual convention as stated in §5, the monoclinic polar axis b would be called the Z-axis. To avoid confusion we adopt Jaffe's suggestion that it still be called the X-axis, the rhombic Y-axis remaining unchanged, being now the same as the monoclinic Y-axis with sign reversed. The a-axis of the monoclinic crystal then makes a small angle β with the negative direction of the rhombic Y-axis. The rhombic Z-axis coincides with the monoclinic X- (or c-) axis.

This convention requires a revision of the subscripts of the piezoelectric constants with respect to Voigt's usage. It is brought about by

exchanging the index 1 with 3, and 4 with 6. The tabulation of constants then becomes, instead of that given in §131,

$$\begin{matrix} d_{11} & d_{12} & d_{13} & d_{14} & 0 & 0 \\ 0 & 0 & 0 & 0 & d_{25} & d_{26} \\ 0 & 0 & 0 & 0 & d_{35} & d_{36} \end{matrix}$$

The tabulation includes five new constants in addition to d_{14}, d_{25}, and d_{36}. No search for them seems to have been made beyond the experiments described in §§464 and 483. The chief difficulty in their detection and measurement lies in eliminating stray effects due to the large d_{14}.

The angle β between the c-axis and the orthogonal Z-axis is simply the angle of shear y_z imposed upon the domain by its own spontaneous field in the absence of an external field. This angle varies with temperature between the Curie points, having a maximum of the order of 3′ at about 5°C. Reversal of the polarity of the domain by application of an external field reverses the direction of the polar axis and changes the sign of β.

It is not surprising that so small a departure from the orthogonal relation has escaped notice, especially since goniometric measurements have presumably been made with crystals in which there were complexes of opposing domains. The point to emphasize is that the structure of Rochelle salt is essentially that of the domain, for which β has a value different from zero. In Jaffe's paper are mentioned other instances of recognized transitions from one crystal classification to another in which the changes in parameters are very small.

From these considerations it follows that between the Curie points an ordinary Rochelle-salt crystal with its complex of positively and negatively oriented domains is to be regarded as twinned, the twinning being of the Dauphiné (orientational) type, like that in low quartz produced by cooling from uniform high quartz (electrical twinning).

The Curie points are inversion points from monoclinic to rhombic hemihedral symmetry. For this inversion the piezoelectric effect is responsible. An isolated unit cell would be rhombic at all temperatures, but between the Curie points the interaction between the dipoles (or their equivalent) in neighboring cells is such as to produce an internal field with attendant deformation, making the domain as a whole monoclinic.

482. In §436 it was pointed out that the coercive field E_c has a value of about 200 volts/cm at 0°C, approaching zero at the two Curie points, We can now go a step further in the explanation, recognizing E_c as a measure of the energy required to reverse the polar axis of the crystal. That E_c is so small at all temperatures is because the transition temperatures are so close together. When the field E reaches the critical value

E_c, the dipoles that are responsible for the spontaneous polarization become reversed from their stable state in one direction to that in the opposite direction. As they do so, the angle β changes sign. Midway between the two stable states, then, is the configuration of higher (rhombic) symmetry, for which $\beta = 0$. As either Curie point is approached the stable states come nearer and nearer to the higher symmetry; this explains why the energy necessary to effect the reversal approaches zero. Now a finite change in strain and polarization caused by an electric field of vanishing magnitude means that at the Curie points both d_{14} and η_x approach infinity. Experimental evidence (§474) tends to confirm this conclusion.

The angle β referred to above is the *spontaneous strain* y_z^0 that was discussed in §§403 and 452. To Vigness[566] belongs the credit for the first experimental work from which its magnitude could be calculated, while Jaffe first recognized it as a characteristic feature of Rochelle salt and treated its theoretical significance in the manner outlined above. From Vigness's data Jaffe calculated $y_z^0 = 8(10^{-4})$ at temperatures from 0 to 10°C, whence $\beta = 2.7'$. Vigness's crystal showed distinct unipolarity; yet it is unlikely that he happened to have a strictly single-domain specimen. Hence the foregoing value is probably too small rather than too large.

From the observations of Hinz shown in Fig. 114 an estimate can be made of y_z^0 on the assumption that, by analogy with the spontaneous polarization P^0, y_z^0 can be calculated from the remanent strain when $E = 0$. In this manner one finds, at 18.5°C, $y_z^0 = 0.95(10^{-4})$, a value smaller than would be expected from Vigness's results, even after making allowance for the greater nearness to the Curie point; but the reason may lie in the multi-domain structure.

Mueller[380] made a direct measurement of the variation with temperature of the angle between the Y- and Z-faces of a Rochelle-salt block. He found no temperature effect above the upper Curie point but observed an angular change beginning at θ_u which amounted to about

$$3'(y_z^0 = 8.7 \times 10^{-4})$$

at 11°C and to 3′45″ ($y_z^0 = 10.9 \times 10^{-4}$) at 0°C.

Finally, from Eq. (494), $y_z^0 = b_{14}P^0$, the spontaneous strain can be computed by taking b_{14} and P^0 from Fig. 146. At 0°C, $b_{14} = 6.8(10^{-7})$, $P^0 = 740$, whence $y_z^0 = 5.03(10^{-4})$. This value agrees as well as can be expected with the results of Vigness and of Mueller, considering the differences in domain structure of the specimens employed.

Although observations of spontaneous strain in the neighborhood of the lower Curie point θ_l are still to be made, there is little reason to doubt that the relation between spontaneous strain and temperature

can be represented by a curve similar to that for P^0 in Fig. 147, with a maximum for y_z^0 of the order of 10^{-3}.

From the thermal point of view, the spontaneous strain would be described as due to an anomaly in the coefficients of thermal deformation (§407). A discussion of thermal expansion in monoclinic crystals will be found in Voigt* and in Wooster.[B56]

Induced Monoclinic Properties. In an important sense Rochelle salt takes on monoclinic properties even outside the Curie points, *viz.*, in an electric field. The class to which any crystal is normally assigned depends on goniometric measurements on specimens that are unstressed, either mechanically or electrically. The change in crystallographic symmetry in a crystal under stress is mentioned in §531, and more especially in §464. As an example of an effect theoretically observable with monoclinic but not with rhombic crystals and that nevertheless has been found above the upper Curie point in Rochelle salt, we may cite the linear electro-optic effect discussed in §535.

483. *A Search for Monoclinic Coefficients by Hydrostatic Pressure.* If, as is indicated in the footnote on page 613, there is a detectable monoclinic piezoelectric effect in monoclinic Rochelle salt between the Curie points, independent of morphic effects, its presence should be revealed by means of hydrostatic pressure. According to the axial system adopted in §481, the piezoelectric constants that would play a part in such an effect are d_{11}, d_{12}, and d_{13}. A uniform hydrostatic pressure Π would then produce, through the direct effect, a polarization given by Eq. (193):

$$-P_x = (d_{11} + d_{12} + d_{13})\Pi$$

An X-cut plate immersed in insulating oil, with electrodes connected to a measuring device, should respond to a change in pressure of the oil. An advantage in this method is that it entirely eliminates disturbing effects from d_{14}, since no shear is caused by hydrostatic pressure.

A preliminary investigation of this sort has been made by A. C. Grosvenor.† An X-cut Rochelle-salt plate 4.2 mm thick, area 8.3 cm², was connected to a d-c amplifier. Substantially the same results were obtained with a second crystal. There was no difficulty in obtaining a deflection of the milliammeter when a pressure of a few kgs/cm² was applied to the paraffin oil surrounding the crystal in a metal container. The difficulty lay in interpreting the results. In the temperature range under investigation Rochelle salt is pyroelectric. The adiabatic heating of the oil and of the crystal itself when pressure is applied causes a pyroelectric contribution to the deflection. Now the pyroelectric effect is greatest at the Curie points, having opposite signs at these points and

* Pp. 289–294.

† A. C. Grosvenor, master's thesis, Wesleyan University, 1940.

passing through zero in the neighborhood of 0°C. It should therefore be possible to eliminate the pyroelectric disturbance by applying the pressure at a temperature sufficiently below 0°C so that the net pyroelectric polarization, due to the rise in temperature on application of pressure, would be zero.

At present only preliminary results have been obtained by this method, indicating a value of $(d_{11} + d_{12} + d_{13})$ of the order of $3(10^{-11})$.

It was also observed that at 11.3°C the deflection was zero. On the assumption that the pyroelectric and piezoelectric effects at this temperature were equal and opposite, a crude calculation of $(d_{11} + d_{12} + d_{13})$ was made by estimating for the pyroelectric coefficient p the value of about 20 by the method indicated in §521 and calculating the rise in temperature due to compression. Owing particularly to the fact that the crystal plate used had presumably a multi-domain structure, for which the assumed value of p may have been many times too large, the calculation would be expected to yield too high a value of

$$(d_{11} + d_{12} + d_{13})$$

The value by this method was, in fact, of the order of a thousand times greater than that obtained by the first method.

It is possible that a repetition of these experiments with greater refinement, coupled with a thorough pyroelectric investigation of the specimen, would prove of value in the attack on the problem of Rochelle salt. And let the observer not forget to use several different specimens!

CHAPTER XXVI

INTERNAL-FIELD THEORY OF SEIGNETTE-ELECTRIC CRYSTALS

Doch im Innern scheint ein Geist gewaltig zu ringen . . .

—GOETHE.

484. Although doubt has been thrown on the importance of the orientation of free dipoles in explaining the nature of the Seignette-electrics, still the dipole theory, which involves the concept of the internal field, has figured so prominently in the literature—and may still continue to do so in a modified form—that it is advisable to survey the subject briefly, with special reference to the work of Kurchatov,[B32,263] Mueller,[376] and Busch.[88] At the end of the chapter an account is given of the attempts to calculate the dipole moment of Rochelle salt.

The outstanding differences between the internal-field and the interaction theories are these: (1) The polarization P is expressed as a cubic function of the internal field F by the former theory and as a cubic function of the ordinary field $E = V/e$ by the latter. (2) The two Curie points and the properties of the crystal in the region between them are attributed in the former theory to small changes in the molecular polarizability and in the latter to small changes in the susceptibility of the clamped crystal. Further comparisons between the two theories will be found in the following paragraphs.

From Eqs. (171) and (174) it is seen that the polarization may be expressed as

$$P = N\alpha_{ea}F + P_0L(a) \qquad (530)$$

where $L(a)$ is the Langevin function, P_0 is the polarization in infinite field, α_{ea} is the polarizability by distortion (electronic plus atomic), and $a = \mu F/KT$. If $L(a)$ is written in the generalized approximate form of Eq. (562), one finds*

$$P = \left(N\alpha_{ea} + \frac{P_0p\mu}{KT}\right)F - \frac{P_0q\mu^3}{(KT)^3}F^3 \qquad (530a)$$

* In §552 it is stated that the value of the coefficient p depends on the restrictions imposed on the degrees of orientational freedom of the dipoles, *i.e.*, on the quantum number n. For unrestricted orientation $n = \infty$ and the equation becomes the original Langevin function, Eq. (556) or (556a), with $p = \frac{1}{3}$. If the orientation is restricted to parallel and antiparallel positions with respect to a single direction, $n = \frac{1}{2}$ and

It was shown in Eq. (168) that

$$F = E + \gamma P \tag{531}$$

By means of this equation, (530a) could be converted into a theoretical expression for polarization in terms of applied field E, which would include both the non-linearity and the dependence on temperature. Although a step in this direction was taken by Busch, still the various parameters and the dependence of N and P_0 on temperature are so little known that such an expression could not be put to experimental test.

485. Mueller's Internal-field Theory. This theory, an elaboration of that of Debye and Kurchatov, assumes the existence of a field F, related to P by an empirical equation of the same form as (530a),

$$P = \alpha_M F - \beta F^3 \tag{532}$$

where α_M is the *polarizability per unit volume* in small fields (to avoid confusion with the *molecular* polarizability, we write α_M in place of Mueller's α). α_M includes the effects of dipoles, as well as that due to piezoelectric deformation; the theory is phenomenological to the extent that the constituents of α_M do not appear in the equations.

Both α_M and β are dependent on temperature.* The kernel of Mueller's theory is the assumption that α_M may be expressed by

$$\alpha_M = \frac{\theta(T)}{\gamma T} \tag{533}$$

where γ is the internal field constant of Eq. (531), T the absolute temperature, and $\theta(T)$ is a function which Mueller calls the "Curie temperature." Although $\theta(T)$ is of the nature of a temperature, equal to θ_u or θ_l at the Curie points, still it might more properly be called the *Mueller function*, in order to avoid confusion with the Curie *point*, which is often referred to as the Curie temperature. At present there is no convincing theoretical expression for $\theta(T)$ that can be put to quantitative test.†

$p = 1$. Since the dielectric anomalies in Rochelle salt have to do with the X-direction alone, one might be led to set $p = 1$ in Eq. (530a). The objection to this form of the function is that it requires absolute quantization with respect to one direction, an assumption for which there is no theoretical justification in solid dielectrics. Yet it may well be that $p = 1$ comes closer to the truth than $p = \frac{1}{3}$. Too little is known of the numerical values of N, μ, F, and γ to decide this question. For the present we must remain content with the assumption that for not too large values of the field the relation between μ and α, and correspondingly the relation between polarization and field, can be represented by a cubic equation like (530a) in which the constants have to be determined empirically.

* Mueller shows that the saturation coefficient B of his later papers is identical with $\beta\gamma^4$.

† Busch[88] derived a theoretical relation between $\theta(T)$ and T, but it contains parameters whose numerical values are still unknown.

Since in Rochelle salt the anomalies are present only with fields in the X-direction, we are concerned with the value of γ in this direction only. Rochelle salt may be expected to be anisotropic with respect to γ, which presumably has different values parallel to the three axes.

Unlike Mueller, Busch, whose work is based largely on Mueller's internal-field theory, makes explicit use of the Langevin function. It will perhaps aid both in interpreting the theory and in emphasizing the ferromagnetic analogy if we follow here the method outlined in §550 for ferromagnetism. If P and F in Eq. (532) are plotted as ordinate and abscissa, respectively, a curve similar to that in Fig. 165 results. That which corresponds to the "Weiss lines" is obtained by writing Eq. (531) in the form

$$P = \frac{F}{\gamma} - \frac{E}{\gamma} \tag{534}$$

At higher temperatures, down to a few degrees above the upper Curie point, we have the purely parelectric region. In this region, as has been suggested by Scherrer,[451] the dipole system behaves like a dipolar gas embedded in a polarizable matrix.

The upper Curie point θ_u is the temperature at which, with small fields, the slope of the Weiss line is the same as that of the curve:

$$\frac{\partial P}{\partial F} = \alpha_M = \frac{1}{\gamma} = \frac{\theta(T)}{\gamma\theta_u}$$

Since $\theta(T) = \theta_u$ at the Curie point, it follows that at this critical temperature $\alpha_M = 1/\gamma$. As the temperature falls below θ_u, the slope of the Weiss line diminishes, thus accounting for the spontaneous polarization, as illustrated, for the magnetic case, by the point P' in Fig. 165.

In order to account for the lower Curie point θ_l, Busch elaborates upon Kurchatov's theory of the variability of the number of free dipoles with temperature and deduces a different Langevin curve for each temperature. θ_l is then the temperature at which the Weiss line again becomes tangential to the curve at the origin. Mueller, who does not make explicit use of the number of free dipoles, simply assumes $\gamma\alpha_M = 1$ at each Curie point.*

The significance of the quantity $\gamma\alpha_M$ is shown by writing, from Eqs. (531) and (532),

$$E = (1 - \gamma\alpha_M)F + \gamma\beta F^3 \tag{535}$$

* Debye (ref. B15, p. 89) predicts large values of the dielectric constant of polar liquids when the quantity $(4\pi/3)N(\alpha_{ea} + \alpha_d)$ approaches unity. Since $4\pi/3$ corresponds to γ and $N(\alpha_{ea} + \alpha_d)$ to α_M, it is evident that Mueller's assumption that $\gamma\alpha_M = 1$ at the Curie points is the analogue for Rochelle salt to Debye's condition for liquids. Mueller's piezoelectric constituent of α_M supplies the amount needed to make $\gamma\alpha_M = 1$, thus yielding an infinite dielectric constant at certain temperatures.

Outside the Curie points, $\gamma\alpha_M < 1$, F vanishes when $E = 0$, and Rochelle salt behaves like an ordinary dielectric. In the region where $\gamma\alpha_M > 1$, the inner field has two real values, differing from zero, thus accounting for the spontaneous polarization. The Seignette-electric region is that in which α_M is slightly greater than $1/\gamma$. According to this theory, a small and gradual change in α_M with temperature is responsible for the anomalies, just as in the later interaction theory (§468) the anomalies are attributed to a small and gradual change in the clamped susceptibility

The cubic equation (535) corresponds to Eq. (496): $E = \chi' P + BP^3$. For $P \approx \alpha_M F$ from Eq. (532), $\eta' = 1/\chi' = \alpha_M/(1 - \gamma\alpha_M)$ from Eq. (536) below, while, as has been stated, $B = \beta\gamma^4$.

Obviously, the numerical value of α_M depends on that of γ (Mueller's f). As we have seen in §113, in all crystals one would expect γ to be of the same order of magnitude as the theoretical Lorentz factor $4\pi/3$ At present, a theoretical calculation of γ for Rochelle salt is impossible; moreover, as Busch points out, γ may be expected to have different values for the lattice and the dipoles. Without making this distinction, Mueller derives γ empirically from Eq. (536), as will be seen. The point to emphasize here is that it is not necessary, as in ferromagnetism (§549), to postulate a very great value of γ in order to account for the large internal field in the Seignette-electrics. Moreover, since the X-ray observations of Warren and Krutter[579] indicate no change in the lattice structure of Rochelle salt over the entire temperature range, it can safely be assumed that γ is not appreciably affected by temperature.

486. The Curie-Weiss law for Rochelle salt outside the Curie points is derived from Eqs. (531) to (533). We thus find, for the free crystal in small fields, where the second term in Eq. (532) can be omitted,

$$\eta' = \frac{P}{E} = \frac{\alpha_M}{1 - \gamma\alpha_M} = \frac{\theta(T)}{\gamma[T - \theta(T)]} \tag{536}$$

This equation is a special form of the general relation between dielectric susceptibility and polarizability given in Eq. (173).* $\theta(T)$ signifies the "Curie temperature," which in §434 is denoted by t_c. The quantity $\theta(T)/\gamma$ is the theoretical equivalent of the experimental C in Eqs. (490) and (524). For a few degrees above the upper Curie point θ_u, $\theta(T) = \theta_u$. Equation (536) then becomes (written in reciprocal form for comparison with the earlier equations)

$$\chi' = \frac{1}{\eta'} = \frac{\gamma(T - \theta_u)}{\theta_u} \tag{537}$$

* When Eq. (536) is written $-1/\eta' = -\chi' = \gamma - 1/\alpha_M$, it is analogous to Eq. (497): $-\chi' = a_{14}b_{14} - \chi_1$. Mueller[580] calls $a_{14}b_{14}$ (in his notation f_{14}^2/c_{44}) the "apparent Lorentz factor." χ_1 is analogous to $1/\alpha_M$. Numerical equality is not to be expected, since γ is the factor for the *internal* field.

At higher temperatures $\theta(T)$ assumes values differing somewhat from θ_u, as is indicated in the discussion of Eq. (490).

By analogy with ferromagnetic theory one may say that the experimental confirmation of the Curie-Weiss law expressed by Eq. (537) by Mueller and by Hablützel (§465) indicates that, if the effect is due to dipoles, the latter must be nearly all free at temperatures outside the Curie points.

Since Mueller found experimentally that for all temperatures above 34°C the relation between $1/\eta'$ and T was very exactly linear, he was able to derive from Eq. (536) a value for the internal field constant γ, namely $\gamma = 2.19$.

It should be observed that the internal-field theory, together with the basic assumption expressed in Eq. (533), provides a theoretical basis for the Curie-Weiss law in Eq. (536). In this respect the internal-field theory is more potent than the interaction theory, which provides no theoretical relation between susceptibility and temperature, simply accepting the Curie-Weiss law as an experimental fact (see §465).

In the Seignette-electric region, also, the internal-field theory predicts a Curie-Weiss law that agrees with observation. For small fields and for temperatures distant by not over a few degrees from the Curie points, one finds by the same process that is used in §552 for deriving Eq. (566) that the initial susceptibility is given by

$$\chi_s' = \frac{1}{\eta_s'} = \frac{2\gamma(\theta_u - T)}{3T - 2\theta_u} \tag{538}$$

From this expression it follows that the susceptibility between the Curie points is given theoretically by

$$\eta_s' = \frac{T}{2\gamma(\theta_u - T)} - \frac{1}{\gamma} \tag{538a}$$

an equation that is in approximate agreement with experiment.

Comparison of Eq. (538a) with (537) shows that the initial susceptibility varies about twice as rapidly with temperature below the upper Curie point as above it, as has already been pointed out in §465; for the ferromagnetic case see Fig. 166. In Eqs. (529) and (529a) we have seen that the same relation holds for the piezoelectric constant.

The infinite value of the susceptibility of the free crystal at the Curie points follows from Eq. (536) or (538) on setting $\gamma\alpha_M = 1$.

487. Theoretical expressions for the spontaneous internal field F^0 and the spontaneous polarization P^0 are found by setting $E = 0$ in Eqs. (535) and (531):

$$F^{0s} = \frac{\gamma\alpha_M - 1}{\gamma\beta} = \frac{\theta(T) - T}{\gamma\beta T} \tag{539}$$

$$P^{0s} = \frac{F^{0s}}{\gamma^2} = \frac{\gamma\alpha_M - 1}{\beta\gamma^3} = \frac{\theta(T) - T}{\beta\gamma^3 T} \tag{539a}$$

Mueller's original paper[376] must be consulted for the ingenious manner in which he combined the results of both dielectric and electro-optic measurements at different temperatures and different field strengths, in order to derive the values of the various unknown quantities. It must suffice here to say that, in addition to the data already mentioned, an estimate was made of the value of β (2.5×10^{-9}), whence, from Eqs. (539) and (539a), F^0 and P^0 could be calculated for any temperature. For example, at 0°C, $F^0 \sim 2{,}600$ esu = 770,000 volts/cm, and $P^0 \sim 1{,}200$ esu. This latter value agrees as well as can be expected with the values of P^0 from pyroelectric and oscillographic data.

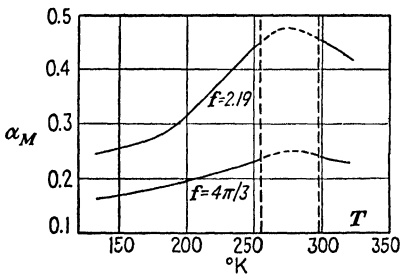


FIG. 149.—Polarizability α_M per unit volume as function of temperature, from Mueller's data.

From Mueller's observations we have plotted values of α_M as a function of T, both for $\gamma = 2.19$ and $\gamma = 4\pi/3$; the result is shown in Fig. 149.

In general, it may be said that Mueller's internal-field theory is in good quantitative agreement with experiment in the parelectric regions and in qualitative agreement in the Seignette-electric region. It was only by making explicit use of the piezoelectric effects in his interaction theory that Mueller was able to obtain quantitative agreement between theory and observation over the entire temperature range. A unification of the two theories remains as a problem for the future.

488. While the internal-field theory as outlined above deals explicitly only with dielectric properties, still it can be used to describe the elastic and piezoelectric properties also. For this purpose one may employ the method indicated in §189 for treating the problem in terms of the internal field F, with equations analogous to those in Table XX. Corresponding to a_{14} and b_{14} of the polarization theory, or e_{14} and d_{14} of Voigt's formulation, are the internal-field piezoelectric constants, which may be called a^F_{14} and b^F_{14}. The latter are easily shown to be very nearly proportional to a_{14} and b_{14}. b^F_{14} is related to d_{14} by the equation $d_{14} = (1 + \gamma\eta')b^F_{14}$, where γ is the internal field constant.

The only application that we find of the internal-field theory to piezoelectric observations is that of Norgorden,[393] whose experiments

have been described in §424 and whose work appeared before the advent of the interaction theory. Norgorden finds b_{14}^{F} (his d_{14}) practically independent of temperature from 14 to 33°C, with a very slight increase as the field strength increases. Now from the relation given above between d_{14} and b_{14}^{F}, together with $d_{14} = \eta' b_{14}$ from Eq. (495*b*), it follows that $b_{14} = (1/\eta' + \gamma) b_{14}^{F}$. Since η' is large, it is evident that the approximate independence of b_{14}^{F} on temperature and field lends support to the conclusion already reached that b_{14} is essentially constant. Norgorden's experimental data could, of course, be discussed entirely in terms of the polarization theory, without reference to the internal field, but this seems hardly necessary.

489. Correlation between the Theories of Mueller, Kurchatov, and Fowler. In his application of Debye's theory (§445), Kurchatov assumes that the Clausius-Mosotti relation

$$\frac{k_0 - 1}{k_0 + 2} = \frac{4\pi}{3} N\alpha \tag{540}$$

can be extended to include the case in which the molecular polarizability α contains a dipole term. k_0 is the initial dielectric constant of the free crystal, and N the number of molecules per cubic centimeter. In order to express the dependence of $N\alpha$ on temperature, he writes

$$\frac{k_0 - 1}{k_0 + 2} T = \frac{4\pi}{3} N\alpha T \tag{540a}$$

In comparing this equation with Mueller's corresponding Eq. (533), we recall first that Mueller's α (which we have denoted by α_M) is the polarizability *per unit volume*. Equation (533) may be put in the form

$$\theta(T) = \gamma \alpha_M T \tag{541}$$

If for the field constant γ the value $4\pi/3$ is taken, (541) becomes identical with (540*a*), and $\alpha_M \equiv N\alpha$.

The excellent agreement between Kurchatov and Mueller in their measurements of k_0 is attested by the close similarity in their diagrams. Kurchatov plots $(k_0 - 1)T/(k_0 + 2)$ as function of T in Fig. 9 of the French edition of his book,[B32] while Mueller calculates α_M from Eq. (536), and then from Eq. (533) plots $\theta(T)$ in terms of T (Fig. 25 of his paper[376]). The latter diagram contains two curves for $\theta(T)$, corresponding to $\gamma = 4\pi/3$ and $\gamma = 2.19$.* It is the one with $\gamma = 4\pi/3$ that should be compared with Kurchatov's curve. Mueller's assumption that $\gamma\alpha_M > 1$ in the Seignette-electric region corresponds to writing $4\pi N\alpha/3 > 1$ in

* As was pointed out in §485, the numerical value of α_M (and of α) depends on the choice of γ. Values of α_M in terms of temperature are shown in Fig. 149.

Eq. (540*a*).* Although it is not stated explicitly by Kurchatov, it is implicit in his equations and diagrams that in the Seignette-electric region $4\pi N\alpha/3 > 1$.

Kurchatov does not discuss the theoretical significance of the fact that letting $4\pi N\alpha/3$ become greater than unity on the right side of Eq. (540*a*) leads to *negative* values of k_0. Mueller's interaction theory also introduces the concept of a negative dielectric constant, the relation of which to the actual dielectric constant between the Curie points is explained in §454.

From Kurchatov's data we have calculated the values of $N\alpha$ for several temperatures. When plotted in Fig. 149 they fall very nicely on Mueller's curve.

Although Fowler's treatment gives no observational data, still it is possible to ascertain whether his theory predicts a relation like Mueller's between $\theta(T)$ and T. The expression that corresponds to Mueller's $\theta(T)$ is Fowler's $T_d^0 g$,† which when plotted with T as abscissa yields a curve of the same general characteristics as Mueller's.

The chief limitation in the theories of Kurchatov and of Fowler lies in their neglect of the piezoelectric contribution to the dielectric constant. By taking this effect into account, together with the non-linear effects in large fields, Mueller was able, as we have seen, to trace the dielectric anomalies of Rochelle salt back to their origin in the clamped crystal.

490. Calculation of the Moment of Rochelle-salt Dipoles. Much of the theoretical work on Rochelle salt has centered in the hypothesis of rotatable dipoles, which are most commonly considered to be the molecules of the water of crystallization. It seems desirable, therefore, to show how the dipole moment can be estimated, even though, as will be seen in §542, it is likely that the dielectric peculiarities are due to hydrogen bonds rather than to rotating dipoles.

In estimating the dipole moment, only the formulas for weak fields need be used. We begin with Mueller's Eq. (533), in which α_M is the polarizability *per unit volume*. α_M may be expressed in terms of Eq. (177), with the assumption that N_1 and N_2 are the number of lattice elements and permanent dipoles, respectively, per unit volume:

$$\frac{\theta(T)}{T} = \gamma\alpha_M = N_1\gamma\alpha_{ae} - N_2\gamma\frac{p\mu^2}{KT} \tag{542}$$

Appropriate values for the molecular field coefficient γ and the coefficient

* The identity of Kurchatov's Eq. (540*a*) with Mueller's formulation is quickly shown by setting $\gamma = 4\pi/3$ and $k_0 = 1 + 4\pi\eta'$ in Eq. (536).

† Ref. B18, p. 818.

p of the generalized Langevin function (§114) will be introduced later. For the present purpose it is not necessary to discriminate between the different values that should, in view of §485, be assigned to γ in the two terms of Eq. (542).

If we agree with Kurchatov and others in regarding the dipole moments as residing in the H_2O molecules, there may be four such separate moments for each Rochelle-salt molecule. But if the Rochelle-salt molecule is a single dipole, the number N_2 will, at least at sufficiently high temperatures, be the same as the number of molecules per cubic centimeter, $3.8(10^{21})$. N_2 will then be either $3.8(10^{21})$ or $15(10^{21})$ according to whether n, the number of dipoles associated with the molecules, is 1 or 4.

At either Curie point Eq. (542) becomes equal to unity. It is necessary in calculating μ to use the *upper* temperature $\theta = 296.7°$ abs, since only then are we justified in assigning to N_2 the values given above.

A further step that must be taken before μ can be found is to determine the magnitude of the first term in Eq. (542). This can be done by means of Kurchatov's data[B32] on the susceptibilities of crystals grown from a mixture of Rochelle salt with its isomorphic relative sodium–ammonium tartrate (§491). This latter is not of itself Seignette-electric. In the mixed crystals Kurchatov found that, if the Rochelle-salt component did not amount to more that 41 per cent of the whole, the quantity $(k_0 - 1)/(k_0 + 2)$ in Eq. (540a) was independent of temperature, indicating that only the lattice polarization, represented by the first term in Eq. (542), is then effective. From the experimental data, and on the assumption that the lattice polarizability is the same for all isomorphic mixtures, including pure Rochelle salt itself, it is found that $N_1\gamma\alpha_{ae} \approx 0.6$ at the upper Curie point. This value is deduced directly from the susceptibility [for example by means of Eq. (536)] and does not require any knowledge of N_1, γ, or α_{ae} separately.

Recalling that, by §485, $\gamma\alpha_M = 1$ at the Curie point θ_u, and setting $T = \theta_u$ in Eq. (542), one finds $N_2\gamma p\mu^2/K\theta_u = 1 - 0.6 = 0.4$, whence

$$\mu^2 = \frac{0.4K\theta_u}{N_2\gamma p} \tag{543}$$

In Table XXXV are given values of μ calculated from Eq. (543) for $n = 1$ or 4 dipoles per Rochelle salt molecule, for $\gamma = 4\pi/3$ or 2.19 (Mueller's value), and for $p = \frac{1}{3}$ or 1 (§484). In order to show what the dipole moment would be if the polarizability were due to the dipoles alone, the column designated as $\mu' = \mu/\sqrt{0.4}$ has been added, obtained by omitting the factor 0.4 in Eq. (543).

All the values of μ below are of the order of magnitude commonly accepted for polar molecules. All things considered, for Rochelle salt the value printed in boldface type is perhaps the most acceptable.

TABLE XXXV.—CALCULATED VALUES OF DIPOLE MOMENTS
(In esu)

γ	p	n	μ^2	μ	μ'	$\frac{\mu}{\bar{\mu}}$
			$\times 10^{-36}$	$\times 10^{-18}$	$\times 10^{-18}$	
$\frac{4\pi}{3}$	$\frac{1}{3}$	1	2.98	1.73	2.74	9
		4	0.75	0.86	1.37	17
	1	1	0.99	1.00	1.58	5
		4	0.25	0.50	0.79	10
2.19	$\frac{1}{3}$	1	5.69	2.38	3.78	12
		4	1.43	1.20	1.89	25
	1	1	1.89	1.38	2.18	7
		4	0.47	**0.69**	1.09	14

Still another estimate of μ can be made by making use of Mueller's value of $\beta = 2.5(10^{-9})$ [see §487 and Eq. (532)]. We assume that (532) can be represented by a Langevin function of the type given in Eq. (176). When the latter equation is solved for P and compared with (532), it is found that at the Curie point $\alpha_M = Np\mu^2/KT$, $\beta = Nq\mu^4/K^3T^3$, whence $\mu^2 = \beta pK^2\theta_u^2/q\alpha_M$. The value of μ depends on the choice of p and q. If the original Langevin function given by Eq. (175) is accepted, $q/p = \frac{1}{15}$. Or, using Eq. (176), $q/p = \frac{1}{3}$ (see §§552, 484). With $\beta = 2.5(10^{-9})$, $\alpha_M = 0.257$, $K = 1.37(10^{-16})$, there results $\mu = 12(10^{-18})$ or $5.2(10^{-18})$, respectively. These values indicate at least the right order of magnitude, with the odds in favor of the second formula.

From the observed spontaneous polarization an estimate can be made of $\bar{\mu} = P/N_2$, the average component of dipole moment in the direction of the field (§548). This quantity is a function of both field and temperature, but only the value at 0°C and $E = 0$ need be considered. P is then the spontaneous polarization P^0 at 0°C, at which temperature it has its greatest experimental value of 740 esu. Using the values of N_2 given above, one finds $\bar{\mu} = 0.20(10^{-18})$ or $0.049(10^{-18})$ according to whether the number of dipoles per molecule is 1 or 4. Values about twice as large as this are obtained if for P^0 one uses the theoretical value derived from Eq. (539*a*).

In any case, it appears that the maximum spontaneous polarization

is but a small fraction, $P^0/P_{max} = \bar{\mu}/\mu$, of the absolute maximum

$$P_{max} = N_2\mu$$

which would be present if all the dipoles lay in the same direction parallel to the field. The reciprocal of this fraction is given in the last column of Table XXXV. It follows that on the Langevin diagram (Fig. 165) the operating point is never far from the origin, so that even with the strongest electric fields that Rochelle salt can withstand the first two terms in the development of the Langevin function should suffice. This is in marked contrast to the spontaneous polarization in iron, which, as stated in §553, has at room temperature a value not very far below the theoretical maximum at 0° abs. The reason for this difference between Rochelle salt and iron is that Rochelle salt has a *lower Curie point* that lies near enough to the upper Curie point so that there is no temperature in the region of spontaneous polarization at which we are not fairly close to one or other of these points.

CHAPTER XXVII

OTHER SEIGNETTE-ELECTRIC CRYSTALS

Ich werde dies Projekt niemals vollendet sehen, aber die Nachwelt kann es erleben, wenn sie den Plan weiter verfolgt und sich der geeigneten Mittel für die Ausfuhrung bedient.
—FREDERICK THE GREAT.

Except Rochelle salt, the only substances known at present that have dielectric properties analogous to ferromagnetism are certain mixed crystals isomorphic with Rochelle salt, and a few tetragonal phosphates and arsenates. These two groups of crystals will now be considered.

491. Crystals Isomorphic with Rochelle Salt, and Mixed Tartrates. The substances thus far investigated are those in which the K of Rochelle salt is replaced by NH_4, Rb, or Tl. The crystals have molecular radii and axial ratios sufficiently alike so that mixed crystals can be grown in any proportion.

Pure crystals of $NH_4NaC_4H_4O_6{\cdot}4H_2O$, $RbNaC_4H_4O_6{\cdot}4H_2O$, or $TlNaC_4H_4O_6{\cdot}4H_2O$ have quite normal dielectric behavior. From the point of view of the ferromagnetic analogy they are, down to the lowest temperatures investigated, parelectric rather than Seignette-electric. If they have Curie points, they must come at extremely low temperatures. For example, the dielectric constant k_x of the ammonium salt is about 10[B32] and independent of temperature. As we have seen in §144, the piezoelectric constants of this crystal, though large, show no anomalies at least down to $-17°C$, and from the constancy in k_x down to very low temperatures one can feel fairly confident that a like constancy obtains with the piezoelectric coefficients.

Peculiar effects are observed with crystals that have been grown from solutions containing mixtures with the KNa salt of any one of the three isomorphic salts named above. The first papers on the subject were those of B. Kurchatov and M. Eremeev[133,292] in 1932. The present account is based on their work, together with the following: B. and I. Kurchatov,[293] Bloomenthal,[55] Evans,[140] and especially the book by I. Kurchatov.[B32] Investigations have been chiefly with Rochelle salt containing the NH_4Na admixture, as described below. Results with the rubidium and thallium salts, as far as they go, are at least qualitatively similar.

Some of the principal results with crystals containing various proportions of $NH_4NaC_4H_4O_6{\cdot}4H_2O$ are shown in Fig. 150, from ref. B32.

Since the field strength is not given, the values of the dielectric constant must be regarded as only of relative significance. The addition to the pure Rochelle salt of only 1 per cent of the NH_4 salt (molar ratio) reduces the temperature range of the Seignette-electric region by about one-half. An addition of 3 per cent (curve marked 97 per cent) completely eliminates the Seignette-electric properties, leaving only a maximum in the curve. Further increase in NH_4 makes this maximum lower and flatter, rising again slightly at 83 per cent of Rochelle salt.

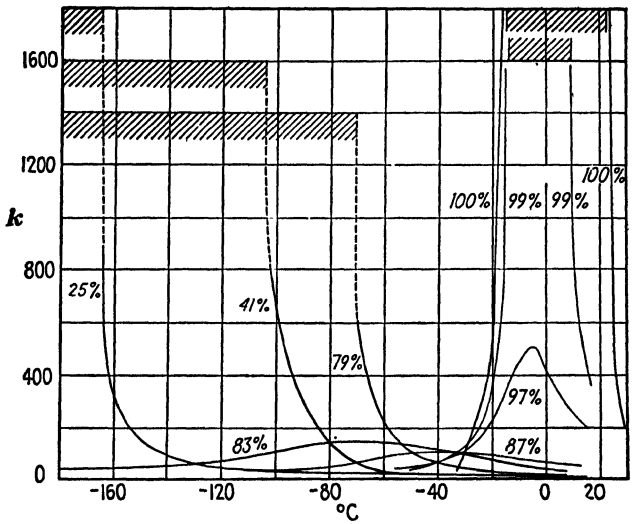


FIG. 150.—Dielectric constant of mixed crystals of potassium and ammonium Rochelle salt, from I. Kurchatov. The percentages indicate the relative numbers of molecules of the potassium salt in the mixture.

Further reduction in the Rochelle-salt content to 79 per cent ushers in a second Seignette-electric region at low temperature, which persists down to 25 per cent. Kurchatov's explanation of this curious behavior may be somewhat freely summarized as follows: It is assumed that the rotatable dipoles are chiefly those of the Rochelle salt. Small admixtures of the NH_4Na salt raise the lower Curie point only slightly, but larger admixtures loosen the forces that bind the dipoles in the local groups that characterize the lower Curie point, releasing a number of dipoles sufficient to allow the product $4\pi N\alpha/3$ to become greater than unity. One may also predict that the large values of the dielectric constant in this region are attended by correspondingly large values of d_{14}.*

* Bloomenthal in his theoretical treatment of mixed crystals takes account of the piezoelectric effect on the susceptibility by an equation like (516) and (516a), but his experimental data are insufficient to help in the present case.

In a more general manner it may be suggested that for a certain range of percentages of the NH_4Na salt there are certain temperatures at which the settling of the system into a state of minimum energy (§473) is attended by a change in crystal structure to a configuration of lower symmetry, with a spontaneous polarization, as the temperature falls below a critical value.

Further Measurements of the Dielectric Constant in the X-direction. Evans[140] measured the dielectric constant for various molecular percentages of the ammonium salt mixed with Rochelle salt, at temperatures between 16 and 17°C and frequencies chiefly from 400 to 2,000 kc/sec. At these frequencies there was no disturbance from resonant vibrations. The maximum voltage was 45, but the maximum field strength, crystal dimensions, and range of variation of field strength are not stated. The results were as follows:

Molecular percentage of ammonium salt	0	10	20	30	40	50	100
Dielectric constant	114	25.0	15.8	13.0	11.8	9.9	8.2

From Evans's remarks concerning the precision of his observations it is apparent that the uncertainty in his data may amount to at least 10 per cent. The value 114 for pure Rochelle salt has already been recorded in Table XXXIV. The small magnitude of the dielectric constant from Evans's observations, in comparison with the values shown in Fig. 150, is of course due to the high frequency.

The temperature at which Evans obtained his data lay in the Seignette-electric range for the pure Rochelle salt, but with this exception the ammonium content was such that the material was parelectric. The only correlation that can be made between the work of Evans and that of the Russian investigators is in the value of k_x for the pure ammonium salt: here Evans's value of 8.2 at high frequency agrees well enough with Kurchatov's l-f value of 10 mentioned above.

In the Russian edition of his book,[B32] Kurchatov gives some values of the dielectric constant of mixed KNa and TlNa salts, for various molecular percentages, measured at 500 volts/cm. At 0°C the results were as follows:

Percentage Tl	0	0.25	0.5	1	2.5
Dielectric constant	10,000	2,300	1,200	600	120

The results at −10°C and +10°C are not essentially different.

Dielectric hysteresis in the NH_4Na + KNa mixture has been investigated by Eremeev and B. Kurchatov.[133,*] As with Rochelle salt, there

* See also ref. B32.

is no hysteresis, fatigue, or lag above the Curie point, and the $P:E$ relation becomes linear at a temperature not far above this point.

In the low-temperature Seignette-electric regions the width of the hysteresis loop and the magnitude of the coercive field E_c increase as the temperature diminishes below the Curie point, and many seconds may be required for the attainment of equilibrium. That there is no evidence of a lower Curie point is shown by the fact that the saturation polarization ("knee" of the polarization curve) increases with decreasing temperature down to the lowest recorded temperature, −190°C, while at the same time the field strength necessary for saturation increases also. For example, in a crystal containing 45 molecular per cent of KNa salt, the saturation field was 10,000 volts/cm (for Rochelle salt it is less than 200!), while the saturation polarization was 3,000 esu, several times greater than in pure Rochelle salt.

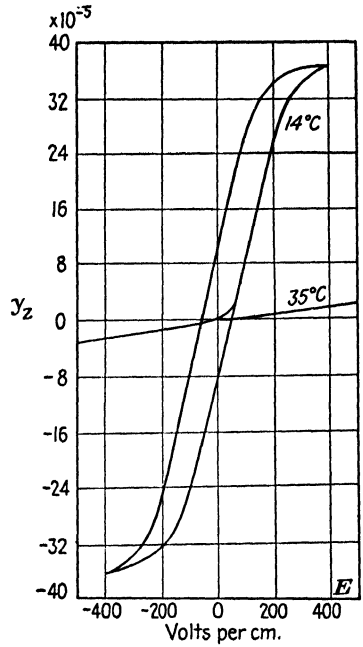


FIG. 151.—Converse effect in Rochelle salt containing 0.37 per cent of TlNa tartrate, at temperatures below and above the Curie point, from Bloomenthal. The strain y_z is calculated from the observed change in length of a 45° X-cut bar.

Kurchatov used the vanishing of E_c to determine the Curie point, obtaining a value in agreement with that from the Curie-Weiss law. At any temperature in this region there is an initial value of k_x such that over a certain range of field strengths there is no hysteresis; this range is greater the lower the temperature and the higher the percentage of the ammonium salt. Hysteresis is observed as soon as the peak value of the field exceeds this critical value (point B in Fig. 148), the critical field being greater as the content of NH_4Na is increased.

492. *Piezoelectric Properties.* Not even qualitative tests seem to have been made of the piezoelectric properties of the pure RbNa and TlNa tartrates. Mandell's measurements on the NH_4Na tartrate have been mentioned above. As for mixed crystals, Eremeev and Kurchatov[133] obtained a piezoelectric hysteresis loop below the Curie point by the *direct effect*, by applying to a 45° X-cut crystal containing 26.7 molecules of the NH_4Na tartrate to 100 molecules of the KNa tartrate

a succession of stresses up to 18 kg/cm², decreasing again to zero. Above the Curie point the polarization:stress relation was linear, with no hysteresis, obeying a Curie-Weiss law.

The *converse effect* in mixed crystals has been investigated by Bloomenthal,[55] by the method described in §422, at temperatures from 10 to 35°C. The plates were 45° X-cut, of the order of 30 by 8 by 1 mm, coated with thin tin foil. The hysteresis loop obtained at 14°C with a crystal containing 0.37 per cent of the TlNa tartrate is shown in Fig. 151. The form of the loop is very similar to that for pure Rochelle salt at 18.5° in Fig. 114, and at the same field strengths the strains are nearly

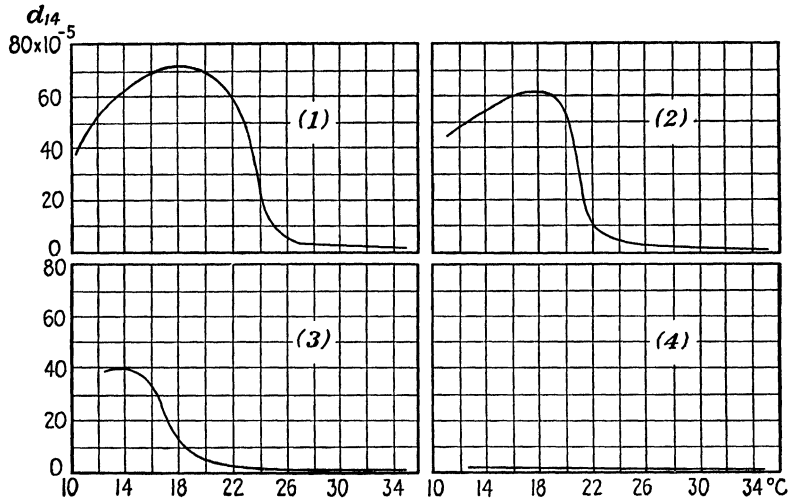


FIG. 152.—d_{14} for Rochelle salt and isomorphic mixtures, by the converse effect, from Bloomenthal. Curve (1) pure Rochelle salt; (2) Rochelle salt with 0.37 per cent $C_4H_4O_6TlNa \cdot 4H_2O$; (3) with 1.0 per cent $C_4H_4O_6NH_4Na \cdot 4H_2O$; (4) with 3.7 per cent $C_4H_4O_6TlNa \cdot 4H_2O$.

as large. The curve for 35°C, in the parelectric region, shows practically a linear relation between y_z and E, with no hysteresis.

Bloomenthal secured similar data at other temperatures, for pure Rochelle salt and for the mixtures shown in Fig. 152. In this figure $d_{14} = dy_z/dE$, which is the same as y_z/E at those temperatures where the relation is linear. In the non-linear Seignette-electric region

$$d_{14} = \frac{dy_z}{dE} = \text{slope of the straight portion of the loop}$$

The figure makes evident the decrease in d_{14} of Rochelle salt on adding a small amount of the TlNa salt, as well as the lowering of the upper Curie point with increasing amounts of TlNa salt. The thallium salt

does not appear to have as profound an effect as the ammonium salt. For example, 1 per cent of TlNa tartrate reduces the upper Curie point to about 21°C, while from Fig. 150 it is seen that the same percentage of the NH_4Na tartrate reduces it to 10°C.

493. Seignette-electric Properties of Phosphates and Arsenates. Hitherto we have considered the dielectric analogy to ferromagnetism in the case of Rochelle salt and crystals isomorphic with it.

Attention will now be given to another group of crystals that have been found to possess similar properties. They are the primary phosphates and arsenates of potassium and ammonium, isomorphic members of the tetragonal sphenoidal Class 11, symmetry V_d. The piezoelectric constants are the same as for Rochelle salt, *viz.*, d_{14}, d_{25}, and d_{36}, only now $d_{14} = d_{25}$. The unique axis, parallel to the field direction for which the Seignette-electric anomalies exist, is the crystallographic *c*- (or *Z*-) axis: thus the anomalous piezoelectric constant is d_{36}, and the anomalous susceptibility is η_z. Quantitative data on the piezoelectric properties of KH_2PO_4 are given in §146. Qualitatively, piezoelectric properties were detected in $NH_4H_2PO_4$ by Giebe and Scheibe,[164] and in KH_2PO_4, KH_2AsO_4, and $NH_4H_2AsO_4$ by Elings and Terpstra (see footnote, page 232). In all cases measurements over wide ranges of stress and temperature are greatly to be desired.

Quantitative observations have been published on the dielectric constants and specific heats k_x and k_z of all four salts, the spontaneous polarization P_z^0 and the spontaneous Kerr effect in the potassium salts, and some of the elastic properties of KH_2PO_4. Dielectric observations have been made both above and below the Curie points of the potassium salts, but with the ammonium salts only observations above the upper Curie point were possible. In all cases the anomalies occur at liquid-air temperatures.

TABLE XXXVI

Property	KH_2PO_4	KD_2PO_4	KH_2AsO_4	$NH_4H_2PO_4$	$NH_4H_2AsO_4$
Molecular weight.....	136.13	138.14	180.02	115.08	158.97
Density.....	2.34	2.34	2.87	1.803	2.311
Melting point, °C.....	252.6	—	288	~190*	~300*
Axial ratio c/a.....	0.938	0.973	0.938	1.008	1.004
Curie point, °K.....	122.0	213	95.6	147.9	216.1
Max. P°, esu cm^{-2}.....	14,100	14,500	15,000	—	—

* Decomposes with evolution of ammonia and water.

Studies in this field began with a paper on "a new Seignette-electric substance" (KH_2PO_4)* by Busch and Scherrer in 1935.[90] This paper

* It is of historical interest that isomorphism in crystals was first discovered by Mitscherlich in 1819 between the phosphate and arsenate of potassium.

was followed in 1938 by Busch's more complete investigation[88] and in the succeeding years by a series of papers by Busch and his colleagues at Zurich, to which reference will be made below.* Busch's theoretical treatment has been considered in §485. The data summarized in

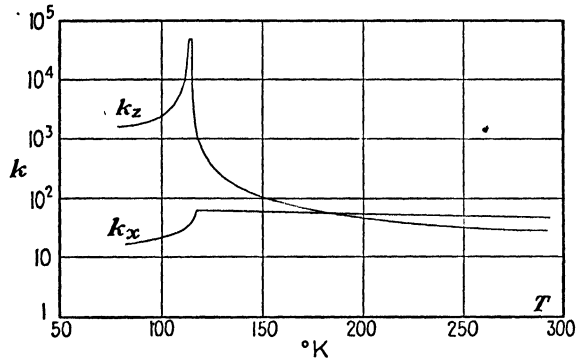


FIG. 153.—Dielectric constants k_z and k_x of KH_2PO_4, from Busch. E = 200 volts/cm, frequency 800 cycles.

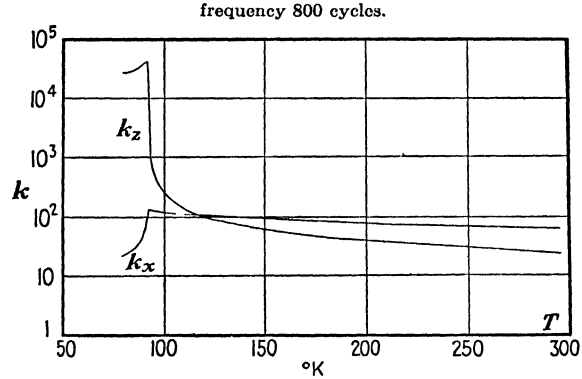


FIG.154.—Dielectric constants k_z nd k_x of KH_2AsO_4, from Busch. E = 200 volts/cm, frequency 800 cycles.

Table XXXVI are assembled from these papers and from the "Handbook of Chemistry and Physics."

The method of growing these crystals is described by Busch[88] and by Bantle.[22]

494. The results of Busch's measurements of the dielectric constants k_x and k_z for the potassium salts are shown in Figs 153 and 154. A capacity bridge was used. The maxima in k_z at the Curie points are the distinguishing feature of Seignette-electrics. The maxima in k_x are unexpected: in Rochelle salt, k_y and k_z have normal values with no anomaly in the neighborhood of the Curie point. Busch's explanation

* In Busch's first paper is the erroneous statement that $d_{25} = d_{36}$.

is that the number of free dipoles increases rapidly as the Curie point is approached from the low-temperature side.*

Busch finds that the potassium salts, like Rochelle salt, obey a Curie-Weiss law.

In a later paper[89] Busch and Ganz discuss the theory and measurement of the complex dielectric constants of KH_2PO_4 and KH_2AsO_4 parallel to Z, which they call ϵ_c^*. The measurements, made with a 50-cycle capacity bridge, differ from the curves in Figs. 153 and 154 in that ϵ_c^*, which is practically the same as k_x outside the Curie points where the losses are negligible, remains at a high level over a wide range of temperature below θ_u. The value for KH_2PO_4 is not far from $3(10^4)$ from the upper Curie point down to about 80°K, where it begins to fall rapidly to a value around 40 at 50°K, with still further decrease at lower temperatures. The curve for KH_2AsO_4 has a similar course, the largest value† being $1.95(10^4)$.

As a measure of the spontaneous polarization P_x^0, Busch took the saturation value at the peak of the hysteresis loop, instead of the more commonly adopted remanent value. In the case of KH_2PO_4 the difference is small except close to the Curie point;‡ but with KH_2AsO_4, which has a much narrower loop, the remanent value is a small fraction of the peak value. If the remanent value were used, P_x^0 for KH_2AsO_4 would be considerably smaller than for KH_2PO_4. In any event, the spontaneous polarization in these salts is far greater than in Rochelle salt, the ratio, from Table XXXVI, being of the order of 20:1 in the case of KH_2PO_4.

The dielectric constants of the *ammonium salts* were measured by Busch.[88] Observations could be made only down to −53°C with the arsenate and −118°C with the phosphate. At these temperatures the crystals became converted to an inhomogeneous microcrystalline mass. Busch records the following dependence on temperature:

* From Prof. Hans Mueller the author learns that he finds a sufficient explanation of the large value of k_x at the Curie point in the large internal field, without any hypothesis concerning dipoles. The absence of such an effect to a perceptible extent in k_y and k_z for Rochelle salt is attributable to the fact that in Rochelle salt the internal field is very much smaller than in the phosphates.

† It will be noted that the largest values of ϵ_c^* for both salts are much lower than the peak values shown in Figs. 153 and 154. The reason is doubtless that Busch and Ganz used a much higher voltage (2,400 volts/cm for KH_2PO_4, 3,300 volts/cm for KH_2AsO_4) than did Busch in his earlier measurements. At high voltages the polarization is brought nearer to the saturation value. Moreover, considerations mentioned in §480 make it evident that the observed persistence of a relatively large dielectric constant over a wide range of temperature below θ_u is what one would expect when the applied voltage is large.

‡ The value of P^0 for KH_2PO_4 in Table XXXVI is taken from a later paper by Arx and Bantle.[10]

(1) $NH_4H_2PO_4$—k_x increases from 55 at room temperature to 90 at $-118°C$; k_z increases from 14.5 at room temperature to 20 at $-118°C$.

(2) $NH_4H_2AsO_4$–k_x increases from 126 at room temperature to 145 at $-53°$; $k_z = 12$ from $+27°$ to $-53°C$.

495. *Spontaneous Polarization P^0, Coercive Field E_c, and Lower Curie Point θ_l.* It will be recalled that with Rochelle salt P^0 and E_c vanish outside the Curie points, rising to maxima at about 5°C, and that the free dielectric constant rises to a sharp maximum at θ_l just as at θ_u. The Seignette-electric phosphates and arsenates have critical temperatures with the same properties as at the *upper* Curie point in Rochelle salt. Insofar as they can be said to have a lower Curie point at all, this point differs in important particulars from that in Rochelle salt.

The evidence is based mostly on observations on KH_2PO_4. With this crystal, P^0 rises very rapidly from its zero value at θ_u to a value of the order of 14000 esu, without appreciable diminution down to 95°K, the lowest temperature recorded (Arx and Bantle[10]). The dielectric constant decreases continuously as the temperature goes below θ_u, without again having a maximum anywhere. The coercive field increases enormously with decreasing temperature, approaching zero only at θ_u (Bantle, Busch, Lauterburg, and Scherrer[25]). The only thing resembling a lower Curie point is the disappearance of hysteresis, which Busch and Ganz[89] found to take place at about 58°K. With a 50 $\sim$ field having a peak value of 3,000 volts/cm they found hysteresis to be present from 58 to 123.5°K, the loops having maximum area at about 62°K.

In Rochelle salt the disappearance of hysteresis at temperatures below θ_l is associated with the *vanishing* of the coercive force at θ_l. On the other hand, in KH_2PO_4 the coercive force was still very large at the temperature at which the hysteresis ceased to be measurable in the experiments mentioned above. As long as the temperature was above this value, Arx and Bantle's peak voltage was sufficient for a hysteresis loop with appreciable area to be traced. From this temperature on downward, the coercive force was so great that their apparatus recorded only a small portion of a complete loop: what was recorded was the reversible permittivity k_r (§430). The hysteresis loop had degenerated to a straight line through the origin. If they had used a higher voltage, they would pretty certainly have observed hysteresis at temperatures below 58°K.

Evidently the disappearance of hysteresis cannot be taken as a criterion for the presence of a lower Curie point. Arx and Bantle very properly refrain from making any such claim in the discussion of their results.

All the evidence supports the view first advanced by Bantle, Busch, Lauterburg, and Scherrer, that the spontaneous polarization does not

vanish at any temperature below the "upper Curie point," but that there is nevertheless a certain (or perhaps uncertain, since the Zurich investigators seem nowhere to specify it clearly) temperature at which the elementary domains refuse to be reversed by an applied field. Herein lies the contrast with Rochelle salt. The spontaneous polarization becomes—perhaps somewhat gradually—frozen. The decrease in k_s, the increase in E_c, and the absence of a sudden anomaly either in the specific heat or in the Kerr effect* all support this view. As far as the evidence goes, the same is true also of KH_2AsO_4 and KD_2PO_4 (see below).

In terms of the interaction theory, the persistence of P^0 indicates that the susceptibility η_z'' of the clamped crystal remains greater than the product $a_{36}b_{36}$ at all temperatures below θ_u (see §453). According to the internal-field theory (§485) one would say that the product $\gamma\alpha_M$ remained greater than unity.

The temperature at which P^0 becomes "frozen" does not seem to be sharply definable in terms of any observed physical effect. To call such a temperature the "lower Curie point" seems arbitrary and misleading.†

The spontaneous polarization P^0 and coercive field E_c are not very different in KD_2PO_4 and KH_2PO_4. The spontaneous Kerr effect has been investigated by Zwicker and Scherrer,[602] whose results agree with those of Bantle, Busch, Lauterburg, and Scherrer on KH_2PO_4 and KH_2AsO_4 in that there is an anomalous change in double refraction at θ_u but not at any lower temperature.

496. *Deuterium Potassium Phosphate,* KD_2PO_4. We saw in §444 that the replacing of H by D in Rochelle salt raises the upper Curie point by about 11°C. An even greater isotopic effect is exhibited by KD_2PO_4.

The present treatment is based on the work of Bantle[22] and of Zwicker and Scherrer.[602] Bantle measured k_z with a 1,000-cycle per sec bridge, the field strength being 40 volts/cm. The upper Curie point is indicated by a sharp maximum in k_z at 213°K (−60°C). From this maximum, k_z diminishes to about 82 at 300°K and 46 at 100°K. The curve has a slight bend at 158°K, which Bantle takes as the lower Curie point. Except for the shift in the Curie point, the dielectric behavior of KD_2PO_4 runs parallel to that of KH_2PO_4. The hysteresis loops have an appreciable area only between 105 and 213°K. The value 213° for θ_u seems well

* See also Zwicker and Scherrer.[602]

† As instances of the use of this term by the Zurich investigators may be mentioned the paper by Bantle, Busch, Lauterburg, and Scherrer, in which 70°K is given as the lower Curie point of KH_2AsO_4, with no statement as to the basis for this value; and Bantle's paper,[22] discussed in §496, in which he mentions the lower Curie point of KD_2PO_4.

established; with regard to the lower temperature the same comment may be made as for KH_2PO_4 in the preceding section.

497. *Specific Heats and Internal Field Constants.* In §409 it was shown that in Rochelle salt the anomaly in specific heat is extremely small at both Curie points. From the relatively large values of P^0 for the phosphates discussed above and the marked dependence of P^0 on temperature, one might expect a more pronounced anomaly for them. This expectation has been fulfilled by Bantle[22] for all three phosphates and by Stephenson and Hooley[481] and J. and K. Mendelssohn[364] for KH_2PO_4. Very recently, the specific heats of KH_2PO_4, KH_2AsO_4, $NH_4H_2PO_4$, and $NH_4H_2AsO_4$ were measured over a very wide range of temperatures by Stephenson and his associates.[480–483] They found no anomaly except at the upper Curie point. From their results, which are probably the most precise, we find the following values for the normal specific heat C_n at θ_u (derived from the course of the curve above and below θ_u), the peak value C_θ at θ_u, and the difference $\Delta C = C_\theta - C_n$, all in cal mole^{-1} deg^{-1}, and also the heat of transition ΔH in cal mole^{-1}:

	C_θ	C_n	ΔC	ΔH
KH_2PO_4	118	16	102	87 ± 6
KH_2AsO_4	76	15	61	84 ± 4
$NH_4H_2PO_4$	274	20	254	154 ± 5
$NH_4H_2AsO_4$	279	29	250	220 ± 15
KD_2PO_4*	134	29	105	100.3

* Data for KD_2PO_4 are from Bantle.[22]

As has been shown in §409, the internal field constant γ can be calculated when ΔC and the temperature variation of P^0 are known. Bantle thus finds the following values of γ: for KH_2AsO_4, 0.5; for KH_2PO_4, 0.37 (in contrast with Stephenson and Hooley's value of 0.7); for KD_2PO_4, 0.68.

Although the phosphates here considered have only small internal field constants, the large values of P^0 make it certain that the internal fields themselves must be much greater than in Rochelle salt. For example, the product γP^0 for KD_2PO_4 yields a value of the internal field of about 3,000,000 volts/cm.

498. *Domain Structure.* It was stated in §494 that, on cooling below certain definite temperatures, $NH_4H_2PO_4$ (at −118°C) and $NH_4H_2AsO_4$ (at −53°C) broke down to a microcrystalline mass. When this fact is compared with Busch's remark that the potassium salts tended to become cracked when heated through the upper Curie point, there appears some probability that the temperatures recorded above are close to the Curie points for the ammonium salts. If this assumption is

made, the shattering of the crystals can be attributed to the stresses attending the commencement of a domain structure as the Seignette region is approached. The temperatures recorded as "Curie points" of the ammonium salts in Table XXXVI are those for the maximum values of the specific heat, as measured by Stephenson and Adams[480] and by Stephenson and Zettlemoyer.[483] These temperatures are a few degrees lower than those at which Busch's crystal plates broke down. It seems just possible that, if this breakdown could have been avoided, the dielectric constants (values of which are given in §494) might have risen to high values at the Curie points.

Further evidence of domain structure, at least in KH_2PO_4 and KD_2PO_4, is afforded by the experiments of Zwicker and Scherrer,[602] in which the change in double refraction under an electric field, at temperatures below θ_u, takes place in steps, in a manner analogous to the Barkhausen effect in iron. In a discussion of this paper, Quervain and Zwicker[432] reach the conclusion that the domains themselves are microscopic but that they fall into groups some millimeters in extent. They find that sudden cooling through θ_u causes minute cracks perpendicular to the Z-axis, which disappear on warming.

499. *Technical Applications.* The potassium and ammonium salts mentioned in the preceding paragraphs seem to offer considerable promise of useful applications. The only member of the group for which definite mention of applications has hitherto appeared in the literature is KH_2PO_4. In both its elastic and piezoelectric properties this crystal, like the others in the group, stands between quartz and Rochelle salt. Its piezoelectric effect at room temperature (§146) is about seven times as great as in quartz, while it is much more stable than Rochelle salt and has no water of crystallization. At ordinary temperatures it is so far above its Curie point as to be free from such fantastic behavior as that shown by Rochelle salt in the neighborhood of 24°C. It is practically devoid of hysteresis. Some of its elastic temperature coefficients, however, are considerably greater than those of quartz.

Experiments with KH_2PO_4 resonators are described by Bantle and Lüdy,[27] by Lüdy,[323] and by Bantle.[23] Lüdy measured the values of the elastic constants s_{11} and s_{33}, as recorded in §89. Bantle and Lüdy studied lengthwise vibrations in thin rods, using frequency modulation to sweep rapidly and repeatedly through the resonant frequency. From the curves recorded by means of a cathode-ray oscillograph they found the resonant frequency, effective elastic constant, and damping, at different temperatures down to the Curie point, where certain of the elastic constants had very large temperature coefficients. The only numerical data published thus far are in Bantle's paper. Using Z-cuts he finds, for different modes, temperature coefficients of frequency from

$-205(10^{-6})$ to $-290(10^{-6})$ and considers the possibility of securing cuts with zero temperature coefficient.

Since the matrices of the elastic and piezoelectric constants have the same form as for Rochelle salt, the rules for exciting various vibrational modes are exactly the same as for that crystal.

Matthias and Scherrer[354] have called attention to the advantages of KH_2PO_4 for band-pass filters.

CHAPTER XXVIII

MISCELLANEOUS APPLICATIONS OF PIEZOELECTRICITY

Was man an der Natur Geheimnisvolles pries,
Das wagen wir verständig zu probieren,
Und was sie sonst organisieren liess,
Das lassen wir kristallisieren.

—GOETHE.

In dealing with technical applications the discussion will be confined mainly to the types of crystal commonly used, their cuts, electrodes, and general performance. Space forbids detailed descriptions of circuits and of mechanical features.

The application of piezoelectric crystals in electric filters of various types will first be considered. In filter circuits the crystal operates as a resonator; the conversion of electrical into mechanical energy and back, though essential to its performance, is only incidental from the point of view of the filtering action.

The remainder of the chapter will be devoted to the large and important group of applications in which the crystal functions as a transducer, converting mechanical movements into electrical energy or the converse. The first subdivision in this group comprises the *non-resonant* applications, in which the crystal is in a state of forced vibration at a frequency which is usually far below that of any of its normal modes. In the second subdivision the crystal usually vibrates at or near a resonant frequency and is used for emitting or receiving h-f acoustic radiation. The practical applications include submarine signal and echo work, the acoustic interferometer, and intense ultrasonic beams for physical, chemical, biological, and industrial uses.

One of the most interesting effects of ultrasonic waves is their ability to diffract a beam of light. Some of the applications of this effect, especially in the measurement of elastic constants, light relays, and television, will be described.

500. The Crystal Filter. The use of piezoelectric crystals as couplers and sharply tuned circuit elements was first proposed in 1921.* For use as a piezoelectric coupler the crystal is provided with two pairs of electrodes, connecting the output of one circuit with the input of another. The crystal then operates as a filter element, transmitting energy only

*Ref. 91; also W. G. Cady, U.S. patent 1,450.246 (1923) and reissue 17,355 (1929).

at a resonant frequency. The theory of the coupler has been investigated by Watanabe.[581] Its use as a tuned coupling between tubes is described by Rohde and Handrek.[438] Of greater importance is its use in electric filters, to which we now turn. Filters employing crystals were first described by L. Espenschied.* The evolution of the filter is described by Buckley in the reference at the end of this chapter.

All electric filters depend for their operation on the change in reactance within a certain band of frequencies. Filters constructed from coils and condensers are limited in usefulness partly by their variability with temperature and partly by the fact that the band width cannot be made sufficiently narrow to meet modern requirements in communication circuits, owing to the unavoidable resistances of the coils. Properly designed crystal filters avoid both these difficulties. In fact, the selectivity of crystals is so great that for many purposes the band width is too narrow, requiring the use of coils associated with the crystals.

In a band-pass filter the width of the band is approximately the frequency interval $(f_p - f_s)$ illustrated in Fig. 62. From Eq. (401) this interval is approximately equal to $f_s C/2C_1$. The ratio C_1/C is therefore a measure of the excellence of the filter. From Eq. (450a), it can be seen that either a capacitance C_2 in series with the resonator $RLCC_1$ or a capacitance C_3 in parallel with it has the effect of reducing the value of $(f_p - f_s)$. Use is made of this fact in the design of filters of very narrow band width.

Most crystal filters in use today in filter circuits are of quartz, with zero gap, the thin metallic electrodes being deposited directly on the quartz. The quartz plates may be supported by the lead wires, which are soldered to the electrodes at nodal points. Some filter circuits require the use of pairs of matched crystal units of identical frequency. In such cases a single crystal plate with two pairs of electrodes can be used. Much ingenuity has been shown in the placing and interconnecting of the electrodes and in the provision of a narrow metallic strip plated to the crystal to serve as a screen between the electrode pairs. Such arrangements are described by Mason and Sykes,[342,343] Mason,[B35] and Rohde.[436,437]

For the higher frequencies, thickness vibrations must be used. From 50 to 500 kc/sec compressional vibrations in the direction of length or breadth of the plate are ordinarily employed. For lower frequencies, use is made of flexural vibrations; the NT-cut described in §359 can be used from 50 down to 4 kc/sec, while Rohde and Handrek[438] describe flexural filter crystals for frequencies as low as 1,000 cycles/sec.

As an example of the band width obtainable without the use of auxiliary condensers may be mentioned the 18.5° cut, for which, from

* U.S. patent 1,795,204, filed 1927 and issued in 1931.

Table XXX, $C_1/C = 138$. From this one finds $(f_p - f_s)/f_s = 0.36$ per cent. For this cut, as well as the $-5°$ cut, see §357.

In some lattice filters two crystals of slightly different frequency are used, the resonant value f_s of one coinciding with the antiresonant value f_p of the other. In such cases the band width is twice that of one crystal alone.

Filter elements have also been made from Rochelle salt. For a time, composite resonators consisting of metallic bars with Rochelle-salt crystals attached were tried, but this method has been abandoned. For the lower frequencies 45° bars may be used; to avoid the anomalies that beset the X-cut, the cuts may be made normal to the Y- or Z-axis. Filters of higher frequency employ thickness shear vibrations of oblique plates,* some formulas for which are given in §77.

Whichever type of crystal is chosen, an all-important requirement is the absence, over as wide a range as possible, of all disturbing resonant frequencies.

An attempt by Guerbilsky† to broaden the band by using a wedge-shaped crystal was based on an erroneous concept of the nature of vibrations in solids. The experiments of Zacek and Petrzilka[597] showed, as would be expected, that such a resonator has a large number of closely adjacent frequencies; the subject is also discussed by Wagner.[578]

Crystals can be connected to serve as elements in high-pass, low-pass, or band filters. They are used commercially in pilot channel filters for carrier systems and for separating carrier from side-band frequencies in radio. They have also found application in acoustics, for analyzing the components of complex sounds. Finally may be mentioned their use in radio receiving sets, in which they are commonly placed in a bridge in the i-f amplifier.

A fully equipped section of coaxial cable for carrier communication, with 400 circuits, requires 12,800 crystals for channel filters, in addition to those for channel supply filters.‡

501. Crystals as Mechanical and Acoustic Transducers. For the *measurement of pressures*, plates or blocks of quartz or Rochelle salt are chiefly used, and to a small extent tourmaline. There is a great variety of devices, ranging from quartz or tourmaline plates, used singly or in stacks, for measuring violent explosion pressures, down to delicate apparatus for recording blood pressures. Among the references at the end of the chapter will be found descriptions of piezoelectric methods for

* W. P. Mason, U.S. patent 2,303,375. See also Z. Kamayachi, T. Ishikawa, and E. Kamizcki, *Nippon Elec. Comm. Eng.*, January 1941, p. 195, and M. Monji and I. Kuwayama, *Electrotech. Jour. Japan*, vol. 4, p. 235, 1940.

† A. Guerbilsky, *Jour. phys. rad.*, vol. 8, pp. 165–168, 1937.

‡ A. J. Gill, in discussion of paper by Booth.[69]

measuring pressures in internal-combustion engines and in various types of firearms and artillery; pressures produced by cutting tools; transient pressures resulting from impact; piezoelectric oscillographs; and applications of piezoelectric manometric devices in biology. Many of the articles cited contain further references to the literature. Applications of optical phenomena produced by vibrating crystals are considered later.

Piezoelectric devices have come into extensive use for the *measurement of vibrations*, especially in machinery, and for analyzing the degree of smoothness of finished surfaces. Owing to its large piezoelectric effect, Rochelle salt is well suited to these purposes. Some references are given at the end of the chapter.

Space forbids an account of the various crystal cuts and mountings that are used for the measurement of stresses and vibrations. It must suffice to say that, in devices employing quartz, X-cuts are commonly used, with either the longitudinal or the transverse effect. Rochelle-salt devices are described in §503. With few exceptions resonance in the crystal or in the assemblage of crystals is avoided. This is usually not difficult, since in most cases the crystal frequency is much higher than any frequency associated with the effect being investigated. Moreover, the mounting can be made in such a way as to tend to damp out any crystal vibrations.

Some of the papers cited at the end of the chapter contain a theoretical treatment of the devices for measurement of pressures and vibrations, for example, those by Gohlke, Kluge and Linckh, Webster, and Zeller.

502. Rochelle-salt Non-resonant Transducers. Rochelle salt is used at the present time more than any other crystal in electroacoustic and electromechanical devices. The operating frequencies are usually well removed from the resonant frequencies of the crystal units, and in any case the construction is such as to tend to damp out all resonances. The outstanding advantage of Rochelle salt, at least in the X-cut commonly employed, is of course the large piezoelectric constant. This advantage carries with it a train of difficulties, due to the great sensitiveness of the piezoelectric property to mechanical constraint, the variability with temperature, the presence of hysteresis, and the large dielectric constant. It is a fortunate circumstance that the constraints imposed on the crystal units by cement, electrodes, clamping, and waterproofing not only suppress resonant frequencies, but at the same time greatly reduce the effects of temperature and hysteresis and lower the dielectric constant to a value approximately that of a completely clamped crystal. The price that has to be paid is a great diminution in the effective values of d_{14} and e_{14}.

Some Rochelle-salt transducers operate as motors, others as generators. The *motor* devices are most sensitive in the neighborhood

of the Curie point, 24°C. By suitable mounting it is possible, however, to restrict the response within a few decibels over the allowable temperature range from −40° to +54°C (−40° to +130°F). It is of the utmost importance never to let the temperature rise above this upper limit, owing to the disintegration of Rochelle salt at 55.6°C. The upper limit of useful operation is 45°C, since above this temperature leakage becomes objectionable.

The dielectric constant of a clamped Rochelle-salt crystal in the X-direction is of the order of 100. The high parallel capacitance thus conferred on a thin plate would be a serious handicap if the purpose were to convert as much mechanical into electrical energy as possible. In most applications, however, in which the crystal acts as a *generator* to produce electrical energy, the crystal is connected to a very high impedance. It is then almost on open circuit; and since stress and temperature affect the dielectric constant in approximately the same manner as they affect the piezoelectric constant, it follows that the potential difference that a given stress on the crystal impresses on the outer circuit is not far from proportional to the stress under all circumstances. Moreover, less trouble is experienced from the capacitance of long lead wires than if the dielectric constant of the crystal were low. The open-circuit output of these generator devices is practically independent of temperature.

The fact that with a high external electrical impedance the crystal is practically on open circuit has a bearing on the theoretical treatment of this form of transducer. When the crystal is on open circuit and well below resonance, its electrical state under mechanical stress is substantially the same as that of a bare crystal with an infinite gap. The polarization remains nearly zero at all strains. Since, as shown in §375, the stiffness at infinite gap is very nearly independent of temperature and stress, it follows that the crystal when connected to a high external impedance is comparatively free from the effects of the usual anomalies of the X-cut. This is especially true when the crystal is also in a state of partial constraint.

In the theoretical treatment of the Rochelle-salt transducer it is convenient to use the equations of the polarization theory, with the coefficients a_{14} and b_{14}, which vary comparatively little with temperature, in place of e_{14} and d_{14}. This is virtually the method followed by Mason[B35] in his treatment of the problem, although he employs the "charge" theory; as explained in §191, the charge and polarization theories lead to almost identical results.

503. Leaving out of account certain experiments on acoustic effects with crystals in 1917 and 1918, it appears that the first published work was that of Nicolson[391] in 1919. He used entire crystals, 2 in. or more in extent, with variously disposed electrodes. Although the crystal

structure and the electric field were far from uniform, Nicolson was able to make use of the relative displacements of the faces normal to the Z-axis in such a way as to make the crystals serve as microphones and reproducers. Unpublished experiments in Scott laboratory following Nicolson's work soon showed that equally sensitive units could be made in the form of thin X-cut bars, cut after the manner of Pockels with lengths bisecting the angle between the Y- and Z-axes. These plates were from 1 to 2 cm long, 0.4 to 1 cm wide, and 0.1 to 0.2 cm thick. When the ends were cemented between diaphragms and rigid backings they acted as microphones and reproducers; such plates were also tested successfully as phonograph pickups.*

Much more effective are the Rochelle-salt "bimorphs"† of Sawyer.[448] These devices generally consist of two X-cut Rochelle-salt plates cemented face to face, usually with a thin metallic electrode interposed.

In the "bender" type, plates are rectangular, square, or trapezoidal, the major axes of the plates making angles of $\pm 45°$ with the Y- and Z-axes. The X-axes of the two plates are so oriented that as one plate dilates in either direction the other contracts. This type of element is therefore somewhat similar to the "Curie strip" described in §354. There is, however, this important difference, that while in the quartz Curie strip with length parallel to Y the only strain (the small change in thickness of the component plates being ignored) is in the direction of length, with none at all in the direction of breadth, the piezoelectric effect in Rochelle salt is such that both length and breadth are affected (if the element is square either dimension of the major surfaces may be called the "length"). If an applied electric field tends to make one plate longer and narrower, the other plate tends to become shorter and wider. As a result, the element as a whole does not become bent to a cylindrical form but tends to become saddle-shaped; when one surface is convex in the length direction it is concave in the breadth direction.

The foregoing remarks apply to the unconstrained element. If one end of the rectangle is clamped and an alternating field is applied, the other end moves to and fro (*single clamping*). If both ends are clamped, the curvature in the breadth direction is largely suppressed and the central portion vibrates like a diaphragm (*double clamping*). Either of these methods of mounting may be used to make the element act as a transducer for transforming electrical into mechanical energy or the converse.

A second type of bimorph is called the "twister." The two component X-cut plates are square or rectangular, with edges parallel to

* See also Schwartz.[454]

† The information concerning bimorphs and their applications was kindly furnished by the Brush Development Company.

Y and Z, or trapezoidal (tapered element), with the two parallel edges AB and CD (Fig. 155) in the direction of Y or Z. When a voltage is applied to the combination, the two plates tend to become sheared in opposite directions, according to the formula $y_s = d_{14}E_x$. If the element is clamped at one end, as at AB, then since the plates are cemented together the small end face CD rotates in its own plane. The end P of a pointer attached to CD moves in a circular arc in the plane of this end face. Twister elements are often mounted and used in this manner. Another common method of mounting the twister element is to clamp it at three corners, the fourth being left free to move.

The principle of the twister is illustrated in Fig. 156, which shows a Rochelle-salt motor that has been found useful for demonstration. By proper design of the ratchet and pawl the device could be made to serve as a synchronous low-speed motor.

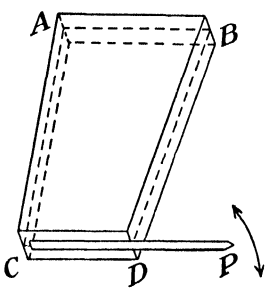


FIG. 155.—A bimorph "twister."

Bender and twister elements are made commercially under the trade name "Bimorph" in sizes from $\frac{7}{32}$ by $\frac{7}{32}$ by 0.015 in. to $2\frac{1}{2}$ by $2\frac{1}{2}$ by $\frac{1}{4}$ in., depending on the uses to which they are put. Among the applications for such elements are pickups and recorders for phonographs, microphones, earphones, vibration meters, oscilloscopes, direct inking oscillographs, light valves, stethoscopes, and pickups to be placed on musical instruments. Rochelle salt has also been used in loud-speakers but is now superseded by the more rugged electrodynamic drive. An instrument known as the "surface analyzer" consists of a combination of crystal pickup, amplifier, and crystal oscillograph that makes a direct record in ink of the surface contour of the test specimen.

Crystal microphones and earphones usually employ either a twister element with three-corner mounting or a long narrow bender element with double end clamping. The free corner of the twister or the center of the bender is coupled to a small acoustic diaphragm.

Another type of microphone is known as the "sound-cell" microphone. The sound cell employs two approximately square bender bimorphs placed close together so as to form a flat airtight cell, with a small gap between them. The elements are supported at the centers of two opposite edges so that they are free to partake of the saddle-shaped curvature. The two elements are so oriented and electrically connected in parallel that their voltages are in phase when sound waves strike the cell, while the device is insensitive to mechanical shock or vibration. Two or more sound cells can be combined in a single microphone; in one type the number is 24. A typical sound cell has elements $\frac{7}{16}$ by

$\frac{7}{16}$ by 0.02 in. with a flat response from 30 to 10,000 cycles/sec. A laboratory type has elements only $\frac{7}{32}$ by $\frac{7}{32}$ by 0.015 in. with a resonant frequency of 45,000 and a flat response to 17,000 cycles/sec.

Vibration meters of the displacement type employ bender or twister elements mounted to a convenient support and arranged for the active portion of the element to be driven by the vibrating object. Both

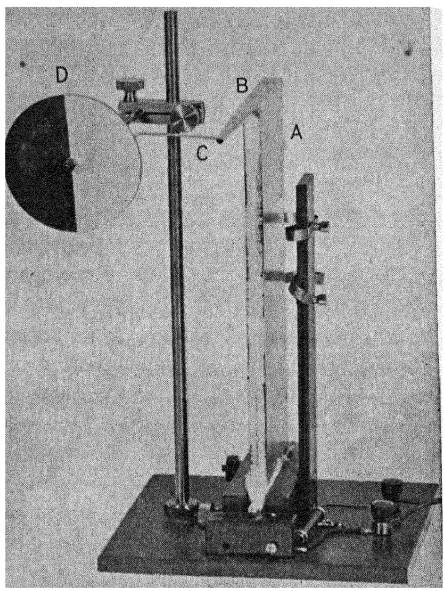


FIG. 156.—Rochelle-salt motor. *A* is a bimorph "twister" consisting of two *X*-cut plates, each 4.5 mm thick, cemented together with a tin-foil electrode between, which is connected to one terminal of the 60-cycle 115-volt supply. The length, parallel to *Z*, is 25 cm, and the breadth, parallel to *Y*, is 7.5 cm. The two outer tin-foil electrodes are connected together and to the other terminal of the supply, through a high resistance for safety. The lower end of the twister is fixed. When the field is applied, the upper end twists about the vertical axis, rotating the arm *B* and the light spring *C*, which acts as a pawl on the knurled circumference of the wheel *D*. The alternating field causes *D* to rotate slowly.

bender and twister elements are used also in the acceleration type, the accelerating force being applied to the holder and the deformation of the element taking place through inertia. This type of pickup is especially useful for measuring mechanical vibrations of relatively high frequency. The voltage generated by the crystal element is proportional to the acceleration; for the same amplitude it increases with the square of the frequency. The frequencies investigated must lie well below the resonant frequency of the element in its mounting.

The voltages involved in the operation of bimorph crystal elements

vary over a large range depending on the uses to which the elements are put. The voltage developed by a laboratory sound-cell microphone may be far less than 1 mv, while the output of a typical phonograph pickup may be as high as 10 volts. One or two volts is sufficient to produce comfortable volume in crystal earphones, while about 700 volts is required to drive a crystal-actuated direct-inking oscillograph at full amplitude.

504. A Rochelle salt transducer of quite a different type is the *L*-cut.[108] This is a plate making equal angles with all three crystallographic axes, as described in §140. A field normal to the plate causes a change in *thickness*, while through the direct piezoelectric effect a normal compression produces polarization charges. Plates of this type have been used experimentally as emitters and receivers of sound waves and also as generators of ultrasonic waves. They have recently found application by Groth and Liebermann[190] as microphones in the measurement of the velocity of sound.

505. Ultrasonics. The study of acoustic waves of frequencies above the range of human audibility began late in the nineteenth century. Koenig's longitudinally vibrating steel rods appeared in 1874, and his ultra-audible tuning forks in 1899. Other early sources of very short acoustic waves were the Galton whistle (1883) and in 1907 Altberg's application of the oscillatory spark discharge, by means of which he recorded acoustic frequencies of over 300,000 vibrations per second. Wavelengths were usually measured by means of the Kundt dust figures.

Although some of these sources were fairly intense, they could emit only decaying wave trains, and they were practically point-sources, radiating in all directions.

Leaving aside certain attempts in the First World War to produce h-f sounds electrostatically from vibrating condenser plates, it may be said that the modern science of ultrasonics* began with the introduction of an entirely new source of h-f sound waves by Langevin—a device that also serves for detecting these waves. Langevin conceived the brilliant idea of making use of the piezoelectric property of quartz crystals to cause them to emit a continuous flow of undamped acoustic waves when connected to a h-f electric generator. Moreover, by the use of a mosaic of crystal plates of large area, he was able to produce a system of approximately *plane* waves, resulting in an ultrasonic beam of great intensity, concentrated within a small angle of divergence.

The immediate purpose of Langevin's invention was the detecting and locating of distant objects under water by means of echoes. A

* The word "supersonics" is in wide use as a synonym for "ultrasonics." The author's reason for the use of the latter term is twofold: the word "ultrasonic" is analogous to "ultraviolet" in optics, and it conforms to the usage in other languages.

principle so novel and so suggestive could not fail to excite the interest of many physicists. Numerous researches were begun, leading to several applications of considerable importance in both pure and applied science.

A second source of continuous ultrasonic waves is the magnetostriction oscillator, introduced by Pierce in 1928,* and developed further by him and by many others. It can generate more intense radiation than the vibrating crystal; but its practicable upper limit of frequency comes at about 60 kc/sec, and it is not so well adapted to the production of some of the effects described below. Descriptions of the magnetostriction oscillator and its uses will be found in the books listed at the end of the chapter.

506. Langevin's Quartz-Steel Oscillator. It has been shown in earlier chapters that an X-cut quartz plate dilates or contracts in the direction of its thickness when an electric field in the X-direction is applied by means of electrodes covering its major surfaces, and that by application of an alternating voltage of suitable frequency it can be set into resonant compressional thickness vibration. Quartz plates of reasonable thickness have resonant frequencies too high to be suitable for submarine signaling and echo production. To surmount this difficulty Langevin cemented a quartz plate a few millimeters thick between two massive slabs of steel. The thickness of these slabs was so chosen that the over-all frequency of the entire "sandwich" was of the desired value. The slabs served also as electrodes. When the unit was vibrating in thickness resonance in air, a system of stationary waves was set up in it, the thickness of the entire unit corresponding to a half wavelength of the compressional wave. When mounted for immersion in water, one steel slab was in direct contact with the water and emitted ultrasonic radiation, while the other slab, in contact with air, reflected the wave energy without appreciable loss.

In his first experiments Langevin used a Poulsen arc generator for his h-f source. This type of generator was soon superseded by the vacuum-tube oscillator.

In order to radiate more energy and at the same time to concentrate the energy in a narrow beam, Langevin increased the lateral dimensions of the steel slabs to 20 cm or more and cemented between them a mosaic of quartz X-cut plates, all carefully ground to the same thickness. In this manner small pieces of crystal could be used for building an ultrasonic emitter of any desired area.

Although the vibrations are heavily damped by radiation into the water, it is none the less important to excite the oscillator at or near its

* G. W. Pierce, *Proc. Am. Acad. Arts Sci.*, vol. 63, pp. 1–47, 1928.

resonating frequency. For example, if 50,000 volts were required to produce a desired amplitude by forced vibrations far from resonance, 2,500 volts would suffice at the frequency of resonance. Moreover, since the oscillator usually serves also as a detector for waves reflected from distant objects, it is of enormous advantage to have it tuned to the emitted frequency.

The best size and frequency for an underwater source of concentrated radiation is determined by the following considerations: Like all other media, water absorbs sound energy to an extent depending on the distance traversed and also on the frequency. The rate of absorption increases with the square of the frequency. Waves in the audible range suffer very little absorption. Langevin points out that at a frequency of 40,000 the energy is reduced to one-third of its original value in about 30 km, while at 100,000 cycles/sec the same reduction takes place in about 5 km. If the radiation took place in air instead of water, two-thirds of the energy at this higher frequency would be absorbed in a few meters.

The second consideration has to do with the fact that a plane source of sound comes closer to emitting plane waves, and hence a highly concentrated beam, the greater its lateral dimensions in comparison with the wavelength of the sound. An oscillator designed for 100,000 cycles/sec, with a diameter of 20 cm, producing a wavelength in water of about 1.5 cm, would emit a beam with very sharply directional properties. For the observation of echoes from distant objects such a beam would be inconveniently narrow, and moreover at this frequency the relatively great absorption of energy by the water would be objectionable. For echo detection it is desirable to have most of the energy confined to a cone with total aperture of about 20°. This requirement is met when the diameter of the radiating surface is around six times the wavelength in the medium.

A compromise must be sought between the greater penetrating ability of l-f waves and the requirement of relatively large area to make the beam sufficiently directive. Very fortunately such a compromise is found at frequencies around 40,000. The wavelength is then about 3.5 cm, and a suitable diameter of the radiating surface is about 20 cm. Langevin's calculations showed that for emission of radiation at the rate of 1 watt/cm^2 the amplitude of vibration must be about $5(10^{-5})$ cm. The returning echo may have an amplitude as low as 10^{-10} cm, only $\frac{1}{500}$ of the diameter of a molecule. Even this minute motion is enough for detection when the wave frequency is the same as the resonating frequency of the oscillator. Various devices have been developed for observing or automatically recording both the direction of a submerged object and, from the time interval between the emission and return of a

short signal, its distance. The maximum range in echo work is of course limited by the inverse fourth-power law.

In his experiments Langevin transmitted signals over distances as great as 9 km and received echoes from submerged objects 2,000 meters from the oscillator. He described the use of a small quartz crystal as a "probe" to explore the sound field in the neighborhood of the oscillator. The radiated power was as high as 10 watts/cm^2.

By turning the submerged oscillator so that it radiated vertically downward, he received echoes from the ocean bottom. Even in shallow water, at depths as small as 1 m, records could still be made. This device is of great value in depth sounding, since it enables a survey of the bottom to be made, revealing the location of reefs and sunken wrecks; moreover it can be operated on a vessel in motion.

A more complete account of the quartz-steel oscillator, its theory, and its uses in echo detection and depth sounding is given in the sources listed at the end of the chapter.

507. Piezoelectric Emitters of Ultrasonic Waves. As in the Langevin oscillator just described, flat crystal plates vibrating in a compressional thickness mode are most commonly used. For most of the work described below, the desired frequencies are so high that one can employ a fairly thin plate vibrating at its own fundamental resonant frequency or at one of its odd overtones. For the highest frequencies the plates are excited at very high overtones. In place of Langevin's massive metallic slabs, various types of electrodes are used, as described below. Frequencies have been used up to 50,000 kc/sec. For frequencies below 200 kc/sec, however, single plates or stacks of plates in lengthwise vibration are employed.

If Nature had paid more attention to the production of large and perfect tourmaline crystals, instead of giving birth to so many quartz twins, all who are concerned in the applications of piezoelectricity would be deeply appreciative. Especially in ultrasonics is this true, for large Z-cut tourmaline plates would make almost ideal emitters.

With the world as it is, tourmaline has been used but little in ultrasonics. Rochelle salt as a possible emitter has been discussed by Hiltscher[228] and Cady.[108] For mechanical and thermal reasons Rochelle salt is unsuited to the production of very intense radiation. For demonstration of the optical diffraction effects described below, as well as for other purposes where low power is sufficient, the author[108] has had good success with the Rochelle salt L-cut described in §§140 and 504. Like quartz, this cut can vibrate in a compressional thickness mode, which recommends it where a large area is desired, whether for emitting or receiving. Its application in the detection of acoustic waves is mentioned in §504.

Almost all the work in ultrasonics described in the literature has been done with X-cut quartz plates, except some of that which lies within the range of the magnetostriction oscillator. The plate is usually circular, though in a few cases the Straubel contour (§360) has been used, since the radiation is then somewhat more uniformly distributed over the surface and higher voltages can be applied without danger of fracture.*

For experiments in non-conducting liquids, such as xylol, transformer oil, or paraffin oil, the simplest arrangement consists in laying the quartz plate on a sheet or block of lead at the bottom of the vessel, the lead serving as one electrode. A lead support is less likely to cause fracture of the quartz than a harder metal. The other electrode is a thin sheet of metal resting on the quartz, through which the radiation passes with little loss. This is the arrangement used by Wood and Loomis in their experiments.[B55] Wire gauze has been used as an upper electrode by Lindberg. The front surface of the crystal can also be plated, contact being made by a narrow brass ring resting on the crystal at its circumference.

A more efficient use is made of the vibrational energy of the crystal by having one of its sides in contact with a layer of air. The compressional waves in the crystal are practically totally reflected at the boundary between crystal and air, all loss by radiation from the rear of the oscillator being thus eliminated. Several arrangements are possible, some of which are very simple and convenient for demonstration and for approximate measurements of ultrasonic velocities and wavelengths.

508. In Fig. 157*a* is shown a crystal bar C for lengthwise vibrations at the lower ultrasonic frequencies. The bar has tin-foil or plated electrodes and is cemented to a metal plate a few tenths of a millimeter thick. This plate closes the end of a glass or metal tube T. R is a movable piston for reflecting the radiation and producing stationary waves. The effective impedance of the crystal varies with the position of the piston, passing from one maximum to another as the piston moves through a half wavelength. This periodic change in impedance is observed as a series of changes in the anode current of the tube by which the crystal is driven. This experiment illustrates the principle of the ultrasonic interferometer. It can also be performed in free air without the enclosing tube. An advantage of the tube, however, is that if it contains a fine powder the particles of powder collect at the nodal regions, as in the well-known Kundt experiment, giving visible evidence of the shortness of the wavelengths.

Figure 157*b* shows a similar device, but with the crystal C in the form of a plate for thickness vibrations, to cover the higher range of frequencies. The rear electrode can be of tin foil or a plated film. At a

* Ref. B5, p. 39.

frequency of 10^6 cycles/sec, the wavelength in air is of the order of 0.03 cm, so that for high frequencies a micrometer control is needed for the piston *R*.

If the medium is a liquid instead of a gas, the tube *T* may be vertical with the crystal at the bottom. This method is convenient for demonstrating the optical diffraction effects described below. If a piston is to be used, it should be an air cell, in the form of a pillbox with thin metal front, in order to prevent the transmission of radiation.

Experiments with liquids can also be carried out with an open trough or tank in place of the tube. The crystal may be cemented to the inside of a small flat-sided can of thin metal, as shown in Fig. 157*c*, which may be moved about at will in the liquid. Since the beam from such an oscillator diverges considerably, reflections from the side walls take place, so that the container is filled with a three-dimensional array of maxima and minima of intensity. This acoustic field can be explored by means of a second crystal in a small open can. Or, better, the exploring crystal, which serves as a microphone, can be a small *X*-cut 45° block or bar of Rochelle salt, of the order of 0.5 by 1 by 1 cm with tin-foil electrodes, immersed in oil inside of a tube of rubber or thin metal closed at the bottom by a cork, as in Fig. 157*d*. This crystal is connected between grid and filament of the tube in a low-power oscillating circuit of frequency sufficiently removed from that of the ultrasonic emitter to produce an audible beat note in a telephone receiver or loud-speaker.

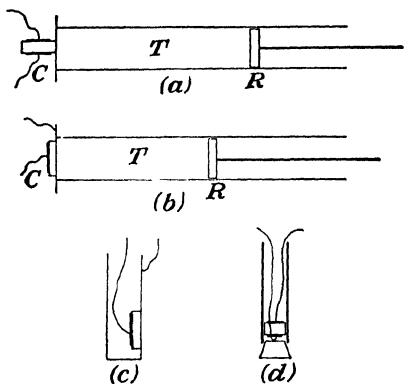


FIG. 157.—Simple arrangements for producing ultrasonic waves. *a* and *b* are for use with air as the medium. The containers shown in *c* and *d* are for immersion in a liquid.

Even with a low-power oscillator, "dust patterns" can be produced in a tube or trough of liquid. In the course of experiments in 1918 the author had occasion to let a small oscillator radiate continuously for several hours at a frequency around 25,000, at one end of a trough of somewhat turbid water several meters in length. The particles suspended in the water settled in nodal bands crossing the bottom of the trough. A similar effect has been recorded by Ardenne (reference at end of chapter) and by Boyle.[74]

In Fig. 157*b* and *c*, direct radiation from the crystal plate into the liquid can be brought about by having in the metal sheet to which the

crystal is cemented an opening nearly as large as the crystal. The front face of the crystal is then plated and electrically connected to the metal sheet.

A great advantage in having one side of the crystal plate insulated from the surrounding liquid is that the liquid itself need not be an insulator.

Some experimenters have taken pains to support the crystal at points halfway between the two major surfaces, as is sometimes done with quartz resonators (see §344). Unless the plate radiates to the same extent in both directions—as is rarely the case—this is largely wasted effort, because when the impedances of the media in contact with the two surfaces are different the median plane of the plate is no longer a nodal plane.

The radiation from the surface of the quartz is usually far from uniform in intensity and direction. The complication that this fact introduces in quantitative work is somewhat reduced by the use of the Straubel contour mentioned above. A considerable amount of research has been devoted to the study of the acoustic radiation field in the neighborhood of the oscillator.

Theoretically, a piezoelectric plate can be excited to any desired amplitude of vibration at any frequency, however far from resonance, provided that a sufficiently high voltage is applied. Apart from the danger of puncturing the dielectric when in a strong field, it may be said that the danger of mechanical fracture is no greater with forced vibrations at high voltage than with resonant vibrations at low voltage. Still, even if it were economical to drive the crystal by a strong field at a non-resonant frequency, the crystal would almost certainly be fractured, even when damped by radiation into a liquid, if the frequency by any mischance happened to pass through resonance. In practice, resonant frequencies are commonly employed. The experimenter should remember that a resonant voltage that is safe when the crystal is in contact with a liquid can easily shatter the crystal in air.

For concentrating a large amount of ultrasonic energy in a small region, Gruetzmacher's concave quartz oscillator[192,193] may be used (see also the references at the end of the chapter to J. G. Lynn, Zwemer, and Chick, and to Tumanski). The radiating surface of a large circular *X*-cut plate is made slightly concave, thus emitting a convergent beam. By this means, with frequencies from 638 to 1,000 kc/sec, Tumanski has produced jets of oil 70 cm high, projected upward from the free surface of the liquid.

For ultrasonic effects in air the crystal may be connected in a Pierce circuit, but in liquids the crystal is too heavily damped to operate in this way. A suitable and much used source for all purposes is the Hartley

tube generator; in some cases two tubes in push-pull connection have been used. To the output of the generator is coupled a coil connected to the crystal. By proper choice of inductance the circuit can be made to operate as a Tesla transformer, supplying a high voltage to the crystal.

An interesting demonstration of interference between the waves from two ultrasonic sources has been described by Müller and Kraefft.[383] Two quartz plates of slightly different dimensions are excited in compressional vibration from independent sources. The plates are a few centimeters apart, with radiating surfaces opposed, and the frequency difference lies in the audible range. Under these conditions a beat note can be heard. When the distance between the plates is varied, the pitch of this note changes by an amount proportional to the relative velocity, thus demonstrating the Doppler effect.

The extreme range of frequencies hitherto attained with ultrasonic waves is from 20 to 500,000 kc/sec. This is a range of about 15 octaves in frequency. The corresponding range of wavelengths in air is from 1.6 cm to $6(10^{-5})$ cm. The maximum power that can be radiated without breaking the crystal depends on mounting, frequency, and medium. Wood and Loomis recorded a value as high as 35 watts/cm^2. This is an extreme case; usually 10 watts/cm^2 is considered the upper limit, and even here there is danger of fracture. Ten watts per square centimeter is 10^9 times greater than the output from an average loud-speaker (80 db). At this power, with a frequency of $3(10^8)$ cycles/sec, the amplitude of pressure in the medium is ± 5 atm, maximal acceleration 10^5 times gravity, maximal velocity 40 cm/sec, and radiation pressure 1,300 dynes/cm^2 = 0.0013 atm.

509. Effects Produced by Intense Ultrasonic Radiation. Although a few of the effects mentioned below had already been observed with oscillators of the Langevin type, it remained for Wood and Loomis to explore the possibilities of the new tool that had been placed at the disposal of science. The spectacular success of their experiments was due to the combination of great intensity with high frequency.

One of the most important consequences of this combination is the generation of large stresses in the irradiated medium, as the following considerations will show: As we saw in the preceding paragraph, extremely high accelerations are produced, with correspondingly large forces on the particles of the medium or on small objects immersed in it. These forces cause compressions and rarefactions in the medium, and since the wavelength is very small it is evident that the stresses are large.

An important result of the large stresses in the liquid is *cavitation.* Its presence in liquids traversed by ultrasonic waves was first investigated by Boyle and his associates. The term "cavitation" is applied both to the liberation from the liquid of bubbles of air or other absorbed

gases and to the tearing apart of the liquid itself with the production of hollow spaces filled with vapor. These hollow spaces, in the form of layers a wavelength apart, collapse with great violence, owing to the external pressure, as do also to some extent the bubbles of absorbed gas. Cavitation is accompanied by the generation of intense local electric fields, a process that is thought to account for the accelerating effect of intense ultrasonic fields on certain chemical reactions and also for the luminescence sometimes observed.

At pressure zero, and also under high hydrostatic pressure, there is no cavitation. The optimal pressure for pronounced cavitation effects is about 2 atm. At atmospheric pressure the effect sets in at a power of the order of 0.03 watt/cm^2.

Examples of the applications of intense ultrasonic waves are the production of finely dispersed emulsions; the destruction of bacteria and other biological effects; the acceleration of chemical reactions; the degassing of liquids; metallurgical applications; and the dissipation of fogs. Emulsification is feeble, and in some cases impossible, unless absorbed gas is present in the liquid medium.

510. The Ultrasonic Interferometer. The formation of stationary waves in air between a vibrating quartz plate and a reflecting surface was first observed by G. W. Pierce[424] in 1925, who measured wavelengths in air and CO_2 and made the first observation of the high absorption of CO_2 for ultrasonic waves. Pierce's method has been developed by J. C. Hubbard, W. H. Pielemeier, and others,[B5,B24] into an instrument of high precision for the measurement of the velocity and absorption of sound in gases and liquids.

511. Optical Effects of Ultrasonic Vibrations and Waves. The first optical method to be applied in the study of vibrating crystals was the piezo-optic effect, according to which the amount of light transmitted through an optical system containing a vibrating crystal between a polarizer and an analyzer varies with the strain in the crystal. By this means Tawil[505] in 1926 investigated the strains in a quartz bar, as already stated in §368. In the same paper he also foresaw the applications of optical effects in piezoelectric crystals to light relays and television. The piezo-optic method has been applied by Tawil[516] to the measurement or registration of very short time intervals; by R. A. Houstoun to the measurement of the velocity of light, following a suggestion originated by Grant; and by D. W. R. McKinley to the measurement of small optical activities; see also the paper by C. O. Browne.*

In Tawil's second method of observation[511] he used a vibrating quartz with frequency sufficiently high to produce in the surrounding air a

* The papers by the foregoing authors are listed at the end of the chapter.

system of very short waves. It has long been known that sound waves can be observed and photographed by taking advantage of the difference in refractive index between compressed and rarefied regions. This method, originated by Toepler and known as the "schlieren method," was applied to these ultrasonic waves by Tawil. For the lower frequencies he used a quartz-steel composite resonator. The schlieren method has been further developed and refined by Tawil and others, especially for investigating the sound field in the neighborhood of the emitter.

The idea that the closely spaced regions of condensation and rarefaction would make the medium serve as an *optical diffraction grating* occurred independently and almost simultaneously to Debye and Sears[122] and to Lucas and Biquard.[321] The simplest case is that of a transparent liquid in which a system of plane waves, either progressive or stationary, is generated. A collimated beam of light from a slit parallel to the wave fronts is passed through the liquid in a direction normal to the direction of propagation of the waves and becomes diffracted according to a law similar to that for the ordinary plane diffraction grating. When the emergent light is focused on a screen, a system of parallel lines is observed, consisting of a central image and on each side the spectra—or, in the case of monochromatic light, the diffraction lines—of various orders. The effect is easily demonstrated, with xylol as liquid, using thickness vibrations of an *X*-cut quartz plate or of an *L*-cut Rochelle-salt plate. A simple mounting for the crystal is that shown in Fig. 157*b*. From the frequency, the geometry of the system, and the spacing of the lines, the velocity of sound in the liquid and the adiabatic compressibility can be calculated.

512. The diffraction method has been extended and modified in many ways for special purposes and has become an important research tool. For its numerous applications and the literature to which it has given rise the references at the end of the chapter must be consulted. One great advantage of the method as compared with the interferometer is that results almost as accurate are obtained with very small samples of material in a very short time. By the use of high frequencies the wavelengths are so short that even in a specimen of volume no greater than a cubic centimeter the waves behave as if in an infinite medium, so that boundary conditions can be ignored.

Schaefer and Bergmann have applied the diffraction method with great success to the measurement of the elastic constants of transparent solids, both amorphous and crystalline. When the ultrasonic waves pass through a crystal, a diffraction pattern can be photographed that reveals the elastic symmetry of the crystal and also the presence of the three types of elastic waves that the crystal can transmit. From photo-

graphs made with the sound beam and the light in suitable orientations, all the elastic constants can be calculated. A cube of the material to be investigated is excited by a quartz plate cemented to one side or simply pressed against it with a layer of oil between. A frequency close to a resonant frequency of the quartz is selected, for which stationary waves are set up in the cube. Through the combined action of thickness and lengthwise motions of the quartz, all possible vibrational modes are excited in the cube.

Even in the case of *opaque* solids the elastic constants can be determined optically, as was proved by experiments by Schaefer and Bergmann after the theory of the method had been given by Ludloff. Advantage is taken of the fact that the surface of a solid subjected to ultrasonic radiation is set into a state of vibration, producing a characteristic diffraction pattern when a beam of light is reflected from it.

513. Piezoelectric Light Relays. The earliest use of a vibrating quartz crystal for controlling the intensity of a beam of light was made by Tawil, by both of the methods described in §511. The second method has been used in the design of a stroboscope for the observation of progressive waves.*

A more effective form of relay, first described independently by Biquard and by Karolus,† makes use of the diffraction effect described in §511. The light beam is passed through a liquid subjected to ultrasonic radiation, as in the Debye-Sears experiment. At zero amplitude all the light energy is in the central image (spectrum of zero order). With increasing amplitude the spectra of the first and higher orders grow in intensity at the expense of the central image. In the light relay the central image is cut out by a narrow opaque diaphragm, so that the amount of light transmitted depends on the total intensity in the portion that is diffracted. Thus the transmitted light is very nearly proportional to the amplitude of vibration of the crystal, and its intensity can be modulated by modulating the current that drives the crystal. For rapid modulation the vibrations of the crystal must be highly damped by the liquid. A liquid that combines good characteristics for this purpose with high transparency is carbon tetrachloride.

Piezoelectric relays have marked advantages over Kerr cells for controlling light beams. They respond well at higher frequencies; they can be used with ultraviolet light; and they require much less power, with lower voltages. Their chief limitation is that if the voltage on the crystal is to remain reasonably low the frequency must remain near resonance.

* Ref. B24, p. 210.

† P. Biquard, French patent 752,910 (1932); A. Karolus, U.S. patent 2,084,201 (1932).

Still another type of light relay, making use of the electro-optical effect in quartz, was described by Ardenne in 1939 (reference at end of chapter).

514. *Ultrasonics in Television Reception.* Television images formed on fluorescent screens by means of cathode rays are very limited in both size and brightness. All the light has to be produced by the rapidly moving cathode-ray beam, and the light from any one element of the picture is of very short duration. By using a powerful electric lamp as the light source and modulating the light beam in accordance with the television signals corresponding to the brightness of the various picture elements, the size and brightness of the television images can be vastly increased. One method of such light modulation, which makes use of an ultrasonic light modulator, is known as the Scophony Supersonic Television System and was originated by Jeffree.* A progressive train of waves is propagated along a column of liquid from a quartz plate at one end, as in the Debye-Sears experiment. At the other end of the column the waves are absorbed in order to prevent reflection and the formation of stationary waves. The quartz plate serving as emitter is driven approximately at its resonant frequency by a voltage that is modulated by the received signals. In the liquid there is then an ultrasonic carrier wave similarly modulated. To a given element of the picture there corresponds a short train of waves of a certain amplitude, which progresses with little attenuation along the column.

The light from the lamp, made parallel as it passes across the liquid cell in a direction parallel to the wave fronts, is diffracted. The central image is stopped out by a small barrier, so that only the diffracted light is transmitted; this light is approximately proportional to the amplitude of the quartz and therefore to the brightness of the picture element in question. At any instant different amounts of light are transmitted by different regions in the cell, corresponding to a series of successive picture elements. By means of a lens system an enlarged image of the cell is formed in a certain image plane on a viewing screen. As the wave train for a given element traverses the cell, the image that it produces sweeps across the viewing screen.

In order to fix the position of the individual picture elements on the viewing screen a small drum with a series of mirror faces around its periphery, rotated at high speed, is placed in the path of the light; the mirrors, by their rotation, reflect the light in such a way as to counteract the motion of the image and to hold each picture element at the right location on the line that is being projected onto the screen.

From the foregoing description it is seen that the image corresponding to a single picture element, instead of being projected onto the screen

* J. H. JEFFREE, ref. 20 at end of chapter.

only for the extremely short time during which the element is being received, continues to be projected during the entire time for the train of waves to run the length of the cell (of the order of one-fifth of a microsecond for a picture of 525 lines). During this time the image is "stored" in the cell and continues to contribute to the brightness of the picture. At any instant a large number of picture elements are thus stored simultaneously, corresponding to as much as an entire line across the screen.

In order to resolve the successive lines into the actual picture, a second mirror drum is used, revolving at relatively low speed.

The ultrasonic cells may have liquid columns from 2.5 to 10 cm in length. At an ultrasonic frequency of 18 megacycles/sec, the wavelength, when water is used as the liquid, is about 0.08 mm [velocity of sound in water about $1.5(10^5)$ cm/sec]. Several hundred picture elements may be stored simultaneously. For the high-speed mirror system a 30-sided polygon of stainless steel about 5 cm in diameter is used, rotated at 31,500 rpm for a picture of 525 lines. The 30 faces of the polygon are polished mirror surfaces, each about 5 by 3 mm. Glass polygons have also been used. Pictures up to 18 ft in width have been projected on screens in motion-picture theaters, using a high-intensity motion-picture arc lamp as light source. For further details and modifications the references at the end of the chapter may be consulted.

REFERENCES

The Use of Crystals in Filters

Books

Mason,[B35] Vigoureux.[B50,B51]

Starr, A. T.: "Electric Circuits and Wave Filters," Sir Isaac Pitman & Sons, Ltd., London, 1944, 475 pp.

Vilbig, Fritz: "Lehrbuch der Hochfrequenztechnik," Akademische Verlagsgellschaft m. b. H., Leipzig, 1937, 775 pp.

Periodicals

Bechmann,[37,38] Booth,[69] Booth and Sayers,[71] Mason,[332,334,339] Mason and Sykes,[342] Metschl,[365] Rohde,[436,437] Rohde and Handrek.[438]

Buckley, O. E.: The Evolution of the Crystal Wave Filter, *Jour. Applied Phys.*, vol. 8, pp. 40–47, 1937.

Builder, G.: Resistance-balancing in Wave Filters, *A.W.A Tech. Rev.*, vol. 3, pp. 83–100, 1938.

Burns, G. K.: Manufacture of Quartz Crystal Filters, *Bell System Tech. Jour.*, vol. 19, pp. 516–532, 1940.

Chakravarti, S. P., and N. L. Dutt: On a Wide Band-pass Effect in Crystals Associated with Negative-impedance Elements, and the Development of Wide-band Low-loss Crystal Band-pass filters, *Indian Jour. Phys.*, vol. 14, pp. 295–310, 1940.

D'Heedene, A. R.: Effects of Manufacturing Deviations on Crystal Units for Filters, *Bell System Tech. Jour.*, vol. 23, pp. 260–281, 1944.

Flint, W. A.: New Double-crystal Band-pass Filters, *Electronics and Television and Short-wave World*, vol. 13, pp. 552–554, 1940.

Gardiner, E. L.: Crystal Band-pass Filters, *Wireless World and Radio Rev. (London)*, vol. 43, pp. 382–384, 407–408, 447–448, 463–464, 1938; *T. and R. Bull. (London)*, vol. 15, pp. 75–79, 141–144, 178–179, 213–216, 251–253, 1939.

Hudec, E.: Calculation and Construction of a Quartz Bridge Filter, and Various Circuits for Quartz Bridge Filters, *Elek. Nachr.-Tech.*, vol. 18, pp. 265–276, 1941; vol. 19, pp. 16–25, 1942.

Kamayachi, Z, and T. Ishikawa: On Quartz Crystal Vibrators as Elements for Electrical Wave-filters, *Nippon Elec. Comm. Eng.*, no. 18, pp. 103–106, 1939.

Kamayachi, Z., and T. Ishikawa: Longitudinal Mode of Vibration, *Electrotech. Jour. (Japan)*, vol. 4, pp. 243–246, 1940.

Kautter, W.: Wide-band Adjustable Quartz Filters, *Telef. Hausmitt.*, vol. 18, pp. 42–50, 1937.

Knox, R. E.: The Use of Quartz Crystals in Wave Filters, *Electronics*, vol. 13, pp. 78*f.*, November, 1940.

Lane, C. E.: Limitations in Band Filter Design, *Bell Labs. Record*, vol. 16, pp. 56–61, October, 1937.

Lane, C. E.: Crystal Channel Filters for the Cable Carrier System, *Elec. Eng.*, vol. 57, pp. 245–249, 1938.

Mason, W. P.: Quartz Crystal Filters, *Bell Labs. Record*, vol. 13, pp. 305–311, 1935.

Mason, W. P.: Resistance Compensated Band-pass Crystal Filters for Use in Unbalanced Circuits, *Bell System Tech. Jour.*, vol. 16, pp. 423–436, 1937.

Pöhlmann, W.: Investigations of Crystal Band-pass Filters, *Telegraphen Fernsprech Tech. (Berlin)*, vol. 30, pp. 285–295 and 324–329, 1941.

Stanesby, H.: A Simple Narrow-band Crystal Filter, *Post Office Elec. Eng. Jour.*, vol. 35, pp. 4–7, April, 1942.

Stanesby, H., and E. R. Broad: A Narrow Band Filter Using Crystal Resonators, *Post Office Elec. Eng. Jour.*, vol. 33, pp. 176–182, 1941.

Waltz, W. W.: Crystal Filter Design, *Radio Engineering*, vol. 16, pp. 7–10 (January), 14–17 (Febuary), 16–17 (March), 12–14, (April), 1936.

White, G. J.: Crystal I.F. Coupling and Filters, *Proc. I.R.E. Australia*, vol. 1, pp. 50–56, 1938.

Willis, E. S.: Channel Crystal Filters for Broad-band Carrier Systems, *Bell Labs. Record*, vol. 17, pp. 62–65, 1938.

Wilson, J. E.: The Crystal Filter Treated as an Impedance Bridge Circuit, *Communications*, vol. 21, pp. 18, 20, April, 1941.

Crystal Filters for Receiving Sets

Books

"Documents du Comité Consultatif International des Radio Communications," 3ème réunion, Lisbon, 1934; Bern, 1935.

"Radio Amateurs' Handbook," American Radio Relay League, West Hartford, Conn.

Periodicals

Bacon, D.: Improving Crystal Filter Performance, *QST*, vol. 24, pp. 58*f.*, December, 1940.

BATCHER, R. R.: Application of Piezoelectric Crystals to Receivers, *Electronics*, vol. 3, pp. 57–58, August, 1931.

BENSON, J. E.: Crystal Control of the Mixer Oscillator in a Superheterodyne Receiver, *A.W.A. Tech. Rev.*, vol. 4, pp. 127–137, 1939; vol. 5, pp. 29–40, 1940.

BENSON, J. E.: A Note on the History of Piezoelectric Crystal Filters, *A.W.A. Tech. Rev.*, vol. 5, pp. 191–192, 1941.

BUILDER, G., and J. E. BENSON: Simple Quartz-crystal Filters of Variable Bandwidth, *A.W.A. Tech. Rev.*, vol. 5, pp. 93–103, 1941; also in *Wireless Eng. Exptl. Wireless (London)*, vol. 20, pp. 183–189, 1943.

COLEBROOK, F. M.: A Theoretical and Experimental Investigation of High Selectivity Tone-corrected Receiving Circuits, *Radio Res. Board, Nat. Phys. Lab., Spec. Rept.* 12, London, 1932.

CROSBY, M. G.: Communication by Phase Modulation, *Proc. I.R.E.*, vol. 27, pp. 126–136, 1939.

FISCHER, H. B.: A Crystal Control Superheterodyne Receiver, *Bell Labs. Record*, vol. 11, pp. 273–278, 1933.

GRAMMER, G.: A Crystal Filter and Noise-silencer for the "High-performance" Super, *QST*, vol. 20, pp. 28*f.*, October, 1936.

KAUTTER, W.: Quartz Filters with Continuously Variable Band Breadth, *Telefunken Z.*, vol. 18, pp. 22–41, 1937.

KEALL, O. E.: Analysis of Bridge Circuit for Piezoelectric Quartz Resonators, *Marconi Rev.*, no. 59, pp. 19–29, March–April, 1936.

LAMB, J. J.: Short-wave Receiver Selectivity to Match Present Conditions, *QST*, vol. 16, pp. 9–20, 90, August, 1932.

LAMB, J. J.: Developments in Crystal Filters for S-S Superhets, *QST*, vol. 17, pp. 21–24, November, 1933.

LAMB, J. J.: Receiver Selectivity Characteristics, *QST*, vol. 19, pp. 37–41, May, 1935.

LAMB, J. J.: A New I.F. Coupling System for Superhet Receivers, *QST*, vol. 21, pp. 28–30, April, 1937.

LAMB, J. J.: And Now We Have Full-range Superhet Selectivity, *QST*, vol. 21, pp. 16*f.*, June, 1937.

MILLEN, J., and D. BACON: Modern Design of High-frequency Stages for the Amateur Superhet, *QST*, vol. 19, pp. 13*f.*, January, 1935.

MIZOKAMI, K., and T. FUJITA: Automatic Tuning Control by Means of a Quartz Crystal, *Nippon Elec. Comm. Eng.*, pp. 443–444, November, 1937.

MORRISON, H.: Ten-frequency Receiver, *Bell Labs. Record*, vol. 19, pp. 307–309, 1941.

ORAM, D. K.: Full-range Selectivity with 455-kc. Quartz Crystal Filters, *QST*, vol. 22, pp. 33*f.*, December, 1938.

Radio News Staff: A Modern Receiver for Short Waves and "Ham" Communication, *Radio News*, vol. 16, pp. 603*f.*, 1935.

Radio News Staff: Ultra-selectivity with Crystal Filters, *Radio News*, vol. 15, pp. 477*f.*, 1934; vol. 16, pp. 603*f.*, 1935.

ROBINSON, J.: The Stenode Radiostat, *Radio News*, vol. 12, pp. 590*f.*, 1931. More on this device will be found in *Electronics*, *Radio News*, *Wireless Eng. Exptl. Wireless*, and *Wireless World* from 1931 on.

ROESCHEN, E.: Measurements and Investigations on Quartz Crystals for Receiver Control, *Elek. Nachr.-Tech.*, vol. 13, pp. 187–197, 1936.

THIELE, K.: New Developments for the Single-span Superheterodyne Receiver, *Funktech. Monatshefte*, January, 1938, pp. 19–23.

YODA, H., and B. KATO: Filters Employing YT-cut Quartz Plates, *Electrotech. Jour. (Japan)*, vol. 3, pp. 142–143, 1939.

ZIEGLER, A. W.: Channel Crystal Filters for Broad-band Carrier Systems: Physical Features. *Bell Labs. Record*, vol. 17, pp. 66–70, 1938.

ACOUSTIC APPLICATIONS OF CRYSTALS

CADY,[95] NICOLSON.[391]

ALDOUS, D. W.: A New Temperature-controlled Crystal Cutting-head, *Electronic Eng.*, vol. 14, p. 605, 1942.

BALLANTINE, S.: A Piezo-electric Loud Speaker for the Higher Audio Frequencies, *Proc. I.R.E.*, vol. 21, pp. 1399–1408, 1933.

BALLANTINE, S.: High Quality Radio Broadcast Transmission and Reception (Rochelle salt "sound-cell"), *Proc. I.R.E.*, vol. 22, pp. 564–629, 1934.

BEERWALD, P., and H. KELLER: Piezoelectric Crystal Elements for Electro-acoustical Purposes (including bimorph Rochelle-salt systems: equivalent circuits and quantitative results), *Funktech. Monatshefte*. no. 11, pp. 345–348, 1938.

BEERWALD, P., and H. KELLER: Theory and Practice of the Piezo-electric "Sound Cell" Microphone, *Funktech. Monatshefte*, no. 12, pp. 187–190, 1941.

BEGUN, S. J.: Some Problems of Disk Recording, *Proc. I.R.E.*, vol. 28, pp. 389–398, 1940; *Jour. Soc. Motion-Picture Eng.*, vol. 36, pp. 666–674, 1941.

BIRD, J. R.: Recent Improvements in Crystal Pickup Devices, *Proc. I.R.E.*, vol. 25, p. 660, 1937.

CELLERIER, J. F.: On the Scientific Analysis of Musical Sounds, *Compt. rend.*, vol. 190, pp. 45–47, 1930.

COOK, R. K.: Absolute Pressure Calibrations of Microphones (use of tourmaline disk), *Bur. Standards Jour. Research*, vol. 25, pp. 489–505, 1940.

ELLIS, W. G.: New Electrophones for High-fidelity Sound Reproduction, *Radio Eng.*, vol. 13, pp. 18*f.*, Oct. 1933.

FERRARI, A.: Problem of "Touch" in the Pianoforte, *Alta Frequenza*, vol. 4, pp. 582–602, 1935.

GOLDSMITH, F. H.: A Noise and Wear Reducing Phonograph Reproducer with Controlled Response, *Jour. Acous. Soc. Am.*, vol. 13, pp. 281–283, 1942.

KELLER, H.: The Piezoelectric "Flexural Strip" as Electromechanical Converter, *Hochfrequenztech. Elektroakustik*, vol. 60, pp. 5–10, 1942.

LYNCH, T. E., and S. J. BEGUN: General Considerations of the Crystal Cutter, *Communications*, vol. 20, pp. 9*f.*, Dec. 1940.

PIERCE, G. W.: The Songs of Insects, *Jour. Franklin Inst.*, vol. 236, pp. 141–146, 1943 (see also *Radio Rev. Australia*, vol. 5, p. 303, 1937).

SAWDEY, R. S., JR.: "Bimorph" Rochelle Salt Crystals and Their Applications, *Radio*, pp. 23*f.*, September, 1943.

SAWYER, C. B.: The Use of Rochelle Salt Crystals for Electrical Reproducers and Microphones, *Proc. I.R.E.*, vol. 19, pp. 2020–2029, 1931.

SCHAEFER, O.: The Electrical Equivalent Circuit of Piezoelectric Sound-Receivers, *Akust. Z.*, vol. 6, pp. 326–328, 1941.

SENGEWITZ, L.: The Rochelle Salt Crystal and Its Application in the Field of Telephony, *Elektrotech. Z.*, vol. 62, pp. 463–465, 1941.

SIVIAN, L. J.: Absolute Sound Pressure Measurements with Tourmaline (abst), *Jour. Acous. Soc. Am.*, vol. 92, p. 462, 1941.

SUGIMOTO, T.: Rochelle Salt Crystal Microphone and Under-water Acoustic Receiver, *Rep. Radio Research Japan*, vol. 6, absts. pp. 9–10, 1936.

TIBBETTS, R. W.: Rochelle Salt Crystal Devices of Low Impedance (loud-speaker and oscilloscope), *Electronics*, vol. 16, pp. 88*f.*, April, 1943.

VERMEULEN, R.: Perspectives in the Development of the Violin, *Philips Tech. Rev.*, vol. 5, pp. 36–41, February, 1940.

WILLIAMS, A. L.: Piezo-electric Loudspeakers and Microphones, *Electronics*, vol. 4, pp. 166–167, May, 1932; see also *Jour. Soc. Motion-picture Eng.*, vol. 25, pp. 196*f.*, 1934, and *Proc. I.R.E.*, vol. 23, pp. 1420–1421, 1935.

WILLIAMS, A. L., and J. P. ARNDT: Crystal Microphone Design for Single-direction Pickup, *Electronics*, vol. 8, pp. 242–243, August, 1935.

PIEZOELECTRIC TRANSDUCERS FOR THE MEASUREMENT OF PRESSURES, ACCELERATIONS, AND VIBRATIONS

AMBRONN, R.: A New Registering Acceleration Meter with Quartz Plates, *Z. Feinmechanik Präcision*, vol. 39, pp. 199–204, 1931.

ANDREEVSKI, N.: A Piezo-quartz Dynamometer for Measuring Impact Stresses, *Jour. Tech. Phys. (U.S.S.R.)*, vol. 9, pp. 680–686, 1939.

BARTELS, H.: Application of Piezoelectric Methods to the Measurement of Forces in Machines, *Werkstattstechn.*, vol. 31, pp. 187–188, 1937.

BAUMZWEIGER, B.: Application of Piezoelectric Vibration Pick-ups to Measurement of Acceleration, Velocity and Displacement, *Jour. Acous. Soc. Am.*, vol. 11, pp. 303–307, 1940.

BAXTER, H. W.: A Recording Instrument for Transient Pressures, *Electrician*, vol. 113, pp. 121–122, 1934.

BÉKÉSY, G. VON: On the Piezoelectric Measurement of the Absolute Threshold of Audibility in Bone Conduction, *Akust. Z.*, vol. 4, pp. 113–125, 1939.

BERNARD, P.: Reversibility of Piezoelectric Phenomena (quartz manometer), *Compt. rend.*, vol. 199, pp. 1388–1389, 1934; see also vol. 200, pp. 222–223, 1935.

BISANG, L.: On the Development of the Quartz Engine Indicator and Its Application, *Kraftfahrtech. Forschungsarb.*, no. 8, pp. 82–90, 1937 (Stuttgart).

BLOCH, A.: New Methods for Measuring Mechanical Stresses at Higher Frequencies, *Nature*, vol. 136, pp. 223–224, 1935; see also *Electronics*, vol. 8, pp. 212–213, 1935.

DAVY, N., J. H. LITTLEWOOD, and M. MCCRAIG: The Force-Time Law Governing the Impact of a Hammer on a Stretched String, *Phil. Mag.*, vol. 27, pp. 133–143, 1939.

EBIHARA, K.: Researches on the Piston Ring, *Sci. Papers Inst. Phys. Chem. Research (Tokyo)*, vol. 10, pp. 107–185, 1929.

ERVIN, C. T.: A Piezoelectric Gauge for Recording the Instantaneous Pressure in Shotguns, *Jour. Franklin Inst.*, vol. 213, pp. 503–514, 1932.

FAHRENTHOLZ, S., J. KLUGE, and H. E. LINCKH: Quartz Piezoelectric Pressure Gauges, *Physik. Z.*, vol. 38, pp. 73–78, 1937.

FEHR, R. O.: Quartz-crystal Accelerometer, *Gen. Elec. Rev.*, vol. 45, pp. 269–272, 1942.

GOHLKE, W.: Measurement of the Natural Frequency of Piezoelectric Pressure-measuring Devices, *Z. Instrumentenk.*, vol. 61, pp. 197–198, 1941; *Z. Ver. deut. Ing.*, vol. 84, pp. 663–666, 1940.

GOMEZ, M., and A. LANGEVIN: On the Use of Piezoelectric Quartz for the Study of Certain Biological Phenomena and Especially for the Study of Variations of Pressure in Blood Vessels, *Compt. rend.*, vol. 199, pp. 890–893, 1934.

GONDET, H., and P. BEAUDOUIN: Piezoelectric Vibrograph-Accelerograph, *Rev. gén. élec.*, vol. 37, pp. 499–508, 1935; see also *Génie civil*, vol. 109, pp. 552–554, 574–577, 1936.

GRAVLEY, C. K.: An Instrument for Measuring Surface Roughness, *Electronics*, vol. 15, pp. 70–73, 1942.

GUERBILSKY, A.: Piezoelectric Dynamometers of the Resonance Type, *Compt. rend.*, vol. 197, pp. 399–401, 1933.

HAYNES, J. R.: Apparatus for the Direct Measurement of Force/Displacement Characteristics of Mechanical Systems at Audio-frequencies, *Jour. Acous. Soc. Am.*, vol. 13, p. 332, 1942.

HELDT, P. M.: Piezoelectric Indicators, *Automotive Ind.*, vol. 70, pp. 657–658 and 660, 1934.

HELLMANN, R. K.: Piezoelectric Measuring Apparatus, *Archiv tech. Messen.*, vol. 85, J.766-1, 1938.

HERRMANN, A.: Piezoelectric Seismographs, *Beiträge angew. Geophysik*, vol. 4, pp. 296–301, 1934.

HERRMANN, A., and O. MEISSER: A Piezoelectric Acceleration-meter, *Z. Geophysik*, vol. 11, pp. 152–153, 1937.

HERRMANN, P. K.: Piezoelectric Measurement Apparatus (for engines), *A E G Mitt.*, no. 12, pp. 497–502, 1939.

HULL, G. F.: Some Applications of Physics to Ordnance Problems, *Jour. Franklin Inst.*, vol. 192, pp. 327–347, 1921.

IIDA, K.: Determining Young's Modulus and the Solid Viscosity Coefficients of Rocks by the Vibration Method, *Bull. Earthquake Research Inst. Japan*, vol. 17, pp. 79–91, 1939. (In English.)

ILLGEN, H.: Recent Applications of Piezoelectric Methods in Ballistics, *Z. tech. Phys.*, vol. 18, pp. 470–474, 1937.

JUNGNICKEL, H.: Piezoelectric Indicator for High-speed Internal-combustion Motors, *Z. Ver. deut. Ing.*, vol. 80, pp. 80–81, 1936.

KARCHER, J. C.: A Piezoelectric Method for the Instantaneous Measurement of High Pressures, *Jour. Franklin Inst.*, vol. 194, pp. 815–816, 1922.

KATO, Y., and S. NAKAMURA: On the Piezoelectric Accelerometer and Its Use in the Measurement of the Velocity of the Elastic Waves Produced by Artificial Shocks, *Sci. Repts. Tohoku Univ.*, vol. 19, ser. 1, pp. 761–772, 1930; *Proc. Imp. Acad. (Tokyo)*, vol. 6, pp. 272–274, 1930.

KELLER, H.[255]

KENT, R. H.: The Piezoelectric Gauge—Its Use in the Measurement of Gun Pressures, *Army Ordnance (Washington)*, vol. 18, pp. 281*f.*, 1938; see also *Trans. A.S.M.E.*, vol. 61, pp. 197*f.*, 1939.

KEYS, D. A.: Piezoelectric Method of Measuring Explosion Pressures, *Phil. Mag.*, vol. 42, pp. 473–488, 1921.

KLUGE, J., and H. E. LINCKH: The Measurement of Compression- and Acceleration-forces by Piezoelectric Methods, *Z. Ver. deut. Ing.*, vol. 73, pp. 1311–1314, 1929; see also vol. 74, p. 887, 1930; vol. 75, p. 115, 1931; also *Z. tech. Mechanik Thermodynamik*, vol. 2, pp. 153–164, 1931; *Arch. tech. Messen*, vol. 2, Lieferung 15, pp. V132–133, 1932; *Electrotech. Z.*, vol. 54, pp. 158–159, 1933; *Forsch. Gebiete Ingenw.*, vol. 2, pp. 153–164, 1931 (abst. in *Electronics*, vol. 3, p. 115, 1931), and vol. 4, pp. 177–182, 1933.

LANGEVIN, A.: The Use of Piezoelectric Quartz for the Study of Varying Pressures and Vibrations at High Frequencies, *Rev. gén. élec.*, vol. 37, pp. 3–10, 1935.

LANGEVIN, A., H. MURAOUR, and G. AUNIS: Study of Methods of Measuring Explosive Pressures, *Jour. phys. rad.*, vol. 7, pp. 448–452, 1936.

LAWSON, A. W., and P. H. MILLER, JR.: Piezometer for Transient Pressures (crystals of tartaric acid, tourmaline, and sucrose), *Rev. Sci. Instruments*, vol. 13, pp. 297–298, 1942.

LUND, H.: The Measurement of Accelerations of Motors, etc., by a Piezoelectric Equipment, *A E G Mitt.*, vol. 27, pp. 694–697, 1931.

MASON, C. A., and B. B. RAY: Piezoelectric Vibration Meter: Its Use for the Detection of Bearing Vibrations, *Electrician*, vol. 117, pp. 565–567, 1936.

MEURER, S.: Contribution to the Construction of Piezoelectric Indicators, *Forsch. Gebiete Ingenw.*, vol. 8, pp. 249–360, 1937.

MURAOUR, H., A. LANGEVIN, and G. AUNIS: Comparison of Pressure-Time Curves Derived: (a) from Fracture by the "Crusher"; (b) from Registration with a Piezoelectric Quartz, *Journal Physique*, vol. 7, pp. 450–452, 1936.

NIELSEN, H.: The Piezoelectric Indicator, *Arch. tech. Messen.*, vol. 5, pp. T9–10, J. 137-3, 1936.

NOLZEN, H.: Piezoelectric Pressure Measurement, *Deutsche Techniker*, vol. 6, pp. 4–6, 1938.

OKOCHI, M., S. HASHIMOTO, and S. MATSUI: High Speed Internal Combustion Engine and Piezoelectric Pressure Indicator, *Bull. Inst. Phys. Chem. Research (Tokyo)* vol. 4, pp. 85–97, 1925.

OKOCHI, M., and K. EBIHARA: "P.C.R." Piston Ring and the Packing Ring Tester, *Sci. Papers Inst. Phys. Chem. Research (Tokyo)*, vol. 6, pp. 67–80, 1927.

OKOCHI, M., and M. OKOSHI: New Method for Measuring the Cutting Force of Tools and Some Experimental Results, *Sci. Papers Inst. Phys. Chem. Research (Tokyo)*, vol. 5, pp. 261–301, 1927; see also vol. 12, pp. 167–192, 1930.

OKOCHI, M., and M. OKOSHI: Deflection of a Continuous Beam and Force Exerted on the Support by a Moving Load, *Bull. Inst. Phys. Chem. Research (Tokyo)*, vol. 7, pp. 659–667, 1928.

OKOCHI, M., and T. MIYAMOTO: Balancing Machine Utilizing Piezoelectricity, *Bull. Inst. Phys. Chem. Research (Tokyo)*, vol. 7, pp. 383–391, 1928; see also vol. 9, pp. 6–10, 1930.

RASUMIKHIN, V.: The Measurement of Alternating Pressure by the Piezoelectric Method, *Jour. Tech. Phys. (U.S.S.R.)*, vol. 8, pp. 447–452, 1938.

ROTHÉ, E.: Piezoelectric Quartz Seismograph, *Union géodés. géophys. intern., travaux scientifiques*, no. 15, pp. 152–164, 1937.

SAWDEY, R. S., JR.: Piezoelectric Surface Analyzer, *Radio*, March, 1943, pp. 20–23.

SCHILLING, W.: Vibration-width Amplitude and Vibration-Acceleration Measurements with Crystal Transmitter, *A E G Mitt.*, nos. 3–4, pp. 86–87, 1940.

SCOTT, H. H.: A General Purpose Vibration Meter, *Jour. Acous. Soc. Am.*, vol. 13, pp. 46–50, 1941.

SEIDL, F.: Piezoelectric Determination of the Breaking Strength of Thin Metal, Glass and Quartz Fibers, *Z. Physik*, vol. 75, pp. 735–740, 1932.

SEIFERT, E.: Piezoelectric Pressure Indicator, *Automobil tech. Z.*, vol. 40, pp. 144–146, 1937.

SIGRIST, W., and C. MEYER: Ballistic Investigation Employing a Recording Piezo-quartz Pressure Gauge, *Helv. Phys. Acta*, vol. 9, pp. 646–648, 1936.

TEICHMANN, H.: Methods for the Determination of the Velocity of Projectiles, *Electrotech. Z.*, vol. 58, pp. 627–628, 1937.

THOMPSON, L.: Shock Waves in Air and Characteristics of Instruments for Their Measurement (discharge of heavy artillery, use of quartz, Rochelle salt, and tourmaline), *Jour. Acous. Soc. Am.*, vol. 12, pp. 198–204, 1940.

THOMSON, J. J.: Piezoelectricity and Its Applications (quartz and tourmaline for explosion pressures), *Engineering*, vol. 107, pp. 543–544, 1919.

TSCHAPPAT, W. H.: New Instruments for Physical Measurements (pressure gauge for interior ballistics), *Mech. Eng.*, vol. 45, pp. 673–678, 1923; see also vol. 48, pp. 821–825, 1926.

WATANABE, S.: A New Design of Cathode Ray Oscillograph and Its Applications to Piezoelectric Measurements, *Sci. Papers Inst. Phys. Chem. Research (Tokyo)*, vol. 12, pp. 82–98, 1929; see also *Proc. World Eng. Congr., Tokyo*, vol. 5, Paper No. 632.

WATANABE, S.: Study on Impact Test by Means of Piezoelectric and Cathode Ray Oscillograph, *Sci. Papers Inst. Phys. Chem. Research (Tokyo)*, vol. 12, pp. 99–112, 251–267, 1929–1930; see also *Bull. Inst. Phys. Chem. Research (Tokyo)*, vol. 8, pp. 735–745, 1929.

WATSON, H. G. I., and D. A. KEYS: A Piezoelectric Method of Measuring the Pressure Variations in Internal Combustion Engines, *Can. Jour. Research*, vol. 6, pp. 322–331, 1932.

WEBSTER, R. A.: Piezoelectric Gauge and Amplifier (pile of 21 quartz plates, for pressures up to 30,000 lb/in.^{2}), *Jour. Franklin Inst.*, vol. 211, pp. 607–615, 1931.

WEBSTER, R. A.: Piezoelectric versus Mechanical Spring Pressure Gauge, *Jour. Applied Phys.*, vol. 10, pp. 890–891, 1939.

WOOD, H. O.: On a Piezoelectric Accelerograph, *Bull Seismol. Soc. Am.*, vol. 11, pp. 15–57, 1921.

YAMAGUCHI, K.: An Accelerometer Utilizing Piezoelectricity, *Bull. Inst. Phys. Chem. Research (Tokyo)*, vol. 8, pp. 157–163, 1929.

ZELLER, W.: Experimental and Theoretical Investigation of Vibration Meters for Traffic Vibrations, *Z. Bauwesen*, vol. 80, pp. 171–184, 1930.

MISCELLANEOUS APPLICATIONS OF PIEZOELECTRICITY

BAZZONI, C. B.: The Piezo-electric Oscillograph, *Radio News*, vol. 7, pp. 142–143, 233–237, August, 1925.

BECKER, H. E. R., W. HANLE, and O. MAERCKS: Modulation of Light by Means of a Vibrating Quartz, *Physik. Z.*, vol. 37, pp. 414–415, 1936.

CURIE, J., and P. CURIE: Hemihedral Crystals with Oblique Faces as Constant Sources of Electricity (Electrometer), *Compt. rend.*, vol. 93, p. 204, 1881 (also in "Œuvres," p. 22).

GALITZIN, B.: Apparatus for Direct Determination of Accelerations, *Proc. Roy. Soc., (London)*, vol. 95, p. 492, 1919.

GOLAY.[178]

GRUETZMACHER, J.: Piezoelectric Relays (Electrostatic Attraction between Vibrating Crystal and Its Electrode), *Arch. Elektrotech.*, vol. 30, pp. 122–126, 1936.

HARTLEY, J. J., and R. H. RINALDI: Demonstration of the Application of Piezoelectric Properties of a Rochelle Salt Crystal and the Three-electrode Valve to the Determination of Impact Stresses in Granular Material, *Proc. Phys. Soc. (London)*, vol. 38, p. 273, 1926.

HOUSTOUN, R. A.: A New Method of Measuring the Velocity of Light (Fizeau's method, using quartz crystal), *Nature*, vol. 142, p. 833, 1938; see also *Proc. Roy. Soc. Edinburgh*, A, vol. 61, pp. 102–114, 1941, vol. 62, pp. 58–63, 1943–1944, and *Phil. Mag.*, vol. 35, pp. 192–202, 1944.

HUBBARD, J. C.: The Crevasse Phenomenon in Piezoelectric Quartz and Its Application in Physical Measurements (ultramicrometer), *Jour. Acous. Soc. Am.*, vol. 10, pp. 87–88, 1938.

KAZANSKI, V.: A Piezo-quartz Oscillograph, *Jour. Tech. Phys. (U.S.S.R.)*, vol. 9, pp. 673–679, 1939.

MUTH, H., and H. ROOSENSTEIN: A Method of Generating Electric Waves (oscillations from powdered quartz particles), German patent 706,799 (1941); *Hochfrequenztech. Electroakustik*, vol. 59, p. 30, 1942.

MYERS, L. M.: A Piezoelectric Peak Voltmeter, *Marconi Rev.*, November–December, 1934, pp. 4–8.

OFFNER, F.: Recorder for Electrical Potentials. Damping of Piezo-electric Systems, *Jour. Applied Phys.*, vol. 11, pp. 347–352, 1940.

PHILIPPOFF, W. VON: The Piezoelectric Oscillograph, *Arch. tech. Messen*, vol. 2, p. 184, December, 1932; *Electrotech. Z.*, vol. 53, pp. 405–408, 1932.

PLASENCIA, H. T.: Spanish Standard for the Roentgen (piezoelectric device for standard charge), *Radiology*, vol. 34, pp. 82–94, January, 1940.

STEVENS, H. C., and J. M. SNODGRASS: A Piezoelectric Myograph (for measurement of contracting muscle), *Proc. Soc. Exptl. Biol. Med.*, vol. 30, pp. 939–943, 1933.

SYNGE, E. H.: Application of Piezoelectricity to Microscopy, *Phil. Mag.*, vol. 13, pp. 297–300, 1932.

TAKENAKA, S.: On a Piezoelectric Method for the Investigation of the Contraction of Muscles, *Japan. Jour. Phys.*, vol. 12, pp. 81–82, 1938.

TAWIL.[516]

TIBBETTS, R. W.: Rochelle Salt Crystal Devices of Low Impedance (loud-speaker and oscilloscope), *Electronics*, vol. 16, pp. 88*f.*, April, 1943.

WOLOGDIN, V.: Frequency Multiplication by Means of Condenser with Rochelle Salt Dielectric (makes use of non-linear properties), *Z. tech. Physik*, vol. 13, pp. 82–84, 1932.

WOOD, A. B.: The Piezoelectric Oscillograph, *Phil. Mag.*, vol. 50, pp. 631–637, 1925.

WOOD, A. B., G. A. TOMLINSON, and L. ESSEN: The Effect of the Fitzgerald-Lorentz Contraction on the Frequency of Longitudinal Vibration of a Rod (two quartz oscillators, one stationary and one rotating), *Proc. Roy. Soc. (London) A*, vol. 158, pp. 606–633, 1937.

WYNN-WILLIAMS, C. E.: A Piezoelectric Oscillograph, *Phil. Mag.*, vol. 49, pp. 289–313, 1925.

ULTRASONICS

Most of the literature down to 1938 is referred to in the books by Bergmann and by Hiedemann. The following references supplement them and include some of the more recent papers that are of interest from the standpoint of applied piezoelectricity.

Numbers in brackets apply to the special references below.

Books and General Articles. BERGMANN,[B5] HIEDEMANN,[B24] WOOD,[B55] BOYLE,[74] HUBBARD.[237] [15], [30], [34], [41], [42], [46], [51].

The Quartz "Sandwich" for Submarine Use. B51, [11], [23], [24].

Apparatus and Circuits. B5, B24, B35, B55, 145, 146, 192, 228, 445, 474, 511, [1], [5], [6], [7], [10], [25], [28], [31], [38], [40], [48], [49], [51].

Theory of the Ultrasonic Oscillator as a Transducer. B35, 474.

The Acoustic Field Close to the Crystal Oscillator. B5, B24, 145, 192, 422, 445, 511, [9], [22], [28], [36], [49].

Cavitation. [42].

The Ultrasonic Interferometer. 190, 236, 424, [12], [17], [18], [19], [37], [41].

Piezo-optic Effects. 505, 511, 516, [8], [16], [32], [33].

Diffraction Effects. 122, 321, [27], [42], [47].

Measurement of Velocities and Absorption. 145, 190, [1], [4], [13], [14], [25], [42], [45], [48], [50].

Measurement of Elastic Constants. [3], [13], [27].

Light Relays. 505, 511, [2], [21].

Television. B38, [2], [20], [29], [35], [39], [43], [44].

Ultrasonic Sounds in Nature. [26]; see also G. W. Pierce, The Songs of Insects, *J. Franklin Inst.*, vol. 236, pp. 141–146, 1943.

Special References

[1] ARDENNE, M. VON: The Construction of Apparatus for the Generation of Ultrasonic Waves, *Funktech. Mon.*, no. 8, pp. 285–288, 1935.

[2] ARDENNE, M. VON: A New Large-surface Light Relay for Intensity, Color, or Plane-of-polarization Control, *Telegraphen Fernsprech Tech. (Berlin)*, vol. 28, no. 6, pp. 226–231, June, 1939.

[3] BÄR, R.: Supersonic Measurement of Elastic Constants of Isotropic Solids, *Helv. Phys. Acta*, vol. 13, pp. 61–76, 1940.

[4] BENDER, D.: Ultrasonic Velocities in Nitrogen, Nitric Oxide, and Carbon Monoxide between 20° and 200°C, Measured by a New Process (Emission from Both Surfaces of Quartz Plate), *Ann. Physik*, vol. 38, pp. 199–214, 1940.

[5] BOSCH, W. C. and W. G. ALLÉE, JR.: Circuit Details for a Small Supersonic Oscillator of the Piezoelectric Type, *Am. Phys. Teacher*, vol. 6, pp. 272–273, 1938.

[6] BOYLE, R. W., J. F. LEHMANN, and S. C. MORGAN: Some Measurements of Ultrasonic Velocities in Liquids, *Trans. Roy. Soc. Can.*, vol. 22, sec. 3, pp. 371–378, 1928.

[7] BRIGGS, H. B.: A Supersonic Cell Fluorometer, *Jour. Optical Soc. Am.*, vol. 31, pp. 543–549, 1941.

[8] BROWNE, C. O.: Demonstration of High-frequency Fluctuations in the Intensity of a Beam of Light, *Proc. Phys. Soc. (London)*, vol. 40, p. 36, 1927.

[9] CEROVSKA, J.: Ultrasonic Optical Phenomena in the Circular Hole in a Quartz Plate, *Jour. Phys. rad.*, vol. 10, pp. 97–103, 1939.

[10] COCHRAN, D., and R. W. SAMSEL: Ultrasonics—A Method of Determining the Acoustic Properties, Absorption and Velocity, for Materials to be Used as Ultrasonic Windows, Lenses, and Reflectors, *Gen. Elec. Rev.*, vol. 47, pp. 39–41, 1944.

[11] FLORISSON, C.: Ultra-sound and Its Applications, *Bull. Soc. belge électriciens*, vol. 52, pp. 165–170, 263–278, 339–348, 1936.

[12] FOX, F. E.: Ultrasonic Interferometry for Liquid Media, *Phys. Rev.*, vol. 52, pp. 973–981, 1937.

[13] FOX, F. E., and G. D. ROCK: An Ultrasonic Stroboscope for Measuring Sound Wave-length in Liquids, *Rev. Sci. Instruments*, vol. 10, pp. 345–348, 1939.

[14] FOX, F. E., and G. D. ROCK: Ultrasonic Absorption in Water, *Jour. Acous. Soc. Am.*, vol. 12, pp. 505–510, 1941.

[15] FREEHAFER, J. E.: Supersonic Vibrations, *Newark Eng. Notes*, vol. 5, no. 1, pp. 18–19, December, 1941.

[16] GRANT, K.: High-frequency Interruption of Light, Nature, vol. 120, p. 586, 1927.

[17] HERGET, C. M.: A Constant Path Acoustic Interferometer for Gases at Variable Pressure, *Rev. Sci. Instruments*, vol. 11, pp. 37–39, 1940.

[17a] HOUSTOUN, R. A.: The Ultrasonic Diffraction Grating, *Phil. Mag.*, vol. 35, pp. 192–202, March, 1944.

[18] HUBBARD, J. C.: Sound Velocity and Absorption by Ultrasonic Interferometry, *Phys. Rev.*, vol. 59, p. 935, 1941.

[19] HUBBARD, J. C., and I. F. ZARTMAN: A Fixed Path Acoustic Interferometer for the Study of Matter, *Rev. Sci. Instruments*, vol. 10, pp. 382–386, 1939.

[20] JEFFREE, J. H.: The Scophony Light Control, *Television and Short-wave World*, vol. 9, pp. 260*f.*, 1936; see also Brit. patent 439,236 (1934).

[21] KHARIZOMENOV, V. K.: The Modulation of Light by Supersonic Waves, *Jour. Tech. Phys.* (*U.S.S.R.*), vol. 7, no. 8, pp. 844–860, 1937.

[22] LABAW, L. W.: Wave Front Determination in a Supersonic Beam (abst.), *Phys. Rev.*, vol. 66, p. 354, 1944.

[23] LANGEVIN, P.: Sounding by Means of Sound Waves, *Bur. hydrogr. internat., Spec. Pub.* 3, Monaco, 1924.

[24] LANGEVIN, P., and C. CHILOWSKY: Echo Sounding, *Nature*, vol. 115, pp. 689–690, 1925; also *Bur. hydrogr. internat., Spec. Pub.* 14, Monaco, August, 1926.

[25] LINDBERG, A.: Ultrasonic Absorption in Liquids, Measured Optically, *Physik. Z.*, vol. 41, pp. 457–467, 1940.

[26] LITTLE, E. P.: Supersonic Sounds in Nature, *Gen. Radio Experimenter*, vol. 9, pp. 5–8, February, 1935.

[27] LUDLOFF, H. F.: Ultrasonics and Elasticity, *Jour, Acous. Soc. Am.*, vol. 12, pp. 193–197, 1940.

[28] LYNN, J. G., R. L. ZWEMER, and A. J. CHICK: The Biological Application of Focused Ultrasonic Waves, *Science*, vol. 96, pp. 119–120, July, 1942; see also *Sci. American*, vol. 168, p. 115, March, 1943, and *Jour. Gen. Physiol.*, vol. 24, pp. 179–193, 1942.

[29] MAERCKS, O.: Ultrasonic Waves as Optical Shutter, *Z. Physik*, vol. 109, pp. 598–605, 1938.

[30] MAYBERRY, W.: Supersonics, *Electronics*, vol. 10, pp. 7–9, July, 1937.

[31] MCGRATH, J. W., and A. R. KURTZ: Isolation of an Ultrasonic Crystal Radiator from Conducting Liquids, *Rev. Sci. Instruments*, vol. 13, p. 128, 1942.

[32] MCKINLEY, D. W. R.: Application of Quartz Crystals to the Modulation of Light, *Can. Jour. Research*, sec. A, vol. 16, pp. 77–81, 1938.

[33] MCKINLEY, D. W. R.: Measurement of Small Optical Activities with the Quartz Crystal Light Modulator, *Can. Jour. Research*, vol. 17, pp. 202–207, October, 1939.

[34] METSCHL, E. C.: The Nature and Employment of Supersonic Waves (Survey), *Elektrotech. Z.*, vol. 60, no. 2, pp. 33–40, 1939.

[35] OKOLICSANYI, F.: The Wave-slot, an Optical Television System, *Wireless Eng. Exptl. Wireless* (*London*) vol. 14, pp. 527–536, October, 1937.

[36] OSTERHAMMEL, K.: The Optical Examination of the Sound Field of a Quartz Plate Oscillating as a Piston, *Akust. Z.*, March, 1941, pp. 73*f*.

[37] PIELEMEIER, W. H., H. L. SAXTON, and D. TELFAIR: Supersonic Effects of Water Vapor in CO_2 and Their Relation to Molecular Vibrations, *Jour. Chem. Phys.*, vol. 8, pp. 106–115, 1940.

[38] PITT, A., and W. J. JACKSON: Measurement of the Velocity of Sound in Low Temperature Liquids at Ultrasonic Frequencies, *Can. Jour. Research*, vol. 12, pp. 686–689, 1935.

[39] POGODAEV, K. N.: The Relationship between the Voltages Applied to a Quartz Crystal and the Light Intensity Distribution in the Diffraction Spectra Caused by the Supersonic Waves so Produced, *Jour. Tech. Phys.* (*U.S.S.R.*), vol. 11, pp. 474–478, 1941.

[40] PORTER, B. H.: The Supersonic Oscillator, *Ind. Eng. Chem.*, vol. 12, pp. 748–749, 1940.

[41] RICHARDS, W. T.: Recent Progress in Supersonics, *Jour. Applied Phys.*, vol. 9, pp. 298–306, 1938.

[42] RICHARDS, W. T.: Supersonic Phenomena, *Rev. Modern Phys.*, vol. 11, pp. 36–64, 1939.

[43] ROBINSON, D. M.: The Supersonic Light Control and Its Application to Television with Special Reference to the Scophony Television Receiver, *Proc. I.R.E.*, vol. 27, pp. 483–486, 1939; also papers by J. Sieger (pp. 487–492), G. Wikkenhauser (pp. 492–496), and H. W. Lee (pp. 496–500).

[44] ROSENTHAL, A. H.: Storage in Television Reception, *Electronics*, vol. 14, pp. 46*f.*, October, 1941; also *Electronic Eng.* (British), January, 1942, pp. 578*f.*

[45] SHAPOSHNIKOV, I. G.: The Propagation of Sound in a Crystal Possessing Piezoelectric Properties, *Jour. Exptl. Theoret. Phys. U.S.S.R.*, vol. 11, pp. 332–339, 1941.

[46] SIEGEL, S.: Review of Supersonic Methods for Measuring Elastic and Dissipative Properties of Solids, *Jour. Acous. Soc. Am.*, vol. 6, pp. 26–30, 1944.

[47] SMITH, A. W., and L. M. EWING: The Diffraction of Light by Supersonic Waves in Liquids; Apparatus for Demonstration and for an Intermediate Laboratory Experiment, *Am. Jour. Phys.*, vol. 8, pp. 57–59, 1940.

[48] TELFAIR, D., and W. H. PIELEMEIER: An Improved Apparatus for Supersonic Velocity and Absorption Measurements, *Rev. Sci. Instruments*, vol. 13, pp. 122–126, 1942.

[49] TUMANSKI, S. S.: The Generation of Supersonic Oscillations by Piezo-quartz Lenses, *Jour. Tech. Phys.* (*U.S.S.R.*), vol. 7, pp. 2049–2052, 1937.

[50] WILLARD, G. W.: Ultrasonic Absorption and Velocity Measurements in Numerous Liquids, *Jour. Acous. Soc. Am.*, vol. 12, pp. 438–449, 1941.

[51] ZWIKKER, C.: Oscillating Quartz Crystals and Their Use in Ultra-acoustics, *Nederland Tijdschr. Natuurkunde*, vol. 8, pp. 311–326, 1941; *Tijdschr. Nederland Radiogen.*, vol. 9, pp. 107–122, 1941.

CHAPTER XXIX

PYROELECTRICITY

Un phénomène a au moins la symétrie de ses causes, mois il peut être plus symétrique.
—PERRIER and DE MANDROT.

515. The early history of pyroelectricity has already been sketched in Chap. I. Among later investigators, both experimental and theoretical, may be mentioned Friedel and J. Curie (who in 1883 first recognized the distinction between the effects of uniform and non-uniform heating), Ackermann, Boguslawski, Gaugain, Hankel, Hayashi, Traube, Kundt, Riecke, Röntgen, and Voigt. References to some of these, as well as to other authors mentioned in the text, are at the end of the chapter.

Pyroelectricity can mean any one of several things. First one must distinguish between *vectorial* and *tensorial* pyroelectricity. Vectorial pyroelectricity is the type usually encountered, and it forms the chief subject matter of this chapter. Mathematically, it is a relation between a scalar (temperature) and a vector (polarization). Physically, it is *the change with temperature of positive and negative polarization charges on certain portions of crystals belonging to certain classes.* This phenomenon is the *direct* pyroelectric effect, represented by the arrow $\vartheta \rightarrow P$ in Fig. 10. The *converse,* or electrocaloric, effect, described in §523, is represented by the arrow $E \rightarrow \delta Q$.

The practically negligible tensorial effect is described in §525.

The vectorial effect is complicated by the fact that every pyroelectric crystal is also piezoelectric: a change in temperature of an unconstrained crystal causes a deformation, and this in turn produces a secondary polarization of piezoelectric origin superposed on the primary pyroelectric polarization. The terms *primary* and *secondary* are preferable to the commonly employed "true" and "false." Primary pyroelectricity is that which would be observed in a completely clamped crystal.

The secondary pyroelectric effect must be subdivided according to whether the heating is uniform or not. For non-uniform heating the term "false pyroelectricity of the first kind" has sometimes been used, while the secondary effect of uniform heating has been called "false pyroelectricity of the second kind." We shall restrict the term *secondary* to the effect of the "second kind," and for the case of non-uniform heating we suggest the term *tertiary pyroelectricity,* although it is only a special manifestation of the secondary type.

The distinction is by no means trivial. All the 10 classes listed below that possess *primary* pyroelectricity are of course subject also to secondary and tertiary effects. On the other hand, those crystals, like quartz, which are not included in any of these 10 classes can show only the *tertiary* effect. They become polarized by heating or cooling only in those regions where there is a *temperature gradient.* The reason follows from the fact that such crystals do not, like those in the 10 classes of "true" pyroelectricity, have a single unique polar axis (the direction of the spontaneous polarization). For example, quartz has three equivalent polar axes, but no one of them is unique. Although the application of a scalar agent, like uniform heating, cannot give rise to a polarization in a unique direction, still the *gradient* of temperature is a vector quantity, which can produce a polarization dependent on the direction of the gradient.

In interpreting the extensive literature on pyroelectric observations it is important to keep these distinctions in mind. Only rarely does uniform heating seem to have been employed in qualitative observations. The observed results have therefore in most cases been due largely, if not chiefly, to the tertiary effect, proving merely that the crystals were piezoelectric. Too often has there been reason to suspect that spurious effects of frictional electricity or of a layer of ions deposited from the flame or other heating agent may have been mistaken for pyroelectricity. Even when all spurious effects have been eliminated, one cannot expect more than crude qualitative results unless the specimen is of a definite geometrical form (parallelepiped or sphere), free from defects, cracks, and twinning, and cut in a known orientation with respect to the crystal axes.

It is not even certain that the primary effect is strong enough to be observed in any crystal. Its separation from the secondary effect is extremely difficult, requiring a precise knowledge of the elastic and piezoelectric constants (§520).

516. Theory of the Vectorial Pyroelectric Effect. In its broadest sense the vectorial effect includes primary, secondary, and tertiary pyroelectricity and the converse, or electrocaloric, effect. The theory as presented here does not include the tertiary type. The primary and secondary effects may theoretically be present in the following 10 classes, designated by $\underline{P}$ in Table I: Classes 1, 3, 4, 7, 9, 10, 16, 19, 23, and 26, with symmetries C_1, C_2, C_{1h}, C_{2v}, S_4, C_4, C_3, C_{3v}, C_6, and C_{6v}. In these classes the symmetry is such that there is a single polar, or "electric," axis, with the possibility of a permanent (spontaneous) polarization along this axis.*

* In Voigt's "Lehrbuch," p. 252, the number of pyroelectric classes is erroneously stated as eleven instead of ten.

In the present treatment we shall follow the method initiated by Lord Kelvin and adopted by Voigt, according to which a pyroelectric crystal behaves as if it had a spontaneous polarization, the variation of which with temperature constituted the primary pyroelectric effect. That this is not the only possible hypothesis will be seen in §545.

Following the same procedure as with elastic and piezoelectric phenomena, we take as starting point for the formulation of the direct and converse pyroelectric effects Eq. (1). It is found experimentally, at least within small ranges of temperature, that the polarization charges on a pyroelectric crystal are proportional to the change in temperature $\Delta T \equiv \vartheta$. The crystal is assumed to be uniformly heated so that there is no temperature gradient at either the initial or the final temperature. At the initial temperature the polarization charges are assumed to have been neutralized by slow leakage or by artificial means, so that the entire surface is at zero potential. The charges are due to a change with temperature of the polarization, the constant of proportionality being p_m.

The derivative of the energy ζ per unit volume, given in Eq. (1), is to be taken with respect to E and T. The latter derivative leads to the electrocaloric effect (§523). Considering E first, we have (see §105)

$$\frac{\partial \zeta}{\partial E_m} = P_m = \sum_k^3 \eta'_m E_m - \sum_h^6 d_{mh} X_h + \vartheta p'_m \tag{544}$$

where p'_m is the primary pyroelectric constant.

In the dielectric term, E_m is a component of any stray field, including the depolarizing field due to the polarization charges.

In Eq. (544), X_h is a component of the stress due to change in temperature. According to Eqs. (6) we write $X_h = -\sum_i^6 c^E_{ih} x_i$. Since x_i is a component of the thermal expansion, we have $x_i = \vartheta a_i$. Then from Eq. (191) the piezoelectric term in Eq. (544) becomes $-\vartheta \sum_i^6 e_{mi} a_i$.

When the pyroelectric constant is determined experimentally, the field E_m can be eliminated by suitable compensation. Hence in the following the first term in Eq. (544) is omitted. P_m is then due to the combined effects of stress and temperature change. Equation (544) now becomes, on writing ΔT for ϑ,

$$\Delta P_m = \Delta T \left(\sum_i^6 e_{mi} a_i + p'_m \right) \equiv \Delta T (p''_m + p'_m) \tag{545}$$

where $p''_m \equiv \sum_i^6 e_{mi}a_i$ is a component of the pyroelectric constant due to strain. This piezoelectric contribution to the total pyroelectric polarization is the secondary pyroelectric effect, illustrated in Fig. 10 by the path $\vartheta \rightarrow x \rightarrow P$. The primary pyroelectric effect, independent of the effects of strain, is illustrated by the path $\vartheta \rightarrow P$.

We shall call $p_m \equiv p'_m + p''_m$ the *total* pyroelectric constant, where p'_m and p''_m are the primary and secondary constants for the m-direction and m is the direction of one of the crystallographic axes X, Y, Z. p_m does not include the tertiary effect, since uniform heating is assumed. In the most general case the values for $m = 1$, 2, and 3 all differ from zero, and the direction of the "pyroelectric axis," as well as the magnitude of p_m, varies with temperature. Those crystals for which p_m has been measured, including tourmaline and Rochelle salt, have, at least for the primary effect, only a single value of m.

The pyroelectric coefficient p_m has the dimensions (electric moment per unit volume) per degree change in temperature. p_m is positive when an increase in temperature causes a pyroelectric polarization in that direction which is adopted as positive for the crystal in question.

The equation for p_m follows from Eq. (545):

$$p_m = p'_m + p''_m = \frac{\Delta P_m}{\Delta T} \tag{546}$$

In experimental work if the counterpolarization due to the field created by the polarization charges [first term in Eq. (544)] is not compensated, the observed p_m will be too small. A calculation of the correction for E_m would be difficult, as it depends in a complicated manner on boundary conditions.

517. Tourmaline. Tourmaline has been the object of more study than any other pyroelectric crystal. Considering the variable composition of this crystal (§13) it is surprising that the quantitative results by different investigators and with different specimens show so little variation. It is commonly found that the pyroelectric constant is lower for dark than for light varieties and that the conductivity of black tourmaline is so great that no pyroelectric observations can be made with it. The largest values are observed with pink varieties (Ackermann, Hayashi).

At ordinary temperatures the analogous end (§13) becomes positive on heating. The direction of the spontaneous polarization is from the analogous to the antilogous end, so that heating *decreases* the spontaneous polarization.

The pyroelectric property can be demonstrated in several ways. In all such tests the surface of the crystal should be clean and dry.

1. Kundt's method, by sprinkling over the heated crystal a mixture of powdered sulphur and red lead,* or Bürker's powder.† Positive regions become yellow; negative regions, red. These charged regions are at the ends of the crystal, but they are also detected wherever there are cracks along the sides, owing to local strains.

2. An "electric compass" can be made by suspending an elongated specimen horizontally from a fine thread or fiber, subjecting it to a change in temperature, and holding it near a charged body or between the plates of a condenser connected to an electrostatic machine.

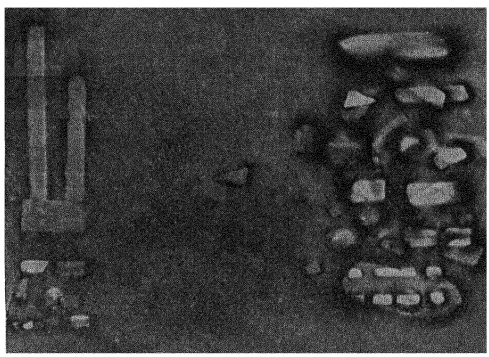


FIG. 158.—Dust patterns from tourmaline crystals. The photograph shows a portion of a white painted shelf in a mineralogical cabinet at Wesleyan University after the tourmalines had been removed. The crystals had lain undisturbed for many years, except that on one occasion they were rearranged, thus accounting for the overlapping effects. A long cyrstal near the border of the picture had been broken into several segments, to the ends of which the dust particles were attracted.

3. When a crystal has been cooled in liquid air, ice filaments from the moisture of the air in the room form at the two ends, like iron filings at the ends of a magnet. Small particles of ice sometimes shoot from one end to the other.‡

Even the small fluctuation in temperature of the air in a room will in time cause dust figures at the ends of tourmaline crystals. An instance of this effect is shown in Fig. 158. Particles of dust tend to move into regions where the electric field is strongest. On touching a crystal, they are repelled, like pith balls from a rubbed rod, and lodge on the adjacent portion of the shelf.

If a tourmaline crystal is laid on a white card in a location in the room where the air is comparatively stagnant but subject to ordinary variations in temperature, a faint smudge on the card begins to be visible at the ends of the crystal in a few months.

Numerical data on tourmaline are considered below.

* For details see the "Lehrbuch," p. 230.

† K. BÜRKER, *Ann. Physik.*, vol. 1, p. 474, 1900. 1 part carmine and 5 parts sulphur are rubbed together and then mixed with 3 parts lycopodium (by volume). See "Lehrbuch," p. 232.

‡ L. BLEEKRODE, *Ann. Physik.*, vol. 12, pp. 218–223, 1903; M. E. MAURICE, *Proc. Cambridge Phil. Soc.*, vol. 26, pp. 491–495, 1930; C. M. FOCKEN, *Nature*, vol. 129, p. 168, 1932. Miss Maurice also found that a tourmaline heated to 140°C, discharged by passing it through a flame, and then allowed to cool in a smoke of NH_4Cl showed the formation of similar filaments.

518. Pyroelectric Constants of Various Crystals. Quantitative measurements have been made by a number of observers, notably Ackermann,[1] Hayashi,[210] Riecke,[B20] Röntgen,[439] and Veen.[563] References to their work and that of others, including qualitative results, are given in the "International Critical Tables."[B29,*] Only a few outstanding results need be discussed here.

The most complete investigation is that of Ackermann. Over a range of temperature extending in some instances from −250° to +375°C he measured p_m (primary plus secondary effects; care was taken to have the temperature always uniform) for tourmaline, lithium sulphate, lithium selenate, potassium tartrate, lithium trisodium selenate, potassium lithium sulphate, ammonium tartrate, lithium sodium sulphate, and strontium acid tartrate. In all cases p_m appeared to approach zero at the absolute zero of temperature. With increasing temperature p_m increased slowly at first, then more rapidly, and in some cases it approached a saturation value at the highest temperatures. The theory of Ackermann's results has been treated by Boguslawski,[60,61] who discusses the similarity of the p_m: T curves to the curves relating temperature to specific heat and coefficient of thermal expansion. The work of both Ackermann and Boguslawski was discussed later by Born.†

All numerical values given below are in cgs electrostatic units.

519. *Tourmaline.* The pyroelectric axis is in the Z-direction; hence the symbol p signifies p_3.

The following values of p are from Ackermann:

Temperature, deg C	Color		
	Yellow-green	Rose-red	Blue-green
−250	0.08	0.08	0.04
+ 20	1.28	1.31	1.06
+648	1.86	1.94	1.52

Hayashi's results, at 18°C, are in good agreement with Ackermann's. He finds for a yellow-green crystal $p = 1.275$; pink, 1.324; blue-green,

* The section on Electroelastic and Pyroelectric Phenomena in the "International Critical Tables" was published also in *Proc. I.R.E.*, vol. 18, pp. 1247–1262, 1930. In the references at the end of these publications the following errors occur: ref. (43.5) should be the same as (43), in which the year should be 1882, not 1884. In the "International Critical Tables" are also these further errors, which were corrected in the *Proc. I.R.E.*: ref. (18), the pages should read "444, 471"; Ref. (39) should read "vol. 46, p. 607, 1928." The *Proc. I.R.E.* version has an error in ref. (80), in which the journal reference should be to 188 (*Nachr. Göttingen Math.-physik. Klasse*) instead of 88.

† M. Born, *Physik. Z.*, vol. 23, pp. 125–128, 1922.

1.057. Both Hayashi and Ackermann, whose work was done under Voigt, used Brazilian tourmalines.

Röntgen observed from −252.5 to +40.5°C with a light-green Brazilian crystal. His results, obtained from crystals of various colors, are in general somewhat lower than Ackermann's. At room temperature the light-green specimen gave $p = 1.03$.

Riecke[B20] measured p and its temperature coefficient in the neighborhood of room temperature, for several Brazilian crystals. From the average of his results Voigt derived the equation

$$p = 1.13 + 0.0104(t - 18°\text{C}).$$

In Voigt's "Lehrbuch,"* is the statement, based on the data then available, that p changes sign at the temperature of liquid air. This statement is evidently not confirmed by the measurements of Ackermann and of Röntgen, which were made a few years after the appearance of the "Lehrbuch."

The spontaneous polarization of tourmaline. When a tourmaline crystal is broken across the Z-axis, a little time must always elapse before the charges are compensated by conduction effects. The main experimental support of the hypothesis of a permanent spontaneous polarization P^0 is the fact that the charges thus observed are proportional to the area exposed and independent of the length of the segment.

Voigt estimated the value of P^0 at 24°C by quickly immersing the two parts, into which a crystal had just been broken, in mercury cups connected to an electrometer. In cgs electrostatic units the value was found to be about 33. According to Voigt's view, this value is only a lower limit, especially since tourmaline does not show distinct cleavage, so that on different portions of a surface of fracture there may be ultimate charges of opposite signs. In contrast with this view is Larmor's theory of pyroelectricity, treated in §545.

520. *Does Tourmaline Possess Measurable Primary Pyroelectricity?* With any crystal that theoretically possesses primary pyroelectricity, the answer to the question concerning the relative magnitudes of the primary p'_m and the secondary p''_m requires the evaluation of the piezoelectric term in Eq. (545). It is therefore necessary to know the piezoelectric, elastic, and thermal-expansion constants, as well as the total p_m, and these should be measured on the same specimen, or at least on specimens from the same mother crystal.

In general, the principal uncertainty may be expected to lie in the observation of the total pyroelectric constant p_m. If the primary p'_m is small, a slightly too low value of p_m may be sufficient to lead to the conclusion that p'_m is altogether negligible.

* P. 245.

Voigt's measurements in 1898[570] with tourmaline indicated that the primary effect contributed about one-fifth of the total pyroelectric constant.* In 1914, Röntgen, on the basis of his observations quoted above, in which p_m was found to be relatively low, came to the conclusion that all the observable pyroelectricity in tourmaline is secondary. This conclusion was promptly contested by Voigt,[572] who still defended his former observations. The matter was later discussed by Lindman,† whose measurements of the coefficients of expansion, when substituted for those used by Voigt, led to the conclusion that about 12 per cent of the total effect is primary. On the whole, the best evidence at present favors the view that the part played by the primary effect in tourmaline, though small, is not negligible.

521. *Rochelle Salt.* As we have said in Chap. I, the pyroelectric effect in Rochelle salt was discovered by Brewster.‡ Qualitative tests have also been reported by Hankel and Lindenberg, Valasek, and Körner.§ The only quantitative experiments are those of H. Mueller and his pupils. A general account of the subject is given by Mueller,[382] on which most of the following statements are based.

It is only between the Curie points, where Rochelle salt is monoclinic, that there can be primary pyroelectricity, and even here the recorded effects are chiefly due to secondary pyroelectricity, influenced possibly also by the tertiary type.

Pyroelectric tests offer the most convincing proof of the existence of domains of opposite sign in Rochelle salt, as well as a means for estimating their size and distribution and the magnitude of the spontaneous polarization P_x^0.

Qualitative tests have been made by Dr. Jaffe and the author, both on complete crystals a few centimeters in size, of the form shown in Fig. 2, and on X-cut plates. Best results are obtained on heating rather than on cooling, probably owing to the avoidance of the condensation of moisture that takes place on cooling. After the crystal has been kept for 2 hr or more at a cool temperature (15 to 20°C), it is heated approximately to the Curie point and then dusted with the mixture of sulphur and red lead.

In the case of an *entire crystal*, the Z-axis should be vertical. The c-face may or may not show a pattern. That which is characteristic is the alternate stripes of red and yellow along the prismatic faces,

* For details see the "Lehrbuch," p. 924.

† K. F. LINDMAN, *Ann. Physik*, vol. 62, pp. 107–112, 1920. See also Geiger and Scheel, ref. B19, vol. 13, p. 315.

‡ D. BREWSTER, *Edinburgh Jour. Science*, 1824.

§ W. G. HANKEL and H. LINDENBERG, *Sächs. Abh.*, vol. 18, pp. 359–406, 1892; J. VALASEK;[543] H. KÖRNER, *Z. Physik*, vol. 103, pp. 170–190, 1936.

parallel to the Z-axis. Corresponding stripes, with colors interchanged, can often be identified at opposite ends of the X-axis. The indication is that the domains tend to be in the form of laminae from 1 to 8 mm thick in the Y-direction and 1 cm or more in extent parallel to X and Z. Different tests on the same specimen give essentially the same pattern.

A small *X-cut plate* 1 cm or so in size may well consist of a single domain. Larger plates may show a checkerboard pattern, each element of which on one side has its counterpart, with opposite sign, on the other side.

The dust patterns offer convincing evidence of a permanent polarization in the X-direction, present only between the Curie points. The sense of the polarization, for each domain, cannot be permanently reversed even after the crystal has been cooled from a high temperature while in a strong opposing electric field or heated almost to the disintegration point between successive tests.

The total pyroelectric constant p and its dependence on temperature have been measured by L. Tarnopol and by H. O. Saunders in Prof. Mueller's laboratory, using a modification of Ackermann's method. Small crystals gave results agreeing within 20 per cent. The constant has upper limits of opposite sign at the Curie points, decreasing to zero and changing sign at about 5°C.

By means of Eq. (546), using the value of p observed for a series of small values of ΔT between the Curie points, one can construct a curve relating P^0 to T. It is here assumed that $P^0 = 0$ at each Curie point. By this process Mueller[376,382] found good agreement with the P^0:T curve in Fig. 147.

The maximum value of P^0 in Rochelle salt, about 640, is more than ten times that which Voigt estimated for tourmaline. To produce such a polarization by an external field in an ordinary insulator of low dielectric constant would require a field of the order of 1,000,000 volts/cm.

The primary pyroelectric effect in Rochelle salt. Data are not available for a precise determination of the relative values of p_x' and p_x'' (Eq. (545)) such as Voigt attempted in the case of tourmaline. Nevertheless, a rough estimate can be made, which is perhaps worth while even if not yet conclusive. When applied to Rochelle salt, Eq. (545) becomes

$$\frac{\Delta P_x^0}{\Delta T} = e_{14}a_{14} + p_x'$$

For small ΔT, $\Delta P_x^0/\Delta T$ can be found from the slope of the curve for P_x^0 in Fig. 147. e_{14} is taken from Fig. 146. a_4 is the thermal coefficient of the shear y_z. It can be calculated from the rate of change of the spontaneous strain y_z^0 with temperature. We take Mueller's value $y_z^0 = 10.9(10^{-4})$ at 0°C from §482 and assume that the curve relating y_z^0 to temperature is similar to that for P_x^0.

In this manner we find, for small ΔT in the neighborhood of 18°C,

$$p_x = \Delta P_x^0/\Delta T \approx 50; a_4 \approx 4.5(10^{-5}); e_{14} \approx 9.1(10^5); e_{14}a_4 = p_x'' \approx 41;$$

and finally $p_x' = p_x - p_x'' \approx 9$.

While this calculation is necessarily crude and the fact that the ratio p_x'/p_x is nearly the same as that which Voigt found for tourmaline is obviously only a coincidence, still it is an indication that the greater part of the pyroelectricity of Rochelle salt is secondary.

522. Other Crystals. *Zinc Sulphide.* This substance is mentioned partly to correct an error in the "International Critical Tables,"* where it is indicated that sphalerite is both piezoelectric and pyroelectric. Zinc sulphide exists in two modifications. Wurtzite, or α-ZnS, crystallizes in the hexagonal hemimorphic Class 26, symmetry C_{6v}. It is stable above 1020°C and metastable below. Sphalerite, or β-ZnS, also called zinc blende, crystallizes in the cubic hemimorphic Class 31, symmetry T_d. It is the more common form, stable at ordinary temperature.† Thus, while both forms are piezoelectric, only wurtzite is pyroelectric. If Veen's value of $p = 0.13$, cited in the "International Critical Tables," was obtained with sphalerite, he must have used non-uniform heating.

Quartz does not belong to a pyroelectric class; hence it possesses only tertiary pyroelectricity, which is observed on non-uniform heating. The direction of the temperature gradient must always be considered in interpreting the pyroelectric patterns on quartz shown in some books. Any results observed on uniform heating must be attributed to causes other than pyroelectricity, as when Röntgen[439] traced his results to expansion of the silver coating on his crystal. The precautions that should be observed in pyroelectric tests of quartz have been described by Van Dyke.[558]

Topaz is usually classified as rhombic holohedral, symmetry V_h, and as such it should posses neither piezo- nor pyroelectricity. Nevertheless, various authors have reported pyroelectric properties, with such qualifications as that the properties are "confused and uncertain" and that different specimens have polar axes in different directions.‡ The last statement suggests that if topaz is pyroelectric at all the effect is tertiary, dependent on the direction of the temperature gradient, and that Neumann's principle may be invoked for placing topaz in Class 6, symmetry V, like Rochelle salt outside the Curie points. One may also raise the

*Vol. 6, p. 210.

† On the two types of ZnS see Geiger and Scheel, ref. B19, vol. 24, part 2, p. 269, 1933.

‡ See, for example, N. A. Alston and J. West, *Proc. Roy. Soc.* (*London*) (*A*), vol. 121, pp. 358–367, 1928.

question whether the irregular pyroelectric results, together with the externally holohedral form, may not be the result of twinning.*

It is well recognized that the discordant results with certain crystals, for example *picric acid*, are due to varying degrees of twinning.† The same is true of *axinite*.‡

Among the papers of recent years should be mentioned those by Martin and by Orelkin and Lonsdale,§ which describe the experimental technique as well as the results with various crystals.

A practical application of pyroelectricity in the detection of feeble radiation, especially in the infrared, has been proposed by Yeou Ta.‖ From his experiments with tourmaline and with tartaric acid,¶ which is several times as strongly pyroelectric as tourmaline, Ta finds that he can detect an increase in the temperature of the radiated face of the crystal as small as (10^{-6})°C.

523. The Electrocaloric Effect. When Lord Kelvin applied the principles of thermodynamics to the pyroelectric effect in 1877, he was led, on the assumption of reversibility, to predict the converse effect. This is the electrocaloric effect, or the change in temperature of a pyroelectric crystal caused by a change in the electric field. Like the magnetocaloric effect (§556) it is very minute and is mentioned here chiefly because of its relation to the properties of Rochelle salt.

We seek an expression for $\partial T/\partial E$ in terms of the pyroelectric coefficient $p = \partial P/\partial T$. The change in energy per unit volume accompanying small variations in the electric and thermal conditions is the exact differential $dU = E\,dP + T\,dS$ where S is the entropy. From this expression one finds, in terms of density ρ, mechanical equivalent

$$J = 4.18(10^7)$$

and specific heat C in joule gm^{-1} deg^{-1}, the following equation for the electrocaloric coefficient q:

$$q = \frac{\partial T}{\partial E} = \frac{-pT}{\rho C J} \text{ deg statvolt}^{-1} \text{ cm}^{-1} \tag{547}$$

* W. A. Wooster, ref. B56, p. 230.

† L. Brugnatelli, *Z. Krist*, vol. 24, pp. 274–280, 1894–1895; G. Greenwood, *Z. Krist*, vol. 96, pp. 81–84, 1937; Wood and McCale.[591]

‡ W. A. Wooster, ref. B56, p. 230.

§ A. J. P. Martin, A New Method for the Detection of Pyroelectricity, *Mineral. Mag.*, vol. 22, pp. 519–523, 1931; B. Orelkin and K. Lonsdale, The Structure of Symm. (1-3-5) Triphenylbenzene, *Proc. Roy. Soc.* (*London*), vol. 144, pp. 630–642, 1934.

‖ Yeou Ta, *Compt. rend*, vol. 207, pp. 1042–1044, 1938.

¶ For tartaric acid see "International Critical Tables"[B29] or F. Hayashi.[210]

This equation can also be derived by taking the derivative of Eq. (1) with respect to temperature [*cf.* Eq. (544)]. Equation (547) states that, when p is positive, q is negative, so that a positive increment ΔE in field strength leads to a decrease in temperature. This is the case, for example, with tourmaline, the spontaneous polarization of which is in the $+Z$-direction (from antilogous to analogous pole) and increases with rising temperature. The density of tourmaline is approximately 3, $C = 0.2$, $p = 1.2$ (§519), whence at 300°K the theoretical value of q is roughly $-1.4(10^{-5})°$ per esu of field strength. This value has been verified within a few per cent by Lange.* The electrocaloric coefficient of Rochelle salt near the Curie points is many times greater than this, as is shown in the next section.

524. *The Electrocaloric Effect in Rochelle Salt.* The earliest observations of a linear effect were those of Kobeko and Kurchatov,[263] who also were the first to predict the effect in Rochelle salt from theoretical grounds. As was stated in §515, this is the converse of the pyroelectric effect, and its presence in Rochelle salt—always assuming reversibility—is a necessary consequence of the dependence of the spontaneous polarization of Rochelle salt upon temperature. Since q in Eq. (547) is proportional to p, it is evident that the electrocaloric coefficient, like the pyroelectric coefficient (§521), has its greatest values, with opposite signs, just within the two Curie points, passing through zero in the neighborhood of 0°C.

With a field strength of various values up to 1,200 volts/cm Kobeko and Kurchatov observed, at the upper Curie point, a proportional increase in temperature (a few hundredths of a degree for the strongest fields, independent of the direction of the field) and a decrease in temperature of the same order of magnitude at the lower Curie point, all in conformity with theory.

There is also theoretically in Rochelle salt, as in all dielectrics, a *quadratic* electrocaloric effect due to electrostriction, which according to Debye and Sack[B16] has been detected experimentally. It is of a lower order of magnitude than the linear effect except in fields at least as large as 30,000 volts/cm.

525. Tensorial Pyroelectricity. This is an excessively minute effect, theoretically observable with all crystal classes except the cubic. It manifests itself in the production of small charges of *like* sign at edges occurring at the ends of certain axes, when the crystal is heated uniformly. In the case of crystals that have vectorial (ordinary) pyroelectricity, the two effects are superposed, making the detection of tensorial pyroelectricity especially difficult.

* F. Lange, dissertation, Jena, 1905. Further details are given in Voigt's "Lehrbuch," p. 259.

In a crystal with a polar axis, the polarization produced by changes in temperature or mechanical stress is a vector. In general, crystals possess also quadrupole moments, which under the influence of temperature or stress give rise to a polarization that is tensorial rather than vectorial and is characterized by central symmetry. Uniform heating causes changes in the field in the immediate neighborhood of the quadrupoles, with the result that double layers of electricity appear at the surface. The accompanying expansion produces a tensorial *piezoelectric* effect, which by analogy with vectorial pyroelectricity might be called a *secondary tensorial pyroelectric* effect. The total observed tensorial pyroelectricity is therefore the sum of the primary effect due to heating alone and this secondary effect.

Voigt* looked for the effect by experiments with the following crystals, all non-piezoelectric in order to exclude disturbing effects: calcite, dolomite, beryl, topaz, barite, and celestite. His conclusion was that the real existence of the effect was "very probable."

In the "Lehrbuch,"† Voigt discusses briefly the *tensorial piezoelectric effect*, which, though necessarily minute, is theoretically possible with all crystals and even with isotropic dielectrics. Like tensorial pyroelectricity and elasticity, it involves the relations between two tensors, in this case the tensorial electric field and the elastic stress. Voigt claims to have demonstrated experimentally the probable existence of the effect.‡

526. Actino-electricity. This term was introduced by Hankel,§ to designate an electrification observed by him along the prismatic edges of a quartz crystal exposed to radiant heat. It was soon shown convincingly by Friedel and Curie‖ that the effect could be fully explained as due to piezoelectric deformation (tertiary pyroelectricity, §515).

Recently the term has been revived, in connection with the production of an emf in certain crystals under the influence of light.¶ Such effects have to do probably with internal photoelectricity rather than piezoelectricity.

REFERENCES

General. International Critical Tables,[B29] Geiger and Scheel (vol. 13),[B19] Graetz,[B20] Poynting and Thomson,[B42] Voigt,[B52] Wien and Harms (vol. 10),[B53] Winkelmann (vol. 4, part 1),[B54] Voigt.[569–572,574,575]

Theory. Debye and Sack,[B16] "Encyclopadie der mathematischen Wissenschaften" [vol. 5, part 2 (by F. Pockels)],[B17] Geiger and Scheel (vol. 24, part 2, 1933),[B19] Graetz [vol. 1 (by E. Riecke)],[B20] Boguslawski,[59–61] Heckmann,[213] Larmor.[308]

* W. Voigt,[591] "Lehrbuch," p. 303.

† Page 944.

‡ See also Voigt's later papers.[574,575] The subject is further discussed by Pockels,[B17] Falkenhagen,[B19] and Born[B6] and also in "Problems of Atomic Dynamics," Massachusetts Institute of Technology, Cambridge, Mass, 1926.

§ W. G. Hankel, *Wiedemann's Ann.*, vol. 10, p. 618, 1880, vol. 19, pp. 818–844, 1883; *Sächs. Ber.*, vol. 33, pp. 52–63, 1881; *Sächs. Abh.*, vol. 12, pp. 457–548, 1883.

‖ C. Friedel and J. Curie, *Bull. soc. française minéral.*, vol. 5, pp. 282–296, 1882; *Compt. rend.*, vol. 96, pp. 1262, 1389, 1883. *Cf.* also W. C. Röntgen, *Wiedemann's Ann.*, vol. 19, pp. 513–518, 1883.

¶ See. for example, J. J. Brady and W. H. Moore, *Phys. Rev.*, vol. 55, pp. 308–311, 1939.

Measurements. GEIGER and SCHEEL,[B19] VOIGT,[B52] WOOSTER,[B56] ACKERMANN,[1] LE QUÉRÉ,[315] MUELLER,[382] RÖNTGEN,[439] WOOD and MCCALE.[591]

Tourmaline. HINTZE,[B25] MEISSNER and BECHMANN,[362] RIECKE,[434] WOROBIEFF.[592]

Quartz. KOLENKO.[286]

The numerous investigations of Hankel in pyro- and piezoelectricity are described in his collected works: Wilhelm Gottlieb Hankel, "Elektrische Untersuchungen," S. Hirzel, Leipzig, 1856–1899, 3 vols. A partial list of his papers is given in ref. 203. Hankel's investigations were mostly qualitative and are now chiefly of historical value.

A few additional references to various authors are given in footnotes in this chapter.

CHAPTER XXX

PIEZO-OPTIC, ELECTRO-OPTIC, AND OTHER OPTICAL EFFECTS

Lass dir von den Spiegeleien
Unsrer Physiker erzählen,
Die am Phänomen sich freuen,
Mehr sich mit Gedanken quälen.

Spiegel hüben, Spiegel drüben,
Doppelstellung, auserlesen;
Und dazwischen ruht im Trüben
Als Krystall das Erdewesen.

—GOETHE.

527. Introduction. Although it is assumed that the reader is acquainted with the principles of physical optics, still it may be helpful, in order to point the way to the special properties of crystals that are now to be treated, to summarize briefly certain features of the subject. Detailed proofs must be sought elsewhere. We shall have to do chiefly with the laws of double refraction for the various crystal systems, as represented by the optical ellipsoids. A discussion of wave surfaces in crystals is omitted, although it is an important feature in crystal optics, since it is not essential for the present purpose.

We deal first with transparent crystals in the normal state, free from mechanical and electric stresses. It is recalled that the electric field vector E is perpendicular to the *ray* and to the magnetic vector H, while the electric displacement D is perpendicular to the *wave normal* and to H. The *vibration direction* is that of D. It is customary to describe the optical properties of crystals in terms either of the *Fresnel ellipsoid* or of the *index ellipsoid* (Fletcher ellipsoid). The representation of physical properties of crystals by an ellipsoidal surface is a device that we have already encountered in the discussion of dielectric properties (§112) and of elasticity (§28). Indeed, the analogies of these properties with optical phenomena are far-reaching. The equations for the optical ellipsoids are given below.

The Fresnel Ellipsoid. To any given crystal there corresponds, for a given wavelength and temperature, a certain ellipsoidal surface with axes definitely oriented with respect to the crystal lattice, such that the major and minor semiaxes of the ellipse forming the intersection of the surface by any plane through the center are proportional to the velocities

of the two polarized rays that can be propagated in the direction normal to the plane. The phenomenon is that of *double refraction.* The electric vectors of the two rays are parallel to the major and minor axes of the ellipse. This ellipsoid is the Fresnel ellipsoid. In the most general case it is triaxial; its principal semiaxes a, b, c are called the *principal velocities** of light in the crystal, the symbols being so chosen that $a > b > c$. It is customary to take as unit vector the velocity of light in vacuum, whence a, b, and c are to be regarded as *relative* velocities and therefore dimensionless.

The equation of the Fresnel ellipsoid is

$$\frac{x^2}{a^2} + \frac{y^2}{b^2} + \frac{z^2}{c^2} = 1 \tag{548}$$

The axes of reference for the ellipsoid are parallel, respectively, to the principal velocities a, b, and c. In an unstrained crystal, except in the

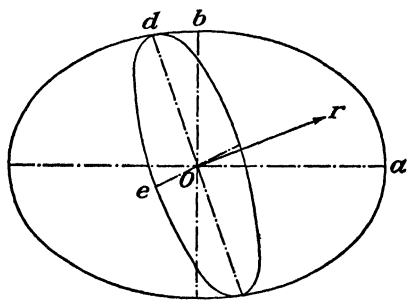


FIG. 159.—Fresnel ellipsoid. The c-axis is perpendicular to the paper. The ray *Or* is normal to an elliptical section, the principal axes of which are represented by *Od* and *Oe*.

triclinic and monoclinic systems, these axes are identical with the crystallographic a-, b-, c- (or X-, Y-, Z-) axes, but not necessarily in the same order; nor is there any fixed relation between the relative lengths of the principal axes of the ellipsoid and the crystallographic axial ratios.

528. The *principal refractive indices,* denoted by n_1, n_2, n_3 or by α, β, γ are the reciprocals of a, b, and c, respectively. Of these, γ has the maximum value for the crystal and α the minimum. Since for transparent crystals the magnetic permeability $\mu = 1$, the Fresnel ellipsoid is identical with the ellipsoid of the reciprocal square roots of the dielectric constants at optical frequencies (§112).

Figure 159 represents a Fresnel ellipsoid in which *Or* is a ray in any arbitrary direction. The plane through O normal to *Or* intersects the ellipsoid in an ellipse. According to the statements made above, the

* In this chapter the symbols a, b, c represent in general the principal velocities, not, as heretofore, the crystallographic axes.

principal axes *Od* and *Oe* of this ellipse are proportional to the velocities of the two polarized rays that can be propagated along *Or*, while the directions of *Od* and *Oe* are those of the electric vectors of the two rays.

Figure 159 may be used also to illustrate another property of the Fresnel ellipsoid, *viz.*, that all rays lying in a given plane, such as that perpendicular to the vector *Or*, fall into two categories: those polarized so as to have the electric vector in the plane, and those having the electric vector perpendicular to the plane, parallel to *Or*. For all rays in the latter group, whatever their direction in the plane, there is a common velocity, given by the length of *Or*. This property explains why, in tables of principal refractive indices of crystals, the symbols n_a, n_b, n_c stand for the indices for all rays having vibration directions parallel to *a*, *b*, or *c*. In the general case, for example, rays parallel to *c* may have either of the two indices n_a or n_b. If, as is the case with unstrained crystals of Rochelle salt, the *a*-, *b*-, *c*-axes of the ellipsoid coincide with the *X*-, *Y*-, *Z*-axes of the crystal, (though not necessarily in the same order), the principal indices may be denoted by n_x, n_y, and n_z. $(n_a - n_b)/\lambda$ is a measure of the double refraction in the *c*-direction for wavelength λ.

In unstrained *cubic* crystals the axes of the Fresnel ellipsoid are equal, the ellipsoid becomes a sphere, and all directions are optically, as well as elastically, equivalent, as in isotropic solids.

It is sometimes convenient to express the optical properties of crystals in terms of the *index ellipsoid*, which is the "reciprocal" of the Fresnel ellipsoid, having as principal axes $1/a$, $1/b$, and $1/c$; that is, its axes are the three principal refractive indixes. For *waves* whose normals are in the direction of any radius vector, the two refractive indices are the principal axes of the ellipse in which the ellipsoid is intersected by a plane perpendicular to this radius vector. The directions of these principal axes are those of the electric displacement, *i.e.*, the vibration directions.

The equation of the index ellipsoid is

$$a^2x^2 + b^2y^2 + c^2z^2 = 1 \tag{549}$$

All symbols have here the same meaning as for the Fresnel ellipsoid.

The number of parameters needed to fix the lengths and orientations of the axes of the Fresnel and index ellipsoids decreases as the crystalline symmetry increases. These parameters are the polarization constants discussed below. With triclinic crystals the number is six—three for the axial lengths, and three for the orientation. Monoclinic crystals require four parameters; rhombic crystals, three. These three systems comprise the *biaxial* crystals, for which the velocities *a*, *b*, and *c* are all different.

529. Confining ourselves for the moment to the three systems of lowest symmetry, we distinguish between the primary and secondary *optic axes.* The two *primary optic axes* are those directions for which the two wave velocities are equal; there are also two *secondary* optic axes, usually very close to the primary, for which the *ray* velocities are equal. The primary axes are the normals to the two circular sections that can be drawn through the center of the index ellipsoid, while the secondary axes are normal to the two circular sections of the Fresnel ellipsoid. The line bisecting the acute angle (the *axial angle* of the mineralogist) between the primary (or secondary) optic axes is the *acute bisectrix.* It is necessarily parallel to either the α- or the γ-axis of the index ellipsoid. A crystal is called *positive* or *negative* according to whether the acute bisectrix is parallel to γ or to α, respectively.

We pass to the consideration of *uniaxial crystals,* which include quartz. Like biaxial crystals they are doubly refracting except along one direction called the *optic axis;* we are here ignoring circular double refraction, which is treated below. All crystals in the tetragonal, trigonal, and hexagonal systems are uniaxial; two of the axes of the ellipsoid are equal, and the two optic axes merge into one. The Fresnel and index ellipsoids are now ellipsoids of revolution, the rays corresponding to the two axes becoming the single ordinary ray, the remaining ray being the extraordinary.

530. The Optical Polarization Constants. In describing the effects of external influences on the optical properties of crystals it is desirable to use an orthogonal axial system. For all classes except triclinic and monoclinic Eq. (549) can be used as it stands; with these two classes a transformation is necessary, leading to an equation for the index ellipsoid in terms of six parameters. For the sake of completeness the expressions for these parameters will be given in full, although they are not all needed in the treatment of those classes with which we are concerned here.

The X-, Y-, Z-orthogonal axes are chosen to coincide with the crystallographic axes of all classes from rhombic symmetry upward. In general form, in the notation of Pockels, Eq. (549) becomes

$$a_{11}^0x^2 + a_{22}^0y^2 + a_{33}^0z^2 + 2a_{23}^0yz + 2a_{31}^0zx\ \ 2a_{12}^0xy = 1$$

The superscript 0 designates the unstrained state of the crystal. a_{11}^0 . . . a_{12}^0 are the six *polarization constants,* defined in terms of a, b, c and the direction cosines α_1 . . . γ_3 by Eqs. (550) below.

	X	Y	Z
X'	α_1	α_2	α_3
Y'	β_1	β_2	β_3
Z'	γ_1	γ_2	γ_3

The direction cosines are given in the adjoining matrix. In the general case, as has already been pointed out, six parameters are needed for the complete specification of the ellipsoid.

$$\left.\begin{aligned} a^0_{11} &= a^2\alpha_1^2 + b^2\beta_1^2 + c^2\gamma_1^2 \\ a^0_{22} &= a^2\alpha_2^2 + b^2\beta_2^2 + c^2\gamma_2^2 \\ a^0_{33} &= a^2\alpha_3^2 + b^2\beta_3^2 + c^2\gamma_3^2 \\ a^0_{23} &= a^2\alpha_2\alpha_3 + b^2\beta_2\beta_3 + c^2\gamma_2\gamma_3 \\ a^0_{31} &= a^2\alpha_3\alpha_1 + b^2\beta_3\beta_1 + c^2\gamma_3\gamma_1 \\ a^0_{12} &= a^2\alpha_1\alpha_2 + b^2\beta_1\beta_2 + c^2\gamma_1\gamma_2 \end{aligned}\right\} \qquad (550)$$

The quantities a^0_{mn} are the components of a symmetrical tensor, analogous to the elastic strain or stress tensor and to the dielectric susceptibility tensor.

The statement in §527, that in all systems except the triclinic and monoclinic the directions of the principal velocities a, b, c coincide with the three rectangular crystallographic axes, is valid as long as the crystals are unstrained. The last three equations in (550) then vanish, while each of the first three is reduced to a single term, which represents the reciprocal of the square of the principal refractive index in the corresponding direction, since $a^0_{11} = a^2$, $a^0_{22} = b^2$, $a^0_{33} = c^2$. As will be seen, under certain elastic or electric stresses the optical ellipsoid of a crystal may suffer both a deformation and a rotation, which can cause all the polarization coefficients to assume values different from zero. Then a_{23}, a_{31}, and a_{12} do not vanish but become parameters of the new ellipsoid.

Leaving aside the monoclinic and triclinic systems (even these may be included by arbitrarily letting the X, Y, Z axial system coincide in direction with a, b, c), we may write for the surviving terms in Eqs. (550), for an unstrained crystal, $a^0_{11} \equiv a_0^2$, $a^0_{22} \equiv b_0^2$, $a^0_{33} \equiv c_0^2$. a_0, b_0, and c_0 are the principal axes of the Fresnel ellipsoid, parallel (though not necessarily respectively) to the orthogonal crystal axes.

For the *uniaxial systems* (tetragonal, hexagonal, and trigonal), a_0, b_0, c_0 coincide in direction with the X, Y, Z crystal axes, respectively, and $a_0 = b_0$. We then have, calling $o = 1/n_o$ and $e = 1/n_e$ the velocities of the ordinary and extraordinary rays, n_o and n_e being the corresponding refractive indices, $a^0_{11} = a^0_{22} = o^2 = 1/n_o^2$ and $a^0_{33} = c^2 = 1/n_e^2$.

The parameters of the optical ellipsoids are in general functions of wavelength and temperature.

531. The Piezo-optic Effect. This effect consists in a change in the refractive indices of materials under mechanical strain. Singly refracting substances become doubly refracting, while in doubly refracting substances the optical constants are altered by the strain. It was discovered in both crystalline and amorphous substances by Brewster

about 1815, and under the name of *photoelasticity* it has come to be of great importance in engineering. The special phenomena in crystals are commonly termed *elasto-optic* or *piezo-optic* effects. They are present in *all* crystals. Their theory, together with observations on several cubic and uniaxial crystals, was given by Pockels in 1889 and 1890. A summary of this work is in his textbook on crystal optics.[B41] The assumption is made that the optical effects are *linear* functions of the strain.

A full discussion of piezo-optics would be very complicated and quite beyond the scope of this work. We can only summarize and interpret the main points, in order that the nature of the electro-optic effect may be better understood.

In general, a mechanical stress both deforms and rotates the index ellipsoid, with consequent changes in birefringence and in the directions of the optic axes. An electric field, as shown below, has a like effect; but whereas piezo-optic effects are universal, the linear electro-optic effect is possible only in piezoelectric crystals.

The fundamental equations are relations between the components of two tensors, *viz.*, the polarization constants a_{mn} and either the components x_h of elastic strain or those of elastic stress X_h. The piezo-optic strain and stress coefficients are designated by Pockels as p_{mn} and π_{mn}, respectively. Their matrices for the various classes are the same as for the elastic constants, except that it is not in general true that $p_{mn} = p_{nm}$. The latter relation in elasticity is derived from thermodynamic considerations that are not applicable to the piezo-optic phenomena. The maximum number of independent constants (triclinic) is thus raised from 21 to 36, the 15 additional values appearing below the diagonal of the elastic matrix in §26 or 29, with reversed subscripts. For all systems except triclinic, monoclinic, and rhombic, however, Pockels stated that $p_{21} = p_{12}$, hence $\pi_{21} = \pi_{12}$, and in addition, for the cubic system, that $p_{31} = p_{13}$, hence $\pi_{31} = \pi_{13}$. This statement of Pockels rests on the tacit assumption that the symmetry of the crystal is not perceptibly altered by pressure.

From more recent observations on cubic crystals* it has become apparent that this assumption of Pockels is not justified. The explanation, as pointed out by Mueller, is that deformation lowers the symmetry, thus increasing the number of non-vanishing coefficients p_{hk} and π_{hk}; the magnitude of these deformation-induced coefficients is not constant but is *proportional to the stress.* For effects of this nature Mueller suggests the term "morphic" (§464). It follows that the

* H. B. MARIS, *Jour. Optical Soc. Am.*, vol. 15, pp. 194–200, 1927, and Y. KIDANI, *Proc. Phys.-Math. Soc. Japan*, vol. 21, pp. 457*f.*, 1939. See also the discussion by H. Mueller.[381]

piezo-optic effect, which according to Eqs. (551) and (551*a*) should be strictly linear, requires (at least for systems of higher symmetry) correction terms involving the square of the stress. The present treatment omits this second-order effect.

The piezo-optic equations in terms of strain are

$$\left.\begin{aligned}
a_{11} - a_{11}^0 &= p_{11}x_x + p_{12}y_y + p_{13}z_z + p_{14}y_z + p_{15}z_x + p_{16}x_y \\
a_{22} - a_{22}^0 &= p_{21}x_x + p_{22}y_y + p_{23}z_z + p_{24}y_z + p_{25}z_x + p_{26}x_y \\
a_{33} - a_{33}^0 &= p_{31}x_x + p_{32}y_y + p_{33}z_z + p_{34}y_z + p_{35}z_x + p_{36}x_y \\
a_{23} - a_{23}^0 &= p_{41}x_x + p_{42}y_y + p_{43}z_z + p_{44}y_z + p_{45}z_x + p_{46}x_y \\
a_{31} - a_{31}^0 &= p_{51}x_x + p_{52}y_y + p_{53}z_z + p_{54}y_z + p_{55}z_x + p_{56}x_y \\
a_{12} - a_{12}^0 &= p_{61}x_x + p_{62}y_y + p_{63}z_z + p_{64}y_z + p_{65}z_x + p_{66}x_y
\end{aligned}\right\} \quad (551)$$

where a_{mn}^0 is the value of a_{mn} for the unstrained crystal, *i.e.*, the value as defined in Eq. (550).

In terms of stress the equations are:

$$\left.\begin{aligned}
-(a_{11} - a_{11}^0) &= \pi_{11}X_x + \pi_{12}Y_y + \pi_{13}Z_z + \pi_{14}Y_z \\
&\qquad + \pi_{15}Z_x + \pi_{16}X_y \\
&\cdots\cdots\cdots\cdots\cdots\cdots\cdots\cdots \\
&\cdots\cdots\cdots\cdots\cdots\cdots\cdots\cdots \\
-(a_{23} - a_{23}^0) &= \pi_{41}X_x + \pi_{42}Y_y + \pi_{43}Z_z + \pi_{44}Y_z \\
&\qquad + \pi_{45}Z_x + \pi_{46}X_y \\
&\cdots\cdots\cdots\cdots\cdots\cdots\cdots\cdots \\
&\cdots\cdots\cdots\cdots\cdots\cdots\cdots\cdots
\end{aligned}\right\} \quad (551a)$$

The coefficients p_{mn} are dimensionless, while the π_{mn} have the dimensions of an elastic compliance.

The first three equations in (551) and (551*a*) express a change in the principal velocities, which can be measured by observations on rays parallel to the three axes, respectively, by the usual methods for measuring small changes in the refractive index. For example, if the only applied stress is Y_z and if $\pi_{14} \neq 0$, then the product $\pi_{14}Y_z$ may be interpreted as expressing the change in the refractive index n_1 caused by Y_z, in accordance with the relation $(a_{11} - a_{11}^0) = (1/n_1^2 - 1/n_1^{0^2}) = \pi_{14}Y_z$, where n_1 and n_1^0 are the values of this particular principal refractive index with and without the application of stress. The last three equations in (551*a*) represent a rotation of the optical ellipsoid around its axes. This rotation is determined by measuring the change in refractive index under stress with light perpendicular to any one axis and bisecting the angle between the other two. From the change in length of the corresponding radius vector of the ellipsoid the amount of rotation is calculated, from which the coefficients can be determined.*

* Ref. B41, p. 468.

The piezo-optic coefficients are related to the elastic coefficients c and s by the equations

$$p_{hk} = \sum_{i=1}^{6} \pi_{hi} c_{ki} \qquad \pi_{hk} = \sum_{i=1}^{6} p_{hi} s_{ki} \tag{552}$$

The parameters of the optical ellipsoids are in general functions of wavelength and temperature.

532. *Cubic* crystals become uniaxial for pressures normal to cube or octahedron faces and biaxial for all other types of stress.* Crystals of the *trigonal* system become biaxial under any pressure not parallel to the optic axis. If the pressure is *normal* to the original optic axis, one of the principal axes of the index ellipsoid is parallel to the pressure, while a second remains very near the original optic axis. The two optic axes lie in the plane of these two principal axes if the difference $\pi_{12} - \pi_{11}$ of the piezo-optic constants has the same sign as the velocity difference $o - e$. With a pressure of 1 kg/mm² the axial angle was found by Pockels to be 5°54′ for *quartz*.

Following are the piezo-optic constants of quartz and Rochelle salt, from Pockels,[B41,428] who used sodium light. Pockels' values in mm²/gm are here converted into cm²/dyne:

Quartz (for optical constants see §534).

π_{11}	π_{12}	π_{13}	π_{14}	π_{31}	π_{33}	π_{44}	π_{41}
1.11	2.50	1.97	−0.097	2.77	0.183	−1.015	−0.320, all $\times 10^{-13}$

Rochelle salt (for optical constants see §535). The experimental difficulties were so great that the following results indicate only the order of magnitude. Pockels' values for π_{nn}, converted to square centimeters per dyne, are

$$\pi_{44} = -9 \qquad \pi_{55} = +19 \qquad \pi_{66} = -17 \quad (\text{all} \times 10^{-14})$$

From Hinz's values of the elastic constants in Table IV, we find by the use of Eqs. (552)

$$p_{44} = -0.009 \qquad p_{55} = +0.006 \qquad p_{66} = -0.015$$

Piezo-optic observations on quartz have also been made by Günther.[194] His observations were restricted to the determination of the phase retardation for polarized light in the Y-direction, under a mechanical stress X_x up to 30 kg/cm², and yielded a value which in Pockels' notation would be represented by $n_o^3\pi_{31}/2 - n_o^3\pi_{11}/2$. The numerical value of this quantity, about $10(10^{-13})$ cm²/dyne, is in excellent agreement with Günther's theory,† but it is about three times as great as that calculated from Pockels' experimentally determined coefficients.

* The piezo-optic properties of cubic crystals have been treated in a theoretical paper by H. Mueller (reference at end of chapter).

† Günther develops a theory of the piezo-optic and electro-optic effects, based on various properties of quartz, including characteristic frequencies in the infrared and

The piezo-optic effect in quartz can be demonstrated by mounting a polished *Z*-cut plate in convergent light between a polarizer and analyzer so that the usual concentric circular rings are seen. When the plate is compressed in any direction normal to the optic axis, the circles become ellipses, the orientations of whose axes depend on the direction of the pressure. If in place of compression an electric field normal to the optic axis is applied, a similar result is observed, thus demonstrating the electro-optic effect.

533. Electro-optic Effects. These effects deserve a brief treatment here because of a certain parallelism with piezoelectricity and electrostriction. We first investigate the question as to the manner in which a static electric field may be expected to influence the optic behavior of a transparent crystal. The phenomenon is described in terms of the effect of the electric vector on the symmetrical tensor of the optical polarization constants (§530).

The most general assumption is that the field will change both the magnitudes and the directions of the principal axes of this tensor. A uniaxial crystal becomes biaxial. The difference between the original and the deformed tensors is again a symmetrical tensor. The electro-optic effect is a *symmetrical-tensorial* effect of the electric field. Theory shows that one may expect a *linear* electro-optic effect with exactly the same symmetry conditions as the converse piezoelectric effect, and a *quadratic* electro-optic effect (Kerr effect, §536) corresponding to quadratic electrostriction.

The Linear Electro-optic Effect. This effect is possible with all piezoelectric crystals, and with them only. The relationship between the linear electro-optic effect and piezoelectricity is so close that Kundt and Röntgen, who in 1883 were the first to make a careful study of the former phenomenon, believed that it was only a secondary result of the piezoelectric deformation; the effect of a deformation on the refractive indices is the *piezo-optic* effect discussed above.

The question was decided by Pockels in his classical investigation of 1894, which is still the principal source of our knowledge of the linear electro-optic effect. Pockels found a *direct* influence of the electric field on the optical constants; *i.e.*, the refractive indices of a crystal deformed by an electric field are different from those of a crystal deformed to the same extent by mechanical forces.

Pockels computed the "direct" effect by subtracting from the observed total effect the secondary, or "indirect," effect due to deformation, making use of the known piezoelectric and piezo-optic constants.

---

ultraviolet. His theory predicts the magnitudes of both effects. Since his observations were made with a single plate, his results cannot yet be regarded as a confirmation of his theory, especially since for the electro-optic effect (§534) his theoretical value of the constant r_{11} is 60 per cent higher than that which he found experimentally.

The relation of this indirect to the direct effect is quite analogous to that between "false" and "true" pyroelectricity discussed in §520.

Pockels' theory relates the change in the optical polarization constants to the electric polarization P by means of 18 coefficients. In accordance with §530 it is assumed that the axes of reference are parallel to the principal axes of the normal ellipsoid. The equations for the change in optical polarization constants caused by the electric field may then be written with a_0^2 in plate of a_{11}^0, etc., in accordance with §530. From Pockels' theory these equations are

$$\left.\begin{aligned} a_{11} - a_0^2 &= r_{11}P_x + r_{12}P_y + r_{13}P_z \\ a_{22} - b_0^2 &= r_{21}P_x + r_{22}P_y + r_{23}P_z \\ a_{33} - c_0^2 &= r_{31}P_x + r_{32}P_y + r_{33}P_z \\ a_{23} &= r_{41}P_x + r_{42}P_y + r_{4}P_z \\ a_{31} &= r_{51}P_x + r_{52}P_y + r_{53}P_z \\ a_{12} &= r_{61}P_x + r_{62}P_y + r_{63}P_z \end{aligned}\right\} \tag{553}$$

These expressions are strictly analogous to Eq. (190) or to Eq. (*vii*) in Table XX for the converse piezoelectric effect.* The quantities on the left side of the equations can be determined from observations of the refractive indices by standard methods with polarized light. From them and the known electric field strength the coefficients r_{mn} may be calculated.

The matrices for these coefficients are exactly the same as those for the piezoelectric coefficients, in §131. In the most general case there are 18 electro-optic constants.

In the following paragraphs we shall use the symbol r for the observed, or over-all, electro-optic effect. The indirect effect will be designated by r', and the direct effect by $r'' = r - r'$; r'' is the true electro-optic coefficient.

534. Experimental Results in Electro-optics. Data are available only for quartz, tourmaline, sodium chlorate, and Rochelle salt. Until the recent work by Ny Tsi-Ze and Günther on quartz and of Mueller on Rochelle salt, the only observations beyond the earlier work of Röntgen, Kundt, and Czermak were those of Pockels in 1890. In all cases the observations of the dependence of double refraction upon field yield the over-all values of the electro-optic coefficients r_{nm}, including the effect of piezoelectric deformation (indirect effect). The latter contribution,

* Following the convention adopted by Mueller,[381] we write r_{mn} in place of Pockels' e_{mn} in order to avoid confusion with the piezoelectric constants. The order of subscripts is the same as with Pockels: the *second* digit in the subscript indicates the direction of the polarization. In his experiments Pockels observed the field $E = \eta' P$; hence in Eqs. (553) P requires a knowledge of the dielectric susceptibility η' of the free crystal. In all experiments hitherto, P has been parallel to E.

which we shall call r'_{mn}, is calculated from the piezoelectric, elastic, and piezo-optic constants, just as in the case of pyroelectricity. The direct electro-optic coefficients may then be expressed as $r''_{mn} = r_{mn} - r'_{mn}$. It is easily proved from Eqs. (551), (551*a*), (189), and (190) that

$$\eta'_m r'_{nm} = \sum_{i=1}^{6} p_{ni} d_{mi} = \sum_{i=1}^{6} \pi_{ni} e_{mi} \tag{554}$$

Quartz. The electro-optic constants are $r_{11} = -r_{21} = -r_{62}$ and $r_{41} = -r_{52}$.

Principal refractive indices for the ordinary and extraordinary rays (Na, 18°C): $n_o = 1.54425$; $n_e = 1.55336$. On the optical activity of quartz see §538.

Only the component of field perpendicular to the optic axis is effective. The crystal becomes biaxial, the angle between the two optic axes and the magnitude of the effect being given by r_{11}. The coefficient r_{41} has an influence only on rays oblique to all three axes. In accordance with §5, for the crystal class to which quartz belongs, Eqs. (550) reduce to $a_{11} - o^2 = r_{11}P_x$; $a_{22} - o^2 = -r_{11}P_x$; $a_{33} = e^2 = 0$; $a_{23} = r_{41}P_x$; $a_{31} = -r_{41}P_y$; $a_{12} = -r_{11}P_y$. As in §530 the symbols o and e represent the principal light velocities, ordinary and extraordinary.

The equation for r_{11} becomes

$$r_{11} = \frac{\partial a_{11}}{\partial P_x} = \frac{\partial}{\partial P_x}\frac{1}{n_o} \approx -\frac{1}{n_o^2}\frac{\Delta n_o}{\Delta P_x} \tag{555}$$

where n_o is the refractive index for the ordinary ray and Δn_o is the observed change in n_o for a change ΔP_x in polarization.

For the total effect, using Na light, Pockels found $r_{11}\eta'_x = 1.40(10^{-8})$, $r_{41}\eta'_x = 0.59(10^{-8})$. The effect of quadratic electrostriction upon the results was ruled out, as being small in comparison with the errors of observation. The direct effect was found by subtracting from these values the calculated effect due to deformation alone. The direct coefficients thus obtained are $r''_{11}\eta'_x = 0.73(10^{-8})$ and $r''_{41}\eta'_x = 0.14(10^{-8})$. For the over-all effect the change in n_o per esu of field (300 volts/cm) parallel to the X-axis is only $\Delta n_o/\Delta E_x = 3.3(10^{-8})$; for the direct effect the calculated value is $1.74(10^{-8})$.

The only other observations that have been made on the electro-optic effect in quartz are those of Tsi-Ze and of Günther.* The obser-

* L. M. Myers (*Marconi Rev.*, no. 52, pp. 16–25, February, 1935; no. 53, pp. 9–18, April, 1935) has also described experiments on the optical effects in electrically stressed quartz. Apparently unaware of the work of Pockels, Myers thinks his results to be of purely mechanical origin, *i.e.*, due to piezoelectric deformations. He comes to the practical conclusion that electrically stressed quartz is inferior to an ordinary Kerr cell for controlling light intensity. On this point see §513 concerning the ultrasonic light relay.

vations of Günther, reduced to the foregoing units, yield for the total effect $r_{11}\eta_x' = 1.45(10^{-8})$, in good agreement with Pockels. From Tsi-Ze's paper one finds, by a somewhat roundabout calculation,

$$r_{11}\eta_x' = -1.18(10^{-8})$$

If we ignore the discrepancy in sign, which may be due to a difference in polarity of field or to enantiomorphism, it appears that Tsi-Ze's result is at least of the order of magnitude of the other observers.* Although the calculations of the indirect effect by both Günther and Tsi-Ze are open to question on theoretical grounds, they at least confirm Pockels' conclusion as to the reality of the direct effect.

It may be added that Tsi-Ze also recorded the observation of an electro-optic effect for the *extraordinary* ray in quartz, which is quite contrary to Pockels' theory, since this effect involves the coefficients r_{31}, r_{32}, r_{33}, all of which vanish for quartz.

535. Rochelle Salt. Principal refractive indices† $n_x = \gamma = 1.4954$; $n_y = \beta = 1.4920$; $n_z = \alpha = 1.4900$. Valasek's observations[543] indicate no great change in these values from $-70°$ to $+40°$C, but his observations were not sufficiently precise to record the small anomalies reported by Mueller.[376] The crystal is optically active: rotation of plane of polarization, for Na light, 1.35°/mm for each axis.‡ The *a*-, *b*-, *c*-axes of the Fresnel ellipsoid are parallel, respectively, to the *Z*, *Y*, *X* crystal axes. The plane of the optic axes is the *XZ*-plane (010), the *X*-axis being the acute bisectrix. The angle between the optic axes is 69°40′ (Groth, for "yellow" light).

The electro-optic coefficients for crystals of this class (Class 6, symmetry *V*) are $a_{11} = a_0^2 = 1/\gamma^2$, $a_{22} = b_0^2 = 1/\beta^2$, $a_{33} = c_0^2 = 1/\alpha^2$, $a_{23} = r_{41}P_x$, $a_{31} = r_{52}P_y$, $a_{12} = r_{63}P_z$.

Just as the three piezoelectric coefficients for Rochelle salt have to do with *shears* with respect to the crystal axes, so in the *linear* electro-optic effect a field parallel to any one of the axes rotates the Fresnel ellipsoid slightly around this axis without affecting its shape. Since the principal axes of the ellipsoid coincide with the crystal axes, it follows that the refractive indices, for light parallel to any one of the axes, should remain unchanged.

For electric fields parallel to the *Y*- and *Z*-axes, and Na light, Pockels found $r_{52}\eta_y' = -5.1(10^{-8})$ and $r_{63}\eta_z' = +0.95(10^{-8})$. From §408 we may

* Günther's selection of data from Tsi-Ze's Table XI to compare with his own (and thereby to show that Tsi-Ze was in error) seems to be based on a misconception. The proper data to use are those in Table VII of Tsi-Ze; the discrepancy between the results of the two investigators is then greatly reduced. Günther also made a slight numerical error in the reduction of Pockels' observations.

† LANDOLT-BÖRNSTEIN, "Tabellen," 5th ed. At 20°, Na light.

‡ H. DUFET, *Jour. phys. rad.*, vol. 3, pp. 757–765, 1904.

call $\eta'_y = 0.70$, $\eta'_z = 0.65$. The two electro-optic constants are then $r_{52} = -7.3(10^{-8})$ and $r_{63} = +1.5(10^{-8})$; they include both the direct and the indirect effects. To calculate the indirect coefficient r'_{52} we must find a_{31} from Eqs. (551) for the piezoelectric strain z_x, remembering that for rhombic crystals $a^0_{31} = 0$. Calling this value a'_{31}, we have $r'_{52}P_y = a'_{31} = p_{55}z_x = p_{55}d_{25}E_y$, whence $r'_{52} = p_{55}d_{25}/\eta'_y$. Similarly,

$$r'_{63} = \frac{p_{66}d_{36}}{\eta'_z}$$

The values of p_{55} and p_{66} are given in §532, while for d_{25} and d_{36} we use the values from Eq. (207); we thus obtain $r'_{52} = -1.4(10^{-8})$,

$$r'_{63} = -0.8(10^{-8})$$

On subtracting these values from those of r_{52} and r_{63} above, there results for the direct effect $r''_{52} = -5.9(10^{-8})$, $r''_{63} = +2.3(10^{-8})$.

The fact that the electro-optic constant involves both the dielectric susceptibility and the piezoelectric constant makes the determination of r_{41} for Rochelle salt very inexact. The only recorded measurements are those of Pockels, who found $\eta'_x r_{41} = -6(10^{-8})$, a value of the same order of magnitude as r_{52} and r_{63}. An accurate determination of r_{41} and r'_{41} would demand the same careful attention to temperature control, suitable electrodes, and freedom from mechanical constraint as are needed for dielectric and piezoelectric investigations with this crystal. Without a knowledge of the exact conditions in Pockels' experiments, one can only guess that d_{14} was of the order of $500(10^{-8})$, in which case η' should be around 10. Using these values, one finds $r_{41} \sim -0.56(10^{-8})$ and $r'_{41} \sim -0.42(10^{-8})$. With considerable reservation the coefficient of the true electro-optic effect in Rochelle salt may be taken as

$$r''_{41} = r_{41} - r'_{41} = -0.14(10^{-8}).$$

The indirect effect, expressed by r'_{41}, is apparently very large. This conclusion agrees with Mueller's results, discussed in §536; qualitatively at least it agrees also with Mandell's findings.[326]

536. *The Quadratic Electro-optic Effect.* This is the well-known Kerr effect, which can occur in all substances. Among all crystals hitherto investigated Rochelle salt is the only one in which it amounts to more than a second-order effect. In this crystal the Kerr effect is about a million times greater than the electric double refraction in most liquids. A pronounced effect has recently been found with other Seignette-electrics (see §495).

This effect in Rochelle salt was first detected by Pockels. In his study of the linear effect, with the electric field in the X-direction and the light beam at 45° to the Y- and Z-axes, he found the magnitude of the

electro-optic effect to be considerably different for opposite signs of field. In order to separate this apparently non-linear effect from the linear, he prepared an X-cut plate with two pairs of faces normal to the Y- and Z-axes of the crystal. He found that a field in the X-direction had a marked effect on the phase difference for light in the Y- and Z-directions. This effect did not reverse its sign with reversal of the field and was therefore interpreted as a quadratic, or Kerr, effect. The symmetry conditions for the Kerr effect are identical with those for the piezo-optic effect (relation of tensor to tensor) and permit a change in the refractive index along all three axes with the field parallel to one axis.

The Kerr effect in Rochelle salt has been very thoroughly studied by H. Mueller,[376,381] who found a close correlation between the optical and the dielectric properties, including the presence of hysteresis. His observations were made with the field in the X-direction. He observed the differences between refractive indices, $n_a - n_b$, $n_b - n_c$, or $n_c - n_a$, for light parallel to Z, X, or Y, as a function of field and temperature. The outstanding experimental results are as follows: (1) The order of magnitude with a field of 5,000 volts/cm is 0.1λ phase difference per centimeter path. (2) The effect does not change sign with the field. (3) It is quadratic in the field at temperatures well above the upper Curie point; complicated near the Curie points; roughtly linear between the Curie points, except when the field is less than the coercive field E_c.

It has been pointed out by Jaffe[245] that this linear effect between the Curie points is to be regarded as a *true linear electro-optic effect* if Rochelle salt is accepted as being *monoclinic* in this range of temperature (§481). From this point of view the failure of the effect to reverse its sign with the field is due to a reversal of the crystallographic a-axis when the field changes sign, owing to the reversal of the domains.

In the earlier of his two papers Mueller's theoretical treatment was in terms of his internal-field theory. In the later paper[381] Mueller replaces his internal-field theory by the polarization theory (change in double refraction dependent on P_x rather than on F_x). He adopts in principle Jaffe's view that Rochelle salt is to be regarded as monoclinic in the Seignette-electric range, and by introducing the second power of the polarization he obtains expressions that satisfactorily describe the peculiarities in the dependence of the electro-optic effect upon temperature and electric field. Even in the absence of an external field he found, between the Curie points, a *spontaneous Kerr effect* due to the internal spontaneous polarization.*

* The experimental evidence of this effect is a bend, at each Curie point, in the curve relating birefringence to temperature.

Mueller gives evidence that the Kerr effect in unconstrained crystals of Rochelle salt is due in part, at least, to deformation (the piezo-optic effect). The only measurements of the photoelastic constants of Rochelle salt are those of Pockels, on the assumption that the crystal is rhombic; they do not suffice for computing the piezo-optic contribution to the Kerr effect when the crystal is in the monoclinic form.

537. Extinction and Optical Activity. *Determination of Axial Directions by Means of Optical Extinction.* This method is useful for making a preliminary examination of irregular pieces of doubly refracting crystal and, within limits, for identifying axial directions. It is applicable to all crystals except those of the cubic system.

In general, when a doubly refracting transparent crystal is viewed between crossed polarizer and analyzer, the field of view is more or less illuminated. Except under certain special circumstances it is found, however, that when the specimen is rotated about the beam as an axis a minimum of illumination is encountered for every 90° of rotation, with maxima between. In most practical cases, even with white light, the minima are regions of complete darkness; these are the extinction positions. As we shall see, when white light is used, the emergent light for the intermediate positions may be colored.

It was shown in §527 that along any direction in the crystal two waves of different velocities may be propagated, the vibration directions being parallel to the major and minor axes of the ellipse in which the plane normal to the wave direction cuts the index ellipsoid at its center, and the two refractive indices being proportional to these axes. It is when these vibration directions are parallel to those of the polarizer and analyzer that extinction occurs. If the two indices happen to be equal, as is the case for light parallel to an optic axis in any crystal that is not optically active (§538), the field remains dark for all angular positions of the crystal.

If plane-polarized light of wavelength λ cm and intensity I_0 is incident normally on a plane-parallel plate of any orientation, whose thickness is e cm, the indices of refraction for light in the given direction being n_1 and n_2, then if polarizer and analyzer are crossed the emergent light has the intensity*

$$I = I_0 \sin^2 2\alpha \sin^2 \left[\pi \frac{e}{\lambda} (n_2 - n_1) \right]$$

where α is the angle between the vibration direction of the polarizer and that corresponding to n_1. An inspection of this equation verifies the general statements made above, and in addition it shows that for

* Ref. B41, p. 213.

any α the illumination varies periodically as e is gradually increased. The variation of I with λ gives rise to the color effects mentioned above when white light is used. Very thin plates—the thickness depending on $(n_2 - n_1)$—fail to show color, because the phase difference between the two waves is too small. If the plate is sufficiently thick, the colors of different orders overlap to such an extent that the emergent light, except in positions of extinction, is sensibly white. With quartz plates parallel to the optic axis, colors are seen only for thicknesses less than a millimeter; with X-cut Rochelle-salt plates, the limiting values of thickness are about 0.2 mm and 3 mm.

Both quartz and Rochelle salt have *parallel extinction:* when the optic axis of quartz or any one of the three crystallographic axes of Rochelle salt is at right angles to the beam, extinction occurs when this axis is *parallel* to the vibration direction of either the polarizer or the (crossed) analyzer.

Extinction can be observed with entire crystals or irregular fragments; it can be used for finding approximately the directions (though not the sense) of the crystal axes. Its application to *quartz* is considered in §333. If a plate of *Rochelle salt* is known to be cut perpendicular to one of the crystal axes, extinction tests quickly give the approximate directions of the other two axes, since the field remains dark when either of the two is parallel or at right angles to the vibration direction of the polarizer. In general, one cannot by this test discriminate between the two axes without the use of auxiliary devices.

In one special case, at least, it is possible to make this discrimination. The author has observed that when a Rochelle-salt X-cut plate whose thickness is such as to show colors in white light between polaroids is rotated about the Y-axis away from the position in which the X-axis is parallel to the beam, the colors persist until the angle of rotation is almost 90°, whereas they disappear after about 20° when the rotation is about the Z-axis.

538. *Optical Activity.* This phenomenon, known also as "circular double refraction" and "rotatory polarization," is a special property of certain crystals, not derivable from the Fresnel ellipsoid. It is observed by means of an analyzer when plane-polarized light traverses the crystal parallel to the optic axis (or parallel to either of the two optic axes in biaxial crystals). If the velocities of the two oppositely circularly polarized rays into which the incident light can be resolved are appreciably different, the plane of polarization of the emergent light is found to be rotated by an amount depending on the *rotatory power* (angle in degrees per millimeter of path for some specified wavelength) and on the thickness of the specimen. If the incident light is white, the emergent light shows the well-known characteristic tints (rotatory dispersion, *i.e.*,

variation of rotatory power with wavelength). The emergent light is not affected by rotation of the crystal about its optic axis.

Crystals belonging to 15 classes may be optically active.* They are all devoid of a center of symmetry; they are also all piezoelectric except one (cubic enantiomorphous hemihedral, symmetry *O*). Many crystals in these 15 classes, however, have an activity too small to be detected. All enantiomorphous crystals are optically active, the right and left forms rotating the plane of polarization in opposite directions.

From the molecular point of view there are two types of optically active crystals. One consists of individual molecules having no center of symmetry. If such a crystal is melted or dissolved, the liquid also shows circular double refraction; the sense of rotation depends on the solvent. Conversely, a compound whose melt or solution rotates the plane of polarization must crystallize in an enantiomorphous class (Pasteur's law). This first type is exemplified by Rochelle salt. The second type has molecules or ions of high individual symmetry, the low symmetry of the crystal being due to the lattice arrangement. α-quartz and $NaClO_3$ are examples of this type. From a solution of a left-crystal of $NaClO_3$, left- and right-crystals grow with equal probability.

In a right-crystal, the direction of rotation of the plane of polarization appears clockwise to an observer looking into the analyzer [against the beam (§326)]; this is also the direction in which the analyzer would have to be turned to keep the field dark if the thickness of the crystal were increased progressively, assuming the polarizer and analyzer to have been crossed initially.

Observations of the optical activity of quartz are useful for determining the direction of the optic axis in a plate and for detecting Brazilian twinning, as well as for distinguishing between right- and left-crystals. As stated in §15, optical tests can reveal only Brazilian (optical) twinning. Tests are best made in monochromatic light, for which a color screen is sufficient. Tests of quartz crystals by this method, and also in convergent light, are described in §333.

The *true* rotatory power of uniaxial crystals is found to be unaffected by *mechanical strain*. Nevertheless, under certain types of strain the *apparent* rotatory power is changed, but this effect is due to the fact that the crystal becomes biaxial under stress, so that there is double refraction in the direction of the original optic axis, in accordance with the laws of piezo-optics discussed above. The same effects would take place in inactive crystals. Herein lies the explanation of the optical effects recorded by Tawil (§368) for polarized light parallel to the optic axis in vibrating quartz plates. The operation of the author's "optically

* Ref. B41, p. 316.

controlled piezo oscillator" (§398) is also based on the double refraction induced by strain.

REFERENCES

BORN,[B7] GEIGER and SCHEEL,[B19] POCKELS,[B41] ROGERS and KERR,[B44] SOSMAN,[B47] TUTTON,[B48] WOOSTER,[B56] BOND,[64] GÜNTHER,[194] MUELLER,[376,377,381] TSI-ZE.[524]

BHAGAVANTAM, S.: Photo-elastic Effect in Crystals, *Proc. Indian Acad. Sci.*, vol. 16, pp. 359–365, 1942.

CHAPTER XXXI

PIEZOELECTRICITY IN THE LIGHT OF ATOMIC THEORY

Wenn nach der Entdeckung der Gebrüder Curie Deformationen von Kristallen elektrische Erregungen derselben bewirken, und wenn für dieselben, wie ich dargetan habe, je nach der Gruppe, welcher der Kristall angehört, höchst mannigfaltige Gezetze gelten, so ist damit für jede Theorie der Konstitution der Moleküle ein klares und fundamentales Problem aufgestellt. —VOIGT.

In spite of the fact that molecular or atomic theories of piezoelectricity began to appear very soon after the Curies' discovery, a satisfactory theoretical treatment of the phenomenon can hardly be said to have passed the initial stage. The resources of modern lattice dynamics are still unequal to the task of predicting anything better than a rough approach to the order of magnitude of the piezoelectric effect, even for the simplest structures. Incomplete though the story is, however, it offers much of interest on both the theoretical and the experimental side.

The piezoelectric effect is, of course, intimately related to the general subject of crystal structure. We shall therefore consider first the atomic structures of some of the more important piezoelectric crystals, as revealed by X-rays, and then summarize such progress as has been made in accounting for the piezoelectric properties. References are given at the end of the chapter.

539. The Binding Forces in Crystals. For the present purpose, the chief types of chemical bond may be listed as follows:

1. *Ionic* bonds, also called *polar* or *heteropolar*. The substance is held together by the electrostatic Coulomb attraction between ions of opposite sign. Each positive ion is surrounded by negatives, and there are no individual molecules. If the substance is a crystalline solid, the entire crystal is to be regarded as a single molecule. An example is NaCl, in which the binding is entirely ionic. Many of the simpler minerals are of this type.

2. *Valence* bonds, also called *covalent* or *electron-pair*. The pair of electrons is shared between two electropositive or two electronegative atoms. With the former case, *viz.*, the metals, we are not concerned. Valence bonding between two electronegative atoms is called *homopolar* (or non-polar) bonding. These bonds have the property of saturation and tend to form discrete and stable molecules. For example, in organic compounds the carbon uses its four available valence electrons to hold four other atoms. Such compounds may take the form of chains, sheets, or three-dimensional structures of indefinitely large extent, as do also various minerals, silicates, and refractory materials.

3. *Van der Waals bonds.* Comparatively weak forces act between molecules, due to the mutual polarization of the molecules. If only forces of this type are present, the result is a gas, a liquid, or a mechanically weak solid of low melting point. Crystals thus bonded are called *molecular crystals.*

4. *Hydrogen bonds.* In recent years it has become recognized that two electronegative atoms may be bound by a single intervening hydrogen nucleus. The bond between the H^+ and each of the negative atoms is often ionic in character and is stronger the more electronegative the atoms are. This type of bond is present in many compounds, and it plays a part in the theory of such physical properties as melting and boiling points and the dielectric constant. Sometimes, as in ice, it is the only bonding agent.

Two or more different types of bond are very commonly present in the same substance. Both ionic and valence types are thought to be present in α-quartz (Wei, Pauling), while β-quartz is a purely ionic crystal. The part played by hydrogen bonds in the Seignette-electric phosphates is discussed below, as well as the problem of Rochelle salt.

Relations between Crystal Structure and Piezoelectric Properties. If the molecule is asymmetric, the crystal is likely to have the asymmetry necessary to make it piezoelectric. For example, if, as in tartaric acid or Rochelle salt, there are asymmetric C atoms in the molecule, the crystal must lack a center of symmetry. The only exception to this rule would be with such crystals as meso- or racemic tartaric acid, where the asymmetric atoms or molecules compensate one another.

Simple ionic salts cannot be expected to be piezoelectric, unless the radii of the constituent atoms are decidedly unlike.

Simple semipolar compounds (containing both ionic and valence bonds) tend to be piezoelectric. Crystals of the zinc blende type fall under this rule. Decidedly homopolar compounds (little or no ionic binding) often have highly symmetrical structures, for example the pyrite type. This subject is further discussed by Wooster.[B56]

We turn next to those features of the structure of quartz and of Rochelle salt that are related to the purpose of this book. For the X-ray methods used in determining the structures the reader may consult the references at the end of this chapter.

540. The Structure of Quartz. In 1914 W. H. Bragg published the first X-ray analysis of quartz and offered the hypothesis of the three interpenetrating lattices mentioned below. The first investigation of the relative positions of the atoms in α- and β-quartz by X-rays was that of Bragg and Gibbs (1925). This work was extended by Gibbs (1926) and especially by Wyckoff (1926), who completely determined the structural parameters of β-quartz. One such parameter is needed for β-quartz and four for α-quartz. References to the later determinations of the parameters are given at the end of the chapter.*

The space-groups for the two enantiomorphous forms of β-quartz are D_6^4 and D_6^5. For α-quartz they are D_3^4 and D_3^6.

* An excellent account of the work of Bragg and Gibbs, with diagrams, is given by Sosman.[B47]

The crystallization of SiO_2 in three principal forms, as quartz (including the α- and β-modifications), tridymite, and cristobalite, has been mentioned in §10. All three forms have the same basic structure, *viz.*, a tetrahedral group of four oxygen atoms with a silicon atom in the center. The arrangement of the groups is what distinguishes one form from another. Our interest is in α-quartz and β-quartz. In each of these modifications the structure is based on three interpenetrating hexagonal lattices.

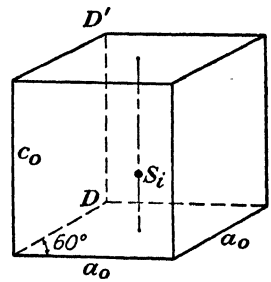


FIG. 160.—The unit cell of α- and β-quartz, with one of the three silicon atoms.

In order to visualize this type of crystal architecture we start with the unit cell of one of the three component lattices, as illustrated in Fig. 160. The unit cell has the form of a right prism of height c_0, having as its base a 60° rhombus. The vertical edges are parallel to the principal (Z-) axis, while the sides of the base are parallel to two X-axes. It contains one Si and two O atoms. We have arbitrarily placed the Si atom at a distance $c_0/3$ above the center of the base, in order to make it fit into the final scheme. The positions of the oxygens will be considered later.

Suppose cells of this type to be packed regularly in all three dimensions, forming a lattice. A projection on the basal plane, viewed from

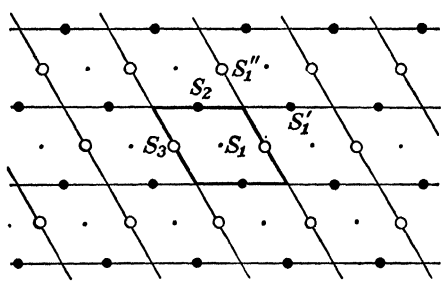


FIG. 161.—Projection, on a plane perpendicular to the optic axis, of the three interpenetrating hexagonal simple lattices, showing the silicon atoms in the configuration for β-quartz.

above, will look like Fig. 161, in which the projection of each unit cell has at its center a silicon atom, indicated by a small dot S_1, corresponding to Si in Fig. 160. The entire array of S_1 dots has hexagonal symmetry, forming a hexagonal lattice. Now imagine two other lattices identical with the first, but rotated about one of the prismatic edges, say DD' in Fig. 160, by 120° and −120°, respectively. In Fig. 161, the axis of rotation may be taken as perpendicular to the paper. In the pro-

jection, the Si atoms will appear in the positions shown by the large dots S_1' and the open circles S_1''. Then let these two lattices be displaced vertically, the first downward by $c_0/3$ and the other upward by the same distance (we anticipate by remarking that the result will be right- or left-quartz according to which of the two lattices is displaced upward). The projection of each unit cell now has, in addition to a Si at its center, four others at the edges, located at two different levels. Of the five silicons, any three at different levels may be selected as belonging properly to the unit cell. We choose arbitrarily the three marked S_1, S_2, and S_3 for the cell indicated by heavy lines; the other two silicons then belong to adjacent cells, although bonded to certain oxygens in the indicated cell.

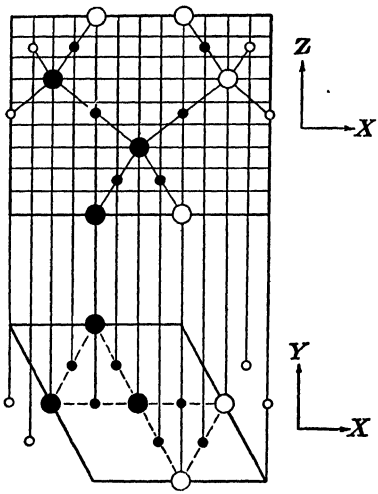


FIG. 162.—The unit cell of β-quartz, in elevation and plan. Large black circles are silicons belonging to this cell, the basal outline of which is the outer rhombus. Large open circles are silicons from some of the adjacent cells. Small black circles are oxygens belonging to this cell; small open circles are oxygens from adjacent cells.

The final structure is the interpenetrating hexagonal lattice system characteristic of β-quartz. The unit cell of the complete structure still has the form and dimensions shown in Fig. 160, but it now contains three Si and six O atoms, as indicated in Fig. 162.

The positions of the O atoms have been a matter of uncertainty. From the work of Wei and of Machatschki their most probable location is as follows: For both α- and β-quartz their projections on the basal plane are at distances $a_0/4$ on either side of the Si, in the a_0-direction. In β-quartz, which has hexagonal symmetry, all the O's are at multiples of $c_0/6$ above the basal plane, as shown in Fig. 162.

Bragg and Gibbs showed that the structural change at the α-β point, to which the crystallographic and physical differences between β- and α-quartz are due, involves only small displacements of the atoms. The movement of the Si atoms is about 0.3 Å. The corresponding modification of Fig. 162 to make it represent the unit cell of α-quartz requires rotating adjacent triangles of Si atoms, as seen in the basal projection in Fig. 162, in opposite directions by about 8° in the plane of the paper. In the upper portion of Fig. 162 the oxygens at the left of the center are raised by $c_0/18$; those at the right of the center are

lowered by $c_0/18$. The hexagonal symmetry of β-quartz thus becomes changed to the trigonal symmetry of α-quartz. The dimensions of the unit cell also undergo a slight alteration. For α-quartz there have been two recent determinations. According to Bradley and Jay, $a_0 = 4.90288$ Å, $c_0 = 5.39328$ Å; Miller and Du Mond* found

$$a_0 = 4.91267 \pm 0.00009 \text{ Å}$$

and $c_0 = 5.40459 \pm 0.00011$ Å, at 25°C. For β-quartz, Wyckoff found $a_0 = 5.01$ Å, $c_0 = 5.47$ A.

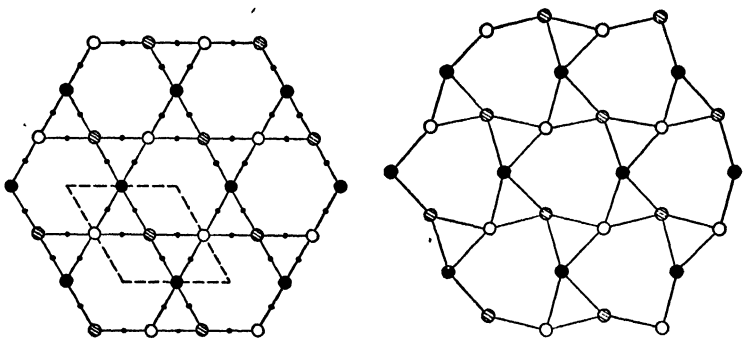


FIG. 163.—Projection, on a plane perpendicular to the optic axis, of the lattices of β-quartz (a) and α-quartz (b), adapted from Bragg and Gibbs.

The complete lattice for β-quartz is shown in projection in Fig. 163a, in which the outline of the unit cell is indicated by dotted lines. Considering three layers of silicon atoms in planes parallel to the paper, we represent the atoms in the first, or lowest, layer (farthest from the observer) by large open circles and those in the third, or uppermost, layer by large black circles. The intermediate layer is indicated by shaded circles. The oxygen atoms are in layers between the silicon atoms. Each oxygen is bonded to the two nearest silicons. Each Si is bonded to four oxygens, two above and two below it. These latter are the four oxygen atoms that form the tetrahedral group referred to above. This interconnecting of all the tetrahedra produces a three-dimensional framework of great rigidity.

In Fig. 163b is the corresponding projection for α-quartz, in which only the Si atoms are represented. The structure is now symmetrical about the X-axis, but no longer about the Y-axis. The X-axis has become a polar axis, and the crystal has acquired the piezoelectric constants d_{11}, d_{12}, and d_{26}.

If the layers of atoms are considered as continued indefinitely in the

* P. H. MILLER, JR., and J. W. M. DU MOND, *Phys. Rev.*, vol. 57, pp. 198–206, 1940.

direction perpendicular to the paper, it becomes evident from Fig. 162 that all the silicons appearing in the projection at the vertices of any one of the small triangles in Fig. 163 form a helix with axis parallel to the principal axis of the crystal. The crystal is of the left or right form according to whether or not the helix advances in the direction of a right-handed screw. The structure shown in Fig. 162 is that for *right*-quartz, since to an observer looking down at the paper the helix appears to wind in a clockwise direction. This statement corresponds to the fact that in a left-quartz the rotation of a beam of polarized light parallel to the principal axis is counterclockwise, as seen when looking through the analyzer toward the source of light.

It has been pointed out by Machatschki that the helical structure is revealed in a more fundamentally significant manner by taking as the axis of the helix a line through the center of a *hexagon* in Fig. 163. About this axis there is a continuous helix of *tetrahedra*, winding in a direction opposite to the silicon helix.

541. *Theory of the Piezoelectric Effect in Quartz.* The first attempt at an atomic theory was that of Lord Kelvin,[256] who in 1893 proposed a model in which the silicon atoms were clustered in groups of three. His guess as to the geometrical arrangement and the effect of mechanical pressure on internal structure came remarkably close to the facts as revealed by X-rays thirty years later. The probable seat of the piezoelectric effect was considered by Bragg and Gibbs (1925) and by Gibbs (1926) on the basis of their X-ray investigations. They express the view that mechanical pressure in the X- or Y-direction distorts the triangles shown in Fig. 163*b*, resulting in a polarization parallel to X. Gibbs attempted an estimate of the magnitude of the effect, assuming quartz to be an ionic crystal containing effective dipoles. Such an estimate is necessarily defective, since quartz is no longer considered to be purely ionic. Nevertheless, Gibbs arrived at the right order of magnitude. His analysis of the pyroelectric effect in quartz suffers from the failure to discriminate between secondary and tertiary pyroelectricity.

542. The Structure of Rochelle Salt. The complete crystal structure has been determined by Beevers and Hughes, by applying Fourier and Patterson methods to their X-ray observations. The original paper should be consulted for details and for the diagram showing a projection of the structure on the (001) plane. The unit cell contains four molecules. The structure does not change perceptibly on passing through the Curie points, since at these points it is only hydrogen nuclei that change their positions. Of present interest is the conjecture of Beevers and Hughes concerning the origin of the anomalies, which they attribute to repeated zigzag chains containing O (or OH) and H_2O groups, running in the X-direction.

From their discussion one may draw the following conclusions: The peculiar dielectric properties are attributed to the effect of the impressed electric field on the chains; in particular, the normal direction of the bonds can be *reversed* by a field in the proper direction. The disappearance of the anomalies outside the Curie points is thought to be due to a breaking of some of the contacts in the chains.

These authors do not mention the spontaneous polarization. Indeed, their diagram pictures adjacent chains in the unit cell as polarized in opposite directions. One can extend their reasoning by following Jaffe's suggestion[245] that the unit cell is orthorhombic outside the Curie points and, if isolated, would remain orthorhombic between these points. Between the Curie points each unit cell in a domain tends to become polarized and slightly deformed under the influence of neighboring cells. In the Seignette-electric region a majority of the chains in a given domain become polarized the same way, just as in the Kurchatov and Fowler theories dipoles were supposed to become rotated into parallelism. The existence of a spontaneous polarization and its dependence on temperature could thus be accounted for.

If these views are accepted, it is possible still to apply in substance Mueller's internal-field theory given in Chap. XXVI. A function corresponding to the Langevin function can still be used, with the dipoles quantized in the X-direction.

The space-group of Rochelle salt is V^3. The *unit cell* is orthorhombic, containing four molecules. The unit cell has the following dimensions according to Beevers and Hughes: $a_0 = 11.93$ Å, $b_0 = 14.30$ Å, $c_0 = 6.17$ Å. These values may be compared with those of Warren and Krutter, who found $a_0 = 11.85$ Å, $b_0 = 14.25$ Å, $c_0 = 6.21$ Å. From these data the axial ratio is $a:b:c = 0.8343:1:0.4315$ according to Beevers and Hughes and $0.8316:1:0.4358$ according to Warren and Krutter. From Staub's X-ray measurements* we find

$$a:b:c = 0.8317:1:0.4330$$

The mean value of the axial ratio, from the three sources just mentioned, is

$$a:b:c = \mathbf{0.8325:1:0.4334}$$

The value given in Groth[B22] is $0.8317:1:0.4296$.

Further X-ray Investigations on Rochelle Salt. Kirkpatrick and Ross† conclude that Rochelle-salt crystals have a very uniform structure, since the rocking curve widths are as narrow as those of high-grade calcite. Staub and Németh have studied the effects of an electric field on X-ray

* H. Staub, *Helv. Phys. Acta*, vol. 7, pp. 3–45, 1934.

† P. Kirkpatrick and P. A. Ross, *Phys. Rev.*, vol. 43, pp. 596–600, 1933.

intensities by the Bragg method, and Staub also measured intensities at different temperatures.* Staub found that, between the Curie points, the reflections from the (111) plane (parallel to any one of the faces marked *o* in Fig. 2) were increased by about 10 per cent when a field of the order of 500 volts/cm was applied. In stronger fields the effect was absent, owing, as Staub thought, to the destruction of the lattice by the field. The change in intensity was not altered when the crystal was vibrated in resonance (see §261).

Németʼs observations were made with reflections from faces normal to the *X*-, *Y*-, and *Z*-axes. In each case fields up to 700 volts/cm parallel to all three axes were applied. All observations were at room temperature. In all cases the curves relating intensity to field strength showed saturation and, at the strongest fields, a tendency for the intensity to decrease with increasing field, in agreement with Staub. The effect was most pronounced at the (100) faces, where the maximum increase in intensity amounted to as much as 40 per cent. Endwise pressure on an *X*-cut 45° plate did not affect the intensity of the reflections. The great sensitiveness of Rochelle salt to an electric field stands in sharp contrast to quartz, which Német found to give negative results, and ice, which showed an increase in intensity of 2 or 3 per cent in a field of 1,300 volts/cm.

Staub investigated the change in intensity of reflection from the (111) plane over a wide range of temperatures in the absence of an external field.† Between the Curie points the intensity increased by about 10 per cent. Staub regarded this effect as evidence for the existence of a large internal field, which stabilized the lattice against the effect of thermal agitation. For his theoretical treatment, based on Debyeʼs theory, the original papers should be consulted.

543. A complete discussion of the dielectric and piezoelectric properties of Rochelle salt in terms of the Beevers-Hughes model would require accounting for all three of the piezoelectric constants d_{14}, d_{25}, and d_{36}. In this connection it is of interest to consider a model of the arrangement of dipoles in the unit cell as conceived by Staub,[479] at a time when Rochelle salt was thought to contain free dipoles.‡ This model is shown in Fig. 164; it is applicable to all rhombic crystals of the digonal holoaxial class and has the simplest distribution of charges compatible with this type of symmetry. While it offers a simple qualitative interpretation of the piezoelectric and diclectric effects in Rochelle salt, it is only a model, and as such must be taken *cum*

* H. Staub, *Physik. Z.*, vol. 34, pp. 292–296, 1933, vol. 35, pp. 720–725, 1934; *Helv. Phys. Acta*, vol. 7, pp. 3–45, 480–482, 1934. A. Német, *Helv. Phys. Acta*, vol. 8, pp. 97–116, 117–151, 1935.

† See also S. Miyake, *Proc. Phys.-Math. Soc. Japan*, vol. 23, pp. 378–395, 1941.

‡ For earlier treatment of the "electric axes" of Rochelle salt see Riecke, in Graetz, vol. 1, also W. G. Hankel and H. Lindenberg, *Z. Krist.*, vol. 27, pp. 515–517, 1897.

grano salis (*tartari natronati*). Four dipoles in the directions of the diagonals are assumed, the positive direction of each being indicated by an arrow. Upon application of mechanical stress or of an electric field the dipoles become rotated.

Outside the Curie points the effects of the dipoles, subject to thermal agitation, neutralize one another so that there is no permanent resultant polarization of the cell. Compression along any one of the axes produces no polarization at any temperature. But a compression applied *diagonally* in a plane perpendicular to any axis causes a polarization parallel to that axis. For example, let the compression be such as to bring the edges EH and BC closer together. This causes a shearing strain, and the deformation is the same as if the face $EFGH$ were slid parallel to itself in the direction EF. The originally rectangular faces $ABFE$ and $OCGH$ become parallelograms, and the dipoles become rotated in such a way as to polarize the cell in the

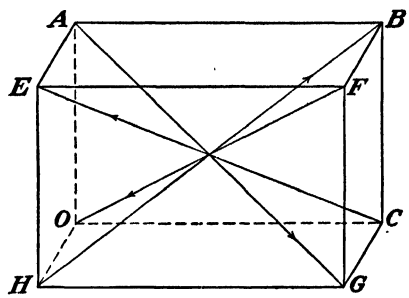


FIG. 164.—Staub's model of the unit cell of Rochelle salt.

drection OA, the face $ABFE$ having a positive polarization charge. This describes the direct piezoelectric effect for which the equation is $P_x = -d_{14}Y_z$ (d_{14} is positive, and the stress Y_z is negative when the strain, as assumed above, is positive). According to the *converse* effect, it is evident from the figure that a field applied in the direction from O to A will rotate the dipoles so as to cause a positive shearing strain in the YZ-plane. The freer the dipoles are to rotate, the greater will be the dielectric constant.

In reality, the relation between strain and positions of the dipoles cannot be as simple as this. For example, the symmetry in Fig. 164 is such that the three coefficients d_{14}, d_{25}, and d_{36} all ought to have the same sign. Pockels found that d_{14} and d_{36} are both positive but that d_{25} is *negative*. This can be "explained" only by assuming the configuration of atoms in the cell, and the forces between them, to be such that a positive shearing strain in the ZX-plane is associated with a *negative* polarization along the Y-axis, or else by attributing the effect to interactions between adjacent cells.

In order to reconcile the model with the properties of Rochelle salt between the Curie points one may postulate that the configurations of the cells and their mutual interactions are such that there is a tendency for the dipoles to become aligned more or less closely along the X-axis instead of along the diagonals. Then, when the temperature is sufficiently low, spontaneous polarization sets in, accompanied by a spontaneous strain. This takes the form of a shear y_z and is the ground for the view advanced in §481 that in the region of spontaneous polarization Rochelle salt should properly be classified as monoclinic rather than orthorhombic. The spontaneous strain, however, is so small that the structure as revealed by X-rays appears orthorhombic at all temperatures.

The same model can be used to illustrate the longitudinal effect when the field is

oblique to all three axes (§140). For example, if a compression is applied along *OF*, the strain will rotate the dipoles so as to produce a polarization in the *FO*-direction.

544. The Structure of Primary Potassium Phosphate, KH_2PO_4. An X-ray analysis of this crystal was made in 1930 by West,* who found phosphate groups consisting of a phosphorus atom tetrahedrally surrounded by four oxygens. Each group is surrounded tetrahedrally by four other groups. Neighboring PO_4 groups are connected by hydrogen bonds.

Recently, this analysis has been further treated by Slater, by the use of statistical methods. He considers the possible arrangements of the H atoms, finding that each phosphate group is likely to have two of its neighboring hydrogens close to it, forming $(H_2PO_4)^-$ dipoles. At low temperatures, in the state of lowest energy the dipoles tend to become oriented one way or the other along the *c*- (*Z*-) axis, thus accounting for the spontaneous polarization. Above the Curie point (*cf.* §445), the dipoles assume random orientations. Slater derives an expression for the dielectric susceptibility at small fields, indicating a Curie-Weiss law.

Slater's theory predicts that the transition at the Curie point is a phase change of the first kind, with latent heat and a discontinuous jump from the polarized state at low temperatures to the unpolarized state at higher temperatures. On the other hand, the experiments recorded in §497 indicate that the transition, while confined to a narrow temperature range, is not abrupt. Slater considers that the discrepancy between theory and experiment is due to the fact that the theory—like the fundamental theory of Rochelle salt treated in Chaps. XXIII and XXIV—applies only to the individual domain. As the temperature falls below the Curie point, the crystal breaks up into many domains, with opposing polarizations and opposing spontaneous shearing stresses in adjacent domains. The result is the appearance of stresses of varying magnitude at the boundaries between domains, which tend to lower the transition point by varying amounts, thus giving a continuous transition process instead of an abrupt change. In explaining that the transition is trying to be one of the first kind, Slater points to the fact that the analogous transitions in potassium arsenate and in ammonium phosphate are much sharper than in potassium phosphate.

From his observations on the specific heats of KH_2AsO_4, KH_2PO_4, and KD_2PO_4, Bantle[22] finds changes in entropy at the upper Curie points of the order of magnitude predicted by Slater's theory. Accepting the O—H—O combination as the dipole responsible for the Seignette-

* J. West, *Z. Krist.*, vol. 74, pp. 306–332, 1930. See also M. Avrami, *Phys. Rev.*, vol. 54, pp. 300–303, 1938.

electric properties and assuming two dipoles per molecule, Bantle calculates for the molecular electric moment μ the value $0.74(10^{-18})$.

545. Atomic Theories of Piezoelectricity. The theory of the piezoelectric effect is a part of the theory of the solid state. This subject is much too large for treatment here. We can only point out some of the historical milestones in the journey, which is still far from complete.

Prior to the discovery of piezoelectricity, the molecular theory of pyroelectricity had been the object of much speculation (see references at the end of Chap. XXIX). One contribution was made by *J. and P. Curie* themselves,* following Lord Kelvin's suggestion of permanently polarized molecules.

Lord Kelvin's theory of piezoelectricity (1893) has already been referred to in §541. He made a rough quantitative estimate of the piezoelectric effect, based on the assumption that the potential differences between molecules are of the same order as the macroscopic contact potentials between different metals. He thus calculated a value of d_{11} for quartz of the right order of magnitude.

At about the same time Riecke (in 1892) published a somewhat elaborate molecular theory of piezoelectricity for crystals of all symmetries (see Graetz†). He assumed the piezoelectric effect to be due to a change in electric Coulomb interaction between molecules, brought about by a mechanical deformation of the crystal lattice. In the light of the later investigations described below, this theory must now be regarded as obsolete. It was an ingenious theory, involving five types of "pole systems" to account for the piezoelectric constants of all classes of crystals. His pole system for crystals of symmetry V led to a model like that of Staub shown in Fig. 164.

An advance more in step with the progress of modern physics was made by *Schrödinger* in 1912. He extended Debye's kinetic theory of dielectrics to anisotropic solids. While his paper has to do mainly with melting points, it discusses piezo- and pyroelectricity as well, with particular reference to quartz and tourmaline, and at some points it has a bearing on the theory of Seignette-electrics. His estimate of d_{11} for quartz is of the right order of magnitude. By the use of an approximate Langevin function he reaches the right order of magnitude for the pyroelectric constant of tourmaline. The chief weakness in his theory lies in his assumption of freely rotating dipoles in all crystals.

The theory of piezo- and pyroelectricity was also discussed in 1921 by *Larmor*. The chief importance of this paper for us lies in the emphasis on the correct treatment of the *surface layer* for the piezo- and pyroelectric

* J. and P. Curie, *Compt. rend.*, vol. 92, p. 350, 1881; *Jour. phys.* (2), vol. 1, p. 245, 1882.

† Ref. B20, vol. 1, 1918.

effects. Born (see below) deals only with the infinite lattice, ignoring the conditions at the surface. Larmor's theory indicates that it is not necessary to postulate a spontaneous polarization in order to account for the pyroelectric effect. He points out that, if the positive and negative ionic charges in the crystal are not uniformly spaced, a change in temperature will alter their relative spacing. Although this alteration is very minute, it is sufficient to account for the observed surface charges. without the existence of a permanent internal polarization. The charge observed on a freshly fractured surface depends on whether more positive or more negative ions are exposed.

Larmor goes so far as to doubt the existence of a spontaneous polarization in any crystal. Without accepting this thesis, one may at least grant that if there are crystals possessing a spontaneous polarization, as seems well established, for example, in the case of Rochelle salt, still the amount of charge observed on a freshly fractured surface may be modified to a considerable extent by the precise position of the fractured surface with respect to the crystal lattice. This possibility has been pointed out in §519 in the case of tourmaline.

The same consideration also suggests an explanation of the author's failure to detect a charge on the freshly fractured surfaces of a bar of Rochelle salt, the length of which was in the X-direction.

546. *The Piezoelectric Effect According to Lattice Dynamics.* Modern atomic dynamics had its beginning at the hands of Madelung in 1909. In 1912 the first work of M. Born appeared, in collaboration with Th. v. Kármán, on vibrations in space-lattices. Born's first treatment of the piezoelectric and pyroelectric effects was in his "Dynamik der Kristallgitter" in 1915. Eight years later came the "Atomtheorie des festen Zustandes," in which the treatment was extended and simplified. The chapter on the dynamic lattice theory of crystals by Born and Goeppert-Mayer in the second edition of the "Handbuch der Physik"[B19] is practically a new edition of the "Atomtheorie."

Born's theory assumes pure central forces between the atom centers. Considering the advances that have been made in atomic dynamics in more recent years, it is remarkable that his piezoelectric computations could lead even to an approach to the right order of magnitude.

Only for very simple lattices did Born find it possible to make a quantitative estimate of the relation between strain and electric field. He applied his theory to crystals of the cubic system having a diagonal lattice, in which all the particles lie on diagonals of the unit cube. An example of this structure is zinc blende, ZnS, symmetry T_d (see §170). Crystals of this symmetry have only one independent piezoelectric constant, $e_{14} = e_{25} = e_{36}$. For such a structure Born found the following relation between e_{14}, the dielectric constant k at low frequency, k_0 at

optical frequencies ($k_0 = n^2$), and the elastic constants c_{12} and c_{44}:

$$e_{14}^2 = \frac{k - k_0}{4\pi}(c_{12} - c_{44})\frac{c_{44}}{c_{12}}$$

For ZnS, Born thus calculated $e_{14} \sim -23(10^4)$ esu, about five times greater than the observed value of $-4.2(10^4)$ recorded in §170. At Born's suggestion, Heckmann in 1925 attempted to improve the theory by considering the polarizability of the ions, but the numerical value of e_{14} for ZnS was not improved thereby. Further advances in atomic dynamics must be awaited before agreement can be expected between the theoretical and experimental values of the piezoelectric constant.

In general the piezoelectric stress constant e_{hk} may be considered as of more fundamental significance than the strain constant d_{hk}. Not only is it the constant given by the atomic theory, but it relates mechanical to electric stress in the equation $X_k = -e_{hk}E_h$ and mechanical to electric strain in the equation $P_h = e_{hk}x_k$. Moreover, as has been shown in §474, in Rochelle salt e_{14} remains finite at all temperatures, instead of becoming infinite at the Curie points, as is the case with the piezoelectric strain constant.

REFERENCES

No attempt has been made to compile a complete list of references on matters treated in this chapter. Those references have been selected which were most useful in the preparation of the chapter.

BRAGG,[B8] DAVEY,[B14] GEIGER and SCHEEL,[B19] SOSMAN.[B47]

KELVIN, LORD: "Baltimore Lectures," C. J. Clay & Sons, London, 1904; "Mathematical and Physical Papers," vol. 5, Cambridge University Press, London, 1911; *Phil. Mag.*, vol. 36, pp. 331, 342, 384, 414, 453, 1893.

PAULING, L.: "The Nature of the Chemical Bond," Cornell University Press, Ithaca, N.Y., 1939.

BEEVERS and HUGHES,[48] BRAGG and GIBBS,[75] GIBBS,[157] LARMOR,[308] WARREN and KRUTTER.[579]

BRADLEY, A. J., and A. H. JAY: Quartz as a Standard for Accurate Lattice-spacing Measurements, *Proc. Phys. Soc.* (*London*), vol. 45, pp. 507–522, 1933.

BRILL, R., C. HERMANN, and C. PETERS: X-ray Fourier Synthesis of Quartz, *Ann. Physik*, vol. 41, pp. 233–244, 1942.

HECKMANN, G.: On the Lattice Theory of Deformable Ions, *Z. Physik*, vol. 31, pp. 219–223, 1925; *Z. Krist.*, vol. 61, pp. 250–292, 1925.

HYLLERAAS, E. A.: Gleichgewichtslage der Atome, Doppelbrechung und Optisches Drehungsvermögen von β-Quarz, *Z. Physik*, vol. 44, pp. 871–886, 1927.

MACHATSCHKI, F.: Die Kristallstruktur von Tiefquarz SiO_2 und Aluminiumorthoarsenat $AlAsO_4$, *Z. Krist.*, vol. 94, pp. 222–230, 1936.

MAUGUIN, C.: Possible Use of Diffraction Patterns from X-rays for the Complete Determination of the Structure of Quartz, *Compt. rend*, vol. 173, pp. 719–724, 1921.

SCHRÖDINGER, E.: Studien über Kinetik der Dielektrika, den Schmelzpunkt, Pyro- und Piezoelektrizität, *Sitzber. Akad. Wiss. Wien, Math.-naturw. Klasse*, vol. 121, pp. 1937*f.*, 1912.

SLATER, J. C.: Theory of Transition in KH_2PO_4, *Jour. Chem. Phys.*, vol. 9, pp. 16-33, 1941.

UBBELOHDE, A. R., and I. WOODWARD: Isotope Effect in Potassium Dihydrogen Phosphate, *Nature*, vol. 144, p. 632, 1939.

WEI, P'EI-HSIU: Structure of α-Quartz, *Z. Krist.*, vol. 92, pp. 355–362, 1935.

WYCKOFF, R. W. G.: The Crystal Structure of the High Temperature (β-) Modification of Quartz, *Am. Jour. Sci.*, vol. 11, pp. 101–112, 1926; Kriterien für Hexagonale Raumgruppen und die Kristallstruktur von β-Quarz, *Z. Krist.*, vol. 63, pp. 507–537. 1926.

APPENDIX

FERROMAGNETISM

547. In the discussion of the properties of Rochelle salt and of the other Seignette electrics in Chaps. XX to XXVII, there is frequent reference to the analogies that exist between these dielectric phenomena and the magnetic properties of such substances as iron. As a background for this discussion the pertinent features of the theory of paramagnetism and ferromagnetism are here summarized.* Emphasis will be laid especially on the dependence of magnetic properties upon temperature, with particular reference to the Curie point, and upon the nature of those minute regions of spontaneous magnetization known as *domains*. Some of the effects of mechanical strain upon magnetism will be considered, as well as magnetic hysteresis. For more complete details of ferromagnetic theory the references cited in the footnote may be consulted.

Following the early theory of Weber, and Ewing's successful attempt at a qualitative explanation of residual magnetism and hysteresis by means of his model of small elementary magnets, the basis for the mathematical formulation was laid by H. A. Lorentz's equations for the internal field (§113), which are applicable equally to dielectric and magnetic substances. In the meantime P. Curie had experimentally established the law relating the susceptibility of paramagnetics to temperature (now known as Curie's law) and had made his famous study of the temperature of transition from the ferromagnetic to the paramagnetic state (the Curie point), which for iron is around 770°C.

The Curie law in its original form expressed the relation between mass susceptibility k_m and absolute temperature T by the equation $k_m = C/T$, C being a constant.† With many substances it has been found that the relation is given more precisely by $k_m = C/(T - \theta)$, where for paramagnetic materials the constant θ has a small positive or negative value. A positive θ implies the possibility of a ferromagnetic state; in the ferromagnetic metals θ has relatively large positive values.

548. *Paramagnetism.* The modern theory of paramagnetism is due chiefly to Langevin. By his method the degree of magnetization of a paramagnetic substance is expressed in terms of the ratio $\bar{\mu}/\mu$, where μ is the magnetic moment of the elementary dipole and $\bar{\mu}$ the average component of μ in the direction of the applied field.‡ From classical statistical mechanics Langevin found an expression for $\bar{\mu}/\mu$

* For the theory of ferromagnetism see, for example, F. Bitter, "Introduction to Ferromagnetism," New York, 1937; R. M. Bozorth, *Bell System Tech. Jour.*, vol. 15, pp. 63–91, 1936; F. Bloch, in "Handbuch der Radiologie," 2d ed., vol. 6, part 2, Leipzig, 1934; E. C. Stoner, "Magnetism and Matter," London, 1934, or "Magnetism," London, 1936; R. Becker, "Theorie der Elektrizität," vol. 2, Leipzig, 1933.

† Custom sanctions the use of the symbol k for *volume susceptibility*, defined as (magnetic moment per unit volume)/(field strength). The Curie law is usually expressed in terms of *mass susceptibility*, designated as $\chi = k/\rho$. Since in this book the symbol χ is employed for the reciprocal of the dielectric susceptibility, we shall designate the magnetic mass susceptibility by k_m.

‡ The symbol μ must not be confused with magnetic *permeability*, a quantity for which no symbol will be needed in this discussion.

as a function of the quantity $\mu F/KT$. The numerator of this quantity is a measure of the directive effect of the molecular field F acting on the dipole, while the denominator ($K = 1.37 \times 10^{-16}$ erg deg^{-1} = Boltzmann constant; T = absolute temperature) measures the tendency of the dipoles to be kept in a state of disorder by thermal agitation. With paramagnetic substances under all ordinary conditions, F is practically identical with the impressed field H.

Writing a for $\mu F/KT$, we have Langevin's equation for paramagnetism, in which the symbol L is used to denote the Langevin function:

$$\frac{I}{I_0} = \frac{\bar{\mu}}{\mu} = L(a) = \coth a - \frac{1}{a} \tag{556}$$

where $I_0 = N\mu$ is the saturation value of the intensity of magnetization $I = N\bar{\mu}$ (magnetic moment per unit volume); N is the number of dipoles per cubic centimeter. Equation (556) is valid for both para- and ferromagnetic substances and also for dielectrics. It is represented graphically in Fig. 165.

If $a << 1$, as is usually the case with paramagnetic substances, (556) may be written in the approximate form

$$\frac{I}{I_0} = \frac{\bar{\mu}}{\mu} \approx \tfrac{1}{3}a - \tfrac{1}{45}a^3 \tag{556a}$$

The small magnitude of a means that in paramagnetic phenomena, at least at ordinary fields and temperatures, the effect of thermal agitation is large in comparison with the magnetic directive force. Under extremely large fields Eq. (556) and Fig. 165 indicate an approach to saturation. This effect has been detected in gadolinium sulphate.

It is important to point out that the form of the Langevin function in Eqs. (556) and (556a) is based on the assumption that in the absence of an external field all orientations of dipoles are equally probable. When the spatial quantization of dipole directions is considered, this assumption is no longer valid and the function has to be modified. We shall revert to this in §552. So far as the general outline of ferromagnetic theory is concerned, it suffices to consider the Langevin function in its original form.

549. *Ferromagnetism.* Langevin's paramagnetic theory was applied by Debye in his treatment of electric dipoles. We come now to the contributions of Weiss, whose theory of ferromagnetism, combined with Debye's dipole theory, has become the basis of the theory of Rochelle salt.

Langevin's original theory has to do only with feebly magnetizable substances, in which it is assumed that the magnetic dipoles do not interact, but, like the molecules of a gas, are free to rotate in the field H, while subject also to thermal agitation. The theory requires that the magnetic susceptibility increase indefinitely with decreasing temperature—a requirement that is met experimentally, at least until very low temperatures are reached. The chief problems that confronted Weiss were to account for the high magnetizability of ferromagnetic materials and for the existence of the high Curie temperature, at which the material passes from the ferromagnetic to the paramagnetic state. He made the radical assumption that the effective magnetic field strength F acting upon the elementary magnetic particle is given by the equation

$$F = H + \gamma I \tag{557}$$

in which γ, the *Weiss molecular field constant*, instead of being of the order of $4\pi/3$, as in dielectrics (§113) or in diamagnetic substances, has a value of several thousand.

In ferromagnetic theory γ is sometimes considered as having different values in different directions in the crystal. It is shown in §485 that the same is true of Rochelle salt. For the present purpose we may disregard the possible anisotropy of γ.

The value of F under ordinary conditions is determined chiefly by the second term, which is proportional to the intensity of magnetization I already present.* The coefficient γ has the same value in both the para- and ferromagnetic ranges.

The requirement that γ must be large follows from the high polarization produced in ferromagnetic materials by applied fields of ordinary magnitude. It is evident that such fields must be able to align the magnetic dipoles to a very considerable degree. This is possible only if, in the Langevin parameter a, the quantity μF is not too small in comparison with KT. Taking iron as an example, we may assign to μ the order of magnitude 2 (10^{-20}). Since at room temperature $KT = 4$ (10^{-14}) ergs, it follows that F must be of the order of magnitude of 2 (10^6) oersteds. On substituting this value in Eq. (557), together with the representative value 2,000 for I (H being relatively small), we see that γ must be at least of the order of 1,000.

This abnormally large value of γ remained without theoretical justification until in 1928 Heisenberg explained it as due to exchange forces analogous to those which occur in the theory of molecular binding. The ultimate magnetic particle is assumed to be the spinning electron, which has as its magnetic moment one Bohr magneton.† According to quantum mechanics the spins in adjacent atoms must be either parallel or antiparallel. In ferromagnetic materials, the relative distances and grouping of electrons in the atom and the distances between atoms are such that the electron spins and charges can influence one another so as to bring about the parallel orientation. The spinning electrons responsible for electromagnetism are always those in *incomplete* shells.

Heisenberg finds that these exchange forces ("forces of interaction") provide a molecular field F of the right magnitude to overcome thermal agitation and thus to account for the phenomena of ferromagnetism. F may thus be thought of as equivalent to a magnetic field due to parallel spins, the forces that make the spins parallel being more nearly of electrostatic than of magnetic origin. In paramagnetic materials the electrons, of course, also have spins, but the exchange forces are negligible, and the polarization is due entirely to the alignment of magnetic dipoles by the impressed field. The pure magnetic force between dipoles is very feeble; on the other hand, as is shown in Chap. XXVI, in the Seignette analogy the *electric* dipole forces suffice to account completely for the strong internal field.

550. Following the procedure of Weiss, we substitute for I in Eq. (557) its equivalent $\bar{\mu}N$, where N is the number of elementary magnets (dipoles) per unit volume. If then both sides of (557) are divided by $\gamma\mu N$ and F is replaced by KTa/μ, there results the equation

$$\frac{\bar{\mu}}{\mu} = \frac{KT}{\gamma N \mu^2} a - \frac{H}{\gamma N \mu} \tag{558}$$

Analytically, by the use of Eq. (557) and the expression $I = \bar{\mu}N$, a may be eliminated between Eqs. (556) and (558), whence $\bar{\mu}/\mu$ or I may be expressed directly in terms of H, μ, T, and γ. A procedure analogous to this in the Seignette-electric case is mentioned in §484. It is simpler and more illuminating to use the customary graphical method of Fig. 165. In this figure the curve represents the Langevin

*We shall also refer to I as the *magnetic polarization* or simply the *polarization*.

† A discussion of the Heisenberg theory may be found in the references given in §547 and also in ref. B49.

function, while the straight lines W_p and W_f from Eq. (558) are drawn for temperatures corresponding to the paramagnetic and ferromagnetic cases, respectively. For brevity, we shall call the lines determined by Eq. (558) the *Weiss lines*. Line W_f is drawn through the origin in order to represent the state of affairs when $H = 0$. Equation (556a) shows that at the origin, where $a = \mu F/KT$ vanishes, the slope of the curve is 1/3.

The value of $\bar{\mu}/\mu$, and therefore of the intensity of magnetization I, under any given conditions, is determined by the intersection of the straight line with the curve.

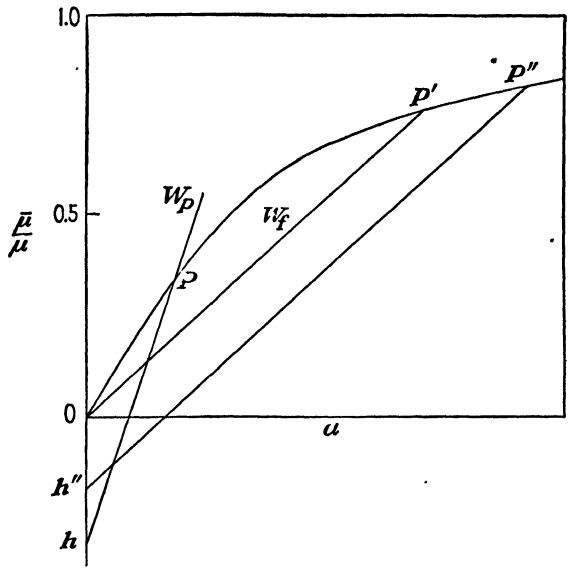


FIG. 165.—The Langevin function. The curve represents Eq. (556). Lines W_p and W_f are from Eq. (558); their slopes depend on T, while the ordinate intercepts are proportianal to H.

The higher the temperature, the greater the slope $KT/\gamma N\mu^2$ of the straight line, from Eq. (558).

For slopes greater than 1/3 the substance is *paramagnetic* (line W_p) The intercept $Oh = H/\gamma N\mu$ represents the applied field, and the value of $\bar{\mu}$ is that corresponding to the point P. If H were equal to zero, the line would touch the curve only at the origin, at which $\bar{\mu} = 0$, showing that paramagnetic materials are unpolarized in the absence of an external polarizing field.

As the temperature is decreased from a high value, for which the substance is paramagnetic, the slope of the Weiss lines diminishes until, from a certain critical temperature on, the lines for $H = 0$ begin to intersect the Langevin curve at points beyond the origin. Below this critical temperature the material has *ferromagnetic* properties and is characterized by a *spontaneous magnetization*, $\bar{\mu}$ no longer vanishing when there is no applied field. For example, the spontaneous magnetization for the temperature corresponding to the line W_f is determined by the point P'.

The critical temperature, called the *Curie temperature* and designated by θ, is

found by equating the coefficient of a in Eq. (558) to 1/3, the slope of the Langevin curve at the origin. We thus find

$$\theta = \frac{\gamma N \mu^2}{3K} \tag{559}$$

For iron, the value of θ is around 770°C, while $\gamma \approx 3{,}500$.

According to Eq. (559) the high values of the Curie points for ferromagnetic substances are due to the large values of γ. For paramagnetic materials, for which γ is of the order of $4\pi/3$, the Curie point, if it exists at all, must be sought extremely close to the absolute zero of temperature.

That such materials should become ferromagnetic at very low temperatures was predicted by Debye. Recently the transition has been found by Kürti, Lainé, and Simon* in the case of iron alum. This substance shows hysteresis and the characteristic anomaly in the specific heat (§556) at temperatures below 0.034°K, which is regarded as the Curie point.

551. *The Curie-Weiss Law.* We consider next the characteristic equation for the paramagnetic region, which also plays a part in the theory of Rochelle salt. At temperatures sufficiently above the Curie point the second term on the right side of (556*a*) may, for all ordinarily attainable fields, be ignored, and from (556*a*), (558), and (559) there results

$$\frac{\bar{\mu}}{\mu} = \frac{\mu H}{3K(T - \theta)} \tag{560}$$

and for the *mass susceptibility* we have the *Curie-Weiss law*

$$k_m = \frac{\bar{\mu} N}{II} = \frac{\mu^2 N}{3K(T - \theta)} = \frac{\theta}{\gamma(T - \theta)} \tag{561}$$

The linear relation expressed in Eq. (561) is illustrated by the straight line in Fig. 166. This law is commonly written in the form mentioned in §547, $k_m = C/(T - \theta)$. The value of θ that satisfies this equation for observed values of k_m with ferromagnetic materials above the Curie point often differs by several degrees from the actual transition point at which ferromagnetism disappears. Equation (560) shows that at these high temperatures the polarization varies linearly with H. On the other hand, at temperatures only slightly above the Curie point the dependence of polarization upon field strength is not linear. The equation corresponding to (561) for temperatures below the Curie point is (566).

Most significant is the fact that Eq. (561) predicts *infinite susceptibility* at the Curie point, where $T = \theta$. Sharp and very high maxima have indeed been observed at this point. Above the Curie point thermal agitation prevails over the exchange forces, and the quantity $a = \mu F/KT$ in Eqs. (556) and (556*a*) is relatively small. This state of disorder becomes one of comparative order below the Curie point, where the internal field F gains the upper hand. Close to the critical temperature is a narrow region of instability, where a very small applied field strength can effect a large amount of rotation of dipoles. Herein lies the physical explanation of the rapid increase in susceptibility at the Curie point. At this critical temperature the word "susceptibility" in the ordinary sense loses its meaning. There is no *abrupt* change in observed magnetic phenomena at any temperature. Indeed, the Curie "point" is usually determined by extrapolation from observations of susceptibility or of the magnetocaloric effect at temperatures considerably removed from this

* N. Kürti, P. Lainé, and F. Simon, *Compt. rend*, vol. 204, pp. 675–677, 754–756, 1937.

critical temperature and is therefore somewhat dependent on the temperature at which observations are made.

In general, it may be said that the outstanding property of ferromagnetic materials is a spontaneous polarization which disappears above a certain critical temperature. From this premise the other features follow in logical sequence. Herein lies also the essence of the analogy with Rochelle salt.

552. *Generalization of the Langevin Function.* The term "Langevin function" has come to be applied generically to any function relating the quantity a in Eq. (556) with $\bar{\mu}/\mu$. A number of variations of the original function have been derived to meet certain conditions of directional quantization. In fact, Eq. (556) is that member of the family for which the quantum number is infinity, the orientation of dipoles being unrestricted.

In its most general form the function may be written

$$L_n(a) = \frac{\bar{\mu}}{\mu} = \frac{I}{I_0} = \frac{\sum_{s=-n}^{n} \frac{s}{n} \epsilon^{(s/n)a}}{\sum_{s=-n}^{n} \epsilon^{(s/n)a}} \qquad (s = -n),\ -n+1,\ -n+2,\ \cdots\ n)$$

where $a = \mu F/KT$ and $I_0 = N\mu$; n, the quantum number, may be any integral multiple of $\frac{1}{2}$. For $n = \infty$ the expression above reduces to Eq. (556), while, for $n = \frac{1}{2}$, it corresponds to parallel or antiparallel orientation in a single direction.

Whatever the form of a polarization function may be, when it is developed in a power series the first two terms can always be written $pa - qa^3$, where p and q are constants. It is easily proved that the coefficient p, which is the initial slope of the curve, is related to n by the equation $p = \frac{1}{3} + 1/3n$. For example, when $n = \frac{1}{2}$ (§484), $p = 1$, and $q = \frac{1}{3}$.

For $a << 1$ we may therefore write the following approximate equation, of which Eq. (556*a*), the original Langevin function, is a special case:

$$\frac{I}{I_0} = \frac{\bar{\mu}}{\mu} = L_n(a) = pa - qa^3 \tag{562}$$

The coefficients p and q become $\frac{1}{3}$ and $\frac{1}{45}$, respectively, in Eq. (556*a*). We shall consider only the general expression for the Curie-Weiss law with small fields, at temperatures in the neighborhood of the Curie point. The discussion has a bearing on Signette-electric phenomena as well as on magnetism.

a. Above the Curie point, over the range for which Eq. (562) is valid, it is easily proved that

$$\frac{I}{I_0} = \frac{\bar{\mu}}{\mu} = p\frac{\mu H}{K(T-\theta)} \tag{563}$$

This equation is the generalized form of Eq. (560). It shows that the association of Weiss's Eq. (557) with any form of the Langevin function [*i.e.*, with any values of p and q in the cubic equation (562) relating the intensity of magnetization I with the molecular field F] leads to a Curie-Weiss law above the Curie point. From Eq. (563) the reciprocal susceptibility is found to be

$$\frac{1}{k_m} = \frac{H}{\bar{\mu}N} = \frac{K(T-\theta)}{p\mu^2 N} = \gamma\frac{T-\theta}{\theta} \tag{564}$$

The last part follows from Eq. (565). This relation, as well as Eq. (561), is illustrated by the straight line in Fig. 166.

b. At the Curie point, the generalized form of Eq. (559) is

$$\theta = p\gamma \frac{N\mu^2}{K} \tag{565}$$

For any given Langevin function it follows that the value assigned to μ (or to γ) must depend on p.

c. Below the Curie point there is a Curie-Weiss law, valid for small values of H (this condition is imposed by the fact that below the Curie point the phenomenon of saturation at large H makes the susceptibility a function of H) and for temperatures not far below the Curie point. We seek an expression for the initial susceptibility k_m^0. This is $\partial I/\partial H$ for $H \to 0$ and is found by taking the derivative of Eq. (562). Then from Eqs. (557), (558), and (565), one finds

$$\frac{1}{k_m^0} = 2\gamma \frac{\theta - T}{3T - 2\theta} \tag{566}$$

In contrast to the relation for $T > \theta$, this equation is not linear in T but is represented by the curve in Fig. 166. Like Eq. (561) it is independent of the special form of the Langevin function. It must be emphasized that Eq. (566) is valid only for temperatures slightly below θ and furthermore that it is characteristic of the single domain and fails to agree accurately with observed values.

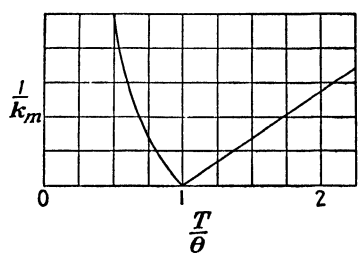


FIG. 166.—Reciprocal initial magnetic susceptibility near the Curie point.

Of chief interest from the point of view of the Seignette analogy is the similarity of Fig. 166 to Fig. 120, especially as regards the relative slopes of the lines above and just below the Curie point. From Eq. (566) the initial slope at $T = \theta$ for the curve at the left in Fig. 166 is $-2\gamma/\theta$, numerically just twice as great as for $T > \theta$, and independent of the special form of the Langevin function.

The manner in which the domain theory explains the high observed magnetic susceptibilities of ferromagnetic materials will be considered below.

553. *Domains.* Neither the Weiss theory as outlined above nor Heisenberg's theory predicts the existence of discrete "domains." It was to account for the great magnetizability of iron and for the fact that unmagnetized iron shows no external polarity that Weiss made the additional assumption that iron is composed of small regions, each magnetized to a saturation value dependent only upon the temperature, the polarities of the various regions having random orientations in the absence of a magnetizing field. Today there is convincing evidence of their reality. Their origin has been the object of much speculation, especially in relation to the problem of secondary crystal structure and the configuration for minimum energy.

So far as iron is concerned, the evidence at present indicates that each of the minute crystals of which ordinary iron is composed consists of still smaller domains, each having a volume of the order of 10^{-8} cm^3 and containing 10^{14} to 10^{15} atoms.* The three cubic axes of iron are "directions of easy magnetization," and in each domain the spins associated with the atoms tend to become aligned parallel to one

* R. M. BOZORTH, *Bell System Tech. Jour.*, vol. 19, pp. 1–39, 1940.

of these directions, in accordance with Heisenberg's theory. The result is the spontaneous polarization. In polycrystalline material the separate crystals themselves have random orientation.

The spontaneous polarization within each domain, which is zero at the Curie temperature, increases at first rapidly with decreasing temperature and gradually approaches a saturation value at 0°K, when all the atoms are similarly oriented.

The Langevin function [Eq. (556)] applies only to the individual domain. For iron at room temperature the polarization of the domain is not far from complete saturation. This state is represented by point P' in Fig. 165. If now a magnetizing field H is applied, represented by Oh'' in Fig. 165, the polarization is increased from P' to P''. This increment is small, owing to the high polarization already present and also to the fact that on the scale to which such diagrams are drawn the distance Oh'', even for large applied fields, is very small. From these considerations it follows that, except near the Curie point, the susceptibility of the individual domain is very low. The observed high permeability of ferromagnetic substances is therefore not a property of the domain but is due, as will be explained in §555, to alterations in the directions of polarization in the domains.

As is seen in §521, the domain structure of Rochelle salt can be superficially explored by dusting powdered sulphur and red lead over a freshly heated crystal. There is a certain degree of analogy between this and the recent technique, employed by Bitter and others, in which a finely divided ferromagnetic powder in the colloidal state is allowed to settle on the surface of a ferromagnetic substance. This method brings to light great complexities in the crystalline structure, the finest details of which have a magnitude in agreement with that which on other grounds is attributed to the magnetic domains. A typical magnetic domain appears to be of the form of either a rod or a flat plate. The fact that a change in temperature (the pyroelectric effect) must be used in the experiments with Rochelle salt, while it is unnecessary in the magnetic case, is of course due to electric conduction in the salt crystal, which, when the temperature is left unchanged, soon causes compensating charges which mask those due to the spontaneous polarization. Nothing like this exists in magnetism.

When we pass from consideration of the single domain to that of aggregates of many domains, as is necessary in order to explain the form of the magnetization and hysteresis curves, we can no longer make use of the Langevin function alone. Its importance in ferromagnetism, as also in the theory of Rochelle salt, lies chiefly in helping to interpret the nature of the Curie point, which is definitely a property of the domain.

554. *Magnetism and Strain.* Just as in piezoelectric crystals, and especially in Rochelle salt, the dielectric properties are affected by the state of strain, so in ferromagnetic materials the magnetism is closely related to strain. The *magnetostrictive effect*, discovered by Joule, is now believed to consist in a deformation of the domain by an applied magnetic field. The converse effect, a change in magnetic properties when the material is stressed, has become of great importance in understanding the nature of magnetization. At first sight these phenomena might appear to be the counterparts of the converse and direct piezoelectric effects, respectively. The effects are somewhat analogous, it is true; but the relations between strain and polarization, both in magnitude and direction, are very much more complicated in the case of magnetism.

The analogue of piezoelectricity is the piezomagnetism discussed in §557. This linear effect is theoretically absent in crystals of the class to which iron belongs.

555. *The Hysteresis Loop.* We now consider briefly the form of the curves of magnetization and of hysteresis. It was the observation of strikingly similar curves

for the electric polarization of Rochelle salt that first led to the idea of the "ferromagnetic analogy." The simplest possible case would be that of an ideal crystal consisting of a single domain with a single axis of easy magnetization, the susceptibility along the other axes being very small. In conformity with the Weiss theory, such a crystal has a permanent spontaneous intensity of magnetization I_1, the magnitude of which is a function of temperature, but independent of the impressed H, while the direction may be either + or −. Starting with I_1 negative, there is a critical H_1 at which the magnetic polarity is abruptly reversed, as indicated in Fig. 167. Under an alternating impressed field, a rectangular hysteresis loop is produced. Loops approximating to this form have been observed with certain pyrrhotite crystals and also with permalloy. Various degrees of magnetic anisotropy have been found in a number of substances.

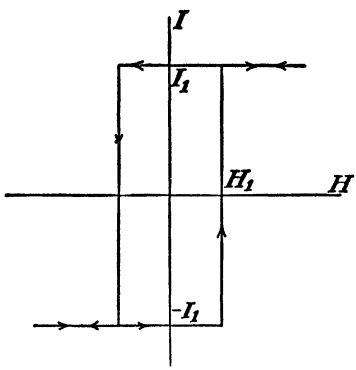


FIG. 167.—The three stages of magnetization in an ideal ferromagnetic crystal.

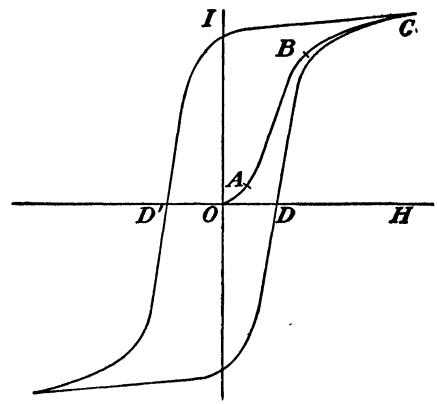


FIG. 168.—Typical magnetization curve and hysteresis loop.

In most ferromagnetic materials there are many domains, whose polarities neutralize one another when the specimen is in the demagnetized state.

As is well known, a typical virgin curve has three stages, shown in Fig. 168. The form of the portion OA, corresponding to the "initial permeability," is dependent on the magnetostrictive effect between adjacent domains, which, when a small external field is applied, leads to the growth of those domains which happen to be magnetized the right way at the expense of their neighbors. This process is called "translational magnetization." Along the portion AB, the directions of spontaneous magnetization of groups of domains are being changed abruptly from one stable position to another, as is made evident by the Barkhausen effect. At the approach to saturation we have the third stage BC, in which, under the influence of the large H, the direction of polarization of each domain is turned away from the direction of easy magnetization and becomes more and more nearly parallel to the direction of H. By way of analogy it may be added that with Rochelle salt the direction of spontaneous magnetization is actually *reversed* by strong fields, although in the case of Rochelle salt there is evidence that this reversal is only temporary. In contrast with iron, Rochelle salt has only one axis of easy polarization, and its domains are enormously large in comparison with those of ordinary ferromagnetic substances.

The form of the hysteresis loop obtained with an alternating magnetic field, like

that of the virgin curve, varies greatly with composition, heat treatment, external and internal stress, and other factors. In the case of single crystals the direction of the field relative to the crystal axes also plays a part. Along the steep portions of the curve the Barkhausen discontinuities find a simple explanation in terms of the domain theory. It is also in agreement with theory that changes in magnetization with temperature proceed smoothly. A useful index to the magnetic properties is the coercive force, represented by OD or OD' in Fig. 168, which is thought to depend on inhomogeneous strains. Permalloy with composition $FeNi_3$, for example, has a coercive force of the order of only 0.05 oersted, while for its permeability, owing to the absence of internal strains, values of over 1,000,000 have been observed. Although the effects of mechanical strain on the magnetic state are very complicated, involving considerations not present in dielectric phenomena, still they offer a striking correspondence between ferromagnetic and Seignette-electric substances.

556. There are two closely related *thermal effects* which play an important part in ferromagnetic theory and to which Rochelle salt offers at least slight analogies. The first of these is the anomaly in the *specific heat* of iron, which is related by theory to the variation of spontaneous polarization with temperature and which Weiss and his associates found to rise to a sharp maximum at the Curie point. The second is the *magnetocaloric effect*, also discovered by Weiss. This consists in a small rise in temperature upon the application of a magnetizing field and is the converse of the change in magnetic moment with temperature. The latter is the analogue of the *pyroelectric* effect, while the former corresponds to the *elcctrocaloric* effect discussed in §523. One may take as the magnetic analogue of any pyroclectric crystal either a single domain or a permanent magnet.

A change in temperature upon application of a magnetizing field is characteristic of both ferro- and paramagnetic substances. Indeed, it is the fall in temperature of certain paramagnetic substances upon removal of the magnetizing field that is now used for the attainment of temperatures near the absolute zero. The agreement between the theory of the magnetocaloric effect and the experimental results affords convincing proof of the essential correctness of Weiss's concept of the internal field. From the experimental results have been derived the most reliable values of the internal field constant γ and of the Curie temperature.

557. Piezomagnetism. For its theoretical interest and its analogy to piezoelectricity we mention this subject briefly. It involves a relation between II, an axial vector, and the symmetrical elastic tensor. By the method of the thermodynamic potential Voigt* derives the fundamental equations for the piezomagnetic "constants" n and "moduli" m. These are analogous to the piezoelectric e and d. The matrices for the various crystal classes, however, are not the same as for piezoelectricity but are related to those for the elastic groups; they comprise all classes except Nos. 29, 31, and 32. Voigt's theory, couched in the language of 1901, assumes that a small magnetic polarization accompanies the change in molecular orientation caused by strain.

Voigt made experimental tests of his theory with quartz and pyrite; the looked-for effect was smaller than the observational errors, so that only an upper limit could be set to the size of the coefficients.

* "Lehrbuch," p. 938.

GENERAL BIBLIOGRAPHY

The bibliography is in two sections. First comes the list of books, to most of which reference has been made in the text. The reference numbers of books are prefixed by the letter B.

The second part contains articles from periodicals. It would be several times longer if it contained all references that bear on the subject, including publications in the various technical, popular, and radio periodicals, reports of scientific and engineering congresses, and annual reports of national laboratories.

At the ends of some of the chapters are classified lists of references. These lists consist in part of items in the General Bibliography and in part of books or articles on those special topics with which the particular chapters are concerned.

A fairly complete bibliography on piezoelectricity was published by the author in 1928.[99] Many of the references in that bibliography are here omitted. Those of chief historical interest have been retained, together with certain ones to which reference is made in the text.

The 1928 bibliography contained also a list of patents bearing on the subject. Since then a vast number of patents have been issued in various countries, ranging all the way from inventions of fundamental importance to trifling details. A few of them are mentioned in the text.

ABBREVIATIONS OF NAMES OF PERIODICALS

Abh. Gött.	Abhandlungen der Gesellschaft der Wissenschaften zu Göttingen
Abh Sächs.	Abhandlungen der mathematischen-physikalischen Klasse der Sächsischen Akademie der Wissenschaften zu Leipzig
Alta freq.	Alta frequenza
An. chim. phys.	Annales de chimie et de physique
An. fr. chron.	Annales françaises de chronométrie
An. Phk.	Annalen der Physik (from 1824 to 1899, Annalen der Physik und Chemie)
An. Phq.	Annales de physique
Ann. soc. sci. Brux.	Annales de la société scientifique de Bruxelles
Anz. Wien	Anzeiger der Akademie der Wissenschaften zu Wien, mathematisch-naturwissenschaftliche Klasse
A.P.T.	American Physics Teacher
Arch. sci. phys. nat.	Archives des sciences physiques et naturelles. Geneva
A.W.A. Tech. Rev.	A.W.A. Technical Review. Published by Amalgamated Wireless (Australasia), Ltd., Sydney, Australia
Bell Labs. Rec.	Bell Laboratories Record
Bell Syst. T.J.	Bell System Technical Journal
Ber. Sächs.	Berichte der Königlichen Sächsischen Gesellschaft der Wissenschaften (mathematisch-physikalische Klasse)

Ber. Wien	Sitzungsberichte der Akademie der Wissenschaften zu Wien (mathematisch-naturwissenschaftliche Klasse)
Brit. Rad. Ann.	British Radio Annuals
Bull. soc. min. fr.	Société française de minéralogie, bulletin. Until 1885, société minéralogique de France
Can. J. Res.	Canadian Journal of Research
C.R.	Comptes rendus hebdomadaires des séances de l'académie des sciences
C.R. congrès int. d'élec	Comptes rendus du congrès international d'électricité, Paris, 1932
C.R. (Russ.)	Comptes rendus (Doklady), Akademia Nauk, S.S.S.R., Leningrad; published in both a Russian edition and a French-English-German edition with French title
Dati e mem.	Dati e memorie sulle radiocomunicazioni, Rome
Denki Hyoron	Denki Hyoron (Kyoto) (in Japanese)
Elec. Comm.	Electrical Communication
Elec. Rev. (Jap.)	Electrical Review (Japan) (Electrotechnical Laboratory Tokyo)
Electrotech. Jour. (Jap.)	Journal of the Electrotechnical Laboratory, Ministry of Communications, Tokyo, Japan
ENT	Elektrische Nachrichten-Technik, Berlin
ENW	Elektrisches Nachrichtenwesen, Berlin
Ergeb. exakt. Naturwiss.	Ergebnisse der exakten Naturwissenschaften, Herausgegeben von der Schriftleitung der "Naturwissenschaften," Verlag von Julius Springer, Berlin
ETZ	Elektrotechnische Zeitschrift
F. M. Mag.	Frequency Modulation Magazine
Funktech. Mon.	Funktechnische Monatshefte
G.E. Rev.	General Electric Review
Helv. Ph. Ac.	Helvetica Physica Acta
Hfr. u. El. ak.	Hochfrequenztechnik und Elektroakustik, Jahrbuch der Drahtlosen Telegraphie und Telephonie (formerly Zeitschrift für Hochfrequenztechnik)
Izv. El. Slab. Toka	Izvestiia Elektromyshlennosti Slabogo Toka, Leningrad and Moscow
J.A.S.A.	Journal of the Acoustical Society of America
J. Am. Chem. Soc.	Journal of the American Chemical Society
J. Appl. Ph.	Journal of Applied Physics
J. Appl. Ph. (Russian)	Journal of Applied Physics, Leningrad and Moscow (in Russian)
J. Exp. Th. Ph. U.S.S.R.	Journal of Experimental and Theoretical Physics, Leningrad
J. Frank. Inst.	Journal of the Franklin Institute
J.I.E.E. (Japan)	Journal of the Institute of Electrical Engineers of Japan
J.I.E.E. (London)	Journal of the Institution of Electrical Engineers (England)
J.I.T.T.E. Jap.	Journal of Institute of Telegraph and Telephone Engineers of Japan (in Japanese)

J.O.S.A.	Journal of the Optical Society of America
J. Ph. U.S.S.R.	Journal of Physics of the U.S.S.R.
J. phq.	Journal de physique et le radium. Until 1919, Journal de physique théorique et appliquée
J. Res. N.B.S.	Journal of Research of the National Bureau of Standards (from 1928 to 1934, Bureau of Standards Journal of Research)
J. Russ. Ph.-Chem. Soc.	Journal of the Russian Physical Chemical Society, Leningrad (in Russian)
J. Sci. Instr.	Journal of Scientific Instruments, London
J. Tech. Phys.	Journal of Technical Physics (in Russian)
Konink. Akad. Amst.	Koninklijke Akademie van Wetenschappen te Amsterdam, Proceedings
L'Elettrot.	L'Elettrotecnica, Milan
L'Onde élec.	L'Onde électrique
Luftfahrt-F.	Luftfahrtforschung
Nachr. Gött.	Gesellschaft der Wissenschaften zu Göttingen, Nachrichten, mathematisch-physikalische Klasse
Naturwiss.	Die Naturwissenschaften, Berlin
Neues Jahrb. Min.	Neues Jahrbuch für Mineralogie, Geologie und Paläontologie
Nippon Elec. Comm. Eng.	Nippon Electrical Communication Engineering, Institute of Electrical Communication Engineers of Japan, Tokyo
Phil. Mag.	Philosophical Magazine
Phys. Rev.	Physical Review
Phys. ZS	Physikalische Zeitschrift
Phys. ZS. d. Sowjetunion	Physikalische Zeitschrift der Sowjetunion
P.O.E.E.J.	Post Office Electrical Engineers' Journal, London
Proc. A.A.A.S.	Proceedings of the American Academy of Arts and Sciences
Proc. A.I.E.E.	Proceedings of the American Institute of Electrical Engineers
Proc. I.R.E.	Proceedings of the Institute of Radio Engineers
Proc. Nat. Acad. Sci.	Proceedings of the National Academy of Sciences of the United States of America
Proc. Ph. Soc.	Proceedings of the Physical Society, London
Proc. Roy. Soc.	Proceedings of the Royal Society of London, *A*, papers of mathematical or physical character
Proc. World Eng. Cong., Tokyo	Proceedings of the World Engineering Congress, Tokyo
QST	QST, published by the American Radio Relay League
QST fr.	QST français
Radio-Centrum	Radio-Centrum, journal of the Nederlandsche vereeniging voor radiotelegraphie, The Hague
Rass. P.T.T	Rassegna delle Poste, dei Telegrafi e dei Telefoni, Rome
Rep. El. Res. Inst. Tokyo	Reports of the Electrical Research Institute of the Tokyo Municipality
Rev. d'opt.	Revue d'optique, théorique et instrumentale, Paris
Rev. gén. de l'élec.	Revue générale de l'électricité
R.R.R.W. Jap.	Reports of Radio Researches and Works in Japan

R.S.I.	Review of Scientific Instruments
Sci.	Science
Sci. Pap. Bur. St.	Scientific Papers of the Bureau of Standards, Washington
Tech. Phys. U.S.S.R.	Technical Physics of the U.S.S.R., Leningrad
Telef. Hausmitt.	Telefunken Hausmitteilungen
Telef.-Z.	Telefunken-Zeitung
T.R. Bull.	T. and R. Bulletin, Official Journal of the Radio Society of Great Britain
Trans. A.I.E.E.	Transactions of the American Institute of Electrical Engineers
Trans. Conn. Acad.	Transactions of the Connecticut Academy of Arts and Sciences
Trans. Roy. Soc. Can.	Transactions of the Royal Society of Canada
U.R.S.I. Gen. Assem.	Proceedings of the General Assembly, International Scientific Radio Union
V.D.I.	Zeitschrift des Vereines Deutscher Ingenieure, Berlin
Wied. An.	Wiedemann's Annalen
W.E.	The Wireless Engineer and Experimental Wireless. Originally, Experimental Wireless, then Experimental Wireless and the Wireless Engineer, London
W. World	Wireless World and Radio Review, London
Zentr. f. Min.	Zentralblatt für Mineralogie, Geologie und Paläontologie, Abt. A
ZS. Elektrochem.	Zeitschrift für Elektrochemie
ZS. Hfr.	Zeitschrift für Hochfrequenztechnik (see Hochfrequenztechnik und Elektroakustik)
ZS. Instr.	Zeitschrift für Instrumentenkunde, Berlin
ZS. Kr.	Zeitschrift für Kristallographie
ZS. Ph.	Zeitschrift für Physik
ZS. ph. Chem.	Zeitschrift für physikalische Chemie
ZS. tech. Ph.	Zeitschrift für technische Physik

BOOKS

B1. AUERBACH, F., and W. HORT: "Handbuch der physikalischen und technischen Mechanik," vol. 3, J. A. Barth, Leipzig, 1927, 468 pp.

B2. BARTON, EDWIN H.: "A Text-Book on Sound," Macmillan & Co., Ltd., London, 1919, 687 pp.

B3. BEDEAU, F.: "Le Quartz piézo-électrique et ses applications dans la technique des ondes hertziennes" (Memorial des sciences physiques, Fasc. VI), Gauthier-Villars & Cie, Paris, 1928, 64 pp.

B4. BERGMANN, L.: "Schwingende Kristalle und ihre Anwendung in der Hochfrequenz-und Ultraschalltechnik," B. G. Teubner, Leipzig, 1937, 47 pp.

B5. BERGMANN, DR. LUDWIG: "Der Ultraschall und seine Anwendung in Wissenschaft und Technik," Berlin, VDI-Verlag G.m.b.H., 1937, 230 pp; 2d ed., 1939, 358 pp.; 3d ed., 1942, 445 pp.; English translation of the 1st edition entitled "Ultrasonics and Their Scientific and Technical Applications," by Dr. H. Stafford Hatfield, George Bell & Sons, Ltd., London, John Wiley & Sons, Inc., New York, 1939, 264 pp.

B6. BORN, MAX: "Atomtheorie des festen Zustandes," 2d ed., B. G. Teubner, Leipzig and Berlin, 1923, 262 pp.

B7. BORN, MAX: "Optik, ein Lehrbuch der elektromagnetischen Lichttheorie," Verlag Julius Springer, Berlin, 1933, 591 pp. (Chapter on Crystal Optics.)

B8. BRAGG, W. L.: "Atomic Structure of Minerals," Cornell University Press, Ithaca, New York, 1937, 292 pp.

B9. CRANDALL, IRVING B.: "Theory of Vibrating Systems and Sound," D. Van Nostrand Company, Inc., New York, 1926, 272 pp.

B10. CURIE, P.: "Œuvres de Pierre Curie," Gauthier-Villars & Cie, Paris, 1908, 621 pp.

Contains reprints of following papers on piezoelectricity (pages in the "Œuvres" are printed in boldface type): (*a*) *C.R.*, vol. 91, p. 294, 1880 (**6**); (*b*) *C.R.*, vol. 91, p. 383, 1880 (**10**); (*c*) *C.R.*, vol. 92, p. 186, 1881 (**15**); (*d*) *C.R.*, vol. 92, p. 350, 1881; *Jour. d. phys.*, 2d ser., vol. 1, p. 245, 1882 (**18**); (*e*) *C.R.*, vol. 93, p. 204, 1881; *Jour. d. phys.*, 2d ser., vol. 1, p. 245, 1882 (**22**); (*f*) *C.R.*, vol. 93, p. 1137, 1881 (**26**); (*g*) *C.R.*, vol. 95, p. 914, 1882 (**30**); (*h*) *Bulletin des séances de la société française de physique*, 1887 p. 47, (**33**); (*i*) *C.R.*, vol. 106, p. 1287, 1888; *Jour. d. phys.*, 2d ser., vol. 8, p. 149, 1889 (**35**); (*j*) *An. chim. Phys.*, 6th ser., vol. 17, p. 392, 1889 (**554**); (*k*) *Jour. d. phys.*, 3d ser., vol. 3, p. 393, 1894 (**118**). References (*h*) and (*k*) are by P. Curie; (*j*) by J. Curie; the remainder by P. and J. Curie.

B11. CURIE, MME. P.: "Traité de Radioactivité," vol. 1, Gauthier-Villars & Cie, Paris, 1910; "Die Radioaktivität," (German translation by B. Finkelstein), vol. 1, Akademische Verlagsgesellschaft m.b.H., Leipzig, 1912, 420 pp.

B12. DAKE, H. C., F. L. FLEENER, and B. H. WILSON: "Quartz Family Minerals," Whittlesey House, New York, 1938, 304 pp.

B13. DALE, A. B.: "The Form and Properties of Crystals," University Press, Cambridge, London, 1932, 186 pp.

B14. DAVEY, WHEELER P.: "A Study of Crystal Structure and Its Applications," McGraw-Hill Book Company, Inc., New York, 1934, 695 pp.

B15. DEBYE, P.: "Polar Molecules," Chemical Catalog Company, Inc., New York, 1929, 172 pp.

B16. DEBYE, P., and H. SACK: "Theorie der elektrischen Molekulareigenschaften," Handbuch der Radiologie, 2d ed., vol. 6, part 2, pp. 69–204, 1934; also issued as a separate publication by the Akademische Verlagsgesellschaft m.b.H., Leipzig, 1934.

B17. "Encyclopädie der mathematischen Wissenschaften," edited by A. Sommerfeld, vol. 5, B. G. Teubner, Leipzig, 1903–1926.

B18. FOWLER, R. H.: "Statistical Mechanics," 2d ed., Cambridge University Press, London, 1936, 864 pp.

B19. GEIGER, H., and K. SCHEEL: "Handbuch der Physik," Verlag Julius Springer, Berlin. Vol. 6, 1927: F. Pfeiffer, Theory of Vibrations (including crystals), pp. 334–403; J. W. Geckeler, Elasticity of Crystals (with references and numerical data), pp. 404-427. Vol. 8, 1927: H. Lichte, Piezoelectric Transmitters for Sound Waves, pp. 332–335. Vol. 12, 1927: A. Güntherschulze, Electrostriction, pp. 555–559. Vol. 13, 1928: H. Falkenhagen, Pyro- and Piezoelectricity (with some applications), pp. 291–331.

B20. GRAETZ, L.: "Handbuch der Elektricität und des Magnetismus," vol. 1, J. A. Barth, Leipzig, 1918: R. v. Hirsch, Electrostriction, pp. 262–270; E. Riecke, Pyro- and Piezoelectricity, pp. 342–419.

B21. GRAMONT, A. DE: "Recherches sur le quartz piézoélectrique," Éditions de la Revue d'optique théorique et instrumentale, Paris, 1935, 113 pp.

B22. GROTH, P.: "Physikalische Krystallographie," Wilhelm Engelmann, Leipzig, 1905, 820 pp.; also "Elemente der physikalischen u. chemischen Krystallographie," R. Oldenbourg, Munich and Berlin, 1921, 363 pp.
B23. HANDEL, P. VON: "Grundlagen der Kurzwellen-Sendung," in "Hochfrequenztechnik in der Luftfahrt," edited by H. Fassbender, Verlag Julius Springer, Berlin, 1932, pp. 228–248.
B24. HIEDEMANN, EGON: "Grundlagen und Ergebnisse der Ultraschallforschung," Walter de Gruyter & Company, Berlin, 1939, 287 pp.
B25. HINTZE, C.: "Handbuch der Mineralogie," Veit, Leipzig, 1897–1933.
B26. HONESS, A. P.: "The Nature, Origin and Interpretation of the Etch Figures on Crystals," John Wiley & Sons, Inc., New York, 1927, 171 pp.
B27. HUND, AUGUST: "Hochfrequenzmesstechnik," 2d ed., Verlag Julius Springer, Berlin, 1928, 526 pp.
B28. HUND, AUGUST: "High-frequency Measurements," McGraw-Hill Book Company, Inc., New York, 1933, 491 pp.
B29. "International Critical Tables," vol. 6, pp. 207–212, Electroelastic and Pyroelectric Phenomena, McGraw-Hill Book Company, Inc., New York, 1929.
B30. JOFFÉ, A. F.: "The Physics of Crystals," 1st ed., McGraw-Hill Book Company, Inc., New York, 1928, 198 pp.
B31. KOGA, I.: "Elements of Piezoelectric Oscillating Crystal Plate," Institute of Electrical Engineers of Japan, 1933, 76 pp., (in Japanese).
B32. KURCHATOV, I. V.: "Seignette Electricity," Moscow, 1933, 104 pp. (in Russian); French translation, abbreviated, entitled "Le Champ moléculaire dans les diélectriques (le sel de Seignette)," by I. V. Kourtschatov, Hermann & Cie, Paris, 1936, 47 pp..
B33. LAMB, HORACE: "The Dynamical Theory of Sound," Edward Arnold & Co., London, 1910, 303 pp.
B34. LOVE, A. E. H.: "A Treatise on the Mathematical Theory of Elasticity," 4th ed., Cambridge University Press, London, 1934, 643 pp.
B35. MASON, WARREN P.: "Electromechanical Transducers and Wave Filters," D. Van Nostrand Company, Inc., New York, 1942, 333 pp.
B36. MARX, DR. ERICH: "Handbuch der Radiologie," Leipzig, 2d ed., vol. 6, published by Dr. Erich Marx, Akademische Verlagsgesellschaft m.b.H., Die Theorien der Radiologie, 1934.
B37. MOULLIN, E. B.: "The Theory and Practice of Radio Frequency Measurements," 2d ed., Charles Griffin & Company, Ltd., London, 1931, 487 pp.
B38. MYERS, L. M.: "Television Optics: An Introduction," Pitman Publishing Corporation, New York, 1936, 338 pp.
B39. PETRZILKA, V., and J. B. SLAVIK: "Piezoelektrina—A Jeji Pouziti V Technicke Praxi," Jednoty ceskych matematiku a fysiku, Prague, 1940, 117 pp.
B40. POCKELS, F.: "Uber den Einfluss des elektrostatischen Feldes auf das optische verhalten piezoelektrischer Krystalle," Dieterisch'sche Verlagsbuchhandlung, Göttingen, 1894, 204 pp.
B41. POCKELS, F.: "Lehrbuch der Kristalloptik," B. G. Teubner, Leipzig and Berlin, 1906, 519 pp.
B42. POYNTING, J. H., and J. J. THOMSON: "A Text-book of Physics," vol. 4, Electricity and Magnetism, part 1, London, 1920; Pyroelectricity and Piezoelectricity, pp. 148–163.
B43. RAYLEIGH, LORD: "The Theory of Sound," Macmillan & Company, Ltd., London, 1926, vol. 1, 480 pp.; vol. 2, 504 pp.
B44. ROGERS, AUSTIN F., and PAUL F. KERR: "Optical Mineralogy," McGraw-Hill Book Company, Inc., New York, 1942, 390 pp.

B45. SCHEIBE, DR. A.: "Piezoelektrizität des Quarzes," Theodor Steinkopf, Dresden and Leipzig, 1938, 233 pp.
B46. SHUBNIKOV, A. V.: "Quartz and Its Applications," Press of the Academy of Science of the U.S.S.R., Moscow and Leningrad, 1940, 194 pp. (in Russian).
B47. SOSMAN, R. B.: "The Properties of Silica," Chemical Catalog Company, Inc., New York, 1927, 856 pp.
B48. TUTTON, A. E. H.: "Crystallography and Practical Crystal Measurement," 2d ed., Macmillan & Company, Ltd., London, 1922, 2 vols., 746 and 699 pp.
B49. VAN VLECK, J. H.: "The Theory of Electric and Magnetic Susceptibilities," Oxford, Clarendon Press, New York, 1932, 384 pp.
B50. VIGOUREUX, P.: "Quartz Resonators and Oscillators," His Majesty's Stationery Office, London, 1931, 217 pp.
B51. VIGOUREUX, P.: "Quartz Oscillators and Their Applications," His Majesty's Stationery Office, London, 1939, 131 pp.
B52. VOIGT, W.: "Lehrbuch der Kristallphysik," B. G. Teubner, Leipzig, 1st ed., 1910, 964 pp.; 2d ed., 1928, 978 pp., identical with the first except for the addition of an appendix on secondary effects in the flexure and torsion of circular cylinders, based on refs. 573 and 576.
B53. WIEN, W., and F. HARMS: "Handbuch der Experimentalphysik," Akademische Verlagsgesellschaft m.b.H., Leipzig. Vol. 10, 1930: G. Hoffmann, Electrostriction, pp. 262–267; Pyro- and Piezoelectricity (with brief statement of applications), pp. 327–345. Vol. 13, part 2, 1928: H. Rothe, Quartz Resonators, pp. 437–453. Vol. 17, part 1, 1934: H. Schmidt, Vibrations of Solids (including crystals), pp. 285–454; E. Grossmann, Ultrasonics, pp. 469–534.
B54. WINKELMANN, A.: "Handbuch der Physik," Leipzig, vol. 4, part 1, 1905: L. Graetz, Electrostriction, pp. 162–168; F. Pockels, Pyro- and Piezoelectricity, pp. 766–791.
B55. WOOD, R. W.: "Supersonics, the Science of Inaudible Sounds," Charles K. Colver Lectures, 1937, Brown University, Providence, R.I., 1939, 158 pp.
B56. WOOSTER, W. A.: "A Text-book on Crystal Physics," Cambridge University Press, London, 1938, 295 pp.
B57. WYCKOFF, R. W. G.: "The Analytical Expression of the Results of the Theory of Space-groups," Carnegie Institute of Washington, 1922, 180 pp.; 2d edition, 1930, 180 pp.

PERIODICALS

1. ACKERMANN, W.: Dependence of Pyroelectricity on Temperature, *An. Phk.*, vol. 46, pp. 197–220, 1915.
2. AMARI, S.: On the Frequency Variation of Quartz-controlled Short-wave Radio Transmitters, *R.R.R.W. Jap.*, vol. 6, absts, p. 9, 1936.
3. ANDERSON, J. E.: Frequency Characteristics of Piezoelectric Oscillators, *Electronics*, vol. 11, pp. 22–24, August, 1938.
4. ANDREEFF, A., V. FRÉDERICKSZ, and I. KAZARNOWSKY: The Dependence of the Piezoelectric Constants of Quartz upon Temperature, *ZS. Ph.*, vol. 54, pp. 477–483, 1929.
5. ANGRISANO, G.: Experimental Arrangement for the Determination of the Resonance Curves of Piezoelectric Resonators, *L'Elettrot.*, vol. 17, pp. 678–679, 1930.
6. ANTSELIOVICH, E. S.: On the Stability of Oscillators, *Izv. El. Slab. Toka*, no. 6, pp. 28–39, 1935.
7. ANTSELIOVICH, E. S.: The Frequency Stability of Crystal-controlled Valve Oscillators, *Izv. El. Slab. Toka*, no. 9, pp. 1–9, 1935.

8. ARKHANGEL'SKAYA, A.: Measurement of the Parameters of Quartz Plates, *Izv. El. Slab. Toka*, nos. 8/9, pp. 28–35, 1938.
9. ARNULF, A.: Examination of Raw Quartz Crystals by Immersion, *Rev. d'opt.*, vol. 10, pp. 453–473, 1931.
10. ARX, A. VON, and W. BANTLE: Polarization and Specific Heat of KH_2PO_4, *Helv. Ph. Ac.*, vol. 16, pp. 211–214, 1943.
11. ARX, A. VON, and W. BANTLE: The Converse Piezoelectric Effect in KH_2PO_4, *Helv. Ph. Ac.*, vol. 16, pp. 416–418, 1943.
12. ATANASOFF, J. V., and P. J. HART: Dynamical Determination of the Elastic Constants and Their Temperature Coefficients for Quartz, *Phys. Rev.*, vol. 59, pp. 85–96, 1941.
13. ATANASOFF, J. V., and E. KAMMER: A Determination of the c_{44} Elastic Constant for Beta-quartz, *Phys. Rev.*, vol. 59, pp. 97–99, 1941.
14. AWENDER, H., and E. BUSSMAN: A Heterodyne Adaptor Unit for 1.6 m Wavelength with and without Crystal Control, *Funktech. Mon.*, no. 12, pp. 441–442, 1936.
15. BAHRS, S. and J. ENGL: On the Piezoelectric Effect with Ammonium Chloride Crystals Having a Transition Point at 30.5°, *ZS. Ph.*, vol. 105, pp. 470–477, 1937.
16. BALDWIN, C. F.: Quartz Crystals, *G.E. Rev.*, vol. 43, pp. 188–194, 237–243, 1940.
17. BALDWIN, C. F.: Quartz Crystals in Radio, *Communications*, vol. 22, pp. 20*f.*, October, 1942.
18. BALDWIN, F. C., and S. A. BOKOVOY: Practical Operating Advantages of Low Temperature-Frequency Coefficient Crystals, *QST*, vol. 19, pp. 26, 27, 92, January, 1935.
19. BALZER, K.: A Contribution to the Problem of Multiple Waves in Piezoelectric Quartz Plates, *ZS. tech. Ph.*, vol. 18, pp. 169–170, 1937.
20. BANCROFT, D.: The Effect of Hydrostatic Pressure on the Susceptibility of Rochelle Salt, *Phys. Rev.*, vol. 53, pp. 587–590, 1938.
21. BANCROFT, D.: The Velocity of Longitudinal Waves in Cylindrical Bars, *Phys. Rev.*, vol. 59, pp. 588–593, 1941.
22. BANTLE, W.: The Specific Heat of Seignette-electric Substances. Dielectric Measurements on KD_2PO_4 Crystals, *Helv. Ph. Ac.*, vol. 15, pp. 373–404, 1942.
23. BANTLE, W.: Artificial Crystals of KH_2PO_4 as Frequency Stabilizers, *Helv. Ph. Ac.*, vol. 16, pp. 207–209, 1943.
24. BANTLE, W., and G. BUSCH: Dielectric Investigations of Rochelle Salt, *Helv. Ph. Ac.*, vol. 10, pp. 261–264, 1937.
25. BANTLE, W., G. BUSCH, B. LAUTERBURG, and P. SCHERRER: The Spontaneous Kerr Effect in KH_2PO_4 and KH_2AsO_4 Crystals, *Helv. Ph. Ac.*, vol. 15, pp. 324–325, 1942.
26. BANTLE, W., and C. CAFLISCH: The Piezoelectric Effect of the KH_2PO_4 Crystal, Akin to Rochelle Salt, *Helv. Ph. Ac.*, vol. 16, pp. 235–250, 1943.
27. BANTLE, W., and W. LÜDY: The Elastic Properties of Seignette-electric Substances, *Helv. Ph. Ac.*, vol. 15, pp. 325–327, 1942.
28. BANTLE, W., B. MATTHIAS, and P. SCHERRER: The Dependence of Piezoelectric Resonant Frequencies of the Seignette-electrics on Field Strength, *Helv. Ph. Ac.*, vol. 16, pp. 209–211, 1943.
29. BANTLE, W., and P. SCHERRER: Anomaly of the Specific Heat of Potassium Dihydrogen Phosphate at the Upper Curie Point, *Nature*, vol. 143, p. 980, 1939.
30. BAUMGARDT, E.: Velocity of Propagation of Elastic Waves in Piezoelectric Crystals, *C.R.*, vol. 206, pp. 1887–1890, 1938.

31. BECHMANN, R.: Development of Quartz Control for the Telefunken High-power Transmitter, *Telef.-Z.*, vol. 14, pp. 17–29, 1933.
32. BECHMANN, R.: The Temperature Coefficients of the Natural Frequencies of Piezoelectric Quartz Plates and Bars, *Hfr. u. El. ak.*, vol. 44, pp. 145–160, 1934.
33. BECHMANN, R.: The Crystal Control of Transmitters, *W.E.*, vol. 11, pp. 249–253, 1934.
34. BECHMANN, R.: Measurement of the Velocity of Sound in Anisotropic Media, Particularly in Quartz, by Means of Piezoelectric Excitation, *ZS. Ph.*, vol. 91, pp. 670–678, 1934.
35. BECHMANN, R.: Investigations on the Elastic Vibrations of Piezoelectrically Excited Quartz Plates, *ZS. tech. Ph.*, vol. 16, pp. 525–528, 1935.
36. BECHMANN, R.: Quartz Oscillators, *Telef.-Z.*, vol. 17, pp. 36–45, 1936.
37. BECHMANN, R.: Quartz Resonators, *Telef.-Z.*, vol. 18, pp. 5–15, 1937.
38. BECHMANN, R.: On Circuits for Piezoelectric Quartz Oscillators and Resonators for Frequency Stabilization and Filters, *Telef. Hausmitt.*, vol. 19, pp. 60–69, March, 1938.
39. BECHMANN, R.: Thickness Vibrations of Piezoelectrically Excited Crystal Plates, *Hfr. u. El. ak.*, vol. 56, pp. 14–21, 1940.
40. BECHMANN, R.: Elastic Vibrations of an Anisotropic Body in the Form of a Rectangular Parallelepiped, *ZS. Ph.*, vol. 117, pp. 180–197, 1941.
41. BECHMANN, R.: Lengthwise Vibrations of Square Quartz Plates, *ZS. Ph.*, vol. 118, pp. 515–538, 1942.
42. BECHMANN, R.: Lengthwise Vibrations of Rectangular Quartz Plates, *ZS. Ph.*, vol. 120, pp. 107–120, 1942.
43. BECHMANN, R.: Properties of Quartz Oscillators and Resonators in the Range from 300 to 5000 kc/s, *Hfr. u. El. ak*, vol. 59, pp. 97–105, 1942.
44. BECHMANN, R.: Quartz Oscillators and Resonators in the Region from 50 to 300 kc/s., *Hfr. u. El. ak.*, vol. 61, pp. 1–12, 1943.
45. BECKER, H. E. R.: The Reaction of the Surrounding Liquid on the Vibrations of a Quartz Plate, *An. Phk.*, vol. 25, pp. 359–372, 1936.
46. BECKER, H. E. R.: On the Vibration Mechanism of a Quartz Plate in Liquids, *An. Phk.*, vol. 26, pp. 645–658, 1936.
47. BECKERATH, H.: The Vibrating Quartz in Communications Technique. Part I —The Mechanical and Electrical Properties of the Vibrating Quartz (Survey), *ENT*, vol. 19, pp. 45–62, 1942.
48. BEEVERS, C. A., and W. HUGHES: The Crystal Structure of Rochelle Salt (Sodium Potassium Tartrate Tetrahydrate $NaKC_4H_4O_6 \cdot 4H_2O$), *Proc. Roy. Soc.*, vol. 177, pp. 251–259, 1941.
49. BENOIT, J.: The Various Modes of Vibration of Piezoelectric Quartz, *L'Onde élec.*, vol 18, pp. 22–36, 1938.
50. BENSON, J. E.: A Piezoelectric Calibrator, *A.W.A. Tech. Rev.*, vol. 5, pp. 47–50, 1940.
51. BENSON, J. E.: Modes of Vibration and Design of *V*-cut Quartz Plates for Medium Broadcast Frequencies, *A.W.A. Tech. Rev.*, vol. 6, pp. 73–89, 1943.
52. BERGMANN, L.: A Simple Method for Detecting the Piezoelectricity of Crystals, *Phys. ZS.*, vol. 36, pp. 31–32, 1935; *Zentralblatt f. Mineralogie* (*A*), pp. 213–222, 1935.
53. BERGMANN, L.: On the Natural Frequencies of Piezoelectric Quartz Plates When Excited in Thickness Vibration, *An. Phk.*, vol. 21, pp. 553–563, 1935.
54. BIOT, A.: Testing Quartz Plates Cut at Right Angles to the Optic Axis, *Ann. soc. sci. Brux.*, vol. 58, pp. 98–100, 1938.

55. Bloomenthal, S.: The Converse Piezoelectric Effect in Mixed Crystals Isomorphous with Rochelle Salt, *Physics*, vol. 4, pp. 172–177, 1933.
56. Boella, M.: On the Performance of the Piezo-oscillator in Relation to the Resonance Curve of the Quartz, *L'Elettrot.*, vol. 17, pp. 672–678, 1930.
57. Boella, M.: Influence of the Decrement of the Quartz on the Oscillation Frequency of Piezo-oscillators, *L'Elettrot.*, vol. 17, pp. 734–736, 1930; *Proc. I.R.E.*, vol. 19, pp. 1252–1273, 1931.
58. Boella, M.: Piezo-oscillators with Neutralization of the Quartz, *Alta freq.*, vol. 8, pp. 512–515, 1939.
59. Boguslawski, S.: Theory of Dielectrics; Temperature Coefficient of the Dielectric Constants; Pyroelectricity, *Phys. ZS.*, vol. 15, pp. 283–288, 1914.
60. Boguslawski, S.: Pyroelectricity on the Basis of the Quantum Theory, *Phys. ZS.*, vol. 15, pp. 569–572, 1914.
61. Boguslawski, S.: On W. Ackermann's Measurements of the Temperature Coefficient of Pyroelectric Excitation, *Phys. ZS.*, vol. 15, pp. 805–810, 1914.
62. Bokovoy, S. A.: Quartz Crystals—Development and Application, *Elec. Comm.*, vol. 21, pp. 233–246, 1944.
63. Bond, W. L.: Etch Figures of Quartz, *ZS. Kr.*, vol. 99, pp. 488–498, 1938.
64. Bond, W. L.: The Mathematics of the Physical Properties of Crystals, *Bell Syst. T.J.*, vol. 22, pp. 1–72, 1943.
65. Bond, W. L.: A Mineral Survey for Piezoelectric Materials, *Bell Syst. T.J.*, vol. 22, pp. 145–152, 1943.
66. Bond, W. L.: Methods for Specifying Quartz Crystal Orientation and Its Determination by Optical Means, *Bell Syst. T.J.*, vol. 22, pp. 224–262, 1943.
67. Bond, W. L.: Processing Quartz, *Bell Labs. Rec.*, vol. 22, pp. 359–361, 1944.
68. Bond, W. L., and E. J. Armstrong: The Use of X-rays for Determining the Orientation of Quartz Crystals, *Bell Syst. T.J.*, vol. 22, pp. 293–337, 1943.
69. Booth, C. F.: The Application and Use of Quartz Crystals in Telecommunications, *J.I.E.E.*, vol. 88, part 3, pp. 97–128, 1941; discussion, pp. 128–144.
70. Booth, C. F., and E. J. C. Dixon: Crystal Oscillators for Radio Transmitters: An Account of Experimental Work Carried Out by the Post Office, *W.E.*, vol. 12, pp. 198–200, 1935; *J.I.E.E.*, vol. 77, pp. 197–236, discussion pp. 237–244, 1935; *Proc. Wireless Sec., I.E.E.*, vol. 10, pp. 129–168, discussion, pp. 169–176, 1935.
71. Booth, C. F., and C. F. Sayers: The Production of Quartz Resonators for the London-Birmingham Coaxial Cable System, *P.O.E.E.J.*, vol. 32, pp. 7–15, 88–93, 1939.
72. Borsarelli, C.: A New Piezo-oscillator, *Alta freq.*, vol. 5, pp. 763–772, 1936.
73. Bosshard, W., and G. Busch: The Damping of Piezoelectric Vibrations, *Helv. Ph. Ac.*, vol. 10, pp. 329–330, 1937; *ZS. Ph.*, vol. 108, pp. 195–199, 1938.
74. Boyle, R. W.: Ultrasonics, *Science Progress*, vol. 23, pp. 75–105, 1928.
75. Bragg, W., and R. E. Gibbs: The Structure of Alpha- and Beta-quartz, *Proc. Roy. Soc.*, vol. 109, pp. 405–427, 1925.
76. Brown, H. A.: Oscilloscope Patterns of Damped Vibrations of Quartz Plates and *Q* Measurements with Damped Vibrations, *Proc. I.R.E.*, vol. 29, pp. 195–199, 1941.
77. Brown, S. L., and S. Harris: Measurements of Temperature Coefficient and Pressure Coefficient of Quartz Crystal Oscillators, *R.S.I.*, vol. 2, pp. 180–183, 1931.
78. Brown, W. F., Jr.: Interpretation of Torsional Frequencies of Crystal Specimens, *Phys. Rev.*, vol. 58, pp. 998–1001, 1940.
79. Bücks, K., and H. Müller: On Some Observations of Vibrating Piezo-quartz Plates and Their Acoustic Radiation Field, *ZS. Ph.*, vol. 84, pp. 75–86, 1933.

80. BUILDER, G.: Quartz Crystals for the Control and Measurement of Frequency, *A.W.A. Tech. Rev.*, vol. 2, pp. 104–105, 1936.
81. BUILDER, G.: A Note on the Determination of the Equivalent Electrical Constants of a Quartz-crystal Resonator, *A.W.A. Tech. Rev.*, vol. 5, pp. 41–45, 1940.
82. BUILDER, G., and J. E. BENSON: Precision Frequency-control Equipment Using Quartz Crystals, *A.W.A. Tech. Rev.*, vol. 3, pp. 157–214, 1938; *Proc. World Radio Convention*, Sydney, Australia, 1938.
83. BUILDER, G., and J. E. BENSON: Contour-mode Vibrations in *Y*-cut Quartz-crystal Plates, *Proc. I.R.E.*, vol. 29, pp. 182–185, 1941; *A.W.A. Tech. Rev.*, vol. 5, pp. 181–189, 1941.
84. BUILDER, G., and J. E. BENSON: Simple Quartz-crystal Filters of Variable Bandwidth, *A.W.A. Tech. Rev.*, vol. 5, pp. 93–103, 1941.
85. BUISSON, H.: Method of Observing the Optical Purity of Quartz Crystals, *J. phq.*, vol. 8, pp. 25–31, 1919.
86. BUNING, DE C.: Quartz Crystals with Low Temperature Coefficients, *Radio-Centrum*, vol. 1, pp. 25–28, 1935.
87. BUSCH, G.: Anomalous Dispersion of the Dielectric Constants of Rochelle Salt, *Helv. Ph. Ac.*, vol. 6, pp. 315–336, 1933.
88. BUSCH, G.: New Seignette-electrics, *Helv. Ph. Ac.*, vol. 11, pp. 269–298, 1938.
89. BUSCH, G., and E. GANZ: Dielectric Measurements on KH_2PO_4 and KH_2AsO_4 at Low Temperatures, *Helv. Ph. Ac.*, vol. 15, pp. 501–508, 1942.
90. BUSCH, G., and P. SCHERRER: A New Seignette-electric Substance, *Naturwiss.*, vol. 23, p. 737, 1935.
91. CADY, W. G.: The Piezoelectric Resonator (abst.), *Phys. Rev.*, vol. 17, p. 531, 1921.
92. CADY, W. G.: Theory of Longitudinal Vibrations of Viscous Rods, *Phys. Rev.*, vol. 19, pp. 1–6, 1922.
93. CADY, W. G.: The Piezoelectric Resonator, *Proc. I.R.E.*, vol. 10, pp. 83–114, 1922.
94. CADY, W. G.: A Method of Testing Plates from Piezoelectric Crystals, *J.O.S.A.*, vol. 6, pp. 183–185, 1922.
95. CADY, W. G.: Piezoelectrically Driven Tuning-forks and Rods, *Phys. Rev.*, vol. 21, pp. 371–372, 1923.
96. CADY, W. G.: An International Comparison of Radio Wavelength Standards by Means of Piezoelectric Resonators, *Proc. I.R.E.*, vol. 12, pp. 805–816, 1924.
97. CADY, W. G.: Piezoelectric Standards of High Frequency, *J.O.S.A.*, vol. 10, pp. 475–489, 1925.
98. CADY, W. G.: A Shear Mode of Crystal Vibration (abst.), *Phys. Rev.*, vol. 29, p. 617, 1927.
99. CADY, W. G.: Bibliography on Piezoelectricity, *Proc. I.R.E.*, vol. 16, pp. 521–535, 1928.
100. CADY, W. G.: Some Electromechanical Properties of Rochelle Salt Crystals (abst.), *Phys. Rev.*, vol. 33, pp. 278–279, 1929.
101. CADY, W. G.: Electroelastic and Pyro-electric Phenomena, *Proc. I.R.E.*, vol. 18, pp. 1247–1262, 1930.
102. CADY, W. G.: Piezoelectric Terminology, *Proc. I.R.E.*, vol. 18, pp. 2136–2142, 1930.
103. CADY, W. G.: Low Frequency Vibrations in Rochelle Salt and Quartz Plates (abst.), *Phys. Rev.*, vol. 39, p. 862, 1932.
104. CADY, W. G.: Quartz Oscillator with Optical Control, *C.R. congrès int. d'élec.*, vol. 11, sec. 9, pp. 40–48, Paris, 1932.

105. CADY, W. G.: The Application of Methods of Geometrical Inversion to the Solution of Certain Problems in Electrical Resonance, *Proc. A.A.A.S.*, vol. 68, pp. 383–409, 1933.
106. CADY, W. G.: The Potential Distribution between Parallel Plates and Concentric Cylinders Due to any Arbitrary Distribution of Space Charge, *Physics*, vol. 6, pp. 10–13, 1935.
107. CADY, W. G.: The Piezoelectric Resonator and the Effect of Electrode Spacing upon Frequency, *Physics*, vol. 7, pp. 237–259, 1936.
108. CADY, W. G.: The Longitudinal Piezoelectric Effect in Rochelle Salt Crystals, *Proc. Ph. Soc.*, vol. 49, pp. 646–653, 1937.
109. CADY, W. G.: A Survey of Piezoelectricity, *A.P.T.*, vol. 6, pp. 227–242, 1938.
110. CADY, W. G., and K. S. VAN DYKE: Proposed Standard Conventions for Expressing the Elastic and Piezoelectric Properties of Right- and Left-quartz, *Proc. I.R.E.*, vol. 30, pp. 495–499, 1942.
111. CHAIKIN, S.: On a Direct Method for the Measurement of Small Decrements of Piezo-crystal Resonators, *Hfr. u. El. ak.*, vol. 35, pp. 6–9, 1930.
112. CLAY, J., and J. KARPER: Piezoelectric Constant of Quartz, *Physica*, vol. 4, pp. 311–315, 1937.
113. CORTEZ, S. H.: Interferometer Method for Measuring the Amplitude of Vibration of Quartz Bar Crystals, *J.O.S.A.*, vol. 24, pp. 127–129, 1934; erratum, vol. 24, p. 194, 1934.
114. COSTER, D., K. S. KNOL, and J. A. PRINS: Differences in Intensity of *X*-ray Reflection from the Two 111-Faces of Zinc Blende, *ZS. Ph.*, vol. 63, pp. 345–369, 1930.
115. CROSSLEY, A.: Piezoelectric Crystal-controlled Transmitter, *Proc. I.R.E.*, vol. 15, pp. 9–36, 1927.
116. CROSSLEY, A.: Modes of Vibration in Piezoelectric Crystals, *Proc. I.R.E.*, vol. 16, pp. 416–423, 1928.
117. CURIE, J., and P. CURIE: Development by Pressure of Polar Electricity in Hemihedral Crystals with Inclined Faces, *Bull. soc. min. de France*, vol. 3, pp. 90–93, 1880. This paper, read at the meeting of Apr. 8, 1880, contained the first announcement of the discovery of piezoelectricity.
118. CZERMAK, P.: On the Electric Behavior of Quartz, *Ber. Wien*, vol. 96, pp. 1217–1244, 1887.
119. DAVID, R.: The Dependence of the Dielectric Properties of Rochelle Salt on Mechanical Conditions, *Helv. Ph. Ac.*, vol. 8, pp. 431–484, 1935.
120. DAVIES, R. M.: On the Determination of Some of the Elastic Constants of Rochelle Salt by a Dynamical Method, *Phil. Mag.*, vol. 16, pp. 97–124, 1933.
121. DAWSON, L. H.: Piezoelectricity of Crystal Quartz, *Phys. Rev.*, vol. 29, pp. 532–541, 1927.
122. DEBYE, P., and F. W. SEARS: Scattering of Light by Supersonic Waves, *Proc. Nat. Acad. Sci.*, vol. 18, pp. 409–414, 1932.
123. DIJL, B. VAN: The Application of Ricci-calculus to the Solution of Vibration Equations of Piezoelectric Quartz, *Physica*, vol. 3, pp. 317–326, 1936.
124. DOERFFLER, H.: Flexural and Shear Vibrations in Piezoelectrically Excited Quartz Plates, *ZS. Ph.*, vol. 63, pp. 30–53, 1930.
125. DOHERTY, W. H.: Synchronized FM Transmitter, *F.M. Mag.*, vol. 1, pp. 21–25, December, 1940.
126. DRUESNE, M. A. A.: Quartz Crystals, *Communications*, vol. 23, pp. 46*f.*, September, 1943.
127. DYE, D. W.: Piezoelectric Quartz Resonator and Equivalent Electrical Circuit, *Proc. Ph. Soc.*, vol. 38, pp. 399–457; discussion, pp. 457–458, 1926.

128. DYE, D. W.: The Modes of Vibration of Quartz Piezoelectric Plates as Revealed by an Interferometer, *Proc. Roy. Soc.*, vol. 138, pp. 1–16, 1932.
129. ECCLES, W. H., and W. A. LEYSHON: Some New Methods of Linking Mechanical and Electrical Vibrations, *Proc. Ph. Soc.*, vol. 40, pp. 229–232, 1928.
130. EICHHORN, K.: Photoelastic Investigations of the Piezoelectrically Excited Flexural Oscillations of Quartz Bars, *ZS. tech. Ph.*, vol. 17, pp. 276–279, 1936.
131. EKSTEIN, H.: Free Vibrations of Anisotropic Bodies, *Phys. Rev.*, vol. 66, pp. 108–118, 1944.
132. ENGL, J., and I. P. LEVENTER: On a New Method for Measuring the Piezoelectric Effect in Powdered Crystals, *An. Phk.*, vol. 29, pp. 369–385, 1937; abst. in *Naturwiss.*, vol. 24, pp. 217–218, 1936.
133. EREMEEV, M., and B. KURCHATOV: Electric Properties of the Isomorphic Crystals $NaKC_4H_4O_6 \cdot 4H_2O$ and $NaNH_4C_4H_4O_6 \cdot 4H_2O$, *Phys. ZS. d. Sowjetunion*, vol. 3, pp. 304–320, 1933; *J. Exp. Th. Ph. U.S.S.R.*, vol. 2, pp. 329–338, 1932.
134. ERRERA, J.: Dispersion of Hertz Waves in Solids, *Phys. ZS.*, vol. 32, pp. 369–373, 1931.
135. ESSEN, L.: Description of the Quartz Control of a Transmitter at 1785 Kilocycles per Second, *J.I.E.E.*, vol. 74, pp. 595–597, 1934; *Proc. Wireless Sec., I.E.E.*, vol. 9, pp. 167–169, 1934.
136. ESSEN, L.: Examples of the Electrical Twinning of Quartz, *J. Sci. Instr.*, vol. 12, pp. 256–257, 1935.
137. ESSEN, L.: Oscillations of Hollow Quartz Cylinders, *Nature*, vol. 135, p. 1076, 1935.
138. ESSEN, L.: The Dye Quartz Ring Oscillator as a Standard of Frequency and Time, *Proc. Roy. Soc.*, vol. 155, pp. 498–519, 1936.
139. ESSEN, L.: A New Form of Frequency and Time Standard, *Proc. Ph. Soc.*, vol. 50, pp. 413–423; discussion, pp. 423–426, 1938.
140. EVANS, R. C.: The Dielectric Constant of Mixed Crystals of Sodium Ammonium and Sodium Potassium Tartrates, *Phil. Mag.*, vol. 24, pp. 70–79, 1937.
141. FAIR, I. E.: Using High Crystal Harmonics for Oscillator Control, *Bell Labs. Rec.*, vol. 21, pp. 237–242, 1943.
142. FOWLER, R. H.: A Theory of the Rotations of Molecules in Solids and of the Dielectric Constants of Solids and Liquids, *Proc. Roy. Soc.*, vol. 149, pp. 1–28, 1935.
143. FOX, G. W., and G. A. FINK: The Piezoelectric Properties of Quartz and Tourmaline, *Physics*, vol. 5, pp. 302–306, 1934.
144. FOX, G. W., and W. G. HUTTON: Experimental Study of Parallel-cut Piezoelectric Quartz Plates, *Physics*, vol. 2, pp. 443–447, 1932.
145. FOX, F. E., and G. D. ROCK: The Ultrasonic Radiation Field of a Quartz Disk Radiating into Liquid Media, *Phys. Rev.*, vol. 54, pp. 223–228, 1938.
146. FOX, F. E., and G. D. ROCK: An Ultrasonic Source of Improved Design: Optical Studies of Ultrasonic Waves in Liquids, *R.S.I.*, vol. 9, pp. 341–345, 1938.
147. FOX, F. E., and G. D. ROCK: A Quartz Plate with Coupled Liquid Column as a Variable Resonator, *Proc. I.R.E.*, vol. 30, pp. 29–33, 1942.
148. FOX, G. W., and M. UNDERWOOD: On the Piezoelectric Properties of Tourmaline, *Physics*, vol. 4, pp. 10–13, 1933.
149. FRAYNE, J. G.: Reversible Inductivity of Rochelle Salt Crystals, *Phys. Rev.*, vol. 21, pp. 348–359, 1923.
150. FRÉDERICKSZ, V., and G. MIKHAILOV: The Dependence of the Piezoelectric Constant of Quartz upon Temperature, *ZS. Ph.*, vol. 76, pp. 328–336, 1932.
151. FRIEDEL, G.: On the Forms of Quartz Crystals, *Bull. soc. min. fr.*, vol. 46, pp. 79–95, 1923.

152. FUJIMOTO, T.: On the Determination of the Piezoelectric Constant of a Quartz Resonator at High Frequency, *Proc. World Eng. Cong., Tokyo, Paper* 369, pp. 399–416, 1929.
153. GALOTTI, F.: Luminous Quartz Resonators, *Alta freq.*, vol. 6, pp. 809–824, 1937.
154. GAUDEFROY, C.: Orientation of Crystals, Especially Quartz, by Means of Etch Figures, *C.R.*, vol. 192, pp. 1113–1116, 1931.
155. GAUGAIN, J. M.: Note on the Electricity of Tourmaline, *An. chim. phys.*, vol. 57, pp. 5–39, 1859.
156. GERTH, F., and H. ROCHOW: The Temperature Dependence of the Frequency of Quartz Resonators, ENT, vol. 5, pp. 549–551, 1928.
157. GIBBS, R. E.: Structure of Alpha Quartz, *Proc. Roy. Soc.*, vol. 110, pp. 443–455, 1926.
158. GIBBS, R. E., and V. N. THATTE: Temperature Variation of the Frequency of Piezoelectric Oscillations of Quartz, *Phil. Mag.*, vol. 14, pp. 682–694, 1932.
159. GIBBS, R. E., and L. C. TSIEN: The Production of Piezoelectricity by Torsion, *Phil. Mag.*, vol. 22, pp. 311–322, 1936.
160. GIEBE, E.: Luminous Piezoelectric Resonators as High-frequency Standards, *ZS. tech. Ph.*, vol. 7, p. 235, 1926.
161. GIEBE, E., and E. BLECHSCHMIDT: Experimental and Theoretical Investigations on Extensional Vibrations of Rods and Tubes, I, *An. Phk.*, vol. 18, pp. 417–456; II, *An. Phk.*, vol. 18, pp. 457–485, 1933.
162. GIEBE, E., and E. BLECHSCHMIDT: On Torsional Vibrations of Quartz Rods and Their Use as Standards of Frequency, *Hfr. u. El. ak.*, vol. 56, pp. 65–87, 1940.
163. GIEBE, E., and A. SCHEIBE: Luminous Effects of High-frequency Longitudinal Vibrations in Piezoelectric Crystals, *ZS. Ph.*, vol. 33, pp. 335–344, 1925.
164. GIEBE, E., and A. SCHEIBE: A Simple Method for Qualitative Indication of Piezoelectricity of Crystals, *ZS. Ph.*, vol. 33, pp. 760–766, 1925.
165. GIEBE, E., and A. SCHEIBE: Luminous Piezoelectric Resonators as High-frequency Standards, *ETZ*, vol. 47, pp. 380–385, 1926.
166. GIEBE, E., and A. SCHEIBE: Piezoelectric Excitation of Elastic Vibrations, *ZS. Hfr.*, vol. 30, pp. 32–33, 1927.
167. GIEBE, E., and A. SCHEIBE: Activity of the Phys.-tech. Reichsanstalt in the Year 1926, *ZS. Instr.*, vol. 46, pp. 269–297, June, 1927.
168. GIEBE, E. and A. SCHEIBE: Piezoelectric Crystals as Standards of Frequency, *ENT*, vol. 5, pp. 65–82, 1928.
169. GIEBE, E., and A. SCHEIBE: Piezoelectric Excitation of Extensional, Flexural, and Torsional Vibrations of Quartz Rods, *ZS. Ph.*, vol. 46, pp. 607–652, 1928.
170. GIEBE, E., and A. SCHEIBE: Flexurally Vibrating Luminous Resonators as Frequency Standards in the Range from 1000 to 20000 Hertz, *ZS. Hfr.*, vol. 35, pp. 165–177, 1930.
171. GIEBE, E., and A. SCHEIBE: On the Series Relationships of the Natural Elastic Frequencies of Quartz Rods, *An. Phk.*, vol. 9, pp. 93–175, 1931.
172. GIEBE, E., and A. SCHEIBE: On Luminous Resonators as Standards of High Frequency, *Hfr. u. El. ak.*, vol. 41, pp. 83–96, 1933.
173. GOCKEL, H.: Decrement of Damping in Piezoelectric Crystals, *Phys. ZS.*, vol. 37, pp. 657–659, 1936.
174. GOEDECKE, H.: The Dielectric Constant of Rochelle Salt in an Electric Field, as a Function of Time, *ZS. Ph.*, vol. 94, pp. 574–589, 1935.
175. GOENS, E.: Determination of Young's Modulus from Flexural Oscillations, *An. Phk.*, vol. 11, pp. 649–678, 1931.
176. GOENS, E.: On Flexural and Torsional Vibrations of a Thin Crystal Rod of any Crystallographic Orientation, *An. Phk.*, vol. 15, pp. 455–484, 1932.

177. GOENS, E.: On the Calculation of Velocity of Propagation of Elastic Waves in Crystals, *An. Phk.*, vol. 29, pp. 279–285, 1937.
178. GOLAY, M. J. E.: A Rochelle Salt Electrometer, *R.S.I.*, vol. 8, pp. 228–230, July, 1937.
179. GOODMAN, B.: Keying the Crystal Oscillator, *QST*, vol. 25, pp. 10–13, May, 1941.
180. GRAMONT, A. DE: On the Movements of a Quartz Crystal in an Electrostatic Field, *C.R.*, vol. 196, pp. 1705–1707, 1933.
181. GRAMONT, A. DE: On Various Types of Vibration of a Quartz Parallelepiped, *C.R.*, vol. 197, pp. 101–103, 1933.
182. GRAMONT, A. DE: Clock Controlled by Means of Piezoelectric Quartz, *An. fr. chron.*, no. 1, pp. 37–43, 1937.
183. GRAMONT, A. DE, and D. BÉRETZKI: A New Method for Temperature Control of Quartz Crystals, *ETZ*, vol. 53, pp. 1039–1040, 1932.
184. GRAMONT, A. DE, and D. BÉRETZKI: Stabilization of Beat Frequency by Temperature-coefficient Compensation, *C.R.*, vol. 200, pp. 1558–1560, 1935.
185. GRAMONT, A. DE, and D. BÉRETZKI: On the Generation of Acoustic Waves by Means of Piezoelectric Quartz, *C.R.*, vol. 202, pp. 1229–1232, 1936.
186. GRAMONT, A. DE, and D. BÉRETZKI: Determination of the Area of a Piezoelectric Plate as Function of Frequency (optimal ratio of diameter to thickness for high-frequency piezo-oscillators), *C.R.*, vol. 204, pp. 459–462, 1937.
187. GRANT, K.: High-frequency Interruption of Light, *Nature*, vol. 120, p. 586, 1927.
188. GREENIDGE, R. M. C.: The Mounting and Fabrication of Plated Quartz Crystal Units, *Bell Syst. T.J.*, vol. 23, pp. 234–259, 1944.
189. GROSSMANN, E., and M. WIEN: On the Effect of Surroundings on the Frequency of a Quartz Resonator, *Phys. ZS.*, vol. 32, pp. 377–378, 1931.
190. GROTH, E. J., and L. N. LIEBERMANN: Precision Measurement of the Velocity of Sound at Supersonic Frequencies Using a Microphone (abstr.), *Phys. Rev.*, vol. 65, p. 350, 1944.
191. GRUETZMACHER, J.: Piezoelectric Crystal with Very Low Natural Frequency, *ENT*, vol. 12, p. 257, 1935.
192. GRUETZMACHER, J.: Piezoelectric Crystal with Ultrasonic Convergence, *ZS. Ph.*, vol. 96, pp. 342–349, 1935.
193. GRUETZMACHER, J.: Directed Supersonic Radiator, *ZS. tech. Ph.*, vol. 17, pp. 166–167, 1936.
194. GÜNTHER, N.: Investigation of the Effect of Mechanical and Electrical Forces on the Double Refraction of Quartz, *An. Phk.*, vol. 13, pp. 783–801, 1932.
195. GÜNTHER, R.: On a Measurement of the Equivalent Electrical Constants of Piezoelectric Crystals, *Hfr. u. El. ak.*, vol. 45, pp. 185–186, 1935.
196. GÜNTHER, R.: The Equivalent Electrical Constants of Piezoelectric Crystals and Their Measurement, *Hfr. u. El. ak.*, vol. 50, pp. 200–203, 1937.
197. GÜNTHER, R.: The Internal Friction in Quartz Crystals, *ENT*, vol. 16, pp. 53–62, 1939.
198. HABLÜTZEL, J.: Anomalous Expansion of Rochelle Salt, *Helv. Ph. Ac.*, vol. 8, pp. 498–499, 1935.
199. HABLÜTZEL, J.: Dielectric Investigations of Heavy-water Rochelle Salt, *Helv. Ph. Ac.*, vol. 12, pp. 489–510, 1939.
200. HANDEL, P. VON: Investigations of Quartz-controlled Oscillations, *ENT*, vol. 7, pp. 34–40, 1930.
201. HANDEL, P. VON: Investigations of the Behavior of Quartz-controlled Transmitters, *Luftfahrt-F.*, vol. 8, pp. 121–140, 1930.

202. HANDEL, P. VON, K. KRÜGER, and H. PLENDL: Quartz Control for Frequency Stabilization in Short-wave Receivers, *Proc. I.R.E.*, vol. 18, pp. 307–320, 1930; *Hfr. u. El. ak.*, vol. 34, pp. 12–18, 1929.
203. HANKEL, W. G.: Following are references to a few of the more important of Hankel's many papers on pyro- and piezoelectricity. Abstracts of all are in *ZS. Kr.* and *Neues Jahrb. Min.* (*a*) *Abh. Sächs.*, vol. 10, pp. 345*f.*, 1872. (*b*) *Abh. Sächs.*, vol. 12, pp. 457–548, 1881. (*c*) *Abh. Sächs.*, vol. 12, pp. 549–596, 1882. (*d*) *Abh. Sächs.*, vol. 24, pp. 467–497, 1899. (*e*) *Ber. Sächs.*, vol. 33, pp. 52–63, 1881. (*f*) *An. Phk.*, vol. 10, pp. 618*f.*, 1880. (*g*) *An. Phk.*, vol. 19, pp. 818–844, 1883. It was in papers (*b*) and (*e*) that the term "piezoelectricity" was introduced.
204. HARDING, J. W., and F. W. G. WHITE: On the Modes of Vibration of a Quartz Crystal, *Phil. Mag.*, vol. 8, pp. 169–179, 1929.
205. HARRISON, J. R.: Piezoelectric Resonance and Oscillatory Phenomena with Flexural Vibrations in Quartz Plates, *Proc. I.R.E.*, vol. 15, pp. 1040–1054, 1927.
206. HARRISON, J. R.: Piezoelectric Oscillator Circuits with Four-electrode Tubes, *Proc. I.R.E.*, vol. 16, pp. 1455–1467, 1928; discussion, pp. 1467–1470.
207. HARRISON, J. R.: Push-pull Piezoelectric Oscillator Circuits, *Proc. I.R.E.*, vol. 18, pp. 95–100, 1930.
208. HARRISON, J. R., and I. P. HOOPER: The Striated Luminous Glow of the Piezoelectric Quartz Resonator at Flexural Vibration Frequencies, *Phys. Rev.*, vol. 55, p. 674, 1939.
209. HATAKEYAMA, K.: Frequency Variation of Quartz Resonator Due to Heating by Its Vibration, *J.I.T.T.E. Jap.*, no. 109, pp. 522–532, 1932; *R.R.R.W. Jap.*, vol. 2, supp., p. 6, 1932.
210. HAYASHI, F.: Observations on Pyroelectricity, disscrtation, Göttingen, 48 pp., 1912.
211. HAYASI, T., and S. AKASI: Quick Building-up of the Electron-coupled Quartz Oscillator, *Electrotech. Jour.* (*Jap.*), vol. 3, pp. 219–222, 1939.
212. HEATON, V. E., and E. G. LAPHAM: Quartz Plate Mountings and Temperature Control for Piezo Oscillators, *Proc. I.R.E.*, vol. 20, pp. 261–271, 1932; discussion, p. 1064; *J. Res. N.B.S.*, vol. 7, pp. 683–690, 1931.
213. HECKMANN, G.: The Lattice Theory of Solids, *Ergeb. exakt. Naturwiss.*, vol. 4, pp. 100–153, 1925.
214. HEEGNER, K.: On Measurements with Piezoelectric Crystals, *ZS. Hfr.*, vol. 29, pp. 177–180, 1927.
215. HEEGNER, K.: On the Pierce Crystal Oscillator, *ENT*, vol. 10, pp. 357–371, 1933.
216. HEEGNER, K.: Coupled Self-excited Circuits and Crystal Oscillators, *ENT*, vol. 15, pp. 359–368, 1938.
217. HEHLGANS, F. W.: On Plates of Piezoelectric Quartz as Transmitters and Receivers of High-frequency Sound-waves, *An. Phk.*, vol. 86, pp. 587–627, 1928.
218. HEIERLE, J.: The Frequency Constancy of Tourmaline-controlled Ultra-short-wave Transmitters, *Helv. Ph. Ac.*, vol. 10, pp. 345–346, 1937.
219. HENDERSON, J. T.: Properties of Tourmaline Crystals Used as Piezoelectric Resonators, *Trans. Roy. Soc. Can.*, vol. 22, pp. 127–131, 1928.
220. HERLINGER, E.: On a New Photogoniometer, *ZS. Kr.*, vol. 66, pp. 282–296, 1927.
221. HETTICH, A.: Piezoelectric Experiments According to the Principle of the Method of Giebe and Scheibe, *ZS. Ph.*, vol. 65, pp. 506–511, 1930.
222. HETTICH, A.: On Ammonium Salts at Low Temperatures, *ZS. ph. Chem. A*, vol. 168, pp. 353–362, 1933.

223. HETTICH, A., and A. SCHLEEDE: Polarity and Piezoelectric Excitation, *ZS. Ph.*, vol. 46, pp. 147–148, 1927.
224. HETTICH, A., and A. SCHLEEDE: Contributions to the Methods for Determining Crystal Classes, *ZS. Ph.*, vol. 50, pp. 249–265, 1928.
225. HIGHT, S. C.: Wind from Quartz Crystals, *Bell Labs. Rec.*, vol. 14, pp. 121–123, 1935.
226. HIGHT, S. C.: Quartz Plates for Frequency Sub-standards, *Bell Labs. Rec.*, vol. 16, pp. 21–25, 1937.
227. HIGHT, S. C., and G. W. WILLARD: A Simplified Circuit for Frequency Substandards Employing a New Type of Low-frequency Zero-temperature-coefficient Quartz Crystal, *Proc. I.R.E.*, vol. 25, pp. 549–563, 1937.
228. HILTSCHER, R.: Piezoelectric Vibration Experiments with Rochelle Salt Crystals, *ZS. Ph.*, vol. 104, pp. 672–680, 1937.
229. HINZ, H.: Elastic Deformations of Rochelle Salt, *ZS. Ph.*, vol. 111, pp. 617–632, 1939.
230. HITCHCOCK, R. C.: The Dimensions of Low-frequency Quartz Oscillators, *R.S.I.*, vol. 1, pp. 13–21, 1930.
231. HOLDEN, A. N., and W. P. MASON: Constants of Heavy-water Rochelle Salt, *Phys. Rev.*, vol. 57, pp. 54–56, 1940.
232. HOLMAN, W. F.: Piezoelectric Excitation of Cane Sugar, *An. Phk.*, vol. 29, pp. 160–178, 1909.
233. HOLTON, G. J.: Rodometric Examination of Quartz Crystals, *Electronics*, vol. 17, pp. 114*f.*, 1944.
234. HORTON, J. W., and W. A. MARRISON: Precision Determination of Frequency, *Proc. I.R.E.*, vol. 16, pp. 137–154, 1928.
235. HOVGAARD, O. M.: Application of Quartz Plates to Radio Transmitters, *Proc. I.R.E.*, vol. 20, pp. 767–782, 1932.
236. HUBBARD, J. C.: The Acoustic Resonator Interferometer, I, *Phys. Rev.*, vol. 38, pp. 1011–1019, 1931; II, *Phys. Rev.*, vol. 41, pp. 523–535, 1932; *errata*, vol. 46, p. 525, 1934.
237. HUBBARD, J. C.: Ultrasonics—A Survey, *Am. Jour. Phys.*, vol. 8, pp. 207–221, 1940.
238. HUND, A.: Uses and Possibilities of Piezoelectric Oscillators, *Proc. I.R.E.*, vol. 14, pp. 447–469, 1926.
239. HUND, A.: Notes on Quartz Plates, Air Gap Effect and Audio-frequency Generation, *Proc. I.R.E.*, vol. 16, pp. 1072–1078, 1928.
240. HUND, A.: Generator for Audio Currents of Adjustable Frequency with Piezoelectric Stabilization, *Sci. Pap. Bur. St.*, vol. 22, pp. 631–637, 1928 (No. 569); *QST fr.*, vol. 9, pp. 16–19, 1928.
241. HUND, A.: Note on a Piezoelectric Generator for Audiofrequencies, *J. Res. N.B.S.*, vol. 2, pp. 355–358, 1929.
242. HUND, A., and R. B. WRIGHT: New Piezo-oscillations with Quartz Cylinders Cut along the Optical Axis, *Proc. I.R.E.*, vol. 18, pp. 741–761, 1930; *J. Res. N.B.S.*, vol. 4, pp. 383–394, 1930.
243. ISELEY, F. C.: The Relation between the Mechanical and Piezoelectrical Properties of a Rochelle Salt Crystal, *Phys. Rev.*, vol. 24, pp. 569–574, 1924.
244. JACKSON, C. H.: Development of an Improved Crystal Exciter Unit, *Civil Aeronautics Authority (U.S.A.), Tech. Development Rept.* 26, pp. 1–14, July, 1940.
245. JAFFE, H.: Polymorphism of Rochelle Salt, *Phys. Rev.*, vol. 51, pp. 43–47, 1937.
246. JAFFE, H.: Crystalline Transitions and Dielectric Constant (abst.), *Phys. Rev.*, vol. 53, p. 917, 1938.

247. JEFFERSON, H.: The Pierce Piezoelectric Oscillator, *W.E.*, vol. 18, pp. 232–237, 1941.
248. JIMBO, S.: An International Comparison of Frequency by Means of a Luminous Quartz Resonator, *Proc. I.R.E.*, vol. 18, pp. 1930–1934, 1930; *Elec. Rev.* (*Jap.*), vol. 18, pp. 185–194, 1930; *Researches Electrotech. Lab., Tokyo*, March, 1930.
249. KAMAYACHI, Z., and H. WATANABE: On Ultra-short-wave Quartz Crystal Vibrators, *Electrotech. Jour.* (*Jap.*), vol. 5, pp. 19–20, 1941.
250. KAMIENSKI, S.: Spherical Piezoelectric Resonators, *Wiadomosci i Prace* (*WPPIT*), vol. 7, pp. 54–58, 1936.
251. KAMMER, E. W., and J. V. ATANASOFF: A Determination of the Elastic Constants of Beta-quartz, *Phys. Rev.*, vol. 62, pp. 395–400, 1942.
252. KAO, P. T.: Relaxation Oscillations Produced by a Quartz Piezoelectric Oscillator, *C.R.*, vol. 191, pp. 932–934, 1930.
253. KAO, P. T.: A Phenomenon Produced in Polarized Light by Quartz in Vibration, *C.R.*, vol. 200, pp. 563–565, 1935.
254. KARCHER, J. C.: A Piezoelectric Method for the Instantaneous Measurement of High Pressures, *Sci. Pap. Bur. St.*, vol. 18, pp. 257–264, 1922 (No. 445); *J. Frank. Inst.*, vol. 194, pp. 815–816 (abst.), 1922.
255. KELLER, H.: Piezoelectric Flexural Strip as an Electromechanical Transducer, *Hfr. u. El. ak.*, vol. 60, pp. 5–10, 1942.
256. KELVIN, LORD: On the Piezoelectric Property of Quartz, *Phil. Mag.*, vol. 36, pp. 331, 342, 384, 453, 1893.
257. KEYS, D. A.: Adiabatic and Isothermal Piezoelectric Constants of Tourmaline, *Phil. Mag.*, vol. 46, pp. 999–1001, 1923.
258. KHOL, F.: A Method for the Measurement of Elastic Constants, *ZS. Ph.*, vol. 108, pp. 225–231, 1938.
259. KHOL, F.: Elastic Constants and Phase Velocities of Transverse and Longitudinal Waves, *ZS. Ph.*, vol. 111, pp. 450–453, 1939.
260. KISHPAUGH, A. W., and R. E. CORAM: Low Power Radio Transmitters for Broadcast Requirements for 100 to 1000 Watts, *Proc. I.R.E.*, vol. 21, pp. 212–227, 1933.
261. KLUGE, M., and H. SCHÖNFELD: Electric Barkhausen Effect in Rochelle Salt Crystals, *Naturwiss.*, vol. 21, p. 194, 1933.
262. KNOL, K. S.: Measurement of the Piezoelectric Modulus of Zinc Blende, *Konink. Akad. Amst.*, vol. 35, pp. 99–106, 1932.
263. KOBEKO, P., and I. KURCHATOV: Dielectric Properties of Rochelle Salt Crystals, *ZS. Ph.*, vol. 66, pp. 192–205, 1930; *J. Russ. Ph.-Chem. Soc.*, vol. 62, p. 251, 1930.
264. KOBEKO, P., and J. G. NELIDOV: The Discontinuity in the Specific Heat of Rochelle Salt, *Phys. ZS. d. Sowjetunion*, vol. 1, pp. 382–386, 1932.
265. KOBZAREV, J.: On the Parameters of Piezoelectric Resonators, *J. Appl. Ph.* (*Russian*), vol. 6, pp. 17–37, 1929.
266. KOGA, I.: On the Piezoelectric Oscillator, *Denki Hyoron*, vol. 15, p. 547, 1927.
267. KOGA, I.: Tuning Fork Made of Quartz Crystal, *J.I.E.E.* (*Japan*), vol. 48, p. 100, 1928; *Rep. El. Res. Inst. Tokyo*, series 1, pp. 213–221, 1928.
268. KOGA, I.: Characteristics of Piezoelectric Quartz Oscillators, *Proc. I.R.E.*, vol. 18, pp. 1935–1959, 1930.
269. KOGA, I.: Note on the Piezoelectric Quartz Oscillating Crystal Regarded from the Principle of Similitude, *Proc. I.R.E.*, vol. 19, pp. 1022–1023, 1931.
270. KOGA, I.: Thickness Vibrations of Piezoelectric Oscillating Crystals, *Physics*, vol. 3, pp. 70–80, 1932; *R.R.R.W. Jap.*, vol. 2, pp. 157–173, 1932; *J.I.T.T.E. Jap.*, no. 115, pp. 1223–1253, 1932.

271. KOGA, I.: Vibration of Piezoelectric Oscillating Crystal, *Phil. Mag.*, vol. 16, pp. 275–283, 1933.
272. KOGA, I.: Thermal Characteristics of Piezoelectric Oscillating Quartz Plates, *U.R.S.I. Gen. Assembly, Document* 33, *Comm.* I, London, 1934; *R.R.R.W. Jap.*, vol. 4, pp. 61–76, 1934.
273. KOGA, I.: On the Temperature-coefficients of Quartz Plates for Long Waves, *ENT*, vol. 12, pp. 1–2, 1935.
274. KOGA, I.: Notes on Piezoelectric Quartz Crystals, *Proc. I.R.E.*, vol. 24, pp. 510–531, 1936.
275. KOGA, I.: Young's Modulus of a Crystal in any Direction, *Proc. I.R.E.*, vol. 24, pp. 532–533, 1936.
276. KOGA, I.: Vibrating Piezoelectric Quartz Plates without Variation of Frequency with Temperature, *L'Onde élec.*, vol. 15, pp. 457–468, 498–507, 1936.
277. KOGA, I.: A Portable Standard Frequency Oscillator, *R.R.R.W. Jap.*, vol. 7, pp. 219–225, 1937.
278. KOGA, I.: An Ultra-short-wave Quartz Crystal Oscillator, *R.R.R.W. Jap.*, vol. 7, pp. 227–229, 1937.
279. KOGA, I.: Equivalence of Two Piezoelectric Oscillating Quartz Crystals of Symmetrical Outlines with Respect to a Plane Perpendicular to an Electrical Axis, *Phil. Mag.*, vol. 27, pp. 640–643, 1939.
280. KOGA, I.: Variable Resistance Device and Its Application Especially to the Frequency Modulation of Quartz Crystal Oscillator, *Electrotech. Jour.* (*Jap.*), vol. 4, no. 5, pp. 99–107, 1940.
281. KOGA, I., and M. SHOYAMA: Contour Vibration of Rectangular X-cut Oscillating Quartz Plate, *J.I.E.E.* (*Japan*), vol. 56, p. 852, 1936.
282. KOGA, I., and M. SHOYAMA: Transient Frequency Variation of Crystal Oscillator (abst.), *R.R.R.W. Jap.*, vol. 8, p. 6, 1938; *Electrotech. Jour.* (*Jap.*), vol. 2, pp. 199–201, 1938.
283. KOGA, I., and M. TATIBANA: Anomalies of Thickness Vibration of Quartz Plates Due to Non-uniform Thickness, *Electrotech. Jour.* (*Jap.*), vol. 3, pp. 81–85, 1939.
284. KOGA, I., and W. YAMAMOTO: Beat-frequency Crystal Oscillator, *Electrotech. Jour.* (*Jap.*), vol. 4, pp. 134–137, 1940.
285. KOGA, I., W. YAMAMOTO, H. NISIO, O. HARASIMA, and S. IKEZAWA: 250-Watt Pentode Crystal Oscillator, *Electrotech. Jour.* (*Jap.*), vol. 3, pp. 92–94, 1939.
286. KOLENKO, B. VON: Pyroelectricity of Quartz with Respect to Its Crystalline System, *ZS. Kr.*, vol. 9, pp. 1–28, 1884.
287. KÖRNER, H.: Growing Rochelle-salt Crystals for Reproducible Measurements, *ZS. Ph.*, vol. 94, pp. 801–807, 1935.
288. KÖRNER, H.: Dielectric Constant, Conductivity and Piezo-effect of Rochelle-salt Crystals, *ZS. Ph.*, vol. 103, pp. 170–190, 1936.
289. KOTLYAREVSKI, M. L., and E. YA. PUMPER: Investigations of the Oscillations of Piezo-quartz Plates by the Interferometer Method, *J. Ph. U.S.S.R.*, vol. 4, pp. 67–78, 1941.
290. KRISTA, F.: Dependence of the Velocity of Propagation of Flexural Vibrations upon Frequency, *ZS. Ph.*, vol. 112, pp. 326–338, 1939.
291. KÜHNHOLD, W.: The Control by Means of Tourmaline Crystals of Ultra-short Waves Excited in any Type of Circuit, *Hfr. u. El. ak.*, vol. 46, pp. 82–85, 1935.
292. KURCHATOV, B., and M. EREMEEV: On the Electrical Properties of Rochelle-salt Mixed Crystals, *Phys. ZS. d. Sowjetunion*, vol. 1, pp. 140–154, 1932.
293. KURCHATOV, B., and I. KURCHATOV: The Lower Curie-point in Rochelle Salt, *Phys. ZS. d. Sowjetunion*, vol. 3, pp. 321–334, 1933.

294. KURCHATOV, I.: Unipolarity of Polarization in Rochelle-salt Crystals, *Phys. ZS. d. Sowjetunion*, vol. 4, pp. 125–129, 1933.
295. KURCHATOV, I.: Rochelle Salt in the Region of Spontaneous Orientation, *Phys. ZS. d. Sowjetunion*, vol. 5, pp. 200–211, 1934.
296. KURCHATOV, I., and A. SHAKIROV: Inversion Phenomena in the Polarization of Rochelle Salt, *Phys. ZS. d. Sowjetunion*, vol. 7, pp. 631–638, 1935 (in German). KURTSCHATOW—see KURCHATOV.
297. KUSUNOSE, Y., and S. ISHIKAWA: Frequency Stabilization of Radio Transmitters, *Proc. I.R.E.*, vol. 20, pp. 310–339, 1932; *R.R.R.W. Jap.*, vol. 1, pp. 157–183, 1931.
298. LACK, F. R.: Observations on Modes of Vibration and Temperature-coefficients of Quartz Crystal Plates, *Proc. I.R.E.*, vol. 17, pp. 1123–1141, 1929; *Bell Syst. T.J.*, vol. 8, pp. 515–535, 1929.
299. LACK, F. R., G. W. WILLARD, and I. E. FAIR: Some Improvements in Quartz Crystal Circuit Elements, *Bell Syst. T.J.*, vol. 13, pp. 453–463, 1934.
300. LAMB, J. J.: A More Stable Crystal Oscillator of High Harmonic Output, *QST*, vol. 17, pp. 30–32, June, 1933.
301. LAMB, J. J.: Tritet Multi-band Crystal Control, *QST*, vol. 17, pp. 9–15, October, 1933.
302. LAMB, J. J.: A Practical Survey of Pentode and Beam Tube Crystal Oscillators for Fundamental and Second Harmonic Output, *QST*, vol. 21, pp. 31–38, 106, 107, April, 1937.
303. LANE, C. T.: Magnetic Properties of Rochelle Salt, *Phys. Rev.*, vol. 45, p. 66, 1934.
304. LANGEVIN, A.: On the Variation of the Piezoelectric Modulus of Quartz with Temperature, *J. phq.*, vol. 7, pp. 95–100, 1936.
305. LANGEVIN, A.: Absolute Value of the Principal Piezoelectric Modulus of Quartz, *C.R.*, vol. 209, pp. 627–630, 1939.
306. LANGEVIN, A., and A. MOULIN: On the Variation of the Piezoelectric Modulus of Quartz with Temperature, *J. phq.*, vol. 8, pp. 257–259, 1937.
307. LANGEVIN, P., and J. SOLOMON: On the Laws of the Liberation of Electricity by Torsion in Piezoelectric Bodies, *C.R.*, vol. 200, pp. 1257–1260, 1935.
308. LARMOR, J.: Electro-crystalline Properties as Conditioned by Atomic Lattices, *Proc. Roy. Soc.*, vol. 99, pp. 1–10, 1921.
309. LAUE, M. v.: Piezoelectrically Excited Vibrations of Quartz Rods, *ZS. Ph.*, vol. 34, pp. 347–361, 1925.
310. LAWSON, A. W.: The Piezoelectricity of Beta-quartz, *Science*, vol. 92, p. 419, 1940.
311. LAWSON, A. W.: A Determination of the Elastic Modulus s_{13} of Beta-quartz, *Phys. Rev.*, vol. 59, pp. 608–612, 1941.
312. LAWSON, A. W.: Comment on the Elastic Constants of Alpha-quartz, *Phys. Rev.*, vol. 59, p. 838, 1941.
313. LAWSON, A. W.: The Vibration of Piezoelectric Plates, *Phys. Rev.*, vol. 62, pp. 71–76, 1942.
314. LEITHÄUSER, G., and V. PETRZILKA: On Standards for Measurement of Ultrashort Waves, *Funktech. Mon.*, no. 9, 1932.
315. LE QUÉRÉ, H.: An Apparatus Designed for the Determination of the Pyroelectric Effect, *Bull. soc. min. fr.*, vol. 59, pp. 137–142, 1936.
316. LIPPMANN, G.: Principle of the Conservation of Electricity, *C.R.*, vol. 92, pp. 1049–1051, 1149–1152, 1881; *J. phq.*, vol. 10, pp. 381–394, 1881; *An. chim. phys., ser.* 5, vol. 24, pp. 145–178, 1881 (prediction of the converse piezoelectric effect).

317. LISSÜTIN, A.: The Vibrations of a Quartz Plate, *ZS. Ph.*, vol. 59, pp. 265–273, 1930.
318. LLEWELLYN, F. B.: Constant Frequency Oscillators, *Bell Syst. T.J.*, vol. 11, pp. 67–100, 1932; *Proc. I.R.E.*, vol. 19, pp. 2063–2094, 1931.
319. LONN, E.: Theory of Oscillation of Crystal Plates, *An. Phk.*, vol. 30, pp. 420–432, 1937.
320. LUCAS, H. J.: Some Developments of the Piezoelectric Crystal as a Frequency Standard, *J.I.E.E.* (*London*), vol. 68, pp. 855–872, 1930; reprinted in *Wireless Section*, vol. 5, pp. 151–163, 1930; discussion, pp. 163–168.
321. LUCAS, R., and P. BIQUARD: New Optical Properties of Liquids Subjected to Ultra-sonic Waves, *C.R.*, vol. 194, pp. 2132–2134, 1932; more fully in *J. phq.*, vol. 3, pp. 464–477, 1932.
322. LÜDY, W.: The Piezoelectricity of Potassium Phosphate, *ZS. Ph.*, vol. 113, pp. 302–305, 1939; *Helv. Ph. Ac.*, vol. 12, pp. 278–279, 1939.
323. LÜDY, W.: Effect of Temperature on the Dynamic-elastic Behavior of Substances like Rochelle Salt, *Helv. Ph. Ac.*, vol. 15, pp. 527–552, 1942.
324. MACKINNON, K. A.: Crystal Control Applied to the Dynatron Oscillator, *Proc. I.R.E.*, vol. 20, pp. 1689–1714, 1932.
325. MALLETT, E., and V. J. TERRY: The Quartz Oscillator, *W. World*, vol. 16, pp. 630–636, 1925.
326. MANDELL, W.: The Determination of the Elastic Moduli of the Piezoelectric Crystal Rochelle Salt by a Statical Method, *Proc. Roy. Soc.*, vol. 116, pp. 623–636, 1927.
327. MANDELL, W.: The Change in Elastic Properties on Replacing the Potassium Atom of Rochelle Salt by the Ammonium Group, *Proc. Roy. Soc.*, vol. 121, pp. 122–130, 1928.
328. MANDELL, W.: The Determination of the Piezoelectric Moduli of Ammonium Seignette Salt, *Proc. Roy. Soc.*, vol. 121, pp. 130–140, 1928.
329. MANDELL, W.: Resonance in Crystal Beams of Sodium-ammonium Seignette Salt, *Proc. Roy. Soc.*, vol. 165, pp. 414–431, 1938.
330. MARRISON, W. A.: A High Precision Standard of Frequency, *Proc. I.R.E.*, vol. 17, pp. 1103–1122, 1929; *Bell Syst. T.J.*, vol. 8, pp. 493–514, 1929.
331. MARRISON, W. A.: The Crystal Clock, *Proc. Nat. Acad. Sci.*, vol. 16, pp. 496–507, 1930.
332. MASON, W. P.: Electrical Wave Filters Employing Quartz Crystals as Elements, *Bell Syst. T.J.*, vol. 13, pp. 405–452, 1934.
333. MASON, W. P.: The Motion of a Bar Vibrating in Flexure, Including the Effects of Rotary and Lateral Inertia, *J.A.S.A.*, vol. 6, pp. 246–249, 1935.
334. MASON, W. P.: An Electromechanical Representation of a Piezoelectric Crystal Used as a Transducer, *Proc. I.R.E.*, vol. 23, pp. 1252–1263, 1935; *Bell. Syst. T.J.*, vol. 14, pp. 718–723, 1935.
335. MASON, W. P.: A Dynamic Measurement of the Elastic, Electric and Piezoelectric Constants of Rochelle Salt, *Phys. Rev.*, vol. 55, pp. 775–789, 1939.
336. MASON, W. P.: A New Quartz-crystal Plate, Designated the GT, Which Produces a Very Constant Frequency over a Wide Temperature Range, *Proc. I.R.E.*, vol. 28, pp. 220–223, May, 1940.
337. MASON, W. P.: Low Temperature Coefficient Quartz Crystals, *Bell Syst. T.J.*, vol. 19, pp. 74–93, 1940.
338. MASON, W. P.: The Location of Hysteresis Phenomena in Rochelle Salt Crystals, *Phys. Rev.*, vol. 58, pp. 744–756, 1940.
339. MASON, W. P.: Electrical and Mechanical Analogies, *Bell Syst. T.J.*, vol. 20, pp. 405–414, 1941.

340. MASON, W. P.: Quartz Crystal Applications, *Bell Syst. T.J.*, vol. 22, pp. 178–223, 1943.
341. MASON, W. P., and I. E. FAIR: A New Direct Crystal-controlled Oscillator for Ultra-short-wave Frequencies, *Proc. I.R E.*, vol. 30, pp. 464–472, 1942.
342. MASON, W. P., and R. A. SYKES: Electrical Wave Filters Employing Crystals with Normal and Divided Electrodes, *Bell Syst. T.J.*, vol. 19, pp. 221–248, 1940.
343. MASON, W. P., and R. A. SYKES: Low Frequency Quartz-crystal Cuts Having Low Temperature Coefficients, *Proc. I.R.E.*, vol. 32, pp. 208–215, 1944.
344. MATSUMURA, S., and K. HATAKEYAMA: Comparison between Oscillations of Short Wave Length Produced by Means of Quartz Resonator with Reference to the Effect of the Air Gap, *J.I.T.T.E. Jap.*, no. 87, pp. 575–580, 1930.
345. MATSUMURA, S., and K. HATAKEYAMA: On a Discontinuity in Wave Length of an X-cut Quartz Resonator Depending on the Dimensional Relation, *J.I.T.T.E. Jap.*, no. 91, pp. 946–952, October, 1930.
346. MATSUMURA, S., and K. HATAKEYAMA: On a Discontinuity in Wave Length of an X-cut Quartz Resonator of Rectangular Form and Method of Determining the Most Suitable Dimensions, *J.I.T.T.E. Jap.*, no. 97, pp. 469–477, April, 1931.
347. MATSUMURA, S., and K. HATAKEYAMA: Relation between the Wave Length Constant and Dimension of Rectangular X-cut Quartz Resonators, *J.I.T.T.E. Jap.*, no. 101, pp. 984–989, August, 1931.
348. MATSUMURA, S., and S. ISHIKAWA: On Tourmaline Oscillators, *R.R.R.W. Jap.*, vol. 3, pp. 1–5, 1933.
349. MATSUMURA, S., S. ISHIKAWA, and S. KANZAKI: Effect of Temperature on Piezoelectric Vibration of Tourmaline Plate, *J.I.E.E. (Japan)*, vol. 53, p. 199, 1933; *Monthly Bibliographical. Ref. U.R.S.I.*, p. 10, May, 1933.
350. MATSUMURA, S., and S. KANZAKI: On the Temperature Coefficient of Natural Frequency of Y-waves in X-cut Quartz Plates, *R.R.R.W. Jap.*, vol. 2, pp. 35–48, 157–173, 1932.
351. MATSUMURA, S., and S. KANZAKI: On a Method of Reducing the Temperature Coefficient of a Piezo-resonator, *J.I.T.T.E. Jap.*, no. 111, pp. 834–842, 1932; *J.I.E.E. (Japan)*, vol. 52, suppl. issue, pp. 172–174, 929, 1932.
352. MATSUMURA, S., and S. KANZAKI: Quartz Plates with a Very Small Temperature-coefficient of Oscillation Frequency, *U.R.S.I. Gen. Assembly, Document* 34, *Comm.* I, London, 1934; *Elec. Rev. (Jap.)*, vol. 21, pp. 24*f.*, 1933; *R.R.R.W. Jap.*, vol. 4, pp. 105–108, 1934; abstr. in *J.I.E.E. (Japan)*, vol. 52, p. 932, 1932, vol. 53, p. 201, 1933.
353. MATTHIAS, B.: On the Piezoelectric ΔE-effect in the Seignette-electrics, *Helv. Ph. Ac.*, vol. 16, pp. 99–135, 1943.
354. MATTHIAS, B., and P. SCHERRER: Crystal Band Pass Filters, *Helv. Ph. Ac.*, vol. 16, pp. 432–434, 1943.
355. MATTIAT, O.: On Vibrating Crystals of Rochelle Salt, *Hfr. u. El. ak.*, vol. 50, pp. 115–120, 1937.
356. MCSKIMIN, H. J.: Theoretical Analysis of Modes of Vibration for Isotropic Rectangular Plates Having All Surfaces Free, *Bell Syst. T.J.*, vol. 23, pp. 151–177, 1944.
357. MEACHAM, L. A.: The Bridge-stabilized Oscillator, *Proc. I.R.E.*, vol. 26, pp. 1278–1294, 1938; *Bell Syst. T.J.*, vol. 17, pp. 574–591, 1938; short account in *Bell Labs. Rec.*, suppl. to vol. 18, January, 1940.
358. MEAHL, H. R.: Quartz Crystal Controlled Oscillator Circuits, *Proc. I.R.E.*, vol. 22, pp. 732–737, 1934.
359. MEISSNER, A.: Piezoelectric Crystals at High Frequency, *ZS. tech. Ph.*, vol. 7,

pp. 585–592, 1926, vol. 8, pp. 74–77, 1927; *ENT*, vol. 3, pp. 401–408, 1926; *ZS. Hfr.*, vol. 29, pp. 20–24, 1927.

360. MEISSNER, A.: Piezoelectric Crystals at Radio Frequencies, *Proc. I.R.E.*, vol. 15, pp. 281–296, 1927.
361. MEISSNER, A.: Investigations on Quartz, *Phys. ZS.*, vol. 28, pp. 621–625, 1927.
362. MEISSNER, A., and R. BECHMANN: Investigation and Theory of Pyroelectricity, *ZS. tech. Ph.*, vol. 9, pp. 175–186, 1928.
363. MELIKIAN, A. B., and E. K. PIETROVA: On a Method for the Determination of Parameters of Piezo-resonators, *Izv. El. Slab. Toka*, no. 3, pp. 40–51, 1935.
364. MENDELSSOHN, J., and K. MENDELSSOHN: Specific Heat of a Substance Showing Spontaneous Electric Polarization, *Nature*, vol. 144, p. 595, 1939.
365. METSCHL, E. C.: The Nature and Applications of Piezoelectricity, *ETZ*, vol. 59, pp. 819–825, 1938.
366. MIKHAILOV, G.: The Influence of Temperature on the Frequency of Piezoelectric Oscillations in Rochelle Salt, *Tech. Phys. U.S.S.R.*, vol. 3, pp. 511–518, 1936.
367. MIKHAILOV, G.: The Investigations of Elastic Vibration in a Piezocrystal of Rochelle Salt, *Tech. Phys. U.S.S.R.*, vol. 3, pp. 652–661, 1936.
368. MIKHAILOV, G.: Influence of Temperature on the Dynamic Piezo-modulus of Rochelle Salt, *Tech. Phys. U.S.S.R.*, vol. 4, pp. 461–465, 1937.
369. MILLER, J. M.: Quartz Crystal Oscillators, *U.S. Navy Radio Sound Rept.*, issue of Apr. 1, May 1, June 1, 1925, pp. 53–64.
370. MITSUI, H.: Broadcast Frequency Monitor Employing Luminous Quartz Resonator, *Nippon Elec. Comm. Eng.*, no. 1, pp. 86–87, September, 1935.
371. MODRAK, P.: Quartz and Tourmaline, *W.E.*, vol. 14, pp. 127–134 and 175–183, 1937.
372. MOENS, R., and J. E. VERSCHAFFELT: Optical Phenomena Exhibited by Quartz When Vibrating Piezoelectrically, *C.R.*, vol. 185, pp. 1034–1036, 1927.
373. MÖGEL, H.: Control of Operation of Short-wave Transmitters, *ENT*, vol. 7, pp. 333–348, 1930; *Telef.-Z.*, vol. 11, pp. 8–21, 1930.
374. MÖGEL, H.: Monitoring the Operation of Short-wave Transmitters, *Proc. I.R.E.*, vol. 19, pp. 214–232, 1931.
375. MORRISON, J. F.: A New Broadcast Transmitter Circuit Design for Frequency Modulation, *Proc. I.R.E.*, vol. 28, pp. 444–449, 1940.
376. MUELLER, H.: Properties of Rochelle Salt, *Phys. Rev.*, vol. 47, pp. 175–191, 1935.
377. MUELLER, H.: Determination of Elasto-optical Constants with Supersonic Waves, *ZS. Kr.*, vol. 99, pp. 122–141, 1938.
378. MUELLER, H.: Properties of Rochelle Salt, II, *Phys. Rev.*, vol. 57, pp. 829–839, 1940.
379. MUELLER, H.: Influence of Electrostatic Fields on the Elastic Properties of Rochelle Salt, *Phys. Rev.*, vol. 57, pp. 842–843, 1940.
380. MUELLER, H.: Properties of Rochelle Salt, III, *Phys. Rev.*, vol. 58, pp. 565–573, 1940.
381. MUELLER, H.: Properties of Rochelle Salt, IV, *Phys. Rev.*, vol. 58, pp. 805–811, 1940.
382. MUELLER, H.: The Dielectric Anomalies of Rochelle Salt, *Ann. N.Y. Acad. Sci.*, vol. 40, pp. 321–356, 1940.
383. MÜLLER, H., and T. KRAEFFT: Doppler Effect with Piezoelectric Quartz, *Phys. ZS.*, vol. 33, pp. 305–306, 1932.
384. MURPHY, E. J., and S. O. MORGAN: The Dielectric Properties of Insulating Materials, *Bell Syst. T.J.*, vol. 16, pp. 493–512, 1937, vol. 17, pp. 640–669, 1938.

385. MYERS, L. M.: Application of the Electrometer Triode to the Determination of Piezoelectric Constants, *Brit. Rad. Ann.*, pp. 15–20, 1934–5.
386. NACHTIKAL, F.: Proportionality between Piezoelectric Moment and Pressure, *Nachr. Gött.*, pp. 109–118, 1899.
387. NACKEN, R.: Etching Experiments with Spheres of Quartz and α-quartz, *Neues Jahrb. Min.*, vol. 1, pp. 71–82, 1916.
388. NAMBA, S., and S. MATSUMURA: Piezoelectric Properties of Quartz and Its Value as a Frequency Standard, *J.I.T.T.E. Jap.*, no. 70, pp. 817–833, November, 1928; *Researches Electrotech. Lab.* (*Tokyo*), no. 248, April, 1929 (in English); also in abbreviated form in *ZS. Hfr.*, vol. 34, pp. 198–200, 1929.
389. NAMBA, S., and S. MATSUMURA: Piezoelectric Quartz Resonator with a Small Temperature Coefficient, *J.I.E.E.* (*Japan*), vol. 49, suppl. issue, pp. 9–10, 1929.
390. NELSON, E. L.: Radio Broadcasting Transmitters and Related Transmission Phenomena, *Bell Syst. T.J.*, vol. 9, pp. 121–140, 1930.
391. NICOLSON, A. M.: The Piezoelectric Effect in the Composite Rochelle Salt Crystal, *Trans. A.I.E.E.*, vol. 38, pp. 1467–1485, 1919; *Proc. A.I.E.E.*, vol. 38, pp. 1315–1333, 1919; *Electrician* (*London*), vol. 83, pp. 32*f.*, 1919.
392. NIESSEN, K. F.: Frequency-stability of Some Resonators, *Physica*, vol. 8, pp. 1077–1093, 1941.
393. NORGORDEN, O.: The Inverse Piezoelectric Properties of Rochelle Salt at Audio Frequencies, *Phys. Rev.*, vol. 49, pp. 820–828, 1936.
394. NORGORDEN, O.: The Piezoelectric Properties of Rochelle Salt, *Phys. Rev.*, vol. 50, p. 782, 1936 (letter to the editor).
395. NUSSBAUMER, B.: Measurement of the First Piezoelectric Modulus of Quartz, *ZS. Ph.*, vol. 78, pp. 781–790, 1932.
NY TSI-ZE—see TSI-ZE.
396. ONNES, H. K., and A. BECKMAN: Piezoelectric and Pyroelectric Properties of Quartz at Low Temperatures, *Konink. Akad. Amst.*, vol. 15, pp. 1380–1383, 1913; *Communication* 132*f Phys. Lab. Leyden.*
397. OPLATKA, G.: A New Method of Determining the Static Dielectric Constants of Semiconductors, and Measurements of the Dielectric Constant of Rochelle Salt, *Phys. ZS.*, vol. 34, pp. 296–300, 1933.
398. OSTERBERG, H.: An Interferometer Method of Observing the Vibrations of an Oscillating Quartz Plate, *Proc. Nat. Acad. Sci.*, vol. 15, pp. 892–896, 1929.
399. OSTERBERG, H.: An Interferometer Method of Studying the Vibrations of an Oscillating Quartz Plate, *J.O.S.A.*, vol. 22, pp. 19–35, 1932.
400. OSTERBERG, H.: A Triple Interferometer for Distinguishing Flexural and Longitudinal Vibrations in Quartz, *J.O.S.A.*, vol. 23, pp. 30–34, 1933.
401. OSTERBERG, H.: A Multiple Interferometer for Analyzing the Vibrations of a Quartz Plate, *Phys. Rev.*, vol. 43, pp. 819–829, 1933.
402. OSTERBERG, H.: A Refracting Interferometer for Examining Modes of Vibration in Quartz Plates, *R.S.I.*, vol. 5, pp. 183–186, 1934.
403. OSTERBERG, H., and J. W. COOKSON: Piezoelectric Stabilization of High Frequencies, *R.S.I.*, vol. 5, pp. 281–286, 1934.
404. OSTERBERG, H., and J. W. COOKSON: Some Piezoelectric and Elastic Properties of β-quartz, *J. Frank. Inst.*, vol. 220, pp. 361–371, 1935.
405. OSTERBERG, H., and J. W. COOKSON: A Theory of Two-dimensional Longitudinal and Flexural Vibrations in Rectangular Isotropic Plates, *Physics*, vol. 6, pp. 234–246, 1935.
406. OSTERBERG, H., and J. W. COOKSON: Longitudinal, Shear and Transverse Modes of Vibration in Quartz and Tourmaline, *Physics*, vol. 6, pp. 246–256, 1935.

407. OSTERBERG, H., and J. W. COOKSON: An Interference Method for Measuring the Piezoelectric Moduli of Alpha-quartz: The Moduli, *R.S.I.*, vol. 6, pp. 347–356, 1935.
408. PAVLIK, B.: Two Transmitting Circuits with Octode, *ENT*, vol. 12, pp. 53–54, 1935.
409. PAVLIK, B.: Contribution to the Theoretical and Experimental Investigation of Flexural Vibrations in Rectangular Plates with Free Borders, *An. Phk.*, vol. 27, pp. 532–542, 1936.
410. PAVLIK, B.: Contribution to the Investigation of Flexural Vibrations of Plates in the Form of Parallelograms with Free Edges, *An. Phk.*, vol. 28, pp. 353–360, 1937.
411. PAVLIK, B.: The Possibility of Exciting Simple Modes of Vibration in Piezoelectric Crystals of Low Symmetry, *ZS. Kr.*, vol. 100, pp. 414–419, 1938.
412. PERRIER, A.: Hypotheses Concerning Spontaneous Dielectric Polarization, and Some Experimental Results, *Arch. sci. phys. nat.*, vol. 41, pp. 492*f.*, 1916.
413. PERRIER, A., and R. DE MANDROT: Elasticity and Symmetry of Quartz at High Temperatures, *Mém. société vaudoise sci. nat.*, vol. 1, pp. 333–363, 1922–1924; *C.R.*, vol. 175, pp. 622–624, 1006, 1922; abst. in *Arch. sci. phys. nat.*, vol. 4, pp. 367–369, 1922.
414. PETRZILKA, V.: On the Relation between the Optical and Piezoelectric Properties of Vibrating Quartz Crystals, *An. Phk.*, vol. 11, pp. 623–632, 1931.
415. PETRZILKA, V.: Tourmaline Resonators for Short and Ultra-short Waves, *An. Phk.*, vol. 15, pp. 72–88, 1932.
416. PETRZILKA, V.: Longitudinal and Flexural Vibrations of Tourmaline Plates, *An. Phk.*, vol. 15, pp. 881–902, 1932.
417. PETRZILKA, V.: Longitudinal Oscillations of Circular Quartz Plates, *An. Phk.*, vol. 23, pp. 156–168, 1935.
418. PETRZILKA, V.: Longitudinal Vibrations of Rectangular Quartz Plates, *ZS. Ph.*, vol. 97, pp. 436–454, 1935.
419. PETRZILKA, V.: Control of Transmitters by Lengthwise Vibrations of Tourmaline Plates, *Hfr. u. El. ak.*, vol. 50, pp. 1–5, 1937.
420. PETRZILKA, V., and W. FEHR: On Steady-state Oscillating Conditions in Quartz-controlled Single and Two-circuit Transmitters, *ENT*, vol. 9, pp. 283–292, 1932.
421. PETRZILKA, V., and L. ZACHOVAL: Direct Observation of Oscillations of a Quartz Plate by Means of the Schlieren Method, *ZS. Ph.*, vol. 90, pp. 700–702, 1934.
422. PIELEMEIER, W. H.: Acoustical Detection of Electrically Weak Vibrations in Quartz Plates, *J.A.S.A.*, vol. 9, pp. 212–216, 1938.
423. PIERCE, G. W.: Piezoelectric Crystal Resonators and Crystal Oscillators Applied to the Precision Calibration of Wavemeters, *Proc. A.A.A.S.*, vol. 59, pp. 81–106, 1923.
424. PIERCE, G. W.: Piezoelectric Crystal Oscillators Applied to the Precision Measurement of the Velocity of Sound in Air and Carbon Dioxide at High Frequencies, *Proc. A.A.A.S.*, vol. 60, pp. 277–302, 1925.
425. PINCIROLI, A.: On a New Piezoelectric Oscillator, *Alta freq.*, vol. 11, pp. 341–343, 1942.
426. PITT, A., and D. W. R. MCKINLEY: Variation with Temperature of the Piezoelectric Effect in Quartz, *Can. J. Res., A*, vol. 14, pp. 57–65, 1936.
427. POCKELS, F.: On the Changes in Optical Behavior and Elastic Deformations of Dielectric Crystals in an Electric Field, *Neues Jahrb. Min.*, vol. 7 (supplementary vol.), pp. 201–231, 1890.
428. POCKELS, F.: On the Effect of an Electrostatic Field on the Optical Behavior

of Piezoelectric Crystals, *Abh. Gött.*, vol. 39, pp. 1–204, 1894 (also in book form[B40]).

429. PONTECORVO, P.: Piezo-oscillators of High Frequency Stability Obtained by the Simultaneous Use of Positive and Negative Feedback, *Alta freq.*, vol. 7, pp. 365–381, 1938.
430. POPPELE, J. R., F. W. CUNNINGHAM, and A. W. KISHPAUGH: Design and Equipment of a Fifty-kilowatt Broadcast Station for WOR, *Proc. I.R.E.*, vol. 24, pp. 1063–1081, 1936.
431. POWERS, W. F.: Temperature Coefficient of Frequency of Quartz Resonators (abst.), *Phys. Rev.*, vol. 23, p. 783, 1924.
432. QUERVAIN, M. DE, and B. ZWICKER: Observations of the Elementary Electric Domains in the Seignette-electrics, *Helv. Ph. Ac.*, vol. 16, pp. 216–218, 1943.
433. RAYNER, E. H.: The Researches of the Late Dr. D. W. Dye on the Vibrations of Quartz, *J.I.E.E. (London)*, vol. 72, pp. 519–527, 1933; *Proc. Wireless Sec., I.E.E.*, vol. 8, pp. 99–107, 1933.
434. RIECKE, E.: Molecular Theory of the Piezoelectricity of Tourmaline, *Phys. ZS.*, vol. 13, pp. 409–415, 1912; *Nachr. Gött.*, pp. 253–266, 1912.
435. RIECKE, E., and W. VOIGT: Piezoelectric Constants of Quartz and Tourmaline, *Nachr. Gött.*, pp. 247–255, 1891; *Wied. An.*, vol. 45, pp. 523–552, 1892.
436. ROHDE, L.: New Types of Quartz Master-oscillators and Filters, *ZS. tech. Phys.*, vol. 20, pp. 75–80, 1939.
437. ROHDE, L.: Audio-frequency Quartz Oscillators and Filters, *ZS. tech. Phys.*, vol. 21, pp. 30–34, 1940.
438. ROHDE, L., and H. HANDREK: The Properties of Quartz Resonators at Audio- and Intermediate Frequencies, *ZS. tech. Phys.*, vol. 21, pp. 401–405, 1940.
439. RÖNTGEN, W. C.: Pyro- and Piezoelectric Investigations, *An. Phk.*, vol. 45, pp. 737–800, 1914.
440. RÖNTGEN, W. C., and A. JOFFÉ: On the Electric Conductivity of Certain Crystals and the Effect of Radiation Thereupon, *An. Phk.*, vol. 41, pp. 449–498, 1913.
441. RUSTERHOLZ, A. A.: Anomaly in the Specific Heat of Rochelle Salt, *Helv. Ph. Ac.*, vol. 7, pp. 643–644, 1934, vol. 8, pp. 39–54, 1935.
442. RZIANKIN, A. G.: Attenuation of Oscillations in Piezoelectric Quartz Crystals, *J. Tech. Phys.*, vol. 4, pp. 1282–1294, 1934.
443. SABAROFF, S.: A Voltage Stabilized High-frequency Crystal Oscillator Circuit, *Proc. I.R.E.*, vol. 25, pp. 623–629, 1937.
444. SABBATINI, A.: Multiple Oscillations of Piezoelectric Crystals and Their Dependence upon Circuit Conditions, *Dati e mem.*, vol. 2, pp. 618–636, 1930.
445. SALISBURY, W. W., and C. W. PORTER: An Efficient Piezoelectric Oscillator, *R.S.I.*, vol. 10, pp. 269–270, 1939.
446. SANDERS, E. W.: Modes of Fracture in Piezoelectric Crystals, *QST*, vol. 21, pp. 17–18, 84, 1937.
447. SANDERS, E. W.: Wave Propagation in Shearing Quartz Oscillators of High Frequency, *J. Appl. Ph.*, vol. 11, pp. 299–300, 1940.
448. SAWYER, C. B.: The Use of Rochelle Salt Crystals for Electrical Reproducers and Microphones, *Proc. I.R.E.*, vol. 19, pp. 2020–2029, 1931.
449. SAWYER, C. B., and C. H. TOWER: Rochelle Salt as a Dielectric, *Phys. Rev.*, vol. 35, pp. 269–273, 1930.
450. SCHAAFFS, W.: A Schlieren Test of the Vibrations of a Thin Quartz Plate, *ZS. Ph.*, vol. 105, pp. 576–578, 1937.
451. SCHERRER, P.: Investigations of the Dielectric Behavior of Rochelle Salt and Related Materials, *ZS. Elektrochem.*, vol. 45, pp. 171–174, 1939.

452. SCHIFFERMÜLLER, R.: On the Multiplicity of Vibrations in Thin Piezoelectric Quartz Plates, *ZS. tech. Ph.*, vol. 19, pp. 469–475, 1938.
SCHUBNIKOW—see SHUBNIKOV
SCHULWAS—see SHULVAS.
453. SCHUMACHER, R. O.: Investigations on Transversally Vibrating Quartz Plates, *Telef.-Z.*, vol. 18, pp. 16–21, 1937.
454. SCHWARTZ, E.: Experimental Investigations of the Piezoelectric and Dielectric Properties of Rochelle Salt, *ENT*, vol. 9, pp. 481–495, 1932.
455. SEIDL, F.: An Interesting Crack in Piezoelectric Quartz, *Naturwiss.*, vol. 17, pp. 781–782, 1929.
456. SEIDL, F.: Conductivity of Loaded Piezoelectric Quartz, *ZS. Ph.*, vol. 75, pp. 488–503, 1932.
457. SEIDL, F.: Action of Radium and X-rays on Piezoelectric Quartz, *Ber. Wien*, vol. 142, pp. 467–469, 1933.
458. SEIDL, F.: The Electrical Behavior of Rochelle Salt Single Crystals Produced from a Saturated Solution in an Electric Field, *Anz. Wien*, no. 11, pp. 92–93, 1936.
459. SEIDL, F.: The Anomalous Charging Current in Rochelle Salt Crystals, *Phys. ZS.*, vol. 39, pp. 714–716, 1938.
460. SEIDL, F., and E. HUBER: Effect of X-rays and Gamma-rays on Piezoelectric Crystals, *ZS. Ph.*, vol. 97, pp. 671–680, 1935.
461. SHAW, H. S.: Oscillating Crystals, *QST*, vol. 7, pp. 30*f.*, July, 1924.
462. SHORE, S. X.: A series of articles on the grading and orientation of quartz crystals and the sawing, lapping, finishing, and testing of quartz plates, *Communications*, vol. 23, October–December, 1943, vol. 24, January, February, 1944.
463. SHUBNIKOV, A.: On Impact-patterns on Quartz, *ZS. Kr.*, vol. 74, pp. 103–104, 1930.
464. SHULVAS-SOROKINA, R. D.: Is It Possible to Determine the Piezoelectric Constant at High Temperature by the Statical Method? *Phys. Rev.*, vol. 34, pp. 1448–1450, 1929.
465. SHULVAS-SOROKINA, R. D.: Piezoelectric Properties of Rochelle Salt Crystals, *ZS. Ph.*, vol. 73, pp. 700–706, 1932.
466. SHULVAS-SOROKINA, R. D.: On a Characteristic Temperature in Rochelle Salt Crystals, *ZS. Ph.*, vol. 77, pp. 541–546, 1932.
467. SHULVAS-SOROKINA, R. D.: Relaxation Time in Rochelle Salt Crystals, II, *J. Exp. Th. Ph. U.S.S.R.*, vol. 7, pp. 1440–1447, 1937; *Phys. ZS. d. Sowjetunion*, vol. 12, pp. 685–700, 1937.
468. SHULVAS-SOROKINA, R. D.: Polarization of Rochelle Salt Crystals at Low Voltages, *J. Tech. Phys.*, vol. 11, pp. 947–958, 1941.
469. SHULVAS-SOROKINA, R. D., and M. V. POSNOV: The Time of Relaxation in Crystals of Rochelle Salt, *Phys. Rev.*, vol. 47, pp. 166–174, 1935.
470. SKELLETT, A. M.: A Visual Method for Studying Modes of Vibration of Quartz Plates, *J.O.S.A.*, vol. 17, pp. 308–317, 1928.
471. SKELLETT, A. M.: Modes of Vibration of a Round Plate Cut from a Quartz Crystal, *J.O.S.A.*, vol. 20, pp. 293–302, 1930.
472. SMIRNOV, V. A.: The Effect of the Parameters of a Piezoelectric Quartz Oscillator on Its Operation, and the Maximum Permissible Power Rating for Such an Oscillator, *J. Tech. Phys.*, vol. 6, pp. 493–513, 1936.
473. SOKOLOV, S. J.: Oscillations of Piezoelectric Quartz Rods in Non-uniform Fields, *ZS. Ph.*, vol. 50, pp. 385–394, 1928.
474. SPEIGHT, J. W.: The Electrodynamic Characteristics of the Quartz Piezoelectric Oscillator, *Can. J. Res.*, vol. 12, pp. 812–819, 1935.

475. STAMFORD, N. C.: The Production of Rochelle Salt Piezoelectric Resonators Having a Pure Longitudinal Mode of Vibration, *Proc. I.R.E.*, vol. 25, pp. 465–471, 1937.
476. STARR, A. T.: Electro-acoustic Reactions, W.E., vol. 17, pp. 247–256, 303–309, 1940.
477. STAUB, H.: Investigation of the Dielectric Properties of Rochelle Salt by Means of X-rays, *Helv. Ph. Ac.*, vol. 7, pp. 3–45, 1934; *Phys. ZS.*, vol. 34, pp. 292–296, 1933; thesis, 1934.
478. STAUB, H.: Evidence for the Internal Electric Field of Rochelle Salt by Means of X-rays, *Helv. Ph. Ac.*, vol. 7, pp. 480–482, 1934; *Phys. ZS.*, vol. 35, pp. 720–725, 1934.
479. STAUB, H.: Dielectric Anomalies of Rochelle Salt, *Naturwiss.*, vol. 23, pp. 728–733, 1935.
480. STEPHENSON, C. C., and H. E. ADAMS: The Heat Capacity of Ammonium Dihydrogen Arsenate from 15 to 300°K. The Anomaly at the Curie Temperature, *J. Am. Chem. Soc.*, vol. 66, pp. 1409–1412, 1944.
481. STEPHENSON, C. C., and J. G. HOOLEY: The Heat Capacity of Potassium Dihydrogen Phosphate from 15 to 300°K. The Anomaly at the Curie Temperature, *J. Am. Chem. Soc.*, vol. 66, pp. 1397–1401, 1944.
482. STEPHENSON, C. C., and A. C. ZETTLEMOYER: The Heat Capacity of Potassium Dihydrogen Arsenate from 15 to 300°K. The Anomaly at the Curie Temperature, *J. Am. Chem. Soc.*, vol. 66, pp. 1402–1405, 1944.
483. STEPHENSON, C. C., and A. C. ZETTLEMOYER: The Heat Capacity of Ammonium Dihydrogen Phosphate from 15 to 300°K. The Anomaly at the Curie Temperature, *J. Am. Chem. Soc.*, vol. 66, pp. 1405–1408, 1944.
484. STRAUBEL, H.: Piezoelectric Quartz Oscillators, *Phys. ZS.*, vol. 32, p. 222, 1931.
485. STRAUBEL, H.: Some Experiments in Supersonics, *Phys. ZS.*, vol. 32, pp. 379–381, 1931.
486. STRAUBEL, H.: Piezoelectric Oscillators, *Phys. ZS.*, vol. 32, pp. 586–587, 1931.
487. STRAUBEL, H.: Direct Crystal Control for Ultra-short Waves, *Phys. ZS.*, vol. 32, pp. 937–941, 1931.
488. STRAUBEL, H.: Oscillation Form and Temperature Coefficient of Quartz Oscillators, *ZS. Hfr.*, vol. 38, pp. 14–27, 1931.
489. STRAUBEL, H.: Crystal Control of Ultra-short Wave Transmitters, *V.D.I.*, vol. 76, pp. 873–874, 1932.
490. STRAUBEL, H.: Modes of Vibration of Piezoelectric Crystals, *Phys. ZS.*, vol. 34, pp. 894–896, 1933.
491. STRAUBEL, H.: Temperature Coefficient, Mode of Vibration, and Amplitude of Piezoelectric Oscillators, *Phys. ZS.*, vol. 35, pp. 179–181, 1934.
492. STRAUBEL, H.: The Temperature Coefficient of Quartz Oscillators, *Phys. ZS.*, vol. 35, pp. 657–658, 1934.
493. STRAUBEL, H.: The Temperature Coefficient of Quartz Oscillators, *ZS. tech. Ph.*, vol. 15, pp. 607–608, 1934.
494. STRAUBEL, H.: Crystal Control of Decimeter Waves, *ZS. tech. Ph.*, vol. 16, pp. 627–629, 1935.
495. STRAUBEL, H.: Crystal Control of Ultra-short Waves, *Hfr. u. El. ak.*, vol. 46, pp. 4–6, 1935.
496. STRAUBEL, H.: Crystal Control of Decimeter Waves, *Hfr. u. El. ak.*, vol. 47, pp. 152–154, 1936.
497. STRONG, J. A.: New Method of Investigating the Modes of Vibration of Quartz Crystals, *Nature*, vol. 129, p. 59, 1932.

498. SYKES, R. A.: Modes of Motion in Quartz Crystals, the Effects of Coupling and Methods of Design, *Bell Syst. T.J.*, vol. 23, pp. 52–96, 1944.
499. SYKES, R. A.: Principles of Mounting Quartz Plates, *Bell Syst. T.J.*, vol. 23, pp. 178–189, 1944.
500. SZÉKELY, A.: A Simple Method for Determining the First Piezoelectric Modulus of Quartz from Measurements on a Quartz Resonator, *ZS. Ph.*, vol. 78, pp. 560–566, 1932.
501. TAKAGI, N., and Y. MIYAKE: Thickness Vibrations of a Rochelle Salt Plate, *Electrotech. Jour.* (*Jap.*), vol. 4, p. 120, 1940.
502. TAKAGI, N., and H. NAKASE: New Characteristics of Pentode Quartz Oscillator, *Electrotech. Jour.* (*Jap.*), vol. 2, pp. 22–23, 1938.
503. TAMARU, T.: Determination of the Piezoelectric Constants of Tartaric Acid Crystals, *Phys. ZS.*, vol. 6, p. 379, 1905.
504. TASCHEK, R., and H. OSTERBERG: Crystalline Symmetry and Shear Constants of Rochelle Salt, *Phys. Rev.*, vol. 50, p. 572, 1936.
505. TAWIL, E. P.: On the Variations of the Optical Properties of Piezoelectric Quartz under the Action of High-frequency Electric Fields, *C.R.*, vol. 183, pp. 1099–1101, 1926.
506. TAWIL, E. P.: Observations on Piezoelectric Quartz at Resonance, *C.R.*, vol. 185, pp. 114–116, 1927.
507. TAWIL, E. P.: The Vibrations of Piezoelectric Quartz Made Visible by Polarised Light, *Bull. soc. min. fr.*, p. 129S, Nov. 16, 1928.
508. TAWIL, E. P.: New Method for the Development of Electricity by the Torsion of Quartz Crystals, *C.R.*, vol. 187, pp. 1042–1044, 1928.
509. TAWIL, E. P.: The Vibrations of Piezoelectric Quartz Made Visible by Polarized Light, *Rev. gén. de l'élec.*, vol. 25, p. 58, 1929.
510. TAWIL, E. P.: On the Vibrations along the Optical Axis in an Oscillating Piezoelectric Quartz Crystal, *C.R.*, vol. 189, pp. 163–164, 1929.
511. TAWIL, E. P.: Stationary Ultrasonic Waves Made Visible in Gases by the Method of Striations, *C.R.*, vol. 191, pp. 92–95, 1930.
512. TAWIL, E. P.: Liberation of Electricity in Quartz Crystals by Flexure, *C.R.*, vol. 192, pp. 274–277, 1931.
513. TAWIL, E. P.: Laws of the Liberation of Electricity by Torsion in Quartz, *C.R.*, vol. 199, pp. 1025–1026, 1934.
514. TAWIL, E. P.: Remarks on the Liberation of Electricity by Torsion in Quartz, *C.R.*, vol. 200, pp. 1088–1090, 1935.
515. TAWIL, E. P.: Remarks on the Liberation of Electricity by Torsion in Quartz and on the Reciprocal Phenomenon, *C.R.*, vol. 200, pp. 1306–1308, 1935.
516. TAWIL, E. P.: On a Piezoelectric Chronograph, *C.R.*, vol. 202, pp. 1016–1018, 1936.
517. TERRY, E. M.: The Dependence of the Frequency of Quartz Piezoelectric Oscillators upon Circuit Constants, *Proc. I.R.E.*, vol. 16, pp. 1486–1506, 1928.
518. THOMSON, W. T.: Effect of Rotary and Lateral Inertia on Flexural Vibration of Prismatic Bars, *J.A.S.A.*, vol. 11, pp. 198–204, 1939.
519. THURSTON, G. M.: Flatness and Parallelism in Quartz Plates, *Bell Labs. Rec.*, vol. 22, pp. 435–439, 1944.
520. THURSTON, G. M.: A Crystal Test Set, *Bell Labs. Rec.*, vol. 22, pp. 477–480, 1944.
521. TOLANSKY, S.: Topography of a Quartz Crystal Face, *Nature*, vol. 153, pp. 195–196, 1944.
522. TOURNIER, M.: History and Applications of Piezoelectricity, *Elec. Comm.*, vol. 15, pp. 312–327, 1937; *ENT*, vol. 15, pp. 320–334, 1937.

523. Tsi-Ze, Ny: Electric Deformations of Quartz, *C.R.*, vol. 184, pp. 1645–1647, 1927.
524. Tsi-Ze, Ny: Experimental Study of the Deformations and of the Changes in the Optical Properties of Quartz under the Influence of an Electric Field, *J. phq.*, vol. 9, pp. 13–37, 1928; *C.R.*, vol. 185, pp. 195–197, 1927.
525. Tsi-Ze, Ny: The Transverse Circular Vibration of a Hollow Quartz Cylinder, *C.R.*, vol. 204, pp. 226–228, 1937.
526. Tsi-Ze, Ny, and S. Keng-Yi: Vibrations in Quartz Plates Cut in Different Planes Around the Optic Axis, *C.R.*, vol. 204, pp. 1059–1060, 1937.
527. Tsi-Ze, Ny, and Chung Ming-San: States of Vibration of a Hollow Quartz Cylinder, *J. phq.*, vol. 9, pp. 52–56, 1938.
528. Tsi-Ze, Ny, and F. Sun-Hung: On the Circumferential Vibration of a Hollow Cylindrical Quartz Oscillator, *Chinese J. of Phys.*, vol. 2, pp. 145–153, 1936.
529. Tsi-Ze, Ny, and F. Sun-Hung: On the Transverse Circular Vibrations of a Hollow Quartz Cylinder, *C.R.*, vol. 203, pp. 461–463, 1936.
530. Tsi-Ze, Ny, and Ling-Chao Tsien: Oscillations with Hollow Quartz Cylinders Cut along the Optical Axis, *Nature*, vol. 134, pp. 214–215, 1934.
531. Tsi-Ze, Ny, and Ling-Chao Tsien: Electrification by Torsion in Quartz Crystals, *C.R.*, vol. 198, pp. 1395–1396, 1934.
532. Tsi-Ze, Ny, and Ling-Chao Tsien: The Laws of Liberation of Electricity by Torsion in Quartz Crystals, *C.R.*, vol. 199, pp. 1101–1102, 1934.
533. Tsi-Ze, Ny, and Ling-Chao Tsien: Oscillations of a Hollow Quartz Cylinder, *C.R.*, vol. 200, pp. 565–567, 1935.
534. Tsi-Ze, Ny, and Ling-Chao Tsien: On the Laws of Production of Electrification by Torsion in Quartz, *C.R.*, vol. 200, pp. 732–733, 1935.
535. Tsi-Ze, Ny, and Ling-Chao Tsien: Electrification by Torsion in Quartz Crystal, *Chinese J. of Phys.*, vol. 1, pp. 41–53, October, 1935.
536. Tsi-Ze, Ny, Ling-Chao Tsien, and Fang Sun-Hung: Oscillations of Hollow Quartz Cylinders Cut along the Optic Axis, *Proc. I.R.E.*, vol. 24, pp. 1484–1494, 1936.
537. Tykocinski-Tykociner, J., and M. W. Woodruff: Flexural Vibrations of Piezoelectric Quartz Bars and Plates, *Univ. Illinois Bull.*, vol. 34, 33 pp., Jan. 8, 1937 (No. 291).
538. Uda, H., and H. Watanabe: Ultra-short-wave Quartz Oscillator, *Electrotech. Jour. (Jap.)*, vol. 2, pp. 94–95, 1938.
539. Ust'yanov, V. I.: On the Effect of a Layer of Gold Deposited on a Quartz Crystal on the Logarithmic Decrement of the Crystal, *Izv. El. Slab. Toka*, no. 4, pp. 44–48, 1938.
540. Usui, R.: The Circle Diagrams of the Quartz Oscillator, *J.I.E.E. (Japan)*, vol. 54, pp. 201–213, 1934; English summary, pp. 21–24.
541. Valasek, J.: Piezoelectricity and Allied Phenomena in Rochelle Salt, *Phys. Rev.*, vol. 17, pp. 475–481, 1921.
542. Valasek, J.: Piezoelectric Activity of Rochelle Salt under Various Conditions, *Phys. Rev.*, vol. 19, pp. 478–491, 1922.
543. Valasek, J.: Properties of Rochelle Salt Related to the Piezoelectric Effect, *Phys. Rev.*, vol. 20, pp. 639–664, 1922.
544. Valasek, J.: Dielectric Anomalies in Rochelle Salt Crystals, *Phys. Rev.*, vol. 24, pp. 560–568, 1924.
545. Valasek, J.: Note on the Piezoelectric Effect in Rochelle Salt Crystals, *Science*, vol. 65, pp. 235–236, 1927.
546. Valasek, J.: Infrared Absorption by Rochelle Salt Crystals, *Phys. Rev.*, vol. 45, pp. 654–655, 1934.

547. VAN DYKE, K. S.: The Electric Network Equivalent of a Piezoelectric Resonator (abst.), *Phys. Rev.*, vol. 25, p. 895, 1925.
548. VAN DYKE, K. S.: The Use of the Cathode Ray Oscillograph in the Study of Resonance Phenomena in Piezoelectric Crystals (abst.), *Phys. Rev.*, vol. 31, p. 303, 1928.
549. VAN DYKE, K. S.: Some Experiments with Vibrating Quartz Spheres (abst.), *Proc. I.R.E.*, vol. 16, pp. 706–707, 1928; *Phys. Rev.*, vol. 31, pp. 1113, 1133, 1928 (absts.).
550. VAN DYKE, K. S.: The Piezoelectric Resonator and Its Equivalent Network, *Proc. I.R.E.*, vol. 16, pp. 742–764, 1928.
551. VAN DYKE, K. S.: The Measurement of the Decrement of Piezoelectric Resonators (abst.), *Proc. I.R.E.*, vol. 18, p. 1989, 1930.
552. VAN DYKE, K. S.: The Electric Network Equivalent of a Piezoelectric Resonator (abst.), *Phys. Rev.*, vol. 40, p. 1026, 1932.
553. VAN DYKE, K. S.: Temperature Variation of Viscosity and of the Piezoelectric Constant of Quartz (abst.), *Phys. Rev.*, vol. 42, p. 587, 1932.
554. VAN DYKE, K. S.: A Determination of Some of the Properties of the Piezoelectric Quartz Resonator, *Proc. I.R.E.*, vol. 23, pp. 386–392, 1935. *Document* AG, No. 24, *Comm.* I., *U.R.S.I. Gen. Assem.*, 1934.
555. VAN DYKE, K. S.: Note on a Peculiar Case of Fracture of a Quartz Resonator, *J. Appl. Ph.*, vol. 8, pp. 567–568, 1937.
556. VAN DYKE, K. S.: Some Unusual Demonstrations with Piezoelectric Resonators (abst.), *Phys. Rev.*, vol. 53, p. 686, 1938.
557. VAN DYKE, K. S.: Vibration Modes of Low Decrement for a Quartz Ring (abst.), *Phys. Rev.*, vol. 53, p. 945, 1938.
558. VAN DYKE, K. S.: On the Right- and Left-handedness of Quartz and Its Relation to Elastic and Other Properties, *Proc. I.R.E.*, vol. 28, pp. 399–406, 1940.
559. VAN DYKE, K. S., and A. M. THORNDIKE: The Three-crystal Method of Quartz Resonator Measurement (abst.), *Phys. Rev.*, vol. 57, p. 560, 1940.
560. VECCHIACCHI, F.: Frequency-stability of Piezoelectric Standards, *L'Elettrot.*, vol. 15, pp. 462–468, 1928.
561. VECCHIACCHI, F.: Piezo-oscillators with Great Frequency-stability, *L'Elettrot.*, vol. 18, pp. 79–82, 1931; *Livorno Publication* 55.
562. VECCHIACCHI, F.: Advances in Piezoelectric Frequency Standards and Stabilizers, *Rass. P.T.T.*, vol. 10, pp. 5–8, October 1931.
563. VEEN, A. L. W. E. VAN DER: Symmetry of Diamond, thesis, Delft, 1911. *ZS. Kr.*, vol. 51, pp. 545–590, 1913.
564. VENKOV, M. M.: Principles in Designing a Crystal Holder for a Piezo-quartz Stabilizer, *Izv. El. Slab. Toka*, no. 6, pp. 39–44, no. 7, pp. 35–41, 1935.
565. VIGNESS, I.: Inverse Piezoelectric Properties of Rochelle Salt, *Phys. Rev.*, vol. 46, pp. 255–257, 1934.
566. VIGNESS, I.: Dilatations in Rochelle Salt, *Phys. Rev.*, vol. 48, pp. 198–202, 1935.
567. VIGOUREUX, J. E. P.: Development of Formulas for the Constants of the Equivalent Electrical Circuit of a Quartz Resonator in Terms of Elastic and Piezoelectric Constants, *Phil. Mag.*, vol. 6, pp. 1140–1153, 1928.
568. VIGOUREUX, J. E. P.: The Valve-maintained Quartz Oscillator, *J.I.E.E. (London)*, vol. 68, pp. 265–295, 1930; discussion, pp. 867–872; *Proc. Wireless Section, I.E.E.*, vol. 5, pp. 41–71, 1930; discussion, pp. 163–168.
569. VOIGT, W.: General Theory of the Piezo- and Pyroelectric Properties of Crystals, *Abh. Gött.*, vol. 36, pp. 1–99, 1890.
570. VOIGT, W.: Can the Pyroelectricity of Crystals Be Attributed Entirely to

Piezoelectric Effects? *Nachr. Gött.*, pp. 166–194, 1898; *An. Phk.*, vol. 66, pp. 1030–1060, 1898.

571. VOIGT, W.: On Pyroelectricity in Centro-symmetrical Crystals, *Nachr. Gött.*, pp. 394–437, 1905.
572. VOIGT, W.: Remarks on Some New Investigations on Pyro- and Piezoelectricity of Tourmaline, *An. Phk.*, vol. 46, pp. 221–230, 1915.
573. VOIGT, W.: Theory and Experiments on Piezoelectric Excitation of a Cylinder by Torsion and Bending, *An. Phk.*, vol. 48, pp. 433–448, 1915.
574. VOIGT, W.: Questions on the Pyro- and Piezoelectricity of Crystals, *Phys. ZS.*, vol. 17, pp. 287–293, 307–313, 1916.
575. VOIGT, W.: Pyro- and Piezoelectricity. Experimental Determination of Permanent Centro-symmetrical Moments, *Phys. ZS.*, vol. 18, pp. 59–67, 1917.
576. VOIGT, W., and V. FRÉEDERICKSZ: Piezoelectric Excitation of a Cylinder by Torsion and Bending, *An. Phk.*, vol. 48, pp. 145–176, 1915.
577. WACHSMUTH, R., and H. AUER: Mechanical Vibrations of Piezoelectrically Excited Quartz, *ZS. Ph.*, vol. 47, pp. 323–329, 1928.
578. WAGNER, K. W.: Wedge-shaped Piezoelectric Resonators, *Hfr. u. El. ak.*, vol. 47, p. 28, 1936.
579. WARREN, B. E., and H. M. KRUTTER: X-ray Study of Crystal Structure of Rochelle Salt and Effect of Temperature (abst.), *Phys. Rev.*, vol. 43, p. 500, 1933.
580. WATAGHIN, G., and G. SACERDOTE: Optical Examination of the Surface of Piezoelectric Quartz in Vibration; Doppler Effect of Acceleration, *Atti. accad. sci. Torino*, vol. 66, pp. 424–427, 1930–1931.
581. WATANABE, Y.: Piezoelectric Resonator in High-frequency Oscillation Circuits, *Proc. I.R.E.*, vol. 18, pp. 695–717, 862–893, 1930; *ENT*, vol. 5, pp. 45–64, 1928.
582. WHEELER, L. P.: An Analysis of a Piezoelectric Oscillator Circuit, *Proc. I.R.E.*, vol. 19, pp. 627–646, 1931.
583. WHEELER, L. P., and W. E. BOWER: A New Type of Standard Frequency Piezoelectric Oscillator, *Proc. I.R.E.*, vol. 16, pp. 1035–1044, 1928.
584. WILLARD, G. W.: Raw Quartz, Its Imperfections and Inspection, *Bell Syst. T.J.*, vol. 22, pp. 338–361, 1943.
585. WILLARD, G. W.: Inspecting and Determining the Axis Orientation of Quartz Crystals, *Bell Labs. Rec.*, vol. 22, pp. 320–326, 1944.
586. WILLARD, G. W.: Use of the Etch Technique for Determining Orientation and Twinning in Quartz Crystals, *Bell Syst. T.J.*, vol. 23, pp. 11–51, 1944.
587. WILLIAMS, N. H.: Modes of Vibration of Piezoelectric Crystals, *Proc. I.R.E.*, vol. 21, pp. 990–995, 1933.
588. WILSON, A. J. C.: The Heat Capacity of Rochelle Salt between −30° and +30°C., *Phys. Rev.*, vol. 54, pp. 1103–1109, 1938.
589. WOLF, K.: Flexural Oscillations in a Thin Rod, *Ber. Wien*, vol. 143, pp. 79–86, 1934.
590. WOLOGDIN, V.: Frequency Multiplication by the Use of a Condenser with Rochelle Salt Dielectric, *ZS. tech. Ph.*, vol. 13, pp. 82–84, 1932.
591. WOOD, R. G., and C. H. MCCALE: Simple Apparatus for Detecting the Pyroelectric Effect in Crystals, *J. Sci. Instr.*, vol. 17, pp. 225–226, 1940.
592. WOROBIEFF, V. VON: Crystallographic Studies of Tourmaline from Ceylon and Several Other Sources, *ZS. Kr.*, vol. 33, pp. 263*f.*, 1900.
593. WRIGHT, J. W.: The Piezoelectric Crystal Oscillator, *Proc. I.R.E.*, vol. 17, pp. 127–142, 1929.
594. WRIGHT, R. B., and D. M. STUART: Some Experimental Studies of the Vibrations of Quartz Plates, *J. Res. N.B.S.*, vol. 7, pp. 519–553, 1931.

595. YODA, H.: Thermal Characteristics of Piezoelectric Oscillating AT-cut and YT-cut Plates, *R.R.R.W. Jap.*, vol. 5, pp. 77–87, 1935.
596. YODA, H.: YT-cut Quartz Plates, *Electrot. Jour.* (*Jap.*), vol. 2, p. 96, 1938.
597. ZACEK, A., and V. PETRZILKA: On Wedge-shaped Piezoelectric Resonators, *Hfr. u. El. ak.*, vol. 46, pp. 157–159, 1935; *Czech. Inst. Elec. Eng.*, vol. 24, 1935.
598. ZACEK, A., and V. PETRZILKA: Radial and Torsional Vibrations of Annular Quartz Plates, *Phil. Mag.*, vol. 25, pp. 164–175, 1938.
599. ZAKS, E. S., and V. P. UFTIUJANINOV: Low-frequency Luminous Piezo-quartz Resonators, *Izv. El. Slab. Toka*, no. 1, pp. 32–40, January–February, 1934.
ZE, NY TSI—see TSI-ZE.
600. ZELENY, A., and J. VALASEK: Variation of the Dielectric Constant of Rochelle Salt Crystals with Frequency and Applied Field Strength, *Phys. Rev.*, vol. 46, pp. 450–453, 1934.
601. ZELYAKH, E. V., and Y. I. VELIKIN: Equivalent Circuits of the Four-electrode Quartz Resonator, *Izv. El. Slab. Toka*, no. 3, pp. 46–50, 1938.
602. ZWICKER, B., and P. SCHERRER: Electro-optical Behavior of KH_2PO_4 and KD_2PO_4 Crystals, *Helv. Ph. Ac.*, vol. 16, pp. 214–216, 1943.

NAME INDEX

The following list includes only authors named in the text and footnotes. For other authors, see the General Bibliography and the special bibliographies at the ends of chapters.

A

Ackermann, W., 704
Adams, E. P., 234
Adams, H. E., 665
Alston, N. A., 232, 708
Altheim, O. G., von, 413
Anderson, J. A., 514, 537, 567
Andreeff, A., 220, 222, 390
Ardenne, M. von, 680
Armstrong, E., 427
Arndt, J. P., 530
Arx, A. von, 209, 661, 662
Atanasoff, J. V., 104, 106, 121, 135–141, 158, 315, 320, 442, 446
Auer, H., 440, 465
Auerbach, F., 155
Austen, A. E. W., 413
Awender, H., 506

B

Bahrs, S., 230
Bain, G. W., 484
Balamuth, L., 486
Baldwin, C. F., 457
Bancroft, D., 525, 557, 573–575, 622
Bantle, W., 209, 572, 573, 660–665, 740
Barkhausen, H., 632, 754
Barrett, C. S., 329, 330
Baumgardt, E., 312
Bechmann, R., 104, 136–138, 144–146, 153, 216, 234, 306–314, 432–439, 454–460
Becker, H. E. R., 396, 397
Becker, R., 745
Beckman, A., 221
Bedeau, F., 501
Beevers, C. A., 736–738
Benoit, J., 451
Benson, J. E., 407, 455, 502
Béretzki, D., 500–502
Bergmann, L., 233, 244, 446, 684, 685
Bertsch, C. V., 329
Biot, A., 406, 419
Biquard, P., 6, 684, 685
Bitter, F., 745
Blechschmidt, E., 138, 157, 329, 439, 450, 451, 484
Bleekrode, L., 703
Bleuler, K., 330
Bloch, F., 745
Bloomenthal, S., 523, 538, 540, 654–658
Boas, W., 329
Boella, M., 502
Boguslawski, S., 704
Bokovoy, S. A., 457
Bond, W. L., 184, 232, 417, 422, 427, 458
Booth, C. F., 394, 411, 419, 421, 431, 438, 445, 506, 669
Borel, C., 514
Born, M., 230, 704, 711, 742
Bosshard, W., 397
Bower, W. E., 502
Boyle, R. W., 486, 680, 682
Bozorth, R. M., 745, 751
Bradford, E. B., 557, 626, 628
Bradley, A. J., 735
Brady, J. J., 711
Bragg, W. H., 7, 732–736
Brain, K. R., 234
Bravais, A., 12, 23
Brewster, D., 706
Bridgman, P. W., 126, 127, 139, 410
Brouwer, D., 504
Brown, E. W., 504
Brown, H. A., 397
Brown, R. L., 440
Brown, W. F., Jr., 486
Browne, C. O., 683

Bruce, W. A., 330
Brugnatelli, L., 709
Bruhat, G., 199
Bruninghaus, L., 465
Bücks, K., 440, 464, 465
Bürker, K., 703
Builder, G., 405, 407, 455, 457, 502
Busch, G., 208, 397, 481, 523–529, 572, 573, 617, 619, 643–645, 659–663
Bussman, E., 506
Butterworth, S., 333
Byrnes, I. F., 500

C

Cady, W. G., 124, 125, 287, 407, 426, 476, 484, 582, 678
Caflisch, C., 209
Carr, P. H., 329
Chaikin, S., 397
Chick, A. J., 681
Christoffel, E. W., 104–106, 480
Christopher, J. H., 523
Clay, J., 217, 220, 222
Coblentz, W. W., 329
Colby, M. Y., 329, 330
Cook, R. C., 227
Cookson, J. W., 138, 156, 158, 199, 217–219, 465, 484, 501
Cork, J. M., 329
Cortez, S. H., 390
Coster, D., 229
Crandall, I. B., 101
Crossley, A., 465, 498
Curie, J., 2–4, 180, 181, 217, 230, 711, 741
Curie, M., 181
Curie, P., 2–4, 7, 217, 230, 741
Czermak, P., 217, 722

D

Darmois, E., 413
David, R., 524, 529, 554–569, 635
Davies, R. M., 102, 120–131, 476
Dawson, L. H., 218, 222, 244, 416
Day, A. L., 412
Debye, P., 171, 176, 580, 631, 645, 684, 710
Dixon, E. J. C., 431, 445, 506
Doborzynski, D., 414
Doerffler, H., 111, 112, 449
Dolejsek, V., 330
Dorfman, J., 631
Duhem, P., 5, 251
Du Mond, J. W. M., 412, 735
Dye, D. W., 244, 334, 345, 353, 361, 373, 400, 403, 439, 444, 445, 465

E

Eaton, J. E., 486
Eccles, W. H., 501
Eguchi, M., 233
Eichhorn, K., 465
Ekstein, H., 110, 439
Elings, S. B., 232, 659
Engl, J., 230, 233
Eremeev, M., 557, 573, 615, 654–657
Errera, J., 528, 557, 572, 636
Espenchied, L., 668
Essen, L., 432, 452, 504
Eucken, A., 620
Evans, R. C., 526, 572, 654, 656
Ewing, M., 234

F

Fair, I. E., 372, 394, 454, 502
Fairbairn, H. W., 410
Falkenhagen, H., 711
Ferroni, E. von, 462
Fink, G. A., 218, 227
Focken, C. M., 703
Fowler, R. H., 515, 575, 580–582, 649, 650
Fox, G. W., 157, 218, 227, 329, 487, 501
Frayne, J. G., 556, 557, 566, 572
Fréedericksz, V., 140, 141, 218–222, 390, 449
Friedel, C., 711
Fujimoto, T., 220, 390
Fukushima, E., 330

G

Ganz, E., 661, 662
Gaudefroy, C., 424
Gemant, A., 234
Gerber, P. D., 424
Gerlash, E., 234
Gibbs, R. E., 7, 219, 411, 732–736
Giebe, E., 138, 156, 157, 231, 232, 303, 314, 439, 448–452, 463, 484, 486, 659

Gill, A. J., 669
Gockel, H., 397, 462, 479
Goedecke, H., 528, 548
Goeppert-Mayer, M., 742
Gohlke, W., 670
Good, W. M., 234, 486
Gorelik, B., 521
Gramont, A. de, 218, 411, 424, 441, 500, 501
Grant, K., 465
Green, G., 43, 104, 107
Greenwood, G., 232, 233, 709
Greninger, A. B., 426
Grime, G., 486
Gross, E., 107
Grossmann, E., 439
Grosvenor, A. C., 641
Groth, E. J., 675
Groth, P., 230, 232, 420, 737
Gruetzmacher, J., 449, 681
Günther, R., 215, 217, 396, 720–724
Guerbilsky, A., 669

H

Hablützel, J., 207, 517, 518, 528, 557–579, 615, 635, 647
Hagen, J. P., 462
Handel, P. von, 492
Handrek, H., 460, 494, 668
Hankel, W. G., 3, 706, 711, 738
Harding, J. W., 440
Harms, F., 199
Harris, S., 329, 330
Harrison, E. P., 517
Harrison, J. R., 448, 500, 501
Hart, P. J., 104, 106, 121, 135–137, 139–141, 315, 320, 442, 446
Hatakeyama, K., 445
Hawk, H. W. N., 411
Hayashi, F., 217, 704, 709
Heaps, C. W., 548
Heaton, V. E., 432
Heckmann, G., 743
Hedvall, J. A., 516, 620
Heegner, K., 394, 492, 502
Hehlgans, F. W., 303
Heierle, J., 506
Heisenberg, W., 747
Heising, R. A., 452
Henderson, J. T., 484
Herlinger, E., 424
Herrmann, K., 234
Herschel, W., 406
Hertel, E., 232
Hettich, A., 232, 233
Hicks, J. F G., 516, 520
Hight, S. C., 440, 455, 457, 493
Hiltscher, R., 124, 125, 476, 480, 522, 678
Hinz, H., 120–129, 522–526, 538–542, 627, 640, 720
Hippel, A. von, 413
Hirschhorn, S. I., 442
Holden, A. N., 133, 207, 526, 575–579
Holmann, W. F., 201
Holton, G. J., 426
Honess, A. P., 421
Hooley, J. G., 516, 520, 664
Hort, W., 155
Horton, J. W., 494
Hostetter, J. C., 412
Houstoun, R. A., 683
Howe, C. E., 329, 330
Hubbard, J. C., 683
Hubbell, H. H., Jr., 426
Huber, E., 523, 529
Hughes, W., 736–738
Hulsizer, R. I., 440
Hund, A., 450, 500, 501
Hunter, L., 486

I

Ichikawa, S., 410
Iseley, F. C., 129, 533, 547, 610, 617
Ishikawa, S., 157, 492, 669

J

Jaeger, F. M., 414
Jaffe, H., 230, 518, 637, 640, 737
Jahoda, M., 330
Jauncey, G. E. M., 330
Jay, A. H., 412, 735
Jeans, J. H., 199
Jeffree, J. H., 686
Joffé, A., 156, 217, 222, 413
Johnson, K. S., 358

K

Kakiuchi, Y., 330
Kamayachi, Z., 501, 669

Kamienski, S., 458
Kamizeki, E., 669
Kammer, E. W., 140, 141, 158
Kanzaki, S., 453
Kao, P. T., 465, 501
Karcher, J. C., 220
Kármán, Th. von, 742
Karolus, A., 685
Karper, J., 217–222
Kazarnowsky, I., 220, 222, 390
Kelvin, Lord, 1, 5, 161, 701, 709, 736, 741
Kennelly, A. E., 336
Kent, G. H., 131
Keys, D. A., 227, 228
Khol, F., 156, 484
Kidani, Y., 718
Kirkpatrick, P., 737
Kjellgren, B., 522
Klein, E., 132
Kluge, M., 631, 670
Knol, K. S., 217, 229
Kobeko, P., 528, 563–567, 580, 710
Kobzarew, J., 314
Koch, P. P., 228
Körner, H., 526–533, 706
Koga, I., 104, 136–143, 307, 314, 407, 426, 439, 444, 445, 454, 456, 484, 487, 500, 501
Kraefft, T., 682
Krüger, K., 492
Krutter, H. M., 646, 737
Kürti, N., 749
Kundt, A., 721, 722
Kurchatov, B., 520, 555, 557, 565, 615, 654–657
Kurchatov, I. V., 515, 520–529, 547, 551–557, 563–567, 573–582, 632, 643, 649–656, 710
Kusunose, Y., 492
Kuwayama, I., 669

L

Lack, F. R., 452, 454
Laimböck, J., 223
Lainé, P., 749
Lamb, J. J., 501
Lane, C. T., 521
Lange, F., 710
Langevin, A., 217, 222
Langevin, P., 5, 219, 287, 451, 485, 580, 581, 675–678, 745
Lapham, E. G., 432
Larmor, J., 741, 742
Laue, M. von, 99, 305, 314
Lauterburg, B., 662, 663
Lawson, A. W., 135–140, 158, 201, 229, 271, 307, 315, 323
Leventer, I. P., 233
Leyshon, W. A., 501
Liebermann, L. N., 675
Linckh, H. E., 670
Lindberg, A., 679
Lindenberg, H., 706, 738
Lindman, K. F., 706
Lippmann, G., 4, 182, 283
Lissauer, W., 221, 228
Llewellyn, F. [illegible] 493, 506
Lonn, E., 439, 484
Lonsdale, K., 709
Loomis, A. L., 679, 682
Love, A. E. H., 104, 107
Lowry, H. H., 527
Lucas, R., 6, 232, 684
Ludloff, H. F [illegible]
Lüdy, W., 134, [illegible]9, 217, 242, 665
Lynn, J. G., 6[illegible]

Machatschki, F., 734, 736
MacNair, D., 412
Mallett, E., 341, 494
Mandell, W., 119–134, 208, 483, 524, 525, 532, 547, 627, 725
Mandrot, R. de, 137, 140, 147, 148, 158
Mare, J. de, 501
Maris, H. B., 718
Mark, H., 232
Marrison, W. A., 452, 494
Martin, A. J. P., 709
Mason, W. P., 101, 104, 110, 120–137, 153, 204, 207, 220, 245, 250, 251, 272, 292, 305, 328, 372, 390, 394, 407, 411, 438, 439, 449–460, 473–478, 480, 486, 494, 502, 515, 518, 526, 532, 548, 557, 572–579, [illegible]93, 603, 616, 622–629, 635, 668
Matsumoto, T., 413
Matsumura, S., 157, 445, 453
Matthias, B., 471, 479, 480, 614, 666

Mattiat, O., 120, 125, 131, 476, 479
Maurer, R. J., 413
Maurice, M. E., 703
McCale, C. H., 710
McKinley, D. W. R., 221, 683
Meacham, L. A., 503
Meissner, A., 154, 216, 234, 244, 394, 440, 441
Mendelssohn, J., 664
Mendelssohn, K., 664
Meyer, O., 420
Mikhailov, G., 124–131, 140, 141, 220, 222, 387, 390, 476, 477, 481, 505, 628
Miller, J. M., 494
Miller, P. H., Jr., 201, 412, 735
Miller, W. H., 23
Miyake, S., 738
Miyake, Y., 126, 480
Modrak, P., 484
Moens, R., 465
Monji, M., 669
Moore, R. W., 522
Moore, W. H., 711
Morgan, S. O., 176, 527
Moulin, A., 221
Mueller, [illegible] 120 [illegible], 242, 245, 251, 252, [illegible] 471, 3473, 478–481, 515–521, 527, 529, 548, 557–570, 575–585, 593, 595, 604, 607, 610, 613, 615–621, 626–632, 636, 640, 643–650, 661, 706, 707, 718–727
Müller, H., 440, 464, 465, 682
Murphy, E. J., 176
Myers, L. M., 242, 723

N

Nachtikal, F., 217, 227
Nacken, R., 424, 426
Nakamura, K., 415
Namba, S., 445
Nelidov, J. G., 519
Német, A., 737, 738
Neuman, F., 11
Newark, A. F., 394
Nicolson, A. M., 287, 514, 515, 671, 672
Nishikawa, A., 234
Nix, F. C., 412
Norgorden, O., 538, 543, 548, 618, 648, 649
Norrman, E., 462
Nukiyama, D., 234
Nussbaumer, B., 220, 390, 394

O

Onnes, H. K., 221
Oplatka, G., 520, 554
Orelkin, B., 709
Osterberg, H., 138, 156, 158, 199, 217–221, 390, 465, 481, 484, 501, 638

P

Palmer, H. C., 484
Pancholy, M., 309
Pande, A., 309
Parthasarathy, S., 309
Pauling, L., 732
Pauly, R. W., 620
Pauthenier, M., 199
Pavlik, B., 201, 483
Peabody, E. T., 394
Penfield, S. L., 420
Perrier, A., 137, 140, 147, 148, 158, 222, 637
Petrzilka, V., 156, 157, 439, 451, 464, 465, 484, 506, 669
Pielemeier, W. H., 683
Pierce, G. W., 6, 306, 494, 500, 505, 676, 683
Pitt, A., 221
Plendl, H., 492
Pockels, F., 5, 204, 205, 217–219, 229, 251, 514, 532, 711, 716, 718, 720–725
Posnov, M. V., 548, 566
Powers, W. F., 438
Poynting, J. H., 283
Prins, J. A., 229

Q

Quervain, M. de, 665
Quimby, S. L., 101, 486

R

Radmanèche, R., 413
Rahimi, N. G., 413
Ream, J. H., 528
Riecke, E., 217–219, 227, 228, 704, 705, 738, 741

Rivlin, R. S., 411, 425
Rochow, E. G., 413
Rock, G. D., 487
Röntgen, W. C., 217, 222, 227, 704–711, 721, 722
Rohde, L., 460, 494, 501, 668
Rosani, S., 244
Rose, F. C., 486
Ross, P. A., 737
Ruedy, R., 102
Rusterholz, A. A., 519
Rziankin, A. G., 397

S

Sabbatini, A., 501
Sack, H., 176, 710
Saegusa, H., 413, 415
Sakisaka, Y., 330
Sanders, E. W., 411, 465
Sawyer, C. B., 242, 525, 529, 538, 542, 543, 560, 561, 567, 569, 672
Schaaffs, W., 465
Schaefer, V. J., 420, 684, 685
Scheibe, A., 138, 156, 231, 232, 244, 314, 438, 439, 448–451, 462, 463, 486, 659
Scherrer, P., 515, 645, 659, 662–666
Schleede, A., 232
Schenk, D., 486
Schneider, K., 232
Schneider, W., 232
Schönfeld, H., 631
Schrödinger, E., 741
Schuler, M., 462
Schwartz, E., 522, 526–534, 546, 552–557, 565–567, 672
Scott, G. W., Jr. 440
Sears, F. W., 6, 684
Seidl, F., 217, 410, 413, 523, 529
Seifert, H., 232
Shakirov, A., 554
Shaw, H. S., 442
Shea, T. E., 334, 358
Shimizu, S., 413
Shubnikov, A., 411
Shulvas-Sorokina, R. D., 515, 532–536, 548, 559, 565, 566
Siegel, S., 486
Simon, F., 749
Slater, J. C., 740
Sokolov, S. J., 303, 306, 437
Solomon, J., 219, 451
Sosman, R. B., 32, 156, 218, 406, 410–415, 732
Sproule, D. O., 486
Stamford, N. C., 526
Starr, A. T., 304, 305
Staub, H., 329, 524, 526, 548, 737, 738
Steinmetz, H., 232, 233
Stephenson, C. C., 664, 665
Stilwell, W. S., 633
Stoner, E. C., 745
Stranathan, J. D., 234
Straubel, H., 157, 411, 440, 444, 454, 458, 462, 465, 484, 501, 506, 679
Strong, J. A., 465
Stuart, D. M., 155, 156, 410, 440, 463
Sumoto, I., 330
Sun-Hung, F., 501
Sutton, R. M., 485
Sykes, R. A., 110, 412, 456, 457, 494, 668
Szćkely, A., 394

T

Takagi, N., 126, 480, 481
Tamaru, T., 201
Taschek, R., 481, 638
Tatibana, M., 426, 456
Tawil, E. P., 440, 441, 451, 465, 683–685, 729
Terpstra, P., 201, 232, 659
Terry, E. M., 506
Terry, V. J., 494
Thiessen, P. A., 234
Thomson, W. T., 283, 449
Thorndike, A. M., 396
Thorndike, E. M., 390
Tomboulian, D., 232, 233
Tower, C. H., 242, 529, 538, 542–544, 560, 561, 567, 569
Tsien, L., 219, 411, 451, 501
Tsi-Ze, N., 217, 220, 221, 244, 451, 501, 722–724
Tumanski, S. S., 681
Tykociner, J., 449

U

Uda, H., 501
Underwood, M., 157, 501
Usui, R., 507

V

Vadilov, P., 522
Valasek, J., 175, 204, 205, 329, 511, 515, 520, 527, 529, 532–537, 551–556, 566, 567, 573, 580, 638, 706, 724
Van Dyke, K. S., 220, 222, 334, 390, 396, 397, 406, 407, 411, 422, 424, 432, 441, 462, 479, 708
Van Leeuwen, J. D., 516
Van Vleck, J. H., 176
Veen, A. L. W. E. van der, 208, 217, 225–229, 232, 704
Verschaffelt, J. E., 465
Vigness, I., 517, 521, 526, 538–548, 640
Vigoureux, P., 99, 244, 292, 444, 445, 460, 497, 501, 506
Voigt, W., 3, 5, 8, 135, 155, 156, 190, 194, 197, 201, 217–219, 227, 228, 251, 265, 267, 276, 278, 409, 410, 448, 449, 641, 700, 701, 706, 711, 754

W

Wachsmuth, R., 440, 464, 465
Wagner, K. W., 669
Walstrom, J. E., 394
Warren, B. E., 646, 737
Watanabe, Y., 334, 358, 393, 439, 491–497, 501, 507, 668
Webster, R. A., 670
Wei, P., 732, 734
Weigle, J., 330
Weiss, P., 580, 746, 754
Weissenberg, K., 232
Wertli, A., 501
West, J., 232, 708, 740
Wheeler, L. P., 502
White, F. W. G., 440
Whitehead, S., 413
Wien, W., 199, 439
Wildberger, A., 519
Willard, G. W., 407, 424, 425, 454, 455, 493
Williams, A. L., 529
Williams, N. H., 303, 442
Wilson, A. J. C., 519
Winkel, A., 234
Wologdin, V., 470
Wood, R. G., 709
Wood, R. W., 679, 682
Woodruff, M. W., 449
Wooster, W. A., 184, 232, 641, 709, 732
Worobieff, V. von, 30
Wright, R. B., 155, 156, 410, 440, 450, 463, 501
Wyckoff, R. W. G., 732, 735

Y

Yamamoto, W., 501
Yeou Ta, 709
Yoda, H., 457, 501

Z

Zacek, A. 451, 669
Zachoval, L., 465
Zeleny, A., 573
Zeller, W., 670
Zettlemoyer, A. C., 665
Ziegler, A. W., 432
Zottu, P. D., 481
Zwemer, R. L., 681
Zwicker, B., 663, 665

SUBJECT INDEX

A

Actino-electricity, 1, 711
Activity of resonator, 298
Adiabatic heating, 42, 641
Air blast (*see* Quartz wind)
Air gap (*see* Gap)
Alternating current notation, 288
Ammonium arsenate (*see* Arsenates)
Ammonium chloride, 230
Ammonium phosphate (*see* Phosphates)
Ammonium tartrate (*see* Tartrates)
Analogous end, 30
Antilogous end, 30
Antiresonance (*see* Resonance)
Applications, technical, 665–698
Arsenates, 208, 659–666, 740
Asparagine, 483
Atomic theory, 731–744
  (*See also* Unit cell)
Attenuation constant, 89
Axial ratio, 13
  quartz, 27
  Rochelle salt, 21, 737
  tourmaline, 30
Axinite, 709
Axis, Bravais, 16
  crystal, 13, 16, 27
  Millerian, 16
  orthogonal, 15–17
  piezoelectric, 194
    I.R.E. system, 217, 407–410, 458
  polar, 15, 30
  quartz, 406–410, 415–427

B

Bar, composite, 391
  (*See also* Constants, piezoelectric; Resonator; Vibrations, lengthwise)
Barium antimonyl tartrate (*see* Tartrates)
Beet sugar, 483
Bender, 672
Benzil, 225
Bimorph, 239, 672
Body forces, 46, 185, 312
Bonds, chemical, 731
Boracite, 230
Boundary conditions, 262, 265
Bravais-Miller system, 16
Bravais symbols, 28
  system, 16
Brushite, 201

C

Camphor, 232
  patchouli, 225
Capacitance, parallel, of resonator, 333–336, 342–346, 353, 354, 357, 370, 392, 397, 461, 478
Clamped crystal, 161, 254, 262, 264, 270, 276, 279, 311, 328, 397
  Rochelle salt, 512, 513, 593, 598–602, 606, 620–625, 646
Classes, crystal, 13, 17, 19, 53
  piezoelectric, 190–192
  pyroelectric, 700
Cleavage, 27, 410, 525, 705
Click method, 231, 385
Clinohedrite, 233
Constants, dielectric, 44, 160–176
    clamped, 311, 414, 585
    complex, 325–329, 661
    cross-constants, 162
    definitions of, 550, 551, 586, 587
    effective, 329, 437, 473–475
    lengthwise vibrations, 291, 304, 473–475
    mixed tartrates, 655–657
    phosphates and arsenates, 659–662
    piezoelectric contribution, 267
    quartz, 413–415
    resonator, 304
    thickness vibrations, 311
  elastic, 43, 49, 53
    adiabatic, 63, 120–146, 157, 158, 437, 460, 477

Constants, elastic, constant displacement, 263, 264, 269
constant field, 41, 263, 272, 316
constant normal displacement, 270, 313, 318, 478
constant polarization, 269, 272, 273
cross-constants, 58
isagric, 41, 263, 272, 316
lengthwise vibrations, 316
measurement of, 116–119, 317–320
piezoelectric contribution, 269–275
quartz, 134–156
best values, 137
Rochelle salt, 119–133, 627–629
best values, 123
sodium-ammonium tartrate, 125
sodium chlorate, 159
thickness vibrations, 316
tourmaline, 156, 157
transformation equations, 68–79, 272
zinc blende, 159
equivalent electric, 296, 304, 305, 333–383
Rochelle salt, 474, 475, 478
mechanical, of resonator, 98, 475
piezoelectric, 44, 178–193, 200–233
cross-constants, 193
measurement of, 241–243, 387–392, 531
quartz, 144, 145, 217–223, 409, 736
Rochelle salt, 204–207, 546, 604, 627–636
tourmaline, 227, 228
zinc blende, 742, 743
(*See also* Measurement; Piezoelectricity; Pyroelectricity; Quartz; Rochelle salt; Stiffness; Tourmaline)
Contour, Straubel, 458
(*See also* Vibrations, contour)
Conversion factors, 188, 189, 253
Coupler, piezoelectric, 668
Coupling effects, 438, 454, 456, 466, 467, 482
Crevasse, 393, 401
Cronstedtite, 233
Cross section, effect of, 102, 439
Crystallography, 9–38
Cubic crystals, 16, 20
elastic properties of, 158, 159
optical properties of, 715, 718, 720
piezoelectric properties of, 229–231
Curie-Weiss law, 749
mixed tartrates, 657
phosphates and arsenates, 661
Rochelle salt, 557, 559, 614–618, 623, 646, 647
(*See also* Ferromagnetism)
Cuts, crystal, 80
(*See also* Quartz, Rochelle salt)
Cycles, elastic, 281–283

D

Damping constant, 89–100, 372
Decrement, logarithmic, 89, 90, 92
(*See also* Damping constant)
Demonstrations, 231, 243, 385–387, 416–422, 424–426, 440–442, 462–465, 485, 486, 490, 495, 499, 674, 678–683, 703, 706, 721, 727–730
Deuterium phosphate (*see* Phosphates)
Dextrogyrate, 21
Dielectric properties of crystals, 160–176
comparison with elastic properties, 260
effect, 34
energy, 166, 174–176
impermeability, 163
losses, 174, 479
stiffness, 163
(*See also* Constants)
Dimensions, 89, 702, 719
piezoelectric, 184, 188, 253
Dipole, 171–174, 580–582, 645, 650–653, 739
Direction cosines, 65, 69, 83, 194
Dispersion, 107
anomalous, 176, 325
Displacement, electric, 160–164, 167, 168, 247, 250
mechanical, 88, 106
Dissonance, 92
Distance, electrical, 277
Double refraction, elastic, 107
Double strip, 181, 500, 672

E

Edingtonite, 233
Effect, converse, 4, 178, 187
direct, 4, 178, 187
electrocaloric, 709
longitudinal, 180, 193

Effect, primary, 40, 183, 699, 701, 707
quadratic, 585, 612–614
secondary, 40
piezoelectric, 260–283
tertiary, 699, 708
thermal expansion, 34
thermoclastic, 40, 44
transverse, 180, 193
(*See also* Pyroelectricity)
Elasticity, 34, 39–64
compliance, 48, 49
compressibility, 63, 126
correlation with dielectrics, 260
geometrical representation, 79
susceptibility, 49
(*See also* Constants; Groups; Shear; Strain; Stress)
Electret, 233–235
Electrocaloric effect, 40, 709, 710
Electrodes, location of, on crystal, 236–240
optimum length, 305
short, 237, 301–305
(*See also* Rochelle salt)
Electromechanical relations, 247, 265
(*See also* Ratio)
Electro-optic effect, 721–727
(*See also* Optical effects)
Electrostriction, 4, 198, 199, 614
Ellipsoids, 52, 107, 169, 170
Enantiomorphism, 20, 26, 31, 217, 406–409, 510, 516, 729
Energy in dielectrics, 174–176, 283, 625
Energy equations, 44, 184, 249, 252, 589, 701
Epistilbite, 233
Epsomite, 233
Equivalent, electrical, 333–383, 491
(*See also* Network)
Etch figures, 33
quartz, 420–424
Rochelle salt, 516
Etching tests, 37
quartz, 419–426
reflection method, 424
refraction method, 424

F

Fatigue, (*see* Rochelle salt)
Ferromagnetic analogy, 511, 753
Ferromagnetism, 745–754
Curie law, 745
Curie point, 748–754
Curie-Weiss law, 749–751
domains, 751–753
hysteresis, 752–754
magnetocaloric effect, 754
magnetostriction, 752
paramagnetism, 745, 746, 748
piezomagnetism, 754
spontaneous magnetization, 748–753
susceptibility, 745, 749
Fiducial circle, 339, 368
Filter, 394, 667–669, 687–690
Flexure, 59, 60, 239
(*See also* Vibrations, flexural)
Frequency, 87
critical, 94, 347, 354, 355
fundamental, 92
harmonic, 92, 106, 302, 303, 308, 372
natural, 87
resonant, 398
response, 336, 366
temperature coefficient, 452 (*see also* Quartz; Rochelle salt; Tourmaline)
Frequency calibration, 339, 346
Frequency modulation, 509
Friction, internal, 34, 306
Frictional factor, 88, 89, 97, 99, 108

G

Gadolinium sulphate, 746
Gap, effect of, on equivalent constants, 357–361, 368, 387
on frequency, 301, 322, 324, 439, 445
on polarization, 167
on stiffness, 277, 278, 279, 299, 300, 316, 445
when large, 369
network with, 335
resonance diagram with, 362, 398–405
Rochelle salt, 480
Graphical methods, 336–383, 398
Groups, 33, 34
elastic, 53, 54, 119, 134, 157, 158

H

Hexagonal crystals, 16, 20
optical properties of, 716, 717

Hexagonal crystals, piezoelectric properties of, 228
beta-quartz, 228
(*See also* Quartz, beta)
Hydrostatic pressure, piezoelectric effects of, 194, 227
Rochelle salt, 573–575, 641
Hysteresis, 283
mixed tartrates, 656, 657
phosphates and arsenates, 662, 663
Rochelle salt, 479, 511, 513, 541, 559–571, 577, 579, 597, 598, 634, 635
(*See also* Ferromagnetism)

I

Impurities on surfaces, 168, 169, 526, 527
Indices, rational, 13
Bravais, 16, 17
Miller, 14–17
quartz, 28
Inertia, lateral, 102
Internal field constant, 170, 582
magnetic, 746, 754
phosphates and arsenates, 664
Inversion, α-β, 139
geometrical, 339, 344, 347, 363
Iodyrite, 232, 233
Iron, 749, 754
Isomorphism, 33, 654
Isothermal process, 41, 182, 246, 267
Isotropic solid, 45, 55, 57, 103

K

Kerr effect, 725–727
Key-tapping method, 385, 386

L

Lag (*see* Rochelle salt)
Langbeinite, 233
Langevin function, 172, 173, 643, 645, 652, 653, 746–752
Lattice, 10, 733, 734
dynamics, 742, 743
Lenz's law, 280
Leucophanite, 233
Levogyrate, 21, 25
Lithium selenate, 704
Lithium sodium sulphate, 704
Lithium sulphate, 201, 704
Lithium trisodium molybdate, 228
Lithium trisodium selenate, 704

M

Magnetism, 42, 745–754
Mass, equivalent, 98
Measurement, dynamic, 120, 127, 132, 384–405
equivalent network, 392–405
elastic, 116
piezoelectric, 210, 218, 241–244, 384–392, 531
static, 120
pyroelectric, 712
(*See also* Transducer; Constants)
Meliphanite, 233
Mixtures, isomorphic, 33, 654–659
Model, quartz, piezoelectric, 215
Rochelle salt, elastic, 127
Rochelle salt, unit cell, 738–740
Modes, normal, 86
(*See also* Vibrations)
Molecular field theory, (*see* Theory, internal field)
Momentum, angular, 108
Monitor, crystal, 504, 505
Monoclinic crystals, 16, 19
optical properties of, 715–718, 726
piezoelectric properties of, 201
Rochelle salt, 585, 638, 641
Morphic effects, 613, 614, 621, 718
Motional admittance, 381

N

Network, equivalent, 298, 392, 490, 491
(*See also* Constants; Equivalent, electrical)
Neumann's principle, 11
Nickel sulphate, 209

O

Optical effects, 713–730
activity, 728–730
biaxial, 715, 720, 723
electro-optic, linear, 34, 721–727

Optical effects, electro-optic, quadratic, 725–727
ellipsoids, 713–715, 717–720, 722, 724, 727
extinction, 727, 728
optic axes, 716, 720, 724
piezo-optic, 34, 717–721, 726
polarization constants, 716, 717, 722
quartz, 720, 722–724, 728, 729
refractive index, 714, 723, 724, 726
Rochelle salt, 720, 722, 724, 725, 728, 729
sodium chlorate, 722, 729
tourmaline, 722
uniaxial, 716, 717, 720
Oscillator, piezo, 286, 489–509
bridge-stabilized, 503
early types of, 493
high frequency, 501
light-controlled, 502
low frequency, 500
modifications, 498
performance of, 507
Pierce circuit, 494–500
Pierce-Miller circuit, 494–500
push-pull, 499
theory of, 506, 507
tourmaline, 501, 506, 509
Rochelle salt, 505
sound-controlled, 502
standard-frequency, 503–505, 508
Oscillograph, 559, 560

P

Parelectric, 511, 558, 591, 596
Pentaerythritol, 232
Permalloy, 754
Permittivity, 160, 550
complex, 176, 548
(*See also* Constant, dielectric; Dielectric properties)
Phosphates, 208, 659–666, 740
structure of KH_2PO_4, 740
Picric acid, 709
Piezoelectricity classes, 34, 190–194
converse effect, 4
discovery of, 2
equations, fundamental, 44, 183–188, 246–252
excitation, 236–241
Piezoelectricity, miscellaneous crystals, 231
noncrystalline materials, 234
principles, 177–199
qualitative tests, 243
strain coefficients, 183, 184, 217, 219, 220
stress coefficients, 183, 184, 310
surfaces, 196–198, 215
susceptibility, 183, 184
tensorial, 711
Voigt's theory, 182–189, 249, 257
alternative formulations, 245–259
(*See also* Constants; Effect)
Piezomagnetism, 34, 754
Piezo-optic effect, (*see* Optical effects)
Point-groups, 12
Poisson's ratio, 58, 156, 438, 439
Polarizability, 170, 171, 644, 649
Polarization, 160–167
longitudinal, 197
molecular theory of, 170–174
spontaneous, 174, 189, 252, 254, 471
transverse, 197
by uniform field, 216
by uniform pressure, 214
Polarized light, use of, with quartz, 416–419, 465, 468, 713–730
Potassium arsenate (*see* Arsenates)
Potassium iodate, 232
Potassium lithium sulphate, 704
Potassium phosphate (*see* Phosphates)
Potassium tartrate (*see* Tartrates)
Potential, thermodynamic, 39–43, 246, 252
(*See also* Energy equations)
Powder method, 231
Projection, stereographic, 29, 34, 36
Pyrite, 754
Pyroelectricity, 1, 44, 699–711
axis, 702, 704
constant, 39
primary, 699, 701, 705, 707
secondary, 699, 702
tertiary, 699, 702
effect, 34, 625, 700–709
electrocaloric effect, 709, 710
miscellaneous crystals, 708, 709
quartz, 708, 712
Rochelle salt, 637, 706–708, 710
tensorial, 710, 711

Pyroelectricity, theory of, 700–711
tourmaline, 702–706, 712
Pyrrhotite crystals, 753

Q

Quality factor Q, 89, 90
quartz, 462
Quartz, 22, 23, 37, 134–157
artificial, 25
axes, 406–410, 415–427, 434
clock, 503, 508
conductivity, electrical, 413
thermal, 411
crushing strength, 410
cutting and finishing, 427, 434
density, 411
dielectric constant, 413–415
elasticity, 134–156
secondary effects, 274, 281
temperature coefficients, 136–145
electric strength, 413
etching, 419–426
expansion, thermal, 412
fracture, 410
frequency temperature coefficient, 444, 451–459
geology, 434
hardness, 410
high Q, 462
imperfections, 434
inspection, 434
luminescence, 411
mountings and holders, 428–434
optical tests, 416–427, 434
piezoelectric constants, 217–223
effect, of stress, 220
of temperature, 221
properties of, 406–427, 434
radiation, effect of, 434
resonator, 434–468
aging, 433
luminous, 463, 467
numerical data, 460, 461
reduced friction of, 442, 462
ring-shaped, 452, 467, 504
rotational effects, 441
special cuts, 451–461
wave patterns, 463–466
right and left, 26–28, 406–410
shear, 444, 452–455
Quartz, specific heat, 411
sphere, 422–424, 441, 458
structure, 732–736
technique, 427–433
vibrations, flexural, 446–449, 460, 467
torsional, 449–451, 467
wind, 440, 441
(*See also* Atomic theory; Constants; Vibrations)
Quartz, alpha (*see* Quartz)
Quartz, beta, 24, 30, 140, 157, 412, 734, 735
(*See also* Resonator)
Quartz cuts, oblique, 451–461, 466
AC-cut, 454
AT-cut, 453–459, 461, 466, 502, 505
BC-cut, 454
BT-cut, 453–459, 461, 466, 502
CT-cut, 453, 455, 456, 458, 459, 466
DT-cut, 453, 455, 456, 458, 459, 466
ET-cut, 457
FT-cut, 457
GT-cut, 452, 453, 456, 458, 459, 466, 504
MT-cut, 453, 456–459
NT-cut, 453, 456–459, 668
V-cut, 457, 467
X-cut, 443, 444, 461, 505, 669, 670
Y-cut, 444, 452, 454, 461
YT-cut, 457
−5°-cut, 453, 458, 459, 669
18.5°-cut, 453, 458, 459, 668

R

Radium, effect of, on quartz, 223
Ratio, capacitance, 298, 305, 324, 353, 354, 370, 392, 453, 460, 478, 668
electromechanical, 297, 322, 324, 354
Reactance, equivalent parallel, 346
equivalent series, 345
mechanical, 99
(*See also* Resonator)
Reciprocity theorem, 247
Relaxation time (*see* Rochelle salt)
Resistance, effect of, on resonator, 377
equivalent parallel, 346
equivalent series, 345
mechanical, 99
(*See also* Resonator)

Resonance, 94, 96, 97
antiresonance, 348, 355, 389, 395, 493, 496
circle, 336–382, 401, 402
impedance circle, 346, 348, 404
quadrantal points, 350
curve, 374
parallel, 336, 348–352, 366, 367
series, 336, 348, 349, 350, 366, 367
Resonator, 284–329
admittance, 351, 352, 368, 369, 379
beta-quartz, 228, 466
composite, 484–488
crystals, various, 483
current, 292–298, 321, 324
energy, 357
flexural, 239, 397, 482
history, 287
impedances, 346, 378, 380
lengthwise vibrations, 290–306
forces applied locally, 100
mountings and holders, 428–433
parallel capacitance, 365
phase relations, 356
polarization in, 292–298, 313
potential, distribution, 372
quartz-liquid, 487
Rochelle salt, 469–483, 487
wave patterns, 482
sources of error, 241
theories, comparison of, 382
torsional, 483
tourmaline, 484
(*See also* Constants; Resonance; Resonance circle; Vibrations)
Rhamnose, 483
Rhombic crystals, 16, 19, 73–76
elastic properties of, 119–134
optical properties of, 718
piezoelectric properties of, 201
(*See also* Rochelle salt)
Rigidity, modulus, 155
Rochelle salt, anomalies, 470, 510, 584
coercive force, 562, 578, 597, 628, 635, 639
converse effect, 511, 538–546
crystallography, 21, 36, 37
Curie point, 511, 558, 585, 594, 639, 644, 645
cutting, 524
Rochelle salt, dielectric constant, 473–475, 518, 556–559, 571–573, 576, 597, 614, 635, 671
dielectric observations, 549–579
dielectric properties, 512
direct effect, 511, 531–538, 544–546
domains, 470, 513, 553, 583, 631–642, 706, 737
elastic theory, 609–614, 616, 617
electrodes, 528–530
etch figures, 516
flaws, 525
grinding and finishing, 526–528
growth, 522, 523, 633
heavy water, 133, 207, 575–579
high frequency, 476
historical, 3, 6, 7, 513
interaction theory, 580–602
L-cut, 204, 481, 675
lag and fatigue, 546–548, 552–554
monoclinic clamping, 587, 599
normal method, 587, 588, 601, 602
orientation, 204
piezoelectric constants, 204–207, 546, 604, 627–636
observations, 531–548
theory, 603–630
polarization theory, 256, 585, 589, 608, 629, 630, 671
polymorphism, 637
properties of, general, 515–521
quadratic effect, 612–614
relaxation times, 175, 522, 540, 547, 548
reversibility, 545
rhombic clamping, 586, 587, 590–594, 619
rhombic method, 587, 588, 592
saturation coefficient, 588 *ff.*
secondary effects, 274, 281
specific heat, 519
spontaneous polarization, 513, 566, 578, 594–599, 601, 616, 627, 628, 634, 638, 646, 647, 648, 652, 706, 707, 737, 739
spontaneous strain, 252, 540, 586, 589, 619, 640
stereographic projection, 36
structure, 736–740
surface impurities, 555
temperature effects, 129, 477, 532–536, 561–579, 592–600

Rochelle salt, expansion, 517, 641
unipolarity, 537, 540, 555, 556, 632
(*See also* Atomic theory; Clamped crystal; Constants; Curie-Weiss law; Hydrostatic pressure; Hysteresis; Optical effects; Pyroelectricity; Resonator; Susceptibility; Transducer; Vibrations)
Rod (*see* Vibrations, lengthwise; Bar)
Rodometer, 426
Rodoscope, 425
Rotation of axes, 65–83
piezoelectric constants, 194–226
positive sense defined, 67, 409
quartz, 141–155, 164, 409
dielectric equations, 164, 166
Rubidium tartrate (*see* Tartrates)

S

Scale value, admittance, 338, 363
frequency, 341, 379, 399
impedance, 344
Schönflies symbols, 18
Scolecite, 233
Seignette-electrics, 7, 510–666
origin of term, 581
theory between Curie points, 618–625
Shear, 50–53
piezoelectric excitation, 238
rule for signs, 51
(*See also* Vibrations; Quartz)
Shortite, 233
Sodium-ammonium tartrate (*see* Tartrates)
Sodium chlorate, 229, 722, 729
Sodium tartrate (*see* Tartrates)
Space charge, 314
Space-groups, 12
Space-lattices, 12
Specific heat, phosphates and arsenates, 664
(*See also* Rochelle salt)
Sphalerite, 229, 708
Stabilizer, 286, 489–492
Stibiotantalite, 233
Stiffness, 63, 105, 113, 114
coefficients, 49
effective, 293, 312–317, 361
(*See also* Constants, elastic)
Strain, 47–53
rules for signs, 48, 51
Stress, 45–47, 50–53, 65
driving, 90, 290, 320
effect of, on elastic constants, 129
rules for signs, 47, 51
(*See also* Resonator)
Strontium tartrate (*see* Tartrates)
Struvite, 233
Sugar, 201
Susceptibility, 160–164, 268
definitions of, 550, 551
Rochelle salt, 473–475, 558, 559, 573–575, 577, 597, 615, 626
(*See also* Piezoelectricity; Ferromagnetism)
Symmetry, crystal, 17, 18
Systems, crystallographic, 15, 16, 19, 162

T

Tartaric acid, 201
Tartrate, ammonium 201, 704
ammonium-sodium, 208, 483, 654–659
barium antimonyl, 208
mixed, 651, 654–659
dielectric constants, 655–657
piezoelectric properties of, 657–659
potassium, 201, 704
rubidium, 225
sodium, 201
strontium, 704
thallium-sodium, 654–659
Temperature coefficients, 129–133, 136–140, 452
(*See also* Quartz; Rochelle salt; Tourmaline)
Tetragonal crystals, 16, 19, 208, 209
optical properties, 716, 717
Thallium-sodium tartrate (*see* Tartrates)
Theory, charge, 249, 250, 253
displacement, 248–253
internal fields, 247–251, 643–653
polarization, 206, 220, 247–259, 274, 473
(*See also* Rochelle salt)
Thickness, effective, 315, 316
Tiemannite, 233
Topaz, 232, 708

Torsion, 61, 240
compliance, 61
stiffness, dynamic, 113
static, 114
(*See also* Vibrations, torsional)
Tourmaline, 3, 30, 38, 225, 227, 228, 464, 484, 710, 722
density of, 484
dielectric constant, 484
oscillator, 506
resonator, 484
temperature coefficient, 506
wave patterns of, 464, 484
(*See also* Optical effects; Resonator)
Transducer, 285, 669–698
acoustic, 671–675, 690, 691
measurement of pressures, accelerations, and vibrations, 669, 670, 691–695
miscellaneous applications, 694–698
quartz-steel oscillator, 676–678, 695
Rochelle salt, 670–675
(*See also* Ultrasonics)
Transformation (*see* Constants; Rotation of axes)
Triclinic crystals, 16, 19, 179
optical properties, 715–718
Trigonal crystals, 716
optical properties, 716, 717, 720
piezoelectric properties, 209–228
(*See also* Quartz; Tourmaline)
Tuning fork, 486
Twinning, 27, 31, 32
quartz, 417, 421, 422, 434
Rochelle salt, 639
Twister, 240, 672

U

Ultrasonics, 5, 675–685, 695–698
crystal generator, 678–686, 695
effects of intense radiation, 682
interferometer, 679, 683, 695
light relays, 685, 695
optical effects, 683–687, 695
television, 686, 687, 695
(*See also* Transducer)
Unit cell, 10, 12, 733–735, 737, 739
Unit face, 13
Urotropine, 483

V

Velocity, 94
at end of bar, 298
of waves, 87, 89, 110
Vibrations, 84–115
compressional, 86, 115, 238
contour, 108, 286, 455, 467, 500
Rochelle salt, 481
damped free, 94
face shear, 455
flexural, 86, 111–113, 115, 239, 500
(*See also* Quartz; Resonator)
forced, 90–92
free, 356
harmonic, 92–106, 114, 158, 295–324, 353–359, 371, 372, 438, 463, 502
lengthwise, 88–103, 115, 238, 286, 290–306, 359, 387, 435–442, 466, 476
damping, 295
Rochelle salt, 626–629
unsymmetrical effects, 439
normal modes, 86
overtone, 92, 110, 112, 446–449
shear, 86, 106, 108, 444, 452–455
thickness, 103–108, 115, 238, 286, 306–324, 358, 359, 371, 389, 397
damped, 107
electrical constants, 320–324
quartz, 141, 442–446, 451–455, 466
Rochelle salt, 127, 480
torsional, 86, 113–115, 240, 500, 501
(*See also* Quartz; Resonator)

W

Wave constant, 460
Wavelength, 87, 89, 95, 96
constant, 89
Waves, compressional, 154
equation, 88, 108
shear, 106, 108
(*See also* Quartz; Resonator; Rochelle salt; Vibration)
Wurtzite, 229, 233, 708

X

X-rays, effect of vibrations on, 329–331
orientation by, 426, 434
Rochelle salt structure, 646, 737, 738

Y

Young's modulus, 72, 88, 111, 124–126, 133, 134, 140, 147, 150, 155, 409, 437, 440, 458, 485
(*See also* Constants)

Z

Zinc blende, 229, 708, 742, 743
structure, 742
Zinc sulphide, 708
Zone, 15
Zunyite, 233